Scientific and Technical Aerospace Reports

STAR

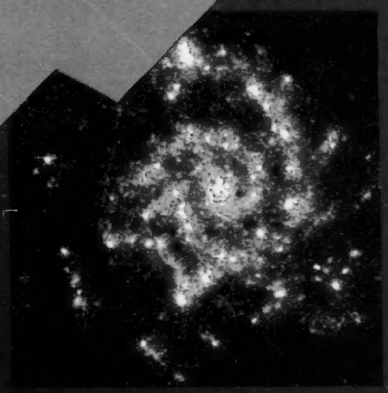

An Abstract Journal

NASA STI PROGRAM SCIENTIFIC & TECHNICAL INFORMATION

Volume 31, Number 1
January 1993
N93-10001 to N93-10960

Scientific and Technical Aerospace Reports

Scientific and Technical Aerospace Reports (STAR) is an abstract journal that provides comprehensive coverage of worldwide aerospace-related reports. It is a major product of the International Aerospace Database managed by the NASA Scientific and Technical Information (STI) Program. The coverage includes reports on aeronautics, space, and supporting disciplines. *STAR* lists current, publicly available reports entered into the NASA STI Database during the 4-week period preceding publication. A typical citation and abstract appear on page viii. They explain how to read the items that are announced in this journal.

NASA sponsors a companion journal, *International Aerospace Abstracts (IAA) (NOVA* for internal NASA use) that lists abstracts of the open literature on aerospace subjects available worldwide. *IAA* is available for sale through the AIAA.

Entries found in *STAR* and *IAA* are available through NASA's online service, RECON, as the International Aerospace Database and through DIALOG as the Aerospace Database.

Information on aerospace and related subjects is gathered by the NASA STI Program through national and international agreements and exchanges and is made available to the NASA community as well as to the public in many forms through various outlets. The section on NASA STI Program Products and Services contains additional information.

For further information please contact:
NASA Center for AeroSpace Information (CASI)
P.O. Box 8757
Baltimore, Maryland 21240-0757
(301) 621-0390

US ISSN 0036-8741

Volume 31 Number 1 / January 1993

TABLE OF CONTENTS

AERONAUTICS For related information see also *Astronautics.*

01 AERONAUTICS (GENERAL) 1

02 AERODYNAMICS 2
Includes aerodynamics of bodies, combinations, wings, rotors, and control surfaces; and internal flow in ducts and turbomachinery. For related information see also *34 Fluid Mechanics and Heat Transfer.*

03 AIR TRANSPORTATION AND SAFETY ..... N.A.
Includes passenger and cargo air transport operations; and aircraft accidents. For related information see also *16 Space Transportation* and *85 Urban Technology and Transportation.*

04 AIRCRAFT COMMUNICATIONS AND NAVIGATION 6
Includes digital and voice communication with aircraft; air navigation systems (satellite and ground based); and air traffic control. For related information see also *17 Space Communications, Spacecraft Communications, Command and Tracking* and *32 Communications and Radar.*

05 AIRCRAFT DESIGN, TESTING AND PERFORMANCE 8
Includes aircraft simulation technology. For related information see also *18 Spacecraft Design, Testing and Performance* and *39 Structural Mechanics.* For land transportation vehicles see *85 Urban Technology and Transportation.*

06 AIRCRAFT INSTRUMENTATION ..... N.A.
Includes cockpit and cabin display devices; and flight instruments. For related information see also *19 Spacecraft Instrumentation* and *35 Instrumentation and Photography.*

07 AIRCRAFT PROPULSION AND POWER 9
Includes prime propulsion systems and systems components, e.g., gas turbine engines and compressors; and onboard auxiliary power plants for aircraft. For related information see also *20 Spacecraft Propulsion and Power, 28 Propellants and Fuels,* and *44 Energy Production and Conversion.*

08 AIRCRAFT STABILITY AND CONTROL 10
Includes aircraft handling qualities; piloting; flight controls; and autopilots. For related information see also *05 Aircraft Design, Testing and Performance.*

09 RESEARCH AND SUPPORT FACILITIES (AIR) ..... N.A.
Includes airports, hangars and runways; aircraft repair and overhaul facilities; wind tunnels; shock tubes; and aircraft engine test stands. For related information see also *14 Ground Support Systems and Facilities (Space).*

ASTRONAUTICS For related information see also *Aeronautics.*

12 ASTRONAUTICS (GENERAL) ..... N.A.
For extraterrestrial exploration see *91 Lunar and Planetary Exploration.*

13 ASTRODYNAMICS ..... N.A.
Includes powered and free-flight trajectories; and orbital and launching dynamics.

14 GROUND SUPPORT SYSTEMS AND FACILITIES (SPACE) ..... N.A.
Includes launch complexes, research and production facilities; ground support equipment, e.g., mobile transporters; and simulators. For related information see also *09 Research and Support Facilities (Air).*

15 LAUNCH VEHICLES AND SPACE VEHICLES 12
Includes boosters; operating problems of launch/space vehicle systems; and reusable vehicles. For related information see also *20 Spacecraft Propulsion and Power.*

16 SPACE TRANSPORTATION ..... N.A.
Includes passenger and cargo space transportation, e.g., shuttle operations; and space rescue techniques. For related information see also *03 Air Transportation and Safety* and *18 Spacecraft Design, Testing and Performance.* For space suits see *54 Man/System Technology and Life Support.*

17 SPACE COMMUNICATIONS, SPACECRAFT COMMUNICATIONS, COMMAND AND TRACKING ... 12
Includes telemetry; space communications networks; astronavigation and guidance; and radio blackout. For related information see also *04 Aircraft Communications and Navigation* and *32 Communications and Radar.*

N.A.—no abstracts were assigned to this category for this issue.

18 SPACECRAFT DESIGN, TESTING AND PERFORMANCE **12**
Includes satellites; space platforms; space stations; spacecraft systems and components such as thermal and environmental controls; and attitude controls. For life support systems see *54 Man/System Technology and Life Support.* For related information see also *05 Aircraft Design, Testing and Performance, 39 Structural Mechanics,* and *16 Space Transportation.*

19 SPACECRAFT INSTRUMENTATION **14**
For related information see also *06 Aircraft Instrumentation* and *35 Instrumentation and Photography.*

20 SPACECRAFT PROPULSION AND POWER **15**
Includes main propulsion systems and components, e.g., rocket engines; and spacecraft auxiliary power sources. For related information see also *07 Aircraft Propulsion and Power, 28 Propellants and Fuels, 44 Energy Production and Conversion,* and *15 Launch Vehicles and Space Vehicles.*

CHEMISTRY AND MATERIALS

23 CHEMISTRY AND MATERIALS (GENERAL) **27**

24 COMPOSITE MATERIALS **27**
Includes physical, chemical, and mechanical properties of laminates and other composite materials. For ceramic materials see *27 Nonmetallic Materials.*

25 INORGANIC AND PHYSICAL CHEMISTRY **29**
Includes chemical analysis, e.g., chromatography; combustion theory; electrochemistry; and photochemistry. For related information see also *77 Thermodynamics and Statistical Physics.*

26 METALLIC MATERIALS **33**
Includes physical, chemical, and mechanical properties of metals, e.g., corrosion; and metallurgy.

27 NONMETALLIC MATERIALS **35**
Includes physical, chemical, and mechanical properties of plastics, elastomers, lubricants, polymers, textiles, adhesives, and ceramic materials. For composite materials see *24 Composite Materials.*

28 PROPELLANTS AND FUELS **41**
Includes rocket propellants, igniters and oxidizers; their storage and handling procedures; and aircraft fuels. For related information see also *07 Aircraft Propulsion and Power, 20 Spacecraft Propulsion and Power,* and *44 Energy Production and Conversion.*

29 MATERIALS PROCESSING ..... **N.A.**
Includes space-based development of products and processes for commercial application. For biological materials see *55 Space Biology.*

ENGINEERING For related information see also *Physics.*

31 ENGINEERING (GENERAL) **43**
Includes vacuum technology; control engineering; display engineering; cryogenics; and fire prevention.

32 COMMUNICATIONS AND RADAR **67**
Includes radar; land and global communications; communications theory; and optical communications. For related information see also *04 Aircraft Communications and Navigation* and *17 Space Communications, Spacecraft Communications, Command and Tracking.* For search and rescue see *03 Air Transportation and Safety,* and *16 Space Transportation.*

33 ELECTRONICS AND ELECTRICAL ENGINEERING **70**
Includes test equipment and maintainability; components, e.g., tunnel diodes and transistors; microminiaturization; and integrated circuitry. For related information see also *60 Computer Operations and Hardware* and *76 Solid-State Physics.*

34 FLUID MECHANICS AND HEAT TRANSFER **77**
Includes boundary layers; hydrodynamics; fluidics; mass transfer and ablation cooling. For related information see also *02 Aerodynamics* and *77 Thermodynamics and Statistical Physics.*

35 INSTRUMENTATION AND PHOTOGRAPHY **85**
Includes remote sensors; measuring instruments and gauges; detectors; cameras and photographic supplies; and holography. For aerial photography see *43 Earth Resources and Remote Sensing.* For related information see also *06 Aircraft Instrumentation* and *19 Spacecraft Instrumentation.*

36 LASERS AND MASERS **87**
Includes parametric amplifiers. For related information see also *76 Solid-State Physics.*

37 MECHANICAL ENGINEERING **91**
Includes auxiliary systems (nonpower); machine elements and processes; and mechanical equipment.

38 QUALITY ASSURANCE AND RELIABILITY **93**
Includes product sampling procedures and techniques; and quality control.

39 STRUCTURAL MECHANICS **94**
Includes structural element design and weight analysis; fatigue; and thermal stress. For applications see *05 Aircraft Design, Testing and Performance* and *18 Spacecraft Design, Testing and Performance.*

GEOSCIENCES For related information see also *Space Sciences.*

42 GEOSCIENCES (GENERAL) ..... **N.A.**

43 EARTH RESOURCES AND REMOTE SENSING **102**
Includes remote sensing of earth resources by aircraft and spacecraft; photogrammetry; and aerial photography. For instrumentation see *35 Instrumentation and Photography.*

44 ENERGY PRODUCTION AND CONVERSION **103**
Includes specific energy conversion systems, e.g., fuel cells; global sources of energy; geophysical conversion; and windpower. For related information see also *07 Aircraft Propulsion and Power, 20 Spacecraft Propulsion and Power,* and *28 Propellants and Fuels.*

45 ENVIRONMENT POLLUTION **104**
Includes atmospheric, noise, thermal, and water pollution.

46 GEOPHYSICS **105**
Includes aeronomy; upper and lower atmosphere studies; ionospheric and magnetospheric physics; and geomagnetism. For space radiation see *93 Space Radiation.*

47 METEOROLOGY AND CLIMATOLOGY **125**
Includes weather forecasting and modification.

48 OCEANOGRAPHY **128**
Includes biological, dynamic, and physical oceanography; and marine resources. For related information see also *43 Earth Resources and Remote Sensing.*

LIFE SCIENCES

51 LIFE SCIENCES (GENERAL) **129**

52 AEROSPACE MEDICINE **130**
Includes physiological factors; biological effects of radiation; and effects of weightlessness on man and animals.

53 BEHAVIORAL SCIENCES **132**
Includes psychological factors; individual and group behavior; crew training and evaluation; and psychiatric research.

54 MAN/SYSTEM TECHNOLOGY AND LIFE SUPPORT **133**
Includes human engineering; biotechnology; and space suits and protective clothing. For related information see also *16 Space Transportation.*

55 SPACE BIOLOGY ..... **N.A.**
Includes exobiology; planetary biology; and extraterrestrial life.

MATHEMATICAL AND COMPUTER SCIENCES

59 MATHEMATICAL AND COMPUTER SCIENCES (GENERAL) **134**

60 COMPUTER OPERATIONS AND HARDWARE **134**
Includes hardware for computer graphics, firmware, and data processing. For components see *33 Electronics and Electrical Engineering.*

61 COMPUTER PROGRAMMING AND SOFTWARE **135**
Includes computer programs, routines, algorithms, and specific applications, e.g., CAD/CAM.

62 COMPUTER SYSTEMS **140**
Includes computer networks and special application computer systems.

63 CYBERNETICS **141**
Includes feedback and control theory, artificial intelligence, robotics and expert systems. For related information see also *54 Man/System Technology and Life Support.*

64 NUMERICAL ANALYSIS **143**
Includes iteration, difference equations, and numerical approximation.

65 STATISTICS AND PROBABILITY **146**
Includes data sampling and smoothing; Monte Carlo method; and stochastic processes.

66 SYSTEMS ANALYSIS **147**
Includes mathematical modeling; network analysis; and operations research.

67 THEORETICAL MATHEMATICS ..... **N.A.**
Includes topology and number theory.

PHYSICS For related information see also *Engineering.*

70 PHYSICS (GENERAL) ..... **N.A.**
For precision time and time interval (PTTI) see *35 Instrumentation and Photography;* for geophysics, astrophysics or solar physics see *46 Geophysics, 90 Astrophysics,* or *92 Solar Physics.*

71 ACOUSTICS **147**
Includes sound generation, transmission, and attenuation. For noise pollution see *45 Environment Pollution.*

72 ATOMIC AND MOLECULAR PHYSICS **153**
Includes atomic structure, electron properties, and molecular spectra.

73 NUCLEAR AND HIGH-ENERGY PHYSICS **155**
Includes elementary and nuclear particles; and reactor theory. For space radiation see *93 Space Radiation.*

74 OPTICS **157**
Includes light phenomena and optical devices. For lasers see *36 Lasers and Masers.*

75 PLASMA PHYSICS **159**
Includes magnetohydrodynamics and plasma fusion. For ionospheric plasmas see *46 Geophysics.* For space plasmas see *90 Astrophysics.*

76 SOLID-STATE PHYSICS **164**
Includes superconductivity. For related information see also *33 Electronics and Electrical Engineering* and *36 Lasers and Masers.*

77 THERMODYNAMICS AND STATISTICAL PHYSICS **169**
Includes quantum mechanics; theoretical physics; and Bose and Fermi statistics. For related information see also *25 Inorganic and Physical Chemistry* and *34 Fluid Mechanics and Heat Transfer.*

SOCIAL SCIENCES

80 SOCIAL SCIENCES (GENERAL) **171**
Includes educational matters.

81 ADMINISTRATION AND MANAGEMENT ..... **N.A.**
Includes management planning and research.

82 DOCUMENTATION AND INFORMATION SCIENCE **171**
Includes information management; information storage and retrieval technology; technical writing; graphic arts; and micrography. For computer documentation see *61 Computer Programming and Software.*

83 ECONOMICS AND COST ANALYSIS ..... **N.A.**
Includes cost effectiveness studies.

84 LAW, POLITICAL SCIENCE AND SPACE POLICY ..... **N.A.**
Includes NASA appropriation hearings; aviation law; space law and policy; international law; international cooperation; and patent policy.

85 URBAN TECHNOLOGY AND TRANSPORTATION ..... **N.A.**
Includes applications of space technology to urban problems; technology transfer; technology assessment; and surface and mass transportation. For related information see *03 Air Transportation and Safety, 16 Space Transportation,* and *44 Energy Production and Conversion.*

SPACE SCIENCES For related information see also *Geosciences.*

88 SPACE SCIENCES (GENERAL) ..... **N.A.**

89 ASTRONOMY **177**
Includes radio, gamma-ray, and infrared astronomy; and astrometry.

90 ASTROPHYSICS **178**
Includes cosmology; celestial mechanics; space plasmas; and interstellar and interplanetary gases and dust. For related information see also *75 Plasma Physics.*

91 LUNAR AND PLANETARY EXPLORATION **189**
Includes planetology; and manned and unmanned flights. For spacecraft design or space stations see *18 Spacecraft Design, Testing and Performance.*

92 SOLAR PHYSICS **190**
Includes solar activity, solar flares, solar radiation and sunspots. For related information see *93 Space Radiation.*

93 SPACE RADIATION **192**
Includes cosmic radiation; and inner and outer earth's radiation belts. For biological effects of radiation see *52 Aerospace Medicine.* For theory see *73 Nuclear and High-Energy Physics.*

GENERAL

Includes aeronautical, astronautical, and space science related histories, biographies, and pertinent reports too broad for categorization; histories or broad overviews of NASA programs.

99 GENERAL **192**

SUBJECT INDEX **I-1**

PERSONAL AUTHOR INDEX **I-75**

CORPORATE SOURCE INDEX **I-83**

CONTRACT NUMBER INDEX **I-95**

REPORT NUMBER INDEX **I-97**

APPENDIX **A-1**

TYPICAL CITATION AND ABSTRACT

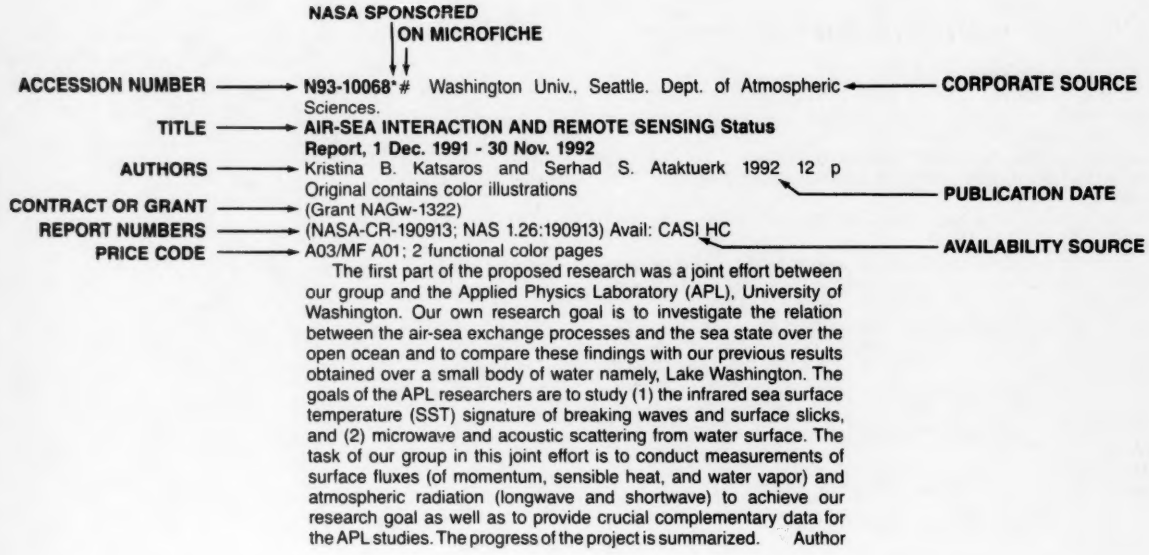
NASA SPONSORED
ON MICROFICHE
ACCESSION NUMBER
N93-10068* # Washington Univ., Seattle. Dept. of Atmospheric Sciences.
CORPORATE SOURCE
TITLE
AIR-SEA INTERACTION AND REMOTE SENSING Status Report, 1 Dec. 1991 - 30 Nov. 1992
AUTHORS
Kristina B. Katsaros and Serhad S. Ataktuerk 1992 12 p
Original contains color illustrations
PUBLICATION DATE
CONTRACT OR GRANT
(Grant NAGw-1322)
REPORT NUMBERS
(NASA-CR-190913; NAS 1.26:190913) Avail: CASI HC
AVAILABILITY SOURCE
PRICE CODE
A03/MF A01; 2 functional color pages
The first part of the proposed research was a joint effort between our group and the Applied Physics Laboratory (APL), University of Washington. Our own research goal is to investigate the relation between the air-sea exchange processes and the sea state over the open ocean and to compare these findings with our previous results obtained over a small body of water namely, Lake Washington. The goals of the APL researchers are to study (1) the infrared sea surface temperature (SST) signature of breaking waves and surface slicks, and (2) microwave and acoustic scattering from water surface. The task of our group in this joint effort is to conduct measurements of surface fluxes (of momentum, sensible heat, and water vapor) and atmospheric radiation (longwave and shortwave) to achieve our research goal as well as to provide crucial complementary data for the APL studies. The progress of the project is summarized. Author

VOLUME 31 NUMBER 1 / JANUARY 1993

Scientific and Technical Aerospace Reports

A Monthly Publication of the National Aeronautics and Space Administration

01 AERONAUTICS (GENERAL)

N93-10073* National Aeronautics and Space Administration, Washington, DC.
AERONAUTICAL ENGINEERING: A CONTINUING BIBLIOGRAPHY WITH INDEXES (SUPPLEMENT 276)
Mar. 1992 194 p
(NASA-SP-7037(276); NAS 1.21:7037(276)) Avail: CASI HC A09

This bibliography lists 705 reports, articles, and other documents introduced into the NASA scientific and technical information system in Feb. 1992. Subject coverage includes: design, construction, and testing of aircraft and aircraft engines; aircraft components, equipment, and systems; ground support systems; and theoretical and applied aspects of aerodynamics and general fluid dynamics. Author

N93-10074* National Aeronautics and Space Administration, Washington, DC.
AERONAUTICAL ENGINEERING: A CONTINUING BIBLIOGRAPHY WITH INDEXES (SUPPLEMENT 279)
Jun. 1992 207 p
(NASA-SP-7037(279); NAS 1.21:7037(279)) Avail: CASI HC A10

This bibliography lists 759 reports, articles, and other documents introduced into the NASA scientific and technical information system in May 1992. Subject coverage includes: design, construction, and testing of aircraft and aircraft engines; aircraft components, equipment, and systems; ground support systems; and theoretical and applied aspects of aerodynamics and general fluid dynamics. Author

N93-10351* National Aeronautics and Space Administration, Washington, DC.
AERONAUTICAL ENGINEERING: A CUMULATIVE INDEX TO A CONTINUING BIBLIOGRAPHY (SUPPLEMENT 274)
Feb. 1992 642 p
(NASA-SP-7037(274); NAS 1.21:7037(274)) Avail: CASI HC A99

This publication is a cumulative index to the abstracts contained in supplements 262 through 273 of Aeronautical Engineering: A Continuing Bibliography. The bibliographic series is compiled through the cooperative efforts of the American Institute of Aeronautics and Astronautics (AIAA) and the National Aeronautics and Space Administration (NASA). Seven indexes are included: subject, personal author, corporate source, foreign technology, contract number, report number, and accession number. Author

N93-10352* National Aeronautics and Space Administration, Washington, DC.
AERONAUTICAL ENGINEERING: A CONTINUING BIBLIOGRAPHY WITH INDEXES (SUPPLEMENT 281)
Aug. 1992 167 p
(NASA-SP-7037(281); NAS 1.21:7037(281)) Avail: CASI HC A08

This bibliography lists 596 reports, articles, and other documents introduced into the NASA scientific and technical information system in Jul. 1992. Subject coverage includes: design, construction, and testing of aircraft and aircraft engines; aircraft components, equipment, and systems; ground support systems; and theoretical and applied aspects of aerodynamics and general fluid dynamics. Author

N93-10644 Aerospace Industries Association of Canada, Ottawa (Ontario).
AEROSPACE INDUSTRIES ASSOCIATION OF CANADA Annual Report, 1991
1992 48 p Original contains color illustrations
(CTN-92-60590) Avail: CASI HC A03/MF A01

The Aerospace Industries Association of Canada is charged with providing a voice for the industry before government and public, coordinating and developing industry views, advising and assisting governments in developing programs and implementing policies, promoting the role of the industry as a major exporter, participating in long- and short-term planning with governments, and ensuring that the Canadian aerospace industry continues to progress and prosper. About 150 companies are members, and a listing of members is appended. Activities of the Association for 1991 are summarized, including the work of committees specializing in such fields as airworthiness, customs and traffic, defence and marketing, electronics systems, human resources, trade, productivity, space, and technical standards. Some industry statistics and forecasts are also presented for the years 1988-1994. CISTI

N93-10647*# National Academy of Sciences - National Research Council, Washington, DC.
AERONAUTICAL TECHNOLOGIES FOR THE TWENTY-FIRST CENTURY
1992 311 p
(Contract NASw-4003)
(NASA-CR-190918; NAS 1.26:190918; LC-92-64197;
ISBN-0-309-04732-3) Avail: CASI HC A14/MF A03

This study gives an overview of the future technologies in aeronautics. This collaborative effort relies upon the input of numerous experts from around the country. Specific issues covered include subsonic transport aircraft, high-speed civil transport aircraft short-haul aircraft, environmental issues, operational issues, aerodynamics, propulsion, materials and structures, avionics and control, and cognitive engineering. The appendices include bibliography, abbreviations and acronyms, and NASA fiscal year 1992 aeronautics funding (table) and participants. The forward states that over the last decade, foreign aircraft manufacturers have made significant inroads into the global aircraft market, to the detriment of U.S. interests. Recommendations are made to counter that trend. R.L.B.

N93-10651# Industry, Science and Technology Canada, Toronto (Ontario).
AEROSPACE INDUSTRY PROFILE, 1990-1991 [PROFIL DE L'INDUSTRIE AEROSPATIALE, 1990-1991]
1991 22 p In ENGLISH and FRENCH Original contains color illustrations
(CTN-92-60513) Avail: CASI HC A03/MF A01

In 1988, the Canadian aerospace industry employed 63,650 people and had sales worth $6 billion, of which $4 billion were exports. Companies in Ontario and Quebec accounted for 89 percent of the total industry value of production. These companies form a 3-tiered system, with the first tier consisting of the largest

companies and accounting for 45 percent of annual output. These large companies have integrated capabilities for complete aircraft, aero-engines, space systems, or avionics systems. The second tier also accounts for 45 percent of industry output and comprises about 40 medium-sized companies that primarily supply proprietary products and build-to-print components, most of which are sold to foreign aerospace principal manufacturers. This tier also includes companies providing repair and overhaul services. The third tier consists of over 100 smaller companies that mainly supply subcontract products and services. During the decade ending in 1988, the industry had an average annual sales growth of 9 percent. Strengths and weaknesses of the industry are discussed in terms of such issues as the degree of foreign ownership, research and development expenditures, the relatively small size of Canadian companies, the risks of new product development, availability of trained labor, the barriers to trade with the United States, the forecast reductions in defense budgets, and international competition. CISTI

N93-10652# Industry, Science and Technology Canada, Toronto (Ontario). Aeronautics Branch.
AEROSPACE AND DEFENCE-RELATED INDUSTRIES STATISTICAL SURVEY REPORT, 1991
Mar. 1992 22 p Original contains color illustrations
(CTN-92-60514) Avail: CASI HC A03/MF A01

Graphs and tables are presented showing the state of the Canadian aerospace and defence industries in 1991, as determined by survey data received from 48 companies. Information is included on the following: sales according to such categories as exports, customer, product category, industry subsector, and geographical area; employment; costs of sales; materials and labor costs; imported content of sales and purchases; new investment; research and development funding; capital assistance; repayment of federal government contributions; and value of inventories. Many of the graphs include forecast data for 1991-1995. Industry growth is projected for each year to 1995. CISTI

02 AERODYNAMICS

Includes aerodynamics of bodies, combinations, wings, rotors, and control surfaces; and internal flow in ducts and turbomachinery.

For related information see also *34 Fluid Mechanics and Heat Transfer.*

N93-10069*# Georgia Inst. of Tech., Atlanta. Signature Technology Lab.
LV SOFTWARE FOR SUPERSONIC FLOW ANALYSIS Final Technical Report, Oct. 1991 - Oct. 1992
William A. Bell Oct. 1992 19 p
(Grant NAG3-1215)
(NASA-CR-190911; NAS 1.26:190911) Avail: CASI HC A03/MF A01

The NASA Lewis Research Center (LeRC) maintains a leadership position in research into advanced aerospace propulsion systems. For the next generation of aircraft, engine designs continue to involve complex, high-speed flows. Performing the detailed flow diagnostics to properly evaluate these designs requires advanced instrumentation to probe these highly turbulent flows. The hostile flow environment often requires nonintrusive measurement techniques such as the laser velocimeter (LV). Since the LV is a proven instrument for nonintrusive flow measurement, it can provide quantitative velocity data with minimal interference to the flow. Based on anticipated flow conditions, laser velocimeter systems were procured from TSI, Inc. The initial system utilized counter processor technology, but later procurements this past year include a more advanced, correlator-based processor, which significantly improves the overall LV performance. To meet the needs of advanced research into propulsion, this instrument must be integrated into an existing VAX/VMS computer system for data acquisition, processing, and presentation. The work done under this grant before this period concentrated on developing the software required to setup and acquire data from the TSI MI-990 multichannel interface, and the RMR 1989 rotating machinery resolver. With the basis established for controlling the operation of the LV system, software development this past year shifted in emphasis from instrumentation control and data acquisition to data analysis and presentation. The progress of the program is reported. Author

N93-10071*# National Aeronautics and Space Administration. Langley Research Center, Hampton, VA.
PITOT SURVEY OF EXHAUST FLOW FIELD OF A 2-D SCRAMJET NOZZLE AT MACH 6 WITH AIR OR FREON AND ARGON USED FOR EXHAUST SIMULATION
William J. Monta Oct. 1992 34 p
(RTOP 505-59-40-03)
(NASA-TM-4361; L-17021; NAS 1.15:4361) Avail: CASI HC A03/MF A01

A pitot-rake survey of the simulated exhaust of a half-span scramjet nozzle model was conducted in the Langley 20-Inch Mach 6 Tunnel to provide an additional data set for computational fluid dynamics (CFD) code comparisons. A wind-tunnel model was tested with a 26-tube pitot rake that could be manually positioned along the mid-semispan plane of the model. The model configuration had an external expansion surface of 20 degrees and an internal cowl expansion of 12 degrees; tests were also performed with a flow fence. Tests were conducted at a free-stream Reynolds number of approximately 6.5 x 10(exp 6) per foot and a model angle of attack of -0.75 degrees. The two exhaust gas mediums that were tested were air and a Freon 12-argon mixture. Each medium was tested at two jet total pressures at approximately 28 and 14 psia. This document presents the flow-field survey results in graphical as well as tabular form, and several observations concerning the results are discussed. The surveys reveal the major expected flow-field characteristics for each test configuration. For a 50-percent freon 12 and 50-percent argon mixture by volume (Fr-Ar), the exhaust jet pressures were slightly higher than those for air. The addition of a flow fence slightly raised the pitot pressure for the Fr-Ar mixture, but it produced little change for air. For the Fr-Ar exhaust, the plume was larger and the region between the shock wave and plume was smaller. Author

N93-10097*# Institute for Computer Applications in Science and Engineering, Hampton, VA.
UNSTRUCTURED MESH ALGORITHMS FOR AERODYNAMIC CALCULATIONS Final Report
D. J. Mavriplis Jul. 1992 35 p Submitted for publication
(Contracts NAS1-18605; NAS1-19480; RTOP 505-90-52-01)
(NASA-CR-189685; NAS 1.26:189685; ICASE-92-35) Avail: CASI HC A03/MF A01

The use of unstructured mesh techniques for solving complex aerodynamic flows is discussed. The principle advantages of unstructured mesh strategies, as they relate to complex geometries, adaptive meshing capabilities, and parallel processing are emphasized. The various aspects required for the efficient and accurate solution of aerodynamic flows are addressed. These include mesh generation, mesh adaptivity, solution algorithms, convergence acceleration, and turbulence modeling. Computations of viscous turbulent two-dimensional flows and inviscid three-dimensional flows about complex configurations are demonstrated. Remaining obstacles and directions for future research are also outlined. Author

N93-10098*# Old Dominion Univ., Norfolk, VA. Dept. of Mechanical Engineering and Mechanics.
NAVIER-STOKES DYNAMICS AND AEROELASTIC COMPUTATIONS FOR VORTICAL FLOWS, BUFFET AND AEROELASTIC APPLICATIONS Progress Report, 1 Oct. 1991 - 30 Sep. 1992
Osama A. Kandil Sep. 1992 38 p
(Grant NAG1-648)
(NASA-CR-190692; NAS 1.26:190692) Avail: CASI HC A03/MF A01

The accomplishments achieved during the period include

conference and proceedings publications, journal papers, and abstracts which are either published, accepted for publication or under review. Conference presentations and NASA highlight publications are also included. Two of the conference proceedings publications are attached along with a Ph.D. dissertation abstract and table of contents. In the first publication, computational simulation of three-dimensional flows around a delta wing undergoing rock and roll-divergence motions is presented. In the second publication, the unsteady Euler equations and the Euler equations of rigid body motion, both written in the moving frame of reference, are sequetially solved to simulate the limit-cycle rock motion of slender delta wings. In the dissertation abstract, unsteady flows around rigid or flexible delta wings with and without oscillating leading-edge flaps are considered. L.R.R.

N93-10306 Tennessee Univ., Knoxville.
A GLOBALLY WELL-POSED ACCURATE AND EFFICIENT FINITE ELEMENT CFD ALGORITHM FOR COMPRESSIBLE AERODYNAMICS Ph.D. Thesis
Giuseppe Settimo Iannelli 1991 391 p
Avail: Univ. Microfilms Order No. DA9133745

For the reliable determination of aerodynamic flows, a minimally dissipative generalized curvilinear-coordinate flux vector splitting implicit algorithm is developed within an optimal finite element integral statement for the two-demensional (2-D) and axisymmetric compressible Navier-Stokes equations for ideal and reacting gases. Hypersonic-flow dissociated real air is modeled via a neutral mixture of five species: nitric oxide, and molecular and atomic oxygen and nitrogen. The associated thermodynamic state is then determined via an original solution procedure for the classical chemical equilibrium equation system. The analysis develops the curvilinear-coordinate flux vector Jacobian matrices and associated characteristics equations. For any equation of state, the eigenvalues are the contravariant components of velocity in combination with the sound speed. Hence, the flow wave propagation in curvilinear space is rigorously represented using a tensor-field resolution of the flux vector into essentially kinematic and kinetic components. The streamwise semi-discretization is achieved using a Lyapunov-stable, Galerkin finite element integral statement for an eigenvalue-based 'companion conservation law system', permitting classical test and trial space definitions. Thereafter, the accurate computation of the unsteady flow evolution is attained utilizing an implicit Runge-Kutta time-integration scheme, which is nonlinearly stable and 2nd order accurate. Subsequently, a matrix tensor product factorization permits efficient numerical linear algebra handling for large Courant number. For 2-D and axisymmetric transonic, supersonic, and hypersonic inviscid and viscous flows, including real gas effect simulation, the algorithm is verified to yield reliable determination of velocity, pressure, and temperature fields by generating accurate and monotone, essentially non-oscillatory numerical solutions in the presence of weak and strong shocks, attached and detached, and in boundary layer-inviscid flow interactions. Dissert. Abstr.

N93-10320 Texas A&M Univ., College Station.
ANALYSIS OF WING-BODY JUNCTION FLOWFIELDS USING THE INCOMPRESSIBLE NAVIER-STOKES EQUATIONS, VOLUMES 1 AND 2 Ph.D. Thesis
Bernard P. Paul, Jr. 1991 492 p
Avail: Univ. Microfilms Order No. DA9133985

An incompressible three dimensional Navier-Stokes flow solver has been developed for the analysis of wing-body junction flowfields on general aviation, light twin-engined aircraft. The numerical scheme used in the code is based on the cell-centered finite volume multistage Runge-Kutta time stepping scheme originally developed by Jameson et al. for the Euler equations and extended to viscous flows by Martinelli (two dimensions) and Vatsa (three dimensions). The code, INCRK3D, uses the techniques of local time stepping, implicit residual averaging, and multigridding to accelerate the solution to convergence. The development of the code was performed by taking the three dimensional compressible Navier-Stokes solver of Vatsa and extensively modifying the code and making it applicable to incompressible flow thru the use of the artificial compressibility concept. The code was then applied to a series of wing-body junction flow test cases for verification, the simplified wing-body junction that was experimentally analyzed by Dickinson, the Cougar wind tunnel model geometry, and the Cougar flight vehicle geometry. The numerical results obtained for the Dickinson test case agreed very well with the experimental data and demonstrated that the code had the ability to simulate the physics of junction flows. The comparison of the numerical and experimental pressure coefficients on the wing surface for the Cougar test cases yielded mixed results, with the wind tunnel results comparing poorly and the flight test results comparing very well. The new code has been found to be numerically efficient and accurate and applicable to simplified wing-body junction geometries. Its development constitutes the initial step in the process of developing an analytical tool capable of aiding in the design of junction drag reduction devices such as flow energizers. Dissert. Abstr.

N93-10340# University of Southern California, Los Angeles. Dept. of Aerospace Engineering.
CONTROL OF LIFT AND DRAG IN UNSTEADY FLOWS Final Technical Report, 15 May 1990 - 14 May 1992
Chih-Ming Ho 1 Jul. 1992 75 p
(Contract F49620-90-C-0038)
(AD-A253146; AFOSR-92-0675TR) Avail: CASI HC A04/MF A01

The response of delta wings with different aspect ratios and a 2-D wing in unsteady free stream was investigated. It was found that the characteristics of the lift forces depend on the existence of leading-edge vortex shedding. For delta wings with attached leading-edge vortex, the time-averaged lift force was found to be independent of reduced frequency since there is no intrinsic vortex convection time scale. With increasing angle of attack or aspect ratio, vortex shedding can occur, and the time required to convect along the chord becomes an intrinsic time scale. The appearance of the intrinsic convection time scale on the delta wing corresponds to increased lift with increasing reduced frequency, just like the 2-D wing. Flow visualizations of vortex breakdown position around the trailing edge does not affect the lift force. For the 2-D wing, the aerodynamic performance in the poststall region shows a maximum at an optimum frequency. Very high lift coefficients exceeding 10 can be observed at this reduced frequency. GRA

N93-10342# Aeronautical Research Labs., Melbourne (Australia).
DESIGN AND IMPLEMENTATION OF DIGITAL FILTERS FOR ANALYSIS OF F/A-18 FLIGHT TEST DATA
W. Waldman May 1992 35 p
(AD-A253447; ARL-STRUC-TM-555; DODA-AR-006-678) Avail: CASI HC A03/MF A01

This technical memorandum describes the methods and computer programs used to specify, design, and implement time-domain and frequency-domain FIR digital filters for use in the analysis of F/A-18 flight test data. Two bandpass filters covering the 10-20 Hz and 32-52 Hz frequency bands have been developed, and they can be used for analyzing the two dominant modes of structural vibration response occurring on the F/A-18 empennage. A highpass filter with a cutoff frequency of 8 Hz was also designed for filtering strain gauge data for use in producing fatigue load sequences for coupon testing. The effects of bandpass filtering on the transient response of short-term vibrations lasting about one second have also been investigated, leading to the conclusion that FIR digital filters have a negligible effect on the transient response characteristics of short bursts of vibration. GRA

N93-10349*# National Aeronautics and Space Administration. Langley Research Center, Hampton, VA.
INTERACTIVE GRID GENERATION PROGRAM FOR CAP-TSD
Samuel R. Bland Oct. 1990 29 p
(RTOP 505-63-21-01)
(NASA-TM-102705; NAS 1.15:102705) Avail: CASI HC A03/MF A01

A grid generation program for use with the CAP-TSD transonic

small disturbance code is described. The program runs interactively in FORTRAN on the Sun Workstation. A fifth-degree polynomial is used to map the grid index onto the computational coordinate. The grid is plotted to aid in the assessment of its quality and may be saved on file in NAMELIST format. Author

N93-10375# Naval Postgraduate School, Monterey, CA.
A METHOD OF TESTING TWO-DIMENSIONAL AIRFOILS M.S. Thesis
Richard K. Joyce Mar. 1992 77 p
(AD-A253210) Avail: CASI HC A05/MF A01

The Naval Postgraduate School Aeronautics and Astronautics Department conducts research and development for the Navy's Unmanned Air Vehicle program. NPS currently lacks the capability of testing two-dimensional airfoils to obtain lift, drag and pitching moment coefficients. This thesis consists of the design and calibration of a method of measuring these coefficients using strain gages, and the method of obtaining purely two-dimensional flow over the airfoil. During the calibration process, two amplifiers were tested in an attempt to minimize system drift and to ensure repeatability during successive runs. These desired characteristics were not achieved, however. The final phase was to be validation of the design by testing an NACA 0012 airfoil and comparing measured airfoil data with established reference data. This final phase was not completed due to structural failure of the airfoil. GRA

N93-10648# Cincinnati Univ., OH. Dept. of Aerospace Engineering and Applied Mechanics.
LDV MEASUREMENTS OF UNSTEADY FLOW FIELDS IN RADIAL TURBINE Final Report
W. Tabakoff and M. Pasin Jul. 1992 165 p
(Contract DAAL03-90-G-0129)
(AD-A253592; ASE/EM-92-105) Avail: CASI HC A08/MF A02

Detailed measurements of an unsteady flow field within the inlet guide vanes (IGV) and the rotor of a radial inflow turbine were performed using a three component Laser Doppler Velocimeter (LDV) system together with a rotary encoder. The mean velocity, the flow angle and the turbulence contours for IGV passages are presented at four blade-to-blade planes for different rotor positions to give three dimensional, unsteady behavior of the IGV flow field. These results are compared with the measurements obtained in the same passage in the absence of the rotor. The flow field of the IGV passage was found to be affected by the presence of the rotor. The ratio of the tangential normal stresses to the radial normal stresses at the exit of the IGV was found to be more than doubled when compared to the case without the rotor. The rotor flow field measurements are presented as relative mean velocity and turbulence stress contours at various cross section planes throughout the rotor. The cross flow and turbulence stress levels were found to be influenced by the incidence angle. Transportation of the high turbulence fluid by the cross flow was observed downstream in the rotor blade passages. GRA

N93-10707# Air Force Inst. of Tech., Wright-Patterson AFB, OH. Foreign Aerospace Science and Technology Center.
RESEARCH ON THE ASYMMETRICAL AERODYNAMIC FORCES OF REENTRY VEHICLES
Lumin Zhang 6 Feb. 1992 16 p Transl. into ENGLISH from Yuhang Xuebao (China), no. 4, 1989 p 45-50
(AD-A254307; FASTC-ID(RS)T-0789-91) Avail: CASI HC A03/MF A01

This article goes through numerical trajectory equations with six degrees of freedom to simulate reentry vehicle or body asymmetrical aerodynamic forces and asymmetrical static and dynamic derivative influences on abnormalities in the rolls and turns of bodies or vehicles. It illucidates the mechanisms which produce asymmetrical aerodynamic forces and asymmetrical static and dynamic derivatives. This article makes use of approximate calculations and numerical value calculation methods. It calculates classical asymmetrical aerodynamic forces for reentry bodies. It does qualitative analyses of the patterns or rules associated with aerodynamic forces as they follow changes in the geometrical parameters of vehicles or bodies, having important reference value for the design of reentry bodies or vehicles. GRA

N93-10753# Wright Lab., Wright-Patterson AFB, OH.
HYDRODYNAMIC INVESTIGATION OF VORTICAL FLOWS FOR AN ATTAC CONFIGURATION WITH CANARDS
Lawrence W. Rogers and Michael G. Alexander Jun. 1992 44 p
(AD-A253928; WL-TM-92-332) Avail: CASI HC A03/MF A01

Hydrodynamic investigation was conducted on an ATTAC Fighter model to qualitatively determine the nature of forebody/Canard/LEX/wing vortex systems. Dye flow visualization was accomplished for angles of attack from 5 to 40 degrees and Canard deflections from +10 to -20 degrees. A Canard Deflection of -10 degrees created least disturbance to the vortex systems. GRA

N93-10811# Army Armament Research, Development and Engineering Center, Picatinny Arsenal, NJ.
WIND TUNNEL SPIN DATA REDUCTION TO OBTAIN AERODYNAMIC SPIN DAMPING COEFFICIENTS BY USING NONLINEAR EQUATION OF MOTION
Chiu H. Ng and Seungeuk Han Aug. 1992 36 p
(AD-A253880; ARAED-TR-92011) Avail: CASI HC A03/MF A01

A compute program, SPINFIT, is designed for extracting the linear and nonlinear spin damping coefficients by fitting calculated values to the observed wind tunnel spin data. The approach used in this program was developed at NASA Ames. The example given in this report showed significant improvement in fitting with the nonlinear spin damping term in the equation of motion when compared to this exponential fit. GRA

N93-10824*# National Aeronautics and Space Administration. Langley Research Center, Hampton, VA.
EFFECT OF PLANFORM AND BODY ON SUPERSONIC AERODYNAMICS OF MULTIBODY CONFIGURATIONS
S. Naomi McMillin, Steven X. S. Bauer, and Dorothy T. Howell Sep. 1992 281 p
(RTOP 505-59-30-01)
(NASA-TP-3212; L-16976; NAS 1.60:3212) Avail: CASI HC A13/MF A03

An experimental and theoretical investigation of the effect of the wing planform and bodies on the supersonic aerodynamics of a low-fineness-ratio, multibody configuration has been conducted in the Langley Unitary Plan Wind Tunnel at Mach numbers of 1.60, 1.80, 2.00, and 2.16. Force and moment data, flow-visualization data, and surface-pressure data were obtained on eight low-fineness-ratio, twin-body configurations. These configurations varied in inboard wing planform shape, outboard wing planform shape, outboard wing planform size, and presence of the bodies. The force and moment data showed that increasing the ratio of outboard wing area to total wing area or increasing the leading-edge sweep of the inboard wing influenced the aerodynamic characteristics. The flow-visualization data showed a complex flow-field system of shocks, shock-induced separation, and body vortex systems occurring between the side bodies. This flow field was substantially affected by the inboard wing planform shape but minimally affected by the outboard wing planform shape. The flow-visualization and surface-pressure data showed that flow over the outboard wing developed as expected with changes in angle of attack and Mach number and was affected by the leading-edge sweep of the inboard wing and the presence of the bodies. Evaluation of the linear-theory prediction methods revealed their general inability to consistently predict the characteristics of these multibody configurations. Author

N93-10845 Kansas Univ., Lawrence.
DEVELOPMENT OF NONLINEAR AERODYNAMIC MODELS FOR UNSTEADY RESPONSES Ph.D. Thesis
Suei Chin 1991 102 p
Avail: Univ. Microfilms Order No. DA9210033

In the current study, a method based on Fourier analysis is developed to analyze the force and moment data obtained in large amplitude forced oscillation tests at high angles of attack. The aerodynamic models for normal force, lift, drag and pitching moment coefficients are built up from a set of aerodynamic responses to harmonic motions at different frequencies. Based on the aerodynamic models of harmonic data, the indicial responses are formed. The final expressions for the models involve time integrals of the indicial type advocated by Tobak and Schiff. Results from linear two- and three-dimensional unsteady aerodynamic theories as well as test data for a 70-deg delta wing as used to verify the models. It is shown that the present modeling method is accurate in producing the aerodynamic responses to harmonic motions and the ramp type motions. The model also produces correct trend for a 70-deg delta wing in harmonic motion with different mean angles-of-attack. However, the current model cannot be used to extrapolate data to higher angles-of-attack than that of the harmonic motions which form the aerodynamic model. For linear ramp motions, a special method is used to calculate the corresponding frequency and phase angle at a given time. The calculated results from modeling show higher lift peak for linear ramp motion than for harmonic ramp motion. The current model also shows reasonably good results for the lift responses at different mean angles of attack. To the author's knowledge, the current methodology of aerodynamic modeling is the first to produce the harmonic oscillation responses at high angle-of-attack and the ramp type motions. Dissert. Abstr.

N93-10856# Air Force Inst. of Tech., Wright-Patterson AFB, OH. Foreign Aerospace Science and Technology Center.
ONE TYPE OF AUTOMATICALLY ADJUSTED DIFFERENCE SCHEME WITH ARTIFICIAL VISCOSITY TO CALCULATE ABLATED EXTERIOR SHAPES
Maozhao Yang 17 Jan. 1992 14 p Transl. into ENGLISH from Yuhang Xuebao (China), no. 3, 1988 p 55-60
(AD-A254108; FASTC-ID(RS)T-0786-91) Avail: CASI HC A03/MF A01

In the calculation of the exterior form of ablated reentry nose tips, through automatic wave filter processing with reference to the shape of the object, a type of explicit difference scheme with added artificial viscosity quantities was created. This type of scheme reaches first order accuracy in areas where shape change is wavy and second order accuracy in areas where it is smooth. Tests with numerical values clearly show that this type of method is effective in guaranteeing the accuracy of exterior shape calculations, enlarging time increments and saving computer time. GRA

N93-10858# Air Force Inst. of Tech., Wright-Patterson AFB, OH. Foreign Aerospace Science and Technology Center.
ARGUMENTS CONCERNING WIND TUNNEL TEST STUDIES OF THE TRIM CHARACTERISTICS OF OBJECTS WITH SMALL ASYMMETRIES'
Mingxi Feng 17 Jan. 1992 7 p Transl. into ENGLISH from Yuhang Xuebao (China), no. 4, 1988 p 87-88
(AD-A254111; FASTC-ID(RS)T-0788-91) Avail: CASI HC A02/MF A01

The experimental methods and results set out in the discussions of the referenced earlier work are all correct. However, the mathematical methods and formulae set down in the referenced work are not appropriate. This article brings out some different ideas about this and supplies discussion. GRA

N93-10877 Maryland Univ., College Park.
CONTRIBUTIONS TO THE EXPERIMENTAL INVESTIGATION OF ROTOR/BODY AERODYNAMIC INTERACTIONS Ph.D. Thesis
Naipei Bi 1991 358 p
Avail: Univ. Microfilms Order No. DA9133035

A series of tests were successfully conducted in both hover and forward flight to investigate the mutual aerodynamic interactions between a four-bladed, fully articulated rotor and a helicopter like fuselage. Comprehensive measurements were made of the forces and moment on the body, the thrust and power on the rotor, the time-averaged body pressures and the unsteady pressures on the body. Measurements of the total pressures and corresponding induced velocities below and behind the rotor were made using 7-hole probes. The wide-field shadowgraph technique was also used to visualize the rotor wake vortices. Experiments were conducted at various combinations of rotor thrust, advance ratio and tip path plane angle. Measurements were made on the isolated body, the body with the hub rotating but without the blades, and on the rotor/body combination. It was found that the mutual aerodynamic interactions occurring between the rotor and body were very complicated and highly unsteady. The presence of the rotor significantly affected the time-averaged and unsteady loads on the body. The rotor performance was also affected by the presence of the body, although mainly at low advance ratios. Four basic types of unsteady pressure signatures on the body surface were identified due to: (1) blade passage effected, (2) close wake vortex/body interactions, (3) wake impingement interactions, and (4) post wake-impingement interactions. This classification was supported by unsteady potential flow theory and by flow visualization using the side-field shadowgraph method. The tip vortex behavior near the body surface was also investigated. Dissert. Abstr.

N93-10889 Air Force Inst. of Tech., Wright-Patterson AFB, OH.
HIGH-RESOLUTION TVD SCHEMES FOR THE ANALYSIS OF: 1. INVISCID SUPERSONIC AND TRANSONIC FLOWS. 2. VISCOUS FLOWS WITH SHOCK-INDUCED SEPARATION AND HEAT TRANSFER Ph.D. Thesis
Mark Anthony Driver 1991 170 p
Avail: Univ. Microfilms Order No. DA9210354

Application of Total Variation Diminishing (TVD) schemes to both inviscid and viscous flows is considered. The mathematical and physical basis of TVD schemes is discussed. First and second-order accurate TVD schemes, and a second-order accurate Lax-Wendroff scheme, are used to compute solutions to the Riemann problem in order to investigate the capability of each to resolve shocks, rarefactions, and contact surfaces. Second-order finite-volume and finite-difference TVD schemes are used to obtain solutions to inviscid supersonic and transonic cascade flow problems. TVD schemes are shown to be superior to the Lax-Wendroff family of schemes for both transient and steady-state computations. TVD methodology is extended to the solution of viscous flow problems. A first-order time accurate, second-order space accurate algorithm is contrasted against a second-order time and space accurate algorithm for the solution of the viscous Burgers'equation. Necessity of using the fully second-order accurate algorithm at low Reynolds numbers is shown. Solutions are computed to the problems of laminar shock-boundary-layer interaction and unsteady, laminar, shock-induced heat transfer using the new algorithms. These algorithms provide the capability to accurately predict separation, reattachment, and pressure and skin friction profiles for shock-boundary-layer interaction. Additionally, extremely accurate comparison with theory and experiment is evident for the unsteady shock-induced heat transfer problem. These solutions are contrasted against solutions computed with the Beam-Warming algorithm, and the TVD solutions are shown to be vastly superior. Dissert. Abstr.

N93-10012 General Electric Co., Cincinnati, OH. Aircraft Engines Div.
HYPERSONIC INLET EFFICIENCY REVISITED
Paul H. Kutschenreuter, J. A. Davis, and R. J. Gaeta, Jr. *In* JHU, The 1992 JANNAF Propulsion Meeting, Volume 1 Feb. 1992 p 203-214 (For primary document see N93-10001 01-20)
Avail: CPIA, 10630 Little Patuxent Pkwy., Suite 202, Columbia, MD, 21044-3200 HC

N93-10544 Ecole Polytechnique, Montreal (Quebec). Dept. of Mechanical Engineering.
A COMPARATIVE STUDY OF SEMI-EMPIRICAL DYNAMIC STALL MODELS

R. Botez, O. Marchand, and I. Paraschivoiu *In* Carleton Univ., Proceedings of the Twelfth Canadian Congress of Applied Mechanics, Volumes 1 and 2 May 1989 p 586-587 (For primary document see N93-10466 01-31)
Copyright Avail: Canadian Society for Mechanical Engineering, 2050 Mansfield St., Suite 700, Montreal, Quebec H3A 1Z7 Canada

N93-10547 Ecole Polytechnique, Montreal (Quebec). Dept. of Mechanical Engineering.
A FIELD PANEL METHOD FOR TRANSONIC FLOWS
C. Masson, L. Lamarche, O. Marchand, and I. Paraschivoiu *In* Carleton Univ., Proceedings of the Twelfth Canadian Congress of Applied Mechanics, Volumes 1 and 2 May 1989 p 598-599 (For primary document see N93-10466 01-31)
Copyright Avail: Canadian Society for Mechanical Engineering, 2050 Mansfield St., Suite 700, Montreal, Quebec H3A 1Z7 Canada

N93-10549 University of Western Ontario, London.
FLOW OVER A LEADING EDGE WITH DISTRIBUTED ROUGHNESS
J. M. Floryan and U. Dallmann (Institut fuer Theoretische Stroemungsmechanik, Goettingen, Germany) *In* Carleton Univ., Proceedings of the Twelfth Canadian Congress of Applied Mechanics, Volumes 1 and 2 May 1989 p 660-661 (For primary document see N93-10466 01-31)
Copyright Avail: Canadian Society for Mechanical Engineering, 2050 Mansfield St., Suite 700, Montreal, Quebec H3A 1Z7 Canada

N93-10550 Moncton Univ., Edmundston (New Brunswick).
EXPERIMENTAL INVESTIGATION OF FLOWS BEHIND DIFFERENT LARGE-EDDY BREAKUP (LEBU) DEVICES IN THICK BOUNDARY LAYERS
D. Vo-Ngoc, J. R. Longval, V. D. Nguyen (Laval Univ., Quebec), and J. Dickinson (Laval Univ., Quebec) *In* Carleton Univ., Proceedings of the Twelfth Canadian Congress of Applied Mechanics, Volumes 1 and 2 May 1989 p 662-663 (For primary document see N93-10466 01-31)
Copyright Avail: Canadian Society for Mechanical Engineering, 2050 Mansfield St., Suite 700, Montreal, Quebec H3A 1Z7 Canada

N93-10551 Sherbrooke Univ. (Quebec). Dept. of Mechanical Engineering.
HARMONIC ANALYSIS OF THE AERODYNAMIC FORCES ON A DARRIEUS ROTOR [ANALYSE HARMONIQUE DES FORCES AERODYNAMIQUES SUR UN ROTOR DARRIEUS]
Abdelkrim Mazouzi, Andre Laneville, and Pierre Vittecoq *In* Carleton Univ., Proceedings of the Twelfth Canadian Congress of Applied Mechanics, Volumes 1 and 2 May 1989 p 680-681 In FRENCH (For primary document see N93-10466 01-31)
Copyright Avail: Canadian Society for Mechanical Engineering, 2050 Mansfield St., Suite 700, Montreal, Quebec H3A 1Z7 Canada

03 AIR TRANSPORTATION AND SAFETY

Includes passenger and cargo air transport operations; and aircraft accidents.

For related information see also *16 Space Transportation* and *85 Urban Technology and Transportation.*

No abstracts in this category.

04 AIRCRAFT COMMUNICATIONS AND NAVIGATION

Includes digital and voice communication with aircraft; air navigation systems (satellite and ground based); and air traffic control.

For related information see also *17 Space Communications, Spacecraft Communications, Command and Tracking* and *Communications and Radar.*

N93-10065# Federal Aviation Administration, Cambridge, MA. National Transportation Systems Center.
ADVANCED TERRAIN DISPLAYS TO TRANSPORT CATEGORY AIRCRAFT Final Report, Jan. - Sep. 1991
J. K. Kuchar and R. J. Hansman Feb. 1992 88 p Prepared in cooperation with Massachusetts Inst. of Tech., Cambridge
(Contract DTRS57-88-C-00078)
(PB92-197136; DOT-VNTSC-FAA-92-4; DOT/FAA/RD-92/4; AD-A252495) Avail: CASI HC A05/MF A01

A preliminary evaluation of terrain information presentation methods was conducted in a part-task simulation study. Pilots qualified on autoflight aircraft used both paper and prototypical electronic instrument approach plate formats to obtain terrain information. Approaches were flown using the MIT Aeronautical Systems Laboratory Advanced Cockpit Simulator. During the simulation, terrain situational awareness was tested by issuing erroneous vectors into terrain. Pilots successfully detected and avoided terrain hazards only 3 out of 52 times (6 percent). This low-hazard recognition rate is thought to be due to high level of confidence in Air Traffic Control (ATC) clearances, and highlighted the fact that current terrain depiction methods appear to be inadequate. To evaluate the increased effectiveness of advanced terrain depiction methods on electronic displays, several terrain situation display formats were designed and evaluated in a second simulation study. Spot elevation and smoothed contour terrain presentation techniques were examined using a separate moving map display dedicated to terrain information. In addition, a prototypical Graphical Ground Proximity Warning System (GGPWS) was developed and used to solicit pilot opinions and comments. Experimental methodology followed that of the preliminary terrain depiction study closely - erroneous vectors were again given by ATC, and pilot performance and opinion data were recorded. When given vectors into terrain, there was an overall 50 percent hazard recognition rate when pilots used the spot elevation display, and a 78 percent recognition rate with the contour display. Author

N93-10265# Army Engineer Topographic Labs., Fort Belvoir, VA.
GPS AZIMUTH DETERMINATION USING SHORT BASELINE CARRIER WAVE INTERFEROMETRY
Mahlon C. Hawker Dec. 1991 11 p
(AD-A254257; TEC-R-172) Avail: CASI HC A03/MF A01

The U.S. Army Topographic Engineering Center (TEC) is involved in research regarding the determination of azimuth by measurement of the carrier phase of GPS satellite signals between two or more antennas. TEC awarded three contracts to develop a GPS Azimuth Determining System (GPS ADS). A discussion of the three approaches and test data from limited Government tests are presented. GRA

N93-10323# Systems Control Technology, Inc., Arlington, VA.
ROTORCRAFT EN ROUTE ATC ROUTE STANDARDS Final Report
Raymond H. Matthews and Brian M. Sawyer Aug. 1991 50 p
(Contract DTFA01-87-C-00014)
(AD-A249129; SCT-90-RR67; DOT/FAA/RD-90/19) Avail: CASI HC A03/MF A01

Constraints on helicopter operations in the en route environment as they relate to visual flight rules (VFR), special visual flight rules (SVFR), and instrument flight rules (IFR) are identified. However, since there is relatively little VFR/SVFR interaction between helicopters in the en route environment, the report concentrates on IFR operations and recommends

modifications to route development standards using existing and planned navigation capabilities that will ultimately maximize the use of NAS en route airspace, enhance capacity, and accommodate the unique operational capabilities and requirements of helicopters. This is the second in a series of three reports that address rotorcraft/helicopter standards, route structures, and procedures applied by FAA air traffic facilities. The series consists of: (1) Rotorcraft Terminal ATC Route Standards, DOT/FAA/RD-90/18, (2) Rotorcraft En Route ATC Route Standards, DOT/FAA/RD-90/19, and (3) Rotorcraft ATC Route Standards - Implementation Guidelines, DOT/FAA/RD-90/20. GRA

N93-10424# Army Engineer Topographic Labs., Fort Belvoir, VA.

GPS ARMY RESEARCH AND APPLICATIONS

Richard B. Marth, Sr. 31 Jan. 1992 7 p

(AD-A254262; TEC-R-155) Avail: CASI HC A02/MF A01

The NAVigation Satellite Timing and Ranging (NAVSTAR) Global Positioning System (GPS) is a tool used to support military and civil needs for positioning, navigation and precise timing. The U.S. Army Topographic Engineering Center (TEC) is studying tactical and civil applications of GPS to Army missions. For the tactical Army, TEC is investigating GPS for use as a precise surveying tool and for accurate use of azimuth. The integration of GPS with an inertial navigation system is also being studied as a potential improvement for tactical navigation and positioning. For the civil missions of the U.S. Army Corps of Engineers (USACE), TEC is investigating the application of Differential GPS (DGPS) to photogrammetry and hydrographic surveying needs. Code-phase DGPS and carrier-phase DGPS are being studied with the goal of achieving real-time accuracies of 1-3 meters and .1 meter with the respective approaches. GRA

N93-10442# Lockheed Engineering and Sciences Co., Las Vegas, NV. Environmental Programs Office.

GLOBAL POSITIONING SYSTEMS TECHNOLOGY AND ITS APPLICATION IN ENVIRONMENTAL PROGRAMS

R. Puterski, J. A. Carter, M. J. Hewitt, H. F. Stone, and L. T. Fisher Feb. 1992 71 p Sponsored in part by Enviromental Monitoring Systems Lab., Las Vegas, NV

(Contract EPA-68-CO-0050)

(PB92-169358; EPA/600/R-92/036; GIS-TM-3) Avail: CASI HC A04/MF A01

Global Positioning Systems (GPS) are a location determination technology that offers significant opportunities for obtaining highly accurate locational data at low cost. In order for the technology to perform up to its capabilities in Agency applications, Environmental Protection Agency (EPA) staff will need to develop a greater understanding of the technology itself, coordinate systems, surveying, and basic geodesy. The EPA has been developing expertise in the use of the technology over the last 3 years via pilot use of GPS systems to enhance locational control in Agency projects. In order to operationalize the use of the technology within EPA, there also exists a need to develop concise standard operational procedures and methodologies for its use. The document is a beginning toward fulfillment of these needs. It is intended to be an introductory reference that describes the technology and how it could be employed in EPA work. It provides an overview of survey methods from initial planning to data reduction and postprocessing. Ancillary but important issues such as reference datums and use with geographic information systems are covered in order to provide the reader additional context regarding the use of the spatial information in a project environment. Case studies performed by the Environmental Monitoring Systems Laboratory, Las Vegas, are also included in the document as auxiliary background that may provide helpful techniques. Author

N93-10459# Federal Aviation Administration, Atlantic City, NJ.

AIR TRAFFIC CONTROL VISUAL SCANNING Report, Jan. 1991 - Jan. 1992

Earl S. Stein Jul. 1992 108 p

(Contract FAA-F2003-C)

(DOT/FAA/CT-TN92/16) Avail: CASI HC A06/MF A02

Air traffic controllers scan multiple displays to gather information necessary to make critical decisions in order to separate aircraft flying in the National Airspace System (NAS). When controllers make an error, they often respond that they did not see a piece of information that was right in front of them. Little is known about how controllers systematically scan their displays. This study was undertaken to determine whether there were patterns of scanning that characterized personnel with different levels of skill. Ten FAA controllers from a very active Terminal Radar Approach Control Facility (TRACON) participated in this study in which they controlled simulated radar traffic while their eye movements were monitored with an oculometer. This device allowed the computation of fixation frequencies and saccade duration during dynamic operations. Results indicated that the more experienced personnel had higher fixation frequencies than those who were in training. There were also significant changes in scanning behavior over time that the controllers worked. This occurred irrespective of experience and indicated that it takes between 5 and 10 minutes for the controller to establish a pattern which continues for the remainder of the work period. This suggests the importance of systematic relief period as personnel come on to control position. Author

N93-10738# Federal Aviation Administration, Washington, DC. Office of System Engineering.

A DESCRIPTION OF THE MODE SELECT BEACON SYSTEM (MODE S) AND ITS ASSOCIATED BENEFITS TO THE NATIONAL AIRSPACE SYSTEM (NAS) Final Report

P. Douglas Hodgkins Aug. 1992 43 p

(DOT/FAA/SE-92/6) Avail: CASI HC A03/MF A01

This report describes the operation of the Mode S subsystem and identifies benefits that the Mode S system provides to the National Airspace System (NAS) for surveillance and data link operations. These benefits include a reduction in asynchronous interference, reduced sensitivity to synchronous garble, more accurate and reliable surveillance, and support of air-ground data link operations. The benefits of using the mode select (Mode S) beacon system as an alternative for replacement of existing air traffic control beacon interrogators are addressed. Author

N93-10745*# National Aeronautics and Space Administration. Ames Research Center, Moffett Field, CA.

APPRAISAL OF DIGITAL TERRAIN ELEVATION DATA FOR LOW-ALTITUDE FLIGHT

Richard E. Zelenka and Harry N. Swenson Jan. 1992 12 p

(RTOP 505-64-36)

(NASA-TM-103896; A-91241; NAS 1.15:103896) Avail: CASI HC A03/MF A01

The use of terrain elevation databases in advanced guidance and navigation systems has greatly expanded. However, the limitations and accuracies of these databases must be considered and established prior to safe system flight evaluation. A simple approach to quantify reasonable flight limits is presented and evaluated for a helicopter guidance system dependent on a terrain database. The flight test evaluated involved a helicopter equipped with a Global Positioning System (GPS) receiver and radar altimeter, and a ground station GPS receiver which provided improved helicopter positioning. The precision navigation and radar altimeter data was acquired while flying low-altitude missions in south-central Pennsylvania. The aircraft-determined terrain elevations were compared with the terrain predicted by the Defense Mapping Agency (DMA) Level 1 terrain elevation data for the same area. The results suggest a safe set clearance altitude of 220 ft for flight testing of a DMA-based guidance avionic in the same area. Author

N93-10833# Federal Aviation Administration, Atlantic City, NJ.

WEATHER MESSAGE SWITCHING CENTER REPLACEMENT (WMSCR) OPERATIONAL TEST AND EVALUATION (OT/E)/INTEGRATION TEST PLAN

Frances A. Mackuse, William Benner, and Maureen Varani Sep. 1992 95 p

(DOT/FAA/CT-TN90/59) Avail: CASI HC A05/MF A01

The Weather Message Switching Center Replacement (WMSCR) will serve as the Federal Aviation Administration (FAA) gateway for the receipt and distribution of weather data and Notice to Airmen (NOTAM) within the National Airspace System (NAS). In December 1981, the FAA chartered a comprehensive NAS Plan for modernizing and improving air traffic control (ATC) and airway facilities through the year 2000. As part of the NAS Plan in 1983, the Air Traffic Service operation and requirements for the WMSCR were published. The purpose of the WMSCR system is to replace the current Weather Message Switching Center (WMSC) system in Kansas City, Missouri. It will support all functions related to weather processing presently performed by the WMSC. In addition, the WMSCR will collect NOTAM's from the Automated Flight Service Station (AFSS) environment for processing by the Consolidated NOTAM System Processor (CNSP) and will store and distribute the processed NOTAM's received from the CNSP. The WMSCR will be comprised of two identical nodes and the national Weather Service Telecommunications Gateway (NWSTG) WMSCR Interface Device (NWID). The nodes will be located at the National Aviation Weather Processing Facility (NAWPF) sites at Salt Lake City, Utah and at Atlanta, Georgia. The NWID will be located at Leesburg, Virginia. Each node will have the capability of servicing the entire geographical airspace system 24 hours a day, 7 days a week. Author

N93-10898# Army Engineer Topographic Labs., Fort Belvoir, VA.
DYNAMIC POSITIONING SYSTEMS PHOTOGRAMMETRIC
Anthony Niles 1991 7 p
(AD-A254250; TEC-R-178) Avail: CASI HC A02/MF A01

Many electronic dynamic positioning systems that use a variety of technologies, such as laser ranging, UHF signal ranging, and satellite ranging, are currently available. With the advances in technology, these systems are undoubtedly becoming more and more accurate. In fact, real-time submeter accuracy using the different-Lal Global Positioning System (GPS) in a boat, aircraft, or ground vehicle is not unrealistic. However, verifying positional accuracy at this level of accuracy of a moving platform is difficult. Close-range terrestrial photogrammetry offers a proven and accepted method for this verification, using mostly off-the shelf components and technology. Such a system is being developed at the U.S. Army Engineer Topographic Laboratories. GRA

05 AIRCRAFT DESIGN, TESTING AND PERFORMANCE

Includes aircraft simulation technology.

For related information see also *18 Spacecraft Design, Testing and Performance* and *39 Structural Mechanics*.For land transportation vehicles see *85 Urban Technology and Transportation*.

N93-10322 Southampton Univ. (England).
AN EXPERIMENTAL AND A THEORETICAL INVESTIGATION OF ROTOR PITCH DAMPING USING A MODEL ROTOR Ph.D. Thesis
Constantinos Panteli Sotiriou 1990 456 p
Avail: Univ. Microfilms Order No. BRDX93277

An experimental investigation was conducted to study rotor pitch damping in hover, axial flight (climb speed to tip speed ratios: 0-0.0549), and low speed forward flight (advance ratios: 0.05-0.088), for a variation in rotor thrust coefficient 0.001-0.0.13, and for the range of flapping frequency ratios squared 1.0-1.11. The tests were conducted at the following oscillation ratio frequencies, (frequency of oscillation divided by rotor angular speed), 0.186 for hover and axial flight and 0.1068 for low speed forward flight and in hover for the case of flapping frequency equal to unity. The nature of the damping of the rig was investigated since it was found that frictional effects contaminated the estimates of the rotor aerodynamic damping. To do this, a parameter estimation method, based on a nonlinear minimization procedure, was developed that does not require a large amount of data to identify the viscous and frictional damping coefficients from the free response of the rotor. A theoretical model for low frequency coupled rotor body dynamics was developed, and the effects of rotor and inflow degrees of freedom on rotor damping were investigated. Results indicate that both rotor and inflow degrees of freedom are required in the mathematical description of low frequency coupled rotor-body dynamics for the adequate estimation of rotor damping. The dynamic inflow degrees of freedom were described by using momentum theory and by assuming a nonuniform distribution for the steady induced velocity given by a Glauert wake. A blade flexibility study was conducted to define the flapping frequency for blade-linear spring configurations producing both time invariant and time dependent boundary conditions at the spring location. Comparison of theoretical damping estimates with the experimental data in hover and axial flight shows that at oscillation ratio frequency 0.186, the no-inflow model is in reasonable agreement with the experimental data and that the inclusion of dynamic inflow theory produces no improvement in the experimental data correlation. In hover and in low speed forward flight at oscillation frequency ratio 0.1068, the inclusion of dynamic inflow theory provides an improvement in the experimental data correlation indicating that for these conditions inflow degrees of freedom are also required for the adequate prediction of rotor pitch damping. Dissert. Abstr.

N93-10420# RAND Corp., Santa Monica, CA.
MAINTAINING FUTURE MILITARY AIRCRAFT DESIGN CAPABILITY
Jeffrey A. Drezner, Giles K. Smith, Lucille E. Horgan, Curt Rogers, and Rachel Schmidt 1992 87 p
(Contract F49620-91-C-0003)
(AD-A253963; RAND/R-4199-AF) Avail: CASI HC A05/MF A01

This research addresses one element of this broad issue: the continuing ability to design and develop manned aircraft systems. Many studies and review committees have examined the industrial base, focusing primarily on the ability to produce items under various conditions. Other studies have examined the organization and funding of the underlying technology base. But having the basic technology and a production base does not ensure the ability to design and develop a new system in an effective manner. Although other studies have examined weapon system development in terms of acquisition strategies, we were surprised to find that little attention has been devoted to the design and development process with respect to industry posture and capability. It is this design capability, as affected by diminishing budgets and new project starts, that is the focus of this research. GRA

N93-10803# Royal Aircraft Establishment, Farnborough (England).
FLIGHT TEST AND ANALYSIS PROCEDURES FOR NEW HANDLING CRITERIA
M. T. Charlton and S. S. Houston 5 May 1989 54 p Presented at the Royal Aeronautical Society Conference on Helicopter Handling Qualities and Control, London, England, Nov. 1988
(RAE-TM-FM-26; BR111319) Copyright Avail: CASI HC A04/MF A01

There is work underway to revise the US MIL-H-8501 and the UK Def-Stan 00970 design requirements for the specification of handling qualities for military rotorcraft. Current RAE research activities in support of the two programs are reported. The focus of this work has been an extensive series of flight trials to investigate handling and performance requirements for low level-nap-of-earth operations. Results of trials on two different aircraft in a small amplitude, high gain pitch tracking task, and for two discrete moderate amplitude maneuvers are introduced and discussed. Author

N93-10842# Massachusetts Inst. of Tech., Cambridge. Technology Lab. for Advanced Composites.
NONLINEAR AEROELASTICITY OF COMPOSITE STRUCTURES Final Report, 1 Jul. 1986 - 31 Jan. 1991

Peter E. Dunn and John Dugundji Oct. 1991 24 p
(Contract F49620-86-C-0066)
(AD-A254285; AFOSR-92-0807TR) Avail: CASI HC A03/MF A01

The nonlinear, stalled, aeroelastic behavior of rectangular, graphite/epoxy, cantilevered plates with varying amounts of bending-torsion stiffness coupling and with NACA 0012 Styrofoam airfoil shapes is investigated for low Reynolds number flow (less than 200,000). A general Rayleigh-Ritz formulation is used to calculate point load static deflections, and nonlinear static vibration frequencies and mode shapes for varying tip deflections. Nonlinear lift and moment aerodynamics are used in the context of the Rayleigh-Ritz formulation to calculate static airload deflections. The nonlinear, stalled ONERA model using non-constant coefficients - initially developed by Tran and Petot - is reformulated into a harmonic balance form and compared against a time-marching Runge-Kutta scheme. Low angle-of-attack, linear flutter calculations are done by applying Fourier analysis to extract the harmonic balance method and a Newton-Raphson solver to the resulting nonlinear. GRA

N93-10900 Illinois Inst. of Tech., Chicago.
CONTROL OF PANEL FLUTTER AT HIGH SUPERSONIC SPEED Ph.D. Thesis
Seoud Ahmed Abou-Amer 1991 117 p
Avail: Univ. Microfilms Order No. DA9222167

The exterior panels of flight vehicles travelling through the atmosphere at supersonic speed are often susceptible to the occurrences of limit-cycle type self-excited vibrations called flutter. The development of methods for the prevention and control of flutter, without adversely affecting the weight and cost, is desirable, and is the objective of this thesis. The two methods for suppressing flutter investigated in this study involve the use of damping treatment and piezoelectric actuators. The effect of both aerodynamic loading and damping, the structural damping, in-plane applied loads, the thermal stresses, and the cavity pressure are investigated through parametric study. Viscoelastic damping layers have been used in existing studies for noise and vibration control, and they are employed here to control panel flutter. Two different methods of damping are used. Modified formulations of the plate equations of motion with viscoelastic and constraining layers are represented, and the flutter behavior of the plate with and without damping are compared for both methods. A new advanced technique to control the plate flutter using a distributed piezoelectric material is developed and the modified formulation is derived. The values of the control voltage and the effect of piezoelectric material properties are investigated. Both methods give good results and succeed in suppressing the plate flutter at its operating condition. Dissert. Abstr.

N93-10011 National Aero-Space Plane Joint Program Office, Wright-Patterson AFB, OH.
A CONFIGURATION DEVELOPMENT STRATEGY FOR THE NASP
Curtis D. Snyder and S. Zane Pinckney (Lockheed Engineering and Sciences Co., Hampton, VA.) *In* JHU, The 1992 JANNAF Propulsion Meeting, Volume 1 Feb. 1992 p 195-202 Previously announced in IAA as A91-56156 and A92-17830 (For primary document see N93-10001 01-20)
Avail: CPIA, 10630 Little Patuxent Pkwy., Suite 202, Columbia, MD, 21044-3200 HC

06 AIRCRAFT INSTRUMENTATION

Includes cockpit and cabin display devices; and flight instruments.

For related information see also *19 Spacecraft Instrumentation* and *35 Instrumentation and Photography.*

No abstracts in this category.

07 AIRCRAFT PROPULSION AND POWER

Includes prime propulsion systems and systems components, e.g., gas turbine engines and compressors; and onboard auxilliary power plants for aircraft.

For related information see also *20 Spacecraft Propulsion and Power, 28 Propellants and Fuels,* and *44 Energy Production and Conversion.*

N93-10348*# Garrett Turbine Engine Co., Phoenix, AZ.
COMPOUND CYCLE ENGINE FOR HELICOPTER APPLICATION Final Report
Jere Castor, John Martin, and Curtiss Bradley 30 Sep. 1987 188 p
(Contract NAS3-24346; DA Proj. 1L1-61102-AH-45)
(NASA-CR-180824; NAS 1.26:180824; GTEC-21-5854-1; AVSCOM-TR-87-C-30) Avail: CASI HC A09/MF A02

The compound cycle engine (CCE) is a highly turbocharged, power-compounded, ultra-high-power-density, lightweight diesel engine. The turbomachinery is similar to a moderate-pressure-ratio, free-power-turbine gas turbine engine and the diesel core is high speed and a low compression ratio. This engine is considered a potential candidate for future military helicopter applications. Cycle thermodynamic specific fuel consumption (SFC) and engine weight analyses performed to establish general engine operating parameters and configurations are presented. An extensive performance and weight analysis based on a typical 2-hour helicopter (+30 minute reserve) mission determined final conceptual engine design. With this mission, CCE performance was compared to that of a contemporary gas turbine engine. The CCE had a 31 percent lower-fuel consumption and resulted in a 16 percent reduction in engine plus fuel and fuel tank weight. Design SFC of the CCE is 0.33 lb/hp-hr and installed wet weight is 0.43 lb/hp. The major technology development areas required for the CCE are identified and briefly discussed. Author

N93-10456*# National Aeronautics and Space Administration. Lewis Research Center, Cleveland, OH.
COMPARISON OF ALL-ELECTRIC SECONDARY POWER SYSTEMS FOR CIVIL SUBSONIC TRANSPORTS
David D. Renz 1992 6 p Presented at the 27th Intersociety Energy Conversion Engineering Conference, San Diego, CA, 3-7 Aug. 1992; sponsored by SAE, ACS, AIAA, ASME, IEEE, AIChE, and ANS
(RTOP 538-01-10)
(NASA-TM-105852; E-7300; NAS 1.15:105852) Avail: CASI HC A02/MF A01

Three separate studies have shown operational, weight, and cost advantages for commercial subsonic transport aircraft using an all-electric secondary power system. The first study in 1982 showed that all-electric secondary power systems produced the second largest benefit compared to four other technology upgrades. The second study in 1985 showed a 10 percent weight and fuel savings using an all-electric high frequency (20 kHz) secondary power system. The last study in 1991 showed a 2 percent weight savings using today's technology (400 Hz) in an all-electric secondary power system. This paper will compare the 20 kHz and 400 Hz studies, analyze the 2 to 10 percent difference in weight savings and comment on the common benefits of the all-electric secondary power system. Author

N93-10537 Technical Univ. of Istanbul (Turkey).
VIBRATIONS OF NONLINEARLY PRETWISTED ASYMMETRICAL THICK TURBINE BLADES
V. Karadag *In* Carleton Univ., Proceedings of the Twelfth Canadian Congress of Applied Mechanics, Volumes 1 and 2 May 1989 p 464-465 (For primary document see N93-10466 01-31)
Copyright Avail: Canadian Society for Mechanical Engineering, 2050 Mansfield St., Suite 700, Montreal, Quebec H3A 1Z7 Canada

N93-10539 Toronto Univ. (Ontario). Dept. of Mechanical Engineering.
THEORETICAL AND EXPERIMENTAL INVESTIGATIONS CONCERNING THE STRUCTURAL INTEGRITY OF AEROENGINE COMPRESSOR DISCS
S. A. Meguid, B. Theobald (Rolls-Royce Ltd., Derby, England), and J. Wiseman (Rolls-Royce Ltd., Bristol, England) *In* Carleton Univ., Proceedings of the Twelfth Canadian Congress of Applied Mechanics, Volumes 1 and 2 May 1989 p 484-485 (For primary document see N93-10466 01-31)
Copyright Avail: Canadian Society for Mechanical Engineering, 2050 Manstield St., Suite 700, Montreal, Quebec H3A 1Z7 Canada

08 AIRCRAFT STABILITY AND CONTROL

Includes aircraft handling qualities; piloting; flight controls; and autopilots.

For related information see also *05 Aircraft Design, Testing and Performance.*

N93-10070*# National Aeronautics and Space Administration. Langley Research Center, Hampton, VA.
DESIGN, TEST, AND EVALUATION OF THREE ACTIVE FLUTTER SUPPRESSION CONTROLLERS
William M. Adams, Jr., David M. Christhilf (Lockheed Engineering and Sciences Co., Hampton, VA.), Martin R. Waszak, Vivek Mukhopadhyay, and S. Srinathkumar (National Aeronautical Lab., Bangalore, India) Oct. 1992 41 p
(RTOP 505-64-20-01)
(NASA-TM-4338; L-17041; NAS 1.15:4338) Avail: CASI HC A03/MF A01

Three control law design techniques for flutter suppression are presented. Each technique uses multiple control surfaces and/or sensors. The first method uses traditional tools (such as pole/zero loci and Nyquist diagrams) for producing a controller that has minimal complexity and which is sufficiently robust to handle plant uncertainty. The second procedure uses linear combinations of several accelerometer signals and dynamic compensation to synthesize the model rate of the critical mode for feedback to the distributed control surfaces. The third technique starts with a minimum-energy linear quadratic Gaussian controller, iteratively modifies intensity matrices corresponding to input and output noise, and applies controller order reduction to achieve a low-order, robust controller. The resulting designs were implemented digitally and tested subsonically on the active flexible wing wind-tunnel model in the Langley Transonic Dynamics Tunnel. Only the traditional pole/zero loci design was sufficiently robust to errors in the nominal plant to successfully suppress flutter during the test. The traditional pole/zero loci design provided simultaneous suppression of symmetric and antisymmetric flutter with a 24-percent increase in attainable dynamic pressure. Posttest analyses are shown which illustrate the problems encountered with the other laws. Author

N93-10319 Pennsylvania State Univ., University Park.
CHARACTERIZATION OF AND ACTIVE CONTROL OF FLEXIBLE STRUCTURES, USING PIEZOCERAMICS AS SENSORS AND ACTUATORS Ph.D. Thesis
Chia-Chi Sung 1991 160 p
Avail: Univ. Microfilms Order No. DA9127429

This thesis presents the first detailed study of the active control of various truss structures and clamped shafts in pure bending, pure torsion and combined bending/torsional vibration. The important features of the work presented here are (1) exploitation of the d sub 15 coefficient in piezoelectric lead zirconate titanate (PZT) sensors and actuators to respond to shear stress and shear strain, (2) design and preparation of such shear mode transducers in either the ring or shell type configuration, (3) finite element simulation of the structures studied to verify that the new transducers indeed sense shear stress/strain, and (4) the study of the effect of mounting discrete piezoelectric sensors and actuators on the structural dynamics of the system be controlled. The PZT sensors output an electrical signal proportional to the mechanical strain as detected by the vibration response of a structure. This signal is input into an analog velocity feedback control circuit and then used to drive the PZT actuator. The actuator outputs a mechanical displacement that is equal in amplitude and opposite in phase to the vibration disturbance. The superposition of the vibration disturbance and the actuator displacement results in vibration reduction because of the destructive interference principle. Two vibration modes, the thickness mode and shear mode, of piezoceramics are investigated. The coupled piezoelectric coefficients for thickness mode and shear mode excitation are d sub 31 and d sub 15, respectively. The experimental structures used for thickness mode driven actuators include the cantilever beam, T-beam, Y-beam, and Y-bar beam. Two shear mode driven piezoceramics are considered--the ring type and shell type. Both are used as sensors and/or actuators for pure torsion control of cylindrical tube structures. Single mode, time responses (transients) are measured. Transfer functions are used to measure the extended frequency bands. Single as well as multimode experimental vibration performance comparisons between the undamped and actively damped structures are given. The finite element code ANSYS is used for mode-frequency analysis of the structures. Experimental results of the structure dynamics are compared with and without damping. The validity of the research methods is confirmed using this analysis. Dissert. Abstr.

N93-10374 Composite Aircraft Products Ltd. (Canada).
PITCH CONTROL TRIMMING SYSTEM FOR CANARD DESIGN AIRCRAFT Patent Application
Hugh O. Thomas, inventor (to Composite Aircraft Products Ltd.) 28 Nov. 1991 28 p
(CA-Patent-Appl-SN-2013236; Int-Patent-Class-B64C-17/00; Int-Patent-Class-B64D-27/08; Int-Patent-Class-B64C-13/00; CTN-92-60362) Copyright Avail: Micromedia Ltd., Technical Information Centre, 165 Hotel de Ville, Place du Portage, Phase 2, Hull, Quebec J8X 3X2, Canada HC/MF

A pitch control trimming system for a canard design aircraft has the ability to reposition the center of gravity of the aircraft along the longitudinal axis. The design permits trimming of the aircraft without external trim tabs and permits flaps to be used on a canard design aircraft without forward pitching moment occurring. The aircraft has a substantial mass associated with the aircraft, preferably the engine, which is movable substantially along the longitudinal axis of the aircraft, and includes an actuator to move the mass forward and aft on the longitudinal axis to reposition the center of gravity of the aircraft. In one embodiment of the invention, the canard design aircraft is of the pusher type wherein the aircraft engine represents the mass which is moved forward or aft along the aircraft's longitudinal axis. In another embodiment, a pressure sensor is positioned to measure the thrust of the engine and provide the pilot with an indication of engine thrust during flight or static conditions. Author (CISTI)

N93-10704# Air Force Inst. of Tech., Wright-Patterson AFB, OH. Foreign Technology Div.
METHODS OF GUIDANCE FLIGHT DYNAMICS
Zhu Wenxuan 29 Nov. 1991 26 p Transl. into ENGLISH from Yuhang Xuebao (China), no. 4, 1989 p 30-38
(AD-A254248; FTD-ID(RS)T-0544-91) Avail: CASI HC A03/MF A01

Setting up and solving ballistic type rocket kinetic equations in inertial coordinate systems with directions which do not vary, it is possible not to consider dragging inertial or centrifugal forces or coriolis inertial forces and set up inertial guidance on a convenient and simple, quick and clear foundation. This is different from what has been published in the past, where studies have been done of various types of flight mechanics problems in coordinate systems which turn, following along with the earth. We illucidate the initial take off conditions as rockets leave the surface of the earth, and analyze, in detail, the air or atmospheric effects associated with air being pulled along by the gravity of the earth as it turns and

the treatment methods for aerodynamic forces on rockets moving in an inertial space. We derive a formula for calculating the geographical location of movement parameters, used for rockets in inertial coordinate systems, and a formula for dynamic coordinate system movement parameters. GRA

N93-10741*# National Aeronautics and Space Administration. Ames Research Center, Moffett Field, CA.
INITIAL PILOTED SIMULATION STUDY OF GEARED FLAP CONTROL FOR TILT-WING V/STOL AIRCRAFT
Lourdes M. Guerrero and Lloyd D. Corliss Oct. 1991 39 p (RTOP 505-61-51)
(NASA-TM-103872; A-91175; NAS 1.15:103872) Avail: CASI HC A03/MF A01

A simulation study of a representative tilt wing transport aircraft was conducted in 1990 on the Ames Vertical Motion Simulator. This simulation is in response to renewed interest in the tilt wing concept for use in future military and civil applications. For past tilt wing concepts, pitch control in hover and low-speed flight has required a tail rotor or reaction jets at the tail. Use of mono cyclic propellers or a geared flap have also been proposed as alternate methods for providing pitch control at low speed. The geared flap is a subject of this current study. This report describes the geared flap concept, the tilt wing aircraft, the simulation model, the simulation facility and experiment setup, the pilots' evaluation tasks and procedures, and the results obtained from the simulation experiment. The pilot evaluations and comments are also documented in the report appendix. Author

09 RESEARCH AND SUPPORT FACILITIES (AIR)

Includes airports, hangars and runways; aircraft repair and overhaul facilities; wind tunnels; shock tubes; and aircraft engine test stands.

For related information see also *14 Ground Support Systems and Facilities (Space).*

N93-10046*# National Aeronautics and Space Administration. John F. Kennedy Space Center, Cocoa Beach, FL.
GENERIC PROPELLANT TRANSFER UNIT
Chuck L. Davis *In* JHU, The 1992 JANNAF Propulsion Meeting, Volume 1 Feb. 1992 p 703-718 (For primary document see N93-10001 01-20)
Avail: CPIA, 10630 Little Patuxent Pkwy., Suite 202, Columbia, MD, 21044-3200 HC

N93-10047 Hughes Space and Communications Group, El Segundo, CA. Propulsion Product Line.
LOADING OPERATIONS FOR SPACECRAFT PROPULSION SUBSYSTEMS
G. P. Purohit, H. O. Nordeng, and J. R. Ellison *In* JHU, The 1992 JANNAF Propulsion Meeting, Volume 1 Feb. 1992 p 719-731 (For primary document see N93-10001 01-20)
Avail: CPIA, 10630 Little Patuxent Pkwy., Suite 202, Columbia, MD, 21044-3200 HC

N93-10668# German Air Force, Bonn (Germany). Planning Div.
POSSIBILITIES AND LIMITATIONS OF FLYING TRAINING IN THE GERMAN AIR FORCE
H. Rueggeberg *In* AGARD, Combat Aircraft Noise Apr. 1992 6 p (For primary document see N93-10666 01-71)
Copyright Avail: CASI HC A02/MF A03

12 ASTRONAUTICS (GENERAL)

For extraterrestrial exploration see *91 Lunar and Planetary Exploration.*

No abstracts in this category.

13 ASTRODYNAMICS

Includes powered and free-flight trajectories; and orbital and launching dynamics.

N93-10499 Cornell Univ., Ithaca, NY. Dept. of Theoretical and Applied Mechanics.
COMPUTER ALGEBRA AND THE ELLIPTIC RESTRICTED PROBLEM OF THREE BODIES
Richard H. Rand and Bhaskar Viswanadham *In* Carleton Univ., Proceedings of the Twelfth Canadian Congress of Applied Mechanics, Volumes 1 and 2 May 1989 p 248-249 (For primary document see N93-10466 01-31)
Copyright Avail: Canadian Society for Mechanical Engineering, 2050 Mansfield St., Suite 700, Montreal, Quebec H3A 1Z7 Canada

14 GROUND SUPPORT SYSTEMS AND FACILITIES (SPACE)

Includes launch complexes, research and production facilities; ground support equipment, e.g., mobile transporters; and simulators.

For related information see also *09 Research and Support Facilities (Air).*

N93-10021*# National Aeronautics and Space Administration. Marshall Space Flight Center, Huntsville, AL.
FACILITY FOR COLD FLOW TESTING OF SOLID ROCKET MOTOR MODELS
D. L. Bacchus, O. E. Hill, and R. Harold Whitesides (Engineering Research and Consulting, Inc., Huntsville, AL.) *In* JHU, The 1992 JANNAF Propulsion Meeting, Volume 1 Feb. 1992 p 353-363 (For primary document see N93-10001 01-20)
(Contract NAS8-37505)
Avail: CPIA, 10630 Little Patuxent Pkwy., Suite 202, Columbia, MD, 21044-3200 HC

N93-10953# Imperial Coll. of Science and Technology, London (England).
A MULTIPURPOSE VACUUM-ULTRAVIOLET TEST FACILITY
R. C. M. Learner, A. Thorne, J. Maxwell, C. R. Young (Chelsea Instruments Ltd., East Molesey, England), and R. P. Glover (RGC Technical Consultancy, London, England) *In* ESA, Solar Physics and Astrophysics at Interferometric Resolution May 1992 p 291-294 Sponsored in part by ESTEC (For primary document see N93-10901 01-90)
Copyright Avail: CASI HC A01/MF A03

15 LAUNCH VEHICLES AND SPACE VEHICLES

Includes boosters; operating problems of launch/space vehicle systems; and reusable vehicles.

For related information see also *20 Spacecraft Propulsion and Power.*

N93-10106# Science Applications International Corp., Shalimar, FL.
MEASUREMENT OF ACCELERATION USING AN INSTRUMENTED RAILGUN PROJECTILE Final Report, Apr. 1990 - Apr. 1991
Donald M. Littrell, Keith A. Jamison, Roger D. Hudson, Michael J. Fernandez, and Scott A. Ager Jun. 1992 30 p
(Contract F08635-87-C-0003; AF Proj. 1203)
(AD-A253366; WL/MN-TR-91-76) Avail: CASI HC A03/MF A01

An instrumented package has been accelerated in a railgun projectile to measure the inbore acceleration as a function of time. Direct, continuous acceleration profiles have been repeatedly obtained with this package during electromagnetic launch and downrange soft catch. These proof-of-principle experiments were conducted using a square bore railgun and off-the-shelf components for the in situ measurement, digitization, and storage of acceleration data. A continuous record of the entire launch event clearly shows gas injection, electromagnetic propulsion, and downrange deceleration in a soft catch recovery system. The launch package was subject to peak accelerations of nearly 30 kilogees (2.8 x 105 m/sq. sec) in the electromagnetic propulsion phase of the launch. Velocity and position data obtained through integration of this data are correlated with velocity data derived from conventional static diagnostic (e.g., magnetic flux loops) to validate the technique. The peak acceleration was slightly more than anticipated from the electrical current delivered to the railgun, and this deviation is examined. The paper presents a description of the experimental apparatus, acquired data, a comparison of the data with code simulations, and suggestions for future work. GRA

N93-10814# Air Force Inst. of Tech., Wright-Patterson AFB, OH. Foreign Technology Div.
BURN PHASE CORRECTIONS OF MANEUVER BALLISTIC MISSILES WITH STAR LIGHT
Gongxun Shen and Zhiming Zhou 3 Dec. 1991 15 p Transl. into ENGLISH from Hangkong Xuebao (China), v. 11, no. 5, p A288-A293 1990
(AD-A254105; FTD-ID(RS)T-1471-90) Avail: CASI HC A03/MF A01

In this paper, the maneuver ballistic missile parametric correction in the burning phase with star light is studied, when the maneuver ballistic missile is launched under the condition that the initial position is not exactly defined and the inertial navigation platform is not completely leveled and aligned. GRA

16 SPACE TRANSPORTATION

Includes passenger and cargo space transportation, e.g., shuttle operations; and space rescue techniques.

For related information see also *03 Air Transportation and Safety* and *18 Spacecraft Design, Testing and Performance.* For space suits see *54 Man/System Technology and Life Support.*

No abstracts in this category.

17 SPACE COMM., SPACECRAFT COMM., COMMAND & TRACKING

Includes telemetry; space communications networks; astronavigation and guidance; and radio blackout.

For related information see also *04 Aircraft Communications and Navigation* and *32 Communications and Radar.*

N93-10236# Range Commanders Council, White Sands Missile Range, NM. Telemetry Group.
TRANSDUCER WORKSHOP NO. 16
Jun. 1991 237 p Workshop held in San Antonio, TX, 18-20 Jun. 1991
(AD-A248047) Avail: CASI HC A11/MF A03

This document is published as the proceedings of the transducer workshop sponsored by the Vehicular Instrumentation/Transducer Committee of the Telemetry Group. The committee apprises the Telemetry Group of significant progress in the field of transducers used in telemetry systems; maintains any necessary liaison between the group and the National Bureau of Standards and their transducers' programs or other related telemetry transducer efforts. GRA

18 SPACECRAFT DESIGN, TESTING AND PERFORMANCE

Includes satellites; space platforms; space stations; spacecraft systems and components such as thermal and environmental controls; and attitude controls.

For life support systems see *54 Man/System Technology and Life Support.* For related information see also *05 Aircraft Design, Testing and Performance, 39 Structural Mechanics,* and *16 Space Transportation.*

N93-10081# General Accounting Office, Washington, DC. Information Management and Technology Div.
SPACE STATION: NASA'S SOFTWARE DEVELOPMENT APPROACH INCREASES SAFETY AND COST RISKS. REPORT TO THE CHAIRMAN, COMMITTEE ON SCIENCE, SPACE, AND TECHNOLOGY, HOUSE OF REPRESENTATIVES
19 Jun. 1992 33 p
(GAO/IMTEC-92-39; B-247878) Avail: CASI HC A03/MF A01; GAO, PO Box 6015, Gaithersburg, MD 20877 HC

The House Committee on Science, Space, and Technology asked NASA to study software development issues for the space station. How well NASA has implemented key software engineering practices for the station was asked. Specifically, the objectives were to determine: (1) if independent verification and validation techniques are being used to ensure that critical software meets specified requirements and functions; (2) if NASA has incorporated software risk management techniques into program; (3) whether standards are in place that will prescribe a disciplined, uniform approach to software development; and (4) if software support tools will help, as intended, to maximize efficiency in developing and maintaining the software. To meet the objectives, NASA proceeded: (1) reviewing and analyzing software development objectives and strategies contained in NASA conference publications; (2) reviewing and analyzing NASA, other government, and industry guidelines for establishing good software development practices; (3) reviewing and analyzing technical proposals and contracts; (4) reviewing and analyzing software management plans, risk management plans, and program requirements; (4) reviewing and analyzing reports prepared by NASA and contractor officials that identified key issues and challenges facing the program; (5) obtaining expert opinions on what constitutes appropriate independent V-and-V and software risk management activities; (6) interviewing program officials at NASA headquarters in Washington, DC; at the Space Station Program Office in Reston, Virginia; and at the three work package centers; Johnson in Houston, Texas; Marshall in Huntsville, Alabama; and Lewis in Cleveland, Ohio; and (7) interviewing contractor officials doing work for NASA at

Johnson and Marshall. The audit work was performed in accordance with generally accepted government auditing standards, between April 1991 and May 1992. Author

N93-10308 Colorado Univ., Boulder.
NUMERICAL SIMULATION OF LARGE ACTIVELY CONTROLLED SPACE STRUCTURES Ph.D. Thesis
Ralph W. Quan 1991 158 p
Avail: Univ. Microfilms Order No. DA9132604

A unique combination of methods for the simulation of controller-structure interaction is developed from a first order viewpoint. These algorithms unify a structural finite element model, state estimator, actuator dynamics, and sensor dynamics into one linear system. It is show that the stability of the numerical simulation is equivalent to the stability of the closed loop system. Nested linked lists are used to exploit the sparsity of the system matrices. Algorithms are developed for sparse matrix algebra involving the addition, multiplication, and factorization of nested linked list matrices. A software package was written which combines these ideas to simulate the reduced order model control of a structure. Dissert. Abstr.

N93-10365 Colorado Univ., Boulder.
MODEL REFERENCE ADAPTIVE CONTROL IN LARGE SPACE STRUCTURES Ph.D. Thesis
Shin-Ching Liang 1991 109 p
Avail: Univ. Microfilms Order No. DA9132590

On line adaptive control is essential for large space structure (LSS) where the model parameters are poorly known, due to modeling error and changing or variable configuration. Yet most of the adaptive control methods need some precise a priori structural information of the plant (at least the order). This is unsatisfactory for LSS adaptive control. In this paper, the Model Reference Adaptive Control (MRAC) for LSS using direct and indirect schemes base on a Reduced-Order Model (ROM) are obtained. In the direct MRAC scheme, the hyperstability theory is used for stability analysis, this approach provides greater flexibility in choosing adaptive laws and avoids the shortcomings of Lyapunov's method. For improving the sensors and actuators noncollocated problem, the almost strict positive realness condition is established. The indirect MRAC scheme, are based on an Auto Regressive Moving Average (ARMA) model, the spillover from the unmodel dynamics is compensated by Residual Mode Filter (RMF). The results of both schemes have been used to design an ROM-Based controller and tested successfully via computer simulation; the direct adaptive controller has been tested successfully via a flexible robot manipulator experiment. Dissert. Abstr.

N93-10705# Air Force Inst. of Tech., Wright-Patterson AFB, OH. Foreign Aerospace Science and Technology Center.
ECHO CHARACTERISTIC ANALYSIS OF THE NONEQUILIBRIUM WAKES OF REENTRY VEHICLE
Niu Jiayu 13 Jan. 1992 19 p Transl. into ENGLISH from Konqqidonglixue Xuebao (China), v. 8, no. 3, 1990 p 286-292
(AD-A254249; FASTC-ID(RS)T-0784-91) Avail: CASI HC A03/MF A01

The article makes use of a method to calculate the flow fields of pure air nonequilibrium reentry vehicle wakes. It analyzes the effects of wake plasma body fields on radar wave frequencies. In conjunction with this, it takes a step further in calculations of radar scattering cross sections under several types of elevation conditions. It explains several important factors influencing cross section size and distribution. Analyses and calculations clearly show that, after taking the Reynolds number, which is verified with the diameter of the bottom section or base of the object and environmental parameters, and arriving at turning point or transition values in fully developed turbulent flow wakes, it is possible to show the appearance of the phenomenon of abrupt increase in scattering cross sections. GRA

N93-10737*# National Academy of Sciences - National Research Council, Washington, DC.
GUIDELINES FOR DEVELOPING SPACECRAFT MAXIMUM ALLOWABLE CONCENTRATIONS FOR SPACE STATION CONTAMINANTS
1992 122 p
(Contract NASw-3749; NAGw-2239)
(NASA-CR-190748; NAS 1.26:190748) Avail: CASI HC A06/MF A02

The National Aeronautics and Space Administration (NASA) is preparing to launch a manned space station by the year 1996. Because of concerns about the health, safety, and functioning abilities of the crews, NASA has requested that the National Research Council (NRC) through the Board on Environmental Studies and Toxicology (BEST) provide advice on toxicological matters for the space-station program. The Subcommittee on Guidelines for Developing Spacecraft Maximum Allowable Concentrations for Space Station Contaminants was established by the Committee on Toxicology (COT) to address NASA's concerns. Spacecraft maximum allowable concentrations (SMAC's) are defined as the maximum concentrations of airborne substances (such as gas, vapor, or aerosol) that will not cause adverse health effects, significant discomfort, or degradation in crew performance. Author

N93-10744*# National Aeronautics and Space Administration. Langley Research Center, Hampton, VA.
EXTRAVEHICULAR ACTIVITY COMPATIBILITY EVALUATION OF DEVELOPMENTAL HARDWARE FOR ASSEMBLY AND REPAIR OF PRECISION REFLECTORS
Walter L. Heard, Jr., Mark S. Lake, Harold G. Bush, J. Kermit Jensen (Lockheed Engineering and Sciences Co., Hampton, VA.), James E. Phelps (Lockheed Engineering and Sciences Co., Hampton, VA.), and Richard E. Wallsom (Lockheed Engineering and Sciences Co., Hampton, VA.) Sep. 1992 62 p
(RTOP 506-43-41-02)
(NASA-TP-3246; L-17062; NAS 1.60:3246) Avail: CASI HC A04/MF A01

This report presents results of tests performed in neutral buoyancy by two pressure-suited test subjects to simulate Extravehicular Activity (EVA) tasks associated with the on-orbit construction and repair of a precision reflector spacecraft. Two complete neutral buoyancy assemblies of the test article (tetrahedral truss with three attached reflector panels) were performed. Truss joint hardware, two different panel attachment hardware concepts, and a panel replacement tool were evaluated. The test subjects found the operation and size of the truss joint hardware to be acceptable. Both panel attachment concepts were found to be EVA compatible, although one concept was judged by the test subjects to be considerably easier to operate. The average time to install a panel from a position within arm's reach of the test subjects was 1 min 14 sec. The panel replacement tool was used successfully to demonstrate the removal and replacement of a damaged reflector panel in 10 min 25 sec. Author

N93-10841*# National Aeronautics and Space Administration. Lewis Research Center, Cleveland, OH.
ACCEPTANCE TESTING OF THE PROTOTYPE ELECTROMETER FOR THE SAMPIE FLIGHT EXPERIMENT
G. Barry Hillard Sep. 1992 24 p
(RTOP 589-01-1B)
(NASA-TM-105880; E-7343; NAS 1.15:105880) Avail: CASI HC A03/MF A01

The Solar Array Module Plasma Interaction Experiment (SAMPIE) has two key instruments at the heart of its data acquisition capability. One of these, the electrometer, is designed to measure both ion and electron current from most of the samples included in the experiment. The accuracy requirement, specified by the project's Principal Investigator, is for agreement within 10 percent with a calibrated laboratory instrument. Plasma chamber testing was performed to assess the capabilities of the prototype

design. Agreement was determined to be within 2 percent for electron collection and within 3 percent for ion collection. Author

N93-10511 Cambridge Univ. (England). Dept. of Engineering.
A NEW DEPLOYABLE MAST
A. Kwan and S. Pellegrino *In* Carleton Univ., Proceedings of the Twelfth Canadian Congress of Applied Mechanics, Volumes 1 and 2 May 1989 p 334-335 (For primary document see N93-10466 01-31)
Copyright Avail: Canadian Society for Mechanical Engineering, 2050 Mansfield St., Suite 700, Montreal, Quebec H3A 1Z7 Canada

N93-10521 British Columbia Univ., Vancouver. Dept. of Mechanical Engineering.
EXPERIMENTAL DEMONSTRATION OF OFFSET CONTROL WITH AN APPLICATION TO THE TETHERED PAYLOAD
V. J. Modi, P. K. Lakshmanan, A. K. Misra (McGill Univ., Montreal, Quebec), R. J. Picha, S. Chan, and S. Vakil *In* Carleton Univ., Proceedings of the Twelfth Canadian Congress of Applied Mechanics, Volumes 1 and 2 May 1989 p 402-403 (For primary document see N93-10466 01-31)
Copyright Avail: Canadian Society for Mechanical Engineering, 2050 Mansfield St., Suite 700, Montreal, Quebec H3A 1Z7 Canada

19 SPACECRAFT INSTRUMENTATION

For related information see also *06 Aircraft Instrumentation* and *35 Instrumentation and Photography.*

N93-10960*# Lockheed Engineering and Sciences Co., Houston, TX.
REQUIREMENTS ANALYSIS NOTEBOOK FOR THE FLIGHT DATA SYSTEMS DEFINITION IN THE REAL-TIME SYSTEMS ENGINEERING LABORATORY (RSEL)
Richard B. Wray Dec. 1991 117 p
(Contract NAS9-17900)
(NASA-CR-185698; NAS 1.26:185698; LESC-29702) Avail: CASI HC A06/MF A02

A hybrid requirements analysis methodology was developed, based on the practices actually used in developing a Space Generic Open Avionics Architecture. During the development of this avionics architecture, a method of analysis able to effectively define the requirements for this space avionics architecture was developed. In this methodology, external interfaces and relationships are defined, a static analysis resulting in a static avionics model was developed, operating concepts for simulating the requirements were put together, and a dynamic analysis of the execution needs for the dynamic model operation was planned. The systems engineering approach was used to perform a top down modified structured analysis of a generic space avionics system and to convert actual program results into generic requirements. CASE tools were used to model the analyzed system and automatically generate specifications describing the model's requirements. Lessons learned in the use of CASE tools, the architecture, and the design of the Space Generic Avionics model were established, and a methodology notebook was prepared for NASA. The weaknesses of standard real-time methodologies for practicing systems engineering, such as Structured Analysis and Object Oriented Analysis, were identified. Author

N93-10929# European Space Agency, Paris (France).
ATTACHED PAYLOADS ON SPACE STATION FREEDOM AND COLUMBUS
G. P. Haskell and H. Olthof *In its* Solar Physics and Astrophysics at Interferometric Resolution May 1992 p 167-169 (For primary document see N93-10901 01-90)
Copyright Avail: CASI HC A01/MF A03

N93-10933# Imperial Coll. of Science and Technology, London (England).
IFTS: THE IMAGING FOURIER TRANSFORM SPECTROMETER
A. P. Thorne *In* ESA, Solar Physics and Astrophysics at Interferometric Resolution May 1992 p 191-195 (For primary document see N93-10901 01-90)
Copyright Avail: CASI HC A01/MF A03

N93-10934# Eidgenoessische Technische Hochschule, Zurich (Switzerland). Inst. of Astronomy.
POLARIMETRY WITH AN IMAGING FTS
J. O. Stenflo and S. K. Solanki *In* ESA, Solar Physics and Astrophysics at Interferometric Resolution May 1992 p 197-200 (For primary document see N93-10901 01-90)
Copyright Avail: CASI HC A01/MF A03

N93-10935# Norges Tekniske Hoegskole, Trondheim.
FOURIER TRANSFORM SPECTROMETER PROCESSING: DATA REDUCTION AND PROCESSOR DESIGN
K. Andreassen and P. A. Armbruster (European Space Agency. European Space Research and Technology Center, ESTEC, Noordwijk, Netherlands) *In* ESA, Solar Physics and Astrophysics at Interferometric Resolution May 1992 p 201-204 (For primary document see N93-10901 01-90)
Copyright Avail: CASI HC A01/MF A03

N93-10937# Rutherford Appleton Lab., Chilton (England).
DETECTORS FOR THE SIMURIS PAYLOAD
B. E. Patchett, M. K. Carter, and P. D. Read *In* ESA, Solar Physics and Astrophysics at Interferometric Resolution May 1992 p 211-213 (For primary document see N93-10901 01-90)
Copyright Avail: CASI HC A01/MF A03

N93-10938# Turin Univ. (Italy). Ist. di Fisica.
EUV COMPLEMENTARY INSTRUMENTATION FOR SIMURIS
Ester Antonucci *In* ESA, Solar Physics and Astrophysics at Interferometric Resolution May 1992 p 215-220 (For primary document see N93-10901 01-90)
Copyright Avail: CASI HC A02/MF A03

N93-10939*# Harvard-Smithsonian Center for Astrophysics, Cambridge, MA.
OBTAINING HIGH RESOLUTION XUV CORONAL IMAGES
L. Golub and E. Spiller (IBM Watson Research Center, Yorktown Heights, NY.) *In* ESA, Solar Physics and Astrophysics at Interferometric Resolution May 1992 p 221-224 Sponsored by NASA, Washington (For primary document see N93-10901 01-90)
Copyright Avail: CASI HC A01/MF A03

N93-10954# Messerschmitt-Boelkow-Blohm G.m.b.H., Munich (Germany).
ACCOMMODATION ASPECTS OF SIMURIS ON SPACE STATION FREEDOM
U. Lemmer, E. Schulz-Luepertz, and K. Thoermer *In* ESA, Solar Physics and Astrophysics at Interferometric Resolution May 1992 p 295-297 (For primary document see N93-10901 01-90)
Copyright Avail: CASI HC A01/MF A03

N93-10956# European Space Agency. European Space Research and Technology Center, ESTEC, Noordwijk (Netherlands). Structures and Mechanisms Div.
MECHANICAL AND THERMAL DESIGN OF THE SUN INSTRUMENT
J. Pang and R. Bureo *In its* Solar Physics and Astrophysics at Interferometric Resolution May 1992 p 303-308 (For primary document see N93-10901 01-90)
Copyright Avail: CASI HC A02/MF A03

20 SPACECRAFT PROPULSION AND POWER

Includes main propulsion systems and components, e.g., rocket engines; and spacecraft auxilliary power sources.

For related information see also *07 Aircraft Propulsion and Power, 28 Propellants and Fuels, 44 Energy Production and Conversion,* and *15 Launch Vehicles and Space Vehicles.*

N93-10001 Johns Hopkins Univ., Columbia, MD. Chemical Propulsion Information Agency.
THE 1992 JANNAF PROPULSION MEETING, VOLUME 1
Debra S. Eggleston, ed. Feb. 1992 771 p Meeting held in Indianapolis, IN, 24-27 Feb. 1992; sponsored by the Joint NASA, Army, Navy, Air Force Interagency Propulsion Committee
(Contract N00014-91-C-0001)
(CPIA-Publ-580-Vol-1) Avail: CPIA, 10630 Little Patuxent Pkwy., Suite 202, Columbia, MD, 21044-3200 HC

This volume, the first of four volumes, is a collection of 60 unclassified/unlimited distribution papers which were presented at the 1992 Joint Army-Navy-NASA-Air Force (JANNAF) Propulsion Meeting. Specific subjects discussed include solid propellant grain nozzle flow field analysis, hypersonic propulsion, solid and liquid propellant guns, liquid rocket engine and component development, thrust vector control, rocket nozzle design and testing, electric propulsion, advanced polymers, upper-stage propulsion, and altitude control systems. For individual titles, see N93-10002 through N93-10049.

N93-10002 United Technologies Corp., San Jose, CA. Chemical Systems Div.
INSTRUMENTED PROPELLANT BLOCK TEST AND STRESS ANALYSIS COMPARISON
Richard E. Thompson and Steven E. Perkins *In* JHU, The 1992 JANNAF Propulsion Meeting, Volume 1 Feb. 1992 p 33-45 (For primary document see N93-10001 01-20)
(Contract F04611-87-C-0062)
Avail: CPIA, 10630 Little Patuxent Pkwy., Suite 202, Columbia, MD, 21044-3200 HC

There is an on-going need to experimentally measure bond stresses in both termination stress and low-gradient stress areas of solid propellant rocket motors employing composite cases and having complex geometries. These measurements are needed to verify the finite element-predicted structural margins and environmental operating limits for these advanced tactical, strategic, and space motors. Chemical Systems Division undertook a program to develop stress transducers usable in low stress gradient regions and in termination, or high stress gradient, regions. The various transducers were evaluated in propellant blocks tested in tension and compression in the laboratory prior to being placed into structural test vehicles. Finite element analyses of the propellant test blocks were also performed to predict transducer response. The results of the instrumented propellant block tests are presented. Author

N93-10003 Phillips Lab., Hanscom AFB, MA.
A THREE-DIMENSIONAL ANALYSIS OF THE EFFECT OF LOCAL STRESS DISTRIBUTION NEAR CRACK TIP **c39**
Chi-Tsieh Liu and Minh D. Le *In* JHU, The 1992 JANNAF Propulsion Meeting, Volume 1 Feb. 1992 p 47-53 (For primary document see N93-10001 01-20)
Avail: CPIA, 10630 Little Patuxent Pkwy., Suite 202, Columbia, MD, 21044-3200 HC

A three-dimensional elastic analysis of crack-defect interaction was conducted using finite element methods. In the analysis, two different types of defects, void and damage, were considered. The effect of crack-defect interaction on the mode 1 stress intensity factor and the stress distribution near the crack tip was investigated, and the results were discussed. Author

N93-10004 Naval Weapons Center, China Lake, CA.
IMPACT SENSITIVITY REDUCTION VIA EXO-ELECTRON CONTROL **c28**
Robert A. Rhein, Russell Reed, and Ngo Q. Vu *In* JHU, The 1992 JANNAF Propulsion Meeting, Volume 1 Feb. 1992 p 103-109 (For primary document see N93-10001 01-20)
Avail: CPIA, 10630 Little Patuxent Pkwy., Suite 202, Columbia, MD, 21044-3200 HC

Many materials, upon fracturing, emit electrons (exo-electrons) by a process called fracto-emission. For a substance or mixture that can deflagrate or detonate upon impact or friction, these exo-electrons may contribute to the initiation of deflagration or detonation. Some materials, such as p-type semiconductors, can absorb exo-electrons and, as used as additives, can reduce the impact or friction sensitivity of propellants or explosives. It was found that the addition of 1 percent p-type silicon powder did decrease the impact sensitivity of a propellant consisting of ammonium perchlorate in a polybutadiene matrix, but did not reduce the impact sensitivity of powdered cyclotetramethylene tetranitramine (HMX), cyclotrimethylene trinitramine (RDX), and pentaerythritol trinitrate (PETN). Author

N93-10005 Olin Corp., Cheshire, CT.
SYNTHESIS AND CHARACTERIZATION OF ENERGETIC POLYMERS **c27**
Eugene Rothgery, R. Hani, R. Dumas, M. Shen, D. Gavin, R. Day, J. Necessary, and Gerry Traylor *In* JHU, The 1992 JANNAF Propulsion Meeting, Volume 1 Feb. 1992 p 111-117 Prepared in cooperation with Olin Corp., Brandenburg, KY (For primary document see N93-10001 01-20)
Avail: CPIA, 10630 Little Patuxent Pkwy., Suite 202, Columbia, MD, 21044-3200 HC

We would like to report the results of our synthesis and characterization efforts of the last several years, which have resulted in the production of two series of energetic polymers. The purpose was to provide binder material for use in new, minimum smoke, insensitive rocket propellant formulations. One series consists of a family of polyesters made by the reaction of nitramine-containing diacids with energetic or non-energetic diols. The second series consist of a series of polyethers synthesized from substituted 2,4-dinitrazahexane and energetic or non-energetic diols. For each polymer prepared, we have determined the glass transition Tg, the molecular weight, decomposition temperature, and estimated heat of formation. Additionally, we have measured the heat of combustion for some of the materials. Both melt and solution polymerizations were employed as synthetic methods. This has provided a range of molecular weights and Tg's for the resulting polymers, thus allowing a tailoring of polymer properties to meet the required formulation needs. The molecular weights obtained have ranged from about 1000 to 6000 and Tg's as low as -35 C. The decomposition temperatures observed have ranged as high as 256 C. One of the energetic polyesters was produced in our pilot plant in Brandenburg, KY. The polymer was produced in a 30 gallon glass lined reactor in multi-pound quantities. Facilities are available for an additional 20 fold scale-up of this energetic polyester. Author

N93-10006 Naval Weapons Center, China Lake, CA.
THE EFFECT OF ELEVATED TEMPERATURES ON THE PROPERTIES OF THERMALLY STABLE SILICON-BASED ELASTOMERS FOR ADHESIVES, SEALANTS, AND INSULATOR APPLICATIONS **c27**
Robert A. Rhein and James C. Baldwin *In* JHU, The 1992 JANNAF Propulsion Meeting, Volume 1 Feb. 1992 p 119-141 (For primary document see N93-10001 01-20)
Avail: CPIA, 10630 Little Patuxent Pkwy., Suite 202, Columbia, MD, 21044-3200 HC

Viscous liquid poly(methylvinylsiloxane) (PMVS) and silphenylene- methylvinylsiloxane copolymer (SILCOP), both alternating and random, were prepared with silane (Si-H) terminal groups. These polymers were cured by hydrosilylation (using a platinum catalyst) to elastomers. Their mechanical properties were determined both before and after exposure to elevated

temperatures and were compared to the mechanical properties of commercial polysiloxanes. Exposure temperatures to 800 C were employed. Lap-shear tests at elevated temperatures were also conducted. Whereas commercial polysiloxanes became soft and weak upon exposure to elevated temperatures, the elastomers composed of PMVS and SILCOP became hard by the mechanism of thermal crosslinking. The influence of various types of fillers (both treated and untreated silica and silicon carbide) was studied; it was found that silicon carbide powder, when used as filler, aided in high-temperature resistance. The application to high-temperature adhesives was described. Homopolymers and copolymers based upon oxo-1,4-disila- 1,4-dimethyl-2,5-cyclo-hexadiene were prepared. These polymers included the homopolymer and the copolymers with oxo-p-bis-dimethylsilylbenzene, dimethylsiloxane, methylphenylsiloxane, and tetramethyldisiloxane. These polymers were terminated with Si-H and underwent self-curing to elastomers by addition of a platinum catalyst and heating overnight at 70 C. Small samples of each of these elastomers were subjected to heating, in an argon atmosphere, from 50 to 800 C. All turned brittle and glassy upon heating. After the polymers were heated to 800 C, the lowest weight loss, around 10 percent, was found for the homopolymer; the weight loss for the copolymers was about 20 percent.

Author

N93-10007 Materials Sciences Corp., Blue Bell, PA.

TRANSVERSE TENSION, TRANSVERSE COMPRESSION, AND INPLANE SHEAR JANNAF ROUND ROBIN TEST METHODS STANDARDIZATION RESULTS **c39**

Ron B. Bucinell, D. Moy, and Terry Vandiver (Army Missile Command, Redstone Arsenal, AL.) *In* JHU, The 1992 JANNAF Propulsion Meeting, Volume 1 Feb. 1992 p 143-151 (For primary document see N93-10001 01-20)

(Contract DAAL04-89-C-0023)

Avail: CPIA, 10630 Little Patuxent Pkwy., Suite 202, Columbia, MD, 21044-3200 HC

The uniqueness of the filament winding process has led to the development of hoop wound tube test methods for transverse tension, transverse compression, and inplane shear properties. A round robin testing program is being used to evaluate the precision of these test methods. At this time, only five of the six test sites have reported data. Preliminary evaluations of the reported data indicate that the material response appears indistinguishable between test sites. This suggests that the precision of the test methods are adequate for standardization. The test methods are currently being considered for both Military and ASTM standardization.

Author

N93-10008 Naval Research Lab., Washington, DC. Lab. for Computational Physics and Fluid Dynamics.

NUMERICAL SIMULATION OF UNSTEADY FLOW IN A NOZZLE **c34**

Ravi Ramamurti, K. Kailasanath, and R. Loehner (George Washington Univ., Washington, DC.) *In* JHU, The 1992 JANNAF Propulsion Meeting, Volume 1 Feb. 1992 p 153-163 Sponsored by SSPO (For primary document see N93-10001 01-20)

Avail: CPIA, 10630 Little Patuxent Pkwy., Suite 202, Columbia, MD, 21044-3200 HC

A finite-element scheme coupled with the Flux-Corrected Transport Algorithm in axisymmetric coordinates is employed to compute unsteady flow in a nozzle. Stationary and moving shocks are captured using an adaptive remeshing technique. In order to accommodate moving frames of reference associated with moving grids, an Arbitrary Lagrangian-Eulerian form of the governing equations is employed. A simple model is also incorporated to study the effects of variable ratio of specific heats. Several calculations are performed by varying the clearance between the nozzle exit and the aft-shield and other initial conditions in the nozzle. Results are compared with experiments and generally good agreement is obtained in both the pressure levels and the location of the shock at different times.

Author

N93-10009 Air Force Inst. of Tech., Wright-Patterson AFB, OH.

SUPERSONIC CONFINED JET NOZZLES **c34**

Milt E. Franke *In* JHU, The 1992 JANNAF Propulsion Meeting, Volume 1 Feb. 1992 p 165-169 (For primary document see N93-10001 01-20)

Avail: CPIA, 10630 Little Patuxent Pkwy., Suite 202, Columbia, MD, 21044-3200 HC

Two-dimensional and axisymmetric confined jet nozzles that operate in various stable flow conditions are described. When used for propulsion purposes, these confined jet nozzles are sometimes referred to as confined jet thrust vector control nozzles. Supersonic flow leaves the nozzle in an axial direction but with control flow can be made to attach to a diverging wall, thus vectoring the supersonic flow in the confined region. Axial and vectored performance and some of the operating characteristics of the nozzles are described.

Author

N93-10010*# National Aeronautics and Space Administration. Langley Research Center, Hampton, VA.

A BUILDING-BLOCK APPROACH FOR TURBULENCE MODEL VALIDATION/UPGRADE FOCUSSED ON HIGH-SPEED JET FLOWFIELDS **c34**

Stanford M. Dash (Science Applications International Corp., Fort Washington, PA.), B. J. Walker (Army Missile Command, Redstone Arsenal, AL.), and J. M. Seiner *In* JHU, The 1992 JANNAF Propulsion Meeting, Volume 1 Feb. 1992 p 171-193 (For primary document see N93-10001 01-20)

Avail: CPIA, 10630 Little Patuxent Pkwy., Suite 202, Columbia, MD, 21044-3200 HC

A building-block approach for turbulence model validation/upgrade is described whereby blocks of unit problem data of increasing complexity are implemented. This approach requires filling in gaps in the data base and remedying deficiencies in the turbulence model before moving to the next block of data. The previous utilization of this approach to develop a hybrid axisymmetric jet turbulence model, and, its current utilization (with an improved data base and recently formulated compressible-dissipation concepts) to develop an improved turbulence model are described. Building-block data of specific interest to the jet/acoustics and missile/plume communities were gathered over the years and are being utilized to support current turbulence modeling efforts.

Author

N93-10011 National Aero-Space Plane Joint Program Office, Wright-Patterson AFB, OH.

A CONFIGURATION DEVELOPMENT STRATEGY FOR THE NASP **c05**

Curtis D. Snyder and S. Zane Pinckney (Lockheed Engineering and Sciences Co., Hampton, VA.) *In* JHU, The 1992 JANNAF Propulsion Meeting, Volume 1 Feb. 1992 p 195-202 Previously announced in IAA as A91-56156 and A92-17830 (For primary document see N93-10001 01-20)

Avail: CPIA, 10630 Little Patuxent Pkwy., Suite 202, Columbia, MD, 21044-3200 HC

Characteristics of airframe-integrated scramjet (AIS) aerospacecraft are studied using elementary and a recently developed AIS analysis code. Of principal interest is the definition of the AIS and what concepts offer the most potential. One of the concepts is selected for a limited optimization study aimed at defining the relationship of exhaust area to performance potential. The study shows that, if the AIS vehicle is to be fully constrained within the 'optimum' flowpath envelope, large values of exhaust-area-to-capture-area ratio are desired. A benefit of this choice is that performance at the very highest airbreather speeds is improved and, thus, may delay the need to switch to rocket power.

Author

N93-10012 General Electric Co., Cincinnati, OH. Aircraft Engines Div.

HYPERSONIC INLET EFFICIENCY REVISITED **c02**

Paul H. Kutschenreuter, J. A. Davis, and R. J. Gaeta, Jr. *In JHU, The 1992 JANNAF Propulsion Meeting, Volume 1* Feb. 1992 p 203-214 (For primary document see N93-10001

01-20)
Avail: CPIA, 10630 Little Patuxent Pkwy., Suite 202, Columbia, MD, 21044-3200 HC

The problem of inlet efficiency parameter definition for hypersonic scramjet propulsion at double-digit Mach numbers less than 20 is addressed. At such flight conditions, the inlet compression process is no longer adiabatic. Real gas chemistry takes on extra importance, and the combined effects of entropy layer and viscous effects lead to highly nonuniform flow profile characteristics at the combustor entrance. The concept of using inlet entropy increase is proposed, evaluated, and compared against traditional inlet parameters. Examples of its use in dealing with the problems of real gas chemistry, combustor entrance profile nonuniformity, and nonadiabatic compression are illustrated. Freestream Mach number 18 inlet CFD results are used as an example in computing the overall inlet entropy increase compared to results obtained from superposition of leading edge bluntness effects, friction, and inviscid shock losses - all calculated separately by simpler methods. Although CFD 'nose-to-tail' analysis capability has progressed significantly in the last few years, both numerical and physical accuracy requirements (as well as economics) are currently taxed significantly by double-digit Mach number applications. Thus, there remains a practical need to estimate high Mach number scramjet engine performance by less sophisticated techniques. Consequently, this paper concludes with an application of the inlet entropy increase approach based on an example nonuniform flow combustor entrance profile in order to permit a one-dimensional calculation of scramjet propulsion performance. Author

N93-10013 General Dynamics Corp., San Diego, CA. Space Systems Div.
PLUG NOZZLE PROPULSION SYSTEM
Dan A. Heald *In* JHU, The 1992 JANNAF Propulsion Meeting, Volume 1 Feb. 1992 p 263-270 (For primary document see N93-10001 01-20)
Avail: CPIA, 10630 Little Patuxent Pkwy., Suite 202, Columbia, MD, 21044-3200 HC

General Dynamics studied a vertical takeoff/vertical landing fully reusable single-stage-to-orbit (SSTO) concept for medium payload missions. A hydrogen oxygen plug nozzle main engine integrates well in the wide aft end. The principal driver for its selection was the promise of very high I(sub SP), 480 seconds vacuum. Further, preliminary design and analysis with Rocketdyne showed uncertainties and performance losses degrading this number to 467.4 seconds. Nevertheless, this SSTO configuration appears to be optimum for a plug nozzle main engine system. The merits and risks of this propulsion system are discussed. Continued development is recommended. Author

N93-10014 GenCorp Aerojet, Sacramento, CA. Aerojet Propulsion Div.
CRITICAL ENGINE SYSTEM DESIGN CHARACTERISTICS FOR SSTO VEHICLES
Thomas J. Fanciullo, D. C. Judd, and C. J. OBrien *In* JHU, The 1992 JANNAF Propulsion Meeting, Volume 1 Feb. 1992 p 271-283 (For primary document see N93-10001 01-20)
(Contract SDIO84-90-C-0030)
Avail: CPIA, 10630 Little Patuxent Pkwy., Suite 202, Columbia, MD, 21044-3200 HC

Engine system design characteristics are summarized for typical vertical take-off and landing (VTOL) and vertical take-off and horizontal landing (VTHL) Strategic Defense Initiative Organization (SDIO) single stage to orbit (SSTO) vehicles utilizing plug nozzle configurations. Power cycle selection trades involved the unique modular platelet engine (MPE) with the use of (1) LO2 and LH2 at fixed and variable mixture ratios, (2) LO2 and propane or RP-1, and (3) dual fuels (LO2 with LH2 and C3H8). The number of thrust cells and modules were optimized. Dual chamber bell and a cluster of conventional bell nozzle configurations were examined for comparison with the plug configuration. Thrust modulation (throttling) was selected for thrust vector control. Installed thrust ratings were established to provide an additional 20 percent overthrust capability for engine out operation. Turbopumps were designed to operate at subcritical speeds to facilitate a wide range of throttling and long life. A unique dual spool arrangement with hydrostatic bearings was selected for the LH2 turbopump. Controls and health monitoring with expert systems for diagnostics are critical subsystems to ensure minimum maintenance and supportability for a less than seven day turnaround. The use of an idle mode start, in conjunction with automated health condition monitoring, allows the rocket propulsion system to operate reliably in the manner of present day aircraft propulsion. Author

N93-10015 Garrett Fluid Systems Co., Tempe, AZ.
PNEUMATIC MOTOR POWERED THRUST VECTOR CONTROL (TVC) FOR LIQUID PROPELLED LAUNCH VEHICLES
Mark C. Malone and P. S. Evans *In* JHU, The 1992 JANNAF Propulsion Meeting, Volume 1 Feb. 1992 p 285-294 (For primary document see N93-10001 01-20)
(Contract F04701-85-C-0019)
Avail: CPIA, 10630 Little Patuxent Pkwy., Suite 202, Columbia, MD, 21044-3200 HC

Recent studies performed for the Titan 4 launch vehicle indicate significant potential advantages in replacing the current stage 1 and 2 recirculating hydraulic TVC (thrust vector control) system with a PMA (pneumatic mechanical actuation) system. Some of the advantages of a PMA system over the recirculating hydraulic system include reduced part count and weight, reduced maintenance and life-cycle cost, and improved mission reliability. PMA technology, used in aircraft applications since the 1960s, is well suited in launch vehicle TVC applications where an existing pneumatic pressure source is available. A typical pneumatic motor TVC consists of a pneumatic power source, a dual rotor pneumatic motor, a gear box, a ball screw actuator, and the associated closed-loop servo-control elements. One key issue with implementing this mechanical approach is designing a TVC system to withstand large load transient disturbances during liquid engine starting. Hydraulic actuator transient loads have exceeded 60,000 lb(sub f) for a 30,000 lb(sub f) stall design actuator during ground starts of the Titan 3B, Stage 1 engine. A PMA TVC system must also withstand these start transients without imparting excessive reaction loads to the engine nozzle and thrust structure. Work completed to date with Martin Marietta to examine pneumatic motor powered TVC options and technology benefits is presented. The load transient issue is discussed along with potential solutions and the associated trades. General background on PMA technology and experience base is also presented. Author

N93-10016*# National Aeronautics and Space Administration. Lewis Research Center, Cleveland, OH.
COMBUSTION-WAVE IGNITION FOR ROCKET ENGINES
Larry C. Liou *In* JHU, The 1992 JANNAF Propulsion Meeting, Volume 1 Feb. 1992 p 295-311 Previously announced as N92-20043 (For primary document see N93-10001 01-20)
Avail: CPIA, 10630 Little Patuxent Pkwy., Suite 202, Columbia, MD, 21044-3200 HC

The combustion wave ignition concept was experimentally studied in order to verify its suitability for application in baffled sections of a large booster engine combustion chamber. Gaseous oxygen/gaseous methane (GOX/GH4) and gaseous oxygen/gaseous hydrogen (GOX/GH2) propellant combinations were evaluated in a subscale combustion wave ignition system. The system included four element tubes capable of carrying ignition energy simultaneously to four locations, simulating four baffled sections. Also, direct ignition of a simulated Main Combustion Chamber (MCC) was performed. Tests were conducted over a range of mixture ratios and tube geometries. Ignition was consistently attained over a wide range of mixture ratios. At every ignition, the flame propagated through all four element tubes. For GOX/GH4, the ignition system ignited the MCC flow at mixture ratios from 2 to 10 and for GOX/GH2 the ratios is from 2 to 13. The ignition timing was found to be rapid and uniform. The total ignition delay when using the MCC was under 11 ms, with the tube-to-tube, as well as the run-to-run, variation under 1 ms. Tube

geometries were found to have negligible effect on the ignition outcome and timing. Author

N93-10017 Marotta Scientific Controls, Inc., Tustin, CA.
LAM ACTUATED PROPELLANT FLOW CONTROL DEVICE
Robert H. Reinicke and Kevin M. Cust *In* JHU, The 1992 JANNAF Propulsion Meeting, Volume 1 Feb. 1992 p 313-322 Prepared in cooperation with Marotta Scientific Controls, Inc., Montville, NJ (For primary document see N93-10001 01-20)
Avail: CPIA, 10630 Little Patuxent Pkwy., Suite 202, Columbia, MD, 21044-3200 HC

An advanced design LAM (limited angle motor) positions an integral flow control element for bi-level flow control of storable propellants. The LAM incorporates permanent magnet latching to maintain the flow control element in either the low or high flow position without continuous electrical energization. The LAM stator and rotor are fully sheathed within stainless steel. This construction method permits the LAM to control storable propellants without using dynamic seals to isolate the LAM from the propellants. All welded construction prevents external leakage. The design concept selection rationale and the computer FEA (finite element analysis) methods employed to optimize design characteristics are presented. Correlations of analyses to test results are described. Author

N93-10018*# Aerojet-General Corp., Sacramento, CA. Propulsion Div.
FORMED PLATELETS FOR LOW COST REGENERATIVELY COOLED ROCKET COMBUSTION CHAMBERS
Wendel M. Burkhardt *In* JHU, The 1992 JANNAF Propulsion Meeting, Volume 1 Feb. 1992 p 323-328 (For primary document see N93-10001 01-20)
(Contract NAS8-37456)
Avail: CPIA, 10630 Little Patuxent Pkwy., Suite 202, Columbia, MD, 21044-3200 HC

The ongoing work performed to demonstrate the fabrication feasibility of a formed platelet regeneratively cooled combustion chamber liner is described. The combustion chambers are fabricated in three or four axial sections from formed platelet stacks joined together. The platelets are etched, stacked, and bonded into flat panels that contain the regen passages. The flat panels are formed into the final contour with a die. The formed platelet approach takes advantage of the inherent low cost, high accuracy, and thin wall capability of photoetched platelet technology to fabricate long life, low cost rocket combustion chambers. Combustion chamber liner sections were fabricated with extremely thin (tw = 0.20 mm (0.008-in.)) hot gas side walls and very high aspect ratio coolant channels (aspect ratio greater than 10:1). Combustion chamber liner sections were formed of both Zr-Cu and stainless steel. The results of both the forming of individual panels and the joining of panels together are discussed. Work performed demonstrating the feasibility of rocket combustion chamber liners from formed platelets is described. A discussion of the benefits of chamber liners so constructed and of a chamber producing 176,000 N (40 Klbf) of thrust currently fabricated is presented. The results of a study examining the forming of large scale platelet panels for an Space Shuttle Main Engine (SSME) Main Combustion Chamber (MCC) liner are included. Author

N93-10019*# National Aeronautics and Space Administration. Lewis Research Center, Cleveland, OH.
THERMAL STRATIFICATION POTENTIAL IN ROCKET ENGINE COOLANT CHANNELS
Kenneth J. Kacynski *In* JHU, The 1992 JANNAF Propulsion Meeting, Volume 1 Feb. 1992 p 329-338 Previously announced as N92-25616 (For primary document see N93-10001 01-20)
Avail: CPIA, 10630 Little Patuxent Pkwy., Suite 202, Columbia, MD, 21044-3200 HC

The potential for rocket engine coolant channel flow stratification was computationally studied. A conjugate, 3-D, conduction/advection analysis code (SINDA/FLUINT) was used. Core fluid temperatures were predicted to vary by over 360 K across the coolant channel, at the throat section, indicating that the conventional assumption of a fully mixed fluid may be extremely inaccurate. Because of the thermal stratification of the fluid, the walls exposed to the rocket engine exhaust gases will be hotter than an assumption of full mixing would imply. In this analysis, wall temperatures were 160 K hotter in the turbulent mixing case than in the full mixing case. The discrepancy between the full mixing and turbulent mixing analyses increased with increasing heat transfer. Both analysis methods predicted identical channel resistances at the coolant inlet, but in the stratified analysis the thermal resistance was negligible. The implications are significant. Neglect of thermal stratification could lead to underpredictions in nozzle wall temperatures. Even worse, testing at subscale conditions may be inadequate for modeling conditions that would exist in a full scale engine. Author

N93-10020*# National Aeronautics and Space Administration. Lewis Research Center, Cleveland, OH.
HOT FIRE TEST RESULTS OF SUBSCALE TUBULAR COMBUSTION CHAMBERS
John M. Kazaroff, Robert S. Jankovsky, and Albert J. Pavli (Sverdrup Technology, Inc., Brook Park, OH.) *In* JHU, The 1992 JANNAF Propulsion Meeting, Volume 1 Feb. 1992 p 339-352 (For primary document see N93-10001 01-20)
Avail: CPIA, 10630 Little Patuxent Pkwy., Suite 202, Columbia, MD, 21044-3200 HC

Advanced subscale tubular combustion chambers have been built and test fired with Hydrogen-Oxygen propellants to assess the increase in fatigue life that can be obtained with this type of construction. Two chambers were tested; one ran for 637 cycles without failing compared to a predicted life of 200 cycles for a comparable smooth-wall milled-channel liner configuration. The other chamber failed at 256 cycles, compared to a predicted life of 118 cycles for a comparable smooth-wall milled-channel liner configuration. Post-test metallographic analysis determined that the strain relieving design (structural compliance) of the tubular configuration was the cause of this increase in life. Author

N93-10021*# National Aeronautics and Space Administration. Marshall Space Flight Center, Huntsville, AL.
FACILITY FOR COLD FLOW TESTING OF SOLID ROCKET MOTOR MODELS **c14**
D. L. Bacchus, O. E. Hill, and R. Harold Whitesides (Engineering Research and Consulting, Inc., Huntsville, AL.) *In* JHU, The 1992 JANNAF Propulsion Meeting, Volume 1 Feb. 1992 p 353-363 (For primary document see N93-10001 01-20)
(Contract NAS8-37505)
Avail: CPIA, 10630 Little Patuxent Pkwy., Suite 202, Columbia, MD, 21044-3200 HC

A new cold flow test facility was designed and constructed at NASA Marshall Space Flight Center for the purpose of characterizing the flow field in the port and nozzle of solid propellant rocket motors (SRM's). A National Advisory Committee was established to include representatives from industry, government agencies, and universities to guide the establishment of design and instrumentation requirements for the new facility. This facility design includes the basic components of air storage tanks, heater, submicron filter, quiet control valve, venturi, model inlet plenum chamber, solid rocket motor (SRM) model, exhaust diffuser, and exhaust silencer. The facility was designed to accommodate a wide range of motor types and sizes from small tactical motors to large space launch boosters. This facility has the unique capability of testing ten percent scale models of large boosters such as the new Advanced Solid Rocket Motor (ASRM), at full scale motor Reynolds numbers. Previous investigators have established the validity of studying basic features of solid rocket motor development programs include the acquisition of data to (1) directly evaluate and optimize the design configuration of the propellant grain, insulation, and nozzle; and (2) provide data for validation of the computational fluid dynamics, (CFD), analysis codes and the performance analysis codes. A facility checkout model was designed, constructed, and utilized to evaluate the performance characteristics of the new facility. This model consists of a cylindrical chamber and converging/diverging nozzle with

appropriate manifolding to connect it to the facility air supply. It was designed using chamber and nozzle dimensions to simulate the flow in a 10 percent scale model of the ASRM. The checkout model was recently tested over the entire range of facility flow conditions which include flow rates from 9.07 to 145 kg/sec (20 to 320 lbm/sec) and supply pressure from 5.17 x 10 exp 5 to 8.27 x 10 exp 6 Pa. The performance of the self-pumping exhaust diffuser was verified down to exhaust pressures of 1.379 x 10 exp 4 Pa. The facility was successfully operated over the entire range of design pressures and flowrates and is available for national use by industry and government agencies requiring facilities capable of testing SRM cold flow models to support development programs or resolve problems arising on operational flight systems. Author

N93-10022 Air Force Academy, CO.
A SIMPLIFIED MODEL FOR HYBRID ROCKET PERFORMANCE PREDICTION
Robert S. Wolf and John W. Wagner *In* JHU, The 1992 JANNAF Propulsion Meeting, Volume 1 Feb. 1992 p 365-369 (For primary document see N93-10001 01-20)
Avail: CPIA, 10630 Little Patuxent Pkwy., Suite 202, Columbia, MD, 21044-3200 HC

A computer code to predict hybrid rocket performance was developed and validated. The algorithm used is a simplification of the model derived by Marxman and Wooldridge. This model assumes the fuel regression rate to be controlled by convective heat transfer to the solid fuel from a relatively thin diffusion flame in a turbulent boundary layer. The model further assumes that the Reynolds analogy applies with mass addition at the wall. The computer code incorporates variable combustion product properties (temperature, molecular weight, and ratio of specific heats) as a function of the instantaneous global oxidizer/fuel ratio. The code was validated by constructing and firing a hybrid rocket motor. This motor used gaseous oxygen and hydroxyl-terminated polybutadiene as propellants. The oxygen flow rate used in the test was given as an input to the computer code, which then calculated chamber pressures and thrust. The agreement between test data and computer predictions was excellent. Author

N93-10023*# Atlantic Research Corp., Gainesville, VA.
FEASIBILITY EVALUATION OF THE MONOLITHIC BRAIDED ABLATIVE NOZZLE
Mark N. Director and Douglass J. McPherson, Sr. *In* JHU, The 1992 JANNAF Propulsion Meeting, Volume 1 Feb. 1992 p 371-385 (For primary document see N93-10001 01-20)
(Contract NAS8-38237)
Avail: CPIA, 10630 Little Patuxent Pkwy., Suite 202, Columbia, MD, 21044-3200 HC

The feasibility of the monolithic braided ablative nozzle was evaluated as part of an independent research and development (IR&D) program complementary to the National Aeronautics and Space Administration/Marshall Space Flight Center (NASA/MSFC) Low-Cost, High-Reliability Case, Insulation and Nozzle for Large Solid Rocket Motors (LOCCIN) Program. The monolithic braided ablative nozzle is a new concept that utilizes a continuous, ablative, monolithic flame surface that extends from the nozzle entrance, through the throat, to the exit plane. The flame surface is fabricated using a Through-the-Thickness braided carbon-fiber preform, which is impregnated with a phenolic or phenolic-like resin. During operation, the braided-carbon fiber/resin material ablates, leaving the structural backside at temperatures which are sufficiently low to preclude the need for any additional insulative materials. The monolithic braided nozzle derives its potential for low life cycle cost through the use of automated processing, one-component fabrication, low material scrap, low process scrap, inexpensive raw materials, and simplified case attachment. It also has the potential for high reliability because its construction prevents delamination, has no nozzle bondlines or leak paths along the flame surface, is amenable to simplified analysis, and is readily inspectable. In addition, the braided construction has inherent toughness and is damage-tolerant. Two static-firing tests were conducted using subscale, 1.8 - 2.0-inch throat diameter, hardware. Tests were approximately 15 seconds in duration, using a conventional 18 percent aluminum/ammonium perchlorate propellant. The first of these tests evaluated the braided ablative as an integral backside insulator and exit cone; the second test evaluated the monolithic braided ablative as an integral entrance/throat/exit cone nozzle. Both tests met their objectives. Radial ablation rates at the throat were as predicted, approximately 0.017 in/sec; these rates are comparable to those for tapewrapped carbon phenolic materials. The maximum temperature rise on the outside surface occurred one inch from the nozzle exit plane and was less than 50 F at the end of the test. Further development for this concept is scheduled as part of phase 2 on the NASA/MSFC LOCCIN Program. During this effort, the nozzle materials, architecture, and processing will be optimized and tested in nozzles with 3- and 10-inch diameter throats. Further, a design and manufacturing plan for a full-scale, 20-inch-diameter throat, nozzle will be developed. Author

N93-10024 Thiokol Corp., Huntsville, AL.
MOLDED NOZZLE TECHNOLOGY FOR LARGE SOLID ROCKET MOTORS
Mark L. Fox and R. C. Laramee *In* JHU, The 1992 JANNAF Propulsion Meeting, Volume 1 Feb. 1992 p 387-397 (For primary document see N93-10001 01-20)
Avail: CPIA, 10630 Little Patuxent Pkwy., Suite 202, Columbia, MD, 21044-3200 HC

Trade studies conducted during the Advanced Launch System and National Launch System Programs selected nozzles manufactured from PAN based carbon cloth phenolic molding compound. This was one component of large solid rocket boosters that could provide for significant cost reduction and still maintain high reliability. Molded nozzle technology is not new and is currently employed in several small tactical systems now in production. What is needed is to determine the feasibility of this technology in larger systems such as NLS. The NASA's MNASAM solid rocket motor was chosen as a 1/4 to 1/2 scale representation of a proposed future ALS/NLS size solid rocket booster nozzle. Design and fabrication accomplishments, process development, acceptance testing, structural load testing, char motor testing results, and thermal and mechanical property data are presented and discussed. Also, cost reduction is discussed relative to the conventional tape wrapped nozzle technology currently employed for the MNASAM. Author

N93-10025 Minnesota Mining and Mfg. Co., Saint Paul. Industrial Chemical Products Div.
GAP BENEFITS **c27**
Peter F. Aiello and Anthony P. Manzara *In* JHU, The 1992 JANNAF Propulsion Meeting, Volume 1 Feb. 1992 p 399-405 (For primary document see N93-10001 01-20)
Avail: CPIA, 10630 Little Patuxent Pkwy., Suite 202, Columbia, MD, 21044-3200 HC

The Industrial Chemical Products Division of 3M has been involved in the development and production of Glycidyl Azide Polymer (GAP) since 1979. Recent developments in polymer and plasticizer technology have led to GAP gumstocks of improved mechanical properties. The benefits of GAP are discussed.
Author

N93-10026*# Jet Propulsion Lab., California Inst. of Tech., Pasadena.
INVESTIGATION OF THE STIMULATED RELEASE OF GASEOUS AMMONIA FROM AMMONIUM PERCHLORATE BY HTPB SOLID PROPELLANT BONDING AGENTS **c28**
James C. McComb *In* JHU, The 1992 JANNAF Propulsion Meeting, Volume 1 Feb. 1992 p 407-418 Sponsored by NASA, Washington (For primary document see N93-10001 01-20)
Avail: CPIA, 10630 Little Patuxent Pkwy., Suite 202, Columbia, MD, 21044-3200 HC

The stimulated release of gaseous ammonia by the reactions of HTPB solid propellant bonding agents with ammonium perchlorate (AP) was studied in chloroform/AP suspensions of the bonding agents and in live propellant smears. Polyamine

bonding agents such as tepanol were found to evolve ammonia over a sustained time period (2-4 hours) when reacted with AP in chloroform. For propellant containing 0.15 percent (w/w) tepanol the total weight of ammonia generated per unit weight of propellant was equivalent to 120 ppm. Successful application of these bonding agents is therefore dependent on how well the ammonia by-product can be dissipated from the mix before the isocyanate curing agent is introduced. Ammonia generation by the bifunctional aziridine-based bonding agent system HX-752 was found to be twenty-five times less severe (on a w/w basis) than by tepanol. Ammonia generation by HX-752 was slow and sustained, requiring up to 18-20 hours to reach completion. The level of ammonia generation by HX-752 was sufficiently low, however, that no effort to remove ammonia contamination was necessary to obtain propellant with good end-product physical properties. HX-752 is therefore better suited to applications where removal of ammonia is impractical, such as continuous process mixing. The epoxy-based bonding agent, XU238, generated only trace amounts of ammonia (3 ppm for 0.3 percent XU238 propellant), but required the presence of a reactive polyamine, diethylene triamine (DETA), to reduce the propellant viscosity to processible levels (less than 25 kP). DETA generated up to five times as much ammonia (on a w/w basis) as tepanol in chloroform/AP slurries, but required less than 2 hours to react completely. The effects of mix procedure, aluminum type, and pre-mix reaction time on the ammonia generating properties of these three bonding agent systems in HTPB solid propellant are described. Author

N93-10027*# Thiokol Corp., Brigham City, UT.
EFFECTS OF THE RSRM GRAIN DEFORMATION ON BALLISTIC PERFORMANCE **c28**
Boyd J. Hutchison and P. J. Downey *In* JHU, The 1992 JANNAF Propulsion Meeting, Volume 1 Feb. 1992 p 419-426 (For primary document see N93-10001 01-20)
(Contract NAS8-30490)
Avail: CPIA, 10630 Little Patuxent Pkwy., Suite 202, Columbia, MD, 21044-3200 HC

Grain deformation of a solid rocket motor is an important factor in accurately modeling its performance. Deformation can effect maximum pressure and thrust, burn time, performance trace shape, and tailoff. Motor parameters such as propellant web thickness, case strength and diameter, propellant mechanical properties, and grain geometry will determine the extent of the effects that deformation will have on performance. Early in the Space Shuttle solid booster program, grain deformation was not modeled. Adjustment factors were estimated based on historical large motor data. After several static test firings, two adjustment factors were determined for the redesigned solid rocket motor (RSRM) to account for the unknown parameters. These two factors, the Surface Burn Rate Error (SBRE) curve and scale factor, were used to help predict the performance of the motor for future firings. SBRE is applied to the instantaneous burn rate. Scale factor is applied to the reference burn rate. These two factors and the burn rate were consistent and therefore, the ballistic predictions were accurate. In an effort to better understand the SBRE curve and determine the true burn rate of the RSRM, coupled analyses were done on the grain deformation. These analyses included finite element structural analyses to determine actual grain configuration, propellant burn back geometry analyses, and ballistic performance analyses. The results of the analyses showed the web thickness is reduced and therefore, the burn rate is actually lower. The current nominal RSRM burn rate is 0.368 in/sec at 625 psi and 60 F. These analyses showed the burn rate is 0.358 in/sec. The SBRE curve, which includes errors caused by directional burn rate bias as well as geometry modeling errors, was reduced slightly during the first half of motor operation. It appears that directional burn rate bias is the primary contributor to the SBRE for the RSRM. It should be noted that the pressure loads applied in the structural studies were at the rollover pressure, which is the pressure just after the maximum pressure spike of the RSRM. The loads did include a significant pressure drop that occurs down the bore of the motor. After 50 seconds of the motor burn, the pressure level drops to roughly two-thirds the rollover pressure. Also at this time, the bore diameter has opened up enough to nearly eliminate the pressure drop. A lower motor pressure will obviously change the grain deformation. An iterative and coupled structural and ballistic analyses using the motor pressure at different burned back configurations would increase the accuracy of the results. Author

N93-10028 Jet Propulsion Lab., California Inst. of Tech., Pasadena.
ALTERNATIVES IN CLEAN PROPELLANTS FOR LARGE SCALE MAN-RATED SOLID ROCKET MOTORS **c28**
James C. McComb *In* JHU, The 1992 JANNAF Propulsion Meeting, Volume 1 Feb. 1992 p 427-438 (For primary document see N93-10001 01-20)
Avail: CPIA, 10630 Little Patuxent Pkwy., Suite 202, Columbia, MD, 21044-3200 HC

Development work conducted in-house at JPL and within the solid propellant industry in the area of clean burning (low HCl) solid propellant over the last 15 years is reviewed within the context of the performance requirements for large scale man-rated booster systems such as the Advanced Solid Rocket Motor (ASRM) for the Space Shuttle. Alternate approaches are critically compared in terms of the tradeoffs of delivered I(sub sp), HCl emission, safety considerations, processing difficulties, ballistic and combustion stability properties, and end-product mechanical properties. Theoretical calculations for several alternate reduced-HCl propellants are presented. The results suggest that as much as one half of the total HCl emission could be eliminated with an overall 2.2 percent gain in I(sub sp) x density by including sodium perchlorate (NaClO4) as a co-oxidizer in ammonium perchlorate/aluminum/HTPB propellant. A smaller, but significant increase (approximately 0.5 percent) in I(sub sp) x density is predicted if half of the ammonium perchlorate oxidizer is replaced by potassium perchlorate. Complete replacement of AP with NaClO4 virtually eliminates HCl generation, with an overall gain in theoretical I(sub sp) x density of 3.5 percent, but the flame temperature of the propellant is raised considerably. An alternate clean propellant formulation which reduces the HCl content of the exhaust plume to 3 percent by weight is also suggested, based on ammonium perchlorate, sodium nitrate, HMX, aluminum, and HTPB as the propellant ingredients. This formulation has a theoretical I(sub sp) that is within 3.5 percent that of the conventional AP/HTPB propellant formulation proposed for the ASRM. Greater reductions in HCl content are achievable; they are accompanied by larger reductions in propellant performance. Author

N93-10029 Aerospace Corp., Los Angeles, CA.
ELECTRIC PROPULSION APPLICATIONS
Jeffrey W. Ramos, D. M. Sutton, M. G. McLain, and K. P. Zondervan *In* JHU, The 1992 JANNAF Propulsion Meeting, Volume 1 Feb. 1992 p 439-502 (For primary document see N93-10001 01-20)
Avail: CPIA, 10630 Little Patuxent Pkwy., Suite 202, Columbia, MD, 21044-3200 HC

The mission enhancing applications of electric propulsion in the integrated satellite system are presented. Applications considered are orbit transfer, on-orbit maneuvering, and effects on launch vehicle selection. Parametric orbit transfer performance is presented for solar powered arcject, ion, resistojet, and hybrid configured upper stages. Mission specific performance is compared for a DSP class spacecraft. Significant reductions in propellant requirements lead to a large increase in net payload capability using electric propulsion, albeit, at transfer times on the order of months. On-orbit applications investigated include control of the right ascension of the ascending note (RAAN), inclination change, station relocation, station keeping, and threat avoidance. On-orbit maneuvers benefit in terms of propellant and/or time savings as compared to conventional chemical systems. Maneuvers such as RAAN control, for making orbits sun-synchronous, are made possible using high specific impulse ion engines. A variety of medium and heavy launch vehicles are paired with both conventional chemical upper stages and electric orbit transfer

systems. The role of an EOTV in the current mission model is to enhance and enable missions in the class of payloads which fall between current Medium Launch Vehicle (MLV) and Heavy Launch Vehicle (HLV) capabilities. This performance gap can be filled by an MLV/Electric Orbit Transfer Vehicle (EOTV) which has the potential to carry between 5,000 and 8,000 pounds into geosynchronous orbit. This effort was accomplished in support of DOD objectives to identify mission enhancing applications of electric propulsion to space launch systems. Author

N93-10030 TRW Space and Defense Sector, Redondo Beach, CA.
ELECTRIC PROPULSION SPACE EXPERIMENT (ESEX): SPACECRAFT DESIGN ISSUES FOR HIGH-POWER ELECTRIC PROPULSION
Mary M. Kriebel and Terry M. Sanks *In* JHU, The 1992 JANNAF Propulsion Meeting, Volume 1 Feb. 1992 p 503-516 Prepared in cooperation with Phillips Lab., Edwards AFB, CA (For primary document see N93-10001 01-20)
(Contract F04611-90-C-0005)
Avail: CPIA, 10630 Little Patuxent Pkwy., Suite 202, Columbia, MD, 21044-3200 HC

Electric propulsion provides high specific impulses, and low thrust when compared to chemical propulsion systems. Therefore, electric propulsion offers improvements over chemical systems such as increased station-keeping time, prolonged on-orbit maneuverability, low acceleration of large structures, and increased launch vehicle flexibility. The anticipated near-term operational electric propulsion system for an electric orbit transfer vehicle is an arcjet propulsion system. Towards this end, the USAF's Phillips Laboratory (PL) has awarded a prime contract to TRW Space & Technology Group to design, build, and space qualify a 30-kWe class arcjet as well as develop and demonstrate, on the ground, a flight-qualified arcjet propulsion flight unit. The name of this effort is the 30 kWe Class Arcjet Advanced Technology Transition Demonstration (Arcjet ATTD) program. Once the flight unit has completed its ground qualification test, it will be given to the Space Test and Transportation Program Office of the Air Force's Space Systems Division (ST/T) for launch vehicle integration and space test. The flight unit's space test is known as the Electric Propulsion Space Experiment (ESEX). ESEX's mission scenario is 10 firings of 15 minutes each. The objectives of the ESEX flight are to measure arcjet plume deposition, electromagnetic interference, thermal radiation, and acceleration in space. Plume deposition, electromagnetic interference, and thermal radiation are operational issues that are primarily being answered for operational use. This paper describes the Arcjet ATTD flight unit design and identifies specifically how the diagnostic data will be collected as part of the ESEX program. Author

N93-10031 Rocket Research Corp., Redmond, WA.
A 26 kW ARCJET SYSTEM FOR ON-ORBIT DEMONSTRATION
R. Joe Cassady, C. E. Vaughan, and R. S. Aadland *In* JHU, The 1992 JANNAF Propulsion Meeting, Volume 1 Feb. 1992 p 517-526 (For primary document see N93-10001 01-20)
Avail: CPIA, 10630 Little Patuxent Pkwy., Suite 202, Columbia, MD, 21044-3200 HC

Design and testing of a 26 kW ammonia arcjet system for the Air Force Laboratory's Electric (Propulsion) Space EXperiment (ESEX) demonstration mission are described in this paper. The design philosophy of the arcjet thruster and the ammonia propellant feed subsystem is presented. A third system element, the Power Conditioning Unit (PCU), is also discussed. The purpose of the ESEX demonstration is to validate ground based measurements of 26 kW ammonia arcjet performance and operational characteristics. This is an important first step toward eventual application of ammonia or hydrogen arcjet thrusters for satellite orbit transfer missions. The data gathered by the ESEX flight will provide user confidence in the critical areas of performance, spacecraft interfaces, and arcjet/spacecraft interactions. The arcjet and PCU designs will serve as the basis for the eventual Electric Orbit Transfer Vehicle (EOTV) thruster systems. While thruster performance can be readily measured in ground test facilities, other user concerns such as Electromagnetic Interference (EMI) are difficult to characterize due to a lack of adequate ground test facilities. A space test also provides the opportunity to verify the thermal modelling and the plume species predictions in the actual space environment. The spacecraft requirements for an arcjet thruster operating at 26 kW demand careful thermal and structural design. The electrode geometry was determined in the Endurance Test program and fixed in this program. The design effort focused on minimizing the heat conducted through the thruster into the PCU and the spacecraft, while maintaining a structure capable of withstanding launch vibration loads. Careful design practice was also applied to minimize radiated EMI. A significant part of the thruster design was a unique power cable to carry the 260 amperes from the PCU to the arcjet. The propellant feed subsystem presented several design challenges. The design requirements include providing ammonia vapor to the arcjet at a controlled pressure and mass flow rate under milli-gee accelerations. An approach was pursued which minimized the qualification requirements by utilizing previously qualified components. The details of the design and test results are presented in the paper. Author

N93-10032 Pacific Electro Dynamics, Redmond, WA.
POWER CONDITIONING UNIT FOR 30 kWe CLASS ARCJET FLIGHT EXPERIMENT
C. M. Golden, J. R. Fisher, and Robert J. Kay *In* JHU, The 1992 JANNAF Propulsion Meeting, Volume 1 Feb. 1992 p 527-537 (For primary document see N93-10001 01-20)
Avail: CPIA, 10630 Little Patuxent Pkwy., Suite 202, Columbia, MD, 21044-3200 HC

The requirements, design, and operation of a 30 kilowatt (kWe) class arcjet power conditioning unit (PCU) are described by this paper. The PCU provides conditioned power to operate an ammonia-propellant arcjet thruster system for a low-earth orbit demonstration program. This arcjet Advanced Technology Transition Demonstration (ATTD) program is sponsored by the U.S. Air Force Phillips Laboratory. The purpose of the program is to develop an experiment package to operate and characterize the performance of a high-power arcjet thruster. Author

N93-10033*# National Aeronautics and Space Administration. Lewis Research Center, Cleveland, OH.
10 kW POWER ELECTRONICS FOR HYDROGEN ARCJETS
John A. Hamley, Luis R. Pinero, and Gerald M. Hill *In* JHU, The 1992 JANNAF Propulsion Meeting, Volume 1 Feb. 1992 p 539-553 (For primary document see N93-10001 01-20)
Avail: CPIA, 10630 Little Patuxent Pkwy., Suite 202, Columbia, MD, 21044-3200 HC

A combination of emerging mission considerations such as launch on schedule, resource limitations, and the development of higher power spacecraft busses has resulted in renewed interest in high power hydrogen arcjet systems with specific impulses greater than 1000 s for Earth-space orbit transfer and maneuver applications. Solar electric propulsion systems with about 10 kW appear to offer payload benefits at acceptible trip times. The design and development of 10 kW hydrogen arcjet power electronics and the results of arcjet integration testing are discussed. The power electronics incorporated a full bridge switching topology similar to that employed in state of the art 5 kW power electronics, and the output filter included an output current averaging inductor with an integral pulse generation winding for arcjet ignition. Phase shifted, pulse width modulation with current mode control was used to regulate the current delivered to the arcjet; a low inductance power stage minimized switching transients. Hybrid power MOSFET's were used to minimize conduction losses. Switching losses were minimized using a fast response, optically isolated, totem-pole gate drive circuit. The input bus voltage for the unit was 150 V, with a maximum output voltage of 225 V. The switching frequency of 20 kHz was a compromise between mass savings and higher efficiency. Power conversion efficiencies in excess of 0.94 were demonstrated, along with steady state load current regulation of 1 percent. The power electronics were successfully integrated with a 10 kW laboratory hydrogen arcjet, and reliable,

non-destrusive starts, and transitions to steady state operation were demonstrated. The estimated specific mass for a flight packaged unit was 2 kg/kW. Author

N93-10034 Lawrence Livermore National Lab., CA.
SELECTION OF ROCKET PROPULSION SYSTEMS
George P. Sutton *In* JHU, The 1992 JANNAF Propulsion Meeting, Volume 1 Feb. 1992 p 555-565 (For primary document see N93-10001 01-20)
Avail: CPIA, 10630 Little Patuxent Pkwy., Suite 202, Columbia, MD, 21044-3200 HC

A process for selecting the most suitable rocket propulsion for each particular application is described. Starting with mission requirements, the propulsion requirements are derived and from them one obtains the criteria against which candidate propulsion systems can be evaluated. Although the emphasis is on liquid propellant rocket engines and solid propellant rocket motors, other propulsion systems, including electric propulsion systems, are also discussed. Detailed tables are presented for three aspects of the selection process, and they can serve as check lists during design. A comparison of liquid propellant versus solid propellant rocket propulsion systems is given. Typical criteria for selecting the best rocket propulsion system from amongst the competing candidate systems are given. Various interfaces between the propulsion system and the flying vehicle or missile are also included. Author

N93-10035 Rockwell International Corp., Canoga Park, CA. Rocketdyne Div.
OPERATIONALLY EFFICIENT SPACE-BASED INTEGRATED PROPULSION MODULE
Timothy Harmon, C. Erickson, and R. Pauckert *In* JHU, The 1992 JANNAF Propulsion Meeting, Volume 1 Feb. 1992 p 567-576 (For primary document see N93-10001 01-20)
Avail: CPIA, 10630 Little Patuxent Pkwy., Suite 202, Columbia, MD, 21044-3200 HC

Space-based propulsion systems, for lunar and Mars missions, will require operability to be a prime design requirement. Since the rocket engine propulsion system represents one of the most complex systems in a space-based vehicle, a study was made to identify propulsion system operational problems. This paper uses descriptions of major operations problems encountered in today's launch vehicles as a point of departure for this study. Lessons learned from the Space Shuttle, expendable launch vehicles, and satellite maintenance reveal activities that are time consuming, costly, difficult, and potentially dangerous. Operational functions are much more difficult in space, have a large impact on cost, and unscheduled operations could result in a missed launch window. Launch and satellite flight certification problems are related to projected space-based propulsion system operations issues. Space-based propulsion systems may be reusable with long periods of space exposure and storage between firings. The space-based propulsion system operability study approach is described, and tradeoffs are presented on operability. Operations driven requirements focus on minimizing or eliminating processing and checkout operations. This paper presents a concept description of a zero maintenance, space-based, integrated propulsion module system. This system is operationally efficient, minimizing operational activities. The resulting propulsion system is simpler, more reliable, has enhanced component out capability, and is more operable than a conventional unintegrated engine system. Author

N93-10036*# National Aeronautics and Space Administration. Lyndon B. Johnson Space Center, Houston, TX.
UPRATED OMS ENGINE STATUS: ALTITUDE TESTING RESULTS
Richard J. Schoenberg *In* JHU, The 1992 JANNAF Propulsion Meeting, Volume 1 Feb. 1992 p 589-597 (For primary document see N93-10001 01-20)
Avail: CPIA, 10630 Little Patuxent Pkwy., Suite 202, Columbia, MD, 21044-3200 HC

The current Space Shuttle Orbital Maneuvering Engine (OME) is pressure fed, utilizing storable propellants. Performance uprating of this engine, through the use of a gas generator driven turbopump to increased operating pressure, is being pursued by the NASA Johnson Space Center (JSC). Component level design, fabrication, and test activities on this engine system began at Aerojet in 1984. More recently, a complete engine, designated the Integrated Component Test Bed (ICTB), was tested at simulated altitude conditions at the NASA White Sands Test Facility (WSTF). A description of the test hardware, and results of the altitude test program are presented. These results, which include the test condition operating envelope, confirm the capability of the selected Uprated OME (UOME) configuration to meet or exceed performance and operational requirements. Engine flexibility, demonstrated through testing at two different operational mixture ratios, along with a summary of projected Space Shuttle performance enhancements using the UOME, are discussed. Planned future activities and recommendations for further engine development are also discussed. Author

N93-10037 Pratt and Whitney Aircraft, West Palm Beach, FL.
ALTITUDE COMPENSATING NOZZLE EVALUATION
R. C. Parsley and Kenneth J. VanStelle *In* JHU, The 1992 JANNAF Propulsion Meeting, Volume 1 Feb. 1992 p 599-604 (For primary document see N93-10001 01-20)
(Contract F04611-87-C-0069)
Avail: CPIA, 10630 Little Patuxent Pkwy., Suite 202, Columbia, MD, 21044-3200 HC

Typically, the nozzle area ratio selected for booster applications is a compromise between optimum performance at lift off and optimum performance at altitude. If nozzle area ratio could be tailored for different altitudes, without significant weight increase, vehicle payload performance can be enhanced. This is particularly true for single-stage-to-orbit (SSTO) applications where the nozzle must operate both at sea level and in space. For conventional bell nozzles, altitude compensation is accomplished most effectively by varying the exit areas of the nozzle during ascent. There are two fundamental approaches to varying nozzle exit area. The first is to physically retract the aft skirt of the nozzle allowing operation at the truncated exit area; the skirt is then deployed to allow full nozzle expansion at altitude. The second approach is to design a fixed geometry nozzle to the full and final area ratio and to induce controlled and stable separation at reduced 'effective' exit areas inside the nozzle. This separation is controlled by allowing passive inflow of ambient air. As altitude increases the vent will be closed to prevent outflow of combustion products and to support expansion to a larger effective exit area. This paper summarizes the proof-of-concept evaluation and testing of a passively ventilated altitude compensating nozzle (ACN) concept. The scheme was tested on a modified RL10 under Air Force contract F04611-87-C-0069 in August 1990. This data complements an earlier Air Force ACN activity completed in the early 1970's, under Air Force contract F04611-68-C-0002. In this program the XLR-129 demonstrated significant altitude compensation performance for a two-position translating skirt. Author

N93-10038*# National Aeronautics and Space Administration. Lewis Research Center, Cleveland, OH.
HOT FIRE FATIGUE TESTING RESULTS FOR THE COMPLIANT COMBUSTION CHAMBER
Al J. Pavli (Sverdrup Technology, Inc., Brook Park, OH.), John M. Kazaroff, and Robert S. Jankovsky *In* JHU, The 1992 JANNAF Propulsion Meeting, Volume 1 Feb. 1992 p 605-614 (For primary document see N93-10001 01-20)
Avail: CPIA, 10630 Little Patuxent Pkwy., Suite 202, Columbia, MD, 21044-3200 HC

A hydrogen-oxygen subscale rocket combustion chamber was designed incorporating an advanced design concept to reduce strain and increase life. The design permits unrestrained thermal expansion in a circumferential direction and, thereby, provides structural compliance during the thermal cycling of hot-fire testing. The chamber was built and test fired at a chamber pressure of 4137kn/sq m (600 psia) and a mixture ratio of 6.0. Compared to a conventional milled-channel configuration, the new structurally

compliant chamber had a 134 or 287 percent increase in fatigue life depending on the life predicted for the conventional configuration. Author

N93-10039*# National Aeronautics and Space Administration. Lewis Research Center, Cleveland, OH.
A SURVEY OF INSTABILITIES WITHIN CENTRIFUGAL PUMPS AND CONCEPTS FOR IMPROVING THE FLOW RANGE OF PUMPS IN ROCKET ENGINES c34
Joseph P. Veres *In* JHU, The 1992 JANNAF Propulsion Meeting, Volume 1 Feb. 1992 p 615-629 Previously announced as N92-18280 (For primary document see N93-10001 01-20)
Avail: CPIA, 10630 Little Patuxent Pkwy., Suite 202, Columbia, MD, 21044-3200 HC

Design features and concepts that have primary influence on the stable operating flow range of propellant-feed centrifugal turbopumps in a rocket engine are discussed. One of the throttling limitations of a pump-fed rocket engine is the stable operating range of the pump. Several varieties of pump hydraulic instabilities are mentioned. Some pump design criteria are summarized and a qualitative correlation of key parameters to pump stall and surge are referenced. Some of the design criteria were taken from the literature on high pressure ratio centrifugal compressors. Therefore, these have yet to be validated for extending the stable operating flow range of high-head pumps. Casing treatment devices, dynamic fluid-damping plenums, backflow-stabilizing vanes, and flow-reinjection techniques are summarized. A planned program was undertaken at LeRC to validate these concepts. Technologies developed by this program will be available for the design of turbopumps for advanced space rocket engines for use by NASA in future space missions where throttling is essential. Author

N93-10040 Phillips Lab., Hanscom AFB, MA. Propulsion Directorate.
THE APPLICATION OF LIQUID CRYSTAL POLYMERS TO TURBOMACHINERY
Mark A. Mueller and Ed E. Schmidt *In* JHU, The 1992 JANNAF Propulsion Meeting, Volume 1 Feb. 1992 p 631-638 (For primary document see N93-10001 01-20)
Avail: CPIA, 10630 Little Patuxent Pkwy., Suite 202, Columbia, MD, 21044-3200 HC

The Advanced Materials for Turbomachinery program is investigating the use of thermotropic Liquid Crystal Polymers (LCP's) as a housing material in turbopump assemblies. A requirement for this application is the compatibility of the LCP's with the working fluids (propellants) of the turbopump. A study was therefore undertaken to assess the physical and chemical properties of several commercial thermotropic LCP's in both storable and cryogenic propellants. Compatibility tests in storable propellants showed the LCP's to be incompatible with monomethyl hydrazine due to the breakdown of ester linkages in the polymer chains. Several LCP's were found to be compatible with nitrogen tetroxide under ambient conditions. Compatibility tests in oxygen environments determined that, although they have high autoignition temperatures, thermotropic LCP's are sensitive to ignition by means of mechanical impact and have high flame propagation rates. Pneumatic burst testing under ambient and cryogenic (liquid nitrogen) conditions showed that burst pressures generally increased at cryogenic temperatures. However, the burst pressure data showed large standard deviations leading to the conclusion that the mechanical properties of thermotropic LCP's are extremely sensitive to material processing parameters. Author

N93-10041*# National Aeronautics and Space Administration. Marshall Space Flight Center, Huntsville, AL.
NLS CARGO TRANSFER VEHICLE PROPULSION SYSTEM
Hank C. Hearn (Lockheed Missiles and Space Co., Huntsville, AL.) and G. K. Langford *In* JHU, The 1992 JANNAF Propulsion Meeting, Volume 1 Feb. 1992 p 639-649 (For primary document see N93-10001 01-20)
Avail: CPIA, 10630 Little Patuxent Pkwy., Suite 202, Columbia, MD, 21044-3200 HC

The propulsion system of the Cargo Transfer Vehicle is designed to meet a wide range of requirements associated with the National Launch System (NLS) resupply function for Space Station Freedom. It provides both orbit adjustment and precise vehicle control capability, and is compatible with close proximity operation at the space station as well as return on the shuttle for ground refurbishment and reuse. Preliminary trade studies have resulted in designing and sizing an integrated biropellant system using monomethyl hydrazine and nitrogen tetroxide. Design and analysis activities are continuing, and the design will evolve and mature as part of the NLS program. Author

N93-10042*# National Aeronautics and Space Administration. Lyndon B. Johnson Space Center, Houston, TX.
LONG LIFE MONOPROPELLANT HYDRAZINE THRUSTER EVALUATION FOR SPACE STATION FREEDOM APPLICATION
Christopher G. Popp, Joseph C. Cook, Brenda L. Ragland, and Leah R. Pate *In* JHU, The 1992 JANNAF Propulsion Meeting, Volume 1 Feb. 1992 p 651-662 (For primary document see N93-10001 01-20)
Avail: CPIA, 10630 Little Patuxent Pkwy., Suite 202, Columbia, MD, 21044-3200 HC

In support of propulsion system thruster development activity for Space Station Freedom (SSF), NASA Johnson Space Center (JSC) conducted a hydrazine thruster technology demonstration program. The goal of this program was to identify impulse life capability of state-of-the-art long life hydrazine thrusters nominally rated for 50 pounds thrust at 300 psia supply pressure. The SSF propulsion system requirement for impulse life of this thruster class is 1.5 million pound-seconds, corresponding to a throughput of approximately 6400 pounds of propellant. Testing at JSC was completed on the thruster designs to quantify life while simulating expected thruster firing duty cycles and durations for SSF. This paper presents a review of the SSF propulsion system hydrazine thruster requirements, the three long life thruster designs procured by JSC, and acceptance test results for each thruster, the JSC thruster life evaluation test program, and the results of the JSC test program. Author

N93-10043*# Jet Propulsion Lab., California Inst. of Tech., Pasadena.
A COMPARISON OF MULTIMEGAWATT ELECTRIC PROPULSION OPTIONS FOR MARS MISSIONS
Robert H. Frisbee *In* JHU, The 1992 JANNAF Propulsion Meeting, Volume 1 Feb. 1992 p 663-678 Sponsored by NASA, Washington (For primary document see N93-10001 01-20)
Avail: CPIA, 10630 Little Patuxent Pkwy., Suite 202, Columbia, MD, 21044-3200 HC

An evaluation of multimegawatt (MMW) nuclear electric propulsion (NEP) and solar electric propulsion (SEP) for a piloted Mars exploration scenario is summarized. The figures of merit used in this study were total initial mass in low Earth orbit (IMLEO) and the trip time. We compared the MMW NEP and SEP systems to an aerobraked chemical (O2/H2) propulsion system. A good performance compromise between a low IMLEO and short trip time can be obtained using MMW NEP systems; they can be both lighter and faster than the baseline chemical system. However, a MMW SEP system does not appear capable of providing as short a trip time as MMW NEP, in part due to the higher specific mass of the overall system and the non-constant power output of a SEP system. Author

N93-10044*# National Aeronautics and Space Administration. Lewis Research Center, Cleveland, OH.
EFFECTS OF ANODE MATERIAL ON ARCJET PERFORMANCE
John M. Sankovic, F. M. Curran, and C. A. Larson (Air Force Academy, CO.) *In* JHU, The 1992 JANNAF Propulsion Meeting, Volume 1 Feb. 1992 p 679-691 (For primary document see N93-10001 01-20)
Avail: CPIA, 10630 Little Patuxent Pkwy., Suite 202, Columbia, MD, 21044-3200 HC

Anodes fabricated from four different materials were tested in a modular arcjet thruster at the 1 kW power level on nitrogen/hydrogen mixtures. A two-percent thoriated tungsten

anode served as the control. Graphite was chosen for its ease in fabrication, but experienced severe erosion in the constrictor and diverging side. Hafnium carbide and lanthanum hexaboride were chosen for their low work functions but failed due to thermal stress and reacted with the propellant. When compared to the thoriated tungsten nozzle, thruster performance was significantly lower for the lanthanum hexaboride insert and the graphite nozzle, but was slightly higher for the hafnium carbide nozzle. Both the lanthanum hexaboride and hafnium carbide nozzle operated at higher voltages. An attempt was made to duplicate higher performance hafnium carbide results, but repeated attempts at machining a second anode insert were unsuccessful. Graphite, hafnium carbide, and lanthanum hexaboride do not appear viable anode materials for low power arcjet thrusters. Author

N93-10045*# National Aeronautics and Space Administration. Lewis Research Center, Cleveland, OH.

TANK CHILLDOWN ANALYSIS AND VERIFICATION WITH A FLIGHTWEIGHT, 175 CU FT TANK UNDER NORMAL GRAVITY WITH LIQUID HYDROGEN **c28**

Naseem H. Saiyed *In* JHU, The 1992 JANNAF Propulsion Meeting, Volume 1 Feb. 1992 p 693-702 (For primary document see N93-10001 01-20)

Avail: CPIA, 10630 Little Patuxent Pkwy., Suite 202, Columbia, MD, 21044-3200 HC

In a typical No-Vent Fill (NVF) process the receiver tank wall is cooled to a target temperature before filling proceeds. One way to cool the tank wall is to use the Charge-Hold-Vent (CHV) approach. The three phases of the CHV process--Charge, Hold, and Vent--influence the tank chilldown in very different ways. The enthalpy inflow and the evaporation of the liquid dominate the Charge phase. Direct tank wall to vapor heat transfer, free convection on earth, and mostly conduction in low-g, determines the Hold phase. In the Vent phase the enthalpy outflow and forced convection are the dominant factors. An analysis that encompasses all phases of the CHV approach is developed. The resulting equations are easily programmable. Transient modeling of the CHV process is achieved by evaluating the equations at discrete time intervals. The analysis is compared with data from a CHV demonstration. The trends in the calculated profiles for the tank wall temperature, vapor temperature, and tank pressure match those from the data; however, the calculated profiles are offset from the data. The demonstration does not have sufficient information for properly modeling the parameters that influence the heat transfer processes to reduce the offset. Further research is recommended concerning heat transfer during Charge and Vent phases to improve the analysis. Author

N93-10046*# National Aeronautics and Space Administration. John F. Kennedy Space Center, Cocoa Beach, FL.

GENERIC PROPELLANT TRANSFER UNIT **c09**

Chuck L. Davis *In* JHU, The 1992 JANNAF Propulsion Meeting, Volume 1 Feb. 1992 p 703-718 (For primary document see N93-10001 01-20)

Avail: CPIA, 10630 Little Patuxent Pkwy., Suite 202, Columbia, MD, 21044-3200 HC

Currently, most satellite programs use dedicated hypergolic propellant ground servicing equipment. These 'carts' are typically program specific, non-interchangeable, costly, and not Department of Transportation (DOT) compliant. They require safety waivers when used on government property and must be emptied before transport over public highways. Large amounts of hazardous wastes are generated by these carts. NASA, KSC, has initiated the Generic Propellant Transfer Unit (GPTU) project as a method of resolving these problems. The ultimate goal of the project is to reduce program costs by developing a multi-use satellite servicing cart that will be part of the launch-site infrastructure. KSC polled users for their cart requirements which defined the design envelope of the GPTU system. DOT codes were reviewed to determine what class packaging system the GPTU would be and if exemptions are required. The survey and subsequent GPTU design effort resulted in a DOT 51 portable tank system with a capacity of 1893 liters (500 gallons) and 2068 kpa (300 psi) working pressure to meet the needs of NASA programs. Any volume down to 454 liters (120 gallons) can be built within DOT 51 code parameters. Two tanks can be connected together to double usable volume. A trailer and thermal conditioning unit are envisioned for the overall GPTU system. KSC plans to construct a small fleet of GPTU's which will provide a wide variety of NASA users with a safe, reliable, cost effective, and environmentally sensitive hypergolic propellant servicing system. VAFB has indicated an interest in establishing a West Coast GPTU fleet. The GPTU project was well received by the local safety offices and some of the user community. Others will need to be convinced of the advantages of the KSC GPTU, or a similar system, over current methods before it is widely accepted. Author

N93-10047 Hughes Space and Communications Group, El Segundo, CA. Propulsion Product Line.

LOADING OPERATIONS FOR SPACECRAFT PROPULSION SUBSYSTEMS **c09**

G. P. Purohit, H. O. Nordeng, and J. R. Ellison *In* JHU, The 1992 JANNAF Propulsion Meeting, Volume 1 Feb. 1992 p 719-731 (For primary document see N93-10001 01-20)

Avail: CPIA, 10630 Little Patuxent Pkwy., Suite 202, Columbia, MD, 21044-3200 HC

A broad overview of loading operations for pressurized blowdown monopropellant and pressure regulated integral bipropellant propulsion subsystems used in geosynchronous communication satellites is provided. Propellant chemical composition, cleanliness, processing, and handling requirements are addressed. Ground servicing equipment (GSE) and propellant transfer procedures for the various loading configurations are discussed. Effects of helium solubility and helium saturation levels in both GSE carts and propellant tanks are examined. Predicted equilibrium pressures for actual postload tank pressures are compared against extensive loading data on Hughes bipropellant spacecraft. Helium tank pressurization and manifold pressurization practices are described. Propellant loading facility requirements and safety requirements are discussed. Author

N93-10048 TRW, Inc., Redondo Beach, CA. Space and Technology Group.

DSP PROPULSION SYSTEM LAUNCH CONFIGURATION AND RELATED TESTING

Neil F. Dipprey and S. D. Tingle (Aerospace Corp., El Segundo, CA.) *In* JHU, The 1992 JANNAF Propulsion Meeting, Volume 1 Feb. 1992 p 733-742 (For primary document see N93-10001 01-20)

Avail: CPIA, 10630 Little Patuxent Pkwy., Suite 202, Columbia, MD, 21044-3200 HC

Spacecraft propulsion systems using hydrazine propellant, that are launched with dry propellant lines, may be susceptible to explosive hazards. The literature suggests that explosive hazards, such as vapor detonation and runaway liquid decomposition, can be caused by rapid compression ('adiabatic heating') of hydrazine vapor and pressurant gas. The Defense Support Program (DSP) Satellite 016 was recently launched on STS-44 with dry lines. Prior to launch, the potential for rapid compression induced decomposition and detonation was investigated through analysis and testing. Testing involved accelerating hydrazine into simulated line ullages for several ullage pressure conditions and dead-head temperatures. These efforts demonstrated that the DSP system is not susceptible to explosive hazards of hydrazine. Operationally, a technique to manage ullage gas before and after propellant line priming was developed; on-orbit initialization ultimately went smoothly. Analysis, test, and operational results are presented along with concluding remarks. Author

N93-10049*# National Aeronautics and Space Administration. Lyndon B. Johnson Space Center, Houston, TX.

DESIGN AND OPERATION OF THE US SPACE STATION FREEDOM PROPULSION SYSTEM

Joseph S. Morano (McDonnell-Douglas Space Systems Co., Huntington Beach, CA.) and Rex A. Delventhal *In* JHU, The 1992 JANNAF Propulsion Meeting, Volume 1 Feb. 1992

p 743-750 Previously announced in IAA as A91-44063 (For primary document see N93-10001 01-20)
Avail: CPIA, 10630 Little Patuxent Pkwy., Suite 202, Columbia, MD, 21044-3200 HC

The propulsion functions for the U.S. Space Station Freedom (SSF) are accomplished by two separate systems, the Primary Propulsion System and the Supplemental Reboost System (SRS). The Primary Propulsion System includes self-contained hydrazine modules for station reboost, attitude control, and contingency maneuvers. These Propulsion Modules contain reboost and attitude control thrusters, propellant storage, thermal conditioning, and electronic controls. The modules are serviced on the ground and launched on the Space Shuttle as replacements for the on-orbit modules which have expended their propellant. The expended modules are returned to the ground for reservicing and subsequent reuse. The Supplemental Reboost System includes a Waste Gas Assembly and Resistojet Modules which are used for reboost maneuvers only. The Waste Gas Assembly contains waste gas storage, compressors, and dryers, and the Resistojet Modules contain multipropellant resistojet thrusters, electronic pressure regulators and power conditioning equipment. Author

N93-10086*# Sverdrup Technology, Inc., Brook Park, OH.
SPECIES AND TEMPERATURE MEASUREMENT IN H2/O2 ROCKET FLOW FIELDS BY MEANS OF RAMAN SCATTERING DIAGNOSTICS Interim Report
Wim A. deGroot and Jonathan M. Weiss (Pennsylvania State Univ., University Park.) Jul. 1992 20 p Presented at the 28th Joint Propulsion Conference and Exhibit, 6-8 Jul. 1992, Nashville, TN; cosponsored by AIAA, SAE, ASME, and ASEE
(Contract NAS3-25266; RTOP 506-42-31)
(NASA-CR-189217; E-7246; NAS 1.26:189217; AIAA Paper 92-3353) Avail: CASI HC A03/MF A01

Validation of Computational Fluid Dynamics (CFD) codes developed for prediction and evaluation of rocket performance is hampered by a lack of experimental data. Non-intrusive laser based diagnostics are needed to provide spatially and temporally resolved gas dynamic and fluid dynamic measurements. This paper reports the first non-intrusive temperature and species measurements in the plume of a 110 N gaseous hydrogen/oxygen thruster at and below ambient pressures, obtained with spontaneous Raman spectroscopy. Measurements at 10 mm downstream of the exit plane are compared with predictions from a numerical solution of the axisymmetric Navier-Stokes and species transport equations with chemical kinetics, which fully model the combustor-nozzle-plume flowfield. The experimentally determined oxygen number density at the centerline at 10 mm downstream of the exit plane is four times that predicted by the model. The experimental number density data fall between those numerically predicted for the exit and 10 mm downstream planes in both magnitude and radial gradient. The predicted temperature levels are within 10 to 15 percent of measured values. Some of the discrepancies between experimental data and predictions result from not modeling the three dimensional core flow injection mixing process, facility back pressure effects, and possible diffuser-thruster interactions. Author

N93-10197*# National Aeronautics and Space Administration. Lewis Research Center, Cleveland, OH.
EFFECTS OF ANODE MATERIAL ON ARCJET PERFORMANCE
John M. Sankovic, Frank M. Curran, and C. A. Larson (Air Force Academy, CO.) 1992 15 p Presented at the 1992 JANNAF Propulsion Meeting, Indianapolis, IN, 24-28 Feb. 1992
(RTOP 506-42-31)
(NASA-TM-105799; E-6873; NAS 1.15:105799) Avail: CASI HC A03/MF A01

Anodes fabricated from four different materials were tested in a modular arcjet thruster at 1 kW power level on nitrogen/hydrogen mixtures. A two-percent thoriated tungsten anode served as the control. Graphite was chosen for its ease in fabrication, but experienced severe erosion in the constrictor and diverging side. Hafnium carbide and lanthanum hexaboride were chosen for their low work functions but failed due to thermal stress and reacted with the propellant. When compared to the thoriated tungsten nozzle, thruster performance was significantly lower for the lanthanum hexaboride insert and the graphite nozzle, but was slightly higher for the hafnium carbide nozzle. Both the lanthanum hexaboride and hafnium carbide nozzle operated at higher voltages. An attempt was made to duplicate higher performance hafnium carbide results, but repeated attempts at machining a second anode insert were unsuccessful. Graphite, hafnium carbide, and lanthanum hexaboride do not appear viable anode materials for low power arcjet thrusters. Author

N93-10258# Phillips Lab., Edwards AFB, CA.
SYNCHROTRON RADIATION CONSIDERATIONS IN THE DENSE PLASMA FOCUS (DPF) MAGNETOPLASMADYNAMIC (MPD) THRUSTER Final Report, 16 May - 12 Jun. 1991
Larry T. Cox, Jr. Jul. 1992 44 p
(AF Proj. 3058)
(AD-A254188; AD-E201166; PL-TR-92-3035) Avail: CASI HC A03/MF A01

The Dense Plasma Focus (DPF) computer model has been modularized and updated. The code now assumes an inherent value beta = 1 upon which further calculations are based. The DPF model is using deuterium (D) and Helium-3 as the fuels and hydrogen as the propellant. D-D side reactions have been included. I(sub sp) values in the range of 900-1000 have been obtained for operating temperatures in the tens of keV's regime, as well thrust-to-weight ratios on the order of 0.0001. The majority of the work has been devoted to the synchrotron radiation emissions from the DPF. It has been shown that for beta = 1, no synchrotron radiation will be emitted. If the beta value is less than 1, then reabsorption of the synchrotron radiation will become a concern for plasma operating temperatures exceeding approximately 62 keV. Calculations have been made assuming a plasma pinch mass density of 0.0022 kg/cu m. The characteristic synchrotron radiation absorption length, lambda sub o, for a beta = 1 case has been found to be less than the radius of the plasma pinch. GRA

N93-10350*# Rockwell International Corp., Canoga Park, CA. Rocketdyne Div.
SPACE TRANSPORTATION ENGINE PROGRAM (STEP), PHASE B Progress Report, Jul - Sep. 1990
31 Oct. 1990 18 p
(Contract NAS8-38160)
(NASA-CR-184062; NAS 1.26:184062) Avail: CASI HC A03/MF A01

The Space Transportation Engine Program (STEP) Phase 2 effort includes preliminary design and activities plan preparation that will allow smooth and time transition into a Prototype Phase and then into Phases 3, 4, and 5. A Concurrent Engineering approach using Total Quality Management (TQM) techniques, is being applied to define an oxygen-hydrogen engine. The baseline from Phase 1/1' studies was used as a point of departure for trade studies and analyses. Existing STME system models are being enhanced as more detailed module/component characteristics are determined. Preliminary designs for the open expander, closed expander, and gas generator cycles were prepared, and recommendations for cycle selection made at the Design Concept Review (DCR). As a result of July '90 DCR, and information subsequently supplied to the Technical Review Team, a gas generator cycle was selected. Results of the various Advanced Development Programs (ADP's) for the Advanced Launch Systems (ALS) were contributive to this effort. An active vehicle integration effort is supplying the NASA, Air Force, and vehicle contractors with engine parameters and data, and flowing down appropriate vehicle requirements. Engine design and analysis trade studies are being documented in a data base that was developed and is being used to organize information. To date, seventy four trade studies were input to the data base. Author

N93-10457*# National Aeronautics and Space Administration. Lewis Research Center, Cleveland, OH.
SYSTEM MODEL DEVELOPMENT FOR NUCLEAR THERMAL PROPULSION

James T. Walton, Nelson A. Hannan (Argonne National Lab., IL.), Ken R. Perkins (Brookhaven National Lab., Upton, NY.), John H. Buksa (Los Alamos National Lab., NM.), Brian A. Worley (Oak Ridge National Lab., TN.), and Dean Dobranich (Sandia National Labs., Albuquerque, NM.) Aug. 1992 15 p Presented at the World Space Congress, Washington, DC, 2-5 Sep. 1992; sponsored by AIAA
(RTOP 593-71-00)
(NASA-TM-105761; E-7178; NAS 1.15:105761) Avail: CASI HC A03/MF A01

A critical enabling technology in the evolutionary development of nuclear thermal propulsion (NTP) is the ability to predict the system performance under a variety of operating conditions. This is crucial for mission analysis and for control subsystem testing as well as for the modeling of various failure modes. Performance must be accurately predicted during steady-state and transient operation, including startup, shutdown, and post operation cooling. The development and application of verified and validated system models has the potential to reduce the design, testing, and cost and time required for the technology to reach flight-ready status. Since Oct. 1991, the U.S. Department of Energy (DOE), Department of Defense (DOD), and NASA have initiated critical technology development efforts for NTP systems to be used on Space Exploration Initiative (SEI) missions to the Moon and Mars. This paper presents the strategy and progress of an interagency NASA/DOE/DOD team for NTP system modeling. It is the intent of the interagency team to develop several levels of computer programs to simulate various NTP systems. The first level will provide rapid, parameterized calculations of overall system performance. Succeeding computer programs will provide analysis of each component in sufficient detail to guide the design teams and experimental efforts. The computer programs will allow simulation of the entire system to allow prediction of the integrated performance. An interagency team was formed for this task to use the best capabilities available and to assure appropriate peer review. Author

N93-10638# Rockford Technology Associates, Inc., Champaign, IL.
CRITICAL TECHNOLOGY DEMONSTRATION OF PLASMA FOCUS TYPE MPD THRUSTERS Final Report, 4 Apr. - 4 Oct. 1991
George H. Miley, Jonathon Nadler, Brian Temple, Scott Bolt, and Hanoch Kislev May 1992 78 p
(Contract F29601-91-C-0036)
(AD-A252428; PL-TR-91-3111; AD-E201089) Avail: CASI HC A05/MF A01

The technical objective of the Phase 1 work was to study the optimization and scaling of a plasma focus type MPD thruster device in order to design a MJ-scale test facility for construction in Phase 2. This report describes studies done to develop the capacitor bank and electrode design for the MJ facility. A modular design is proposed which would allow construction and testing of a 1/4-MJ facility in Phase 2 with the addition of the remaining modules to be done in Phase 3. Details of thruster electrode design studies for use in the 1/4-MJ device and the facility specifications are given in this report. Key items include a fast gas-injection system, control system and timing circuits, advanced target design concepts, and switching circuits. GRA

N93-10721# Air Force Inst. of Tech., Wright-Patterson AFB, OH. Foreign Technology Div.
STUDIES ON THE COMBUSTION EFFICIENCY OF LIQUID FUEL ROCKETS WITH VARIABLE THRUST
Li Xiaobin, Qizhi Chen, and Yunqin Chen 3 Dec. 1991 29 p Transl. into ENGLISH from Yuhan Xuebao (China), no. 3, 1986 p 61-72
(AD-A254232; FTD-ID(RS)T-0571-91) Avail: CASI HC A03/MF A01

This article carries out studies on the stability characteristics of liquid fuel rocket engines within a relatively large range of variations. The research work was carried out centering around the speed and efficiency characteristics of combustion chambers. This article sets out the results of relevant experiments and theoretical calculations. From the angle of the combustion processes within combustion chambers, there were clear indications of the status of the effects of various processes (for example, evaporation or vaporization, mixing, chemical reactions, etc.) following along with changes in the operational status of variable thrust engine combustion efficiency. GRA

N93-10734*# National Aeronautics and Space Administration. Lewis Research Center, Cleveland, OH.
POWER SYSTEM MONITORING AND SOURCE CONTROL OF THE SPACE STATION FREEDOM DC POWER SYSTEM TESTBED
Greg L. Kimnach and Anastacio N. Baez Aug. 1992 9 p Presented at the 27th Intersociety Energy Conversion Engineering Conference, San Diego, CA, 3-7 Aug. 1992; cosponsored by SAE, ACS, AIAA, ASME, IEEE, AIChE, and ANS
(RTOP 474-42-10)
(NASA-TM-105841; E-7284; NAS 1.15:105841) Avail: CASI HC A02/MF A01

Unlike a terrestrial electric utility which can purchase power from a neighboring utility, the Space Station Freedom (SSF) has strictly limited energy resources; as a result, source control, system monitoring, system protection, and load management are essential to the safe and efficient operation of the SSF Electric Power System (EPS). These functions are being evaluated in the DC Power Management and Distribution (PMAD) Testbed which NASA LeRC has developed at the Power System Facility (PSF) located in Cleveland, Ohio. The testbed is an ideal platform to develop, integrate, and verify power system monitoring and control algorithms. State Estimation (SE) is a monitoring tool used extensively in terrestrial electric utilities to ensure safe power system operation. It uses redundant system information to calculate the actual state of the EPS, to isolate faulty sensors, to determine source operating points, to verify faults detected by subsidiary controllers, and to identify high impedance faults. Source control and monitoring safeguard the power generation and storage subsystems and ensure that the power system operates within safe limits while satisfying user demands with minimal interruptions. System monitoring functions, in coordination with hardware implemented schemes, provide for a complete fault protection system. The objective of this paper is to overview the development and integration of the state estimator and the source control algorithms. Author

N93-10743*# National Aeronautics and Space Administration. Lewis Research Center, Cleveland, OH.
HOT FIRE FATIGUE TESTING RESULTS FOR THE COMPLIANT COMBUSTION CHAMBER
Albert J. Pavli (Sverdrup Technology, Inc., Brook Park, OH.), John M. Kazaroff, and Robert S. Jankovsky Sep. 1992 12 p
(RTOP 593-12-21)
(NASA-TP-3223; E-6850; NAS 1.60:3223) Avail: CASI HC A03/MF A01

A hydrogen-oxygen subscale rocket combustion chamber was designed incorporating an advanced design concept to reduce strain and increase life. The design permits unrestrained thermal expansion of a circumferential direction and, thereby, provides structural compliance during the thermal cycling of hot-fire testing. The chamber was built and test fired at a chamber pressure of 4137 kN/sq m (600 psia) and a hydrogen-oxygen mixture ratio of 6.0. Compared with a conventional milled-channel configuration, the new structurally compliant chamber had a 134 or 287 percent increase in fatigue life, depending on the life predicted for the conventional configuration. Author

N93-10756*# Alabama Univ., Huntsville. Dept. of Mechanical and Aerospace Engineering
IMPROVE SSME POWER BALANCE MODEL Final Report
Gerald R. Karr 9 Sep. 1992 83 p
(Contract NAS8-36955)
(NASA-CR-184464; NAS 1.26:184464) Avail: CASI HC A05/MF A01

Effort was dedicated to development and testing of a formal strategy for reconciling uncertain test data with physically limited computational prediction. Specific weaknesses in the logical structure of the current Power Balance Model (PBM) version are described with emphasis given to the main routing subroutines BAL and DATRED. Selected results from a variational analysis of PBM predictions are compared to Technology Test Bed (TTB) variational study results to assess PBM predictive capability. The motivation for systematic integration of uncertain test data with computational predictions based on limited physical models is provided. The theoretical foundation for the reconciliation strategy developed in this effort is presented, and results of a reconciliation analysis of the Space Shuttle Main Engine (SSME) high pressure fuel side turbopump subsystem are examined. Author

N93-10813# Air Force Inst. of Tech., Wright-Patterson AFB, OH. Foreign Technology Div.
A PERSONAL VIEWPOINT ON THE DEVELOPMENT OF CHINA'S LIQUID PROPELLANT ROCKET ENGINES
Ninchang Zhu 3 Dec. 1991 15 p Transl. into ENGLISH from Zhuang Xuebao (China), no. 3, 1990 p 5-9
(AD-A254104; FTD-ID(RS)T-0545-91) Avail: CASI HC A03/MF A01

An attempt, on the basis of launch vehicle and spacecraft requirements, is made to analyze development trends in liquid rocket propulsion technology. A simple introduction of the Long March (Chang Zheng) launch vehicle liquid propulsion system's current status and technological development is given. A discussion of various types of liquid rocket motor development processes is presented. GRA

23 CHEMISTRY AND MATERIALS (GENERAL)

N93-10465# Pittsburgh Univ., PA. Surface Science Center.
HYDROCARBON SURFACE CHEMISTRY ON Si(100)
C. C. Cheng, P. A. Taylor, R. M. Wallace, H. Gutleben, and M. L. Clemen 1 Jun. 1992 33 p
(Contract N00014-82-C-0280)
(AD-A252803; TR-45) Avail: CASI HC A03/MF A01

The interaction of various hydrocarbon species with the Si(100) surface has been investigated using several surface science techniques. The efficiency of carbon deposition is related to the efficiency of SiC thin film formation. The hydrocarbon species studied include acetylene (C2H2), ethylene (C2H4), and the adsorbed methyl group (CH3(a)). In the case of the chemisorption of acetylene and ethylene, the pi-bond of the olefinic molecules interacts with the dimer unit (Si2) on the Si(100)-(2x1) surface. One monolayer of both acetylene and ethylene on Si(100) has been achieved by saturating the surface at 105 K, and a di-sigma bonding structure is proposed for one molecule per Si2 dimer unit at monolayer coverage. Upon heating, the majority (greater than 95 percent) of the adsorbed acetylene undergoes dissociation to produce chemisorbed carbon and H2(g). In contrast, chemisorbed ethylene desorbs intact from Si(100) at -550 K, with approximately two percent of the monolayer undergoing dissociation. The low activation energy for desorption (E(sub d) deg (C2H4) = 38 kcal/mol) allows C2H4 to desorb prior to significant decomposition. GRA

24 COMPOSITE MATERIALS

Includes physical, chemical, and mechanical properties of laminates and other composite materials.
For ceramic materials see *27 Nonmetallic Materials.*

N93-10254# California Univ., Santa Barbara. Dept. of Materials.
SENSOR AND ACTUATOR MATERIALS FOR HIGH PERFORMANCE COMPOSITES Final Report
A. G. Evans and D. R. Clarke 1991 132 p
(Contract N00014-91-J-4024)
(AD-A254178) Avail: CASI HC A07/MF A02

The residual stresses in sapphire fibers embedded in a number of ceramic and inter-metallic matrices are measured non-destructively and in-situ using the stress-induced frequency shift in fluorescence from chromium dopants in the fibers. The stresses as a function of depth into the fibers from the free surface are measured and from the depth profile we have determined the interfacial shear stresses between the fibers and the matrices. The stress distributions provide a validation of the shear lag mechanics models of Hutchinson and Jensen, as well as a test of finite element computations. GRA

N93-10272# Naval Research Lab., Washington, DC.
ULTRASONIC CHARACTERIZATION OF HIGHLY ATTENUATIVE THICK COMPOSITES
Narendra K. Batra 24 Jul. 1992 43 p
(AD-A253347; NRL/MR/6385-92-7102) Avail: CASI HC A03/MF A01

Thick composites manufactured from various fiber and matrix materials are being increasingly used for structural components. Conventional ultrasonic methods cannot be used to characterize nondestructively these highly attenuative materials. In this report we define the term 'THICK' from a nondestructive evaluation (NDE) point of view which pertains to poor signal-to-noise (S/N) ratio of the received propagated signal in contrast to 'THICK' as referred to the load-bearing limit. Ultrasonic nondestructive evaluation of such composites may involve analyzing the interaction of elastic waves with the physical properties of the material constituents. We developed ultrasonic transmission techniques which, when used in conjunction with specimens in the shape of wedges, steps or parallel plates, allow accurate measurement of attenuation and consequently evaluation of flaws in these materials. We will describe several ultrasonic methods developed for application to determine the variations in the attenuation to characterize thick composites. GRA

N93-10277# Washington Univ., Seattle. Dept. of Mechanical Engineering.
DAMAGE ACCUMULATION PROCESS IN ADVANCED METAL MATRIX COMPOSITE UNDER THERMAL CYCLING Final Report, 16 Oct. 1990 - 15 Nov. 1991
Minoru Taya, William D. Armstrong, and Marty Dunn 20 Nov. 1991 91 p
(Grant AF-AFOSR-0234-91)
(AD-A248674; UW-ME-91-002; AFOSR-92-0256TR) Avail: CASI HC A05/MF A01

This research was intended the second stage of thermal cycling damage in metal matrix composites where progressive dimensional change along the fiber is observed. This dimensional change was documented by SEM-image analysis technique in terms of damage area distribution along the matrix-fiber interface. The progressive dimensional change was then predicted by using elastic/plastic/creep analytical model, resulting in a good agreement. Based on the analytical study, we designed a new type of MMC which possesses higher thermal cycling resistance and where additional short fibers are embedded in the matrix to make a MMC hybrid MMC. It was found that the main mechanisms for higher thermal cycling resistance in the hybrid MMC are as follows. (1) The apparent CTE of the matrix modified with additional short fibers is closer to that of the main fibers, resulting in smaller CTE mismatch, which would be a weaker driving force for thermal cycling damage. (2) Additional short fibers in the matrix give rise

to higher density of dislocations which are punched out from the interface between the matrix and these short fibers, enhancing the in-situ mechanical properties of the matrix. GRA

N93-10325# Northrop Corp., Hawthorne, CA. Aircraft Div.
COMPOSITE FAILURE ANALYSIS HANDBOOK. VOLUME 2: TECHNICAL HANDBOOK. PART 2: ATLAS OF FRACTOGRAPHS Final Report, Jan. 1987 - Oct. 1990
R. J. Kar Feb. 1992 499 p
(Contract F33616-87-C-5212)
(AD-A249130; WL-TR-91-4032-Vol-2-Pt-2; DOT/FAA/CT-91-23-Vol-2-Pt-2) Avail: CASI HC A21/MF A04

The objective was to create a comprehensive handbook for use in conducting failure analysis investigations on failed composite structure. This program builds upon previous efforts as documented. The purpose of creating this handbook was to document the techniques, the fractographic and material property data and case history studies currently being utilized in the analysis of failed composite structure. The major tasks on this program included: (1) procedural guidelines for field investigation techniques; (2) an expanded fractographic data base for carbon/epoxy materials tested under known conditions; (3) a fractographic data base for resin based composite materials other than carbon/epoxy; (4) fractographic documentation of composite material and processing defects; (5) documentation of fracture characteristics in adhesive and mechanical joint failures; (6) compilation of material property data for composite materials; and (7) documentation of case histories recently conducted on failed composite structure. GRA

N93-10344# University of Southern Illinois, Carbondale. Dept. of Mechanical Engineering and Energy Processes.
OXIDATION PROTECTION SYSTEMS FOR CARBON-CARBON COMPOSITES FORMED BY CHEMICAL VAPOR DEPOSITION AND PLASMA ASSISTED CHEMICAL VAPOR DEPOSITION TECHNIQUES Final Report, 1 Mar. 1988 - 28 Feb. 1991
Yongyi Shi, Jean L. Stojak, Jun He, Jarlen Don, and Maurice A Wright 22 Apr. 1992 409 p
(Grant AF-AFOSR-0130-88)
(AD-A253450) Avail: CASI HC A18/MF A04

A final report written in three sections. (1) 'CVI Densification of Carbon-Carbon Composites' deals with the densification of porous preforms of carbonized carbon-resin mixtures using various methane and hydrogen gas mixtures. The experimental conditions include temperatures between 1000 C and 1200 C and total pressures between 5 and 15 torr. The resulting solid was characterized using optical and electron microscopy. (2) 'Oxidation Protection of Carbon-Carbon Composites Using Pack Cementation' deals with formation of oxidation protective films formed from combinations of boron carbide, silicon carbide and zirconium carbide. Films were processed using a reactive process called pack cementation. The effects of initial powder composition and temperature were correlated with microstructure and oxidation resistance. (3) In 'The Formation of Oxidation Protective Coatings on Carbon-Carbon Composites Using a Chemical Vapor Deposition (CVD) Technique' four types of CVD coatings were investigated: SiC, ZrB ZrB /SiC multilayer and graded SrC/ZrC. Coatings were produced as a function of temperature, pressure and gas flow rates. The resulting coatings were then characterized in terms of microstructure and oxidation resistance. GRA

N93-10391# Sandia National Labs., Albuquerque, NM.
REACTIONS OF Ti AND Zr WITH AlN AND Al2O3
R. E. Loehman and A. P. Tomsia (Pask Research and Engineering, Inc., Pinole, CA.) 1991 25 p Presented at the International Symposium on Metal/Ceramic Interfaces, Irsee (Germany), 30 Jun. - 5 Jul. 1991
(Contract DE-AC04-76DP-00789)
(DE92-016234; SAND-91-1080C; CONF-9106236-3) Avail: CASI HC A03/MF A01

We studied the reactions of Ti and Zr with AlN, 99.8 percent Al2O3, and 95 percent Al2O3. The substrates were chosen to represent a simple nitride (AlN), a simple oxide (99.8 percent Al2O3), and a simple oxide with a silicate grain boundary phase (95 percent Al2O3). The activities of the Ti and the Zr were varied by dissolving them at 1 and 5 wt percent in the 72Ag-28Cu eutectic composition, which is otherwise unreactive with the ceramics. Reactions were studied by measuring the variation of the alloy contact angle on the ceramic with time at temperature and by determining the compositions of interfacial reaction products. Contact angles were lower for Ti alloys than for those containing Zr. Reaction products were primarily the nitrides of Zr or Ti for reaction with AlN and the respective oxides for reaction with Al2O3. Complex alloy phases were found in the metal away from the ceramic-metal reaction zone. DOE

N93-10742*# National Aeronautics and Space Administration. Ames Research Center, Moffett Field, CA.
DOCUMENTATION OF THE DETAILED RADIATION PROPERTY DATA FOR THE RADIATION-ABLATION CODE RASLE
William D. Henline Jun. 1991 25 p
(RTOP 506-43-31)
(NASA-TM-103848; A-91097; NAS 1.15:103848) Avail: CASI HC A03/MF A01

This report is a documentation of the necessary radiation property input data for the radiating shock layer simulation code RASLE. The tabulated data are required to simulate systems which are composed of oxygen, nitrogen, carbon, hydrogen, and silicon. These data are needed to compute the flowfield effects of many practical ablative, hypersonic vehicle heat shield materials. A brief outline description is provided for the RASLE code. A more detailed discussion is provided for the RASLE code non-grey gas spectral radiation model. This model is related to the required radiation property data which are tabulated at the end of the report. Other correlations needed for the RASLE simulations are not discussed, since these are automatically included in the program and no input data are required. Author

N93-10896# Rensselaer Polytechnic Inst., Troy, NY.
MECHANICS OF COMPOSITE MATERIALS FOR SPACECRAFT Final Report
George J. Dvorak, Mark S. Shephard, and Yehia A. Bahei-El-Din Jul. 1992 265 p
(Contract N00014-85-K-0733)
(AD-A254217) Avail: CASI HC A12/MF A03

This report presents the work performed under ONR contract number N00014-85-K-0733 during the period 1985-1990. The main objective of the project was to develop a computational facility for inelastic analysis of fibrous composite materials based on micromechanics. The theoretical work focused on development of micromechanical models for thermoplastic and thermoviscoplastic fibrous composites based on experimental observations of certain phenomena found in unreinforced and fiber reinforced metals. Implementation of the material models in computational procedures for analysis of composite materials and structures was an important part of the research. Accomplishments in these areas and in development of a layer-wise composite shell element, also performed under this contract, are described. GRA

N93-10508 Missouri Univ., Rolla.
ANALYSIS OF FAILURE MODES IN CERAMIC MATRIX COMPOSITE
L. Chai and L. R. Dharani *In* Carleton Univ., Proceedings of the Twelfth Canadian Congress of Applied Mechanics, Volumes 1 and 2 May 1989 p 322-323 (For primary document see N93-10466 01-31)
Copyright Avail: Canadian Society for Mechanical Engineering, 2050 Mansfield St., Suite 700, Montreal, Quebec H3A 1Z7 Canada

N93-10509 Ohio State Univ., Columbus. Dept. of Civil Engineering.
CONSISTENT SHEAR CONSTITUTIVE RELATIONS FOR LAMINATED PLATES
Soon-Jo Hong, Ranbir S. Sandhu, and Harpal S. Chohan *In* Carleton Univ., Proceedings of the Twelfth Canadian Congress of

Applied Mechanics, Volumes 1 and 2 May 1989 p 324-325 (For primary document see N93-10466 01-31)
Copyright Avail: Canadian Society for Mechanical Engineering, 2050 Mansfield St., Suite 700, Montreal, Quebec H3A 1Z7 Canada

N93-10510 Florida Univ., Gainesville. Dept. of Aerospace Engineering, Mechanics and Engineering Science.
INVESTIGATION OF LAMINATED COMPOSITE PLATES UNDER IMPACT DYNAMIC LOADING BY USING A THREE-DIMENSIONAL HYBRID STRESS FINITE ELEMENT METHOD
C. T. Sun and W. J. Liou (Feng Chia Univ., Taichung, Taiwan) *In* Carleton Univ., Proceedings of the Twelfth Canadian Congress of Applied Mechanics, Volumes 1 and 2 May 1989 p 328-329 (For primary document see N93-10466 01-31)
Copyright Avail: Canadian Society for Mechanical Engineering, 2050 Mansfield St., Suite 700, Montreal, Quebec H3A 1Z7 Canada

N93-10525 Virginia Polytechnic Inst. and State Univ., Blacksburg. Dept. of Engineering Science and Mechanics.
DYNAMIC STABILITY OF LAMINATED TRANSVERSELY-ISOTROPIC COMPOSITE PLATES SUBJECTED TO PARAMETRIC EXCITATIONS
L. Librescu and S. Thangjitham *In* Carleton Univ., Proceedings of the Twelfth Canadian Congress of Applied Mechanics, Volumes 1 and 2 May 1989 p 414-415 (For primary document see N93-10466 01-31)
Copyright Avail: Canadian Society for Mechanical Engineering, 2050 Mansfield St., Suite 700, Montreal, Quebec H3A 1Z7 Canada

25 INORGANIC AND PHYSICAL CHEMISTRY

Includes chemical analysis, e.g., chromatography; combustion theory; electrochemistry; and photochemistry.

For related information see also *77 Thermodynamics and Statistical Physics.*.

N93-10101# Dayton Univ. Research Inst., OH.
ALTERNATE SPECTROMETRIC OIL ANALYSIS TECHNIQUES Final Report, May 1988 - Sep. 1990
Costandy S. Saba, Hoover A. Smith, and Robert E. Kauffman Apr. 1992 216 p
(Contract F33615-87-C-2714)
(AD-A253355; UDR-TR-91-156; WL-TR-92-2017) Avail: CASI HC A10/MF A03

Oil analysis results from currently used AE and AA techniques are compared with those from various other techniques such as ICP, DCP, graphite furnace AA, ferrography, and particle size distribution using the acid dissolution method (ADM). The effect of fine filtration on the analysis capability of the various methods was investigated using a test rig equipped with a 3-micron operational in-depth type oil filter. This investigation also includes studies related to ICP sample introduction systems, overloading of ICP sources, and the use of different diluents for improving ICP analyses. Considering the data from all sample groups, all analysis techniques investigated (except ferrography and the acid dissolution method) were iron particle size sensitive. None of the techniques offered any improvement over the currently used AE with respect to analyzing large particles, monitoring capability with or without microfiltration, analysis time, or analysis cost or person-power. The study also indicated that microfiltration could have a small effect on spectrometric oil analysis results. GRA

N93-10207# Army Armament Research, Development and Engineering Center, Watervliet, NY. Weapons Lab.
DETERMINATION OF SANDOZ BLACK ALUMINUM COLORING DYE, OLIVE ALUMINUM COLORING DYE, AND SODIUM DICHROMATE ALUMINUM SEALING SOLUTIONS BY UV-VISIBLE SPECTROPHOTOMETRY Final Report
Samuel Sopok May 1992 22 p
(AD-A253639; ARCCB-MR-92022) Avail: CASI HC A03/MF A01

The chemical literature lacks an acceptable method to determine and adequately control Sandoz black aluminum coloring dye, olive aluminum coloring dye, and sodium dichromate aluminum sealing solutions in aluminum finishing processes. Specific methods are presented here that provide acceptable finishing processes. The optimum operating range of the Sandoz black aluminum coloring dye solution is 12.5 g/l maximum with resulting precisions in the 0.5 to 0.9-g/l range. The optimum operating range of the Sandoz olive aluminum coloring dye solution is 4.5 g/l maximum with resulting precisions in the 0.2 to 0.4-g/l range. The optimum operating range of the Sandoz sodium dichromate aluminum sealing solution is 50.0 g/l maximum with resulting precisions in the 1.5 to 2.0-g/l range. These methods provided adequate control of the three processes supported by six years of testing. GRA

N93-10224# Arnold Engineering Development Center, Arnold Air Force Station, TN.
EMISSION TOMOGRAPHY OF SODIUM IN A HYDROGEN-AIR FLAME Final Report, Oct. 1990 - Sep. 1991
W. J. Phillips and R. Y. Walker Jul. 1992 30 p
(AD-A253530; AEDC-TR-92-2) Avail: CASI HC A03/MF A01

An investigation into the use of emission computed tomography for gas diagnostics is presented. The radiative transfer equations necessary for the determination of temperature and number density from emission data are examined. Assumptions required to cast the radiative transform equations in a form amenable for use in emission computed tomography are discussed. The Donner computed tomography algorithms are utilized to perform reconstructions of sodium 589-nm spectral line emissions from a hydrogen-air flame utilizing a square, flat flame burner. GRA

N93-10263# Aerospace Corp., El Segundo, CA. Technology Operations.
VIBRATIONAL RELAXATION OF H2O BY H2, HCl, AND H2O AT 295 K
P. F. Zittel and D. E. Masturzo 16 Jun. 1992 26 p
(Contract F04701-88-C-0089)
(AD-A252800; TR-0091(6940-07)-1; SSD-TR-92-14) Avail: CASI HC A03/MF A01

A laser-induced fluorescence method has been used to measure rate constants for vibrational relaxation of the equilibrated nu(1) and nu(3) stretching level reservoir, the 2nu(2) bending overtone level, and the nu(2) bending level of H2O by H-2 and HCl at 295 K. The rate constants for relaxation by H2 were found to be 8.0 +/- 1.1, 29 +/- 4, and 13 +/- 2 x 10(-13) cu cm molecule(-1) s(-1), respectively. For relaxation by HCl, the rate constants were 8.4 +/- 1.2, 47 +/- 7, and 24 +/- 4 x 10(-12) cu cm molecule(-1) s(-1), respectively. Relaxation by intermolecular V to V transfer was experimentally determined to account for less than 8 percent of the rate constant for relaxation of the H2O stretching levels by HCl, and was estimated to contribute less than 16 percent of the rate constant for relaxation of the bending overtone level. For both collision partners, the H2O stretching levels were relaxed predominantly to the 2nu(2) level, and the 2nu(2) level was relaxed predominantly to nu(2). Following direct laser excitation, the rate constant for relaxation of the equilibrated nu(1) + nu(2) and nu(3) + nu(2) combination vibrational levels Of H2O by H2O was measured to be 1.6 +/- 0.2 x 10(-10) cu cm molecule(-1) s(-1). Direct relaxation to the nu(1)and nu(3) fundamental levels was experimentally determined to account for less than 40 percent of the relaxation rate constant. GRA

N93-10266# Pittsburgh Univ., PA. Surface Science Center.
ATOMIC HYDROGEN: A REAGENT FOR THE EXTRACTION OF CHEMICAL SPECIES FROM SILICON SURFACES
J. T. Yates, Jr., C. C. Cheng, Q. Gao, M. L. Colaianni, and W. J. Choyke 1 Jun. 1992 27 p
(Contract N00014-82-C-0280)
(AD-A252804; TR-46) Avail: CASI HC A03/MF A01

The surface chemistry of adsorbed halogen atoms on Si(100) has been studied using several surface science methods. It has been found that Cl atoms bond to dangling bonds on symmetric Si2 dimer sites, and that the Si-Cl bond angle is tilted from the normal in the vertical plane containing the Si2 dimer bond. The covalently-bonded halogens Cl, Br, and I have been studied on Si(100) using atomic hydrogen bombardment at low substrate temperatures (300 - 630 K). In all cases, facile elimination of the hydrogen halide occurs, and the coverage of halogen may be driven to zero by moderate exposure to atomic hydrogen. The halogen extraction process is almost non-activated, suggesting that the chemical reaction to produce hydrogen halide species is driven by the potential energy carried by the atomic hydrogen species. This is an example of an Eley-Rideal reaction process and provides a potentially useful new approach for controlling atomic layer chemistry on semiconductors. GRA

N93-10281# Pittsburgh Univ., PA. Surface Science Center.
COMPARISON OF Cl AND HCl ADSORPTION ON Si(100)-(2 X 1)
Q. Gao, C. C. Cheng, P. J. Chen, W. J. Choyke, and J. T. Yates, Jr. 1 Jun. 1992 23 p
(Contract N00014-82-C-0280)
(AD-A252802; TR-47) Avail: CASI HC A03/MF A01

The chemisorption and reaction of Cl2 and HCl on Si(100)-(2x1) have been studied using a variety of measurement methods. At 100 K, both Cl2 and HCl dissociatively chemisorb on the dangling bonds of Si(100). At saturation coverage, the surface concentration of Cl is about one Cl atom per Si atom while HCl can produce a Cl coverage only one fourth of that achieved with Cl2. This is the first report of a self-site-blocking effect in adsorption on a semiconductor surface. High resolution electron energy loss (HREEL) spectra indicate that both Cl2 and HCl adsorption at 100 K give a monochloride surface species with a Si-Cl stretching frequency of approximately 550-600 cm(exp -1). Digital electron-stimulated de sorption ion angular distribution (ESDIAD) measurements reveal that the Si-Cl bond angle for the monochloride from both Cl2 and HCl adsorption is oriented on the vertical plane containing the Si-Si dimer bond and is inclined from the surface normal. The etching products of Si(100) by Cl2 at elevated temperatures are SiCl2 at approximately 800 K and a small amount of SiCl4 at approximately 500 K. For HCl, the only observed etching product is SiCl2. GRA

N93-10400# Rochester Univ., NY.
TRANSITION METAL ACTIVATION AND FUNCTIONALIZATION OF CARBON-HYDROGEN BONDS
W. D. Jones Jun. 1992 37 p
(Contract DE-FG02-86ER-13569)
(DE92-014809; DOE/ER-13569/7) Avail: CASI HC A03/MF A01

We are investigating the fundamental thermodynamic and kinetic factors that influence carbon-hydrogen bond activation at homogeneous transition metal centers and the conversion of hydrocarbons into functionalized products of potential use to the chemical industry. Advances have been made in both understanding the interactions of hydrocarbons with metals and in the functionalization of hydrocarbons. We have found that RhCl(PR3)2(CNR) complexes can catalyze the insertion of isonitriles into the C-H bonds or arenes upon photolysis. The mechanism of these reactions was found to proceed by way of initial phosphine dissociation, followed by C-H activation and isonitrile insertion. We have also examined reactions of a series of arenes with (C5Me5)Rh(PMe3)PhH and begun to map out the kinetic and thermodynamic preferences for arene coordination. The effects of resonance, specifically the differences in the Hueckel energies of the bound vs free ligand, are now believed to fully control the C-H activation/eta(sup 2)-coordination equilibria. We have begun to examine the reactions of rhodium isonitrile pyrazolylborates for alkane and arene C-H bond activation. A new, labile, carbodiimide precursor has been developed for these studies. We have completed studies of the reactions of (C5Me5)Rh(PMe3)H2 with D2 and PMe3 that indicate that both eta(sup 5) yields eta(sup 3) ring slippage and metal to ring hydride migration occur more facilely than thermal reductive elimination of H2. We have examined the reactions of heterocycles with (C5Me5)Rh(PMe3)PhH and found that pyrrole and furan undergo C-H or N-H activation. Thiophene, however, undergoes C-S bond oxidative addition, and the mechanism of activation has been shown to proceed through sulfur coordination prior to C-S insertion. DOE

N93-10401# Calm (James M.), Arlington, VA.
ARTI REFRIGERANT DATABASE
J. M. Calm 30 Apr. 1992 56 p
(Contract DE-FG02-91CE-23810)
(DE92-015122; DOE/CE-23810/2G) Avail: CASI HC A04/MF A01

The Refrigerant Database consolidates and facilitates access to information to assist industry in developing equipment using alternative refrigerants. The underlying purpose is to accelerate phase out of chemical compounds of environmental concern. The database provides bibliographic citations and abstracts for publications that may be useful in research and design of air-conditioning and refrigeration equipment. The complete documents are not included, though some may be added at a later date. The database identifies sources of specific information on R-32, R-123, R-124, R-125, R-134a, R-141b, R142b, R-143a, R-152a, R-290 (propane), R-717 (ammonia), ethers, and others as well as azeotropic and zeotropic blends of these fluids. It addresses polyalkylene glycol (PAG), ester, and other lubricants. It also references documents addressing compatibility of refrigerants and lubricants with metals, plastics, elastomers, motor insulation, and other materials used in refrigerant circuits. DOE

N93-10414# North Carolina Univ., Chapel Hill. Dept. of Chemistry.
PRE-OXIDATION ANNEAL KINETICS: INTERFACE DEGRADATION OF THIN SiO2 FILMS ON SILICON
J. C. Polar and E. A. Irene 13 Jul. 1992 8 p
(Contract N00014-89-J-1178)
(AD-A253142; TR-48) Avail: CASI HC A02/MF A01

The high temperature anneal of hydrogen terminated silicon has been shown to etch and roughen its surface. We attempt to describe the degree of this roughness and the time scale on which it occurs using several electrical measurements: excess direct tunneling currents, dielectric breakdown, and the oscillations in the Fowler-Nordheim tunneling currents. From these results we draw conclusions on the time and water content dependence of pre-oxidation annealing on the microroughness of the Si/SiO2 interface. GRA

N93-10416# State Univ. of New York, Stony Brook. Dept. of Chemistry.
CLUSTER BEAM STUDIES OF METAL COMBUSTION Final Report, 1 Jul. 1985 - 31 Oct. 1991
Scott L. Anderson 21 Jul. 1992 14 p
(Contract N00014-85-K-0678)
(AD-A253952; SBIL-002) Avail: CASI HC A03/MF A01

This report outlines the goals, approach, and accomplishments for the Stony Brook Cluster Beam program. We have developed the Cluster Beam method for examining the primary chemistry that occurs in high temperature attack on metal or semi-metal surfaces. The method has been applied to boron, aluminum, and carbon combustion chemistry, and we have been able to identify reactions and products, derive thermochemical information, and convert the data to reaction probabilities that can be fed into combustion models. The report also describes construction and

initial operation of a new experiment designed to study the energetics and mechanism of strain energy release in strained hydrocarbon fuel molecules. GRA

N93-10423# Wisconsin Univ., Milwaukee. Dept. of Mechanical Engineering.
A MULTI-FLUID MODEL OF TURBULENCE FOR LI-SF6 SUBMERGED COMBUSTION Technical Report, 15 Jul. - 1 Aug. 1991
S. H. Chan and M. M. Abou-Ellail 1 Aug. 1992 28 p
(Contract N00014-89-J-1267)
(AD-A253973) Avail: CASI HC A03/MF A01

Liquid metal combustion has been used as the primary energy source for underwater vehicle propulsion because of its energetic and closed-cycle characteristics. This can be achieved by injecting gaseous oxidizer (SF6) in a molten metal (Li) bath. The present paper describes a new multi-fluid (MF) combustion model for multiphase submerged diffusion flames. Each fluid has separate transport equations which are linked to other fluids' transport equations by additional source terms. The present MF model results for a submerged Li(l)-SF6(g) flame gave a much longer plume length compared to the corresponding locally-homogeneous flow (LHF) model results and is in good agreement with the experimentally measured plume length. GRA

N93-10436# Colorado State Univ., Fort Collins.
STUDY OF IMPROVED METHODS FOR PREDICTING CHEMICAL EQUILIBRIA
T. G. Lenz and J. D. Vaughan Jun. 1992 30 p
(Contract DE-FG02-86ER-13582)
(DE92-016974; DOE/ER-13582/6) Avail: CASI HC A03/MF A01

The objective of our research has been to develop computational methods that have the capability of accurately predicting equilibrium constants of typical organic reactions in gas and liquid solution phases. We have chosen Diels-Alder reactions as prototypic systems for the investigation, chiefly because there are an adequate number of reported equilibrium constants for the candidate reactions in both gas and solution phases, which data provides a suitable basis for tests of the developed computational methods. Our approach has been to calculate the standard enthalpies of formation ((Delta)H(sub f)(sup 0)) at 298.15 K and the standard thermodynamic functions (S(sup 0), Cp(sup 0), and (H(sup 0)-H(sub 0)(sup 0))/T) for a range of temperatures for reactants and products, and from these properties to calculate standard enthalpies, entropies, Gibbs free energies, and equilibrium constants ((Delta)H(sub T)(sup 0), (Delta)S(sub T)(sup 0), and K(sub a)) at various temperatures for the chosen reaction. DOE

N93-10437# California Inst. of Tech., Pasadena. Graduate Aeronautical Labs.
COMBUSTION IN TURBULENT JETS AND BUOYANT FLAMES Annual Report, 1 Jan. - 31 Dec. 1991
Paul E. Dimotakis and James E. Broadwell 25 Jun. 1992 35 p
(Contract GRI-5087-260-1467)
(PB92-211481; GRI-92/0213) Avail: CASI HC A03/MF A01

Results are reported from an ongoing investigation of the entrainment and mixing mechanisms in momentum-dominated turbulent jets and flows which undergo a transition from the momentum to buoyancy-driven regime. The investigation also addresses the effects of molecular diffusion rates (Schmidt number) and combustion heat release on these mechanisms and incorporates these mechanisms into modeling and predictive techniques for practical natural gas flames. The gas-phase, chemically reacting jet experiments in the High Pressure Combustion Facility are completed. These experiments investigated the effects of Reynolds number on turbulent jet diffusion flame length, free of buoyancy, and radiation effects. To ensure that the flows were free of buoyancy, experiments were conducted in which the reacting jet was no longer momentum-dominated. This preliminary investigation of buoyancy provided results against which turbulent jet combustion models may be compared. GRA

N93-10460# Grambling State Univ., LA.
NQR-NMR STUDIES OF HIGHER ALCOHOL SYNTHESIS Cu-Co CATALYSTS
17 Dec. 1991 11 p
(Contract DE-FG22-89PC-89761)
(DE92-015783; DOE/PC-89761/T6) Avail: CASI HC A03/MF A01

The primary objective of the project is to examine the relations between the catalytic and magnetic properties of the copper-cobalt higher alcohol synthesis catalysts. We have undertaken to investigate the magnetic character by studying the Nuclear Quadrupole resonance of copper and (Zerofield) Nuclear Magnetic Resonance of cobalt in copper cobalt catalysts. DOE

N93-10712# Massachusetts Inst. of Tech., Cambridge. Dept. of Physics.
OPTICAL METROLOGY OF MAGNETICALLY TRAPPED HYDROGEN Final Report, 1 Feb. 1991 - 31 Jan. 1992
Daniel Kleppner 31 Jan. 1992 2 p
(Grant AF-AFOSR-0127-90)
(AD-A253229; AFOSR-92-0695TR) Avail: CASI HC A01/MF A01

During the period of this grant, 2/1/91-1/31/92, we completed the new version of our cold hydrogen trap and brought into operation our highly stabilized 243 nm laser system. The new trap has provisions for passing laser light through it, and reflecting it back by a steerable mirror. The light is brought to a focus on the axis of the trap where the hydrogen density is highest. Servo systems control the frequency of the laser light to within a few kilocycles of the frequency of a reference cavity, and also the position of the light beam in the cell. The excited atoms are detected by quenching them with a small electric field and observing the radiated Lyman-alpha photons with a microchannel plate detector mounted on the bottom of the trap. We had one test run in which we searched for an optical signal from the cold trapped hydrogen, without success. Considering that this represented the first attempt to integrate laser spectroscopy with trapped hydrogen, it is not remarkable that we ran into a problem on our first attempt. GRA

N93-10794# Missouri Univ., Rolla. Dept. of Chemistry.
MOBILITY OF TOLUENE IN POLYSTYRENE-TOLUENE SOLUTIONS: A NMR STUDY Interim Report, 1 Jul. 1990 - 1 Jul. 1992
Byaprorn naNagara, Robert D. OConnor, and Frank D. Blum 1 Jul. 1992 38 p
(Contract N00014-89-J-1274)
(AD-A253203; UMR-FDB-25) Avail: CASI HC A03/MF A01

Self-diffusion coefficients, longitudinal (T(sub 1)) and transverse (T(sub 2))NMR relaxation times of toluene in polystyrene-toluene solutions were determined at concentrations up to 50 percent polymer at room temperature to ca. -70 C. The self-diffusion coefficients were used to calculate the fraction of motionally-altered toluene based on deviations from the Maxwell-Fricke approximation of the obstruction effect. The fraction of motionally-altered toluene was found to be nearly constant with temperature for the lower polymer concentrations, but increased with decreasing temperature for the higher polymer concentrations. The relaxation times of the motionally-altered toluene were calculated using the two-fraction fast-exchange model and used to estimate the mean correlation times from a log-normal distribution of correlation times. The dependence of correlation times on temperature was found to be the Arrhenius type and the activation energies increased with polymer concentration. The activation energies for translational diffusion ranged from 12 to 22 kJ/mol and those of the motionally altered solvent's rotational motion from 11 to 42 kJ/mol. GRA

N93-10843# California Inst. of Tech., Pasadena.
SHOCK ENHANCEMENT AND CONTROL OF HYPERSONIC COMBUSTION Annual Technical Report, 1 Apr. 1991 - 31 Mar. 1992
Frank E. Marble and Edward E. Zukoski 18 Jun. 1992 21 p

(Grant AF-AFOSR-0804-92)
(AD-A254295; AFOSR-92-0804TR) Avail: CASI HC A03/MF A01

Experiments concerning the details of combustion in large vortices in the Caltech Unsteady Combustion Facility, using simultaneous measurements of pressure, shadowgraphy, and chemiluminescence are now about 50 percent complete. The detail of these results document a very different ignition mechanism and combustion pattern than previous experiments have suggested. Shock tube studies of shock enhanced mixing of helium into air, utilizing the Rayleigh scattering technique have been completed. Because of their greater sensitivity in the low concentration range, these measurements are significantly more accurate than those obtained with laser induced fluorescence and demonstrate that mixing is considerably more rapid and more complete than reported previously. Preliminary results have been obtained from experiments on the interaction of shock induced mixing with shear layers in the GALCIT M = 2.5 supersonic wind tunnel. GRA

N93-10852*# North Carolina State Univ., Raleigh. Analytical Instrumentation Facility.

ANALYSIS OF INTERPLANETARY DUST EXPERIMENT DETECTORS AND OTHER WITNESS PLATES Semiannual Report, 1 Jan. - 30 Jun. 1992

D. P. Griffis and J. J. Wortman 30 Jun. 1992 34 p
(Grant NAG1-1214)
(NASA-CR-190818; NAS 1.26:190818) Avail: CASI HC A03/MF A01

The development of analytical procedures for identifying the chemical composition of residue from impacts that occurred on the Interplanetary Dust Experiment (IDE) detectors during the flight of Long Duration Exposure Facility (LDEF) and the carrying out of actual analysis on IDE detectors and other witness plates are discussed. Two papers on the following topics are presented: (1) experimental analysis of hypervelocity microparticle impact sites on IDE sensor surfaces; and (2) contaminant interfaces with secondary Ion Mass Spectrometer (SIMS) analysis of microparticle impactor residues on LDEF surfaces. For individual titles, see N93-10853 through N93-10854.

N93-10853*# Institute for Space Science and Technology, Inc., Gainesville, FL.

ELEMENTAL ANALYSES OF HYPERVELOCITY MICROPARTICLE IMPACT SITES ON INTERPLANETARY DUST EXPERIMENT SENSOR SURFACES

C. G. Simon, J. L. Hunter (North Carolina State Univ., Raleigh.), D. P. Griffis (North Carolina State Univ., Raleigh.), V. Misra (North Carolina State Univ., Raleigh.), D. A. Ricks (North Carolina State Univ., Raleigh.), J. J. Wortman (North Carolina State Univ., Raleigh.), and D. E. Brownlee (Washington Univ., Seattle.) *In* North Carolina State Univ., Analysis of Interplanetary Dust Experiment Detectors and Other Witness Plates 30 Jun. 1992 15 p (For primary document see N93-10852 01-25)
Avail: CASI HC A03/MF A01

The Interplanetary Dust Experiment (IDE) had over 450 electrically active ultra-high purity metal-oxide-silicon impact detectors located on the six primary sides of the Long Duration Exposure Facility (LDEF). Hypervelocity microparticles (approximately 0.2 to approximately 100 micron diameter) that struck the active sensors with enough energy to breakdown the 0.4 or 1.0 micron thick SiO2 insulator layer separating the silicon base (the negative electrode), and the 1000 A thick surface layer of aluminum (the positive electrode) caused electrical discharges that were recorded for the first year of orbit. The high purity Al-SiO2-Si substrates allowed detection of trace (ppm) amounts of hypervelocity impactor residues. After sputtering through a layer of surface contamination, secondary ion mass spectrometry (SIMS) was used to create two-dimensional elemental ion intensity maps of microparticle sites on the IDE sensors. The element intensities in the central craters of the impacts were corrected for relative ion yields and instrumental conditions and then normalized to silicon. The results classification resulted from the particles' origins as 'manmade', 'natural', or 'indeterminate'. The last classification resulted from the presence of too little impactor residue, analytical interference from high background contamination, the lack of information on silicon and aluminum residues, or a combination of these circumstances. Several analytical 'blank' discharges were induced on flight sensors by pressing down on the sensor surface with a pure silicon shard. Analyses of these blank discharges showed that the discharge energy blasts away the layer of surface contamination. Only Si and Al were detected inside the discharge zones, including the central craters, of these features. Thus far, a total of 79 randomly selected microparticle impact sites from the six primary sides of the LDEF were analyzed: 36 from tray C-9 (Leading (ram), or east, side), 18 from tray C-3 (Trailing (wake), or west, side), 12 from tray B-12 (north side), 4 from tray D-6 (south side), 3 from tray H-11 (space end), and 6 from tray G-10 (earth end). Residue from manmade debris was identified in craters on all trays (aluminum oxide particle residues were not detectable on the Al/Si substrates). These results were consistent with the IDE impact record which showed highly variable long term microparticle impact flux rates on the west, space, and Earth sides of the LDEF which could not be ascribed to astronomical variability of micrometeorite density. The IDE record also showed episodic bursts of microparticle impacts on the east, north, and south sides of the satellite, denoting passage through orbital debris clouds or rings. Author

N93-10854*# Institute for Space Science and Technology, Inc., Gainesville, FL.

CONTAMINANT INTERFERENCES WITH SIMS ANALYSES OF MICROPARTICLE IMPACTOR RESIDUES ON LDEF SURFACES

C. G. Simon, D. Batchelor (North Carolina State Univ., Raleigh.), D. P. Griffis (North Carolina State Univ., Raleigh.), J. L. Hunter (North Carolina State Univ., Raleigh.), V. Misra (North Carolina State Univ., Raleigh.), D. A. Ricks (North Carolina State Univ., Raleigh.), and J. J. Wortman (North Carolina State Univ., Raleigh.) *In* North Carolina State Univ., Analysis of Interplanetary Dust Experiment Detectors and Other Witness Plates 30 Jun. 1992 11 p (For primary document see N93-10852 01-25)
Avail: CASI HC A03/MF A01

Elemental analyses of impactor residues on high purity surface exposed to the low earth orbit (LEO) environment for 5.8 years on Long Duration Exposure Facility (LDEF) has revealed several probable sources for microparticles at this altitude, including natural micrometeorites and manmade debris ranging from paint pigments to bits of stainless steel. A myriad of contamination interferences were identified and their effects on impactor debris identification mitigated during the course of this study. These interferences included pre-, post-, and in-flight deposited particulate surface contaminants, as well as indigenous heterogeneous material contaminants. Non-flight contaminants traced to human origins, including spittle and skin oils, contributed significant levels of alkali-rich carbonaceous interferences. A ubiquitous layer of in-flight deposited silicaceous contamination varied in thickness with location on LDEF and proximity to active electrical fields. In-flight deposited (low velocity) contaminants included urine droplets and bits of metal film from eroded thermal blankets. Author

N93-10553 California Univ., Berkeley.

PULSED JET PLUME COMBUSTION: AN EXOTHERMIC PROCESS UNDER FLUID MECHANICAL CONTROL

A. K. Oppenheim *In* Carleton Univ., Proceedings of the Twelfth Canadian Congress of Applied Mechanics, Volumes 1 and 2 May 1989 p 736-737 (For primary document see N93-10466 01-31)
Copyright Avail: Canadian Society for Mechanical Engineering, 2050 Mansfield St., Suite 700, Montreal, Quebec H3A 1Z7 Canada

26 METALLIC MATERIALS

Includes physical, chemical, and mechanical properties of metals, e.g., corrosion; and metallurgy.

N93-10072*# National Aeronautics and Space Administration. Marshall Space Flight Center, Huntsville, AL.
TENSILE PROPERTIES OF CAST TITANIUM ALLOYS: TITANIUM-6Al-4V ELI AND TITANIUM-5Al-2.5Sn ELI
E. E. Billinghurst, Jr. Oct. 1992 16 p
(NASA-TP-3288; M-699; NAS 1.60:3288) Avail: CASI HC A03/MF A01

This work was performed to determine the tensile properties of cast, hot isostatic pressed (HIP'ed), and annealed titanium alloys, Ti-6Al-4V ELI and Ti-5Al-2.5Sn ELI, that are candidate materials for the space transportation main engine (STME) liquid hydrogen turbopump impeller. Samples of the cast alloys were HIP'ed, annealed, and machined into tensile specimens. The specimens were tested in air at ambient temperature (70 F) and also at -423 F in liquid hydrogen. The Ti-6Al-4V alloy had an average ultimate strength of 129.1 ksi at 70 F and 212.2 ksi at -423 F. The Ti-5Al-2.5Sn alloy had an average ultimate strength of 108.4 ksi at 70 degrees F and 185.0 ksi at -423 F. The ductility, as measured by reduction of area, for the Ti-6Al-4V averaged 15.2 percent at 70 F and 8.7 percent at -423 F, whereas for the Ti-5Al-2.5Sn alloy average reduction of area was 24.6 percent at 70 F and 11.7 percent at -423 F. Author

N93-10100# State Univ. of New York, Stony Brook. Dept. of Materials Science and Engineering.
A STUDY OF THE EFFECT OF NITROGEN AND MOLYBDENUM IN THE CORROSION INHIBITION OF AUSTENITIC STAINLESS STEEL Ph.D. Thesis Final Report
Clive R. Clayton and Donggil Kim 1992 198 p
(Contract N00014-85-K-0437)
(AD-A253354) Avail: CASI HC A09/MF A03

The synergistic effect of nitrogen and molybdenum in remarkably improving the corrosion resistance of austenitic stainless steels in chlorine ions containing solution has been investigated. Electrochemical techniques in conjunction with X-ray Photoelectron Spectroscopy (XPS) were utilized to elucidate the mechanism by which N and Mo influence the passivation behavior of austenitic stainless steel. Since nitrates and nitrites are known to be powerful corrosion inhibitors, the possibility that alloyed nitrogen was capable of oxidizing to either of these species was considered. While no evidence could be found of NO3 formation by XPS, it was decided to further clarify this issue by considering the stability of NO3 ions on the surface of pure chromium and a variety of molybdenum bearing stainless steels polarized through an extensive range of potentials. Nitrate was found to be unstable at all potentials considered provided that the metal was exposed directly to the solution. This resulted in clear evidence that alloyed nitrogen does not oxidize to NO3 or NO2. Indeed a new mechanism by which nitrates inhibit corrosion was uncovered. GRA

N93-10395# Ohio State Univ., Columbus. Dept. of Materials Science and Engineering.
EFFECT OF ALLOYING ELEMENTS ON PASSIVITY AND BREAKDOWN OF PASSIVITY OF Fe- AND Ni-BASED ALLOYS MECHANISTICS ASPECTS
Z. Szklarska-Amialowska Jun. 1992 23 p
(Contract DE-FG02-87ER-45293)
(DE92-017316; DOE/ER-45293/5) Avail: CASI HC A03/MF A01

On the basis of the literature data and the current results, the mechanism of pitting corrosion of Al-alloys is proposed. An assumption is made that the transport of Cl- ions through defects in the passive film of aluminum and aluminum alloys is not a rate determining step in pitting. The pit development is controlled by the solubility of the oxidized alloying elements in acid solutions. A very good correlation was found between the pitting potential and the oxidized alloying elements for metastable Al-Cr, Al-Zr, Al-W, and Al-Zn alloys. We expect that the effect of oxidized alloying elements in other passive alloys will be the same as in Al-alloys. To verify this hypothesis, susceptibility to pitting in the function of alloying elements in the binary alloys and the composition of the oxide film has to be measured. We propose studying Fe- and Ni-alloys produced by a sputtering deposition method. Using this method one-phaseous alloy can be obtained, even when the two metals are immiscible using conventional methods. Another advantage to studying sputtered alloys is to find new materials with superior resistance to localized corrosion. DOE

N93-10411# California Univ., Berkeley. Lawrence Berkeley Lab.
ELECTRONIC AND STRUCTURAL PROPERTIES OF METALLIC MICROCLUSTERS Ph.D. Thesis
A. Maiti Apr. 1992 110 p
(Contract DE-AC03-76SF-00098)
(DE92-016917; LBL-32185) Avail: CASI HC A06/MF A02

The first part of this thesis presents a first-order pseudopotential calculation at T = O of the total energy of small sodium clusters of size N less than 800. The calculation is based on a local-pseudopotential scheme and local-density correlation and exchange. A temperature-size (T-N) phase-diagram is then derived using the T = O results and Lindemann's criterion for melting. The phase-diagram contains three regions of stability: (1) a liquid (jellium) phase at temperatures above the melting line T(sub M)(N) where cluster-stability occurs at electronic magic numbers; (2) a phase related to complete geometrical shells of body-centered-cubic structure at temperatures below the melting line; and (3) a close-packed structure at very low temperatures and sufficiently large N. The melting line drops to T(sub M)(N) = O for N less than 65, where electronic magic numbers are stable even at T = 0. The phase diagram reduces asymptotically to the known phases of sodium as N yields infinity, including the known martensitic transformation at T approximately 5 K. The second and the last part of this thesis consists of a study of small-cluster many-body systems by means of an on-site 'local' chemical potential which allows the continuous variation of local electron-density. This method yields a criterion to distinguish particular features of a small cluster that are likely to survive in the large-N thermodynamic limit from those discontinuities that arise only from finite-size effects. DOE

N93-10706# Air Force Inst. of Tech., Wright-Patterson AFB, OH. Foreign Aerospace Science and Technology Center.
PROTECTIVE COATINGS FOR NIOBIUM ALLOYS AND THEIR PROPERTIES
Ye. L. Geraseva, A. N. Sokolov, A. S. Stroyev, N. F. Lashko, and M. N. Kozlova 6 Feb. 1992 18 p Transl. into ENGLISH from Zharostoikie Teplostoikie Pokrytiya (USSR, Tr Vses Soveshch), 1968 p 139-152
(AD-A254252; FASTC-ID(RS)T-0919-91) Avail: CASI HC A03/MF A01

Niobium alloys cannot be used at high temperatures without protective coatings. Superficial alloying of niobium alloys with only one element (aluminum, silicon, or chromium) does not make it possible to obtain a coating which reliably protects the alloy for a prolonged period of time. The development of complex coatings is still proceeding only by empirical means, since the chemistry of their formation reactions is unknown. This work studied chromium-aluminum-silicon and chromium-titanium-silicon coatings which were applied to alloys VN-2A and VN-4 in two stages. First, the alloys were subjected to saturation with chromium, aluminum, or chromium and titanium, and then siliconing was performed. The chemical and phasal composition of the coating were determined by the method of by-layer phasal analysis and the method of microprobe. A metallographic analysis was also performed, heat-resistance curves were plotted, and certain mechanical properties were determined. GRA

N93-10717# Rhode Island Univ., Kingston. Dept. of Mechanical Engineering and Applied Mechanics.
MECHANISMS AND MODELLING OF ENVIRONMENT-DEPENDENT FATIGUE CRACK GROWTH IN A NICKEL BASED SUPERALLOY Final Report, 1989 - 1991

H. Ghonem and D. Zheng 12 Dec. 1991 252 p
(Grant AF-AFOSR-0285-89)
(AD-A253967; URI-MSL-921; AFOSR-92-0787TR) Avail: CASI HC A12/MF A03

At loading frequencies below that of the transitional frequency level, which is typical of mission cycles of jet engines, the elevated temperature fatigue crack growth process in Alloy 718 is viewed to be fully environment-dependent. Of all the crack growth stages, this process, while is the most critical in high temperature application due to its highly accelerated crack growth rate, is the least studied or understood. The objective of this research program is to focus on the understanding or the mechanism controlling this oxidation-dependent stage in order to develop the ability to predict its associated crack growth performance under different environment conditions. For this purpose, three major studies have been carried out; the first was to provide evidence of the existence of the fully environment-dependent stage in which the crack growth rate would be equal to the oxygen penetration rate at the crack tip. The second study was to establish a crack tip oxidation mechanism on the basis of material, environmental and loading parameters interactions in the crack tip region. The last objective of this program is to establish a micromechanical based quantitative model to predict the environmentally-dominated crack growth stage. GRA

N93-10752# Pennsylvania State Univ., University Park. Dept. of Engineering Science and Mechanics
INHIBITING CORROSION IN Gr/Al AND Gr/Mg METAL MATRIX COMPOSITES USING NONEQUILIBRIUM ALLOYING TECHNIQUES Annual Report, 1 Apr. 1991 - 31 Mar. 1992
B. A. Shaw, T. R. Schrecengost, W. C. Moshier, and R. G. Wendt Jun. 1992 102 p
(Contract N00014-91-J-1196)
(AD-A253923) Avail: CASI HC A06/MF A02

Metal matrix composites (MMC's) have been heavily studied over the cast thirty years. During that period, many proposals have been made to develop a matrix alloy that was compatible with the reinforcing phase. However, for one reason or another, the technology has continued to focus on conventional alloys and fabrication practices. Although tremendous advances have been made on composite materials, the basic technology remains similar to systems studied twenty years ago. This work represents the first program where new alloys are being developed for graphite reinforced composites which are tailored to a novel processing technology for manufacturing corrosion resistant graphite reinforced composites. GRA

N93-10789# Oak Ridge National Lab., TN.
ATOMIC SHORT RANGE ORDER AND SPIN DENSITY WAVE PROPAGATION IN CuMn
J. W. Cable and Y. Tsunoda (Osaka Univ., Toyonaka, Japan) 1992 6 p Presented at the International Conference on the Physics of Transition Metals, Darmstadt (Germany), 20-24 Jul. 1992
(Contract DE-AC05-84OR-21400)
(DE92-016903; CONF-920762-3) Avail: CASI HC A02/MF A01

Neutron scattering studies of the atomic short range order (ASRO) and spin density waves (SDW) were carried out for a Cu-35 percent Mn sample with an unusually high degree of ASRO that develops mostly in a single tetragonal domain. The SDW peaks show a distinctly non-cubic distribution that is readily correlated with the ASRO and which corresponds to the propagation of SDW only in the c plane of the tetragonally based ASRO. The high degree of ASRO and single domain character of this carefully heat-treated sample produces an unusually stable SDW with a higher transition temperature and a larger correlation length than is observed for quenched alloys of the same Mn content. Since SDW stability depends on structural features in the conduction electron susceptibility and on flat, parallel sections of the Fermi surface, these observations suggest that the degree of ASRO and/or the presence of single domain ASRO influences the sharpness of the relevant Fermi surface features in these alloys. DOE

N93-10802# Royal Aircraft Establishment, Farnborough (England).
THE MICROSTRUCTURAL CHARACTERIZATION OF AN Al-Li-Cu-Mg ALLOY (8090) METAL-MATRIX COMPOSITE
C. J. Gilmore and A. W. Bowen 25 Oct. 1989 7 p
(RAE-TM-MAT/STR-1139; BR112718) Copyright Avail: CASI HC A02/MF A01

The results of a preliminary investigation into the microstructure of a metal matrix composite (MMC) containing 20 (vol) percent of SiC particles in an Al-Li-Cu-Mg (8090) alloy matrix are described. Transmission electron microscopy and energy dispersive spectroscopy were used to characterize changes in the matrix, and at matrix/SiC interfaces resulting from the hot-rolling schedule and from a typical heat treatment cycle of solution heat treatment at 530 C followed by water quenching and artificial aging for 24 h at 170 C. Author

N93-10880# California Univ., Los Angeles.
ATOMIC FORCE MICROSCOPE STUDIES OF CuCl ISLAND FORMATION ON CaF2(111) SUBSTRATES
W. M. Tong, E. J. Snyder, R. S. Willims, A. Yanase, and Y. Segawa 20 May 1992 20 p
(Contract N00014-90-J-1178)
(AD-A252499; TR-18) Avail: CASI HC A03/MF A01

We have grown by molecular beam epitaxy (MBE) CuCl thin films at various thickness and substrate temperatures on CaF2 (111) substrates. Atomic Force Microscope (AFM) topographs reveal that islanding is the dominant growth mechanism. Quantitative analysis of the AFM data enabled us to determine the amount of the substrate remaining exposed after the deposition as well as the total amount of CuCl deposited. We calculated the reciprocal-space height correlation function, ((the absolute value of h(q,t))exp 2) for each of our films and compared them to the predictions of the Shadowing Growth Theory, which enabled us to extract the important kinetic parameter of surface diffusion length for the growth condition of each of the four films. GRA

N93-10579*# National Aeronautics and Space Administration. Marshall Space Flight Center, Huntsville, AL.
SELECTED RESULTS FOR METALS FROM LDEF EXPERIMENT A0171
Ann F. Whitaker *In* NASA. Langley Research Center, LDEF Materials Workshop 1991, Part 2 Sep. 1992 p 467-478 (For primary document see N93-10578 01-27)
Avail: CASI HC A03/MF A03

N93-10580*# European Space Agency. European Space Research and Technology Center, ESTEC, Noordwijk (Netherlands).
SOME RESULTS OF THE OXIDATION INVESTIGATION OF COPPER AND SILVER SAMPLES FLOWN ON LDEF
A. deRooij *In* NASA. Langley Research Center, LDEF Materials Workshop 1991, Part 2 Sep. 1992 p 479-490 (For primary document see N93-10578 01-27)
Avail: CASI HC A03/MF A03

N93-10581*# Boeing Co., Seattle, WA. Defense and Space Group.
CHANGES IN OXIDATION STATE OF CHROMIUM DURING LDEF EXPOSURE
Johnny L. Golden *In* NASA. Langley Research Center, LDEF Materials Workshop 1991, Part 2 Sep. 1992 p 491-500 (For primary document see N93-10578 01-27)
Avail: CASI HC A02/MF A03

27 NONMETALLIC MATERIALS

Includes physical, chemical, and mechanical properties of plastics, elastomers, lubricants, polymers, textiles, adhesives, and ceramic materials.

For composite materials see *24 Composite Materials*.

N93-10082# Keramont Corp., Tucson, AZ.
REINFORCEMENTS FOR HIGH TEMPERATURE CERAMICS
C. I. Kyriacou, J. L. Sepulveda, and M. A. Watson Apr. 1992 56 p Prepared in cooperation with Keramont Corp., Tucson, AZ
(Contract DE-AC05-84OR-21400)
(DE92-014815; ORNL/Sub-90-SB688/1) Avail: CASI HC A04/MF A01

A method has been investigated and developed to grow TiB2 whiskers by the VLS mechanism. The reaction was carried out in a 3-inch diameter, 30-inch long quartz tube at about 1150 C in the presence of a catalyst. The basic experimental parameters, a substrate, and a catalyst for the growth of the whiskers have been defined. The produced whiskers have shown variable size and morphology depending on the experimental conditions and location of the whiskers from the input port. The corrosion of the catalyst by the gas environment and the gas distribution profile in the furnace had a serious effect on the reproducibility of the experimental results and the overall yield of whiskers. DOE

N93-10084# Iowa State Univ. of Science and Technology, Ames.
MATERIALS COMPATIBILITY AND LUBRICANTS RESEARCH ON CFC-REFRIGERANT SUBSTITUTE: MISCIBILITY OF LUBRICANTS WITH REFRIGERANTS
M. B. Pate, S. Zoz, and L. Berkenbosch Apr. 1992 7 p Prepared for Air-Conditioning and Refrigeration Technology Inst., Inc., Arlington VA
(Contract DE-FG02-91CE-23810)
(DE92-015118; DOE/CE-23810/2C) Avail: CASI HC A02/MF A01

During this reporting period, modifications were made to the experimental apparatus in preparation for performing the experiments required in this project. In addition, new procedures for charging the lubricant and refrigerant into the cells for high temperature tests have been adopted. All of the refrigerants (10 different types) and lubricants (seven different types) have been ordered from the manufacturers. To date, the data obtained includes that for R-134a and four lubricants, namely, two esters and two polypropylene glycols (PAG's). Methods for quantifying immiscibility based on observation by different lab workers have been developed. DOE

N93-10205# American Ceramic Society, Westerville, OH.
CERAMIC TRANSACTIONS. VOLUME 21: PROCEEDINGS OF THE SYMPOSIUM ON MICROWAVE THEORY AND APPLICATION IN MATERIALS PROCESSING ANNUAL MEETING NO. 23 IO ON APRIL 29-MAY 3 1991 Final Report, 28 Apr. 1991 - 27 Apr. 1992
David E. Clark, Frank D. Gac, and Willard H. Sutton 27 Apr. 1992 620 p Meeting held in Cincinnati, OH, 29 Apr. - 3 May 1991
(Grant AF-AFOSR-0229-91)
(AD-A253631; AFOSR-92-0670TR-Vol-21) Avail: CASI HC A99/MF A06

The symposium was held during the 93rd Annual Meeting of The American Ceramic Society in Cincinnati, OH, April 29-May 3, 1991. One objective was to assemble the experts in this emerging technology for the purpose of identifying problem areas and defining potential solutions. A second objective was to explore new applications where microwave energy can have significant impact. A third objective was to bring together researchers, materials fabricators, and microwave equipment manufacturers for the purpose of expediting technology transfer and commercialization of important discoveries in this field. Participants from 7 countries presented 80 papers at the symposium. A combination of keynote, invited, and contributed presentations provided excellent overviews of existing programs, microwave/materials interactions, measurements, equipment design, modeling, and applications. GRA

N93-10221# Dayton Univ., OH. Research Inst.
DETERMINATION OF THE DYNAMIC UNLOAD/RELOAD CHARACTERISTICS OF CERAMICS Final Report, Oct. 1988 - Mar. 1992
G. Abfalter, N. Brar, and D. Jurick Jun. 1992 65 p
(Contract DAAL03-88-K-0203)
(AD-A253513; UDR-TR-92-72; ARO-26169.11-MS-A) Avail: CASI HC A04/MF A01

Ballistic impacts on ceramics give rise to many complex phenomena. The common features of target response include the following: (1) compressive failure; (2) followed by shear and/or tensile failure; and (3) finally, bulk motion (flow) of damaged material. The University of Dayton Research Institute (UDRI) has studied the behavior of ceramics subjected to these unusual loading conditions. To investigate these phenomena we developed, modified, and/or improved a set of impact tests to exercise ceramics in stress states and stress histories that are characteristic of ballistic impact. This set included the transverse gauge technique, bar impacts, reverberation technique, unload/reload technique, etc. We used these experiments to gain insight into the behavior of ballistic ceramics important to DARPA research groups. Included in the ceramics studied were TiB2 B4C and AlN. We developed correlations, based upon empirical data, between the material properties and the ballistic properties of ceramics. The correlations included the relation of Tate target strength (Rt) to the Hugoniot elastic limit (HEL) and the relation of the loss of shear strength to the ballistic performance of brittle solids. GRA

N93-10230# Carnegie-Mellon Univ., Pittsburgh, PA.
EPITAXIAL MAGNETIC OXIDES Final Technical Report, 11 Nov. 1988 - 30 Apr. 1992
M. H. Kryder, D. D. Stancil, D. E. Laughlin, W. Wang, and M. Ramesh 30 Jun. 1992 149 p
(Grant AF-AFOSR-0097-89)
(AD-A253667; AFOSR-92-0721TR) Avail: CASI HC A07/MF A02

Research was carried out on the heteroepitaxial growth of magnetic oxides (garnets and hexaferrites) on a variety of substrates. These new materials technologies are being used for the development of novel microwave, millimeter wave, and optical signal processing devices. Liquid phase epitaxy (LPE) sputtering and pyrolysis (thermal decomposition of spin coated material) were used to grow these materials. For integrated microwave and optical signal processing devices, two-layer LPE grown garnets with one layer having a narrow resonance linewidth (less than 1 Oe) and the other a high Faraday rotation (greater than 0.1 deg/micron) were developed. Silicon-on-garnet technology was developed and demonstrated capable of producing high quality integrated semiconductor and magnetic devices on a common substrate. Sputter deposition and pyrolysis were developed as alternative lower temperature processes capable of depositing garnets onto nongarnet substrates, and thin film hexaferrites with near-bulk values of magnetization and uniaxial anisotropy were grown by sputter deposition. GRA

N93-10231# National Inst. of Standards and Technology, Gaithersburg, MD.
MOIRE-FRINGE IMAGES OF TWIN BOUNDARIES IN CHEMICAL VAPOR DEPOSITED DIAMOND Interim Report
D. Shechtman, A. Feldman, M. D. Vaudin, and J. L. Hutchison 10 Jul. 1992 12 p
(Contract N00014-90-F-0011)
(AD-A253729; NIST-TR-14) Avail: CASI HC A03/MF A01

Features in lattice image micrographs of chemical vapor deposited diamond can be interpreted as Moire fringes that occur when viewing twin boundaries that are inclined to the electron beam. The periodicities in images of inclined twin boundaries with Sigma = 3 and Sigma = 9 misorientations have been modeled by computer graphic simulation. GRA

N93-10243# Colorado State Univ., Fort Collins. Dept. of Chemistry.
INFRARED INVESTIGATIONS OF PRISTINE POLYPYRROLE. IS THE POLYMER CALLED POLYPYRROLE REALLY POLY (PYRROLE-CO-HYDROXYPYRROLE)?
Junting Lei and Charles R. Martin 30 Apr. 1992 15 p
(Contract N00014-82-K-0612)
(AD-A249746; CSU-TR-67) Avail: CASI HC A03/MF A01

Polypyrrole (PPy) is one of the most extensively investigated of the electronically conductive polymers. Nevertheless, there is still much we don't understand about this interesting and useful material. One of the most persistent mysteries involves simple chemical composition. Doped PPy should have the empirical formula C4H3NX(z) where X is the dopant counterion and z is the fractional doping level; z is typically on the order of 0.3. However, elemental analyses of PPy typically show empirical formulas like C4H3NX(z)0(y) where y ranges from 0.3 to 0.7 unaccounted for oxygen atoms per pyrrole ring. This paper presents IR spectral data which suggests that the oxygen in PPy is present as covalently-bound hydroxide. Analogous IR investigations of poly(N-methylpyrrole) films show that this polymer is also hydroxylated. The hydroxy substitution present in these polymers undoubtedly results from nucleophilic attack by water on the nascent polycationic chains. GRA

N93-10244# Seville Univ. (Spain).
THE THIRD WORKSHOP ON NON-CRYSTALLINE SOLIDS, PROGRAMME AND ABSTRACTS
Nov. 1991 102 p Workshop held in Matalascanas, (Spain), 5-8 Nov. 1991
(AD-A250739) Avail: CASI HC A06/MF A02

Abstracts of the papers presented at the third Workshop on Non-Crystalline Solids are compiled along with the conference schedule. Some of the topics covered include intermetallic phases, nanocrystalline alloys, metallic and non-metallic glasses, amorphous ferromagnets, and polymeric solids. Author

N93-10246# Indiana Univ.-Purdue Univ., Indianapolis. Dept. of Chemistry.
WATER SOLUBLE POLYSILOXANES WITH PENDANT 1-OXYPYRIDIN-3-YL GROUPS
Martel Zeldin, Slawomir Rubinsztajn, and Wilmer K. Fife 15 May 1992 11 p
(Contract N00014-91-J-1434)
(AD-A250637; TR-15) Avail: CASI HC A03/MF A01

Polysiloxanes with 1-oxypyridin-3-yl groups bonded to silicon were prepared by base catalyzed hydrolysis-polycondensation of dialkoxy silane monomers. The polymers were characterized by IR, IH- and 13C-NMR spectra. Polymers bearing 1-oxypyridin-3-yl functions were soluble in organic solvents like CH2Cl2. The solubility in hydrogen bonding solvents, such as H20 and MeOH, increased with increase in molecular weight. The distribution coefficient for materials with different molecular weight in a water/CHCl3 mixture is reported. Quasi-elastic light scattering data indicate that the Stokes diameter for the polymer with molecular weight 9000 increases in the order H20 less than MeOH less than CH2Cl2. Structural ramifications of the solvent effect are suggested. GRA

N93-10287# National Inst. for Research in Inorganic Materials, Tokyo (Japan).
DEVELOPMENTAL RESEARCH ON ULTRA ABRASION-RESISTANT MATERIALS
27 Nov. 1991 47 p
(DE92-531066; ETDE/JP-MF-92531066) Avail: CASI HC A03/MF A01

Research development on abrasion resistant materials presented by the Inorganic Material Research Institute for the fiscal year 1991 activities is summarized. This research, with an intention of developing novel materials for processing ceramics at high accuracy and efficiency, discusses elucidating the sintering mechanisms in diamond and cBN (cubic crystal boron nitride) and synthesizing conditions and cutting tool characteristics used for sintered bodies. The research clarified infiltrating behavior of Co working as an auxiliary sintering agent in the infiltration process utilized to synthesize diamond sinters, as well as the effects of the working conditions and the ultrafine joint structure. Uniform and dense sinters were successfuly synthesized using additives of ultrafine diamond particles having sizes 1 micrometer or less, as well as BN sinters without auxiliary sintering agents, which proves the possibility of new tool materials. Additionally, other tests on the characteristics of these cutting tools provided valuable knowledge and information. DOE

N93-10343# Northwestern Univ., Evanston, IL. Basic Industry Research Lab.
OXYGEN BARRIER OXIDES Final Report, Jun. 1989 - Oct. 1990
Rheal Turcotte, Doreen Edwards, and Jill Jonkouski Mar. 1992 77 p
(Contract F33615-87-C-5339)
(AD-A253683; WL-TR-91-4059) Avail: CASI HC A05/MF A01

A series of mixed oxides with composition Zr3M4O12 were prepared as candidate high-melting-point ceramics for composite applications. The oxides selected should have significantly reduced oxygen diffusion coefficients compared to cubic-stabilized zirconia. Colloidal processing and conventional sintering produced samples with densities near 98 percent of theoretical. Zr3M4O12 compositions with M = Sc, Y, La, and Gd, as well as Y2O3 and cubic-stabilized zirconia, were studied using the 18O-exchange method to measure diffusivity in the range 900 to 1200 C. The materials span about three orders of magnitude in diffusivity, with D ranging from 10(exp -7) to 10(exp -10) sq cm/s at 1135 C. Zr3Sc4O12 and Y2O3 were found to have the lowest diffusivity, and the temperature dependence for all of the rare earth containing ceramics was similar. For the mixed oxides, there is no apparent trend correlating diffusivity and the crystal lattice dimensions. Porous microstructures in some of the materials, especially cubic-ZrO2 and Zr3Gd4O12, led to experimental O-18 exchange versus time curves which could not be easily fit to theoretical curves. Doping studies of SC(3+) and Ta(5+) in Zr3La4O12 showed no significant effect on diffusivity at 1135 C. GRA

N93-10399# Sandia National Labs., Albuquerque, NM.
SIMPLE SHEARING FLOW OF A 3D FOAM
A. M. Kraynik and D. A. Reinelt (Southern Methodist Univ., Dallas, TX.) 1992 3 p Presented at the 11th International Congress of Rheology, Brussels, Belgium, 17-21 Aug. 1992
(Contract DE-AC04-76DP-00789)
(DE92-011151; SAND-92-0429C; CONF-920852-3) Avail: CASI HC A01/MF A01

Foams, like most highly structured fluids, exhibited rheological behavior that is both fascinating and complex. We have developed microrheological models for uniaxial extension and simple shearing flow of a 'dry', perfectly ordered, three-dimensional foam composed of thin films with uniform surface tension, T, and negligible liquid content. We neglect viscous flow in the thin films and examine large elastic-plastic deformations of the foam. The primitive undeformed foam structure is composed of regular space-filling tetrakaidecahedra, which have six square and eight hexagonal surfaces. This structure possesses the film-network topology that is necessary to satisfy equilibrium: three films meet at each edge, which corresponds to a plateau border, and four edges meet at a vertex. However, to minimize surface energy, the films must meet at equal angles of 120 degrees and the edges must join at equal tetrahedral angles of cos exp -1(-1/3) approximately = 10.947 degrees. No film in an equilibrium foam structure can be a planar polygon because no planar polygon has all angles equal to the tetrahedral edge. In the equilibrium foam structure known as Kelvin's minimal tetrakaidecahedron, the 'squares' are planar quadrilateral surfaces with curved edges and the 'hexagons' are nonplanar saddle surfaces with zero mean curvature. As the foam structure evolves with the macroscopic flow, each film maintains zero mean curvature because the pressure is the same in every bubble. In general, the shape of each thin film, defined by z = h(x,y), satisfies 1/R(sub 1) + 1/R(sub 2) = del x ((del h)/(1 +

the absolute value of (del h))exp 1/2) where R sub 1(exp -1) and R sub 2(exp -2) are the principal curvatures. The appropriate boundary conditions correspond to three films meeting at equal angles. For the homogeneous deformations under consideration, the center of each film moves affinely with the flow. DOE

N93-10439# Pennsylvania State Univ., University Park. Center for Advanced Materials.

MECHANICAL BEHAVIOR OF OPEN CELL CERAMICS Topical Report, 1 Jun. 1986 - 31 Aug. 1990

R. M. Orenstein and D. J. Green Dec. 1991 122 p

(Contract GRI-5084-238-1302)

(PB92-212984; CAM-9007; GRI-91/0025) Avail: CASI HC A06/MF A02

The report describes the response of alumina-mullite foams subjected to severe thermal shock. Specimens of heated 92 percent alumina open cell foams were thermally shocked by immersion in water or oil. Two distinct temperature profiles were found during liquid quenching: (1) across the bulk foam due to heating of the fluid during infiltration into the foam; and (2) across the individual struts. The thermal shock resistance was quantified as the probability of crack extension in a strut as a function of quench severity (for one geometry), and the temperature difference required for a 10 percent reduction in bulk foam stiffness (for all geometries). For one series of thermally shocked specimens, it was shown that retained foam stiffness correlated with retained foam strength in bending and compression. The peak thermal stresses were coupled with the two-parameter Weibull distribution of the strut strengths to calculate the probability of crack extension on a strut, and with the mean strut strengths to calculate the thermal shock resistance parameters. Good agreement between the predicted and the measured crack extension probabilities was found. Thermal shock resistances of the open cell ceramics increased with increasing relative density and increasing cell size. GRA

N93-10578*# National Aeronautics and Space Administration. Langley Research Center, Hampton, VA.

LDEF MATERIALS WORKSHOP 1991, PART 2

Bland A. Stein, comp. and Philip R. Young, comp. Washington Sep. 1992 291 p Workshop held in Hampton, VA, 19-22 Nov. 1991

(RTOP 506-48-91-08)

(NASA-CP-3162-Pt-2; L-17135-Pt-2; NAS 1.55:3162-Pt-2) Avail: CASI HC A13/MF A03

The LDEF Materials Workshop 1991 was a follow-on to the Materials Sessions at the First LDEF Post-Retrieval Symposium held in Kissimmee, Florida, June 1991. The workshop comprised a series of technical sessions on materials themes, followed by theme panel meetings. Themes included materials, environmental parameters, and data bases; contamination; thermal control and protective coating and surface treatments; polymers and films; polymer matrix composites; metals, ceramics, and optical materials; lubricants adhesives, seals, fasteners, solar cells, and batteries. This document continues the LDEF Space Environmental Effects on Materials Special Investigation Group (MSIG) pursuit to investigate the effects of LEO exposure on materials which were not originally planned to be test specimens. Papers from the technical sessions are presented. For individual titles, see N93-10579 through N93-10592.

N93-10579*# National Aeronautics and Space Administration. Marshall Space Flight Center, Huntsville, AL.

SELECTED RESULTS FOR METALS FROM LDEF EXPERIMENT A0171 **c26**

Ann F. Whitaker *In* NASA. Langley Research Center, LDEF Materials Workshop 1991, Part 2 Sep. 1992 p 467-478 (For primary document see N93-10578 01-27)

Avail: CASI HC A03/MF A03

Metal specimens in disk type and ribbon configurations of interest to various programs at the Marshall Space Flight Center were exposed to the LEO environment for 5.8 years on Long Duration Exposure Facility (LDEF) Experiment A0171. Most of the metals flown were well heat sunk in the LDEF experiment tray which experienced benign temperatures, but a few metals were thermally isolated allowing them to experience greater thermal extremes. All metal specimens whose preflight weights were known showed a weight change as a result of exposure. Optical property and mass changes are attributed principally to atomic oxygen exposures. Silver and copper were grossly affected whereas tantalum, molybdenum, and several preoxidized alloys were the least affected. Metals contained in this experiment are shown. Results including mass, surface morphology, and optical property changes from selected evaluations of these metals are presented. Author

N93-10580*# European Space Agency. European Space Research and Technology Center, ESTEC, Noordwijk (Netherlands).

SOME RESULTS OF THE OXIDATION INVESTIGATION OF COPPER AND SILVER SAMPLES FLOWN ON LDEF **c26**

A. deRooij *In* NASA. Langley Research Center, LDEF Materials Workshop 1991, Part 2 Sep. 1992 p 479-490 (For primary document see N93-10578 01-27)

Avail: CASI HC A03/MF A03

The Long Duration Exposure Facility (LDEF) Mission provides a unique opportunity to study the long term effects of the space environment on materials. The LDEF has been deployed in orbit on 7 April 1984 by the shuttle Challenger in an almost circular orbit with a mean altitude of 477 km and an inclination of 28.5 degrees. It was retrieved from its decayed orbit of 335 km by the shuttle Columbia on 12 January 1990 after almost 6 years in space. The LDEF is a 12-sided, 4.267 m diameter, and 9.144 m long structure. The experiments, placed on trays, are attached to the twelve sides and the two ends of the spacecraft. The LDEF was passively stabilized with one end of the spacecraft always pointing towards the earth center and one of the sides (row 9) always facing the flight direction. The materials investigated originate from the Ultra-Heavy Cosmic Ray Experiment (UHCRE). The main objective is a detailed study of the charge spectra of ultraheavy cosmic-ray nuclei from zinc to uranium and beyond, using solid-state track detectors. Besides the aluminium alloy used for the experiment, UHCRE comprises several other materials. The results of space exposure for two of them, the copper grounding strips and the thermal covers (FEP Teflon/Ag/Inconel) painted black on the inner side (Chemglaze Z306), are presented. Author

N93-10581*# Boeing Co., Seattle, WA. Defense and Space Group.

CHANGES IN OXIDATION STATE OF CHROMIUM DURING LDEF EXPOSURE **c26**

Johnny L. Golden *In* NASA. Langley Research Center, LDEF Materials Workshop 1991, Part 2 Sep. 1992 p 491-500 (For primary document see N93-10578 01-27)

Avail: CASI HC A02/MF A03

The solar collector used for the McDonnell-Douglas Cascade Variable Heat Pipe, Experiment A0076 (Michael Grote - Principal Investigator) was finished with black chromium plating as a thermal control coating. The coating is metallic for low emittance, and is finely microcrystalline to a dimension which yields its high absorptivity. An underplate of nickel was applied to the aluminum absorber plate in order to achieve optimal absorptance characteristics from the black chromium plate surface. Experiment A0076 was located at tray position F9, receiving a projected 8.7 x 10 exp 21 atomic oxygen atoms/sq cm and 11,200 ESH solar radiation. During retrieval, it was observed that the aluminized kapton thermal blankets covering most of the tray were severely eroded by atomic oxygen, and that a 'flap' of aluminum foil was overlaying a roughly triangular shaped portion of the absorber panel. The aluminum foil 'flap' was lost sometime between the Long Duration Exposure Facility (LDEF) retrieval and deintegration. At deintegration, the black chromium was observed to have discolored where it had been covered by the foil 'flap'. A summary of the investigation into the cause of the discoloration is presented. Author

N93-10582*# National Aeronautics and Space Administration. Langley Research Center, Hampton, VA.
EFFECT OF SPACE EXPOSURE ON PYROELECTRIC INFRARED DETECTORS **c35**
James B. Robertson *In its* LDEF Materials Workshop 1991, Part 2 Sep. 1992 p 501-506 (For primary document see N93-10578 01-27)
Avail: CASI HC A02/MF A03

Pyroelectric detectors are one of the many different types of infrared radiation detectors. Pyroelectric detectors are of interest for long-term space use because they do not require cooling during operation. Also, they can detect at very long wavelengths and they have a relatively flat spectral response. A disadvantage is that the radiation must be chopped in order to be detected by a pyroelectric detector. The objective of the experiment was to determine the effects of launch and space exposure on the performance of commercially available pyroelectric detectors. The approach was to measure performance parameters of the detectors before and after flight on the Long-Duration Exposure Facility (LDEF) and determine the loss of detector performance. The experiment was passive; no data was taken during flight. Author

N93-10583*# Boeing Co., Seattle, WA. Defense and Space Group.
LONG DURATION EXPOSURE FACILITY (LDEF) OPTICAL SYSTEMS SIG SUMMARY AND DATABASE **c74**
Gail Bohnhoff-Hlavacek *In* NASA. Langley Research Center, LDEF Materials Workshop 1991, Part 2 Sep. 1992 p 507-512 (For primary document see N93-10578 01-27)
Avail: CASI HC A02/MF A03

The main objectives of the Long Duration Exposure Facility (LDEF) Optical Systems Special Investigative Group (SIG) Discipline are to develop a database of experimental findings on LDEF optical systems and elements hardware, and provide an optical system overview. Unlike the electrical and mechanical disciplines, the optics effort relies primarily on the testing of hardware at the various principal investigator's laboratories, since minimal testing of optical hardware was done at Boeing. This is because all space-exposed optics hardware are part of other individual experiments. At this time, all optical systems and elements testing by experiment investigator teams is not complete, and in some cases has hardly begun. Most experiment results to date, document observations and measurements that 'show what happened'. Still to come from many principal investigators is a critical analysis to explain 'why it happened' and future design implications. The original optical system related concerns and the lessons learned at a preliminary stage in the Optical Systems Investigations are summarized. The design of the Optical Experiments Database and how to acquire and use the database to review the LDEF results are described. Author

N93-10584*# Aerospace Corp., El Segundo, CA.
POLYMER MATRIX COMPOSITES ON LDEF EXPERIMENTS M0003-9 AND M0003-10
Gary L. Steckel, Thomas Cookson (General Dynamics Corp., San Diego, CA.), and Christopher Blair (Lockheed Missiles and Space Co., Sunnyvale, CA.) *In* NASA. Langley Research Center, LDEF Materials Workshop 1991, Part 2 Sep. 1992 p 515-542 (For primary document see N93-10578 01-27)
(Contract F04701-88-C-0089)
Avail: CASI HC A03/MF A03

Over 250 polymer matrix composites were exposed to the natural space environment on Long Duration Exposure Facility (LDEF) experiments M0003-9 and 10. The experiments included a wide variety of epoxy, thermoplastic, polyimide, and bismalimide matrix composites reinforced with graphite, glass, or organic fibers. A review of the significant observations and test results obtained to date is presented. Estimated recession depths from atomic oxygen exposure are reported and the resulting surface morphologies are discussed. The effects of the LDEF exposure on the flexural strength and modulus, short beam shear strength, and coefficient of thermal expansion of several classes of bare and coated composites are reviewed. Lap shear data are presented for composite-to-composite and composite-to-aluminum alloy samples that were prepared using different bonding techniques and subsequently flown on LDEF. Author

N93-10585*# Boeing Co., Seattle, WA. Defense and Space Group.
SPACE ENVIRONMENTAL EFFECTS ON LDEF LOW EARTH ORBIT EXPOSED GRAPHITE REINFORCED POLYMER MATRIX COMPOSITES
Pete George *In* NASA. Langley Research Center, LDEF Materials Workshop 1991, Part 2 Sep. 1992 p 543-570 (For primary document see N93-10578 01-27)
Avail: CASI HC A03/MF A03

The Long Duration Exposure Facility (LDEF) was deployed on April 7, 1984 in low earth orbit (LEO) at an altitude of 482 kilometers. On board experiments experienced the harsh LEO environment including atomic oxygen (AO), ultraviolet radiation (UV), and thermal cycling. During the 5.8 year mission, the LDEF orbit decayed to 340 kilometers where significantly higher AO concentrations exist. LDEF was retrieved on January 12, 1990 from this orbit. One experiment on board LDEF was M0003, Space Effects on Spacecraft Materials. As a subset of M0003 nearly 500 samples of polymer, metal, and glass matrix composites were flown as the Advanced Composites Experiment M0003-10. The Advanced Composites Experiment is a joint effort between government and industry with the Aerospace Corporation serving as the experiment integrator. A portion of the graphite reinforced polymer matrix composites were furnished by the Boeing Defense and Space Group, Seattle, Washington. Test results and discussions for the Boeing portion of M0003-10 are presented. Experiment and specimen location on the LDEF are presented along with a quantitative summary of the pertinent exposure conditions. Matrix materials selected for the test were epoxy, polysulfone, and polyimide. These composite materials were selected due to their suitability for high performance structural capability in spacecraft applications. Graphite reinforced polymer matrix composites offer higher strength to weight ratios along with excellent dimensional stability. The Boeing space exposed and corresponding ground control composite specimens were subjected to post flight mechanical, chemical, and physical testing in order to determine any changes in critical properties and performance characteristics. Among the more significant findings are the erosive effect of atomic oxygen on leading edge exposed specimens and microcracking in non-unidirectionally reinforced flight specimens. Author

N93-10586*# Toronto Univ. (Ontario). Inst. for Aerospace Studies.
ADDITIONAL RESULTS ON SPACE ENVIRONMENTAL EFFECTS ON POLYMER MATRIX COMPOSITES: EXPERIMENT A0180
R. C. Tennyson *In* NASA. Langley Research Center, LDEF Materials Workshop 1991, Part 2 Sep. 1992 p 571-592 (For primary document see N93-10578 01-27)
Avail: CASI HC A03/MF A03

Additional experimental results on the atomic oxygen erosion of boron, Kevlar, and graphite fiber reinforced epoxy matrix composites are presented. Damage of composite laminates due to micrometeoroid/debris impacts is also examined with particular emphasis on the relationship between damage area and actual hole size due to particle penetration. Special attention is given to one micrometeoroid impact on an aluminum base plate which resulted in ejecta visible on an adjoining vertical flange structure. Author

N93-10587*# Toronto Univ. (Ontario). Inst. for Aerospace Studies.
PROPOSED TEST PROGRAM AND DATA BASE FOR LDEF POLYMER MATRIX COMPOSITES
R. C. Tennyson, Pete George (Boeing Co., Seattle, WA.), Gary L. Steckel (Aerospace Corp., El Segundo, CA.), and D. G. Zimcik (Canadian Space Agency, Ottawa, Ontario) *In* NASA. Langley Research Center, LDEF Materials Workshop 1991, Part 2 Sep.

1992 p 593-600 (For primary document see N93-10578 01-27)
Avail: CASI HC A02/MF A03

A survey of the polymer matrix composite materials that were flown on Long Duration Exposure Facility (LDEF) is presented with particular attention to the effect of circumferential location (alpha) on the measured degradation and property changes. Specifically, it is known that atomic oxygen fluence (AO), VUV radiation dose, and number of impacts by micrometeoroids/debris vary with alpha. Thus, it is possible to assess material degradation and property damage changes with alpha for those materials that are common to three or more locations. Once the alpha-dependence functions were defined, other material samples will provide data that can readily be used to predict damage and property changes as a function of alpha as well. What data can be realistically obtained from these materials, how this data can be obtained, and the scientific/design value of the data to the user community is summarized. Finally, a proposed test plan is presented with recommended characterization methodologies that should be employed by all investigators to ensure consistency in the data base that will result from this exercise. Author

N93-10588*# Boeing Aerospace Co., Seattle, WA.
IDENTIFICATION AND EVALUATION OF LUBRICANTS, ADHESIVES, AND SEALS USED ON LDEF
Bruce Keough *In* NASA. Langley Research Center, LDEF Materials Workshop 1991, Part 2 Sep. 1992 p 603-618 (For primary document see N93-10578 01-27)
Avail: CASI HC A03/MF A03

A variety of lubricants, adhesives, and seals were flown on Long Duration Exposure Facility (LDEF). They were used in the fabrication and assembly of the experiments similar to other spacecraft applications. Typically, these materials were not exposed to U.V. radiation or atomic oxygen, except possibly around the perimeter of the joints. Most of these materials were of secondary interest and were only investigated by visual examination and a 'Did they fall?' criteria. Because of this role, most applications had only a few specimens, not enough for statistical data generation. Often, no control samples were kept, and documentation of what was used was occasionally sketchy.
Author

N93-10589*# Boeing Aerospace Co., Seattle, WA.
RESULTS FROM THE TESTING AND ANALYSIS OF LDEF BATTERIES **c33**
Steve Spear, Harry Dursch, and Chris Johnson *In* NASA. Langley Research Center, LDEF Materials Workshop 1991, Part 2 Sep. 1992 p 619-631 (For primary document see N93-10578 01-27)
Avail: CASI HC A03/MF A03

Batteries were used on the Long Duration Exposure Facility (LDEF) to provide power to both the active experiments and the experiment support equipment such as the Experiment Initiative System, Experiment Power and Data System (data acquisition system), and the Environment Exposure Control Canisters. Three different types of batteries were used: lithium sulfur dioxide (LiSO2), lithium carbon monofluoride (LiCF), and nickel cadmium (NiCd). A total of 92 LiSO2, 10 LiCF, and 1 NiCd batteries were flown on the LDEF. In addition, approximately 20 LiSO2 batteries were kept in cold storage at NASA LaRC. The various investigations and post-flight analyses of the flight and control batteries are reviewed. The primary objectives of these studies was to identify degradation modes (if any) of the batteries and to provide information useful to future spacecraft missions. Systems SIG involvement in the post-flight evaluation of LDEF batteries was two-fold: (1) to fund SAFT (original manufacturer of the LiSO2 batteries) to perform characterization of 13 LiSO2 batteries (10 flight and 3 control batteries); and (2) to integrate investigator results. Author

N93-10590*# Boeing Aerospace Co., Seattle, WA.
EFFECTS OF LONG-TERM EXPOSURE ON LDEF FASTENER ASSEMBLIES **c37**
Steve Spear and Harry Dursch *In* NASA. Langley Research Center, LDEF Materials Workshop 1991, Part 2 Sep. 1992 p 633-648 (For primary document see N93-10578 01-27)
Avail: CASI HC A03/MF A03

This presentation summarizes the Systems Special Investigations Group (SIG) findings from testing and analysis of fastener assemblies used on the Long Duration Exposure Facility (LDEF) structure, the tray mounting clamps, and by the various experimenters. The LDEF deintegration team and several experimenters noted severe fastener damage and hardware removal difficulties during post-flight activities. The System SIG has investigated all reported instances, and in all cases examined to date, the difficulties were attributed to galling during installation or post-flight removal. To date, no evidence of coldwelding was found. Correct selection of materials and lubricants as well as proper mechanical procedures is essential to ensure successful on-orbit or post-flight installation and removal of hardware.
Author

N93-10591*# Boeing Aerospace Co., Seattle, WA.
RESULTS FROM TESTING AND ANALYSIS OF SOLAR CELLS FLOWN ON LDEF **c44**
Harry Dursch *In* NASA. Langley Research Center, LDEF Materials Workshop 1991, Part 2 Sep. 1992 p 649-660 (For primary document see N93-10578 01-27)
Avail: CASI HC A03/MF A03

A brief discussion of the solar cell experiments flown on the Long Duration Exposure Facility (LDEF) is provided. The information presented is a collation of results published by the various experimenters. This process of collation and documentation is an ongoing Systems Special Investigation Group (SIG) effort. There are four LEO environments, operating individually and/or synergistically, that cause performance loss in solar cells: meteoroid and space debris, atomic oxygen, ultraviolet radiation, and charged particle radiation. In addition, the effects of contamination caused by outgassing of materials used on the specific spacecraft play a role in decreasing the light being transmitted through the coverglass and adhesive to the solar cell. From the results presented on the solar cells aboard LDEF, the most extensive degradation of the solar cells came from impacts and the resulting cratering. The extent of the damage to the solar cells was largely dependent upon the size and energy of the meteoroids or space debris. The other cause of degradation was reduced light reaching the solar cell. This was caused by contamination, UV degradation of coverglass adhesive, and/or atomic oxygen/UV degradation of antireflection coatings. Author

N93-10592*# Centre National d'Etudes Spatiales, Toulouse (France).
SYSTEM RELATED TESTING AND ANALYSIS OF FRECOPA **c37**
Christian Durin *In* NASA. Langley Research Center, LDEF Materials Workshop 1991, Part 2 Sep. 1992 p 661-676 (For primary document see N93-10578 01-27)
Avail: CASI HC A03/MF A03

Results from the French Cooperative Payload (FRECOPA) system analysis are presented. It was one of the numerous experiments which were flown on the Long Duration Exposure Facility (LDEF) satellite. In our flight configuration (LEO orbit, trailing edge), the environment was a better vacuum than the leading edge, with many thermal cycles (32000) and a large amount of UV radiation (11100 equivalent sun hours). Also, the satellite was mainly bombarded by micro-particles. It saw a low atomic flux and minor doses of protons and electrons. Author

N93-10627# Ibiden Co. Ltd., Ogaki (Japan).
CONDUCTIVE TITANATE FIBER AND ITS PRODUCTION METHOD
Yoshiya Matsuno and Ryo Enomoto 1991 11 p Transl. into ENGLISH of Japanese Patent No. SHO-63(1988)-252928 (20 Oct. 1988) Prepared for Oak Ridge National Lab., TN
(Contract DE-AC05-84OR-21400)
(DE92-014738; ORNL/TR-91/39) Avail: CASI HC A03/MF A01

This invention is concerned with a conductive titanium fiber and its production method; in addition a patent is applied for techniques related to a fiber having good reinforcement and surface smoothness, and that is especially suitable as a filler for conductive plastics. This patent application describes the invention, a conductive fiber, and associated process for fabrication. DOE

N93-10632# Brown Univ., Providence, RI.
HIGH TEMPERATURE FATIGUE CRACK GROWTH IN CERAMICS AND CERAMIC COMPOSITES
S. Suresh 29 Jun. 1992 4 p
(Contract DE-FG02-84ER-45167)
(DE92-016835; DOE/ER-45167/7) Avail: CASI HC A01/MF A01

This three-year program (8/1990-7/1993) is aimed at developing a detailed quantitative understanding of the elevated temperature fracture properties of ceramics and ceramic-matrix composites. In the second year (8/1991-7/1992), considerable progress had been made in our experimental studies and numerical modelling of deformation and fracture in ceramics composites at ambient and elevated temperatures. As part of this effort, new experimental techniques have already been developed for the study of elevated temperature fracture in brittle materials in direct tension loading. The newly set-up facility is now in operation. Furthermore, new experimental results based on quantitative transmission electron microscopy are obtained on high-temperature phase transformations in SiC-whisker-reinforced alumina which have important implications for high-temperature fracture properties. The initially proposed work on the role of glass phase on the high-temperature fracture and fatigue response has been completed. Finite element analyses of cyclic damage zones ahead of tensile and compressive fatigue cracks in ceramic materials have been completed using several different constitutive models for matrix materials. DOE

N93-10727# Massachusetts Inst. of Tech., Cambridge. Dept. of Chemistry.
SYNTHESIS OF SIDE CHAIN LIQUID CRYSTAL POLYMERIZATION BY LIVING RING OPENING METATHESIS POLYMERIZATION. REPORT 1: INFLUENCE OF MOLECULAR WEIGHT, POLYDISPERSITY, AND FLEXIBLE SPACER LENGTH (N=2-8) ON THE THERMOTROPIC BEHAVIOR OF THE RESULTING POLYMERS
Zen Komiya, Coleen Pugh, and Richard R. Schrock 31 Mar. 1992 39 p
(Contract N00014-89-J-1542)
(AD-A248699; TR-13-Rept-1) Avail: CASI HC A03/MF A01

The living ring opening metathesis polymerization of 5-carbo (n-((4'-methoxy-4-biphenylyl)oxy)alkyl) bicyclo(2.2.1)hept-2-ene (1-n, n=2-8) by Mo(CH-t-Bu)(NAr)(0-t-Bu)2 (Ar=2,6-C6H3-t-Pr2) is described. Polymers with degrees of polymerization from 5 to 100 and narrow molecular weight distributions (M sub w / M sub n = 1.05-1.24) were obtained in high yield. All polymers exhibit an enantiomorphic nematic mesophase. Glass transition and isotropization temperatures increase with increasing molecular weight and become independent at approximately 30-50 repeat units. The change in enthalpy of isotropization is relatively independent of molecular weight. Using polymer blends, it was shown that polydispersity has no effect on either the transition temperatures or the temperature range of isotropization. Isotropization alternates in an odd-even manner up to spacer lengths of n=6, and then levels off. Living ring opening metathesis polymerization, GRA

N93-10748# Pittsburgh Univ., PA. Dept. of Chemistry.
TRANSFORMATION OF Cl BONDING STRUCTURES ON Si(100)-(2X1)
C. C. Cheng, Q. Gao, W. J. Choyke, and J. T. Yates, Jr. 22 Jun. 1992 24 p
(Contract N00014-82-C-0280)
(AD-A253739; TR-48) Avail: CASI HC A03/MF A01

The digital electron stimulated desorption ion angular distribution (ESDIAD) method has been used to observe the existence and the irreversible thermal transformation between different bonding structures for Cl on the Si(100)(2x1) surface. The ESDIAD pattern produced from dissociative chemisorption of Cl2 at 120 K shows intense normal emission of Cl+, plus lower intensity of Cl+ emission focused along the (011) and (011) axes (the axes of Si2 dimer orientations in two domains). Upon annealing to higher temperatures (T less than or equal to 673 K), the Cl+ -ESDIAD pattern is irreversibly transformed into a four-beam pattern with a two-fold azimuthal symmetry in the plane of each dimer axis, indicative of Si-Cl bonds inclined 25 deg + or - 4 deg from the surface normal. This irreversible thermal behavior indicates that the four-beam ESDIAD pattern represents the lower-energy bonding configuration for Cl on the Si(100)-(2x1) surface. The broad temperature range (delta T approx. 300 K) associated with the complete transformation suggests that a kinetic process, involving a constant activation energy and preexponential factor, is not appropriate for describing the structural conversion process. GRA

N93-10766# Pennsylvania Univ., Philadelphia. Dept. of Materials Science and Engineering.
PLASTICITY OF SINGLE CRYSTALLINE Al3X INTERMETALLIC COMPOUNDS Final Report, 1 Nov. 1988 - 31 Dec. 1991
V. Vitek, D. P. Pope, and D. E. Luzzi 29 Jun. 1992 16 p
(Grant AF-AFOSR-0062-89)
(AD-A254282; AFOSR-92-0765TR) Avail: CASI HC A03/MF A01

Single crystals of six different compositions were grown, five of Al3Ti + Fe and one of Al3TI + Cr. The flow stress was measured as a function of temperature, orientation and composition. Al2Ti precipitates are the major strengthening phase and form platelets on the 100 planes of the L12 matrix. Deformation occurs primarily by group of zone axes (110) 111 slip, with SISF dissociation at low temperatures and by APB dissociation at high temperatures. Simulations of dislocation cores using many body potentials have revealed a variety of core configurations in the L12 and DO22 form, all of which are sessile and one of which provides a twinning mechanism. GRA

N93-10770# Air Force Inst. of Tech., Wright-Patterson AFB, OH.
MEASUREMENT OF AERODYNAMIC SHEAR STRESS USING SIDE CHAIN LIQUID CRYSTAL POLYMERS M.S. Thesis
Carlo G. Demandante 1992 75 p
(AD-A254312; AFIT/CI/CIA-92-067) Avail: CASI HC A04/MF A01

A novel concept was proposed exploiting the optical property response of liquid crystalline materials to various external effects. This study determined the feasibility of using side chain liquid crystal polymers as aerodynamic shear sensors. A method was developed to observe and measure the optical birefringent response of film coatings made from these polymer materials due to applied shear. Different polymers were synthesized, spray-coated, and tested for their shear-sensing potential. Empirical results confirmed the promise of this method on future aerodynamic testing. GRA

N93-10778# National Inst. of Standards and Technology, Gaithersburg, MD.
GROWTH DEFECTS IN DIAMOND FILMS
D. Shechtman, J. L. Hutchison, L. H. Robins, E. N. Farabaugh, and A. Feldman 9 Jul. 1992 27 p
(Contract N00014-90-F-0011)
(AD-A253618; NIST-TR-13) Avail: CASI HC A03/MF A01

Growth defects in diamond films grown by plasma-assisted chemical vapor deposition (CVD) were studied by high resolution electron microscopy. Several features of the microstructure were resolved and their importance to the growth of the diamond film was evaluated. The observations included various twin boundaries of the type sigma=3 as well as sigma=9, sigma=27 and sigma=81, which form by an interaction of lower order twins. These higher order boundaries, are loci of intersection points of

growing planes on two adjacent twins and can serve as an indicator for the local crystal growth direction. The central nucleation site for the growing planes in many cases can be traced back to a quintuplet twin point. A twin quintuplet has five reentrant angles and thus serves as a preferred nucleation site for new planes as the crystal grows. GRA

N93-10779# National Inst. of Standards and Technology, Gaithersburg, MD. Ceramics Div.
A FUNDAMENTAL UNDERSTANDING OF THE EFFECTS OF CERAMIC PROCESSING ON PRODUCT MICROSTRUCTURE Interim Report
Gabrielle Long, James Cline, and Jose Ritter 15 Feb. 1992 57 p
(Contracts ARO-MIPR-120-89; ARO-MIRO-120-90)
(AD-A253660; ARO-26126.3-MS) Avail: CASI HC A04/MF A01

This is the final report arising from our research program involving the investigation of processing/microstructure relationships in selected ceramic systems. The first year of this program was dedicated to the development and detailed assessment of the novel neutron scattering and x-ray diffraction techniques required for the measurement of ceramic microstructure evolution as a function of sintering and chemistry. The next two years of the program were used to study several systems in detail, and has led to some remarkable conclusions which have changed the way in which the sintering stages in different systems are understood. The sintering behavior of a ceramic body and the properties of the ceramic product depend directly on the internal microstructure. The goal of our research program with the ARO has been to investigate well-characterized systems and to measure microstructure evolution during ceramic processing in order to obtain an improved understanding of the relationships between processing and microstructure. This approach has led to progress in improving process models and to improved predictability of product microstructure. GRA

N93-10783# Research Triangle Inst., Research Triangle Park, NC.
RESEARCH AND DEVELOPMENT OF TWO MARINE-DEGRADABLE BIOPOLYMERS Report, 1 Oct. 1989 - 30 Sep. 1990
Anthony L. Andrady, Jan E. Pegram, and Todd M. Olson Mar. 1992 49 p
(AD-A254051; DTRC/SME-CR-19-90) Avail: CASI HC A03/MF A01

The Navy is developing a biopolymeric film material suitable for fabrication into marine-disposable trash bags so that it can comply with impending national and international requirements which will prohibit the discharge of plastics into the sea. Two biopolymers, chitosan and regenerated cellulose, were selected and tested to meet this need. After 6 weeks of marine exposure, regenerated cellulose samples disappeared; after 10 weeks, chitosan samples became brittle and separated. While chitosan showed greater anaerobic degradation than regenerated cellulose in soil studies, the opposite occurred in the marine sediment environment. Aerobic degradation was much higher than anaerobic degradation for both biopolymers. To improve flexibility, 50 plasticizers were tested in chitosan. Ten percent lithium bromide and 5 percent lithium acetate/10 percent PEG 400 in chitosan were the most effective plasticizers. Regenerated cellulose films treated with lithium salt solutions also showed improved flexibility. Incorporating urea and potassium phosphate into cellulose showed that degradation could be increased in soil. Tests are ongoing to further accelerate the rate of biodegradation by increasing the availability of nitrogen and phosphorus. Fabricating trash bags will require adhesive bonding. Five adhesives were evaluated with regenerated cellulose. Covinax 220, JW 2-47, and Adcote 333T proved acceptable. Chitosan requires further development to be produced and processed into bags efficiently. With minor adjustments, regenerated cellulose presently meets this requirement; thus, it is the more promising film. Progress towards our goal of developing a biopolymeric film material meeting the Navy's requirements is continuing. GRA

N93-10825# Case Western Reserve Univ., Cleveland, OH. Dept. of Macromolecular Science.
HIERARCHICAL STRUCTURE IN POLYMERIC SOLID AND ITS INFLUENCE ON PROPERTIES Final Report, 15 Jul. 1988 - 31 Mar. 1992
Eric Baer, A. Hiltner, J. X. Li, and S. Bazhenov 11 Jun. 1992 11 p
(Contract DAAL03-88-K-0097)
(AD-A253818; ARO-25193.9-MS) Avail: CASI HC A03/MF A01

The research project involves two interrelated areas of investigation which are directed toward obtaining a fundamental understanding of the interrelationships between the structure and mechanical function of the collagen network of the intestine. The approach is soundly based on knowledge gained over the past 10 years in the study of tendon. Current studies of the hierarchical organization of intestinal collagen were extended in order to develop mechanical models which consider the actual multicomposite structure of the structural protein. This approach led to an understanding of the age-dependence of mechanical properties and of structural changes at the various levels of organization. A comparison of different tissues which function under a variety of stress conditions is extremely important for developing a fundamental understanding of the relationships between the organization of structural proteins. GRA

N93-10005 Olin Corp., Cheshire, CT.
SYNTHESIS AND CHARACTERIZATION OF ENERGETIC POLYMERS
Eugene Rothgery, R. Hani, R. Dumas, M. Shen, D. Gavin, R. Day, J. Necessary, and Gerry Traylor *In* JHU, The 1992 JANNAF Propulsion Meeting, Volume 1 Feb. 1992 p 111-117 Prepared in cooperation with Olin Corp., Brandenburg, KY (For primary document see N93-10001 01-20)
Avail: CPIA, 10630 Little Patuxent Pkwy., Suite 202, Columbia, MD, 21044-3200 HC

N93-10006 Naval Weapons Center, China Lake, CA.
THE EFFECT OF ELEVATED TEMPERATURES ON THE PROPERTIES OF THERMALLY STABLE SILICON-BASED ELASTOMERS FOR ADHESIVES, SEALANTS, AND INSULATOR APPLICATIONS
Robert A. Rhein and James C. Baldwin *In* JHU, The 1992 JANNAF Propulsion Meeting, Volume 1 Feb. 1992 p 119-141 (For primary document see N93-10001 01-20)
Avail: CPIA, 10630 Little Patuxent Pkwy., Suite 202, Columbia, MD, 21044-3200 HC

N93-10025 Minnesota Mining and Mfg. Co., Saint Paul. Industrial Chemical Products Div.
GAP BENEFITS
Peter F. Aiello and Anthony P. Manzara *In* JHU, The 1992 JANNAF Propulsion Meeting, Volume 1 Feb. 1992 p 399-405 (For primary document see N93-10001 01-20)
Avail: CPIA, 10630 Little Patuxent Pkwy., Suite 202, Columbia, MD, 21044-3200 HC

28 PROPELLANTS AND FUELS

Includes rocket propellants, igniters, and oxidizers; their storage and handling procedures; and aircraft fuels.

For related information see also *07 Aircraft Propulsion and Power, 20 Spacecraft Propulsion and Power,* and *44 Energy Production and Conversion.*

N93-10216# Arkansas Univ., Fayetteville.
BIOLOGICAL PRODUCTION OF ETHANOL FROM COAL
1991 29 p
(Contract DE-AC22-89PC-89876)

(DE92-016116; DOE/PC-89876/T14; PETC-2-5-91) Avail: CASI HC A03/MF A01

Research is continuing in attempting to increase both the ethanol concentration and product ratio from the C. ljungdahlii fermentation. Both batch and continuous reactors are being used for this purpose. The purpose of this report is as follows. (1) The data presented in PETC Report No. 2-4-91 (June-September 1991) are analyzed and interpreted using normalized specific growth and production rates. This technique eliminates experimental variation due to the differences in inoculum history. (2) The effects of the sulfur gases H2S and COS on the performance of C. ljungdahlii are presented and discussed. Although these are preliminary results, they illustrate the tolerance of the bacterium to low levels of sulfur gases. (3) The results of continuous stirred tank reactor studies are presented, where cell and product concentrations are shown as a function of agitation rate and gas flow rate. Finally, additional data are presented showing the performance of C. ljungdahlii in a CSTR with cell recycle. DOE

N93-10267# California Univ., San Diego.
THEORY OF COMBUSTION OF LIQUID PROPELLANTS BASED ON HYDROXYLAMMONIUM NITRATE Final Report
Forman A. Williams 29 Jan. 1992 7 p
(Contract DAAL03-89-K-0011)
(AD-A248445) Avail: CASI HC A02/MF A01

Deflagration velocities of liquid propellants based on hydroxylammonium nitrate are controlled by the chemistry of decomposition of this oxidizer in aqueous solutions. Theory was developed for the deflagration velocity and its dependence on oxidizer concentration, giving excellent agreement with experiment and suggesting that the rate of the initial proton-transfer step determines the deflagration rate. Nitramine deflagration also was considered, with two-phase flow in the reaction zone taken into account, employing empirical one-step Arrhenius chemistry. Although excellent agreement of theoretical deflagration rates with experiment was obtained from 0.5 to 10(exp 3) atmospheres, attempts to relate the one-step rate constants to rates of known elementary steps were only partially successful. Asymptotic analysis was also completed for the structure and burning velocity of carbon monoxide-nitrous oxide flames, which have some relevance to propellant deflagration. For these last flames, there is good agreement with numerical integrations, and differences from experiment are explicable. In general, the research advances our understanding of homogeneous propellant deflagration. GRA

N93-10268# Dayton Univ. Research Inst., OH.
POLYNITRO POLYCYCLIC CAGE COMPOUNDS Interim Report, 1 Nov. 1989 - 30 Apr. 1991
Suresh C. Suri Mar. 1992 20 p
(Contract F04611-88-C-0020)
(AD-A252889; UDR-TR-91-20; PL-TR-91-3089; AD-E201061)
Avail: CASI HC A03/MF A01

The objective of this project is to synthesize advanced propellant ingredients of the propulsion system. This task is divided into two categories: Synthesis of new strained molecules; Study of thermochemical properties of new strained molecules. This report covers the efforts towards synthesis of new pentanitrobis-homocubane and its isomer. During the course of this synthetic endeavor a novel base-promoted eliminative cyclization was observed which lead to the synthesis of two new functionalized strained ring systems: Tetracyclo(6.2.1.0(2,7).0(4,10)) - undecane and Tetracyclo(5.3.0.0(2,6).0(5,9)) decane. GRA

N93-10313 Georgia Inst. of Tech., Atlanta.
MULTIDIMENSIONAL EFFECTS IN COMPOSITE PROPELLANT COMBUSTION Ph.D. Thesis
Sung-Taick Lee 1991 180 p
Avail: Univ. Microfilms Order No. DA9206099

This research was directed toward clarification of the combustion of oxidizer-fuel complexes in heterogeneous solid propellant combustion. Earlier studies used edge burning of oxidizer-fuel laminae as a means to geometrically simplify the details of solid propellant combustion. In the present studies, different sizes of AP particles (10 microns, 33.5 microns, and 41 microns) were included in the binder lamina to investigate how individual AP particles burn and how their combustion couples with the rather well studied sandwich results. In such experiments, the oxidizer laminae played the role of large AP particles, and the AP-filled lamina corresponds to the AP-filled matrix between large particles in the solid propellant. It was relatively easy to test the effects of AP to binder ratio in the lamina (5:5 and 7:3), the effect of AP particle sizes, and of thickness of the matrix lamina. Combustion photography was used for the measurement of sample burning rates at different pressures for several AP-filled binder thicknesses. Optical and scanning electron microscopes were employed to provide information on the surface details of AP particles in the AP-filled binder, the interface region between the oxidizer and AP-filled binder, and surface profiles of the samples. It was observed that the establishment of individual oxidizer-binder flames does not occur for small AP particles and/or low pressure, whereas the AP particle flame was established for large AP particles and/or high pressure. Roles of the LEFs in more complex systems than conventional sandwiches and flamelet interaction were also investigated. Insights into the different modes of burning of heterogeneous systems resulting from pressure effects, AP particle size effects, and different AP/binder mix ratios were also investigated. The burning rates of 5:5 (10 microns), 5:5 (33.5 microns), 7:3 (10 micrometers), and 7:3 (33.5 micrometers) AP-filled sandwiches were plotted as a function of matrix thickness, and compared with each other at 300, 500, and 1000 psi. Considering the role of the LEF's, flamelet interaction between large and small AP particles, different modes of burning of heterogeneous systems resulting from pressure effects, AP particle size effects, and different AP/binder mix ratios, the qualitative theory of a flame complex described earlier for PBAN binder was developed for the case of AP particles in the binder. This new expanded flame theory is able to qualitatively predict the burning rate trends, overall surface profiles, and multidimensional flame structures at each pressure and matrix combination. Dissert. Abstr.

N93-10329# Morgantown Technology Center, WV.
TEMPERATURE-PROGRAMMED OXIDATION OF ETHANE AND ETHYLENE IN THE PRESENCE AND ABSENCE OF C-13 LABELED METHANE
A. Shamsi 1992 19 p Presented at the US DOE Contractor Review Meeting on Natural Gas Research and Development, Morgantown, WV, 5-6 May 1992
(DE92-015048; DOE/METC-C/92/7017; CONF-920584-20)
Avail: CASI HC A03/MF A01

The objective of this project is to perform short- and long-term studies to identify new concepts and technological barriers for the development of a process to convert natural gas to liquid fuels. Temperature-programmed oxidation of ethane and ethylene in the presence and absence of C-13 labeled methane was conducted to determine the relative reactivity of ethane and ethylene compared to methane. DOE

N93-10336# Aerospace Corp., El Segundo, CA. Technology Operations.
RATE CONSTANTS FOR REACTIONS OF HYDRAZINE FUELS WITH O(P-3)
Valerie I. Lang 15 Feb. 1992 22 p
(Contract F04701-88-C-0089)
(AD-A252813; TR-0091(6940-07)-2; SSD-TR-92-20) Avail: CASI HC A03/MF A01

Room temperature rate constants for the reactions of three hydrazine fuels with O(P-3) were measured. A laser-photolysis resonance fluorescence technique was used in the experiments. The reactions were monitored by the decay of 131 nm, O((S-3)(P-3)) resonance fluorescence under both high pressure (-50 Torr) and low pressure (1 to 3 Torr) conditions. The measured rate constants were 0.99 (+/- 0.12 x 10(exp -11) cubic cm molecule(sup -1) s(sup -1) for N2H4, 1.6 (+/- 0.34) x 10(exp -11) cubic cm molecule(sup -1) s(sup -1) for CH3HN2H2, and 2.3 (+/- 0.34) x 10(exp -11) cubic cm molecules(sup -1) s(sup -1) for (CH3)2N2H2,

all at 296 K. The rate constants increase with the number of hydrogen atoms per hydrazine molecule. GRA

N93-10608# Arkansas Univ., Fayetteville.
BIOLOGICAL PRODUCTION OF ETHANOL FROM COAL
1991 27 p
(Contract DE-AC22-89PC-89876)
(DE92-016114; DOE/PC-89876/T12; PETC-2-2-91) Avail: CASI HC A03/MF A01

Previously studies have shown the importance of both medium composition and concentration and medium pH on ethanol production of Clostridium ljungdahlii in fermenting CO, CO2, and H2 in synthesis gas. Four additional batch experiments involving medium composition and concentration were carried out in modified basal medium without yeast extract at pH 4.0. These experiments indicate that basal medium with only small amounts of B-vitamins can yield significant cell growth while yielding ethanol as the major product. Product ratios as high as 11.0 g ethanol per g acetate were obtained with half strength B-vitamins. Further experiments indicates that Ca-pantothenate may be necessary for the growth of C. ljungdahlii and that growth and ethanol production can occur simultaneously. DOE

N93-10636# Pharmakon Research International, Inc., Waverly, PA.
LIMITED TOXICITY AND MUTAGENICITY TESTING OF FIVE UNICHARGE PROPELLANT COMPOUNDS Final Report, 20 Sep. - 31 Dec. 1991
Vincent B. Ciofalo and Victor T. Mallory 31 Jan. 1992 36 p
(Contract DAMD17-91-C-1140)
(AD-A252339) Avail: CASI HC A03/MF A01

Bis (2,2-dinitropropyl) acetal/formal (-50/50 mixture) +/diphenyl amine stabilizer (BDNPA/F+/-DPA) were tested for oral toxicity. Groups of ten rats per dose level were fasted and administered the test article orally by gavage. Animals were observed for clinical signs and mortality at 1 and 4 hours after dosing and once daily for 14 days. Based upon the results of these assays, the definitive acute oral LD50 (combined sexes) for BDNPA/F+DPA was determined to be 4791.1 mg/kg with 95 percent confidence limits of 3057.7 to 7507.2 mg/kg. The definitive acute oral LD50 for BDNPA/F-DPA was determined to be 3718.3 mg/kg with 95 percent confidence limits of 3311.2 to 4175.3 mg/kg. GRA

N93-10004 Naval Weapons Center, China Lake, CA.
IMPACT SENSITIVITY REDUCTION VIA EXO-ELECTRON CONTROL
Robert A. Rhein, Russell Reed, and Ngo Q. Vu *In* JHU, The 1992 JANNAF Propulsion Meeting, Volume 1 Feb. 1992 p 103-109 (For primary document see N93-10001 01-20)
Avail: CPIA, 10630 Little Patuxent Pkwy., Suite 202, Columbia, MD, 21044-3200 HC

N93-10026*# Jet Propulsion Lab., California Inst. of Tech., Pasadena.
INVESTIGATION OF THE STIMULATED RELEASE OF GASEOUS AMMONIA FROM AMMONIUM PERCHLORATE BY HTPB SOLID PROPELLANT BONDING AGENTS
James C. McComb *In* JHU, The 1992 JANNAF Propulsion Meeting, Volume 1 Feb. 1992 p 407-418 Sponsored by NASA, Washington (For primary document see N93-10001 01-20)
Avail: CPIA, 10630 Little Patuxent Pkwy., Suite 202, Columbia, MD, 21044-3200 HC

N93-10027*# Thiokol Corp., Brigham City, UT.
EFFECTS OF THE RSRM GRAIN DEFORMATION ON BALLISTIC PERFORMANCE
Boyd J. Hutchison and P. J. Downey *In* JHU, The 1992 JANNAF Propulsion Meeting, Volume 1 Feb. 1992 p 419-426 (For primary document see N93-10001 01-20)
(Contract NAS8-30490)
Avail: CPIA, 10630 Little Patuxent Pkwy., Suite 202, Columbia, MD, 21044-3200 HC

N93-10028 Jet Propulsion Lab., California Inst. of Tech., Pasadena.
ALTERNATIVES IN CLEAN PROPELLANTS FOR LARGE SCALE MAN-RATED SOLID ROCKET MOTORS
James C. McComb *In* JHU, The 1992 JANNAF Propulsion Meeting, Volume 1 Feb. 1992 p 427-438 (For primary document see N93-10001 01-20)
Avail: CPIA, 10630 Little Patuxent Pkwy., Suite 202, Columbia, MD, 21044-3200 HC

N93-10045*# National Aeronautics and Space Administration. Lewis Research Center, Cleveland, OH.
TANK CHILLDOWN ANALYSIS AND VERIFICATION WITH A FLIGHTWEIGHT, 175 CU FT TANK UNDER NORMAL GRAVITY WITH LIQUID HYDROGEN
Naseem H. Saiyed *In* JHU, The 1992 JANNAF Propulsion Meeting, Volume 1 Feb. 1992 p 693-702 (For primary document see N93-10001 01-20)
Avail: CPIA, 10630 Little Patuxent Pkwy., Suite 202, Columbia, MD, 21044-3200 HC

29 MATERIALS PROCESSING

Includes space-based development of products and processes for commercial applications.

For biological materials see *55 Space Biology*.

No abstracts in this category.

31 ENGINEERING (GENERAL)

Includes vacuum technology; control engineering; display engineering; cryogenics; and fire prevention.

N93-10314# Polish Academy of Sciences, Warsaw. Inst. Podstawowych Problemow Techniki.
SHORTENED TEST HEATING SEASON (STHS) [SKROCONY TESTOWY SEZON GRZEWICZY (STSG)]
Elzbieta Kossecka, Krzysztof Loskot, and Zbigniew Pretczynski 1992 29 p In POLISH
Avail: CASI HC A03/MF A01

A suggested package of 14 days of hourly meteorological data substituting a set of data representing the climate of Warsaw for the entire heating season is presented. This package is described as the Shortened Test Heating Season (STHS). STHS is suggested to be applied in computer-aided studies of heat transfer through structural partitions. Author

N93-10397# National Inst. of Standards and Technology, Gaithersburg, MD. Thermophysics Div.
MATERIALS COMPATIBILITY AND LUBRICANTS RESEARCH ON CFC-REFRIGERANT SUBSTITUTES: THERMOPHYSICAL PROPERTIES
R. F. Kayser Apr. 1992 9 p Prepared for Air-Conditioning and Refrigeration Technology Inst., Inc., Arlington, VA
(Contract DE-FG02-91CE-23810)
(DE92-015116; DOE/CE-23810/2A) Avail: CASI HC A02/MF A01

Numerous fluids have been identified as promising alternative refrigerants, but much of the information needed to predict their behavior as pure fluids and as components in mixtures does not exist. In particular, reliable thermophysical properties data and models are needed to predict the performance of the new refrigerants in heating and cooling equipment, and to design and optimize equipment to be reliable and energy efficient. The objective of this project is to provide highly accurate, selected thermophysical

properties data for refrigerants 32, 123, 124, and 125, and to use these data to fit simple and complex equations of state and detailed transport property models. The new data will fill in the gaps in existing data sets and resolve the problems and uncertainties that exist in and between the data sets. The progress made during the first quarter of this fifteen-month project, which was initiated in late January, 1992 is described. DOE

N93-10398# Air-Conditioning and Refrigeration Technology Inst., Inc., Arlington, VA.

CHEMICAL AND THERMAL STABILITY OF REFRIGERANT-LUBRICANT MIXTURE WITH METAL

D. F. Huttenlocher 31 Mar. 1992 28 p Prepared for Spauchus Associates, Inc., Atlanta, GA

(Contract DE-FG02-91CE-23810)

(DE92-015117; DOE/CE-23810/2B) Avail: CASI HC A03/MF A01

This report presents completed sealed tube stability test results for the R-123/mineral oil mixture and preliminary results for seven of the eighteen contracted refrigerant-lubricant mixtures. The R-123 mixture was tested at 105, 150, and 175 C. The results obtained indicate that prolonged exposure to temperatures of about 150 C and higher will lead to rapid chemical deterioration of the R-123/mineral oil system. Chlorotrifluoroethane (R-133a) and trifluoroethane (R-143a) have been identified as decomposition products of R-123. Testing at 150 and 175 C have been completed for the HCFC refrigerants R-22, R-124, and R-142b with either mineral oil or alkylbenzene lubricants. These mixtures were very stable at the indicated temperatures. Testing at a higher temperature level will be necessary to define their upper temperature limits. Similarily, partial test results are available for HFC refrigerants R-32, R-125, R-134a (two esters), and R-143a with pentaerythritol ester lubricants at the 150 and 175 C temperature levels. Again, all five mixtures were found to be extremely stable at the test temperatures and additional testing will be needed to establish their upper temperature limits. DOE

N93-10466 Carleton Univ., Ottawa (Ontario).

PROCEEDINGS OF THE TWELFTH CANADIAN CONGRESS OF APPLIED MECHANICS, VOLUMES 1 AND 2

M. A. Erki, ed. and J. Kirkhope, ed. May 1989 949 p Congress held in Ottawa, Ontario, 28 May - 2 Jun. 1989

(ISBN-0920049-03; CTN-92-60512) Copyright Avail: Canadian Society for Mechanical Engineering, 2050 Mansfield St., Suite 700, Montreal, Quebec H3A 1Z7 Canada

These proceedings cover a wide range of topics of interest to mechanical engineers, including developments in modeling and theory, analytical and numerical techniques, investigations into the behavior of engineering materials, and special applications of mechanics. Sessions focusing on modeling and theory covered the following topics: (1) dynamics and vibration of structures; (2) structural stability; (3) fracture and fatigue; (4) dynamic fracture mechanics; (5) elastic, viscoelastic, and plastic behavior of materials; (6) vibration in plates and shells; (7) applications of the finite element method to plate and shell analysis; (8) investigation of fracture mechanics and structural dynamics of using strings, rods, beams, membranes, plates, and shell structures; (9) heat transfer in porous media; (10) application of computer algebra in mechanics; and (11) application of stochastic methods in mechanics. For individual titles, see N93-10467 through N93-10577.

N93-10467 Stanford Univ., CA. Dept. of Mechanical Engineering.

NEW DIRECTIONS IN COMPUTATIONAL MECHANICS **c34**

Thomas J. R. Hughes *In* Carleton Univ., Proceedings of the Twelfth Canadian Congress of Applied Mechanics, Volumes 1 and 2 May 1989 p 22-46 (For primary document see N93-10466 01-31)

Copyright Avail: Canadian Society for Mechanical Engineering, 2050 Mansfield St., Suite 700, Montreal, Quebec H3A 1Z7 Canada

A few areas of computational mechanics are identified in which considerable progress has occurred. Recent developments in general purpose large-scale nonlinear problem solving capabilities are reviewed. Emphasis is placed upon the recent introduction of highly vectorized iterative solution strategies which have dramatically increased efficiency in three dimensional implicit calculations. Contemporary developments in finite element methods for fluids are reviewed. Attention is devoted to adaptive meshing strategies, and the construction of new classes of methods which possess provable mathematical convergence properties. These latter methods, which go under the names SUPG and Galerkin / least squares, are the first finite element methods with satisfactory theoretical properties for fluid dynamics equations. Elementary examples of steady and unsteady space-time formulations of first order hyperbolic equations are presented. Two applications of the Galerkin / least squares procedure to solids and structures are discussed. One application deals with kinematically constrained media in general, and incompressible elasticity in particular. The other application concerns spacetime finite element algorithms for second order systems, such as the equations of structural dynamics. Author (CISTI)

N93-10468 Nottingham Univ. (England). Dept. of Theoretical Mechanics.

DEVELOPMENT IN THE ELASTIC ANALYSIS OF LAMINATED PLATES **c39**

A. J. M. Spencer *In* Carleton Univ., Proceedings of the Twelfth Canadian Congress of Applied Mechanics, Volumes 1 and 2 May 1989 p 47-53 (For primary document see N93-10466 01-31)

Copyright Avail: Canadian Society for Mechanical Engineering, 2050 Mansfield St., Suite 700, Montreal, Quebec H3A 1Z7 Canada

Some developments in three dimensional analyses of stress and deformation in laminated plates are described. They are based on work by Michell published in 1900. For isotropic and homogeneous plates, Michell obtained a number of classes of exact solutions of the three dimensional elasticity equations which satisfy zero traction conditions on the lateral surfaces of a moderately thick plate. Firstly, for laminates in which the laminae are different isotropic materials, generalizations of Michell's solutions are outlined. Then a more general problem of extending Michell's solutions to materials in which the elastic moduli vary through the plate thickness is considered. The results are then recovered in a direct and simple manner by specializing to the case in which the elastic moduli are piecewise constant through the thickness. For advanced composite materials applications, the main interest is in laminates whose laminae are anisotropic. Michell's solutions cannot be generalized, in closed form, to anisotropic elastic plates. However, the concept of using solutions of the two dimensional thin plate equations to generate relevant solutions of the three dimensional elasticity equations remains valid, although the three dimensional solutions can no longer be presented in closed form. Recent developments along these lines are outlined. Author (CISTI)

N93-10469 Texas Univ., Austin.

SMART ALGORITHMS AND ADAPTIVE METHODS IN COMPUTATIONAL FLUID DYNAMICS **c34**

J. Tinsley Oden *In* Carleton Univ., Proceedings of the Twelfth Canadian Congress of Applied Mechanics, Volumes 1 and 2 May 1989 p 54-74 (For primary document see N93-10466 01-31)

Copyright Avail: Canadian Society for Mechanical Engineering, 2050 Mansfield St., Suite 700, Montreal, Quebec H3A 1Z7 Canada

A review is presented of the use of smart algorithms which employ adaptive methods in processing large amounts of data in computational fluid dynamics (CFD). Smart algorithms use a rationally based set of criteria for automatic decision making in an attempt to produce optimal simulations of complex fluid dynamics problems. The information needed to make these decisions is not known beforehand and evolves in structure and form during the numerical solution of flow problems. Once the code makes a decision based on the available data, the structure of the data may change, and criteria may be reapplied in order to direct the

analysis toward an acceptable end. Intelligent decisions are made by processing vast amounts of data that evolve unpredictably during the calculation. The basic components of adaptive methods and their application to complex problems of fluid dynamics are reviewed. The basic components of adaptive methods are: (1) data structures, that is what approaches are available for modifying data structures of an approximation so as to reduce errors; (2) error estimation, that is what techniques exist for estimating error evolution in a CFD calculation; and (3) solvers, what algorithms are available which can function in changing meshes. Numerical examples which demonstrate the viability of these approaches are presented. Author (CISTI)

N93-10470 Concordia Univ., Montreal (Quebec). Dept. of Mechanical Engineering.
AXISYMMETRIC VIBRATIONS OF ROTATING CIRCULAR PLATES USING CHARACTERISTIC ORTHOGONAL POLYNOMIALS **c39**
A. Kaushal and R. B. Bhat *In* Carleton Univ., Proceedings of the Twelfth Canadian Congress of Applied Mechanics, Volumes 1 and 2 May 1989 p 94-95 (For primary document see N93-10466 01-31)
Copyright Avail: Canadian Society for Mechanical Engineering, 2050 Mansfield St., Suite 700, Montreal, Quebec H3A 1Z7 Canada

Vibration characteristics of rotating circular plates are of interest in the design of turbine discs, circular saws, and other rotating structures. Centrifugal forces are set up in these structures due to their rotation which cause in-plane strains resulting in the stiffening of the structure. Due to the change in structural characteristics with the speed of rotation, the natural frequencies of free vibration will be different from those under non-rotating conditions. Axisymmetric free behavior of rotating circular plates with varying thickness was studied using the characteristic orthogonal polynomials. The variation of natural frequencies with the speed of rotation was obtained for several parameter combinations such as ratio of the inner/outer radii, ratio of inner/outer thickness, etc. The results are presented for free (inner), free (outer), and clamped (inner) free (outer) plates. Cases corresponding to uniform thickness and to linear variation in thickness and to parabolic thickness variation are presented.
Author (CISTI)

N93-10471 Manchester Univ. (England).
VIBRATION OF ORTHOTROPIC CYLINDRICAL SHELL PANELS WITH ARBITRARY SUPPORTED CURVED EDGES **c39**
C. B. Sharma and I. A. Al-Khayat *In* Carleton Univ., Proceedings of the Twelfth Canadian Congress of Applied Mechanics, Volumes 1 and 2 May 1989 p 100-101 (For primary document see N93-10466 01-31)
Copyright Avail: Canadian Society for Mechanical Engineering, 2050 Mansfield St., Suite 700, Montreal, Quebec H3A 1Z7 Canada

Vibration characteristics of thin orthotropic circular cylindrical panels with rectangular planform are analyzed. The curved edges are arbitrarily supported. Transverse shear deformation and rotary inertia are included due to their importance in composite materials. The formulations are based on a general laminated shell theory which includes shear deformation and rotary inertia terms. Axial dependence of modal forms is assumed in the form of simple Fourier series. Stokes' transformation is used to legitimize the derivatives of Fourier series as well as to enforce those geometric boundary conditions that are not identically satisfied and to release those which are forced to zero due to the nature of the assumed series. The method is used to solve the problems with arbitrarily supported curved edges in an overall sense. The constraints to satisfy the boundary conditions of a chosen base problem result in a general eigenvalue formulation. The influence of boundary conditions on the vibration characteristics was studied. The effects of changes in geometrical and material parameters of a panel on its overall vibration response (natural frequencies, mode shapes and modal forces) were studied. Some results for a given panel with clamped curved edges are presented. Author (CISTI)

N93-10472 Old Dominion Univ., Norfolk, VA.
A FINITE ELEMENT METHOD FOR NONLINEAR PANEL FLUTTER **c39**
Chuh Mei and Carl E. Gray, Jr. (National Aeronautics and Space Administration. Langley Research Center, Hampton, VA.) *In* Carleton Univ., Proceedings of the Twelfth Canadian Congress of Applied Mechanics, Volumes 1 and 2 May 1989 p 118-119 (For primary document see N93-10466 01-31)
Copyright Avail: Canadian Society for Mechanical Engineering, 2050 Mansfield St., Suite 700, Montreal, Quebec H3A 1Z7 Canada

Panel flutter is the self excited oscillations of a plate in supersonic flow. Linear theory gives no information about the panel's deflections and stresses. Hence, the service life of the panel cannot be predicted by linear methods. Nonlinear structural theory determines the limit cycle oscillating frequency, and also panel deflections and stresses. Panel fatigue life, therefore, can be predicted. For a more thorough understanding of panel flutter behavior, the geometric nonlinearity effects due to large deflections must be considered in the formulation. The Galerkin's method was used in the investigation of limit cycle oscillations of panels in supersonic flow in the spatial domain, and the panel deflections. All nonlinear flutter methods and results presently available were limited to a linear or linearized aerodynamic theory. Extension of the finite element flutter formulation to include nonlinear hypersonic aerodynamic loading and finite element nonlinear panel flutter results are presented. Author (CISTI)

N93-10473 Virginia Polytechnic Inst. and State Univ., Blacksburg.
VIBRATION OF LAMINATED COMPOSITE PLATES USING VARIOUS PLATE THEORIES: ANALYTICAL AND FINITE ELEMENT RESULTS **c39**
J. N. Reddy and A. A. Khdeir *In* Carleton Univ., Proceedings of the Twelfth Canadian Congress of Applied Mechanics, Volumes 1 and 2 May 1989 p 120-121 (For primary document see N93-10466 01-31)
Copyright Avail: Canadian Society for Mechanical Engineering, 2050 Mansfield St., Suite 700, Montreal, Quebec H3A 1Z7 Canada

Analytical and finite element solutions of the classical, first-order, and third-order laminate theories are developed to study free vibrations of cross-ply rectangular composite laminates under various boundary conditions. The analytical solutions are developed using the space-state approach. The effects of side to thickness ratio, aspect ratio, and lamination schemes on the fundamental frequencies are investigated for the theories. The Levy type solution procedure and finite element model developed was used to evaluate the natural frequencies of antisymmetric, cross-ply, rectangular laminates. The effect of orthotropy and number of layers on the non-dimensional fundamental frequency of simply supported square laminates is investigated, and the numerical results obtained using various plate theories are compared. The fundamental frequencies increase with increasing orthotropy as well as the number of layers. In all cases, the classical plate theory over-predicts the frequencies compared to the shear deformation theories. Author (CISTI)

N93-10474 Glasgow Univ. (Scotland).
NON-LINEAR THERMOELASTICITY OF RUBBERLIKE SOLIDS **c39**
R. W. Ogden *In* Carleton Univ., Proceedings of the Twelfth Canadian Congress of Applied Mechanics, Volumes 1 and 2 May 1989 p 126-127 (For primary document see N93-10466 01-31)
Copyright Avail: Canadian Society for Mechanical Engineering, 2050 Mansfield St., Suite 700, Montreal, Quebec H3A 1Z7 Canada

A modified entropic formulation is used in order to examine from a fresh standpoint certain features arising in the modeling of

the thermoelastic response of rubberlike solids. The basic equations are described and then applied to particular models. Special attention is focused on circumstances in which volume changes accompanying large deformation and large temperature changes are small. Author (CISTI)

N93-10475 Akron Univ., OH.
FAILURE PROCESSES IN ELASTOMERIC COMPOSITES **c39**
A. N. Gent *In* Carleton Univ., Proceedings of the Twelfth Canadian Congress of Applied Mechanics, Volumes 1 and 2 May 1989 p 130-131 (For primary document see N93-10466 01-31)
Copyright Avail: Canadian Society for Mechanical Engineering, 2050 Mansfield St., Suite 700, Montreal, Quebec H3A 1Z7 Canada

It has been shown that a small cavity is formed in rubber near, but not at, the surface of a well-bonded rigid spherical inclusion when the elastomeric material containing the inclusion is subjected to a sufficiently high tensile stress. This phenomenon has been attributed to internal rupture of the elastomer under the action of triaxial tension set up near the poles of the inclusion. Attention is focused here on the formation of cavities in well bonded systems by internal failure of the elastomer. A hypothetical mechanism is proposed for internal rupture involving the expansion of preexisting microvoids. Investigation of conditions under which this type of failure occurs are reported and an attempt is made to interpret the failure characteristics on the basis of the hypothesis. Author (CISTI)

N93-10476 California Univ., Livermore. Lawrence Livermore Lab.
CHRONORHEOLOGICAL CHARACTERIZATION OF ELASTOMERS **c39**
William W. Feng *In* Carleton Univ., Proceedings of the Twelfth Canadian Congress of Applied Mechanics, Volumes 1 and 2 May 1989 p 132-133 (For primary document see N93-10466 01-31)
Copyright Avail: Canadian Society for Mechanical Engineering, 2050 Mansfield St., Suite 700, Montreal, Quebec H3A 1Z7 Canada

Elastomers often exhibit chronorheological (rheological and aging) behavior. The magnitudes of the property change with time, and are often large enough that they cannot be neglected. The chronorheological effects of elastomers are studied theoretically and experimentally. An interpretation of chronorheological properties of an elastomer was obtained. The constitutive equations and a method for determining these material properties were also presented. In the formulation, the geometric nonlinearity as well as the material nonlinearity were included. The theoretical value for the strains can be as large as needed; for practical applications, however, these values are limited by the fracture strength and are usually less than a few hundred percent. The method described is for the temperature aging; however, the constitutive equations and the method for obtaining the material properties can be extended readily to other types of aging. Author (CISTI)

N93-10477 Alcoa Foundation, Pittsburgh, PA.
INTEGRATED FINITE ELEMENT MODEL OF COMPOSITE MATERIALS **c39**
Jan L. Teply and William C. Herbein *In* Carleton Univ., Proceedings of the Twelfth Canadian Congress of Applied Mechanics, Volumes 1 and 2 May 1989 p 138-139 (For primary document see N93-10466 01-31)
Copyright Avail: Canadian Society for Mechanical Engineering, 2050 Mansfield St., Suite 700, Montreal, Quebec H3A 1Z7 Canada

Two problems traditionally addressed in the area of micromechanics of composite materials can be briefly summarized as follows: (1) for a macroscopically uniform volume of composite material, which is subjected to macroscopically uniform boundary tractions, displacements or heat influx, find overall thermomechanical properties in terms of the thermomechanical properties of the individual constituents; and (2) for the same material volume and boundary conditions as above, find the local stress, strain, and temperature fields in the constituents and on the interfaces. Two different types of micromechanical models are usually applied to the solutions of these two types of problems. For linear elastic materials, the micromechanical models to solve problem (1) offer simple solutions of overall thermomechanical properties either in terms of bound which are derived from periodic or random microstructures, or in terms of single estimates, which are derived from a solution of an isolated inclusion. The finite element variational approaches are applied to integrate the solutions of problems (1) and (2) into one model. The application of displacement and equilibrium variational approaches to the calculation of overall elastic-plastic properties, are extended to the solution of the second problem. The integrated model is then applied to calculate the overall properties and local stress and strain fields of boron-aluminum composites subjected to transverse tension, in-plane shear and bending. Author (CISTI)

N93-10478 Virginia Polytechnic Inst. and State Univ., Blacksburg.
COMPRESSION BUCKLING OF THICK ORTHOTROPIC PLATES WITH A STEP THICKNESS CHANGE **c39**
Eric R. Johnson and Carlos G. Davila *In* Carleton Univ., Proceedings of the Twelfth Canadian Congress of Applied Mechanics, Volumes 1 and 2 May 1989 p 140-141 (For primary document see N93-10466 01-31)
Copyright Avail: Canadian Society for Mechanical Engineering, 2050 Mansfield St., Suite 700, Montreal, Quebec H3A 1Z7 Canada

The influence of transverse shearing deformations on the buckling of thick, specially orthotropic laminated plates with a step change in thickness is shown. An example problem involving a rectangular plate subjected to uniaxial compression with the step perpendicular to the load axis, spanning the width of the plate, and symmetric about the middle plane of the plate is examined. Buckling coefficients are presented for a simply supported square plate with a centrally located step as the thickness of one half, t(sub 1), is decreased relative to the thickness of the other half, t(sub 2), for a plate of constant weight. Values of the dimensionless buckling coefficient K as a function of t(sub 1)/t(sub 2) for classical laminated plate theory (CLT) and shear deformation theory (SDT) are computed. It is shown that the buckling modes can be significantly different for SDT with respect to CLT.

Author (CISTI)

N93-10479 Stanford Univ., CA. Dept. of Aeronautics and Astronautics.
CONTACT PROBLEM IN DELAMINATION-BUCKLING OF LAMINATED COMPOSITE SHELLS Abstract only **c39**
Fukuo Chang and Zafer Kutlu *In* Carleton Univ., Proceedings of the Twelfth Canadian Congress of Applied Mechanics, Volumes 1 and 2 May 1989 p 142 (For primary document see N93-10466 01-31)
Copyright Avail: Canadian Society for Mechanical Engineering, 2050 Mansfield St., Suite 700, Montreal, Quebec H3A 1Z7 Canada

The objective was to develop an analytical model for analyzing delamination buckling of composite shells with consideration of the interface contact and slip condition. The model consists of a stress analysis and a failure analysis. Stresses, strains, and deformations of the delaminated structures were calculated by a nonlinear finite element analysis developed based on the large deformation theory. Delamination growth in the structures was determined by a crack extension formulation based on fracture mechanics. The Lagrange Multiplier technique was adopted for modeling the interaction between interfaces of delaminations during loading. No friction was assumed at the delamination interfaces. Based on the model, the interaction between the global response of the structures and the local behavior of the delaminated sublaminates in the structure can be analyzed. Experiments involving graphite epoxy prepregs were also performed to provide materials data needed for the model and to generate test data for verifying the analysis. Based on the results of the investigation, it can be concluded that the introduction of interface contact

condition is essential for analyzing delamination buckling failure of composite shells. The actual contact and the condition along the delamination interfaces strongly depends on the curvature and ply orientation of the structures and the location and size of delamination. Author (CISTI)

N93-10480* National Aeronautics and Space Administration. Langley Research Center, Hampton, VA.
COMPARISON OF FULL 3-D, THIN-FILM 3-D, AND THIN-FILM PLATE ANALYSES OF A POSTBUCKLED EMBEDDED DELAMINATION
John D. Whitcomb *In* Carleton Univ., Proceedings of the Twelfth Canadian Congress of Applied Mechanics, Volumes 1 and 2 May 1989 p 144-145 (For primary document see N93-10466 01-31)
Copyright Avail: Canadian Society for Mechanical Engineering, 2050 Mansfield St., Suite 700, Montreal, Quebec H3A 1Z7 Canada

Strain-energy release rates are often used to predict when delamination growth will occur in laminates under compression. Because of the inherently high computational cost of performing such analyses, less rigorous analyses such as thin-film plate analysis were used. The assumptions imposed by plate theory restrict the analysis to the calculation of total strain energy, G(sub t). The objective is to determine the accuracy of thin-film plate analysis by comparing the distribution of G(sub t) calculated using fully three dimensional (3D), thin-film 3D, and thin-film plate analyses. Thin-film 3D analysis is the same as thin-film plate analysis, except 3D analysis is used to model the sublaminate. The 3D stress analyses were performed using the finite element program NONLIN3D. The plate analysis results were obtained from published data, which used STAGS. Strain-energy release rates were calculated using variations of the virtual crack closure technique. The results demonstrate that thin-film plate analysis can predict the distribution of G(sub t) quite well, at least for the configurations considered. Also, these results verify the accuracy of the strain-energy release rate procedure for plate analysis.
Author (CISTI)

N93-10481 Virginia Polytechnic Inst. and State Univ., Blacksburg.
ON THE BEHAVIOR OF A HIGHER-ORDER PLATE BENDING ELEMENT **c39**
R. C. Averill and J. N. Reddy *In* Carleton Univ., Proceedings of the Twelfth Canadian Congress of Applied Mechanics, Volumes 1 and 2 May 1989 p 146-147 (For primary document see N93-10466 01-31)
Copyright Avail: Canadian Society for Mechanical Engineering, 2050 Mansfield St., Suite 700, Montreal, Quebec H3A 1Z7 Canada

The third-order shear deformation plate theory developed by Reddy is used to develop a displacement finite element model to analyze laminated composite plates. The element's behavior in thin plate applications is investigated to determine if and when locking occurs. Both the number and type of constraints imposed on the element in the thin plate limit are defined, and the effect of using low-order integration rules to evaluate various portions of the element stiffness matrix are examined. The displacement finite element model based on the third-order shear deformation theory of Reddy exhibits very good behavior when applied to plates with a wide range of span to thickness ratios. A 2 by 2 Gauss-Legendre rule should be employed to evaluate the entire element stiffness matrix in order to alleviate locking and to reduce computational expense. In contrast to underintegrated first-order elements, the present element requires no additional modifications in order to maintain proper rank of the element stiffness matrix.
Author (CISTI)

N93-10482 Arizona Univ., Tucson. Dept. of Civil Engineering and Engineering Mechanics.
INTERFACE CRACKS IN AN ORTHOTROPIC LAYERED HALF-SPACE UNDER IMPACT LOADING **c39**
T. Kundu and M. R. Karim *In* Carleton Univ., Proceedings of the Twelfth Canadian Congress of Applied Mechanics, Volumes 1 and 2 May 1989 p 176-177 (For primary document see N93-10466 01-31)
Copyright Avail: Canadian Society for Mechanical Engineering, 2050 Mansfield St., Suite 700, Montreal, Quebec H3A 1Z7 Canada

The plane problem of two interface cracks in a layered orthotropic half-space excited by a time harmonic antiplane impact loading applied at a point on the surface is investigated. Using the representation theorem for the displacements, the boundary value problem is formulated in terms of singular integral equations for the displacement jump (COD) across the cracks. An appropriate expansion of the unknown COD function into Chebychev polynomials leads to a system of algebraic equations for the expansion coefficients. As an example, a layered half-space with two cracks loaded by a line load at the surface are considered and numerical results are presented. Author (CISTI)

N93-10483 Clarkson Univ., Potsdam, NY.
AN OPEN OR CLOSED CRACK TERMINATING AT A BI-MATERIAL INTERFACE: POWER-LOGARITHMIC SINGULARITIES **c39**
John P. Dempsey *In* Carleton Univ., Proceedings of the Twelfth Canadian Congress of Applied Mechanics, Volumes 1 and 2 May 1989 p 178-179 (For primary document see N93-10466 01-31)
Copyright Avail: Canadian Society for Mechanical Engineering, 2050 Mansfield St., Suite 700, Montreal, Quebec H3A 1Z7 Canada

An open or closed crack terminating at a material interface is modeled by considering a bi-material tri-sector geometry. The eigenvalue equation in lambda for each case is examined to reveal the possible existence of power logarithmic stress singularities given certain material combinations and crack termination angles. The primary emphasis is on predicting the dominant singular behavior that may exist in the vicinity of a crack-tip terminating at a material interface. No requirements are imposed on the behavior (decay rate) of the elastostatic field quantities at infinity. Rather, emphasis is on describing the possible local asymptotic character of these quantities. Results that confirm the possible existence of power logarithmic corner singularities for open or closed cracks terminating at a bi-material interface are presented. The above singularities are stronger than the conventional power-type singularities and for this reason numerical analysts should be aware of their possible occurrence. Author (CISTI)

N93-10484 Sandia National Labs., Albuquerque, NM.
ENRICHED ELEMENT ANALYSIS OF BIMATERIAL INTERFACE CRACKS **c39**
E. P. Chen *In* Carleton Univ., Proceedings of the Twelfth Canadian Congress of Applied Mechanics, Volumes 1 and 2 May 1989 p 180-181 (For primary document see N93-10466 01-31)
Copyright Avail: Canadian Society for Mechanical Engineering, 2050 Mansfield St., Suite 700, Montreal, Quebec H3A 1Z7 Canada

Application of an enriched finite element method to the solution of stress intensification around interface cracks are reviewed. This method includes the effects of a singularity in the element by enriching the conventional displacement assumption with terms that give the proper singularity at the singular node. This procedure works very well for isotropic elasticity problems where extremely accurate predictions on the stress intensity factor for various crack geometries and loading conditions have been obtained. To extend the enriched element method to interface crack problems, crack-tip stress, and displacement, expressions were derived for the several interface crack geometries. An enriched element method was implemented in the PAPST finite element program, a special purpose fracture mechanics code which handles axisymmetric and planar geometries with a 12-node quadrilateral isoparametric element. Comparisons between the results from the modified PAPST program with analytical and other numerical methods show good agreement. Author (CISTI)

N93-10485 Colorado Univ., Boulder. Dept. of Mechanical Engineering.

ELASTIC WAVE SCATTERING BY AN INTERFACIAL CRACK IN A PLATE **c39**

S. K. Datta, R. L. Bratton, and A. H. Shah (Manitoba Univ., Winnipeg.) *In* Carleton Univ., Proceedings of the Twelfth Canadian Congress of Applied Mechanics, Volumes 1 and 2 May 1989 p 182-183 (For primary document see N93-10466 01-31)

Copyright Avail: Canadian Society for Mechanical Engineering, 2050 Mansfield St., Suite 700, Montreal, Quebec H3A 1Z7 Canada

Characterization of potential flaws and joints in Al cladded graphite epoxy material by nondestructive evaluation methods may be obtained by use of anti-plane shear waves generated and detected by electromagnetic acoustic transducers. A hybrid method is presented for studying the diffraction of horizontally polarized shear (SH) waves by delamination cracks in plates. The technique replaces a bounded region containing the scatterers by finite elements. This allows such inclusions as slanted surface breaking cracks, buried cavities, and delaminations between two materials to be modeled. Moreover, the materials can be isotropic and anisotropic as well as layered. In the exterior regions, the field is written as a modal sum. Continuity conditions at the boundary between the interior and exterior regions are imposed. Although the presented results are for an interfacial crack, the method can be used for other defects like, canted, buried, or surface breaking cracks. Author (CISTI)

N93-10486 Carleton Univ., Ottawa (Ontario).

INDENTATION OF A PRECOMPRESSED PENNY-SHAPED CRACK **c39**

A. P. S. Selvadurai, B. M. Singh, and M. C. Au *In its* Proceedings of the Twelfth Canadian Congress of Applied Mechanics, Volumes 1 and 2 May 1989 p 184-185 (For primary document see N93-10466 01-31)

Copyright Avail: Canadian Society for Mechanical Engineering, 2050 Mansfield St., Suite 700, Montreal, Quebec H3A 1Z7 Canada

The elastostatic problem which deals with a penny-shaped crack was extended to cover effects such as anisotropy, nonhomogeneity, localized loading, effects of localized plastic flow, and dynamic loading. This presents a useful technique for the examination of fracture and crack propagation in brittle elastic solids. The problem of a penny-shaped crack which is subjected to both a precompression normal to the plane of the crack and an indentation by a rigid disc over one of its plane faces is considered. Due to the presence of the precompression, the crack experiences closure at the crack tips. For certain combinations of the precompression and the indenting stress, the crack remains closed over a finite annular region. In this closed position, only mode 2 type stress intensity factors occur at the crack tip. The analysis allows the evaluation of the indenting stress necessary to initiate the flaw opening mode stress intensity factors at the crack tip.

Author (CISTI)

N93-10487 Technische Hochschule, Vienna (Austria).

NONSTATIONARY RANDOM VARIATIONS OF MODERATELY THICK PLATES USING BEM **c39**

H. Irschik and R. Heuer *In* Carleton Univ., Proceedings of the Twelfth Canadian Congress of Applied Mechanics, Volumes 1 and 2 May 1989 p 192-193 (For primary document see N93-10466 01-31)

Copyright Avail: Canadian Society for Mechanical Engineering, 2050 Mansfield St., Suite 700, Montreal, Quebec H3A 1Z7 Canada

The analysis of nonstationary random vibrations in linear elastic polygonal plates of moderate thickness is addressed. An expression based on Mindlin's theory is developed for deflection due to uniform harmonic support excitation. The boundary value problem is solved by an advanced boundary element method (BEM) using Green's function of finite rectangular domains in the kernels of the integrals. Forced vibrations in damped structures is considered by splitting the complex frequency response function into an analytical part to account for the singularities due to resonance and a regular part to account for the influence of the higher complex resonances not considered in the truncated analytical expression. The analytical part is solved for by the boundary element method. The complex frequency response is evaluated numerically by elastic-viscoelastic correspondence. Author (CISTI)

N93-10488 Houston Univ., TX.

NUMERICAL SIMULATION OF TRANSIENT CRACK GROWTH **c39**

T.-J. Shiue and K. Ravi-Chandar *In* Carleton Univ., Proceedings of the Twelfth Canadian Congress of Applied Mechanics, Volumes 1 and 2 May 1989 p 198-199 (For primary document see N93-10466 01-31)

Copyright Avail: Canadian Society for Mechanical Engineering, 2050 Mansfield St., Suite 700, Montreal, Quebec H3A 1Z7 Canada

Transient crack growth under stress wave loading is simulated using a fine grid finite element mesh. The simulations duplicate exactly the loading conditions and crack growth observations reported by other investigators. The results of the simulation were used to determine the range of dominance of asymptotic singular field and also examine the optical method of caustics. Analytical results from the literature which also address the same problems and the present numerical simulations are also used for comparison. Results from the three approaches were compared for two different crack growth cases. The comparisons were proper only before the dilatational wave reflected from the boundary arrives at the crack tip. All three methods agreed very well before the crack started running; after that, the experimental stress intensity factor grew continuously, the analytical one showed a drop followed by a slight increase, and the numerical one showed oscillations when the loads are large, but fell between experiments and theory. The oscillations are probably due to the discrete nature of the nodal release procedure. It is also possible that three dimensional inertial constraint is important in such highly transient problems.

Author (CISTI)

N93-10489 Clarkson Univ., Potsdam, NY. Dept. of Civil and Environmental Engineering.

DYNAMIC CRACK DIVISION IN BRITTLE SOLIDS **c39**

John P. Dempsey *In* Carleton Univ., Proceedings of the Twelfth Canadian Congress of Applied Mechanics, Volumes 1 and 2 May 1989 p 200-201 (For primary document see N93-10466 01-31)

Copyright Avail: Canadian Society for Mechanical Engineering, 2050 Mansfield St., Suite 700, Montreal, Quebec H3A 1Z7 Canada

A review of recent and ongoing analytical and numerical research on dynamic crack branching in brittle solids is presented. The idealizations inherent in the mathematical models under investigation are emphasized. The analytical and numerical schemes that have recently yielded several dynamic crack branching solutions are discussed. It is apparent from experimental evidence that the dynamic branching event is inherently three dimensional. Multibranching invariably occurs during crack propagation but most microcracks are arrested. The crack branching mechanism is arguably governed by the nucleation, coalescence, and subsequent interaction of advanced microcracks. The detailed three dimensional situation is very difficult to model. The process zone may be asssumed to be small compared to any characteristic length. Analytically, the process zone is modeled as a point. Correct analytical and numerical approaches to elastodynamic self-similar crack branching problems in homogeneous, isotropic, and elastic brittle solids are available for some cracking conditions. Recent work has presented solutions for the branching of a propagating crack into a stress field that is not self-similar. Finally, new directions and the needs of future research are emphasized. Author (CISTI)

N93-10490 Naval Academy of Greece, Athens.
INTEGRAL TRANSFORM APPROACH TO AN INERTIAL VISCOELASTIC PROBLEM INVOLVING MOVING SINGULARITIES **c39**
H. G. Georgiadis and S. C. Mouskos *In* Carleton Univ., Proceedings of the Twelfth Canadian Congress of Applied Mechanics, Volumes 1 and 2 May 1989 p 204-205 (For primary document see N93-10466 01-31)
Copyright Avail: Canadian Society for Mechanical Engineering, 2050 Mansfield St., Suite 700, Montreal, Quebec H3A 1Z7 Canada

The transient stress field in the vicinity of singular points in moving crack and punch problems is of considerable interest in elastodynamics. Moreover, only very few solutions of the above type exist for viscoelastic materials. Such a solution is presented in this work for an inertial viscoelastic problem by utilizing an integral transform approach. The specific problem considered is the transient motion of a fixed-length crack in an infinite strip made of a linearly viscoelastic material. However, the adopted procedure is also suitable for any symmetrical crack or punch in a linearly viscoelastic solid. The solution is obtained by utilizing Sih's integral transform procedure and a numerical technique for the Laplace transform inversion. The suitability of the Crump inversion technique for inertial viscoelastic problems is emphasized. This technique uses the complex form of the intensity function which is to be inverted in the time domain. A complex form of the intensity function is always the case in transient viscoelastodynamics of moving singularities. Author (CISTI)

N93-10491 Naval Research Lab., Washington, DC. Mechanics of Materials Branch.
STRESS PATTERNS IN THE DYNAMIC TEAR TEST **c39**
V. Gensheimer DeGiorgi *In* Carleton Univ., Proceedings of the Twelfth Canadian Congress of Applied Mechanics, Volumes 1 and 2 May 1989 p 206-207 (For primary document see N93-10466 01-31)
Copyright Avail: Canadian Society for Mechanical Engineering, 2050 Mansfield St., Suite 700, Montreal, Quebec H3A 1Z7 Canada

The importance of specific stress waves in the dynamic fracture process occurring in studies involving the dynamic tear (DT) test is well known. The current work is another step in the full transient study of a DT tear test modeled as a plane strain process. The major goals were to incorporate nonlinear material effects into the full finite element (FE) method transient solution of the DT tear test and to examine the state of stress at the notch. The form and magnitude of the notch region operating mode stress field prior to dynamic fracture can be divided into five distinct stages. At the experimentally determined fracture initiation time, the notch tip is the primary stress concentrator and the stresses calculated by the FE computational simulation have reached the magnitude required for fracture. Author (CISTI)

N93-10492 Cornell Univ., Ithaca, NY. Dept. of Theoretical and Applied Mechanics.
DYNAMIC MEASUREMENT OF THE J INTEGRAL IN DUCTILE METALS USING THE OPTICAL METHOD OF CAUSTICS **c39**
Alan T. Zehnder and Ares J. Rosakis (California Inst. of Tech., Pasadena.) *In* Carleton Univ., Proceedings of the Twelfth Canadian Congress of Applied Mechanics, Volumes 1 and 2 May 1989 p 208-209 (For primary document see N93-10466 01-31)
Copyright Avail: Canadian Society for Mechanical Engineering, 2050 Mansfield St., Suite 700, Montreal, Quebec H3A 1Z7 Canada

Experiments were performed using the optical method of reflected caustics in conjunction with high speed photography to measure the J integral dynamically. Interpretation of the caustics was made possible by the results of other investigators which provide a relationship between the J integral and the caustic diameter. The tested specimens were three point bend specimens made of heat treated 4340 steel, loaded dynamically in a drop weight tower. Values for J were obtained by measuring the caustic diameter, D, for each time interval and then determining J. The complete time history of the J integral as measured with caustics was obtained. An estimated value of J corresponding to crack tunnelling is believed to most accurately reflect overall fracture toughness. Author (CISTI)

N93-10493 California Inst. of Tech., Pasadena. Graduate Aeronautical Labs.
STATUS OF DYNAMIC FRACTURE IN BRITTLE SOLIDS **Abstract only** **c39**
W. G. Knauss and P. D. Washabaugh *In* Carleton Univ., Proceedings of the Twelfth Canadian Congress of Applied Mechanics, Volumes 1 and 2 May 1989 p 210 (For primary document see N93-10466 01-31)
Copyright Avail: Canadian Society for Mechanical Engineering, 2050 Mansfield St., Suite 700, Montreal, Quebec H3A 1Z7 Canada

Techniques to examine dynamically propagating cracks in brittle media have progressed sufficiently to allow investigators to examine material behavior near the crack tip in regions where two dimensional assumptions are no longer valid. Boundary conditions can be prescribed to allow ample viewing time of near tip deformation. Refinements in high speed detectors and illumination sources have allowed clear measurement of full field quantities. These measurements have been done with the visible light on the transmissive and reflective properties of crack tip deformation. Commensurate with the experimental activity, advances in numerical capability have allowed the three dimensional and wave nature of the fracture region to be modeled. A brief review of the more significant findings resulting from this work, especially those resulting from crack visualization, is presented. Author (CISTI)

N93-10494 Ecole Polytechnique Federale de Lausanne (Switzerland).
EVOLUTION OF HYBRID-TREFFTZ FE MODEL: STATE OF THE ART AND FUTURE TRENDS **c39**
J. Jirousek *In* Carleton Univ., Proceedings of the Twelfth Canadian Congress of Applied Mechanics, Volumes 1 and 2 May 1989 p 212-213 (For primary document see N93-10466 01-31)
Copyright Avail: Canadian Society for Mechanical Engineering, 2050 Mansfield St., Suite 700, Montreal, Quebec H3A 1Z7 Canada

Several finite element (FE) models are presented that are based on the application of displacement and/or stress trial functions that fail to satisfy either the equilibrium or the compatibility. One modeling approach is to base the element formulation on assumed displacements. The displacement field is chosen so as to satisfy a priori the governing differential equations (equilibrium) while the interelement continuity and the boundary conditions are enforced. This is the so-called Trefftz-type approach. Its application in a FE formulation is natural (it amounts to solving each element accurately for the prescribed load and then tying them together) but it also presents important computational advantages over the conventional elements. The hybrid-Trefftz (HT) model is based on assuming over the element subregion simultaneously two distinct displacement fields: the nonconforming Trefftz field and the auxiliary conforming displacement field. A review of the principles behind this approach is presented along with a discussion of the state of the art and future trends. Author (CISTI)

N93-10495 Calgary Univ. (Alberta). Dept. of Mechanical Engineering.
A MULTILAYERED SHELL FINITE ELEMENT **c39**
Marcelo Epstein *In* Carleton Univ., Proceedings of the Twelfth Canadian Congress of Applied Mechanics, Volumes 1 and 2 May 1989 p 214-215 (For primary document see N93-10466 01-31)
Copyright Avail: Canadian Society for Mechanical Engineering, 2050 Mansfield St., Suite 700, Montreal, Quebec H3A 1Z7 Canada

Work undertaken in the area of multilayered finite elements is discussed. The goal was to develop a clear and precise underlying theory, a simple finite element model, and an effective programming

strategy. A brief review is given of an oriented continuum approach and a direct integration approach for multilayered shell theory. In an oriented continuum, the configurations are specified by the coordinates of the material points plus a number of vector fields which are interpreted physically in each application. A simple, 4 node, isoparametric bilinear finite element model is outlined. An easily programmed master routine, called ELIVW, containing the raw expressions for the internal virtual work in an element is described. All element integrations, with the exception of shear like terms, are performed numerically by means of a 2 by 2 Gaussian quadrature. Shear like terms are calculated with a 1-point reduced integration. A variety of codes were developed for the use of linear, nonlinear, static, dynamic, and stability analyses of multilayered shells. Author (CISTI)

N93-10496 Puerto Rico Univ., Mayaguez.
A NEW NON-GAUSSSIAN APPROXIMATION TECHNIQUE FOR RANDOM VIBRATION OF GENERAL HYSTERESIS c39
H. Davoodi and M. Noori (Worcester Polytechnic Inst., MA.) *In* Carleton Univ., Proceedings of the Twelfth Canadian Congress of Applied Mechanics, Volumes 1 and 2 May 1989 p 224-225 (For primary document see N93-10466 01-31)
Copyright Avail: Canadian Society for Mechanical Engineering, 2050 Mansfield St., Suite 700, Montreal, Quebec H3A 1Z7 Canada

The problem of the random vibration of hysteretically degrading nonlinear systems has attracted considerable attention. This is due to the significance of hysteresis in the dynamic response analysis of structural or mechanical systems. Non-Gaussian response analysis of general hysteresis has to date received little attention. Information on the higher order statistics for hysteretically yielding structures is very useful in the reliability and random vibration analysis of these systems. A non-Gaussian closure for the random vibration of general hysteresis is presented. Results show that the non-Gaussian responses are in better agreement with the Monte Carlo simulation than the linearized statistics. These statistics were also compared with the simulated 4th order moments for displacement and velocity. These plots show a good agreement between predicted and simulated response statistics.
Author (CISTI)

N93-10497 Pacific Northwest Lab., Richland, WA.
FRACTALS AND MULTIFRACTALS IN FRACTURE c39
R. E. Williford *In* Carleton Univ., Proceedings of the Twelfth Canadian Congress of Applied Mechanics, Volumes 1 and 2 May 1989 p 230-231 (For primary document see N93-10466 01-31)
Copyright Avail: Canadian Society for Mechanical Engineering, 2050 Mansfield St., Suite 700, Montreal, Quebec H3A 1Z7 Canada

In many disciplines, the occurrence of a linear correlation on a log-log plot is being interpreted as the existence of a fractal dimension describing either a structure or a dynamical process; the slope of the line is the fractal dimension and corresponds to the exponent in a power law. A model for relating distributions of microfracture energies to the distributions of fractal dimensions for fracture surfaces is presented, and progress toward developing the model for engineering applications is reviewed. The model provides a characterization of complex damage morphologies and estimates of fracture energies for heterogeneous or mixed fracture processes. That is, interactions between the two fundamental processes are automatically accounted for in the model. A means for verifying the model for each material is given. The fracture energy can be estimated from the measured fracture surface roughness, or from a replica of the surface. Author (CISTI)

N93-10498 Purdue Univ., West Lafayette, IN. School of Aeronautics and Astronautics.
ENTROPY OF DISORDER IN THERMOMECHANICS OF DAMAGE IN HETEROGENEOUS SOLIDS c39
Martin Ostoja-Starzewski *In* Carleton Univ., Proceedings of the Twelfth Canadian Congress of Applied Mechanics, Volumes 1 and 2 May 1989 p 232-233 (For primary document see N93-10466 01-31)
Copyright Avail: Canadian Society for Mechanical Engineering, 2050 Mansfield St., Suite 700, Montreal, Quebec H3A 1Z7 Canada

Development of a mesomechanics type continuum damage mechanics (CDM) model which takes into account the fractal morphology and the random character of damage evolution is reported. A two dimensional model of a solid body in x(1), x(2)-space is considered. The microstructure of the body is represented by a planar simple and finite graph. This micromechanical theory of cumulative damage can be extended to three dimensional systems. Quantitative and qualitative results were obtained for effective moduli of Voronoi type elastic microstructures. The graph model is capable of explaining two commonly observed effects: decrease of scatter in strength with the increase in specimen size, and decrease of average strength with increase of specimen size. These results hinge on the properties of correlated and uncorrelated percolation in spatially distributed systems. Further advantages of the use of such geometric ideas in damage analysis are discussed.
Author (CISTI)

N93-10499 Cornell Univ., Ithaca, NY. Dept. of Theoretical and Applied Mechanics.
COMPUTER ALGEBRA AND THE ELLIPTIC RESTRICTED PROBLEM OF THREE BODIES c13
Richard H. Rand and Bhaskar Viswanadham *In* Carleton Univ., Proceedings of the Twelfth Canadian Congress of Applied Mechanics, Volumes 1 and 2 May 1989 p 248-249 (For primary document see N93-10466 01-31)
Copyright Avail: Canadian Society for Mechanical Engineering, 2050 Mansfield St., Suite 700, Montreal, Quebec H3A 1Z7 Canada

Perturbation solutions of differential equations typically involve power series expansions in a small parameter. Computer algebra has proven to be a useful tool for the treatment of perturbation problems due to the large quantities of algebra involved. As an example, a problem which was previously handled both by numerical integration and by hand-derived perturbation analysis is treated by computer algebra. The elliptic restricted problem of three bodies describing the planar motion of a particle (the third body) under the gravitational attraction of two masses (the primaries) which move about their common center of mass in elliptical orbits is examined. Specifically, the stability of the L(sub 4) equilibrium, located at the vertex of an equilateral triangle which is positioned so that the primaries lie at the other two vertices is determined. It is shown that the use of computer algebra yields a vast increase in the number of terms obtained in the perturbation expansion, and raises new questions concerning the convergence of the derived series. Author (CISTI)

N93-10500 Columbia Univ., New York, NY. Dept. of Civil Engineering and Engineering Mechanics.
HEXAGONAL AND OCTAGONAL FINITE ELEMENTS c64
Andre Publico and Gautam Dasgupta *In* Carleton Univ., Proceedings of the Twelfth Canadian Congress of Applied Mechanics, Volumes 1 and 2 May 1989 p 252-253 (For primary document see N93-10466 01-31)
Copyright Avail: Canadian Society for Mechanical Engineering, 2050 Mansfield St., Suite 700, Montreal, Quebec H3A 1Z7 Canada

Computer algebra problems are particularly suited for manipulating polynomials, rationalizing expressions, and evaluating derivatives of Taylor and Pade sequences. Thus, all the algebraic chores pertaining to the finite element formulation for local stiffness and mass matrices do not pose any difficulty when the boundary geometry exceeds the traditional complexity bounds of isoparametric (quadrilateral) elements. Attention is focused on furnishing closed form expressions for shape functions associated with polygons with an arbitrary number of sides. The same procedure holds good for polyhedra and convex shaped domains in higher dimensional (hyper-) spaces. It is anticipated that with the emergence of powerful microcomputers, where the symbolic

manipulator, MATHMATICA, is furnished within the standard operating system, finite elements of better mathematical precision could evolve since literally hundreds of pages of algebraic substitution do not qualify anymore for an equal amount of text book pages (which indeed has been the de facto definition of the intricacy of the method). Author (CISTI)

N93-10501 Clarkson Univ., Potsdam, NY. Dept. of Mechanical and Industrial Engineering.
AN ASSESSMENT OF THE CORRESPONDENCE PRINCIPLE IN COMPARISON TO NONLINEAR VISCOELASTIC THEORY: A CASE STUDY **c39**
E. Sancaktar *In* Carleton Univ., Proceedings of the Twelfth Canadian Congress of Applied Mechanics, Volumes 1 and 2 May 1989 p 290-291 (For primary document see N93-10466 01-31)
Copyright Avail: Canadian Society for Mechanical Engineering, 2050 Mansfield St., Suite 700, Montreal, Quebec H3A 1Z7 Canada

The general form of the correspondance principle states that if the solution of an elastic problem is known, the Laplace transform of the solution to the corresponding linear viscoelastic problem may be found by replacing the elastic constants with their linear viscoelastic counterparts, and the actual loads by their Laplace transforms. This modified transform is inverted subsequently to obtain the solution in time domain. Solutions describing the time variation of the maximum adhesive shear stress in double lap joints using linear correspondance principle and nonlinear compliance method for comparison purposes are presented. The nonlinear solution involves a quasi-elastic method utilizing iteration by successive differentiation as described by Weitsman.
Author (CISTI)

N93-10502 Cagliari Univ. (Italy).
DAMAGE DUE TO PLASTIC DEFORMATION IN ELASTIC-PLASTIC MATERIALS: THE THERMODYNAMICAL CONNECTION **c39**
A. Paglietti *In* Carleton Univ., Proceedings of the Twelfth Canadian Congress of Applied Mechanics, Volumes 1 and 2 May 1989 p 294-295 (For primary document see N93-10466 01-31)
Copyright Avail: Canadian Society for Mechanical Engineering, 2050 Mansfield St., Suite 700, Montreal, Quebec H3A 1Z7 Canada

A continuum damage mechanics approach is provided to the analysis of the relationship between plastic deformation and damage in severely deformed metals. The damage in the material is described by a single scalar variable. It is then shown that the damage produced by plastic strain during isothermal processes at constant stress cannot exceed a limit that is precisely determined by thermodynamics. A means of determining the minimum plastic deformation increment, that is needed to produce a given increment in damage, is provided as well as an expression which sets the upper bound to damage produced by a given plastic deformation. The formulae show that the smaller the stress, the less the damage to be expected from plastic deformation. This is in agreement with the loss of ductility exhibited in dynamic plasticity by metals under uniaxial tests at increased stress levels. The analysis predicts the limit damage beyond which rupture will occur. Author (CISTI)

N93-10503 Sherbrooke Univ. (Quebec). Dept. of Civil Engineering.
SINGULAR STRESS DISTRIBUTIONS AT CIRCULAR HOLES IN COMPOSITE LAMINATES **c39**
Antoine E. Lahoud and Otmane Bouksour *In* Carleton Univ., Proceedings of the Twelfth Canadian Congress of Applied Mechanics, Volumes 1 and 2 May 1989 p 308-309 (For primary document see N93-10466 01-31)
Copyright Avail: Canadian Society for Mechanical Engineering, 2050 Mansfield St., Suite 700, Montreal, Quebec H3A 1Z7 Canada

Assuming the existence of a singularity in the stress distribution at a hole in a composite plate, the numerical determination of the strength of such a singularity using the finite element method with mesh refinement is reported. A finite element program using 20-node quadratic solid isoparametric elements was written to investigate the stresses in a rectangular composite plate with a circular hole in its center. Using this program, a graphite epoxy composite and other laminates were evaluated for the strength of the stress singularity in the vicinity of a circular hole. The resulting values were very similar to those obtained analytically for singularities near a straight edge. This leads to the conclusion that the free edge singularity is the same whether the edge is straight or circular. This result opens the possibility of using singular finite elements for an accurate and efficient determination of the free edge stresses in laminates with straight or curved edges.
Author (CISTI)

N93-10504 Southern Methodist Univ., Dallas, TX.
THERMAL BUCKLING OF HEATED LAMINATED COMPOSITE CIRCULAR CYLINDRICAL SHELLS **c39**
Marion W. Wilcox and S. F. Ma *In* Carleton Univ., Proceedings of the Twelfth Canadian Congress of Applied Mechanics, Volumes 1 and 2 May 1989 p 310-311 (For primary document see N93-10466 01-31)
Copyright Avail: Canadian Society for Mechanical Engineering, 2050 Mansfield St., Suite 700, Montreal, Quebec H3A 1Z7 Canada

The development of an energy method to treat the thermal buckling of a heated composite circular cylindrical shell is adressed. The governing differential equations of the shell for predicting this response are based on the total potential energy of this system and derived by means of the applicable variational principle. This study investigates the effects of ply orientations, number of layers, geometric aspect ratios, and various temperature functions on the critical buckling temperature. Approximate solutions are obtained by applying the Galerkin's method, and numerical results are concentrated on simply supported, antisymmetric angle-ply, and unsymmetric cross-ply laminated composite circular cylindrical shells subjected to non-uniform temperature distribution around the circumference. The temperature changes are taken as constant through the shell thickness. The principal conclusions can be summarized as follows: (1) buckling values of temperature monotonically decrease with increasing ply angles; (2) the expectation of the composite circular cylindrical shell is that the coupling effect between bending and compression decrease with increasing number of plies; (3) the buckling values of temperature monotonically decreases with an increase of such; and (4) the combination of a variational approach together with the Galerkin method, is a very effective way of treating eigenvalue problems.
Author (CISTI)

N93-10505 Chung Shan Inst. of Science and Technology (Taiwan).
FAILURE ANALYSIS OF LAMINATED COMPOSITES BY USING ITERATIVE THREE-DIMENSIONAL FINITE ELEMENT METHOD **c39**
W. C. Hwang and C. T. Sun *In* Carleton Univ., Proceedings of the Twelfth Canadian Congress of Applied Mechanics, Volumes 1 and 2 May 1989 p 314-315 (For primary document see N93-10466 01-31)
Copyright Avail: Canadian Society for Mechanical Engineering, 2050 Mansfield St., Suite 700, Montreal, Quebec H3A 1Z7 Canada

A failure analysis of laminated composites is accomplished by using an iterative three-dimensional finite element method. Based on Tsai-Wu failure theory, three different modes of failure are proposed: fiber breakage, matrix cracking, and delamination. The first ply failure load is then evaluated. As the applied load exceeds the first ply failure load, localized structural failure occurs and the global structural stiffness should change. The global stiffness matrix is modified by taking nonlinearity due to partial failures within a laminate into consideration. The first ply failure load is analyzed by using a iterative mixed field method in solving the linear part of the finite element equations. The progressive failure problem is solved numerically by using Newton-Raphson iterative schemes for the solution of nonlinear finite element equations. Numerical

examples include angle-ply symmetric Thornel 300 graphite/934 resin epoxy laminates under uniaxial tension. First ply failure loads as well as the final failure loads are evaluated. Good correlation between analytical results and experimental data are observed. Numerical results also include the investigation of composite specimens with a centered hole, under uniaxial tension. Excellent correlation with the experimental data is observed.

Author (CISTI)

N93-10506 McDonnell-Douglas Corp., Saint Louis, MO.
ANALYSIS OF A BUFFER STRIP LAMINATE WITH A CUTOUT **c39**

E. S. Meyer and L. R. Dharani (Missouri Univ., Rolla.) *In* Carleton Univ., Proceedings of the Twelfth Canadian Congress of Applied Mechanics, Volumes 1 and 2 May 1989 p 316-317 (For primary document see N93-10466 01-31)

Copyright Avail: Canadian Society for Mechanical Engineering, 2050 Mansfield St., Suite 700, Montreal, Quebec H3A 1Z7 Canada

Stress concentration at holes results in a loss of strength of composite structures, as much as one-third in tension and one-half in compression. A model based on the classical shear lag theory for predicting the fracture behavior of a unidirectional laminate with a pair of (hybrid) buffer strips and with a transverse crack in the form of broken fiber is extended to include a circular cutout. An assessment of the buffer strips, soft or stiff, is presented. A simplified model consisting of two half-planes and three finite-width unidirectional strips is analyzed. The basic solution required in the analysis of this problem is the solution of a unidirectional half-plane with a circular cutout and a longitudinal matrix split between two arbitrary fibers. By letting the split length approach infinity, the solution of the finite-width strip with a circular cutout is obtained. The final solution to the buffer strip laminate is obtained by making use of the half-plane and the finite-width strip solutions. The results show that the use of softening strips in composite laminates with circular cutouts will reduce the stress concentration at the hole. However, the stress concentration in the undamaged main panel is increased with a decrease in the buffer strip stiffness; thus, there is a cutoff after which further softening of the buffer strip will not increase the notched strength of the laminate.

Author (CISTI)

N93-10507 Florida Univ., Gainesville. Dept. of Aerospace Engineering, Mechanics and Engineering Science.
ELASTICITY ANALYSIS OF ORTHOTROPIC BEAMS UNDER THREE-PART BENDING **c39**

S. Hu and B. V. Sankar *In* Carleton Univ., Proceedings of the Twelfth Canadian Congress of Applied Mechanics, Volumes 1 and 2 May 1989 p 318-319 (For primary document see N93-10466 01-31)

Copyright Avail: Canadian Society for Mechanical Engineering, 2050 Mansfield St., Suite 700, Montreal, Quebec H3A 1Z7 Canada

An approximate, but closed-form solution for the stresses in an orthotropic beam under three-point bending is proposed. The solution is obtained as the superposition of stresses in an orthotropic half-plane and in an orthotropic beam. The stress concentration effects due to the small loading area are mostly accounted for by the half-plane solution. The half-plane solution is exact and can be expressed in closed-form. The second part of the solution involves stresses in a beam, which is derived by a combination of beam theory solution and elasticity solution. The loading on the beam is obtained by solving the problem of contact between a rigid, smooth indenter, and an orthotropic beam. The proposed method was applied to the case of three-point bending of an orthotropic beam. The results were compared with a finite element solution. The present method also has application in computing stresses due to low-velocity impact. The effect of material properties on the shear stress concentration was studied by considering glass/epoxy, graphite/epoxy, and boron/epoxy as examples. It was found that the shear concentration very much depend on the contact length. Author (CISTI)

N93-10508 Missouri Univ., Rolla.
ANALYSIS OF FAILURE MODES IN CERAMIC MATRIX COMPOSITE **c24**

L. Chai and L. R. Dharani *In* Carleton Univ., Proceedings of the Twelfth Canadian Congress of Applied Mechanics, Volumes 1 and 2 May 1989 p 322-323 (For primary document see N93-10466 01-31)

Copyright Avail: Canadian Society for Mechanical Engineering, 2050 Mansfield St., Suite 700, Montreal, Quebec H3A 1Z7 Canada

A micromechanics analytical model, a two phase consistent shear lag model, is developed for predicting the failure modes in a fiber reinforced unidirectional ceramic matrix composite. The model is based on a modified shear lag theory that accounts for the relatively large matrix stiffness. The fiber and matrix stresses are established as functions of the applied stress, crack geometry, and most importantly, the microstructural properties of the constituents. From the predicted stresses, the modes of failure are established. The following specific damage configurations in a unidirectional ceramic matrix composite subject to uniaxial tensile loading parallel to the fibers are addressed: a transverse crack formed by fracture of both the fiber and the matrix phases with no interface damage, and with interface damage (mode-1) and a transverse matrix crack bridged by intact fibers with no interface damage, and with interface damage (mode-2). A comparison of stresses between mode-1 and mode-2 shows that the maximum stresses corresponding to mode-1 are much higher than those of mode-2. Therefore, a brittle matrix reinforced by fibers which are of higher failure strain than that of the matrix results in a more desirable composite system as it would exhibit crack bridging failure mode. The crack propagation for the failure mode-2 under the constant applied load is of steady state cracking and that for failure mode-1 is that of unstable cracking. The preliminary predictions show that a transition from one failure mode to another is possible. Author (CISTI)

N93-10509 Ohio State Univ., Columbus. Dept. of Civil Engineering.
CONSISTENT SHEAR CONSTITUTIVE RELATIONS FOR LAMINATED PLATES **c24**

Soon-Jo Hong, Ranbir S. Sandhu, and Harpal S. Chohan *In* Carleton Univ., Proceedings of the Twelfth Canadian Congress of Applied Mechanics, Volumes 1 and 2 May 1989 p 324-325 (For primary document see N93-10466 01-31)

Copyright Avail: Canadian Society for Mechanical Engineering, 2050 Mansfield St., Suite 700, Montreal, Quebec H3A 1Z7 Canada

Using a mixed variational formulation of linear elastostatics it is shown that the shearing force in any lamina may depend upon the shear deformation of that lamina as well as others. Existing theories of homogeneous as well as laminated plates are seen to arise as specializations/approximations of the general theory. The free vibration problem of a sandwich plate with simply supported edges was solved using a finite element procedure. A square plate composed of three layers was considered. Three different sets of material properties were considered for the orthotropic plate. Non dimensionalized fundamental frequencies of the orthotropic laminate computed using the consistent theory and the existing theory are provided. For all cases, the consistent shear deformation theory proposed gave values closer to the exact solution. Author (CISTI)

N93-10510 Florida Univ., Gainesville. Dept. of Aerospace Engineering, Mechanics and Engineering Science.
INVESTIGATION OF LAMINATED COMPOSITE PLATES UNDER IMPACT DYNAMIC LOADING BY USING A THREE-DIMENSIONAL HYBRID STRESS FINITE ELEMENT METHOD **c24**

C. T. Sun and W. J. Liou (Feng Chia Univ., Taichung, Taiwan) *In* Carleton Univ., Proceedings of the Twelfth Canadian Congress of Applied Mechanics, Volumes 1 and 2 May 1989 p 328-329 (For primary document see N93-10466 01-31)

Copyright Avail: Canadian Society for Mechanical Engineering, 2050 Mansfield St., Suite 700, Montreal, Quebec H3A 1Z7 Canada

The objective of this paper is to investigate the dynamic response of laminated composite plates impacted by a projectile with a known velocity. A blunt ended circular cylinder 2.54 cm in length, 0.9525 cm in diameter and 0.01475 kg is assumed to hit a square laminate clamped around the four edges with a side length of 14 cm. In order to solve the dynamic impact problem a three dimensional hybrid stress isoparametric element in conjunction with the Newmark direct integration method was used. The method is very powerful in analyzing dynamic response of composite structural elements impacted by the projectile. It can provide some valuable information about the initiation of delamination cracks of laminated composites subject to impact load. Author (CISTI)

N93-10511 Cambridge Univ. (England). Dept. of Engineering.

A NEW DEPLOYABLE MAST **c18**

A. Kwan and S. Pellegrino *In* Carleton Univ., Proceedings of the Twelfth Canadian Congress of Applied Mechanics, Volumes 1 and 2 May 1989 p 334-335 (For primary document see N93-10466 01-31)

Copyright Avail: Canadian Society for Mechanical Engineering, 2050 Mansfield St., Suite 700, Montreal, Quebec H3A 1Z7 Canada

It is envisaged that deployable masts will act as actuators for the deployment of solar panel arrays, telescopes and antennas in space, and subsequently become fully effective structural components of the whole assembly. Several schemes for a new type of deployable mast, which contains cable segments as well as rods were investigated. All the cables are in a state of pretension when the mast is in its deployed state, and hence are able to carry both tensile and compressive axial forces resulting from external loads acting on the mast. During deployment/folding all cables are slack and, because the distance between points connected by a cable never exceeds the length of the cable, only the rods affect the process. Unlike existing designs, masts based on this concept are stress-free in their folded configuration and need much fewer and simpler mechanical hinges than the more conventional schemes which have been proposed in the past. Author (CISTI)

N93-10512 Osaka Univ., Suita (Japan). Dept. of Precision Engineering.

VIBRATIONS OF A FLEXIBLE TIMOSHENKO BEAM UNDER GRAVITY **c39**

T. Yokayama *In* Carleton Univ., Proceedings of the Twelfth Canadian Congress of Applied Mechanics, Volumes 1 and 2 May 1989 p 340-341 (For primary document see N93-10466 01-31)

Copyright Avail: Canadian Society for Mechanical Engineering, 2050 Mansfield St., Suite 700, Montreal, Quebec H3A 1Z7 Canada

A study was carried out to investigate the gravity effect on the vibration behavior of flexible space structures. The generic structural element chosen for this study is a flexible Timoshenko beam. The governing equations for free vibrations of the vertically hanging beam under gravity are derived from Hamilton's principle. The effects of gravity, shear deformation and rotatory inertia are incorporated into a finite element model for determining the vibration characteristics of the hanging beam. The natural frequencies are given for the classical Euler-Bernoulli beam, which is a special case of the present model, and compared with the existing experimental and numerical results. The results provide a better understanding of the dynamic characteristics of a large flexible space beam under gravity. Author (CISTI)

N93-10513 Indian Inst. of Tech., New Delhi. Dept. of Applied Mechanics.

ORTHOTROPIC CIRCULAR PLATE ON NONLINEAR ELASTIC SUBGRADE **c39**

Rakesh Kumar Jain and Yogendra Nath *In* Carleton Univ., Proceedings of the Twelfth Canadian Congress of Applied Mechanics, Volumes 1 and 2 May 1989 p 352-353 (For primary document see N93-10466 01-31)

Copyright Avail: Canadian Society for Mechanical Engineering, 2050 Mansfield St., Suite 700, Montreal, Quebec H3A 1Z7 Canada

Circular plates made of composite materials are extensively used in civil, marine and aeronautical industries. There are several situations in which the plate structure must be analyzed by taking into account the interaction with the surrounding elastic subgrade. A cubic nonlinear spring model for the interaction force is assumed and the orthotropic circular plates on elastic subgrades undergoing moderately large axisymmetric elastic deformation are analyzed. Finite degree Chebyshev series and implicit Houbolt scheme are employed for the spatial and temporal discretizations of dynamic analogue of Von Karman type partial differential equations of motion. The effects of nonlinear stiffness orthotropy and damping of the plate material on the central response of clamped and simply supported plates were investigated. Author (CISTI)

N93-10514 University of South Florida, Tampa. Dept. of Civil Engineering and Mechanics.

COMPARISON OF THE MAXIMUM STRESS AND THE STRESS INTENSITY APPROACH IN THE ANALYSIS OF BONDED JOINTS **c39**

William C. Carpenter *In* Carleton Univ., Proceedings of the Twelfth Canadian Congress of Applied Mechanics, Volumes 1 and 2 May 1989 p 368-369 (For primary document see N93-10466 01-31)

Copyright Avail: Canadian Society for Mechanical Engineering, 2050 Mansfield St., Suite 700, Montreal, Quebec H3A 1Z7 Canada

Predictions of the strength of an adhesive joint are often based on maximum stresses as predicted by theories such as that of Goland and Reissner. A recent approach has been to examine the joint configuration as an eigenvalue problem. Failure prediction is then based on determining critical values of the undetermined coefficients (or stress intensities) associated with those eigenvectors which give infinite stresses as the joint edges are approached. This paper examines the prediction of joint strength with the maximum stress theory of Goland and Reissner and with a fracture mechanics approach. The methodology of the two approaches is first described. Then a lap joint is studied in detail using the two approaches. Except for very small lap lengths, maximum stresses in the adhesive from the theory of Goland and Reissner depend on the applied moments and axial forces at the edges of the joint and are only insignificantly affected by the shear force applied to the edge of the joint. Applied axial forces, moments, and shears seem to have more of an equal affect on the stress intensities. Both the maximum adhesive stresses from the theory of Goland and Reissner and the stress intensities are relatively unaffected by increased lap length after a critical lap length. Author (CISTI)

N93-10515 Reims Univ. (France).

EXPERIMENTAL AND THEORETICAL BEHAVIOR OF ADHESIVELY BONDED COMPOSITE STRUCTURES UNDER TENSILE STRESS AT THE EDGE VICINITY [COMPORTEMENT EXPERIMENTAL ET THEORIQUE, AU VOISINAGE DES EXTREMITES, D'ASSEMBLAGES COMPOSITES COLLES, SOLLICITES AU CISAILLEMENT PAR TRACTION] **c39**

Y. Gilibert and Michel L. L. Klein (Ecole Nationale Superieure de Techniques Avancees, Paris, France) *In* Carleton Univ., Proceedings of the Twelfth Canadian Congress of Applied Mechanics, Volumes 1 and 2 May 1989 p 374-375 In FRENCH (For primary document see N93-10466 01-31)

Copyright Avail: Canadian Society for Mechanical Engineering, 2050 Mansfield St., Suite 700, Montreal, Quebec H3A 1Z7 Canada

This paper presents the first results obtained during a study of the mechanical behavior of an adhesively bonded, symmetrical, double lap joint in a composite structure under simple tensile stress at 20 C. The experimental results on glass epoxy composites are

compared with those obtained in earlier work involving an identical set of tests on steel plates having the same dimensions and bonded using the same adhesive. The results are interpreted using a simple model which potentially could be used in industrial applications. In both studies stress concentrations were noted in the neighborhood of the free and loaded extremities. This situation arises from edge effects engendered by the shape of the substratum. Similar global elastic behavior resulting from tensile stress at ambient temperatures was observed at the macroscopic level for both cases. The model of surface contraction at the free extremity of lap joints has been modified to produce adequate agreement between theory and experiment. Author (CISTI)

N93-10516 Ecole Nationale Superieure de Techniques Avancees, Paris (France).
EXPERIMENTAL AND NUMERIC ANALYSIS OF CONSTRAINTS IN A BONDED STEPPED LAP JOINT SUBJECTED TO TRACTION [ANALYSE EXPERIMENTALE ET NUMERIQUE DES CONSTRAINTES DANS UN ASSEMBLAGE COLLE EN ESCALIER SOLLICITE A LA TRACTION] **c39**
Yvon Gilibert and Alain Rigolot *In* Carleton Univ., Proceedings of the Twelfth Canadian Congress of Applied Mechanics, Volumes 1 and 2 May 1989 p 376-377 In FRENCH (For primary document see N93-10466 01-31)
Copyright Avail: Canadian Society for Mechanical Engineering, 2050 Mansfield St., Suite 700, Montreal, Quebec H3A 1Z7 Canada

The analysis of the constraints on glued stepped lap joints is not sufficiently advanced that predictions on the fracture or fatigue behavior of such joints can be made. This report presents an experimental and numeric analysis of such joints. The experimental setup involved a four step steel member adhesively joined to a glass epoxy member by Eponal adhesive. The mechanical properties of the components of the assembly were measured by elastic extensiometry. The evolution of acoustic emissions and the surface deformation of the members were measured simultaneously. It is notable that the first acoustic emission event coincided with the first change in the slope of the deformation - constraint curve. A material resistance approximation based on the elongation of each step and on weakness in the width of the joint was used in the numerical analysis. Author (CISTI)

N93-10517 Waterloo Univ. (Ontario). Dept. of Mechanical Engineering.
DYNAMICS OF SYSTEMS WITH TIME-VARYING INERTIAL PROPERTIES **c39**
John J. McPhee *In* Carleton Univ., Proceedings of the Twelfth Canadian Congress of Applied Mechanics, Volumes 1 and 2 May 1989 p 392-393 (For primary document see N93-10466 01-31)
Copyright Avail: Canadian Society for Mechanical Engineering, 2050 Mansfield St., Suite 700, Montreal, Quebec H3A 1Z7 Canada

A classification scheme is presented for a general materials system that has time varying inertial properties, as well as a control volume formulation of the governing equations of motion. Inertial problems may vary with time by means of capture or release of mass, change in configuration, or mass redistribution. Translational and rotational variable mass equations are developed and applied to the falling string problem. As illustrated by an example, the power of this formulation lies in its systematic nature: once the analyst has defined the control volume (that may translate, rotate, and deform in three dimensional space) the equations of translational and rotational motions can be directly applied.
Author (CISTI)

N93-10518 Technische Univ., Hamburg (Germany).
AN ELASTIC OBLATE AXISYMMETRIC REFERENCE GYRO FOR ATTITUDE STUDIES **c35**
V. Schlegel, A. Guran (Toronto Univ., Ontario), and F. P. J. Rimrott (Toronto Univ., Ontario) *In* Carleton Univ., Proceedings of the Twelfth Canadian Congress of Applied Mechanics, Volumes 1 and 2 May 1989 p 396-397 (For primary document see N93-10466 01-31)
Copyright Avail: Canadian Society for Mechanical Engineering, 2050 Mansfield St., Suite 700, Montreal, Quebec H3A 1Z7 Canada

For real gyros deformations due to inertial forces are inevitable. If such deformations are small, one can often predict attitude drift and attitude stability of the gyro. This paper sets out to gain an understanding of the motion of a torque-free gyro, where the elastic deformations are not necessarily small. To that end, an elastic oblate axisymmetric gyro model has been devised. The model is as simple as possible, yet designed to have all characteristics required to study its behavior at any nutation angle. By studying the behavior of the reference gyro, it is concluded that the assumption of near-rigidity plays an important role in prediction of the motion of axisymmetric gyros. For large elastic deformations, the full nonlinear analysis shows that several equilibrium states exist. In an attempt to study the stability of the equilibrium states, comparisons were made of the value of the total energy of the system for a given nutation angle on different branches. It has been observed that depending on the oblateness of the gyro the total energy may attain its minimum on one branch or the other. This observation is based on numerical experiments.
Author (CISTI)

N93-10519 British Columbia Univ., Vancouver. Dept. of Mechanical Engineering.
DYNAMICS OF AN ORBITING FLEXIBLE MANIPULATOR **c37**
J. K. Chan and V. J. Modi *In* Carleton Univ., Proceedings of the Twelfth Canadian Congress of Applied Mechanics, Volumes 1 and 2 May 1989 p 398-399 (For primary document see N93-10466 01-31)
Copyright Avail: Canadian Society for Mechanical Engineering, 2050 Mansfield St., Suite 700, Montreal, Quebec H3A 1Z7 Canada

A mobile remote manipulator system (MRMS) is an integral part of the proposed Space Station. The manipulator is also inherently flexible; this flexibility complicates the dynamics of the system and presents challenging problems in stability and control. The coupling of the MRMS between the flexibilities of the arm and the joint was investigated. This may lead to pointing inaccuracies and undesired accelerations of the payload at the tip of the manipulator arm. This paper studies, numerically, the effects of the flexible joint on the system dynamics which is, in general, governed by highly nonlinear, nonautonomous and coupled hybrid equations of motion. An approximate analytic solution is also obtained to provide better physical appreciation of the response. The system response for a tip deflection equal to 10 percent of the arm length was evaluated. The response of both the generalized coordinates consist of a characteristic low frequency with a high frequency modulation superposed. With larger initial conditions the numerical response indicated the high frequency component to have periodic modulation. The analytic solution, derived from the assumption that the system is quasi-linear, is unable to predict the nonlinear effect. However, the closed form solution yields an average value for the high frequency such that no error is accumulated after one cycle of the low frequency mode. When damping is included at the joint, the high frequency component decays rapidly while the low frequency oscillation is only slightly affected. From the time constants in the analytic solution, the settling times for pointing error of acceleration can be easily calculated with good accuracy. Author (CISTI)

N93-10520 Thomson-CSF, Ottawa (Ontario).
EFFECT OF MOUNTING OFFSET ON THE DYNAMICS OF DEPLOYING FLEXIBLE APPENDAGES **c39**
S. Kalaycioglu, B. A. Kalaycioglu, Z. R. Irani, and A. K. Misra *In* Carleton Univ., Proceedings of the Twelfth Canadian Congress of Applied Mechanics, Volumes 1 and 2 May 1989 p 400-401 (For primary document see N93-10466 01-31)
Copyright Avail: Canadian Society for Mechanical Engineering, 2050 Mansfield St., Suite 700, Montreal, Quebec H3A 1Z7 Canada

This paper presents the effect of offset of the mounting point

of deploying flexible beams from the center of rotation on their dynamics. The response characteristics of the system configuration are investigated taking into account the role played by non-linear axial shortening effect when undergoing a 3-D rotational motion. It is observed that due to the root offset, large tip deflections of the beams may result during steady yaw and roll of the system for several deployment schemes. Author (CISTI)

N93-10521 British Columbia Univ., Vancouver. Dept. of Mechanical Engineering.
EXPERIMENTAL DEMONSTRATION OF OFFSET CONTROL WITH AN APPLICATION TO THE TETHERED PAYLOAD c18
V. J. Modi, P. K. Lakshmanan, A. K. Misra (McGill Univ., Montreal, Quebec), R. J. Picha, S. Chan, and S. Vakil *In* Carleton Univ., Proceedings of the Twelfth Canadian Congress of Applied Mechanics, Volumes 1 and 2 May 1989 p 402-403 (For primary document see N93-10466 01-31)
Copyright Avail: Canadian Society for Mechanical Engineering, 2050 Mansfield St., Suite 700, Montreal, Quebec H3A 1Z7 Canada

A control law for tethered satellite systems was proposed that uses a boom-trolley arrangement that allows the point of attachment of the tether to be moved in three orthogonal directions. This means that the position, velocity and acceleration of the tether attachment point, become specified quantities in the dynamical formulation. The accelerations are integrated along each axis to obtain the corresponding velocities and positions. A tethered satellite system model was developed to demonstrate the offset control strategy in real time. A variety of tether configurations, retrieval rates, and initial conditions were employed to systematically test the controller's effectiveness. Even at large initial conditions the controller proved very successful in bringing the tether to its equilibrium configuration. This clearly demonstrated the robustness of the control algorithm. The effectiveness increased as the tether length diminished which makes it particularly attractive in situations where other controllers have limitations. It is expected that a hybrid control strategy with thruster/tension control at large tether lengths followed by offset control near the platform end during the final stages of retrieval would be most effective.
Author (CISTI)

N93-10522 New Brunswick Univ., Fredericton. Dept. of Mechanical Engineering.
PROBABILITY DENSITY FUNCTIONS FOR RANDOM NONLINEAR OSCILLATION c71
Huw G. Davies and Qiang Liu *In* Carleton Univ., Proceedings of the Twelfth Canadian Congress of Applied Mechanics, Volumes 1 and 2 May 1989 p 404-405 (For primary document see N93-10466 01-31)
Copyright Avail: Canadian Society for Mechanical Engineering, 2050 Mansfield St., Suite 700, Montreal, Quebec H3A 1Z7 Canada

This paper reviews recent work done by the authors on the response of nonlinear systems to random excitation. The systems are of first order with fairly general nonlinear elements and the excitation is either modulated white noise or a narrow band random noise. Particular attention is paid to the probability density function (PDF) of the envelope of the response. Stationary and nonstationary approximate solutions of appropriate Fokker Planck equations are obtained for the PDF, and the approximate results are compared with extensive numerical simulations.
Author (CISTI)

N93-10523 University of Western Ontario, London.
ON TECHNIQUES FOR DIGITAL SIMULATION OF RANDOM RESPONSE OF NONLINEAR OSCILLATORS c61
C. W. S. To and S. W. Zhang (Beijing Agricultural Univ., China) *In* Carleton Univ., Proceedings of the Twelfth Canadian Congress of Applied Mechanics, Volumes 1 and 2 May 1989 p 406-407 (For primary document see N93-10466 01-31)
Copyright Avail: Canadian Society for Mechanical Engineering, 2050 Mansfield St., Suite 700, Montreal, Quebec H3A 1Z7 Canada

In the study of dynamical systems, digital simulation (DS) is often used for the solving of nonlinear equations of motion whose inhomogeneous parts are expressed as random processes. When DS results of nonlinear oscillators excited by Gaussian stationary or time modulated white noise are required, numerical integration methods, such as Runge-Kutta fourth order (RK4) or the central difference scheme, is frequently employed. This paper presents the results of studies on how the use of time stepping on the RK4 and central difference schemes effects the accuracy of the response. A third technique based on sampling functions is proposed along with a strategy to ensure accurate simulation results and to circumvent the problem of integrating the white noise excitation. The Duffy oscillator is used to illustrate this work.
Author (CISTI)

N93-10524 University of Western Ontario, London.
EVOLUTIONARY SPECTRA OF TIME-DEPENDENT DISCRETIZED SYSTEMS TO TIME-FREQUENCY MODULATED RANDOM EXCITATIONS c39
C. W. S. To *In* Carleton Univ., Proceedings of the Twelfth Canadian Congress of Applied Mechanics, Volumes 1 and 2 May 1989 p 412-413 (For primary document see N93-10466 01-31)
Copyright Avail: Canadian Society for Mechanical Engineering, 2050 Mansfield St., Suite 700, Montreal, Quebec H3A 1Z7 Canada

Closed form solutions employing the theory of evolutionary spectrum have been developed for nonstationary random response analysis of linear time invariant multiple degree of freedom (MDOF) systems in the area of structural dynamics. The closed form solutions are capable of handling discretized systems such as those encountered in finite element analysis. This paper extends the formulation and makes use of the closed form solutions to deal with MDOF systems with deterministic parametric and autoparametric excitations. Each of the latter can be represented as a product of a deterministic frequency modulating function, a deterministic time modulating function, and a stationary random process. Thus, the frequency composition of the excitation process can be controlled by the frequency modulating function. The method makes use of the results of normal mode analysis and requires no numerical integration. Examples of the application include analysis of response of a helicopter rotor blade excited spanwise by turbulence, plate structures subjected to distributed random loadings and in-plane deterministic forces, and cylindrical shell structures with distributed random and deterministic axial forces. Author (CISTI)

N93-10525 Virginia Polytechnic Inst. and State Univ., Blacksburg. Dept. of Engineering Science and Mechanics.
DYNAMIC STABILITY OF LAMINATED TRANSVERSELY-ISOTROPIC COMPOSITE PLATES SUBJECTED TO PARAMETRIC EXCITATIONS c24
L. Librescu and S. Thangjitham *In* Carleton Univ., Proceedings of the Twelfth Canadian Congress of Applied Mechanics, Volumes 1 and 2 May 1989 p 414-415 (For primary document see N93-10466 01-31)
Copyright Avail: Canadian Society for Mechanical Engineering, 2050 Mansfield St., Suite 700, Montreal, Quebec H3A 1Z7 Canada

The dynamic instability of simply supported shear deformable laminated composite plates subjected to parametric excitation by compressive edge loadings was investigated. The analysis is performed both in linear and nonlinear formulation. While the former formulation allows determination of the boundaries of the instability domains, the latter one is used to obtain the frequency-amplitude response behavior. Towards the end of investigating these problems, a higher-order geometrically nonlinear theory of symmetrically laminated plates is used. The results obtained within this theory are compared with their first order and classical counterparts and a number of conclusions concerning their range of applicability and the influence of various parameters are presented. The numerical results allow one to infer the following. The increase of transverse shear flexibilities yields a decrease in

size and a shift towards the domain of lower excitation frequencies of the parametric stability regions. The account of transverse shear flexibilities results in higher amplitudes and bifurcation points which are farther apart than in their classical counterparts and shifted toward the domain of lower excitation frequencies. Classical theory overestimates the size of the stability domains and underestimates the response amplitudes when compared with their first order transverse shear deformation (FTSD) and high order geometrically nonlinear theory counterparts. Author (CISTI)

N93-10526 California Univ., Davis. Dept. of Civil Engineering.
RESPONSE OF A BEAM TO TRANSVERSE IMPULSIVE AND HIGH FREQUENCY LOADS **c39**
James R. Hutchinson *In* Carleton Univ., Proceedings of the Twelfth Canadian Congress of Applied Mechanics, Volumes 1 and 2 May 1989 p 418-419 (For primary document see N93-10466 01-31)
Copyright Avail: Canadian Society for Mechanical Engineering, 2050 Mansfield St., Suite 700, Montreal, Quebec H3A 1Z7 Canada

Rapid position adjustments required of control systems in certain space structures have the potential of exciting the higher modes of the structure. The purpose of this paper was to investigate the importance of the higher modes of a simplified structure, a free beam. The beam was characterized by Timoshenko beam theory which accounts for shear deformation and rotary inertia effects. The transverse displacement response of a Timoshenko beam to a centrally applied point load was found. The forcing function was considered as both an impulsive load and as a sinusoidal load. Damping was included as linear viscous damping in each mode, except for the rigid body mode which was considered to be undamped. The damping is considered to be the same in each of the flexural modes. The response is found by modal superposition of up to five hundred modes. The early time response to impulsive forces is little effected by low damping levels. The high frequency steady state response shows a localized effect which is greatly affected by low level damping. Author (CISTI)

N93-10527 California State Univ., Long Beach. Dept. of Mechanical Engineering.
VIBRATION OF A DAMPED DOUBLE-BEAM SYSTEM **c39**
H. V. Vu and B. H. Karnopp (Michigan Univ., Ann Arbor.) *In* Carleton Univ., Proceedings of the Twelfth Canadian Congress of Applied Mechanics, Volumes 1 and 2 May 1989 p 426-427 (For primary document see N93-10466 01-31)
Copyright Avail: Canadian Society for Mechanical Engineering, 2050 Mansfield St., Suite 700, Montreal, Quebec H3A 1Z7 Canada

This paper presents an exact analytical method of solving the vibration of a damped double-beam system. The viscous damping and the applied forcing function can be completely arbitrary. The damping is assumed neither small nor proportional, and the forcing function can be either continuous or concentrated. The system consists of a main beam, with a force acting on it, and an auxiliary beam with a viscoelastic material between the two. The method uses a simple manipulation of variables to decouple the equations first, then the solution is solved by means of modal analysis. With this method, both the viscous damping and the applied forcing function are completely arbitrary. The damping is neither small nor proportional to the mass and stiffness, and the forcing function can be either continuous or concentrated, periodic or not. At present, the Bernoulli-Euler model is used for transverse vibrations of the two beams, and the viscoelastic material is modeled simply as a distributed spring and dashpot in parallel. As a demonstration of the method, a case study of simply supported beams is considered. Although the boundary conditions of the two beams may be arbitrary, it is necessary that they are identical if they are on the same side of the system. Author (CISTI)

N93-10528 Manitoba Univ., Winnipeg. Dept. of Mechanical Engineering.
OVERVIEW OF THE VIBROIMPACT DAMPING OF PACKAGED PARTICLES **c39**
N. Popplewell, C. Pang, and S. E. Semercigil *In* Carleton Univ., Proceedings of the Twelfth Canadian Congress of Applied Mechanics, Volumes 1 and 2 May 1989 p 428-429 (For primary document see N93-10466 01-31)
Copyright Avail: Canadian Society for Mechanical Engineering, 2050 Mansfield St., Suite 700, Montreal, Quebec H3A 1Z7 Canada

Impact damping utilizes the principle of momentum exchange and the energy dissipation usually arising from the collisions of a lightly damped, resonant primary system with a smaller secondary mass. It has been used to successfully attenuate the excessive vibrations of turbine blades, antennae and aircraft wings. Various forms have been considered to make the standard integral secondary mass more effective. A sophisticated version involves packaging particles in a resilient plastic bag. This form has shown to be generally superior for a given weight and a resonant frequency of the primary system around 20 Hz. The tightness and the no longer constant dimensions of the bag itself are complicating factors. Experimentally observed effects of various bag tightnesses are summarized at individual optimum clearances. Differences between horizontal and vertical motions are qualified over a range of frequencies. The benefit of making a vertical motion analogous to a horizontal one is illustrated by introducing a magnetic bias to counteract gravity. This demonstration potentially expands the application of impact damping to flexible robot arms.
Author (CISTI)

N93-10529 Toronto Univ. (Ontario). Inst. for Aerospace Studies.
MODE LOCALIZATION IN A SIMPLE CONTINUUM MODEL **c39**
C. J. Damaren *In* Carleton Univ., Proceedings of the Twelfth Canadian Congress of Applied Mechanics, Volumes 1 and 2 May 1989 p 430-431 (For primary document see N93-10466 01-31)
Copyright Avail: Canadian Society for Mechanical Engineering, 2050 Mansfield St., Suite 700, Montreal, Quebec H3A 1Z7 Canada

The phenomenon of mode localization is investigated wherein the characteristic vibrations of a structure are confined to small spatial regions. Typically, structures that are perturbed from a nominal configuration consisting of weakly-coupled, identical substructures are susceptible to mode localization. The present work investigates the case where the substructures and coupling agents are continua (possess many degrees of freedom). The structure is a simple model of a wrap-rib antenna. The mode shapes in the lightly coupled uniform case extend throughout the structure for all values of the coupling parameters. Where the rib bending stiffnesses are randomly perturbed from their nominal values the modes are localized within certain regions of the structure. The alpha(th) mode localizes around the beam with the alpha(th) lowest bending stiffness where alpha represents the circumferential index. The shape of each beam is almost identical to the first bending mode of a uniform, cantilevered beam. Other results show that as the amount of disorder is increased, the degree of localization increases. Furthermore, higher radial mode numbers exhibit the same behaviour, although each beam takes on the shape of the bending mode corresponding to the radial number. These results did not change significantly when finer approximations for the mesh were used. Simulations of the response to a point force that acts impulsively in time show that the vibrations become confined to the region where the force acted, whereas for the perfect structure they propagated throughout. Author (CISTI)

N93-10530 Lakehead Univ., Port Arthur (Ontario). Dept. of Mechanical Engineering.
EXPERIMENTAL INVESTIGATION OF SIMPLE SUPPORT CONDITION IN FREE VIBRATION ANALYSIS OF PLATES **c39**
H. T. Saliba and D. Ciszewski *In* Carleton Univ., Proceedings of the Twelfth Canadian Congress of Applied Mechanics, Volumes 1 and 2 May 1989 p 436-437 (For primary document see N93-10466 01-31)

Copyright Avail: Canadian Society for Mechanical Engineering, 2050 Mansfield St., Suite 700, Montreal, Quebec H3A 1Z7 Canada

Simply supported plates do not lend themselves well to experimental investigations. Difficulties encountered in satisfying all of the requirements of a simple support under laboratory conditions are largely responsible for the current lack of experimental data. The aim of the present experiment is to produce a satisfactory working model of the simple support for the experimental study of plate vibration. Data obtained using this model are compared with existing rectangular plate eigenvalues. Simply supported trapezoidal plates are also investigated and results are compared with those of reference. Simple support theoretically requires that only the reactive forces, and not moments, be transmitted between the plate and its support. From a practical point of view it means that the edge of the plate must be restrained from lateral motion while permitting free rotation of the plate about the supported edge. This study makes use of a modified hinge. Preliminary experimental eigenvalues obtained for simply supported rectangular plates show excellent agreement with known theoretical values. This suggests that the modified hinge model of simple support is performing well. Author (CISTI)

N93-10531 Industrial Marine Products Group Ltd., Halifax (Nova Scotia).

FLEXURAL VIBRATION OF BEAMS WITH VARYING SECTION PROPERTIES **c39**

R. Jategaonkar and D. S. Chehil (Nova Scotia Technical Coll., Halifax.) *In* Carleton Univ., Proceedings of the Twelfth Canadian Congress of Applied Mechanics, Volumes 1 and 2 May 1989 p 438-439 (For primary document see N93-10466 01-31)

Copyright Avail: Canadian Society for Mechanical Engineering, 2050 Mansfield St., Suite 700, Montreal, Quebec H3A 1Z7 Canada

A procedure has been developed for calculating the natural frequencies for a beam with inertia, area and mass varying in a general manner. This procedure developed the concept of effective inertia, effective area and effective mass. It also enabled determination of natural frequencies of a beam with varying section properties using a simple formula similar to the one used in practice for computing the natural frequencies for a uniform beam. This work has been extended to cover nonuniform beams with other classical boundary conditions. In each case the procedure leads to a formula similar to the one used for computing the natural frequencies for a uniform beam. The concept of effective inertia and effective area (or mass) may be applied whenever there is a need to idealize a non-uniform structural member by an equivalent uniform member. The proposed procedure is general and not restricted to any particular cross-section of a beam. In this paper, the necessary expressions are derived for hollow sections with a linear taper. Author (CISTI)

N93-10532 Missouri Univ., Rolla. Dept. of Mechanical and Aerospace Engineering.

NATURAL VIBRATIONS OF MULTILAYERED DOUBLY CURVED SHELLS **c39**

K. Chandrashekhara *In* Carleton Univ., Proceedings of the Twelfth Canadian Congress of Applied Mechanics, Volumes 1 and 2 May 1989 p 440-441 (For primary document see N93-10466 01-31)

Copyright Avail: Canadian Society for Mechanical Engineering, 2050 Mansfield St., Suite 700, Montreal, Quebec H3A 1Z7 Canada

In the present work, the effect of inplane inertia and rotary inertia are included in the vibration of the doubly curved laminated shell and first order shear deformation is accounted for using an extension of Sanders shell theory. Numerical results are presented using a doubly curved shell element to study the influence of various important aspects of the problem such as change in shell geometry, orientation of layers, material parameters, and boundary conditions on the frequencies. The variety of case studies performed aid in identifying the effect of boundary conditions, number layers through the thickness and ply orientation on shell vibrations. Author (CISTI)

N93-10533 Communications Research Centre, Ottawa (Ontario).

FREE VIBRATIONS OF THE THICK CIRCULAR CYLINDRICAL SHELLS AND RINGS **c39**

R. K. Singal and K. Williams (Saskatchewan Univ., Saskatoon.) *In* Carleton Univ., Proceedings of the Twelfth Canadian Congress of Applied Mechanics, Volumes 1 and 2 May 1989 p 442-443 (For primary document see N93-10466 01-31)

Copyright Avail: Canadian Society for Mechanical Engineering, 2050 Mansfield St., Suite 700, Montreal, Quebec H3A 1Z7 Canada

Theories predicting the vibrational behavior of circular cylindrical shells deal only with thin shells and are inconsistent in their predictions. This paper describes briefly an energy method of analysis based on the three dimensional theory of elasticity. The analysis can be applied to thick as well as thin circular cylindrical shells and rings. The paper also describes the various experimental models. The measured experimental values of the resonant frequencies are compared with the calculated frequencies for the purpose of verifying the validity of the analysis. For all circumferential modes, the value of the lowest resonant frequency associated with the symmetric longitudinal mode ($m=0$), can be considered to be independent of the length. All higher order frequencies are length dependent and the variation is nonlinear. For special modes $n=0$ and $n=1$, the lowest resonant frequency associated with symmetric longitudinal modes is length dependent. For all circumferential modes, including the special modes, the values of the lowest resonant frequency associated with the antisymmetric longitudinal mode ($m=1$) is not the same for all the models. All frequencies are length dependent and the variation is nonlinear. The lowest resonant frequency of a circular cylindrical shell and ring is associated with the circumferential mode $n=2$. The analysis provides the values of the resonant frequencies of shells and rings for all circumferential modes of vibration with very good accuracy. Author (CISTI)

N93-10534 Texas Univ., El Paso. Dept. of Mechanical and Industrial Engineering.

VIBRATION FREQUENCIES OF A CONSTRAINED CANTILEVER WEDGE **c39**

W. Lionel Craver, Jr. and Yangshan Lu *In* Carleton Univ., Proceedings of the Twelfth Canadian Congress of Applied Mechanics, Volumes 1 and 2 May 1989 p 444-445 (For primary document see N93-10466 01-31)

Copyright Avail: Canadian Society for Mechanical Engineering, 2050 Mansfield St., Suite 700, Montreal, Quebec H3A 1Z7 Canada

This paper presents the solution for the natural frequencies of a beam tapered in one direction, or a wedge, with both a rotational and a translational constraint at a position along the length of the beam. The eigenfrequencies were determined using an incremental search and bisection method, accurate to the fourth decimal place. The taper ratio was varied from 1.4 to 5.0 and the dimensionless spring constants were varied from 0 to 1000. Graphs are provided to illustrate some results. Author (CISTI)

N93-10535 Waterloo Univ. (Ontario). Dept. of Systems Design Engineering.

ON THE VIBRATION OF AXISYMMETRIC SHELLS **c39**

G. R. Heppler and L. Wahl *In* Carleton Univ., Proceedings of the Twelfth Canadian Congress of Applied Mechanics, Volumes 1 and 2 May 1989 p 446-447 (For primary document see N93-10466 01-31)

Copyright Avail: Canadian Society for Mechanical Engineering, 2050 Mansfield St., Suite 700, Montreal, Quebec H3A 1Z7 Canada

The application of nonconventional basis functions to the linear vibration problem is explored. By employing shell coordinates the elements allow the exact geometrical modelling of shells of revolution with arbitrary meridians and the elements are able to reproduce strain free states under an arbitrary rigid body motion

due to the use of these special basis functions. A generalization of the Reissner Mindlin plate theories is used because they have a broader range of applicability than the usual thin/shallow shell theories and also the trial functions need only be of class C(sup 0). The geometry treated is a hyperbola of revolution, in two configurations. Author (CISTI)

N93-10536 Communications Research Centre, Ottawa (Ontario).
THE VIBRATIONS OF ANNULAR DISCS: A COMPARISON OF EXPERIMENTAL AND TWO ANALYTICAL TECHNIQUES **c39**
R. K. Singal, E. Haseganu-Zamfirescu (Saskatchewan Univ., Saskatoon.), H. Wong (Saskatchewan Univ., Saskatoon.), and K. Williams *In* Carleton Univ., Proceedings of the Twelfth Canadian Congress of Applied Mechanics, Volumes 1 and 2 May 1989 p 452-453 (For primary document see N93-10466 01-31)
Copyright Avail: Canadian Society for Mechanical Engineering, 2050 Mansfield St., Suite 700, Montreal, Quebec H3A 1Z7 Canada

The vibrational behavior of circular annular discs or plates is of considerable engineering importance as such plates have numerous applications such as flywheels, turbine rotors, and gears. Several investigators have predicted the resonant frequencies of circular annular plates (rings). However, all these analytical models have limited applications. This paper describes briefly two methods of analysis. The first is an energy method based on the three dimensional theory of elasticity. The second method utilizes an educational version of the commercial finite element package ANASYS. In order to assess the accuracy of the analysis based on the energy and finite element methods, extensive experimental data was acquired using eight models from a thin ring to a solid disc made of mild steel. The analyses were tested on a range of models comprising both thin and thick rings. They have been found in all cases considered, to predict the resonant frequencies for all the circumferential modes of vibration, including the breathing and beam-type modes. Both the energy method and the refined finite element analysis yielded agreement with an accuracy which is adequate for most engineering calculations. For the energy method excellent agreement, generally better than two percent, exist for all modes up to n=7 for all eight modes tested. Likewise the finite element technique confirmed the results in all cases where a refined sectored model was employed. Author (CISTI)

N93-10537 Technical Univ. of Istanbul (Turkey).
VIBRATIONS OF NONLINEARLY PRETWISTED ASYMMETRICAL THICK TURBINE BLADES **c07**
V. Karadag *In* Carleton Univ., Proceedings of the Twelfth Canadian Congress of Applied Mechanics, Volumes 1 and 2 May 1989 p 464-465 (For primary document see N93-10466 01-31)
Copyright Avail: Canadian Society for Mechanical Engineering, 2050 Mansfield St., Suite 700, Montreal, Quebec H3A 1Z7 Canada

The influence of the nonlinearity of blade pretwist and cross sectional properties on the vibration frequencies and mode shapes of turbine blades was investigated by the finite element method. It was shown that the nonlinearity of pretwist of a blade can change the vibration characteristics of turbine blades considerably. Thin and thick beam theories were incorporated into the analysis. Twelve and twenty degrees of freedom, thin and thick beam finite element models are used in the analysis of thin and thick beam theories, respectively. Higher order polynomials were used in representing the nonlinear pretwist and cross sectional properties along the blade and the blade elements. These polynomials are the same both along the blade and the blade finite elements. Bending displacements and slopes, shear force displacements and slopes, torsional and longitudinal displacements have been choosen as degrees of freedom at each end of the thick beam finite elements. In the thin beam theory analysis, the shear force displacements and slopes were neglected. The influence of the nonlinearity of the pretwist on the vibration characteristics of asymmetrical turbine blades is high and the representation of the nonlinearity of the pretwist and cross sectional properties along the blade is very important. The influence on the mode shapes is very small. Using one main polynomial for nonlinearity continuous cases along the blade is a better representation and gives satisfactory results. Both thin and thick beam theories results are supported by each other in all of the cases. Author (CISTI)

N93-10538 Technische Hogeschool, Eindhoven (Netherlands).
A SPLINE FINITE STRIP METHOD FOR ANALYSING LOCAL AND DISTORTIONAL BUCKLING OF THIN-WALLED BEAMS UNDER ARBITRARY LOADING **c39**
G. M. vanErp and C. M. Menken *In* Carleton Univ., Proceedings of the Twelfth Canadian Congress of Applied Mechanics, Volumes 1 and 2 May 1989 p 474-475 (For primary document see N93-10466 01-31)
Copyright Avail: Canadian Society for Mechanical Engineering, 2050 Mansfield St., Suite 700, Montreal, Quebec H3A 1Z7 Canada

As part of a research project concerning the interactive buckling of thin-walled beams, a spline finite strip program was developed to determine the buckling loads and modes of these structural elements under arbitrary loading. In this paper, the theory is briefly outlined and a typical example is presented. The influence of the number of strips in a cross section and the number of subdivisions along the length, on the local and distortional buckling loads of folded plate structures loaded in bending and/or shear was studied. The buckling load and mode of a simply supported I-beam loaded by a concentrated force is determined with the spline finite strip method. The example indicates that the spline finite strip method is an efficient tool for analyzing the local and distortional buckling of flat plate assemblies loaded in bending andor shear. The simplicity of the conventional finite strip method is preserved, while the problems of dealing with non-periodic buckling modes, shear and non-simple support are eliminated. Due to the high order of approximation, which is achieved with only four degrees of freedom per section of knot, the spline finite strip method displays considerable computing economy compared with the standard finite element methods. Author (CISTI)

N93-10539 Toronto Univ. (Ontario). Dept. of Mechanical Engineering.
THEORETICAL AND EXPERIMENTAL INVESTIGATIONS CONCERNING THE STRUCTURAL INTEGRITY OF AEROENGINE COMPRESSOR DISCS **c07**
S. A. Meguid, B. Theobald (Rolls-Royce Ltd., Derby, England), and J. Wiseman (Rolls-Royce Ltd., Bristol, England) *In* Carleton Univ., Proceedings of the Twelfth Canadian Congress of Applied Mechanics, Volumes 1 and 2 May 1989 p 484-485 (For primary document see N93-10466 01-31)
Copyright Avail: Canadian Society for Mechanical Engineering, 2050 Mansfield St., Suite 700, Montreal, Quebec H3A 1Z7 Canada

The dovetail regions of aeroengine compressor discs are critical regions for which lifetime certification is necessary. Attention is devoted here to features and interface conditions in the dovetail region upon the least damage fail-safe design criterion. These features include inner and outer fillet radii R(sub 1) and R(sub 2), flank length and angle, and the coefficient of friction at the blade-disc interface. Three aspects of the work were examined. The first was concerned with the stressing of a given disc, the second with the initiation and subsequent propagation of cracks in regions exhibiting maximum stress concentration, and the third with the minimum principal stress criterion. Finally, the results were compared with photoelastic spin tests using the stress freezing technique. Author (CISTI)

N93-10540 Ecole Polytechnique, Montreal (Quebec). Dept. of Mechanical Engineering.
AN EVALUATION OF THE CUMULATIVE DAMAGE EFFECT UNDER CREEP LOADING **c39**
R. Gomuc, T. Bui-Quoc, and A. Biron *In* Carleton Univ., Proceedings of the Twelfth Canadian Congress of Applied Mechanics, Volumes 1 and 2 May 1989 p 486-487 (For primary document see N93-10466 01-31)

Copyright Avail: Canadian Society for Mechanical Engineering, 2050 Mansfield St., Suite 700, Montreal, Quebec H3A 1Z7 Canada

Structural components operating at high temperature are usually subjected to a fluctuation of stress and/or temperature. Experimental conditions cannot cover all possible combinations of these important parameters and, in addition, systematic investigations on cumulative creep damage are very limited due to long-term testing. There is a need to establish a reliable procedure for evaluating the cumulative creep damage effect under nonsteady stresses or temperatures. The aim of this paper is to present a technique to analyze the experimental data under multistep loading taking into account the order effect; it may then be used for predicting the cumulative damage effect in order to obtain the remaining life under creep loading. An interaction effect consideration is introduced in the cumulative creep damage concept in order to account for the strong sequence effect of loading for some materials. The procedure, using the non-dimensional stress, may be extended for cases involving a change of stresses and/or of temperatures. The agreement between experimental results and predictions is reasonably good. Author (CISTI)

N93-10541 Ecole Polytechnique, Montreal (Quebec). Dept. of Mechanical Engineering.

ON THE DEVELOPMENT OF A NEW FRACTURE TOUGHNESS PROCEDURE **c39**

M. Bernard and J. W. Provan (McGill Univ., Montreal, Quebec) *In* Carleton Univ., Proceedings of the Twelfth Canadian Congress of Applied Mechanics, Volumes 1 and 2 May 1989 p 488-489 (For primary document see N93-10466 01-31)

Copyright Avail: Canadian Society for Mechanical Engineering, 2050 Mansfield St., Suite 700, Montreal, Quebec H3A 1Z7 Canada

The present ASTM test procedure for plane strain fracture toughness is time consuming, expensive, includes specimen thickness requirements, and provides no assurance of a valid K(sub IC). An attempt to circumvent the thickness limitations and to develop a simple, inexpensive method to determine plane strain fracture toughness is reported. A novel disc-shaped specimen geometry was investigated for the determination of the plane strain fracture toughness of metallic materials. The specimen has an axisymmetric notch on its upper face, is clamped on its periphery and is uniformly and perpendicularly loaded around the notch. The frozen stress photoelasticity method was applied to Araldite specimens with fatigue precracked notches to determine the stress intensity factors and the fracture mode. One configuration was retained and using the crack profile from the test, a finite element study was performed to determine the compliance of the specimen geometry. Finally, the fracture toughness of aluminium Al7075-T651 was determined by applying the critical load obtained from rupture tests. Author (CISTI)

N93-10542 Toronto Univ. (Ontario). Dept. of Mechanical Engineering.

FATIGUE CRACK PROPAGATION IN THE PRESENCE OF SHOT-PEENING RESIDUAL STRESSES **c39**

S. A. Meguid *In* Carleton Univ., Proceedings of the Twelfth Canadian Congress of Applied Mechanics, Volumes 1 and 2 May 1989 p 490-491 (For primary document see N93-10466 01-31)

Copyright Avail: Canadian Society for Mechanical Engineering, 2050 Mansfield St., Suite 700, Montreal, Quebec H3A 1Z7 Canada

This study is part of an investigation into fatigue fracture in the presence of residual stresses and the lifetime of two contrasting materials: aluminium zinc alloy and medium carbon steel. The work was extended to assess the potential of re-peening treatment for the restoration of faded residual stresses and the consequent fatigue life improvement. Accordingly, two aspects of the material behavior under constant amplitude cyclic loading were examined: (1) the extent of fading of the residual stress profile due to partial fatigue; and (2) the extent of fatigue life enhancement associated with re-peening treatment after partial fatigue. For this purpose, room temperature rotating-bend fatigue tests were conducted on peened and re-peened cylindrical components made from the aforementioned materials. In the case of the steel specimens, further enhancement of the life was achieved by re-peening. This, however, was not the case for the aluminium specimens. Typically, re-peening of the steel after being partially fatigued by 70 percent of its mean fatigue life showed complete rejuvenation. The re-peening of the aluminium specimens did not show any improvement. Author (CISTI)

N93-10543 Carleton Univ., Ottawa (Ontario). Dept. of Mechanical and Aeronautical Engineering.

IMPROVEMENTS TO THE AC POTENTIAL DROP METHOD OF CRACK MEASUREMENT **c39**

P. R. Frise and R. Bell *In its* Proceedings of the Twelfth Canadian Congress of Applied Mechanics, Volumes 1 and 2 May 1989 p 504-505 (For primary document see N93-10466 01-31)

Copyright Avail: Canadian Society for Mechanical Engineering, 2050 Mansfield St., Suite 700, Montreal, Quebec H3A 1Z7 Canada

The alternating current potential drop (ACPD) method of crack detection and sizing has gained widespread acceptance in experimental fatigue and fracture mechanics. Much of the ACPD work to date has used only one or two reference potential drop values in the crack depth calculation. This calculation is valid based on the assumption that the electrical field induced on the surface of the specimen is uniform in the region of the crack measurement. To investigate the implied assumption that the voltage drop between probes is independent of the position of the probes on the specimen surface, the electrical field induced by an AC current in a rectangular bar was examined. Different numbers of probes and configurations of probes were tested. The results clearly indicated the induced electric field was not uniform at the centerline of the test specimen. A new test method was developed to minimize the effect of this nonuniformity of test results. A comparison was made of the accuracy of the measurements made using the improved method with that obtained by the standard method of the development of fatigue crack coalescence at the root of a notch in a V notched plate. The improved technique enhanced the accuracy of the crack depth measurement obtained using the ACPD technique. Author (CISTI)

N93-10544 Ecole Polytechnique, Montreal (Quebec). Dept. of Mechanical Engineering.

A COMPARATIVE STUDY OF SEMI-EMPIRICAL DYNAMIC STALL MODELS **c02**

R. Botez, O. Marchand, and I. Paraschivoiu *In* Carleton Univ., Proceedings of the Twelfth Canadian Congress of Applied Mechanics, Volumes 1 and 2 May 1989 p 586-587 (For primary document see N93-10466 01-31)

Copyright Avail: Canadian Society for Mechanical Engineering, 2050 Mansfield St., Suite 700, Montreal, Quebec H3A 1Z7 Canada

Dynamic stall is more difficult to predict than static stall due to its dependence on a much larger number of parameters such as airfoil shape, reduced frequency, mean angle, Mach number, Reynolds number, type of motion, three dimensional and turbulence level effects. Several semi empirical methods have been developed based on experimental data for use in the helicopter industry. These methods are used for estimating the forces and moments on oscillating airfoils. These methods are summarized and compared. The UTRC method uses a direct and simple procedure for calculating unsteady aerodynamic loads, but it has the disadvantage of requiring extensive tests to provide the body of the tabulated data for each airfoil. Work is being done on developing analytical expressions to replace the tabulated data. The GORMONT, MIT, MODIFIED MIT and SIKORSKY methods have the great advantage of requiring only steady state airfoil data for their applications. ONERA method is based on a set of algebraic equations containing parameters that must be determined from the available synthesized experimental data. A comparison was made of the variation of the coefficient of lift with the angle of

attack results estimated by the GORMONT, SIKORSKY, and URTC models with those obtained experimentally in preliminary tests for an oscillating airfoil. The SIKORSKY method gave the best results. The GORMONT case gave larger hysteresis in the curve than the two other methods. In the high angle regions the moment computed for each of the three methods was poor in comparison with the experimental results. Author (CISTI)

N93-10545 Ecole Polytechnique, Montreal (Quebec). Dept. of Mechanical Engineering.

STREAM FUNCTION-VORTICITY FINITE ELEMENT FORMULATIONS OF UNSTEADY INCOMPRESSIBLE NAVIER-STOKES EQUATIONS **c34**

K. F. Tchon, W. Ghaly, and I. Paraschivoiu *In* Carleton Univ., Proceedings of the Twelfth Canadian Congress of Applied Mechanics, Volumes 1 and 2 May 1989 p 588-589 (For primary document see N93-10466 01-31)

Copyright Avail: Canadian Society for Mechanical Engineering, 2050 Mansfield St., Suite 700, Montreal, Quebec H3A 1Z7 Canada

A study was carried out to determine the finite element solution of the unsteady incompressible Navier-Stokes equations, using a stream function-vorticity formulation in which the solid boundary conditions are easily introduced. The resulting numerical solver will eventually be used to simulate the dynamic stall of an oscillating airfoil, and complement experimental results in order to enhance the understanding of the physical phenomenon. In this paper the formulation and the preliminary tests used to validate the steady state part of the solver are presented. Using the flow around a cylinder as a test case, the validation of the resulting numerical solver has been undertaken. The computed stream lines match closely with the experimentally visualized ones. Author (CISTI)

N93-10546 Toronto Univ. (Ontario). Inst. for Aerospace Studies.

SHOCK WAVE DIFFRACTIONS OVER SEMI-CIRCULAR AND HALF-DIAMOND CYLINDERS **c34**

I. I. Glass, J. Kaca, and D. L. Zhang *In* Carleton Univ., Proceedings of the Twelfth Canadian Congress of Applied Mechanics, Volumes 1 and 2 May 1989 p 596-597 (For primary document see N93-10466 01-31)

Copyright Avail: Canadian Society for Mechanical Engineering, 2050 Mansfield St., Suite 700, Montreal, Quebec H3A 1Z7 Canada

Interferometric investigations were conducted of shock-wave diffractions over semi-circular and half-diamond cylinders, with varying time, over a wide range of initial shock-wave Mach numbers and initial pressures using infinite-fringe interferograms. In addition, the effects of surface roughness were also studied for the half-diamond cylinders using sandpaper, a spongy plastic and a sawtooth model. Long-duration flow-effects were investigated by using smaller-size models. The results indicate that the flow systems become progressively more complex with time. The effects of surface roughness on the half-diamond cylinders affected mainly the front (wedge) part of the cylinder. Major disturbances were caused by the saw-tooth (1 mm deep by 2 mm pitch) roughness elements. The long-duration half-size flow model showed how the diffracted shock wave reflects from the shock-tube wall and undergoes regular or Mach reflection. It then interacts with the contact surface and the vortex produced by the sharp apex. In the case of the semi-circular cylinder surface roughness effects were not investigated. However, the long-duration flow effects were very similar. The highest loads occur at the front of the cylinders, behind the initial shock wave, and decrease with increasing time of travel of the shock wave such that the smallest loads occur on the rear face of the cylinders. The inviscid numerical simulation agrees quite well with the experimental results. The significant lambda-shock interaction with the boundary layer at the front stagnation region is not reproduced numerically. However, the isopycnic values are reasonably well represented. Author (CISTI)

N93-10547 Ecole Polytechnique, Montreal (Quebec). Dept. of Mechanical Engineering.

A FIELD PANEL METHOD FOR TRANSONIC FLOWS **c02**

C. Masson, L. Lamarche, O. Marchand, and I. Paraschivoiu *In* Carleton Univ., Proceedings of the Twelfth Canadian Congress of Applied Mechanics, Volumes 1 and 2 May 1989 p 598-599 (For primary document see N93-10466 01-31)

Copyright Avail: Canadian Society for Mechanical Engineering, 2050 Mansfield St., Suite 700, Montreal, Quebec H3A 1Z7 Canada

This study concerns the development and implementation of a numerical method for the design and analysis of wings in transonic regime. A new approach, called the Field Panel Method, is used. It combines the advantages of panel methods (e.g., arbitrary configurations and boundary conditions) with solution techniques appropriate for the nonlinear transonic regime. It offers the possibility of treating very complex configurations and eases the handling of the boundary conditions such as design conditions, solid and porous wall conditions. A 2-D formulation is presented which is the first step in the development of a 3-D numerical method and computer code for the design and analysis of wings. The chosen integral formulation will permit evaluation of aerodynamic characteristics of the arbitrary configurations in flows up to the nonlinear transonic regime where discontinuous solutions (shock waves) can occur. Author (CISTI)

N93-10548* National Aeronautics and Space Administration. Lewis Research Center, Cleveland, OH.

A LEAST-SQUARES FINITE ELEMENT METHOD FOR INCOMPRESSIBLE NAVIER-STOKES PROBLEM **c34**

Bonan Jiang (Cleveland State Univ., OH.) and Louis A. Povinelli *In* Carleton Univ., Proceedings of the Twelfth Canadian Congress of Applied Mechanics, Volumes 1 and 2 May 1989 p 602-603 (For primary document see N93-10466 01-31)

Copyright Avail: Canadian Society for Mechanical Engineering, 2050 Mansfield St., Suite 700, Montreal, Quebec H3A 1Z7 Canada

Most finite element schemes for solving the Navier-Stokes equations can be categorized into the Galerkin mixed method and the penalty method. The mixed method leads to a saddle-point problem. In order to guarantee the existence of a solution, the combination of velocity and pressure interpolations requires satisfaction of the Ladyzhenskaya Babuska Brezzi (LBB) consistency condition which precludes the use of equal order interpolations and many seemingly natural pairs of velocity and pressure elements. In a previous paper a least-squares finite element method based on the first order velocity-pressure-vorticity formulation for the Stokes problem was proposed. This method leads to a minimization problem. The choice of combination of elements is thus not subject to the LBB condition. The numerical experiments exhibit the optimal rate of convergence for all variables with equal order interpolations. A theoretical error analysis supports the numerical results. In this paper the least-squares finite element method is extended to solving the incompressible Navier-Stokes problem. Author (CISTI)

N93-10549 University of Western Ontario, London.

FLOW OVER A LEADING EDGE WITH DISTRIBUTED ROUGHNESS **c02**

J. M. Floryan and U. Dallmann (Institut fuer Theoretische Stroemungsmechanik, Goettingen, Germany) *In* Carleton Univ., Proceedings of the Twelfth Canadian Congress of Applied Mechanics, Volumes 1 and 2 May 1989 p 660-661 (For primary document see N93-10466 01-31)

Copyright Avail: Canadian Society for Mechanical Engineering, 2050 Mansfield St., Suite 700, Montreal, Quebec H3A 1Z7 Canada

Analysis of flow near a leading edge is of primary importance since this is where the boundary layer originates and where the disturbances could first penetrate into it. The purpose of this paper is to analyze modifications of the stagnation flow caused by presence of surface roughness. The resulting nonuniform flow might be subject to an instability mechanism which is different from the

classical one. The results provide initial conditions necessary for tracking effects of surface roughness further downstream. Further applications include determination of increase of heat transfer due to the presence of roughness, and determination of shear and normal stress increases with applications to erosion and ablation. Numerical results show that the fluid is forced to flow away from the stagnation line and away from the peaks of roughness. The flow can be described as corresponding to the upper half of a layer of counter rotating vortex pairs, with vortex centers overlapping with the surface of the plate. An increase in shear acts on the peaks of roughness in the x-direction and a decrease in the shear acts on the valleys. An additional shear acts in the spanwise direction from the peak towards the valley position. The effects of roughness on heat transfer on an isothermal plate is such that there is an increase of heat transport through the peak area. Author (CISTI)

N93-10550 Moncton Univ., Edmundston (New Brunswick).
EXPERIMENTAL INVESTIGATION OF FLOWS BEHIND DIFFERENT LARGE-EDDY BREAKUP (LEBU) DEVICES IN THICK BOUNDARY LAYERS **c02**

D. Vo-Ngoc, J. R. Longval, V. D. Nguyen (Laval Univ., Quebec), and J. Dickinson (Laval Univ., Quebec) *In* Carleton Univ., Proceedings of the Twelfth Canadian Congress of Applied Mechanics, Volumes 1 and 2 May 1989 p 662-663 (For primary document see N93-10466 01-31)

Copyright Avail: Canadian Society for Mechanical Engineering, 2050 Mansfield St., Suite 700, Montreal, Quebec H3A 1Z7 Canada

The current study was initiated to assess the influence of the state of the large-eddy breakup (LEBU) boundary layer on the local distribution of C(sub f) downstream of the device. Studies were carried out in a 1 m by 2 m wind tunnel equipped with vortex generators at the entrance, which results in a boundary layer thickness on the order of 50 cm, three meters downstream, at free stream velocities around 10 m/s. The vortex generators have a mean velocity profile following a 0.1 exponent law. The very extensive boundary layers permit the use of large LEBU devices, possessing both more easily controllable geometries and measurable secondary boundary layers and separating wakes. The different shapes of turbulence moderators on LEBUs were chosen comprising a cylinder, rectangular blades with and without chamferings of the leading and trailing edges, and a 15 m chord NACA-0015 profile. Measurements of mean velocity profiles and local C(sub f) distribution were conducted at a number of downstream stations. Turbulence skin friction was determined. Some of the preliminary results are presented. Author (CISTI)

N93-10551 Sherbrooke Univ. (Quebec). Dept. of Mechanical Engineering.
HARMONIC ANALYSIS OF THE AERODYNAMIC FORCES ON A DARRIEUS ROTOR [ANALYSE HARMONIQUE DES FORCES AERODYNAMIQUES SUR UN ROTOR DARRIEUS] **c02**

Abdelkrim Mazouzi, Andre Laneville, and Pierre Vittecoq *In* Carleton Univ., Proceedings of the Twelfth Canadian Congress of Applied Mechanics, Volumes 1 and 2 May 1989 p 680-681 In FRENCH (For primary document see N93-10466 01-31)

Copyright Avail: Canadian Society for Mechanical Engineering, 2050 Mansfield St., Suite 700, Montreal, Quebec H3A 1Z7 Canada

This article presents a harmonic analysis of aerodynamic forces measured on the vertical blades of a Darrieus type rotor in rotation. A new similarity parameter was developed and the relationship between this parameter and the aerodynamic coefficients of force makes it possible to distinguish the zone of dynamic stall. A new cyclical representation as a function of the variable Lambda (theta), where theta is the azimuthal position, is proposed to facilitate the presentation of certain aerodynamic phenomena. A model of the aerodynamic coefficients was formulated. A comparison with experimental results shows that only the first five harmonics are necessary to describe the aerodynamic forces. Author (CISTI)

N93-10552 University of Western Ontario, London.
STRUCTURE OF THERMOCAPILLARY FLOW IN NARROW CAVITIES **c34**

J. Krol and J. M. Floryan *In* Carleton Univ., Proceedings of the Twelfth Canadian Congress of Applied Mechanics, Volumes 1 and 2 May 1989 p 718-719 (For primary document see N93-10466 01-31)

Copyright Avail: Canadian Society for Mechanical Engineering, 2050 Mansfield St., Suite 700, Montreal, Quebec H3A 1Z7 Canada

Potentials for improving different crystal growth techniques by utilizing low-g environments are currently being explored. Surface tension forces are among the dominant factors limiting possible gains in size and quality of crystals. The limitations may manifest themselves either by the occurrence of the capillary instability or by the occurrence of natural convection driven by surface tension gradients. Such gradients are known to exist in the presence of thermal gradients along the interface (Marangoni effect) and in the presence of chemical contamination of the interface. A model of flow inside a gravity free tube was developed based on an incompressible Newtonian fluid and employing Navier Stokes continuity and energy equations. The flow structure was analyzed based on arbitrary interface temperature. Results show that the flow structure in a narrow cavity corresponds to a single column of vortices if the temperature has an antisymmetric component and to two columns of vortices if the temperature is symmetric. While the flow in the surface layer is strongly affected by the surface temperature, the transition between the outer and inner flow structures is rapid and occurs at a depth no greater than the cavity width. The study forms a part of a long term investigation aimed at identification of the means of containment of the convection or at least its reduction to an acceptable level, either through appropriate tailoring of heat fluxes at the interface or through chemical contamination of the interface. Author (CISTI)

N93-10553 California Univ., Berkeley.
PULSED JET PLUME COMBUSTION: AN EXOTHERMIC PROCESS UNDER FLUID MECHANICAL CONTROL **c25**

A. K. Oppenheim *In* Carleton Univ., Proceedings of the Twelfth Canadian Congress of Applied Mechanics, Volumes 1 and 2 May 1989 p 736-737 (For primary document see N93-10466 01-31)

Copyright Avail: Canadian Society for Mechanical Engineering, 2050 Mansfield St., Suite 700, Montreal, Quebec H3A 1Z7 Canada

In conventional reciprocating piston, internal combustion engines, the spatial and temporal distribution of the specific exothermic power as well as the residence time of reacting particles in the zone of the most effective chemical activity are virtually beyond control. These drawbacks can be obviated by combustion executed within a turbulent plume of a pulsed jet, the pulsed jet plume combustion (PJPC) system. Its salient features are presented, and this is followed by the description of the PJPC generators for premixed (gasoline) as well as non-premixed (diesel) charge engines. A plume is formed by a jet issuing from the orifice of a generator located on the side of the combustion chamber such that a turbulent plume is made out of turbulent shear layers consisting of large scale eddies. The most important property of PJPC is that the exothermic reaction is initiated in the middle of the elementary turbulent eddy forming the plume so that it is virtually decoupled from its outer contour, an interface that acts primarily as a contact discontinuity between the burnt gas and the unburnt charge, rather than a flame. It is this property that permits full control over the distribution of the specific exothermic power over the compressed charge, as well as the residence time of particles in the zone of essential chemical activity. Author (CISTI)

N93-10554 Carleton Univ., Ottawa (Ontario). Dept. of Mechanical and Aeronautical Engineering.
AN ADAPTIVE MESH-MANAGEMENT ALGORITHM FOR THREE-DIMENSIONAL AUTOMATIC FINITE ELEMENT ANALYSIS **c64**

J. M. McDill, J. A. Goldak, and A. S. Oddy (Canada Centre for Mineral and Energy Technology, Ottawa, Ontario) *In its* Proceedings of the Twelfth Canadian Congress of Applied Mechanics, Volumes 1 and 2 May 1989 p 766-767 (For primary document see N93-10466 01-31)

Copyright Avail: Canadian Society for Mechanical Engineering, 2050 Mansfield St., Suite 700, Montreal, Quebec H3A 1Z7 Canada

In current finite element analysis (FEA), the program is unable to improve the FEA approximation (input file) and provides little indication of the error. Automatic FEA (AFEA) will improve the quality and reduce its cost. For transient analysis, near optimal meshes will be generated for each increment. Robust a posteriori error estimates will be reported to guide adaptive changes in the mesh. The algorithm will be most useful in FEA of problems with moving singularities. Elements undergo refinement in the vincinity of the load, and coarsen after the load has passed. A rule-based adaptive mesh management algorithm was developed. Appropriate data structures are arrays and a 3-D tree. The algorithm handles complex situations and provides an important contribution to AFEA. Author (CISTI)

N93-10555 Aeronautical Development Establishment, Bangalore (India).

DESIGN OPTIMIZATION FOR UNIFORM DYNAMIC STRENGTH UNDER MULTI-MODAL RESPONSE **c39**

M. K. Padmanablan, S. Suryanarayan, and M. S. S. Prabhu *In* Carleton Univ., Proceedings of the Twelfth Canadian Congress of Applied Mechanics, Volumes 1 and 2 May 1989 p 768-769 (For primary document see N93-10466 01-31)

Copyright Avail: Canadian Society for Mechanical Engineering, 2050 Mansfield St., Suite 700, Montreal, Quebec H3A 1Z7 Canada

In this study the problem of structrual design optimization under a multi-modal response is presented. Spectral response in a beam with uniform width and variable depth was investigated. Both cantilever and simply supported (SS) end conditions were studied. The spectral contents of the excitation were used to decide the extent of participation of each mode of vibration in the overall dynamic response of the structure. Excitation spectra were chosen so as to give various combinations of participation of the first three modes of the structure in the overall response. Cases of individual modal response as well as typical combinations were studied. Two important, typical constraints, mass and stiffness, were investigated. The mode shapes and the distribution of strain energy (SE) and kinetic energy (KE) over the span differs considerably for the two boundary conditions. While the study was successful for cantilever boundary condition, it was found to be more difficult and iterative for SS end condition. In all the cases wherein the full realization of the optimization goals is not achieved, the role of frequency constraints in limiting the process is clearly seen. Spatial distribution of excitation was shown to accentuate the higher modes. Author (CISTI)

N93-10556 Alberta Univ., Edmonton. Dept. of Civil Engineering.

VARIATIONAL FORMULATION OF A MIXED METHOD FOR SECOND ORDER FRAME ANALYSIS **c64**

T. M. Hrudey *In* Carleton Univ., Proceedings of the Twelfth Canadian Congress of Applied Mechanics, Volumes 1 and 2 May 1989 p 772-773 (For primary document see N93-10466 01-31)

Copyright Avail: Canadian Society for Mechanical Engineering, 2050 Mansfield St., Suite 700, Montreal, Quebec H3A 1Z7 Canada

A hybrid treatment, combining the classical force method with the direct stiffness method, was recently developed to overcome the difficulties of applying computer analysis to the classical force method. In the present paper, a variational finite element formulation is developed that produces essentially the same system of equations as the hybrid method. This serves to establish the relationship between that method's mixed formulation and mixed finite element procedures used in other problem areas such as plates and shells. The present formulation also has the advantage that the equations governing equilibrium and compatibility are generated directly from the variational procedure at the member level and the process of constructing the final equations that govern the complete frame, follow the usual steps in finite element matrix assembly. Author (CISTI)

N93-10557 Naples Univ. (Italy).

A VARIATIONAL APPROACH FOR COUPLED CREEPING-FLOW PROBLEMS **c39**

P. Luchini and A. Pozzi *In* Carleton Univ., Proceedings of the Twelfth Canadian Congress of Applied Mechanics, Volumes 1 and 2 May 1989 p 774-775 (For primary document see N93-10466 01-31)

Copyright Avail: Canadian Society for Mechanical Engineering, 2050 Mansfield St., Suite 700, Montreal, Quebec H3A 1Z7 Canada

The majority of the available solutions of the Stokes equations refer to inflow and/or outflow boundary conditions assigned at a given station. In practice, the entrance of a flow field is always the exit of some other flow field, and therefore coupling of two infinite flow regions of different shape is of interest. In coupled creeping flow problems, a singularity arises on the boundaries at the transition point which makes it difficult to attack them by standard techniques. Here, the coupling problem is treated by an approximate analytical method based on a variational principle. This method is flexible enough to deal with a wide range of geometries and allows the introduction of singular terms describing correctly the local behavior of the solution, which makes even a few-term approximation accurate. The variational approach is applied to an example case of an infinite array of parallel ducts (of which only one is depicted) discharging in free space. Author (CISTI)

N93-10558 Laval Univ. (Quebec). Dept. of Mechanical Engineering.

A BOUNDARY ELEMENT AND MATHEMATICAL PROGRAMMING APPROACH FOR UNILATERAL CONTACT PROBLEMS **c64**

A. Gakwaya and D. Lambert *In* Carleton Univ., Proceedings of the Twelfth Canadian Congress of Applied Mechanics, Volumes 1 and 2 May 1989 p 788-789 (For primary document see N93-10466 01-31)

Copyright Avail: Canadian Society for Mechanical Engineering, 2050 Mansfield St., Suite 700, Montreal, Quebec H3A 1Z7 Canada

Modern design and service conditions require a continued increase in loading and speed of various mechanical components, so the interaction of the involved normal and tangential contact forces becomes of utmost importance in establishing their operating performance. The analysis of contact problems may require solution of the combined friction problems in which tangential stress bounds depend on the normal pressure. In this paper, a general three dimensional boundary numerical procedure for the solution of the combined friction-normal contact problem using a piecewise linear Coulomb's friction law is presented. Local elastic contact conditions are derived using a quadratic boundary element formulation and finite dimensional global contact equations are formulated as a linear complementary problem of mathematical programming for their actual numerical solution. Author (CISTI)

N93-10559 Carleton Univ., Ottawa (Ontario). Dept. of Civil Engineering.

A NEW QUADRILATERAL ELEMENT FOR THE ELASTIC AND PLASTIC ANALYSIS OF SHELLS **c39**

A. Ghani Razaqpur, Omer Aziz, and Mostafa Nofal *In its* Proceedings of the Twelfth Canadian Congress of Applied Mechanics, Volumes 1 and 2 May 1989 p 790-791 (For primary document see N93-10466 01-31)

Copyright Avail: Canadian Society for Mechanical Engineering, 2050 Mansfield St., Suite 700, Montreal, Quebec H3A 1Z7 Canada

The basic concept in the development of a flat shell element is simple; a membrane is combined with a plate bending element,

and the result is a flat shell element. In the present study a refined four node plane quadilateral is combined with an accurate quadrilateral bending element to produce a four noded flat shell element. Since the membrane element has drilling degrees of freedom, as well as the usual displacement freedoms, the present shell element does not suffer from lack of stiffness and thus no artificial stiffness is needed for coplanar elements. The comparison of the finite element results and a theoretical solution shows excellent agreement. The latter observation indicates that the quadrilateral finite shell element (QFSE) is a competitive element for the analysis of materially nonlinear structures. An efficient quadrilateral flat shell element for linear and nonlinear problems was derived which can model any shell structure with arbitrary geometry. The element converges very rapidly and behaves well in most of the cases tested by the authors. Author (CISTI)

N93-10560 Kansas Univ., Lawrence. Dept. of Mechanical Engineering.

THREE DIMENSIONAL CURVED BEAM ELEMENTS WITH LARGE TRANSLATIONS AND ROTATIONS **c39**

Karan S. Surana, Deane E. Ackers, and Robert M. Sorem *In* Carleton Univ., Proceedings of the Twelfth Canadian Congress of Applied Mechanics, Volumes 1 and 2 May 1989 p 792-793 (For primary document see N93-10466 01-31)

Copyright Avail: Canadian Society for Mechanical Engineering, 2050 Mansfield St., Suite 700, Montreal, Quebec H3A 1Z7 Canada

This paper presents a geometrically nonlinear (GNL) formulation for the three dimensional curved beam elements using the total Lagrangian approach. The element displacement field, which is fully compatible with the isoparametric curved shell elements, is described using three translations in the global directions and three rotations about the local axes at the element nodes. The formulation permits large translations as well as large rotations between two successive load increments. This is accomplished by retaining nonlinear nodal rotation terms in the definition of the element displacement field and the consistent derivation of the element properties. Numerical examples are presented to demonstrate the superiority of the present formulation in terms of large load steps, large rotations between two load steps, and extremely good convergence characteristics during equilibrium iterations. Author (CISTI)

N93-10561 Exeter Univ. (England).

A REAPPRAISAL OF COMPOUND EQUILIBRIUM FINITE ELEMENTS **c39**

E. A. W. Maunder *In* Carleton Univ., Proceedings of the Twelfth Canadian Congress of Applied Mechanics, Volumes 1 and 2 May 1989 p 796-797 (For primary document see N93-10466 01-31)

Copyright Avail: Canadian Society for Mechanical Engineering, 2050 Mansfield St., Suite 700, Montreal, Quebec H3A 1Z7 Canada

Pure equilibrium elements have the advantages, in finite element analysis, of providing alternative bounds in elasto-plastic analyses, and providing more directly to the designer information on statically admissible stress fields. Recently, families of membrane equilibrium elements with edge node variables were generated by combining 3 or 4 triangular regions into compound triangular or quadrilateral elements, thus inhibiting spurious kinematic modes. In this paper these families of elements are reappraised, particularly when quadratic stress fields are used. The existence of kinematic and hyperstatic modes in quadrilateral elements is considered in relation to the geometry of the element subdivision. The extension to plate and shell elements is also considered. A general procedure is proposed for a more direct formulation of element flexibility matrices. Author (CISTI)

N93-10562 Newcastle-upon-Tyne Univ. (England).

EVALUATION OF THE TRIANGULAR PLATE ELEMENT OF ZIENKIEWCZ AND LEFEBVRE [EVALUATION DE L'ELEMENT PLAQUE TRIANGULAIRE DE ZIENKIEWCZ ET LEFEBVRE] **c39**

P. Bettes, B. Peseux, and J. P. Quevat *In* Carleton Univ., Proceedings of the Twelfth Canadian Congress of Applied Mechanics, Volumes 1 and 2 May 1989 p 798-799 In FRENCH (For primary document see N93-10466 01-31)

Copyright Avail: Canadian Society for Mechanical Engineering, 2050 Mansfield St., Suite 700, Montreal, Quebec H3A 1Z7 Canada

A new triangular finite element characterized by interpolation which is independent of normal displacements, of rotation, and of strong forces is proposed. This element allows the treatment of bending problems with the Kirchhoff hypothesis as well as with the Reissner-Mindlin hypothesis. In addition, it satisfies the patch test for the three fields. To evaluate the performance of this element, it was used to treat problems in statics and of vibration of plates in water and in air. Triangular element results are compared with those obtained on the same problem using the Mindlin 8 node quadrilateral, the 9 node heterosis quadrilateral, the Ahmad-type 9 node quadrilateral, and Bogner 4 node rectangular elements. In addition, it was evaluated against experimental results for coupled fluid structure problems. For static comparisons, displacements and constraints were calculated for a perforated circular plate. For dynamic calculations, vibration modes of a rectangular free-free plate were derived. The mixed triangular element was found to be effective and sufficiently precise in all cases. Author (CISTI)

N93-10563 Sheffield Univ. (England). Dept. of Mechanical and Process Engineering.

ON THE USE OF COUPLED FINITE ELEMENT BOUNDARY ELEMENT MODELS IN NUMERICAL DESIGN ANALYSIS **c64**

J. L. Wearing, M. A. Sheikh, and A. J. Hickson *In* Carleton Univ., Proceedings of the Twelfth Canadian Congress of Applied Mechanics, Volumes 1 and 2 May 1989 p 802-803 (For primary document see N93-10466 01-31)

Copyright Avail: Canadian Society for Mechanical Engineering, 2050 Mansfield St., Suite 700, Montreal, Quebec H3A 1Z7 Canada

The use of coupled finite element boundary elements for the analysis of linear elastic problems is discussed. These models allow simultaneous use of the finite element and boundary element methods so that the particular advantage of each method can be used in an optimal manner. A few examples of such models are presented. These employ the boundary element method to discretize the bulk of the problems with regions of finite elements in those areas where the analysis is more complex or critical. Author (CISTI)

N93-10564 Vermont Univ., Burlington.

NUMERICAL CONSIDERATIONS FOR STRUCTURAL SYSTEM IDENTIFICATION FROM MODAL INFORMATION **c39**

Jean-Guy Beliveau *In* Carleton Univ., Proceedings of the Twelfth Canadian Congress of Applied Mechanics, Volumes 1 and 2 May 1989 p 808-809 (For primary document see N93-10466 01-31)

Copyright Avail: Canadian Society for Mechanical Engineering, 2050 Mansfield St., Suite 700, Montreal, Quebec H3A 1Z7 Canada

Efficient algorithms are required to estimate physical parameters such as mass and member stiffness of large structures from modal information in the form of resonant frequencies, mode shapes of vibration, and the modal damping ratios associated with energy dissipation. In this paper numerical aspects of partial eigenvalue calculation and eigenvector sensitivity, which are needed to utilize the modal information in obtaining estimates to physical parameters associated with mass or stiffness characteristics, are presented. The efficient calculation of the lowest natural frequencies of vibration and the associated mode shapes as well as their sensitivity with respect to physical parameters makes it possible to correlate measured dynamic data with finite element models. Concurrently, the recent advances in modal testing procedures make modal information readily available from a large variety of tests. These two developments should help structural engineers in evaluating their structures. Author (CISTI)

N93-10565 University of South Florida, Tampa. Dept. of Civil Engineering and Mechanics.

AN IMPROVED TECHNIQUE FOR DETERMINING HIGHER ORDER EIGENVECTOR COEFFICIENTS **c64**

William C. Carpenter and Curtis Byers *In* Carleton Univ., Proceedings of the Twelfth Canadian Congress of Applied Mechanics, Volumes 1 and 2 May 1989 p 810-811 (For primary document see N93-10466 01-31)

Copyright Avail: Canadian Society for Mechanical Engineering, 2050 Mansfield St., Suite 700, Montreal, Quebec H3A 1Z7 Canada

Much of the effort of computational fracture mechanics has been directed towards developing numerical algorithms for determining coefficients associated with eigenvectors of the problem. Knowledge of the higher order coefficients (those associated with eigenvalues whose real part is positive and less than one) may be useful in developing an understanding of the behavior of a configuration subject to displacements or traction boundary conditions. This paper extends the reciprocal work contour integral method (RWCIM) so that any number of eigenvector coefficients can be found (the number being limited only by the number of known eigenvalues). The method is not sensitive to idealization error introduced by the finite element method. The method has the added advantage that the numerical effort to obtain the higher order coefficients is not great. Thus, while the higher order may not often be required, they are so computationally inexpensive with the RWCIM that they can be routinely calculated. The method was calculated on several problems of known solution. The algorithm gave excellent prediction of the eigenvector coefficients when stresses and displacements from an eigenvector generation routine were used as input as well as when results from a finite element analysis of the configuration were used. The method was found to be insensitive to finite element idealization error which makes the method preferable to the collocation method for determining eigenvector coefficents, that method being very sensitive to idealization error.

Author (CISTI)

N93-10566 Sheffield Univ. (England). Dept. of Mechanical and Process Engineering.

A BOUNDARY ELEMENT SUPER-ELEMENT METHOD FOR COUPLING WITH THE FINITE ELEMENT METHOD OF SUBSTRUCTURES **c64**

J. L. Wearing and M. A. Sheikh *In* Carleton Univ., Proceedings of the Twelfth Canadian Congress of Applied Mechanics, Volumes 1 and 2 May 1989 p 816-817 (For primary document see N93-10466 01-31)

Copyright Avail: Canadian Society for Mechanical Engineering, 2050 Mansfield St., Suite 700, Montreal, Quebec H3A 1Z7 Canada

The two most common numerical techniques for the analysis of structural and other field problems, the finite element method (FEM) and the boundary element method (BEM) have different strengths and weaknesses. The ideal analysis would combine both methods. The usual derivation of the BEM gives rise to a system of equations which relate to tractions and displacements and as such are not directly compatible with the FEM which relate to nodal forces and displacements. A BE super-element was, therefore, developed which modifies an indirect BEM and produces a final system of equations analogous to that of the FEM. The equations for the BE region can then be used by a standard FE program as a substructure or super-element. The technique allows a stiffness matrix and nodal force contributions for a sub-region to be calculated using BEM and then linked with a standard FEM in the same way as a finite element substructuring strategy. A major attraction of this technique is that as many existing FE program suites have super-element capability it would be possible to link in a BE super-element without any major modifications to the FE programs.

Author (CISTI)

N93-10567 Vermont Univ., Burlington.

PARTIAL SOLUTION OF THE GENERALIZED EIGENVALUE PROBLEM USING THE WOODBURY TRANSFORMATION **c64**

Jean-Guy Beliveau and B. Marcos (Sherbrooke Univ., Quebec) *In* Carleton Univ., Proceedings of the Twelfth Canadian Congress of Applied Mechanics, Volumes 1 and 2 May 1989 p 822-823 (For primary document see N93-10466 01-31)

Copyright Avail: Canadian Society for Mechanical Engineering, 2050 Mansfield St., Suite 700, Montreal, Quebec H3A 1Z7 Canada

The dynamic modelling of large structural systems leads to large dimensional mass and stiffness matrices. Physical reality is such that only a limited frequency range is of interest. Partial eigensolution techniques are used to solve an eigenproblem. A new approach based on a modified Rayleigh quotient is presented. The Woodbury transformation is used to arrive at an efficient algorithm which requires the decomposition of only one large dimensional matrix, the original stiffness matrix. Imposing the normality constraint on a modified Rayleigh quotient and using the particular characteristics of the eigenvalue problem, it is shown that the partial eigensolution of large generalized symmetric matrix systems may be iteratively solved with the decomposition of only the original stiffness matrices. The procedure converges on the smallest eigenvalue satisfying the constraints and is competitive with the two methods currently used.

Author (CISTI)

N93-10568 Calgary Univ. (Alberta). Dept. of Mechanical Engineering.

NUMERICAL SIMULATION OF THE PROPAGATION OF COUPLED THERMOMECHANICAL WAVES IN INELASTIC SOLIDS **c39**

I. R. Orisamolu and M. C. Singh *In* Carleton Univ., Proceedings of the Twelfth Canadian Congress of Applied Mechanics, Volumes 1 and 2 May 1989 p 824-825 (For primary document see N93-10466 01-31)

Copyright Avail: Canadian Society for Mechanical Engineering, 2050 Mansfield St., Suite 700, Montreal, Quebec H3A 1Z7 Canada

A constitutive model for studying the propagation of coupled thermomechanical waves in inelastic solids was developed. The incorporation of dissipative effects such as heat generation, heat flow, irrecoverable energy storage, and thermomechanical coupling rendered the nonlinear model sophisticated so that analytical procedures cannot be employed for its implementation. In this study, two numerical solutions to the propagation of coupled thermomechnical waves in inelastic solids are presented, one based on a modified McCormack scheme and one based on an application of the constant-time technique of the numerical method of characteristics. All results involving the propagation of shock waves show excellent shock resolution profiles for the method of characteristics whereas there are evidences of shock smearing in the McCormack finite difference scheme due to the phenomenon of numerical dispersion. For the cases involving acceleration waves excellent agreement was observed between the two algorithms. For both algorithms the time step was found to be sensitive to the values of the thermal relaxation time and the magnitude of the plastic strain rate.

Author (CISTI)

N93-10569 Calgary Univ. (Alberta). Dept. of Mechanical Engineering.

DISCONTINUOUS INITIAL VALUE PROBLEM OF NONLINEAR ELASTICITY BY SIMILARITY APPROACH **c64**

W. Frydrychowicz and M. C. Singh *In* Carleton Univ., Proceedings of the Twelfth Canadian Congress of Applied Mechanics, Volumes 1 and 2 May 1989 p 836-837 (For primary document see N93-10466 01-31)

Copyright Avail: Canadian Society for Mechanical Engineering, 2050 Mansfield St., Suite 700, Montreal, Quebec H3A 1Z7 Canada

The study of quasilinear hyperbolic partial differential equations presents difficulties such as the nonexistence of globally defined smooth solutions. This represents physical phenomena such as development of shocks. No strong a priori estimates were discovered for systems of more one than equation, so that the system is not amenable to functional analytic techniques. The application of continuous groups of transformation of the p-system

is considered: (1) (epsilon(sub t)) - upsilon(sub x) = 0, and (2) (upsilon(sub t)) + p(epsilon(sub x = 0)), where p(epsilon) is a given function and assumes the form p(epsilon) = -1/rho times sigma(epsilon) = -1/(rho)(q) x (B)(epsilon(sup q)), where B and q are greater than 0, and sigma denotes stress while epsilon denotes strain. Such systems arise in the study of nonlinear wave phenomena such as shocks. The present paper develops the similarity solution on the basis of group theory for problems involving these equations. It was found that it was thus possible to reduce the p-system with discontinuous initial conditions to the ordinary differential equations with given fixed initial conditions. In some cases a closed solution can be obtained, in others numerical analysis is recommended. All physical quantities like strain, velocity, stress, and speed of discontinuity can be determined.

Author (CISTI)

N93-10570 University of Western Ontario, London.
OPTIMAL ROBOT TRAJECTORY PLANNING **c61**
R. O. Buchal *In* Carleton Univ., Proceedings of the Twelfth Canadian Congress of Applied Mechanics, Volumes 1 and 2 May 1989 p 858-859 (For primary document see N93-10466 01-31)
Copyright Avail: Canadian Society for Mechanical Engineering, 2050 Mansfield St., Suite 700, Montreal, Quebec H3A 1Z7 Canada

In order to achieve the objectives of off-line robot programming and automatic program synthesis, an effective trajectory planning method is required. A method is presented for determining optimal robot trajectories subject to the constraints of collision avoidance, joint displacement limits, and joint actuator force limits. The constraints are represented by penalty functions, and a discrete gradient approach is used to optimize the equivalent unconstrained objective functional. The model includes the dynamic equations of motion, which were generated for the planar four-link manipulator using the MACSYMA symbolic algebra package. In the current implementation, the user interactively specifies a number of different starting trajectories so that several alternative locally optimal trajectories are generated. Author (CISTI)

N93-10571 Laval Univ. (Quebec). Dept. of Mechanical Engineering.
EFFECTIVE FORMULATION OF THE DYNAMICS OF A MANIPULATOR BASED ON THE APPELL EQUATIONS [FORMULATION EFFICACE DE LA DYNAMIQUE D'UN MANIPULATEUR A L'AIDE DES EQUATIONS D'APPELL] **c64**
B. Levesque and M. J. Richard *In* Carleton Univ., Proceedings of the Twelfth Canadian Congress of Applied Mechanics, Volumes 1 and 2 May 1989 p 860-861 In FRENCH (For primary document see N93-10466 01-31)
Copyright Avail: Canadian Society for Mechanical Engineering, 2050 Mansfield St., Suite 700, Montreal, Quebec H3A 1Z7 Canada

The formulation of dynamic equations for robot manipulators plays a dominant role in the effectiveness of algorithms used in computer simulation and for real-time control of manipulators. The Appell equations were originally developed to treat dynamic problems in nonholonomic systems. These equations are in a form which is similar to the Lagrange equations. They are based on a calculation of the energy of acceleration which is equivalent to the kinetic energy in the acceleration domain. The best results currently available for the Appell equations are some way from permitting real-time operation. A new method for deriving the equations of dynamics of a manipulator based on the Appell equations has been developed. Starting with this model, four formulations of these equations were evaluated along with the algorithms which are derived from them. The analytical method proposed here permits a reduction, by a factor of 3 in relation to current Appell formulations, of the number of operations necessary to calculate the universal forces for a manipulator possessing 6 degrees of freedom in rotation. Author (CISTI)

N93-10572 Missouri Univ., Rolla. Dept. of Mechanical and Aerospace Engineering.
MODELLING AND CONTROL OF ROBOTIC ARMS FABRICATED FROM ORTHOTROPIC MATERIALS **c37**
K. Krishnamurthy, K. Chandrashekhara, and S. Roy *In* Carleton Univ., Proceedings of the Twelfth Canadian Congress of Applied Mechanics, Volumes 1 and 2 May 1989 p 864-865 (For primary document see N93-10466 01-31)
Copyright Avail: Canadian Society for Mechanical Engineering, 2050 Mansfield St., Suite 700, Montreal, Quebec H3A 1Z7 Canada

A dynamic model for single-link robotic manipulators fabricated from orthotropic composite materials is presented. The equations of motion are derived using Hamilton's principle and include the coupling between the rigid body motion and elastic motion. An optimal controller is designed for rest-to-rest maneuvers without large starting or stopping transients and with minimum residual vibration. Results presented for aluminum, steel, graphite/epoxy, and boron/epoxy indicate that the motion induced vibration is significantly less for the composite robotic arms, and that substantial savings in energy are achieved. Furthermore, it was seen that the magnitude of the control spillover effects, an issue of great concern in designing control systems for flexible structures, was very small for the composite robotic arms. Author (CISTI)

N93-10573 Waseda Univ., Tokyo (Japan). Dept. of Mechanical Engineering.
MODELLING OF FLEXIBLE MULTIBODY DYNAMICS AND A COMPUTER METHOD VIA THE BOND GRAPH METHOD **c37**
Hiroaki Yoshimura, Katsuhide Fujita, Hideo Nakano (Sagami Inst. of Tech., Fujisawa, Japan), and Takehiko Kawase *In* Carleton Univ., Proceedings of the Twelfth Canadian Congress of Applied Mechanics, Volumes 1 and 2 May 1989 p 866-867 (For primary document see N93-10466 01-31)
Copyright Avail: Canadian Society for Mechanical Engineering, 2050 Mansfield St., Suite 700, Montreal, Quebec H3A 1Z7 Canada

Much of the difficulty in the modelling of flexible multibody systems such as a space manipulator lies in setting up the complex kinematical and dynamical relations to generate a large number of system equations. A modelling method for flexible multibody systems is proposed. The method utilizes the bond graphical technique which fully entails the structural information of the system in a systematic way and hence is quite suitable for the symbolic manipulation of the equations on the computer and is finalized as a symbolic generation scheme SYMBOG which enables derivation of the system equations at any reticulation level of the system for the objectives of setting such system equations. Some numerical simulation results by the system equations generated by the proposed scheme are presented which show the effectiveness of the proposed modelling method. Author (CISTI)

N93-10574 Waterloo Univ. (Ontario). Dept. of Mechanical Engineering.
CHAOTIC OSCILLATION OF A HIGH SPEED FLEXIBLE ARM ROBOT **c37**
M. F. Golnaraghi *In* Carleton Univ., Proceedings of the Twelfth Canadian Congress of Applied Mechanics, Volumes 1 and 2 May 1989 p 872-873 (For primary document see N93-10466 01-31)
Copyright Avail: Canadian Society for Mechanical Engineering, 2050 Mansfield St., Suite 700, Montreal, Quebec H3A 1Z7 Canada

In this paper the existence of chaotic oscillations associated with nonlinearities due to Coriolis and centripetal forces in a multi-degree of freedom high speed flexible arm robot are considered. Numerical studies indicate that these nonlinearities indeed cause chaotic solutions. The routes to chaos contain subharmonic bifurcations and quasi-periodic motions. It is shown that chaotic solutions do occur in the forced resonance regions obtained using perturbation methods. At resonance, chaos occurs when the cyclic forcing amplitude is increased. Author (CISTI)

N93-10575 Nanyang Univ. (Singapore).
A SOLUTION SCHEME FOR THE DEFLECTION EQUATIONS OF FLEXIBLE ARMS WITH TIME-DEPENDENT BOUNDARY CONDITIONS **c63**
K. H. Low and R. N. Dubey (Waterloo Univ., Ontario) *In* Carleton Univ., Proceedings of the Twelfth Canadian Congress of Applied Mechanics, Volumes 1 and 2 May 1989 p 878-879 (For primary document see N93-10466 01-31)
Copyright Avail: Canadian Society for Mechanical Engineering, 2050 Mansfield St., Suite 700, Montreal, Quebec H3A 1Z7 Canada

The system equations of flexible arms consist of two sets of equations: the joint equations and the deflection equations. Only the latter, which are associated with time dependenat boundary conditions, are considered. The objective of this work is to solve the deflection equations with time dependent boundary conditions by making use of existing methods. The resulting model is suitable for simulations. Author (CISTI)

N93-10576 University of Western Ontario, London.
AUTOMATED MULTI-BODY SYSTEM DYNAMICS VIA BOND GRAPH MODELLING AND INTERACTIVE GRAPHICS **c39**
J. B. McInnis and W. H. ElMaraghy *In* Carleton Univ., Proceedings of the Twelfth Canadian Congress of Applied Mechanics, Volumes 1 and 2 May 1989 p 880-881 (For primary document see N93-10466 01-31)
Copyright Avail: Canadian Society for Mechanical Engineering, 2050 Mansfield St., Suite 700, Montreal, Quebec H3A 1Z7 Canada

For all but the simplest multi-body systems, it is necessary to solve the kinematics and dynamics by computer simulation. The development of algorithms for automating the modelling process for general multi-body systems via the bond graph formalism and the implementaion of these algorithms in a computer program for multi-body dynamical analysis and simulation are discussed. The program, which is implemented to operate in the Sun Suntools environment, encompasses the entire range of operations required for analyzing multi-body systems, from interpretation of a physical model description, through the bond graph representation, to the determination and presentation of results. Interactive graphics, automatic bond graph generation, automatic graph indexing, power flow, and casual assignment are employed to generate the equations of motion for a wide range of mechanical systems. Equations of motion are written in advanced continuous simulation language (ACSL) format, so that solution of these equations of motion can be carried out in a convenient fashion. The program was used to model and study the kinematic and dynamic behavior of robotic manipulators and is being employed in the analysis of other multi-body systems. Author (CISTI)

N93-10577 Nanyang Technological Inst. (Singapore).
A DERIVATION FOR THE KINEMATIC EQUATIONS OF FLEXIBLE ROBOTS WITH APPROPRIATE TRANSFORMATION MATRICES **c64**
K. H. Low and R. N. Dubey *In* Carleton Univ., Proceedings of the Twelfth Canadian Congress of Applied Mechanics, Volumes 1 and 2 May 1989 p 886-887 (For primary document see N93-10466 01-31)
Copyright Avail: Canadian Society for Mechanical Engineering, 2050 Mansfield St., Suite 700, Montreal, Quebec H3A 1Z7 Canada

Coordinate transformations are essential tools for the kinematic and dynamic analyses of robots. In cases of flexible arms the transform matrices are, in general, functions of the corresponding joint displacement and the elastic slopes due to deformation of the links. A derivation for the kinematic equations of flexible robots is first presented. A general transformation matrix associated with the elastic deformation is then introduced. The possibilities of simplifying the expression of the matrix is also investigated from the assumption that the strain components and elastic slopes are small compared to unity. In the above, a general form of kinetic equations for flexible robots, which are in terms of the transformation matrices, was developed. Regarding the transformation matrix associated with the elastic slopes, the possibilities of simplifying the expression are discussed.
Author (CISTI)

N93-10649# Ohio State Univ., Columbus. Dept. of Electrical Engineering.
AUTOMATED HANDLING AND ASSEMBLING OF NON-RIGID OBJECTS Semiannual Report No. 5, 16 Jan. - 15 Jul. 1992
Yuan F. Zheng 15 Jul. 1992 155 p
(Contract N00014-90-J-1516)
(AD-A253605) Avail: CASI HC A08/MF A02

This is the fifth semi-annual report of the project entitled 'Automated Handling and Assembling of Non-Rigid Objects'. This report covers the period from January 16, 1992 to July 15, 1992. The objective of this research project is to identify mechanisms for automated handling and assembling of non-rigid objects. To accomplish the goal, four aspects of the problem have been identified in our original proposal. These are: (1) Study the deformation characteristics of non-rigid materials; (2) Investigate optimal tool structures for handling non-rigid objects; (3) Develop sensing mechanisms to locate non-rigid objects; and (4) Develop motion control mechanisms for the host machines. GRA

N93-10653# Industry, Science and Technology Canada, Toronto (Ontario).
DEFENCE ELECTRONICS INDUSTRY PROFILE, 1990-1991 [PROFIL DE L'INDUSTRIE ELECTRONIQUE DE DEFENSE, 1990-1991]
1991 22 p In ENGLISH and FRENCH Original contains color illustrations
(CTN-92-60515) Avail: CASI HC A03/MF A01

The defense electronics industry profiled in this review comprises an estimated 150 Canadian companies that develop, manufacture, and repair radio and communications equipment, radars for surveillance and navigation, air traffic control systems, acoustic and infrared sensors, computers for navigation and fire control, signal processors and display units, special-purpose electronic components, and systems engineering and associated software. Canadian defense electronics companies generally serve market niches and end users of their products are limited to the military, government agencies, or commercial airlines. Geographically, the industry is concentrated in Ontario and Quebec, where about 91 percent of the industry's production and employment is found. In 1989, the estimated revenue of the industry was $2.36 billion, and exports totalled an estimated $1.4 billion. Strengths and weaknesses of the industry are discussed in terms of such factors as the relatively small size of Canadian companies, the ability of Canadian firms to access research and development opportunities and export markets in the United States, the dependence on foreign-made components, and international competition. CISTI

N93-10710# Army Engineer Waterways Experiment Station, Vicksburg, MS. Geotechnical Lab.
STABILITY OF OPEN-GRADED BASES UNDER WHEEL LOADS USING A MODEL TESTING APPROACH Final Report
Carlos R. Gonzalez May 1992 43 p
(AD-A253209; WES/MP/GL-92-11) Avail: CASI HC A03/MF A01

The stability of open-graded bases of various gradations and types of aggregates were examined when subjected to traffic. A small scale test box was designed and constructed to contain the base materials to be tested. Traffic was applied with a tire load directly on top of the bases. Rut depths at the deepest point of the wheel path were taken and used as a measurement of the stability of the material. Six different gradations of two types of materials were tested and compared with the performance of the US Army Corps of Engineers standard crushed stone base coarse gradation. Recommendations are given as to the type of material and gradation that would be most stable under direct traffic.
GRA

32 COMMUNICATIONS AND RADAR

Includes radar; land and global communications; communications theory; and optical communications.

For related information see also *04 Aircraft Communications and Navigation* and *17 Space Communications, Spacecraft Communications, Command and Tracking.* For search and rescue see *03 Air Transportation and Safety,* and *16 Space Transportation.*

N93-10092# Massachusetts Inst. of Tech., Cambridge. Research Lab. of Electronics.
BASIC AND APPLIED RESEARCH IN THE FIELD OF ELECTRONICS AND COMMUNICATIONS Final Report, 1 Nov. 1988 - 31 Oct. 1991
Jonathan Allen Jul. 1992 23 p
(Contract DAAL03-89-C-0001)
(AD-A253593; ARO-26213.137-EL) Avail: CASI HC A03/MF A01

Results of the research done under this contract are described in the articles or presented at the meetings enumerated in the attached List of Publications. The topics covered include atomic physics, communications, electromagnetics, electronics, lasers, microwaves, molecular physics, and quantum electronics. GRA

N93-10096# Department of the Navy, Washington, DC.
LIGHTWEIGHT DEPLOYABLE ANTENNA SYSTEM Patent Application
Paul Mileski, inventor (to Navy) and Jeffrey Kornblith, inventor (to Navy) 25 Feb. 1992 8 p
(AD-D014746; US-Patent-5,091,732; US-Patent-Appl-SN-579455; US-Patent-Class-343-797) Avail: CASI HC A02/MF A01

A deployable antenna assembly is discussed. The assembly includes a canister providing an elongated chamber and an elongated hollow mast with a mounting member on its upper end. A coaxial cable extends into the hollow mast to provide radio signals to the antenna assembly. Four antenna members of resiliently deflectable wire are spaced at 90 deg intervals about the periphery of the mounting plate. The members comprise a generally helical coil and elongate arms extending downward along the inner wall of the canister. Each opposed pair comprises a dipole. A pair of baluns are connected to the coaxial cable and placed adjacent to the mounting member. A phase shifter is connected between the coaxial cable and one of the baluns. The central conductor of the balsun is connected to the coil of one of the antenna members of a dipole. The conductive shield is connected to the coil of the other antenna member of a dipole. A sealing medium is provided about the baluns, and phase shifter. The coils of the antenna members are flexed when the arms are extending downward within the canister, and the canister is slidable relative to the mast and antenna members to free the arms therefrom for extension into a horizontal position. GRA

N93-10111 Canadian Marconi Co. Ltd., Montreal (Quebec).
BEAM FORMING ANTENNA SYSTEM Patent
Andrew J. Lait, inventor (Canadian Marconi Co. Ltd.) 30 Jan. 1990 21 p
(Patent-1-265-236; Int-Patent-Class-H01Q-25/00; Int-Patent-Class-H01Q-3/40; CTN-91-60130) Copyright Avail: Micromedia Ltd., Technical Information Centre, 165 Hotel de Ville, Place du Portage, Phase 2, Hull, Quebec J8X 3X2, Canada HC/MF

A multiple beam forming antenna system suitable for use with surveillance radar is described. The system includes beam forming circuitry coupled to linear, circular, planar or three dimensional arrays to supply signals to the antenna elements so that multiple beams are formed on transmit, or to receive signals from the corresponding multiple beams. The system may thus use separate beams to measure the azimuth bearing and the elevation angle (height) of a target. The system comprises a plurality of antenna array elements and of beam forming networks. The outputs from each of the beam forming networks are connected together at simple junctions behind each radiating element of the array. The antenna system is low power loss in that it obtains isolation between beams by applying orthogonality principles. CISTI

N93-10199# Surveillance Research Lab., Salisbury (Australia).
SOFTWARE FOR PREDICTION AND ANALYSIS OF GROUND WAVE PROPAGATION LOSS
M. J. Whitington and R. M. Thomas Apr. 1992 28 p
(AD-A253474; SRL-0073-TM; DODA-AR-006-744) Avail: CASI HC A03/MF A01

This document describes a variety of in-house and externally written software which was used in the High Frequency Radar Division for the prediction and analysis of ground wave propagation losses. Applications of the software have included the determination of sizes of HF array buffer zones and intersite separations between transmitter and receiver for Over-The-Horizon Radars of the Jindalee Operational Radar Network. The same software may also be useful for communications and broadcasting applications, and can be made available upon consultation with the authors. GRA

N93-10203# Electronics Research Lab., Adelaide (Australia).
METEOR BURST COMMUNICATIONS SYSTEM TRIAL, 1990-1991
John A. Hackworth Jun. 1992 26 p
(AD-A253625; ERL-0596-RE; DODA-AR-006-928) Avail: CASI HC A03/MF A01

This report describes a series of three Meteor Burst Communication (MBC) trials conducted over the eastern and northern regions of the Australian continent during 1990/91, using commercially available MBC equipment. Also included in the report is a comparison between the performances of the commercial equipment and an MBC system developed at DSTO Salisbury and trialed during 1989 and 1990. GRA

N93-10223# Michigan Univ., Ann Arbor. Radiation Lab.
MILLIMETER WAVE MEASUREMENT AND MODELING OF TERRAIN SCATTERING Final Report, 1 Feb. 1989 - 31 Jan. 1992
Fawwaz T. Ulaby 15 Feb. 1992 110 p
(Contract DAAL03-89-K-0056)
(AD-A253525; Rept-026247-1-F; ARO-26224.8-GS) Avail: CASI HC A06/MF A02

A summary of the results realized, over the past three years, with regard to improved characterization of radar backscatter from terrain is provided. The papers and reports published under this program cover three types of contributions: (1) techniques for measuring the polarimetric scattering response of distributed targets using coherent-on-receive systems; (2) theoretical models for polarimetric scattering from tree canopies and snow-covered terrain; and (3) extensive experimental measurements at 35, 94, and 140 GHz for model targets (such as small trees) under laboratory conditions as measurements for natural surfaces from truck-mounted platforms. GRA

N93-10253# Carnegie-Mellon Univ., Pittsburgh, PA. Software Engineering Inst.
ANALYSIS OF RESERVATION-BASED DUAL-LINK NETWORKS FOR REAL-TIME APPLICATIONS Final Report
Lui Sha, Shirish S. Sathaye, and Jay K. Strosnider Jun. 1992 33 p
(Contract F19628-90-C-0003)
(AD-A254176; CMU/SEI-92-TR-10; ESD-TR-92-10) Avail: CASI HC A03/MF A01

Next-generation networks are expected to support a wide variety of services. Some services such as video, voice, and plant control traffic have explicit timing requirements on a per-message basis rather than on the average. In this paper we develop a general model of reservation-based dual-link networks to support real-time communication. We examine the desirable properties of this network and the difficulties in achieving these properties. We then introduce the concept of coherence and develop a theory of coherent dual-link networks. We show that a coherent dual-link network can be analyzed as though it is a centralized system. We then discuss practical considerations in implementing a dual-link

network, and implications of this work to address problems observed in the IEEE 802.6 metropolitan area network standard. GRA

N93-10260# Naval Postgraduate School, Monterey, CA.
LINK-11 COMMUNICATIONS M.S. Thesis
Thor A. Simensen Mar. 1992 61 p
(AD-A252766) Avail: CASI HC A04/MF A01

This thesis provides the reader with an overview of the Link-11 system and what telecommunication assets are needed to operate the system. Fundamental aspects of High Frequency (HF), Ultra High Frequency (UHF), and communication configurations are reviewed. An examination of the Link-11 equipment operations is presented. This includes a description of the Tactical Data Set (TDS) computer and encryption device. The thesis also contains an in-depth review of the Data Terminal Set (DTS). The specific operations of the DTS that are studied are Error Detection and Correction (EDAC), audio signal generation, link control, NTDS computer interface, and digital/analog conversion. Distinctive Link-11 communication features are discussed. These features consist of Phase Shift Keying (PSK), signal generation, signal structure, and binary coding. The protocol, consisting of the frame structure, control codes, and net operation, which operates the net automatically is introduced. A review of radio equipment and its management concludes the thesis. GRA

N93-10301# Illinois Univ., Champaign.
PROCEEDINGS OF THE ANTENNA APPLICATIONS SYMPOSIUM, VOLUME 1 Final Report
Paul Mayes Feb. 1992 259 p Symposium held 25-27 Sep. 1991
(Contract F30602-88-D-0028)
(AD-A253681; RL-TR-92-42-Vol-1) Avail: CASI HC A12/MF A03

A collection of state-of-the-art papers relating to phased array antennas, multibeam antennas, satellite antennas, microstrip antennas, reflector antennas, HF, VHF, UHF and various other antennas are collected. GRA

N93-10302# Illinois Univ., Champaign.
PROCEEDINGS OF THE ANTENNA APPLICATIONS SYMPOSIUM, VOLUME 2 Final Report
Paul Mayes Feb. 1992 116 p Symposium held 25-27 Sep. 1991
(Contract F30602-88-D-0028)
(AD-A253682; RL-TR-92-42-Vol-2) Avail: CASI HC A06/MF A02

State-of-the-art papers relating to phased array antennas, multibeam antennas, satellite antennas, microstrip antennas, reflector antennas, HF, VHF, UHF, and various other antennas are addressed. GRA

N93-10358# Arcon Corp., Waltham, MA.
APPLICATION OF VOLUMETRIC MULTIPLE-SCATTERING APPROXIMATIONS TO FOLIAGE MEDIA Interim Report
Douglas Tamasanis Dec. 1991 44 p
(Contract F19628-89-C-0186)
(AD-A253337; RL-TR-91-433) Avail: CASI HC A03/MF A01

Representation of natural terrain growth as a complex dielectric slab with some arbitrary thickness equivalent to the mean height of the vegetation is a common modeling simplification technique. The vegetation medium may be viewed as two or more different types of dielectric scatterers arranged in a random geometric configuration in a surrounding 'host' medium. Based on this assumption, the foliage is treated as a continuous medium, with the propagation of the waves governed by an effective dielectric constant, (epsilon*). Several volumetric multiple-scattering models were used to determine the effective dielectric constants representative of foliage media. A brief discussion of the Average T-Matrix Approximation (ATA) and the Coherent Potential Approximation (CPA) is presented. The ATA represents the field at an individual scattering center in terms of an equivalent field produced by the other scatterers but includes no provision for the interaction between scatterers. The CPA neglects the difference between the external excitation field and the average field and includes interaction effects between scatterers. GRA

N93-10366# Price (M. A.), Windsor Junction (Nova Scotia).
MATHEMATICAL ANALYSIS OF MULTI-SENSOR CROSS-CORRELATION PROCESSING FOR SOURCE LOCALIZATION
M. A. Price Nov. 1989 48 p
(Contract DREA-W7707-8-0176)
(DREA-CR-89-433; CTN-92-60356) Avail: CASI HC A03/MF A01

This work examines source localization by passive means when signals from multiple sensors are available. Each of the two localization techniques presented search over a grid of hypothesized source locations to find the location that best explains the observed measurement. The first technique finds the best location that yields the greater cross correlation sum. This sum comprises weighed values of the correlations obtained at time delays at which the hypothesized location would induce a peak. Variants of the technique allow for multipaths to be handled under both coherent and incoherent assumptions. The second technique uses Time Differences of Arrival (TDOA) between signal reception at multiple sensors. It minimizes the square of the error between the observed delays and those that a source at the hypothesized location would produce. In this document, a Cramer-Rao lower bound is presented to delineate the limit of performance for a multisensor, multipath scenario with sensor position inaccuracy. Simulations for a restricted number of scenarios are used to check the validity of the Cramer-Rao Bound calculations and to compare the two estimators. Author (CISTI)

N93-10380# Drexel Univ., Philadelphia, PA. Dept. of Electrical and Computer Engineering.
NONLINEAR SIGNAL PROCESSING SCHEMES FOR ROBUST TARGET DETECTION AND AUTOMATIC CLUTTER REJECTION IN RADAR Final Technical Report, 1 Apr. 1986 - 31 Dec. 1991
Nihat M. Bilgutay, Kevin D. Donohue, and Jafar Saniie 22 Jul. 1992 14 p
(Contract N00014-86-K-0520)
(AD-A253546) Avail: CASI HC A03/MF A01

The application of a technique called Split-Spectrum Processing, which was developed to achieve frequency diversity in one-dimensional (A-scan) ultrasonic application, to radar was examined. The major highlights and accomplishments of the project are: (1) adaptive techniques for determination of optional processing parameters; (2) robust techniques for target detection; (3) non-parametric target detection techniques; (4) rank determination for order statistic filters; and (5) order statistic characterization and signal processing for nonparametric robust and adaptive detection systems. I.I.C.

N93-10394# Sandia National Labs., Albuquerque, NM.
OPEN SKIES TREATY IMAGING RADAR TECHNOLOGY ISSUES
M. B. Sandoval Jun. 1992 9 p Presented at the Arms Control and Verification Technology, Williamsburg, VA, 2-4 Jun. 1992
(Contract DE-AC04-76DP-00789)
(DE92-016548; SAND-92-1372C; CONF-9206179-2) Avail: CASI HC A02/MF A01

This paper discusses the imaging radar technology requirements for the Open Skies regime, including the unresolved issues to be discussed at future Open Skies Consultative Commission (OSCC) meetings. Compliance with international rules on shared technology is addressed and some of the practical considerations for operational deployment of the radar imaging equipment in an Open Skies aircraft are presented. The Open Skies Treaty requirements and validation methodologies for imaging radars that were agreed on and those that will require future OSCC review are discussed. DOE

N93-10418# Syracuse Univ., NY. Dept. of Electrical and Computer Engineering.
ANALYSIS OF A MEDIUM SIZE BOR RADOME Final Technical Report
A. Rahhalarabi and E. Arvas Aug. 1992 13 p
(Contract N00014-90-J-1224)
(AD-A253954) Avail: CASI HC A03/MF A01

A brief summary of a simple moment solution is presented for the problem of analyzing a medium size BOR (body of revolution) radome. The radome is excited by a plane wave (receive mode) and we are interested in finding the total far scattered field and the total internal field that is transmitted into the radome. A medium size radome is one which is not much larger than the wavelength of the exciting field. Using a simple spherical dielectric shell as a model, it is shown that one can obtain accurate results with BOR formulation where the necessary computer CPU and storage is much less than those required by arbitrary surface formulation that was used in an earlier report. GRA

N93-10430# National Telecommunications and Information Administration, Boulder, CO. Inst. for Telecommunication Sciences.
ANALYSIS OF RECEPTION VARIABILITY DUE TO TERRAIN MULTIPATH ON MICROWAVE COMMON CARRIER LINKS
E. J. Dutton, T. G. Hoople, and M. P. Roadifer Jan. 1992 41 p
(NTIA-92-283) Avail: CASI HC A03/MF A01

The error variability of received phase shift keying (minimum shift keying SK), quadrature amplitude modulation, and quadrature partial response modulations on digital microwave common carrier links resulting from transmitted power variations and the dispersive effects of terrain multipath using a two-ray model is analyzed. The results and an earlier prediction of long-term (annual) average symbol error rate (SYE) for the above modulations are used to predict median annual received SYE. Since the average SYE was used earlier to represent median conditions, average and new median SYE's are compared. Year-to-year variability of received power and bit error rate (BER) of common carrier microwave transmissions caused by variation of annual refractivity gradient distributions on off-axis paths is also analyzed, and it is concluded that this variability is not significant vis-a-vis the annual variability discussed above. GRA

N93-10440# National Inst. of Standards and Technology, Boulder, CO. Electronics and Electrical Engineering Lab.
GRADIOMETER ANTENNAS FOR TUNNEL DETECTION
David A. Hill Jun. 1992 38 p Sponsored by Army Belvoir Research, Development and Engineering Center
(PB92-205400; NISTIR-3990) Avail: CASI HC A03/MF A01

The use of gradiometer antennas for detection of long conductors and detection of empty tunnels is analyzed. For reception in vertical boreholes, the gradiometer consists of two vertical electric or magnetic dipoles with a vertical separation. Both sum and difference responses are useful, but the difference responses has the potential advantage of suppressing the primary field and making the scattered field easier to detect. The difference response is most effective in suppressing the primary field for a parallel scan where the transmitting antenna and receiving gradiometer are always at the same height. Gradiometers are most advantageous at low frequencies where the scattered field is small compared to the primary field. GRA

N93-10657# Mission Research Corp., Santa Barbara, CA.
ACIRF USER'S GUIDE FOR THE GENERAL MODEL (VERSION 3.5) Technical Report, 1 Dec. 1990 - 30 Jun. 1991
Roger A. Dana 1 Jun. 1992 214 p
(Contract DNA001-91-C-0010)
(AD-A254068; MRC-R-1358; DNA-TR-91-162) Avail: CASI HC A10/MF A03

Design and evaluation of Radio Frequency (RF) systems that must operate through ionospheric disturbances require an accurate channel model. Such a model can be used to construct realizations of the received signal for use in digital simulations of transionospheric communications links and radars or hardware channel simulators. This report describes the Fortran program ACIRF (Version 3.5) that generates realizations of the channel impulse response functions at the outputs of multiple antennas with arbitrary beamwidths, pointing angles, and relative positions. A general model that varies smoothly between the frozen-in and turbulent models is used for the temporal fluctuations of the impulse response functions. Examples are given which illustrate the effects on the received signal of the variation from the turbulent to frozen-in models, and the effects of antennas with arbitrary sizes and pointing angles. ACIRF inputs and outputs are described. GRA

N93-10695# Wright Lab., Wright-Patterson AFB, OH.
ELEVEN YEARS OF IONOSPHERIC SCINTILLATION FADING DATA FROM TWENTY GREENLANDIC STATIONS Final Report, Jan. 1980 - Jan. 1990
Allen L. Johnson May 1992 52 p
(AD-A253271; WL-TR-92-1050) Avail: CASI HC A04/MF A01

Radio communications in the polar region are subject to periodic outages due to rapid density fluctuations in the Arctic ionosphere. In order to evaluate the effect of solar activity on these outages, the messages from an extensive network of unmanned automatic meteorological stations in Greenland were recorded. In a joint project between the Danish Meteorological Institute and the U.S. Air Force Wright Laboratory, the recorded data were reduced and analyzed to derive bit-error-rate and missed message statistics. These data are summarized in hourly, daily, monthly, and yearly plots for 20 mid-latitude, auroral, and polar station around Greenland. This report describes the results of the-experiment. The appendices (WL-TR-92-1051) contains 100 station years of data. GRA

N93-10701# Air Force Inst. of Tech., Wright-Patterson AFB, OH. Foreign Technology Div.
CHINESE SPACE SCIENCE AND TECHNOLOGY (SELECTED ARTICLES)
3 Dec. 1991 65 p Transl. into ENGLISH from Zhongguo Kongjian Kexue Jishu (China), v. 10, no. 1, 1990 p 14-20, 21-27, 28-35, 60-66, and title page
(AD-A254099; FTD-ID(RS)T-1274-90) Avail: CASI HC A04/MF A01

This article carries out a technical summary for communication satellites. It describes limiting conditions in the process of designing communications satellites, and it details primary technical design characteristics of sub-systems on satellites, for example, effective loading, attitudes, and orbit controls, as well as power sources, measurement control, structures, and heat control, along with other similar items. GRA

N93-10728# Massachusetts Inst. of Tech., Cambridge.
MICROWAVE PROPAGATION AND ATTENUATION IN MAGNETOPLASMAS Final Report, 1 Jun. 1990 - 30 Nov. 1991
Min-Chang Lee 30 Nov. 1991 10 p
(Grant AF-AFOSR-0263-90)
(AD-A250197; AFOSR-92-0275TR) Avail: CASI HC A02/MF A01

Under the sponsorship of the Air Force Office of Scientific Research Profs. Min-Chang Lee and Ronald R. Parker's research team has conducted experimental studies of anomalous absorption of radio waves in turbulent magnetized plasmas. This research program includes laboratory experiments with the newly constructed Versatile Toroidal Facility (VTF) at the MIT Plasma Fusion Center and the field experiments using orbiting satellites and ground-based radars at Arecibo, Puerto Rico. The design and construction of the Versatile Toroidal Facility involved five graduate students and twenty-two UROP (Undergraduate Research Opportunity Program) students. This student-oriented project was reported in the 1991 March 6 issue of the MIT Tech Talk. The detailed documentation and discussions of this VTF plasma device are presented in the M.S. theses of Robert F. Duraski (1991) and Chan Yoo (1991). Attached are the abstracts of these two graduate theses. GRA

N93-10747# Massachusetts Inst. of Tech., Cambridge. Dept. of Electrical Engineering and Computer Science.
INTERACTION OF ELECTROMAGNETIC FIELDS WITH CHONDROCYTES IN GEL CULTURE Final Report, 14 Jan. 1991 - 14 Jan. 1992
Alan J. Grodzinsky, Michael D. Buschmann, and Yehezkiel A. Gluzband 14 Jan. 1992 26 p
(Grant AF-AFOSR-0153-91)
(AD-A253727; AFOSR-92-0742TR) Avail: CASI HC A03/MF A01

The specific objectives of this research period were: (1) to quantify the effect of applied electric fields on chondrocyte metabolism, using a range of stimulation frequencies and amplitudes; (2) to compare the chondrocyte biosynthetic response to applied fields at early times in agarose gel culture before an extracellular matrix has accumulated and at later times after significant deposition of matrix around and between the cells; and (3) to begin to interpret the biosynthetic response to applied fields in terms of models of physical mechanisms. The results of these studies suggest that electric fields applied to chondrocytes in agarose can modulate the synthesis of proteoglycans and protein constituents. Biosynthesis may be inhibited or stimulated depending on the amplitude of the applied current density. In addition, the presence of extracellular matrix may enhance the ability of normal chondrocytes and cells in intact cartilage to respond to electric fields, although the presence of matrix was not required for the stimulatory response to be observed with Swarm rat chondrosarcoma cells. GRA

N93-10800*# National Aeronautics and Space Administration. Goddard Space Flight Center, Greenbelt, MD.
DATA SYNTHESIS AND DISPLAY PROGRAMS FOR WAVE DISTRIBUTION FUNCTION ANALYSIS
L. R. O. Storey and K. J. Yeh Jun. 1992 18 p
(NASA-TM-108009; NAS 1.15:108009;
NSSDC/WDC-A-R/S-92-05) Avail: CASI HC A03/MF A01

At the National Space Science Data Center (NSSDC) software was written to synthesize and display artificial data for use in developing the methodology of wave distribution analysis. The software comprises two separate interactive programs, one for data synthesis and the other for data display. Author

N93-10865# California Univ., Berkeley. Lawrence Berkeley Lab.
MODELLING OF 3-D ELECTROMAGNETIC RESPONSES USING THE TIME-WAVENUMBER METHOD Ph.D. Thesis
S. Lee Dec. 1991 97 p
(Contract DE-AC03-76SF-00098)
(DE92-017025; LBL-31970) Avail: CASI HC A05/MF A02

The diffusion of electromagnetic fields in time and the three spatial dimensions can be modelled using a new numerical algorithm that is tailored for geophysical applications. The novel feature of the algorithm is that a large part of the computation is done in the wavenumber domain. Here, the spatial Fourier transforms of the vertical magnetic field and the vertical current density are used to define two scalar potentials. For either a vertical electric or a vertical magnetic dipole source at the subsurface these wavenumber potentials can be represented by a simple Gaussian distribution function. In the air, the fields satisfy the Laplace equation. The flow of this algorithm is as follows: the potentials are defined in the wavenumber domain as an initial condition depending on the source configuration, the vector current density J in space is obtained from the potentials using the inverse Fourier transform, the vector electric field E is obtained by multiplying J by resistivity, and the updated potentials are then obtained from the forward Fourier transform of E. Using the updated potential as a subsequent initial condition these steps are repeated until the solution reaches the final time. Since spatial derivatives can be exactly evaluated in the wavenumber domain by simple multiplications, this algorithm requires far less memory than the conventional finite difference (FD) method. The conventional FD method needs finer discretization in space in order to minimize the numerical dispersion caused by numerical differentiation in space. The conductivity distribution for this algorithm is piece-wise continuous and bounded in the wavenumber domain. DOE

33 ELECTRONICS AND ELECTRICAL ENGINEERING

Includes test equipment and maintainability; components, e.g., tunnel diodes and transistors; microminiaturization; and integrated circuitry.

For related information see also *60 Computer Operations and Hardware* and *76 Solid-State Physics.*

N93-10091# Mitre Corp., Bedford, MA.
FAR-ZONE FIELD OF A MONOPOLE ELEMENT ON A DISK GROUND PLANE ABOVE FLAT EARTH
Melvin M. Weiner Jun. 1992 148 p
(AD-A253580; MTR-92B0000090) Avail: CASI HC A07/MF A02

Richmond's moment-method analysis for the current distribution and input impedance of a monopole element on a disk ground plane above flat Earth is used to obtain the far-zone field in the free-space region. Numerical results for directivity and radiation efficiency are presented as separate entities, unlike previously reported results based on Monteath's compensation theorem or Sommerfeld's attenuation function that give only the product of the directivity and radiation efficiency. GRA

N93-10215# Naval Research Lab., Washington, DC.
SIMULATION OF ELECTRON BEAM TRANSPORT IN ION-FOCUSED REGIME CONDITIONING CELLS
R. F. Hubbard, S. P. Slinker, R. F. Fernsler, G. Joyce, and M. Lampe 21 Jul. 1992 63 p
(AD-A253352; NRL/MR/4790-92-6983) Avail: CASI HC A04/MF A01

The resistive hose instability can disrupt propagation of self-pinched beams in dense gas. To reduce growth of the instability, beams can be conditioned prior to propagation. The objectives of beam conditioning are to center the beam in order to reduce initial transverse perturbations which seed the hose instability, and to tailor the beam emittance in order to detune the head-to-tail coherence of the instability. Emittance tailoring can be performed by transporting the beam through a passive ion-focused regime (IFR) cell, which induces a head-to-tail taper of the beam radius; the radius taper is then converted to an emittance taper by passing the beam through a thick exit foil which scatters the beam. Beam centering can be accomplished by transporting the beam through either: (1) a passive IFR cell which is narrow enough to provide wall guiding, or (2) a laser-ionized active IFR cell, or (3) a wire cell in which the centering is provided by a current-carrying wire. We report here on axisymmetric particle simulation studies of IFR tailoring cells, alone and in tandem with each of these types of centering cells, and also on the effect of supplementary focusing lenses and conducting foils. We discuss the parameter choices that are conducive to effective beam conditioning. The emphasis is on conditioning configurations and beam parameters that have actually been tested in experiments with the ATA and SuperIBEX accelerators. GRA

N93-10233# Cree Research, Inc., Durham, NC.
DEVELOPMENT OF 6H-SiC CMOS TRANSISTORS FOR INSERTION INTO A 350 C OPERATIONAL AMPLIFIER Technical Report, 16 May - 15 Jul. 1992
John W. Palmour 22 Jul. 1992 8 p
(Contract N00014-92-C-0053)
(AD-A253760) Avail: CASI HC A02/MF A01

Device parameter measurements have been made on n-channel MOSFET devices that were fabricated prior to this contract. These parameters were to be used to simulate circuits using the Simulation Program with Integrated Circuit Emphasis (SPICE). The devices had I-V curves characteristic of normal MOSFET's. However, the gate leakage of these devices was too high to allow meaningful

data to be taken at very low drain biases. Therefore, the wafers currently in process must be finished, and must have sufficiently low gate leakage, before a significant modeling effort can be undertaken. GRA

N93-10240# California Univ., Irvine. Dept. of Electrical and Computer Engineering.
MAGNETOSTATIC WAVES-BASED INTEGRATED OPTIC BRAGG CELL MODULES WITH APPLICATIONS TO RF SIGNAL PROCESSING Annual Technical Report No. 2, 1 Jul. 1991 - 30 Jun. 1992
Chen S. Tsai 30 Jun. 1992 30 p
(Contract N00014-90-J-4039)
(AD-A254035) Avail: CASI HC A03/MF A01

Two major achievements were made during the second program year (July 1, 1991 to June 30, 1992). First, a complete analysis on guided-wave magnetooptic (MO) Bragg diffraction in a YIG-GGG layer structure aimed at the key parameters and guidelines for design of high-performance MO Bragg cells was performed. Second, an integrated MO Bragg cell module was realized, for the first time, using a YIG-GGG tapered waveguide structure. GRA

N93-10241# Naval Surface Warfare Center, Silver Spring, MD.
RESONANCE APPARATUS OPERATING MANUAL
Gilbert F. Lee 15 Sep. 1991 40 p
(AD-A254040; NAVSWCMP91-644) Avail: CASI HC A03/MF A01

This manual presents the following material: (1) a detailed description of the resonance apparatus; (2) a step-by-step electrical hookup of the equipment; and (3) the use of computer program QCP. The material is given in three tutorials. Operating diagnostics are also given. GRA

N93-10250# SRI International Corp., Menlo Park, CA.
DEVELOPMENT OF ELECTROSUPERCAPACITORS Final Report
Digby D. MacDonald and Subhash C. Narang Nov. 1991 54 p
(Contract DAAL01-88-C-0840)
(AD-A252208) Avail: CASI HC A04/MF A01

Nonfluorinated proton conducting superionic molecular tunnel electrolytes (PSMTE) exhibiting high proton conductivity (approximately 10 exp -2 S/cm) have been synthesized. The highly hygroscopic nature of these polymers yielding deliquescent films has precluded their use in supercapacitors. Fluorinated analogs of these PSMTE's were synthesized to provide higher conductivity and greater hydrophobicity. Fluorinated PSMTE's exhibit higher conductivity than Nafion (1.3 x 10 exp -2 vs. 2.1 x 10 exp -4 S/cm) under identical conditions of relative humidity and temperature. Fluorinated PSMTE's show good film forming properties suitable for fabrication of supercapacitors. However, these materials have not yet been utilized in supercapacitors. Polymer films of aniline and its various derivatives having electron donating (-OCH3) and electron withdrawing groups (-SO3H, -NO2) were formed electrochemically using platinum and nickel substrates. These films were characterized by cyclic voltammetry (CV) and electrochemical impedance spectroscopy (EIS). The electron withdrawing groups (-SO3H, -NO2) increased the voltage at which the redox reaction occurs for aniline. The electron donating groups (-OCH3) moved the redox potential in the negative direction. The monomers were also deposited on Nafion coated Pt. These films gave multiple oxidation-reductions peaks and better discharge characteristics as compared to films on bare Pt. They also exhibited electrochromic behavior. To demonstrate 'proof of concept', different combinations of the polymers and Pt black were used as electrodes with a thin (0.001 in.) Nafion membrane to form a capacitor/battery. The capacity and the energy density were determined for the cells. The cells were able to pulse charge-discharge for times as low as 0.1 ms. GRA

N93-10255# Harry Diamond Labs., Adelphi, MD.
DESIGN AND EVALUATION OF A QUASI-ACTIVE DELAY-LINE LIMITER/FILTER RF PROTECTION DEVICE Final Report, Mar. 1990 - Feb. 1992
Chance M. Glenn May 1992 65 p
(AD-A254179; HDL-TM-92-9) Avail: CASI HC A04/MF A01

A compact, quasi-active delay-line limiter/filter (QUADLF) was designed to limit high-power, fast-rise-time pulses and prevent spike leakage, which is common to conventional limiting techniques. The QUADLF design incorporates both waveguide and microstrip technologies. Over the operating frequency range, from 0.8 to 1.2 GHz, experimental results showed less than 2-dB transmission loss below 10-mW input power and greater than 20-dB in-band isolation above 5.0-W input power. Design procedures are outlined and experimental data are presented that demonstrate feasibility and applicability. Data on frequency response, temporal response, and isolation characteristics are also shown. GRA

N93-10273# Pennsylvania State Univ., University Park. Materials Research Lab.
PIEZOELECTRIC AND ELECTROSTRICTIVE MATERIALS FOR TRANSDUCERS APPLICATIONS, VOLUME 1 Final Report, 1 Feb. 1991 - 31 Jan. 1992
L. E. Cross, R. E. Newnham, A. S. Bhalla, J. P. Dougherty, J. H. Adair, V. K. Varadan, and V. V. Varadan 31 Jan. 1992 151 p
(Contract N00014-89-J-1689)
(AD-A250889) Avail: CASI HC A08/MF A02

Highlights of the past year's activities include: An increased emphasis upon the flextensional (moonie) type actuators, modeling both the internal stress distribution as a function of geometry, and the very interesting resonant mode structure of the composites; a more refined focus upon the performance of piezoelectric ceramic transducers, particularly under high drive levels is developing with concern for the extrinsic domain and phase boundary contributions to response. Measurement and modelling are being used to explore the nonlinearity and the frequency response and to examine the phase partitioning at the rhombohedral:tetragonal morphotropic phase boundary in the PZT system. Phenomena limiting lifetime in polarization and phase switching actuators are being explored to separate surface and volume effects and those due to grain size and flaw population differences. New work has been initiated to examine Acoustic Emission as a technique, in combination with Barkhausen current pulse analysis, to separate and evaluate domain switching and microcracking in polarization switching systems. GRA

N93-10276# Pennsylvania State Univ., University Park. Materials Research Lab.
PIEZOELECTRIC AND ELECTROSTRICTIVE MATERIALS FOR TRANSDUCERS APPLICATIONS, VOLUME 2 Final Report, 1 Feb. 1991 - 31 Jan. 1992
L. E. Cross, R. E. Newnham, A. S. Bhalla, J. P. Dougherty, J. H. Adair, V. K. Varadan, and V. V. Varadan 31 Jan. 1992 174 p
(Contract N00014-89-J-1689)
(AD-A250890) Avail: CASI HC A08/MF A02

The topics discussed are as follows: Ceramic-Metal Composite Actuator; Effects of Surface Layers on the Physical Properties of Lanthanum Doped Lead Zirconate Titanate Ceramic; The Influence of Surface Contamination on Electric Fatigue of Ferroelectrics; Fatigue Effects in High Strain Actuators; Acoustic Emission in Ferroelectric Lead Titanate Ceramics; Origin and Recombination of Microcracks; Morphotropic Phase Boundary in the Pb(ZrxTi1-x)O3 System; Theory of Tetragonal Twin Structure in Ferroelectric Perovskites with a First-Order Phase Transition; The Extrinsic Nature of Nonlinear Behavior Observed in Lead Zirconate Titanate Ferroelectric Ceramic; Electromechanical Nonlinearity of Ferroelectric Ceramics and Related Non-180* Domain Wall Motions; Stress and Electric Displacement Distribution Near Griffith's Type III Crack Tips in Piezoceramics; Stress Induced Shift of the Curie Point in Epitaxial PbTiO3 Thin Films; and X-ray and Phenomenological Study of Lanthanum-Modified Lead Zirconate-Titanates in the Vicinity of the Relaxor Phase Transition Region. GRA

N93-10279# Sandia National Labs., Albuquerque, NM.
LONG CONDUCTION TIME PLASMA OPENING SWITCH EXPERIMENTS AT SANDIA NATIONAL LABS
M. E. Savage, W. W. Simpson, G. W. Cooper (New Mexico Univ., Albuquerque.), and M. A. Usher (General Technology Corp., Albuquerque, NM.) 1992 6 p Presented at the 9th International Conference on High Power Particle Beams, Washington, DC, 25-29 May 1992
(Contract DE-AC04-76DP-00789)
(DE92-015003; SAND-92-0080C; CONF-920515-4) Avail: CASI HC A02/MF A01

Sandia National Labs has undertaken an ambitious program to reduce the size and cost of large pulsed power drivers. The program basis is inductive energy storage and Plasma Opening Switches (POS). Inductive energy storage has well known advantages, including increased efficiency and reduced stress on the vacuum interface. The Sandia approach is to retain the reliable and efficient Marx generator and the temporal pulse compression of the water dielectric capacitor. A triggered closing switch, developed at Sandia, transfers the capacitor charge into the energy storage inductor. This approach has several advantages, including relaxed requirements on Marx jitter and inductance, and must faster current risetime in the energy storage inductor. The POS itself is the key to the Sandia program. The switch design uses an auxiliary magnetic field to inject the plasma and hold it in place during conduction. After opening begins, the self magnetic field of the power pulse pushes on the plasma to increase the opened gap. We use magnetic pressure because we desire POS gaps of several cm. Erosion POS devices typically open much less than that. Improved opening allows more efficient energy transfer to loads. DOE

N93-10280# Pennsylvania State Univ., University Park. Materials Research Lab.
PIEZOELECTRIC AND ELECTROSTRICTIVE MATERIALS FOR TRANSDUCERS APPLICATIONS, VOLUME 3 Final Report, 1 Feb. 1991 - 31 Jan. 1992
L. E. Cross, R. E. Newnham, A. S. Bhalla, J. P. Dougherty, J. H. Adair, V. K. Varadan, and V. V. Varadan 31 Jan. 1992 167 p
(Contract N00014-89-J-1689)
(AD-A250891) Avail: CASI HC A08/MF A02

The topics discussed are as follows: Distribution Functions of Coexisting Phases in a Complete Solid Solution System; The Glassy Behavior of Relaxor Ferroelectrics; The Dielectric Relaxation of Lead Magnesium Niobate Relaxor Ferroelectrics; An Elastic Relaxation and Internal Strain in Lead Magnesium Niobate Relaxors; Dipolar-Glass Model for Lead Magnesium Niobate; Ferroelectric Properties of Lead Barium Niobate Compositions Near the Morphotropic Phase Boundary; Pyroelectric Properties of Lead Barium Niobate Single Crystals; Microstructure-Property Relations in Tungsten Bronze Lead Barium Niobate, Pb(1-x)BaxNb2O6; An Investigation of the Lead Scandium Tantalate-Lead Titanate Solid Solution System; Pyroelectric Response and Depolarization Behavior of (1-x)Pb(Sc(1/2)Ta(1/2)O3 - (x)PbTiO3 Materials; Pyroelectric and Dielectric Properties of PMN-Based Ceramics Under DC Bias; Chemical Reactions of Lead Magnesium Niobate Titanate in the Presence of a Glass; La2Ti2O7 Ceramics; Effects of pH and H2O2 Upon Coprecipitated PbTiO3 Powders; and Kinetics of the Hydrothermal Crystallization of the Perovskite Lead Titanate. GRA

N93-10282# Pennsylvania State Univ., University Park. Materials Research Lab.
PIEZOELECTRIC AND ELECTROSTRICTIVE MATERIALS FOR TRANSDUCERS APPLICATIONS, VOLUME 4 Final Report, 1 Feb. 1991 - 31 Jan. 1992
L. E. Cross, R. E. Newnham, A. S. Bhalla, J. P. Dougherty, J. H. Adair, V. K. Varadan, and V. V. Varadan 31 Jan. 1992 59 p
(Contract N00014-89-J-1689)
(AD-A250892) Avail: CASI HC A04/MF A01

The topics discussed are as follows: A Study of Y1Ba2Cu3O(7-x) Thick Films on Ferroelectric Substrates; Y1Ba2Cu30(7-x) as an Electrode Material for Ferroelectric Devices; Polarization Reversal and High Dielectric Permittivity in Lead Magnesium Niobate Titanate Thin Films; Ferroelectric Switching in Lead Zirconate-Lead Zinc Niobate Thin Films; Lead Zirconate Titanate Stannate Thin Films for Large Strian Microactuator Applications; Ferroelectric Thin Film Ultrasonic Micromotors; and Piezoelectric Micromotors for Microrobots. GRA

N93-10357# Westinghouse Electric Corp., Baltimore, MD. Electronic Systems Group.
ADVANCED TECHNOLOGY COMPONENT DERATING Final Report, Jun. 1989 - Sep. 1991
Timothy A. Jennings Feb. 1992 198 p
(Contract F30602-89-C-0095)
(AD-A253334; RL-TR-92-11) Avail: CASI HC A09/MF A03

A technical study performed to determine the derating criteria of advanced technology components is summarized. The study covered existing criteria from AFSC Pamphlet 800-27 and the development of new criteria based on data, literature searches, and the use of advanced technology prediction methods developed in RADC-TR-90-72. The devices that were investigated were as follows: VHSIC, ASIC, MIMIC, Microprocessor, PROM, Power Transistors, RF Pulse Transistors, RF Multi-Transistor Packages, Photo Diodes, Photo Transistors, Opto-Electronic Couplers, Injection Laser Diodes, LED, Hybrid Deposited Film Resistors, Chip Resistors, and Capacitors and SAW devices. The results of the study are additional derating criteria that extend the range of AFSC Pamphlet 800-27. These data will be transitioned from the report to AFSC Pamphlet 800-27 for use by government and contractor personnel in derating electronics systems yielding increased safety margins and improved system reliability. GRA

N93-10359# Kings Coll., London (England). Dept. of Physics.
NUMERICAL MODELLING OF FRINGING FIELDS AND THEIR USE FOR COMPLEX PERMITTIVITY MEASUREMENTS AT HIGH FREQUENCIES Annual Technical Report, Feb. 1991 - Feb. 1992
Camelia Gabriel Mar. 1992 22 p
(Grant AF-AFOSR-0122-91)
(AD-A253994; AFOSR-97-0747TR) Avail: CASI HC A02/MF A01

Interest in the use of open ended coaxial probes for dielectric measurements stems from their suitability to a variety of applications in material science, chemical, biochemical, and biomedical fields. This report deals with the theoretical principles involved in the implementation of this technique and the simplifying assumptions adopted in practice. A rigorous formulation based on transmission line theory is derived and compared to a number of simpler models reported in the literature and used for dielectric measurements with various degrees of success. GRA

N93-10368 Koa Oil Co. Ltd. (Japan).
AIR CELL Patent Application
Okiyoshi Okamura, inventor (to Koa Oil Co. Ltd.), Masayuki Wakasa, inventor (to Koa Oil Co. Ltd.), and Yoshihito Tamanoi, inventor (to Koa Oil Co. Ltd.) 24 Apr. 1991 18 p
(CA-Patent-Appl-SN-2001346; Int-Patent-Class-H01M-12/00; Int-Patent-Class-H01M-4/04; Int-Patent-Class-B29C-41/18; CTN-92-60390) Avail: Micromedia Ltd., Technical Information Centre, 165 Hotel de Ville, Place du Portage, Phase 2, Hull, Quebec J8X 3X2, Canada HC/MF

The present invention relates to an air cell. This air cell provides a compact light-weight power source for model aircraft permitting them to fly for an extended period so that they may be used for such practical purposes as crop dusting, surveying, and photographing. The cell is comprised of a current collector so disposed between a magnesium, zinc, or aluminum alloy cathode and a petroleum graphite anode that it is in contact with the anode. The anode is formed by adding polytetrafluoroethylene dispersion liquid in a mixture of active carbon and graphite powder, pouring the mixture into a mold and heating it to form the anode. It is fabricated by a plurality of anode sections and is formed with at least one hole so that it can provide a cell which is compact in size and light in weight yet is capable of generating a high output.

The anode, the cathode, and a separator are wetted by an electrolytic liquid. The electrolyte is continuously supplied through the life of the cell. CISTI

N93-10405# SRI International Corp., Menlo Park, CA.
FIELD-EMITTER ARRAYS FOR RF VACUUM MICROELECTRONICS Quarterly Report No. 2, 1 Jan. - 31 Mar. 1992
C. A. Spindt and A. Rosengreen Jun. 1992 12 p
(Contract MDA972-91-C-0029; ARPA Order 8162; SRI Proj. 2743)
(AD-A253396) Avail: CASI HC A03/MF A01

SRI International has completed the second quarter of a program to develop field-emitter arrays for vacuum microelectronics. The goals of the effort are 5 mA total current at 5 A/sq. cm for at least 1 hour, and demonstrated modulation of the emission at 1 GHz. Improved vendor deposition of the oxide layer indicated that a cathode achieving 1000 A/cm2 shows very brittle oxide that tends to break up and flake off under the pressure of the contact leads. Low-capacitance cathode fabrication studies were temporarily discontinued after equipment failure. To date, 1000-tip cathodes have been operated with carefully processed, closed-spaced nickel anodes, presently at 15 mA and 22.8 A/cm2, for over 2700 hours. Major effort was directed toward detailed design of the apparatus required for microwave measurements, and on developing technologies for assembling microstrip lines and lead bonding them to SMA coaxial connectors and cathode arrays. GRA

N93-10417# Georgia Inst. of Tech., Atlanta. School of Electrical Engineering.
TWO-DIMENSIONAL SIGNAL PROCESSING, OPTICAL INFORMATION STORAGE AND PROCESSING, AND ELECTROMAGNETIC MEASUREMENTS Annual Report, 1 Jan. - 31 Dec. 1991
R. W. Schafer 15 Jul. 1992 92 p
(Contract DAAL03-90-C-0004)
(AD-A253953) Avail: CASI HC A05/MF A01

This is an annual report on research conducted under the auspices of the Joint Services Electronics Program. Specific topics covered are: multidimensional digital signal processing, signal restoration and detection, morphological systems for multidimensional signal processing, multidimensional processing for sensory arrays, multiprocessor systems and tools for digital signal processing, linear and nonlinear image processing, two-dimensional optical storage and processing, semiconductor quantum wave devices, electromagnetic measurements in the time and frequency domains, and automated radiation measurements for near- and far-field transformations. GRA

N93-10421# General Atomic Co., San Diego, CA.
TWENTY-FIVE KA, 5000V SOLID STATE OPENING SWITCH FOR INDUCTIVE ENERGY STORES Final Report, Apr. 1990 - Apr. 1992
Mark W. Heyse, James B. Cornette, Nolan E. Taconi, E. Bowles, and W. G. Homeyer Jul. 1992 11 p
(Contract F08635-90-C-0241)
(AD-A253968; WL-TP-92-006) Avail: CASI HC A03/MF A01

A self-commutated solid state switch has been developed for use as an opening device for an inductive energy store. A 25 kA, 5000 V operation has been obtained in a compact switch module. The switch topology is a two-stage hybrid consisting of an SCR-FET/SCR-IGBT combination. The switch is designed to charge an inductive energy store and repetitively commutate the current to a dynamic load. A 25 kA switch module has been built and tested on a battery test stand at General Atomics. The theory of operation, circuit topology, and test results are given. GRA

N93-10426# Thin Film Concepts, Inc., Elmsford, NY.
NOVEL Si-YBCuO REACTIVE PATTERNING TECHNIQUE FOR MANUFACTURE OF LARGE AREA HIGH Tc SUPERCONDUCTING ELECTRONIC DEVICES Final Report, 1 Sep. 1991 - 31 Mar. 1992
7 Apr. 1992 23 p
(Contract F49620-91-C-0069)
(AD-A250740; AFOSR-92-0295TR) Avail: CASI HC A03/MF A01

A technique to pattern YBCuO, utilizing rapid thermal annealing to intermix layers such as silicon with the superconductor, was analyzed. Films were prepared using laser ablation and e-beam deposition. Areas that intermixed destroyed the superconductivity and allowed 10 micron lines to be fabricated. The system was evaluated using SEM, Auger, XPS, and x-ray diffraction. Another technique was investigated in which silicon films were deposited and patterned over existing YBCuO films. The silicon was patterned and then annealed to define micron-sized superconducting patterns. This technique is relevant to producing large-area superconducting patterns such as delay lines, microwave devices, and packaging interconnects. GRA

N93-10656# North Carolina Univ., Chapel Hill. Dept. of Chemistry.
SPECTROSCOPIC DIFFERENTIAL REFLECTANCE AS AN ANALYTICAL PROBE FOR MICROELECTRONIC PROCESSING
T. M. Burns, E. A. Irene, S. Chevacharoeukul, and G. E. McGuire 13 Jul. 1992 38 p
(Contract N00014-89-J-1178)
(AD-A253134; TR-47) Avail: CASI HC A03/MF A01

It is important in microelectronics to be able to measure damage and monitor processing during or following the many different processes. To this end, a simple and universal technique is desirable. In this paper, differential reflectance (DR) is examined as a tool for studying several processes including implantation, preamorphization, solid phase epitaxy, and rapid thermal annealing. DR is found to be able to measure small differences between samples, and the amount of damage is qualitatively assessed by the intensity and broadening of the silicon interband transitions. More quantitative information about damage layer thickness can be obtained if interference bands are present. DR results were in good agreement with transmission electron microscope (TEM), findings, and in some cases DR spectra suggested residual damage where TEM found annealing to be complete. Preamorphized samples had different interband transition peak broadening and responded differently to annealing compared to their nonpreamorphized counterparts. Distinctive DR spectra features were also obtained for heavily doped silicon samples, and the features were related to dopant species size. GRA

N93-10663# Florida Univ., Gainesville.
ADVANCED PROCESSING AND CHARACTERIZATION TECHNOLOGIES. FABRICATION AND CHARACTERIZATION OF SEMICONDUCTOR OPTOELECTRONIC DEVICES AND INTEGRATED CIRCUITS. FINAL CONFERENCE PROCEEDINGS NO. 10
Paul H. Holloway Jul. 1992 236 p Presented at the American Vacuum Society Series 10, Clearwater, FL, 8-10 May 1991
(Contract DAAL03-91-G-0142)
(AD-A254162; ARO-28953.1-EL-CF) Avail: CASI HC A11/MF A03

The Topics include: Focused-Ion-Beam Micromachining: A Fabrication Tool for Prototypal Semiconductor Lasers; A Novel Vacuum Lithography with SiN(x) Resist by Focused Ion Beam Exposure and Dry Etching Development; ECR Plasma Etching of III-V Optoelectronic Devices; Influence of SiCl4 Reactive Ion Etching on the Electrical Characteristics of GaAs; Electron-beam Writing System for Holographic Optical Elements; Micro Dry Etching Process for Vertical Cavity Surface Emitting Lasers; Sulfide Treatment on III-V Compound Surfaces; Sulfur Passivation of GaAs Surfaces; Direct Observation of GaAs Surface Cleaning Process Under Hydrogen Radical Beam Irradiation; Near Surface Type Conversion of p-type, Single Crystal InP by Plasma Exposure; Advances in Controlling Electrical Contacts for Optoelectronics; Indium Ohmic Contacts to n-ZnSe; A New Method of Zn Diffusion into InP for Optical Device Fabrication; Open Tube Double Diffusion for the Fabrication of Bipolar Transistor Waveguide Optical Switch; and Full-Water Technology for Laser Fabrication and Testing. GRA

N93-10702# Air Force Inst. of Tech., Wright-Patterson AFB, OH. Foreign Aerospace Science and Technology Center.
STRESS AND STRAIN OF SLAB TYPE AMPLIFIERS
Liming Ding and Fumin Yang 9 Jan. 1992 12 p Transl. into ENGLISH from Zhonggou Jiguang (China), v. 16, no. 11, 1989 p 687-689
(AD-A254246; FASTC-ID(RS)T-1476-90) Avail: CASI HC A03/MF A01

The test production of high repetition rate, high power slab configuration solid state laser devices is, at the present time, both inside China and abroad, a topic which interests scientists. In order to make slab amplifiers capable of supporting high powers and high energies simultaneously, and, in order to reduce double refraction, and improve the luminosity of laser output, the important thing is that there must be research on the status of the stresses and strains produced by laser amplifiers. Besides this, in order to raise slab amplifier anti-explosive capabilities, besides factors associated with laser materials themselves, it is also necessary to find a type of installation method which does not produce stress. In order to do this, we designed four types of installation systems, improving the seal materials as well as the installation methods and obtaining relatively good results. GRA

N93-10715# Illinois Univ., Urbana. Coordinated Science Lab.
VLSI DESIGN FOR RELIABILITY - HOT ELECTRON Final Report, Mar. 1990 - Mar. 1991
Sung-Mo Kang, Yusuf Leblebici, Ping Li, Ibrahim Hajj, and Carlos Diaz May 1992 46 p
(Contract F30602-88-D-0028)
(AD-A253942; RL-TR-92-106) Avail: CASI HC A03/MF A01

This report describes the accomplishments during the contract period (March 27, 1990 to March 26, 1991) on the computer-aided analysis of CMOS device and circuit degradation due to hot-electron effects. The task involved four subtasks: (1) modeling of the gate oxide degradation in n-channel MOS transistor; (2) modeling of n-channel MOS transistor behavior with localized oxide damage; (3) simulation of gate oxide degradation during long-term circuit operation; and (4) determination of overall circuit performance after hot-electron stress. For the modeling of the gate oxide degradation in nMOS transistor, a localized triangular charged density distribution function has been introduced in the drain end of the channel. This model was effective in explaining the local electric potential near the drain, especially on the flatband voltage and also the changes in the local channel electron mobility. To model the behavior of nMOS transistor with local oxide damages, a new one-dimensional I-V equation has been derived and implemented in a generic circuit simulator, iSMILE program. For the modeling of gate oxide degradation process, the rate equations governing the generation of interface states have been implemented for dynamic circuit operating conditions. With these mechanisms implemented, the iSMILE program has been able to simulate the degradation of circuit performances dynamically. For large scale reliability simulation, simpler models have been devised and used in the iDSIM2 program. GRA

N93-10718# Massachusetts Inst. of Tech., Lexington.
COVALENT ELECTRON TRANSFER THEORY OF SUPERCONDUCTIVITY
Gerald F. Dionne 19 Jun. 1992 170 p
(Contract F19628-90-C-0002)
(AD-A253975; MIT-TR-885; ESD-TR-91-092) Avail: CASI HC A08/MF A02

Following a brief review of phenomenological origins, a comprehensive discussion of the physics and chemistry of super-conducting perovskite systems is presented. The covalent transfer theory developed in 1987, which was based on the normal-state electrical behavior of large polarons, is refined to include a molecular-orbital analysis of the electron transfer probability (assumed to be unity in the original model). An examination of the local magnetic superexchange interactions between Cu2-O2-Cu2+ ions indicates that preconditions for the onset of superconduction include a breakdown in static antiferromagnetic order to eliminate the exchange contribution to the polaron trap energy. The occurrence of magnetic frustration is explained by the existence of mobile polaron ions in zero-spin states. By comparing the covalent transfer and electron hopping mechanisms, a new two-fluid function is derived for the temperature-dependent distribution of normal and superelectrons. From the population of carriers that are not thermally activated (hopping), condensation to the superconducting state occurs in the form of dynamic ferroelectric chains of ordered dipoles, with the condensation energy directly proportional to the square of the supercarrier population. With this relation, it is then possible to derive direct expressions between the measurable superconduction parameters and the effective supercarrier density as functions of temperature. Based on these concepts, computed values of critical temperature, magnetic field, and current density, as well as specific heat, penetration depth, coherence length, and microwave surface resistance all compare favorably with measured values, both in magnitude and as functions of temperature. GRA

N93-10731# Brookhaven National Lab., Upton, NY.
A NOVEL CHARGE SENSITIVE PREAMPLIFIER WITHOUT THE FEEDBACK RESISTOR
G. Bertuccio (Politecnico di Milano, Italy), P. Rehak, and D. Xi 1992 20 p Presented at the 6th European Symposium on Semiconductor Detectors, Milano, 24-27 Feb. 1992
(Contract DE-AC02-76CH-00016)
(DE92-015842; BNL-47525; CONF-920299-3) Avail: CASI HC A03/MF A01

A novel charge sensitive preamplifier which has no resistor in parallel with the feedback capacitor is presented. No external device or circuit is required to discharge the feedback capacitor. The detector leakage and signal current flows away through the gate of the first JFET which works with its gate to source junction slightly forward biased. The DC stabilization of the preamplifier is accomplished by an additional feedback loop, which permits to equalize the current flowing through the forward baised gate to source junction and the current coming from the detector. An equivalent noise charge of less than 20 electrons r.m.s. has been measured at room temperature by using an input JFET with a transconductance to gate capacitance ratio of 4 mS/5.4 pF. DOE

N93-10751# Missouri Univ., Saint Louis. Dept. of Physics.
QUANTUM 1/f NOISE IN HIGH TECHNOLOGY APPLICATIONS INCLUDING ULTRASMALL STRUCTURES AND DEVICES Annual Report No. 3, 15 Jun. 1991 - 14 Jun. 1992
Peter H. Handel 14 Jul. 1992 44 p
(Grant AF-AFOSR-0416-89)
(AD-A253922; AFOSR-92-0746TR) Avail: CASI HC A03/MF A01

The practical application of the quantum 1/f effect to quartz resonators and to infrared detectors present in this report allows us for the first time to understand and to extend the stability limits of quartz resonators. It also explains 1/f noise in most semiconductor devices and in infrared detectors considered in this report in the presence of radiation, although 1/f noise has been already successfully pushed below background in PtSi on p-type Si Schottky diodes at RADC-Hanscomb. A fundamental breakthrough was performed through the first direct derivation of the coherent quantum 1/f effect from a special quantum-electrodynamic propagator, and from the author's general sufficient 1/f chaos criterion presented in the previous yearly report. Finally, the quantum 1/f cross-correlations derived by the author have been used to recalculate and to graph the quantum 1/f mobility fluctuations in Si and gallium arsenide samples as a function of temperature and doping, in good agreement with the measurements of Tacano in Japan and Hooge in the Netherlands. GRA

N93-10755# GTE Labs., Inc., Waltham, MA.
SEMICONDUCTOR-METAL EUTECTIC COMPOSITES FOR HIGH POWER SWITCHING Final Report
Q. Nguyen, P. Rossoni, M. Levinson, and B. M. Ditchek 1992

110 p
(Contract N00014-86-C-0595)
(AD-A253930) Avail: CASI HC A06/MF A02

This report reviews the accomplishments of a research program that sought to develop a totally new material for high-power transistor switching. The material, which we have generally referred to as SME for semiconductor-metal eutectic, is a composite with a high density of aligned, micron-sized metallic rods embedded in a matrix of a semiconductor. This material differs dramatically from silicon, the material used to fabricate almost all other conventional high-power transistors. Silicon is a single-phase pure material. Devices are fabricated from this material through the use of thin film techniques to incorporate junctions in the surface which enable switching. The composite material contains internal junctions throughout the bulk of the material. Further, it consists of a two-phase equilibrium structure, which because of concerns for defects in the semiconductor, has never before been demonstrated to be of electronic quality, that is, suitable for the fabrication of high-quality devices like high-voltage transistors. GRA

N93-10785# Johns Hopkins Univ., Laurel, MD. Applied Physics Lab.
A NEW MODEL FOR INTERPRETING EXPERIMENTAL DATA FROM A CIRCULAR WAVEGUIDE CAVITY
William A. Huting 7 Aug. 1992 20 p
(Contract N00039-91-C-6099)
(AD-A254067; JHU/APL-TG-1383) Avail: CASI HC A03/MF A01

Progress is described in the testing of circular TE(01) waveguide using a resonant cavity technique. A new model has been developed for extrapolating insertion loss values from experimental cavity Q data. This model is compared with a previous model, and experiments are described that involve both cavities with mechanically adjustable lengths and cavities with fixed lengths. Data are also presented for waveguide bend cavities. In all cases, the extrapolated traveling wave losses were in good agreement with the theory. GRA

N93-10786# Jet Propulsion Lab., California Inst. of Tech., Pasadena.
ACTIVATED TRANSPORT IN AMTEC ELECTRODES
R. M. Williams, B. Jeffries-Nakamura, M. A. Ryan, M. L. Underwood, D. OConnor, and S. Kikkert 1992 6 p Presented at the 27th Intersociety Energy Conversion Engineering Conference, San Diego, CA, 3-7 Aug. 1992
(Contract DE-AI01-86CE-90237)
(DE92-016810; CONF-920801-8) Avail: CASI HC A02/MF A01

Transport of alkali metal atoms through porous cathodes of alkali metal thermal-to-electric converter (AMTEC) cells is responsible for significant, reducible losses in the electrical performance of these cells. Experimental evidence for activated transport of metal atoms at grain surfaces and boundaries within some AMTEC electrodes has been derived from temperature dependent studies as well as from analysis of the detailed frequency dependence of ac impedance results for other electrodes, including thin, mature molybdenum electrodes which exhibit transport dominated by free molecular flow of sodium gas at low frequencies or dc conditions. Activated surface transport will almost always exist in parallel with free molecular flow transport, and the process of alkali atom adsorption/desorption from the electrode surface will invariably be part of the transport process, and possibly a dominant part in some cases. Little can be learned about the detailed mass transport process from the ac impedance or current voltage curves of an electrode at one set of operating parameters, because the transport process includes a number of important physical parameters that are not all uniquely determined by one experiment. The temperature dependence of the diffusion coefficient of the alkali metal through the electrode in several cases provides an activation energy and pre-exponential, but at least two activated processes may be operative, and the activation parameters should be expected to depend on the alkali metal activity gradient that the electrode experiences. In the case of Pt/W/Mn electrodes operated for 2500 hours, limiting currents varied with electrode thickness, and the activation parameters could be assigned primarily to the surface/grain boundary diffusion process. DOE

N93-10790# California Univ., Berkeley. Lawrence Berkeley Lab.
SIGNAL AND NOISE ANALYSIS OF a-Si:H RADIATION DETECTOR-AMPLIFIER SYSTEM Ph.D. Thesis
Gyuseong Cho Mar. 1992 161 p
(Contract DE-AC03-76SF-00098)
(DE92-016928; LBL-32218) Avail: CASI HC A08/MF A02

Hydrogenated amorphous silicon (a-Si:H) has potential advantages in making radiation detectors because of its deposition capability on a large-area substrate and its high radiation resistance. Position-sensitive radiation detectors can be made out of a 1-d strip or a 2-d pixel array of a Si:H pin diodes. In addition, signal processing electronics can be made by thin-film transistors on the same substrate. The calculated radiation signal, based on a simple charge collection model agreed well with results from various wave length light sources and 1 MeV beta particles on sample diodes. The total noise of the detection system was analyzed into shot noise, 1/f noise from a detector diode, thermal noise, and 1/f noise from the frontend TFT of a charge-sensitive preamplifier. The effective noise charge calculated by convoluting these noise power spectra with the transfer function of a CR-RC shaping amplifier showed a good agreement with the direct measurements of noise charge. The derived equations of signal and noise charge can be used to design an a-Si:H pixel detector amplifier system optimally. Signals from a pixel can be readout using switching TFT's, or diodes. Prototype tests of a double-diode readout scheme showed that the storage time and the readout time are limited by the resistances of the reverse-biased pixel diode and the forward biased switching diodes respectively. A prototype charge-sensitive amplifier was made using poly-Si TFT's to test the feasibility of making pixel-level amplifiers which would be required in small-signal detection. The measured overall gain-bandwidth product was approximately 400 MHz and the noise charge approximately 1000 electrons at a 1 micro-sec shaping time. When the amplifier is connected to a pixel detector of capacitance 0.2 pF, it would give a charge-to-voltage gain of approximately 0.02 mV/electron with a pulse rise time less than 100 nsec and a dynamic range of 48 dB. DOE

N93-10792# RAND Corp., Santa Monica, CA.
A CHANGE OF COURSE: THE IMPORTANCE TO DOD OF INTERNATIONAL STANDARDS FOR ELECTRONIC COMMERCE
Judith E. Payne 1991 78 p
(Contract MDA903-90-C-0004)
(AD-A253199; RAND/R-4088-PL; ISBN-0-8330-1168-5) Avail: CASI HC A05/MF A01

The U.S. Department of Defense (DoD) is committed to using electronic commerce in the future with the over 300,000 vendors interested in doing business with DoD. Electronic commerce will move DoD from a paper-based world to one based on electronic transactions enabled by the exchange of formatted, electronic messages referred to as electronic data interchange (EDI). With electronic commerce, DoD plans to reduce costs, increase effectiveness, and make it easier for vendors to deal with DoD. Benefits from electronic commerce are enhanced when many businesses use the same standards for EDI messages themselves and their transmission. The fewer standards used, the less time and resources must be spent translating messages and agreeing on how to use different standards. To enhance benefits and smooth the transition to electronic commerce for itself and its vendors, DoD has chosen to use the widely accepted American National Standards Institute (ANSI) X12 standards for EDI messages, coupled with international standards for delivering messages and organizing addresses. In the past 18 months, EDI standards sponsored by a United Nations body and serving the same purpose as ANSI X12 message standards have begun to gain wider acceptance internationally. GRA

N93-10829# Harvard Univ., Cambridge, MA. Div. of Applied Sciences.
JOINT SERVICES ELECTRONICS PROGRAM Annual Progress Report No. 106, 1 Aug. 1991 - 31 Jul. 1992
Michael Tinkham Jul. 1992 119 p
(Contract N00014-89-J-1023)
(AD-A253842) Avail: CASI HC A06/MF A02

An annual report of the JSEP (Joint Services Electronics Program) in solid state electronics, quantum electronics, information electronics, control and optimization, and electromagnetic phenomena is presented. Results of the research to date are summarized and significant accomplishments are discussed. GRA

N93-10830 Auburn Univ., AL.
OHMIC CONTACTS TO COMPOUND SEMICONDUCTORS Ph.D. Thesis
John Bernard Crofton 1992 152 p
Avail: Univ. Microfilms Order No. DA9225351

Ohmic contacts to compound semiconductors were studied both theoretically and experimentally. The specific contact resistance of an n-type GaAs ohmic contact was calculated using an improved method to compute the electron tunneling probability through the Schottky barrier. Techniques to experimentally measure the specific contact resistance are discussed. The linear and circular transmission line methods were studied and were found to exhibit a geometry dependent specific contact and modified sheet resistance. Appropriate geometries are presented to minimize this effect. Experimental studies of ohmic contacts to 6H-SiC are presented. The alloys TiW and NiCr are found to produce ohmic contacts to n-type 6H-SiC while Al is found to produce an ohmic contact to p-type 6H-SiC. Characterization of SiC ohmic contacts included specific contact resistance measurements, barrier height measurements using C-V techniques, and RBS and Auger analysis. Dissert. Abstr.

N93-10831# Argonne National Lab., IL.
ASSESSMENT STUDY OF SUPERCONDUCTING FAULT-CURRENT LIMITERS OPERATING AT 77 K
R. F. Giese and M. Runde (Electric Power Research Inst., Trondheim, Norway) 1992 13 p Presented at the Summer Power Meeting of the Institute of Electrical and Electronic Engineers (IEEE) Power Engineering Society (PES), Seattle, WA, 12-16 Jul. 1992
(Contract W-31-109-eng-38)
(DE92-015273; ANL/CP-75500; CONF-920713-1) Avail: CASI HC A03/MF A01

The possible impact of nitrogen-cooled superconductors on the design and cost of superconducting fault-current limiters is assessed by considering the technical specifications such devices must meet and by comparing material properties of 77 K and 4 K superconductors. The main advantage of operating superconductors at 77 K is that the refrigeration operating cost is reduced by a factor of up to 25, and the refrigeration capital cost is reduced by a factor of up to 10. The heat capacity of 77 K is several orders of magnitude larger than at 4 K. This phenomenon increases conductor stability against flux jumps but makes switching from the superconducting to normal state slow and difficult. Consequently, a high critical current density, probably at least 10(exp 5) A/sq cm, is required. DOE

N93-10836# Sandia National Labs., Albuquerque, NM.
THERMAL MANAGEMENT IN HIGH AVERAGE POWER PULSED COMPRESSION SYSTEMS
R. W. Wavrik, K. W. Reed, H. C. Harjes, G. J. Weber, M. Butler, K. J. Penn, and E. L. Neau 1992 4 p Presented at the 20th International Power Modulator Symposium, Myrtle Beach, SC, 23-25 Jun. 1992
(Contract DE-AC04-76DP-00789)
(DE92-017055; SAND-92-0372C; CONF-920671-5) Avail: CASI HC A01/MF A01

High average power repetitively pulsed compression systems offer a potential source of electron beams which may be applied to sterilization of wastes, treatment of food products, and other environmental and consumer applications. At Sandia National Laboratory, the Repetitive High Energy Pulsed Power (RHEPP) program is developing a 7 stage magnetic pulse compressor driving a linear induction voltage adder with an electron beam diode load. The RHEPP machine is designed to deliver 350 kW of average power to the diode in 60 ns FWHM, 2.5 MV, 3 kJ pulses at a repetition rate of 120 Hz. In addition to the electrical design considerations, the repetition rate requires thermal management of the electrical losses. Steady state temperatures must be kept below the material degradation temperatures to maximize reliability and component life. The optimum design is a trade off between thermal management, maximizing overall electrical performance of the system, reliability, and cost effectiveness. Cooling requirements and configurations were developed for each of the subsystems of RHEPP. Finite element models that combine fluid flow and heat transfer were used to screen design concepts. The analysis includes one, two, and three dimensional heat transfer using surface heat transfer coefficients and boundary layer models. Experiments were conducted to verify the models as well as to evaluate cooling channel fabrication materials and techniques in Metglas wound cores. DOE

N93-10882# Varian Associates, Palo Alto, CA. Microwave Power Tube Products.
EXTENDED-INTERACTION KLYSTRON FOR THE AN/TPS-43-E RADAR SYSTEM Final Report, Sep. 1983 - Aug. 1991
Jun. 1992 41 p
(Contract F30602-83-C-0161)
(AD-A253166; F1776; RL-TR-92-183) Avail: CASI HC A03/MF A01

This effort was directed at developing and demonstrating a form, fit, and functional extended-interaction klystron replacement for the VA-145E Twystron in the AN/TPS-43E radar system. A suitable extended-interaction output circuit had already been demonstrated under Contract F30602-78-C-0029. A total of three tubes were built and tested under this program. All performed to full specifications when tested under normal factory test conditions. However, none of the three tubes performed satisfactorily in a simulated AN/TPS-43-E system (a Westinghouse TPS-3 system). Unstable tube operation was caused by the rotary joint, which has a severe mismatch near the operating frequency band. After this condition was discovered with tube S/N 001, tubes S/N 002 and S/N 003 were built in an attempt to overcome this near-short-circuit condition by reducing the output resonator impedence near the problem frequencies. This solution was only partially successful. These later tubes operated satisfactorily at some orientations of the rotary joint but would become unstable at the worst mismatch points. The task of designing a special tube that would include novel features for overcoming the severe system mismatch problem was determined to be outside the scope of this contract and this effort was concluded. GRA

N93-10888# Westinghouse Science and Technology Center, Pittsburgh, PA.
IMPROVED GALLIUM NITRIDE AND ALUMINUM NITRIDE ELECTRONIC MATERIALS Annual Report, 20 Feb. 1991 - 19 Feb. 1992
W. D. Partlow, W. J. Choyke, R. P. Devaty, John T. Yates, Jr., and Karl-Heinz Bornschauer 20 Apr. 1992 44 p
(Contract F49620-91-C-0032)
(AD-A253785; WGD-12523-CE; AFOSR-92-0720TR) Avail: CASI HC A03/MF A01

This report describes the progress in the first year of a three-year program to improve the quality of gallium and aluminum nitride electronic materials. In this period, the experimental apparatus for the ultrahigh vacuum characterization of nitride growth processes was upgraded to increase the capability for experimental control and characterization of growth surfaces. These improvements include the addition of a cooled atomic hydrogen source and a reverse view LEED apparatus. Vibrational studies of the methyl radical on Si(100) surfaces were completed, increasing the understanding of the kinetics and stability of this radical, important

for understanding growth from alkyl precursors. Cathodoluminescence and infrared reflectometry measurements were performed on numerous samples of epitaxial aluminum nitride to build up a base for materials quality determination. GRA

N93-10897# Naval Ocean Systems Center, San Diego, CA.
PROTOTYPE SUPERCONDUCTING PLANAR TRANSFORMERS USING HIGH-Tc THIN AND THICK FILMS Final Report, Sep. 1988 - Oct. 1991
W. C. McGinnis, J. S Briggs, T. E. Jones, and L. J. Johnson Jan. 1992 45 p
(AD-A254230; NOSC/TR-1479) Avail: CASI HC A03/MF A01

This report describes a prototype on-chip electrical transformer that was developed using high-transition-temperature superconducting films. Two approaches for making high-T films were pursued: melt-processing of thick films and sputter deposition of thin films. It is concluded that further optimization of production procedures (particularly for YBa2CU3O7 thin films) will lead to films with much higher critical currents. Practical microelectronic transformers and other inductive devices will require such high-quality films as well as the ability to deposit multiple superconducting and insulating layers. GRA

N93-10589*# Boeing Aerospace Co., Seattle, WA.
RESULTS FROM THE TESTING AND ANALYSIS OF LDEF BATTERIES
Steve Spear, Harry Dursch, and Chris Johnson *In* NASA. Langley Research Center, LDEF Materials Workshop 1991, Part 2 Sep. 1992 p 619-631 (For primary document see N93-10578 01-27)
Avail: CASI HC A03/MF A03

34 FLUID MECHANICS AND HEAT TRANSFER

Includes boundary layers; hydrodynamics; fluidics; mass transfer; and ablation cooling.

For related information see also *02 Aerodynamics* and *77 Thermodynamics and Statistical Physics.*

N93-10050# Von Karman Inst. for Fluid Dynamics, Rhode-Saint-Genese (Belgium).
RADIAL TURBINES
1992 495 p Lecture series held in Rhode-Saint-Genese, Belgium, 6-10 Apr. 1992
(VKI-LS-1992-05; ETN-92-92166) Copyright Avail: CASI HC A21/MF A04

The basic theory of radial turbines, the choice of appropriate nondimensional parameters for design selection and performance assessment, basic design concepts, and performance correlations and predictions, are reviewed. Advanced turbine design requires the extensive use of computational methods. Inviscid and viscous flow analysis methods were reviewed and the trade off between various levels of complexity from stream line curvature analysis to three dimensional viscous time marching techniques was demonstrated. Inverse design methods were discussed and their effectiveness was illustrated by comparison with experimental results. Radial turbines are designed on the basis of steady state flow assumptions even when operated in unsteady conditions as is the case of turbocharger turbines. Measurement techniques for both steady and unsteady flow operation were described. For individual titles, see N93-10051 through N93-10062.

N93-10051# Imperial Coll. of Science and Technology, London (England). Dept. of Mechanical Engineering.
INTRODUCTION TO RADIAL TURBINE TECHNOLOGY
N. C. Baines *In* VKI, Radial Turbines 1992 30 p (For primary document see N93-10050 01-34)
Copyright Avail: CASI HC A03/MF A04

An introduction to radial turbine stage technology, where the radial stage is differentiated from an axial stage by having the fluid undergo a significant radius stage in passing through the rotor, is presented. Reasons for selecting a radial turbine are outlined. A basic analysis of a stage is given. Radial turbine efficiency and incidence, friction, passage, tip clearance, and windage losses are described. The volute, nozzle, and related flows are described. ESA

N93-10052# Imperial Coll. of Science and Technology, London (England). Dept. of Mechanical Engineering.
PERFORMANCE PARAMETERS AND ASSESSMENT
N. C. Baines and H. Chen *In* VKI, Radial Turbines 1992 32 p (For primary document see N93-10050 01-34)
Copyright Avail: CASI HC A03/MF A04

Some of the basic performance parameters for radial turbines, and the influence which the overall turbine design has on them, are considered. Particular attention is paid to the concept of stage loading, which is a somewhat neglected parameter in radial turbine design. Having established the loading coefficient definition, it is possible to use test data from a range of turbines to fix preliminary values. On this basis a simple one dimensional optimization procedure is derived which uses a minimum of empirical input. ESA

N93-10053# Bath Univ. (England).
NON-DIMENSIONAL CONCEPTUAL DESIGN OF RADIAL INFLOW TURBINES. PART A: APPLICATION OF FUNDAMENTAL FLUID MECHANICS
A. Whitfield *In* VKI, Radial Turbines 1992 33 p (For primary document see N93-10050 01-34)
Copyright Avail: CASI HC A03/MF A04

A nondimensional design procedure is developed to provide the overall dimensions, including the leading and trailing edge blade angles, of a radial inflow turbine rotor. The procedure includes consideration of the adoption of nonradial blades at the rotor inlet. The design procedure initially assumes a good order of magnitude efficiency for the turbine stage for subsequent assessment through the application of empirical loss correlations in order to predict the efficiency. ESA

N93-10054# Bath Univ. (England).
NON-DIMENSIONAL CONCEPTUAL DESIGN OF RADIAL INFLOW TURBINES. PART B: APPLICATION OF EMPIRICAL CORRELATIONS
A. Whitfield *In* VKI, Radial Turbines 1992 10 p (For primary document see N93-10050 01-34)
Copyright Avail: CASI HC A02/MF A04

Empirical loss models and correlations are considered in order to derive the rotor efficiency and optimize the nondimensional design developed to provide the overall dimensions, including the leading and trailing edge blade angles, of a radial inflow turbine rotor. The design procedure included consideration of the adoption of nonradial blades at rotor inlet. ESA

N93-10055# University Coll., London (England). Dept. of Mechanical Engineering.
NUMERICAL METHODS FOR INVISCID AND VISCOUS FLOW ANALYSIS
M. Zangeneh *In* VKI, Radial Turbines 1992 33 p (For primary document see N93-10050 01-34)
Copyright Avail: CASI HC A03/MF A04

A review of some of the available flow analysis methods and their application to radial inflow turbines is presented. Because of the nature of the problem and the different types of approximations for it, there are a large number of available methods for analysis of flow through turbomachinery vanes and blades. The basic approaches used for the solution of the flow analysis problem are outlined. One or two methods are cited as examples of how these approaches are implemented in computer programs. The axisymmetric methods, which offer the most approximate (and computationally efficient) approach to the flow analysis problem, are considered. Quasi-three-dimensional inviscid and viscous methods are reviewed. Developments in analyzing the three-dimensional viscous flow through multistage turbomachinery

are discussed. Particular emphasis is placed on the limitations of the methods, their accuracy and efficiency, as well as their applicability to different stages of the design process. ESA

N93-10056# Holset Engineering Co., Turnbridge (England).
AERODYNAMIC INVESTIGATION OF RADIAL TURBINES USING COMPUTATIONAL METHODS
S. T. Kitson *In* VKI, Radial Turbines 1992 45 p (For primary document see N93-10050 01-34)
Copyright Avail: CASI HC A03/MF A04

A demonstration of how computational methods can be used to enable a designer to understand the flow phenomenon which takes place inside the machine is presented. Unfortunately the complicated three dimensional viscous programs take a prohibitive length of time to be used for every design iteration. Simpler, less CPU (Central Processor Unit) intensive programs, will continue to be used for some time in design. Therefore in order to assess the tradeoff between various levels of complexity of computational methods an interesting turbine flow is studied. The methods investigated are a simple streamline curvature analysis, a potential flow solver, an Euler code, and a three dimensional time marching viscous technique. In a time and computer limited design environment it is hoped to provide a guide on how to obtain the most CPU effective use of the range of computational methods available. The radial inflow turbine used was analyzed at 2.1:1 expansion ratio with an inlet prerotation set at 15.88 sq m/s. This results in an average of -33 deg of incidence onto the leading edge. ESA

N93-10057# University Coll., London (England). Dept. of Mechanical Engineering.
AN INVERSE DESIGN METHOD FOR RADIAL TURBOMACHINES
M. Zangeneh *In* VKI, Radial Turbines 1992 47 p (For primary document see N93-10050 01-34)
Copyright Avail: CASI HC A03/MF A04

The calculation of compressible flow by computing the velocities and density throughout the three dimensional flow field is described. A second, approximate approach to solve the compressible flow problem is presented. In this approach the variation of density in the pitchwise direction is neglected and an approximate form of the continuity equation is used. In order to evaluate the method experimentally and assess the practical feasibility of the application of three dimensional blade geometries, a high speed small diameter radial inflow turbine was designed. The performance of this turbine is compared with that of three baseline impellers. The method is validated numerically by computing the flow through the designed impeller using inviscid and viscous flow analysis methods. ESA

N93-10058# Ulstein Turbine A/S, Kongsberg (Norway).
THE INTEGRATION OF GEOMETRIC MODELING INTO AN INVERSE DESIGN METHOD AND APPLICATION OF A PC-BASED INVERSE DESIGN METHOD AND COMPARISON WITH TEST RESULTS
Ivar Helge Skoe *In* VKI, Radial Turbines 1992 87 p (For primary document see N93-10050 01-34)
Copyright Avail: CASI HC A05/MF A04

An 'engineering' approach to the inverse design problem where both aerodynamic and mechanical criteria are imposed is described. A novel exducer configuration, with slanted trailing edge, evolves during the iterative design procedure based on the introduction of the following: a realistic loss distribution; a prescribed rotor exit spanwise total pressure distribution; and with the imposed geometric restrictions. For a gas generator turbine, 'back to back' traverse results show reduced loss for the novel design as compared with a conventionally designed radial inflow turbine. Through extensive use of Bezier curves for the aerodynamically defined three dimensional geometry, the same 'solid model' is used to prepare the input files for the structural analysis ('meshing' for the finite element method) as well as the geometry definition for production. ESA

N93-10059# Imperial Coll. of Science and Technology, London (England). Dept. of Mechanical Engineering.
PARTIAL ADMISSION AND UNSTEADY FLOW IN RADIAL TURBINES
N. C. Baines *In* VKI, Radial Turbines 1992 31 p (For primary document see N93-10050 01-34)
Copyright Avail: CASI HC A03/MF A04

The twin problems of partial admission (with stator nozzles and with vaneless stator) and unsteady flow in radial turbines are discussed. The performance of radial turbines is concluded to be significantly influenced by partial admisssion inlet conditions. Turbines with vaned nozzles are suitable for circumferentially divided housings, but suffer significant end of sector and windage losses under partial admission. Housings with a meridional division are more approximate to nozzleless turbines, and the major influence is the interaction between the two streams as they mix upstream of the nozzle. Experiments have shown that the point of maximum efficiency occurs, not at equal admission, but when the flow is biased towards the shroud side of the turbine. It is believed that this is connected with a strong secondary vortex in the rotor passage near the leading edge, which such a biased inlet flow can help to counter. When the inlet flow is unsteady, but varying at relatively low frequency, the turbine rotor behaves in a quasi steady manner and the working fluid remains in dynamic equilibrium. However, if the turbine housing has significant volume, this acts as a reservoir which introduces a time delay into the system, and makes the unsteady performance of the turbine depart from the steady flow by as much as 10 to 15 percent efficiency. ESA

N93-10060# Imperial Coll. of Science and Technology, London (England). Dept. of Mechanical Engineering.
TESTING TECHNIQUES
N. C. Baines *In* VKI, Radial Turbines 1992 31 p (For primary document see N93-10050 01-34)
Copyright Avail: CASI HC A03/MF A04

A survey of some of the testing techniques used for radial turbines, including the test rig arrangements, instrumentation, and data reduction methods available, is presented. The increasingly important subject of unsteady flow performance is addressed and some of the techniques developed to measure performance and unsteady flows are highlighted. ESA

N93-10061*# National Aeronautics and Space Administration. Lewis Research Center, Cleveland, OH.
RADIAL TURBINE COOLING
Richard J. Roelke *In* VKI, Radial Turbines 1992 38 p (For primary document see N93-10050 01-34)
Copyright Avail: CASI HC A03/MF A04

The technology of high temperature cooled radial turbines is reviewed. Aerodynamic performance considerations are described. Heat transfer and structural analysis are addressed, and in doing so the following topics are covered: cooling considerations, hot side convection, coolant side convection, and rotor mechanical analysis. Cooled rotor concepts and fabrication are described, and the following are covered in this context: internally cooled rotor, hot isostatic pressure bonded rotor, laminated rotor, split blade rotor, and the NASA radial turbine program. ESA

N93-10062# Dresser Industries, Inc., Liberty Corner, NJ.
STRUCTURAL ANALYSIS: FATIGUE LIFE ASSESSMENT **c39**
William D. Marscher *In* VKI, Radial Turbines 1992 73 p (For primary document see N93-10050 01-34)
Copyright Avail: CASI HC A04/MF A04

Lectures on the structural analysis of turbomachinery covering fatigue life assessment, stresses due to centrifugal, pressure, and thermal loads, and blade disc vibration and rotor dynamics, are presented. Concepts and techniques, modeling methods, and structural design evaluation and optimization are desribed. ESA

N93-10087*# National Aeronautics and Space Administration. Lewis Research Center, Cleveland, OH.
EVALUATION AND APPLICATION OF THE BALDWIN-LOMAX TURBULENCE MODEL IN TWO-DIMENSIONAL, UNSTEADY, COMPRESSIBLE BOUNDARY LAYERS WITH AND WITHOUT SEPARATION IN ENGINE INLETS
Barbara Sakowski, Douglas Darling, Robert L. Roach (Georgia Inst. of Tech., Atlanta.), and Allan vandeWall (Case Western Reserve Univ., Cleveland, OH.) 1992 11 p Presented at the 28th Joint Propulsion Conference and Exhibit, Nashville, TN, 6-8 Jul. 1992; cosponsored by AIAA, SAE, ASME, and ASEE
(RTOP 505-62-20)
(NASA-TM-105810; E-7241; NAS 1.15:105810) Avail: CASI HC A03/MF A01

There is a practical need to model high speed flows that exist in jet engine inlets. The boundary layers that form in these inlets may be turbulent or laminar and either separated or attached. Also, unsteady supersonic inlets may be subject to frequent changes in operating conditions. Some changes in the operating conditions of the inlets may include varying the inlet geometry, bleeds and bypasses, and rotating or translating the centerbody. In addition, the inlet may be either started or unstarted. Therefore, a CFD code, used to model these inlets, may have to run for several different cases. Also, since the flow conditions through an unsteady inlet may be continually fluctuating, the CFD code which models these flows may have to be run over many time steps. Therefore, it would be beneficial that the code run quickly. Many turbulence models, however, are cumbersome to implement and require a lot of computer time to run, since they add to the number of differential equations to be solved to model a flow. The Baldwin-Lomax turbulence model is a popular model. It is an algebraic, eddy viscosity model. The Baldwin-Lomax model is used in many CFD codes because it is quick and easy to implement. In this paper, we will discuss implementing the Baldwin-Lomax turbulence model for both steady and unsteady compressible flows. In addition, these flows may be either separated or attached. In order to apply this turbulence model to flows which may be subjected to these conditions, certain modifications should be made to the original Baldwin-Lomax model. We will discuss these modifications and determine whether the Baldwin-Lomax model is a viable turbulence model that produces reasonably accurate results for high speed flows that can be found in engine inlets.
Author

N93-10094# Princeton Univ., NJ. Dept. of Mathematics.
MATHEMATICAL ANALYSIS OF STRONG FLUID MECHANICAL EFFECTS AT HIGH MACH NUMBER IN REACTIVE AND NONREACTIVE FLOW Final Report, 1 Jan. 1989 - 31 Mar. 1992
Andrew J. Majda 12 May 1992 4 p
(Contract DAAL03-89-K-0013)
(AD-A253617; ARO-26113.19-MS) Avail: CASI HC A01/MF A01

The following topics have been studied during this three year period: transition to instability for unstable one-dimensional detonations; development of the first asymptotic model to incorporate the self-stretching of vortex filaments in high Reynolds number fluid flows; and development of the first rigorous model with exact renormalization for turbulent transport. GRA

N93-10220# Wisconsin Univ., Madison.
FINITE DIFFERENCE METHODS FOR INCOMPRESSIBLE VISCOUS FLOW IN SCIENTIFIC COMPUTING Final Report, 15 Mar. 1991 - 14 Apr. 1992
John C. Strikwerda Jun. 1992 4 p
(Contract DAAL03-91-G-0094)
(AD-A253512; ARO-28025.4-MA) Avail: CASI HC A01/MF A01

Research centered around three topics in computational fluid dynamics is presented. The topics are as follows: (1) schemes for the time-dependent Navier-Stokes equations; (2) improved methods for the steady Navier-Stokes equations; and (3) domain decomposition methods. The progress that was made on these topics was significant. GRA

N93-10232# Georgia Inst. of Tech., Atlanta. School of Mechanical Engineering.
COMPUTATIONAL STUDIES OF VORTEX BREAKDOWN Final Report, 1 Nov. 1990 - 30 Nov. 1991
G. P. Neitzel and John P. Watson 5 Jun. 1992 26 p
(Grant AF-AFOSR-0047-91)
(AD-A253759; AFOSR-92-0758TR) Avail: CASI HC A03/MF A01

Axisymmetric vortex breakdown was simulated numericaliy within an enclosed circular cylinder with: (1) fixed cylindrical wall-endwall and one rotating lid; and (2) rotating cylindrical wall-endwall with a differentially rotating lid. Variations of the two dynamical parameters permitted the calculation of cases in which incipient vortex breakdown was observed. A vortex breakdown criterion recently proposed by Brown and Lopez was tested against these numerical solutions. GRA

N93-10297# Rockwell International Corp., Thousand Oaks, CA. Science Center.
COMPUTATIONAL FLUID DYNAMICS CAPABILITY FOR INTERNALLY CARRIED STORE SEPARATION Final Report, 26 Sep. 1990 - 26 Sep. 1991
Sukumar R. Chakravarthy and Kuo-Yen Szema Dec. 1991 188 p
(Contract N60530-90-C-0393)
(AD-A253671; SC-71039-TR; NWC-TP-7207) Avail: CASI HC A09/MF A02

The ability to predict safe and effective release of air-launched weapons carried internally in a weapon bay or externally on a pylon/rack is required by the Safety Committee before approval is given for a flight test to validate various store separation characteristics. Because of the novel conditions attendant to test and evaluation (T and E) testing, only limited experimental and flight data are available beforehand to aid in assessing safe weapon release. Computational methods have the potential of resolving, in a timely manner, the store separation problem without these weaknesses. Two areas need to be addressed. First, an accurate computational algorithm is needed to minimize numerical uncertainty as the store is tracked in time. Second, correct physical models must be implemented to model the moving store, including grid capability to provide accurate numerical flow-field predictions for situation of weapon carriage and release from an internal weapons bay. Based on a truly multidimensional unrestricted Essentially Non-Oscillatory (ENO) scheme, a new UNIVERSE (Unification of essentially Non-oscillatory Interpolation techniques with a geometrically VERSatilE) series code was developed at the Rockwell International Science Center. The new ENO concepts are state-of-the-art interpolation schemes that work with arbitrary cell shapes. For example, hexahedral, triangular prism, and tetrahedral elements (conservation cells) can all be covered in a unified manner. this also implies that both structured and unstructured bookkeeping schemes can be employed to conveniently treat complex topologies. A new suite of fully automatic flexible-cell mesh generation methods is also being developed for integration with the new series. GRA

N93-10304 Old Dominion Univ., Norfolk, VA.
EFFECT OF PASSIVE FLOW-CONTROL DEVICES ON TURBULENT LOW-SPEED BASE FLOW Ph.D. Thesis
Farid Heidari-Miandoab 1991 174 p
Avail: Univ. Microfilms Order No. DA9130677

Some configurations of blunt trailing-edge airfoils are known to have a lower pressure drag compared to sharp trailing-edge airfoils. However, this advantage in addition to the structural advantage of a thick trailing-edge airfoil is offset by its high base drag. At subsonic velocities, this is attributed to the low-pressure base flow dominated by a Karman vortex street. In the limiting case, the steady separated flow over a rearward-facing step is attained if the periodically shed vortices from a blunt trailing-edge are suppressed by the addition of a base spiltter-plate. Experimental

studies in the Old Dominion University Low-Speed Closed-Circuit Wind Tunnel were conducted to examine the effect of several passive flow-control devices such as Wheeler doublets and wishbone vortex generators, longitudinal surface grooves, base cavities, and serrations on the characteristics of two- and three-dimensional base flows. Flow over flat-plate airfoil and rearward-facing step models was studied in the turbulent incompressible subsonic flow regime. Models with trailing-edge and step-sweep angles of 0, 30, and 45 degrees with respect to the crossflow direction were considered. Constant-temperature hot-wire anemometry, infrared surface thermography, and pitot-static probes were used to conduct flow measurements. The parameters measured included vortex shedding frequency, convective heat-transfer rates, base pressure, and flow reattachment distance. Surveys of mean velocity profiles in the wake were also conducted. Results have shown that most of the flow control devices tested increased the base pressure of the 2-D and 3-D flat-plate airfoils. Use of longitudinal surface grooves resulted in shorter flow reattachment distances and higher convective heat transfer rates downstream of the 2-D rearward-facing steps. Dissert. Abstr.

N93-10305 Colorado Univ., Boulder.
FORCED UNSTEADY SEPARATED FLOWS ON A 45 DEGREE DELTA WING Ph.D. Thesis
Stephen Albert Huyer 1991 192 p
Avail: Univ. Microfilms Order No. DA9132575

A great deal of current research activities has focused on possible exploitation of forced unsteady separated flows to provide enhanced lift and maneuvering characteristics. The formal and intentional utilization of these flows is currently being manifested in the form of the Advanced Tactical Fighter. The wing planform geometry of the ATF and other fighter aircraft is a delta wing. Under steady conditions, leading edge vortices are formed on each side of a delta wing. These vortices are mostly responsible for the attainment of lift to high angles of attack. Unsteady motion histories will likely alter the characteristics of this vortex as well as its development history. This will then present new difficulties in terms of lift enhancement and control. In order to successfully predict and optimally exploit the flight regimes offered by the ATF, greater understanding of the underlying physical mechanisms responsible for these unsteady flow fields must be obtained. The vortex dominated flow fields produced by an oscillating 45 degree delta wing were examined across a wide range of unsteady motion histories. Still and high speed video photography were employed to document the flow development processes and cortex kinematics. Force balance data recorded the unsteady aerodynamic loading produced. These methods allowed for a thorough qualitative and quantitative examination of the flow fields elicited by a pitching delta wing. The wide range of motion histories employed were found to have a tremendous impact in terms of flow development lift enhancement, drag reduction, and overall aerodynamic performance. Integrations of the data permitted speculation regarding the underlying physical mechanisms responsible for the observed phenomena. Experimental evidence allowed for hypotheses regarding the physical mechanisms of vorticity production, accumulation, convection, and diffusion. Dissert. Abstr.

N93-10309 California Univ., Davis.
IMPROVED NUMERICAL SIMULATION OF EULER EQUATIONS Ph.D. Thesis
David Brucker 1991 161 p
Avail: Univ. Microfilms Order No. DA9125083

Numerical simulation of nonlinear partial differential equations has been viewed as a process by which a discrete solution is sought which satisfies the conservation laws on the discrete level, without requiring that higher order properties of the differential equation are conserved by the discrete system. For example when the two dimensional incompressible Euler equations in conservation form are solved, the discrete solution conserves mass and momentum, but not necessarily vorticity. Standard methods can lead to substantial errors as in the case of a flow over a blunt symmetric body at angle of attack where numerical solution of Euler equations results in substantial lift. In this thesis it is shown that a new algorithm designed to conserve higher order properties, can overcome these shortcomings. The algorithm has been tested for both incompressible and subsonic flows. For irrotational flow, the lift and drag calculated for cylinders and ellipses at angle of attack are zero. Results obtained by this method are superior to any other results available so far. Further study is required to extend the algorithm to three dimensional flows and complex geometries. Dissert. Abstr.

N93-10330# Pittsburgh Energy Technology Center, PA.
TURBULENCE MODELING OF THE FLOW FIELD IN COMBUSTORS USING THE NON-LINEAR k-EPSILON MODEL
C. C. Hwang (Pittsburgh Univ., PA.), G. Zhu (Pittsburgh Univ., PA.), M. Massoudi, and J. M. Ekmann May 1992 26 p
(DE92-014745; DOE/PETC-TR/92/7) Avail: CASI HC A03/MF A01

In swirling turbulent flows, the structure of turbulence is non-homogeneous and anisotropic and it was observed that the assumptions leading to the formulation of the k-(epsilon) model, which is used very often in many engineering applications, are inadequate for highly swirling flows. Furthermore, even with the various modifications made to the k-(epsilon) model, it is still not capable of describing secondary flows in non-circular ducts and it cannot predict non-zero normal-Reynolds-stress differences. Recently a non-linear k-(epsilon) model was developed, which extends the range of validity of the standard k-(epsilon) model while maintaining most of the interesting features of the k-(epsilon) model; for example, the ease of application in existing Computational Fluid Dynamics (CFD) codes. In this work, we will use the non-linear k-(epsilon) closure to model the turbulence in combustors. The particular combustor geometry selected for this study are as follows: (1) the flow in a round pipe entering an expansion into another round pipe; and (2) the flow in two confined co-axial swirling jets. DOE

N93-10369 Iowa Univ., Iowa City.
DEVELOPMENT OF THE FINITE ANALYTIC METHOD FOR TURBULENT FORCED AND FREE CONVECTION Ph.D. Thesis
Richard Allen Bernatz 1991 249 p
Avail: Univ. Microfilms Order No. DA9136900

The finite analytic (FA) method is used to solve turbulent forced and free convective flows. The governing partial differential equations are the primitive variable, ensemble averaged Navier-Stokes and energy equations for two dimensional, incompressible, and constant property fluids. Turbulent characteristics of the flow are simulated using the k-epsilon - Eddy turbulence model. Solutions are found on non-staggered grids using the momentum weighted interpolation method (MWIM). The turbulent flow near solid walls is modeled using a wall function. The square cavity laminar flow problem is solved for Reynolds (Re) numbers of 10(exp 2) and 10(exp 3) to verify the accuracy of the solution procedure incorporating the FA method and MWIM. Model results for both the velocity and thermal fields are consistent with previous experimental and numerical results. Turbulent flow within the square cavity is solved for Re = 200,000, extending the MWIM to turbulent flow problems for the first time. Results for the mean velocity field, and the turbulent fluctuations of the mean velocity field, compare favorably with experimental results. The thermal field predictions for this problem represent new findings for the high Reynolds number square cavity flow. The turbulent, free convective sea breeze flow is solved for a 24 hour heating and cooling cycle using the FA method and MWIM. The model predicts a spatial structure and magnitude for the mean circulation that is in agreement with experimental studies. In terms of turbulent quantities, the model results compare favorably with experimental findings that show the magnitudes of mean velocities and their turbulent fluctuations to be of the same order. Also, the model predicts the rate of turbulent kinetic energy dissipation to be on the order of 100 sq cm/cu sec, which is consistent with experimental measurements. The dynamics of the advancing sea breeze front is correctly simulated by the k-epsilon - Eddy turbulence model as its rate of inland penetration quickens as the land surface begins to cool in the late afternoon. Dissert. Abstr.

N93-10370 Pennsylvania State Univ., University Park.
EXPLICIT NAVIER-STOKES COMPUTATION OF TURBOMACHINERY FLOWS Ph.D. Thesis
Robert Francis Kunz 1991 252 p
Avail: Univ. Microfilms Order No. DA9204236

A new three-dimensional explicit Navier-Stokes procedure has been developed for computation of turbulent turbomachinery flows. Numerical strategies and modelling techniques have been developed and incorporated which enable convergent and accurate predictions of high Reynolds number flowfields across a wide range of Mach numbers. These include incorporation of a compressible low Reynolds number form of the k-epsilon turbulence model in a fully explicit fashion, appropriate stability bound treatment of the transport turbulence model and other physical and solution parameters, eigenvalue and local velocity artificial dissipation scalings, a compact flux evaluation procedure and a hybrid low Reynolds number k-epsilon/algebriac Reynolds stress model. Detailed stability and order of magnitude analyses are performed on the discrete system of seven governing equations. The results of these analyses and corroborative numerical experiments are provided. Conclusions are drawn concerning the influence of system rotation and turbulence transport source terms, grid clustering, effective diffusivity, artificial dissipation, convective acceleration terms, implicit source term treatment and the coupling of the discrete mean flow equation system to the turbulence model equations on the stability of the numerical scheme. Alternative local velocity and flux Jacobian eigenvalue scalings are provided for the dissipation operators. A hybrid k-epsilon/algebraic Reynolds stress model (ARSM) was developed. Two-dimensional results are provided for a supersonic compressor cascade operating at unique incidence condition and a low-subsonic double circular arc compressor cascade. Three-dimensional validation is provided by the results of an incompressible curved duct flow computation. A high Reynolds number axial rotor flow, for which extensive experimental data are also available, was computed. A backswept transonic centrifugal compressor flow, for which L2F meridional passage velocity measurements are available, was computed. Full Navier-Stokes solutions are presented which are shown to capture detailed viscous dominated flow features, including tip clearance and curvature induced and rotation induced secondary motions, with good accuracy. Results of impeller flowfield calculations using the hybrid model with and without the influence of system rotation are also provided and interpreted. Dissert. Abstr.

N93-10371 Case Western Reserve Univ., Cleveland, OH.
THE STRUCTURE AND DEVELOPMENT OF STREAMWISE VORTEX ARRAYS EMBEDDED IN A TURBULENT BOUNDARY LAYER Ph.D. Thesis
Bruce James Wendt 1991 330 p
Avail: Univ. Microfilms Order No. DA9202260

An investigation of the structure and development of streamwise vortices embedded in a turbulent boundary layer was conducted in the test facility CW-22 at NASA Lewis Research Center. The vortices were generated by a single spanwise row of rectangular vortex generator blades. A single embedded vortex was examined, as well as arrays of embedded counter-rotating vortices produced by equally spaced vortex generators. Measurements of the secondary velocity field in the crossplane provided the basis for characterization by four descriptors. The center of each vortex core was located at the spanwise and normal position of peak streamwise vorticity. Vortex concentration was characterized by the magnitude of the peak streamwise vorticity, and the vortex strength by its circulation. Measurements of the secondary velocity field were conducted at two crossplane locations to examine the streamwise development of the vortex arrays. Large initial spacings of the vortex generators produced pairs of strong vortices which tended to move away from the wall region while smaller spacings produced tight arrays of weak vortices close to the wall. The crossplane structure of embedded vortices is observed to be very similar to that exhibited by the two dimensional Oseen vortex with matching descriptors. Quantitative comparisons are established. A model of vortex interaction and development is constructed using the experimental results. The model is based on the structure of the Oseen vortex. Vortex trajectories are successfully modelled by including the convective effects of neighbors, and images to represent the wall. The streamwise decay of circulation is successfully modelled for the single vortex, and for large initial spacings, by accounting for the effects of wall friction. An additional mechanism associated with the turbulent stress field in the near vicinity of the vortex cores is postulated to explain the large losses in the circulation obtained for the smaller initial spacings. The streamwise decay of vortex circulation at the smaller spacings is successfully modelled by summing wall friction losses and 'proximity' losses. These proximity losses are found to be proportional to the gradient in streamwise vorticity occurring between an embedded vortex and its adjacent counter-rotating neighbors. Dissert. Abstr.

N93-10410# Universal Energy Systems, Inc., Dayton, OH.
HIGH-SPEED VISCOUS FLOWS PAST BLUNT BODIES AND COMPRESSION CORNERS WITH FLUX-SPLIT METHODS Final Report, Oct. 1990 - Nov. 1991
Datta Gaitonde Mar. 1992 60 p
(Contract F33615-88-C-2908)
(AD-A253413; WL-TR-92-3018) Avail: CASI HC A04/MF A01

This effort investigates the accuracy of some flux-split algorithms in high-speed viscous flows. Three methods are examined: (1) MacCormack and Candler's (MC) scheme; (2) the van Leer (vL) scheme; and (3) the method of Roe. The problems studied include the blunt body flow at Mach 16 and the flow past a 240 compression corner at Mach 14. Higher order accuracy is obtained with the MUSCL approach. Viscous terms are centered in the full Navier-Stokes cell-centered implicit finite volume simulation. The results indicate a relative similarity of predicted surface pressure with all methods on both flows. However, considerable disparity exists in heat transfer prediction especially on the coarser meshes with van Leer's splitting exhibiting the most overprediction. Generally, however, this disparity-diminishes as the grid is refined. The occurrence of anomalous carbuncle solutions with Roe's scheme may be suppressed with appropriate increase in entropy cutoff with no significant penalty in accuracy. For the ramp flow, the MC method predicts the size of the separated-flow region most accurately, though some overprediction of heat transfer is observed. Roe's algorithm, and on the finer grids, van Leer's method also exhibit comparable results. GRA

N93-10449# Michigan Univ., Ann Arbor. Dept. of Mechanical Research.
MASS TRANSFER IN OSCILLATING FLOWS: EFFICIENT DRYING VIA PULSE COMBUSTORS Final Report, Jan. 1988 - Sep. 1991
V. S. Arpaci and R. Gemmen Apr. 1992 93 p Prepared in cooperation with Sandia National Labs., Albuquerque, NM
(Contract GRI-5088-260-1686)
(PB92-204403; GRI-92/0136) Avail: CASI HC A05/MF A01

Pulse combustors are known to have high rates of heat and mass transfer in the tailpipe because of velocity oscillations created by the acoustic resonance of the combustor. So far, the results reported in the literature are inconclusive. A study of the mass transfer rates in a pulse combustor tailpipe has been conducted. The significant parameters including mean flow rate, frequency, and amplitude of pulsation were varied nearly independently and their effects on the mass transfer were investigated. The mass transfer in the tailpipe is found to be enhanced by the oscillations up to a factor of 2 over steady turbulent flow. A correlation for mass transfer in pulsating turbulent flow is developed using an approach based on the appropriate microscales of turbulence and guided by the physical insight gained from experiments. GRA

N93-10454*# National Aeronautics and Space Administration. Lewis Research Center, Cleveland, OH.
A NEW ENERGY TRANSFER MODEL FOR TURBULENT FREE SHEAR FLOW
William W.-W. Liou Sep. 1992 13 p
(NASA Order C-99066-G; RTOP 505-62-21)

(NASA-TM-105854; ICOMP-92-16; CMOTT-92-09; E-7310; NAS 1.15:105854) Avail: CASI HC A03/MF A01

A new model for the energy transfer mechanism in the large-scale turbulent kinetic energy equation is proposed. An estimate of the characteristic length scale of the energy containing large structures is obtained from the wavelength associated with the structures predicted by a weakly nonlinear analysis for turbulent free shear flows. With the inclusion of the proposed energy transfer model, the weakly nonlinear wave models for the turbulent large-scale structures are self-contained and are likely to be independent flow geometries. The model is tested against a plane mixing layer. Reasonably good agreement is achieved. Finally, it is shown by using the Liapunov function method, the balance between the production and the drainage of the kinetic energy of the turbulent large-scale structures is asymptotically stable as their amplitude saturates. The saturation of the wave amplitude provides an alternative indicator for flow self-similarity. Author

N93-10612# Clarkson Univ., Potsdam, NY. Fluid Mechanics, Heat and Mass Transfer Lab.

HEAT TRANSFER AND PRESSURE DROP FOR AIR FLOW THROUGH ENHANCED PASSAGES

N. T. Obot and E. B. Esen Jun. 1992 119 p

(Contract DE-FG02-89CE-90029)

(DE92-016597; DOE/CE-90029/8) Avail: CASI HC A06/MF A02

An extensive experimental investigation was carried out to determine the pressure drop and heat transfer characteristics for laminar, transitional, and turbulent flow of air through a smooth passage and twenty-three enhanced passages. The internal surfaces of all enhanced passages had spirally shaped geometries; these included fluted, finned/ribbed and indented surfaces. The Reynolds number (Re) was varied between 400 and 50000. The effect of heat transfer (wall cooling or fluid heating) on pressure drop is most significant within the transition region; the recorded pressure drop with heat transfer is much higher than that without heat transfer. The magnitude of this effect depends markedly on the average surface temperature and, to a lesser extent, on the geometric characteristics of the enhanced surfaces. When the pressure drop data are reduced as values of the Fanning friction factor (f), the results are about the same with and without heat transfer for turbulent flow, with moderate differences in the laminar and transition regions. DOE

N93-10629# Michigan State Univ., East Lansing. Turbulence Structure Lab.

A STUDY OF FLOW PROPERTIES OF WET SOLIDS USING LASER INDUCED PHOTOCHEMICAL ANEMOMETRY

R. E. Falco, D. G. Nocera, and S. Buechner 24 Apr. 1992 124 p

(Contract DE-AC22-88PC-88948)

(DE92-015483; DOE/PC-88948/T15; TSL-92-2) Avail: CASI HC A06/MF A02

We have developed the LIPA (Laser Induced Photochemical Anemometry) technique for use in wet-solids and studied model mixtures. Refractive index matched, high Reynolds number (turbulent) solid-liquid flows, composed of silica particle (35-74 micron diameter) in an aqueous solution, were used to enable LIPA measurements of highly loaded wet-solids in a vertical pipe setup. This non-intrusive technique involves use of photoexcitable chemicals, which upon excitation marked the solid-liquid mixture. DOE

N93-10696# Pittsburgh Univ., PA.

INVESTIGATIONS INTO SWIRLING FLOWS OF NEWTONIAN AND NON-NEWTONIAN FLUIDS Final Report, 1 Oct. 1987 - 30 Sep. 1991

Docotr Rajagopal 30 Sep. 1991 27 p

(Grant AF-AFOSR-0045-88)

(AD-A253298; AFOSR-92-0700TR) Avail: CASI HC A03/MF A01

Work carried out under this grant has involved the study of the following problems: (1) flow of non-Newtonian fluids of the rate type between two parallel plates rotating with different angular speeds about a common axis; (2) flow of non-Newtonian fluids of the integral type between parallel plates rotating about distinct axes; (3) flow of non-Newtonian fluids due to torsional and longitudinal oscillations; (4) flow of non-Newtonian fluids in pipes of varying cross-sections; and (5) flow of shear thinning fluid between intersecting planes. GRA

N93-10735*# National Aeronautics and Space Administration. Lewis Research Center, Cleveland, OH.

NAVIER-STOKES TURBINE HEAT TRANSFER PREDICTIONS USING TWO-EQUATION TURBULENCE

Ali A. Ameri and Andrea Arnone Aug. 1992 12 p Presented at the 28th Joint Propulsion Conference and Exhibit, Nashville, TN, 6-8 Jul. 1992; sponsored by AIAA, SAE, ASME, and ASEE

(NASA Order C-99066-G; RTOP 505-62-52)

(NASA-TM-105817; ICOMP-92-14; E-7248; NAS 1.15:105817) Avail: CASI HC A03/MF A01

Navier-Stokes calculations were carried out in order to predict the heat transfer rates on turbine blades. The calculations were performed using TRAF2D which is a two-dimensional, explicit, finite volume mass-averaged Navier-Stokes solver. Turbulence was modeled using q-omega and k-epsilon two-equation models and the Baldwin-Lomax algebraic model. The model equations along with the flow equations were solved explicitly on a non-periodic C grid. Implicit residual smoothing (IRS) or a combination of multigrid technique and IRS was applied to enhance convergence rates. Calculations were performed to predict the Stanton number distributions on the first stage vane and blade row as well as the second stage vane row of the Rocketdyne Space Shuttle Main Engine (SSME) high pressure fuel turbine. The comparison with the experimental results, although generally favorable, serves to highlight the weaknesses of the turbulence models and the possible areas of improving these models for use in turbomachinery heat transfer calculations. Author

N93-10757*# Institute for Computer Applications in Science and Engineering, Hampton, VA.

ON THE COUPLING BETWEEN A SUPERSONIC BOUNDARY LAYER AND A FLEXIBLE SURFACE

Abdelkader Frendi (Analytical Services and Materials, Inc., Hampton, VA.), Lucio Maestrello (National Aeronautics and Space Administration. Langley Research Center, Hampton, VA.), and Alvin Bayliss (Northwestern Univ., Chicago, IL.) Sep. 1992 24 p Submitted for publication

(Contract NAS1-18605; RTOP 505-90-52--01)

(NASA-CR-189697; ICASE-92-42; NAS 1.26:189697) Avail: CASI HC A03/MF A01

The coupling between a two-dimensional, supersonic, laminar boundary layer and a flexible surface is studied using direct numerical computations of the Navier-Stokes equations coupled with the plate equation. The flexible surface is forced to vibrate by plane acoustic waves at normal incidence emanated by a sound source located on the side of the flexible surface opposite to the boundary layer. The effect of the source excitation frequency on the surface vibration and boundary layer stability is analyzed. We find that, for frequencies near the fifth natural frequency of the surface or lower, large disturbances are introduced in the boundary layer which may alter its stability characteristics. The interaction between a stable two-dimensional disturbance of Tollmien-Schlichting (TS) type with the vibrating surface is also studied. We find that the disturbance level is higher over the vibrating flexible surface than that obtained when the surface is rigid, which indicates a strong coupling between flow and structure. However, in the absence of the sound source the disturbance level over the rigid and flexible surfaces are identical. This result is due to the high frequency of the TS disturbance which does not couple with the flexible surface. Author

N93-10793# Georgia Inst. of Tech., Atlanta. School of Aerospace Engineering.
NUMERICAL SOLUTION OF THREE-DIMENSIONAL UNSTEADY VISCOUS FLOWS Progress Report, 1 Dec. 1991 - 31 May 1992
Lakshmi N. Sankar 31 May 1992 57 p
(Contract N00014-89-J-1319)
(AD-A253202) Avail: CASI HC A04/MF A01

The long term objective of the present effort is the development of solution techniques for direct numerical simulation of unsteady 3-D incompressible turbulent flows., The kinetic aspects of this problem are governed by a set of parabolic partial differential equations, which may be efficiently integrated by a variety of time marching schemes. The kinematic aspects of this flow such as the relationship between velocity and vorticity, and the relationship between velocity and pressure are governed by elliptic partial differential equations, which can be solved at any instance in time, only by iterative techniques. Direct and/or large eddy simulation of turbulent flows over submarine configurations, turbomachinery, pumps, ducts and other configurations of interest to the U. S. Navy require efficient solution methods for solving the governing equations. The near term objective of the present research is to investigate and develop efficient time marching schemes for integrating the governing equations, and to evaluate the stability and accuracy of the schemes developed by studying a class of 2-D and 3-D unsteady external flows for which good quality experimental and analytical results are available. GRA

N93-10808*# Institute for Computer Applications in Science and Engineering, Hampton, VA.
PROGRESS IN MULTI-DIMENSIONAL UPWIND DIFFERENCING Final Report
Bram vanLeer (Michigan Univ., Ann Arbor.) Sep. 1992 31 p Presented at the 13th International Conference on Numerical Methods in Fluid Dynamics, Rome, Italy, 6-10 Jul. 1992
(Contracts NAS1-18605; NAS1-19480; RTOP 505-90-52-01)
(NASA-CR-189708; NAS 1.26:189708; ICASE-92-43) Avail: CASI HC A03/MF A01

Multi-dimensional upwind-differencing schemes for the Euler equations are reviewed. On the basis of the first-order upwind scheme for a one-dimensional convection equation, the two approaches to upwind differencing are discussed: the fluctuation approach and the finite-volume approach. The usual extension of the finite-volume method to the multi-dimensional Euler equations is not entirely satisfactory, because the direction of wave propagation is always assumed to be normal to the cell faces. This leads to smearing of shock and shear waves when these are not grid-aligned. Multi-directional methods, in which upwind-biased fluxes are computed in a frame aligned with a dominant wave, overcome this problem, but at the expense of robustness. The same is true for the schemes incorporating a multi-dimensional wave model not based on multi-dimensional data but on an 'educated guess' of what they could be. The fluctuation approach offers the best possibilities for the development of genuinely multi-dimensional upwind schemes. Three building blocks are needed for such schemes: a wave model, a way to achieve conservation, and a compact convection scheme. Recent advances in each of these components are discussed; putting them all together is the present focus of a worldwide research effort. Some numerical results are presented, illustrating the potential of the new multi-dimensional schemes. Author

N93-10810# New Mexico Univ., Albuquerque. Dept. of Mathematics and Statistics.
MATHEMATICAL ANALYSIS OF REACTIVE MULTIPHASE FLOWS Final Report, 31 May 1991 - 30 May 1992
Pedro F. Embid 17 Jul. 1992 6 p
(Contract DAAL03-91-G-0186)
(AD-A253854; ARO-28980.4-MA) Avail: CASI HC A02/MF A01

This work provides a mathematical analysis of a reactive multiphase flow model introduced by Baer and Nunziato in their studies of deflagration to detonation transition (DDT) in reactive granular materials. This work combines asymptotic methods with numerical computations and theoretical analysis. In particular, we derive an asymptotic model to explain the formation and growth of hot spots during DDT in reactive granular materials. The model is founded on nonlinear geometrical optics and high energy asymptotics near choked flow states. Through analysis and numerical simulations, the model is able to reproduce several of the scenarios for DDT previously documented in the literature for the continuum model of Baer and Nunziato. GRA

N93-10846 Pennsylvania State Univ., University Park.
TURBULENT MIXING IN COMPRESSIBLE FREE SHEAR LAYERS Ph.D. Thesis
Manampathy G. Giridharan 1991 216 p
Avail: Univ. Microfilms Order No. DA9127331

For almost twenty years it has been recognized that turbulent shear flows are dominated by large-scale structures. Yet the majority of models for turbulent mixing fail to distinguish the properties of the structures either explicitly or implicitly from the broad band turbulence. A new model for the large-scale structures in a turbulent shear layer is introduced. Two variations on the model are developed that describe the influence of large-scale motions on the turbulent mixing process. The first variation simulates the average behavior by calculating the development of the part of the turbulent spectrum related to the large-scale structures in the flow. The second variation simulates a single realization of the passage of a train of large scale-structures. In both of these treatments, the large scale structures are described by a superposition of instability waves. The local properties of these waves are determined from a quasi-linear, inviscid, stability analysis. The streamwise development of the mean flow is determined from an energy integral analysis. The models contain no empirical constants. The present turbulence models predict the effects of freestream velocity and density ratios and effects of compressibility on the growth of the shear layer. The predictions agree very well with the available experimental data. Calculations are also made for the time-dependent motion of the shear layer in the form of streaklines and iso-vorticity/density contours that agree qualitatively with experimental observations. A successful implementation of the present models requires an understanding of the characteristics of the various modes of instability in compressible shear layers. A detailed spatial stability analysis is performed to fulfill this requirement. Using the traditional normal mode analysis, the various modes of instability in compressible shear layers are characterized and the physical mechanisms that drive these instabilities are described. In addition, an initial value problem is formulated to calculate the development of wave packets in shear layers. The preliminary results obtained from this analysis indicate that the structure of the wave packet in a compressible shear layer depends on the duct aspect ratio and that its development is very different from that of an incompressible shear layer. Dissert. Abstr.

N93-10859# Office National d'Etudes et de Recherches Aerospatiales, Paris (France). Direction de l'Aerodynamique.
NUMERICAL STUDY OF WALL TURBULENCE Final Summary Report [ETUDE NUMERIQUE DE LA TURBULENCE EN PRESENCE DE PAROIS]
S. Rida Nov. 1991 46 p In ENGLISH and FRENCH
(Contract DRET-89-34-001)
(ONERA-RSF-21/3419-AY-126; ETN-92-92176) Avail: CASI HC A03/MF A01

A numerical study considering two aspects of wall turbulence is presented. The turbulent field response at a longitudinal pressure gradient sinusoidally mean variant in time is studied and analyzed for two amplitudes, 0.1 and 0.4, and for two periodic values, 2.6 and 60 s. A Couette-Poiseuille turbulent flow is studied for a critical velocity gradient configuration, showing the role of the velocity-pressure correlation term. A paper on the direct simulation of turbulence pulsed plane channel flows is also reprinted. For individual titles, see N93-10860 through N93-10860.

N93-10860# Office National d'Etudes et de Recherches Aerospatiales, Paris (France).
DIRECT SIMULATION OF TURBULENT PULSED PLANE CHANNEL FLOWS [SIMULATION DIRECTE D'ECOULEMENTS TURBULENTS DE CANAL PLAN PULSE]
S. Rida and K. DangTran *In its* Numerical Study of Wall Turbulence Nov. 1991 p 41-47 Presented at Turbulent Shear Flows, Munich, Germany, 9-11 Sep. 1991 (For primary document see N93-10859 01-34)
Avail: CASI HC A02/MF A01

A study on the behavior of turbulent wall shear flows submitted to time dependent external forces is presented. Experimental studies and theoretical considerations give some insight into the influence of an imposed unsteadiness on turbulent motions in the case of pulsed plane channel and boundary layer flows: the time averaged turbulent quantities seem to be unaffected by the imposed periodical forces, mostly at high frequencies, and the phase averaged quantities follow merely the evolution of the linear viscous Stokes solution on the major part of the flow domain. The completion of these experimental results by means of numerical direct simulation is addressed. This numerical work, completed in the case of a pulsed plane channel flow at a mean Reynolds number 2000 for the steady case, shows that nonlinear interactions can be found between the turbulent flow and the imposed unsteadiness, in the range of low frequencies where the computations were performed. ESA

N93-10868# EG and G Energy Measurements, Inc., Idaho Falls.
FLASH: A FINITE ELEMENT COMPUTER CODE FOR VARIABLY SATURATED FLOW
R. G. Baca and S. O. Magnuson May 1992 62 p
(Contract DE-AC07-76ID-01570)
(DE92-018038; EGG-GEO-10274) Avail: CASI HC A04/MF A01

A numerical model was developed for use in performance assessment studies at the INEL. The numerical model, referred to as the FLASH computer code, is designed to simulate two-dimensional fluid flow in fractured-porous media. The code is specifically designed to model variably saturated flow in an arid site vadose zone and saturated flow in an unconfined aquifer. In addition, the code also has the capability to simulate heat conduction in the vadose zone. This report presents the following: description of the conceptual frame-work and mathematical theory; derivations of the finite element techniques and algorithms; computational examples that illustrate the capability of the code; and input instructions for the general use of the code. The FLASH computer code is aimed at providing environmental scientists at the INEL with a predictive tool for the subsurface water pathway. This numerical model is expected to be widely used in performance assessments for the following: (1) the Remedial Investigation/Feasibility Study process, and (2) compliance studies required by the US Department of Energy. DOE

N93-10874 Concordia Univ., Montreal (Quebec).
CHARACTERISTICS OF SEPARATED FLOWS INCLUDING CAVITATION EFFECTS Ph.D. Thesis
Ramaswami Balachandar 1990 204 p
Avail: Univ. Microfilms Order No. DANN59192

A program of study was performed to obtain the characteristics of two-dimensional separated flows including cavitation effects. The effects of wall interference and cavitation on the characteristics of flow past bluff bodies and backward facing steps were examined. Separated flows so generated can be a major source of flow induced vibration and noise. For non-cavitating flow past sharp-edged bluff bodies, a simplified procedure is developed to determine the effects of wall interference on the drag coefficient. The characteristics related to inception, choking, cavity geometry, and cavity pressure field were determined on the basis of experimental results for cavitating flow past bluff bodies. In this context, models based on theoretical considerations were also developed to determine the inception and choking cavitation characteristics. For sharp-edged bluff bodies, the length of vortex formation region was determined, recognizing it as a significant parameter which precedes the zone where cavitation damage is most probable. Visual observations of the length of formation region supported the view that cavitation stabilizes the vortex against its break-up. The effects of wall interference and cavitation on the frequency of vortex shedding behind bluff bodies were also determined. The absence of the Karman vortex street was noted for flow past bluff bodies which were subject to very severe wall interference effects. At very large Reynolds numbers, the reattachment of two-dimensional separated shear layers downstream of backward facing steps were investigate. Two backward facing steps were used to study the influence of expansion ratio on incipient cavitation indices at various Reynolds numbers. The frequency of vortex shedding and pressure distribution downstream of separation were obtained for both cavitating and non-cavitating flow conditions. Dissert. Abstr.

N93-10875 Kansas Univ., Lawrence.
THE EFFECTS OF STREAMLINE CURVATURE AND SWIRL ON TURBULENT FLOWS IN CURVED DUCTS Ph.D. Thesis
Chih-Hsiung Gary Cheng 1991 201 p
Avail: Univ. Microfilms Order No. DA9210032

A technique for improving the numerical predictions of turbulent flows with the effect of streamline curvature is developed. Separated flows, the flow in a curved duct, and swirling flows are examples of flow fields where streamline curvature plays a dominant role. A comprehensive literature review on the effect of streamline curvature was conducted in the present study. New algebraic formulations for the eddy viscosity incorporating the k-e turbulence model are proposed to account for various effects of streamline curvature. The loci of flow reversal of the separated flows over various backward-facing steps are employed to test the capability of the proposed turbulence model in capturing the effect of local curvature. The inclusion of the effect of longitudinal curvature in the proposed turbulence model is validated by predicting the distributions of the static pressure coefficients in an S-bend duct and in 180 turn-around ducts. The proposed turbulence model embedded with transverse curvature modification is substantiated by predicting the decay of the axial velocities in the confined swirling flows. The numerical predictions of different curvature effects by the proposed turbulence models are also reported.
Dissert. Abstr.

N93-10886# Iowa State Univ. of Science and Technology, Ames. Dept. of Aerospace Engineering.
STUDY OF A VISCOUS SUBLAYER MODEL IN THE ANALYSIS OF 3-D SHOCK/BOUNDARY LAYER INTERACTION FLOW FIELDS Final Report, 1 Oct. 1990 - 31 Dec. 1991
George R. Inger 20 Jun. 1992 25 p
(Grant AF-AFOSR-0049-91)
(AD-A253731; AFOSR-92-0724TR) Avail: CASI HC A03/MF A01

At high Reynolds number, it has been experimentally and computationally well-confirmed that the 3-D interactive physics is vertically organized into the triple-deck type of structure. The governing integral-type equations that characterize the non-reversed flow portion of the interactive wall layer model are formulated in the form of a set of nonlinear partial first order differential equations, including three-dimensional aspects. Also modeled was the splitting of the layer into an upper region of non-reversed flow and an underlying region of slow, reversed flow. The shock structure and nonlinear rotational inviscid flow behavior of the overlying region were explored by means of a suitable 3-D shock/boundary layer approach which include separation. The NASA Langley code 'Laura' was modified to include these new wall layer equations. GRA

N93-10895# California Inst. of Tech., Pasadena. Graduate Aeronautical Labs.
INVESTIGATIONS OF THE MOTION OF DISCRETE-VELOCITY GASES Final Technical Report, 1 Jun. 1989 - 30 Nov. 1991
B. Sturtevant 2 Jun. 1992 9 p
(Grant AF-AFOSR-0369-89)

(AD-A253728; AFOSR-92-0741TR) Avail: CASI HC A02/MF A01

A direct simulation Monte Carlo method for rarefied gasdynamics, patterned after the DSMC of G. A. Bird, in which molecular velocities are discretized to be integers (IDSMC) was developed. The method has been implemented on coarse-grained multi-computers such as the Intel iPSC, Symult 2010, and Intel Gamma with a self-adaptive rectangular mesh to optimize load balancing. A finite-difference method for solving the discrete-velocity (lattice gas) Boltzmann equations has been formulated and implemented. Calculations were made of problems in heat transfer, shock wave structure, and vapor deposition. The applicability of multi-speed discrete-velocity gases to compressible flows has been examined from a fundamental point of view. The equation of state, the anisotropies, and the advection velocities for multi-speed models on the square and triangular lattices were derived. It was shown that the pathologies shown by multi-speed lattice gases can be made rather small. GRA

N93-10008 Naval Research Lab., Washington, DC. Lab. for Computational Physics and Fluid Dynamics.
NUMERICAL SIMULATION OF UNSTEADY FLOW IN A NOZZLE
Ravi Ramamurti, K. Kailasanath, and R. Loehner (George Washington Univ., Washington, DC.) *In* JHU, The 1992 JANNAF Propulsion Meeting, Volume 1 Feb. 1992 p 153-163 Sponsored by SSPO (For primary document see N93-10001 01-20)
Avail: CPIA, 10630 Little Patuxent Pkwy., Suite 202, Columbia, MD, 21044-3200 HC

N93-10009 Air Force Inst. of Tech., Wright-Patterson AFB, OH.
SUPERSONIC CONFINED JET NOZZLES
Milt E. Franke *In* JHU, The 1992 JANNAF Propulsion Meeting, Volume 1 Feb. 1992 p 165-169 (For primary document see N93-10001 01-20)
Avail: CPIA, 10630 Little Patuxent Pkwy., Suite 202, Columbia, MD, 21044-3200 HC

N93-10010*# National Aeronautics and Space Administration. Langley Research Center, Hampton, VA.
A BUILDING-BLOCK APPROACH FOR TURBULENCE MODEL VALIDATION/UPGRADE FOCUSSED ON HIGH-SPEED JET FLOWFIELDS
Stanford M. Dash (Science Applications International Corp., Fort Washington, PA.), B. J. Walker (Army Missile Command, Redstone Arsenal, AL.), and J. M. Seiner *In* JHU, The 1992 JANNAF Propulsion Meeting, Volume 1 Feb. 1992 p 171-193 (For primary document see N93-10001 01-20)
Avail: CPIA, 10630 Little Patuxent Pkwy., Suite 202, Columbia, MD, 21044-3200 HC

N93-10039*# National Aeronautics and Space Administration. Lewis Research Center, Cleveland, OH.
A SURVEY OF INSTABILITIES WITHIN CENTRIFUGAL PUMPS AND CONCEPTS FOR IMPROVING THE FLOW RANGE OF PUMPS IN ROCKET ENGINES
Joseph P. Veres *In* JHU, The 1992 JANNAF Propulsion Meeting, Volume 1 Feb. 1992 p 615-629 Previously announced as N92-18280 (For primary document see N93-10001 01-20)
Avail: CPIA, 10630 Little Patuxent Pkwy., Suite 202, Columbia, MD, 21044-3200 HC

N93-10467 Stanford Univ., CA. Dept. of Mechanical Engineering.
NEW DIRECTIONS IN COMPUTATIONAL MECHANICS
Thomas J. R. Hughes *In* Carleton Univ., Proceedings of the Twelfth Canadian Congress of Applied Mechanics, Volumes 1 and 2 May 1989 p 22-46 (For primary document see N93-10466 01-31)
Copyright Avail: Canadian Society for Mechanical Engineering, 2050 Mansfield St., Suite 700, Montreal, Quebec H3A 1Z7 Canada

N93-10469 Texas Univ., Austin.
SMART ALGORITHMS AND ADAPTIVE METHODS IN COMPUTATIONAL FLUID DYNAMICS
J. Tinsley Oden *In* Carleton Univ., Proceedings of the Twelfth Canadian Congress of Applied Mechanics, Volumes 1 and 2 May 1989 p 54-74 (For primary document see N93-10466 01-31)
Copyright Avail: Canadian Society for Mechanical Engineering, 2050 Mansfield St., Suite 700, Montreal, Quebec H3A 1Z7 Canada

N93-10545 Ecole Polytechnique, Montreal (Quebec). Dept. of Mechanical Engineering.
STREAM FUNCTION-VORTICITY FINITE ELEMENT FORMULATIONS OF UNSTEADY INCOMPRESSIBLE NAVIER-STOKES EQUATIONS
K. F. Tchon, W. Ghaly, and I. Paraschivoiu *In* Carleton Univ., Proceedings of the Twelfth Canadian Congress of Applied Mechanics, Volumes 1 and 2 May 1989 p 588-589 (For primary document see N93-10466 01-31)
Copyright Avail: Canadian Society for Mechanical Engineering, 2050 Mansfield St., Suite 700, Montreal, Quebec H3A 1Z7 Canada

N93-10546 Toronto Univ. (Ontario). Inst. for Aerospace Studies.
SHOCK WAVE DIFFRACTIONS OVER SEMI-CIRCULAR AND HALF-DIAMOND CYLINDERS
I. I. Glass, J. Kaca, and D. L. Zhang *In* Carleton Univ., Proceedings of the Twelfth Canadian Congress of Applied Mechanics, Volumes 1 and 2 May 1989 p 596-597 (For primary document see N93-10466 01-31)
Copyright Avail: Canadian Society for Mechanical Engineering, 2050 Mansfield St., Suite 700, Montreal, Quebec H3A 1Z7 Canada

N93-10548* National Aeronautics and Space Administration. Lewis Research Center, Cleveland, OH.
A LEAST-SQUARES FINITE ELEMENT METHOD FOR INCOMPRESSIBLE NAVIER-STOKES PROBLEM
Bonan Jiang (Cleveland State Univ., OH.) and Louis A. Povinelli *In* Carleton Univ., Proceedings of the Twelfth Canadian Congress of Applied Mechanics, Volumes 1 and 2 May 1989 p 602-603 (For primary document see N93-10466 01-31)
Copyright Avail: Canadian Society for Mechanical Engineering, 2050 Mansfield St., Suite 700, Montreal, Quebec H3A 1Z7 Canada

N93-10552 University of Western Ontario, London.
STRUCTURE OF THERMOCAPILLARY FLOW IN NARROW CAVITIES
J. Krol and J. M. Floryan *In* Carleton Univ., Proceedings of the Twelfth Canadian Congress of Applied Mechanics, Volumes 1 and 2 May 1989 p 718-719 (For primary document see N93-10466 01-31)
Copyright Avail: Canadian Society for Mechanical Engineering, 2050 Mansfield St., Suite 700, Montreal, Quebec H3A 1Z7 Canada

35 INSTRUMENTATION AND PHOTOGRAPHY

Includes remote sensors; measuring instruments and gages; detectors; cameras and photographic supplies; and holography.

For aerial photography see *43 Earth Resources and Remote Sensing.* For related information see also *06 Aircraft Instrumentation,* and *19 Spacecraft Instrumentation.*

N93-10239# State Univ. of New York at Buffalo, Amherst.
ORIENTATION AND PAIR CORRELATION AT HIGH DENSITY BY SUPERRESOLUTION HOLOGRAPHY Final Report

Peter D. Scott 1 Jun. 1992 7 p
(Contract DAAL03-91-G-0144)
(AD-A254034; ARO-28359.1-GS) Avail: CASI HC A02/MF A01

Estimation of the configurational parameters of a particle field requires accurate quantification of the location and orientation of each particle in a test volume at one point in time. In-line holography is a useful technique, but previous reconstruction approaches fail for high density. Here, the feasibility of high density in-line holography is studied in the context of a new superresolving digital reconstruction technique. GRA

N93-10347 Stanford Univ., CA.
DATA REDUCTION ANALYSIS FOR THE STANFORD RELATIVITY GYROSCOPE EXPERIMENT Ph.D. Thesis
Xinhua Qin 1991 169 p
Avail: Univ. Microfilms Order No. DA9206839

This thesis discusses the data reduction simulation and error analysis for the Stanford Relativity Gyroscope Experiment. This experiment is designed to test the Einstein's general theory of relativity. Two untested relativistic effects are predicted for a gyroscope moving in a 650 km polar orbit around the earth: a geodetic effect and a frame-dragging effect. The geodetic effect has a magnitude of 6.602 arcsec/year in the south-north direction. It is due to the orbital motion of a gyroscope in a curve space-time around the earth. The frame-dragging effect has a magnitude of 0.042 arcsec/year in the west-east direction. It is due to the dragging of the 'inertial' frame by the massive rotating earth. The goal of this experiment is to detect these two effects to better than 0.5 milliarcsec/year. A Kalman filter is used to perform the data reduction simulation and error analysis. A two-step Kalman filtering algorithm is developed based on the spectral separation principle. Slowly varying terms are treated as time-invariant in the first step filter. This filter is restarted for every orbital period. The second step filter uses the outputs from the first step filter as pseudo-measurements to estimate the slowly varying terms. This algorithm has the advantages of clearer physical insight, providing intermediate data for dynamical modeling, better numerical performance, and less computation time. A data reduction simulation is performed with realistic spacecraft roll dynamics. The sensitivity to spacecraft roll angle error is investigated. Studies show that data reduction can be successfully performed with only one roll angle measurement as well as one roll rate correction per roll period. Studies also show that spacecraft roll control error starts to have significant influence on the experiment accuracy when its RMS (Root Mean Square) value is bigger than 100 arcsec. The initial gyro spin axis alignment has a significant effect on the experiment accuracy. Studies show that, for a one-year mission, the optimal initial gyro alignment is close to the apparent line-of-sight to the guide star. This analysis is the basis for a newly established fundamental experiment requirement. Data reduction algorithms with a low resolution analog-to-digital converter (12-bit) are also studied. These include a data integration filter and a sigma-delta analog-to-digital converter. These algorithms are tested by simulations. Dissert. Abstr.

N93-10408# North Carolina Univ., Charlotte. Dept. of Electrical Engineering.
HOLOGRAPHIC OPTICAL INTERCONNECTS FOR MULTICHIP MODULES Report, 1 Oct. 1990 - 30 Sep. 1991
Michael R. Feldman 15 Oct. 1991 10 p
(Contract N00014-91-J-4022)
(AD-A253403) Avail: CASI HC A02/MF A01

The primary purpose of this research is the development of a prototype multichip module incorporating high efficiency, high connection density optical interconnects. During the first year, individual components are to be designed, fabricated, and tested. Various methods to achieve and maintain alignment between the components are to be developed and tested experimentally. The results of this work are to be used to develop components for a demonstration system, termed system 1, that is to be completed during the second year. This report describes results of this project for the first 3 months, from Jul. 1, 1991 - Oct. 1, 1991. The work has been divided into 4 tasks: CGH's, photodetectors, laser diode research, and system integration. Preliminary progress has been made in each of these areas. In addition, plans for the coming year are presented. GRA

N93-10444# California Univ., Berkeley. Lawrence Berkeley Lab.
A FOUR CHANNEL 250 MHz VISUAL COUNTER
I. Flores, P. Blando, H. Crawford, J. Engelage, L. Greiner, S. Ko, G. Krebs, and G. Visser Apr. 1992 8 p
(Contract DE-AC03-76SF-00098)
(DE92-016920; LBL-Pub-3097) Avail: CASI HC A02/MF A01

A visual counter rated at 250 mhz with a pulse-pair resolution of 2.6 nanoseconds for nuclear instrument module (NIM) signals was designed. Pulse widths for NIM signals must be equal to or greater than 2 ns. The counter has a separate input for transistor-transistor logic (TTL) signals and for this logic level it operates at rates equal to or less than 190 mhz. TTL pulses must be greater than 4 ns. The design was implemented on a printed circuit card. Four of these cards were packaged into a single unit resulting in a four channel device that can be mounted into a 19 inch rack. Seven units were built; they are presently used in the experimental area and in the Main Control Room of the Bevalac. The counter accepts well defined NIM or TTL signals internally terminated with 50 ohms. All the controls and the signal input connectors are located on the front panel. An Overflow output, Gate, and Reset inputs are located on the back panel. The counters have 8 Light Emitting Diode digit displays which are 20.3 mm high with a viewing distance rating of 10 meters. Light filters are used for the LED displays greatly enhancing their visibility. DOE

N93-10518 Technische Univ., Hamburg (Germany).
AN ELASTIC OBLATE AXISYMMETRIC REFERENCE GYRO FOR ATTITUDE STUDIES
V. Schlegel, A. Guran (Toronto Univ., Ontario), and F. P. J. Rimrott (Toronto Univ., Ontario) *In* Carleton Univ., Proceedings of the Twelfth Canadian Congress of Applied Mechanics, Volumes 1 and 2 May 1989 p 396-397 (For primary document see N93-10466 01-31)
Copyright Avail: Canadian Society for Mechanical Engineering, 2050 Mansfield St., Suite 700, Montreal, Quebec H3A 1Z7 Canada

N93-10582*# National Aeronautics and Space Administration. Langley Research Center, Hampton, VA.
EFFECT OF SPACE EXPOSURE ON PYROELECTRIC INFRARED DETECTORS
James B. Robertson *In its* LDEF Materials Workshop 1991, Part 2 Sep. 1992 p 501-506 (For primary document see N93-10578 01-27)
Avail: CASI HC A02/MF A03

N93-10936# Institut d'Astrophysique, Paris (France).
FIRST RESULTS OF AN IMAGING FTS WITH A NICMOS CAMERA
J. P. Maillard and D. Simons (Canada-France-Hawaii Telescope Corp., Kamuela, HI.) *In* ESA, Solar Physics and Astrophysics at Interferometric Resolution May 1992 p 205-210 (For primary document see N93-10901 01-90)
Copyright Avail: CASI HC A02/MF A03

N93-10952# Technische Physische Dienst TNO-TH, Delft (Netherlands).
THE IMAGING FOURIER TRANSFORM SPECTROMETER: PERFORMANCE AND TOLERANCE ANALYSIS
B. Kruizinga, B. Snijders, B. C. Braam, A. P. Thorne (Imperial Coll. of Science and Technology, London, England), J. Maxwell (Imperial Coll. of Science and Technology, London, England), and L. Dame (Centre National de la Recherche Scientifique, Verrieres-Le Buisson, France) *In* ESA, Solar Physics and Astrophysics at Interferometric Resolution May 1992 p 290 (For primary document see N93-10901 01-90)
Copyright Avail: CASI HC A01/MF A03

36 LASERS AND MASERS

Includes parametric amplifiers.
For related information see also *76 Solid-State Physics.*

N93-10083# Lawrence Livermore National Lab., CA.
THEORETICAL ANALYSIS OF DISCHARGES IN COPPER VAPOR LASERS: A COMPARISON OF Ne AND He
N. Goto (New Technology Research Group, Japan) and K. Nemoto (New Technology Research Group, Japan) 26 Aug. 1991 37 p Transl. into ENGLISH of Japanese document (Japan) p 1-22
(Contract W-7405-eng-48)
(DE92-014739; UCRL-TT-108270; T89036) Avail: CASI HC A03/MF A01

This report describes a theoretical analysis method of the electron transport which has been developed by assuming spatial homogeneity in mixtures of copper vapor and rare gases. This theory gives a more detailed electron transport than use of the Maxwellian. The temperature of discharge tube is an important parameter for discharges, because it gives the pressure of copper vapor and the characteristics of electron transport. Included with one percent of copper vapor, the reduced field for the laser oscillation needs over 8 Td in Ne and 14 Td in He. DOE

N93-10090# Schwartz Electro-Optics, Inc., Orlando, FL.
4.5 MICRON LASER SOURCE Final Report, Mar. - Oct. 1991
M. A. Acharekar and J. Montgomery Jun. 1992 31 p
(Contract F08630-91-C-0006)
(AD-A253367; WL-TR-92-7016) Avail: CASI HC A03/MF A01

This report documents efforts attempted at producing continuous wave (CW) laser power at 4.5 microns. Silver Gallium Selenide (AgGaSe2) was used to frequency double a 9.0 micron CO2 laser. Milliwatts of CW 4.5 micron power were reported. CW damage threshold experiments of AgGaSe2 at 9.0 microns were also conducted. GRA

N93-10201# Columbia Univ., New York, NY. Microelectronics Science Lab.
THE INTERACTION OF UV-LASER RADIATION WITH METAL AND SEMICONDUCTOR SURFACES Final Report, 15 Jan. 1989 - 14 Jan. 1992
Richard M. Osgood, Jr. 26 May 1992 80 p
(Contract DAAL03-89-K-0028)
(AD-A253510; ARO-26223.2-PH) Avail: CASI HC A05/MF A01

This report describes progress in a program to understand the fundamentals of UV laser interactions with solid surfaces. In the first, using previously developed optical probes, we have made the first measurements of the surface photo-dissociation cross section, its yield, its wavelength dependence, and its dependence on surface conditions for two important metal-alkyl precursors. Second, we have successfully initiated a substantial new program in UV-laser photoemission for surface probing. This work has included establishing a new, tunable, two-photon photoemission apparatus including UHV chamber with an electron detection system, demonstration of a new technique to probe buried interfaces, the use of high-resolution, two-photon spectroscopy to probe surface-condition-dependent changes via image states, and the observation of space-charge-limited effects on surface photoionization spectroscopy. GRA

N93-10202# California Univ., Irvine.
SUBPICOSECOND RESOLVED INCIPIENT LASER DAMAGE Final Report, 15 Mar. 1989 - 31 Mar. 1992
W. E. Bron 15 May 1992 17 p
(Contract DAAL03-89-K-0060)
(AD-A253624; ARO-26211.1-PH) Avail: CASI HC A03/MF A01

The overall goal of this line of research is to determine in detail laser induced transient dynamics in condensed matter in the presence of phonons and carriers at concentrations which exceed thermal equilibrium and approach the threshold for incipient damage. Two major problems had to be solved before meaningful data could be obtained and a theoretical basis was achieved with which the observed transient dynamics could be understood. The experimental problem of sufficient signal-to-noise to observe very fast optical transients in the presence of intense laser beams was solved through two unique laser systems. These laser systems consist of dual synchronously pumped and synchronously amplified dye lasers combined with the generation and kilohertz rate amplification of synchronized femtosecond and picosecond laser systems. The development of fast (1 KHz) analogue to digital converter needed to abstract the data and to regulate various components of the laser system was also important. Specifically, this involved the construction of the 1 KHz computerized data acquisition system consisting of before and after sample photodiode beam detection and Raman signal detection, amplification, gated integration, and a/d conversion. This pulse-by-pulse normalized scheme has been used to investigate the absorption properties of the GaP crystal necessary for this experiment. GRA

N93-10211# PCO, Inc., Chatsworth, CA.
LONG WAVELENGTH MULTIPLE QUANTUM WELL LASERS FOR HIGH-SPEED MODULATION APPLICATIONS Final Report
R. M. Ash, D. J. Robbins, and A. K. Wood Feb. 1992 58 p
(Contract F19628-89-C-0136)
(AD-A253348; RL-TR-92-2) Avail: CASI HC A04/MF A01

The goal of this work is the fabrication of quantum well lasers capable of being modulated at high speeds. The intrinsic laser resonance response and parasitic electrical effects combine to limit laser speed. The high gain-slope of multiple quantum well structures was used to overcome the first problem, that is, the fabricated lasers had InGaAsP/InP active regions. Low-pressure MOVPE was used to fabricate the devices. The goal was to design a laser that emits at 1.3 microns, which is the optional wavelength for fiber-optic communications. The first devices fabricated had high threshold current and low efficiency, but they confirmed the accuracy of the chosen model. An eight quantum well structure was chosen to minimize the deleterious effects of damping on the laser's frequency response. The final deliverable product had a threshold current of 10MA and an output power of 20mW. It operated out to 8 GHz and up to 100 deg C. It is believed that diffusion capacitance from the leakage current limits frequency response. GRA

N93-10218# Massachusetts Inst. of Tech., Lexington. Lincoln Lab.
GEOMETRICAL TRANSFORMATION OF LINEAR DIODE-LASER ARRAYS FOR LONGITUDINAL PUMPING OF SOLID-STATE LASERS
J. R. Leger and W. C. Goltsos 26 May 1992 44 p
(Contract F19628-90-C-0002)
(AD-A253415; TR-950; ESD-TR-91-250) Avail: CASI HC A03/MF A01

A 200-stripe linear diode-laser array is geometrically transformed into a two-dimensional, symmetric virtual source with symmetric divergence to end-pump a Nd:YAG laser. The geometrical transformation is performed by two planes of diffractive optical elements separated by a 2.6-cm gap. Discounting optical losses, a TEM00-mode slope efficiency of 56 percent is demonstrated. Methods of increasing the throughput efficiency of the diffractive elements (currently approximately 50 percent per element) are explored. A theoretical model for estimating the maximum useful pump array size in longitudinally pumped rod and fiber lasers shows that this pump geometry is close to optimum. GRA

N93-10228# Arizona Univ., Tucson. Optical Sciences Center.
FELLOWSHIP IN PHYSICS/MODERN OPTICS AND QUANTUM ELECTRONICS Final Report, Nov. 1989 - Feb. 1992
Brian Fluegel 15 May 1992 16 p
(Contract DAAL03-90-G-0006)
(AD-A253666; ARO-27587.10-PH-F) Avail: CASI HC A03/MF A01

Using laser pulses of duration comparable to semiconductor relaxation and dephasing times, the coherent phenomena common to two-level systems were demonstrated in II-VI and III-V

semiconductors. These light-matter interactions are characterized by electrons and holes in their initially excited states and/or a macroscopic polarization that persists after the excitation. GRA

N93-10247# State Univ. of New York, Buffalo. Dept. of Chemistry.
A TIME-RESOLVED TWO-LASER PROBE OF Cr(CO)6 PHOTODISSOCIATION DYNAMICS
William R. Peifer, James F. Garvey, and Robert DeLeon (Calspan Corp., Buffalo, NY.) 1 Jun. 1992 16 p
(Contract N00014-88-K-0483)
(AD-A250930; TR-29) Avail: CASI HC A03/MF A01

We have examined the photodissociation of jet-cooled Cr(CO)6 using a time-resolved, two-laser multiphoton dissociation (MPD) technique with fluorescence detection of the atomic photofragments. We have observed that the rate of appearance of Cr(CO)4 via 248-nm photolysis of Cr(CO)6 is slower if the Cr(CO)6 has first been cooled in a supersonic expansion. We suggest the difference in the observed rates is due to slower intersystem crossing in the transient Cr(CO)5 following impulsive loss of the first CO ligand from the jet-cooled hexacarbonyl. This intersystem crossing is thought to be facilitated by low-energy OC-Cr-CO bending modes, which are probably not accessible by one-photon absorption from the ground state Cr(CO)6. We discuss the utility of our time-resolved MPD/atomic fluorescence technique as a general dynamical probe for metal carbonyl photodissociation. GRA

N93-10251# City Univ. of New York, NY.
LASER AND OPTICAL PHYSICS Final Report, 1 Apr. 1989 - 30 Apr. 1992
Melvin Lax Jul. 1992 16 p
(Contract DAAL03-89-K-0065)
(AD-A253619; ARO-25872.11-PH-SAH) Avail: CASI HC A03/MF A01

This final report summarized significant progress in combining light scattering with decision and estimation theory to determine whether or not aerosols are homogeneous spheres or shell-like (possibly encapsulated). Researchers have succeeded in comparing two parameter spheres with three parameter shells with a reasonable range of permitted radii and indices, and have demonstrated the feasibility of the next step. handling four parameter shells. GRA

N93-10286# Michigan Univ., Ann Arbor. Dept. of Nuclear Engineering.
ADVANCED TRANSPORT SYSTEMS FOR ELECTRON BEAMS IN HIGH-BRIGHTNESS ACCELERATORS AND FEL'S Annual Report, 1 May 1991 - 31 May 1992
R. M. Gilgenbach, T. Kammash, and M. L. Brake 24 Jul. 1992 48 p
(Contract N00014-91-J-1941)
(AD-A253314) Avail: CASI HC A03/MF A01

Research has concentrated on the excitation and stabilization of the beam-breakup (BBU) instability in high current, long-pulse electron beam transport through microwave cavity systems. Electron beams are generated by the Michigan Electron Long Beam Accelerator (MELBA) at parameters: 0.7 to 0.8 MV, I(sub injected) = 40 to 400 A, and pulse length = 0.5 microsec. Major accomplishments include: (1) successful excitation of the beam-breakup (BBU) instability by microwave priming of the first cavity of a ten-RF cavity system; (2) measurements of BBU growth as a function of priming frequency, confirming that the TM(sub 110) BBU mode was responsible for the growth; (3) characterization of the BBU growth rate as a function of magnetic field and e-beam current; (4) the first experiments demonstrating that external-coupled-cavities reduce the growth rate for the BBU instability; and (5) development of a theory for the beam breakup instability in quadrupole and solenoidal electron beam transport systems. GRA

N93-10379 Oregon Graduate Inst. of Science and Technology, Beaverton.
STABILITY OF COUPLED SEMICONDUCTOR DIODE LASERS Ph.D. Thesis
David Jerome Bossert 1992 316 p
Avail: Univ. Microfilms Order No. DA9222644

This dissertation investigates the stability of self and mutually coupled semiconductor diode lasers. Theoretical analysis is based on coupled rate equations which follow from time-dependent coupled mode theory, including complex coupling coefficients describing optical interactions between the lasers. Phase-locking conditions and small signal stability properties are analyzed for the case of two mutually coupled lasers, including self-coupling. These are found to be strongly influenced by both the linewidth enhancement parameter alpha and the phase of the coupling coefficient. A wide locking bandwidth and large mode suppression are shown to be incompatible due to a non-zero alpha. Two different forms of stability are identified. The model is applied to the cases of one and two diode coupled at a distance. Systematic experiments have been designed to study the stability of these systems as a function of coupling magnitude and phase. Careful spectral and coherence measurements are compared directly to numerical simulations from the rate equation model, including nonlinear gain compression and spontaneous emission noise. Modes, mode selection and dynamic stability properties are shown to be well accounted for by the rate equation approach. An accurate comparison is enabled through independent measurements of the model parameters for the experimental devices. Further, techniques to reliably determine the level of optical coupling have been developed. Three distinctive operating regimes are demonstrated with respect to the coupling magnitude. At low coupling level, mode selection is governed by phase stability. While all oscillating modes are stable, phase-locking is found to be limited by spontaneous emission noise throughout most of this regime. These findings are corroborated through numerical integration of an approximate form of the rate equations. In contrast, at large coupling levels, mode selection and dynamic stability are dominated by threshold gain considerations; where the most stable mode minimizes the population inversion. Here, the effect of alpha on the stability properties is minimal. Intermediate levels of coupling are characterized by extreme dynamic instability, resulting in spectral broadening and a near total loss of coherence in the coupled system. This regime is interpreted as a transition between phase- and gain-dominated modes of operation, initiated by the system's inability to damp relaxation oscillations. Dissert. Abstr.

N93-10412# North Carolina Univ., Chapel Hill. Dept. of Chemistry.
THERMO-OPTICAL SWITCHING IN Si BASED ETALONS
S. T. Feng and E. A. Irene 13 Jul. 1992 29 p
(Contract N00014-89-J-1178)
(AD-A253139; TR-43) Avail: CASI HC A03/MF A01

Thermo-optical switching in Si based etalons has been demonstrated in two device structures. In one experiment the switching time of a Si etalon has been reduced from msec. to microsec. by choosing a probe beam of shorter wavelength in an external switching configuration. The switching time has been further improved to the ns range by the use of a 1.06 m Nd:YAG laser pump which is presumed to give rise to a thermo-refractive change in the Si etalon and at the same time the switching threshold energy has been reduced to -1 micron as compared to -1 mJ for a CO2 laser pump. In comparing Si etalons with thicknesses of 400, 72, and 1.5 microns, we find that the 72 micron etalon exhibits the best behavior in terms of low threshold power, high speed, and contrast. In addition, effects of the pump beam intensity on the signal pulse shape has been investigated which indicates a multiple interference fringe shift and transverse thermal relaxation dynamics. The second experiment used a Si/Si3N4 film structure in which the index of the Si3N4 is approximately the square root of the index of the Si, and the optical thickness of the Si3N4 is an odd quarter wavelength multiple of the probe beam. This yielded a minimum in surface reflection. Based on an increase of the optical thickness with pump beam heating, a probe beam reflection

has been switched out with a high contrast ratio (switched on/off) of 61:1. Different structures using different pump beams are discussed and the restriction of the film optical thickness has been investigated. GRA

N93-10429# Oak Ridge National Lab., TN.
RESONANCE IONIZATION OF RUBIDIUM USING SEQUENTIAL DIODE LASER-DRIVEN TRANSITIONS
R. W. Shaw, J. P. Young, and J. M. Ramsey 1992 8 p Presented at the 6th International Symposium on Resonance Ionization Spectroscopy and Its Application, Santa Fe, NM, 24-29 May 1992
(Contract DE-AC05-84OR-21400)
(DE92-014468; CONF-920574-1) Avail: CASI HC A02/MF A01

Diode laser excitation of rubidium atoms at the D2 line followed by (1 + 1) ionization using a pulsed dye laser was examined. Mass-resolved D2 spectra were recorded for both natural isotopes. Excitation using two sequential diode laser photons was accomplished by counterpropagating the beam from the 780 nm laser and one from a 775.8 nm laser; the latter excites Rb from the (sup 5)P(sub 3/2) level to the (sup 5)D(sub 5/2) level at 25704 cm(exp -1). A photon from the R6G laser then ionized the atom. Spectra resulting from scanning the second diode laser--with the first an an off-resonance fixed frequency revealed both two-photon and sequential (1 + 1) processes. DOE

N93-10611# Florida Univ., Gainesville. Dept. of Chemistry.
DEVELOPMENT OF LASER EXCITED ATOMIC FLUORESCENCE AND IONIZATION METHODS
J. D. Winefordner 1991 43 p
(Contract DE-FG05-88ER-13881)
(DE92-016199; DOE/ER-13881/T1) Avail: CASI HC A03/MF A01

Progress made during the period of 1 May 1988 to 31 Dec. 1991 is reported. The topics discussed include the following: (1) theoretical considerations of the ultimate detection powers of laser fluorescence and laser ionization methods; (2) experimental evaluation of laser excited atomic fluorescence; (3) fundamental studies of atomic and molecular parameters in flames and plasmas; and (4) other studies. DOE

N93-10697# Duke Univ., Durham, NC. Dept. of Physics.
UV/XUV FEL STORAGE RING AND LINAC Final Report, 1 Jul. 1988 - 31 Dec. 1991
John M. Madey 31 Dec. 1991 6 p
(Contract F49620-88-C-0100)
(AD-A253307; AFOSR-92-0693TR) Avail: CASI HC A02/MF A01

The following tasks were accomplished: (1) determination of the optical strengths and sensitivities of the quadrupole and sextupole magnets of the ring, and review requirements for the software control system, (2) analysis of the design of the synchrotron radiation absorbers and vacuum components for the FEL and synchrotron radiation straight sections of the ring, (3) design and assembly of the remaining components and subsystems of the proposed UV/XUV storage ring and linac, and (4) installation and testing of the components in the new Duke FEL Laboratory. GRA

N93-10698# University of Western Ontario, London. Dept. of Physics.
MERGED BEAM STUDIES OF LASER STIMULATED RADIATIVE RECOMBINATION Final Report, 1 Jul. 1988 - 31 Dec. 1991
J. B. Mitchell 31 May 1992 15 p
(Grant AF-AFOSR-0327-89; AF Proj. 2301)
(AD-A253308; AFOSR-92-0684TR) Avail: CASI HC A03/MF A01

A brief description is given of a multi-pass cavity assembly, installed recently in the merged beams apparatus. Results for the recombination of molecular ions to give neutrals in specific principal quantum number states are presented. GRA

N93-10703# Air Force Inst. of Tech., Wright-Patterson AFB, OH. Foreign Aerospace Science and Technology Center.
DESIGN OF LASER OPTICAL SYSTEMS
Zhang Ping and Ye Fei 9 Jan. 1992 15 p Transl. into ENGLISH from Jiguang Zazhi (China), v. 11, no. 1, 1990 p 14-18
(AD-A254247; FASTC-ID(RS)T-1478-90) Avail: CASI HC A03/MF A01

This article gives basic rules associated with Gaussian beam transforms in optical systems. It discusses optimum selections for system light passing aperture diameters, and, after researching Gaussian beam diameter system intercepts or truncations, produces rules for diffraction transformations. When designing laser optical systems, it is necessary to study transformations associated with various types of optical instruments or systems with regard to Gaussian beams. This is in order to find out the rules or patterns for transmission and transformation. This is an important topic in the practical applications of lasers. It is also a key question in the design of top quality laser systems. GRA

N93-10720# Oregon State Univ., Corvallis. Dept. of Physics.
MATTER-WAVE INTERFEROMETRY WITH LASER COOLED ATOMS Progress Report
David McIntyre Jul. 1992 12 p
(Contract N00014-91-J-1198)
(AD-A254000) Avail: CASI HC A03/MF A01

The matter wave source for this experiment will be a cold beam of rubidium atoms leaving an atomic funnel. The funnel uses two-dimensional magneto-optic trapping to achieve transverse cooling as well as spatial compression of the beam. With laser beams from all six directions, the atoms are also cooled, but not trapped, along the axis of the magnetic field. We have two ideas we are pursuing for loading atoms into the funnel. The first is to use atoms from the thermal (200 C) beam which are cooled longitudinally with chirped laser cooling. The second is to use a room temperature vapor cell and load atoms from the low velocity tail of the Maxwellian distribution. The second idea would simplify the experiment since the chirped laser cooling could be skipped. The question is whether the vapor cell funnel can produce a beam as intense as the funnel loaded from the cooled atomic beam. GRA

N93-10722# Air Force Inst. of Tech., Wright-Patterson AFB, OH. Foreign Aerospace Science and Technology Center.
INFLUENCE OF FLOW VELOCITY ON THE OUTPUT POWER OF HIGH PRESSURE CW CO2 LASERS
Zexiang Chu, Liyin Chen, and Zhongxiang Wu 9 Jan. 1992 13 p Transl. into ENGLISH from Zhonggou Jiguang (China), v. 17, no. 5, 1990 p 301-304
(AD-A254240; FASTC-ID(RS)T-1477-90) Avail: CASI HC A03/MF A01

This article studies the overall effects of flow speed and pressure on CO2 laser device characteristics within a range of even greater flow speeds and high pressure taking the ocassion to investigate the potential displayed by high pressure instruments. Considering the lens length to be 5 cm and the lens height to be 3 cm, under conditions of relatively high pressure, we select the light cavity or chamber position to be 0.5-5.5 cm. Primary consideration is placed on positions where output light powers are relatively high, lying close to the upper reaches of the gas flow. Besides this, under the low pressures, the range of permissible degrees of output power coupling is relatively large. GRA

N93-10725# Air Force Inst. of Tech., Wright-Patterson AFB, OH.
SYSTEM DESIGN AND RELAXATION OSCILLATIONS OF A TITANIUM-SAPPHIRE LASER M.S. Thesis
William L. Erikson Aug. 1992 113 p
(AD-A254264; AFIT/CI/CIA-92-072) Avail: CASI HC A06/MF A02

A general method for designing a laser system is presented. Using the Ti:sapphire laser as an example, the requirements of stability, astigmatic compensation, and matching of the pump and cavity modes are addressed. Investigations into the relaxation

oscillations of a Ti-sapphire laser are reported. Using four level laser rate equation theory, a technique is developed for analyzing relaxation oscillations exhibited by a laser. This technique presents a new and simple method for measuring the upper state lifetime and intrinsic cavity losses of a laser system. Beam-like vector solutions to Maxwell's equations are also presented. These solutions present a more detailed description of the polarization properties of laser beams. Experimental evidence of these properties is shown using an Argon laser. GRA

N93-10739# Lawrence Livermore National Lab., CA.
MEASUREMENTS AND MODELING OF LASER IRRADIANCE IN THE HIGH-POWER THIRD-HARMONIC NOVA FOCUS. VOLUME A: REPORT
P. Wegner May 1992 35 p
(Contract W-7405-eng-48)
(DE92-016746; UCRL-ID-110480-Vol-A) Avail: CASI HC A03/MF A01

The scope of this report is two-fold. The first objective is to provide useful laser drive data for target physicists. One way to do this is to analyze the beam in detail at all of the sampled planes, assemble the results in an organized fashion and let the experiments pick out the beam parameters that apply to their particular experiments. This approach has advantages in that it fully documents the experiment and provides the individual details of the beam at various planes that may in fact be needed for some experiments. Therefore, a data book has been compiled as a companion document to this report. The data book contains analysis output for the laser irradiance in the 20 focal planes photographed. The analysis consists of irradiance line scans, plots of radially-averaged irradiance, integrated irradiance (power) versus radius, and irradiance probability density and distribution functions. A 16-level grey-scale beam image with overlaid contour plot is provided. A parallel analysis of the Fourier spectrum of the irradiance at each plane is compiled in the second half of the data book. The second objective of this report is to sort out the principle beam characteristics from the details and to relate this information to laser design and performance. The means by which this is accomplished is through the development of a Nova beam model which is tweaked in a controlled fashion until it closely approximates major aspects of the data. The model indicates that much of the beam behavior in the region of focus is due to only a few aberrations. Analysis of the model at best focus and planes up to 1.5 mm on either side of focus show good agreement with the data. The beam model should also prove useful to target-experiment modelers who are interested in simulating the laser irradiance throughout the focal region. DOE

N93-10768# Naval Research Lab., Washington, DC.
STUDIES IMPACTING THE DESIGNS OF FREE ELECTRON LASERS Final Report, Jan. - Jun. 1992
Cha-Mei Tang 4 Aug. 1992 10 p
(AD-A254293) Avail: CASI HC A02/MF A01

The purpose was to investigate the effect of energy spread, emittance, laser pulse shape, and misalignment on x-rays generated by Thomson backscattering using lasers as undulators, and their applications; and to address compact FEL issues. The approach was to formulate Thomson, also known as Compton, backscattered radiation for an electron beam with energy spread and finite emittance and for a laser undulator of arbitrary pulse shape and misalignment. This formulation is to be implemented on the computer. The computer code will be applied to a variety of experimental configurations including Vanderbilt and Duke FEL parameters. We will also evaluate other configurations and medical applications. For FEL's to become a widely utilized laser source, they must become more compact, less expensive, and more user friendly. GRA

N93-10799# Washington State Univ., Pullman. Dept. of Chemistry.
INTERNAL EXPLOSION IN LASER ABLATION OF SUPERCONDUCTING TARGETS Interim Technical Report
D. L. Lin, X. Li, Z. D. Liu, and Thomas F. George Jun. 1992 23 p
(Contract N00014-90-J-1193)
(AD-A253701; TR-90; WSU/92/90) Avail: CASI HC A03/MF A01

The temperature profile inside a superconducting target in laser ablation is calculated for laser pulses of various shapes. The calculation is based on the equation of heat conduction. All parameters characterizing the target material are assumed to be temperature dependent and are determined empirically by extrapolating experimental data to the melting point. The receding velocity of the vapor-solid interface is determined by the dynamical balance of energy. Our calculation shows that, in general, there exist subsurface overheating spots at different instants as long as the laser pulse intensity is strong enough. The dependence of their occurrence on the pulse shape is analyzed, and conditions to avoid them without jeopardizing the deposition process are discussed. GRA

N93-10827# Stanford Univ., CA. Dept. of Physics.
LOW-FREQUENCY NOISE REDUCTION IN SQUID MEASUREMENTS USING LASER SWITCHING Final Report, 15 Jan. 1990 - 15 Jan. 1992
Blas Cabrera Jun. 1992 28 p
(Contract N00014-90-J-1528)
(AD-A253821) Avail: CASI HC A03/MF A01

Reduce SQUID noise in measurements which are intrinsically low frequency or dc. Such low frequency measurements fall below the 1/f knee of the noise energy spectrum and the SQUID performance is degraded substantially below the often quoted white noise levels. We intend to improve the low frequency noise using input circuit modulation at a frequency above the 1/f knee, up-converting the signal in frequency. In our scheme the noise should approach the SQUID white noise floor and the slew rates should approach the original SQUID system slew rate. GRA

N93-10855# Air Force Inst. of Tech., Wright-Patterson AFB, OH. Foreign Technology Div.
LASER JOURNAL
3 Dec. 1991 11 p Transl. into ENGLISH from Jiguang Zazhi (China), v. 10, no. 5, 1989 p 231-232 and title page
(AD-A254106; FTD-ID(RS)T-0847-90) Avail: CASI HC A03/MF A01

The major results of an experimental study of a slab Nd:YAG laser are reported in the article; the laser was successfully developed by the authors. The major findings include the following: (1) a method for cooling the blended flowing air and water, as well the related experimental parameters; (2) by using a crossed lens cavity, the authors further improved the anomalous capability within the compensation cavity of the slab laser, as well as higher insensitivity of the system to maladjustment; and (3) a processing technique and major points of slab YAG laser medium. GRA

N93-10864# California Univ., Berkeley. Lawrence Berkeley Lab.
AN INFRARED FREE-ELECTRON LASER FOR THE CHEMICAL DYNAMICS RESEARCH LABORATORY
D. Vaughan, comp. Apr. 1992 150 p
(Contract DE-AC03-76SF-00098)
(DE92-017018; LBL-Pub-5335) Avail: CASI HC A07/MF A02

This document describes a free-electron laser (FEL) proposed as part of the Chemical Dynamics Research Laboratory (CDRL), a user facility that also incorporates several advanced lasers of conventional design and two beamlines for the ALS. The FEL itself addresses the needs of the chemical sciences community for a high-brightness, tunable source covering a broad region of the infrared spectrum--from 3 to 50 microns. All of these sources, together with a variety of sophisticated experimental stations, will be housed in a new building to be located adjacent to the ALS. The radiation sources can be synchronized to permit powerful two-color, pump-probe experiments that will further our fundamental understanding of chemical dynamics at the molecular level, especially those aspects relevant to practical issues in combustion chemistry. The technical approach adopted in this design makes

use of superconducting radiofrequency (SCRF) accelerating structures. The primary motivation for adopting this approach was to meet the user requirement for wavelength stability equal to one part in 10(exp 4). Previous studies concluded that a wavelength stability of only one part in 10(exp 3) could be achieved with currently available room-temperature technology. In addition, the superconducting design operates in a continuous-wave (CW) mode and hence offers considerably higher average optical output power. It also allows for various pulse-gating configurations that will permit simultaneous multiuser operations. A summary of the comparative performance attainable with room-temperature and superconducting designs is given. The FEL described in this report provides a continuous train of 30-ps micropulses, with 100 micro-J of optical energy per micropulse, at a repetition rate of 6.1 MHz. The device can also deliver pulses at a cw repetition rate of 12.2 MHz, with a peak power of 50 micro-J per micropulse. DOE

37 MECHANICAL ENGINEERING

Includes auxiliary systems (nonpower); machine elements and processes; and mechanical equipment.

N93-10290# Battelle Columbus Labs., OH.
NOVEL SEALS AND SPECIALTY COMPONENT ATTACHMENT MECHANISMS FOR RESPIRATORY PROTECTION SYSTEM (RESPO 21) Final Report
Thomas A. Pettenski Oct. 1992 80 p
(Contract DLA900-86-C-2045)
(AD-A253395) Avail: CASI HC A05/MF A01

To establish the design characteristics of attachment mechanisms for use in the mounting of mask seals and specialty components into the Respiratory Protection System 21 (RESPO 21) was conducted. These design characteristics include but are not limited to keeping the seal/attachment mechanism low in profile, allowing easy seal or component replacement, and incorporating multiple layers of material within the seal and attachment mechanism. Alternative seal concepts were investigated for the interface between the mask and the mask wearer. These concepts include pneumatic bladders, encapsulated gels, laminated foams, and combinations of the above. Prototype seals of the encapsulated gel-type and the pneumatic type were fabricated to demonstrate feasibility and assist with the development of attachment mechanisms. Approaches for attaching a seal to a mask, both hard-shell and soft-shell, were identified. None were fabricated due to time limitations and availability of appropriate seals and masks. GRA

N93-10367 Rahtikone Oy (Finland).
STEERING SYSTEM OF A VEHICLE, SUCH AS A SNOW REMOVING MACHINE FOR AIRFIELDS Patent
Esko T. Rantalahti, inventor (to Rahtikone Oy) 17 Dec. 1991 9 p
(CA-Patent-Appl-SN-1293201; Int-Patent-Class-B62D-5/12; CTN-92-60365) Copyright Avail: Micromedia Ltd., Technical Information Centre, 165 Hotel de Ville, Place du Portage, Phase 2, Hull, Quebec J8X 3X2, Canada HC/MF

An improved steering system is disclosed for a vehicle comprising a cabin with front wheels, which are steered by a steering wheel, and a rearward portion carrying a drive unit and with driven rear wheels. The rearward portion is journalled about a vertical shaft to the forward portion of the vehicle, and a second separate steering mechanism is provided for steering the rearward portion. The second separate steering mechanism of the rearward portion comprises a control unit whereby it may be synchronized to operate in an opposite turning direction to that of the steering movements of the front wheels. The control unit is adapted to lock the rearward portion in a desired position, so that, for example, the vehicle can be driven diagonally with the side first. The second steering mechanism comprises a separate hydraulic system controlled from the control unit. Sensors are connected for sensing the steering angle of both the steering mechanisms, such that signals from the sensors may cause the steering of the rearward portion to follow the steering of the front wheels. The steering system of the invention is particularly applicable to snow removal machines used on airfields. In such machines, the front and rear wheel shafts are often 10-15 m distant from each other, but the invention enables easy and reliable linkage without the need for heavy shafts. The invention also enables a long snow-removing machine to turn on a very small radius, which speeds up movements and operation when clearing airfields. CISTI

N93-10381# Oak Ridge National Lab., TN.
REVIEW AND ANALYSIS OF CHECK VALVE FAILURE DATA
M. D. Todd and D. A. Casada 1992 7 p Presented at the Symposium on Testing of Pumps and Valves in Nuclear Power Plants, Washington, DC, 21-23 Jul. 1992
(Contract DE-AC05-84OR-21400)
(DE92-014462; CONF-920732-3) Avail: CASI HC A02/MF A01

Check valve operating problems in recent years have resulted in significant operating transients, increased cost and decreased system availability. There has been, in response, additional attention given to check valves by utilities, as well as the US Nuclear Regulatory Commission and the American Society of Mechanical Engineers Operation and Maintenance Committee. All these organizations have the fundamental goal of ensuring reliable operation of check valves. A key ingredient to an engineering-oriented reliability improvement effort is a thorough understanding of relevant historical experience. Oak Ridge National Laboratory is currently conducting a detailed review of historical failure data available through the Institute of Nuclear Power Operation's Nuclear Plant Reliability Data System. The focus of the review is on check valve failures that have involved significant degradation of the valve internal parts. A variety of parameters are being considered during the review, including size, age, system of service, method of failure discovery, the affected valve parts, attributed causes, and corrective actions. DOE

N93-10622# Department of Defense, Washington, DC. Safety Diagnostic Div.
EMERGENCY DIESEL GENERATOR RELIABILITY AT DEPARTMENT OF ENERGY (DOE) FACILITIES
Apr. 1992 45 p
(DE92-011888; DOE/DP-0098T) Avail: CASI HC A03/MF A01

This report is the culmination of the first phase of a comprehensive effort by the Department of Energy (DOE) Defense Programs (DP) Office of Self-Assessment and Emergency Management (DP-9) to assess the reliability and availability of emergency power supplies (i.e., standby or backup supplies providing electric power to systems or equipment that perform functions important to safety) at DOE management concerns over the recent number of reported failures of emergency and back-up supplies to provide power when required. Augmented Evaluation Team (AET) on-site reviews were conducted during the week of September 30, 1991 at Rocky Flats (RF), and the week of October 7, 1991 at the Richland (RL) and Savannah River (SR) sites to investigate the failures. The AET reviews focused on Emergency Diesel Generator (EDG) failures because they were identified as the dominant contributor to power supply failures (46 of the 77 failures involved EDG's, as opposed to other sources such as batteries, motor-generator sets, etc.). The RF, RL, and SR sites were chosen because they were among the leaders in numbers of EDG failures. The objectives of the AET investigations were to collect, analyze, and document factual information concerning the causes, conditions, and circumstances surrounding EDG failures, to conduct a preliminary assessment of the safety significance of the failures and the site specific and generic safety implications for DOE facilities, and to identify appropriate follow-on actions necessary to complete the overall assessment of the adequacy of emergency and back-up power sources. This report presents the AET findings concerning the reliability of EDG's at the RF, RL, and SR sites, and the safety significance of EDG failures. DOE

N93-10634# Oak Ridge National Lab., TN.
STRESS MODIFIED WELDING PROCESS FOR IRRADIATED MATERIALS
C. A. Wang (Auburn Univ., AL.), B. A. Chin (Auburn Univ., AL.), and M. L. Grossbeck 1992 14 p Presented at the 3rd International Conference on Trends in Welding Research, Gatlinburg, TN, 1 Jun. 1992
(Contracts DE-AC05-84OR-21400; DE-FG05-91ER-54134)
(DE92-017131; CONF-9206173-4) Avail: CASI HC A03/MF A01

Prior investigations have shown that catastrophic cracking occurs during the repair welding of irradiated material. This cracking has been linked to minute amounts of helium in the material which are produced during irradiation. Experiments have shown that type 316 stainless steel, containing helium levels greater than 2.5 atomic parts per million (appm), is susceptible to cracking upon cooling when welded using the gas tungsten arc (GTA) process under lateral constraint. The cracking has been hypothesized to be caused by stress-assisted helium bubble growth and repture at grain boundaries. In this study, the effects of stress state on the helium bubble growth process were investigated. Autogenous bead-on-plate welds were produced in type 316 stainless steels, containing 256 appm helium. Welds were produced using normal lateral constraint and compressive lateral constraint. The application of a small compressive constraint suppressed previously observed catastrophic cracking. Detailed examinations conducted after welding showed a dramatic change in helium bubble morphology. Grain boundary bubble growth along directions parallel to the weld was suppressed. The results suggest that stress state modification may be used to suppress or eliminate helium-induced cracking encountered during the joining of irradiated materials. DOE

N93-10635# Lawrence Livermore National Lab., CA.
A COMPUTATIONAL STUDY OF PROJECTILE MELT IN IMPACT WITH TYPICAL WHIPPLE SHIELDS
M. L. Alme, P. G. Eltgroth, and C. E. Rhoades, Jr. 20 May 1992 27 p
(Contract W-7405-eng-48)
(DE92-017137; UCRL-ID-110842) Avail: CASI HC A03/MF A01

This report presents the results of computer simulations of the impact of aluminum projectiles onto typical aluminum Whipple shields at speeds of 6 km/s greater. The objective of these simulations, which were performed with the CALE hydrodynamics code, was to determine the extent of projectile and target material melting. The approach was to perform a matrix of computer simulations varying the impact speed from 6 to 14 km/s and varying the areal density of the shield from 5 percent to 80 percent of the centerline areal density of the projectile. The projectile diameter was held fixed at 9.5 mm (3/8 in.) for this matrix. The melt state of the projectile material and the shield material was assessed after release of the initial shock. One significant conclusion from this study is that for 8 km/s impact of an aluminum projectile onto an aluminum shield, a significant fraction of the projectile does not reach the threshold for incipient melt. For aluminum/aluminum impact, a Whipple shield with a thickness of 15 percent of the projectile diameter is very effective against a projectile at this velocity. Taken with our simulation results, we presume this shield effectiveness implies that the projectile material below the incipient melt threshold is fragmented into very small particles. A second conclusion is that for the thicker bumpers considered in the simulation matrix a significant amount of the bumper material that is likely to be ejected into the debris cloud is not melted, even for 10 km/s and 12 km/s impacts. DOE

N93-10740# Washington State Univ., Pullman.
THE DEVELOPMENT OF COMPUTATIONAL METHODS OF ADHESION AND ADHESIVE SCIENCE AND TECHNOLOGY Final Report
William E. Johns 8 Jul. 1992 13 p
(Contract N00014-90-J-1298)
(AD-A253758) Avail: CASI HC A03/MF A01

The development of computational methods for describing the adhesive process was explored. Serious problems currently face the adhesive technologist in that some of the best models for understanding adhesion, i.e., Lewis acid/base neutralization reactions, are based on empirical methods. It was thought that computational methods may show a way for addressing this and provide a first principle basis for understanding adhesion. Current limitations in software, and computer hardware do not yet provide for using computers as a common tool for understanding the adhesive process. HOMO and LUMO values are thought to be directly identified with Lewis acid/base reaction pairs. These values derived using both ab initio and semi-empirical methods for a variety of molecules and docked pairs of molecules yield a unreasonably wide ranges of values and thus, are of very limited value. Further work in our understanding of quantum physics and software to deal with large arrays of atoms in a rigorous manner will be needed before computational methods can directly speak to the problems of adhesion science. GRA

N93-10891*# Texas A&M Univ., College Station. Turbomachinery Lab.
COMPRESSIBLE AND INCOMPRESSIBLE FLUID SEALS: INFLUENCE ON ROTORDYNAMIC RESPONSE AND STABILITY
Howard D. Thames 1 Sep. 1992 31 p Sponsored by NASA. Lewis Research Center
(RF Proj. 4502)
(NASA-CR-190746; NAS 1.26:190746) Avail: CASI HC A03/MF A01

The flow field inside a whirling annular seal operating a Reynolds numbers of 12,000 and 24,000 and a Taylor number of 6,600 was measured. The rotor was mounted eccentric (50 percent) upon the facilities shaft which resulted in a circular orbit at a whirl ratio of 1.0. Three papers which summarize the work were written and are presented. Addition measurements were performed for the annular seal operating at an eccentricity ratio of 10 percent for Re = 24,000 and Ta = 6,600. A labyrinth seal was also installed into the facility and operated at an eccentricity ratio of 50 percent at the same Reynolds and Taylor numbers. These data are currently being reduced and analyzed. For individual titles, see N93-10892 through N93-10894.

N93-10892*# Texas A&M Univ., College Station. Turbomachinery Lab.
EXPERIMENTAL STUDY OF THE FLOW FIELD INSIDE A WHIRLING ANNULAR SEAL
Gerald L. Morrison, Robert E. DeOtte, Jr., and H. Davis Thames, III *In its* Compressible and Incompressible Fluid Seals: Influence on Rotordynamic Response and Stability 1 Sep. 1992 11 p Presented at the 4th International Symposium on Transport Phenomena and Dynamics in Rotating Machinery, Honolulu, HI, 5-8 Apr. 1992 (For primary document see N93-10891 01-37)
(Grant NAG3-181)
Avail: CASI HC A03/MF A01

The flow field inside a whirling annular seal was measured using a 3-D Laser Doppler Anemometer (LDA) system. The seal investigated has a clearance of 1.27 mm, a length of 37.3 mm, and is mounted on a drive shaft with a 50 percent eccentricity ratio. This results in the rotor whirling at the same speed as the shaft rotation (whirl ratio = 1.0). The seal is operated at Reynolds number of 12,000 and a Taylor number of 6,300 (3,600 rpm). The 3-D LDA system is equipped with a rotary encoding system which is used to produce phase averaged measurements of the entire mean velocity vector field and Reynolds stress tensor field from 0.13 mm upstream to 0.13 mm downstream of the seal. The mean velocity field reveals a highly three dimensional flow field with large radial velocities near the inlet of the seal as well as a recirculation zone on the rotor surface. The location of maximum mean axial velocity migrates from the pressure side of the rotor at the inlet to the suction side at turbulence kinetic energy. However, turbulence production and dissipation attain equilibrium fairly quickly with remaining relatively constant over the last half of the seal. Author

N93-10893*# Texas A&M Univ., College Station. Turbomachinery Lab.
TURBULENCE MEASUREMENTS OF HIGH SHEAR FLOW FIELDS IN A TURBOMACHINE SEAL CONFIGURATION
Gerald L. Morrison, Robert E. DeOtte, Jr., and H. Davis Thames, III. *In its* Compressible and Incompressible Fluid Seals: Influence on Rotordynamic Response and Stability 1 Sep. 1992 12 p Presented at the 1992 Conference on Advanced Earth-To-Orbit Propulsion Technology, Huntsville, AL, 19-21 May 1992 (For primary document see N93-10891 01-37)
(Grant NAG3-181)
Avail: CASI HC A03/MF A01

The mean velocity and Reynolds stress tensor throughout a whirling annular seal are presented. The data was collected with a three dimensional laser Doppler velocimeter using phase averaging. Two axial flow conditions (Re = 12,000 and 24,000) were studied at one shaft speed (Ta = 6,600). The eccentricity and whirl ratios were 50 and 100 percent, respectively. There is a region of high axial momentum in this region is higher in the low Reynolds number case due to an axial recirculation zone that occurs on the suction side of the rotor at the inlet. The recirculation zone does not occur in the high Reynolds number case. At both Reynolds numbers, there is a recirculation zone on the rotor surface in the pressure side of the inlet. This recirculation zone extends from 20 to 200 degrees rotor zenith in the tangential direction, and is one third of a clearance wide radially. The high Reynolds number recirculation zone is 1.5 mean clearances long, while the low Reynolds number zone extends 2 mean clearances downstream. When compared to previous studies, it is apparent that the tangential momentum is no greater for a seal with whirl than for one without if other parameters are constant. Areas of high tangential momentum occur in the clearance where the axial momentum is low. Average exit plane tangential velocities in the high Reynolds number case are 1.5 times greater than those in the other flow case. These results are in general agreement with predictions made by other investigators. Author

N93-10894*# Texas A&M Univ., College Station. Turbomachinery Lab.
AN EXPERIMENTAL TECHNIQUE FOR PERFORMING 3-D LDA MEASUREMENTS INSIDE WHIRLING ANNULAR SEALS
Gerald L. Morrison, Mark C. Johnson, Robert E. DeOtte, Jr., H. Davis Thames, III., and Brian G. Wiedner *In its* Compressible and Incompressible Fluid Seals: Influence on Rotordynamic Response and Stability 1 Sep. 1992 7 p Presented at the Sixth International Symposium on Application of Laser Techniques to Fluid Mechanics, Lisbon, Portugal, 20-23 Jul. 1992 Sponsored by NASA. Lewis Research Center (For primary document see N93-10891 01-37)
Avail: CASI HC A02/MF A01

During the last several years, the Fluid Mechanics Division of the Turbomachinery Laboratory at Texas A&M University has developed a rather unique facility with the experimental capability for measuring the flow field inside journal bearings, labyrinth seals, and annular seals. The facility consists of a specially designed 3-D LDA system which is capable of measuring the instantaneous velocity vector within 0.2 mm of a wall while the laser beams are aligned almost perpendicular to the wall. This capability was required to measure the flow field inside journal bearings, labyrinth seals, and annular seals. A detailed description of this facility along with some representative results obtained for a whirling annular seal are presented. Author

N93-10519 British Columbia Univ., Vancouver. Dept. of Mechanical Engineering.
DYNAMICS OF AN ORBITING FLEXIBLE MANIPULATOR
J. K. Chan and V. J. Modi *In* Carleton Univ., Proceedings of the Twelfth Canadian Congress of Applied Mechanics, Volumes 1 and 2 May 1989 p 398-399 (For primary document see N93-10466 01-31)
Copyright Avail: Canadian Society for Mechanical Engineering, 2050 Mansfield St., Suite 700, Montreal, Quebec H3A 1Z7 Canada

N93-10572 Missouri Univ., Rolla. Dept. of Mechanical and Aerospace Engineering.
MODELLING AND CONTROL OF ROBOTIC ARMS FABRICATED FROM ORTHOTROPIC MATERIALS
K. Krishnamurthy, K. Chandrashekhara, and S. Roy *In* Carleton Univ., Proceedings of the Twelfth Canadian Congress of Applied Mechanics, Volumes 1 and 2 May 1989 p 864-865 (For primary document see N93-10466 01-31)
Copyright Avail: Canadian Society for Mechanical Engineering, 2050 Mansfield St., Suite 700, Montreal, Quebec H3A 1Z7 Canada

N93-10573 Waseda Univ., Tokyo (Japan). Dept. of Mechanical Engineering.
MODELLING OF FLEXIBLE MULTIBODY DYNAMICS AND A COMPUTER METHOD VIA THE BOND GRAPH METHOD
Hiroaki Yoshimura, Katsuhide Fujita, Hideo Nakano (Sagami Inst. of Tech., Fujisawa, Japan), and Takehiko Kawase *In* Carleton Univ., Proceedings of the Twelfth Canadian Congress of Applied Mechanics, Volumes 1 and 2 May 1989 p 866-867 (For primary document see N93-10466 01-31)
Copyright Avail: Canadian Society for Mechanical Engineering, 2050 Mansfield St., Suite 700, Montreal, Quebec H3A 1Z7 Canada

N93-10574 Waterloo Univ. (Ontario). Dept. of Mechanical Engineering.
CHAOTIC OSCILLATION OF A HIGH SPEED FLEXIBLE ARM ROBOT
M. F. Golnaraghi *In* Carleton Univ., Proceedings of the Twelfth Canadian Congress of Applied Mechanics, Volumes 1 and 2 May 1989 p 872-873 (For primary document see N93-10466 01-31)
Copyright Avail: Canadian Society for Mechanical Engineering, 2050 Mansfield St., Suite 700, Montreal, Quebec H3A 1Z7 Canada

N93-10590*# Boeing Aerospace Co., Seattle, WA.
EFFECTS OF LONG-TERM EXPOSURE ON LDEF FASTENER ASSEMBLIES
Steve Spear and Harry Dursch *In* NASA. Langley Research Center, LDEF Materials Workshop 1991, Part 2 Sep. 1992 p 633-648 (For primary document see N93-10578 01-27)
Avail: CASI HC A03/MF A03

N93-10592*# Centre National d'Etudes Spatiales, Toulouse (France).
SYSTEM RELATED TESTING AND ANALYSIS OF FRECOPA
Christian Durin *In* NASA. Langley Research Center, LDEF Materials Workshop 1991, Part 2 Sep. 1992 p 661-676 (For primary document see N93-10578 01-27)
Avail: CASI HC A03/MF A03

38 QUALITY ASSURANCE AND RELIABILITY

Includes product sampling procedures and techniques; and quality control.

N93-10307 Council for National Academic Awards (England).
THE DEVELOPMENT OF OPTICAL TECHNIQUES FOR COMPONENT INSPECTION IN THE AEROSPACE INDUSTRY
Ph.D. Thesis
Paul Anthony Irving 1991 176 p
Avail: Univ. Microfilms Order No. BRDX93367

A key requirement discussed within this thesis is feature extraction, in particular line segments. The Hough Transform is an elegant feature extraction technique for image analysis which performs well in noisy scenes and where occlusion may be problematic. Since its inception by P. V. C. Hough in 1962 for the detection of lines in bubble chambers, it has been widely researched, but minimal machine vision applications of the Hough

Transform have been implemented. This lack of an application for the Hough Transform, coupled with the need for experimentation of an optical probe based on a conventional granite bed Coordinate Measuring Machine (CMM) is addressed. This latter requirement is currently fulfilled by mechanical touch trigger probes, or where optical techniques are used, back-illuminated glass tables. The suitability of the Hough Transform for machine vision inspection tasks is analyzed, and conclusions are drawn on whether or not useful results can be obtained by mounting a camera on the head of a CMM coupled with illumination from above. The industrial application addressed a drill and rout template digitizing within the aerospace industry; furthermore, the Hough Transform is also demonstrated for object recognition with a view to automatic component datum setting. New methods are illustrated for efficient, high accuracy Hough Transformation. Techniques are given for peak extraction in Hough space, enabling the isolation of all peaks irrespective of comparative magnitude, thereby eliminating the need for thresholding. Software data structures are shown to be an efficient method for implementing the above, especially with the later processing stages involving component boundary segment parsing. Dissert. Abstr.

N93-10317# *European Space Agency. European Space* Research and Technology Center, ESTEC, Noordwijk *(Netherlands). Product Assurance and Safety Dept.*
RELIABILITY ASSURANCE REQUIREMENTS FOR ESA SPACE SYSTEMS
Mar. 1992 34 p
(ESA-PSS-01-30-Issue-2; ETN-92-91969) Copyright Avail: CASI HC A03/MF A01

The requirements of this specification were tailored by the *European Space Agency to fit the needs and constraints of each* program to which they are applied. In each case, the extent and details of applications of these requirements are described in the applicable Statement Of Work (SOW). The specifications are directly applicable to this specification to the extent specified *therein. The list is as follows: ESA PSS-01-0: product assurance* and safety policy and basic requirements for ESA space systems; *ESA PSS-01-10: product assurance management requirements for* ESA space systems; ESA PSS-01-20: quality assurance requirements for ESA space systems; ESA PSS-01-301: derating requirements and application rules for electronic components; ESA PSS-01-303: failure modes, effects and criticality analysis; ESA PSS-01-40: system safety requirements for ESA space systems; ESA PSS-01-50: maintainability requirements for ESA space systems; ESA PSS-01-401: ESA fracture control requirements; and MIL-HDBK-217: reliability prediction of electronic equipment. Policy and basic approach, reliability program management, reliability tasks testing, demonstration and data collection, the relationship between reliability requirements/activites and program phases, and contractor generated reliability documents, are detailed. ESA

39 STRUCTURAL MECHANICS

Includes structural element design and weight analysis; fatigue; and thermal stress.

For applications see *05 Aircraft Design, Testing and Performance* and *18 Spacecraft Design, Testing and Performance.*

N93-10198# Royal Aircraft Establishment, Farnborough (England).
AN EVALUATION OF A METHOD OF RECONSTITUTING FATIGUE LOADING FROM RAINFLOW COUNTING
B. H. E. Perrett 23 Nov. 1989 49 p
(RAE-TR-89057; BR113381) Copyright Avail: CASI HC A03/MF A01

On-line Rainflow analyses of load histories in structures may be used to reconstitute fatigue load sequences either for cycle-by-cycle damage analysis or for fatigue testing. This report describes work which used Rainflow counting and reversed Rainflow reconstitution to create 'extreme' sequences which have the same Rainflow count as the original sequence but which were intended to maximize and to mimimize the rate at which fatigue damage accumulated. Fatigue life and crack propagation tests have been used to compare 'extreme' sequences derived from the two load sequences standards FALSTAFF and MINITWIST. In addition a method has been used which allows the direction of the Rainflow cycles to be reproduced in the reconstituted sequence in order to recreate the highly structured features of the randomized 'extreme' sequences. Increases in fatigue lives by factors of up to five have been measured for the 'extreme' highly structured reconstituted sequences while all of the randomized reconstituted sequences have been shown to produce fatigue lives which are statistically the same as those under the original sequences FALSTAFF and MINITWIST. Author

N93-10310# Instituto de Pesquisas Espaciais, Sao Jose dos Campos (Brazil).
***A STUDY UPON STRUCTURAL OPTIMIZATION OF ELASTIC* ROTORS FOR MECHANICAL SYSTEMS M.S. Thesis [ESTUDO PARA OTIMIZACAO ESTRUTURAL DE ROTORES FLEXIVEIS EM SISTEMAS MECANICOS]**
Rogerio Lacourt Rodrigues Oct. 1991 129 p In PORTUGESE
(INPE-5376-TDI/471) Avail: CASI HC A07/MF A02

This work presents a methodology for performing structural *optimization of axisymmetric shells. Two kinds of objective functions* are treated: the structure mass or a quotient of its mass per *inertia moment about the symmetry axis. The constraints deal* with the eigenvalue of the fundamental vibration mode, displacements, and stresses at particular points in the structure and also its inertia properties. The structure is analyzed by means of a Finite Element Method, using a three-node axisymmetric shell *element. The design variables are defined as shell thicknesses at* these element nodes. The problem is included in the category of *sizing optimization. The sensitivity analysis is achieved using the* direct differentiation method. The non-linear programming problem thus established is solved employing the modified feasible directions method. The results of the application of this technique in optimizing four different configurations of flywheels for an attitude *control system actuator, a reaction wheel, are shown as* examples. Author

N93-10327# Sandia National Labs., Albuquerque, NM.
***MONITORING STRUCTURAL RESPONSE IN PRESSURIZED* ENVIRONMENTS. PART 2: APPLICATIONS**
D. P. Roach 1992 18 p *Presented at the ASME Pressure* Vessel and Piping Conference, New Orleans, LA, 21-25 Jun. 1992
(Contract DE-AC04-76DP-00789)
(DE92-015034; SAND-92-1028C; CONF-920631-39-Pt-2) Avail: CASI HC A03/MF A01

There are various methods which can be used to monitor the *structural response of electrical components, weapon systems,* pressure vessels, submerged pipelines, deep sea vehicles and offshore structures. Numerous experimental techniques have been developed at Sandia National Labs in order to measure the strain, displacement and acceleration of a structural member. These techniques have been successfully implemented in adverse environments of 25 ksi and 300 F. A separate paper discusses the performance of various instrumentation schemes, the environmental protection of these diagnostics under pressure, and the means by which data is extracted from a closed pressure system. In this paper, specific hydrostatic and dynamic pressure tests are used to demonstrate how these techniques are employed, the problems encountered, and the importance of the data obtained. DOE

N93-10372*# Georgia Inst. of Tech., Atlanta. School of Aerospace Engineering.
SAPNEW: PARALLEL FINITE ELEMENT CODE FOR THIN SHELL STRUCTURES ON THE ALLIANT FX/80
Manohar P. Kamat and Brian C. Watson Feb. 1992 40 p
(Grant NAG3-895)

(NASA-CR-190663; NAS 1.26:190663) Avail: CASI HC A03/MF A01

The results of a research activity aimed at providing a finite element capability for analyzing turbo-machinery bladed-disk assemblies in a vector/parallel processing environment are summarized. Analysis of aircraft turbofan engines is very computationally intensive. The performance limit of modern day computers with a single processing unit was estimated at 3 billions of floating point operations per second (3 gigaflops). In view of this limit of a sequential unit, performance rates higher than 3 gigaflops can be achieved only through vectorization and/or parallelization as on Alliant FX/80. Accordingly, the efforts of this critically needed research were geared towards developing and evaluating parallel finite element methods for static and vibration analysis. A special purpose code, named with the acronym SAPNEW, performs static and eigen analysis of multi-degree-of-freedom blade models built-up from flat thin shell elements. Author

N93-10385# International Centre for Theoretical Physics, Trieste (Italy).

A NONLINEAR OSCILLATORY PROBLEM

Qing-Qing Zhou Oct. 1991 8 p

(DE92-630203; IC-91/337) Avail: CASI HC A02/MF A01

We studied the nonlinear oscillatory problem of orthotropic cylindrical shells. We analyzed the character of the oscillatory system. The stable condition of the oscillatory system is given. DOE

N93-10427# Computer Sciences Corp., Minneapolis, MN.

CALCULATION OF ELASTIC-PLASTIC WAVE PROPAGATION ON THE CONNECTION MACHINE Final Report, Nov. 1990 - Sep. 1991

Mark A. Olson and Kent D. Kimsey (Ballistic Research Labs., Aberdeen Proving Ground, MD.) Jun. 1992 28 p

(Contract DAAL03-89-C-0088; DA Proj. 1L1-62618-AH-80)

(AD-A252429; BRL-TR-3360) Avail: CASI HC A03/MF A01

This report describes the parallel algorithms and data structures for implementing a 2-D multimaterial kernel of the wave-propagation code, HULL, on a Connection Machine. Computational performance is illustrated for a rod-plate impact problem with material strength described through an elastic-perfectly plastic formulation. The hydrodynamic behavior of materials is modeled via the gamma law and Mie-Gruneisen equations of state. GRA

N93-10453*# National Aeronautics and Space Administration. Lewis Research Center, Cleveland, OH.

CALCULATION OF STRESS INTENSITY FACTORS IN AN ISOTROPIC MULTICRACKED PLATE: PART 2: SYMBOLIC/NUMERIC IMPLEMENTATION

S. M. Arnold, W. K. Binienda (Akron Univ., OH.), H. Q. Tan (Akron Univ., OH.), and M. H. Xu (Akron Univ., OH.) Sep. 1992 44 p

(RTOP 510-01-50)

(NASA-TM-105823; E-7254; NAS 1.15:105823) Avail: CASI HC A03/MF A01

Analytical derivations of stress intensity factors (SIF's) of a multicracked plate can be complex and tedious. Recent advances, however, in intelligent application of symbolic computation can overcome these difficulties and provide the means to rigorously and efficiently analyze this class of problems. Here, the symbolic algorithm required to implement the methodology described in Part 1 is presented. The special problem-oriented symbolic functions to derive the fundamental kernels are described, and the associated automatically generated FORTRAN subroutines are given. As a result, a symbolic/FORTRAN package named SYMFRAC, capable of providing accurate SIF's at each crack tip, was developed and validated. Simple illustrative examples using SYMFRAC show the potential of the present approach for predicting the macrocrack propagation path due to existing microcracks in the vicinity of a macrocrack tip, when the influence of the microcrack's location, orientation, size, and interaction are taken into account. Author

N93-10455*# National Aeronautics and Space Administration. Lewis Research Center, Cleveland, OH.

CALCULATION OF STRESS INTENSITY FACTORS IN AN ISOTROPIC MULTICRACKED PLATE. PART 1: THEORETICAL DEVELOPMENT

W. K. Binienda (Akron Univ., OH.), S. M. Arnold, and H. Q. Tan (Akron Univ., OH.) Sep. 1992 21 p

(RTOP 510-01-50)

(NASA-TM-105766; E-7183; NAS 1.15:105766) Avail: CASI HC A03/MF A01

An essential part of describing the damage state and predicting the damage growth in a multicracked plate is the accurate calculation of stress intensity factors (SIF's). Here, a methodology and rigorous solution formulation for SIF's of a multicracked plate, with fully interacting cracks, subjected to a far-field arbitrary stress state is presented. The fundamental perturbation problem is derived, and the steps needed to formulate the system of singular integral equations whose solution gives rise to the evaluation of the SIF's are identified. This analytical derivation and numerical solution are obtained by using intelligent application of symbolic computations and automatic FORTRAN generation capabilities (described in the second part of this paper). As a result, a symbolic/FORTRAN package, named SYMFRAC, that is capable of providing accurate SIF's at each crack tip was developed and validated. Author

N93-10646# Lawrence Livermore National Lab., CA.

DYNA2D: A NONLINEAR, EXPLICIT, TWO-DIMENSIONAL FINITE ELEMENT CODE FOR SOLID MECHANICS: USER MANUAL

R. G. Whirley and B. E. Engelmann Apr. 1992 244 p

(Contract W-7405-eng-48)

(DE92-017310; UCRL-MA-110630) Avail: CASI HC A11/MF A03

This report is the User Manual for the 1992 version of DYNA2D, and also serves as an interim User Guide. DYNA2D is a nonlinear, explicit, finite element code for analyzing the transient dynamic response of two-dimensional solids. The code is fully vectorized and is available on several computer platforms. DYNA2D incorporates a large deformation formulation to allow maximum flexibility in modeling physical problems. Many material models are available to represent a wide range of material behavior, including elasticity, plasticity, composites, thermal effects, and rate dependence. Also, a variety of equations of state are available for modeling the hydrodynamic response of many materials, including explosives and propellants. In addition, DYNA2D has a sophisticated contact interface capability, including frictional sliding, single surface contact, and a new automatic contact option. DYNA2D contains a rezoner to allow nodes to be repositioned when the finite element mesh becomes excessively distorted during a calculation. This rezoner can be used in either an interactive graphics mode or an automatic mode. In addition, DYNA2D now contains a general remeshing option which allows a completely new mesh to be defined for a body during an analysis. A real-time analysis display option allows the analyst to view an evolving graphical display of the analysis results as they are calculated. A material model driver with interactive graphics display is incorporated into DYNA2D to permit accurate modeling of complex material response based on experimental data. This document provides the information necessary to apply DYNA2D to solve a wide range of engineering analysis problems. DOE

N93-10750# Army Armament Research, Development and Engineering Center, Watervliet, NY. Benet Lab.

STRENGTH-TOUGHNESS REQUIREMENTS FOR THICK-WALLED HIGH PRESSURE VESSELS Final Report

Joseph A. Kapp May 1992 18 p

(AD-A253756; ARCCB-TR-92023) Avail: CASI HC A03/MF A01

The strength and toughness requirements of materials used in high pressure vessels has been the subject of some discussion in the meetings of the Materials Task Group of the Special Working Group - High Pressure Vessels. A fracture mechanics analysis

has been performed to theoretically establish the required toughness for a high pressure vessel. The analysis is based on the validity requirement for plane-strain fracture of fracture toughness test specimens. This means that at fracture, the crack length, uncracked ligament, and vessel length must each be greater than fifty times the crack tip plastic zone since for brittle fracture to occur. For high pressure piping applications, the limiting physical dimension is the uncracked ligament, since it can be assumed that the other dimensions are always greater than fifty times the crack tip plastic zone. To perform the fracture mechanics analysis, several parameters must be known, including vessel dimensions, material strength, degree of autofrettage, and design pressure. Remarkably, the results of the analysis show that the effects of radius ratio, pressure, and degree of autofrettage can be ignored when establishing strength and toughness requirements for design code purposes. The only parameters that enter into the calculation are yield strength, toughness and vessel thickness. The final results can easily be represented as a graph of yield strength against toughness on which several curves, one for each vessel thickness, are plotted. GRA

N93-10777*# National Aeronautics and Space Administration. Lewis Research Center, Cleveland, OH.
UNIFIED VISCOPLASTIC BEHAVIOR OF METAL MATRIX COMPOSITES
S. M. Arnold, D. N. Robinson (Akron Univ., OH.), and P. A. Bartolotta Nov. 1992 11 p Presented at the American Society of Mechanical Engineers Winter Annual Meeting, Anaheim, CA, 8-13 Nov. 1992; sponsored by ASME
(Grant NAG3-379; RTOP 510-01-50)
(NASA-TM-105819; E-7250; NAS 1.15:105819) Avail: CASI HC A03/MF A01

The need for unified constitutive models was recognized more than a decade ago in the results of phenomenological tests on monolithic metals that exhibited strong creep-plasticity interaction. Recently, metallic alloys have been combined to form high-temperature ductile/ductile composite materials, raising the natural question of whether these metallic composites exhibit the same phenomenological features as their monolithic constituents. This question is addressed in the context of a limited, yet definite (to illustrate creep/plasticity interaction) set of experimental data on the model metal matrix composite (MMC) system W/Kanthal. Furthermore, it is demonstrated that a unified viscoplastic representation, extended for unidirectional composites and correlated to W/Kanthal, can accurately predict the observed longitudinal composite creep/plasticity interaction response and strain rate dependency. Finally, the predicted influence of fiber orientation on the creep response of W/Kanthal is illustrated. Author

N93-10797# California Univ., Berkeley.
INSPECTION AND REPAIR DECISIONS FOR HYDRAULIC STRUCTURES UNDER SYMMETRIC DETERIORATION Interim Technical Report
Jan M. vanNoortwijk Jun. 1992 27 p
(Contract DAAL03-91-G-0046)
(AD-A253621; ARO-27993.4-MA) Avail: CASI HC A03/MF A01

In this report, we will focus on minimizing the cost due to inspection and repair of hydraulic structures. The optimization is based on symmetric properties of the underlying physical deterioration process: the damages per time-unit are exchangeable and the probabilities of preventive repair and failure are obtained by conditioning on the average amount of deterioration with regard to a finite or an infinite time-horizon. By introducing a prior for the average deterioration per time-unit, we can account for uncertainty in the decision problems. Advantages of our Bayesian approach are that we base our mathematical models on an observable quantity, the damage, and that our results are just sums of products which can be easily evaluated. Two examples from the field of hydraulic engineering are studied: the determination of a preventive repair interval when a safety norm is given and a cost-optimal periodic inspection rate if there is a possibility for a preventive repair during each inspection. GRA

N93-10873 Illinois Univ. at Urbana-Champaign, Savoy.
LINEAR AND NONLINEAR ANALYSES OF THICK COMPOSITE CIRCULAR PLATES USING THE FINITE ELEMENT METHOD Ph.D. Thesis
George Henry Thiel 1991 239 p
Avail: Univ. Microfilms Order No. DA9211010

A new finite element for circular plates based on Mindlin's shear deformable plate theory is developed. Unlike conventional plate elements, these new elements may be stacked on top of one another to model laminated plates. The elements assure continuity of the displacements between the layers, but not continuity of the traction vectors. The element does not account for interlaminar slip or debonding between the layers. Each layer in the laminated plate is allowed an independent rotation. Hence, the model gives more accurate results than classical lamination theory models. The plate element is more efficient than solid elements because it accurately models the structure while keeping the degrees of freedom per element to a minimum. Also, if one uses solid elements to model a laminated circular plate, many more elements would have to be used in the model to avoid loss of accuracy due to a large aspect ratio. The new element is also immune from shear locking (at least for radius to thickness ratios up to 500) without having to incorporate complex numerical integration schemes. In fact, the element's stiffness matrix may be integrated in closed form; this is not possible for most plate elements in the literature. The circular plate element is incorporated into a nonlinear finite element code based on the total Lagrangian formulation. The inclusion of the shear deformation allows this finite element to model the large deflection of laminated circular plates accurately and efficiently. Dissert. Abstr.

N93-10003 Phillips Lab., Hanscom AFB, MA.
A THREE-DIMENSIONAL ANALYSIS OF THE EFFECT OF LOCAL STRESS DISTRIBUTION NEAR CRACK TIP
Chi-Tsieh Liu and Minh D. Le *In* JHU, The 1992 JANNAF Propulsion Meeting, Volume 1 Feb. 1992 p 47-53 (For primary document see N93-10001 01-20)
Avail: CPIA, 10630 Little Patuxent Pkwy., Suite 202, Columbia, MD, 21044-3200 HC

N93-10007 Materials Sciences Corp., Blue Bell, PA.
TRANSVERSE TENSION, TRANSVERSE COMPRESSION, AND INPLANE SHEAR JANNAF ROUND ROBIN TEST METHODS STANDARDIZATION RESULTS
Ron B. Bucinell, D. Moy, and Terry Vandiver (Army Missile Command, Redstone Arsenal, AL.) *In* JHU, The 1992 JANNAF Propulsion Meeting, Volume 1 Feb. 1992 p 143-151 (For primary document see N93-10001 01-20)
(Contract DAAL04-89-C-0023)
Avail: CPIA, 10630 Little Patuxent Pkwy., Suite 202, Columbia, MD, 21044-3200 HC

N93-10062# Dresser Industries, Inc., Liberty Corner, NJ.
STRUCTURAL ANALYSIS: FATIGUE LIFE ASSESSMENT
William D. Marscher *In* VKI, Radial Turbines 1992 73 p (For primary document see N93-10050 01-34)
Copyright Avail: CASI HC A04/MF A04

N93-10468 Nottingham Univ. (England). Dept. of Theoretical Mechanics.
DEVELOPMENT IN THE ELASTIC ANALYSIS OF LAMINATED PLATES
A. J. M. Spencer *In* Carleton Univ., Proceedings of the Twelfth Canadian Congress of Applied Mechanics, Volumes 1 and 2 May 1989 p 47-53 (For primary document see N93-10466 01-31)
Copyright Avail: Canadian Society for Mechanical Engineering, 2050 Mansfield St., Suite 700, Montreal, Quebec H3A 1Z7 Canada

N93-10470 Concordia Univ., Montreal (Quebec). Dept. of Mechanical Engineering.
AXISYMMETRIC VIBRATIONS OF ROTATING CIRCULAR PLATES USING CHARACTERISTIC ORTHOGONAL POLYNOMIALS
A. Kaushal and R. B. Bhat *In* Carleton Univ., Proceedings of the Twelfth Canadian Congress of Applied Mechanics, Volumes 1 and 2 May 1989 p 94-95 (For primary document see N93-10466 01-31)
Copyright Avail: Canadian Society for Mechanical Engineering, 2050 Mansfield St., Suite 700, Montreal, Quebec H3A 1Z7 Canada

N93-10471 Manchester Univ. (England).
VIBRATION OF ORTHOTROPIC CYLINDRICAL SHELL PANELS WITH ARBITRARY SUPPORTED CURVED EDGES
C. B. Sharma and I. A. Al-Khayat *In* Carleton Univ., Proceedings of the Twelfth Canadian Congress of Applied Mechanics, Volumes 1 and 2 May 1989 p 100-101 (For primary document see N93-10466 01-31)
Copyright Avail: Canadian Society for Mechanical Engineering, 2050 Mansfield St., Suite 700, Montreal, Quebec H3A 1Z7 Canada

N93-10472 Old Dominion Univ., Norfolk, VA.
A FINITE ELEMENT METHOD FOR NONLINEAR PANEL FLUTTER
Chuh Mei and Carl E. Gray, Jr. (National Aeronautics and Space Administration. Langley Research Center, Hampton, VA.) *In* Carleton Univ., Proceedings of the Twelfth Canadian Congress of Applied Mechanics, Volumes 1 and 2 May 1989 p 118-119 (For primary document see N93-10466 01-31)
Copyright Avail: Canadian Society for Mechanical Engineering, 2050 Mansfield St., Suite 700, Montreal, Quebec H3A 1Z7 Canada

N93-10473 Virginia Polytechnic Inst. and State Univ., Blacksburg.
VIBRATION OF LAMINATED COMPOSITE PLATES USING VARIOUS PLATE THEORIES: ANALYTICAL AND FINITE ELEMENT RESULTS
J. N. Reddy and A. A. Khdeir *In* Carleton Univ., Proceedings of the Twelfth Canadian Congress of Applied Mechanics, Volumes 1 and 2 May 1989 p 120-121 (For primary document see N93-10466 01-31)
Copyright Avail: Canadian Society for Mechanical Engineering, 2050 Mansfield St., Suite 700, Montreal, Quebec H3A 1Z7 Canada

N93-10474 Glasgow Univ. (Scotland).
NON-LINEAR THERMOELASTICITY OF RUBBERLIKE SOLIDS
R. W. Ogden *In* Carleton Univ., Proceedings of the Twelfth Canadian Congress of Applied Mechanics, Volumes 1 and 2 May 1989 p 126-127 (For primary document see N93-10466 01-31)
Copyright Avail: Canadian Society for Mechanical Engineering, 2050 Mansfield St., Suite 700, Montreal, Quebec H3A 1Z7 Canada

N93-10475 Akron Univ., OH.
FAILURE PROCESSES IN ELASTOMERIC COMPOSITES
A. N. Gent *In* Carleton Univ., Proceedings of the Twelfth Canadian Congress of Applied Mechanics, Volumes 1 and 2 May 1989 p 130-131 (For primary document see N93-10466 01-31)
Copyright Avail: Canadian Society for Mechanical Engineering, 2050 Mansfield St., Suite 700, Montreal, Quebec H3A 1Z7 Canada

N93-10476 California Univ., Livermore. Lawrence Livermore Lab.
CHRONORHEOLOGICAL CHARACTERIZATION OF ELASTOMERS
William W. Feng *In* Carleton Univ., Proceedings of the Twelfth Canadian Congress of Applied Mechanics, Volumes 1 and 2 May 1989 p 132-133 (For primary document see N93-10466 01-31)
Copyright Avail: Canadian Society for Mechanical Engineering, 2050 Mansfield St., Suite 700, Montreal, Quebec H3A 1Z7 Canada

N93-10477 Alcoa Foundation, Pittsburgh, PA.
INTEGRATED FINITE ELEMENT MODEL OF COMPOSITE MATERIALS
Jan L. Teply and William C. Herbein *In* Carleton Univ., Proceedings of the Twelfth Canadian Congress of Applied Mechanics, Volumes 1 and 2 May 1989 p 138-139 (For primary document see N93-10466 01-31)
Copyright Avail: Canadian Society for Mechanical Engineering, 2050 Mansfield St., Suite 700, Montreal, Quebec H3A 1Z7 Canada

N93-10478 Virginia Polytechnic Inst. and State Univ., Blacksburg.
COMPRESSION BUCKLING OF THICK ORTHOTROPIC PLATES WITH A STEP THICKNESS CHANGE
Eric R. Johnson and Carlos G. Davila *In* Carleton Univ., Proceedings of the Twelfth Canadian Congress of Applied Mechanics, Volumes 1 and 2 May 1989 p 140-141 (For primary document see N93-10466 01-31)
Copyright Avail: Canadian Society for Mechanical Engineering, 2050 Mansfield St., Suite 700, Montreal, Quebec H3A 1Z7 Canada

N93-10479 Stanford Univ., CA. Dept. of Aeronautics and Astronautics.
CONTACT PROBLEM IN DELAMINATION-BUCKLING OF LAMINATED COMPOSITE SHELLS Abstract only
Fukuo Chang and Zafer Kutlu *In* Carleton Univ., Proceedings of the Twelfth Canadian Congress of Applied Mechanics, Volumes 1 and 2 May 1989 p 142 (For primary document see N93-10466 01-31)
Copyright Avail: Canadian Society for Mechanical Engineering, 2050 Mansfield St., Suite 700, Montreal, Quebec H3A 1Z7 Canada

N93-10481 Virginia Polytechnic Inst. and State Univ., Blacksburg.
ON THE BEHAVIOR OF A HIGHER-ORDER PLATE BENDING ELEMENT
R. C. Averill and J. N. Reddy *In* Carleton Univ., Proceedings of the Twelfth Canadian Congress of Applied Mechanics, Volumes 1 and 2 May 1989 p 146-147 (For primary document see N93-10466 01-31)
Copyright Avail: Canadian Society for Mechanical Engineering, 2050 Mansfield St., Suite 700, Montreal, Quebec H3A 1Z7 Canada

N93-10482 Arizona Univ., Tucson. Dept. of Civil Engineering and Engineering Mechanics.
INTERFACE CRACKS IN AN ORTHOTROPIC LAYERED HALF-SPACE UNDER IMPACT LOADING
T. Kundu and M. R. Karim *In* Carleton Univ., Proceedings of the Twelfth Canadian Congress of Applied Mechanics, Volumes 1 and 2 May 1989 p 176-177 (For primary document see N93-10466 01-31)
Copyright Avail: Canadian Society for Mechanical Engineering, 2050 Mansfield St., Suite 700, Montreal, Quebec H3A 1Z7 Canada

N93-10483 Clarkson Univ., Potsdam, NY.
AN OPEN OR CLOSED CRACK TERMINATING AT A BI-MATERIAL INTERFACE: POWER-LOGARITHMIC SINGULARITIES
John P. Dempsey *In* Carleton Univ., Proceedings of the Twelfth Canadian Congress of Applied Mechanics, Volumes 1 and 2 May 1989 p 178-179 (For primary document see N93-10466 01-31)

Copyright Avail: Canadian Society for Mechanical Engineering, 2050 Mansfield St., Suite 700, Montreal, Quebec H3A 1Z7 Canada

N93-10484 Sandia National Labs., Albuquerque, NM.
ENRICHED ELEMENT ANALYSIS OF BIMATERIAL INTERFACE CRACKS
E. P. Chen *In* Carleton Univ., Proceedings of the Twelfth Canadian Congress of Applied Mechanics, Volumes 1 and 2 May 1989 p 180-181 (For primary document see N93-10466 01-31)
Copyright Avail: Canadian Society for Mechanical Engineering, 2050 Mansfield St., Suite 700, Montreal, Quebec H3A 1Z7 Canada

N93-10485 Colorado Univ., Boulder. Dept. of Mechanical Engineering.
ELASTIC WAVE SCATTERING BY AN INTERFACIAL CRACK IN A PLATE
S. K. Datta, R. L. Bratton, and A. H. Shah (Manitoba Univ., Winnipeg.) *In* Carleton Univ., Proceedings of the Twelfth Canadian Congress of Applied Mechanics, Volumes 1 and 2 May 1989 p 182-183 (For primary document see N93-10466 01-31)
Copyright Avail: Canadian Society for Mechanical Engineering, 2050 Mansfield St., Suite 700, Montreal, Quebec H3A 1Z7 Canada

N93-10486 Carleton Univ., Ottawa (Ontario).
INDENTATION OF A PRECOMPRESSED PENNY-SHAPED CRACK
A. P. S. Selvadurai, B. M. Singh, and M. C. Au *In its* Proceedings of the Twelfth Canadian Congress of Applied Mechanics, Volumes 1 and 2 May 1989 p 184-185 (For primary document see N93-10466 01-31)
Copyright Avail: Canadian Society for Mechanical Engineering, 2050 Mansfield St., Suite 700, Montreal, Quebec H3A 1Z7 Canada

N93-10487 Technische Hochschule, Vienna (Austria).
NONSTATIONARY RANDOM VARIATIONS OF MODERATELY THICK PLATES USING BEM
H. Irschik and R. Heuer *In* Carleton Univ., Proceedings of the Twelfth Canadian Congress of Applied Mechanics, Volumes 1 and 2 May 1989 p 192-193 (For primary document see N93-10466 01-31)
Copyright Avail: Canadian Society for Mechanical Engineering, 2050 Mansfield St., Suite 700, Montreal, Quebec H3A 1Z7 Canada

N93-10488 Houston Univ., TX.
NUMERICAL SIMULATION OF TRANSIENT CRACK GROWTH
T.-J. Shiue and K. Ravi-Chandar *In* Carleton Univ., Proceedings of the Twelfth Canadian Congress of Applied Mechanics, Volumes 1 and 2 May 1989 p 198-199 (For primary document see N93-10466 01-31)
Copyright Avail: Canadian Society for Mechanical Engineering, 2050 Mansfield St., Suite 700, Montreal, Quebec H3A 1Z7 Canada

N93-10489 Clarkson Univ., Potsdam, NY. Dept. of Civil and Environmental Engineering.
DYNAMIC CRACK DIVISION IN BRITTLE SOLIDS
John P. Dempsey *In* Carleton Univ., Proceedings of the Twelfth Canadian Congress of Applied Mechanics, Volumes 1 and 2 May 1989 p 200-201 (For primary document see N93-10466 01-31)
Copyright Avail: Canadian Society for Mechanical Engineering, 2050 Mansfield St., Suite 700, Montreal, Quebec H3A 1Z7 Canada

N93-10490 Naval Academy of Greece, Athens.
INTEGRAL TRANSFORM APPROACH TO AN INERTIAL VISCOELASTIC PROBLEM INVOLVING MOVING SINGULARITIES
H. G. Georgiadis and S. C. Mouskos *In* Carleton Univ., Proceedings of the Twelfth Canadian Congress of Applied Mechanics, Volumes 1 and 2 May 1989 p 204-205 (For primary document see N93-10466 01-31)
Copyright Avail: Canadian Society for Mechanical Engineering, 2050 Mansfield St., Suite 700, Montreal, Quebec H3A 1Z7 Canada

N93-10491 Naval Research Lab., Washington, DC. Mechanics of Materials Branch.
STRESS PATTERNS IN THE DYNAMIC TEAR TEST
V. Gensheimer DeGiorgi *In* Carleton Univ., Proceedings of the Twelfth Canadian Congress of Applied Mechanics, Volumes 1 and 2 May 1989 p 206-207 (For primary document see N93-10466 01-31)
Copyright Avail: Canadian Society for Mechanical Engineering, 2050 Mansfield St., Suite 700, Montreal, Quebec H3A 1Z7 Canada

N93-10492 Cornell Univ., Ithaca, NY. Dept. of Theoretical and Applied Mechanics.
DYNAMIC MEASUREMENT OF THE J INTEGRAL IN DUCTILE METALS USING THE OPTICAL METHOD OF CAUSTICS
Alan T. Zehnder and Ares J. Rosakis (California Inst. of Tech., Pasadena.) *In* Carleton Univ., Proceedings of the Twelfth Canadian Congress of Applied Mechanics, Volumes 1 and 2 May 1989 p 208-209 (For primary document see N93-10466 01-31)
Copyright Avail: Canadian Society for Mechanical Engineering, 2050 Mansfield St., Suite 700, Montreal, Quebec H3A 1Z7 Canada

N93-10493 California Inst. of Tech., Pasadena. Graduate Aeronautical Labs.
STATUS OF DYNAMIC FRACTURE IN BRITTLE SOLIDS
Abstract only
W. G. Knauss and P. D. Washabaugh *In* Carleton Univ., Proceedings of the Twelfth Canadian Congress of Applied Mechanics, Volumes 1 and 2 May 1989 p 210 (For primary document see N93-10466 01-31)
Copyright Avail: Canadian Society for Mechanical Engineering, 2050 Mansfield St., Suite 700, Montreal, Quebec H3A 1Z7 Canada

N93-10494 Ecole Polytechnique Federale de Lausanne (Switzerland).
EVOLUTION OF HYBRID-TREFFTZ FE MODEL: STATE OF THE ART AND FUTURE TRENDS
J. Jirousek *In* Carleton Univ., Proceedings of the Twelfth Canadian Congress of Applied Mechanics, Volumes 1 and 2 May 1989 p 212-213 (For primary document see N93-10466 01-31)
Copyright Avail: Canadian Society for Mechanical Engineering, 2050 Mansfield St., Suite 700, Montreal, Quebec H3A 1Z7 Canada

N93-10495 Calgary Univ. (Alberta). Dept. of Mechanical Engineering.
A MULTILAYERED SHELL FINITE ELEMENT
Marcelo Epstein *In* Carleton Univ., Proceedings of the Twelfth Canadian Congress of Applied Mechanics, Volumes 1 and 2 May 1989 p 214-215 (For primary document see N93-10466 01-31)
Copyright Avail: Canadian Society for Mechanical Engineering, 2050 Mansfield St., Suite 700, Montreal, Quebec H3A 1Z7 Canada

N93-10496 Puerto Rico Univ., Mayaguez.
A NEW NON-GAUSSSIAN APPROXIMATION TECHNIQUE FOR RANDOM VIBRATION OF GENERAL HYSTERESIS
H. Davoodi and M. Noori (Worcester Polytechnic Inst., MA.) *In* Carleton Univ., Proceedings of the Twelfth Canadian Congress of Applied Mechanics, Volumes 1 and 2 May 1989 p 224-225 (For primary document see N93-10466 01-31)
Copyright Avail: Canadian Society for Mechanical Engineering,

2050 Mansfield St., Suite 700, Montreal, Quebec H3A 1Z7 Canada

N93-10497 Pacific Northwest Lab., Richland, WA.
FRACTALS AND MULTIFRACTALS IN FRACTURE
R. E. Williford *In* Carleton Univ., Proceedings of the Twelfth Canadian Congress of Applied Mechanics, Volumes 1 and 2 May 1989 p 230-231 (For primary document see N93-10466 01-31)
Copyright Avail: Canadian Society for Mechanical Engineering, 2050 Mansfield St., Suite 700, Montreal, Quebec H3A 1Z7 Canada

N93-10498 Purdue Univ., West Lafayette, IN. School of Aeronautics and Astronautics.
ENTROPY OF DISORDER IN THERMOMECHANICS OF DAMAGE IN HETEROGENEOUS SOLIDS
Martin Ostoja-Starzewski *In* Carleton Univ., Proceedings of the Twelfth Canadian Congress of Applied Mechanics, Volumes 1 and 2 May 1989 p 232-233 (For primary document see N93-10466 01-31)
Copyright Avail: Canadian Society for Mechanical Engineering, 2050 Mansfield St., Suite 700, Montreal, Quebec H3A 1Z7 Canada

N93-10501 Clarkson Univ., Potsdam, NY. Dept. of Mechanical and Industrial Engineering.
AN ASSESSMENT OF THE CORRESPONDENCE PRINCIPLE IN COMPARISON TO NONLINEAR VISCOELASTIC THEORY: A CASE STUDY
E. Sancaktar *In* Carleton Univ., Proceedings of the Twelfth Canadian Congress of Applied Mechanics, Volumes 1 and 2 May 1989 p 290-291 (For primary document see N93-10466 01-31)
Copyright Avail: Canadian Society for Mechanical Engineering, 2050 Mansfield St., Suite 700, Montreal, Quebec H3A 1Z7 Canada

N93-10502 Cagliari Univ. (Italy).
DAMAGE DUE TO PLASTIC DEFORMATION IN ELASTIC-PLASTIC MATERIALS: THE THERMODYNAMICAL CONNECTION
A. Paglietti *In* Carleton Univ., Proceedings of the Twelfth Canadian Congress of Applied Mechanics, Volumes 1 and 2 May 1989 p 294-295 (For primary document see N93-10466 01-31)
Copyright Avail: Canadian Society for Mechanical Engineering, 2050 Mansfield St., Suite 700, Montreal, Quebec H3A 1Z7 Canada

N93-10503 Sherbrooke Univ. (Quebec). Dept. of Civil Engineering.
SINGULAR STRESS DISTRIBUTIONS AT CIRCULAR HOLES IN COMPOSITE LAMINATES
Antoine E. Lahoud and Otmane Bouksour *In* Carleton Univ., Proceedings of the Twelfth Canadian Congress of Applied Mechanics, Volumes 1 and 2 May 1989 p 308-309 (For primary document see N93-10466 01-31)
Copyright Avail: Canadian Society for Mechanical Engineering, 2050 Mansfield St., Suite 700, Montreal, Quebec H3A 1Z7 Canada

N93-10504 Southern Methodist Univ., Dallas, TX.
THERMAL BUCKLING OF HEATED LAMINATED COMPOSITE CIRCULAR CYLINDRICAL SHELLS
Marion W. Wilcox and S. F. Ma *In* Carleton Univ., Proceedings of the Twelfth Canadian Congress of Applied Mechanics, Volumes 1 and 2 May 1989 p 310-311 (For primary document see N93-10466 01-31)
Copyright Avail: Canadian Society for Mechanical Engineering, 2050 Mansfield St., Suite 700, Montreal, Quebec H3A 1Z7 Canada

N93-10505 Chung Shan Inst. of Science and Technology (Taiwan).
FAILURE ANALYSIS OF LAMINATED COMPOSITES BY USING ITERATIVE THREE-DIMENSIONAL FINITE ELEMENT METHOD
W. C. Hwang and C. T. Sun *In* Carleton Univ., Proceedings of the Twelfth Canadian Congress of Applied Mechanics, Volumes 1 and 2 May 1989 p 314-315 (For primary document see N93-10466 01-31)
Copyright Avail: Canadian Society for Mechanical Engineering, 2050 Mansfield St., Suite 700, Montreal, Quebec H3A 1Z7 Canada

N93-10506 McDonnell-Douglas Corp., Saint Louis, MO.
ANALYSIS OF A BUFFER STRIP LAMINATE WITH A CUTOUT
E. S. Meyer and L. R. Dharani (Missouri Univ., Rolla.) *In* Carleton Univ., Proceedings of the Twelfth Canadian Congress of Applied Mechanics, Volumes 1 and 2 May 1989 p 316-317 (For primary document see N93-10466 01-31)
Copyright Avail: Canadian Society for Mechanical Engineering, 2050 Mansfield St., Suite 700, Montreal, Quebec H3A 1Z7 Canada

N93-10507 Florida Univ., Gainesville. Dept. of Aerospace Engineering, Mechanics and Engineering Science.
ELASTICITY ANALYSIS OF ORTHOTROPIC BEAMS UNDER THREE-PART BENDING
S. Hu and B. V. Sankar *In* Carleton Univ., Proceedings of the Twelfth Canadian Congress of Applied Mechanics, Volumes 1 and 2 May 1989 p 318-319 (For primary document see N93-10466 01-31)
Copyright Avail: Canadian Society for Mechanical Engineering, 2050 Mansfield St., Suite 700, Montreal, Quebec H3A 1Z7 Canada

N93-10512 Osaka Univ., Suita (Japan). Dept. of Precision Engineering.
VIBRATIONS OF A FLEXIBLE TIMOSHENKO BEAM UNDER GRAVITY
T. Yokayama *In* Carleton Univ., Proceedings of the Twelfth Canadian Congress of Applied Mechanics, Volumes 1 and 2 May 1989 p 340-341 (For primary document see N93-10466 01-31)
Copyright Avail: Canadian Society for Mechanical Engineering, 2050 Mansfield St., Suite 700, Montreal, Quebec H3A 1Z7 Canada

N93-10513 Indian Inst. of Tech., New Delhi. Dept. of Applied Mechanics.
ORTHOTROPIC CIRCULAR PLATE ON NONLINEAR ELASTIC SUBGRADE
Rakesh Kumar Jain and Yogendra Nath *In* Carleton Univ., Proceedings of the Twelfth Canadian Congress of Applied Mechanics, Volumes 1 and 2 May 1989 p 352-353 (For primary document see N93-10466 01-31)
Copyright Avail: Canadian Society for Mechanical Engineering, 2050 Mansfield St., Suite 700, Montreal, Quebec H3A 1Z7 Canada

N93-10514 University of South Florida, Tampa. Dept. of Civil Engineering and Mechanics.
COMPARISON OF THE MAXIMUM STRESS AND THE STRESS INTENSITY APPROACH IN THE ANALYSIS OF BONDED JOINTS
William C. Carpenter *In* Carleton Univ., Proceedings of the Twelfth Canadian Congress of Applied Mechanics, Volumes 1 and 2 May 1989 p 368-369 (For primary document see N93-10466 01-31)
Copyright Avail: Canadian Society for Mechanical Engineering, 2050 Mansfield St., Suite 700, Montreal, Quebec H3A 1Z7 Canada

N93-10515 Reims Univ. (France).
EXPERIMENTAL AND THEORETICAL BEHAVIOR OF ADHESIVELY BONDED COMPOSITE STRUCTURES UNDER TENSILE STRESS AT THE EDGE VICINITY [COMPORTEMENT EXPERIMENTAL ET THEORIQUE, AU VOISINAGE DES EXTREMITES, D'ASSEMBLAGES COMPOSITES COLLES, SOLLICITES AU CISAILLEMENT PAR TRACTION]
Y. Gilibert and Michel L. L. Klein (Ecole Nationale Superieure de Techniques Avancees, Paris, France) *In* Carleton Univ., Proceedings of the Twelfth Canadian Congress of Applied Mechanics, Volumes 1 and 2 May 1989 p 374-375 In FRENCH (For primary document see N93-10466 01-31)
Copyright Avail: Canadian Society for Mechanical Engineering, 2050 Mansfield St., Suite 700, Montreal, Quebec H3A 1Z7 Canada

N93-10516 Ecole Nationale Superieure de Techniques Avancees, Paris (France).
EXPERIMENTAL AND NUMERIC ANALYSIS OF CONSTRAINTS IN A BONDED STEPPED LAP JOINT SUBJECTED TO TRACTION [ANALYSE EXPERIMENTALE ET NUMERIQUE DES CONSTRAINTES DANS UN ASSEMBLAGE COLLE EN ESCALIER SOLLICITE A LA TRACTION]
Yvon Gilibert and Alain Rigolot *In* Carleton Univ., Proceedings of the Twelfth Canadian Congress of Applied Mechanics, Volumes 1 and 2 May 1989 p 376-377 In FRENCH (For primary document see N93-10466 01-31)
Copyright Avail: Canadian Society for Mechanical Engineering, 2050 Mansfield St., Suite 700, Montreal, Quebec H3A 1Z7 Canada

N93-10517 Waterloo Univ. (Ontario). Dept. of Mechanical Engineering.
DYNAMICS OF SYSTEMS WITH TIME-VARYING INERTIAL PROPERTIES
John J. McPhee *In* Carleton Univ., Proceedings of the Twelfth Canadian Congress of Applied Mechanics, Volumes 1 and 2 May 1989 p 392-393 (For primary document see N93-10466 01-31)
Copyright Avail: Canadian Society for Mechanical Engineering, 2050 Mansfield St., Suite 700, Montreal, Quebec H3A 1Z7 Canada

N93-10520 Thomson-CSF, Ottawa (Ontario).
EFFECT OF MOUNTING OFFSET ON THE DYNAMICS OF DEPLOYING FLEXIBLE APPENDAGES
S. Kalaycioglu, B. A. Kalaycioglu, Z. R. Irani, and A. K. Misra *In* Carleton Univ., Proceedings of the Twelfth Canadian Congress of Applied Mechanics, Volumes 1 and 2 May 1989 p 400-401 (For primary document see N93-10466 01-31)
Copyright Avail: Canadian Society for Mechanical Engineering, 2050 Mansfield St., Suite 700, Montreal, Quebec H3A 1Z7 Canada

N93-10524 University of Western Ontario, London.
EVOLUTIONARY SPECTRA OF TIME-DEPENDENT DISCRETIZED SYSTEMS TO TIME-FREQUENCY MODULATED RANDOM EXCITATIONS
C. W. S. To *In* Carleton Univ., Proceedings of the Twelfth Canadian Congress of Applied Mechanics, Volumes 1 and 2 May 1989 p 412-413 (For primary document see N93-10466 01-31)
Copyright Avail: Canadian Society for Mechanical Engineering, 2050 Mansfield St., Suite 700, Montreal, Quebec H3A 1Z7 Canada

N93-10526 California Univ., Davis. Dept. of Civil Engineering.
RESPONSE OF A BEAM TO TRANSVERSE IMPULSIVE AND HIGH FREQUENCY LOADS
James R. Hutchinson *In* Carleton Univ., Proceedings of the Twelfth Canadian Congress of Applied Mechanics, Volumes 1 and 2 May 1989 p 418-419 (For primary document see N93-10466 01-31)
Copyright Avail: Canadian Society for Mechanical Engineering, 2050 Mansfield St., Suite 700, Montreal, Quebec H3A 1Z7 Canada

N93-10527 California State Univ., Long Beach. Dept. of Mechanical Engineering.
VIBRATION OF A DAMPED DOUBLE-BEAM SYSTEM
H. V. Vu and B. H. Karnopp (Michigan Univ., Ann Arbor.) *In* Carleton Univ., Proceedings of the Twelfth Canadian Congress of Applied Mechanics, Volumes 1 and 2 May 1989 p 426-427 (For primary document see N93-10466 01-31)
Copyright Avail: Canadian Society for Mechanical Engineering, 2050 Mansfield St., Suite 700, Montreal, Quebec H3A 1Z7 Canada

N93-10528 Manitoba Univ., Winnipeg. Dept. of Mechanical Engineering.
OVERVIEW OF THE VIBROIMPACT DAMPING OF PACKAGED PARTICLES
N. Popplewell, C. Pang, and S. E. Semercigil *In* Carleton Univ., Proceedings of the Twelfth Canadian Congress of Applied Mechanics, Volumes 1 and 2 May 1989 p 428-429 (For primary document see N93-10466 01-31)
Copyright Avail: Canadian Society for Mechanical Engineering, 2050 Mansfield St., Suite 700, Montreal, Quebec H3A 1Z7 Canada

N93-10529 Toronto Univ. (Ontario). Inst. for Aerospace Studies.
MODE LOCALIZATION IN A SIMPLE CONTINUUM MODEL
C. J. Damaren *In* Carleton Univ., Proceedings of the Twelfth Canadian Congress of Applied Mechanics, Volumes 1 and 2 May 1989 p 430-431 (For primary document see N93-10466 01-31)
Copyright Avail: Canadian Society for Mechanical Engineering, 2050 Mansfield St., Suite 700, Montreal, Quebec H3A 1Z7 Canada

N93-10530 Lakehead Univ., Port Arthur (Ontario). Dept. of Mechanical Engineering.
EXPERIMENTAL INVESTIGATION OF SIMPLE SUPPORT CONDITION IN FREE VIBRATION ANALYSIS OF PLATES
H. T. Saliba and D. Ciszewski *In* Carleton Univ., Proceedings of the Twelfth Canadian Congress of Applied Mechanics, Volumes 1 and 2 May 1989 p 436-437 (For primary document see N93-10466 01-31)
Copyright Avail: Canadian Society for Mechanical Engineering, 2050 Mansfield St., Suite 700, Montreal, Quebec H3A 1Z7 Canada

N93-10531 Industrial Marine Products Group Ltd., Halifax (Nova Scotia).
FLEXURAL VIBRATION OF BEAMS WITH VARYING SECTION PROPERTIES
R. Jategaonkar and D. S. Chehil (Nova Scotia Technical Coll., Halifax.) *In* Carleton Univ., Proceedings of the Twelfth Canadian Congress of Applied Mechanics, Volumes 1 and 2 May 1989 p 438-439 (For primary document see N93-10466 01-31)
Copyright Avail: Canadian Society for Mechanical Engineering, 2050 Mansfield St., Suite 700, Montreal, Quebec H3A 1Z7 Canada

N93-10532 Missouri Univ., Rolla. Dept. of Mechanical and Aerospace Engineering.
NATURAL VIBRATIONS OF MULTILAYERED DOUBLY CURVED SHELLS
K. Chandrashekhara *In* Carleton Univ., Proceedings of the Twelfth Canadian Congress of Applied Mechanics, Volumes 1 and 2 May 1989 p 440-441 (For primary document see N93-10466 01-31)
Copyright Avail: Canadian Society for Mechanical Engineering, 2050 Mansfield St., Suite 700, Montreal, Quebec H3A 1Z7 Canada

N93-10533 Communications Research Centre, Ottawa (Ontario).
FREE VIBRATIONS OF THE THICK CIRCULAR CYLINDRICAL SHELLS AND RINGS
R. K. Singal and K. Williams (Saskatchewan Univ., Saskatoon.) *In* Carleton Univ., Proceedings of the Twelfth Canadian Congress of Applied Mechanics, Volumes 1 and 2 May 1989 p 442-443 (For primary document see N93-10466 01-31)
Copyright Avail: Canadian Society for Mechanical Engineering, 2050 Mansfield St., Suite 700, Montreal, Quebec H3A 1Z7 Canada

N93-10534 Texas Univ., El Paso. Dept. of Mechanical and Industrial Engineering.
VIBRATION FREQUENCIES OF A CONSTRAINED CANTILEVER WEDGE
W. Lionel Craver, Jr. and Yangshan Lu *In* Carleton Univ., Proceedings of the Twelfth Canadian Congress of Applied Mechanics, Volumes 1 and 2 May 1989 p 444-445 (For primary document see N93-10466 01-31)
Copyright Avail: Canadian Society for Mechanical Engineering, 2050 Mansfield St., Suite 700, Montreal, Quebec H3A 1Z7 Canada

N93-10535 Waterloo Univ. (Ontario). Dept. of Systems Design Engineering.
ON THE VIBRATION OF AXISYMMETRIC SHELLS
G. R. Heppler and L. Wahl *In* Carleton Univ., Proceedings of the Twelfth Canadian Congress of Applied Mechanics, Volumes 1 and 2 May 1989 p 446-447 (For primary document see N93-10466 01-31)
Copyright Avail: Canadian Society for Mechanical Engineering, 2050 Mansfield St., Suite 700, Montreal, Quebec H3A 1Z7 Canada

N93-10536 Communications Research Centre, Ottawa (Ontario).
THE VIBRATIONS OF ANNULAR DISCS: A COMPARISON OF EXPERIMENTAL AND TWO ANALYTICAL TECHNIQUES
R. K. Singal, E. Haseganu-Zamfirescu (Saskatchewan Univ., Saskatoon.), H. Wong (Saskatchewan Univ., Saskatoon.), and K. Williams *In* Carleton Univ., Proceedings of the Twelfth Canadian Congress of Applied Mechanics, Volumes 1 and 2 May 1989 p 452-453 (For primary document see N93-10466 01-31)
Copyright Avail: Canadian Society for Mechanical Engineering, 2050 Mansfield St., Suite 700, Montreal, Quebec H3A 1Z7 Canada

N93-10538 Technische Hogeschool, Eindhoven (Netherlands).
A SPLINE FINITE STRIP METHOD FOR ANALYSING LOCAL AND DISTORTIONAL BUCKLING OF THIN-WALLED BEAMS UNDER ARBITRARY LOADING
G. M. vanErp and C. M. Menken *In* Carleton Univ., Proceedings of the Twelfth Canadian Congress of Applied Mechanics, Volumes 1 and 2 May 1989 p 474-475 (For primary document see N93-10466 01-31)
Copyright Avail: Canadian Society for Mechanical Engineering, 2050 Mansfield St., Suite 700, Montreal, Quebec H3A 1Z7 Canada

N93-10540 Ecole Polytechnique, Montreal (Quebec). Dept. of Mechanical Engineering.
AN EVALUATION OF THE CUMULATIVE DAMAGE EFFECT UNDER CREEP LOADING
R. Gomuc, T. Bui-Quoc, and A. Biron *In* Carleton Univ., Proceedings of the Twelfth Canadian Congress of Applied Mechanics, Volumes 1 and 2 May 1989 p 486-487 (For primary document see N93-10466 01-31)
Copyright Avail: Canadian Society for Mechanical Engineering, 2050 Mansfield St., Suite 700, Montreal, Quebec H3A 1Z7 Canada

N93-10541 Ecole Polytechnique, Montreal (Quebec). Dept. of Mechanical Engineering.
ON THE DEVELOPMENT OF A NEW FRACTURE TOUGHNESS PROCEDURE
M. Bernard and J. W. Provan (McGill Univ., Montreal, Quebec) *In* Carleton Univ., Proceedings of the Twelfth Canadian Congress of Applied Mechanics, Volumes 1 and 2 May 1989 p 488-489 (For primary document see N93-10466 01-31)
Copyright Avail: Canadian Society for Mechanical Engineering, 2050 Mansfield St., Suite 700, Montreal, Quebec H3A 1Z7 Canada

N93-10542 Toronto Univ. (Ontario). Dept. of Mechanical Engineering.
FATIGUE CRACK PROPAGATION IN THE PRESENCE OF SHOT-PEENING RESIDUAL STRESSES
S. A. Meguid *In* Carleton Univ., Proceedings of the Twelfth Canadian Congress of Applied Mechanics, Volumes 1 and 2 May 1989 p 490-491 (For primary document see N93-10466 01-31)
Copyright Avail: Canadian Society for Mechanical Engineering, 2050 Mansfield St., Suite 700, Montreal, Quebec H3A 1Z7 Canada

N93-10543 Carleton Univ., Ottawa (Ontario). Dept. of Mechanical and Aeronautical Engineering.
IMPROVEMENTS TO THE AC POTENTIAL DROP METHOD OF CRACK MEASUREMENT
P. R. Frise and R. Bell *In its* Proceedings of the Twelfth Canadian Congress of Applied Mechanics, Volumes 1 and 2 May 1989 p 504-505 (For primary document see N93-10466 01-31)
Copyright Avail: Canadian Society for Mechanical Engineering, 2050 Mansfield St., Suite 700, Montreal, Quebec H3A 1Z7 Canada

N93-10555 Aeronautical Development Establishment, Bangalore (India).
DESIGN OPTIMIZATION FOR UNIFORM DYNAMIC STRENGTH UNDER MULTI-MODAL RESPONSE
M. K. Padmanablan, S. Suryanarayan, and M. S. S. Prabhu *In* Carleton Univ., Proceedings of the Twelfth Canadian Congress of Applied Mechanics, Volumes 1 and 2 May 1989 p 768-769 (For primary document see N93-10466 01-31)
Copyright Avail: Canadian Society for Mechanical Engineering, 2050 Mansfield St., Suite 700, Montreal, Quebec H3A 1Z7 Canada

N93-10557 Naples Univ. (Italy).
A VARIATIONAL APPROACH FOR COUPLED CREEPING-FLOW PROBLEMS
P. Luchini and A. Pozzi *In* Carleton Univ., Proceedings of the Twelfth Canadian Congress of Applied Mechanics, Volumes 1 and 2 May 1989 p 774-775 (For primary document see N93-10466 01-31)
Copyright Avail: Canadian Society for Mechanical Engineering, 2050 Mansfield St., Suite 700, Montreal, Quebec H3A 1Z7 Canada

N93-10559 Carleton Univ., Ottawa (Ontario). Dept. of Civil Engineering.
A NEW QUADRILATERAL ELEMENT FOR THE ELASTIC AND PLASTIC ANALYSIS OF SHELLS
A. Ghani Razaqpur, Omer Aziz, and Mostafa Nofal *In its* Proceedings of the Twelfth Canadian Congress of Applied Mechanics, Volumes 1 and 2 May 1989 p 790-791 (For primary document see N93-10466 01-31)
Copyright Avail: Canadian Society for Mechanical Engineering, 2050 Mansfield St., Suite 700, Montreal, Quebec H3A 1Z7 Canada

N93-10560 Kansas Univ., Lawrence. Dept. of Mechanical Engineering.
THREE DIMENSIONAL CURVED BEAM ELEMENTS WITH LARGE TRANSLATIONS AND ROTATIONS
Karan S. Surana, Deane E. Ackers, and Robert M. Sorem *In* Carleton Univ., Proceedings of the Twelfth Canadian Congress of Applied Mechanics, Volumes 1 and 2 May 1989 p 792-793

(For primary document see N93-10466 01-31)
Copyright Avail: Canadian Society for Mechanical Engineering, 2050 Mansfield St., Suite 700, Montreal, Quebec H3A 1Z7 Canada

N93-10561 Exeter Univ. (England).
A REAPPRAISAL OF COMPOUND EQUILIBRIUM FINITE ELEMENTS
E. A. W. Maunder *In* Carleton Univ., Proceedings of the Twelfth Canadian Congress of Applied Mechanics, Volumes 1 and 2 May 1989 p 796-797 (For primary document see N93-10466 01-31)
Copyright Avail: Canadian Society for Mechanical Engineering, 2050 Mansfield St., Suite 700, Montreal, Quebec H3A 1Z7 Canada

N93-10562 Newcastle-upon-Tyne Univ. (England).
EVALUATION OF THE TRIANGULAR PLATE ELEMENT OF ZIENKIEWCZ AND LEFEBVRE [EVALUATION DE L'ELEMENT PLAQUE TRIANGULAIRE DE ZIENKIEWCZ ET LEFEBVRE]
P. Bettes, B. Peseux, and J. P. Quevat *In* Carleton Univ., Proceedings of the Twelfth Canadian Congress of Applied Mechanics, Volumes 1 and 2 May 1989 p 798-799 In FRENCH (For primary document see N93-10466 01-31)
Copyright Avail: Canadian Society for Mechanical Engineering, 2050 Mansfield St., Suite 700, Montreal, Quebec H3A 1Z7 Canada

N93-10564 Vermont Univ., Burlington.
NUMERICAL CONSIDERATIONS FOR STRUCTURAL SYSTEM IDENTIFICATION FROM MODAL INFORMATION
Jean-Guy Beliveau *In* Carleton Univ., Proceedings of the Twelfth Canadian Congress of Applied Mechanics, Volumes 1 and 2 May 1989 p 808-809 (For primary document see N93-10466 01-31)
Copyright Avail: Canadian Society for Mechanical Engineering, 2050 Mansfield St., Suite 700, Montreal, Quebec H3A 1Z7 Canada

N93-10568 Calgary Univ. (Alberta). Dept. of Mechanical Engineering.
NUMERICAL SIMULATION OF THE PROPAGATION OF COUPLED THERMOMECHANICAL WAVES IN INELASTIC SOLIDS
I. R. Orisamolu and M. C. Singh *In* Carleton Univ., Proceedings of the Twelfth Canadian Congress of Applied Mechanics, Volumes 1 and 2 May 1989 p 824-825 (For primary document see N93-10466 01-31)
Copyright Avail: Canadian Society for Mechanical Engineering, 2050 Mansfield St., Suite 700, Montreal, Quebec H3A 1Z7 Canada

N93-10576 University of Western Ontario, London.
AUTOMATED MULTI-BODY SYSTEM DYNAMICS VIA BOND GRAPH MODELLING AND INTERACTIVE GRAPHICS
J. B. McInnis and W. H. ElMaraghy *In* Carleton Univ., Proceedings of the Twelfth Canadian Congress of Applied Mechanics, Volumes 1 and 2 May 1989 p 880-881 (For primary document see N93-10466 01-31)
Copyright Avail: Canadian Society for Mechanical Engineering, 2050 Mansfield St., Suite 700, Montreal, Quebec H3A 1Z7 Canada

42 GEOSCIENCES (GENERAL)

No abstracts in this category.

43 EARTH RESOURCES AND REMOTE SENSING

Includes remote sensing of earth resources by aircraft and spacecraft; photogrammetry; and aerial photography.

For instrumentation see *35 Instrumentation and Photography.*

N93-10063# Instituto de Pesquisas Espaciais, Sao Jose dos Campos (Brazil).
STEREOSCOPY AND PARALAX IN THE VERTICAL DISTANCES DETERMINATION USING AERIAL PHOTOGRAPHS [ESTEREOSCOPIA E PARALAXE NA DETERMINACAO DE DISTANCIAS VERTICAIS MEDIANTE O USO DE FOTOGRAFIAS AEREAS]
Flavio Jorge Ponzoni and Attilio Antonio Disperati Feb. 1992 67 p In PORTUGESE
(INPE-5363-PUD/049) Avail: CASI HC A04/MF A01

This paper is dedicated to students or professionals which have been involved with natural resources survey in which photogrammetry has been a power tool. The main stereoscopic vision aspects and the paralax-vertical measurements relationship considering vertical aerial photographs are presented. The orbital stereoscopic vision possibilities are still presented considering HRV-SPOT imagery. Author

N93-10234# GTE Government Systems Corp., Mountain View, CA. Western Div.
SBS APPLICATIONS STUDY Final Report
Jan. 1992 29 p
(Contract N00014-91-C-0246)
(AD-A253779) Avail: CASI HC A03/MF A01

The thrust of the research was to investigate the potential feasibility of remote sensing applications of stimulated Brillouin scattering (SBS) in water. GRA

N93-10373# Instituto de Pesquisas Espaciais, Sao Jose dos Campos (Brazil).
REMOTE SENSING DATA FOR MONITORING AND EVALUATING BURNED AREAS: CASE OF EMAS NATIONAL PARK (GO) [DADOS SENSORIADOS NO MONITORAMENTO E AVALIACAO DE AREAS QUEIMADAS: O CASO DO PARQUE NACIONAL DE EMAS (GO)]
Yosio Edemir Shimabukuro, Joao RobertodosSantos, David Chung Liang Lee, and Marcos daCostaPereira 1991 28 p In PORTUGESE Submitted for publication
(INPE-5312-PRE/1709) Avail: CASI HC A03/MF A01

In the process of implantation and management of cattle raising and agricultural activities in Brazil, the vegetation cover burning procedure is commonly employed in the Central-West savanna. However, fire action has frequently reached the environmental protection areas such as the Emas National Park (Goias State), which may cause destruction of the habitat and niche, death of smaller animals, and environmental pollution. The objective of this work is an analysis of TM/Landsat and AVHRR/NOAA digital data as a tool for evaluating and monitoring the areas damaged by fire in the National Park. Based on TM images (29 Jul. 1988 and 14 Aug. 1988) and AVHRR data obtained during this period, a monitoring of fire action and the distribution analysis of the burned area related to the vegetation type were made. The change detection techniques such as post-classification comparison and principal components analysis were utilized for TM images. The results show an estimate of 73,884 hectares of burned vegetation areas. The integration of TM (high spatial resolution) and AVHRR (high temporal resolution) data permits the monitoring of the burning process, i.e., from the active fires detection to the burned area estimation. Author

N93-10625# Scotia Group, Inc., Dallas, TX.
RESERVES IN WESTERN BASINS
R. H. Caldwell and B. W. Cotton 1992 9 p Presented at the US Department of Energy Contractor Review Meeting on Natural Gas Research and Development, Morgantown, WV, 5-6 May

1992
(Contract DE-AC21-91MC-28130)
(DE92-014429; DOE/MC-28130/92/C0020; CONF-920584-18)
Avail: CASI HC A02/MF A01

This project requires generation of producible tight gas sand reserve estimates for three western basins. The requirement is to perform such reserve estimates using industry accepted practices so that results will have high credibility and acceptance by the oil and gas industry. The ultimate goal of the project is to encourage development of the tight gas formation by industry through reduction of the technical and economic risks of locating, drilling and completing commercial gas wells. The three geological basins selected for study are the Greater Green River Basin, Uinta Basin and Piceance Basin, located in the Colorado, Utah and Wyoming Rocky Mountain region. DOE

N93-10763# Lawrence Livermore National Lab., CA.
ELECTRICAL RESISTANCE TOMOGRAPHY USED IN ENVIRONMENTAL RESTORATION
A. L. Ramirez, W. Daily, and D. LaBrecque (Arizona Univ., Tucson.) Apr. 1992 8 p Presented at the DOE Information Exchange Meeting on Characterization, Monitoring, and Sensor Technologies, Dallas, TX, 3-4 Jun. 1992
(Contract W-7405-eng-48)
(DE92-018003; UCRL-JC-110356; CONF-9206184-2) Avail: CASI HC A02/MF A01

We are developing a new imaging technique, Electrical Resistance Tomography (ERT), to map subsurface liquids as flow occurs during natural or clean-up processes; ERT can also be used to map geologic structure. Natural processes (such as surface water infiltrating the vadose zone) and clean-up processes (such as air injection in the saturated zone, steam injection, emplacement of subsurface barriers) can create changes in a soil's electrical properties that are readily measured. We use these measurements to calculate tomographs that show the spatial distribution of the subsurface resistivities. The information derived from ERT can be used by remediation projects to do the following: monitor the effectiveness of clean-up processes, characterize hydrologic processes affecting contaminant transport, select appropriate clean-up alternatives, demonstrate regulatory compliance, and to verify the installation and performance of subsurface barriers. DOE

N93-10781# Army Engineer Topographic Labs., Fort Belvoir, VA. Geographic Sciences Lab.
SYSTEM INTEGRATION ISSUES IN DIGITAL PHOTOGRAMMETRIC MAPPING
Daniel Edwards 1992 6 p
(AD-A254046) Avail: CASI HC A02/MF A01

The recent development of the Terrain Information Extraction System (TIES) has provided the U.S. Army with an end-to-end digital photogrammetric mapping testbed. Using components developed by differing vendors, the system provides capabilities for scanning hardcopy imagery, photogrammetrically processing digitized or digital imagery, and interacting with a geographic information system. The process of assembling the components of TIES into a single, functioning system, has raised a number of key issues and provided valuable lessons learned concerning internal data exchange, networking, and quality control. These issues, discussed independently, are analyzed and reviewed from a systems perspective. GRA

N93-10847 Colorado Univ., Boulder.
EVALUATION OF SEASAT/GEOSAT ORBITS AND ALTIMETRY WITH APPLICATION TO LONG-TERM SEA LEVEL CHANGES IN THE NORTH PACIFIC Ph.D. Thesis
Bruce Joseph Haines 1991 188 p
Avail: Univ. Microfilms Order No. DA9132569

Recent studies of the climate over the North Pacific have shown a pronounced change in the past decade leading to an enhancement of the Aleutian low and stronger corresponding surface wind patterns. It has been hypothesized that an attendant change in ocean circulation has occurred, the magnitude of which may have approached 10 to 20 percent of the total mean circulation. Using the geostrophic relationship, one could infer that these circulation changes should be reflected in sea level differences at the decimeter level. Radar altimeter data collected by the Seasat mission in 1978 and by the Geosat mission from 1985-1989 provide a unique opportunity to corroborate the presence of these signals. In this study, Seasat/Geosat altimeter crossover heights were examined for evidence of gyre-scale sea level changes in the North Pacific. A number of issues critical to the success of any intersatellite altimeter investigation were addressed; principal among them is the recomputation of precise orbits using uniform models and standards. A complete re-evaluation of the altimeter correction terms was also conducted. In combination, these steps ensured the establishment of a consistent framework for use in the Seasat/Geosat sea level comparisons. Within this framework, a thorough analysis of the 1987-1978 altimeter sea level change was performed, including an evaluation of the spatial characteristics of the altimeter correction terms in relation to the sea level differences. Finally, tide gauge and hydrographic data were used to corroborate the altimeter results and lend insight on the nature of the oceanic variability for periods during which no altimeter data were collected. Taken together, the altimeter and in situ results provide evidence of large-scale oceanic variability in the North Pacific that is consistent with the observed climatic change. Dissert. Abstr.

N93-10182*# Canada Centre for Remote Sensing, Ottawa (Ontario).
SAR IN SUPPORT OF GEOLOGICAL INVESTIGATIONS OF THE SUDBURY STRUCTURE Abstract Only
V. Singhroy, R. Mussakowski (Ministry of Natural Resources, North York, Ontario), B. O. Dressler (Geological Survey of Canada, Ottawa, Ontario), N. F. Trowell (Geological Survey of Canada, Ottawa, Ontario), and Richard Grieve (Department of Energy, Mines, and Resources, Ottawa, Ontario) *In* Lunar and Planetary Inst., International Conference on Large Meteorite Impacts and Planetary Evolution 1992 p 69 (For primary document see N93-10112 01-46)
Avail: CASI HC A01/MF A01

44 ENERGY PRODUCTION AND CONVERSION

Includes specific energy conversion systems, e.g., fuel cells; global sources of energy; geophysical conversion; and windpower.

For related information see also *07 Aircraft Propulsion and Power, 20 Spacecraft Propulsion and Power,* and *28 Propellants and Fuels.*

N93-10383# Sandia National Labs., Albuquerque, NM.
BOILING BEHAVIOR OF SODIUM-POTASSIUM ALLOY IN A BENCH-SCALE SOLAR RECEIVER
J. B. Moreno, C. E. Andraka, and T. A. Moss 1992 8 p Presented at the 27th Intersociety Energy Conversion Engineering Conference, San Diego, CA, 3-7 Aug. 1992
(Contract DE-AC04-76DP-00789)
(DE92-014947; SAND-91-2801C; CONF-920801-3) Avail: CASI HC A02/MF A01

During 1989-90, a 75-kW(sub t) sodium reflux pool-boiler solar receiver was successfully demonstrated at Sandia National Laboratories. Significant features of this receiver include the following: (1) boiling sodium as the heat transfer medium, and (2) electric-discharge-machined (EDM) cavities as artificial nucleation sites to stabilize boiling. Since this first demonstration, design of a second-generation pool-boiler receiver that will bring the concept closer to commercialization has begun. For long life, the new receiver uses Haynes Alloy 230. For increased safety factors against film boiling and flooding, it has a refined shape and somewhat larger dimensions. To eliminate the need for trace heating, the receiver will boil the sodium-potassium alloy NaK-78 instead of sodium. To reduce manufacturing costs, it will use one

of a number of alternatives to EDM cavities for stabilization of boiling. To control incipient-boiling superheats, especially during hot restarts, it will contain a small amount of inert gas. Before the new receiver design could be finalized, bench-scale tests of some of the proposed changes were necessary. A series of bench-scale pool boilers were built from Haynes Alloy 230 and filled with NaK-78. Various boiling-stabilizer candidates were incorporated into them, including laser-drilled cavities and a number of different sintered-powder-metal coatings. These bench-scale pool boilers have been operated at temperatures up to 750 C, heated by quartz lamps with incident radiant fluxes up to 95 W/sq cm. The effects of various orientations and added gases have been studied. Results of these studies are presented. DOE

N93-10729# Pacific Northwest Lab., Richland, WA.
ADVANCED MATERIALS DEVELOPMENT FOR FOSSIL ENERGY CONVERSION APPLICATIONS
J. L. Bates, L. A. Chick, J. J. Kingsley, L. R. Pederson, W. J. Weber, G. E. Youngblood, J. K. Hurst (Oregon Graduate Inst. of Science and Technology, Beaverton.), A. E. Bell (Oregon Graduate Inst. of Science and Technology, Beaverton.), D. W. Grainger (Oregon Graduate Inst. of Science and Technology, Beaverton.), and S. B. Rananavare (Oregon Graduate Inst. of Science and Technology, Beaverton.) et al May 1992 11 p Presented at the 6th Annual Fossil Energy Materials Conference, Oak Ridge, TN, 12-14 May 1992
(Contract DE-AC06-76RL-01830)
(DE92-015762; PNL-SA-20917; CONF-9205123-5) Avail: CASI HC A03/MF A01

Research activities being conducted as part of this project include: (1) fundamental studies of electrochemical processes occurring at surfaces and interfaces in fuel cells, and (2) development of novel materials synthesis and processing methodologies for fossil energy conversion applications. Complex impedance and dc polarization studies of the electrocatalytic activity at the cathode have allowed intrinsic materials properties to be separated from extrinsic properties related to morphology. Mixed conduction in cathode materials was shown to dramatically enhance electrocatalytic activity with this approach. Combustion synthesis methods were used to prepare multicomponent perovskite catalysts in the La(1-x)Sr(x)Co(1-y)Fe(y)O(3) system. Electronic properties of these catalysts can be altered by adjusting the composition, which affects both catalytic activity and selectivity. Inverse micelles have been utilized to prepare nanosized nickel sulfide particles, which show promise as hydrodesulfurization catalysts for liquefied coal. Self-assembling organic monolayers and derivatized inorganic surfaces have been used to control nucleation and crystal morphology of inorganic phases. DOE

N93-10809*# National Aeronautics and Space Administration. Marshall Space Flight Center, Huntsville, AL.
HUBBLE SPACE TELESCOPE THERMAL CYCLE TEST REPORT FOR LARGE SOLAR ARRAY SAMPLES WITH BSFR CELLS (SAMPLE NUMBERS 703 AND 704)
D. W. Alexander Apr. 1992 21 p
(NASA-TM-108373; NAS 1.15:108373) Avail: CASI HC A03/MF A01

The Hubble space telescope (HST) solar array was designed to meet specific output power requirements after 2 years in low-Earth orbit, and to remain operational for 5 years. The array, therefore, had to withstand 30,000 thermal cycles between approximately +100 and -100 C. The ability of the array to meet this requirement was evaluated by thermal cycle testing, in vacuum, two 128-cell solar cell modules that exactly duplicated the flight HST solar array design. Also, the ability of the flight array to survive an emergency deployment during the dark (cold) portion of an orbit was evaluated by performing a cold-roll test using one module. Author

N93-10591*# Boeing Aerospace Co., Seattle, WA.
RESULTS FROM TESTING AND ANALYSIS OF SOLAR CELLS FLOWN ON LDEF
Harry Dursch *In* NASA. Langley Research Center, LDEF Materials Workshop 1991, Part 2 Sep. 1992 p 649-660 (For primary document see N93-10578 01-27)
Avail: CASI HC A03/MF A03

45 ENVIRONMENT POLLUTION

Includes atmospheric, noise, thermal, and water pollution.

N93-10256*# National Aeronautics and Space Administration. Goddard Space Flight Center, Greenbelt, MD.
THE CURRENT AND FUTURE ENVIRONMENTAL ROLE OF ATMOSPHERIC METHANE: MODEL STUDIES AND UNCERTAINTIES
Joseph P. Pinto (Environmental Protection Agency, Research Triangle Park, NC.), Christoph H. Bruehl (Max-Planck-Inst. fuer Chemie, Mainz, Germany), and Anne M. Thompson 1992 30 p Sponsored in part by EPA
(NASA-CR-190662; NAS 1.26:190662; PB92-188820; EPA/600/A-92/116) Avail: CASI HC A03/MF A01

Concern over increasing levels of methane in the atmosphere centers on its radiative and chemical properties. Methane absorbs terrestrial infrared radiation and contributes to the greenhouse effect. Effects on other greenhouse absorbers (e.g., O3, H2O, and CO2) as the result of its oxidation must also be considered. These indirect effects have made the quantification of the total climatic effects of chemically active gases, such as CH4, much more difficult that if direct radiative effects are considered alone. The oxidation of methane also exerts a controlling influence on atmospheric OH levels and is a major source of carbon monoxide. The variations in OH induced by changing CH4 levels feed back onto the lifetime of methane and the abundance of CO. There is a shortage of intercompared model results documenting the effects of CH4 and nonmethane hydrocarbon (NMHC) additions on tropospheric OH levels. Most analyses to date have relied on analyses of gas phase reaction sequences for methane oxidation without considering the numerous feedbacks on atmospheric chemistry. More complete modeling studies are needed because OH levels also depend on the emissions of CO, NMHCs, and NOy (NOx + NO3 + 2N2O5 + CH3CO3NO2(PAN) + HNO3 + HNO4 + ClNO3 + NO3), where NOx is NO + NO2 and NOy and NX are interchangeable terms. Furthermore, analyses which simulate the role of climate in controlling CH4 emissions from various natural sources (e.g., wetlands) are critical for attempting to predict the response of atmospheric methane levels to future climate change. GRA

N93-10289# North Central Forest Experiment Station, Saint Paul, MN.
THE DEPOSITION AND FATE OF TRACE METALS IN OUR ENVIRONMENT: SYMPOSIUM PROCEEDINGS
Elon S. Verry, ed. and Stephen J. Vermette, ed. 1992 174 p Symposium held in Philadelphia, PA, 8 Oct. 1991
(PB92-189216; FSGTR-NC-150) Avail: CASI HC A08/MF A02

On October 8, 1991, in Philadelphia, the National Atmospheric Deposition Program/National Trends Network (NADP/NTN) Technical Committee hosted a symposium on the deposition and fate of trace metals in the environment. Fourteen papers were prepared by 37 authors with a breadth of experience in trace metal ecology over the last decade. The proceedings are meant to inform the members of the analytic and collection methods for trace metals in precipitation, and the processing of trace metals in the landscape and its biota. It is a solid review of trace metals designed to facilitate an informed discussion about the addition of trace metals to the NADP/NTN network. GRA

N93-10384# Brookhaven National Lab., Upton, NY.
ANALYSIS OF AIR POLLUTION AND GREENHOUSE GASES
C. M. Benkovitz Mar. 1992 108 p
(Contract DE-AC02-76CH-00016)
(DE92-014955; BNL-47274) Avail: CASI HC A06/MF A02

The current objective of the project 'Analysis of Air Pollution

and Greenhouse Gases' is to develop a study of emissions and emission sources that could easily be linked to models of economic activity. Initial studies were conducted to evaluate data currently available linking activity rates and emissions estimates. The emissions inventory developed for the National Acid Precipitation Assessment Program (NAPAP) presents one of the most comprehensive data sets, and was chosen for our initial studies, which are described in this report. Over 99 percent of the SO2 emissions, 98 percent of the NO(x) emission and 57 percent of the VOC emissions from area sources are related to fuel combustion. The majority of emission from these sources are generated by the transportation sector. Activity rates for area sources are not archived with the NAPAP inventory; alternative derivations of these data will be part of the future activities of this project. The availability and completeness of the fuel heat content data in the NAPAP inventory were also studied. Approximately 10 percent of the SO2 emissions, 13 percent of the NO(x) emissions and 46 percent of the VOC emissions are generated by sources with unavailable data for fuel heat content. Initial estimates of pollutant emission rate per unit fuel heat content. Initial estimates of pollutant emission rate per unit fuel heat content were generated. Future studies for this project include the derivation of activity rates for area sources, improved explanations for the default fuel parameters defined in the NAPAP inventory and the development of links to data bases of economic activity. DOE

N93-10432# Environmental Protection Agency, Research Triangle Park, NC. Atmospheric Research and Exposure Assessment Lab.

SENSITIVITY OF MODELED OZONE CONCENTRATIONS TO UNCERTAINTIES IN BIOGENIC EMISSIONS

S. J. Roselle Jun. 1992 212 p

(PB92-192202; EPA/600/R-92/067) Avail: CASI HC A10/MF A03

The study examines the sensitivity of regional ozone (O3) modeling to uncertainties in biogenic emissions estimates. The United States Environmental Protection Agency's (EPA) Regional Oxidant Model (ROM) was used to simulate the photochemistry of the northeastern United States for the period 2-17 Jul. 1988. An operational model evaluation showed that ROM had a tendency to underpredict O3 when observed concentrations were above 70-80 ppb and to overpredict O3 when observed values were below this level. On average, the model underpredicted daily maximum O3 by 14 ppb. Spatial patterns of O3, however, were reproduced favorably by the model. Several simulations were performed to analyze the effects of uncertainties in biogenic emissions on predicted O3 and to study the effectiveness of two strategies of controlling anthropogenic emissions for reducing high O3 concentrations. Biogenic hydrocarbon emissions were adjusted by a factor of 3 to account for the existing range of uncertainty in these emissions. The impact of biogenic emission uncertainties on O3 predictions depended upon the availability of NO(x). In some extremely NO(x)-limited areas, increasing the amount of biogenic emissions decreased O3 concentrations. Two control strategies were compared in the simulations: (1) reduced anthropogenic hydrocarbon emissions; and (2) reduced anthropogenic hydrocarbon and NO(x) emissions. The simulations showed that hydrocarbon emission controls were more beneficial to the New York City area, but that combined NO(x) and hydrocarbon controls were more beneficial to other areas of the Northeast. Hydrocarbon controls were more effective as biogenic hydrocarbon emissions were reduced, whereas combined NO(x) and hydrocarbon controls were more effective as biogenic hydrocarbon emissions were increased. Author

N93-10772# National Oceanic and Atmospheric Administration, Boulder, CO. Environmental Research Labs.

CLIMATE MONITORING AND DIAGNOSTICS LABORATORY
Summary Report No. 19, 1990

Eldon E. Ferguson, ed. and Rita M. Rosson, ed. Dec. 1991 143 p

(PB92-162346) Avail: CASI HC A07/MF A02

The following sections comprise this summary report: CMDL Station Information; Observatory Reports; Atmospheric Radiation Monitoring Group; Carbon Cycle Group, Aerosols, Ozone, and Water Vapor Group; Special Projects; Acquisition and Data Management; Nitrous Oxide and Halocarbons Group; and Cooperative Programs. GRA

46 GEOPHYSICS

Includes aeronomy; upper and lower atmosphere studies; ionospheric and magnetospheric physics; and geomagnetism.

For space radiation see *93 Space Radiation.*

N93-10112*# Lunar and Planetary Inst., Houston, TX. Publications Services Dept.

INTERNATIONAL CONFERENCE ON LARGE METEORITE IMPACTS AND PLANETARY EVOLUTION

1992 93 p Conference held in Sudbury, Ontario, 31 Aug. - 2 Sep. 1992; sponsored by Barringer Crater Co., Falconbridge Ltd., Geological Survey of Canada, Inco Ltd., International Union of Geological Sciences, Laurentian Univ., LPI, and Ontario Ministry of Northern Development and Mines.

(Contract NASw-4574)

(NASA-CR-190677; NAS 1.26:190677; LPI-Contrib-790) Avail: CASI HC A05/MF A01

The papers that were accepted for the International Conference on Large Meteorite Impacts and Planetary Evolution, 31 Aug. - 2 Sep. 1992, are presented. One of the major paper topics was the Sudbury project. For individual titles, see N93-10113 through N93-10196.

N93-10113*# Paris VII Univ. (France).

CARBON AND OXYGEN ISOTOPE STUDY OF CARBONATES FROM HIGHLY SHOCKED CLASTS OF THE POLYMICT BRECCIA OF THE HAUGHTON CRATER (CANADA) **c90**

P. Agrinier, I. Martinez, M. Javoy, and U. Schaerer *In* Lunar and Planetary Inst., International Conference on Large Meteorite Impacts and Planetary Evolution 1992 p 1-2 (For primary document see N93-10112 01-46)

Avail: CASI HC A01/MF A01

It is known that the release of volatiles on impact is an important controlling factor in cratering processes in carbonate terranes and in the mobility of chemical elements. In order to assess the nature and the role of carbon- and oxygen-bearing volatiles during impact-induced metamorphism of sedimentary rocks, the C-13/C-12 and O-18/O-16 ratios and carbonate contents were determined for 30 shocked clasts from the Haughton Crater polymict breccia as well as for some unshocked carbonates from the sedimentary cover adjacent to the crater. Shock-induced CO2 loss during decarbonation of calcite is known to be a function of peak pressure and ambient partial pressure of the volatile species. In our clast samples, shocked from 20 to 60 GPa, we expect about 20 to 100 percent CO2 loss and preferential depletion in C-13 and O-18 in the residual carbonate. Rayleigh model (progressive loss of CO2) and batch model (single-step loss of CO2) curves for this depletion are shown. The magnitudes of the C-13 and O-18 depletions increase with the increase of the CO2 loss. In addition, the isotopic depletions should be correlated with an enrichment in CaO and MgO in the residual solid. Author

N93-10114*# Geological Survey, Iowa City, IA.

RESEARCH CORE DRILLING IN THE MANSON IMPACT STRUCTURE, IOWA **c90**

R. R. Anderson, J. B. Hartung, D. J. Roddy (Geological Survey, Flagstaff, AZ.), and E. M. Shoemaker (Geological Survey, Flagstaff, AZ.) *In* Lunar and Planetary Inst., International Conference on Large Meteorite Impacts and Planetary Evolution 1992 p 2-3 (For primary document see N93-10112 01-46)

Avail: CASI HC A01/MF A01

The Manson impact structure (MIS) has a diameter of 35 km and is the largest confirmed impact structure in the United States. The MIS has yielded a Ar-40/Ar-39 age of 65.7 Ma on microcline

from its central peak, an age that is indistinguishable from the age of the Cretaceous-Tertiary boundary. In the summer of 1991 the Iowa Geological Survey Bureau and U.S. Geological Survey initiated a research core drilling project on the MIS. The first core was beneath 55 m of glacial drift. The core penetrated a 6-m layered sequence of shale and siltstone and 42 m of Cretaceous shale-dominated sedimentary clast breccia. Below this breccia, the core encountered two crystalline rock clast breccia units. The upper unit is 53 m thick, with a glassy matrix displaying various degrees of devitrification. The upper half of this unit is dominated by the glassy matrix, with shock-deformed mineral grains (especially quartz) the most common clast. The glassy-matrix unit grades downward into the basal unit in the core, a crystalline rock breccia with a sandy matrix, the matrix dominated by igneous and metamorphic rock fragments or disaggregated grains from those rocks. The unit is about 45 m thick, and grains display abundant shock deformation features. Preliminary interpretations suggest that the crystalline rock breccias are the transient crater floor, lifted up with the central peak. The sedimentary clast breccia probably represents a postimpact debris flow from the crater rim, and the uppermost layered unit probably represents a large block associated with the flow. The second core (M-2) was drilled near the center of the crater moat in an area where an early crater model suggested the presence of postimpact lake sediments. The core encountered 39 m of sedimentary clast breccia, similar to that in the M-1 core. Beneath the breccia, 120 m of poorly consolidated, mildly deformed, and sheared siltstone, shale, and sandstone was encountered. The basal unit in the core was another sequence of sedimentary clast breccia. The two sedimentary clast units, like the lithologically similar unit in the M-1 core, probably formed as debris flows from the crater rim. The middle, nonbrecciated interval is probably a large, intact block of Upper Cretaceous strata transported from the crater rim with the debris flow. Alternatively, the sequence may represent the elusive postimpact lake sequence. Author

N93-10115*# Witwatersrand Univ., Johannesburg (South Africa). Dept. of Geophysics.

A QUASI-HERTZIAN STRESS FIELD FROM AN INTERNAL SOURCE: A POSSIBLE WORKING MODEL FOR THE VREDEFORT STRUCTURE

L. A. G. Antoine, W. U. Reimold, and W. P. Colliston (Orange Free State Univ., Bloemfontein, South Africa) *In* Lunar and Planetary Inst., International Conference on Large Meteorite Impacts and Planetary Evolution 1992 p 3-4 (For primary document see N93-10112 01-46)
Avail: CASI HC A01/MF A01

The Vredefort structure is a large domal feature about 110 km southeast of Johannesburg, South Africa, situated within and almost central to the large intracratonic Witwatersrand Basin. This structure consists of an Archean core of ca. 45 km in diameter, consisting largely of granitic gneiss, surrounded by a collar of metasedimentary and metavolcanic supracrustal rocks of the Dominian Group, Witwatersrand and Ventersdorp Supergroups, and Transvaal Sequence. The interpretation of images of the gravity and magnetic fields over Vredefort has permitted the delineation of several important features of the structure and of its environment. The outline of the collar strata is a prominent feature of both the gravity and the magnetic fields. The Vredefort structure shares this distinctive geometry with other structures (e.g., Manicouagan, Decaturville, Sierra Madera) of debated impact origin. In all these, successively older strata with steep outward dips are encountered while traversing inward to the center of the structure. A further attribute of these structures is the shortening of the outcrop of a particular stratigraphic unit compared to the original perimeter of that unit. To account for the geometric attributes of the Vredefort structure a mechanical scheme is required where there is radial movement of horizontal strata toward, with uplift in, the center of the Vredefort structure. Two models can be proposed: (1) one in which there is a rapid rise and violent disruption of cover rocks in response to expansion of a fluid accumulation; and (2) one in which there is, in contrast, a nonexplosive, quasi-Hertzian stress field resulting from a diapiric process. Both models can accommodate the geometry and structural components of Vredefort. Author

N93-10116*# Muenster Univ. (Germany). Inst. of Planetology.

SUDBURY PROJECT (UNIVERSITY OF MUENSTER-ONTARIO GEOLOGICAL SURVEY): ORIGIN OF THE POLYMICT, ALLOCHTHONOUS BRECCIAS OF THE ONAPING FORMATION

M. E. Avermann *In* Lunar and Planetary Inst., International Conference on Large Meteorite Impacts and Planetary Evolution 1992 p 4-5 (For primary document see N93-10112 01-46)
Avail: CASI HC A01/MF A01

The Sudbury structure has been interpreted as a deeply eroded remnant of a peak-ring basin. The polymict, allochthonous breccias of the Onaping Formation (OF) occur in the central part of the Sudbury structure, which is surrounded by the 1.85-Ga-old 'Sudbury Igneous Complex' (SIC). From bottom to top the OF can be divided into Basal, Gray, Green, and lower and upper Black members. The breccias were mapped in detail in the east range of the structure. The SIC and the lower part of the OF (Basal Member) are interpreted as the impact melt system. The overlying Gray Member is a breccia unit with a clastic matrix and has a sharp contact to the Basal Member. The Green Member is considered as a continuous uniform breccia layer on top of the Gray Member and comprises the former 'chlorite shard horizon'. The uppermost unit of the OF (Black Member) can be subdivided into a lower and an upper Black Member unit. The lower part (100-150 m thick) still shows petrographic features of suevitic breccias, small fragments of basement rocks, melt particles, chloritized particles, and breccia fragments in a dark, clastic matrix. Author

N93-10117*# Muenster Univ. (Germany).

SUDBURY PROJECT (UNIVERSITY OF MUENSTER-ONTARIO GEOLOGICAL SURVEY): SUMMARY OF RESULTS - AN UPDATED IMPACT MODEL

M. Avermann, L. Bischoff, P. Brockmeyer, D. Buhl (Bochum Univ., Germany), A. Deutsch, B. O. Dressler (Geological Survey of Canada, Toronto, Ontario), R. Lakomy, V. Mueller-Mohr, and D. Stoeffler *In* Lunar and Planetary Inst., International Conference on Large Meteorite Impacts and Planetary Evolution 1992 p 5-6 (For primary document see N93-10112 01-46)
Avail: CASI HC A01/MF A01

In 1984 the Ontario Geological Survey initiated a research project on the Sudbury structure (SS) in cooperation with the University of Muenster. The project included field mapping (1984-1989) and petrographic, chemical, and isotope analyses of the major stratigraphic units of the SS. Four diploma theses and four doctoral theses were performed during the project (1984-1992). Specific results of the various investigations are reported. Selected areas of the SS were mapped and sampled: Footwall rocks; Footwall breccia and parts of the sublayer and lower section of the Sudbury Igneous Complex (SIC); Onaping Formation and the upper section of the SIC; and Sudbury breccia and adjacent Footwall rocks along extended profiles up to 55 km from the SIC. All these stratigraphic units of the SS were studied in substantial detail by previous workers. The most important characteristic of the previous research is that it was based either on a volcanic model or on a mixed volcanic-impact model for the origin of the SS. The present project was clearly directed toward a test of the impact origin of the SS without invoking an endogenic component. In general, our results confirm the most widely accepted stratigraphic division of the SS. However, our interpretation of some of the major stratigraphic units is different from most views expressed. The stratigraphy of the SS and its new interpretation is given as a basis for discussion. Author

N93-10118*# Muenster Univ. (Germany). Inst. of Geology.

STRUCTURAL ASPECTS OF THE ARAGUAINHA IMPACT STRUCTURE (BRAZIL)

L. Bischoff, P. Brockmeyer, U. Jenchen, and R.-M. Swietlik *In* Lunar and Planetary Inst., International Conference on Large

Meteorite Impacts and Planetary Evolution 1992 p 6-7 (For primary document see N93-10112 01-46)
Avail: CASI HC A01/MF A01

The results of two months of field studies carried out in 1988 are presented. During that time the northeast segment was mapped and the structural setting of the central area was studied in detail. In addition, the structure of outer zones of the Araguainha Crater was investigated along three radial sections. Author

N93-10119*# Muenster Univ. (Germany).
SUDBURY PROJECT (UNIVERSITY OF MUENSTER-ONTARIO GEOLOGICAL SURVEY): FIELD STUDIES 1984-1989 - SUMMARY OF RESULTS
L. Bischoff, B. O. Dressler (Geological Survey of Canada, Toronto, Ontario), M. E. Avermann, P. Brockmeyer, R. Lakomy, and V. Mueller-Mohr *In* Lunar and Planetary Inst., International Conference on Large Meteorite Impacts and Planetary Evolution 1992 p 7 (For primary document see N93-10112 01-46)
Avail: CASI HC A01/MF A01

In cooperation between the Ontario Geological Survey and the Institute of Geology and Institute of Planetology, geological, petrological, and geochemical studies were carried out on impact-related phenomena of the Sudbury structure during the last decade. The main results of the field studies are briefly reviewed. Footwall rocks, sublayer, and lower sections of the Sudbury Igneous Complex (SIC) were mainly mapped and sampled in the northern (Levack Township) and western (Trillabelle and Sultana Properties) parts of the north range. Within these mapping areas Sudbury Breccias (SB) and Footwall Breccias (FB) were studied; SB were also investigated along extended profiles beyond the north and south ranges up to 55 km from the SIC. The Onaping Formation (OF) and the upper section of the SIC were studied both in the north range (Morgan and Dowling Townships) and in the southern east range (Capreol and McLennan Townships). Author

N93-10120*# Geological Survey, Denver, CO.
LARGE METEORITE IMPACTS: THE K/T MODEL c90
B. F. Bohor *In* Lunar and Planetary Inst., International Conference on Large Meteorite Impacts and Planetary Evolution 1992 p 8-9 (For primary document see N93-10112 01-46)
(NASA Order T-5715-P)
Avail: CASI HC A01/MF A01

The Cretaceous/Tertiary (K/T) boundary event represents probably the largest meteorite impact known on Earth. It is the only impact event conclusively linked to a worldwide mass extinction, a reflection of its gigantic scale and global influence. Until recently, the impact crater was not definitively located and only the distal ejecta of this impact was available for study. However, detailed investigations of this ejecta's mineralogy, geochemistry, microstratigraphy, and textures have allowed its modes of ejection and dispersal to be modeled without benefit of a source crater of known size and location. Author

N93-10121*# Geological Survey, Denver, CO.
SHOCKED ZIRCONS IN THE ONAPING FORMATION: FURTHER PROOF OF IMPACT ORIGIN c90
B. F. Bohor and W. J. Betterton *In* Lunar and Planetary Inst., International Conference on Large Meteorite Impacts and Planetary Evolution 1992 p 9-10 (For primary document see N93-10112 01-46)
Avail: CASI HC A01/MF A01

The Onaping Formation fills the structural basin at Sudbury, Ontario, Canada. This formation is composed of three members: a basal, coarse, mainly quartzitic breccia (Basal Member); a light-colored, heavily included, polymict middle unit (Gray Member); and a similar but dark-colored upper unit (Black Member). Two different origins were proposed for the Onaping: (1) volcanic ash-flow sheet; and (2) impact fall-back ejecta. These origins are critically discussed in a review paper coauthored by proponents of each view. Author

N93-10122*# Bringemeier (D.), Clausthal-Zellerfeld, (Germany).
SUEVITE SUPERPOSITION ON THE BUNTE BRECCIA IN NOERDLINGER RIES, GERMANY: NEW FINDINGS ON THE TRANSPORT MECHANISM OF IMPACTITES
D. Bringemeier *In* Lunar and Planetary Inst., International Conference on Large Meteorite Impacts and Planetary Evolution 1992 p 10-11 (For primary document see N93-10112 01-46)
Avail: CASI HC A01/MF A01

Research undertaken in the last decades in Noerdlinger Ries, Germany, has repeatedly emphasized the sharp contact between Bunte breccia and suevite. However, extensive investigations into this layer boundary have not yet been possible due to insufficient outcrop ratios. New outcrops enabled an in-depth investigation into the superposition of suevite on the Bunte breccia, which is assigned a key role in interpreting the transport mechanisms of ejecta of large impact. In two quarries lying several kilometers east and south-southwest of the crater, the contact between the suevite and Bunte breccia was recorded in detailed sections on outcrops of over 50 m in length. Author

N93-10123*# Bochum Univ. (Germany). Inst. of Geologie.
SUDBURY PROJECT (UNIVERSITY OF MUENSTER-ONTARIO GEOLOGICAL SURVEY): Sr-Nd IN HETEROLITHIC BRECCIAS AND GABBROIC DIKES
D. Buhl, A. Deutsch (Muenster Univ., Germany), R. Lakomy (Muenster Univ., Germany), P. Brockmeyer (Muenster Univ., Germany), and B. Dressler (Geological Survey of Canada, Toronto, Ontario) *In* Lunar and Planetary Inst., International Conference on Large Meteorite Impacts and Planetary Evolution 1992 p 11-12 (For primary document see N93-10112 01-46)
Avail: CASI HC A01/MF A01

One major objective of our Sudbury project was to define origin and age of the huge breccia units below and above the Sudbury Igneous Complex (SIC). The heterolithic Footwall Breccia (FB) represents a part of the uplifted crater floor. It contains subrounded fragments up to several meters in size and lithic fragments with shock features (greater than 10 GPa) embedded into a fine- to medium-grained matrix. Epsilon(sub Nd)-epsilon(sub Sr) relationships point to almost exclusively parautochthonous precursor lithologies. The different textures of the matrix reflect the metamorphic history of the breccia layer; thermal annealing by the overlying hot impact melt sheet (SIC) at temperatures greater than 1000 C resulted in melting of the fine crushed material, followed by an episode of metasomatic K-feldspar growth and, finally, formation of low-grade minerals such as actinolite and chlorite. Isotope relationships in the Onaping breccias (Gray and Green Member) are much more complex. All attempts to date the breccia formation failed: Zircons are entirely derived from country rocks and lack the pronounced Pb loss caused by the heat of the slowly cooling impact melt sheet (SIC). Rb-Sr techniques using either lithic fragments of different shock stages or the thin slab method, set time limits for the apparently pervasive alkali mobility in these suevitic breccias. The data array and the intercept in the plots point to a major Rb-Sr fractionation around 1.54 Ga ago. This model age is in the same range as the age obtained for the metasomatic matrix of the FB. Rb-Sr dating of a shock event in impact-related breccias seems to be possible only if their matrix had suffered total melting by the hot melt sheet (FB) or if they contain a high fraction of impact melt (suevitic Onaping breccias), whereas the degree of shock metamorphism in rock or lithic fragments plays a minor role. In the Sudbury case, however, the impact melt in the seuvitic breccias is devitrified and recrystallized, which changed Rb/Sr ratios quite drastically. Therefore, the Onaping breccias give only age limits for alteration and low-grade metamorphism. The Sm-Nd system was not reset during the Sudbury event; clasts as well as the matrix in the FB and in the Onaping breccias show preimpact 'Archean' Nd isotope signatures. Author

N93-10124*# Hong Kong Amateur Astronomical Society.
HONG KONG IS AN IMPACT CRATER: PROOF FROM THE GEOMORPHOLOGICAL AND GEOLOGICAL EVIDENCE
Chu-Lok Chan, Siben Wu (Chinese Academy of Geological

Sciences, Beijing.), and Xiuquan Luo (Chinese Academy of Geological Sciences, Beijing.) *In* Lunar and Planetary Inst., International Conference on Large Meteorite Impacts and Planetary Evolution 1992 p 12 (For primary document see N93-10112 01-46)

Avail: CASI HC A01/MF A01

Hong Kong is a city in southern China. The urban districts of Hong Kong, Kowloon, and Victoria Harbour are situated within Hong Kong. Hong Kong is surrounded by mountains with a diameter of 11 km. Three million people live inside the basin. The round structure of the mountains in Hong Kong has been describd as a granite dome that is deeply eroded (batholith). The circularity of the mountains, the existence of a central hill, the inner slope of the mountains being greater than the outer slope, the presence of deep layer rock inside the basin, and the depth-to-diameter ratio were studied. All this evidence shows that the Hong Kong structure satisfies the geomorphological requirement of an impact crater. Some shock metamorphic phenomena of the rocks in Hong Kong such as planar features, microspherilitic silica glass (lechaterlierite), fused margins of rock fragments, concussion fractures, impact glass in which some schlierens are consistent with pyroxene spiculites, etc., were first discoverd in Oct. 1990. In Hong Kong Island, an impact melt sheet was observed from the Victoria Peak to the southern shore. Quenching fractures of quartz in Kowloon fine-grained granite was also discovered. In our work, the K-Ar age (83.34 + 1.26 m.y.) of the impact melt rock, which is younger in comparison to the K-Ar age (117 m.y.) in Hong Kong and Kowloon granite, was measured, and the phenomena indicate that after the granite body formed, there was another geologic event. Maybe it is the Hong Kong cratering event.

Author

N93-10125*# National Aeronautics and Space Administration. Lyndon B. Johnson Space Center, Houston, TX.

MELT PRODUCTION IN LARGE-SCALE IMPACT EVENTS: CALCULATIONS OF IMPACT-MELT VOLUMES AND CRATER SCALING **c90**

Mark J. Cintala and Richard A. F. Grieve (Geological Survey of Canada, Toronto, Ontario) *In* Lunar and Planetary Inst., International Conference on Large Meteorite Impacts and Planetary Evolution 1992 p 13-14 (For primary document see N93-10112 01-46)

Avail: CASI HC A01/MF A01

Along with an apparent convergence in estimates of impact-melt volumes produced during planetary impact events, intensive efforts at deriving scaling relationships for crater dimensions have also yielded results. It is now possible to examine a variety of phenomena associated with impact-melt production during large cratering events and apply them to planetary problems. This contribution describes a method of combining calculations of impact-melt production with crater scaling to investigate the relationship between the two.

Author

N93-10126*# National Aeronautics and Space Administration. Lyndon B. Johnson Space Center, Houston, TX.

MELT PRODUCTION IN LARGE-SCALE IMPACT EVENTS: PLANETARY OBSERVATIONS AND IMPLICATIONS **c90**

Mark J. Cintala and Richard A. F. Grieve (Geological Survey of Canada, Toronto, Ontario) *In* Lunar and Planetary Inst., International Conference on Large Meteorite Impacts and Planetary Evoluation 1992 p 14-16 (For primary document see N93-10112 01-46)

Avail: CASI HC A01/MF A01

Differences in scaling relationships for crater formation and the generation of impact melt should lead to a variety of observable features and phenomena. These relationships infer that the volume of the transient cavity (and final crater) relative to the volume of impact melt (and the depth to which melting occurs) decreases as the effects of gravity and impact velocity increase. Since planetary gravity and impact velocity are variables in the calculation of cavity and impact-melt volumes, the implications of the model calculation will vary between planetary bodies. Details of the model calculations of impact-melt generation as a function of impact and target physical conditions were provided elsewhere, as were attempts to validate the model through ground-truth data on melt volumes, shock attenuation, and morphology from terrestrial impact craters.

Author

N93-10127*# Orange Free State Univ., Bloemfontein (South Africa). Dept. of Geology.

STRUCTURAL REVIEW OF THE VREDEFORT DOME

W. P. Colliston and W. U. Reimold (Witwatersrand Univ., Johannesburg, South Africa) *In* Lunar and Planetary Inst., International Conference on Large Meteorite Impacts and Planetary Evolution 1992 p 16-17 (For primary document see N93-10112 01-46)

Avail: CASI HC A01/MF A01

The structure of the older-than-3.2-Ga Archean basement and Archean-to-Precambrian sedimentary/volcanic rocks (3.07 to ca. 2.2 Ga) in the center of the Witwatersrand Basin to the southwest of Johannesburg (South Africa) is dominated by the ca. 2.0-Ga megascopic Vredefort 'Dome' structure. The effect of the 'Vredefort event' is demonstrably large and is evident within a northerly arc of about 100 km radius around the granitic core of the structure. Northerly asymmetric overturning of the strata is observed within the first 17 km (strata is horizontal in the south), followed by a 40-km-wide rim synclinorium. Fold and fault structures (normal, reverse, and strike-slip) are locally as well as regionally concentrically arranged with respect to the northern and western sides of the structure. The unusual category of brittle deformation, the so-called 'shock deformation', observed in the collar strata has attracted worldwide attention over the past two decades. These deformation phenomena include the presence of coesite and stishovite, mylonites, and pseudotachylites, cataclasis at a microscopic scale, and the ubiquitous development of multiply striated joint surfaces (which include shatter cones, orthogonal, curviplanar, and conjugate fractures). The macroscopic to microscopic deformation features have led to the formulation of various hypotheses to account for the origin of the Vredefort structure: (1) tectonic hypotheses--deep crustal shear model, doming and N-directed thrust fault model, fold interference model, and diapir model; (2) the exogenous bolide impact hypothesis; and (3) the endogenous cryptoexplosion model.

Author

N93-10128*# Toronto Univ. (Ontario). Dept. of Geology.

INTRUSIVE ORIGIN OF THE SUDBURY IGNEOUS COMPLEX: STRUCTURAL AND SEDIMENTOLOGICAL EVIDENCE

E. J. Cowan and W. M. Schwerdtner *In* Lunar and Planetary Inst., International Conference on Large Meteorite Impacts and Planetary Evolution 1992 p 17-18 (For primary document see N93-10112 01-46)

Avail: CASI HC A01/MF A01

In recent years, many geoscientists have come to believe that the Sudbury event was exogenic rather than endogenic. Critical to a recent exogenic hypothesis is the impact melt origin of the Sudbury Igneous Complex (SIC). Such origin implies that the SIC was emplaced before deposition of the Whitewater Group, in contrast to origins in which the SIC postdates the lithification of the Onaping Formation. Structural and sedimentological evidence is summarized herein that supports an intrusion of the SIC after lithification of all Whitewater Group strata, and conflicts with the hypothesis advanced by other researchers.

Author

N93-10129*# Brown Univ., Providence, RI. Dept. of Geological Sciences.

ENHANCED MAGNETIC FIELD PRODUCTION DURING OBLIQUE HYPERVELOCITY IMPACTS

D. A. Crawford and P. H. Schultz *In* Lunar and Planetary Inst., International Conference on Large Meteorite Impacts and Planetary Evolution 1992 p 18-20 (For primary document see N93-10112 01-46)

Avail: CASI HC A01/MF A01

The natural remanent magnetization of the lunar surface as displayed in returned lunar samples and the data returned by the Apollo subsatellite magnetometer has an unexpectedly high magnitude and exhibits spatial variation at all scales. The origin

of the lunar remanent fields may be due to crustal remanence of a core dynamo field occurring early in lunar history prior to extensive modification by impact or remanence of transient fields, particularly associated with impacts, occurring on a local scale throughout lunar history. The presence of an early core dynamo field would have strong consequences for the formation and early evolution of the Moon, yet to deconvolve the role that an internally generated core dynamo field may have had, it is necessary to understand how the magnetic state of the lunar surface has developed through time. Impact-induced magnetism may be an important component of the present magnetic state of the lunar surface. New theoretical considerations suggest that transient magnetic fields within plasma produced by hypervelocity meteorite impacts may have greater significance at larger scales than previously thought. Author

N93-10130*# Houston Univ., TX. Dept. of Geosciences.
IMPACTITE AND PSEUDOTACHYLITE FROM ROTER KAMM CRATER, NAMIBIA
J. J. Degenhardt, Jr. (Texaco, Inc., Houston, TX.), P. C. Buchanan, and A. M. Reid *In* Lunar and Planetary Inst., International Conference on Large Meteorite Impacts and Planetary Evolution 1992 p 20-21 (For primary document see N93-10112 01-46)
Avail: CASI HC A01/MF A01

Pseudotachylite is known to occur in a variety of geologic settings including thrust belts (e.g., the Alps and the Himalayas) and impact craters such as Roter Kamm, Namibia. Controversy exists, however, as to whether pseudotachylite can be produced by shock brecciation as well as by tectonic frictional melting. Also open to debate is the question of whether pseudotachylites form by frictional fusion or by cataclasis. It was speculated that the pseudotachylite at Roter Kamm was formed by extensional settling and adjustment of basement blocks during 'late modification stage' of impact. The occurrence of pseudotachylite in association with rocks resembling quenched glass bombs and melt breccias in a relatively young crater of known impact origin offers a rare opportunity to compare features of these materials. Petrographic, x-ray diffraction, and electron microprobe analyses of the impactites and pseudotachylites are being employed to determine the modes of deformation and to assess the role of frictional melting and comminution of adjacent target rocks. Author

N93-10131*# Muenster Univ. (Germany). Inst. for Planetology.
SUDBURY PROJECT (UNIVERSITY OF MUENSTER-ONTARIO GEOLOGICAL SURVEY): ISOTOPE SYSTEMATICS SUPPORT THE IMPACT ORIGIN
A. Deutsch, D. Buhl (Bochum Univ., Germany), P. Brockmeyer, R. Lakomy, and M. Flucks *In* Lunar and Planetary Inst., International Conference on Large Meteorite Impacts and Planetary Evolution 1992 p 21-22 (For primary document see N93-10112 01-46)
Avail: CASI HC A01/MF A01

Within the framework of the Sudbury project a considerable number of Sr-Nd isotope analyses were carried out on petrographically well-defined samples of different breccia units. Together with isotope data from the literature these data are reviewed under the aspect of a self-consistent impact model. The crucial point of this model is that the Sudbury Igneous Complex (SIC) is interpreted as a differentiated impact melt sheet without any need for an endogenic 'magmatic' component such as 'impact-triggered' magmatism or 'partial' impact melting of the crust and mixing with a mantle-derived magma. Author

N93-10132*# Arizona State Univ., Tempe. Dept. of Geology.
NORIL'SK/SIBERIAN PLATEAU BASALTS AND BAHAMA HOT SPOT: IMPACT TRIGGERED?
R. S. Deitz and J. F. McHone *In* Lunar and Planetary Inst., International Conference on Large Meteorite Impacts and Planetary Evolution 1992 p 22-23 (For primary document see N93-10112 01-46)
Avail: CASI HC A01/MF A01

Twenty-eight years after one of us argued that Sudbury was an astrobleme, this interpretation has only recently attained wide acceptance; not so for the view that the Sudbury Cu/Ni sulfide ores are cosmogenic. Other research has provided the triggering of plateau basalts by super-large impacts a modicum of respectability. The recent apparent successful tying in of the K/T extinctions to the Chicxulub astrobleme in the Yucatan encourages the search for an impact event that may have caused the other two major post-Paleozoic extinctions (P/Tr, Tr/J). This gives us heart to offer two further outrageous hypotheses. The cosmogenic concept for the Sudbury ore deposite remains viable because it is giant, nonultramafic, and unique (except for Noril'sk). The Triassic/Jurassic boundary catastrophic extinctions have been attributed to the Manicouagan asteroidal impact, but recent radiometric dating indicates these events are diachronous (Manicouagan astrobleme 212 +/- 2 Ma and Tr/J boundary 200 Ma). Author

N93-10133*# Melbourne Univ., Carlton (Australia). Dept. of Geology.
MOBILIZATION OF THE PLATINUM GROUP ELEMENTS BY LOW-TEMPERATURE FLUIDS: IMPLICATIONS FOR MINERALIZATION AND THE IRIDIUM CONTROVERSY
Kim Dowling, Reid R. Keays, Malcolm W. Wallace, and Victor A. Gostin (Adelaide Univ., Australia) *In* Lunar and Planetary Inst., International Conference on Large Meteorite Impacts and Planetary Evolution 1992 p 23 (For primary document see N93-10112 01-46)
Avail: CASI HC A01/MF A01

Geochemical investigations on the widely dispersed Late Proterozoic Acraman impact ejecta horizon and its host marine shales in the Adelaide Geosyncline provide strong evidence for low-temperature mobilization of the platinum group elements (PGE), including Ir. The ejecta horizon was formed when the middle Proterozoic dacitic volcanics in the Gawler Ranges, central South Australia, were impacted by a very large (ca. 4 km) meteorite. The resulting structure, now represented by Lake Acraman, is Australia's largest meteorite impact structure. Debris from the impact was blasted for many hundreds of kilometers, some falling into the shallow sea of the Adelaide Geosyncline, some 300 km to the east of the impact site. Author

N93-10134*# New Mexico Univ., Albuquerque. Dept. of Geology.
DOES THE BUSHVELD-VREDEFORT SYSTEM (SOUTH AFRICA) RECORD THE LARGEST KNOWN TERRESTRIAL IMPACT CATASTROPHE?
W. E. Elston *In* Lunar and Planetary Inst., International Conference on Large Meteorite Impacts and Planetary Evolution 1992 p 23-24 (For primary document see N93-10112 01-46)
Avail: CASI HC A01/MF A01

The unique 2.05-Ga Bushveld and Vredefort complexes cover 100,000 sq km (diameter 400 km) on the otherwise stable Kaapvaal craton. Since the 1920's, workers have recognized that they are bracketed by the same units and were probably formed by related processes. Modern field studies and radiometric dates have provided no compelling evidence for different ages. Previous researchers invoked magmatic upthrust. Daly later attributed Vredefort to impact, but never applied his concept to the Bushveld. Subsequently, Vredefort yielded shatter cones, coesite and stishovite, and planar features; pseudotachylite (indistinguishable from Sudbury) was long known to be present. Other research concluded that at least four simultaneous impacts caused the Bushveld-Vredefort system. Three impacts formed overlapping Bushveld basins; the fourth made the Vredefort dome. The nature of intra-Bushveld 'fragments' and the properties of Rooiberg Felsite offer clues. Author

N93-10135*# California Inst. of Tech., Pasadena. Div. of Geological and Planetary Science.
RUTHENIUM/IRIDIUM RATIOS IN THE CRETACEOUS-TERTIARY BOUNDARY CLAY: IMPLICATIONS FOR GLOBAL DISPERSAL AND FRACTIONATION WITHIN THE EJECTA CLOUD
Noreen Joyce Evans, W. D. Goodfellow (Geological Survey of Canada, Toronto, Ontario), D. C. Gregoire (Geological Survey of

Canada, Toronto, Ontario), and J. Veizer (Ottawa Univ., Ontario) *In* Lunar and Planetary Inst., International Conference on Large Meteorite Impacts and Planetary Evolution 1992 p 25 (For primary document see N93-10112 01-46)
Avail: CASI HC A01/MF A01

Ruthenium (Ru) and iridium (Ir) are the least mobile platinum group elements (PGE's) within the Cretaceous-Tertiary (K-T) boundary clay (BC). The Ru/Ir ratio is, therefore, the most useful PGE interelement ratio for distinguishing terrestrial and extraterrestrial contributions to the BC. The Ru/Ir ratio of marine K-T sections (1.77 +/- 0.53) is statistically different from that of the continental sections (0.93 +/- 0.28). The marine Ru/Ir ratios are chondritic (C1 = 1.48 +/- 0.09), but the continental ratios are not. We discovered an inverse correlation of shocked quartz size (or distance from the impact site) and Ru/Ir ratio. This correlation may arise from the difference in Ru and Ir vaporization temperature and/or fractionation during condensation from the ejecta cloud. Postsedimentary alteration, remobilization, or terrestrial PGE input may be responsible for the Ru/Ir ratio variations within the groups of marine and continental sites studied. The marine ratios could also be attained if approximately 15 percent of the boundary metals were contributed by Deccan Trap emissions. However, volcanic emissions could not have been the principal source of the PGE's in the BC because mantle PGE ratios and abundances are inconsistent with those measured in the clay. The Ru/Ir values for pristine Tertiary mantle xenoliths (2.6 +/- 0.48), picrites (4.1 +/- 1.8), and Deccan Trap basalt (3.42 +/- 1.96) are all statistically distinct from those measured in the K-T BC. Author

N93-10136*# Moscow State Univ. (USSR). Dept. of Geology.
DIAPLECTIC TRANSFORMATION OF MINERALS: VOROTILOV DRILL CORE, PUCHEZH-KATUNKI IMPACT CRATER, RUSSIA
V. I. Feldman *In* Lunar and Planetary Inst., International Conference on Large Meteorite Impacts and Planetary Evolution 1992 p 25 (For primary document see N93-10112 01-46)
Avail: CASI HC A01/MF A01

The Vorotilov core was drilled in the central uplift of the Puchezh-Katunki astrobleme to a depth of 5.1 km. Impactites are revealed in the rocks of the core beginning from a depth of 366 m: suevites (66 m), allogenic breccias (112 m), and autogenic breccias (deeper than 544 m). These rocks are represented by shocked-metamorphic gneisses, schists, amphibolites of Archean age, and magmatic rocks (dolerites, olivines, and peridotites) that lie between them. Author

N93-10137*# Stanford Univ., CA. Dept. of Geology.
BRECCIA DIKES FROM THE BEAVERHEAD IMPACT STRUCTURE, SOUTHWEST MONTANA
P. S. Fiske, S. B. Hougen (Princeton Univ., NJ.), and R. B. Hargraves (Princeton Univ., NJ.) *In* Lunar and Planetary Inst., International Conference on Large Meteorite Impacts and Planetary Evolution 1992 p 26 (For primary document see N93-10112 01-46)
Avail: CASI HC A01/MF A01

While shatter cones are generally accepted as indicators of meteorite impact, older petrologic features are not widely recognized in the geologic community. Breccia dikes are one such feature. They are found in many large impact structures occurring over an area at least as extensively as shatter cones. Breccia dikes will survive moderate degrees of metamorphism and tectonism, unlike many other microscopic features (shocked quartz grains, high-pressure polymorphs, etc.) and even large-scale features such as annular or bowl-shaped topographic features. Thus, they are important diagnostic criteria, especially for large, poorly preserved impact structures. The Beaverhead Impact structure is a recently discovered, deeply eroded impact structure in southwestern Montana. The remains of the structure are delineated by the occurrence of shatter cones, found in an area greater than 200 sq km, occurring within the Cabin thrust plate, part of the Cretaceous Sevier fold and thrust system. The distribution of shatter cones is further truncated by Tertiary normal faults. The present remains represent an allochthonous fragment of a larger structure. Author

N93-10138*# National Aeronautics and Space Administration. Goddard Space Flight Center, Greenbelt, MD.
NEW PERSPECTIVES ON THE POPIGAI IMPACT STRUCTURE
J. B. Garvin and A. L. Deino (California Univ., Berkeley.) *In* Lunar and Planetary Inst., International Conference on Large Meteorite Impacts and Planetary Evolution 1992 p 27-28 (For primary document see N93-10112 01-46)
Avail: CASI HC A01/MF A01

The record of large-scale cratering on Earth is scant, and the only currently 'proven' 100-km-class impact structure known to have formed within the Cenozoic is Popigai, located in the Siberian Arctic at 71.5 deg N, 111 deg E. Popigai is clearly a multiringed impact basin formed within the crystalline shield rocks (Anabar) and platform sediments of the Siberian taiga, and estimates of the volume of preserved impact melt typically exceed 1700 cu km, which is within a factor of 2-3 of what would be predicted using scaling relationships. We present the preliminary results of an analysis of the present-day topography of the Popigai structure, together with refined absolute age estimates, in order to reconstruct the pre-erosional morphology of the basin, as well as to quantify the erosion or sediment infill rates in the Popigai region. Author

N93-10139*# National Aeronautics and Space Administration. Goddard Space Flight Center, Greenbelt, MD.
THE ZHAMANSHIN IMPACT FEATURE: A NEW CLASS OF COMPLEX CRATER?
J. B. Garvin and C. C. Schnetzler (Maryland Univ., College Park.) *In* Lunar and Planetary Inst., International Conference on Large Meteorite Impacts and Planetary Evolution 1992 p 28-29 (For primary document see N93-10112 01-46)
Avail: CASI HC A01/MF A01

The record of 10-km-scale impact events of Quaternary age includes only two 'proven' impact structures: the Zhamanshin Impact Feature (ZIF) and the Bosumtwi Impact Crater (BIC). What makes these impact landforms interesting from the standpoint of recent Earth history is their almost total lack of morphologic similarity, in spite of similar absolute ages and dimensions. The BIC resembles pristine complex craters on the Moon to first order (i.e., 'U'-shaped topographic cross section with preserved rim), while the ZIF displays virtually none of the typical morphologic elements of a 13- to 14-km-diameter complex crater. Indeed, this apparent lack of a craterlike surficial topographic expression initially led Soviet geologists to conclude that the structure was only 5.5 to 6 km in diameter and at least 4.5 Ma in age. However, more recent drilling and geophysical observations at the ZIF have indicated that its pre-erosional diameter is at least 13.5 km, and that its age is most probably 0.87 Ma. Why the present topographic expression of a 13.5-km complex impact crater less than 1 m.y. old most closely resembles heavily degraded Mesozoic shield craters such as Lappajarvi is a question of considerable debate. Hypotheses for the lack of a clearly defined craterlike form at the ZIF include a highly oblique impact, a low-strength 'cometary' projectile, weak or water-saturated target materials, and anomalous erosion patterns. The problem remains unresolved because typical erosion rates within the arid sedimentary platform environment of central Kazakhstan in which the ZIF is located are typically low; it would require at least a factor of 10 greater erosion at the ZIF in order to degrade the near-rim ejecta typical of a 13.5-km complex crater by hundreds of meters in only 0.87 Ma, and to partially infill an inner cavity with 27 cu km (an equivalent uniform thickness of infill of 166 m). Our analysis of the degree of erosion and infill at the ZIF calls for rates in the 0.19 to 0.38 mm/yr range over the lifetime of the landform, which are a factor of 10 to 20 in excess of typical rates for the Kazakhstan semidesert. Author

N93-10140*# Bureau of Mineral Resources, Geology and Geophysics, Canberra (Australia).
ASTEROIDS AND ARCHAEAN CRUSTAL EVOLUTION: TESTS OF POSSIBLE GENETIC LINKS BETWEEN MAJOR MANTLE/CRUST MELTING EVENTS AND CLUSTERED EXTRATERRESTRIAL BOMBARDMENTS
A. Y. Glikson *In* Lunar and Planetary Inst., International

Conference on Large Meteorite Impacts and Planetary Evolution 1992 p 29-30 (For primary document see N93-10112 01-46)
Avail: CASI HC A01/MF A01

Since the oldest intact terrestrial rocks of ca. 4.0 Ga and oldest zircon xenocrysts of ca. 4.3 Ga measured to date overlap with the lunar late heavy bombardment, the early Precambrian record requires close reexamination vis a vis the effects of megaimpacts. The identification of microtektite-bearing horizons containing spinals of chondritic chemistry and Ir anomalies in 3.5-3.4-Ga greenstone belts provides the first direct evidence for large-scale Archaean impacts. The Archaean crustal record contains evidence for several major greenstone-granite-forming episodes where deep upwelling and adiabatic fusion of the mantle was accompanied by contemporaneous crustal anatexis. Isotopic age studies suggest evidence for principal age clusters about 3.5, 3.0, and 2.7 (+/- 0.8) Ga, relics of a ca. 3.8-Ga event, and several less well defined episodes. These peak events were accompanied and followed by protracted thermal fluctuations in intracrustal high-grade metamorphic zones. Interpretations of these events in terms of internal dynamics of the Earth are difficult to reconcile with the thermal behavior of silicate rheologies in a continuously convecting mantle regime. A triggering of these episodes by mantle rebound response to intermittent extraterrestrial asteroid impacts is supported by (1) identification of major Archaean impacts from microtektite and distal ejecta horizons marked by Ir anomalies; (2) geochemical and experimental evidence for mantle upwelling, possibly from levels as deep as the transition zone; and (3) catastrophic adiabatic melting required to generate peridotitic komatites. Episodic differentiation/accretion growth of sial consequent on these events is capable of resolving the volume problem that arises from comparisons between modern continental crust and the estimated sial produced by continuous two-stage mantle melting processes. The volume problem is exacerbated by projected high accretion rates under Archaean geotherms. It is suggested that impact shock effects have been largely obscured by (1) outpouring of voluminous basic/ultrabasic lavas, inundating shock-deformed crust and extending beyond the perimeters of impact excavated basins; (2) gravity subsidence and downfaulting of terrestrial maria, accounting for the burial and anatexis of subgreenstone basement; and (3) extensive shearing and recrystallization at elevated temperatures of impact structure, breccias, and mineral deformation features beneath impact-excavated basins, relics of which may be retained in structural windows in high-grade metamorphic terranes. Author

N93-10141*# Adelaide Univ. (Australia). Dept. of Geology and Geophysics.
THE ACRAMAN IMPACT AND ITS WIDESPREAD EJECTA, SOUTH AUSTRALIA
V. A. Gostin, R. R. Keays (Melbourne Univ., Carlton, Australia), and M. W. Wallace (Melbourne Univ., Carlton, Australia) *In* Lunar and Planetary Inst., International Conference on Large Meteorite Impacts and Planetary Evolution 1992 p 30-31 (For primary document see N93-10112 01-46)
Avail: CASI HC A01/MF A01

Discovery of a widespread horizon of shock-deformed volcaniclastic ejecta preserved in Late Proterozoic (approx. 600 Ma) shales in South Australia and its probable link to the Acraman impact structure in the Middle Proterozoic Gawler Range. Volcanics provide a rare opportunity to study the effects of a major terrestrial impact, including the sedimentology and distribution of an ejecta blanket and its precious-metal signature. The ejecta horizon occurs in the Bunyeroo Formation at many localities within the Adelaide Geosyncline, including the Wearing Hills, which are approx. 350 km northeast of the Acraman impact site. Following a search at the same stratigraphic level in other basins in South Australia, the ejecta has been located within the Lower Rodda beds of the Officer Basin, extending the limits of the ejecta to approx. 470 km northwest of the Acraman impact structure. The ejecta is therefore widely dispersed, and provides an important chronostratigraphic marker enabling precise correlation of Late Proterozoic sequences in southern Australia. In summary, the Bunyeroo ejecta is unique as the only known example of a widely dispersed, coarse-grained ejecta blanket that is, moreover, strongly linked to a known major impact structure. The marked Ir-PGE anomalies in the ejecta horizon provide support for the hypothesis that meteorite impact events can produce Ir anomalies interrestrial sediments. The findings also indicate that Ir can be mobilized and concentrated in sediments by low-temperature diagenetic processes. The identification of ejecta horizons in sedimentary rocks therefore should be based on the coincidence of shock-metamorphic features in the detritus and clear Ir anomalies. Author

N93-10142*# Lawrence Livermore National Lab., CA.
OPTICAL AND TEM STUDY OF SHOCK METAMORPHISM FROM THE SEDAN TEST SITE
A. J. Gratz *In* Lunar and Planetary Inst., International Conference on Large Meteorite Impacts and Planetary Evolution 1992 p 31 (For primary document see N93-10112 01-46)
Avail: CASI HC A01/MF A01

Thus far, detailed petrologic studies of shock metamorphism have been performed on samples recovered from laboratory experiments and on a few natural impactites. The loading history of these samples is quite different: In particular, laboratory experiments spend only a short time (less than 1 microsec) at peak pressure, whereas natural impactites may have stress pulses from 0.1 - 1 ms. On the other hand, laboratory experiments have known stress histories; natural impactites do not. Natural samples are also subjected to thousands or millions of years of postshock annealing and/or weathering. A useful intermediate case is that of nuclear detonation. Stress pulses for these events can reach 0.1 ms or higher, and samples are obtained in pristine condition. All three types of loading produce stresses of hundreds of kilobars. Samples studied were taken from the Sedan nulcear test site, and consist of a coarse-grained granodiorite containing quartz, K-feldspar, cordierite, and hornblende. Samples were studied optically in this section, then were thinned with an ion mill and studied by transmission electron microscopy (TEM). Optically, quartz and K-feldspar displayed numerous sets of planar deformation features (PDF's) identical to the nondecorated PDF's seen in laboratory samples and many natural impactites. TEM study showed that the PDF's in quartz and feldspar corresponded to densely packed wide transformation lamellae identical to those described in laboratory studies. The transformation lamellae in both minerals were amorphous, with no sign of high-pressure phases. In the case of K-feldspar only, narrow sublamellae extended outward from some wide lamellae. Quartz, which was more abundant and studied more extensively, contained no shock-induced dislocations. Some planar features were also seen in cordierite, but could not be identified due to rapid beam damage. No shock defects were seen in hornblende in TEM. The shock-induced defects present at the Sedan site are very similar to those seen in shock recovery experiments, and also to those present at certain natural events (e.g., Meteor Crater). This suggests that shock deformation in quartz is not strongly dependent on shock pulse duration, and that laboratory recovery experiments are useful simulations of natural impact events. Author

N93-10143*# Lawrence Livermore National Lab., CA.
SIMULATED METEORITE IMPACTS AND VOLCANIC EXPLOSIONS: EJECTA ANALYSES AND PLANETARY IMPLICATIONS **c90**
A. J. Gratz and W. J. Nellis *In* Lunar and Planetary Inst., International Conference on Large Meteorite Impacts and Planetary Evolution 1992 p 31-32 (For primary document see N93-10112 01-46)
Avail: CASI HC A01/MF A01

Past cratering studies have focused primarily on crater morphology. However, important questions remain about the nature of crater deposits. Phenomena that need to be studied include the distribution of shock effects in crater deposits and crater walls; the origin of mono- and polymict breccia; differences between local and distal ejecta; deformation induced by explosive volcanism; and the production of unshocked, high-speed ejecta that could form the lunar and martian meteorites found on the Earth. To study these phenomena, one must characterize ejecta and crater

wall materials from impacts produced under controlled conditions. New efforts at LLNL simulate impacts and volcanism and study resultant deformation. All experiments use the two-stage light-gas gun facility at LLNL to accelerate projectiles to velocities of 0.2 to 4.3 km/s, including shock pressures of 0.9 to 50 GPa. We use granite targets and novel experimental geometries to unravel cratering processes in crystalline rocks. We have thus far conducted three types of simulations: soft recovery of ejecta, 'frozen crater' experiments, and an 'artificial volcano. Our ejecta recovery experiments produced a useful separation of impactites. Material originally below the projectile remained trapped there, embedded in the soft metal of the flyer plate. In contrast, material directly adjacent to the projectile was jetted away from the impact, producing an ejecta cone that was trapped in the foam recovery fixture. We find that a significant component of crater ejecta shows no signs of strong shock; this material comes from the near-surface 'interference zone' surrounding the impact site. This phenomenon explains the existence of unshocked meteorites on the Earth of lunar and martian origin. Impact of a large bolide on neighboring planets will produce high-speed, weakly shocked ejecta, which may be trapped by the Earth's gravitational field. 'Frozen crater' experiments show that the interference zone is highly localized; indeed, disaggregation does not extend beyond approx. 1.5 crater radii. A cone-shaped region extending downward from the impact site is completely disaggregated, including powdered rock that escaped into the projectile tube. Petrographic analysis of crater ejecta and wall material will be presented. Finally, study of ejecta from 0.9- and 1.3-GPa simulations of volcanic explosions reveal a complete lack of shock metamorphism. The ejecta shows no evidence of PDF's, amorphization, high-pressure phases, or mosaicism. Instead, all deformation was brittle, with fractures irregular (not planar) and most intergranular. The extent of fracturing was remarkable, with the entire sample reduced to fragments of gravel size and smaller. Author

N93-10144*# National Aeronautics and Space Administration. Lyndon B. Johnson Space Center, Houston, TX.

MELT PRODUCTION IN LARGE-SCALE IMPACT EVENTS: IMPLICATIONS AND OBSERVATIONS AT TERRESTRIAL CRATERS

Richard A. F. Grieve (Geological Survey of Canada, Toronto, Ontario) and Mark J. Cintala *In* Lunar and Planetary Inst., International Conference on Large Meteorite Impacts and Planetary Evolution 1992 p 32-33 (For primary document see N93-10112 01-46)

Avail: CASI HC A01/MF A01

The volume of impact melt relative to the volume of the transient cavity increases with the size of the impact event. Here, we use the impact of chondrite into granite at 15, 25, and 50 km s(sup -1) to model impact-melt volumes at terrestrial craters in crystalline targets and explore the implications for terrestrial craters. Figures are presented that illustrate the relationships between melt volume and final crater diameter D(sub R) for observed terrestrial craters in crystalline targets; also included are model curves for the three different impact velocities. One implication of the increase in melt volumes with increasing crater size is that the depth of melting will also increase. This requires that shock effects occurring at the base of the cavity in simple craters and in the uplifted peaks of central structures at complex craters record progressively higher pressures with increasing crater size, up to a maximum of partial melting (approx. 45 GPa). Higher pressures cannot be recorded in the parautochthonous rocks of the cavity floor as they will be represented by impact melt, which will not remain in place. We have estimated maximum recorded pressures from a review of the literature, using such observations as planar features in quartz and feldspar, diaplectic glasses of feldspar and quartz, and partial fusion and vesiculation, as calibrated with estimates of the pressures required for their formation. Erosion complicates the picture by removing the surficial (most highly shocked) rocks in uplifted structures, thereby reducing the maximum shock pressures observed. In addition, the range of pressures that can be recorded is limited. Nevertheless, the data define a trend to higher recorded pressures with crater diameter, which is consistent with the implications of the model. A second implication is that, as the limit of melting intersects the base of the cavity, central topographic peaks will be modified in appearance and ultimately will not occur. That is, the peak will first develop a central depression, due to the flow of low-strength melted materials, when the melt volume begins to intersect the transient-cavity base.

Author

N93-10145*# Geological Survey, Denver, CO.

VENUSIAN IMPACT BASINS AND CRATERED TERRAINS c91

Warren B. Hamilton *In* Lunar and Planetary Inst., International Conference on Large Meteorite Impacts and Planetary Evolution 1992 p 33-35 (For primary document see N93-10112 01-46)

Avail: CASI HC A01/MF A01

The consensus regarding interpretation of Magellan radar imagery assigns Venus a young volcanic surface subjected in many areas to moderate crustal shortening. I infer that, on the contrary, ancient densely cratered terrain and large impact basins may be preserved over more than half the planet and that crustal shortening has been much overestimated. I see wind erosion and deposition as far more effective in modifying old structures. Integration with lunar chronology suggests that most of the surface of Venus may be older than 3.0 Ga and much may be older than 3.8 Ga. Broad volcanos, hug volcanic domes, plains preserving lobate flow patterns, and numerous lesser volcanic features, pocked sparsely by impact craters, are indeed obvious on Magellan imagery. Some of these postvolcanic impact craters have been slightly extended, but only a small portion has been flooded by still younger lavas. Relative ages of the young craters are indicated by the varying eolian removal of their forms and ejecta blankets and flow lobes, and the oldest are much subdued. If these young impact craters, maximum diameter 275 km, include all preserved impact structures, then their quantity and distribution indicate that Venus was largely resurfaced by volcanism approx. 0.5 Ga, subsequent eruptions having been at a much reduced rate. Away from the approx. 0.5 Ga volcanic features, much of Venus is, however, dominated by circular and subcircular features, 50-2000 km in diameter, many of them multiring, that may be mostly older impact and impact-melt structures substantially modified by wind action. Eolian erosion scoured to bedrock old ridges and uplands, including those that may be cratered terrains and the rims and outer-ring depressions of large impact basins, and removed all surficial deposits to the limits of resolution of the imagery. The complementary eolian deposits form not only dunes, wind streaks, and small plains, but also broad radar-dark plains, commonly assumed to be volcanic although lacking flow morphology, whose materials appear to be thick because they are smoothly compacted into buried craters.

Author

N93-10146*# Princeton Univ., NJ. Dept. of Geological and Geophysical Sciences.

WHERE'S THE BEAVERHEAD BEEF?

R. B. Hargraves *In* Lunar and Planetary Inst., International Conference on Large Meteorite Impacts and Planetary Evolution 1992 p 35-36 (For primary document see N93-10112 01-46)

Avail: CASI HC A01/MF A01

Only rare quartz grains with single-set planar (1013) deformation features (PDF's) are present in breccia dikes found in association with uniformly oriented shatter cones that occur over an area 8 x 25 km. This suggests that the Beaverhead shocked rocks come from only the outer part of the central uplift of what must have been a large (greater than 100 km diameter) complex impact structure. An impact event of this magnitude on continental crust (thought to have occurred in late Precambrian or ealy Paleozoic time) could be expected to punctuate local geologic history. Furthermore, although it may now be covered, its scar should remain despite all the considerable subsequent erosion/deposition and tectonism since the impact. The following are three large-scale singularities or anomalies that may reflect the event and mark its source. (1) The Lemhi Arch is a major structural uplift that occurred in late Proterozoic-early Paleozoic time in East Central Idaho and caused the erosion of at least 4 km of sedimentary cover. This may be directly related to the impact. (2) Of the many thrust

sheets comprising the Cordilleran belt, the Cabin plate that carries the shocked rocks is unique in that it alone intersected the crystalline basement. It also now marks the apex of the Southwest Montana Recess in the Sevier front. The basement uplift remaining from the impact may have constituted a mechanical obstacle to the advancing thrust sheets in Cretaceous time, causing the recess. (3) What could be interpreted as a roughly circular aeromagnetic anomaly approx. 70 km in diameter can be discerned in the state aeromagnetic map centered about 20 km southeast of Challis, Idaho, in the Lost River range. It is in approximately the right place, and ignoring the possibility that the anomalies have diverse causes and the circular pattern is coincidental, it may mark what remains of the buried central uplift structure. Author

N93-10147*# Hartung (J.), Des Moines, IA.
REPORT ON THE INTERNATIONAL CAMBODIAN CRATER EXPEDITION, 1992
J. Hartung, C. Koeberl (Wien Univ., Austria), P. Lee (Cornell Univ., Ithaca, NY.), Kuhn Pagnacith (Ministry of Industry, Phnom Penh, Cambodia), and Touch Sambath (Ministry of Industry, Phnom Penh, Cambodia) *In* Lunar and Planetary Inst., International Conference on Large Meteorite Impacts and Planetary Evolution 1992 p 36-37 (For primary document see N93-10112 01-46)
Avail: CASI HC A01/MF A01

It has been proposed that Tonle Sap, a lake in Cambodia, 100 km long and 30 km wide, marks the location of an elongate basin formed by the oblique impact of a comet or asteroid. The impact is considered to have produced melted ejecta found now as tektites over much of southeast Asia and Australia. The location of the lake, its approximate age, its size, and the orientation of its long axis (toward Australia) are consistent with this hypothesis. Our scientific objectives were to find impact or shock metamorphosed rocks unambiguously related to the Tonle Sap basin, to collect samples of rocks that may represent those melted to produce Australasian tektites, and to learn as much as possible about Cambodian geology. Using 1:200,000-scale geologic maps with fairly detailed descriptions of the rock units, we selected a number of acceptable 'phnoms' (hills that rise abruptly out of the surrounding plain) that may contain rocks affected by the postulated Tonle Sap impact. A map of central Cambodia is shown, and the locations of sites where samples were collected are indicated. A list of those sites, together with a description of the rocks reported to be present at each site, is given. No obviously shock-metamorphosed or suevite-like rocks were observed. Recent alluvium surrounding Tonle Sap is judged to be lake sediment deposited when the lake surface was at a higher elevation.
Author

N93-10148*# Hawaii Univ., Honolulu. Dept. of Planetary Geosciences.
THE DISTRIBUTION AND MODES OF OCCURRENCE OF IMPACT MELT AT LUNAR CRATERS **c91**
B. Ray Hawke and J. W. Head (Brown Univ., Providence, RI.) *In* Lunar and Planetary Inst., International Conference on Large Meteorite Impacts and Planetary Evolution 1992 p 37-38 (For primary document see N93-10112 01-46)
Avail: CASI HC A01/MF A01

Numerous studies of the returned lunar samples as well as geologic and remote-sensing investigations have emphasized the importance of impact melts on the surface of the Moon. Information concerning the distribution and relative volumes is important for (1) an improved understanding of cratering processes, (2) kinetic energy estimates and energy partitioning studies, (3) the proper interpretation of melt-bearing lunar samples, and (4) comparative planetology studies. The identification of major flows of fluidized material associated with impact craters on the surface of Venus has increased interest in impact melt flows on the other terrestrial planets. For a number of years, we have been investigating the distribution, modes of occurrence, and relative and absolute amounts of impact melt associated with lunar craters as well as the manner in which melt volumes vary as a function of crater size, morphology, and target characteristics. The results of this effort are presented. Author

N93-10149*# Stockholm Univ. (Sweden). Inst. for Fotogrammetry.
LARGE IMPACTS IN THE BALTIC SHIELD WITH SPECIAL ATTENTION TO THE UPPLAND STRUCTURE
H. Henkel and R. Lilljequist *In* Lunar and Planetary Inst., International Conference on Large Meteorite Impacts and Planetary Evolution 1992 p 38-40 (For primary document see N93-10112 01-46)
Avail: CASI HC A01/MF A01

Within the Baltic Shield several very large structures have been identified and are suspected to be of meteorite impact origin. Some of these deeply eroded circular features are presented with special attention to the Uppland structure, where several indications point toward an impact origin in the mid-Proterozoic. The structures exceed 100 km in diameter and the topographic expression is inferior or absent. An arcuate arrangement of lithologies occurs around the margin of the structures and the central regions show conform magnetic and positive gravity anomalies. The Uppland structure is approximately 320 km in diameter as expressed by morphological, geological, and geophysical concentric patterns. The central part is topographically remarkably flat and is characterized by an unusual irregular fracture pattern. A subcircular central tonalite with density of 2.81 Mg(sup -3) gives a positive gravity anomaly of 35 mgal and the gravimetric profile is very similar to that of Manicouagan and Vredefort. The tonalite constitutes a huge antiform, 80 km in diameter, probably representing a 12-km structural uplift of infracrustal rocks. The flancs of the tonalite are characterized by recrystallized pseudotachylitic breccia dykes and breccia zones. Around the central parts amphibolite-grade metamorphic rocks appear as large fragments within a fine-grained granite interpreted as a thermally annealed melt rock. Several occurrences of breccia dykes and breccia-bearing melts have been identified about 100 km from the gravimetric center of the structure. Impact-related ore deposits are located around the margin of the structure and are interpreted as preexisting downfaulted iron formations, and deposits formed from remobilization of these preimpact occurrences. The so-called ball ores are interpreted to have formed by fluid injection similar to the formation of breccia dykes. The extensive hydrothermal alteration along the outer margin of the structure have created extreme soda and K-enriched rocks ('leptites') from preexisting gneiss granites and supracrustal sedimentary gneisses. Author

N93-10150*# Geological Survey, Albany, NY.
THE PANTHER MOUNTAIN CIRCULAR STRUCTURE, A POSSIBLE BURIED METEORITE CRATER
Y. W. Isachsen, S. F. Wright (Vermont Univ., Burlington.), F. A. Revetta (State Univ. of New York, Potsdam.), and R. J. Duneen (Weston, Roy F., Inc., West Chester, PA) *In* Lunar and Planetary Inst., International Conference on Large Meteorite Impacts and Planetary Evolution 1992 p 40 (For primary document see N93-10112 01-46)
Avail: CASI HC A01/MF A01

Panther Mountain, located near Phoenicia, New York, is part of the Catskill Mountains, which form the eastern end of the Allegheny Plateau in New York. It is a circular mass defined physiographically by an anomalous circular drainage pattern produced by Esopus Creek and its tributary Woodland Creek. The circular valley that rings the mountain is fracture-controlled; where bedrock is exposed, it shows a joint density 5 to 10 times greater than that on either side of the valley. Where obscured by alluvial valley fill, the bedrock's low seismic velocity suggests that this anomalous fracturing is continuous in the bedrock underlying the rim valley. North-south and east-west gravity and magnetic profiles were made across the structure. Terrane-corrected, residual gravity profiles show an 18-mgal negative anomaly, and very steep gradients indicate a near-surface source. Several possible explanations of the gravity data were modeled. We conclude that the Panther Mountain circular structure is probably a buried meteorite crater that formed contemporaneously with marine or fluvial sedimentation during Silurian or Devonian time. An examination of drill core and cuttings in the region is underway to search for ejecta deposits and possible seismic and tsunami effects

in the sedimentary section. Success would result in both dating the impact and furnishing a chronostratigraphic marker horizon.
Author

N93-10151*# Academy of Sciences (USSR), Moscow. Inst. for Dynamics of Geospheres.
GEOMECHANICAL MODELS OF IMPACT CRATERING: PUCHEZH-KATUNKI STRUCTURE
B. A. Ivanov *In* Lunar and Planetary Inst., International Conference on Large Meteorite Impacts and Planetary Evolution 1992 p 40-41 (For primary document see N93-10112 01-46)
Avail: CASI HC A01/MF A01

Impact cratering is a complex natural phenomenon that involves various physical and mechanical processes. Simulating these processes may be improved using the data obtained during the deep drilling at the central mound of the Puchezh-Katunki impact structure. A research deep drillhole (named Vorotilovskaya) has been drilled in the Puchezh-Katunki impact structure (European Russia, 57 deg 06 min N, 43 deg 35 min E). The age of the structure is estimated at about 180 to 200 m.y. The initial rim crater diameter is estimated at about 40 km. The central uplift is composed of large blocks of crystalline basement rocks. Preliminary study of the core shows that crystalline rocks are shock metamorphosed by shock pressure from 45 GPa near the surface to 15-20 GPa at a depth of about 5 km. The drill core allows the possibility of investigating many previously poorly studied cratering processes in the central part of the impact structure. As a first step one can use the estimates of energy for the homogeneous rock target. The diameter of the crater rim may be estimated as 40 km. The models elaborated earlier show that such a crater may be formed after collapse of a transient cavity with a radius of 10 km. The most probable range of impact velocities from 11.2 to 30 km/s may be inferred for the asteroidal impactor. For the density of a projectile of 2 g/cu cm the energy of the impact is estimated as 1E28 to 3E28 erg. In the case of vertical impact, the diameter of an asteroidal projectile is from 1.5 to 3 km for the velocity range from 11 to 30 km/s. For the most probable impact angle of 45 deg, the estimated diameter of an asteroid is slightly larger: from 2 to 4 km. Numerical simulation of the transient crater collapse has been done using several models of rock rheology during collapse. Results show that the column at the final position beneath the central mound is about 5 km in length. This value is close to the shock-pressure decay observed along the drill core. Further improvement of the model needs to take into account the blocky structure of target rocks revealed by drilling. Author

N93-10152*# Laurentian Univ. of Sudbury (Ontario). Dept. of Geology.
THERMOBAROMETRIC STUDIES ON THE LEVACK GNEISSES: FOOTWALL ROCKS TO THE SUDBURY IGNEOUS COMPLEX
R. S. James, W. Peredery (International Nickel Co., Inc., Copper Cliff, Ontario), and J. M. Sweeny (Falconbridge Ltd., Exploration, Ontario) *In* Lunar and Planetary Inst., International Conference on Large Meteorite Impacts and Planetary Evolution 1992 p 41 (For primary document see N93-10112 01-46)
Avail: CASI HC A01/MF A01

Granulite and amphibolite facies gneisses and migmatites of the Levack Gneiss Complex occupy a zone up to 8 km wide around the northern part of the Sudbury Igneous Complex (SIC). Orthopyroxene- and garnet-bearing tonalitic and semipelitic assemblages of granulite facies grade occur within 3 km of the SIC together with lenses of mafic and pyroxenitic rock compositions normally represented by an amphibole +/- cpx-rich assemblage; amphibolite facies assemblages dominate elsewhere in this terrain. These 2.711-Ga gneisses were introduced by (1) the Cartier Granite Batholith during late Archaean to early Proterozoic time and (2) the SIC, at 1.85 Ga, which produced a contact aureole 1-1.5 km wide in which pyroxene hornfelses are common within 200-300 m of the contact. A suite of 12 samples including both the opx-gt and amphibole-rich rock compositions have been studied. Garnets in the semipelitic gneisses are variably replaced by a plg-bio assemblage. Thermobarometric calculations using a variety of barometers and thermometers reported in the literature suggest that the granulite facies assemblages formed at depths in the 21-28 km range (6-8 kbar). Textures and mineral chemistry in the garnet-bearing semipelitic rocks indicate that this terrain underwent a second metamorphic event during uplift to depth in the 5-11 km range (2-3 kbar) and at temperatures as low as 500-550 C. This latter event is distinct from thermal recrystallization caused by the emplacement of the SIC; it probably represents metamorphism attributable to intrusion of the Cartier Granite Batholith. These data allow two interpretations for the crustal uplift of the Levack Gneisses: (1) The gneisses were tectonically uplifted prior to the Sudbury Event (due to intrusion of the Cartier Batholith); or (2) the gneisses were raised to epizonal levels as a result of meteorite impact at 1.85 Ga. Author

N93-10153*# Wien Univ. (Austria). Inst. of Geochemistry.
THE CRETACEOUS-TERTIARY (K/T) IMPACT: ONE OR MORE SOURCE CRATERS?
Christian Koeberl *In* Lunar and Planetary Inst., International Conference on Large Meteorite Impacts and Planetary Evolution 1992 p 41-42 (For primary document see N93-10112 01-46)
Avail: CASI HC A01/MF A01

The Cretaceous-Tertiary (K/T) boundary is marked by signs of a worldwide catastrophe, marking the demise of more than 50 percent of all living species. Ever since Alvarez et al. found an enrichment of IR and other siderophile elements in rocks marking the K/T boundary and interpreted it as the mark of a giant asteroid (or comet) impact, scientists have tried to understand the complexities of the K/T boundary event. The impact theory received a critical boost by the discovery of shocked minerals that have so far been found only in association with impact craters. One of the problems of the K/T impact theory was, and still is, the lack of an adequate large crater that is close to the maximum abundance of shocked grains in K/T boundary sections, which was found to occur in sections in Northern America. The recent discovery of impact glasses from a K/T section in Haiti has been crucial in establishing a connection with documented impact processes. The location of the impact-glass findings and the continental nature of detritus found in all K/T sections supports at least one impact site near the North American continent. The Manson Impact Structure is the largest recognized in the United States, 35 km in diameter, and has a radiometric age indistinguishable from that of the Cretaceous-Tertiary (K/T) boundary. Although the Manson structure may be too small, it may be considered at least one element of the events that led to the catastrophic loss of life and extinction of many species at that time. A second candidate for the K/T boundary crater is the Chicxulub structure, which was first suggested to be an impact crater more than a decade ago. Only recently, geophysical studies and petrological (as well as limited chemical) analyses have indicated that this buried structure may in fact be of impact origin. At present we can conclude that the Manson crater is the only confirmed crater of K/T age, but Chicxulub is becoming a strong contender; however, detailed geochemical, geochronological, and isotopic data are necessary to provide definitive evidence. Author

N93-10154*# Wien Univ. (Austria). Inst. of Geochemistry.
TEKTITE ORIGIN BY HYPERVELOCITY ASTEROIDAL OR COMETARY IMPACT: THE QUEST FOR THE SOURCE CRATERS **c90**
Christian Koeberl *In* Lunar and Planetary Inst., International Conference on Large Meteorite Impacts and Planetary Evolution 1992 p 42-43 (For primary document see N93-10112 01-46)
Avail: CASI HC A01/MF A01

Tektites are natural glasses that are chemically homogeneous, often spherically symmetrical objects several centimeters in size, and occur in four known strewn fields on the surface of the Earth: the North American, moldavite (or Central European), Ivory Coast, and Australasian strewn fields. Tektites found within such strewn fields are related to each other with respect to their petrological, physical, and chemical properties as well as their age. A theory of tektite origin needs to explain the similarity of tektites in respect to age and certain aspects of isotopic and chemical composition within one strewn field, as well as the variety of tektite materials

present in each strewn field. In addition to tektites on land, microtektites (which are generally less than 1 mm in diameter) have been found in deep-sea cores. Tektites are classified into three groups: (1) normal or splash-form tektites, (2) aerodynamically shaped tektites, and (3) Muong Nong-type tektites (sometimes also called layered tektites). The aerodynamic ablation results from partial remelting of glass during atmospheric passage after it was ejected outside the terrestrial atmosphere and quenched from a hot liquid. Aerodynamically shaped tektites are known mainly from the Australasian strewn field where they occur as flanged-button australites. The shapes of splash-form tektites (spheres, droplets, teardrops, dumbbells, etc., or fragments thereof) are the result of the solidification of rotating liquids in the air or vacuum. Mainly due to chemical studies, it is now commonly accepted that tektites are the product of melting and quenching of terrestrial rocks during hypervelocity impact on the Earth. The chemistry of tektites is in many respects identical to the composition of upper crustal material. Author

N93-10155*# Wien Univ. (Austria). Inst. of Geochemistry.

EARLY ARCHEAN SPHERULE BEDS OF POSSIBLE IMPACT ORIGIN FROM BARBERTON, SOUTH AFRICA: A DETAILED MINERALOGICAL AND GEOCHEMICAL STUDY **c90**

Christian Koeberl, Wolf Uwe Reimold (Witwatersrand Univ., Johannesburg, South Africa), and Rudolf H. Boer (Witwatersrand Univ., Johannesburg, South Africa) *In* Lunar and Planetary Inst., International Conference on Large Meteorite Impacts and Planetary Evolution 1992 p 44 (For primary document see N93-10112 01-46)

Avail: CASI HC A01/MF A01

The Barberton Greenstone belt is a 3.5- to 3.2-Ga-old formation situated in the Swaziland Supergroup near Barberton, northeast Transvaal, South Africa. The belt includes a lower, predominantly volcanic sequence, and an upper sedimentary sequence (e.g., the Fig Tree Group). Within this upper sedimentary sequence, Lowe and Byerly identified a series of different beds of spherules with diameters of around 0.5-2 mm. Lowe and Byerly and Lowe et al. have interpreted these spherules to be condensates of rock vapor produced by large meteorite impacts in the early Archean. We have collected a series of samples from drill cores from the Mt. Morgan and Princeton sections near Barberton, as well as samples taken from underground exposures in the Sheba and Agnes mines. These samples seem much better preserved than the surface samples described by Lowe and Byerly and Lowe et al. Over a scale of just under 30 cm, several well-defined spherule beds are visible, interspaced with shales and/or layers of banded iron formation. Some spherules have clearly been deposited on top of a sedimentary unit because the shale layer shows indentions from the overlying spherules. Although fresher than the surface samples (e.g., spherule bed S-2), there is abundant evidence for extensive alteration, presumably by hydrothermal processes. In some sections of the cores sulfide mineralization is common. For our mineralogical and petrographical studies we have prepared detailed thin sections of all core and underground samples (as well as some surface samples from the S-2 layer for comparison). For geochemical work, layers with thicknesses in the order of 1-5 mm were separated from selected core and underground samples. The chemical analyses are being performed using neutron activation analysis in order to obtain data for about 35 trace elements in each sample. Major elements are being determined by XRF and plasma spectrometry. To clarify the history of the sulfide mineralization, sulfur isotopic compositions are being determined. Author

N93-10156*# Royal Ontario Museum, Toronto. Dept. of Geochronology.

U-Pb ISOTOPIC RESULTS FOR SINGLE SHOCKED AND POLYCRYSTALLINE ZIRCONS RECORD 550-65.5-Ma AGES FOR A K-T TARGET SITE AND 2700-1850-Ma AGES FOR THE SUDBURY IMPACT EVENT

T. E. Krogh, S. L. Kamo, and B. F. Bohor (Geological Survey, Denver, CO.) *In* Lunar and Planetary Inst., International Conference on Large Meteorite Impacts and Planetary Evolution 1992 p 44-45 (For primary document see N93-10112 01-46)

Avail: CASI HC A01/MF A01

The refractory mineral zircon develops distinct morphological features during shock metamorphism and retains these features under conditions that would anneal them in other minerals. In addition, weakly shocked zircon grains give primary ages for the impact site, while highly reconstituted (polycrystalline) single grains give ages that approach the age of the impact event. Data for a series of originally coeval grains will define a mixing line that gives both of these ages providing that no subsequent geological disturbances have overprinted the isotopic systematics. In this study, we have shown that the three zircon grain types described by Bohor, from both K-T distal ejecta (Fireball layer, Raton Basin, Colorado) and the Onaping Formation, represent a progressive increase in impact-related morphological change that coincides with a progressive increase in isotopic resetting in zircons from the ejecta and basement rocks. Unshocked grains are least affected by isotopic resetting while polycrystalline grains are most affected. U-Pb isotopic results for 12 of 14 single zircon grains from the Fireball layer plot on or close to a line recording a primary age of 550 +/- 10 Ma and a secondary age of 65.5 +/- 3 Ma. Data for the least and most shocked grains plot closest to the primary and secondary ages respectively. The two other grains each give ages between 300 and 350 Ma. This implies that the target ejecta was dominated by 550-Ma rocks and that the recrystallization features of the zircon were superimposed during the impact event at 65.5 Ma. A predominant age of 550 Ma for zircons from the Fireball layer provides an excellent opportunity to identify the impact site and to test the hypothesis that multiple impacts occurred at this time. A volcanic origin for the Fireball layer is ruled out by shock-related morphological changes in zircon and the fact that the least shocked grains are old. Basement Levack gneisses north of the Sudbury structure have a primary age of 2711 Ma. Data for three single zircons from this rock, which record a progressive increase in shock features, are displaced 24, 36, and 45 percent along a Pb-loss line toward the 1850 +/- 1 Ma minimum age for the impact as defined by the age of the norite. Southeast of the structure three shocked grains from the Murray granite record a primary age of 2468 Ma and are displaced 24, 41, and 56 percent toward the 1853 +/- 4 Ma even as defined by coexisting titanite. Author

N93-10157*# Muenster Univ. (Germany). Inst. fuer Planetologie.

INFLUENCE OF THE PRESHOCK TEMPERATURE ON SHOCK EFFECTS IN QUARTZ

F. Langenhorst and A. Deutsch *In* Lunar and Planetary Inst., International Conference on Large Meteorite Impacts and Planetary Evolution 1992 p 45-46 (For primary document see N93-10112 01-46)

Avail: CASI HC A01/MF A01

Shock metamorphic features are the prime indicators for recognizing impact phenomena on Earth and other planetary bodies. Although the pressure dependence of shock features is well known, information about the influence of the preshock temperature is almost lacking. Especially in the case of large-scale impacts like Sudbury, it is expected that deep-seated crustal rocks were subjected to shock at elevated temperatures. Therefore, we continued to perform shock experiments at elevated temperatures on less than 0.5-mm thin disks of single crystal quartz cut parallel to the (1010) face. All recovered quartz samples were investigated by universal stage, spindle stage, and a newly developed density gradient technique. Errors of refractive index and density measurements are +/- 0.0005 and +/- 0.002 g/cu cm respectively. Our investigations indicate that shock metamorphic features are strongly dependent on the preshock temperature. This statement has far-reaching implications with respect to shock wave barometry that is based on data from recovery experiments at room temperature. These datasets might be applicable only to low-temperature target rocks. Moreover, this study demonstrates that shock recovery experiments are definitely required for understanding the complete pressure-temperature regime of shock metamorphism on planetary bodies. Author

N93-10158*# Cornell Univ., Ithaca, NY. Dept. of Astronomy.
SEARCH FOR A METEORITIC COMPONENT AT THE BEAVERHEAD IMPACT STRUCTURE, MONTANA c90
Pascal Lee and Robert W. Kay *In* Lunar and Planetary Inst., International Conference on Large Meteorite Impacts and Planetary Evolution 1992 p 47 (For primary document see N93-10112 01-46)
Avail: CASI HC A01/MF A01

The Beaverhead impact structure, in southwestern Montana, was identified recently by the presence of shatter cones and impactites in outcrops of Proterozoic sandstones of the Belt Supergroup. The cones occur over an area greater than 100 sq km. Because the geologic and tectonic history of this region is long and complex, the outline of the original impact crater is no longer identifiable. The extent of the area over which shatter cones occur suggests, however, that the feature may have been at least 60 km in diameter. The absence of shatter cones in younger sedimentary units suggests that the impact event occurred in late Precambrian or early Paleozoic time. We have collected samples of shocked sandstone from the so-called 'Main Site' of dark-matrix breccias, and of impact breccias and melts from the south end of Island Butte. The melts, occurring often as veins through brecciated sandstone, exhibit a distinctive fluidal texture, a greenish color, and a cryptocrystalline matrix, with small inclusions of deformed sandstone. Samples of the same type, along with country rock, were analyzed previously for major- and trace-element abundances. It was found that, although the major-element composition as relatively uniform, trace-element composition showed variations between the melt material and the adjacent sandstone. These variations were attributed to extensive weathering and hydrothermal alteration. In a more specific search for a possible meteoritic signature in the breccia and the melt material we have conducted a new series of trace-element analyses on powders of our own samples by thermal neutron activation analysis. Our results indicate that Ir abundances in the breccia, the melts, and the adjacent sandstone clasts are no greater than about 0.1 ppb, suggesting no Ir enrichment of the breccia or the melts relative to the country rock. However, both the breccia and the melt material exhibit notable enrichments in Cr (8- and 10-fold), in U (9- and 5-fold), and in the heavy REE's (1.5- and 3-fold), respectively. Author

N93-10159*# Stockholm Univ. (Sweden).
ORDOVICIAN IMPACTS AT SEA IN BALTOSCANDIA
M. Lindstroem, V. Puura (Academy of Sciences of the Estonian SSR, Tallinn.), T. Floden, and A. Bruun (Geological Survey of Sweden, Stockholm.) *In* Lunar and Planetary Inst., International Conference on Large Meteorite Impacts and Planetary Evolution 1992 p 47 (For primary document see N93-10112 01-46)
Avail: CASI HC A01/MF A01

Northern Europe has an assemblage of Ordovician probable impacts that is exceptional because the structures involved are relatively old yet well preserved because they formed at sea and because they formed within a restricted geological time in a relatively small area. The Tvaren, Kardla, and Lockne structures might not be strictly contemporaneous but all formed near the beginning of the Caradoc Age (about 460 Ma), whereas the Granby structure is about 20 Ma older. The range of diameters is from about 2 km (Tvaren, Granby) to 8 km (Lockne). The stratigraphic succession formed on impact at sea, as uniformly documented by these structures, begins with a breccia lens consisting of basement rocks that are intensely crushed. Owing to expulsion of sea water by the impact, this breccia formed under essentially dry conditions. Later on this breccia was in part hydrothermally altered. It is overlain by backsurge turbidite that formed from fragments of local sedimentary bedrock and crystalline basement when the sea water returned to the crater site. Either the turbidite is simply a Bouma sequence (although quite thick - as much as over 50 m) from very coarse rubble to mud, or it is more complex. After deposition of the backsurge turbidite, or turbidite complex, the craters still remained as 150-200-m-deep holes in the sea bed. Together with the presence of relatively shallow water over the rim wall, this situation created predictable hydrologic conditions for extended histories of sedimentation and biological development at the crater as well as within it. The presence of a concentration of craters within a limited area of well-preserved and accessible Ordovician deposits raises a question about the Ordovician, especially its middle portion, as potentially an age of relatively intense impact activity even in wider areas. In this connection it may be apposite to mention that the only fossil stony meteorites so far recorded in rocks are from the late Early and the Middle Ordovician. Author

N93-10160*# Laurentian Univ. of Sudbury (Ontario). Dept. of Geology.
DOES THE SEDIMENTOLOGY OF THE CHELMSFORD FORMATION PROVIDE EVIDENCE FOR A METEORITE IMPACT ORIGIN OF THE SUDBURY STRUCTURE? Abstract Only
D. G. F. Long *In* Lunar and Planetary Inst., International Conference on Large Meteorite Impacts and Planetary Evolution 1992 p 48 (For primary document see N93-10112 01-46)
Avail: CASI HC A01/MF A01

The post-'event' fill of the Paleoproterozoic Sudbury Basin consists of at least 600 m of deep-water mudrocks of the Onwatin Formation, overlain by 850 m of lithic-arkosic muddy sandstones in the Chelmsford Formation. While mudstones of the Onwatin reflect deposition in a deep-water, anoxic setting, there is no clear evidence of local breccias, conglomerates, or sand bodies to support the concept that the basin was protected by the steep walls of an impact crater. Carbonates in the basal, Vermillion Member are of sedimentary exhalitive origin and were not derived from a shallow marine shelf. Turbidites in the Chelmsford Formation show no evidence of centripetal fill as might be expected from a restricted, circular basin. They appear to have been emplaced by predominantly southwesterly flowing turbidity currents, which showed little to no deflection along the depositional axis of an elongate foreland basin that developed in front of the rising Penokean mountain chain. While the presence of minor sandstone-filled fractures in parts of the Chelmsford Formation suggests the presence of north- or south-directed paleoslopes, no evidence is seen to support the existence of subbasins or a central uplift within the Sudbury Basin. While tilt-corrected paleocurrent orientations are ambiguous, due to postdepositional shortening of strata during cleavage development, strain correction of the observations makes little difference to the net, south-southwest-directed paleoflow. Author

N93-10161*# National Aeronautics and Space Administration. Goddard Space Flight Center, Greenbelt, MD.
IMPACT ORIGIN OF THE SUDBURY STRUCTURE: EVOLUTION OF A THEORY
Paul D. Lowman, Jr. *In* Lunar and Planetary Inst., International Conference on Large Meteorite Impacts and Planetary Evolution 1992 p 48 (For primary document see N93-10112 01-46)
Avail: CASI HC A01/MF A01

This paper reviews the origin, development, and present status of the widely accepted theory, proposed by Robert S. Dietz in 1962, that the Sudbury structure was formed by meteoritic or asteroidal impact. The impact theory for the origin of the Sudbury structure seems supported by a nearly conclusive body of evidence. However, even assuming an impact origin to be correct, at least three major questions require further study: (1) the original size and shape of the crater, before tectonic deformation and erosion; (2) the source of the melt now forming the Sudbury Igneous Complex; and (3) the degree, if any, to which the Ni-Cu-platinum group elements are meteoritic. The history of the impact theory illustrates several under-appreciated aspects of scientific research: (1) the importance of cross-fertilization between space research and terrestrial geology; (2) the role of the outsider in stimulating thinking by insiders; (3) the value of small science, at least in the initial stages of an investigation, Dietz's first field work having been at his own expense; and (4) the value of analogies (here, between the Sudbury Igneous Complex and the maria), which although incorrect in major aspects, may trigger research on totally new lines. Finally, the Sudbury story illustrates the totally unpredictable and, by implication, unplannable nature of basic

research, in that insight to the origin of the world's then-greatest Ni deposit came from the study of tektites and the Moon.

Author

N93-10162*# National Aeronautics and Space Administration. Goddard Space Flight Center, Greenbelt, MD.

IMAGING RADAR INVESTIGATIONS OF THE SUDBURY STRUCTURE

P. D. Lowman, V. H. Singhroy (Canada Centre for Remote Sensing, Ottawa, Ontario), and V. R. Slaney (Canada Centre for Remote Sensing, Ottawa, Ontario) *In* Lunar and Planetary Inst., International Conference on Large Meteorite Impacts and Planetary Evolution 1992 p 49 (For primary document see N93-10112 01-46)

Avail: CASI HC A01/MF A01

This paper reports preliminary results of airborne imaging radar studies of the Sudbury structure carried out in preparation for a CCRS European Remote Sensing Satellite (ERS-1) investigation. The data used were synthetic aperture radar (SAR) C-band (5.66 cm) images acquired from about 6 km altitude in 1987. They cover the Sudbury area in both wide and narrow swath modes, with east-west flight paths and north-south illumination directions. Narrow swath resolution is 6 m in range and azimuth; wide swath resolution is 20 m in range and 10 m in azimuth. The STAR imagery has proven highly effective for field use, providing excellent rendition of topography and topographically expressed structure. Reasons for this include the illumination geometry, notably the look azimuth normal to the long axis of the Sudbury structure and Penokean fold axes, the good spatial resolution, and the short wavelength. Forested areas in the Sudbury area tend to be uniformly rough at C-band wavelength, with backscatter dominated by local incidence angle (i.e., topography). Field work using the SAR imagery has to date been concentrated in the North Range and Superior Province as far north as the Benny greenstone belt. This area was chosen for initial investigation of the original size and shape of the Sudbury structure because the effects of the Penokean Orogeny were minimal there. Field work using SAR indicates that there has been little postimpact deformation of the North Range or adjacent Superior Province rock. There appears to be no evidence for an outer ring concentric with the North Range as indicated by early Landsat imagery. The apparent ring shown by Landsat is visible on the SAR imagery as the intersection of two regional fracture patterns not related to the Sudbury structure. There is no outer ring visible southwest of the structure. This can reasonably be explained by Penokean deformation, but there is no outer ring to the northeast cutting the relatively undeformed Huronian sediments of the Cobalt Embayment.

Author

N93-10163*# Paris VII Univ. (France).

PHASE TRANSFORMATIONS IN 40-60-GPa SHOCKED GNEISSES FROM THE HAUGHTON CRATER (CANADA): AN ANALYTICAL TRANSMISSION ELECTRON MICROSCOPY (ATEM) STUDY

I. Martinez, F. Guyot, and U. Schaerer *In* Lunar and Planetary Inst., International Conference on Large Meteorite Impacts and Planetary Evolution 1992 p 49-50 (For primary document see N93-10112 01-46)

Avail: CASI HC A01/MF A01

In order to better understand phase transformations, chemical migration, and isotopic disequilibrium in highly shocked rocks, we have performed a microprobe and an ATEM study on gneisses shocked up to 60 GPa from the Haughton Crater. This study reveals the following chemical and structural characteristics: (1) SiO2 dominant areas are formed by a mixture of pure SiO2 polycrystalline quartz identified by electron diffraction pattern and chemical analysis and a silica-rich amorphous phase containing minor amounts of aluminium, potassium, and iron; (2) Areas with biotitelike composition are formed by less than 200-nm grains of iron-rich spinels embedded in a silica-rich amorphous phase that is very similar to the one described above; (3) Layers with feldsparlike composition are constituted by 100-200-nm-sized alumina-rich grains (the indexation of the crystalline structure is under progress) and the silica-rich amorphous phase; (4) Zones characterized by the unusual Al/Si ratio close to 1 are formed by spinel grains (200-nm-sized) embedded in the same silica-rich amorphous phase; and (5) The fracturated sillimanites contain domains with a lamellar structure, defined by the intercalation of 100-nm-wide lamellae of mullite crystals and of a silica-rich amorphous phase. These mullite crystals preserved the crystallographical orientation of the preshock sillimanite. All compositional domains, identified at the microprobe scale, can thus be explained by a mixture in different proportion between the following phases: (1) a silica-rich amorphous phase, with minor Al and K; (2) quartz crystals; (3) spinel crystals and alumina-rich crystals; (4) sillimanite; and (5) mullite. Such mixtures of amorphous phases and crystals in different proportions explain disturbed isotope systems in these rocks and chemical heterogeneities observed on the microprobe.

Author

N93-10164*# Karpinsky Geological Research Inst., Saint Petersburg (USSR).

IMPACTITES FROM POPIGAI CRATER **c90**

V. L. Masaitis *In* Lunar and Planetary Inst., International Conference on Large Meteorite Impacts and Planetary Evolution 1992 p 51 (For primary document see N93-10112 01-46)

Avail: CASI HC A01/MF A01

Impactites (tagamites and suevites) from Popigai impact crater, whose diameter is about 100 km, are distributed over an area of 5000 sq km. The continuous sheet of suevite overlies the allogenic polymict breccia and partly authogenic breccia, and may also be observed in lenses or irregular bodies. The thickness of suevites in the central part of the crater is more than 100 m. Suevites may be distinguished by content of vitroclasts, lithoclasts, and crystalloclasts, by their dimensions, and by type of cementation, which reflects the facial settings of ejection of crushed and molten material, its sedimentation and lithification. Tagamites (impact melt rocks) are distributed on the surface predominantly in the western sector of the crater. The most characteristic are thick sheetlike bodies overlying the allogenic breccia and occurring in suevites where minor irregular bodies are widespread. The maximal thickness of separate tagamite sheets is up to 600 m. Tagamites, whose matrix is crystallized to a different degree, include fragments of minerals and gneiss blocks, among them shocked and thermally metamorphosed ones. Tagamite sheets have a complex inner structure; separate horizontal zones distinguish in crystallinity and fragment saturation. Differentiation in the impact melt in situ was not observed. The average chemical compositions of tagamites and suevites are similar, and correspond to the composition of biotite-garnet gneisses of the basement. According to the content of supplied Ir, Ni, and other siderophiles, impact melt was contaminated by 5 percent cosmic matter of collided body, probably ordinary chondrite. The total volume of remaining products of chilled impact melt is about 1750 cu km. Half this amount is represented by tagamite bodies. Though impact melt was in general well homogenized, the trend analysis showed that the concentric zonation is distribution of SiO2, MgO, and Na2O and the bandlike distribution of FeO and Al2O3 content testifies to a certain inheritance and heterogeneity in country rock composition laterally and vertically in the melting zone.

Author

N93-10165*# Arizona State Univ., Tempe. Dept. of Geology.

SUDBURY BRECCIA AND SUEVITE AS GLACIAL INDICATORS TRANSPORTED 800 km TO KENTLAND ASTROBLEME, INDIANA

John F. McHone, Robert S. Dietz, and Walter V. Peredery (International Nickel Co., Inc., Copper Cliff, Ontario) *In* Lunar and Planetary Inst., International Conference on Large Meteorite Impacts and Planetary Evolution 1992 p 51 (For primary document see N93-10112 01-46)

Avail: CASI HC A01/MF A01

A glacial erratic whose place of origin is known by direct comparison with bedrock is known as an indicator. In 1971, while visiting the known astrobleme at Kentland, Indiana, Peredery recognized and sampled in the overlying glacial drift deposits a distinctive boulder of Sudbury suevite (black member, Onaping

Formation) that normally occurs within the Sudbury Basin as an impact fall-back or wash-in deposit. The rock was sampled (but later mislaid) from a farmer's cairn next to a cleared field. Informal reports of this discovery prompted the other authors to recently reconnoiter the Kentland locality in an attempt to relocate the original boulder. Several breccia blocks were sampled but laboratory examination proved most of these probably to be diamictites from the Precambrian Gowganda Formation, which outcrops extensively in the southern Ontario. However, one sample was confirmed as typical Sudbury Breccia, which outcrops in the country rock surrounding the Sudbury Basin. Thus two glacial indicators were transported by Pleistocene continental glaciers about 820 km over a tightly proscribed path and, curiously, from one astrobleme to another. Brecciated boulders in the Illinois/Indiana till plain are usually ascribed to the Gowganda or Mississagi formations in Ontario. But impact-generated rocks need not be confused. The carbonaceous matrix of the suevite, for example, was sufficiently distinctive to assign it to the upper portion of the black Onaping. The unique and restricted source area of these indicators provide an accurate and reliable control for estimating Pleistocene ice movement. Author

N93-10166*# Washington Univ., Saint Louis, MO. Dept. of Earth and Planetary Sciences.

WHAT CAN WE LEARN ABOUT IMPACT MECHANICS FROM LARGE CRATERS ON VENUS? c91

William B. McKinnon and J. S. Alexopoulos *In* Lunar and Planetary Inst., International Conference on Large Meteorite Impacts and Planetary Evolution 1992 p 52-53 (For primary document see N93-10112 01-46)

Avail: CASI HC A01/MF A01

More than 50 unequivocal peak-ring craters and multiringed impact basins have been identified on Venus from Earth-based Arecibo, Venera 15/16, and Magellan radar images. These ringed craters are relatively pristine, and so serve as an important new dataset that will further understanding of the structural and rheological properties of the venusian surface and of impact mechanics in general. They are also the most direct analogues for craters formed on the Earth in Phanerozoic time. Finite-element simulations of basin collapse and ring formation were undertaken in collaboration with V. J. Hillgren (University of Arizona). These calculations used an axisymmetric version of the viscoelastic finite element code TECTON, modeled structures on the scale of Klenova or Meitner, and demonstrated two major points. First, viscous flow and ring formation are possible on the timescale of crater collapse for the sizes of multiringed basins seen on Venus and heat flows appropriate to the plant. Second, an elastic lithosphere overlying a Newtonian viscous asthenosphere results mainly in uplift beneath the crater. Inward asthenospheric flow mainly occurs at deeper levels. Lithospheric response is dominantly vertical and flexural. Tensional stress maxima occur and ring formation by normal faulting is predicted in some cases, but these predicted rings occur too far out to explain observed ring spacings on Venus (or on the Moon). Overall, these estimates and models suggest that multiringed basin formation is indeed possible at the scales observed on Venus. Furthermore, due to the strong inverse dependence of solid-state viscosity on stress, the absence of Cordilleran-style ring faulting in craters smaller than Meitner or Klenova makes sense. The apparent increase in viscosity of shock-fluidized rock with crater diameter, greater interior temperatures accessed by larger, deeper craters, and decreased non-Newtonian viscosity associated with larger craters may conspire to make the transition with diameter from peak-ring crater to Orientale-type multiringed basin rather abrupt. Author

N93-10167*# Muenster Univ. (Germany). Inst. of Planetology.

SUDBURY PROJECT (UNIVERSITY OF MUENSTER-ONTARIO GEOLOGICAL SURVEY): NEW INVESTIGATIONS ON SUDBURY BRECCIA

V. Mueller-Mohr *In* Lunar and Planetary Inst., International Conference on Large Meteorite Impacts and Planetary Evolution 1992 p 53 (For primary document see N93-10112 01-46)

Avail: CASI HC A01/MF A01

Sudbury breccias occur as discordant dike breccias within the footwall rocks of the Sudbury structure, which is regarded as the possible remnant of a multiring basin. Exposures of Sudbury breccias in the North Range are known up to a radial distance of 60-80 km from the Sudbury Igneous Complex (SIC). The breccias appear more frequent within a zone of 10 km adjacent to the SIC and a further zone located about 20-33 km north of the structure. From differences in the structure of the breccias, as for example the size of the breccia dikes, contact relationships between breccia and country rock as well as between different breccia dikes, fragment content, and fabric of the ground mass, as seen in this section, the Sudbury Breccias have been classified into four different types. (1) Early breccias with a clastic/crystalline matrix comprise small dikes ranging in size from approx. 1 cm to max. 20 cm. (2) Polymict breccias with a clastic matrix represent the most common type of Sudbury breccia. The thickness of the dikes varies from several tens of centimeters to a few meters but can also extend to more than 100 m in the case of the largest known breccia dike. Contacts with country rock are sharp or gradational. Heterogenous matrix consisting of a fine-grained rock flour displays nonoriented textures as well as extreme flow lines. Chemical analysis substantiates at least some mixing with allochthonous material. (3) Breccias with a crystalline matrix are a subordinate type of Sudbury breccia. According to petrographical and chemical differences, three subtypes have been separated. (4) Late breccias with a clastic matrix are believed to represent the latest phase of brecciation. Two subtypes have been distinguished due to differences in the fragment content. Author

N93-10168*# Indian School of Mines, Dhanbad. Dept. of Applied Geology.

A HISTORY OF THE LONAR CRATER, INDIA: AN OVERVIEW

V. K. Nayak *In* Lunar and Planetary Inst., International Conference on Large Meteorite Impacts and Planetary Evolution 1992 p 53-54 (For primary document see N93-10112 01-46)

Avail: CASI HC A01/MF A01

The origin of the circular structure at Lonar, India, described variously as cauldron, pit, hollow, depression, and crater, has been a controversial subject since the early nineteenth century. A history of its origin and other aspects from 1823 to 1990 are overviewed. The structure in the Deccan Trap Basalt is nearly circular with a breach in the northeast, 1830 m in diameter, 150 m deep, with a saline lake in the crater floor. Over the years, the origin of the Lonar structure has risen from volcanism, subsidence, and cryptovolcanism to an authentic meteorite impact crater. Lonar is unique because it is probably the only terrestrial crater in basalt and is the closest analog with the Moon's craters. Some unresolved questions are suggested. The proposal is made that the young Lonar impact crater, which is less than 50,000 years old, should be considered as the best crater laboratory analogous to those of the Moon, be treated as a global monument, and preserved for scientists to comprehend more about the mysteries of nature and impact cratering, which is now emerging as a fundamental ubiquitous geological process in the evolution of the planets. Author

N93-10169*# Hawaii Univ., Honolulu. Dept. of Geology and Geophysics.

SUDBURY IGNEOUS COMPLEX: IMPACT MELT OR IGNEOUS ROCK? IMPLICATIONS FOR LUNAR MAGMATISM

Marc D. Norman *In* Lunar and Planetary Inst., International Conference on Large Meteorite Impacts and Planetary Evolution 1992 p 54-55 (For primary document see N93-10112 01-46)

Avail: CASI HC A01/MF A01

The recent suggestion that the Sudbury Igneous Complex (SIC) is a fractionated impact melt may have profound implications for understanding the lunar crust and the magmatic history of the Moon. A cornerstone of much current thought on the Moon is that the development of the lunar crust can be traced through the lineage of 'pristine' igneous rocks. However, if rocks closely resembling those from layered igneous intrusions can be produced by differentiation of a large impact melt sheet, then much of what is thought to be known about the Moon may be called into question.

This paper presents a brief evaluation of the SIC as a differentiated impact melt vs. endogenous igneous magma and possible implications for the magmatic history of the lunar crust. Author

N93-10170*# California Inst. of Tech., Pasadena. Lab. of Experimental Geophysics.
MELTING AND ITS RELATIONSHIP TO IMPACT CRATER MORPHOLOGY
John D. OKeefe and Thomas J. Ahrens *In* Lunar and Planetary Inst., International Conference on Large Meteorite Impacts and Planetary Evolution 1992 p 55-56 (For primary document see N93-10112 01-46)
Avail: CASI HC A01/MF A01

Shock-melting features occur on planets at scales that range from micrometers to megameters. It is the objective of this study to determine the extent of thickness, volume geometry of the melt, and relationship with crater morphology. The variation in impact crater morphology on planets is influenced by a broad range of parameters: e.g., planetary density, thermal state, strength, impact velocity, gravitational acceleration. We modeled the normal impact of spherical projectiles on a semi-infinite planet over a broad range of conditions using numerical techniques. Author

N93-10171*# Geological Survey of Finland, Espoo. Paleomagnetism Lab.
IMPACT CRATERING RECORD OF FENNOSCANDIA
L. J. Pesonen and H. Henkel (Royal Inst. of Tech., Stockholm, Sweden) *In* Lunar and Planetary Inst., International Conference on Large Meteorite Impacts and Planetary Evolution 1992 p 57 (For primary document see N93-10112 01-46)
Avail: CASI HC A01/MF A01

A compilation of circular topographic, morphological, or geophysical structures in Fennoscandia and adjacent areas reveals 62 craterform structures of which 15 appear to be of extraterrestrial origin due to meteorite impact. The majority of the structures are probable and possible impact craters for which there is not yet sufficient proof for impact origin. Four of the proven impact craters contain large volumes of impact melt and many other features of intense shock metamorphism. The age of recognized impact craters vary from prehistoric to late Precambrian. We review the Fennoscandian impact cratering record giving examples of geophysical signatures of impact craters. Author

N93-10172*# Ceskoslovenska Akademie Ved, Prague. Geological Inst.
BOHEMIAN CIRCULAR STRUCTURE, CZECHOSLOVAKIA: SEARCH FOR THE IMPACT EVIDENCE
Petr Rajlich *In* Lunar and Planetary Inst., International Conference on Large Meteorite Impacts and Planetary Evolution 1992 p 57-59 (For primary document see N93-10112 01-46)
Avail: CASI HC A01/MF A01

Test of the impact hypothesis for the origin of the circular, 260-km-diameter structure of the Bohemian Massif led to the discovery of glasses and breccias in the Upper Proterozoic sequence that can be compared to autogeneous breccias of larger craters. The black recrystallized glass contains small exsolution crystals of albite-oligoclase and biotite, regularly dispersed in the matrix recrystallized to quartz. The occurrence of these rocks is limited to a 1-sq-km area. It is directly underlain by the breccia of the pelitic and silty rocks cemented by the melted matrix, found on several tens of square kilometers. The melt has the same chemistry as rock fragments in major and in trace elements. It is slightly impoverished in water. The proportion of melted rocks to fragments varies from 1:5 to 10:1. The mineralogy of melt viens is the function of later, mostly contact metamorphism. On the contact of granitic plutons it abounds on sillimanite, cordierite, and small bullets of ilmenite. Immediately on the contact with syenodiorites it contains garnets. The metamorphism of the impact rock melt seems the most probable explanation of the mineralogy and the dry total fusion of rocks accompanied by the strong fragmentation. Other aspects of this investigation are discussed. Author

N93-10173*# Witwatersrand Univ., Johannesburg (South Africa). Dept. of Geology.
THE VREDEFORT DOME: REVIEW OF GEOLOGY AND DEFORMATION PHENOMENA AND STATUS REPORT ON CURRENT KNOWLEDGE AND REMAINING PROBLEMATICS (FIVE YEARS AFTER THE CRYPTOEXPLOSION WORKSHOP)
W. U. Reimold *In* Lunar and Planetary Inst., International Conference on Large Meteorite Impacts and Planetary Evolution 1992 p 59-60 (For primary document see N93-10112 01-46)
Avail: CASI HC A01/MF A01

The Vredefort structure located in the center of the Witwatersrand basin in South Africa and the Sudbury structure in Canada are widely considered the two oldest and largest impact structures still evident on Earth. Both structures are very similar in a number of geological aspects (e.g., association with major economic ore deposits, similar ages of ca. 2 Ga, abundant pseudotachylite as well as shatter cone occurrences, overturned collar). However, whereas the geological community generally accepts an impact origin for the Sudbury structure, a number of researchers are still reluctant to accept this for the Vredefort Dome. Therefore, the aim of this review is to present new data, highlight the most obvious shortcomings in the current database, and to summarize the major arguments in the genetic controversy. Author

N93-10174*# Witwatersrand Univ., Johannesburg (South Africa). Dept. of Geology.
THE PSEUDOTACHYLITES FROM THE VREDEFORT STRUCTURE AND THE WITWATERSRAND BASIN
W. U. Reimold and W. P. Colliston (Orange Free State Univ., Bloemfontein, South Africa) *In* Lunar and Planetary Inst., International Conference on Large Meteorite Impacts and Planetary Evolution 1992 p 60-61 (For primary document see N93-10112 01-46)
Avail: CASI HC A01/MF A01

Pseudotachylite (PT) from both the Sudbury structure in Ontario and the Vredefort Dome in South Africa have been widely cited as the result of shock (impact)-induced brecciation. In the scientific and popular literature PT has been described as shock melt or even as impact melt rock. In contrast, others have for years requested that a clarification of the definitions for PT and impact melt rock be pursued. We have suggested that, until that time when well-defined criteria for genetically different melt rock types (e.g., generated by impact or tectonic processes) will have been established, the term PT should only be used as a descriptive one and that, wherever genetic implications are discussed, other terms, such as impact melt (rock) or friction melt, should be applied. It is obvious that these suggestions are not only of value for the discussion of terrestrial melt rocks of controversial origin, but also apply to the characterization of melt veins in extraterrestrial materials. Important observations on Vredefort and Witwatersrand pseudotachylite are summarized. Author

N93-10175*# Lunar and Planetary Inst., Houston, TX.
COINCIDENCES IN TIME OF THE IMBRIUM BASIN IMPACT AND APOLLO 15 KREEP VOLCANIC SERIES: IMPACT-INDUCED MELTING?
Graham Ryder *In its* International Conference on Large Meteorite Impacts and Planetary Evolution 1992 p 61-62 (For primary document see N93-10112 01-46)
Avail: CASI HC A01/MF A01

On the Earth there may be no firm evidence that impacts can induce volcanic activity. However, the Moon does provide a very likely example of volcanism induced by an immense impact: the Imbrium Basin-forming event was immediately succeeded by a crustal partial melting event that released KREEP lava flows over a wide area. These two events are presently indistinguishable in radiometric age. The sample record indicates that such KREEP volcanism had not occurred in the region prior to that time, and never occurred again. Such coincidence in time implies a genetic relationship between the two events, and impact-induced partial melting appears to be the only candidate process. This conclusion rests essentially on the arguments that: (1) the Imbrium Basin

event took place 3.86 +/- 0.02 Ga ago; (2) the Apennine Bench Formation postdates Imbrium; (3) the Apollo 15 KREEP basalts are 3.85 +/- 0.03 Ga old; (4) the Apollo 15 KREEP basalts are derived from the Apennine Bench Formation; and (5) the Apollo 15 KREEP basalts are volcanic. Thus, the Apollo 15 KREEP basalts represent a unique volcanic unit that immediately postdates the Imbrium event (within 20 Ma, possibly much less). The evidence for the links in the argument are sketched, and some implications for initial conditions are described. Ramifications of the process for the early history of the Earth are briefly explored. Author

N93-10176*# Lunar and Planetary Inst., Houston, TX.
APOLLO 15 IMPACT MELTS, THE AGE OF IMBRIUM, AND THE EARTH-MOON IMPACT CATACLYSM **c91**
Graham Ryder and G. Brent Dalrymple (Geological Survey, Menlo Park, CA.) *In its* International Conference on Large Meteorite Impacts and Planetary Evolution 1992 p 62-63 (For primary document see N93-10112 01-46)
Avail: CASI HC A01/MF A01

The early impact history of the lunar surface is of critical importance in understanding the evolution of both the primitive Moon and the Earth, as well as the corresponding populations of planetesimals in Earth-crossing orbits. Two endmember hypotheses call for greatly dissimilar impact dynamics. One is a heavy continuous (declining) bombardment from about 4.5 Ga to 3.85 Ga. The other is that an intense but brief bombardment at about 3.85 +/- Ga was responsible for producing the visible lunar landforms and for the common 3.8-3.9 Ga ages of highland rocks. The Apennine Front, the main topographic ring of the Imbrium Basin, was sampled on the Apollo 15 mission. The Apollo 15 impact melts show a diversity of chemical compositions, indicating their origin in at least several different impact events. The few attempts at dating them have generally not produced convincing ages, despite their importance. Thus, we chose to investigate the ages of melt rock samples from the Apennine Front, because of their stratigraphic importance yet lack of previous age definition. Author

N93-10177*# National Aeronautics and Space Administration. Goddard Space Flight Center, Greenbelt, MD.
SEARCH FOR THE 700,000-YEAR-OLD SOURCE CRATER OF THE AUSTRALASIAN TEKTITE STREWN FIELD
C. C. Schnetzler (Maryland Univ., College Park.) and J. B. Garvin *In* Lunar and Planetary Inst., International Conference on Large Meteorite Impacts and Planetary Evolution 1992 p 63-64 (For primary document see N93-10112 01-46)
Avail: CASI HC A01/MF A01

Many tektite investigations have hypothesized that the impact crater that was the source of the extensive Australasian strewn field lies somewhere in or near Indochina. This is due to variations in abundance and size of tektites across the strewn field, variation of thickness of microtektite layers in ocean cores, nature and ablation characteristics across the field, and, above all, the occurrence of the large, blocky, layered Muong Nong-type tektites in Indochina. A recent study of the location and chemistry of Muong Nong-type and splash-form tektites suggests that the source region can be further narrowed to a limited area in eastern Thailand and southern Loas. Satellite multispectral imagery, a digital elevation dataset, and maps showing drainage patterns were used to search within this area for possible anomalous features that may be large degraded impact craters. Four interesting structures were identified from these datasets, and they are presented. Author

N93-10178*# Brown Univ., Providence, RI. Dept. of Geological Sciences.
RECOGNIZING IMPACTOR SIGNATURES IN THE PLANETARY RECORD
Peter H. Schultz and Donald E. Gault (Murphys Center of Planetology, CA.) *In* Lunar and Planetary Inst., International Conference on Large Meteorite Impacts and Planetary Evolution 1992 p 64-65 (For primary document see N93-10112 01-46)
Avail: CASI HC A01/MF A01

Crater size reflects the target response to the combined effects of impactor size, density, and velocity. Isolating the effects of each variable in the cratering record is generally considered masked, if not lost, during late stages of crater modification (e.g., floor uplift and rim collapse). Important clues, however, come from the distinctive signatures of the impactor created by oblique impacts. In summary, oblique impacts allow for the identification of distinctive signatures of the impactor created during early penetration. Such signatures may further allow first-order testing of scaling relations for late crater excavation from the planetary surface record. Other aspects of this study are discussed. Author

N93-10179*# Lunar and Planetary Inst., Houston, TX.
PARADIGM LOST: VENUS CRATER DEPTHS AND THE ROLE OF GRAVITY IN CRATER MODIFICATION **c91**
Virgil L. Sharpton *In its* International Conference on Large Meteorite Impacts and Planetary Evolution 1992 p 65-66 (For primary document see N93-10112 01-46)
Avail: CASI HC A01/MF A01

Previous to Magellan, a convincing case had been assembled that predicted that complex impact craters on Venus were considerably shallower than their counterparts on Mars, Mercury, the Moon, and perhaps even Earth. This was fueled primarily by the morphometric observation that, for a given diameter (D), crater depth (d) seems to scale inversely with surface gravity for the other planets in the inner solar system. The unpredicted depth of fresh impact craters on Venus argues against a simple inverse relationship between surface gravity and crater depth. Factors that could contribute to deep craters on Venus include (1) more efficient excavation on Venus, possibly reflecting rheological effects of the hot venusian environment; (2) more melting and efficient removal of melt from the crater cavity; and (3) enhanced ejection of material out of the crater, possibly as a result of entrainment in an atmosphere set in motion by the passage of the projectile. The broader issue raised by the venusian crater depths is whether surface gravity is the predominant influence on crater depths on any planet. While inverse gravity scaling of crater depths has been a useful paradigm in planetary cratering, the venusian data do not support this model and the terrestrial data are equivocal at best. The hypothesis that planetary gravity is the primary influence over crater depths and the paradigm that terrestrial craters are shallow should be reevaluated. Author

N93-10180*# Geological Survey, Flagstaff, AZ.
K/T BOUNDARY STRATIGRAPHY: EVIDENCE FOR MULTIPLE IMPACTS AND A POSSIBLE COMET STREAM
E. M. Shoemaker and G. A. Izett (Geological Survey, Denver, CO.) *In* Lunar and Planetary Inst., International Conference on Large Meteorite Impacts and Planetary Evolution 1992 p 66-68 (For primary document see N93-10112 01-46)
Avail: CASI HC A01/MF A01

A critical set of observations bearing on the K/T boundary events were obtained from several dozen sites in western North America. Thin strata at and adjacent to the K/T boundary are locally preserved in association with coal beds at these sites. The strata were laid down in local shallow basins that were either intermittently flooded or occupied by very shallow ponds. Detailed examination of the stratigraphy at numerous sites led to the recognition of two distinct strata at the boundary. From the time that the two strata were first recognized, E.M. Shoemaker has maintained that they record two impact events. We report some of the evidence that supports this conclusion. Author

N93-10181*# Oberlin Coll., OH. Dept. of Geology.
GEOLOGICAL EVIDENCE FOR A 2.6-Ga STREWN FIELD OF IMPACT SPHERULES IN THE HAMERSLEY BASIN OF WESTERN AUSTRALIA
Bruce M. Simonson *In* Lunar and Planetary Inst., International Conference on Large Meteorite Impacts and Planetary Evolution 1992 p 68-69 (For primary document see N93-10112 01-46)
Avail: CASI HC A01/MF A01

Sand-sized spherules up to 1.7 mm across with spherulitic,

vesicular, and other crystalline textures that consist mainly of K-feldspar help define a unique horizon in the well-preserved 2.6-Ga Wittenoom Formation in the Hamersley Basin of Western Australia. This layer is informally known as the spherule marker bed. In the northeastern part of the Hamersley Basin, similar spherules again occur at only one horizon, but here they are a minor constituent of a dolomitic debris-flow deposit known as the dolomixtite layer. The dolomixtite layer occurs in the Carawine Dolomite, which is stratigraphically equivalent to the Wittenoom Formation. Moreover, paleocurrent data from closely associated carbonate and volcaniclastic turbidites indicate the spherule marker bed was deposited in deeper-water paleoenvironments than the dolomixtite layer. Therefore, the dolomixtite layer is believed to be a proximal equivalent of the spherule marker bed. The layers that host the spherules are interpreted to be the deposits of a major sediment gravity flow that exhumed and redeposited most of the spherules after shallow burial, although the flow is not believed to have been a direct result of the proposed impact. The most likely site for the proposed impact would have been in the early Precambrian ocean close to the northeastern edge of the Pilbara Craton. Another thin horizon in the overlying Brockman Iron Formation contains spherules that again consist largely of K-feldspar and have internal textures strikingly similar to those of the Wittenoom Formation and Carawine Dolomite. The close resemblance of these spherules to those of the Wittenoom Formation and Carawine Dolomite suggests they also originated as impact melt droplets, even though they are admixed with volcaniclastic detritus. The stratigraphic separation between the two suggests that a second major impact occurred near the Hamersley Basin after a time interval of about 75 m.y. elapsed. This suggests the record of impacts in early Precambrian strata is richer than is generally appreciated.

Author

N93-10182*# Canada Centre for Remote Sensing, Ottawa (Ontario).

SAR IN SUPPORT OF GEOLOGICAL INVESTIGATIONS OF THE SUDBURY STRUCTURE Abstract Only **c43**

V. Singhroy, R. Mussakowski (Ministry of Natural Resources, North York, Ontario), B. O. Dressler (Geological Survey of Canada, Ottawa, Ontario), N. F. Trowell (Geological Survey of Canada, Ottawa, Ontario), and Richard Grieve (Department of Energy, Mines, and Resources, Ottawa, Ontario) *In* Lunar and Planetary Inst., International Conference on Large Meteorite Impacts and Planetary Evolution 1992 p 69 (For primary document see N93-10112 01-46)

Avail: CASI HC A01/MF A01

Imaging radar is an important contributing source of information for a range of geological problems and environments. Airborne SAR and ERS-1 data integrated with other geoscience datasets are being used in an attempt to characterize the crustal fracturing associated with the Sudbury structure. This presentation highlights examples of integrated and composite images aimed at facilitating the interpretation of the Sudbury structure. This work is the result of an ongoing cooperative multidisciplinary SAR study of the basin carried out by the Canada Center for Remote Sensing, Ontario's provincial Remote Sensing Office, the Ontario Geological Survey, and the Geological Survey of Canada. Author

N93-10183*# New Brunswick Univ., Fredericton. Dept. of Geology.

VISCOSITY DETERMINATIONS OF SOME FRICTIONALLY GENERATED SILICATE MELTS: IMPLICATIONS FOR SLIP ZONE RHEOLOGY DURING IMPACT-INDUCED FAULTING

John G. Spray *In* Lunar and Planetary Inst., International Conference on Large Meteorite Impacts and Planetary Evolution 1992 p 69 (For primary document see N93-10112 01-46)

Avail: CASI HC A01/MF A01

Analytical scanning electron microscopy, using combined energy dispersive and wavelength dispersive spectrometry, was used to determine the major-element compositions of some natural and artificial glasses and their crystalline equivalents derived by the frictional melting of acid to intermediate protoliths. The major-element compositions are used to calculate the viscosities of their melt precursors using the model of Shaw at temperatures of 800-1400 C, with Fe(2+)/Fe(tot) = 0.5 and for 1-3 wt percent H2O. These results are then modified to account for suspension effects in order to determine viscosities. The results have implications for the generation of pseudotachylitic breccias as seen in the basement lithologies of the Sudbury and Vredefort structures and possibly certain dimict lunar breccias. Many of these breccias show similarities with the more commonly developed pseudotachylite fault and injection veins seen in endogenic fault zones that typically occur in thicknesses of a few centimeters or less. The main difference is one of scale: Impact-induced pseudotachylite breccias can attain several meters in thickness. This would suggest that they were generated under exceptionally high slip rates and hence high strain rates and that the friction melts generated possessed extremely low viscosities. Author

N93-10184*# Lunar and Planetary Inst., Houston, TX.

THE LARGE IMPACT PROCESS INFERRED FROM THE GEOLOGY OF LUNAR MULTIRING BASINS **c91**

Paul D. Spudis *In its* International Conference on Large Meteorite Impacts and Planetary Evolution 1992 p 69-71 (For primary document see N93-10112 01-46)

Avail: CASI HC A01/MF A01

The nature of the impact process has been inferred through the study of the geology of a wide variety of impact crater types and sizes. Some of the largest craters known are the multiring basins found in ancient terrains of the terrestrial planets. Of these features, those found on the Moon possess the most extensive and diverse data coverage, including morphological, geochemical, geophysical, and sample data. The study of the geology of lunar basins over the past 10 years has given us a rudimentary understanding of how these large structures have formed and evolved. The topics covered include basin morphology, basin ejecta, basin excavation, and basin ring formation. Author

N93-10185*# Muenster Univ. (Germany). Inst. fuer Planetologie.

SUDBURY PROJECT (UNIVERSITY OF MUENSTER-ONTARIO GEOLOGICAL SURVEY): PETROLOGY, CHEMISTRY, AND ORIGIN OF BRECCIA FORMATIONS

D. Stoeffler, A. Deutsch, M. Avermann, P. Brockmeyer, R. Lakomy, and V. Mueller-Mohr *In* Lunar and Planetary Inst., International Conference on Large Meteorite Impacts and Planetary Evolution 1992 p 71-72 (For primary document see N93-10112 01-46)

Avail: CASI HC A01/MF A01

Within the Sudbury Project of the University of Muenster and the Ontario Geological Survey special emphasis was put on the breccia formations exposed at the Sudbury structure (SS) because of their crucial role for the impact hypothesis. They were mapped and sampled in selected areas of the north, east, and south ranges of the SS. The relative stratigraphic positions of these units are summarized. Selected samples were analyzed by optical microscopy, SEM, microprobe, XRF and INAA, Rb-Sr and SM-Nd-isotope geochemistry, and carbon isotope analysis. The results of petrographic and chemical analysis for those stratigraphic units that were considered the main structural elements of a large impact basin are summarized. Author

N93-10186*# Houston Univ., TX. Dept. of Geosciences.

BRONZITE GRANOPHYRE: NEW INSIGHT ON VREDEFORT

A. M. Therriault and A. M. Reid *In* Lunar and Planetary Inst., International Conference on Large Meteorite Impacts and Planetary Evolution 1992 p 72-73 (For primary document see N93-10112 01-46)

Avail: CASI HC A01/MF A01

The Vredefort Dome is located near the center of the Witwatersrand Basin, about 120 km southeast of Johannesburg, South Africa. Its origin is enigmatic, ranging from a major impact event to endogenous processes, either igneous or tectonic. A unique melt rock, the 'Bronzite' Granophyr, occurs in the Vredefort structure as vertical ring dikes along the contact between sedimentary collar and core of Archaean granites, and as vertical dikes extending northwest-southeast and northeast-southwest in

the granitic core. The granophyre rocks have an unusual composition and high content of recrystallized sedimentary inclusions compared to common intrusive igneous rocks with similar SiO2 content (61 to 70 percent by weight). The unique nature of the granophyre has been underlined in previous studies and origin hypotheses as an impact melt or as a highly contaminated intrusive mafic magma have also been discussed. We present new results obtained from a recent detailed petrographic and geochemical study of a very large and texturally diverse suite of 'Bronzite' Granophyre, representing all dikes occurring at Vredefort. Author

N93-10187*# New Brunswick Univ., Fredericton. Dept. of Geology.

A COMPARISON OF THE CHEMISTRY OF PSEUDOTACHYLYTE BRECCIAS IN THE ARCHEAN LEVACK GNEISSES OF THE SUDBURY STRUCTURE, ONTARIO

Lucy M. Thompson and John G. Spray *In* Lunar and Planetary Inst., International Conference on Large Meteorite Impacts and Planetary Evolution 1992 p 73-74 (For primary document see N93-10112 01-46)

Avail: CASI HC A01/MF A01

The Archean Levack Gneisses of the North Range host millimeter-thick veins and centimeter-thick lenses of pseudotachylyte, as well as substantially larger meter-wide, dykelike bodies of pseudotachylytic 'breccia'. The 'breccia' occurs up to several tens of kilometers away from the Sudbury Igneous Complex and is commonly sited within or near joints and other natural weaknesses such as bedding, dyke contacts, and lithological boundaries. The larger 'breccia' dykes comprise a generally dark matrix containing rounded to subrounded and occasionally angular rock fragments derived predominantly from Levack Gneiss. Selected samples of bulk Sudbury Breccia and Sudbury Breccia matrices were chemically analyzed and compared to existing data on the Levack Gneisses and Sudbury Breccia. The matrices are apparently enriched in Fe and, to a lesser extent, Mg, Ti, and Ca compared to the wallrocks and the majority of clasts. This enrichment can be partly explained by the preferential cataclasis and/or frictional melting of hydrous ferromagnesian wallrock minerals, but also appear to require contamination by more basic exotic lithologies. This suggests that certain components of pseudotachylitic Sudbury Breccia have undergone significant transport during their formation. Author

N93-10188*# Max-Planck-Inst. fuer Kernphysik, Heidelberg (Germany).

Ar-40 TO Ar-39 AGES OF THE LARGE IMPACT STRUCTURES KARA AND MANICOUAGAN AND THEIR RELEVANCE TO THE CRETACEOUS-TERTIARY AND THE TRIASSIC-JURASSIC BOUNDARY

M. Trieloff and E. K. Jessberger *In* Lunar and Planetary Inst., International Conference on Large Meteorite Impacts and Planetary Evolution 1992 p 74-75 (For primary document see N93-10112 01-46)

Avail: CASI HC A01/MF A01

Since the discovery of the Ir enrichment in Cretaceous-Tertiary boundary clays in 1980, the effects of a 10-km asteroid impacting on the Earth 65 Ma ago have been discussed as the possible reason for the mass extinction--including the extinction of the dinosaurs--at the end of the Cretaceous. But up to now no crater of this age that is large enough (ca. 200 km in diameter) has been found. One candidate is the Kara Crater in northern Siberia. Kolesnikov et al. determined a K-Ar isochron of 65.6 +/- 0.5 Ma, indistinguishable from the age of the K-T boundary and interpreted this as confirmation of earlier proposals that the Kara bolide would have been at least one of the K-T impactors. Koeberl et al. determined Ar-40 to Ar-39 ages ranging from 70 to 82 Ma and suggested an association to the Campanian-Maastrichtian boundary, another important extinction horizon 73 Ma ago. We dated four impact melts, KA2-306, KA2-305, SA1-302, and AN9-182. Results from the investigation are discussed. Author

N93-10189*# Max-Planck-Inst. fuer Kernphysik, Heidelberg (Germany).

Ar-40 TO Ar-39 DATING OF PSEUDOTACHYLITES FROM THE WITWATERSRAND BASIN, SOUTH AFRICA, WITH IMPLICATIONS FOR THE FORMATION OF THE VREDEFORT DOME

M. Trieloff, J. Kunz, E. K. Jessberger, W. U. Reimold (Witwatersrand Univ., Johannesburg, South Africa), R. H. Boer (Witwatersrand Univ., Johannesburg, South Africa), and M. C. Jackson (Witwatersrand Univ., Johannesburg, South Africa) *In* Lunar and Planetary Inst., International Conference on Large Meteorite Impacts and Planetary Evolution 1992 p 75-77 (For primary document see N93-10112 01-46)

Avail: CASI HC A01/MF A01

The formation of the Vredefort Dome, a structure in excess of 100 km in diameter and located in the approximate center of the Witwatersrand basin, is still the subject of lively geological controversy. It is widely accepted that its formation seems to have taken place in a single sudden event, herein referred to as the Vredefort event, accompanied by the release of gigantic amounts of energy. It is debated, however, whether this central event was an internal one, i.e., a cryptoexplosion triggered by volcanic or tectonic processes, or the impact of an extraterrestrial body. The results of this debate are presented. Author

N93-10190*# Kansas State Univ., Manhattan. Dept. of Geology.

AL UMCHAIMIN DEPRESSION, WESTERN IRAQ: AN IMPACT STRUCTURE?

James R. Underwood, Jr. *In* Lunar and Planetary Inst., International Conference on Large Meteorite Impacts and Planetary Evolution 1992 p 77 (For primary document see N93-10112 01-46)

Avail: CASI HC A01/MF A01

Al Umchaimin, in Arabic 'hiding place' or 'place of ambush', is located at latitude 32 degrees 35.5 N and longitude 39 degrees 25 E. The nearly circular depression averages 2.75 km in diameter and is 33-42 m deep. It is floored with fine-grained, clay-rich deposits, estimated to be 36 m thick, the surface of which shows well-developed desiccation fissures or mudcracks when dry. Because of its nearly circular planimetric shape and its apparent isolation from other surface and subsurface features, it has been considered by some to be a possible meteorite impact structure and by others to be a surface collapse feature that originated following removal of magma from the subsurface as the magma extruded elsewhere. Al Umchaimin was listed in the U.S. Geological Survey tabulation of 110 structures worldwide for which a meteorite impact origin had been suggested. It was placed in Category 6 Structures for which more data are required for classification. It is concluded that, on the basis of the studies that have been made of Al Umchaimin and on the basis of the brief site visit made, Al Umchaimin probably is not an impact structure but most likely resulted from the enlargement and coalescence of sink holes and eventual collapse of the roof material into the resulting cavity. Author

N93-10191*# Alberta Univ., Edmonton. Dept. of Geology.

A LATE DEVONIAN IMPACT EVENT AND ITS ASSOCIATION WITH A POSSIBLE EXTINCTION EVENT ON EASTERN GONDWANA

K. Wang and H. H. J. Geldsetzer (Geological Survey of Canada, Calgary, Alberta) *In* Lunar and Planetary Inst., International Conference on Large Meteorite Impacts and Planetary Evolution 1992 p 77-78 (For primary document see N93-10112 01-46)

Avail: CASI HC A01/MF A01

Evidence from South China and Western Australia for a 365-Ma impact event in the Lower crepida conodont zone of the Famennian stage of the Late Devonian (about 1.5 Ma after the Frasnian/Famennian extinction event) includes microtektitelike glassy microspherules, geochemical anomalies (including a weak Ir), a probable impact crater (greater than 70 k) at Taihu in South China, and an Ir anomaly in Western Australia. A brachiopod faunal turnover in South China, and the 'strangelove ocean'-like c-delta

13 excursions in both Chinese and Australian sections indicate that at least a regional-scale extinction might have occurred at the time of the impact. A paleoreconstruction shows that South China was very close to and facing Western Australia in the Late Devonian. The carbon isotopic excursions, which occur at the same stratigraphic level in both South China and Western Australia cannot be explained as being coincidental. The c-delta 13 excursions and the brachiopod faunal turnover in South China indicate that there might have been at least a regional (possibly global) extinction in the Lower crepida zone. The impact-derived microspherules and geochemical anomalies (especially the Ir) indicate a Lower crepida zone impact event on eastern Gondwana. The location, type of target rocks, and possibly age of the Taihu Lake crater qualify as the probable site of this Late Devonian impact. Author

N93-10192*# New Brunswick Univ., Fredericton. Center for Deformation Studies in the Earth Sciences.

ELECTRON PETROGRAPHY OF SILICA POLYMORPHS ASSOCIATED WITH PSEUDOTACHYLITE, VREDEFORT STRUCTURE, SOUTH AFRICA

J. C. White *In* Lunar and Planetary Inst., International Conference on Large Meteorite Impacts and Planetary Evolution 1992 p 78-79 (For primary document see N93-10112 01-46)

Avail: CASI HC A01/MF A01

High-pressure silica polymorphs (coesite and stishovite) were described from the Vredefort structure in association with pseudotachylite veinlets. In addition to the fundamental significance of the polymorphs to genetic interpretations of the structure, it was additionally argued that the type of pseudotachylite with which they occur forms during the compressional phase of the shock process, while the larger, classic pseudotachylite occurrences are barren of polymorphs and formed during passage of the rarefaction wave. This identification of temporal relationships among transient shock features at a regional scale is similar to observations from the Manicouagan structure, Quebec, where texturally distinct diaplectic plagioclase glasses formed during both compressional and decompressional phases of the shock process. The clarification of such relationships impinges directly on interpretations of natural shock processes and the identification of high probability targets for polymorph searches. Detailed analytical scanning (SEM) and transmission electron microscopy (TEM) were utilized to further establish the nature of both the pseudotachylite and the silica polymorph occurrences in the Vredefort rocks. The results of this investigation are discussed. Author

N93-10193*# Brown Univ., Providence, RI. Dept. of Geological Sciences.

FLOOR-FRACTURED CRATER MODELS OF THE SUDBURY STRUCTURE, CANADA

R. W. Wichman and P. H. Schultz *In* Lunar and Planetary Inst., International Conference on Large Meteorite Impacts and Planetary Evolution 1992 p 79-80 (For primary document see N93-10112 01-46)

Avail: CASI HC A01/MF A01

The Sudbury structure in Ontario, Canada, is one of the oldest and largest impact structures recognized in the geological record. It is also one of the most extensively deformed and volcanically modified impact structures on Earth. Although few other terrestrial craters are recognized as volcanically modified, numerous impact craters on the Moon have been volcanically and tectonically modified and provide possible analogs for the observed pattern of modification at Sudbury. We correlate the pattern of early deformation at Sudbury to fracture patterns in two alternative lunar analogs and then use these analogs both to estimate the initial size of the Sudbury structure and to model the nature of early crater modification at Sudbury. Author

N93-10194*# Brown Univ., Providence, RI. Dept. of Geological Sciences.

VARIATION IN MULTIRING BASIC STRUCTURES AS A FUNCTION OF IMPACT ANGLE

R. W. Wichman and P. H. Schultz *In* Lunar and Planetary Inst., International Conference on Large Meteorite Impacts and Planetary Evolution 1992 p 80-81 (For primary document see N93-10112 01-46)

Avail: CASI HC A01/MF A01

Previous studies have demonstrated that the impact process in the laboratory varies as a function of impact angle. This variation is attributed to changes in energy partitioning and projectile failure during the impact and, in simple craters, produces a sequence of progressively smaller and more asymmetric crater forms as impact angle decreases from approximately 20 degrees. Variations in impact angle can produce differences in the appearance of multiring impact basins. Comparisons of Orientale to the more oblique impact structure at Crisium also suggests that these differences primarily reflect the degree of cavity collapse. The relative changes in massif ring topography, basin scarp relief, and the distribution of peripheral mare units are consistent with a reduction in degree of cavity collapse with decreasing impact angle. The prominent uprange basin scarps and the restriction of tectonically derived peripheral mare units along uprange ring structures also may indicate an uprange enhancement of failure during cavity collapse. Finally, although basin ring faults appear to be preferred pathways for mare volcanism, fault-controlled peripheral mare volcanism occurs most readily uprange of an oblique impact; elsewhere such volcanism apparently requires superposition of an impact structure on the ring fault. Author

N93-10195*# Academia Sinica, Beijing (China). Inst. of Mineral Deposits.

SELF-ORGANIZED ROCK TEXTURES AND MULTIRING STRUCTURE IN THE DUOLUN CRATER

Siben Wu and Jiayun Zhang *In* Lunar and Planetary Inst., International Conference on Large Meteorite Impacts and Planetary Evolution 1992 p 81-82 (For primary document see N93-10112 01-46)

Avail: CASI HC A01/MF A01

The Duolun impact crater is a multiring basin located 200 km north of Beijing. From the center to the edge of the crater there are innermost rim, inner ring, outer rim, and outermost ring. Recently, we have found some self-organized textures or chaos phenomena in shock-metamorphic rocks from the Duolun impact crater, such as turbulence in matrices of impact glass, oscillatory zoning, or chemical chaos of spherulites in spherulitic splashed breccia, fractal wavy textures or self-similar wavy textures with varied scaling in impact glass, and crystallite beams shaped like Lorentz strange attractors. The rare phenomena indicate that the shock-metamorphic rocks from Duolun crater are formed far from equilibrium. If impact cratering generates momentarily under high-pressure and superhigh-temperature, occurrence of those chaos phenomena in shock-metamorphic rock is not surprising. Author

N93-10196*# Academy of Sciences (USSR), Moscow. Inst. of Geochemistry and Analytical Chemistry.

GEOCHEMICAL ASPECT OF IMPACT CRATERING: STUDIES IN VERNADSKY INSTITUTE

O. I. Yakovlev and A. T. Basilevsky *In* Lunar and Planetary Inst., International Conference on Large Meteorite Impacts and Planetary Evolution 1992 p 82 (For primary document see N93-10112 01-46)

Avail: CASI HC A01/MF A01

Studies of the geochemical effects of impact cratering at the Vernadsky Institute in collaboration with the Institute of Dynamics of Geospheres, Moscow State University, Leningrad State University, and some other institutions were fulfilled by several approaches. At the initial stage, three approaches were used: (1) experimental studies of high-temperature vaporization of geological materials (basalts, granites, and so on) in vacuum that was considered as a model of behavior of impact melt and vapor; (2) search of impact-induced geochemical effects in the rock from terrestrial impact craters; and (3) studies of samples of lunar regolith. The next stage of the studies included experiments on quasi-equilibrium vaporization of geological material in Knudsen cells. The results of this investigation are discussed. Author

N93-10262# Texas Technological Univ., Lubbock. Dept. of Electrical Engineering.
HIGH-POWER MICROWAVE BREAKDOWN OF DIELECTRIC INTERFACES Annual Technical Report, 15 Apr. 1991 - 14 Apr. 1992
M. Kristiansen, L. L. Hatfield, and Mark Crawford 15 Jul. 1992 15 p
(Grant AF-AFOSR-0260-91)
(AD-A254200; AFOSR-92-0779TR) Avail: CASI HC A03/MF A01

The objective of this project is to study the electrical breakdown, due to microwaves, which occurs on the surface of vacuum/atmosphere interfaces. This is an annual technical report for AFOSR Grant No. 91-0260, that began in April, 1991 and concluded one year later. This contract was continuing work started on AFOSR Grant No. 88-0102. The final report for that grant was submitted in November, 1991. This report discusses results relating to: placing magnets on the waveguide to prevent the electron beam from hitting the window; frequency measurements of the microwave signal; and the design, construction, and testing of a device for reducing window breakdown. GRA

N93-10318 Illinois Univ., Urbana-Champaign.
THE ROLE OF EDDY FLUXES IN THE RESPONSE OF THE ATMOSPHERE TO TROPICAL THERMAL FORCING Ph.D. Thesis
Huey-Tzu Wu 1991 187 p
Avail: Univ. Microfilms Order No. DA9136769

The applicability of linear models in studying the observed stationary waves is considered. In particular, the time-mean effects of eddy fluxes on the response of the atmosphere to tropical thermal forcing are examined by using a time-dependent, nonlinear, global, baroclinic primitive equation model. It is shown that the lack of proper phase and spatial scale of previous linear simulations can be explained to a large degree by the effects of transient eddy fluxes. In this study, the nonlinear anomaly responses to an isolated region of thermal anomalies is defined as the difference between the perturbation simulation and the basic solution of our forced model. Results indicate that the nonlinear response is a superposition and interaction of two components: A quasi-stationary mode which can be resolved by linear dynamics and a zonally propagating mode which owes its existence to baroclinic instability. Effects of basic state advection by standing eddies, which were included in the linear studies, are responsible for over half the anomaly response amplitude. As a result, the linear dynamics can account for several gross features of the anomaly response. These include the dominance of zonal wavenumbers 1 and 2 in high latitudes, the equivalent barotropic nature of the remote response, and the baroclinic nature of the near source response. Effects of eddy fluxes by nonlinear standing eddies are very small and do not show a clear relationship to the anomaly response. On the other hand, the transient eddies show a substantial impact on the anomaly response, especially for the mid-latitude lower troposphere. Specifically, this study suggests that the transient eddy flux mechanism is responsible for the large zonal scale of the anomaly response. The transient eddies also act to lead the anomaly response, and hence have a significant influence on its phase. In addition, the transient eddy effects are not dissipative, but rather enhance somewhat the amplitude of the anomaly response, especially for zonal wavenumbers 1 and 2 in mid and high latitudes. This suggests that it is unjustified to represent the transient eddy effects by a simple damping term in the linear models. Dissert. Abstr.

N93-10324 Rensselaer Polytechnic Inst., Troy, NY.
EFFECTS OF GRAVITY IN FOLDING Ph.D. Thesis
Donald Howe Minkel 1991 274 p
Avail: Univ. Microfilms Order No. DA9202197

Effects of gravity on buckle folding are studied using a Newtonian fluid finite element model of a single layer embedded between two thicker less viscous layers. The methods allow arbitrary density jumps, surface tension coefficients, resistance to slip at the interfaces, and tracking of fold growth to a large amplitudes. When density increases downward in two equal jumps, a layer buckles less and thickens more than with uniform density. When density increases upward in two equal jumps, it buckles more and thickens less. A low density layer with periodic thickness variations buckles more, sometimes explosively. Thickness variations form, even if not present initially. These effects are greater with; smaller viscosities, larger density jump, larger length scale, and slower shortening rate. They also depend on wavelength and amplitude, and these dependencies are described in detail. The model is applied to the explosive growth of the salt anticlines of the Paradox Basin, Colorado and Utah. There, shale (higher density) overlies salt (lower density). Methods for simulating realistic earth surface erosion and deposition conditions are introduced. Growth rates increase both with ease of slip at the salt-shale interface, and when earth surface relief stays low due to erosion and deposition. Model anticlines grow explosively, attaining growth rates and amplitudes close to those of the field examples. Fastest growing wavelengths are the same as seen in the field. It is concluded that a combination of partial-slip at the salt-shale interface, with reasonable earth surface conditions, promotes sufficiently fast buckling of the salt-shale interface due to density inversion alone. Neither basement faulting, nor tectonic shortening is required to account for the observed structures. Of fundamental importance is the strong tendency of gravity to promote buckling in low density layers with thickness variations. These develop, even if not present initially. Because of this, folds both initiate faster, and grow to much higher amplitude than if density is uniform. Low density layers are ubiquitous in the crust, so these results shed considerable new light on crustal dynamics. Dissert. Abstr.

N93-10376 Columbia Univ., New York, NY.
WORLDWIDE SEISMIC CATALOG AND THE NATURE OF SEISMIC COUPLING Ph.D. Thesis
Javier Francisco Pacheco 1991 233 p
Avail: Univ. Microfilms Order No. DA9221196

An earthquake catalog is compiled for shallow (depth less than 60 km) and large (M(sub s) greater than or equal to 7) earthquakes from 1900 through 1989. The catalog is complete and homogeneous at the magnitude M(sub s) greater than or equal to 7. It is also accompanied by a reference list for all the events with seismic moment determined at periods longer than 20s. The moment determined at long periods combined with that determined by a moment-magnitude relationship is used to produce a seismic moment catalog. This catalog is applied to study the distribution of moment released worldwide. The seismic moment released at subduction zones during this century constitutes 90 percent of all the moment released by large, shallow earthquakes on a global basis. The frequency-size distribution obtained with the catalog shows a break in the b value at a magnitude M(sub s) = 7.4 which corresponds to the smallest size earthquake at a subduction zone capable of breaking the entire width of the seismogenic zone. Using other catalogs we find that this break occurs at lower magnitudes at other tectonic regions. Hence, the break in the b value occurs at a point where the dimension of the event equals the width of the seismogenic layer. The seismic coupling (alpha) for 19 subduction zones is computed from the seismic-slip rates obtained from the catalog and plate-motion rates obtained from a global plate motion model. Better estimates of the downdip width and seismic slip rates improve the accuracy of determinations of alpha and remove several systematic errors in its calculation. The study shows a large variation in seismic coupling along and among subduction zones. These variations are attributed to changes in frictional properties of the material along the plate interface, such as variations in roughness, rock and sediment composition, temperature and effective stress at the plate interface. This study finds no significant correlation between the seismic coupling and subduction parameters such as the age of the oceanic lithosphere that is being subducted, plate convergence rates or absolute velocity of the upper plate in a hot spot reference frame. Such correlation exists, however, for individual subduction zones where other parameters do not vary as much. Dissert. Abstr.

N93-10711# Washington Univ., Seattle. Dept. of Geophysics.
INVESTIGATIONS OF THE DYNAMICS AND THERMODYNAMICS OF THE MESOSPHERE LOWER THERMOSPHERE AND UPPER THERMOSPHERE AT THE POLAR REGIONS WITH OPTICAL GROUND-BASED REMOTE SENSING Annual Report, 15 Apr. 1991 - 14 Apr. 1992
Kenneth C. Clark and G. Hernandez 14 Apr. 1992 4 p
(Grant AF-AFOSR-0316-89)
(AD-A253228; AFOSR-92-0649TR) Avail: CASI HC A01/MF A01

This second year of the grant has been a year of consolidation and staging for the continuing research. The advances made at the end of last year, in particular the proof-of-concept of solid state etalone, are now going through the process of testing and validating the findings made with the prototype devices. Thus far, all of the benchmarks of the electrooptic etalon behavior can be repeated, and we have also found some new characteristics inherent to the device and its operation. For instance, in the non-linearity stage of measurements, it has been found that the reflective coatings are extremely sensitive to the presence of moisture in air. This effect seems to be enhanced by the existence of the electric fields (elrea 20 KV/cm) necessary for the operation of the electrooptic etalon. Operation in a vacuum, or in a controlled atmosphere are the obvious solutions, with the latter being the preferred choice since it preserves the ideal of a lightweight field device. Recoating of the test etalon was necessary. GRA

N93-10714# TRW Space Technology Labs., Redondo Beach, CA. Applied Technology Div.
MODELING OF HF PROPAGATION AND HEATING IN THE IONOSPHERE Final Report, Apr. 1989 - Nov. 1991
Denise Hinkel, Merit Shoucri, Timothy Smith, and Thomas Wagner Feb. 1992 116 p
(Contract F19628-89-C-0031)
(AD-A253941; RL-TR-92-29) Avail: CASi HC A06/MF A02

The purpose of the program of research reported here is to develop and demonstrate a realistic numerical model for self-consistent ionospheric propagation and heating of powerful frequency (HF) waves by conjoining existing, separate numerical models for high frequency wave propagation and ionospheric transport. A comprehensive numerical implementation of plasma geometric optics has been enhanced and adapted to the problem of self-consistent ionospheric propagation of high power, high frequency radar signals. The emphasis in this work is on the realistic and rigorous description of the propagation waves so that geometric and spectral characteristics of nonlinear ionospheric effects can be predicted in detail. The plasma geometric optics code has been used in conjunction with an ionospheric transport code to determine self-consistently the HF radiation field and quasilinear modifications of ionospheric plasma properties due to ohmic dissipation of the HF radiation. This allows detailed study of nonlinear phenomena such as beam self-focusing formation of large-scale density cavities and striations, and induced wave ducting. Overviews of the theory underlying the existing models of radiation propagation and ohmic power deposition are given, and enhancements to these models are described. New results achieved using the enhanced models are shown and the treatment of a self-consistent propagation and heating problem is presented. GRA

N93-10784# Florida Univ., Gainesville. Dept. of Chemistry.
PORTABLE TANDEM MASS SPECTROMETER ANALYZER Final Report, Dec. 1984 - Dec. 1987
R. Yost, Matuszak K. Johnson, and M. Hail Jul. 1991 281 p
(Contract F08635-83-C-0136)
(AD-A254065; ESL-TR-88-74) Avail: CASI HC A13/MF A03

This report documents Phase 1 of a two-phased project to develop a portable tandem mass spectral analyzer to be used in environmental characterizations of contaminated and suspected contaminated sites of Air Force properties. Phase 1 was a laboratory prototyping study and Phase 2 was to entail the construction of an actual portable prototype instrument. Phase 1 accomplishments include the development of an atmospheric pressure ionization source for a compact commercial mass spectrometer, fundamental studies of the atmospheric pressure ionization processes, and the development of rapid gas chromatographic pre-separation methods intended to enhance the instrument's performance when analyzing complex samples. GRA

47 METEOROLOGY AND CLIMATOLOGY

Includes weather forecasting and modification.

N93-10089# National Inst. of Standards and Technology, Gaithersburg, MD.
LIST OF PUBLICATIONS, 1969-1991. PANEL ON WIND AND SEISMIC EFFECTS Final Report
Noel J. Raufaste, ed. (Public Works Research Inst., Tsukuba, Japan) Apr. 1992 97 p
(PB92-201102; NIST/SP-835) Avail: CASI HC A05/MF A02; SOD HC

The Panel on Wind and Seismic Effects was established in 1969. Sixteen U.S. and six Japanese agencies participate with representatives of private sector organizations, to develop and exchange technologies aimed at reducing damages from high winds, earthquakes, storm surge, and tsunamis. This work is produced through collaboration between U.S. and Japanese member researchers working in 11 task committees. Each committee focuses on specific technical issues, e.g., earthquake strong motion data. The panel provides the vehicle to exchange technical data and information on design and construction of civil engineering lifelines, buildings, and water front structures, and to exchange high wind and seismic measurement records. Annual meetings alternate between the U.S. and Japan (even numbered years in the U.S.; odd numbered years in Japan). These one-week technical meetings provide the forum to discuss ongoing research and research results; one-week technical study tours follow the meetings. Author

N93-10108* National Aeronautics and Space Administration. Marshall Space Flight Center, Huntsville, AL.
METHOD AND APPARATUS FOR DETERMINING RETURN STROKE POLARITY OF DISTANT LIGHTNING Patent
Richard J. Blakeslee, inventor (to NASA) and Marx Brook, inventor (to NASA) 6 Oct. 1992 6 p Filed 15 Oct. 1991 Continuation of abandoned US-Patent-7,571,687, issued 23 Aug. 1990
(NASA-Case-MFS-26102-2-CU; US-Patent-5,153,508; US-Patent-7,571,687; US-Patent-Appl-SN-776710; US-Patent-Class-324-72; US-Patent-Class-340-601; Int-Patent-Class-G01W-1/00; Int-Patent-Class-G01R-31/02)
Avail: US Patent and Trademark Office

A method is described for determining the return stroke polarity of distant lightning for distances beyond 600 km by detecting the electric field associated with a return stroke of distant lightning, and processing the electric field signal to determine the polarity of the slow tail of the VLF waveform signal associated with the detected electric field. The polarity of the return stroke of distant lightning is determined based upon the polarity of the slow tail portion of the waveform.
Official Gazette of the U.S. Patent and Trademark Office

N93-10204# Colorado State Univ., Fort Collins. Engineering Research Center.
MESOSCALE SEVERE WEATHER DEVELOPMENT UNDER OROGRAPHIC INFLUENCES Final Report, 1 Feb. 1989 - 31 Mar. 1992
Elmar R. Reiter and Luiz Teixeira 30 Jun. 1992 36 p
(Contract F49620-89-C-0036)
(AD-A253630; AFOSR-92-0730TR) Avail: CASI HC A03/MF A01

Research summarized in this report addresses the lack of response of centralized weather services to specific user needs. Distributed weather prediction on tactical workstations can overcome most of the current barriers. Such a forecasting system,

running on a 486/33 PC, has been developed and tested extensively in Colorado snowstorm and blizzard conditions. The system incorporates a mesoscale numerical prediction model, a detailed geographical database, and a graphics user interface based on Microsoft Windows 3.1. Through this user interface the user can assimilate local observations with simple mouse point-and-click actions. The system can make use of observational data and heuristic rules. A prototype, customized for Colorado, has been tested under real-time and operational conditions. Concepts of object-oriented nowcasting, using artificial intelligence tools, such as 'fuzzy logic' have been developed. GRA

N93-10264# Air Weather Service, Scott AFB, IL.
PROBABILITY FORECASTING: A GUIDE FOR FORECASTERS AND STAFF WEATHER OFFICERS
Dec. 1991 124 p Supersedes AWS Pamphlet 105-51, dated Oct. 1978. Includes change 1, 16 Oct. 1989
(AD-A254216; AWS/TR-91/001) Avail: CASI HC A06/MF A02

Recommended techniques for producing and evaluating probability forecasts are described. A selected number of applications for optimal decision-making are presented. Chapters 1-4 address specific needs of forecasters and supervisors who make and evaluate subjective probability forecasts. Chapters 5-7 address applications of probabilities in decision-making, primarily for staff weather officers and staff meteorologists. GRA

N93-10292# California Univ., Santa Barbara.
AUTOMATIC CLOUD CLASSIFICATION FROM MULTI-SPECTRAL SATELLITE DATA OVER OCEANIC REGIONS Final Report, 15 Jan. 1991 - 14 Jan. 1992
Catherine Gautier 14 Jan. 1992 172 p
(Grant AF-AFOSR-0143-91)
(AD-A253670; AFOSR-92-0726TR) Avail: CASI HC A08/MF A02

This project was aimed at developing an operational expert system to perform the classification of satellite images into cloud types. The approach we have used is based on a number of assumptions. The first one is that such a classification is possible with satellite images of 1 km (or more) resolution. A second assumption, which lays the foundations for all classifications, is that there exists a parameter space wherein some clustering of the data occurs, so the task is to identify this parameter space from the data. An additional assumption necessary to physically interpret the results, but not necessary for the classification itself, is that the clusters found in this parameter space can be related to cloud types or physical features. We chose a Bayesian classifier for our classification. We believe that this type of classifier is best suited for the task because clouds are fuzzy objects which have overlapping characteristics. Also, with a Bayesian classifier, each point in the parameter space has a probability to belong to each class, although this probability may be anywhere between zero and one. GRA

N93-10337# Climate Analysis Center, Camp Springs, MD.
ATLAS OF SOUTHERN HEMISPHERE 500 mb TELECONNECTION PATTERNS DERIVED FROM NATIONAL METEOROLOGICAL CENTER ANALYSES
Vernon E. Kousky and Gerald D. Bell Mar. 1992 95 p
(PB92-203892; NOAA-Atlas-9) Avail: CASI HC A05/MF A01

An atlas of teleconnection patterns, based on monthly mean 500 mb geopotential height anomalies, is presented for the Southern Hemisphere. Height anomalies are computed with respect to the 1979 to 1988 base period monthly means for a 10 degree latitude by 10 degree longitude grid. These anomalies then serve as the basis for a point correlation analysis for the Southern Hemisphere winter (May to September) and summer (November to March) seasons. Author

N93-10363# Florida State Univ., Tallahassee. Geophysical Fluid Dynamics Inst.
NONLINEAR DYNAMICS UNDERLYING ATMOSPHERIC PREDICTABILITY Final Report, 15 Jul. 1989 - 14 Jul. 1992
Richard L. Pfeffer Aug. 1992 23 p
(Grant AF-AFOSR-0462-89)
(AD-A254042; AFOSR-92-0796TR) Avail: CASI HC A02/MF A01

During the three years of this University Research Initiative, 7 papers have been published in quality scientific journals with high standards of review and 3 have been submitted for publication based on full or partial support of AFOSR-89-0462, including the work of four Ph.D. candidates (one of whom received his Ph.D degree within the last two years). There was partial support from this grant on a software package for solving a general second order parameter involved system of elliptic partial differential equations on a two dimensional domain with Dirichlet and/or Neuman boundary conditions. GRA

N93-10377 McGill Univ., Montreal (Quebec).
ANELASTIC MODELLING OF EXPLOSIVE CYCLOGENESIS Ph.D. Thesis
Mark Hedley 1990 116 p
Avail: Univ. Microfilms Order No. DANN67810

This thesis is concerned with the numerical simulations of explosive cyclones using a very high resolution non-hydrostatic model with explicit precipitation physics. Two major aspects of the work are: (1) to explore the importance of various model parameters which lead to the rapid intensification of the surface cyclone through sensitivity tests, and (2) to unravel the cause-effect relations responsible for rapid surface pressure falls through a study of the heat budget, geostrophic vorticity budget, and a Lagrangian trajectory analysis of the simulated cyclone. The results from six experiments are presented. The main conclusions are: (1) By using analytic initial conditions based on typical wintertime conditions prior to explosive cyclogenesis, it is possible to obtain very realistic simulations of rapid cyclogenesis. (2) The use of high horizontal resolution is important in simulating the mesoscale features of rapidly deepening cyclones. In particular, the structure of the intense warm front observed ahead of the cyclone is very sensitive to changes in horizontal resolution. (3) The destabilization of the lower troposphere prior to the period of rapid deepening is essential in the formation of an extremely intense frontal structure, which in turn is instrumental in the rapid spinup of the storm. (4) In the presence of strong surface fluxes, the development of the simulated cyclone is affected by the depth of the planetary boundary layer. A detailed diagnosis of the control case is then presented. Quasi-Lagrangian heat budgets are calculated for several vertical columns about the vortex center. Very large variations in the heating were found to occur over a relatively small horizontal distance of 180 km. The reason for the mesoscale variations was traced to the intense warm front ahead of the cyclone and the bent-back warm front trailing behind the surface vortex. The results of the heat budget were then used in the interpretation of the geostrophic vorticity budget. It was found that the primary mechanism for geostrophic vorticity growth at the surface is through horizontal variations in the horizontal potential temperature advection. In particular, the timing of the most rapid surface geostrophic vorticity growth coincided with the formation of the bent-back warm front. Although the forcing from diabatic heating is large, it is nearly cancelled by the forcing from vertical advection of potential temperature. Instantaneous surface fluxes of sensible heat provide very little direct generation of geostrophic vorticity. The ariflow in the vicinity of the intense warm front was diagnosed by a fully Lagrangian trajectory analysis. A schematic flow diagram is presented which illustrates the overturning of the air in the warm front. Calculation on the evolution of the circulation for closed loops of air parcels indicate that the warm front is responsible for the generation of large vorticity values at the surface. Dissert. Abstr.

N93-10433# Environmental Protection Agency, Research Triangle Park, NC. Atmospheric Research and Exposure Assessment Lab.
METEOROLOGICAL AND SITE INFLUENCES AFFECTING THE COMPARISON OF NEPHELOMETER AND PHOTOGRAPHIC DETERMINATIONS OF LIGHT EXTINCTION AT RURAL SITES IN THE EASTERN US

E. G. Evans, R. J. Tropp, and T. Fitz-Simons 1992 19 p Prepared in cooperation with Alliance Technologies Corp., Chapel Hill, NC
(PB92-195999; EPA/600/A-92/139) Avail: CASI HC A03/MF A01

The level of agreement and the degree of linear correlation between nephelometer and photographic determinations of light extinction were examined from data obtained as part of the Eastern Fine Particle and Visibility Network (EFPVN). Information about the relative equivalence of the two methods was used (along with site-specific topographic features and meteorological factors affecting slide codes and visual range determinations) to assess the significance of various sources of inaccuracy affecting each method. For the EFPVN measurements, significant seasonal and inter-site variation were found in both the level of agreement between seasonal averages and the degree of correlation between short-term (hour to daily) nephelometer and photographic measurements. These differences are examined in terms of seasonal changes, intersite differences, and coding and treatment of photographic measurements for meteorological conditions.
Author

N93-10664# Air Force Inst. of Tech., Wright-Patterson AFB, OH.
ADEQUATE SAMPLING OF A CHAOTIC TIME SERIES M.S. Thesis
Jeffrey A. Doran Dec. 1991 198 p
(AD-A254170; AFIT/CI/CIA-92-054) Avail: CASI HC A09/MF A03

Currently there is some disagreement about what constitutes an adequate sample of a time series with which chaos measures may be quantified. In this thesis, a method for objectively determining such a sample is presented. This method is based on a new, relatively efficient measure, the Histogram Measure, which allows large amounts of data to be considered. This measure also may be used to distinguish the chaotic from the transient, or nonchaotic, portions of the solution that are inherent in any chaotic time series. This is a crucial consideration, since transients contaminate the chaotic characteristics of any time series, be it from observations or models. This measure also leads to a predictability estimate--that of loss of information gain--as functions of sample length and elapsed time. The Histogram Measure is tested with time series generated by the Lorenz (1963) three-component model of Rayleigh-Benard convection. It is shown that the determination of criteria for quantifying adequate samples of data yields a definitive cost/benefit result. In effect, there is a balance between obtaining the greatest possible accuracy and spending the fewest resources; beyond a particular time or number of data points, only a minimal benefit is realized for the increased cost.
GRA

N93-10780# Army Engineer Topographic Labs., Fort Belvoir, VA.
LONG-TERM DATA COLLECTION AND EMPIRICAL BACKGROUND TEMPERATURE MODELING
Alan E. Krusinger 21 Feb. 1992 16 p
(AD-A254044; TEC-R-162) Avail: CASI HC A03/MF A01

At the Research Institute, U.S. Army Topographic Engineering Center (TEC) we are developing empirical models to predict background surface temperatures and thermal contrasts, using continuous, long-term data collection in various climates. We are using a type-day concept to bound and group the values of radiation and other meteorological parameters into typical, somewhat unique weather conditions. Type-days are differentiated mainly by limits on integrated short and long wave incoming radiation, which portray sky cover and atmospheric conditions. The inputs to the models are climate, season, sky cover and whether the bare soil is 'wet' or 'dry'. We believe that existing, energy budget, surface temperature models are too complex in input variables and in operation, and that they cannot be simplified for tactical use. We also think that there is insufficient joint meteorological, radiometric and surface temperature data available.
GRA

N93-10848*# Washington Univ., Seattle. Dept. of Atmospheric Sciences.
MICROWAVE RADIOMETER STUDIES OF ATMOSPHERIC WATER OVER THE OCEANS, VOLUME 2
Kristina B. Katsaros Mar. 1992 73 p
(Grant NAGw-1688)
(NASA-CR-190343; NAS 1.26:190343) Avail: CASI HC A04/MF A01

Since the Seasat carried the Scanning Multichannel Microwave Radiometer (SMMR) into space in July of 1978, shortly followed by the SMMR on Nimbus 7, which operated for almost a decade, a new type of data source on atmospheric water vapor and other meteorological parameters has been available for analysis of weather systems over the ocean. Since 1987, we have had the Scanning Multichannel Microwave/Imager (SSM/I) instrument on Defense Meteorological Satellites providing similar data. We present a collection of our work performed over the last years of the study. For individual titles, see N93-10849 through N93-10851.

N93-10849*# Washington Univ., Seattle. Dept. of Atmospheric Sciences.
SATELLITE DERIVED INTEGRATED WATER VAPOR AND RAIN INTENSITY PATTERNS: INDICATORS OF RAPID CYCLOGENESIS
Lynn McMurdie and Kristina Katsaros *In its* Microwave Radiometer Studies of Atmospheric Water Over the Oceans, Volume 2 Mar. 1992 p 53-56 (For primary document see N93-10848 01-47)
(Contract NAS8-36473)
Avail: CASI HC A01/MF A01

We examine integrated water vapor fields and rain intensity patterns derived from the Scanning Multichannel Microwave Radiometer (SMMR) and Special Sensor Microwave/Imager (SSM/I) for several rapidly deepening and non-rapidly deepening midlatitude cyclones in the North Atlantic. Our goal is to identify features in the satellite data unique to the rapidly deepening cases, and to explore how these data can potentially be used in the analysis and forecasting of these events.
Author

N93-10850*# Centre National d'Etudes Spatiales, Toulouse (France). Groupe de Recherche de Geodesie Spatiale.
COMPARISON OF WIND SPEED MEASUREMENTS OVER THE OCEANS WITH THE SPECIAL SENSOR MICROWAVE/IMAGER AND THE GEOSAT ALTIMETER
Nelly M. Mognard and Kristina B. Katsaros (Washington Univ., Seattle.) *In* Washington Univ., Microwave Radiometer Studies of Atmospheric Water Over the Oceans, Volume 2 Mar. 1992 p 57-61 (For primary document see N93-10848 01-47)
Avail: CASI HC A01/MF A01

In order to compare wind speed estimates from the Geosat altimeter and the Special Sensor Microwave/Imager (SSM/I), 25 colocated passes, within 2 hours of each other, were selected and the SSM/I estimates of wind speed and atmospheric parameters extracted along the Geosat track. Both instruments and their algorithms are described. A statistical comparison of wind speed estimates is presented and the effects of the atmospheric parameters from Geosat are analyzed. Quasi-simultaneous measurements by Geosat and SSM/I, along a Geosat track in the North-East Pacific, are also presented.
Author

N93-10851*# Purdue Univ., West Lafayette, IN. Dept. of Earth and Atmospheric Sciences.
MORNING-EVENING DIFFERENCES IN GLOBAL AND REGIONAL OCEANIC PRECIPITATION AS OBSERVED BY THE SSM/I
Grant W. Petty and Kristina B. Katsaros (Washington Univ., Seattle.) *In* Washington Univ., Microwave Radiometer Studies of Atmospheric Water Over the Oceans, Volume 2 Mar. 1992 p 62-65 (For primary document see N93-10848 01-47)
(Grant NAG5-943)
Avail: CASI HC A01/MF A01

For the present preliminary analysis of oceanic rainfall statistics,

global oceanic SSM/I data were simply scanned for pixels which exhibited a 37 GHz polarization difference (vertically polarized brightness temperatures minus horizontally polarized brightness temperatures) of less than 15 K. Such a low polarization difference over the open ocean is a completely unambiguous indication of moderate to intense precipitation. Co-located brightness temperatures from all seven channels of the SSM/I were saved for each pixel so identified. Bad scans and geographically mislocated block of data were objectively identified and removed from the resulting data base. We collected global oceanic rainfall data for two time periods, each one month in length. The first period (20 July-19 August 1987) coincides with the peak of the Northern Hemisphere summer. The second period (13 January-12 February 1988) coincides with the Northern Hemisphere winter. Author

48 OCEANOGRAPHY

Includes biological, dynamic, and physical oceanography; and marine resources.

For related information see also *43 Earth Resources and Remote Sensing.*

N93-10068*# Washington Univ., Seattle. Dept. of Atmospheric Sciences.
AIR-SEA INTERACTION AND REMOTE SENSING Status Report, 1 Dec. 1991 - 30 Nov. 1992
Kristina B. Katsaros and Serhad S. Ataktuerk 1992 12 p
Original contains color illustrations
(Grant NAGw-1322)
(NASA-CR-190913; NAS 1.26:190913) Avail: CASI HC A03/MF A01; 2 functional color pages

The first part of the proposed research was a joint effort between our group and the Applied Physics Laboratory (APL), University of Washington. Our own research goal is to investigate the relation between the air-sea exchange processes and the sea state over the open ocean and to compare these findings with our previous results obtained over a small body of water namely, Lake Washington. The goals of the APL researchers are to study (1) the infrared sea surface temperature (SST) signature of breaking waves and surface slicks, and (2) microwave and acoustic scattering from water surface. The task of our group in this joint effort is to conduct measurements of surface fluxes (of momentum, sensible heat, and water vapor) and atmospheric radiation (longwave and shortwave) to achieve our research goal as well as to provide crucial complementary data for the APL studies. The progress of the project is summarized. Author

N93-10283# Brookhaven National Lab., Upton, NY.
MOLECULAR BIOLOGY IN STUDIES OF OCEANIC PRIMARY PRODUCTION
J. LaRoche, P. G. Falkowski, and R. Geider 1992 23 p
Presented at the International Symposium on the Measurement of Primary Production from the Molecular to Global Scale, La Rochelle, France, 19-26 Apr. 1992
(Contract DE-AC02-76CH-00016)
(DE92-016101; BNL-47654; CONF-9204164-1) Avail: CASI HC A03/MF A01

Remote sensing and the use of moored in situ instrumentation has greatly improved our ability to measure phytoplankton chlorophyll and photosynthesis on global scales with high temporal resolution. However, the interpretation of these measurements and their significance with respect to the biogeochemical cycling of carbon relies on their relationship with physiological and biochemical processes in phytoplankton. For example, the use of satellite images of surface chlorophyll to estimate primary production is often based on the functional relationship between photosynthesis and irradiance. A variety of environmental factors such as light, temperature, nutrient availability affect the photosynthesis/irradiance (P vs I) relationship in phytoplankton. We present the following three examples showing how molecular biology can be used to provide basic insight into the factors controlling primary productivity at three different levels of complexity. (1) Studies of light intensity regulation in unicellular alga show how molecular biology can help understand the processing of environmental cues leading to the regulation of photosynthetic gene expression. (2) Probing of the photosynthetic apparatus using molecular techniques can be used to test existing mechanistic models derived from the interpretation of physiological and biophysical measurements. (3) Exploratory work on the expression of specific proteins during nutrient-limited growth of phytoplankton may lead to the identification and production of molecular probes for field studies. DOE

N93-10621# Scripps Institution of Oceanography, La Jolla, CA.
MEASUREMENTS OF SURFACE OCEAN CARBON DIOXIDE PARTIAL PRESSURE DURING WOCE
R. F. Weiss 25 Feb. 1992 9 p
(Contract DE-FG03-90ER-60981)
(DE92-011856; DOE/ER-60981/2) Avail: CASI HC A02/MF A01

Progress during the past year of research under 'Measurements of Surface Ocean Carbon Dioxide Partial Pressure During WOCE' has been significant. As was described in our previous progress report, the startup phase of this research was severely frustrated by delays in the US WOCE Hydrographic Program (WHP), which in turn were caused by delays in the mid-life refit of the R/V Knorr. As a result the high latitude southeastern Pacific work (WHP lines P19S and P16S) originally scheduled for the 1990 austral summer has still not been carried out. As a substitute, the smaller R/V Thomas Washington was pressed into service during mid-1991 to carry out lower-latitude portions of the WHP P16 and P17 lines - the TUNES Expedition. Because this ship is much smaller than the R/V Knorr, she could not carry a full complement of WHP programs and seagoing personnel and was restricted by her size and the time of year to lower-latitude work. Our original proposal for carbon dioxide measurements was designed to divide the work between legs in which we participated as part of the WHP dissolved CFC program (under separate NSF funding) and legs in which we entrusted the operation of our system to other CFC or carbon dioxide laboratories with expertise in gas chromatography. Since we were not involved in any CFC work on the substituted Washington expedition, and since all the seagoing programs on the Washington were additionally stressed by a shortage of people and space, this placed our carbon dioxide program at an unwelcome disadvantage. The preliminary results for carbon dioxide and nitrous oxide are shown. We are forced to rely on spotty manual observations and station CTD temperatures to reconstruct our equilibrator temperature solubility corrections for portions of that leg. We did not get our usual reliable data return, but the results were surely worth effort, especially for this vast and rarely-visited region of the world oceans. DOE

N93-10791# Florida State Univ., Tallahassee. Dept. of Meteorology.
AIR-SEA INTERACTION IN REGIONS OF VARYING SURFACE CONDITIONS Final Report
Steven A. Stage Jul. 1992 72 p
(Contract N00014-89-J-1660)
(AD-A253182) Avail: CASI HC A04/MF A01

The Frontal Air-Sea Interaction Experiment (FASINEX) was a field experiment that was primarily performed in the Fall of 1985 and Spring of 1986 in the vicinity of the subtropical oceanic front south of Bermuda. The chief goal of this project was to develop an understanding of the behavior of the Marine Atmospheric Boundary Layer (MABL) in the vicinity of the FASINEX SST front. There were two major components to this work: (1) to study turbulent fluxes and other turbulent statistics in the vicinity of the Sea Surface Temperature (SST) front as measured by FASINEX aircraft (special statistical methods were devised and used to show how these quantities change near the SST front); and (2) to study the structure of the MABL by analysis of results from a two dimensional numerical model. MABL structure was examined as a function of the direction of the synoptic scale geostrophic wind

relative to the front. We also looked at the secondary circulations induced in the MABL by the SST front. GRA

N93-10887# Delaware Univ., Newark. Coll. of Marine Studies.
THE 200TH AMERICAN CHEMICAL SOCIETY GEOCHEMISTRY DIVISION SYMPOSIUM ON PROGRESS IN MARINE CHEMISTRY Final Technical Report, 1 Oct. 1990 - 30 Sep. 1991
Thomas M. Church 15 Jul. 1992 5 p Symposium held in Washington, DC, 28-29 Aug. 1990
(Contract N00014-91-J-1250)
(AD-A253757) Avail: CASI HC A01/MF A01

The meeting included approximately 24 presentations on select topics of physical, inorganic, redox speciation, and organic marine chemistry, about half of which are being published in a special issue of Marine Chemistry. Several noted foreign marine chemists were among the speakers and were supported by this PRF grant. GRA

51 LIFE SCIENCES (GENERAL)

N93-10085*# Purdue Univ., West Lafayette, IN. Chemical Engineering.
DEVELOPMENT OF PHYSICAL AND MATHEMATICAL MODELS FOR THE POROUS CERAMIC TUBE PLANT NUTRIFICATION SYSTEM (PCTPNS)
D. Teh-Wei Tsao, M. R. Okos, J. C. Sager (National Aeronautics and Space Administration. John F. Kennedy Space Center, Cocoa Beach, FL.), and T. W. Dreschel (Bionetics Corp., Cocoa Beach, FL.) Jul. 1992 115 p
(Contract NAS10-11624)
(NASA-TM-107551; NAS 1.15:107551) Avail: CASI HC A06/MF A02

A physical model of the Porous Ceramic Tube Plant Nutrification System (PCTPNS) was developed through microscopic observations of the tube surface under various operational conditions. In addition, a mathematical model of this system was developed which incorporated the effects of the applied suction pressure, surface tension, and gravitational forces as well as the porosity and physical dimensions of the tubes. The flow of liquid through the PCTPNS was thus characterized for non-biological situations. One of the key factors in the verification of these models is the accurate and rapid measurement of the 'wetness' or holding capacity of the ceramic tubes. This study evaluated a thermistor based moisture sensor device and recommendations for future research on alternative sensing devices are proposed. In addition, extensions of the physical and mathematical models to include the effects of plant physiology and growth are also discussed for future research. Author

N93-10109* National Aeronautics and Space Administration. Lyndon B. Johnson Space Center, Houston, TX.
METHOD FOR CULTURING MAMMALIAN CELLS IN A PERFUSED BIOREACTOR Patent
Ray P. Schwarz, inventor (to NASA) and David A. Wolf, inventor (to NASA) 13 Oct. 1992 10 p Filed 28 Jun. 1990 Division of US-Patent-Appl-SN-213559, filed 30 Jun. 1988
(NASA-Case-MSC-21293-2; US-Patent-5,155,035; US-Patent-Appl-SN-545233; US-Patent-Appl-SN-213559; US-Patent-Class-435-240.24; US-Patent-Class-435-240.25; US-Patent-Class-435-240.46; Int-Patent-Class-C12N-5/02) Avail: US Patent and Trademark Office

A bio-reactor system wherein a tubular housing contains an internal circulariy disposed set of blade members and a central tubular filter all mounted for rotation about a common horizontal axis and each having independent rotational support and rotational drive mechanisms. The housing, blade members and filter preferably are driven at a constant slow speed for placing a fluid culture medium with discrete microbeads and cell cultures in a discrete spatial suspension in the housing. Replacement fluid medium is symmetrically input and fluid medium is symmetrically output from the housing where the input and the output are part of a loop providing a constant or intermittent flow of fluid medium in a closed loop.
Official Gazette of the U.S. Patent and Trademark Office

N93-10110* National Aeronautics and Space Administration. Lyndon B. Johnson Space Center, Houston, TX.
METHOD FOR CULTURING MAMMALIAN CELLS IN A HORIZONTALLY ROTATED BIOREACTOR Patent
Ray P. Schwarz, inventor (to NASA), David A. Wolf, inventor (to NASA), and Tinh T. Trinh, inventor (to NASA) 6 Oct. 1992 7 p Filed 15 Apr. 1991 Division of US-Patent-Appl-SN-213558, filed 30 Jun. 1988
(NASA-Case-MSC-21294-2; US-Patent-5,153,133; US-Patent-Appl-SN-687605; US-Patent-Appl-SN-213558; US-Patent-Class-435-240.24; US-Patent-Class-435-240.25; US-Patent-Class-435-240.46; US-Patent-Class-435-240.241; US-Patent-Class-435-818; Int-Patent-Class-C12N-5/02) Avail: US Patent and Trademark Office

A bio-reactor system where cell growth microcarrier beads are suspended in a zero head space fluid medium by rotation about a horizontal axis and where the fluid is continuously oxygenated from a tubular membrane which rotates on a shaft together with rotation of the culture vessel. The oxygen is continuously throughput through the membrane and disbursed into the fluid medium along the length of the membrane.
Official Gazette of the U.S. Patent and Trademark Office

N93-10461# Brookhaven National Lab., Upton, NY.
RESOURCE CAPTURE BY SINGLE LEAVES
S. P. Long May 1992 36 p Presented at the 52nd International Easter School, Resource Capture By Crops, Nottingham, 30 Mar. - 2 Apr. 1992
(Contract DE-AC02-76CH-00016)
(DE92-015847; BNL-47574; CONF-9203160-1) Avail: CASI HC A03/MF A01

Leaves show a variety of strategies for maximizing CO2 and light capture. These are more meaningfully explained if they are considered in the context of maximizing capture relative to the utilization of water, nutrients, and carbohydrates reserves. There is considerable variation between crops in their efficiency of CO2 and light capture at the leaf level. Understanding of these mechanisms indicate some ways in which efficiency of resource capture could be level cannot be meaningfully considered without simultaneous understanding of implications at the canopy level. DOE

N93-10628# Los Alamos National Lab., NM.
SELF-PROGRAMMING OF MATTER AND THE EVOLUTION OF PROTO-BIOLOGICAL ORGANIZATIONS
Steen Rasmussen (Santa Fe Inst., NM.), Rasma Feldberg (Technical Univ. of Denmark, Lyngby.), and Carsten Knudsen (Technical Univ. of Denmark, Lyngby.) 1992 11 p Presented at the Frontiers of Life, Blois (France), Oct. 1991
(Contract W-7405-eng-36)
(DE92-015244; LA-UR-92-1722; CONF-9110388-1) Avail: CASI HC A03/MF A01

We propose a novel class of formal dynamical systems, which are referred to as self-programming or constructive. We believe that these systems form natural models for functional self-organization in prebiotic and proto-biological systems. We shall use the computer as a 'test-tube' to follow the dynamics of these systems and in particular investigate their emergent functional properties. Using the computer as a simulation laboratory to understand such processes in this context based on two fundamental assumptions: (1) That the logic, e.g., the dynamics and the functional organization, of a physical and in particular a living system can be described in terms of mathematics and hence can be studied independent of the molecular hardware that carries this dynamics. (2) That the properties of structures and organizations emerging from the dynamics of self-programming systems reflect aspects of the organizing principles of prebiotic

and proto-biological systems. We shall show that for instance the emergence of complex cooperative structures is part of the natural dynamics of self-programming systems. DOE

N93-10834# Pacific Northwest Lab., Richland, WA.
RADIATION DAMAGE TO DNA
J. H. Miller Apr. 1992 9 p Presented at the 14th Werner Brandt Workshop on Charged Particle Penetration Phenomena, Oak Ridge, TN, 30 Apr. - 1 May 1992
(Contract DE-AC06-76RL-01830)
(DE92-015760; PNL-SA-21039; CONF-9204144-2) Avail: CASI HC A02/MF A01

Our goal is to calculate the probability of ejecting electrons from DNA by charged particles that pass near the macromolecule as they slow down in an aqueous medium that contains DNA in low concentration. This process is illustrated for a particle of charge Ze and velocity v, where impact parameters b(sub 1), b(sub 2), and b(sub 3) indicate the distances between the trajectory and a phosphate group, a base, and a sugar moiety, respectively. In the present state of our theoretical development, we must treat each of these components of DNA as an independent impurity site occupied by electrons in a Slater-type orbital with a characteristic orbital radius and band gap. Determination of these parameters will be discussed below; however, before we turn to that part of the discussion, it is interesting to address the question of multiple ionizations of DNA by the passage of a single charged particle. DOE

N93-10835# Michigan State Univ., East Lansing. Plant Research Lab.
INTERDISCIPLINARY RESEARCH AND TRAINING PROGRAM IN THE PLANT SCIENCES
C. P. Wolk 1992 105 p
(Contract DE-FG02-91ER-20021)
(DE92-015919; DOE/ER-20021/2) Avail: CASI HC A06/MF A02

Our research on plants has continued. The following topics are discussed: molecular basis of symbiotic plant-microbe interactions; enzymatic mechanisms and regulation of plant cell wall biosynthesis; molecular mechanisms that regulate the expression of genes in plants; resistance of plants to environmental stress; studies on hormone biosynthesis and action; plant cell wall proteins; interaction of nuclear and organelle genomes; sensor transduction in plants; molecular mechanisms of trafficking in the plant cell; regulation of lipid metabolism; molecular bases of plant disease resistance mechanisms; biochemical and molecular aspects of plant pathogenesis; developmental biology of nitrogen-fixing cyanobacteria; environmental control of plant development and its relation to plant hormones. DOE

52 AEROSPACE MEDICINE

Includes physiological factors; biological effects of radiation; and effects of weightlessness on man and animals.

N93-10075* National Aeronautics and Space Administration, Washington, DC.
AEROSPACE MEDICINE AND BIOLOGY: A CONTINUING BIBLIOGRAPHY WITH INDEXES (SUPPLEMENT 365)
Aug. 1992 74 p
(NASA-SP-7011(365); NAS 1.21:7011(365)) Avail: CASI HC A04

This bibliography lists 211 reports, articles and other documents introduced into the NASA Scientific and Technical Information System during July 1992. Subject coverage includes: aerospace medicine and physiology, life support systems and man/system technology, protective clothing, exobiology and extraterrestrial life, planetary biology, and flight crew behavior and performance. Author

N93-10076* National Aeronautics and Space Administration, Washington, DC.
AEROSPACE MEDICINE AND BIOLOGY: A CONTINUING BIBLIOGRAPHY WITH INDEXES (SUPPLEMENT 360)
Mar. 1992 78 p
(NASA-SP-7011(360); NAS 1.21:7011(360)) Avail: CASI HC A05

This bibliography lists 217 reports, articles and other documents introduced into the NASA Scientific and Technical Information System during February 1992. Subject coverage includes: aerospace medicine and physiology, life support systems and man/system technology, protective clothing, exobiology and extraterrestrial life, planetary biology, and flight crew behavior and performance. Author

N93-10077* National Aeronautics and Space Administration, Washington, DC.
AEROSPACE MEDICINE AND BIOLOGY: A CONTINUING BIBLIOGRAPHY WITH INDEXES (SUPPLEMENT 364)
Jul. 1992 71 p
(NASA-SP-7011(364); NAS 1.21:7011(364)) Avail: CASI HC A04

This bibliography lists 188 reports, articles and other documents introduced into the NASA Scientific and Technical Information System during June 1992. Subject coverage includes: aerospace medicine and physiology, life support systems and man/system technology, protective clothing, exobiology and extraterrestrial life, planetary biology, and flight crew behavior and performance. Author

N93-10079* National Aeronautics and Space Administration, Washington, DC.
AEROSPACE MEDICINE AND BIOLOGY: A CONTINUING BIBLIOGRAPHY WITH INDEXES (SUPPLEMENT 366)
Sep. 1992 82 p
(NASA-SP-7011(366); NAS 1.21:7011(366)) Avail: CASI HC A05

This bibliography lists 248 reports, articles, and other documents introduced into the NASA Scientific and Technical Information System during Aug. 1992. Subject coverage concentrates on the biological, physiological, psychological, and environmental effects to which humans are subjected during and following simulated or actual flight in the Earth's atmosphere or in interplanetary space. References describing similar effects on biological organisms of lower order are also included. Such related topics as sanitary problems, pharmacology, toxicology, safety and survival, life support systems, exobiology, and personnel factors receive appropriate attention. Applied research receives the most emphasis, but references to fundamental studies and theoretical principles related to experimental development also qualify for inclusion. Author

N93-10080* National Aeronautics and Space Administration, Washington, DC.
AEROSPACE MEDICINE AND BIOLOGY: A CONTINUING BIBLIOGRAPHY WITH INDEXES (SUPPLEMENT 367)
Oct. 1992 73 p
(NASA-SP-7011(367); NAS 1.21:7011(367)) Avail: CASI HC A04

This bibliography lists 205 reports, articles, and other documents introduced into the NASA Scientific and Technical Information System during Aug. 1992. Subject coverage includes the following: aerospace medicine and physiology, life support systems and man/system technology, protective clothing, exobiology and extraterrestrial life, planetary biology, and flight crew behavior and performance. Author

N93-10222# International Atomic Energy Agency, Vienna (Austria).
FORMAT AND STRUCTURE OF A DATABASE ON HEALTH AND ENVIRONMENTAL IMPACTS OF DIFFERENT ENERGY SYSTEMS FOR ELECTRICITY GENERATION
Apr. 1992 232 p

(DE92-634160; IAEA-TECDOC-645) Avail: CASI HC A11/MF A03

There is considerable interest in the application of techniques of comparative risk assessment in the planning of energy mixes for electricity generation, and particularly in the integration of health and environmental impacts in the decision-making process. To assist this it is planned to establish an internationally coordinated database on the health and environmental effects of different energy sources. This document introduces the structure and format of the database, and contains in addition eighteen papers prepared for Technical Committee Meetings to discuss the proposed database. DOE

N93-10271# Pennsylvania Univ., Philadelphia.
COMPUTER SIMULATIONS OF OBJECT DISCRIMINATION BY VISUAL CORTEX
Paul Sajda and Leif H. Finkel 3 Jan. 1992 12 p
(Contract N00014-90-J-1864)
(AD-A253345) Avail: CASI HC A03/MF A01

We present computer simulations of how the visual cortex may discriminate objects based on depth-from-occlusion. We propose neural mechanisms for how the visual system binds edges into contours, and binds contours and surfaces into objects. The model is simulated by a system of physiologically-based neural networks which feature feedback connections from higher to lower cortical areas, a distributed representation of depth, and phase-locked cortical neuronal firing. The system demonstrates psychophysical properties consistent with human perception of real and illusory visual scenes. The model addresses both the binding problem and the problem of object segmentation. GRA

N93-10438# Versar, Inc., Springfield, VA.
DERMAL EXPOSURE ASSESSMENT: PRINCIPLES AND APPLICATIONS Interim Report
Jan. 1992 392 p
(Contract EPA-68-D00101)
(PB92-205665; OHEA-E-367; EPA/600/8-91/011B) Avail: CASI HC A17/MF A04

The purpose of the document is to describe the principles of dermal absorption and show how to apply these principles in actual human exposure scenarios. The primary focus of the document is on dermal contact with water, soils, and vapors. For each of these media, the experimental data on the dermal properties of specific compounds are summarized and methods are provided for predicting these properties when data is lacking. Additionally, scenario factors describing the frequency, duration, and intensity of contact are presented for the soil and water media. GRA

N93-10613# Armed Forces Radiobiology Research Inst., Bethesda, MD.
DOD SPACE RADIATION CONCERNS Annual Program Review No. 3
Michael J. Golightly and Daniel L. Collins 15 Jul. 1992 20 p
(AD-A253135) Avail: CASI HC A03/MF A01

Potential manned military space missions would involve exposing crews to many environmental factors, including ionizing radiation. Ionizing radiation in space comes from several natural and man-made sources. Many parameters influence the radiation dose crews would receive and the biomedical outcome of the exposure. A systematic approach has been developed to examine military space crew doses and its impact on mission objectives. The approach involves determining mission and orbital parameters from analysis of preliminary spaceflight operational concepts and objectives, the types of radiation qualities and dose rates to which crews would be exposed, the critical crew functions, and the resulting impact of the projected radiation exposure. From this analysis and a review of the current space radiobiology database, areas requiring further information or research are identified. An initial space radiobiology research program has been outlined. The resulting Space Radiation Effects Study Program has been incorporated into the current DoD 5-Year Plan for Ionizing Radiation Biomedical Research. GRA

N93-10626# Inhalation Toxicology Research Inst., Albuquerque, NM.
UNDERSTANDING MECHANISMS OF CARCINOGENESIS USING RAT TRACHEAL EPITHELIAL CELLS IN VITRO
David G. Thomassen 1992 7 p Presented at the Symposium on Current Concepts and Approaches on Animal Test Alternatives, Aberdeen Proving Grounds, MD, 4-6 Feb. 1992
(Contract DE-AC04-76EV-01013)
(DE92-013510; CONF-9202107-1) Avail: CASI HC A02/MF A01

In vitro transformation assays are used to increase understanding of mechanisms of carcinogenesis and to determine the transforming potency of individual agents. While these assays can provide information on the mechanism for specific steps in the carcinogenic process or can predict the carcinogenic potency of a given toxicant, the relevance of in vitro endpoints or response for carcinogenesis must be determined. This paper will focus on the utility of an in vitro system for understanding the mechanisms of multistage respiratory carcinogenesis and on considerations that are critical for its use and application. DOE

N93-10650# Loyola Univ., Chicago, IL. Hearing Inst.
AUDITORY PROCESSING OF COMPLEX SOUNDS ACROSS FREQUENCY CHANNELS Final Technical Report, 1 May 1989 - 30 Apr. 1992
William P. Shofner, Raymond H. Dye, and William A. Yost 26 Jun. 1992 24 p
(Grant AF-AFOSR-0335-89)
(AD-A253612; AFOSR-92-0714TR) Avail: CASI HC A03/MF A01

The research supported by this grant is directed towards gaining an understanding how the auditory system processes complex sounds. The results of binaural psychophysical experiments in human subjects suggest (1) that spectrally synthetic binaural processing is the rule when the number of components in the tone complex are relatively few (less than 10) and there are no dynamic binaural cues to aid segregation of the target from the background, and (2) that waveforms having large effective envelope depths are on the average more easily lateralized than those having small effective envelope depths. Psychophysical experiments in human subjects using sinusoidally amplitude modulated narrowband noises and complex patterns of modulation of tonal carriers have been directed toward understanding auditory object perception. Results from experiments and theoretical modelling suggest that slow temporal modulation of different spectral components can be used by the auditory system to fuse these components into one auditory image. The results of psychophysical experiments show that the effects of noise bandwidth on intensity discrimination of noise in chinchillas are similar to data from human subjects; the results can be accounted for by a modification of the ideal energy detector. Neurophysiological experiments have been directed at gaining an understanding of how auditory neurons encode pitch related information in the temporal properties of discharge. The results show that a temporal representation at the level of the cochlear nucleus can account for some, but not of the pitches of rippled noise. GRA

N93-10661# University of Northern Arizona, Flagstaff. Coll. of Health Professions.
EFFECTS OF EARLY BRIGHT, LATE BRIGHT AND DIM ILLUMINATION UPON CIRCADIAN NEUROENDOCRINE, ELECTROPHYSIOLOGICAL AND BEHAVIORAL RESPONSES Final Report, May 1991 - May 1992
Patrick R. Hannon, George Brainard, William Gibson, Jonathan French, and Margaret Hopson 29 Jul. 1992 58 p
(Grant AF-AFOSR-0271-91)
(AD-A254129; AFOSR-92-0793TR) Avail: CASI HC A04/MF A01

This study assessed the effects of bright light on biological and behavioral measures to determine if bright light can reduce fatigue and enhance human work performance. Female subjects (N=37) were exposed to one of 3 lighting conditions in a between groups research design. Subjects in the bright light groups were

exposed to 5000 lux white light from 1800 hrs to 2400 hrs (Early Bright) or from 2400-0600 hrs (Late Bright from 1800-0600 hrs Dim Red). Blood sample were taken every 90 minutes. Repeated measures ANOVA indicated a significant interaction effect (light x time) for tympanic temperature, (F=3.339, p=.001). The bright light conditions maintained higher tympanic temperatures from 2300 hrs through 0400 hrs. Plasma melatonin measures indicated a main effects difference of F=4.009, p=.029. Most importantly, the results showed that the light x time of night interaction for melatonin was significant at F=59.436, p=.000. The suppression of plasma melatonin was greatest from 2230 hrs through 0500 hrs in the Early Bright and Late Bright groups. Cortisol was not affected by the ambient lighting conditions. Dim red light resulted in higher scores on the Stanford Sleep Scale from 2400 hrs through 0500 hrs (light x time, F= 2.595, p=.023). Subjects under the bright light conditions performed better on the cognitive measures of Code Substitution accuracy (F=3.918, p=.030) and Column Addition accuracy (F=4.660, p=.017). These data show some improvements in cognitive performance and alertness associated with bright light exposure and occur with changes in tympanic temperature and plasma melatonin at critical time periods. GRA

N93-10709# Keller Army Community Hospital, West Point, NY.
A PROSPECTIVE EVALUATION OF STRESS FRACTURES/OVERUSE INJURIES IN A POPULATION OF WEST POINT CADETS Annual Report, 1 Dec. 1990 - 30 Nov. 1991
James H. Swain 15 Jan. 1992 4 p
(Contract MIPR-91M1502; DA Proj. 3M2-63002-D-840)
(AD-A252427) Avail: CASI HC A01/MF A01

The study group performed two evaluations during this period. The 175 Cadets remain in the study. Nonparticipant are primarily due to resignation from the Academy. Body fat percent for the men and women has remained the same. The women have increased weight indicating a gain in muscle mass. Lower extremity injuries have equalized in the two groups. There were more injuries in men (32 percent) than in women (27 percent) from January to August 1991. Bone density and laboratory values are being automated presently. GRA

N93-10765# Massachusetts General Hospital, Boston.
COGNITION IN THE BRAIN: INVESTIGATIONS USING POSITRON EMISSION TOMOGRAPHY Final Technical Report
Nathaniel M. Alpert 16 Jul. 1992 17 p
(Grant AF-AFOSR-0029-91)
(AD-A254280; AFOSR-92-0766TR) Avail: CASI HC A03/MF A01

The goal of this workshop was to identify and begin a continuing discussion of the major issues affecting the generation and testing of new hypotheses about cognitive processing. The workshop covered three major topics: (1) anatomic localization of components of cognitive processing; (2) issues of data analysis arising from cognitive function experiments; and (3) task design in cognitive function studies with PET. GRA

N93-10796# Army Medical Center, Fort Gordon, GA.
METABOLIC FACTORS INFLUENCING MYOCARDIAL RECOVERY FROM ACIDOSIS (CIC3) Final Report, 15 Mar. 1991 - 14 Mar. 1992
Joseph I. Shapiro, Jesse Doers, Richard F. Kucera, M. McCormick, and Nancy Elkins 10 Apr. 1992 17 p
(Contract MIPR-91MM1533; NR Proj. 3M1-61102-BS-87)
(AD-A252376) Avail: CASI HC A03/MF A01

The mechanisms involved in cardiac dysfunction during acidosis were explored in an isolated heart model. Metabolic acidosis was observed to cause marked functional and energy metabolic derangement consistent with a primary impairment of energy production. Synergism with hypoxia was also demonstrated in this model. The site of metabolic blockage during acidosis was observed to be at the level of oxidative metabolism and not glycolysis. Isolated cardiac mitochondrial studies, however, did not demonstrate any direct effect of acidosis on mitochondrial respiration or coupling. Studies with respiratory acidosis were complicated by the coexistence of relative hypoxia which affected the model deleteriously. Treatment of acidotic isolated hearts with the experimental buffer, Carbicarb, caused marked increases in intracellular pH as well as functional and metabolic improvements. Isotonic rather than hypertonic Carbicarb was found to be substantially more effective in this model. The superiority of isotonic to hypertonic Carbicarb may be related to the tendency of hypertonic but not isotonic Carbicarb to significantly increase cytosolic sodium concentrations. GRA

53 BEHAVIORAL SCIENCES

Includes psychological factors; individual and group behavior; crew training and evaluation; and psychiatric research.

N93-10278# Rutgers - The State Univ., New Brunswick, NJ. Dept. of Psychology.
EYE MOVEMENTS AND VISUAL INFORMATION PROCESSING Final Report, 1 Apr. 1988 - 30 Sep. 1991
Eileen Kowler 30 Sep. 1991 6 p
(Grant AF-AFOSR-0171-88)
(AD-A250198; AFOSR-92-0268TR) Avail: CASI HC A02/MF A01

The research carried out during the period of the grant continued several lines of investigation on the way in which sensory and high-level influences contribute to the control of smooth and saccadic eye movements and on the perceptual implications of eye movements. We: (1) provided the first clear evidence that symbolic cues determine the direction of anticipatory smooth eye movements, showing that adaptive models, based on algorithms that modify pursuit according to prior performance cannot work; (2) showed that saccades to spatially extended targets are best understood by a serial model, with a selection stage followed by a spatial pooling mechanism; (3) showed that slow control is a velocity, not a position, corrective and; (4) showed that saccades (not shifts of attention) are required for accurate perception of poorly-segregating textures. These results are all consistent with the view that sensory and cognitive influences combine at a relatively high level of processing to provide a single, coherent input to the oculomotor system. Kowler also edited a book, published by Elsevier, containing major reviews and theoretical treatments of eye movements, vision and cognition. GRA

N93-10321# Federal Aviation Administration, Washington, DC. *Office of Aviation Medicine.*
A NEW TEST OF SCANNING AND MONITORING ABILITY: METHODS AND INITIAL RESULTS
A. M. Revzin and P. G. Rasmussen Mar. 1992 19 p
(AD-A249123; DOT/FAA/AM-92/12) Avail: CASI HC A03/MF A01

Most tasks in the FAA's Air Traffic Control (ATC) system involve long duration scanning and monitoring for continuously changing events occurring within a large visual space. Errors occur, so it is important to understand the causes of such errors to minimize or eliminate them by changing task design or improving personnel selection. This study describes a new system for testing scanning and monitoring abilities. The system, as currently implemented, is basically a character identification task. The characters are presented at random intervals and locations within two or more WorkAreas. The WorkAreas are defined as rectangular areas on a microcomputer display screen. They are filled with a constantly changing random dot pattern and may be located anywhere on the screen. The subject's task is to press a designated key on the computer keypad when a specified target character appears. Parametric manipulations can evaluate the effects on performance of many variables, including angular separation of WorkAreas, differential workloads in the WorkAreas, and effects of visual noise. We found a highly significant performance decrement as a function of increasing angular separation of WorkAreas. This is congruent with prior studies, which we interpret

as a validation of our test procedure. We did not find practice effects, fatigue effects, or selective attention effects between WorkAreas. GRA

N93-10658# Retina Foundation, Boston, MA. Eye Research Inst.
PERCEPTION OF LIGHTNESS AND BRIGHTNESS IN COMPLEX PATTERNS Annual Report, 1 May 1991 - 30 Apr. 1992
Lawrence E. Arend, Jr. 30 Jun. 1992 24 p
(Grant AF-AFOSR-0377-89)
(AD-A254093; AFOSR-92-0778TR) Avail: CASI HC A03/MF A01

Perception of surface color plays an important part in many everyday visual tasks. Psychophysical and neurophysiological data on early visual processes suggest a number of potential sensory limitations on the accuracy of surface-color perception. A new paradigm has been used to clarify the relationships between early visual processes and perception of achromatic surface colors (shades of gray). Psychophysical measurements of perceived surface color were made using achromatic stimulus patterns that were complex enough to support unambiguous perception of surfaces and lights. Lightness (apparent reflectance), brightness (apparent luminance) and local brightness contrasts were all measured using the same stimulus patterns. According to a number of models, lightness is closely related to local brightness contrast, but the data indicated that the relationship is more complicated than previously supposed. The brightness contrast data are well described by Stiles' threshold-vs-radiance curve, which is widely thought to be a characteristic of retinal adaptation processes. Both brightness and lightness are slightly higher on dark gray backgrounds than on white backgrounds. This perceptual error appear to be independent of illumination level. GRA

N93-10662# SAM Technology, Inc., San Francisco, CA.
MENTAL WORKLOAD ASSESSMENT IN THE COCKPIT: FEASIBILITY OF USING ELECTROPHYSIOLOGICAL MEASUREMENTS, PHASE 1 Final Technical Report, 1 Sep. 1990 - 28 Feb. 1991
A. S. Gevins and H. M. Leong 30 Apr. 1992 49 p
(Contract F49620-90-C-0077)
(AD-A254138; AFOSR-92-0809TR) Avail: CASI HC A03/MF A01

Limitations in people's ability to process and respond to information have become a limiting factor in advanced military aircraft systems. Accordingly, the USAF OSR has been sponsoring research on measuring mental workload as a prerequisite to developing cockpit systems which take the pilot's mental state into account in optimizing overall system performance. During Phase 1, we performed a feasibility study in which we analyzed physiological data from four USAF fighter test pilots in search of ways to distinguish between two laboratory Mft which had the same stimulus and response components but differed in level of mental workload. Several electrophysiological measures, alone and in combination, were investigated for their discriminating power including regional brain electrical activity, scalp muscle potentials, and hem and eye activity. Measures were restricted to those which could be recorded in the cockpit, and, in the case of brain signals, to those least likely to be contaminated by head, body and eye movement artifacts. Using a neural network algorithm, we achieved an average of 97 percent accuracy in classifying independent testing data for the four subjects as either high or low mental workload. GRA

N93-10719# Institute for Defense Analyses, Alexandria, VA.
RELATING FLYING HOURS TO AIRCREW PERFORMANCE: EVIDENCE FOR ATTACK AND TRANSPORT MISSIONS Final Report, Sep. 1991 - Jun. 1992
Colin P. Hammon and Stanley A. Horowitz Jun. 1992 39 p
(Contract MDA903-89-C-0003)
(AD-A253988; IDA-P-2609; IDA/HQ-91-39384; AD-E501546)
Avail: CASI HC A03/MF A01

This paper describes the development of quantitative relationships between the flight experience of military flying personnel and how well they perform important aspects of their mission. This research responds in part to concerns expressed by the General Accounting Office and Congress about the impact of reductions in the services' flying-hour programs. Research confirms the hypothesis that experience enhances proficiency in two ways: through the short-run honing of skills and through the long-run development of mastery. Measures of experience include flights and flying hours in the previous 7 to 60 days and the number of career flying hours. Econometric models and estimates of the strength of the links between these experience measures and two measures of performance are developed. The performance measures are bombing and tactical airdrop accuracy. In addition, the tradeoff between flying and flight simulator hours is examined for both Marine Corps and C-130 crewmembers. We conclude that although short-run measures are significant, the most important determinant of proficiency is total flying hours. This means that in an emergency it would be difficult to correct long-term deficiencies in accumulated flying hours. GRA

54 MAN/SYSTEM TECHNOLOGY AND LIFE SUPPORT

Includes human engineering; biotechnology; and space suits and protective clothing.

For related information see also *16 Space Transportation.*

N93-10217# Battelle Columbus Labs., OH.
EVALUATION OF LIGHTWEIGHT AND LOW PROFILE COMMUNICATIONS DEVICES FOR RESPIRATORY PROTECTIVE SYSTEM 21 (RESPO 21) Final Report
James E. Dvorsky, G. F. Renner, Kevin M. Taylor, William J. Williams, and Kenneth J. Woodruff Feb. 1992 33 p
(Contract DLA900-86-C-2045)
(AD-A253393) Avail: CASI HC A03/MF A01

The Chemical Research, Development, and Engineering Center (CRDEC) is entering development of the next generation of respiratory protection (RESPO 21) to replace the current M40 series of protective masks. One of the design goals of this development is to improve both face-to-face and electronic communications while wearing respiratory protection. Commercial voice amplification systems being evaluated for this application are too bulky for many field applications. An evaluation of miniaturized communication systems was needed to expand the potential applications of voice enhancement. GRA

N93-10261# Anacapa Sciences, Inc., Fort Rucker, AL.
OPERATOR WORKLOAD PREDICTIONS FOR THE REVISED AH-64A WORKLOAD PREDICTION MODEL, VOLUME 1 Interim Report, Sep. 1988 - Dec. 1991
David B. Hamilton and Carl R. Bierbaum Jul. 1992 39 p
(Contract MDA903-87-C-0523; DA Proj. 2Q2-63007-A-793)
(AD-A254198; ASI690-354-92-I; ARO-RN-92-61) Avail: CASI HC A03/MF A01

Under a previous contract, researchers used a composite scenario to conduct a comprehensive task analysis of the AH-64A attack mission. The analysis produced workload estimates and decision rules for developing an AH-64A workload prediction model. For this research, the task analysis/workload (TAWL) methodology was used to construct a workload prediction model. The TAWL Operator Simulation System (TOSS) was used to implement the model on an IBM-compatible microcomputer, and the original function and task analysis was refined to produce a more accurate simulation of crew task activity. In addition, the original workload rating scales used in the original analysis were replaced with equal-interval scales. The predictions generated by the model constructed for this research indicate that under optimum conditions (1) neither the pilot nor the copilot/gunner experiences excessive workload, (2) the pilot has higher overall workload than the copilot/gunner in most mission segments, and (3) AH-64A workload

is high relative to other Army aircraft that have been analyzed for workload. This model can be used as a baseline for analyzing future modifications to the aircraft. GRA

N93-10288# Battelle Columbus Labs., OH.
EVALUATION OF AN ELECTRONICS SYSTEM CONCEPT FOR RESPIRATORY PROTECTION SYSTEM (RESPO 21) Final Report
Mark T. Byrne, Ronald P. Huck, and Kenneth L. Kimes Apr. 1992 73 p
(Contract DLA900-86-C-2045)
(AD-A253394) Avail: CASI HC A04/MF A01

The primary objective was to develop a preferred electronics system concept for the RESPO-21 mask. This system concept was assembled and integrated with a lightweight mask for demonstration purposes. The demonstration unit was delivered to CRDEC separately. A secondary task objective was to identify component and subsystem enhancements necessary for the final fielded RESPO-21 system. The electronics system evaluation focused on three areas: communications assist, blower control, and power source. This report summarizes the technical approach and results obtained for each subsystem. An appendix to this report contains a detailed technical discussion and manufacturers' data sheets for selected components of the communications assist, blower, and power supply subsystems. GRA

N93-10713# Aeronautical Systems Div., Wright-Patterson AFB, OH.
KC-135 CREW REDUCTION FEASIBILITY DEMONSTRATION SIMULATION STUDY. VOLUME 3: TEST AND EVALUATION Final Report, Oct. 1990 - Oct. 1991
Justin D. Rueb, James M. Barnaba, John A. Hassoun, Ross A. Dudley, and G. F. Ward Mar. 1992 135 p
(AD-A253931; ASD-TR-5004-Vol-3) Avail: CASI HC A07/MF A02

In support of the KC-135 Avionics Modernization Program, a two-person (no-nav) conceptual cockpit design (Vol. 2) was evaluated using man-in-the-loop simulation. This report is Volume 3 of a 3-volume technical report. The objectives of the study were twofold: (1) to demonstrate the feasibility of the design; and (2) given the feasibility, to generate the functional requirements necessary to make such a design work. These requirements could later be used by SPO engineers as an aid in developing specific specifications. The simulation used 10 KC-135 crews and 2 KC-10 crews to demonstrate the feasibility of the design. Each crew was required to fly several missions over a period of 1 week. Subjective and objective measures of performance and workload were taken during and after each flight. The subjective workload measures (Subjective Workload Assessment Technique - SWAT, Subjective Workload Dominance (SWORD) technique and the Modified Cooper-Harper scale - MCH) and the various performance measures (i.e., airspeed, altitude, time control, etc.) provided convergent results supporting the feasibility of the conceptual design. Questionnaire data provided an additional analysis for determining those functions/subsystems deemed necessary for mission success. Recommendations of the functional requirements are discussed. GRA

N93-10890*# National Aeronautics and Space Administration, Washington, DC.
NASA SPACE HUMAN FACTORS PROGRAM
1992 34 p
(NASA-TM-108005; NAS 1.15:108005) Avail: CASI HC A03/MF A01

This booklet briefly and succinctly treats 23 topics of particular interest to the NASA Space Human Factors Program. Most articles are by different authors who are mainly NASA Johnson or NASA Ames personnel. Representative topics covered include mental workload and performance in space, light effects on Circadian rhythms, human sleep, human reasoning, microgravity effects and automation and crew performance. R.L.B.

55 SPACE BIOLOGY

Includes exobiology; planetary biology; and extraterrestrial life.

No abstracts in this category.

59 MATHEMATICAL AND COMPUTER SCIENCES (GENERAL)

N93-10341# Aspen Systems Corp., Rockville, MD.
THE LEVELS OF MATHEMATICS ACHIEVEMENT: INITIAL PERFORMANCE STANDARDS FOR THE 1990 NAEP MATHEMATICS ASSESSMENT, VOLUME 3
Ronald K. Hambleton and Mary Lyn Bourque Nov. 1991 409 p Prepared for National Assessment Governing Board, Washington, DC
(PB92-199421) Avail: CASI HC A18/MF A04

Under the legislation creating the National Assessment Governing Board (NAGB) in 1988, the Board was charged with responsibility for identifying 'appropriate achievement goals for each ... grade in each subject area to be tested under the National Assessment'. In May 1990, after wide public consultation and hearings, the Board unanimously adopted a policy to set achievement levels, defining what students should know and be able to do at different grades, on all National Assessment of Education Program (NAEP) assessments of fourth, eighth, and twelfth graders. Under the plan, three levels---BASIC, PROFICIENT, and ADVANCED---would be set for each grade and subject tested by NAEP. The board voted that levels would first be set, as a trial, on the 1990 national assessment of mathematics. Using information from this experience, the Board resolved that starting in 1992, results for all future assessments would be reported initially and primarily in terms of achievement levels. Author

60 COMPUTER OPERATIONS AND HARDWARE

Includes hardware for computer graphics, firmware, and data processing.

For components see *33 Electronics and Electrical Engineering.*

N93-10804# Royal Signals and Radar Establishment, Malvern (England).
AN EXAMPLE SECURE SYSTEM SPECIFIED USING THE TERRY-WISEMAN APPROACH
C. L. Harrold Jul. 1990 64 p
(RSRE-90011; BR115326) Copyright Avail: CASI HC A04/MF A01

The specification of operations for a secure document handling system (SERCUS) is presented. The specification uses the Terry-Wiseman Security Policy Model and acts as an example of the modeling approach. The specification uses the mathematical notation Z, and consequently also acts as an example of the use of Z in specifying secure systems. However, it must be noted that an appreciation of SERCUS, the model, and modeling approach can usefully be gained even if the formal specifications are not read. The Terry-Wiseman Model and its interpretation are given. Author

N93-10807# Royal Signals and Radar Establishment, Malvern (England).
THE TERRY-WISEMAN SECURITY POLICY MODEL AND EXAMPLES OF ITS USE

C. L. Harrold Mar. 1990 28 p
(RSRE-90001; BR114203) Copyright Avail: CASI HC A03/MF A01

A security model for computer systems where it is essential that the confidentiality of the information is maintained is presented. The model is introduced using a simple analogy; it is then defined formally and its use illustrated by examples. The framework for using the model to achieve high assurance implementations of high functionality systems is also discussed. Author

61 COMPUTER PROGRAMMING AND SOFTWARE

Includes computer programs, routines, alogorithms, and specific applications, e.g., CAD/CAM.

N93-10088 Edgewater Computer Systems, Inc., Carp (Ontario).
INVESTIGATION OF A POSSIBLE STOCHASTIC MODEL FOR THE IEEE P896.1 (FUTUREBUS+) PROTOCOL, INCLUDING THE PROPOSED ENHANCED DISTRIBUTED ARBITER
Duane L. Anderson 31 Mar. 1991 186 p Sponsored by National Defence Headquarters Prepared for Software Kinetics Ltd., Stittsville, Ontario
(CTN-92-60593) Copyright Avail: Micromedia Ltd., Technical Information Centre, 165 Hotel de Ville, Place du Portage, Phase 2, Hull, Quebec J8X 3X2, Canada HC/MF

A model is provided for the stochastic model of the Futurebus+ interface system based on traditional queueing theory analysis. Queueing theory models are derived for each of three arbitration types: the P896.1/D8.3 distributed arbiter, a proposed enhanced distributed arbiter, and the centralized arbiter. In addition, two possible models for the centralized arbiter were considered. It is concluded that the arrival rate of service requests entering the Futurebus+ interface system form a continuous parameter stochastic process which, for many systems, will follow the Poisson distribution. Three different architectures are considered: shared memory, message passing, and input/output. The performance of Futurebus+ is modelled and estimated for all combinations of architecture and arbitration type. A detailed examination of the basic arbitration and data transfer protocols was also carried out. The arbitration service times of the P896.1/D8.3 and the enhanced arbiters, and the data transfer service time distributions for the three architecture schemes, can be approximated by an exponential distribution. Performance estimates were made for each architecture and arbitration type. The Futurebus+ arbitration mechanism may be an impediment to its performance, particularly for use in deterministic priority based (real-time) systems.
Author (CISTI)

N93-10103# Virginia Univ., Charlottesville. Dept. of Electrical Engineering.
INTEGRATED VISION SYSTEM FOR A TARGET SEEKER Final Report
Rafael M. Inigo and E. S. McVey 22 Jul. 1991 117 p
(Contract DASG60-88-C-0030)
(AD-A253359) Avail: CASI HC A06/MF A02

This report summarizes the results of research on An Integrated Vision System for a Target Seeker, (IVS). Detailed explanations of methods, results, simulations, software, etc. can be found in other final reports delivered (A008, A009, A00A, A00B). Figures provided by WL/MNSI on system geometry and requirements are the field of view of from 100 to 300 micron rad/sec of solid angle. The initial distance between weapon and target is of the order of 100 Km with a closing velocity of 6 to 10 Km/hr. The target dimensions can be between 1 m wide-2 m long and 3 m wide-16 m long. Simple geometric considerations show that the above figures are compatible with a feasible system. It is required that the IVS performs in real time and, from the above figures, it is clear that the time from ICBM launching to impact with the intercepting weapon will be just a few seconds. In view of the requirement for real time operation, it was decided that as many parts of the system as possible would be designed using artificial neural networks (ANN's). ANN research has experienced a big increase in activity in the last few years. Among the reasons for this, we can mention the ability of ANN's to recognize patterns even under severe degradation due to noise and other artifacts. In spite of all the research activity on ANN's, progress on their analog VLSI implementation has been very slow. Among the reasons for this are huge numbers of weights (resistors) and connections (and hence a serious routing problem), heat dissipation, etc. GRA

N93-10104# Carnegie-Mellon Univ., Pittsburgh, PA. Software Engineering Inst.
PROCEEDINGS OF THE CASE ADOPTION WORKSHOP Final Report
Cliff Huff, Dennis Smith, Kim Stepien-Oakes, Ed Morris, and Paul Zarrella May 1992 113 p Workshop held in Pittsburgh, PA, 13-14 Nov. 1990
(Contract F19628-90-C-0003)
(AD-A253362; CMU/SEI-91-TR-14; ESD-TR-91-14) Avail: CASI HC A06/MF A02

The Software Engineering Institute (SEI) CASE Technology Project sponsored a workshop to address a number of key CASE adoption issues. The workshop was held at the SEI in Pittsburgh, Pennsylvania on November 13-14, 1990. At the workshop, a representative group of SEI affiliates from industry, government, and academia discussed among themselves such adoption topics as CASE benefits, realistic CASE budget estimates, CASE tool fit, CASE adoption roles, and factors in the project success of CASE. The results of these discussions are summarized in this report.
GRA

N93-10212# Brown Univ., Providence, RI. Dept. of Computer Science.
INTERACTIVE ANIMATION OF FAULT TOLERANT PARALLEL ALGORITHMS
Scott W. Apgar Feb. 1992 37 p
(Contract N00014-91-J-1613)
(AD-A253349; CS-92-10) Avail: CASI HC A03/MF A01

Animation of algorithms makes understanding them intuitively easier. This paper describes the software tool Raft (Robust Animator of Fault Tolerant Algorithms). The Raft system allows the user to animate a number of parallel algorithms which achieve fault tolerant execution. In particular, we use it to illustrate the key Write-All problem. It has an extensive user-interface which allows a choice of the number of processors, the number of elements in the Write-All array, and the adversary to control the processor failures. The novelty of the system is that the interface allows the user to create new on-line adversaries as the algorithm executes. GRA

N93-10214# Carnegie-Mellon Univ., Pittsburgh, PA. Software Engineering Inst.
AN ANALYSIS TECHNIQUE FOR EXAMINING INTEGRATION IN A PROJECT SUPPORT ENVIRONMENT Final Report
Alan W. Brown and Peter H. Feiler Jan. 1992 38 p
(Contract F19628-90-C-0003)
(AD-A253351; CMU/SEI-92-TR-3; ESD-92-TR-3) Avail: CASI HC A03/MF A01

In this paper we describe the use of a Project Support Environment (PSE) services reference model as an analysis technique that helps in describing, understanding, and comparing aspects of integration in a PSE. The model is briefly described, before being used as the basis for discussing a number of issues with regard to PSE integration. A major focus of the paper is a discussion of the interfaces of interest in a PSE-interface within a single service, between services, and between services and the PSE end-users. The paper concludes with a discussion of possible interpretations and developments of the model to suit different user requirements. GRA

N93-10237# Microelectronics and Computer Technology Corp., Austin, TX.
AN MCM/CHIP CONCURRENT ENGINEERING VALIDATION Quarterly Technical Report No. 2, Apr. - Jun. 1992
Hector Moreno 30 Jun. 1992 58 p
(Contract MDA972-92-C-0022; ARPA Order 8363)
(AD-A253783; HVE-171-92) Avail: CASI HC A04/MF A01

A schema to model the information required to do physical design of Multi-Chip Modules was written in the EXPRESS language and mapped into ROSE C++ classes. Software was written in the SKILL language (from Cadence Design Systems) to read and write from/to the Cadence EDGE layout system. C++ code was written to interface the EDGE system to the ROSE C++ classes referred to above. As a result, there now exists a full path in and out of the EDGE system and the information stored by ROSE. GRA

N93-10248# National Inst. of Standards and Technology, Gaithersburg, MD. Semiconductor Electronics Div.
METHODOLOGY FOR THE COMPUTER-AIDED DESIGN OF SILICON MICROMACHINED DEVICES IN A STANDARD CMOS PROCESS
Janet C. Marshall, M. Parmeswaran (Simon Fraser Univ., Burnaby, British Columbia), Mona E. Zaghloul (George Washington Univ., Washington, DC.), and Michael Gaitan May 1992 31 p Submitted for publication Sponsored by Naval Ocean Systems Center and Army Test Measurements and Diagnostic Equipment Activity
(PB92-191246; NISTIR-4845) Avail: CASI HC A03/MF A01

The methodology for implementing the design of silicon-micromachined devices in a standard CMOS foundry process is discussed, and a modified Magic technology file is introduced. The modified technology file is used to design silicon-micromachined devices and circuits that are fabricated using a standard CMOS foundry through the MOSIS service. An additional maskless etch in EDP is required to realize the micromechanical structures once chips are delivered. The modified technology file implements a layer that the authors call 'open' that consists of a combination of active area, contact cut, via, and glass opening. The open area exposes the silicon surface for an anisotropic etch procedure that creates suspended bridges of polysilicon or metal encapsulated in SiO2. Results from fabricated chips are included. GRA

N93-10298# Carnegie-Mellon Univ., Pittsburgh, PA. Software Engineering Inst.
ISSUES AND TECHNIQUES OF CASE INTEGRATION WITH CONFIGURATION MANAGEMENT Final Report
Kurt C. Wallnau Mar. 1992 78 p
(Contract F19628-90-C-0003)
(AD-A253323; CMU/SEI-92-TR-5; ESD-TR-92-5) Avail: CASI HC A05/MF A01

Commercial computer-aided software engineering (CASE) tool technology has emerged as an important component of practical software development environments. Issues of CASE tool integration have received heightened attention in recent years, with various commercial products and technical approaches promising to make inroads into this difficult problem. One aspect of CASE integration that was not adequately addressed is the integration of CASE tools with configuration management (CM) - including both CM policies and systems. Organizations need to address how to make CASE tools from different vendors work effectively with an organization's CM policies and tools (in effect, integrate CASE with CM) within the context of the rapidly evolving state of commercial integration technology. This report describes key issues of the integration of CASE with CM from a third-party integrator's perspective, i.e., how to approach the integration of CASE and CM in such a way as to not require fundamental changes to the implementation of the tools or CM systems themselves. GRA

N93-10300# Carnegie-Mellon Univ., Pittsburgh, PA. Software Engineering Inst.
Ada VALIDATION TESTS FOR RATE MONOTONIC SCHEDULING ALGORITHMS Final Report
Keith A. Kohout, Kent Meyer, and John B. Goodenough Feb. 1992 104 p
(Contract F19628-90-C-0003)
(AD-A253325; CMU/SEI-92-TR-1; ESD-92-TR-1) Avail: CASI HC A06/MF A02

A set of tests for checking whether an Ada runtime system properly supports certain rate monotonic scheduling algorithms, specifically, the basic inheritance, and priority ceiling protocols is addressed. These tests are intended to be used by vendors and by users to validate implementations of these protocols. The report describes the tests and how they are to be used. The source code is available electronically. GRA

N93-10315# European Space Agency, Paris (France). Board for Software Standardization and Control.
GUIDE TO THE USER REQUIREMENTS DEFINITION PHASE
Oct. 1991 43 p
(ESA-PSS-05-02-Issue-1; ETN-92-91967) Copyright Avail: CASI HC A03/MF A01

The software engineering standards to be applied for all deliverable software implemented for the European Space Agency (ESA), either in house or by industry is described. A preliminary phase to the software development life cycle called the 'User Requirements Definition Phase' (URD phase) is defined. Activities and products are examined in the 'UR Review' (UR/R) at the end of the phase. The UR phase can be called the 'problem definition phase' of the life cycle. The phase refines an idea about a task to be performed using computing equipment, into a definition of what is expected from the computer system. This document provides a definition of what user requirements are, suggests how they can be captured, and gives guidelines on how they should be stated in a URD. This guide should be read by all active participants in the user requirements phase, i.e., initiators, user representatives, software project managers and authors, and reviewers of the URD. ESA

N93-10316# European Space Agency, Paris (France). Board for Software Standardization and Control.
GUIDE TO THE SOFTWARE REQUIREMENTS DEFINITION PHASE
Oct. 1991 61 p
(ESA-PSS-05-03-Issue-1; ETN-92-91968) Copyright Avail: CASI HC A04/MF A01

The software engineering standards to be applied for all deliverable software implemented for the European Space Agency (ESA), either in house or by industry , are described. A preliminary phase to the software development life cycle called the 'User Requirements Definition Phase' (UR phase) is defined. The first phase of the software development life cycle is the 'Software Requirements Definition Phase' (SRD phase). Activities and products are examined in the 'SR Review' (SR/R) at the end of the phase. The SR phase can be called the 'problem analysis phase' of the life cycle. The user requirements are analyzed and software requirements are produced that must be as complete, consistent, and correct as possible. This document provides guidance on how to produce the software requirements. This document should be read by all active participants in the SR phase, e.g., initiators, user representatives, analysts, designers, project managers, and product assurance personnel. The SR phase, methods, and tools for software requirements definitions, are discussed. A description of how to write the SRD, starting from the template, is given. The life cycle management activities are summarized. ESA

N93-10361# Texas Univ., Austin. Bureau of Engineering Research.
RECOVERY TECHNIQUES FOR REAL TIME ELECTRONIC SYSTEMS Final Report, 1 Mar. 1988 - 31 Dec. 1991

Jacob A. Abraham 30 Mar. 1992 11 p
(Contract N00014-89-K-0089)
(AD-A254010) Avail: CASI HC A02/MF A01

The objective of this research was to develop new analytical techniques for evaluating the effectiveness of recovery in real time systems and to design novel recovery techniques specifically tailored to real time applications. We have developed a variety of techniques described in more detail. Various checksum codes have been suggested for fault-tolerant matrix computations on processor arrays. Use of these codes is limited due to inflexibility of the encoding schemes and also due to potential numerical problems. Numerical errors may also be construed as errors due to physical faults in the system. We have developed a generalization of the existing schemes as a possible solution to these shortcomings. We have proved that linearity is a necessary and sufficient condition for every code that can be used for fault-tolerant matrix operations such as matrix transposition, addition, multiplication, and matrix-vector multiplication. We also proved that for every linear finite-field code, there exists a real-number code having similar error diagnosing capabilities as the finite-fields code. GRA

N93-10409# Analytics, Inc., Willow Grove, PA.
HANDBOOK FOR OPERATING THE OWLKNEST TECHNOLOGY Interim Report, Sep. 1986 - Jul. 1990
Regina M. Harris, Susan G. Hill, Robert J. Lysaght, and Richard E. Christ Jun. 1992 157 p
(Contract MDA903-86-C-0384)
(AD-A253412; ARI-RN-92-49) Avail: CASI HC A08/MF A02

This handbook offers guidance to users of the operator workload (OWL) knowledge-based expert system tool (OWLKNEST). The handbook is an appropriate foundation for understanding the context within which OWLKNEST can be useful. The handbook describes (1) the concept of workload; (2) problems associated with determining which OWL assessment techniques are most appropriate for any given set of study objectives, system characteristics, and user resource constraints; and (3) the expert system approach to problem solving. The handbook also provides an overview of OWLKNEST and gives detailed instructions and specific examples for operating the tool and interpreting its output. Brief descriptions of each of the 38 OWL assessment techniques included in OWLKNEST and a survey form designed to solicit feedback from OWLKNEST users are in appendixes. GRA

N93-10422# Carnegie-Mellon Univ., Pittsburgh, PA. School of Computer Science.
PRODIGY4.0: THE MANUAL AND TUTORIAL
Jaime G. Carbonell, Jim Blythe, Oren Etzioni, Yolanda Gil, and Robert Joseph Jun. 1992 63 p
(Contract F33615-90-C-1465; ARPA Order 7597)
(AD-A253970; CMU-CS-92-150) Avail: CASI HC A04/MF A01

PRODIGY is a general-purpose problem-solving architecture that serves as a basis for research in planning, machine learning, apprentice-type knowledge-refinement interfaces, and expert systems. This document is a manual for the latest version of the PRODIGY system, PRODIGY4.0, and includes descriptions of the PRODIGY representation language, control structure, user interface, abstraction module, and other features. The tutorial style is meant to provide the reader with the ability to run PRODIGY and make use of all the basic features, as well as gradually learning the more esoteric aspects of PRODIGY4.0. GRA

N93-10441# National Inst. of Standards and Technology, Gaithersburg, MD.
RASTER GRAPHICS VALIDATION
F. E. Spielman May 1992 65 p Sponsored in part by the Assistant Secretary of Defense (Production and Logistics), Washington, DC
(PB92-196070; NISTIR-4848) Avail: CASI HC A04/MF A01

The guidelines for establishing and managing raster graphics validations which include both conformance testing and the issuing of a certificate of validation are described. Raster graphics validation supports the National Institute of Standards and Technology (NIST) initiative to validate products professing to support Federal Information Processing Standard (FIPS) Publication 150, Planned FIPS (ODA Raster DAP), Department of Defense (DoD) Military Standard MIL-STD-1840, and DoD Specification MIL-R-28002. Three functional documents are provided to support raster graphics validation: policy and procedures; description of requirements; and instructions and forms. The policy and procedures document provides the operating policy and procedures that are to be followed in administering validations. The description of requirements document describes the conformance testing environment including the testing system software and procedure for executing the conformance testing system. The instructions and forms document contains the instruction, forms, and information necessary for a testing laboratory to test and report on a raster graphics product. Author

N93-10447# Carnegie-Mellon Univ., Pittsburgh, PA. Software Engineering Inst.
INTRODUCTION TO SOFTWARE PROCESS IMPROVEMENT Final Report
Watts S. Humphrey Jun. 1992 37 p
(Contract F19628-90-C-0003)
(AD-A253326; CMU/SEI-92-TR-7; ESD-92-TR-007) Avail: CASI HC A03/MF A01

While software now pervades most facets of modern life, its historical problems have not been solved. This report explains why some of these problems have been so difficult for organizations to address and the actions required to address them. It describes the Software Engineering Institute's (SEI) software process maturity model, how this model can be used to guide software organizations in process improvement, and some guidelines organizations have found helpful in their improvement efforts. This report concludes with a discussion of the most common process improvements traps and pitfalls, and the steps to take to avoid them. GRA

N93-10448# Carnegie-Mellon Univ., Pittsburgh, PA. Software Engineering Inst.
PARALLELS IN COMPUTER-AIDED DESIGN FRAMEWORK AND SOFTWARE DEVELOPMENT ENVIRONMENT EFFORTS Final Report
Susan A. Dart May 1992 25 p
(Contract F19628-90-C-0003)
(AD-A253327; CMU/SEI-92-TR-9; ESD-TR-92-009) Avail: CASI HC A03/MF A01

An attempt to raise awareness about the similarities between the efforts of the software development environment (SDE) community and the electronic computer-aided design (CAD) framework community is addressed. Apparently, SDE and CAD engineers are not aware of what is happening in each other's fields, yet cross-fertilization of efforts would assist progress. Both communities are addressing the same problems of providing configuration management (CM), tool integration, and process management support in their environment. Each community can benefit from the other since both have similar needs and have found, and are finding, similar solutions. It is particularly useful to consider collaborative efforts as both communities are evolving towards standardization. GRA

N93-10631# Westinghouse Savannah River Co., Aiken, SC.
ADVANCED SCIENTIFIC COMPUTING ENVIRONMENT TEAM
J. P. Church 1992 8 p
(Contract DE-AC09-89SR-18035)
(DE92-016714; WSRC-MS-92-154) Avail: CASI HC A02/MF A01

The mission of the ASCENT (Advanced Scientific Computing EnvironmenT) Team is continually keep pace with, evaluate, and select emerging computing technologies to define and implement prototypic scientific computing environments that maximize the ability of scientists and engineers to manage scientific data. These environments are to be implemented in a manner consistent with the site computing architecture and standards and strategic plans for scientific computing. A broad, long term, goal of the ASCENT Team is to provide a computing environment that will let scientists and engineers function at the higher level of abstraction that is

their actual area of technical expertise. The scientist/engineer should be able to solve problems by interacting with conceptual representations drawn directly from the scientific and engineering domains. In this environment the scientist/engineer (i.e., the 'problem solver') builds the problem model with reusable virtual objects having associated attributes and behaviors, including any real or artificial constraints. The problem solver could then test the model by perturbing it interactively and observing quantitative (archived experimental measurements; simulated or computed data) and/or qualitative (trends, approximations) responses. Such an environment would greatly aid the solution and understanding of scientific and engineering problems. This report discusses the proposed system, program, graphic tools and applications. DOE

N93-10665# Carnegie-Mellon Univ., Pittsburgh, PA. Software Engineering Inst.
THE PAST, PRESENT, AND FUTURE OF CONFIGURATION MANAGEMENT Final Report
Susan A. Dart Jul. 1992 31 p
(Contract F19628-90-C-0003)
(AD-A254175; CMU/SEI-92-TR-8; ESD-TR-92-8) Avail: CASI HC A03/MF A01

Automated support for configuration management (CM) is one aspect of software engineering environments that has progressed over the last 20 years. The progress is seen by the burgeoning interest in CM, many technical papers and conferences involving CM, a large number of CM tool vendors, and new software development environments that incorporate CM capabilities. This paper is about future issues affecting solutions to CM problems. To put the future into perspective, it is necessary to discuss the past and present situation for CM. The past evolves around CM systems built in-house and supplemented with manual procedures and policies for executing the CM functions. The present consists of a better understanding of CM, the beginnings of a common vocabulary for CM, existence of many third-party CM tools and environments supporting CM, and recognition that a single CM system does not solve all CM problems and that there is a need for better understanding of CM process support. GRA

N93-10716# Army Lab. Command, Watertown, MA. Material Technology Lab.
INSTRUMENT DRIVER FOR GENERAL PURPOSE INTERFACE BUS (IEEE-488) Final Report
Bradley M. Taber, III and Patrick J. Sincebaugh May 1992 53 p
(AD-A253947) Avail: CASI HC A04/MF A01

Laboratory automation is invaluable to scientists, engineers, and technicians. It provides a mechanism by which many processes can be interactively controlled. A popular method of connecting and controlling laboratory instrumentation is through the General Purpose Interface Bus (GPIB). The Institute of Electrical and Electronics Engineers (IEEE) standardized this bus under IEEE-488. The objective of this project was to study the IEEE-488 and write instrument drivers in C++ for the GPIB and the Tektronix 2430A Digital Oscilloscope. These drivers contain functions for initialization, command control, and data acquisition. The first section of this paper discusses the IEEE-488 and provides pertinent technical information. The second section of this paper is an instruction manual for the use of the GPIB and Tektronix oscilloscope instrument drivers. Portions of an Input/Output (I/O) module are included to provide a graphical representation for the data acquired with the GPIB and Tektronix modules. A test program is presented which demonstrates the use of these modules. These drivers will be specifically used for ultrasonic data acquisition capabilities for nondestructive testing of materials. The ultrasonic data is generated by an ultrasonic transducer sending a sound pulse through a material. The reflected signal is displayed on a digitizing oscilloscope. GRA

N93-10736*# Research Inst. for Advanced Computer Science, Moffett Field, CA.
AMR ON THE CM-2
Marsha J. Berger (New York Univ., New York.) and Jeff S. Saltzman (Los Alamos National Lab., NM.) Aug. 1992 19 p Submitted for publication Original contains color illustrations
(Contracts NCC2-387; DE-FG02-88ER-25053; W-7405-eng-36; AF-AFOSR-0063-91; NSF ASC-88-58101; NSF DMS-89-19074) (NASA-CR-190747; NAS 1.26:190747; RIACS-TR-92-16) Avail: CASI HC A03/MF A01; 1 functional color page

We describe the development of a structured adaptive mesh algorithm (AMR) for the Connection Machine-2 (CM-2). We develop a data layout scheme that preserves locality even for communication between fine and coarse grids. On 8K of a 32K machine we achieve performance slightly less than 1 CPU of the Cray Y-MP. We apply our algorithm to an inviscid compressible flow problem. Author

N93-10746# Mississippi State Univ., Mississippi State. Engineering Research Center.
ANALYSIS AND CONTROL OF GRID QUALITY IN COMPUTATIONAL SIMULATION Final Report, Mar. 1989 - Sep. 1991
J. F. Thompson, C. W. Mastin, and B. Gatlin Jun. 1992 89 p
(Contract F08635-89-C-0209)
(AD-A253723; WL/MN-TR-91-83) Avail: CASI HC A05/MF A01

The objective of this project was to determine and formulate true measures of grid quality that can be used to evaluate numerically generated grids. Empirical studies were conducted on the relationships between grid metric quantities and actual numerical solution error for physical field problems for which experimental data was available. Correlations of the actual solution error were made for numerical solutions of partial differential equations for which analytical solutions were available. Emphasis was placed on equations that model some aspect of some physical problems. In these studies, detailed localized comparisons were made throughout the field. This is particularly important since certain truncation error relations may be important only in regions of high gradient. Correlations of actual solution error were made for physical field problems. The EAGLE grid and flow codes were used as test beds in this task. General graphical tools for grid analysis and procedures for automatic adjustment of the grid to improve the quality were developed. These tools and procedures were incorporated in the EAGLE code. GRA

N93-10782# Wisconsin Univ., Madison. Dept. of Computer Sciences.
SOFTWARE SUPPORT FOR PROGRAMMING IN THE LARGE Final Report, Jul. 1988 - Dec. 1991
Thomas Reps, Susan Horwitz, and Marvin Solomon 6 Aug. 1992 12 p
(Contract N00014-88-K-0590; ARPA Order 6378)
(AD-A254050) Avail: CASI HC A03/MF A01

The research supported under this contract concerned the design and implementation of interactive environments for computer programming. Activities were carried out in two main areas: Semantics-based program integration. By program integration we mean the merging process that one has to go through when a program's source code diverges into multiple variants (e.g., supporting different features, different operating systems, or incorporating different bug-fixes). The goal of our research is to create a system that tests whether the enhancements made to two or more variants of a program interfere, and - if there is no interference -automatically integrates (combines) the variants so as to incorporate all the different enhancements in one program. This would be applied, for example, when a number of collaborators are collectively producing updates in a large programming project, Logic-based tools for programming-in-the-large The CAPITL program-development environment is an integrated collection to tools supporting cooperative development of moderate to large programs. It includes a database for storing software objects such as program source modules, executable programs, and documentation, as well as arbitrary properties and relationships among objects. The database efficiently supports multiple snapshots or versions of the objects and relationships. A

sophisticated deductive query language-based on Prolog-supports configuration management. GRA

N93-10806# Royal Signals and Radar Establishment, Malvern (England).
CAUSING AND PREVENTING VIRUSES IN COMPUTER SYSTEMS
S. R. Wiseman Jan. 1989 11 p
(AD-A208591; RSRE-Memo-4261; BR109824) Copyright Avail: CASI HC A03/MF A01

Viruses may attack computer systems and carry with them a variety of symptoms. Details of the many ways in which they spread are given and it is shown how this is prevented in conventional systems using procedural controls. More effective measures, which are to be employed in the SMITE secure system are also described. Author

N93-10816# Oak Ridge National Lab., TN.
A LOOK AT SCALABLE DENSE LINEAR ALGEBRA LIBRARIES
J. J. Dongarra, R. A.. vandeGeijn, and D. W. Walker 1992 9 p Presented at the Scalable High Performance Computing Conference, Williamsburg, VA, 26-29 Apr. 1992
(Contract DE-AC05-84OR-21400)
(DE92-017161; CONF-9204106-6) Avail: CASI HC A02/MF A01

We discuss the essential design features of a library of scalable software for performing dense linear algebra computations on distributed memory concurrent computers. The square block scattered decomposition is proposed as a flexible and general-purpose way of decomposing most, if not all, dense matrix problems. An object-oriented interface to the library permits more portable applications to be written, and is easy to learn and use, since details of the parallel implementation are hidden from the user. Experiments on the Intel Touchstone Delta system with a prototype code that uses the square block scattered decomposition to perform LU factorization are presented and analyzed. It was found that the code was both scalable and efficient, performing at about 14 GFLOPS (double precision) for the largest problem considered. DOE

N93-10817# Edgerton, Germeshausen and Grier, Inc., Idaho Falls, ID.
APOLLO: A COMPUTER PROGRAM FOR THE CALCULATION OF CHEMICAL EQUILIBRIUM AND REACTION KINETICS OF CHEMICAL SYSTEMS
H. D. Nguyen Nov. 1991 44 p
(Contract DE-AC07-76ID-01570)
(DE92-017864; EGG-WTD-9876) Avail: CASI HC A03/MF A01

Several of the technologies being evaluated for the treatment of waste material involve chemical reactions. Our example is the in situ vitrification (ISV) process where electrical energy is used to melt soil and waste into a 'glass like' material that immobilizes and encapsulates any residual waste. During the ISV process, various chemical reactions may occur that produce significant amounts of products which must be contained and treated. The APOLLO program was developed to assist in predicting the composition of the gases that are formed. Although the development of this program was directed toward ISV applications, it should be applicable to other technologies where chemical reactions are of interest. This document presents the mathematical methodology of the APOLLO computer code. APOLLO is a computer code that calculates the products of both equilibrium and kinetic chemical reactions. The current version, written in FORTRAN, is readily adaptable to existing transport programs designed for the analysis of chemically reacting flow systems. Separate subroutines EQREACT and KIREACT, for equilibrium and kinetic chemistry respectively, were developed. A full detailed description of the numerical techniques used, which include both Lagrange multiplies and a third-order integrating scheme is presented. Sample test problems are presented and the results are in excellent agreement with those reported in the literature. DOE

N93-10823# Royal Signals and Radar Establishment, Malvern (England).
LATTICES FOR SECURITY POLICIES
S. N. Foley (Cranfield Inst. of Tech., Bedford, England) Apr. 1990 89 p
(RSRE-90005; BR114204) Copyright Avail: CASI HC A05/MF A01

The foundation for a new model and approach for secure information flow is presented. The model is driven by lattice based information flow policy, which describes the permitted dissemination of information in the system. System entities are allowed to handle different classes of information from the flow policy, and information is permitted to flow between entities so long as they do not violate the flow policy. With this conceptually simple notion of security, we can describe many interesting security policies, for example, traditional multi-level policies, aggregation policies, and Chinese walls. Details are given on how secure systems based on the model can be implemented in practice. We also examine how other types of security policies such as integrity and separation of duty can be defined in terms of lattice based policies. Author

N93-10866# Sandia National Labs., Albuquerque, NM.
RHALE: A MMALE SHOCK PHYSICS CODE FOR ARBITRARY MESHES
J. S. Peery and K. G. Budge 1992 6 p Presented at the 7th International Association of Mathematics and Computer Simulation (IMACS) International Conference on Computer Methods for Partial Differential Equations, New Brunswick, NJ, 22-24 Jun. 1992
(Contract DE-AC04-76DP-00789)
(DE92-017051; SAND-92-0032C; CONF-9206185-5) Avail: CASI HC A02/MF A01

RHALE, a two and three-dimensional, multi-material, arbitrary Lagrangian-Eulerian shock physics code written in C++ is described. RHALE is the successor to CTH, Sandia's 3-D Eulerian shock physics code and is capable of solving problems that CTH cannot adequately address. RHALE employs a three step solution algorithm for the equations of motion: a Lagrangian step capable of solving for either structural or hydrodynamic responses, a remesh step to prevent mesh tangling or to facilitate Eulerian hydrodynamic algorithms, and an Eulerian remap step. The Lagrangian step is solved using finite elements on an unstructured grid. RHALE incorporates new Lagrangian capabilities which include arbitrary mesh connectivity, superior artificial viscosity and spurious vorticity control, and improved equations of state. The arbitrary Lagrangian-Eulerian (ALE) algorithm comprises both the remesh and remap steps. The multi-material extension to ALE (MMALE) was generalized for arbitrary grids in both two and three-dimensions in RHALE. The MMALE feature in RHALE provides the accuracy of a Lagrangian code while allowing a calculation to proceed under very large mesh distortions. Coupling an arbitrary connected grid to the MMALE algorithm facilitates modeling of complex shapes with a minimum number of computational cells. RHALE allows regions of a problem to be modeled with Lagrangian, Eulerian, or ALE meshes. In addition, regions can switch from Lagrangian to ALE to Eulerian based on user input or mesh distortion. For arbitrary meshes, new node locations are determined with equipotential schemes. Element quantities are advected with donor, van Leer, or Super-B algorithms. Nodal quantities are advected with second order schemes developed by Benson and Margolin which use the element advection algorithms. DOE

N93-10881# Naval Postgraduate School, Monterey, CA.
AN INDICATOR OF MESSAGE QUALITY FOR A SINGLE OPTICAL SENSOR USING A TEMPLATE BASED TRACKING ALGORITHM M.S. Thesis
Eric R. Bechhoefer Mar. 1992 75 p
(AD-A252704) Avail: CASI HC A04/MF A01

The volume of messages generated by spaced based interceptors (SBI's) resulting from a booster launch can lead to unacceptably great total time for the messages to propagate through the system. In order to help relieve this problem, one might identify the SBI's with the highest quality estimates of the launch information. Message traffic can be sharply reduced if these

SBI's can be identified, and message transmission is restricted to their messages. Launch parameters and position are estimated using a template based tracking algorithm. A single measure of quality based on the estimated covariance matrix of the measured position is proposed and tested using simulation. Results describe possible modifications to the template based tracking algorithm that would reduce error and allow the quality of a message to be determined. GRA

N93-10523 University of Western Ontario, London.
ON TECHNIQUES FOR DIGITAL SIMULATION OF RANDOM RESPONSE OF NONLINEAR OSCILLATORS
C. W. S. To and S. W. Zhang (Beijing Agricultural Univ., China) *In* Carleton Univ., Proceedings of the Twelfth Canadian Congress of Applied Mechanics, Volumes 1 and 2 May 1989 p 406-407 (For primary document see N93-10466 01-31)
Copyright Avail: Canadian Society for Mechanical Engineering, 2050 Mansfield St., Suite 700, Montreal, Quebec H3A 1Z7 Canada

N93-10570 University of Western Ontario, London.
OPTIMAL ROBOT TRAJECTORY PLANNING
R. O. Buchal *In* Carleton Univ., Proceedings of the Twelfth Canadian Congress of Applied Mechanics, Volumes 1 and 2 May 1989 p 858-859 (For primary document see N93-10466 01-31)
Copyright Avail: Canadian Society for Mechanical Engineering, 2050 Mansfield St., Suite 700, Montreal, Quebec H3A 1Z7 Canada

62 COMPUTER SYSTEMS

Includes computer networks and special application computer systems.

N93-10209# Naval Command, Control and Ocean Surveillance Center, San Diego, CA. RDT and E Div.
AN IMPLEMENTATION OF THE MVDR BEAMFORMER ON THE INTEL iWarp SYSTEM Final Report
J. Z. Lou Apr. 1992 38 p
(AD-A253641; NRAD-TD-2282) Avail: CASI HC A03/MF A01

This report discusses the implementation of the minimum Variance Distortionless Response (MVDR) beamformer on the Intel iWarp system. A unidirectional ring and a full connection of processors were used in the implementations. The MVDR computation basically consists of a matrix factorization and a triangular system solver. A parallel Cholesky factorization and a parallel QR factorization were implemented. A fan-in parallel algorithm was used for the triangle system solver. Using the unidirectional ring connection, the QR factorization achieved a 90 percent efficiency on 4 processors and a 64 percent efficiency on 16 processors: the Cholesky factorization achieved a 83 percent efficiency on 4 processors and a 44 percent efficiency on 16 processors. Using the unidirectional ring connection and QR factorization, the MVDR beamformer achieved a 83 percent efficiency on 4 processors and 34 percent on 16 processors. Using the full connection of 4 processors, a 20 percent performance improvement has been obtained on MVDR as compared with the unidirectional ring connection. The parallel processing performance in terms of MFLOPS is still low, which is expected considering the low node performance on a C code using software release 2.3. GRA

N93-10213# Brown Univ., Providence, RI. Dept. of Computer Science.
FAULT-TOLERANT AND EFFICIENT PARALLEL COMPUTATION Ph.D. Thesis
Alexander A. Shvartsman May 1992 163 p
(Contract N00014-91-J-1613)
(AD-A253350; CS-92-23) Avail: CASI HC A08/MF A02

Recent advances in computer technology made parallel machines a reality. Massively parallel systems use many general-purpose, inexpensive processing elements to attain computation speed-ups comparable to or better than those achieved by expensive, specialized machines with a small number of fast processors. In such setting, however, one would expect to see an increased number of processor failures attributable to hardware or software. This may eliminate the potential advantage of parallel computation. We believe that this presents a reliability bottleneck that is among fundamental problems in parallel computation. We investigate algorithmic ways of introducing fault-tolerance in multiprocessors under the constraint of preserving efficiency. This research demonstrates how in certain models of parallel computation it is possible to combine efficiency and fault-tolerance. We show that in the models we study, it is possible to develop efficient parallel algorithms without concern for fault-tolerance, and then correctly and efficiently execute these algorithms on parallel machines whose processors are subject to arbitrary dynamic failstop errors. By ensuring efficient executions for any patterns of failures, the efficiency is also maintained when failures are infrequent, or when the expected number of failures is small. GRA

N93-10219# Mentor Technologies, Inc., Rockville, MD.
TEST RANGE TRACKING NETWORK PROCESSORS Final Technical Report, 20 Jun. 1991 - 5 Mar. 1992
M. Belzer, Y. Cho, and S. Chong 23 Mar. 1992 99 p
(Contract DAAD07-91-C-0153)
(AD-A253511; MTI-R91-004) Avail: CASI HC A05/MF A02

Creating accurate tracks of multiple airborne targets from multiple sensors, in real time, can be a computationally demanding process. Our approach is to perform hypothesis testing based upon the traditional method of Maximum Likelihood, but within a distributed filtering environment. This results in a large reduction in the number of floating point computations required to generate the complete set of likelihood function values. This final report describes results obtained over a 6 month Phase 1 project. The primary mathematical operation performed by the distributed filters is matrix triangularization. Thus, this research focused on understanding algorithms for performing this operation, as well as their parallelization. GRA

N93-10227# Duke Univ., Durham, NC.
IMPLEMENTATION OF PARALLEL ALGORITHMS Quarterly Report, 1 Jan. - 30 Jun. 1992
John H. Reif 30 Jun. 1992 10 p
(Contract N00014-91-J-1985)
(AD-A253638) Avail: CASI HC A02/MF A01

Randomization has been demonstrably useful both in simplifying and in improving the efficiency of sorting algorithms on actual parallel machines. Flashsort RV83,861 and Samplesort HC83 are related parallel sorting algorithms that have been proposed in the literature. Both utilize a sophisticated randomized sub-sampling technique with over-sampling to form a splitter set, but Samplesort differs from Flashsort in that it distributes all the splitters to each processor while Flashsort uses splitter-directed routing. We present B-Flashsort, a new batched-routing variant of Flashsort designed to sort N values using P processors with N greater than P. Like the randomized sorts to which it is related, B-Flashsort performs N/P log N parallel comparisons. The algorithm can be implemented on a wide variety of networks, but we concentrate on its implementation on a d-dimensional toroidal mesh. The algorithm requires only constant space in addition to the input and output. GRA

N93-10242# Oregon State Univ., Newport. Marine Science Center.
PARALLEL PROCESSING AND LEARNING: VARIABILITY AND CHAOS IN SELF-ORGANIZATION OF ACTIVITY IN GROUPS OF NEURONS Final Report, 15 Jan. 1989 - 14 Jan. 1992
George J. Mpitsos 7 Apr. 1992 3 p
(Contract F49620-89-C-0262; AF-AFOSR-0262-89)
(AD-A250290; AFOSR-92-0301TR) Avail: CASI HC A01/MF A01

In view of our previously published findings showing that motor

patterns representing adaptive behaviors may be generated by chaotic activity, we have used computer simulations to examine the ability of simple networks to learn to process chaotic signals and to perform complex operations on them. These studies have shown that even simple networks can be used to understand how networks store information, much of which information can not have been obtained from the more complex biological systems. As one example, an important and unexpected finding is that networks having trainable thresholds, in addition to trainable synapses, can perform computations that trainable synapses alone can not, regardless of the number of synapses that may be included in the network. Another finding is that when networks must learn several tasks simultaneously, the effective size network is self-limiting, and probably does not require special algorithmic rules for limiting the size of successfully computing neural connections. GRA

N93-10299# Hughes Aircraft Co., Culver City, CA. Strategic Systems Div.
DEVELOPMENT OF PARALLEL ARCHITECTURES FOR SENSOR ARRAY PROCESSING ALGORITHMS Semiannual Report
M. M. Jamali and S. C. Kwatra Jul. 1992 204 p
(Contract N00014-91-J-1011)
(AD-A253680; DSPH-2) Avail: CASI HC A10/MF A03

Research for the development of parallel architecture for Multiple Signal Classification (MUSIC) and Estimation of Signal Parameter via Rotational Invariance Technique (ESPRIT) algorithms for the narrow band sources are focused in the first part of this research. The second part is to perform direction-of-arrival (DOA) estimation for the wideband sources using two algorithms. All these algorithms were substituted with computationally efficient modules and converted them to pipelined and parallel algorithms. Parallel Architectures for the computation of these algorithms and architectures were developed. Simulations of these algorithms and architectures were performed and more detailed simulations are in progress. GRA

N93-10334# Oak Ridge National Lab., TN.
PARALLEL SPARSE CHOLESKY FACTORIZATION ALGORITHMS FOR SHARED-MEMORY MULTIPROCESSOR SYSTEMS
E. Rothberg (Stanford Univ., CA.), A. Gupta (Stanford Univ., CA.), E. Ng, and B. Peyton 1992 8 p Presented at the 7th International Association of Mathematics and Computer Simulation (IMACS) International Conference on Computer Methods for Partial Differential Equations, New Brunswick, NJ, 22-24 Jun. 1992
(Contract DE-AC05-84OR-21400)
(DE92-016829; CONF-9206185-2) Avail: CASI HC A02/MF A01

Sparse Cholesky factorization on a multiprocessor system that possesses a globally shared memory is considered. Our algorithm is a parallel version of a serial blocked left-looking factorization algorithm. Unlike previous parallel left-looking algorithms, the new algorithm uses a matrix-matrix multiplication operation to implement its computationally intensive primitives. Consequently, careful implementation of these primitives enables extensive reuse of data in cache for most realistic problems, and thus reduces the volume of traffic to and from main memory. Reducing memory traffic is crucial on many shared-memory multiprocessors because the interconnect to main memory is often a serious bottleneck. We shall compare the performance of the parallel blocked algorithm with an earlier parallel left-looking algorithm studied. DOE

63 CYBERNETICS

Includes feedback and control theory, artificial intelligence, robotics and expert systems.

For related information see also *54 Man/System Technology and Life Support.*

N93-10095# Brown Univ., Providence, RI. Div. of Applied Mathematics.
CENTER FOR INTELLIGENT CONTROL SYSTEMS, BROWN UNIVERSITY COMPONENT: GRADUATE RESEARCH FELLOWSHIPS Final Report
Donald E. McClure 30 Aug. 1991 14 p
(Contract DAAL03-89-G-0010)
(AD-A253620; ARO-26730.1-MA-UIF) Avail: CASI HC A03/MF A01

This report describes the research accomplished with the support of Graduate Research Fellowships at the Center for Intelligent Control Systems, Brown University, during the period 1 July 1989 through 30 June 1991. GRA

N93-10269# Naval Research Lab., Washington, DC.
ARTIFICIAL INTELLIGENCE TECHNICAL PAPER ABSTRACTS, 1991 Abstracts Only
Cathy J. Wiley 8 Jul. 1992 35 p
(AD-A253340; NRL/MR/5510-92-6997) Avail: CASI HC A03/MF A01

Artificial Intelligence Technical Paper Abstracts 1991 documents the accomplishments of projects at the Navy Center for Applied Research in Artificial Intelligence (NCARAI) in machine learning, natural language understanding, intelligent decision aids, and intelligent systems for robotic sensing and control. Points of contact are indicated for acquiring additional technical information about the projects, and an order form is provided for obtaining copies of the publications abstracted. GRA

N93-10346 Stanford Univ., CA.
OPTIMAL SAMPLE POLICIES FOR MULTIRATE DIGITAL CONTROL Ph.D. Thesis
Michael Lee Narigon 1991 207 p
Avail: Univ. Microfilms Order No. DA9205691

The sample frequency at which a digital controller operates affects the performance of the controlled continuous system. For a single rate digital controller, designers often choose the sample frequency to be 10 to 40 times the closed loop bandwidth. This sample frequency gives a reasonable trade-off between performance and the computational load on the control processor. For a multirate digital controller, the selection of sample frequency and its effect on performance is not as clear. This dissertation investigates the effect of sample frequency and sample policy on the performance of digitally controlled continuous systems. It considers both single rate and multirate digital controllers. These controllers regulate the systems driven by white noise. The controllers are designed to minimize some combination of the state errors and control effort while simultaneously requiring low controller computational load. The optimal multirate controller is the basis for the controller design. This dissertation extends previous results of multirate control theory to include analysis of sample phasing and solutions for the current state and predicted state multirate estimator. Additionally, this dissertation develops a cost functional that explicitly defines the effect of sample frequency. A two step parameter optimization and integer programming procedure uses this cost functional to calculate the optimal multirate regulator and estimator gains, sample frequency and sample policy that together minimize the cost functional. The optimization procedure is used to design example controllers for a simple two degree of freedom system consisting of two masses connected by a damped spring. These controllers were used to examine the effect of sample frequency, sample policy, and controller quantization on the closed loop system performance. These examples revealed the important factors contributing to a reasonable sample policy. These factors are the distribution of disturbances in the system, the open loop and closed loop plant frequency characteristics, the control effort, the measurement

process, and the controller implementation. A computer program, OMDPRG, was developed to solve the optimal sample policy multirate control problem. The program was based on MTRLIB, a library of matrix routines. Dissert. Abstr.

N93-10354# Massachusetts Univ., Amherst.
BIOLOGICAL AND THEORETICAL STUDIES OF ADAPTIVE NETWORKS: THE CONDITIONED RESPONSE Final Report, 1 Jun. 1989 - 31 May 1992
John W. Moore 30 Jun. 1992 51 p
(Grant AF-AFOSR-0391-89)
(AD-A253329; AFOSR-92-0678TR) Avail: CASI HC A04/MF A01

Our primary experimental approach was to record from single neurons in awake, behaving animals in order to determine the loci of neurons with conditioning-related activity and to quantitate the relationship of this activity to the expression of the conditioned response. Our theoretical approach was to extend simple computational models of connectionist learning into physiologically plausible neural networks that describe real-time features of conditioned behavior. These network models, and their possible implementations in the brain, suggest experimental tests and provide direction for physiological studies. GRA

N93-10450# National Inst. of Standards and Technology, Gaithersburg, MD. Computer Systems Lab.
OPTIMIZATION OF NEURAL NETWORK TOPOLOGY AND INFORMATION CONTENT USING BOLTZMAN METHODS
C. L. Wilson and O. M. Omidvar (District of Columbia Univ., Washington, DC.) Feb. 1992 13 p
(PB92-205418; NISTIR-4766) Avail: CASI HC A03/MF A01

Reduction in the size and complexity of neural network applications are the driving force behind the current research in network optimization. Most of the known optimization methods heavily rely on weight sharing concepts for pattern separation and recognition. The method used in the research focuses on network topology and information content for optimization. The authors have studied the change in the network topology and its dynamic effects on information content during the optimization of the network. The changes in the network topology were achieved by altering the number of weights. The primary optimization was scaled conjugate gradient and the secondary method of optimization was a Boltzmann method. The findings demonstrate that for a difficult character recognition problem, the number of weights in a fully connected network can be reduced by 90.3 percent with a temperature of 0.55 while achieving training and testing of identical accuracies. Author

N93-10641# Odyssey Research Associates, Inc., Ottawa (Ontario).
THE MECHANICAL VERIFICATION OF A SIMPLE CONTROL SYSTEM
Mark Saaltink Dec. 1989 26 p
(Contract DSS-W7700-88-72093)
(ORA-TR-89-5443-04; CTN-92-60352) Copyright Avail: CASI HC A03/MF A01

This report describes the verification of a simple real-time example control system using the m-EVES system. The example (control of a vehicle moving on a two dimensional plane, acted upon by currents whose position and velocity are measured by sensors and by unpredictable winds) was chosen to illustrate several general points. The system allows initial uncertainty and late resolution of specifications. In the example, the exact definition of the goal of the program and the relationships between parameters are initially unknown. Assumptions about various parameters (such as maximum or minimum values) may be established through some sort of negotiation between the specifier and the implementor. The example problem is decomposed in two different ways: (1) by working in each dimension independently, first developing and verifying the control algorithm; and (2) by verifying its implementation. The example makes use of under specification in the formal description to capture hidden parts of the program's environment. Several idioms are used in developing executable versions of functions. Independent control algorithms are developed for various parameters; the final version interleaves the control algorithms. Ordinals are used for measuring the progress of multi-phase algorithms. The handling of uncertainty in the system is general and would apply to other situations such as the case of unreliable sensors or inaccurate actuators. CISTI

N93-10749# Carnegie-Mellon Univ., Pittsburgh, PA. School of Computer Science.
SELECTIVE PERCEPTION FOR ROBOT DRIVING Ph.D. Thesis
Douglas A. Reece May 1992 210 p
(Contract F33615-90-C-1465; ARPA Order 7597)
(AD-A253740; CMU-CS-92-139) Avail: CASI HC A10/MF A03

Robots performing complex tasks in rich environments need very good perception modules in order to understand their situation and choose the best action. Robot planning systems have typically assumed that perception was so good that it could refresh the entire world model whenever the planning system needed it, or whenever anything in the world changed. Unfortunately, this assumption is completely unrealistic in many real-world domains because perception is far too difficult. Robots in these domains cannot use the traditional planner paradigm, but instead need a new system design that integrates reasoning with perception. In this thesis I describe how reasoning can be integrated with perception, how task knowledge can be used to select perceptual targets, and how this selection dramatically reduces the computational cost of perception. The domain addressed in this thesis is driving in traffic. I have developed a microscopic traffic simulator called PHAROS that defines the street environment for this research. PHAROS contains detailed representations of streets, markings, signs, signals, and cars. It can simulate perception and implement commands for a vehicle controlled by a separate program. I have also developed a computational model of driving called Ulysses that defines the driving task. The model describes how various traffic objects in the world determine what actions that a robot must take. GRA

N93-10828# Carnegie-Mellon Univ., Pittsburgh, PA. School of Computer Science.
SYMBOLIC BOOLEAN MANIPULATION WITH ORDERED BINARY DECISION DIAGRAMS
Randal E. Bryant Jul. 1992 36 p Supersedes CMU-CS-91-162
(AD-A253822; CMU-CS-92-160; CMU-CS-91-162) Avail: CASI HC A03/MF A01

Ordered Binary Decision Diagrams OBDDs represent Boolean functions as directed acyclic graphs. They form a canonical representation, making testing of functional properties such as satisfiability and equivalence straightforward. In most applications, their size remains manageable. A number of operations on Boolean functions can be implemented as graph algorithms on OBDD data structures. Using OBDDs a wide variety of problems can be solved through symbolic analysis. First, the possible variations in system parameters and operating conditions are encoded with Boolean variables. Then the system is evaluated for all variations by a sequence of OBDD operations. Researchers have thus solved a number of problems in digital system design, finite state system analysis, artificial intelligence, and mathematical logic. This paper describes the OBDD data structure, and surveys a number of applications that were solved by OBDD-based symbolic analysis. GRA

N93-10958 Department of the Navy, Washington, DC.
ARTIFICIAL NEURAL NETWORK SYSTEM FOR MEMORY MODIFICATION Patent
David K. Andes, inventor (to Navy), Robert A. Licklider, inventor (to Navy), Donald H. Witcher, inventor (to Navy), Richard M. Swenson, inventor (to Navy), and James F. Barbieri, inventor (to Navy) 7 Apr. 1992 15 p Filed 27 Jun. 1991
(AD-D015354; US-Patent-5,103,496; US-Patent-Appl-SN-722413; US-Patent-Class-395-24) Avail: US Patent and Trademark Office

An artificial neural network, which has a plurality of neurons each receiving a plurality of inputs whose effect is determined by

adjustable weights at synapses individually connecting the inputs to the neuron to provide a sum signal to a sigmoidal function generator determining the output of the neuron, undergoes memory modification by a steepest-descent method. In this method, individual variations in the outputs of the neurons are successively generated by small perturbations imposed on the sum signals. As each variation is generated on the output of a neuron, an overall error of all the neuron outputs in relation to their desired values is measured and compared to this error prior to the perturbation. The difference in these errors, with adjustments which may be changed as the neuron outputs converge toward their desired values, is used to modify each weight of the neuron presently subjected to the perturbation. GRA

N93-10959# Department of the Navy, Washington, DC.
MEMORY MODIFICATION OF ARTIFICIAL NEURAL NETWORKS Patent
David K. Andes, inventor (to Navy), Robert A. Licklider, inventor (to Navy), Donald H. Witcher, inventor (to Navy), Richard M. Swenson, inventor (to Navy), and James F. Barbieri, inventor (to Navy) 24 Dec. 1991 16 p Filed 18 Sep. 1989
(AD-D015356; US-Patent-5,075,868; US-Patent-Appl-SN-410373; US-Patent-Class-395-23) Avail: US Patent and Trademark Office

An artificial neural network, which has a plurality of neurons each receiving a plurality of inputs whose effect is determined by adjustable weights at synapses individually connecting the inputs to the neuron to provide a sum signal to a sigmoidal function generator determining the output of the neuron, undergoes memory modification by a steepest-descent method. In this method, individual variations in the outputs of the neurons are successively generated by small perturbations imposed on the sum signals. As each variation is generated on the output of a neuron, an overall error of all the neuron outputs in relation to their desired values is measured and compared to this error prior to the perturbation. The difference in these errors, with adjustments which may be changed as the neuron outputs converge toward their desired values, is used to modify each weight of the neuron presently subjected to the perturbation. GRA

N93-10575 Nanyang Univ. (Singapore).
A SOLUTION SCHEME FOR THE DEFLECTION EQUATIONS OF FLEXIBLE ARMS WITH TIME-DEPENDENT BOUNDARY CONDITIONS
K. H. Low and R. N. Dubey (Waterloo Univ., Ontario) *In* Carleton Univ., Proceedings of the Twelfth Canadian Congress of Applied Mechanics, Volumes 1 and 2 May 1989 p 878-879 (For primary document see N93-10466 01-31)
Copyright Avail: Canadian Society for Mechanical Engineering, 2050 Mansfield St., Suite 700, Montreal, Quebec H3A 1Z7 Canada

64 NUMERICAL ANALYSIS

Includes iteration, difference equations, and numerical approximation.

N93-10200# Michigan State Univ., East Lansing. Dept. of Electrical Engineering and Systems Science.
UNIFYING THE LANDMARK DEVELOPMENTS IN OPTIMAL BOUNDING ELLIPSOID IDENTIFICATION
J. R. Deller, Jr., M. Nayeri, and M. S. Liu 4 Jun. 1992 43 p
(Contract N00014-91-J-1329)
(AD-A253502) Avail: CASI HC A03/MF A01

A quite general class of Optimal Bounding Ellipsoid (OBE) algorithms including all methods published to date, can be unified into a single framework called the Unified OBE (UOBE) algorithm. UOBE is based on generalized weighted recursive least squares in which very broad classes of 'forgetting factors' and data weights may be employed. Different instances of UOBE are distinguished by their weighting policies and the criteria used to determine their optimal values. A study of existing OBE algorithms, with a particular interest in the tradeoff between algorithm performance interpretability and convergence properties, is presented. Results suggest that an interpretable, converging UOBE algorithm will be found. In this context, a new UOBE technique, the set membership stochastic approximation (SM-SA) algorithm is introduced. SM-SA possesses interpretable optimization measures and known conditions under which its estimator will converge. GRA

N93-10275# Naval Research Lab., Washington, DC.
CONVERGENCE PERFORMANCE OF ADAPTIVE DETECTORS, PART 3 Interim Report
Karl Gerlach 25 Mar. 1992 27 p
(AD-A248415; NRL-9370-Pt-3) Avail: CASI HC A03/MF A01

Two schemes for adaptive detection, Kelly's generalized likelihood ratio test (GLRT) and the mean level adaptive detector (MLAD), are analyzed with respect to the deleterious effect of desired signal contamination of the data used to compute the sampled covariance matrix for the two detectors. The detection probability P(sub D) and false alarm performance (ghosting probability P(sub G)) are predicted for the two schemes under the assumptions that the input noises are Gaussian random variables that are temporally independent but spatially correlated; and the desired signal's amplitude is Rayleigh distributed. P(sub D) and P(sub G) are computed as a function of the false alarm probability P(sub F) with no contamination, the number of input channels, the number of independent samples-per-channel, the matched filtered output signal-to-noise (S/N) power ratio, and the S/N power ratio of the contaminating desired signal. It is shown that both P(sub D) and P(sub G) decrease with increasing levels of contamination. The P(sub G) performance is almost identical for the GLRT and MLAD. The P(sub D) performance shows similar relative performance trends. Significantly, it is shown that the ghosting probability does not exceed P(sub F) in the presence of contamination. GRA

N93-10285# Oak Ridge National Lab., TN.
A LOOK AT SCALABLE DENSE LINEAR ALGEBRA LIBRARIES
J. J. Dongarra (Tennessee Univ., Knoxville.), R. vandeGeijn (Texas Univ., Austin.), and D. W. Walker Jul. 1992 27 p
(Contract DE-AC05-84OR-21400)
(DE92-017805; ORNL/TM-12126) Avail: CASI HC A03/MF A01

The essential design features of a library of scalable software for performing dense linear algebra computations on distributed memory concurrent computers are discussed. A square block scattered decomposition is proposed as a flexible and general-purpose way of decomposing most, if not all, dense matrix problems. An object oriented interface to the library permits more portable applications to be written, and is easy to learn and use, since details of the parallel implementation are hidden from the user. Experiments on the Intel Touchstone Delta system with a prototype code that uses the square block scattered decomposition to perform LU factorization are presented and analyzed. It was found that the code was both scalable and efficient, performing at about 14 Gflop/s (double precision) for the largest problem considered. DOE

N93-10339# Yale Univ., New Haven, CT. Dept. of Computer Science.
ON THE EVALUATION OF BESSEL FUNCTIONS
Gregory Matviyenko 8 May 1992 50 p
(Grant NSF DMS-90-12751)
(AD-A253129) Avail: CASI HC A03/MF A01

In the present paper we describe an algorithm for the evaluation of Bessel functions J(sub nu)x, Y(sub nu)x and H(sub nu, sup j)x (j = 1, 2) of arbitrary positive orders and arguments at a constant CPU time. The algorithm employs Taylor series, the Debye asymptotic expansions and numerical evaluation of the Sommerfeld integral, and is based on the following two observations. (1) The Debye asymptotic expansions, contrary to what appears to be a popular belief, are not expansions in inverse powers of (large) parameter nu but turn out to be uniform expansions in inverse powers of (large) parameter g(sub 1) = (x - nu)/x(sup 1/3) for x

greater than nu and (large) parameter g nu = (nu - x)/nu(sup 1/3) for x less than nu. For x and nu such that both Taylor and Debye expansions do not provide a specified accuracy Bessel functions can be computed at a constant CPU time via (numerical) evaluation of the Sommerfeld integral along contours of steepest descents. In addition, in Appendix B we obtain certain new estimates concerning decay of the functions J(sub nu)x and -1/Y(sub nu)x of fixed x and large nu, and in Appendix C we show that functions J(sub nu)x of integer nu provide the solution for a certain system of coupled harmonic oscillators. GRA

N93-10389# International Centre for Theoretical Physics, Trieste (Italy).
GLOBAL STRUCTURE OF A POLYNOMIAL AUTONOMOUS SYSTEM ON THE PLANE
Nguyen Van Chau Oct. 1991 10 p
(DE92-630230; IC-91/332) Avail: CASI HC A02/MF A01

This note is to study the global behavior of a polynomial autonomous system on the plane with divergence non-positive outside a bounded set. It is shown that in some certain conditions the global structure of such system can be simple. The main result here can be seen as an improvement of the result of Olech and Meister concerning with the global asymptotical stable conjecture of Markur and Yamable and the Jacobian Conjecture. DOE

N93-10407# Maryland Univ., College Park. Inst. for Physical Science and Technology.
THE PROBLEM OF THE SELECTION OF AN a-POSTERIORI ERROR INDICATOR BASED ON SMOOTHENING TECHNIQUES Final Report
Ivo M. Babuska and Rodolfo Rodriguez Aug. 1991 38 p
(Contract N00014-90-J-1030)
(AD-A253401; BN-1126) Avail: CASI HC A03/MF A01

This paper addresses the problem of assessing the quality of an a-posteriori error estimate of a finite element solution. An error estimate based on local L'-projections is analyzed in the case of translation invariant meshes. It is shown that for general meshes this technique does not lead to an asymptotically exact estimator. The problem is analyzed in detail in the one-dimensional setting. It is shown that an asymptotically exact estimator is not the optimal one when the solution is not sufficiently smooth. An optimal estimator for adaptively constructed meshes is given. Finally, a general mathematical framework for the quality assessment of estimators is introduced. GRA

N93-10419# Army Armament Research, Development and Engineering Center, Watervliet, NY.
BOX COUNTING MULTIFRACTAL ANALYSIS
L. V. Meisel, M. A. Johnson, and P. J. Cote Jun. 1992 32 p
(AD-A253960; ARCCB-TR-92025) Avail: CASI HC A03/MF A01

Two box-counting algorithms for the determination of generalized fractal dimensions are described. Results of application of the algorithm to Euclidean curves, quadric islands, Koch symmetric and asymmetric triadic snowflakes, and split snowflake halls are described. Comparison to analytic results for the model curves is provided, and the effectiveness of the algorithms is discussed. GRA

N93-10624# Atomic Energy Corp. of South Africa Ltd., Pretoria.
LABAN-PEL: A TWO-DIMENSIONAL, MULTIGROUP DIFFUSION, HIGH-ORDER RESPONSE MATRIX CODE
E. Z. Mueller Jun. 1991 36 p
(DE92-626845; PEL-309; ISBN-0-86960-888-6) Avail: CASI HC A03/MF A01

The capabilities of LABAN-PEL are described. LABAN-PEL is a modified version of the two-dimensional, high-order response matrix code, LABAN, written by Lindahl. The new version extends the capabilities of the original code with regard to the treatment of neutron migration by including an option to utilize full group-to-group diffusion coefficient matrices. In addition, the code has been converted from single to double precision and the necessary routines added to activate its multigroup capability. The coding has also been converted to standard FORTRAN-77 to enhance the portability of the code. Details regarding the input data requirements and calculational options of LABAN-PEL are provided. DOE

N93-10639# Scopus Technology, Inc., Emeryville, CA.
SOLVING LARGE LINEARIZED SYSTEMS IN MECHANICS Report, Mar. - Nov. 1991
B. Nour-Omid Mar. 1992 45 p
(NR Proj. RM3-3-F-60)
(AD-A252723; NCEL-CR-92001) Avail: CASI HC A03/MF A01

The solution of symmetric linearized systems of equations arising from applications of the finite element method to nonlinear analysis of structures is considered. Two related schemes that are based on Krylov sequences (e.g., Lanczos and conjugate gradient procedures) are examined. The conjugate gradient procedure is derived directly from the Lanczos process. In this derivation it is demonstrated that the conjugate gradient implicitly computes the triangular factors of the reduced tridiagonal system generated by the Lanczos process. The stability of the conjugate gradient procedure depends on that for the triangular factorization that can be guaranteed only for positive definite systems. Loss of orthogonality among the Lanczos vectors is also addressed and the method of partial reorthogonalization is used to maintain orthogonality. This approach improves the robustness of the algorithm but can be expensive for ill-conditioned systems. For such problems, preconditioning can help reduce the number of iterations required for convergence. Three different preconditioning schemes are considered; diagonal, element-by-element (E x E), and substructure-by-substructure (S x S). The above methods were applied to a number of different example problem. The S x S method is more effective than either the diagonal or the E x E methods at reducing both the computation cost and the number of iterations. For ill-conditioned systems the computation cost for E x E was less than that for diagonal preconditioners but as the condition number improved, the cost for the two methods were about the same. GRA

N93-10660# Southern Methodist Univ., Dallas, TX. Dept. of Mathematics.
SINGULAR PERTURBATION METHODS FOR NONLINEAR DYNAMICAL SYSTEMS AND WAVES Final Technical Report, 1 Mar. 1987 - 28 Feb. 1992
Richard Haberman Jul. 1992 18 p
(Grant AF-AFOSR-0134-87)
(AD-A254116; AFOSR-92-0767TR) Avail: CASI HC A03/MF A01

Progress has been made on understanding the complex behavior of physical processes described by nonlinear ordinary and partial differential equations through the use of singular perturbation methods. Modulation equations for the amplitude and phase of dissipatively perturbed strongly nonlinear oscillators and traveling waves have been derived from the action equation using the usual method of multiple scales. Equivalent results have been obtained using the method of averaging developed for the first time for a nonlinear partial differential equation, the Klein-Gordon equation, describing dispersive waves. In another study, Whitham's averaged Lagrangian principle has been generalized to account for arbitrary perturbations of the initial conditions. In other work, Bourland and Haberman analyzed the slow crossing of an uperturbed homoclinic orbit (separatrix) for dynamical systems. Solutions in the neighborhood of the separatrix are matched to the nonlinear slowly varying oscillations, resulting in the determination of accurate analytic formulas for the boundaries of the basin of attraction and connection formulas across the separatrix for the amplitude and phase. Under current investigation are generalizations of the slow crossing of a separatrix to arbitrary Hamiltonian systems and to nonchaotic situations in which small periodic forcing causes the existence of an infinite sequence of resonance layers that coalesce on the separatrix. GRA

N93-10758*# Institute for Computer Applications in Science and Engineering, Hampton, VA.
NUMERICAL STUDY OF THE SMALL SCALE STRUCTURES IN BOUSSINESQ CONVECTION Final Report
E. Weinan (Institute for Advanced Study, Princeton, NJ.) and Chi-Wang Shu (Brown Univ., Providence, RI.) Aug. 1992 40 p Submitted for publication
(Contracts NAS1-18605; NAS1-19480; NAG1-1145; DAAL03-89-K-0039; DAAL03-91-G-0123; AF-AFOSR-0090-90; NSF DMS-91-00383; RTOP 505-90-52-01)
(NASA-CR-189695; NAS 1.26:189695; ICASE-92-40) Avail: CASI HC A03/MF A01

Two-dimensional Boussinesq convection is studied numerically using two different methods: a filtered pseudospectral method and a high order accurate Essentially Nonoscillatory (ENO) scheme. The issue whether finite time singularity occurs for initially smooth flows is investigated. The numerical results suggest that the collapse of the bubble cap is unlikely to occur in resolved calculations. The strain rate corresponding to the intensification of the density gradient across the front saturates at the bubble cap. We also found that the cascade of energy to small scales is dominated by the formulation of thin and sharp fronts across which density jumps. Author

N93-10857# Air Force Inst. of Tech., Wright-Patterson AFB, OH. Foreign Aerospace Science and Technology Center.
A SEMIEMPIRICAL FORMULA FOR CALCULATING THE COEFFICIENTS FOR FIELD EMISSION TIP FORMS
Deqing Yang, Hongjiang Song, Zhi Wang, and Ergang Chen 13 Jan. 1992 15 p Transl. into ENGLISH from Dianzikexue Xuekan (China), v. 12, no. 6, Nov. 1990 p 660-665
(AD-A254109; FASTC-ID(RS)T-0745-91) Avail: CASI HC A03/MF A01

This article presents a formula for calculating the general field emission system tip shape or form coefficient. Using this formula and numerical value calculation methods we carried out, respectively, calculations and comparisons on values for the four types of field emission systems--those with tips presenting semispherical shapes, ellipsoid shapes, rotating parabolic shapes, and hyperbolic shapes. GRA

N93-10870# California Computer Products, Inc., Downey.
ALGEBRA-GEOMETRIC AND DIFFERENTIAL GEOMETRIC METHODS IN SOLID GEOMETRIC MODELING Final Report, 1 Dec. 1987 - 1 Mar. 1992
Peter F. Stiller 24 Apr. 1992 172 p
(Contract DAAL03-88-K-0019)
(AD-A253669; ARO-25187.1-MA-R) Avail: CASI HC A08/MF A02

This research seeks to address problems in geometric modeling that require sophisticated and powerful techniques from two traditional mathematical disciplines: differential geometry and algebraic geometry. It also concerns the search for algorithms to effectively implement theoretical results in the following areas: Geometric Modeling, Splines/Finite Elements, Rational Surfaces, Resultants, Grobner Basis, Wavelets, Generalized Characteristic Polynomial, and Computational Algebraic Geometry. GRA

N93-10500 Columbia Univ., New York, NY. Dept. of Civil Engineering and Engineering Mechanics.
HEXAGONAL AND OCTAGONAL FINITE ELEMENTS
Andre Publico and Gautam Dasgupta *In* Carleton Univ., Proceedings of the Twelfth Canadian Congress of Applied Mechanics, Volumes 1 and 2 May 1989 p 252-253 (For primary document see N93-10466 01-31)
Copyright Avail: Canadian Society for Mechanical Engineering, 2050 Mansfield St., Suite 700, Montreal, Quebec H3A 1Z7 Canada

N93-10554 Carleton Univ., Ottawa (Ontario). Dept. of Mechanical and Aeronautical Engineering.
AN ADAPTIVE MESH-MANAGEMENT ALGORITHM FOR THREE-DIMENSIONAL AUTOMATIC FINITE ELEMENT ANALYSIS
J. M. McDill, J. A. Goldak, and A. S. Oddy (Canada Centre for Mineral and Energy Technology, Ottawa, Ontario) *In its* Proceedings of the Twelfth Canadian Congress of Applied Mechanics, Volumes 1 and 2 May 1989 p 766-767 (For primary document see N93-10466 01-31)
Copyright Avail: Canadian Society for Mechanical Engineering, 2050 Mansfield St., Suite 700, Montreal, Quebec H3A 1Z7 Canada

N93-10556 Alberta Univ., Edmonton. Dept. of Civil Engineering.
VARIATIONAL FORMULATION OF A MIXED METHOD FOR SECOND ORDER FRAME ANALYSIS
T. M. Hrudey *In* Carleton Univ., Proceedings of the Twelfth Canadian Congress of Applied Mechanics, Volumes 1 and 2 May 1989 p 772-773 (For primary document see N93-10466 01-31)
Copyright Avail: Canadian Society for Mechanical Engineering, 2050 Mansfield St., Suite 700, Montreal, Quebec H3A 1Z7 Canada

N93-10558 Laval Univ. (Quebec). Dept. of Mechanical Engineering.
A BOUNDARY ELEMENT AND MATHEMATICAL PROGRAMMING APPROACH FOR UNILATERAL CONTACT PROBLEMS
A. Gakwaya and D. Lambert *In* Carleton Univ., Proceedings of the Twelfth Canadian Congress of Applied Mechanics, Volumes 1 and 2 May 1989 p 788-789 (For primary document see N93-10466 01-31)
Copyright Avail: Canadian Society for Mechanical Engineering, 2050 Mansfield St., Suite 700, Montreal, Quebec H3A 1Z7 Canada

N93-10563 Sheffield Univ. (England). Dept. of Mechanical and Process Engineering.
ON THE USE OF COUPLED FINITE ELEMENT BOUNDARY ELEMENT MODELS IN NUMERICAL DESIGN ANALYSIS
J. L. Wearing, M. A. Sheikh, and A. J. Hickson *In* Carleton Univ., Proceedings of the Twelfth Canadian Congress of Applied Mechanics, Volumes 1 and 2 May 1989 p 802-803 (For primary document see N93-10466 01-31)
Copyright Avail: Canadian Society for Mechanical Engineering, 2050 Mansfield St., Suite 700, Montreal, Quebec H3A 1Z7 Canada

N93-10565 University of South Florida, Tampa. Dept. of Civil Engineering and Mechanics.
AN IMPROVED TECHNIQUE FOR DETERMINING HIGHER ORDER EIGENVECTOR COEFFICIENTS
William C. Carpenter and Curtis Byers *In* Carleton Univ., Proceedings of the Twelfth Canadian Congress of Applied Mechanics, Volumes 1 and 2 May 1989 p 810-811 (For primary document see N93-10466 01-31)
Copyright Avail: Canadian Society for Mechanical Engineering, 2050 Mansfield St., Suite 700, Montreal, Quebec H3A 1Z7 Canada

N93-10566 Sheffield Univ. (England). Dept. of Mechanical and Process Engineering.
A BOUNDARY ELEMENT SUPER-ELEMENT METHOD FOR COUPLING WITH THE FINITE ELEMENT METHOD OF SUBSTRUCTURES
J. L. Wearing and M. A. Sheikh *In* Carleton Univ., Proceedings of the Twelfth Canadian Congress of Applied Mechanics, Volumes 1 and 2 May 1989 p 816-817 (For primary document see N93-10466 01-31)
Copyright Avail: Canadian Society for Mechanical Engineering,

2050 Mansfield St., Suite 700, Montreal, Quebec H3A 1Z7 Canada

N93-10567 Vermont Univ., Burlington.
PARTIAL SOLUTION OF THE GENERALIZED EIGENVALUE PROBLEM USING THE WOODBURY TRANSFORMATION
Jean-Guy Beliveau and B. Marcos (Sherbrooke Univ., Quebec) *In* Carleton Univ., Proceedings of the Twelfth Canadian Congress of Applied Mechanics, Volumes 1 and 2 May 1989 p 822-823 (For primary document see N93-10466 01-31)
Copyright Avail: Canadian Society for Mechanical Engineering, 2050 Mansfield St., Suite 700, Montreal, Quebec H3A 1Z7 Canada

N93-10569 Calgary Univ. (Alberta). Dept. of Mechanical Engineering.
DISCONTINUOUS INITIAL VALUE PROBLEM OF NONLINEAR ELASTICITY BY SIMILARITY APPROACH
W. Frydrychowicz and M. C. Singh *In* Carleton Univ., Proceedings of the Twelfth Canadian Congress of Applied Mechanics, Volumes 1 and 2 May 1989 p 836-837 (For primary document see N93-10466 01-31)
Copyright Avail: Canadian Society for Mechanical Engineering, 2050 Mansfield St., Suite 700, Montreal, Quebec H3A 1Z7 Canada

N93-10571 Laval Univ. (Quebec). Dept. of Mechanical Engineering.
EFFECTIVE FORMULATION OF THE DYNAMICS OF A MANIPULATOR BASED ON THE APPELL EQUATIONS [FORMULATION EFFICACE DE LA DYNAMIQUE D'UN MANIPULATEUR A L'AIDE DES EQUATIONS D'APPELL]
B. Levesque and M. J. Richard *In* Carleton Univ., Proceedings of the Twelfth Canadian Congress of Applied Mechanics, Volumes 1 and 2 May 1989 p 860-861 In FRENCH (For primary document see N93-10466 01-31)
Copyright Avail: Canadian Society for Mechanical Engineering, 2050 Mansfield St., Suite 700, Montreal, Quebec H3A 1Z7 Canada

N93-10577 Nanyang Technological Inst. (Singapore).
A DERIVATION FOR THE KINEMATIC EQUATIONS OF FLEXIBLE ROBOTS WITH APPROPRIATE TRANSFORMATION MATRICES
K. H. Low and R. N. Dubey *In* Carleton Univ., Proceedings of the Twelfth Canadian Congress of Applied Mechanics, Volumes 1 and 2 May 1989 p 886-887 (For primary document see N93-10466 01-31)
Copyright Avail: Canadian Society for Mechanical Engineering, 2050 Mansfield St., Suite 700, Montreal, Quebec H3A 1Z7 Canada

65 STATISTICS AND PROBABILITY

Includes data sampling and smoothing; Monte Carlo method; and stochastic processes.

N93-10107# California Univ., Berkeley.
DE FINETTI REPRESENTATIONS OF SURVIVAL FUNCTIONS LEVEL TO A PRODUCT MEASURE Interim Technical Report
Roger M. Cooke Jun. 1992 19 p
(Contract DAAL03-91-G-0046)
(AD-A253623; ARO-27993.3-MA) Avail: CASI HC A03/MF A01

De Finetti-type representations of survival functions are considered. Exchangeable continuous strictly monotonic infinite-dimensional survival functions whose finite dimensional marginals have the same level sets as a product survival function, can be represented uniquely as mixtures of positive powers of that product survival function. A functional equation characterizes the survival functions which can be represented in this way, and the product measure is extracted using techniques from functional equations. GRA

N93-10208# Naval Command, Control and Ocean Surveillance Center, San Diego, CA. RDT and E Div.
MISCLASSIFICATION RATES OF LIKELIHOOD AND PREDICTIVE DISCRIMINANT FUNCTIONS FOR SMALL SAMPLES Final Report, Oct. 1991 - Jan. 1992
Don Waagen May 1992 40 p
(AD-A253640; NRAD-TD-2277) Avail: CASI HC A03/MF A01

Likelihood and predictive discriminant function misclassification rates are compared when training sets are small (i.e., less than 20). The theoretical foundations for the linear, quadratic, and predictive discriminant functions are described. Simulations are used to compare the classification capability of each discriminant function while varying the variance of the underlying distributions. A multivariate case is also analyzed. GRA

N93-10699# Iowa State Univ. of Science and Technology, Ames.
ORDER STATISTICS AND NONPARAMETRIC STATISTICS Final Report, 1 Dec. 1988 - 30 Jun. 1992
H. A. David 30 Jun. 1992 7 p
(Contract DAAL03-89-K-0010)
(AD-A253574; ARO-25836.17-MA) Avail: CASI HC A02/MF A01

This report covers research performed from December 1, 1988 to June 30, 1992, in the areas of order statistics and nonparametric statistics. The principal topics investigated were the following: (1) Median and Order Statistics Filters; (2) comparison of ranked objects by pairwise matching; (3) concomitants of order statistics in selection procedures; and (4) nonparametric analysis of unbalanced paired-comparison data or ranked data. GRA

N93-10700# Stanford Univ., CA. Dept. of Statistics.
ON WATSON'S ANOVA FOR DIRECTIONS
M. A. Stephens 22 Jun. 1992 21 p
(Contract N00014-92-J-1254)
(AD-A253576; SU-TR-454) Avail: CASI HC A03/MF A01

Watson's ANOVA technique for analyzing unit vectors in p dimensions has been usually used with directional data, with $p = 2$ or 3. It is shown how the one-way ANOVA can be extended to a multiway layout, and an example is given using coal-cleat directions. The accuracy of the techniques is reexamined, and it is shown why this can be expected to be greater for $p = 3$ than for $p = 2$, and possibly also for p greater than 3. Finally, conditional tests for directions are compared with the unconditional ANOVA test. It is shown that a characterization of the gamma distribution permits the conditional significance points to be found from the unconditional points using an argument which, in general, is valid. GRA

N93-10795# Texas A&M Univ., College Station. Dept. of Statistics.
CHANGE ANALYSIS
Emanuel Parzen Jun. 1992 10 p
(Contract DAAL03-90-G-0069; Proj. 6547)
(AD-A253567; TR-172; ARO-27574.9-MA) Avail: CASI HC A02/MF A01

Change Analysis in the strict sense is concerned with the problem of detecting and estimating slow and abrupt changes in the probability distributions of successive observations Y(t) of a variable or system. This paper has two goals (1) introduce an approach to Change problems by introducing analysis of Score Change Process (whose idea is to study if a model to a whole data set fails to fit it by random walking the parameter estimating equations); (2) develop analogies between four basic statistics problems, corresponding to the standard assumptions made about a sequence of observations Y(t), $t = 1, ..., n$; test the hypothesis: Distribution of specified parametric form; Independence; Identical distribution, for a sequence of bivariate observations X((t), Y(t)) one would like to test D: Independence of X and Y. Contents are: Introduction, Change Analysis in the strict sense (test Assumption C), Goodness of fit (test Assumption A), Spectral Analysis (test Assumption B), Four phases of change analysis, Parametric scores change analysis, Nonparametric scores change analysis. GRA

N93-10798# California Univ., Berkeley.
THE TOTAL TIME ON TEST STATISTIC AND AGE-DEPENDENT CENSORING Interim Technical Report
Roger M. Cooke Jun. 1992 25 p
(Contract DAAL03-91-G-0046)
(AD-A253622; ARO-27993.2-MA) Avail: CASI HC A03/MF A01

It is known that observations from any censored life (or competing risk) process can be described by a random censoring (or independent risk) model. On the other hand, it is impossible to verify that the censoring is really random. A class of age-dependent censoring processes are defined and the class of corresponding subsurvival functions is described. Exponential life variables censored by independent variables can also be described by age-dependent censoring models if the censoring variable is DFR. The total time on test statistic consistently estimates the expected life of an exponential life variable under random right censoring. If the censoring is age-dependent, the total time on test statistic will severely overestimate the expected life of the variable of interest. Care should be taken to motivate the application of the total time on test statistic in such situations. GRA

N93-10869# Naval Surface Weapons Center, Dahlgren, VA.
RESISTIVE GRID KERNEL ESTIMATOR (RGKE)
Wendy Poston, George Rogers, Carey Priebe, and Jeffrey Solka Jun. 1992 15 p
(AD-A253520; NSWCDD/TR-92/241) Avail: CASI HC A03/MF A01

The ability to estimate a probability density function from random data has applications in discriminant analysis and pattern recognition problems. A resistive grid kernel estimator (RGKE) is described that is suitable for hardware implementation. The one-dimensional linear RGKE is compared to a kernel estimate using Gaussian kernels, and simulations are presented using both continuous and quantized data. The nonlinear form of the RGKE is shown to have desirable properties, such as the ability to detect discontinuities in the density function. GRA

66 SYSTEMS ANALYSIS

Includes mathematical modeling; network analysis; and operations research.

N93-10822# Royal Signals and Radar Establishment, Malvern (England).
NETWORK STABILITY UNDER VIRAL ATTACK: A GAME ENTITLED, GOD AND THE DEVIL
S. C. Giess Jul. 1990 23 p
(RSRE-Memo-4405; BR115188) Copyright Avail: CASI HC A03/MF A01

The problem of viral attacks on communications networks is explored with an emphasis on the time taken for network recovery. The problem is studied by means of a game which allows for different initial states to the network followed by state evolution according to a fixed rule-set. It is found that only a small percentage of nodes in the network need be equipped with countermeasure software for a near asymptotic recovery time to be achieved. However, for all realistic countermeasure percentages, the time for complete recovery can be long compared to the time for majority recovery - a situation similar to human illness/recuperation time ratios. Author

67 THEORETICAL MATHEMATICS

Includes topology and number theory.

No abstracts in this category.

70 PHYSICS (GENERAL)

For precision time and time interval (PTTI) see *35 Instrumentation and Photography;* for geophysics, astrophysics or solar physics see *46 Geophysics, 90 Astrophysics,* or *92 Solar Physics.*

No abstracts in this category.

71 ACOUSTICS

Includes sound generation, transmission and attenuation. For noise pollution see *45 Environmental Pollution.*

N93-10458*# Cornell Univ., Ithaca, NY.
TILT ROTOR HOVER AEROACOUSTICS
Charles David Coffen Jun. 1992 193 p
(Grant NAG2-554)
(NASA-CR-177598; A-92143; NAS 1.26:177598) Avail: CASI HC A09/MF A03

The methodology, results, and conclusions of a study of tilt rotor hover aeroacoustics and aerodynamics are presented. Flow visualization and hot wire velocity measurement were performed on a 1/12-scale model of the XV-15 Tilt Rotor Aircraft in hover. The wing and fuselage below the rotor cause a complex recirculating flow. Results indicate the physical dimensions and details of the flow including the relative unsteadiness and turbulence characteristics of the flow. Discrete frequency harmonic thickness and the loading noise mechanism were predicted using WOPWOP for the standard metal blades and the Advanced Technology Blades. The recirculating flow created by the wing below the rotor is a primary sound mechanism for a hovering tilt rotor. The effects of dynamic blade response should be included for fountain flow conditions which produce impulsive blade loading. Broadband noise mechanisms were studied using Amiet's method with azimuthally varying turbulence characteristics derived from the measurements. The recirculating fountain flow with high turbulence levels in the recirculating zone is the dominant source of broadband noise for a hovering rotor. It is shown that tilt rotor hover aeroacoustic noise mechanisms are now understood. Noise predictions can be made based on reasonably accurate aerodynamic models developed here. Author

N93-10642# Purcell (Anthony) Consultants, Luenburg (Nova Scotia).
ACOUSTIC NOISE GENERATION AT THE AIR/OCEAN BOUNDARY
Anthony J. Purcell Oct. 1990 60 p
(Contract DREA-W7707-9-0036-01-OSC)
(DREA-CR-90-445; CTN-92-60388) Avail: CASI HC A04/MF A01

The downwash from a hovering aircraft generates acoustic sources at the ocean surface through the same mechanisms as wind generated ambient noise-wave breaking and spray generated radially pulsing bubbles which in turn act as dipole sources because of the pressure release ocean surface. The empirically known dependence of wind generated ambient noise on the wind velocity is used to give the acoustic source strength as a function of the downwash velocity on the ocean surface. The velocity field of the rotor downwash can be deduced through Froude-Rankine actuator disc theory combined with a cylindrical vortex model to account for the ground effect. By integrating the resulting (variable) source strength over the ocean surface, quantities such as the noise level, the received intensity per unit solid angle, and the correlation functions are completely determined. Author (CISTI)

N93-10666# Advisory Group for Aerospace Research and Development, Neuilly-Sur-Seine (France). Propulsion and Energetics Panel.
COMBAT AIRCRAFT NOISE [LE BRUIT GENERE PAR LES AVIONS DE COMBAT]
Apr. 1992 363 p In ENGLISH and FRENCH The 78th meeting was held in Bonn, Fed. Republic of Germany, 23-25 Oct. 1991
(AGARD-CP-512; ISBN-92-835-0667-7; AD-A253108) Copyright Avail: CASI HC A16/MF A03

The Conference Proceedings contain 26 papers presented at the Propulsion and Energetics Panel 78B Specialists' Meeting on 'Combat Aircraft Noise' which was held 23-25 Oct. 1991 in Bonn, Germany. Noise emission from combat aircraft during low-altitude, high-speed training missions over populated areas has led to massive complaints. The purpose of the meeting was to offer a forum for specialists to discuss the latest state of the technology concerned and--if possible--to find solutions for overcoming the problems. The Specialists' Meeting was composed of the following sessions: User's Demand, Experience of Noise Effects; Mechanisms of Noise Generation; Noise Measurements, Predictions Methods; and Noise Reduction. Questions and answers of the discussions follow each paper in the Proceedings. For individual titles, see N93-10667 through N93-10692.

N93-10667# Bundesministerium der Verteidigung, Bonn (Germany).
COMBAT AIRCRAFT OPERATIONS: TRAINING REQUIREMENTS FOR THE GERMAN AIR FORCE TACTICAL FLYING UNITS AND THE NOISE PROBLEM
W. Jertz *In* AGARD, Combat Aircraft Noise Apr. 1992 5 p (For primary document see N93-10666 01-71)
Copyright Avail: CASI HC A01/MF A03

The deterrence potential of an Air Force, and by that the capability to fulfill their mission in times of war, relies on threat oriented training in peacetime. Low level flying is a major tactical means to help aircrews reduce the anticipated threat imposed to them by enemy air defence systems to an acceptable degree. The demand for this capability applies also to air defence tasks against attacking fighter bombers. Military low level flying requires a high degree of proficiency, which can only be reached and maintained by constant training. A high performance level is then the key to air power. The possibilities for this kind of necessary training are restricted by superior demands concerning, amongst others, flying safety and environmental reasons. Too intensive restrictions might reduce the fighting capability of the wings to such an extent, that mission fulfillment could be seriously endangered. Author

N93-10668# German Air Force, Bonn (Germany). Planning Div.
POSSIBILITIES AND LIMITATIONS OF FLYING TRAINING IN THE GERMAN AIR FORCE **c09**
H. Rueggeberg *In* AGARD, Combat Aircraft Noise Apr. 1992 6 p (For primary document see N93-10666 01-71)
Copyright Avail: CASI HC A02/MF A03

Training is the most important task of our Air Force in peacetime, and simulation must be seen as an integral part of it. The rapid progress made in improving and advancing simulation techniques leads to a broader use of simulation in combat aircrew training. Pilots concern about reduction in flying hours in exchange for simulation missions has changed somewhat due to the fact that the total annual flying hours were reduced anyway and low level flying was restricted to 300 meters AGL without having any adequate substitute. Simulators are therefore more and more accepted as a necessary add-on for optimum combat proficiency training in which the simulator training portion will have to grow to approximately 30 to 35 percent of the future training program. The German Air Force has used simulators for all types of aircraft for many years and managed to install one special-to-aircraft type simulator in every wing. The experience gained with those systems should be investigated thoroughly to improve our knowledge of the possible application of simulators in combat training. But before we identify the principle interrelationships and longterm perspectives in a new training and simulation concept, we should collect all available data and analyze the finding from the evaluation and flight testing of the ongoing TORNADO simulator upgrade program. We should identify the shortfalls and initiate the necessary follow-on program and improve the prototype simulator before we come to any decision for the simulators in the TORNADO wings. Author

N93-10669# Royal Air Force, London (England).
COMBAT AIRCRAFT NOISE: THE OPERATOR'S PERSPECTIVE
R. Bogg *In* AGARD, Combat Aircraft Noise Apr. 1992 9 p (For primary document see N93-10666 01-71)
Copyright Avail: CASI HC A02/MF A03

Combat aircraft are not subject to the same noise reduction regulations as civil aircraft. Additionally, combat aircraft are operated closer to their performance limits and at high power settings for extended periods. There is general pressure to reduce noise of all kinds, but particularly noise from low flying aircraft. Although there is little that can be done to quiet in-service engines, operational palliatives, such as noise abatement procedures and restrictions on low flying, have been introduced. Moreover, there has been a concerted education and public relations campaign, and numerous airspace management changes have been introduced to reduce the impact of low flying on the population. These subjects were considered during a Pilot Study into aircraft noise under the auspices of the NATO Committee on the Challenges of Modern Society; the findings of the Study are discussed, giving both the international viewpoint and the UK perspective in particular. Some options for the reduction of low flying are also considered, but so long as military aircraft need to fly low to evade enemy air defences, low flying will remain a principal tactic of NATO air forces, and peacetime training will remain an essential military requirement. Thus, noise from low flying combat aircraft will remain a sensitive issue, and ways of reducing it will continue to be of importance for many years to come. Author

N93-10670# Aerospace Medical Research Labs., Wright-Patterson AFB, OH.
HUMAN NOISE EXPOSURE CRITERIA FOR COMBAT AIRCRAFT TRAINING AREAS
Robert A. Lee, C. Stanley Harris, and Henning E. vonGierke *In* AGARD, Combat Aircraft Noise Apr. 1992 12 p (For primary document see N93-10666 01-71)
Copyright Avail: CASI HC A03/MF A03

An overview of interpretive criteria for the noise exposure conditions associated with low altitude flying operations in the United States is presented. It includes description of single event and cumulative noise characteristics unique to such flying activity and a discussion of rationale for using the measure, onset rated adjusted Day-Night Average Sound Level, for predicting population annoyance. Author

N93-10671# Societe Nationale d'Etude et de Construction de Moteurs d'Aviation, Villaroche (France).
NOISE OF COMBAT AIRCRAFT IN PROXIMITY TO AIR BASES: REVIEW OF THE POSSIBILITIES OF NOISE REDUCTION AT THE SOURCE [BRUIT DES AVIONS DE COMBAT A PROXIMITE DES BASES AERIENNES: REVUE DES POSSIBILITES DE REDUCTION DU BRUIT A LA SOURCE]
D. Collin, J. Julliard, and G. Riou *In* AGARD, Combat Aircraft Noise Apr. 1992 11 p In FRENCH (For primary document see N93-10666 01-71)
Copyright Avail: CASI HC A03/MF A03

The operations carried out by combat aircraft are a source of nuisance for the populations situated in proximity to air bases. The noise of jet aircraft constitutes the dominant source of noise in the operations in question. The authors propose to approach the question of the reduction of the corresponding sonic nuisances by utilizing experience acquired by SNECMA over the course of more than twenty years of research on the noise of civil jet turbine engines, and especially of the Concorde supersonic transport

program. The important experimental database resulting from these studies has permitted the development and evaluation of preview methods and solutions in noise reduction. The different mechanisms and significant sources of noise will therefore be reviewed at the same time as the possibilities for current or future improvement. Author

N93-10672# National Research Council of Canada, Ottawa (Ontario). Inst. for Mechanical Engineering.
NOISE STUDIES FOR ENVIRONMENTAL IMPACT ASSESSMENT OF AN OUTDOOR ENGINE TEST FACILITY
G. Krishnappa *In* AGARD, Combat Aircraft Noise Apr. 1992 8 p (For primary document see N93-10666 01-71)
Copyright Avail: CASI HC A02/MF A03

The potential impact of noise in the community surrounding a proposed outdoor test facility in the Ottawa area was evaluated. The test stand was planned for the testing of high performance gas turbine engines. Theoretical predictions based on the outdoor sound propagation model were made for the noise generated from a General Electric F404 engine. The results were verified by carrying measurements of noise generated from a single engine of a parked CF-18 aircraft. The measured results qualitatively confirmed the validity of theoretical predictions. However, the tests clearly demonstrated the strong influence of the atmospheric conditions in the observed noise levels in the surrounding community. The usefulness of the theoretical predictions in devising noise control measures in the test area and for the scheduling of tests in favorable weather conditions to minimize noise impact in the surrounding area were discussed. Author

N93-10673*# National Aeronautics and Space Administration. Langley Research Center, Hampton, VA.
NON-PROPULSIVE AERODYNAMIC NOISE
William L. Willshire, Jr. and Maureen B. Tracy *In* AGARD, Combat Aircraft Noise Apr. 1992 24 p (For primary document see N93-10666 01-71)
Copyright Avail: CASI HC A03/MF A03

In the first part of the paper, the contribution of airframe noise to total aircraft noise on approach is assessed for a large current technology transport and for the same airframe powered with bypass ratio 10 engines with an additional 5 dB noise suppression applied to the fan and turbine noise sources. The airframe noise of the envisioned advanced subsonic transport is 2 EPNdB less than the largest contributor to the total aircraft noise, the fan inlet. The noise impact of the airframe noise, as measured by noise contour area, is 1/4 that of fan noise. Further fan noise reduction efforts should not view airframe noise as an absolute noise floor. In the second part of the paper, the results from one recent cavity noise wind tunnel experiment is reported. A cavity of dimensions 11.25 in. (28.58 cm) long, 2.5 in. (6.35 cm) wide, and variable depth was tested in the Mach number range of .20 through .90. Reynolds number varied from 5 to 100 million per foot (16 to 328 million per meter). The 1/d ratio was varied from 4.4 to 20.0. The model was tested at yaw angles from 0 to 15 degrees. In general, the deeper the cavity, the greater the amplitude of the acoustic tones. Reynolds number appeared to have little effect on acoustic tone amplitudes. Tone amplitude and bandwidth changed with Mach number. The effect of yaw on acoustic tones varied with Reynolds number, Mach number, 1/h, and mode number. At Mach number 0.90, increased yaw shifted the tone frequencies of the higher modal frequencies to lower frequencies. As cavity depth decreased, the effect of yaw decreased. Author

N93-10674# Deutsche Forschungsanstalt fuer Luft- und Raumfahrt, Brunswick (Germany). Inst. fuer Entwurfsaerodynamik.
COMPARISON OF FLYOVER NOISE DATA FROM AIRCRAFT AT HIGH SUBSONIC SPEEDS WITH PREDICTION
Jan Boettcher and Ulf Michel (Deutsche Forschungsanstalt fuer Luft- und Raumfahrt, Berlin, Germany) *In* AGARD, Combat Aircraft Noise Apr. 1992 12 p Sponsored in part by Bundesminsterium der Verteidigung (For primary document see N93-10666 01-71)
Copyright Avail: CASI HC A03/MF A03

Flyover noise measurements are evaluated for four different military jet aircraft types flying at low altitudes. Flight Mach numbers ranged from 0.5 to 0.9. The analysis shows that noise emission is caused by jet mixing and broadband shock associated noise. Based on the experimental results, existing noise prediction schemes are extended toward higher subsonic flight Mach numbers. The novel prediction schemes describe the observed acoustic signatures quite accurately. This holds for the overall sound pressure level independently of the emission angle, for sound-pressure level time histories and for one-third-octave spectra. Author

N93-10675# Technische Univ., Berlin (Germany).
NOISE EMISSION OF LOW FLYING MILITARY AIRPLANES
H.-D. Marohn *In* AGARD, Combat Aircraft Noise Apr. 1992 11 p (For primary document see N93-10666 01-71)
Copyright Avail: CASI HC A03/MF A03

Until the end of 1990 a great amount of low altitude flying of military airplanes was done in the Federal Republic of Germany. Up to then approximately 80,000 low altitude flights were performed annually. Many of these flights took place at a height from 500 ft to 1500 ft. Nearly 2/3 of the whole area of the Federal Republic of Germany was used for low altitude flights between 500 ft and 1500 ft. In seven distinct low flying areas flights even down to a height of 250 ft above ground were allowed. In a relative densely populated country these low altitude flights caused a great amount of disturbance and annoyance. In order to have some information on noise emission of military airplanes flying at subsonic speed at low altitude a measurement campaign was done in the vicinity of the shooting range in Meppen. A special aim of the campaign was to obtain insight into the influence of operational parameters on the noise emission during low altitude flights. The results of these measurements, for instance noise emission as a function of speed and height above around, will be presented. In general, people affected by low altitude flights would not often receive extremely high noise levels because only a part of the population was exposed to direct overflights. It was therefore of interest to determine the number of occurrences and the statistical distribution of noise levels experienced by people living in low flying areas of Germany. For this purpose a research activity was performed in Germany in the years 1986 and 1990. During six weeks at 16 locations within four low flying areas continuous noise measurements were made. The results, such as relative frequency of noise levels and noise duration, are to be presented. Author

N93-10676# Dassault (E. M.) Co., Saint Cloud (France). Division Acoustique.
COMBAT AIRCRAFT NOISE [BRUIT DES AVIONS DE COMBAT]
M. Sgarbozza and A. Depitre (Direction Generale de l'Aviation Civile, Paris, France) *In* AGARD, Combat Aircraft Noise Apr. 1992 12 p In FRENCH (For primary document see N93-10666 01-71)
Copyright Avail: CASI HC A03/MF A03

A discussion of the characteristics and the noise levels of combat aircraft and of a transport aircraft in taking off and landing are presented. Some methods of noise reduction are discussed, including the following: operational anti-noise procedures; and concepts of future engines (silent post-combustion and variable cycle). Some measurement results concerning the noise generated in flight at great speeds and low altitude will also be examined. Finally, the protection of the environment of French air bases against noise will be described and the possibilities of regulation examined. Author

N93-10677# Office National d'Etudes et de Recherches Aeronautiques, Paris (France).
BOOM AND THE PROBLEMS RELATED TO THE SUPERSONIC FLIGHTS OF MILITARY AIRCRAFT [LE BANG ET LES PROBLEMES LIES AUX VOLS SUPERSONIQUES DES AVIONS MILITAIRES]
Christian Thery and Claude Lecomte *In* AGARD, Combat Aircraft

Noise Apr. 1992 27 p In FRENCH (For primary document see N93-10666 01-71)
Copyright Avail: CASI HC A03/MF A03

The flight of a supersonic projectile is accompanied by a clapping called ballistic detonation. At the same time an aircraft in supersonic flight creates a boom which travels to the ground. The boom represents an impulsional characteristic which provokes a startled reaction in living beings and makes structures vibrate. Because of the elevated altitude of the flight of aircraft the boom is felt along a band of terrain situated along each side of the trajectory of the aircraft, as large as many tens of kilometers. The intensity of the boom essentially depends on the size of the aircraft that creates it, on its altitude, and on the maneuver that it is executing; the maneuvers which are executed by military aircraft provoke locally a very great intensification of booms, these are focalizations and superfocalizations. These phenomena appear especially at the time of transonic acceleration and when turning. The annoyance resulting from these focalized booms is therefore certain and related damage to aging or poorly constructed structures can occur; the sole means of limiting the nuisance which results will be to situate these focalized boom zones over uninhabited regions. A good preview of the affected zones requires precise a priori knowledge of the actual trajectory of the aircraft and the meteorological conditions; in practice therefore, the zones susceptible to being affected by these phenomena are fairly large. Above all, the effects of boom must not be overestimated. The first temporary damages to the auditory system are observed for levels of wave intensity greatly superior to the levels of booms (3000 to 5000 Pa as opposed to 50 or 70 Pa for a boom). The structural effects of normal booms are comparable to those resulting from natural inclemency (wind) or related to modern life (highway traffic). The focalized boom cannot have an impact on sound and well-constructed buildings except by cumulative effect (fatigue). Author

N93-10678# Royal Aircraft Establishment, Farnborough (England). Aerospace Division.
A BRIEF REVIEW OF THE SOURCE NOISE TECHNOLOGY APPLICABLE TO FIXED-WING MILITARY AIRCRAFT
R. A. Pinker *In* AGARD, Combat Aircraft Noise Apr. 1992 14 p (For primary document see N93-10666 01-71)
Copyright Avail: CASI HC A03/MF A03

Although the last two decades have seen major reductions in the noise from civil aircraft, noise from military operations, both around airfields and from low-flying aircraft, continues to be a source of irritation and a potential health hazard. Because of the continuing concern about the noise levels produced by combat aircraft, the following paper is intended to provide some of the background to the main conclusions and recommendations reached in the final report of the NATO/Committee on the Challenges of a Modern Society (CCMS) Pilot Study on aircraft noise. Although biased towards fixed wing combat aircraft noise, the paper also considers other fixed wing military aircraft, but specifically excludes sonic booms and rotary wing aircraft as they both have their own particular noise sources and problems. Author

N93-10679# Office National d'Etudes et de Recherches Aeronautiques, Paris (France).
COMBAT AIRCRAFT JET ENGINE NOISE STUDIES [ETUDES SUR LE BRUIT DES TURBOREACTEURS APPLICABLES AUX AVIONS DE COMBAT]
S. Lewy, G. Fournier, and M. Pianko (Icare, Massy, France) *In* AGARD, Combat Aircraft Noise Apr. 1992 17 p In FRENCH Previously announced in IAA as A92-26353 (For primary document see N93-10666 01-71)
Copyright Avail: CASI HC A03/MF A03

Methods of noise prediction and attenuation based on results obtained in civil applications are presented. Input data for directivity and radiation forecasts are given by measurements of vane and blade pressure fluctuations and by modal analysis of the spinning waves propagating in the inlet duct. Attention is given to sound generation mechanisms for subsonic and supersonic single jets and bypass jets. Prediction methods, based on Lighthill's equation (tensor due to the turbulence), are discussed, and the various means of jet noise reduction are reviewed. The CEPRA 19 anechoic wind tunnel, which is primarily designed for studying the jet noise radiated in the far field with flight effects is described. Author

N93-10680*# National Aeronautics and Space Administration. Langley Research Center, Hampton, VA.
SUPERSONIC ACOUSTIC SOURCE MECHANISMS FOR FREE JETS OF VARIOUS GEOMETRIES
John M. Seiner and Michael K. Ponton *In* AGARD, Combat Aircraft Noise Apr. 1992 12 p (For primary document see N93-10666 01-71)
Copyright Avail: CASI HC A03/MF A03

The aeroacoustic performance of several generic nozzle geometries was tested to evaluate the potential benefits of using non-round jet exit geometries to reduce noise from combat military aircraft. Both the aerodynamics and far field acoustics of several M(sub d) = 1.5 and 2.0 round, elliptic, and rectangular nozzles, including an augmented deflector exhaust nozzle (ADEN), were studied to assess noise emission. The nozzles were operated to jet total temperatures, T(sub 0) = 1160 degree R, and the data scaled to constant thrust. The data were propagated to 1500 ft. and corrected to perceived noise level. The aerodynamic results of the study show that the non-round nozzle geometries mix much faster with the surrounding medium than does an equivalent round nozzle plume. Both the ADEN and elliptic nozzles provide significant reduction of noise, 6 to 7 PNdB, along the major axis direction with little expected impact on nozzle performance. Shock noise processes are eliminated for elliptic nozzles, but are still significant with rectangular nozzles. Comparison of measurements to theoretical predictions of noise using the quasi-linear instability wave model demonstrates good qualitative agreement. Author

N93-10681# Illinois Inst. of Tech., Chicago. Dept. of Mechanical and Aerospace Engineering.
NOZZLE INSTALLATION EFFECTS ON THE NOISE FROM SUPERSONIC EXHAUST PLUMES
R. W. Wlezien *In* AGARD, Combat Aircraft Noise Apr. 1992 11 p (For primary document see N93-10666 01-71)
Copyright Avail: CASI HC A03/MF A03

The sensitivity of screech coupling in supersonic jets to nozzle installation geometry is explored as a function of nozzle shape, spacing, and orientation. The coupling phenomenon is shown to be a function of geometry for a variety of twin axisymmetric and rectangular nozzle configurations as well as for a single jet in proximity to a solid surface. Rapid plume merging or close proximity to a wall are shown to minimize the noise increment due to coupling. Twin impinging supersonic plumes experience more complex aeroacoustic interactions. The acoustic near field is dominated by screech and impingement tones, but the fuselage undersurface dynamic loads are primarily due to impingement of the unsteady upwash fountain flow on the fuselage undersurface. Author

N93-10682*# California Inst. of Tech., Pasadena.
COMBUSTION NOISE AND COMBUSTION INSTABILITIES IN PROPULSION SYSTEMS
F. E. C. Culick, L. Paparizos (Carnegie-Mellon Univ., Pittsburgh, PA.), J. Sterling, and V. Burnley *In* AGARD, Combat Aircraft Noise Apr. 1992 27 p Sponsored in part by NASA, California Inst. of Technology; Navy; and AF (For primary document see N93-10666 01-71)
Copyright Avail: CASI HC A03/MF A03

This paper is concerned with some aspects of non-linear behavior of unsteady motions in combustion chambers. The emphasis is on conditions under which organized oscillations having discrete frequencies may exist in the presence of random motions. In order to treat the two types of motions together, and particularly to investigate coupling between noise and combustion instabilities, the unsteady field is represented as a synthesis of acoustic modes having time-varying amplitudes. Each of the amplitudes are written as the sum of two parts, one associated with the random field and the remainder representing the organized oscillations. After spatial averaging, the general problem is reduced to solution of a

set of second-order ordinary differential equations whose structure depends on the sorts of nonlinear processes accounted for. This formulation accommodates any physical process; in particular, terms are included to represent noise sources, although only limited modeling is discussed. Our results suggest that random sources of noise have only small effects on combustion instabilities and seem not to be a cause of unstable motions. However, the coupling between the two sorts of unsteady motions may be important as an essential process in a proposed scheme for noise control. It is now a familiar observation that many nonlinear deterministic systems are capable of exhibiting apparently random motions called 'chaos.' This is a particularly interesting possibility for systems which also executed non-deterministic random motions. In combustion chambers, a nonlinear deterministic system (acoustical motions) exists in the presence of noise produced by flow separation, turbulent motions, and energy released by combustion processes. The last part of the paper is directed to the matter of discovering whether or not chaotic motions exist in combustion systems. Analysis has not progressed sufficiently far to answer the question. We report here recent results of processing data taken in one combustor to determine the dimensions of any attractors in the motions. No evidence has been found for chaos in the strict sense, but the method seems to be an important means of investigating the nonlinear behavior of combustion systems. Author

N93-10683# Bolt, Beranek, and Newman, Inc., Canoga Park, CA.

AUDIBILITY-BASED ANNOYANCE PREDICTION MODELING

Sanford Fidell and Lawrence S. Finegold (Air Force Systems Command, Wright-Patterson AFB, OH.) *In* AGARD, Combat Aircraft Noise Apr. 1992 9 p (For primary document see N93-10666 01-71)

Copyright Avail: CASI HC A02/MF A03

The effects of rapid onset times and high absolute sound pressures near military training routes (MTR's) including possible startle effects and increased annoyance due to the unpredictable nature of these flights, have been of longstanding concern. A more recent concern is the possibility of increased annoyance due to low ambient noise levels near military flight training operations and differences in expectations about noise exposure in high and low population density areas. This paper describes progress in developing audibility-based methods for predicting the annoyance of noise produced at some distance from aircraft flight tracks. Audibility-based models which take into account near-ground acoustic propagation and ambient noise levels may be useful in assessing environmental impacts of MTR's and Military Operating Areas (MOA's) under some conditions. A prototype Single Event Annoyance Prediction Model (SEAPM) has been developed under USAF sponsorship as an initial effort to address these issues, and work has progressed on a geographic information system (GIS) to produce cartographically referenced representations of aircraft audibility. Author

N93-10684*# Pennsylvania State Univ., University Park. Dept. of Aerospace Engineering.

THE PREDICTION OF NOISE RADIATION FROM SUPERSONIC ELLIPTIC JETS

Philip J. Morris and Thonse R. S. Bhat *In* AGARD, Combat Aircraft Noise Apr. 1992 12 p (For primary document see N93-10666 01-71)

(Grant NAG1-1047)

Copyright Avail: CASI HC A03/MF A03

This paper describes the prediction of noise radiation from supersonic elliptic jets. The noise is associated with the large scale structures in the jet mixing layer. These structures are described as instability waves. The local characteristics of the instability waves are determined from a compressible, linear, analysis. The jet mean velocity and density are described in elliptic cylindrical coordinates. The local eigensolution for the instability waves is determined from a finite difference solution of the non-separable boundary value problem. This inner solution which is formulated in terms of the method of multiple scales is matched with the radiated field using the method of matched asymptotic expansions. The form of the far-field directivity is derived. Predictions are presented for the noise radiation by the several modes of instability in the elliptic jet. The radiated field is not axisymmetric and certain modes radiate strongly in the directions of the major and minor axes of the jet. The extension of the present work to other geometries and flow fields is discussed. Author

N93-10685# Deutsche Forschungsanstalt fuer Luft- und Raumfahrt, Berlin (Germany). Inst. fuer Experimentelle Stroemungsmechanik.

PREDICTION OF JET MIXING NOISE FOR HIGH SUBSONIC FLIGHT SPEEDS

Ulf Michel and Jan Boettcher (Deutsche Forschungsanstalt fuer Luft- und Raumfahrt, Brunswick, Germany) *In* AGARD, Combat Aircraft Noise Apr. 1992 9 p (For primary document see N93-10666 01-71)

Copyright Avail: CASI HC A02/MF A03

A method for the prediction of single stream jet mixing noise in flight is presented that can be used for flight Mach numbers up to 0.9. The method is similar to the empirical SAE method. However, two important results of the theoretical scaling law of Michalke and Michel are incorporated: (1) the total noise of heated jets is separated into quadrupole and dipole noise components because they are influenced differently by the flight Mach number and, (2) the influence of the stretching of the jet plume in flight on the overall sound pressure and the frequency of the emitted sound is considered. A relative velocity exponent law is used to correlate experimental flyover data. The correlation is based on all available data for combat aircraft with fuselage mounted engines and flight Mach numbers between 0.5 and 0.9. The difference between predictions with this new method and measured overall flyover levels is generally less than two decibels. The spectra are also well predicted. Author

N93-10686# Royal Aircraft Establishment, Farnborough (England). Aerospace Div.

IDENTIFYING THE PRINCIPAL NOISE SOURCES OF FIXED-WING COMBAT AIRCRAFT IN HIGH-SPEED FLIGHT

W. D. Bryce, R. A. Pinker, and P. J. R. Strange (Rolls-Royce Ltd., Derby, England) *In* AGARD, Combat Aircraft Noise Apr. 1992 20 p (For primary document see N93-10666 01-71)

Copyright Avail: CASI HC A03/MF A03

Before considering means for alleviating the noise from modern military combat aircraft operating in high-speed low-level flight, it is important to identify the principal noise sources. To this end, a carefully-controlled flight test program has been carried out using a Tornado aircraft (in standard training configuration) operating at flight speeds from 0.5M to 0.8M. The major sources of the aircraft noise, airframe noise, installed jet mixing noise and jet shock noise, have been successfully identified, quantified and correlated. Although the jet mixing noise tends to be the major source at low flight speeds, and the shock noise at high flight speeds, all three sources are comparable in magnitude during the rapid rise-time of the noise signal and at its peak. Indeed, were it possible to reduce greatly both the jet mixing and shock noise, the peak noise levels would only reduce by about 5 dBA. Author

N93-10687# National Physical Lab., Teddington (England).

MEASUREMENT AND PREDICTION OF NOISE FROM LOW-ALTITUDE MILITARY AIRCRAFT OPERATIONS

Bernard F. Barry, Richard C. Payne, Anthony L. Harris, and Ralph J. Weston (Royal Air Force, Halton, England) *In* AGARD, Combat Aircraft Noise Apr. 1992 13 p (For primary document see N93-10666 01-71)

Copyright Avail: CASI HC A03/MF A03

In response to the rapid growth in demand for information on noise levels around military airfields in the UK, NPL developed AIRNOISE, a mathematical model for computing aircraft noise contours. Since its first applications in 1981, the model has been used to determine zones of eligibility within the MoD compensation scheme. The model has been subject to continuous development,

e.g., the incorporation of Harrier V/STOL operations. We have now extended the model to include noise from high-speed, low-level operations. The model predicts not only maximum levels but the complete time-history, so that the time-onset rate can be estimated. To aid refinement and validation of the model, a special exercise has been conducted in which Tornado, Harrier, Jaguar, Hawk, F-15 and F-16 aircraft have flown straight and level at heights between about 100 and 400 feet, at various speeds and engine power settings over an array of microphones. This paper describes the trial and the results obtained. The prediction model is outlined and comparisons made between predictions and measurements. Author

N93-10688# Instituto Nacional de Tecnica Aeroespacial, Madrid (Spain).
MECHANISMS OF SOUND GENERATION IN SUBSONIC JETS
E. Campos and F. Mallen *In* AGARD, Combat Aircraft Noise Apr. 1992 18 p (For primary document see N93-10666 01-71)
Copyright Avail: CASI HC A03/MF A03

This paper gives an overview of some important features of the process of sound generation in subsonic jets. The outstanding aeroacoustic theories are briefly reviewed and some distinguished phenomena relevant to jet noise, like both the effects of source convection and temperature are explained. Finally some mechanisms of sound generation by turbulent jets reported in the literature on the topic are examined. Author

N93-10689# Motoren- und Turbinen-Union Muenchen G.m.b.H. (Germany).
COMBAT AIRCRAFT NOISE REDUCTION BY TECHNICAL MEASURES
M. Wegner, F. Kennepohl, and K. Heinig *In* AGARD, Combat Aircraft Noise Apr. 1992 13 p (For primary document see N93-10666 01-71)
Copyright Avail: CASI HC A03/MF A03

The noise of combat aircraft during low level flight is dominated by the jet. Technical noise reduction measures must therefore reduce the specific thrust of the engine. This can be achieved by altering the engine cycle or by using secondary air to increase the mass flow though the nozzle. In the first part the influence of nozzle area, bypass ratio and variable cycle features on the specific thrust of modern fighter engines is shown. The effects on noise, thrust and fuel consumption are discussed. In the second part ejector-mixer nozzles and the aft-fan are considered. Both reduce the jet velocity by entraining air through secondary inlets and expelling it together with the engine's exhaust flow through a common nozzle. Author

N93-10690# Industrieanlagen-Betriebsgesellschaft m.b.H., Ottobrunn (Germany).
TECHNICAL MEASURES FOR THE ATTENUATION OF AIRCRAFT NOISE AND THEIR APPLICABILITY TO GAF COMBAT AIRCRAFT
H. Toenskoetter, S. Blaeck, and R. Richter *In* AGARD, Combat Aircraft Noise Apr. 1992 8 p (For primary document see N93-10666 01-71)
Copyright Avail: CASI HC A02/MF A03

Possible technical measures for the reduction of aircraft engine noise are evaluated with respect to the noise attenuation potential at take-off, low level flight and landing and their applicability to the combat aircraft of the German Air Force (GAF) is discussed. Based on this analysis short and mid term solutions for Tornado are proposed and investigated with respect to noise attenuation, integration, weight, flight performance, operational impact and safety. The design concept of a 'Low Noise Training-Tornado' with reheatless RB199 engines and ejector nozzles is described. Author

N93-10691# Dornier Luftfahrt G.m.b.H., Friedrichshafen (Germany).
STUDY RESULTS ON COMBAT AIRCRAFT SOURCE NOISE REDUCTION
I. U. Borchers, H. J. Hackstein, and P. Bartels *In* AGARD, Combat Aircraft Noise Apr. 1992 24 p (For primary document see N93-10666 01-71)
Copyright Avail: CASI HC A03/MF A03

For use in combat aircraft noise control, important results of extensive studies on jet noise reduction are presented. The studies covered low-noise nozzle designs such as linear arrays of circular nozzles, inverted profile jets as well as special shape mixing nozzles and coaxial bypass flow configurations. In addition interesting results of systematic research on special acoustic absorbers for propulsion system internal noise reduction and of initial theoretical and experimental studies on promising ejector flow systems are reported. The results of the different investigations are explained and discussed. Furthermore, practical applications, including examples of performed and possible future integrations of the considered noise control measures into aircraft, are presented. It is noted that the implementation of these methods could significantly reduce combat aircraft engine noise. For substantial noise reductions, of the order of 20 dB or more as obtained for civil jet transport aircraft, the integration of advanced ejector flow systems is suggested which are capable of effectively lowering the jet exhaust speed as required and with this strongly reduce the jet noise generation. It is concluded that extensive information and an advanced technology basis for jet engine noise reduction exist. Applying this, by giving the needed noise control equal importance and priority as other critical aircraft aspects, may help resolve the related noise problem. Author

N93-10692# Messerschmitt-Boelkow G.m.b.H., Munich (Germany). Aeroacoustics.
REDUCTION OF PROPELLER NOISE BY ACTIVE NOISE CONTROL
O. Bschorr and D. Kubanke *In* AGARD, Combat Aircraft Noise Apr. 1992 10 p (For primary document see N93-10666 01-71)
Copyright Avail: CASI HC A02/MF A03

Active noise control, a method of cancelling noise by means of interference with a secondary anti-noise source, is now in full development. The first commercial application of this technique is in the case of active electronically controlled head sets. The next step will be the active noise cancellation in air ducts and in passenger cabins. The aim of this paper is to assess the possibilities of the anti-noise technique for reducing propeller noise. First, by a mathematical simulation the theoretical noise reduction on the ground was calculated and found to be promising for further investigations. In the case of the periodic engine and propeller noise, for example, with only a single anti-noise source, the noise foot prints of the lower propeller harmonics can be reduced by up to 10 dB. In laboratory tests the theoretical values will be confirmed experimentally. For cancellation of the periodic noise one can use synchronous anti-noise generators. Compared with the engine and propeller noise the reduction of jet noise by the anti-noise technique is much more difficult. Therefore a sensor and controlling unit are necessary because of the stochastic nature of jet noise. Since aircraft noise is a severe problem, all methods are to be considered. Author

N93-10769# Virginia Polytechnic Inst. and State Univ., Blacksburg. Dept. of Mathematics.
PULSE PROPAGATION IN RANDOM MEDIA Final Technical Report, 1 Mar. 1990 - 30 Jun. 1992
Werner Kohler 31 Jul. 1992 4 p
(Grant AF-AFOSR-0137-90)
(AD-A254294; AFOSR-92-0801TR) Avail: CASI HC A01/MF A01

This report summarizes results obtained in the study of how waves are reflected and transmitted by a randomly layered medium. We assume that temporally pulsed energy (plane wave, beam, or radiated energy from a localized source) illuminates this material. Work that was initially done for the acoustic and electromagnetic problems is being extended in these two areas of application. The fundamental approach is also being applied to the elastic medium problem. GRA

N93-10805# Royal Aircraft Establishment, Farnborough (England).
FURTHER NOISE MEASUREMENTS IN A SLOTTED CRYOGENIC WIND TUNNEL
D. G. Mabey 13 Dec. 1990 34 p
(RAE-TM-AERO-2201; BR116372) Copyright Avail: CASI HC A03/MF A01

Some noise measurements in a cryogenic wind tunnel with slotted walls at subsonic and transonic speeds are described. Pressure fluctuations were measured at three positions on the sidewall of the working section, the downstream end of the plenum chamber, and near the inlet and outlet of the first diffuser. Analysis of the measurements suggests that the diffuser noise field can be represented by the superposition of monopole, dipole, and quadrupole sources. The existence of these sources suggests that the diffuser flow may be separated for a significant portion of its length, either because of poor entry conditions or the presence of the model support strut. As expected, a small model at a small angle of incidence generally has a small effect on the noise measurements in the working section. Recommendations are made for further research. Author

N93-10522 New Brunswick Univ., Fredericton. Dept. of Mechanical Engineering.
PROBABILITY DENSITY FUNCTIONS FOR RANDOM NONLINEAR OSCILLATION
Huw G. Davies and Qiang Liu *In* Carleton Univ., Proceedings of the Twelfth Canadian Congress of Applied Mechanics, Volumes 1 and 2 May 1989 p 404-405 (For primary document see N93-10466 01-31)
Copyright Avail: Canadian Society for Mechanical Engineering, 2050 Mansfield St., Suite 700, Montreal, Quebec H3A 1Z7 Canada

72 ATOMIC AND MOLECULAR PHYSICS

Includes atomic structure, electron properties, and molecular spectra.

N93-10291# Florida Univ., Gainesville. Inst. for Fundamental Theory.
MASS AND MIXING ANGLE PATTERNS IN THE STANDARD MODEL AND ITS MATERIAL SUPERSYMMETRIC EXTENSION
P. Ramond Jan. 1992 17 p
(Contract DE-FG05-86ER-40272)
(DE92-016197; DOE/ER-40272/155; UFIFT-HEP-92-4) Avail: CASI HC A03/MF A01

Using renormalization group techniques, we examined several interesting relations among masses and mixing angles of quarks and lepton in the Standard Model of Elementary Particle Interactions as a function of scale. We extended the analysis to the minimal Supersymmetric Extension to determine its effect on these mass relations. For a heavy to quark, and minimal supersymmetry, most of these relations can be made to agree at one unification scale. DOE

N93-10312# Instituto de Pesquisas Espaciais, Sao Jose dos Campos (Brazil).
PHYSICAL IMPLEMENTATIONS OF AN ANTIMASK IN URA BASED CODED MASK SYSTEMS
Udaya Bhaskaram Jayanthi and Joao Braga Sep. 1991 21 p Submitted for publication
(INPE-5338-PRE/1737) Avail: CASI HC A03/MF A01

X and gamma ray astronomy experiments which employ rectangular URA coded masks alone show artifacts in the images reconstructed due to nonuniform background levels in the detector plane. The employment of a separate antimask in addition to the mask in observations is useful to eliminate this problem. We propose here a method to implement the antimask with the same mask, utilizing the antisymmetric properties in the mask pattern, thereby avoiding the need for a separate antimask in an experiment. Simulations performed with this mask-antimask system are presented to show its advantages. Author

N93-10328# Gosudarstvennyi Komitet po Ispolzovaniyu Atomnoi Energii, Serpukhov (USSR). Inst. Fiziki Vysokikh Ehnergij.
STUDY ON THE PI(SUP -)P YIELDS ETA' PI(SUP 0)N REACTION AT 38 AND 100 GeV/c MOMENTA
D. Alde, F. Binon, and C. Bricman 1991 7 p In RUSSIAN
(DE92-624593; IFVE-OEF-91-88) Avail: CASI HC A02/MF A01

The results of the eta'(pi)(sup 0) system produced in pi(-)p charge-exchange interactions at pi(-)-momenta 38 GeV/c and 100 GeV/c are presented. The 2(gamma) and eta(pi)(sup 0)(pi)(sup 0) modes of eta' decay corresponding to 4(gamma) and 8(gamma)-final state topologies were detected. Background sources and the methods of its suppression are discussed. No statistically significant peaks are observed in the eta'(pi)(sup 0) mass spectrum in the range of 1.2GeV - 2.1GeV. Upper limit for a(sub 2)(sup 0)(1320) yields eta'(pi)(sup 0) branching ratio is obtained, BR less than 6(10)(exp -3). DOE

N93-10332# Oak Ridge National Lab., TN.
TWO-PHOTON COUPLINGS OF QUARKONIA WITH ARBITRARY J(SUP PC)
T. Barnes 1992 13 p Presented at the 9th International Workshop on Photon-Photon Collisions, San Diego, CA, 22-26 Mar. 1992 Prepared in cooperation with Tennessee Univ., Knoxville
(Contract DE-AC05-84OR-21400)
(DE92-016525; CONF-9203159-3; ORNL-CCIP-92-05; UTK-92-3) Avail: CASI HC A03/MF A01

We present theoretical results for the two-photon widths of relativistic quarkonium states with arbitrary angular momenta. These relativistic formulas are required to obtain reasonable agreement with the absolute scale of quarkonium decay rates to two photons, and were previously derived for spin-singlet q(bar-q) states. We also evaluate these formulas numerically for l less than or equal to 3q = u,d states in a Coulomb-plus-linear q(bar-q) potential model. Light-quark higher-l and radially-excited q(bar-q) states should be observable experimentally, as their two-photon widths are typically found to be approximately 1 KeV. The radially-excited (sup 1)S(sub 0) higher-mass quarkonium states such as c(bar-c) and b(bar-b) should also be observable in (gamma)(gamma), but orbitally-excited c(bar-c) states with l greater than 1 and b(bar-b) states with l greater than 0 are expected to have very small two-photon widths. The helicity structure of the higher-l q(bar-q) couplings is predicted to be nontrivial, with both lambda = 0 and lambda = 2(gamma)(gamma) final states contributing significantly; these results may be useful as signatures for q(bar-q) states. DOE

N93-10338# Massachusetts Inst. of Tech., Cambridge. National Magnet Lab.
THE MAGNETOCHEMISTRY OF SUPRAMOLECULAR PARTICLES: THE TRANSITION FROM THE MOLECULAR TO THE SOLID-STATE Final Report
Georgia C. Papaefthymiou May 1992 67 p
(Contract N00014-89-J-1779)
(AD-A253126) Avail: CASI HC A04/MF A01

The magnetic properties of nanometer-sized molecular complexes or clusters that contain an increasing number n of superexchange-coupled iron ions participating in 3-D or lower-dimensional magnetic interactions were examined. The experimental criteria that establish the onset of incipient solid-state magnetic correlation effects in these molecules were emphasized. These chemical structures are beyond the molecular realm but convergence to the bulk has not yet been attained. Thus, they afforded appropriate experimental systems to test theoretical predictions that the onset of incipient solid-state phenomena - such as the emergence of a conduction band in metallic clusters and collective magnetic interactions responsible for magnetic ordering in solids - occurs at the vicinity of n greater than 10, where n is the number of atoms or interacting spins in the cluster. The study provided, by means of Mossbauer spectroscopy with a characteristic measuring time tau(sub m) approx. 10(exp -8) sec

the first experimental observation of the onset of intramolecular magnetic ordering in 10 A diameter clusters whose magnetic exchange interaction network among iron ions was three-dimensional. Owing to the extremely small size of the magnetic domain transitional magnetic behavior and superparamagnetic relaxation phenomena dominated the Mossbauer spectra. GRA

N93-10362# Arizona Univ., Tucson. Dept. of Nuclear and Energy Engineering.
MULTIDIMENSIONAL DETERMINISTIC ELECTRON TRANSPORT CALCULATIONS Final Report, Nov. 1985 - Nov. 1988
W. L. Filippone, B. D. Ganapol, and S. P. Monahan May 1992 96 p
(Contract F30602-81-C-0185)
(AD-A254021; RL-TR-92-47) Avail: CASI HC A05/MF A01

Fast and accurate techniques for determining electron fluxes and energy deposition profile in complex multidimensional microcircuits have been developed. The multidimensional Spencer-Lewis Transport equation is solved deterministically using several special numerical techniques. We begin with the derivation of the Spencer-Lewis equation. Then we discuss SMART scattering theory that enables us to replace the highly anisotropic electron scattering kernal by one that is more amenable to numerical treatment. Next, we describe several transport and diffusion theory solution algorithms. Finally, we present new analytical benchmarking methods that will prove useful in generating more comprehensive benchmarks. GRA

N93-10402# Brookhaven National Lab., Upton, NY.
PARTICLE PRODUCTION AT HIGH p(SUB (PERPENDICULAR)) IN (SUP 28)Si + A COLLISIONS AT 14.6 A x GeV/c
S. G. Steadman (Massachusetts Inst. of Tech., Cambridge.) 1992 8 p Presented at the 8th Winter Workshop on Nuclear Dynamics, Jackson Hole, WY, 18-25 Jan. 1992
(Contract DE-AC02-76CH-00016)
(DE92-016939; BNL-47612; CONF-920113-7) Avail: CASI HC A02/MF A01

Single particle inclusive spectra are presented for particle production in Si + Al and Si + Au reactions at the nucleus-nucleon center-of-mass rapidity for projectiles incident at 14.6 A x GeV/c. The invariant cross sections are all well described by an exponential dependence in the transverse mass. An analysis in terms of different components in p(sub perpendicular}exp 2 shows the importance of resonance production and decay as a reaction mechanism at AGS energies. DOE

N93-10435# Pennsylvania State Univ., University Park. Dept. of Physics.
ELECTRON TRANSFER, IONIZATION, AND EXCITATION IN ATOMIC COLLISIONS
T. G. Winter and S. G. Alston 1992 11 p
(Contract DE-FG02-86ER-13549)
(DE92-017300; DOE/ER-13549/6) Avail: CASI HC A03/MF A01

The ongoing research addresses the fundamental processes of electron transfer, ionization, and excitation in ion-atom (and ion-ion) collisions. The focus is on intermediate- and higher-energy collisions, corresponding to proton energies of about 25 kilo-electron-volts (keV) or larger. At intermediate energies, where the transition probabilities are not small, many states must be coupled in a large calculation, while at higher energies, perturbative approaches may be used. Several studies have been carried out in the current three-year period; most of these treat systems with only one or two electrons, so that fewer approximations need be made and the basic collisional mechanisms can be more clearly described. DOE

N93-10605# Kansas Univ., Lawrence.
RESEARCH IN THEORETICAL PARTICLE PHYSICS
D. W. McKay, H. Munczek, and J. Ralston May 1992 30 p
(Contract DE-FG02-85ER-40214)
(DE92-016181; DOE/ER-40214/1) Avail: CASI HC A03/MF A01

An update of ongoing work at Kansas University is presented. This report discusses the following topics in high energy physics: dynamical symmetry breaking and Schwinger-Dyson equation; consistency bound on the minimal model Higgs mass; tests of physics beyond the standard model; particle astrophysics; the interface between perturbative and non-perturbative QCD; cosmology; anisotropy in quantum networks and integer quantum hall behavior; anomalous color transparency; quantum treatment of solitons; color transparency; quantum stabilization of skyrmions; and casimir effect. DOE

N93-10606# Tufts Univ., Medford, MA.
COHERENT PRODUCTION OF PIONS AND RHO MESONS IN NEUTRINO CHARGED CURRENT INTERACTIONS ON NEON NUCLEI AT THE FERMILAB TEVATRON Ph.D. Thesis
Stephane Willocq May 1992 180 p
(Contract DE-FG02-92ER-40702)
(DE92-015674; DOE/ER-40702/1) Avail: CASI HC A09/MF A02

The coherent production of single pions and rho mesons in charged current interactions of neutrinos and antineutrinos on neon nuclei has been studied. The data were obtained using the Fermilab 15-foot Bubble Chamber, filled with a heavy Ne-H2 mixture and exposed to the Quadrupole Triplet neutrino beam produced by 800 GeV protons from the Tevatron. The average beam energy was 86 GeV. In a sample of 330,000 frames, 1032 two-prong nu(sub mu) + bar-nu(sub mu) charged current interactions were selected. The goal of this study was to investigate the low Q(sup 2) high nu region where the hadron dominance model can be tested. In this model, the vector and axial-vector parts of the weak hadronic current are dominated by the rho and a(sub 1) mesons respectively. Moreover, the Partially Conserved Axial Current (PCAC) hypothesis can be tested by studying the coherent production of single pions. DOE

N93-10730# Brookhaven National Lab., Upton, NY.
PHOTOIONIZATION DYNAMICS AND CATION SPECTROSCOPY WITH COHERENT VUV RADIATION
R. T. Wiedmann, R. G. Tonkyn, M. G. White, and E. R. Grant (Purdue Univ., West Lafayette, IN.) 1992 6 p Presented at the 6th International Symposium on Resonance Ionization Spectroscopy and Its Applications, Santa Fe, NM, 24-29 May 1992
(Contract DE-AC02-76CH-00016)
(DE92-015841; BNL-47617; CONF-920574-5) Avail: CASI HC A02/MF A01

Pulsed field ionization (PFI) has been used in conjunction with coherent VUV radiation to investigate the rotational state distributions of molecular cations following single photon ionization. For photoionization of the H2X (X = O,S) molecules, transitions between asymmetric top levels involving the rotational angular momentum projections, K(sub a) and K(sub c), permit resolution of the photoelectron continua according to symmetry. The observed spectra also clearly demonstrate the importance of the non-spherical nature of the molecular ion potential which leads to photoelectron final states which are unexpected from atomic-like analogies. DOE

N93-10820# Stanford Linear Accelerator Center, CA.
A MEASUREMENT OF THE Z(SUP 0) HADRONIC BRANCHING FRACTION TO BOTTOM QUARKS AND THE CHARGED MULTIPLICITY OF BOTTOM QUARK EVENTS USING PRECISION VERTEX DETECTORS AT E(SUB cm) = 91 GeV Ph.D. Thesis
D. S. Koetke Jun. 1992 296 p
(Contract DE-AC03-76SF-00515)
(DE92-018236; SU-SLAC-396) Avail: CASI HC A13/MF A03

Using the precision vertex detectors of the Mark 2 at the SLC, an impact parameter tag was developed to select a sample of hadronic Z(sup 0) decays enriched in its fraction of bottom

quark events. The nominal tagging method requires that there be at least three tracks whose impact parameters are inconsistent with the track having originated at the electron-position interaction point. A tagging efficiency for b(bar-b) events of 50 percent with a enriched sample purity of 85 percent was achieved. This impact parameter tag was used to measure the fraction hadronic Z(sub 0) decays which produce b(bar-b) events, F(sub b). It is found that F(sub b) = 0.232(sub -0.045)(sup +0.053) (stat) (sub -0.021)(sup +0.025) (syst). This result is consistent with those found using other tagging methods as well as the Standard Model prediction of 0.217. The b(bar-b) -enriched event sample was also used to measure the difference between the average charged multiplicity of b(bar-b) events and that of all hadronic Z(sub 0) decays, delta(bar-n)(sub b) = 2.11 +/- 1.82(stat) +/- 0.57(syst). Using previous measurements of the total hadronic charged multiplicity, the corresponding total multiplicity for b(bar-b) events is (bar-n)(sub b) = 23.05 +/- 1.82 (stat) +/- 0.60 (syst). Subtracting the contribution to the multiplicity from B hadron decays yields the multiplicity of the b(bar-b) non-leading system, (bar-n)(sub nl) = 12.04 +/- 1.82 (stat) +/- 0.63(syst). Comparing this non-leading multiplicity to the total hadronic multiplicity data at lower energy supports the hypothesis that the non-leading particle production is independent of the flavor of the initial quarks. DOE

N93-10840# Syracuse Univ., NY.
RESEARCH PROGRAM IN ELEMENTARY PARTICLE THEORY
A. P. Balachandran, C. Rosenzweig, J. Schechter, and K. C. Wali 1992 67 p
(Contract DE-FG02-85ER-40231)
(DE92-017399; DOE/ER-40231/16) Avail: CASI HC A04/MF A01

A brief account of the work completed by the group during the past year is given. The topics covered here include the following: (1) Effective Lagrangians and Solitons; (2) Chern-Simons and Conformal Field Theories; (3) Spin and Statistics; (4) The Standard Model and Beyond; (5) Non-Abelian Monopoles; (6) The Inflationary Universe; and (7) The Hubbard Model. DOE

N93-10863# California Univ., Berkeley. Lawrence Berkeley Lab.
ELECTRONIC STRUCTURE OF HIGHLY CORRELATED STRUCTURES
L. M. Falicov and J. K. Freericks May 1992 11 p Presented at the 16th International Workshop on Condensed-Matter Theories, San Juan (Puerto Rico), 1-5 Jun. 1992
(Contract DE-AC03-76SF-00098)
(DE92-017017; LBL-32405; CONF-9206214-1) Avail: CASI HC A03/MF A01

Three different but related problems are discussed in this contribution, all related to the so-called Anderson, Hubbard, and t-J Hamiltonians--the prototype Hamiltonians for systems with highly correlated electrons: (1) the relationship, based on the well known canonical (Schrieffer-Wolff) transformation, between the Anderson model (in the small-hybridization and large-Coulomb-interaction regime) and the local moment, the Kondo, the Hubbard, and the t-J models, in particular the phenomena of rare-earth magnetism, intermediate valence, and heavy fermions; (2) the exact solution of these Hamiltonians in the periodic small-cluster approximation and the conditions for the existence of the heavy-fermion phenomenon; and (3) the metamagnetic transition in heavy-fermion systems. DOE

N93-10878# City Coll. of the City Univ. of New York, NY. Dept. of Physics.
RESEARCH IN PARTICLE PHYSICS BEYOND THE STANDARD MODEL
S. Samuel 1992 18 p
(Contract DE-AC02-83ER-40107)
(DE92-012240; DOE/ER-40107/11(B)) Avail: CASI HC A03/MF A01

During the DOE funding period from 1987 to 1991 for Task A, research was carried out in fundamental particle physics in the areas of string field theory, string phenomenology, physics beyond the standard model, and TEV physics. During this five year period, more than 40 articles were published, including contributions to conference proceedings. The overall performance should be regarded as highly successful. The proposed research projects were either discovered to be unfeasible or were successfully completed within a six month period. More than 50 percent of the proposed projects fell into the later category. In addition, many projects were successfully achieved that were not part of DOE proposals, simply because they could not be foreseen. A summary of the research is presented. DOE

N93-10885# National Inst. of Standards and Technology, Gaithersburg, MD.
LASER COOLING AND TRAPPING OF NEUTRAL ATOMS Final Report, 1 Oct. 1989 - 30 Sep. 1992
William D. Phillips Jul. 1992 62 p
(Contract N00014-90-F-0002)
(AD-A253730) Avail: CASI HC A04/MF A01

Our group discovered that sodium atoms could be laser cooled well below the lower limit (the 'Doppler limit') predicted by the then generally accepted theory. Two main consequences of that discovery were a revamping of the theory of laser cooling and a renewed interest in the applications of laser cooling because of the far lower temperatures. Both of these effects are continuing in full force today, and this report is in large part a record of our group's continuing involvement in the new developments in laser cooling during the past three years. The work of the NIST laser cooling group falls functionally into the categories of: investigating laser cooling mechanisms; studies of collisions between laser cooled atoms; development of new trapping techniques for neutral atoms; study of the fluorescent spectrum of laser cooled atoms; manipulation of atoms; and atom optics. GRA

73 NUCLEAR AND HIGH-ENERGY PHYSICS

Includes elementary and nuclear particles; and reactor theory.

For space radiation see *93 Space Radiation.*

N93-10102# Rensselaer Polytechnic Inst., Troy, NY.
D-He-3 SPHERICAL TORUS FUSION REACTOR SYSTEM STUDY M.S. Thesis
William A. Macon, Jr. Apr. 1992 128 p
(AD-A253358) Avail: CASI HC A07/MF A02

This system study extrapolates present physics knowledge and technology to predict the anticipated characteristics of D-He3 spherical torus fusion reactors and their sensitivity to uncertainties in important parameters. Reference cases for steady-state 1000 MWe reactors operating in H-mode in both the 1st stability regime and the 2nd stability regime were developed and assessed quantitatively. These devices would a very small aspect ratio (A=1,2), a major radius of about 2.0 m, an on-axis magnetic field less than 2 T, a large plasma current (80-120 MA) dominated by the bootstrap effect, and high plasma beta (greater than O.6). The estimated cost of electricity is in the range of 60-90 mills/kW-hr, assuming the use of a direct energy conversion system. The inherent safety and environmental advantages of D-He3 fusion indicate that this reactor concept could be competitive with advanced fission breeder reactors and large-scale solar electric plants by the end of the 21st century if research and development can produce the anticipated physics and technology advances. GRA

N93-10333# Los Alamos National Lab., NM.
INTENSE ION BEAM RESEARCH AT LOS ALAMOS
D. J. Rej, R. R. Bartsch, H. A. Davis, R. J. Faehl, D. C. Gautier, J. B. Greenly, I. Henins, T. W. Linton, R. E. Muenchausen, and W. J. Waganaar 1992 9 p Presented at the 9th International Conference on High Power Particle Beams, Washington, DC, 25-29 May 1992

(Contract W-7405-eng-36)
(DE92-015240; LA-UR-92-1642; CONF-920515-11) Avail: CASI HC A02/MF A01

Two new interdisciplinary programs are underway at Los Alamos involving the physics and technology of intense light ion beams. In contrast to high-power ICF applications, the LANL effort concentrates on the development of relatively low-voltage (50 to 800 kV) and long-pulsewidth (0.1 to 1 microsec) beams. The first program involves the 1.2 MV, 300-kJ Anaconda generator which has been fitted with an extraction ion diode. Long pulsewidth ion beams have been accelerated, propagated, and extracted for a variety of magnetic field conditions. The primary application of this beam is the synthesis of novel materials. Initial experiments on the congruent evaporative deposition of metallic and ceramic thin films are reported. The second program involves the development of a 120-keV, 50-kA, 1-microsec proton beam for the magnetic fusion program as an ion source for an intense diagnostic neutral beam. Ultra-bright, pulsed neutral beams will be required to successfully measure ion temperatures and thermalized alpha particle energy distributions in large, dense, ignited tokamaks such as ITER. DOE

N93-10462# Los Alamos National Lab., NM.
ACCELERATOR TECHNOLOGY DIVISION Annual Report, FY 1991
Apr. 1992 114 p
(Contract W-7405-eng-36)
(DE92-016023; LA-12281-PR) Avail: CASI HC A06/MF A02

In fiscal year (FY) 1991, the Accelerator Technology (AT) division continued fulfilling its mission to pursue accelerator science and technology and to develop new accelerator concepts for application to research, defense, energy, industry, and other areas of national interest. This report discusses the following programs: The Ground Test Accelerator Program; APLE Free-Electron Laser Program; Accelerator Transmutation of Waste; JAERI, OMEGA Project, and Intense Neutron Source for Materials Testing; Advanced Free-Electron Laser Initiative; Superconducting Super Collider; The High-Power Microwave Program; (Phi) Factory Collaboration; Neutral Particle Beam Power System Highlights; Accelerator Physics and Special Projects; Magnetic Optics and Beam Diagnostics; Accelerator Design and Engineering; Radio-Frequency Technology; Free-Electron Laser Technology; Accelerator Controls and Automation; Very High-Power Microwave Sources and Effects; and GTA Installation, Commissioning, and Operations. DOE

N93-10618# Brown Univ., Providence, RI. Dept. of Physics.
RESEARCH PROGRAM IN EXPERIMENTAL AND THEORETICAL HIGH ENERGY PHYSICS Progress Report, 1 Jan. - 31 May 1992
R. Brandenberger, D. Cutts, H. M. Fried, G. Guralnik, A. Jevicki, K. King, R. E. Lanou, R. Partridge, C. I. Tan, and M. Widgoff 1 Jun. 1992 50 p
(Contract DE-FG02-91ER-40688)
(DE92-016219; DOE/ER-40688/1) Avail: CASI HC A03/MF A01

This report discusses research at Brown University in experimental and theoretical high energy physics. Some of the research programs conducted are as follows: interactions of leptons and hadrons form accelerator and astrophysical sources; hadron interactions with hydrogen and heavier nuclei; large volume detector at the Gran Sasso Laboratory; GEM collaboration at SSC; and hadron colliders and neutrino physics. DOE

N93-10633# Texas Univ., Austin. Inst. for Fusion Studies.
FAST MAGNETIC FIELD PENETRATION INTO AN INTENSE NEUTRALIZED ION BEAM
R. Armale and N. Rostoker (California Univ., Irvine.) Jun. 1992 8 p
(Contract DE-FG05-80ET-53088)
(DE92-016861; DOE/ET-53088/559; IFSR-559) Avail: CASI HC A02/MF A01

Experiments involving propagation of neutralized ion beams across a magnetic field indicate a magnetic field penetration time determined by the Hall resistivity rather than the Spitzer or Pedersen resistivity. In magnetohydrodynamics the Hall current is negligible because electrons and ions drift together in response to an electric field perpendicular to the magnetic field. For a propagating neutralized ion beam, the ion orbits are completely different from the electron orbits and the Hall current must be considered. There would be no effect unless there is a component of magnetic field normal to the surface which would usually be absent for a good conductor. It is necessary to consider electron inertia and the consequent penetration of the normal component to a depth c/omega(sub p). In addition it is essential to consider a component of magnetic field parallel to the velocity of the beam which may be initially absent, but is generated by the Hall effect. The penetration time is determined by whistler waves rather than diffusion. DOE

N93-10643# Texas Univ., Austin. Inst. for Fusion Studies.
MAGNETIC FUSION WITH HIGH ENERGY SELF-COLLIDING ION BEAMS
N. Rostoker (California Univ., Irvine.), F. Wessel (California Univ., Irvine.), B. Maglich (Advanced Physics Corp., Irvine, CA.), and A. Fisher (Naval Research Lab., Washington, DC.) Jun. 1992 9 p Presented at the 9th International Conference on High Power Particle Beams, Washington, DC, 25-29 May 1992
(Contract DE-FG05-80ET-53088)
(DE92-016860; DOE/ET-53088/558; IFSR-558; CONF-920515-22) Avail: CASI HC A02/MF A01

Field-reversed configurations of energetic large orbit ions with neutralizing electrons have been proposed as the basis of a fusion reactor. Vlasov equilibria consisting of a ring or an annulus have been investigated. A stability analysis has been carried out for a long thin layer of energetic ions in a low density background plasma. There is a growing body of experimental evidence from tokamaks that energetic ions slow down and diffuse in accordance with classical theory in the presence of large non-thermal fluctuations and anomalous transport of low energy (10 keV) ions. Provided that major instabilities are under control, it seems likely that the design of a reactor featuring energetic self-colliding ion beams can be based on classical theory. In this case a confinement system that is much better than a tokamak is possible. Several methods are described for creating field reversed configurations with intense neutralized ion beams. DOE

N93-10732# Brookhaven National Lab., Upton, NY.
TWO-PHOTON PHYSICS AND THE COMING GENERATION OF HEAVY ION COLLIDERS
M. J. Rhoades-Brown 1992 9 p Presented at the 9th International Workshop on Photon-Photon Collisions, San Diego, CA, 22-26 Mar. 1992
(Contract DE-AC02-76CH-00016)
(DE92-015850; BNL-47565; CONF-9203159-2) Avail: CASI HC A02/MF A01

The possibilities for two-photon physics at the coming generation of heavy ion colliders is discussed. Particular attention is given to both e(+),e(-) production and resonance production of the Higgs particle. For e(+),e(-) production the inadequacy of traditional perturbation theory is outlined, and through the introduction of approximations valid for heavy ions it is shown how to sum a class of non-perturbative diagrams. The role of the nuclear form factor in suppressing the cross section for the heaviest resonances is also discussed. It is shown how this latter point affects the two-photon cross sections for W(+),W(-) and Higgs production at RHIC, LHC and SSC energies. DOE

N93-10762# California Univ., Berkeley. Lawrence Berkeley Lab.
GLENN T. SEABORG AND HEAVY ION NUCLEAR SCIENCE
W. Loveland (Oregon State Univ., Corvallis.) Apr. 1992 34 p Presented at the American Chemical Society National Meeting, San Francisco, CA, 5-10 Apr. 1992
(Contract DE-AC03-76SF-00098)

(DE92-016943; LBL-32317; CONF-920444-30) Avail: CASI HC A03/MF A01

Radiochemistry has played a limited but important role in the study of nucleus-nucleus collisions. Many of the important radiochemical studies have taken place in Seaborg's laboratory or in the laboratories of others who have spent time in Berkeley working with Glenn T. Seaborg. Studies of low energy deep inelastic reactions are discussed, and special emphasis is placed on charge equilibration. Additionally, studies of the properties of heavy residues in intermediate energy nuclear collisions and studies of target fragmentation in relativistic and ultrarelativistic reactions are reported. The emphasis will be on the unique information afforded by radiochemistry and the physical insight derived from radiochemical studies. Future roles of radiochemistry in heavy ion nuclear science also will be discussed. DOE

N93-10837# Argonne National Lab., IL.
THERMAL, STRUCTURAL, AND DIFFRACTION ANALYSES OF A GALLIUM-COOLED X RAY MONOCHROMATOR
C. S. Rogers, A. T. Macrander, and D. M. Mills Jun. 1992 11 p Presented at the SPIE International Symposium on Optical Applied Science and Engineering, San Diego, CA, 19-24 Jul. 1992
(Contract W-31-109-eng-38)
(DE92-017063; ANL/CP-76521; CONF-920792-8) Avail: CASI HC A03/MF A01

The next generation of synchrotron radiation sources will produce very high power and power density x-ray beams. For example, the Advanced Photon Source (APS) under construction at Argonne National Laboratory will produce beams containing up to 5 kW of power and peak normal power densities in excess of 150 W/sq mm. Normally, the first optical component to intercept the x-ray beam is a crystal monochromator. This device typically uses a single crystal of silicon or germanium as a band-pass filter according to Braggs' law of diffraction. Under the severe heat loading of modem synchrotron beams, the performance of the monochromator is degraded by reducing the photon throughput and increasing the beam divergence. This paper describes the methods used to calculate the thermally induced deformations in standardly configured monochromator crystals using finite element analysis. The results of these analyses are compared to recent experiments conducted at the Cornell High Energy Synchrotron Source (CHESS) using a high-performance, gallium-cooled crystal. Computer simulations can be used to evaluate the performance of high-heat-load x-ray optics for future synchrotron sources. DOE

N93-10838# Minnesota Univ., Minneapolis.
PION- AND PROTON-NUCLEUS INTERACTIONS AT INTERMEDIATE ENERGY
D. Dehnhard Feb. 1992 21 p
(Contract DE-FG02-87ER-40362)
(DE92-017980; DOE/ER-40362/5) Avail: CASI HC A03/MF A01

The pi-meson and proton beams from the Los Alamos Meson Physics Facility (LAMPF) and the Indiana University Cyclotron Facility (IUCF) were used in scattering and reaction experiments on atomic nuclei. The experimental data allow tests of models of the reaction mechanism and of nuclear structure. For example, the asymmetries observed in a pion scattering experiment on polarized C-13 nuclei were found to contain unique information on the isoscalar spin density. However, further experiments on polarized nuclei of simpler structure are needed to provide the data for a thorough analysis of the reaction mechanism. For this reason a pion scattering experiment on a polarized He-3 target is planned and a high-resolution study on Li-6(pi,pi') will be done. An analysis of pi-triton coincidence events from the He-4(pi,pi't)p reaction yielded evidence for direct triton knock-out from He-4. This work will be continued at higher incident pion energies. Additional work on the He-4(p,n) reaction at IUCF is planned to determine the isovector strength in mass-4 nuclei and the level parameters of Li-4. DOE

N93-10862# Continuous Electron Beam Accelerator Facility, Newport New, VA.
RECENT DEVELOPMENTS IN STORED POLARIZED ELECTRON POSITRON BEAMS
R. Rossmanith Jan. 1992 10 p Presented at the Adriatico Research Conference on Polarization Dynamics in Nuclear and Particle Physics, Trieste (Italy), 7-10 Jan. 1992
(Contract DE-AC05-84ER-40150)
(DE92-016965; DOE/ER-40150/192; CEBAF-PR-92-007; CONF-9201107-2) Avail: CASI HC A02/MF A01

In nearly all electron or positron storage rings the beams are polarized vertically by the Sokolov-Ternov effect. The existence of polarized beams was established both in low energy rings such as ACO (the first storage ring in which the Sokolov-Ternov polarization effect was measured), BESSY, and VEPP2 and in high energy rings such as TRISTAN, HERA, and LEP. As a result beam polarization seems to be an inherent property of electron-positron rings. It should be noted that this free polarization was never used for high energy experiments except in those instances in which exact energy calibration measurements were performed. Proposals for using stored polarized beams for internal target experiments are fairly new. Experiments with polarized longitudinal beams in LEP are still in the stage of planning. The efforts of the last few years are summarized in order to arrive at a better understanding of the spin dynamics in electron positron storage rings and to compare the experimental results with the theory. Polarimeters are not discussed. DOE

74 OPTICS

Includes light phenomena; and optical devices.
For lasers see *36 Lasers and Masers.*

N93-10259# Army Missile Command, Redstone Arsenal, AL.
COMPARISON OF OPTICALLY-ADDRESSED SPATIAL LIGHT MODULATORS Final Report, Oct. 1990 - Dec. 1991
T. D. Hudson, James C. Kirsch, and Don A. Gregory May 1992 19 p
(AD-A254189; AD-E951861; AMSMI/TR-RD-WS-92-10) Avail: CASI HC A03/MF A01

The performance characteristics of three unique optically-addressed spatial light modulator (SLM) structures were investigated. The measured parameters included maximum resolution, visibility, imaging response time, and write light sensitivity. The modulators investigated include two relatively new technologies: the ferroelectric liquid crystal (FLC) SLM from the University of Colorado-Boulder and the amorphous silicon photoconductive twisted nematic liquid crystal SLM from GEC-Marconi Research, and the Hughes Liquid Crystal Light Valve (LCLV), which is a well established industry benchmark. This report is a compilation of the operating parameters and performance of these three modulators. Investigated parameters are conductive to understanding these modulators as input image transducers in optical correlator architectures. GRA

N93-10311# Instituto de Pesquisas Espaciais, Sao Jose dos Campos (Brazil).
SPOT PANCHROMATIC BAND SIMULATION BY LINEAR COMBINATION OF MULTISPECTRAL BANDS
Nelson Delfino DAvil Mascarenhas, Gerald Jean Francis Banon, and Leila Maria Garcia Fonseca Oct. 1991 10 p Submitted for publication
(INPE-5295-PRE/1650) Avail: CASI HC A02/MF A01

The simulation of one or more bands of a multispectral sensor by combination of other bands represents an attractive possibility. For example, it could decrease the data rate of the communications link between the spacecraft and ground. In this work an analysis of the simulation of the spatially degraded SPOT panchromatic band by linear combination of the multispectral bands was performed. Two methods were used for the spectral linear combination: (1) unconstrained least squares; and (2) equality constrained least squares. By using the second method, it is shown

that the signal to noise ratio of the simulated band tends to be better than the signal to noise ratio of each multispectral band. The experiment results have included a spatial simulation of a degraded, 20 m resolution panchromatic band for comparison with the spectrally simulated band. These results demonstrate that a numerically and visually reasonable estimate of the degraded panchromatic band can be obtained. Author

N93-10360# Colsa, Inc., Huntsville, AL.
ALGORITHMS FOR MULTICHANNEL OPTICAL PROCESSOR Final Technical Report, Jan. 1991 - Jan. 1992
Stephen T. Welstead May 1992 40 p
(Contract F30602-88-D-0028)
(AD-A254009; RL-TR-92-78) Avail: CASI HC A03/MF A01

This report discusses several alternative algorithms for implementation in an optical processor to perform adaptive interference cancellation. Estimates of the interference signal are formed in the optical processor by weighting and summing delayed copies of signals which are input from multiple auxiliary antennas. The optical processor is limited in the number of weights that can simultaneously be applied. To address this limitation, a new class of algorithms called limited output weight position algorithms is introduced. One particular algorithm which sequentially applies the output weights is shown to provide good cancellation performance in a number of simulated multipath delay scenarios. GRA

N93-10445# Arizona Univ., Tucson. Dept. of Physics.
POLARIZED LIGHT SCATTERING FROM PERFECT AND PERTURBED SURFACES AND FUNDAMENTAL SCATTERING SYSTEMS Final Report, 1 Mar. 1990 - 29 Feb. 1992
William S. Bickel 29 Feb. 1992 62 p
(Grant AF-AFOSR-0243-90)
(AD-A253186; AFOSR-92-0677TR) Avail: CASI HC A04/MF A01

Following topics are addressed: Light scattering from a sphere on or near a surface; Light scattering from a sphere on or near a surface: Errata; Coherent fluorescent emission and scattering from a uniform cylinder; Coherent fluorescent emission and scattering from a uniform sphere; Light scattering mueller matrix from a fiber as a function of MgO contamination; Experimental light-scattering mueller matrix for a fiber on a reflecting optical surface as a function of incident angle; Light scattering resonances in small spheres; Polarized light scattered from rough surfaces; Stokes vectors, mueller matrices and polarized scattered light; Experimental applications to optical surfaces and all other scatterers; The light scattering mueller for a surface contaminated by a single particle in the Rayleigh limit; Electromagnetic scattering from a sphere; The near field region; Light Scattering from a sphere on or near an interface; The polarized light scattering matrix elements for rough surfaces. GRA

N93-10446# Arizona Univ., Tucson. Optical Sciences Center.
RESEARCH IN THE OPTICAL SCIENCES Final Report, 1 Oct. 1990 - 30 Sep. 1991
R. R. Shannon 17 Feb. 1992 57 p
(Contract F49620-88-C-0009)
(AD-A253188; AFOSR-92-0688TR) Avail: CASI HC A04/MF A01

This report covers special work carried out on the Joint Services Optics Program at the Optical Sciences Center during the period October 1, 1990 through September 30, 1991. The work summarized in the report, and detailed in the appendices, is responsive to request from two sponsors. In each cue the work required system analysis and technical evaluation of the potential in two areas of optical technology: a high-speed video system; and work on membrane mirrors. GRA

N93-10659# Massachusetts Inst. of Tech., Cambridge. Dept. of Physics.
NEW DEVELOPMENTS IN ATOM INTERFEROMETRY Final Report, 1 Apr. 1989 - 30 Apr. 1992
David E. Pritchard Jul. 1992 5 p
(Contract DAAL03-89-K-0082)
(AD-A254094; ARO-26566.5-PH) Avail: CASI HC A01/MF A01

The first true atom interferometer was demonstrated. Using transmission gratings as optical elements for atom deBroglie waves, a three grating atom interferometer was constructed which physically separates atom waves before recombining them. This demonstration was closely followed by two demonstrations of atom interferometers which used laser light as the beam splitters. Atom interferometers will make possible qualitatively new types of experiments involving inertial effects, studies of atomic and molecular properties, tests of basic quantum physics, and may ultimately open the way to make ultra-small structures using atom holograms. GRA

N93-10693# Princeton Univ., NJ.
ARCHITECTURE AND DEVICE DEVELOPMENT FOR OPTICAL NETWORKS Final Technical Report, Mar. 1990 - Mar. 1991
Paul R. Prucnal, John L. Stacy, Mark F. Krol, Raymond K. Boncek, and Steven T. Johns Dec. 1991 35 p Prepared for Calspan-Buffalo Univ. Research Center, NY
(Contract F30602-88-D-0026)
(AD-A253247; RL-TR-91-437) Avail: CASI HC A03/MF A01

This report describes the work accomplished at the Photonics Center, Rome Laboratory in developing an Optical Time Division Multiaccess coder capable of rapidly shifting an optical pulse in time for address recognition. It also describes current and future work being accomplished at the Photonics Center on coincidence detection ('AND' gate) for use in demultiplexing channel information from a multi-gigabit data stream. Part of this effort, dealing with the free-space switching architecture, was primarily accomplished at Princeton University. GRA

N93-10694# Colorado State Univ., Fort Collins. Dept. of Chemistry.
TEMPLATE-SYNTHESIS OF INFRARED-TRANSPARENT METAL MICROCYLINDERS: COMPARISON OF OPTICAL PROPERTIES WITH THE PREDICTIONS OF EFFECTIVE MEDIUM THEORY
C. A. Foss, Jr., M. J. Tierney, and C. R. Martin 20 Jul. 1992 39 p
(Contract N00014-82-K-0612)
(AD-A253267; TR-76) Avail: CASI HC A03/MF A01

Metal-insulator composites of varying metal volume fraction were prepared by electrochemical deposition of gold into porous, aluminum oxide membranes. The cylindrical pore array structure of the host oxide serves as a template for the formation of Au particles ca. 0.26 gm in diameter with lengths ranging from 0.3 gm to 3 gm depending on deposition time. The composites display a significant transparency in the infrared spectrum between 2000 and 4000 cm exp -1. The Au volume fraction and effective medium theory screening parameter K were estimated from scanning electron microscopic analyses of cylinder dimensions and orientations in the composite membranes. Comparison of experimental spectra with those calculated using Maxwell-Garnett or Bruggeman theories indicates that neither approach is entirely satisfactory. The spectra are consistent, however, with retarded polarization effects due to non-negligible Au particle separation distances in the composites. GRA

N93-10708# Logicon Technical Services, Inc., Dayton, OH.
COMPARATIVE STUDY OF THE MTFA, ICS, AND SQRI IMAGE QUALITY METRICS FOR VISUAL DISPLAY SYSTEMS Final Report, Jun. 1990 - Sep. 1991
R. J. Beaton and W. W. Farley Sep. 1991 122 p Prepared in cooperation with Keystone Engineering Ltd., Blacksburg, VA
(Contract F33615-89-C-0532)
(AD-A252116; AL-TR-1992-0001) Avail: CASI HC A06/MF A02

This effort was a review of and analytic comparison between several of the most widely reported display image quality metrics: Modulation Transfer Function Area (MTFA), Integrated Contrast Sensitivity (ICS) metric, and the Square-Root Integral (SQRI) metric. Differences were found with regard to weightings applied to the

psychovisual data which underline each metric. The SQRI metric was found to be sensitive to many variations in display viewing but was also found to exhibit large computational errors which were difficult to bring into control. The MTFA and ICS metrics were found to be somewhat less sensitive to display viewing parameters but also to exhibit greater computational robustness.
GRA

N93-10724# Rome Lab., Griffiss AFB, NY.
ANALYTICAL CHARACTERIZATION OF BISTATIC SCATTERING FROM GAUSSIAN DISTRIBUTED SURFACES Report, Jan. - Jun. 1991
Lisa M. Sharpe Dec. 1991 50 p
(AD-A254253; RL-TR-91-351) Avail: CASI HC A03/MF A01

In a study by Papa and Woodworth, the mean and variance of the diffuse power scattered from a clutter cell were examined as a function of cell size for one-dimensionally rough surfaces. Their study was performed for horizontally polarized incident and scattered fields. Their work is expanded to include vertical and arbitrary linear polarization. Scattering statistics and polarization effects will be examined using a theoretical model based upon physical optics. The present study shows that as the size of the clutter cell is decreased, the statistical distribution of the scattered power deviates from Rayleigh. Also. It Is shown that the tilt angle of the incident linear polarization has little effect on the statistics of the scattered wave. GRA

N93-10812# Air Force Inst. of Tech., Wright-Patterson AFB, OH. Foreign Technology Div.
A SEAM TRACKING MODULATED INFRARED OPTICAL SENSOR FOR USE IN WELDING
Minsheng Wu, Wuzhu Chen, Fangdian He, Bingyi Yan, and Yong Su 3 Dec. 1991 18 p Transl. into ENGLISH from Qinghua Daxue Xuebao (China), v. 30, no. 2, 1990 p 31-36
(AD-A254103; FTD-ID(RS)T-1431-90) Avail: CASI HC A03/MF A01

This article describes a weld seam tracking sensor which has a type of pulse modulated infrared beam as its signal light source. Going through signal reception filters and 'adaptive elimination of noise' processing, it is possible to effectively overcome interference from electric arc light. Making use of the light source pulse driven characteristics, the instantaneous signal power is greatly added to, improving the adaptation of optical sensors to the surfaces of pieces of work. The sensors' structure is simple. Their volume is small. Their sensitivity is high. Additionally, they are capable of realizing, at the same time, automatic tracking of weld seams in the two horizontal and altitude directions. It is capable of precision tracking in both submerged arc and open arc automatic welding.
GRA

N93-10818# Lawrence Livermore National Lab., CA.
UV SPECTRUM SPLITTING MIRROR
G. E. Loomis and R. Chow 10 Oct. 1991 14 p
(Contract W-7405-eng-48)
(DE92-018057; UCRL-CR-108745) Avail: CASI HC A03/MF A01

Five spectrum splitting mirrors were deposited on CaF2 substrates. These mirrors were designed for high reflectance from 165 nm to 200 nm and transmittance from 200 nm to 600 nm. The designed reflectance and transmittance spectral performances are plotted. The peak reflectance is 92 percent and greater than 80 percent from 165 nm to 199 nm except for the region between 187 nm to 194 nm. The measured performance of one mirror from the batch of 5 is shown. The peak reflectance at 45 deg is 77.5 percent at 180 nm. The transmittance is greater than 80 percent from 250 nm to 600 nm. DOE

N93-10583*# Boeing Co., Seattle, WA. Defense and Space Group.
LONG DURATION EXPOSURE FACILITY (LDEF) OPTICAL SYSTEMS SIG SUMMARY AND DATABASE
Gail Bohnhoff-Hlavacek *In* NASA. Langley Research Center, LDEF Materials Workshop 1991, Part 2 Sep. 1992 p 507-512 (For primary document see N93-10578 01-27)
Avail: CASI HC A02/MF A03

N93-10949# Rutherford Appleton Lab., Chilton (England). Space Science Dept.
INVESTIGATIONS OF THE EFFECTS OF CONTAMINATION ON UV OPTICS
Barry J. Kent *In* ESA, Solar Physics and Astrophysics at Interferometric Resolution May 1992 p 283-285 (For primary document see N93-10901 01-90)
Copyright Avail: CASI HC A01/MF A03

N93-10951# Technische Physische Dienst TNO-TH, Delft (Netherlands).
THE IMAGING FOURIER TRANSFORM SPECTROMETER OPTICAL DESIGN
B. Kruizinga, B. Snijders, B. C. Braam, A. P. Thorne (Imperial Coll. of Science and Technology, London, England), J. Maxwell (Imperial Coll. of Science and Technology, London, England), and L. Dame (Centre National de la Recherche Scientifique, Verrieres-Le Buisson, France) *In* ESA, Solar Physics and Astrophysics at Interferometric Resolution May 1992 p 288-289 (For primary document see N93-10901 01-90)
Copyright Avail: CASI HC A01/MF A03

N93-10955# Imperial Coll. of Science and Technology, London (England).
INTERFEROMETER OPTICAL DESIGN FOR THE IMAGING FOURIER TRANSFORM SPECTROMETER (IFTS)
J. Maxwell, A. P. Thorne, J. Wheaton (Chelsea Instruments Ltd., East Molesey, England), and R. P. Glover (RGC Technical Consultancy, London, England) *In* ESA, Solar Physics and Astrophysics at Interferometric Resolution May 1992 p 299-301 Sponsored in part by ESTEC (For primary document see N93-10901 01-90)
Copyright Avail: CASI HC A01/MF A03

75 PLASMA PHYSICS

Includes magnetohydrodynamics and plasma fusion.
For ionospheric plasmas see *46 Geophysics*. For space plasmas see *90 Astrophysics*.

N93-10066*# Southwest Research Inst., San Antonio, TX. Instrumentation and Space Research Div.
SIMULATION STUDY OF INTERACTIONS OF SPACE SHUTTLE-GENERATED ELECTRON BEAMS WITH AMBIENT PLASMAS Final Report
Chin S. Lin 30 Sep. 1992 65 p
(Grant NAGw-1936; SwRI Proj. 15-3399)
(NASA-CR-190843; NAS 1.26:190843) Avail: CASI HC A04/MF A01

This report summarizes results obtained through the support of NASA Grant NAGW-1936. The objective of this report is to conduct large scale simulations of electron beams injected into space. The topics covered include the following: (1) simulation of radial expansion of an injected electron beam; (2) simulations of the active injections of electron beams; (3) parameter study of electron beam injection into an ionospheric plasma; and (4) magnetosheath-ionospheric plasma interactions in the cusp.
Author

N93-10252# Ohio State Univ., Columbus. Dept. of Mechanical Engineering.
FUNDAMENTAL STUDIES ON EROSION IN MPD THRUSTERS Final Report, 30 Sep. 1987 - 30 Sep. 1991
V. V. Subramaniam Apr. 1992 88 p
(Grant AF-AFOSR-0360-87)
(AD-A253900; AFOSR-92-0785TR) Avail: CASI HC A05/MF A01

The purpose of this research is to understand and quantify the mechanisms responsible for evaporative erosion in steady state

magnetoplasmadynamic (MPD) thrusters. This is necessary in order to predict thruster characteristics and lifetimes for a given design. The Back-EMF theory of Onset has been refined and expanded to enable prediction of erosion rates for steady state, self-field MPD thrusters. This theory is capable of explaining both the observed oscillations as well as the increased erosion observed at Onset. This work represents the first time that the plasma discharge and electrode processes have been coupled. GRA

N93-10293# General Atomic Co., San Diego, CA.
HELIUM TRANSPORT IN ENHANCED CONFINEMENT REGIMES ON THE TEXTOR AND D3-D TOKAMAKS
D. L. Hillis, J. T. Hogan, M. R. Wade, C. C. Klepper, P. K. Mioduszewski, K. H. Finken, W. Y. Baek, K. H. Dippel, H. Euringer, and A. Pospieszcyk et al Apr. 1992 33 p Presented at the 10th International Conference on Plasma-Surface Interactions in Controlled Fusion Devices, Monterey, CA, 30 Mar. - 3 Apr. 1992
(Contracts DE-AC03-89ER-51114; DE-AC05-84OR-21400)
(DE92-016247; GA-A-20901; CONF-920311-20) Avail: CASI HC A03/MF A01

Comparisons, of He transport and exhaust in L-mode and in an enhanced confinement regime (H-mode), which is induced by a polarizing electrode, were made for the TEXTOR tokamak. The results showed an increased tendency for He accumulation when bulk plasma energy and particle confinement were improved during the polarization induced H-mode. Since these results imply that a high He pumping efficiency may be necessary for H-mode burning plasmas, we began exploring He transport in a divertor H-mode, similar to that proposed for International Thermonuclear Experimental Reactor (ITER). A collaborative program was initiated to measure He transport and scaling on D3-D during L-mode, H-mode, and ELMing H-mode plasma conditions. To simulate the presence of He ash in D3-D, a 25 ms He puff is injected into a D3-D plasma resulting in a He concentration of approx. = 5 percent. The time dependence of the He(2+) density profiles in the plasma core is measured by charge-exchange recombination spectroscopy at 11 radial locations. DOE

N93-10326# General Atomic Co., San Diego, CA.
DIVERTOR HEAT FLUX REDUCTION BY D2 INJECTION IN DIII-D
T. W. Petrie, R. J. Groebner, A. W. Leonard, S. I. Lippmann, A. M. Mahdavi, W. P. West, D. Buchenauer (Sandia National Labs., Albuquerque, NM.), R. B. Campbell (Sandia National Labs., Albuquerque, NM.), and D. N. Hill (Lawrence Livermore National Lab., CA.) May 1992 18 p Presented at the 10th International Conference on Plasma-Surface Interactions in Controlled Fusion Devices, Monterey, CA, 30 Mar. - 3 Apr. 1992
(Contract DE-AC03-89ER-51114)
(DE92-014232; GA-A-20899; CONF-920311-12) Avail: CASI HC A03/MF A01

D2 gas injected into ELMing H-mode discharges in DIII-D reduced total integrated heat flux to the divertor by approximately 2 times and peak heat flux by approximately 5 times, with only modest degradation to plasma stored energy. Steady gas injection without particle pumping results in eventual degradation in stored energy. The initial reduction in peak heat flux at the divertor tiles may be primarily due to the increase in radiated power from the X-point/divertor region. The eventual formation of a high density region near the X-point appears to play a role in momentum (and energy) transfer from the flux surfaces near the outboard strike point to flux surfaces farther out into the scrapeoff. This may also contribute to further reduction in peak heat flux. DOE

N93-10331# Massachusetts Inst. of Tech., Cambridge. Plasma Fusion Center.
AN ANALYTIC DETERMINATION OF BETA POLOIDAL AND INTERNAL INDUCTANCE IN AN ELONGATED TOKAMAK FROM MAGNETIC PROBE MEASUREMENTS Ph.D. Thesis
J. M. Sorci Feb. 1992 62 p
(Contract DE-FG02-91ER-54109)
(DE92-016294; DOE/ER-54109/T3; PFC/RR-92-6) Avail: CASI HC A04/MF A01

Analytic calculations of the magnetic fields available to magnetic diagnostics are performed for tokamaks with circular and elliptical cross sections. The explicit dependence of the magnetic fields on the poloidal beta and internal inductances is sought. For tokamaks with circular cross sections, Shafranov's results are reproduced and extended. To first order in the inverse aspect ratio expansion of the magnetic fields, only a specific combination of beta poloidal and internal inductance is found to be measurable. To second order in the expansion, the measurements of beta poloidal and the internal inductance are demonstrated to be separable but excessively sensitive to experimental error. For tokamaks with elliptical cross sections, magnetic measurements are found to determine beta poloidal and the internal inductance separately. A second harmonic component of the zeroth order field in combination with the dc harmonic of the zeroth order field specifies the internal inductance. The internal inductance in hand, measurement of the first order, first harmonic component of the magnetic field then determined beta poloidal. The degeneracy implicit in Shafranov's result (i.e., that only a combination of beta poloidal and internal inductance is measurable for a circular plasma cross section) reasserts itself as the elliptic results are collapsed to their circular limits. DOE

N93-10353 Princeton Univ., NJ.
REFLECTION OF PLASMA IONS FROM METALS (AND ITS USE AS A HYPERTHERMAL NEUTRAL BEAM SOURCE) Ph.D. Thesis
John William Cuthbertson 1991 222 p
Avail: Univ. Microfilms Order No. DA9202516

Reflection of ions as neutral atoms at energies below 100 eV has important implications for fusion and other technologies, and can form the basis of a useful hyperthermal neutral beam. Experimental measurements of properties of such reflected atoms are presented. The apparatus developed for this work uses the acceleration of plasma ions across the sheath to a metal reflecting plate biased relative to the plasma potential. Ions are created by a coaxial RF (lower hybrid) plasma source with a 4 kG confining field. The plasma physics determining the characteristics of the ion current to the plate is discussed, and measurements of plasma parameters are presented. Measurements of the energy distribution of reflected atoms were made with a mass spectrometer/cylindrical mirror analyzer in experiments with several gases (Ar, Kr, NE, N, O) and metals (Ta, Mo, steel, Al), at several reflection angles. Peaked distributions were observed where the target atomic mass m(2) exceeded the projectile mass m(1), while only monotonic decreasing 'tails' were seen where m(2) was greater than m(1). The spectrum's peak energy increases with incident energy E(inc), while E(pk)/E(inc) decreases for increasing E(inc) and increases with m(2)/m(1) (but more slowly than for binary collisions). Measurements were also made of the absolute atomic flux for oxygen beams, and the angular distribution, which is forward-peaked. Energy distribution measurements are compared to predictions of the Monte Carlo code TRIM, which uses the sequential binary collision mode. The results differ from TRIM predictions that E(pk)/E(inc) is nearly constant with E(inc) in the observed range and increases faster than observed with m(2)/m(1). The observed behavior of E(pk)/E(inc) implies the projectile is reflected from a collective mass greater than m(2) which increases as E(inc) decreases. An n-body simulation was written to examine the effects of simultaneous interaction with multiple target atoms. The results indicate that projectiles at hyperthermal energies are reflected in a process which is not binary in character, with the effective mass of the target increasing as E(inc) falls and simultaneous interactions become more important. The process is not correctly described by a binary collision model.
Dissert. Abstr.

N93-10390# General Atomic Co., San Diego, CA.
A FORMULA FOR EFFICIENCY OF FAST WAVE CURRENT DRIVE IN FUSION DEVICES
S. C. Chiu, R. W. Harvey, C. F. F. Karney (Princeton Univ., NJ.), and T. K. Mau (California Univ., Los Angeles.) Jun. 1992 4 p Presented at the Topical Conference Meeting on Radio Frequency

Heating and Current Drive of Fusion Devices, Brussels (Belgium), 7-10 Jul. 1992
(Contracts DE-AC03-89ER-53277; DE-AC02-76CH-03073)
(DE92-016152; GA-A-20873; CONF-920717-1) Avail: CASI HC A01/MF A01

Fast wave current drive (FWCD) is a principal candidate for non-inductive current drive schemes in reactors. Major experiments are in progress or planned on D3-D, Joint European Torus (JET), and Tore-Supra. A theory for FWCD was presented by two of the authors and collaborators. To minimize computations required in transport simulations, and for analytical understanding, it is very useful to have a concise analytical efficiency formula. Researchers have obtained empirical formulae that fit numerical results for the Landau limit and Alfven limit; the latter fits results at 1 less than Z(sub i) less than or equal to 2. This paper extends a previous numerical study on FWCD at arbitrary frequencies and Z(sub i). Analytical formulae for FWCD efficiency, valid for all frequencies and Z(sub i), are derived using the adjoint technique in high and low phase velocity regions. A smooth patching between the two regions produces an analytical formula which is accurate for all frequencies, Z(sub i), and phase velocities. Comparison with existing results will be discussed. A corollary of the present calculation is that at low phase velocities and in the Landau limit, the efficiency is the same as that calculated from the Lorentz model collision operator. DOE

N93-10392# General Atomic Co., San Diego, CA.
INVESTIGATION OF THE EFFECT OF LARGE CORE CHANGES IN TOROIDAL PLASMA ROTATION AND RADIAL ELECTRIC FIELD ON CONFINEMENT IN H-MODE DISCHARGES IN THE D3-D TOKAMAK
R. J. LaHaye, R. J. Groebner, A. W. Hyatt, and J. T. Scoville May 1992 4 p Presented at the 14th International Conference on Plasma and 19th EPS Conference on Controlled Fusion and Plasma Physics, Innsbruck (Austria), 29 Jun. - 3 Jul. 1992
(Contract DE-AC03-89ER-51114)
(DE92-016252; GA-A-20909; CONF-920610-4) Avail: CASI HC A01/MF A01

The plasma toroidal rotation and the radial electric field in the core (rho approximately less than 0.9) of H-mode discharges in D3-D are greatly altered by the drag produced by application of static, resonant magnetic field perturbations from an external coil (the n = 1 coil). Transport loss due to turbulent fluctuations can in theory be reduced by E(sub r) shear stabilization or suppression. This is tested experimentally in D3-D by using 'the magnetic breaking' of rotation (with concomitant change in E(sub r)) as an independent control. The magnetic braking produces reversal of the core radial electric field, E(sub r), and E(sub r) shear. However, the plasma maintains a negative edge (rho approximately less than 0.95) E(sub r) and E(sub r) shear and remains in H-mode with insignificant changes in global confinement, density profile, and temperature profiles. The H-mode confinement is remarkably robust to the increasing error fields and the slowed toroidal rotation up to the onset of a locked mode which induces a transition to L-mode, the virtual cessation of plasma rotation and large reconnected islands. DOE

N93-10393# General Atomic Co., San Diego, CA.
POLARIMETRY OF MOTIONAL STARK EFFECT AND DETERMINATION OF CURRENT PROFILES IN D3-D
D. Wroblewski (Lawrence Livermore National Lab., CA.) and L. L. Lao May 1992 35 p Presented at the 9th Topical Conference on High-Temperature Plasma Diagnostics, Santa Fe, NM, 15-19 Mar. 1992
(Contracts DE-AC03-89ER-51114; W-7405-eng-48)
(DE92-016258; GA-A-20881; CONF-920362-34) Avail: CASI HC A03/MF A01

The motional electric field E = v x B, where v is the velocity and B is the tokamak magnetic field, produces a strong Stark effect in spectral lines emitted by hydrogenic neutral beams. The tilt angle of the magnetic field line, a quantity related directly to the distribution of the plasma toroidal current, is deduced from a measurement of the direction of polarization of the Stark components. In the D3-D tokamak, the Balmer-alpha line of deuterium emitted by one of the high-power heating beams is analyzed. A multichord polarimeter measures the magnetic field pitch angle at eight spatial locations covering approximately 0.6 of the nominal plasma diameter at the midplane outboard side. The diagnostic offers 2 to 8 cm resolution in the major radius and 1 ms integration time. The accuracy of the measurement of the polarization direction necessary for an adequate reconstruction of the current profiles is obtained with the use of active polarizing elements which produce high frequency intensity modulation with an amplitude related to the direction of linear polarization of the plasma radiation. The current profiles in highly shaped (non-circular) plasmas cannot be determined solely from the tilt angle measurements because they do not provide any information about the shape of magnetic surfaces. Thus, the polarization measurement are used in conjunction with a large set of external magnetic measurements (magnetic field and flux probes, diamagnetic loops, and Rogowski coils) by the magnetic field equilibrium code EFIT, and provide a constraint on the possible solutions for the current profile. DOE

N93-10413# North Carolina Univ., Chapel Hill. Dept. of Chemistry.
KINETICS OF OXIDATION OF SILICON BY ELECTRON CYCLOTRON RESONANCE PLASMAS
J. Joseph, Y. Z. Hu, and E. A. Irene 13 Jul. 1992 11 p
(Contract N00014-89-J-1178)
(AD-A253140; TR-45) Avail: CASI HC A03/MF A01

In-situ ellipsometry, both single wavelength and spectroscopic, has been used to study the electron cyclotron resonance plasma oxidation of Si. Spectroscopic ellipsometry has been used to establish that the best fit optical model for the oxidation is a two layer model where the interface layer forms early and stabilizes, and the outer layer is SiO2. The interface layer is modeled well as a mixture of a-Si and oxide. The kinetics of film growth were followed using single wavelength ellipsometry at a temperature insensitive wavelength, and the results were in agreement with the Cabrera-Mott theory. GRA

N93-10443# Sandia National Labs., Albuquerque, NM.
FUTURE DIRECTIONS IN PULSED POWER DRIVEN ICF
D. Cook 1992 6 p Presented at the Fusion Power Associates Annual Meeting and Symposium, Pleasanton, CA, 9 Apr. 1992
(Contract DE-AC04-76DP-00789)
(DE92-016233; SAND-92-0942C; CONF-9204146-3) Avail: CASI HC A02/MF A01

The first major round of target experiments driven by intense light ion beams was conducted during August and September 1991. In these experiments, intense proton beams were used to drive two different types of targets. We attempted to obtain information on the two separable issues of ion deposition and implosion hydrodynamics. Ion deposition was studied using a low density hydrocarbon foam contained within a cylindrical gold shell. Implosion hydrodynamics was studied using an ion driven exploding pusher configuration in which the ion beam heated the shell directly, exploding it both outward and inward. One of the main objectives of the experiments was to determine the extent to which we could diagnose the ion deposition and the subsequent behavior of the targets. The diagnostics included time-integrated and time-resolved x-ray pinhole cameras, time-integrated and time-resolved grazing incidence x-ray spectrometers, an 11-channel filtered x-ray diode (XRD) array, an 11-channel PIN diode array, an energy-resolved 1-dimensional imaging x-ray streak camera, a transmission grating spectrometer, an elliptical crystal x-ray spectrograph, and a bolometer. Intense beam diagnostics included an ion movie camera and an off-axis 1D slit imaging magnetic spectrograph for obtaining Rutherford-scattered ion images, momenta, and ion power densities. DOE

N93-10463# General Atomic Co., San Diego, CA.
VH-MODE DISCHARGES IN THE D3-D TOKAMAK
C. M. Greenfield, G. L. Jackson, K. H. Burrell, J. C. DeBoo, L. L. Lao, T. H. Osborne, D. P. Schissel, T. S. Taylor, C. Rettig, and J.

Winter May 1992 4 p Presented at the 14th International Conference on Plasma and 19th EPS Conference on Controlled Fusion and Plasma Physics, Innsbruck, Austria, 29 Jun. - 3 Jul. 1992

(Contract DE-AC03-89ER-51114)
(DE92-016257; GA-A-20917; CONF-920610-8) Avail: CASI HC A01/MF A01

A regime of very high confinement (VH-mode) was observed in divertor discharges in D3-D. The VH-mode, first seen following the initial boronization of the D3-D vessel in 1991, exhibits total energy confinement a factor of 2.5 to 3.5 greater than that predicted by the ITER89-P L-mode scaling relation. Also, confinement of thermal energy alone is greater than 1.6 times that of the JET/D3-D H-mode scaling and in many cases has exceeded twice that amount. VH-mode is observed during a long (less than or equal to 0.8 sec) ELM-free phase of the discharges. At the beginning of the ELM-free period, the plasma appears to be in H-mode, with confinement near that predicted by the JET/D3-D scaling. In the usual H-mode, confinement is observed to decrease or remain constant over time. In the present discharges, confinement was observed to remain nearly constant for up to hundreds of milliseconds, after which the behavior sharply deviates from H-mode as the confinement begins to increase over time. This increase in confinement continues until the occurrence of a beta-related (beta greater than 2.8 I/aB) global MHD event, which rapidly decreases the plasma stored energy with a temperature reduction across the entire profile. Magnetic measurements indicate that at least in some cases, this event includes both an internal n = 1 mode and a more localized high-n mode near the edge. After this event, the plasma relaxes into an ELMing H-mode phase. As a consequence of the boronization, the plasmas in these discharges are unusually clean, with very low radiated power. In previous H-mode discharges, the radiated power increased during the ELM-free, sometimes reaching levels comparable with the input power if the ELM-free period was long enough. Also, Z(sub eff)is constant or decreasing over the length of the discharge, with a central value of approximately 1. It is noted that most of the energy in these discharges is thermal energy, with less than or equal to 10 percent contained in fast ions. DOE

N93-10464# Department of Energy, Washington, DC. Applied Plasma Physics Div.

EXPERIMENTAL PLASMA RESEARCH PROJECT SUMMARIES

Jun. 1992 215 p

(DE92-016274; DOE/ER-0550T) Avail: CASI HC A10/MF A03

This is the latest in a series of Project Summary books that date back to 1976. It is the first after a hiatus of several years. They are published to provide a short description of each project supported by the Experimental Plasma Research Branch of the Division of Applied Plasma Physics in the Office of Fusion Energy. The Experimental Plasma Research Branch seeks to provide a broad range of experimental data, physics understanding, and new experimental techniques that contribute to operation, interpretation, and improvement of high temperature plasma as a source of fusion energy. In pursuit of these objectives, the branch supports research at universities, DOE laboratories, other federal laboratories, and industry. About 70 percent of the funds expended are spent at universities and a significant function of this program is the training of students in fusion physics. The branch supports small- and medium-scale experimental studies directly related to specific critical plasma issues of the magnetic fusion program. Plasma physics experiments are conducted on transport of particles and energy within plasma. Additionally, innovative approaches for operating, controlling, and heating plasma are evaluated for application to the larger confinement devices of the magnetic fusion program. New diagnostic approaches to measuring the properties of high temperature plasmas are developed to the point where they can be applied with confidence on the large-scale confinement experiments. Atomic data necessary for impurity control, interpretation of diagnostic data, development of heating devices, and analysis of cooling by impurity ion radiation are obtained. The project summaries are grouped into the three categories of plasma physics, diagnostic development, and atomic physics. DOE

N93-10615# North Carolina Univ., Chapel Hill. Dept. of Chemistry.

LANGMUIR PROBE AND OPTICAL EMISSION STUDIES OF Ar, O2, AND N2 PLASMAS PRODUCED BY AN ECR MICROWAVE SOURCE

A. A. Shatas, Y. Z. Hu, and E. A. Irene 13 Jul. 1992 24 p

(Contract N00014-89-J-1178)
(AD-A253138; TR-42) Avail: CASI HC A03/MF A01

An understanding of electron cyclotron resonance microwave plasma discharges requires the measurement of plasma parameters. In argon, nitrogen, and oxygen plasmas, cylindrical Langmuir probes were used to determine the variations of plasma parameters (ion density, Ni, floating potential, Vf, plasma potential, Vp, and electron temperature, Te) with applied power (100-300 W) and pressures (1-10 x 10 exp -4 Torr). Simultaneous optical emission (OE) spectra were also obtained, and, using knowledge of excited and neutral peak intensities and transition energies, the electron temperatures were calculated. By the use of the Langmuir probe electron temperature results, the electron temperatures obtained from OE resulted in scaling factors, C, of 2 eV exp -.75, .15 eV exp -.75, and 2 eV exp -.75 for argon, oxygen, and nitrogen, respectively. GRA

N93-10617# California Univ., Irvine. Dept. of Physics.

LARGE ORBIT MAGNETIC CONFINEMENT SYSTEMS FOR ADVANCED FUSION FUELS

N. Rostoker 1992 87 p

(Contract DE-FG03-90ER-54087)
(DE92-016218; DOE/ER-54087/T1) Avail: CASI HC A05/MF A01

The problem of magnetic confinement of plasmas where the majority of ions have large gyro-orbits and do not obey adiabatic particle dynamics is discussed. The electrons are adiabatic. We considered a class of equilibria where large orbit ions dominate; the equilibria are rigorous solutions of the Vlasov/Maxwell equations. For a simple case--the infinitely long, low beta, rotating plasma--a complete stability analysis was carried out. This problem was the basis of the first paper on finite Larmor radius stabilization. In that paper an expansion in epsilon = (bar-alpha(sub i))/r(sub 0) was carried out to the first significant order beyond MHD. In this report the same problem is solved to all orders in epsilon. While this case is of limited applicability to experiments it is rigorous and without approximations, so that it can be used to verify approximations to be developed for more complex and useful cases. The application of the results to small fusion reactors is described in the second paper which was written after the termination of the contract, but is based in part on material developed during the contract period. DOE

N93-10619# General Atomic Co., San Diego, CA.

EDGE ION DYNAMICS IN H-MODE DISCHARGES IN D3-D

R. J. Groebner, K. H. Burrell, P. Gohil, J. Kim, and R. P. Seraydarian May 1992 4 p Presented at the 14th International Conference on Plasma and 19th EPS Conference on Controlled Fusion and Plasma Physics, Innsbruck, Austria, 29 Jun. - 3 Jul. 1992

(Contract DE-AC03-89ER-51114)
(DE92-016255; GA-A-20912; CONF-920610-5) Avail: CASI HC A01/MF A01

The goal of this paper is to present detailed measurements of T(sub i) and E(sub r) at the plasma edge in L- and H-mode with high spatial resolution in order to study the edge ion dynamics. Of primary interest is the relationship between T(sub i) and E(sub r) and the behavior of the edge T(sub i) profile in H-mode. The principle findings are as follows: there appears to be a threshold temperature for T(sub i) required for the transition to occur with T(sub i) at the LCFS in the range of 0.2-0.3 keV at the transition; a correlation between the edge E(sub r) profile and the edge T(sub i) profile was observed; and values of T(sub i) of 2-3 keV within a few cm of the LCFS and of the derivative of T(sub i) with respect to r of up to 1 keV/cm are observed in the transport barrier in H-mode, with the scale length for T(sub i) being of the order of a poloidal gyroradius. DOE

N93-10620# General Atomic Co., San Diego, CA.
THE EFFECT OF CURRENT PROFILE CHANGES ON CONFINEMENT IN THE D3-D TOKAMAK
J. R. Ferron, L. L. Lao, and T. S. Taylor May 1992 4 p Presented at the 14th International Conference on Plasma and 19th EPS Conference on Controlled Fusion and Plasma Physics, Innsbruck, Austria, 29 Jun. - 3 Jul. 1992
(Contract DE-AC03-89ER-51114)
(DE92-016256; GA-A-20913; CONF-920610-7) Avail: CASI HC A01/MF A01

Experiments in the D3-D tokamak have demonstrated that the effect of changes in the current profile on plasma confinement varies with the discharge shape. The results are similar in many respects to those from other tokamaks. In all cases, a rapid change in the plasma current in an L-mode, circular or moderately elongated, discharge was used to produce a transient change in the current density profile. Although the detailed results vary among tokamaks, it is generally observed that during and immediately following a negative plasma current ramp, the stored energy does not follow the L-mode scaling that predicts that confinement should be proportional to the total plasma current. The stored energy changes on the time scale of the relaxation of the current density profile rather than the shorter time scales of the energy confinement time or the change in the total current. Because of the discharge shaping capability of the D3-D tokamak it was possible to extend these current ramp experiments beyond the L-mode, moderate elongation case to highly elongated double-null divertor discharges in H-mode. In separate experiments, a rapid change in the discharge elongation was also used to vary the current density profile. This paper shows that the dependence of the plasma confinement on the current profile changes when the discharge shape is changed. This variation with discharge shape provides evidence for a model that predicts that changes in the local magnetic shear resulting from the changes in the current profile can result in decreased local transport. DOE

N93-10645# Argonne National Lab., IL.
DISPERSION OF SEED VAPOR AND GAS IONIZATION IN AN MHD SECOND STAGE COMBUSTOR AND CHANNEL
S. L. Chang, S. A. Lottes, and J. X. Bouillard 1992 12 p Presented at the 30th Symposium on Engineering Aspects of Magnetohydrodynamics, Baltimore, MD, 29 Jun. - 2 Jul. 1992
(Contract W-31-109-eng-38)
(DE92-016699; ANL/CP-75447; CONF-920677-15) Avail: CASI HC A03/MF A01

An approach is introduced for the simulation of a magnetohydrodynamic system consisting of a second stage combustor, a convergent nozzle, and a channel. The simulation uses an Argonne integral combustion flow computer code and another Argonne channel computer code to predict flow, thermal and electric properties in the seed particle laden reacting flow in the system. The combustion code is a general hydrodynamics computer code for two-phase, two-dimensional, turbulent, and reacting flows, based on mass, momentum, and energy conservation laws for gaseous and condensed phases. The channel code is a multigrid three-dimensional computer code for compressible flow subject to magnetic and electric interactions. Results of this study suggests that (1) the processes of seed particle evaporation, seed vapor dispersion, and gas ionization in the reacting flow are critical to the evaluation of the downstream channel performance, and (2) particle size, loading, and inlet profile have strong effects on wall deposition and plasma temperature development. DOE

N93-10754# Stuttgart Univ. (Germany). Inst. fuer Raumfahrtsysteme.
BASIC PROCESSES OF PLASMA PROPULSION Final Report, 15 Nov. 1990 - 14 Nov. 1991
Herbert O. Schrade, P. C. Sleziona, Thomas Wegmann, and Helmut L. Kurtz Apr. 1992 44 p
(Grant AF-AFOSR-0118-91)
(AD-A253929) Avail: CASI HC A03/MF A01

The report resumes the theoretical and analytical works, which accompanies the experimental development work on plasma thrusters done at the Institute of Space Systems, University of Stuttgart. GRA

N93-10759# General Atomic Co., San Diego, CA.
BORONIZATION IN D3-D
G. L. Jackson, K. H. Burrell, J. C. DeBoo, C. M. Greenfield, R. J. Groebner, T. Hodapp, A. G. Kellman, R. Lee, S. I. Lippman, and J. Phillips et al May 1992 17 p Presented at the 10th International Conference on Plasma-Surface Interactions in Controlled Fusion Devices, Monterey, CA, 30 Mar. - 3 Apr. 1992
(Contract DE-AC03-89ER-51114)
(DE92-016249; GA-A-20904; CONF-920311-19) Avail: CASI HC A03/MF A01

A thin boron film was applied to the D3-D tokamak plasma facing surfaces to reduce impurity influx, particularly oxygen and carbon. A direct result of this surface modification was the observation of a regime of very high energy confinement, VH-mode, with confinement times from 1.5 to 2 times greater than predicted by H-mode scaling relation for the same set of parameters. VH-mode discharges are characterized by low ohmic target densities, low edge neutral pressure, and reduced cycling. These conditions have reduced the collisionality, (nu)*, in the edge region producing a higher edge pressure gradient and a significant bootstrap current, up to 30 percent of the total current. We will describe the edge plasma properties after boronization including reductions in recycling inferred from measurements of (tau)(sub p)*. In particular we will discuss the edge plasma conditions necessary for access to VH-mode including the boronization process and properties of the deposited film. DOE

N93-10760# General Atomic Co., San Diego, CA.
GLOBAL ALFVEN EIGENMODES IN D3-D
A. D. Turnbull, M. S. Chu, E. J. Strait, L. L. Lao, J. M. Greene, T. S. Taylor, W. W. Heidbrink, H. Duong, and M. S. Chance Jun. 1992 4 p Presented at the 14th International Conference on Plasma and 19th EPS Conference on Controlled Fusion and Plasma Physics, Innsbruck, Austria, 29 Jun. - 3 Jul. 1992
(Contracts DE-AC03-89ER-53277; DE-AC02-76CH-03073; DE-AC03-89ER-51114)
(DE92-016250; GA-A-20935; CONF-920610-10) Avail: CASI HC A01/MF A01

Global Alfven modes, such as the Toroidicity-Induced Alfven Eigenmode (TAE), pose a serious threat for strongly-heated tokamaks since they can result in saturation of the achievable beam beta at moderate levels and they may also cause serious alpha-particle losses in future ignited devices. The D3-D tokamak has a unique capability for study of the resonant excitation of these instabilities by energetic beam ions. TAE modes were observed in D3-D over a wide range of operating conditions, including both circular cross-section and elongated (kappa approximately 1.8) discharges. Equilibrium reconstructions of several representative discharges, using all available external magnetic and internal profile data, were done and analyzed in detail. The computed real mode frequencies of the TAE modes are in good agreement with the experimentally observed mode frequencies and differ significantly from the estimated kinetic ballooning mode frequencies. The TAE calculations include coupling to the Alfven and acoustic continuum branches of the MHD spectrum and generally indicate that the simplified circular cross-section, large aspect-ratio assumptions made in analytic calculations are poor approximations to the actual TAE mode structures. In particular, the global TAE modes are almost always coupled to one or more continuum branches by toroidicity, poloidal shaping, and finite (beta) effects. Estimates of the various resonant excitation and damping mechanisms, including continuum damping, were made and the total is found to be in reasonable agreement with the experimental threshold. DOE

N93-10761# General Atomic Co., San Diego, CA.
VARIATIONAL FULL WAVE CALCULATION OF FAST WAVE CURRENT DRIVE IN D3-D USING THE ALCYON CODE

A. Becoulet and D. Moreau Apr. 1992 36 p
(Contract DE-AC03-89ER-51114)
(DE92-016572; GA-A-20846) Avail: CASI HC A03/MF A01

Initial fast wave current drive simulations performed with the ALCYON code for the 60 MHz D3-D experiment are presented. Two typical shots of the 1991 summer campaign were selected with magnetic field intensities of 1 and 2 teslas respectively. The results for the wave electromagnetic field in the plasma chamber are displayed. They exhibit a strong enrichment of the poloidal mode number m-spectrum which leads to the upshift of the parallel wavenumber, kappa(sub parallel), and to the wave absorption. The m-spectrum is bounded when the local poloidal wavenumber reaches the Alfven wavenumber and the (kappa)(sub parallel) upshifts do not destroy the wave directionality. Linear estimations of the driven current are made. The current density profiles are found to be peaked and we find that about 88 kA can be driven in the 1 tesla/1.7 keV phase with 1.7 MW coupled to the electrons. In the 2 tesla/3.4 keV case, 47 kA are driven with a total power of 1.5 MW, 44 percent of which are absorbed on the hydrogen minority, through the second harmonic ion cyclotron resonance. The global efficiency is then 0.18(10)(exp 19) A m(exp -2) W(exp -1) if one considers only the effective power going to the electrons. DOE

N93-10819# MSE, Inc., Butte, MT.
MAGNETOHYDRODYNAMIC PROJECTS AT THE CDIF
1992 18 p
(Contract DE-AC22-88ID-12735)
(DE92-018190; DOE/ID-12735/T23) Avail: CASI HC A03/MF A01

The Component Development and Integration Facility (CDIF) is a major U.S. Department of Energy magnetohydrodynamics (MHD) test facility in Butte, Montana. The CDIF is operated by MSE, Inc. Within the national MHD program, MSE personnel are responsible for performing integration testing of vendor-supplied MHD power train components at the CDIF to support the goal of commercialization. During the second quarter of FY-92, a second external water leak on the iron-core magnet was repaired, and MHD testing was completed on 11 Feb.; this was the final testing of the workhorse hardware. Workhorse hardware was removed, and installation of the proof-of-concept (POC) combustor began. DOE

N93-10839# Sandia National Labs., Albuquerque, NM.
A FIVE-CHANNEL, DIAMOND PHOTOCONDUCTING X RAY DETECTOR ARRAY FOR z-PINCH EXPERIMENTS
R. B. Spielman May 1992 17 p
(Contract DE-AC04-76DP-00789)
(DE92-017345; SAND-92-0580) Avail: CASI HC A03/MF A01

We have built a five-channel, x-ray detector array based on diamond photoconducting detectors (PCD's). The diamond elements have dimensions of 3 mm x 1 mm x 1 mm (or 0.5 mm). We use PCD's for their stability, flat spectral response, and low leakage currents. The good time response of diamond PCD's is due to the 100-ps electron/hole recombination time. Filters were designed to give information in the 1-10 keV spectral region. Calibration of the diamond PCD's showed sensitivities between 4-7 x 10(exp -4) A/W for a bias of 100 V. We shall present data from z-pinch experiments on Saturn. DOE

N93-10861# TRW Space Technology Labs., Redondo Beach, CA. Applied Technology Div.
MHD INTEGRATED TOPPING CYCLE PROJECT Quarterly Technical Progress Report No. 16
Mar. 1992 154 p
(Contract DE-AC22-87PC-90274)
(DE92-016610; DOE/PC-90274/T17; MHD-ITC-92-033) Avail: CASI HC A08/MF A02

The Magnetohydrodynamics (MHD) Integrated Topping Cycle (ITC) Project represents the culmination of the proof-of-concept (POC) development stage in the US Department of Energy (DOE) program to advance MHD technology to the early commercial development stage for utility power applications. The project is a joint effort, combining the skills of three topping cycle component developers: TRW, Avco/TDS, and Westinghouse. TRW, the prime contractor and system integrator, is responsible for the 50 thermal megawatt (50 MW(sub t)) slagging coal combustion subsystem. Avco/TDS is responsible for the MHD channel subsystem (nozzle, channel, diffuser, and power conditioning circuits), and Westinghouse is responsible for the current consolidation subsystem. The ITC Project will advance the state-of-the-art in MHD power systems with the design, construction, and integrated testing of 50 MW(sub t) power train components which are prototypical of the equipment that will be used in an early commercial scale MHD utility retrofit. Long duration testing of the integrated power train at the Component Development and Integration Facility (CDIF) in Butte, Montana will be performed, so that by the early 1990's, an engineering data base on the reliability, availability, maintainability, and performance of the system will be available to allow scaleup of the prototypical designs to the next development level. DOE

76 SOLID-STATE PHYSICS

Includes superconductivity.

For related information, see also *33 Electronics and Electrical Engineering* and *36 Lasers and Masers.*

N93-10093# Washington State Univ., Pullman.
THEORY OF LIGHT-INDUCED DRIFT OF ELECTRONS IN COUPLED QUANTUM WELLS
Mark I. Stockman, Leonid S. Muratov, and Thomas F. George Jul. 1992 24 p
(Contract N00014-90-J-1193)
(AD-A253609; WSU/92/89) Avail: CASI HC A03/MF A01

A theory of the new effect of light-induced drift (LID) in coupled potential wells is developed on the basis of the density-matrix method. The effect appears when light excites intersubband electronic transitions. LID manifests itself as the photocurrent of the 2-D electron gas in the well plane, which depends on coherent electron tunneling between the coupled wells. The theory shows the effect to possess distinctive features such as a characteristic antisymmetric spectral contour consisting of four alternating positive and negative peaks and the change of sign of the LID current with the sign change of the bias normal to the quantum-well plane. The quantitative estimates for GaAs wells show the LID current to be readily detectable. GRA

N93-10099# Naval Research Lab., Washington, DC.
MOLECULAR DYNAMICS OF SHOCKS IN CRYSTALS WITH DEFECTS Interim Report
Lee Phillips, Robert S. Sinkovits, Elaine S. Oran, and Jay P. Boris 15 Jul. 1992 43 p
(AD-A253353; NRL/MR/4440-92-6998) Avail: CASI HC A03/MF A01

We examine, using computational molecular dynamics, shocks launched in two-dimensional crystals by a flying plate. The interaction of the shock with various lattice defects is observed, and is seen to create sites of rapidly growing, thermalized, hot fluid-like phases included within the crystal lattice. We hypothesize that these included fluid-like regions that are the sites of the initial chemical reactions leading to detonation in energetic materials, and that crystallographic defects, therefore, control the sensitivity of single crystal high explosives to shock-initiation. The computations are carried out on the massively parallel Connection Machine using a parallelized version of the MLG algorithm. GRA

N93-10105# Oregon Univ., Eugene. Dept. of Chemistry.
NONLINEAR STUDIES OF SURFACE AND INTERFACES OF ADVANCED SEMICONDUCTOR MATERIALS Final Report, 1 Mar. 1989 - 28 Feb. 1992
Geraldine L. Richmond and Stephen D. Kevan 8 Jul. 1992 4 p
(Contract DAAL03-89-K-0051)
(AD-A253365; ARO-26191-CH) Avail: CASI HC A01/MF A01

A growing interest has developed in the past few years

regarding the role that optical second harmonic generation (SHG) can play in characterization of buried interfaces. This interest arises from the unique sensitivity of SHG to the properties of the interface itself with inherent discrimination against properties of the adjacent bulk media. In UHV studies, it has been used to monitor surface structure, adsorption and desorption of molecules, and surface melting. Much of interest during this time has been to investigate the fundamental aspects of the optical second harmonic generation to the solid/liquid interface and solid/solid junction. In previous electrochemical studies, we have demonstrated the sensitivity of SHG to film growth, molecular and ionic adsorption, and potential dependent effects associated with changes in surface morphology, all on single crystal and smooth polycrystalline surfaces. Our most extensive investigations have involved measuring surface order, surface electronic structure, and thin film deposition in situ on crystalline metal electrodes by analysis of the rotational anisotropy in the polarized SH response. More recently, we have expanded the work to study oxidation of metals and the metallization of semiconductor surfaces. GRA

N93-10206# Stanford Univ., CA. Synchrotron Radiation Lab.
EPITAXIAL GROWTH AND DOPANT INCORPORATION IN DIAMOND Final Report, 1 Feb. 1987 - 30 Sep. 1990
B. B. Pate 30 Jun. 1992 8 p
(Contract N00014-87-K-0262)
(AD-A253636) Avail: CASI HC A02/MF A01

We summarize our experimental studies of the microscopic structure of diamond. We have used Angle Resolved Photo-Electron Spectroscopy (ARPES) to study the electronic structure of the reconstructed (111) 2 x 1 surface and the clean (110) surface which might be topologically similar. We confirm the Pandey pi-bonded structure, of the (111) 2 x 1 surface and find that the clean (110) surface is distinct from the ideal structure. Extended x-ray absorption fine structure (EXAFS) measurements of diamond and graphite demonstrate the applicability of the standard spherical-wave EXAFS analysis in low Z (atomic number) systems such as diamond. This work provides the basis for future Surface EXAFS (SEXAFS) measurements of the local structure of dopants and impurities in/on diamond. Collaboration with M. Geis at MIT Lincoln Labs resulted in an electrical measurement study of the silicon oxide-NEA (negative electron affinity) diamond interface. We showed that there is no electrostatic barrier to electron emission into SiO2 from the diamond conduction band. GRA

N93-10210# Arizona State Univ., Tempe. Coll. of Engineering and Applied Sciences.
SPATIAL LIGHT MODULATORS WITH ARBITRARY QUANTUM WELL PROFILES Annual Report, 14 Jan. 1991 - 1992
George N. Marcas and Krishan K. Bajaj 3 Feb. 1992 42 p
(Grant AF-AFOSR-0118-90)
(AD-A253637; AFOSR-92-0657TR) Avail: CASI HC A03/MF A01

This is the 2nd year technical report for the University Research Initiative (URI) Program, Spatial Light Modulators with Arbitrary Quantum Well Profiles. During the second year of the program, we have continued to optimize optical modulator design, growth, and fabrication. A new method for self-consistent solution of Schroedinger and Poisson equations was developed and used to predict modulator active region performance and vertical cavity surface emitting laser device performance. A comprehensive comparison of asymmetric triangular quantum wells (ATQW) using GaAs/AlGaAs, InGaAs/GaAs, and InGaAs/AlGaAs showed InGaAs/AlGaAs quantum wells to have the highest optical efficiency. A MBE compositional grading technique was used to achieve record narrow photoluminescence linewidths for nonrectangular quantum wells. Bragg reflectors for use in Fabry Perot modulators were measured in-situ by spectroscopic ellipsometry (SE). Advances were made in the growth and fabrication of p-i-n optical modulators, including the development of via hole etching through the substrate for transmission mode modulators. A simple variational method for calculating excitonic properties in quantum confined structures with arbitrary potential profiles in the presence of applied electric and magnetic fields were developed and applied to the study of energy levels of hydrogenic impurities. Also, a theory of radiative transition linewidths due to alloy disordering in semiconductor alloys has been presented and applied to AlGaAs and InGaP bulk alloys. GRA

N93-10225# International Centre for Theoretical Physics, Trieste (Italy).
QUANTUM TUNNELING AND THE CHANGE IN THE SIGNATURE OF THE SPACETIME METRIC
Y. I. Anini Mar. 1992 13 p
(DE92-634877; IC-92/46) Avail: CASI HC A03/MF A01

Three examples where the quantum tunneling process may be viewed as a motion in the Euclidean time are presented. That is, the tunneling object (particle/field/universe) may be viewed to move in a spacetime with Euclidean signature (+ + + +) metric (Riemannian metric) in the classically forbidden region. However, we emphasize the fact that in all three of the examples the quantity that has direct physical meaning is the tunneling probability through the classically forbidden region, i.e., through the potential barrier. DOE

N93-10235# Ghent Univ. (Belgium).
NOVEL OPTOELECTRONIC DEVICES BASED ON COMBINING GaAs AND InP ON Si Interim Report No. 6
P. Demeester 1992 8 p
(Contract DAJA45-90-C-0003)
(AD-A253781; R/D-6291-EE-01) Avail: CASI HC A02/MF A01

We have concentrated on the application of the shadow masked growth technique to the fabrication of optoelectronic devices. We have shown the fabrication of GaAs/AlGaAs and InP/InGaAsP (strained) QW multi-wavelength laser arrays and the use of SMG for the integration of a passive and active waveguiding section in GaAs based materials. On the n-doped substrate (with the shadow mask) we have deposited a 500 nm n-doped lower InP cladding layer and an undoped active region consisting of four InGaAs strained quantum wells with InGaAsP barriers and separate confinement layers. GRA

N93-10245# Pennsylvania State Univ., University Park. Dept. of Chemistry.
FIELD EMISSION CURRENT-VOLTAGE CURVES AS A DIAGNOSTIC FOR SCANNING TUNNELING MICROSCOPE TIPS Technical Report, 1 Jun. 1991 - 30 May 1992
J. A. Meyer, S. J. Stranick, J. B. Wang, and P. S. Weiss 1 Dec. 1991 14 p
(Contract N00014-91-J-1630)
(AD-A251171; TR-1) Avail: CASI HC A03/MF A01

The current-voltage (I-V) characteristics of a low temperature ultrahigh vacuum scanning tunneling microscope (STM) tip positioned greater than 100 A from a planar surface have been recorded. We find curvature in the Fowler-Nordheim plots (log 10 I/V(sup 2) vs. I/V) due to the tip-plane geometry as has been predicted theoretically. Additionally, oscillations and sharp breaks in these I-V curves are observed over a wide voltage range, 50-1000 V. These I-V curves are used to characterize the STM tips prior to tunneling. GRA

N93-10274# Advanced Technology Materials, Inc., Danbury, CT.
IMPLANTED CONTACTS FOR DIAMOND SEMICONDUCTOR DEVICES Final Report, 12 Feb. - 11 Dec. 1991
Soo-Hee Tan and C. P. Beetz, Jr. 27 Jan. 1992 24 p
(Contract DASG60-91-C-0025)
(AD-A245568) Avail: CASI HC A03/MF A01

The key to future diamond semiconductor development are ohmic and Schottky contacts that are stable at high temperatures. Wide bandgap materials, such as diamond (5.5 eV), pose special problems and demand ingenious solutions. Prior to our work, recent research into stable ohmic and Schottky contacts had been primarily limited to e-beam evaporation of carbide forming metals such as Ti, Ta, and Mo. These approaches have been relatively

successful at decreasing the specific contact resistivity to as low as 10(exp -5) ohm sq cm on natural semiconducting diamond with about 10(exp 16) boron atoms/cubic cm. In our Phase 1 SBIR program we investigated metal systems coupled with a shallow Si implant that would form low resistivity, high temperature stable metal silicides. We showed in our Phase 1 results that the barrier height of metals such as Pt, Ti and Mo were reduced when deposited on shallow Si implants and given a heat treatment at 500 C. The barrier height of Pt on diamond was reduced from 1.89 to 0.97 eV by annealing of a sputtered Pt contact on a Si implanted dose of 10(exp 15) cm(exp -2) sq A into the diamond surface. Using the same approach, the barrier height of Ti on diamond was reduced from 2.00 to 1.29 eV. GRA

N93-10284# Texas Univ., Austin. Dept. of Chemistry.
ELECTRON TRANSFER REACTIONS IN MICROPOROUS SOLIDS
T. E. Mallouk May 1992 5 p
(Contract DE-FG05-87ER-13789)
(DE92-016222; DOE/ER-13789/5) Avail: CASI HC A01/MF A01

We have studied electron transfer quenching of the excited state of Ru3(2+) in aqueous suspensions of zeolites Y, L, and mordenite. The internal pore network of the zeolite is ion-exchanged with methylviologen cations, which quench the excited state of the surface-bound sensitizer. A detailed study of the quenching and charge recombination kinetics, using time-resolved luminescence quenching and transient diffuse reflectance spectroscopies, shows two remarkable effects: first, the excited state quenching is entirely dynamic is large-pore zeolites (L and Y), even when they are prepared as apparently 'dry' powders (which still contain significant amounts of internally sited water). Second, a lower limit for the diffusion coefficient of the MV(2+) ion in these zeolites, determined by this technique, is 10(exp -7) sq cm sec, i.e., only about one order of magnitude slower than a typical ion in liquid water, and 2 to 3 orders of magnitude faster than charge transfer diffusion of cations in polyelectrolyte films or membranes such as Nafion. Surface sensitization of internally platinized layered oxide semiconductors such as K(4-x)H(x)Nb6O17 - nH2O(x approx. = 2.5) yields photocatalysts for the production of H2 and I3(-) in aqueous iodide solutions. Layered alkali niobates and titanates form a class of zeolitic wide-bandap semiconductors, and are the first examples of photocatalysts that evolve hydrogen from an electrochemically reversible (i.e., non-sacrificial) electron donor with visible light excitation. DOE

N93-10335# Litton Systems, Inc., Morris Plains, NJ. Airtron Div.
DEVELOPMENT OF GARNET FILMS FOR MAGNETOSTATIC WAVE CHANNELIZED RECEIVERS Final Report, 1 Oct. 1989 - 1 May 1992
R. F. Belt and J. B. Ings 30 Jun. 1992 52 p
(Contract N00014-89-C-2228)
(AD-A252812) Avail: CASI HC A04/MF A01

Single Crystal films of Bi(3-x)Lu(x)Fe5O12 were grown by liquid phase epitaxy on one inch diameter wafers of GGG. Most compositions were centered about X = 2.17 with dopants of Mg(2+) to control the optical absorption. More than 100 experimental films were grown under a variety of growth conditions. The film properties were measured at Airtron and correlated with growth conditions. In addition, measurements of optical absorption, electrical resistivity, resonance linewidth, and Faraday rotation were performed on selected samples. Microwave passband measurements were also conducted at University of Delaware and Westinghouse Research Laboratory to determine the suitability of our films for channelizer devices. Thus far an unknown problem with these films has prevented passband measurements equivalent to pure YIG films. GRA

N93-10345# Pennsylvania State Univ., University Park. Dept. of Electrical Engineering.
SEMICONDUCTOR PHASE CONJUGATION Final Report, Jul. 1988 - Jul. 1991
Iam-Choon Khoo May 1992 18 p
(Contract F29601-88-K-0028)
(AD-A253684; PL-TR-91-1082; AD-E201073) Avail: CASI HC A03/MF A01

The HYWAYS PEP pilot line validated the producibility of long wavelength infrared hybrid sensor arrays with Si:As impurity band conduction detectors and advanced capacitance transimpedance amplifier readouts. The production capacity for processing, packing, and testing 10 hybrids/day was established. Ninety hybrids were delivered. Hybrid sensor arrays designed to Ground-based Surveillance and Tracking System specifications were processed, which satisfied interim proof-of-design requirements. A mathematical model was delivered that estimates the cost of long wavelength infrared hybrid sensor arrays based on format, quantity, and protected yield. GRA

N93-10355# North Carolina State Univ., Raleigh. Dept. of Materials Science and Engineering.
PSEUDOMORPHIC SEMICONDUCTING HETEROSTRUCTURES FROM COMBINATIONS OF AlN, GaN, AND SELECTED SiC POLYTYPES: THEORETICAL ADVANCEMENT AND ITS COORDINATION WITH EXPERIMENTAL STUDIES OF NUCLEATION, GROWTH, CHARACTERIZATION, AND DEVICE DEVELOPMENT Semiannual Report, 1 Jan. - 30 Jun. 1992
Robert F. Davis, K. S. Ailey-Trent, Scott Kern, Young K. Kim, and Philip Grigg Jun. 1992 34 p
(Contract N00014-90-J-1427)
(AD-A253330) Avail: CASI HC A03/MF A01

As an initial step toward the achievement of pseudomorphic heterostructures of nitride materials, thin films of an undoped and p-type doped Al(x)Ga(1-x)N solid solution as well as InN were successfully deposited using a modified gas source MBE system. Application of single layers of the Al(x)Ga(1-x)N solid solution or pure GaN films as UV light photon detectors was achieved. The gain exhibited by these detectors at a forward voltage of 5V was 500 micro-A and 10 mA for the solid solution films deposited on sapphire and alpha(6H)-SiC substrates, respectively. The GaN film deposited on sapphire exhibited a gain of 20 micro-A. Solid solutions and multilayers of AlN and SiC were also grown on 6H-SiC (0001) substrates cut 3-4 deg off-axis to (1120). Evidence is presented which suggests that the AlN-rich solid solutions are cubic. Pseudomorphic heterostructures of 6H-SiC, 2H-AlN, and 3C-SiC were produced for the first time. Each of the layers was monocrystalline, and the interfaces were chemically and structurally sharp and reasonably smooth. Moreover, each layer represents a different crystal structure and bandgap energy. In concert with this research, we are also investigating the chemical interdiffusion of AlN and SiC. Initial results indicate that the interdiffusivity of the four elements is approx. 10-14 sq cm/hr. Finally, initial research concerned with the BN on polycrystalline CVD diamond is reported. GRA

N93-10356# North Carolina State Univ., Raleigh. Dept. of Materials Science and Engineering.
GROWTH, NITROGEN VACANCY REDUCTION, AND SOLID SOLUTION FORMATION IN CUBIC GaN THIN FILMS AND THE SUBSEQUENT FABRICATION OF SUPERLATTICE STRUCTURES USING AlN AND InN Semiannual Report, 1 Jan. - 30 Jun. 1992
Robert F. Davis, K. S. Ailey-Trent, Daniel Kester, Michael J. Paisley, and Bill Perry Jun. 1992 62 p
(Contract N00014-86-K-0686)
(AD-A253331) Avail: CASI HC A04/MF A01

Undoped GaN films have been deposited by gas-source MBE having essentially intrinsic electrical character. Acceptor-type behavior has been achieved with Mg doping. The electrical properties of these latter films were resistivity = 0.5 omega-cm, Hall mobility (holes = 10 sq cm/V-s and carrier concentration = 1(10)(exp 18) cu cm. Photo-assisted gas-source MBE growth of stoichiometric GaN was also achieved using a 500 W Hg lamp. Illumination and Ga cell temperature altered the texture of the polycrystalline GaN in unusual ways, changing the growth habit from (0001) is parallel to (100) to (0001) is parallel to (111) and

back again. Thin films of cubic-BN (c-BN) were also deposited on various substrates via both gas-source MBE and electron beam MBE. The use of Si(100) substrates, the latter technique, and the characterization tools of RHEED, XPS, LEED, SEM, FTIR, and HRTEM resulted in the achievement of an initial amorphous BN layer followed by a layer of turbostratic BN and subsequently by a layer of cubic BN. Cubic BN films were also deposited on polycrystalline diamond films grown via CVD on Si(100). The effect of the bombarding species was examined. Finally, the plans for both a systematic investigation of the ion implantation and contact development and related characterization of AlN and GaN with n- and p-type dopants and the construction and employment of a UV luminescence facility is discussed. GRA

N93-10403# California Univ., Berkeley. Lawrence Berkeley Lab.
STATICS AND KINETICS OF OXYGEN ORDERING IN THE OXIDE SUPERCONDUCTOR YBa2Cu3O(z)
R. McCormack, D. deFontaine, G. Ceder (Massachusetts Inst. of Tech., Cambridge.), and E. Salomons (Commissariat a l'Energie Atomique, Gif-sur-Yvette, France) Mar. 1992 16 p Presented at the Minerals, Metals, and Materials Society (TMS) Annual Meeting and Exhibition, San Diego, CA, 1-5 Mar. 1992
(Contract DE-AC03-76SF-00098)
(DE92-017001; LBL-32164; CONF-920305-12) Avail: CASI HC A03/MF A01

Oxygen ordering in the high-temperature superconductor YBa2Cu3O(z) is well described by a two-dimensional Ising model with anisotropic next-nearest neighbor effective pair interactions, repulsive along the a direction and attractive along b direction. Monte Carlo simulation shows that this marked anisotropy gives rise, particularly at stoichiometric index z close to 7, to large deviations from unity of the ratio D*(sub 11)/D*(sub 22) of tracer diffusion tensor components in the a and b directions. Oxygen ordering kinetics are shown to evolve in a manner which parallels those of the experimentally observed increase with aging time of the superconducting transition temperature of z less than 7.
DOE

N93-10404# Wisconsin Univ., Madison. Dept. of Electrical and Computer Engineering.
VORTICES IN LONG JOSEPHSON JUNCTIONS Final Technical Report, 15 Nov. 1988 - 14 Feb. 1992
James E. Nordman and James B. Beyer 16 Jun. 1992 9 p
(Grant AF-AFOSR-0052-89)
(AD-A253230; AFOSR-92-0696TR) Avail: CASI HC A02/MF A01

This research involved the study of quantized flux lines or vortices in long Josephson junction structures and in superconductive films in the context of electronic device possibilities suggested by these structures. The work encompassed fabrication and low frequency electrical measurement of thin film device configuration coupled with physical device modeling. This was followed by high frequency parameter measurement and creation of circuit models for the devices. In some cases these circuit models were used to model and optimize specific circuits such as amplifiers or oscillators and, when warranted, prototypes were fabricated and tested. The primary structures studied were the long Josephson junction transistors, including the vortex flow transistor (VFT) and the superCIT. In addition, initial success with an exploratory device using a single high Tc superconducting film, the SFFT, led to some concentration on circuit realizations with this device. Comparisons were made of these three devices which were fabricated using a variety of thin film superconductors.
GRA

N93-10415# North Carolina Univ., Chapel Hill. Dept. of Chemistry.
A NEW ELLIPSOMETRY TECHNIQUE FOR INTERFACE ANALYSIS: APPLICATION TO Si-SiO2
E. A. Irene and V. A. Yakovlev 13 Jul. 1992 12 p
(Contract N00014-89-J-1178)
(AD-A253143; TR-46) Avail: CASI HC A03/MF A01

In this paper, we report a new spectroscopic ellipsometry technique that overcomes much of the ambiguity associated with measuring an interface under a film. For this technique we match the refractive index of the overlayer with an immersion liquid and then perform spectroscopic ellipsometry at several angles of incidence. Essentially, the overlayer is optically (not physically) removed, thereby rendering the ellipsometric measurement sensitive to the interfacial layer which is often known to be optically and chemically different than either substrate or film. The Si-SiO2 interface resulting from thermal oxidation of Si, and the evolution of the interface with annealing is studied using the new technique. GRA

N93-10425# Oregon State Univ., Corvallis. Dept. of Electrical and Computer Engineering.
ATOMIC APPROACHES TO DEFECT THERMOCHEMISTRY Final Report, 1 Apr. 1989 - 31 Mar. 1992
James A. VanVechten and John F. Wager 30 Apr. 1992 251 p
(Grant AF-AFOSR-0309-89)
(AD-A254278; AFOSR-92-0782TR) Avail: CASI HC A12/MF A03

We have achieved insight into the role of H in semiconductor crystal growth in processes such as organometallic chemical vapor deposition, OMCVD. If allowed, H will compensate shallow dopants and suppress the formation of other compensators when the Fermi level moves significantly from the intrinsic level at growth or processing temperatures, T. This can be a great advantage because the H can be removed at low T with no rearrangement of other atoms. This has led to the first attainment of good p-type GaN and to improvement of n-type GaN. It should work for any semiconductor. We have improved the thermodynamic analysis of heterojunction band offsets as functions of T and strain. We have done the first fundamental studies of the diffusion equation with boundary conditions appropriate for crystal growth and diffusion and obtained major insights. We devised a simple new experiment to study interstitial impurity diffusion in semiconductors with striking results. We demonstrated that host interstitials play no role in thermal in Si or GaAs and similar low ionicity crystals and have explained the 'U-shaped' profile of transition metal impurities. We have verified that the DX center can be getter out of AlGaAs without reducing donor concentration and studied its properties by various capacitance transient. We have characterized the aging and charge trapping properties of ZnS ACTFEL display materials. We have calculated the entropy of atomic hopping. GRA

N93-10609# Ames Lab., IA.
MODEL FOR THE REVERSIBLE MAGNETIZATION OF HIGH-(KAPPA) TYPE-2 SUPERCONDUCTORS: APPLICATION TO HIGH-TEMPERATURE SUPERCONDUCTOR Ph.D. Thesis
Zhidong Hao Jun. 1992 126 p
(Contract W-7405-eng-82)
(DE92-016297; IS-T-1533) Avail: CASI HC A07/MF A02

This dissertation is divided into five sections, each dealing with an aspect of the response of type-2 superconductors to applied magnetic fields. In Section 1, a generalized variational model of a single vortex is presented, valid in the anisotropic case when the applied magnetic field H is along one of the principal axes. The effects of the anisotropy on pinning forces of individual vortices and on the vortex lattice form are discussed. In Section 2, a variational model of the mixed state is proposed, which permits an analytic calculation of the free energy density F in the Ginzburg-Landau regime. A formula for the reversible magnetization is obtained, valid for the entire field region H(sub c1) less than or equal to H less than or equal to H(sub c2). In Section 3, the reversible magnetization of anisotropic superconductors is considered for the case that H is along an arbitrary direction with respect to the principal axes. In Section 4, it is pointed out the London model for the reversible magnetization M of high-(kappa) type-2 superconductors in the intermediate-field region is quantitatively incorrect. It is also shown that the apparently linear dependence of M versus lnH in the intermediate-field region, a behavior that has been observed experimentally, can be obtained

from the model of Section 2. In Section 5, it is found that the reversible magnetization M can be written to good approximation as -4(pi)M = (H(sub c)(exp 2)/H(sub c2))(Phi)(h) for H much greater than H(sub c1) and (kappa) much greater than 1, where h = H/H(sub c2) is the reduced field and (Phi) is a function of h. DOE

N93-10614# North Carolina Univ., Chapel Hill. Dept. of Chemistry.
SPECTROSCOPIC ELLIPSOMETRIC MEASUREMENTS OF THE DIELECTRIC FUNCTION OF GERMANIUM DIOXIDE FILMS ON CRYSTAL GERMANIUM
Y. Z. Hu, J.-T. Zettler, S. Chongsawangvirod, Y. Q. Wang, and E. A. Irene 13 Jul. 1992 16 p
(Contract N00014-89-J-1178)
(AD-A253137; TR-44) Avail: CASI HC A03/MF A01

From spectroscopic ellipsometry measurements in the 1.5 to 5.7 eV photon energy range we determined the complex dielectric function of thermally grown germanium dioxide in the 1.0 to 6.3 eV range. A Kramers-Kronig consistent dispersion formula utilizing an exponential shaped optical band edge was used in conjunction with both previously published far ultraviolet absorbance data for amorphous GeO2 and our spectra. These measurements show that E2 for GeO2 can be regarded to be zero in the range of E less than 5.5 eV, which differs from a previous report. Using this new optical results for the investigation of oxide growth, we find that GeO2 grows via a parabolic growth law with a growth constant, kp = 1.2 x 10 exp -19 sq. m/sq. sec at 550 C. GRA

N93-10623# Oak Ridge National Lab., TN.
RELIABILITY OF SUBLATTICE OCCUPANCIES DETERMINED BY ALCHEMI
J. Bentley 1992 3 p Presented at the Annual Meeting of the Electron Microscopy Society of America, Boston, MA, 16-21 Aug. 1992
(Contract DE-AC05-84OR-21400)
(DE92-014592; CONF-920819-18) Avail: CASI HC A01/MF A01

The atom location by channeling enhanced microanalysis (ALCHEMI) technique is an attractive method for sublattice (site) occupancy determination, especially in multiphase materials. It has been applied to a wide range of ceramics, minerals, semiconductors and metallic alloys with varying degrees of success. The simplicity of the method originally proposed has not always been borne out in practice; applications of the technique have revealed limitations due to crystallography, microstructure, specimen preparation, ionization delocalization, and weak channeling discrimination. Some of these limitations have been encountered in work at ORNL on ALCHEMI of intermetallic alloys such as L1(sub 2) ordered Ni3Al-based alloys (with additions of Hf, Co and Fe) and L1(sub 0) ordered Cu(50)Au(50-y)(X)(y) alloys with X = Pd or Ni. These applications have been motivated by the technological importance of ordered intermetallic alloys. Commercial materials often have complex compositions with ternary (or higher) additions present at substantial levels. DOE

N93-10630# Rutgers - The State Univ., New Brunswick, NJ. Dept. of Physics.
HIGH PRESSURE AND SYNCHROTRON RADIATION STUDIES OF SOLID STATE ELECTRONIC INSTABILITIES
J. H. Pifer and M. C. Croft Apr. 1992 13 p
(Contract DE-FG05-84ER-45081)
(DE92-015661; DOE/ER-45081/T1) Avail: CASI HC A03/MF A01

This report discusses Eu and General Valence Instabilities; Ce Problem: L(sub 3) Spectroscopy Emphasis; Bulk Property Emphasis; Transition Metal Compound Electronic Structure; Electronic Structure-Phonon Coupling Studies; High Temperature Superconductivity and Oxide Materials; and Novel Materials Collaboration with Chemistry. DOE

N93-10637# Zytron Corp., Saint Paul, MN.
OPTIMIZATION OF RESONANT INTERBAND TUNNEL DEVICES Final Report, 1 Jun. 1991 - 19 May 1992
Mark F. Sweeny 19 May 1992 46 p
(Contract F49620-91-C-0043)
(AD-A252401; AFOSR-92-0526TR) Avail: CASI HC A03/MF A01

We have carried out analytical and numerical studies of resonant interband tunneling. The numerical methods implement a 2 band model, consisting of the conduction band and a single valence band. The valence band can be considered to be the light holes. The numerical methods are described in detail, and can be applied to multiband models too. Analytic estimates are made of the thermionic currents, the effect of stress, and other physical effects not included in the numerical models. The devices simulated are closely modeled after a set of Resonant Interband Tunnel Diodes fabricated at the Varian Research Center in Palo Alto, California. Comparison of the measured and computed results show that our simulator predicts the maximal currents to within a factor of two, for devices with maximal currents varying by a factor of 1000. There are systematic differences which are likely to be due to the very high doping used in the devices. Finally, we describe a graphic user interface, implemented for our device simulator, and a Mathematical package for carrying out symbolic computations upon the operators of the Luttinger model and related multiband models of semiconductors. GRA

N93-10726# Stanford Univ., CA. Lab. of Physics.
SCANNING TUNNELING MICROSCOPY OF SEMICONDUCTOR SURFACES Technical Report, 1 Oct. 1990 - 30 Sep. 1991
A. A. Baski and C. F. Quate Nov. 1991 12 p
(Contract N00014-90-J-1001)
(AD-A246853; SU-GL-4897) Avail: CASI HC A03/MF A01

This report is a summary of our results during the second year of a research program aimed at studying the epitaxial growth of metals on the (111) and (100) surfaces of silicon using scanning tunneling microscopy (STM). The following three systems have been studied in depth during the past year: Al:Si(100), Sn:Si(100), and Yb:Si(111). The room temperature deposition of Al on Si(100) results in the formation of metal dimer rows, similar to the behavior of other group-III metals on Si(100). At elevated temperatures, Al forms 'bow tie' structures which have also been observed on the annealed In:Si(100) surface. In contrast to the group-III metal systems, the annealed Sn:Si(100) system illustrates a complicated phase mixing behavior which involves numerous surface structures. In spite of the complexity of these structures, we believe that many of them can be simply modeled as Sn-Sn dimers. Finally, we have studied the Yb:Si(111) system, which forms two types of reconstructions up to 0.5 ML: (1) a lower coverage 3x1 phase, and (2) higher coverage 'nxl' phases (5x1, 7x1, 2x1). GRA

N93-10733# Wisconsin Univ., Madison.
DEVELOPMENT OF HIGH TEMPERATURE SUPERCONDUCTORS FOR MAGNETIC FIELD APPLICATIONS
D. C. Larbalestier 1991 25 p Presented at the Phenomenology and Applications of High Temperature Superconductivity, Los Alamos, NM, 22-24 Aug. 1991
(Contract DE-FG02-91ER-40643)
(DE92-015930; CONF-9108140-3) Avail: CASI HC A03/MF A01

The key requirement for magnetic field applications of high temperature superconductor (HTS) materials is to have conductors with high transport critical current density available for magnet builders. After 3 or 4 years of being without any such object, conductor makers have had recent success in producing simple conductor prototypes. These have permitted the construction of simple HTS magnets having self fields exceeding 1 tesla at 4K. Thus the scientific feasibility of making powerful HTS magnets has been demonstrated. Attention to the technological aspects of making HTS conductors for magnets with strong flux pinning and reduced superconducting granularity is now sensible and attractive. However, extrinsic defects such as filament sausaging, cracking, misaligned grains and other perturbation to long range current

flow must be controlled at a low level if the benefit of intrinsic improvements to the critical current density is to be maintained in the conductor form. Due to the great complexity of the HTS materials, there is sometimes confusion as to whether a given sample has an intrinsically or extrinsically limited critical current density. Systematic microstructure variation experiments and resistive transition analysis are shown to be particularly helpful in this phase of conductor development. DOE

N93-10764# Michigan Univ., Ann Arbor. Ultrafast Science Lab.
HIGH SENSITIVITY PROBES FOR SILICON VLSI INTERNAL NODE TESTING Final Report, Sep. 1989 - Sep. 1991
Janis A. Valdmanis May 1992 58 p
(Contract F30602-88-D-0028)
(AD-A253924; RL-TR-92-81) Avail: CASI HC A04/MF A01

This contract investigated several new technologies useful for real-time internal node probing of VLSI integrated circuits. Electro-optic, electroabsorptive, photoconductive, and magnetic probe technologies were studied, and their relative merits and drawbacks compared. Testing parameters were less than or equal to 5ns temporal resolution, less than or equal to 50 mV sensitivity, and less than or equal to 2 spatial resolution. Both theoretical and experimental work was performed. Conclusions are drawn indicating the most promising candidates for future in-depth studies. GRA

N93-10871# Illinois Univ., Chicago. Dept. of Physics.
THEORY OF TRANSPORT FOR INTERACTING MANY-BODY SYSTEMS Final Report, 15 Jul. 1991 - 14 Jul. 1992
W. Poetz 15 Jun. 1992 9 p
(Contract DAAL03-91-G-0216)
(AD-A253789; ARO-28464.3-PH) Avail: CASI HC A02/MF A01

An approach to quantum transport in coupled electron-phonon systems has been developed. Application to the polaron problem, two-level systems, and semiconductor double-well structures has been made. We find that dissipative effects in the electronic system can be obtained. Furthermore, a theoretical model for the electronic density of states for (imperfect) semiconductor systems has been developed to aid interpretation of transport data. This model has been successfully applied to ternary alloys, as well as amorphous semiconductor quantum wells. GRA

N93-10879# Litton Systems, Inc., Charlotte, NC. Airtron Div.
SINGLE CRYSTAL GROWTH OF BETA-Al2O3 FOR ISO-INDEX FILTERS Final Report, 1 Aug. 1990 - 1 Feb. 1992
R. F. Belt, M. H. Randles, and J. E. Creamer 31 Mar. 1992 37 p
(Contract N00014-90-C-0006; DARPA Order 7531)
(AD-A252259) Avail: CASI HC A03/MF A01

Single crystals of Beta-Al2O3 with a nominal composition of Na2O.11 Al2O3 were grown from stoichiometric melts contained in an iridium crucible. Seeding was achieved from an Al2O3 single crystal. The growth axis was along a, and x-ray data confirmed the unit cell parameters of a = 5.595 A and c = 22.531 A. The top and bottom lattice constants of the boules were equal to + 0.002 A and indicated a fairly uniform composition. The measured density was 3.25 g/cc. The boules remained physically intact with no major cracks. However, some cleavage progressed on the basal planes as determined by the appearance of interference fringes. Water vapor and CO2 did not enhance the cracking. Crystals were stored in a desiccator but continued to cleave. Ionic diffusions of Na(+), Ag(+), Pb(2+), Rb(+), Ca(2+), Cd(2+), and Tl(+) were performed by immersion of beta-Al2O3 into nitrate or chloride melts at temperatures of 360-7400 C. GRA

77 THERMODYNAMICS AND STATISTICAL PHYSICS

Includes quantum mechanics; theoretical physics; and Bose and Fermi statistics.

For related information see also *25 Inorganic and Physical Chemistry* and *34 Fluid Mechanics and Heat Transfer.*

N93-10226# Weizmann Inst. of Science, Rehovoth (Israel).
SEMICLASSICAL QUANTIZATION OF CHAOTIC BILLIARDS
E. Doron and U. Smilansky (Bristol Univ., England) Sep. 1991 47 p
(DE92-634888; WIS-PH-91-63) Avail: CASI HC A03/MF A01

We derive a semiclassical secular equation which applies for quantized (compact) billiards of any shape. Our approach is based on the fact that the billiard boundary defines two dual problems: (1) the 'inside problem' of the bounded dynamics; and (2) an 'outside problem' which can be looked upon as a scattering from a boundary as an obstacle. This duality exists both on the classical and quantum mechanical levels, and is therefore very useful in deriving a semiclassical quantization rule. We obtain a semiclassical secular equation which is based on classical input from a finite number of classical periodic orbits. We compare our results to secular equations which were recently derived by other means, and provide some numerical data which illustrates our method when applied to the quantization of the Sinai billiard. DOE

N93-10229# Weizmann Inst. of Science, Rehovoth (Israel).
SEMICLASSICAL QUANTIZATION OF INTERACTING ANYONS IN A STRONG MAGNETIC FIELD
S. Levit and N. Sivan (Weizmann Inst. of Science, Rehovoth, Israel) Jan. 1992 12 p
(DE92-634889; WIS-PH-92-1) Avail: CASI HC A03/MF A01

We represent a semiclassical theory of charged interacting anyons in strong magnetic fields. We apply this theory to a number of few anyons systems including two interacting anyons in the presence of an impurity and three interacting anyons. We discuss the dependence of their energy levels on the statistical parameter and find regions in which this dependence follows very different patterns. The semiclassical arguments allow to correlate these patterns with the change in the character of the classical motion of the system. DOE

N93-10249# Arizona State Univ., Tempe. Center for Energy Systems Research.
HEAT TRANSFER ADDITIVES FOR ABSORPTION COOLING SYSTEM FLUIDS Annual Report, Oct. 1990 - Sep. 1991
B. D. Wood, N. S. Berman, K. Kim, D. S. C. Chau, and T. A. Ameel Feb. 1992 109 p
(Contract GRI-5089-260-1874)
(PB92-190354; ASU-CR-R-92020; GRI-92/0051) Avail: CASI HC A06/MF A02

The work was directed towards developing an analytical and physical understanding of the various phenomena, reported in the public literature, that could effect the heat and mass transfer in the absorber of an absorption chiller. Emphasis during the first year of a 3 year study was placed on compiling a comprehensive property data base and doing some simple exploratory experiments. During the second year experimental methods associated with heat and mass transfer in a falling film absorber were emphasized. Significant accomplishments the past year include: surface tension measurements for aqueous LiBr with and without additives, air solubility measurements for LiBr and LiCl, stability observations for a static film absorber, and preliminary tests with the falling film absorber apparatus for 60 wt percent LiBr without surfactant additive. The solubility of surfactants n-Octanol and 2-Ethyl-1-Hexanol in 60 wt percent aqueous LiBr appears to be higher than that for 50 wt percent and the slope of the surface tensions versus log concentration curve is much different for 60 wt percent compared to 50 wt percent and less. Static film experiments showed that the surface films of 60 wt percent LiBr became unstable for concentrations of surfactant for less than the solubility limit found from the surface tension measurements.

The conclusion is that surfactant concentrations equal to or less than that needed to lower the surface tension to that of pure water are necessary to cause instability when mass transfer takes place. Mass transfer correlations were developed for an aqueous LiBr falling film absorber with no additives. This will be used as a reference for the experimental results with additives. GRA

N93-10294# Weizmann Inst. of Science, Rehovoth (Israel).
SYMMETRY BREAKING AND LOCALIZATION IN QUANTUM CHAOTIC SYSTEMS
R. Bluemel (Delaware Univ., Newark.) and U. Smilansky Feb. 1992 11 p
(DE92-634890; WIS-PH-92-13) Avail: CASI HC A03/MF A01

We consider systems which display dynamical localization, and study the effect of breaking an antiunitary symmetry (related to time reversal symmetry) on the localization length. Using semiclassical arguments substantiated by numerical results for the quantum kicked rotor, we establish that localization length increases by a factor of two when the symmetry breaking interaction is sufficiently strong. The transition is not abrupt and we give an approximate expression for the transition function. The semiclassical theory provides also the critical strength of the symmetry breaking interaction which is neccessary to achieve the full factor two increase of the localization length. DOE

N93-10295# Weizmann Inst. of Science, Rehovoth (Israel).
SEMICLASSICAL QUANTIZATION OF INTEGRABLE SYSTEMS OF FEW INTERACTING ANYONS IN A STRONG MAGNETIC FIELD
N. Sivan and S. Levit Jan. 1992 35 p
(DE92-634892; WIS-PH-92-6) Avail: CASI HC A03/MF A01

We present a semiclassical theory of charged interacting anyons in a strong magnetic field. We derive the appropriate generalization of the WKB quantization conditions and determine the corresponding wave functions for nonseparable integrable anyonic systems. This theory is applied to a system of two interacting anyons, two interacting anyons in the presence of an impurity and three interacting anyons. We calculate the dependence of the semiclassical energy levels on the statistical parameter and find regions in which dependence follows very different patterns. The semiclassical treatment allows us to find the correlation between these patterns and the change in the character of the classical motion of the system. We also test the accuracy of the mean field approximation for low and high energy states of the three anyons. DOE

N93-10386# International Centre for Theoretical Physics, Trieste (Italy).
THE CLASS OF THE PATHS IN THE FEYNMAN PATH INTEGRAL ON THE PHASE SPACE
P. P. Fiziev Dec. 1991 7 p
(DE92-630205; IC-91/368) Avail: CASI HC A02/MF A01

The class of the paths in a Feynman phase space path integral was investigated and justified. An infinite dimensional group of homotopical transformations of the phase space paths, which make the classical action invariant, was discovered. A factorization of the volume of this group in the path integral is proposed. DOE

N93-10387# International Centre for Theoretical Physics, Trieste (Italy).
ON THE MEASUREMENT OF TIME-DEPENDENT QUANTUM PHASES
A. O. Barut (Colorado Univ., Boulder.), M. Bozic, S. Klarsfeld (Paris XI Univ., Orsay, France), and Z. Maric (Belgrade Univ., Yugoslavia) Nov. 1991 33 p
(DE92-630206; IC-91/382) Avail: CASI HC A03/MF A01

We have evaluated the exact (Pancharatnam) phase differences between the final state psi(t) greater than and various initial states for a spin 1/2-particle in a rotating magnetic field B(t). For the initial states n;B(sub ef)(0) greater than, which are eigenstates of the spin component along the direction of the initial effective field B(sub ef)(0), the exact phase has an energy dependent part, and an energy independent part. It is shown that these states n;B(sub ef)(0) greater than are cyclic and their corresponding Aharonov-Anandan phases are evaluated. In the adiabatic limit we discuss different choices of time-dependent bases and the relationship between the exact phase, the Born-Fock-Schiff phase and Berry's phase. We propose experiments (neutron) to verify separately the exact and the adiabatic evolution laws, as well as to measure the adiabatic phases associated with different choices of time-dependent basis vectors. DOE

N93-10388# International Centre for Theoretical Physics, Trieste (Italy).
FINITE GROUP ACTIONS AND ELLIPTIC GENERA
J. A. Devoto Dec. 1991 34 p
(DE92-630207; IC-91/394) Avail: CASI HC A03/MF A01

We study the modular properties of a formal power series of elliptic operators that correspond to the S(sup 1)-equivariant index of a hypothetical Dirac operator on loop spaces of a manifold twisted by the action of a group. We also show that this interpretation leads to a natural construction of Virasoro equivariant vector bundles over the loop space of points fixed under the action of the group. DOE

N93-10434# Florida Univ., Gainesville. Dept. of Physics.
WIGGLY RELATIVISTIC STRINGS
Jooyoo Hong, Jaewan Kim, and P. Sikivie 1992 9 p
(Contract DE-FG05-86ER-40272)
(DE92-016461; DOE/ER-40272/158; UFIFT-HEP-92-10) Avail: CASI HC A02/MF A01

We derive the equations of motion for general strings, i.e., strings with arbitrary relation between tension tau and energy per unit length epsilon. The renormalization of tau and epsilon that results from averaging out small scale wiggles on the string is obtained in the general case to lowest order in the amount of wiggliness. For Nambu-Goto strings we find deviations from the equation of state epsilon(tau) = constant in higher orders. Finally we show that under plausible assumptions wiggliness radically modifies the cosmic gauge string scenario. DOE

N93-10604# Texas Univ., Austin. Inst. for Fusion Studies.
STOCHASTIC DIFFUSION AND KOLMOGOROV ENTROPY IN REGULAR AND RANDOM HAMILTONIANS
M. B. Isichenko, W. Horton, D. E. Kim (Korea Advanced Inst. of Science and Technology, Seoul, Republic of Korea), and E. Heo (Korea Advanced Inst. of Science and Technology, Seoul, Republic of Korea) May 1992 38 p
(Contract DE-FG05-80ET-53088)
(DE92-016179; DOE/ET-53088/551; IFSR-551) Avail: CASI HC A03/MF A01

The scalings of the E x B turbulent diffusion coefficient D and the Kolmogorov entropy K with the potential amplitude phi of the fluctuation are studied using the geometrical analysis of closed and extended particle orbits for several types of drift Hamiltonians. The high-amplitude scalings, D proportional to phi(sup 2) or phi(sup 0) and K proportional to log phi, are shown to arise from different forms of a periodic (four-wave) Hamiltonian phi(x,y,t), thereby explaining the controversy in earlier numerical results. For a quasi-random (six-wave) Hamiltonian numerical data for the diffusion D proportional to phi(sup 0.92 +/- 0.04) and the Kolmogorov entropy K proportional to phi(sup 0.56 +/- 0.17) are presented and compared with the percolation theory predictions D(sub p) proportional to phi(sup 0.7), K(sub p) proportional to phi(sup 0.5). To study the turbulent diffusion in a general form of Hamiltonian, a new approach of the series expansion of the Lagrangian velocity correlation function is proposed and discussed. DOE

N93-10787# Brown Univ., Providence, RI.
LOCAL-EQUILIBRIUM FORMALISM APPLIED TO MECHANICS OF SOLIDS
J. Kestin 1992 23 p Presented at the International Symposium on Micromechanics: Homogenization, Heterogenization and Strength, La Jolla, CA, 27-29 Mar. 1992

(Contract DE-FG02-87ER-13687)
(DE92-016852; DOE/ER-13687/8; CONF-9203167-1) Avail: CASI HC A03/MF A01

The lecture starts with an expression of good wishes to George Herrmann on the occasion of his seventieth birthday and continues with a lament that the majority of research workers in the field of solid mechanics have failed to appreciate the power and relevance of 'conventional' thermodynamics which is based on the acceptance of the hypothesis of local equilibrium (principle of local state). The lecture then proceeds to discuss the essential concepts of conventional thermodynamics and emphasizes the differences between the description of nonequilibrium states in physical space and equilibrium states in the Gibbsian phase space. It is asserted that the subject acquires its simplest form by the recognition of the relevance of Bridgman's internal variables. With their aid it is possible to define the accompanying equilibrium state and the accompanying reversible process. An elimination of internal energy between the field equation of energy (First Law) and the Gibbs equation in rate form results in an explicit expression for the local rate of entropy production, theta. It is asserted that the preceding elements supplemented with appropriate rate equations result in a closed system of partial differential equations whose solution, subject to appropriate initial and boundary conditions, constitutes the process ('history') under consideration. DOE

80 SOCIAL SCIENCES (GENERAL)

Includes educational matters.

N93-10270# EG and G Rocky Flats, Inc., Golden, CO.
TOTAL QUALITY MANAGEMENT (TQM) CONCEPTS APPLIED TO INSTRUCTION
E. J. Nuccio 1992 10 p Presented at the 1992 DOE Training Accreditation Program Conference, Phoenix, AZ, 16 Jun. 1992
(Contract DE-AC34-90DP-62349)
(DE92-013399; RFP-4571; CONF-9206164-1) Avail: CASI HC A02/MF A01

Drawing on DOE Order 5700.6C and other industry standards, this document presents several concepts and tools of Total Quality Management (TQM), a brief history of their use at EG&G Rocky Flats, and how they are being applied to address processes of instruction common to TAP. Concepts presented and applied include: statistical process control (SPC), e.g., using control charts, as an evaluation methodology for learners and instructors; TQM conceptual tools, e.g., brainstorming, affinity diagrams, and interrelationship digraphs, as a methodology for planning programs of instruction such as TAP; and team activities to construct instructional process systems. DOE

81 ADMINISTRATION AND MANAGEMENT

Includes management planning and research.

No abstracts in this category.

82 DOCUMENTATION AND INFORMATION SCIENCE

Includes information management; information storage and retrieval technology; technical writing; graphic arts; and micrography.

For computer documentation see *61 Computer Programming and Software.*

N93-10078* National Aeronautics and Space Administration, Washington, DC.
NASA PATENT ABSTRACTS BIBLIOGRAPHY: A CONTINUING BIBLIOGRAPHY. SECTION 1: ABSTRACTS (SUPPLEMENT 41)
Jul. 1992 62 p
(NASA-SP-7039(41)-Sect-1; NAS 1.21:7039(41)-Sect-1) Avail: CASI HC A04

Abstracts are provided for 131 patents and patent applications entered into the NASA scientific and technical information system during the period Jan. 1992 through Jun. 1992. Each entry consists of a citation, an abstract, and in most cases, a key illustration selected from the patent or patent application. Author

N93-10257# Computer Sciences Corp., Research Triangle Park, NC. Applied Technology Div.
GRIDDED MODEL INFORMATION SUPPORT SYSTEM (GMISS) USER'S GUIDE. VOLUME 3: MODEL CONCENTRATION DATA RETRIEVAL SUBSYSTEM
Bennie Sutton 25 Nov. 1991 91 p
(Contract EPA-68-01-7365)
(PB92-190263; EPA/450/4-91/032-Vol-3) Avail: CASI HC A05/MF A01

The Gridded Model Information Support System (GMISS) is a data base management system for selected Regional Oxidant Model (ROM) input data and species concentrations produced by gridded photochemical air pollution models. The Model Concentration Data Retrieval Subsystem allows State and local air pollution control agencies to retrieve these hourly data for use in support of their regulatory programs. These hourly data may be used to calculate initial and boundary conditions for the Empirical Kinetics Modeling Approach (EKMA). They may be used for other modeling application needs as well as to support evaluation of regional emissions controls strategies. Both temporal and spatial subsets of the data may be retrieved. The document describes how to invoke and execute the Model Concentration Data Retrieval Subsystem using the full screen menus. GRA

N93-10382# Oak Ridge National Lab., TN.
TIGER5: EXTRACTION OF GEOGRAPHIC INFORMATION FROM THE TIGER SYSTEM
R. K. Gryder Mar. 1992 74 p
(Contract DE-AC05-84OR-21400)
(DE92-014935; ORNL/TM-12061) Avail: CASI HC A04/MF A01

The need for geographic information in digital form is becoming apparent in many areas, including Emergency Response Planning and Management. The Bureau of Census recognized this need and developed an automated geographic data base, known as Topologically Integrated Geographic Encoding and Referencing (TIGER) System, to produce the geographic products for the 1990 census. The Bureau makes the information available to the public on CD-ROM disks. As distributed, the geographic information is not directly visible, and a program is needed to display the information in a graphic form. MapInfo is a commercially available program that has the capability to display maps and allows the user to perform certain geographic analyses. MapInfo runs on a variety of low-cost platforms that may be found in an average office environment, as well as on high-performance work stations. The TIGER5 program developed by the Emergency Management Information Systems (EMIS) project at Oak Ridge National Laboratory reads files directly from the Census Bureau TIGER/Line CD-ROM and creates MapInfo Exchange Format Files that can be directly imported into MapInfo. The standard default values for

scaling parameters are used, and the resulting map is in the same coordinate system as the world and state maps distributed with MapInfo. DOE

N93-10396# Westinghouse Environmental Management Co. of Ohio, Cincinnati.
QUALITY ASSURANCE PRACTICES FOR DATA ENTRY AND ELECTRONIC DATA TRANSFER
L. M. Tomczak, J. C. Gore, J. W. Nexon, H. B. Spitz (Cincinnati Univ., OH.), J. J. Cardarelli (Cincinnati Univ., OH.), Lia Dai (Cincinnati Univ., OH.), Ning Liu (Cincinnati Univ., OH.), and Sue McGimpsey (Cincinnati Univ., OH.) Jun. 1992 16 p Presented at the 8th Annual Waste Testing and Quality Assurance Symposium, Arlington, VA, 13-17 Jul. 1992
(Contract DE-AC05-86OR-21600)
(DE92-014804; FEMP-2265; CONF-9207100-1) Avail: CASI HC A03/MF A01

The Radiological Environmental Monitoring (REM) group at the Fernald Environmental Management Project is involved in two practices that will result in the improved quality assurance of collected data: the quality assurance program for manually entered data, and electronic data transfer. The first practice focuses on adopting strict quality assurance guidelines for manual database entry. The second practice focuses on electronic data transfer from the recording instrument in order to reduce the manpower normally required for manual data entry. The applications of these two practices can enhance any data collection program where instruments with electronic memories and a signal output are utilized. Organizations employing either or both of these practices, as applicable, can strengthen the quality and efficiency of their data collection program. The use of these practices can assist in complying with quality assurance requirements under ASME NQA-1, RCRA, CERCLA, and DOE Order activities. DOE

N93-10428# Linguistic Research Inst., Boulder, CO.
ANALYSIS OF OBSERVATION REPORT DATABASES/KNOWLEDGE BASES Final Report, Sep. 1989 - Jun. 1991
Dec. 1991 66 p
(Contract F30602-89-C-0152)
(AD-A252636; RL-TR-91-415) Avail: CASI HC A04/MF A01

This project developed software for implementing situation analysis of knowledge bases/data bases based on State of Affairs methodology, using off-the-shelf commercial software as a platform. Capability for event-subevent inferencing and for resource contention analysis were developed. GRA

N93-10431# Science Applications International Corp., San Diego, CA. Foreign Applied Sciences Assessment Center
SOVIET OPTICAL PROCESSING RESEARCH. FSAC TECHNICAL ASSESSMENT REPORT (TAR)
Anthony Vanderlugt (North Carolina State Univ., Raleigh.), Alfred E. Attard (Department of Defense, Washington, DC.), Mark Cronin-Golomb (Tufts Univ., Boston, MA.), Richard L. Hartman (Advanced Optical Systems, Inc., Huntsville, AL.), John N. Lee (Naval Research Lab., Washington, DC.), G. Michael Morris (Rochester Univ., NY.), and William T. Rhodes (Colorado Univ., Boulder.) Apr. 1991 224 p
(PB92-195569) Avail: CASI HC A10/MF A03

Since the 1960s, Soviet researchers have pursued the application of optical processing techniques to transform, manipulate, or transmit information. Soviet capability in optical materials and devices, as well as in applications such as image processing and signal processing/computing is summarized. GRA

N93-10451*# Research Inst. for Computing and Information Systems, Houston, TX.
NASA ELECTRONIC LIBRARY SYSTEM (NELS) DATABASE SCHEMA, VERSION 1.2
Clovis J. Melebeck (I-NET, Inc., Bethesda, MD.) Jul. 1991 33 p Revised
(Contract NCC9-16; RICIS Proj. RB-08)
(NASA-CR-190643; NAS 1.26:190643) Avail: CASI HC A03/MF A01

The database tables used by NELS version 1.2 are discussed. To provide the current functional capability offered by NELS, nineteen tables were created with ORACLE. Each table lists the ORACLE table name and provides a brief description of the tables intended use or function. The following sections cover four basic categories of tables: NELS object classes, NELS collections, NELS objects, and NELS supplemental tables. Also included in each section is a definition and/or relationship of each field to other fields or tables. The primary key(s) for each table is indicated with a single asterisk (*), while foreign keys are indicated with double asterisks (**). The primary key(s) indicate the key(s) which uniquely identifies a record for that table. The foreign key(s) is used to identify additional information in other table(s) for that record. The two appendices are the command which is used to construct the ORACLE tables for NELS. Appendix A contains the commands which create the tables which are defined in the following sections. Appendix B contains the commands which build the indices for these tables. Author

N93-10452*# Research Inst. for Computing and Information Systems, Houston, TX.
A SURVEY OF COMMERCIAL OBJECT-ORIENTED DATABASE MANAGEMENT SYSTEMS
John Atkins (West Virginia Univ., Morgantown.) 4 Jun. 1992 52 p
(Contract NCC9-16; RICIS Proj. SE-43)
(NASA-CR-190645; NAS 1.26:190645) Avail: CASI HC A04/MF A01

The object-oriented data model is the culmination of over thirty years of database research. Initially, database research focused on the need to provide information in a consistent and efficient manner to the business community. Early data models such as the hierarchical model and the network model met the goal of consistent and efficient access to data and were substantial improvements over simple file mechanisms for storing and accessing data. However, these models required highly skilled programmers to provide access to the data. Consequently, in the early 70's E.F. Codd, an IBM research computer scientists, proposed a new data model based on the simple mathematical notion of the relation. This model is known as the Relational Model. In the relational model, data is represented in flat tables (or relations) which have no physical or internal links between them. The simplicity of this model fostered the development of powerful but relatively simple query languages that now made data directly accessible to the general database user. Except for large, multi-user database systems, a database professional was in general no longer necessary. Database professionals found that traditional data in the form of character data, dates, and numeric data were easily represented and managed via the relational model. Commercial relational database management systems proliferated and performance of relational databases improved dramatically. However, there was a growing community of potential database users whose needs were not met by the relational model. These users needed to store data with data types not available in the relational model and who required a far richer modelling environment than that provided by the relational model. Indeed, the complexity of the objects to be represented in the model mandated a new approach to database technology. The Object-Oriented Model was the result. Author

N93-10593# Advisory Group for Aerospace Research and Development, Neuilly-Sur-Seine (France). Technical Information Panel.
SEMINAR ON BASIC DOCUMENTATION PRACTICES [LES PRATIQUES DE BASE EN MATIERE DE DOCUMENTATION]
Aug. 1992 192 p Seminar held in Ankara, Turkey, 3-4 Sep. 1992, in Athens, Greece, 7-8 Sep. 1992, and in Lisbon, Portugal, 10-11 Sep. 1992
(AGARD-R-788; ISBN-92-835-0681-2) Copyright Avail: CASI HC A09/MF A02

Application of new technology to the management of scientific and technical information relies upon a thorough grounding in basic concepts. The acquisition, storage, retrieval, and dissemination of material is becoming ever more complex and is a process which requires an understanding of how knowledge is perceived by the end user, the mechanics of data transfer, and the principles of responsible information exchange. In addition, the proliferation of information and the variety of media currently available make clear objectives and practical solutions essential. The AGARD Technical Information Panel (TIP) has produced a number of publications aimed at establishing and raising the standard of information management. This seminar brings together expert speakers to update the information in these publications and to contribute towards to further improvement in basic documentation practices. For individual titles, see N93-10594 through N93-10603.

N93-10594# Scientific and Technical Research Council of Turkey, Ankara. Documentation Center.
NATIONAL SCENE IN INFORMATION AND DOCUMENTATION ACTIVITIES AND RECENT DEVELOPMENTS IN THE DOCUMENTATION CENTER OF TUBITAK (TURDOK)
Imre Yildiz *In* AGARD, Seminar on Basic Documentation Practices Aug. 1992 3 p (For primary document see N93-10593 01-82)
Copyright Avail: CASI HC A01/MF A02

The first section is based on the evaluation of the survey, conducted by the Documentation Center (TURDOK) of Scientific and Technical Research Council of Turkey (TUBITAK) on the existing national information and documentation activities in Turkey. The second section comprises the recent developments of TURDOK in providing information for universities, governmental institutions, and industry. Author

N93-10595# Hellenic Aerospace Industry, Schimatari (Greece). Technical and Scientific Library.
DOCUMENTATION PRACTICES: THE NATIONAL SCENE (GREECE)
D. Patrinos *In* AGARD, Seminar on Basic Documentation Practices Aug. 1992 10 p (For primary document see N93-10593 01-82)
Copyright Avail: CASI HC A02/MF A02

The information 'explosion' combined with the capabilities offered by the new technologies poses a new challenge to all those involved in documentation work: producers, librarians, documentation and information specialists, and users. An overview of current documentation practices in Greece is presented. It also addresses subjects associated with documentation work, such as standards, telecommunications networks, education and training, and library automation issues. It outlines the progress made in some areas during the recent years and attempts to identify the major problems related to the delayed implementation of modern means and practices in the Greek documentation environment. Author

N93-10596# Laboratorio Nacional de Engenharia e Tecnologia Industrial, Lisbon (Portugal). Centro de Informacao Tecnica para a Industria.
SCIENTIFIC AND TECHNICAL INFORMATION (STI) TOWARDS TECHNOLOGICAL AND INDUSTRIAL DEVELOPMENT: THE CASE OF PORTUGAL
Ana Maria Ramalho Correia *In* AGARD, Seminar on Basic Documentation Practices Aug. 1992 16 p (For primary document see N93-10593 01-82)
Copyright Avail: CASI HC A03/MF A02

As a result of the rapid advancement of science and technology during the last decades, there is a tremendous increase in the accumulation of scientific, technical information (STI) and knowledge. The problem of collecting, cataloging, and accessing information to transfer to those who need it, when they need it, is a challenge faced by all information professionals. The application of information technologies to the management of STI represents an area where promising advancements are taking place, but where the user needs should be the 'push'. An overview is presented of the national scene in Portugal which covers some aspects related to different areas of scientific and technical information (SI) management and the application of new technologies to it. In particular, aspects related to the following are addressed: modernization of libraries; access to foreign databases (online and CD-ROM); advanced training in information management; development of information systems; development of advanced information products; participation in NATO programs in the field of STI; and research in information science in Portugal. Author

N93-10597*# National Aeronautics and Space Administration, Washington, DC.
ESTABLISHING A SCIENTIFIC AND TECHNICAL INFORMATION PROGRAM: PLANNING AND RESOURCE MANAGEMENT
Walter R. Blados *In* AGARD, Seminar on Basic Documentation Practices Aug. 1992 21 p (For primary document see N93-10593 01-82)
Copyright Avail: CASI HC A03/MF A02

In the last 50 years, technological advances have accelerated at a rate unprecedented in history. We are experiencing a tremendous expansion of scientific and technological effort in many directions, and the result is a fantastic increase in the accumulation of scientific and technical information (STI) and knowledge. An integral part of the research and development (R&D) process is the STI associated with it. STI is both a raw material (input) and a product (output) of this process. The topics addressed include the following: the value of STI, management of an STI program, program policy and guidance, organizational structure, data sources, training/orientation, and the current information environment. Author

N93-10598# GEC-Marconi Electronics Ltd., Chelmsford (England).
ACQUISITION 1: STOCK ACQUISITION PROCESSES IN DEFENCE AND AEROSPACE DOCUMENTATION CENTRES
Chris Bigger *In* AGARD, Seminar on Basic Documentation Practices Aug. 1992 9 p (For primary document see N93-10593 01-82)
Copyright Avail: CASI HC A02/MF A02

The acquisition of stock for any library is of course an essential activity, without stock there is no library and no service can be provided. It is sometimes difficult to find or create general rules because every library is different with different budgets, users, user needs, and organizational aims. Some general guidelines will be of some help but most decisions rest with the library after weighing all the evidence. Unless you are running a national library or a very large system it will not be possible to buy or acquire all that is published. Even if it could be acquired there may not be the space to store all stock. You are then forced to be selective due to the limits imposed by your organization. When stock has been selected it must be purchased at reasonable prices and at suitable speed. The acquisition of library stock is covered, and selection and acquisition processes are included, starting with the need for selection policies and moving on to establishing user needs, stock types, evaluation methods, purchase methods, and stock suppliers. Author

N93-10599# North Atlantic Treaty Organization, Brussels (Belgium). System Support Group.
ACQUISITION 2: PROCUREMENT, ACQUISITION, AND MAINTENANCE OF CONFIGURATION MANAGEMENT DOCUMENTATION IN SUPPORT OF A CIS SYSTEM
R. Pool *In* AGARD, Seminar on Basic Documentation Practices Aug. 1992 12 p (For primary document see N93-10593 01-82)
Copyright Avail: CASI HC A03/MF A02

The procedures used by the NATO Communications and Information Systems Agency (NACISA), when acting as host nation for the implementation of a communications and information systems (CIS) project, are outlined. The procurement, acquisition, and maintenance of configuration management documentation required in support of a CIS are addressed. For the purposes of this exercise, configuration management documentation is defined

as specifications, handbooks, drawings, and records that pertain to the design, performance, installation, operation, and maintenance of a CIS. Emphasis is on the activities involved in the acquisition of technical handbooks and drawings required for operation and maintenance, and the various end-users requiring this data are briefly outlined. In addition, the procedures currently used to maintain this documentation during the in-service phase of a CIS are described, and the present storage media utilized and future automation plans are addressed. Author

N93-10600# Federal Armed Forces Documentation and Information Centre, Bonn (Germany).
DOCUMENT PROCESSING
H. Braun *In* AGARD, Seminar on Basic Documentation Practices Aug. 1992 25 p (For primary document see N93-10593 01-82)
Copyright Avail: CASI HC A03/MF A02

Information systems operating a referral-type database, need to produce references for their documents in order to successfully retrieve the information. The same references serve as an initial user information, thereby enabling the users to decide upon the information value of the document contents for their own specific requirements. The various steps in producing such references, the process we call document processing, are addressed: descriptive cataloging deals with the various bibliographic data of documents. Content analysis, subdivided into classifying, indexing, and abstracting, is discussed in some detail. The thesaurus as the main instrument of an indexer, its function, and its structure are described. Finally, the data of the reference are entered into the data base for information retrieval, while the document is stored in the document collection. Author

N93-10601*# National Aeronautics and Space Administration, Washington, DC.
TECHNOLOGY FOR LIBRARIES AND INFORMATION CENTERS: A SEMINAR IN GREECE, PORTUGAL, AND TURKEY
Gladys A. Cotter *In* AGARD, Seminar on Basic Documentation Practices Aug. 1992 36 p (For primary document see N93-10593 01-82)
Copyright Avail: CASI HC A03/MF A02

Information technologies are evolving at a rapid pace in today's world. But the electronic technologies needed to transform today's libraries and information centers into electronic 'libraries without walls', where an end-user has instantaneous access to all the information needed from a desktop workstation, have not yet arrived. Even so, there are many technologies available today that can be applied in the library/information center environment to yield increased productivity. However, not all technologies are right for or successful in every environment. Mission, budget, infrastructure, client profiles, and staff skills are a few of the 'environmental' issues that must be considered when selecting and introducing new technologies into a particular information center. Key technologies used in libraries today are reviewed; it can be used as background for targeting technologies that could be successfully implemented in your own environment to further service goals. Before focusing on a selection of technologies, you must first focus on the strategic goal of your organization. The same technology is not right for every library/information center. An overview of technologies that are readily available and can be applied today is presented. Author

N93-10602# GEC-Marconi Electronics Ltd., Chelmsford (England).
SERVICES: USER SERVICES IN DEFENCE AND AEROSPACE DOCUMENTATION CENTRES
Chris Bigger *In* AGARD, Seminar on Basic Documentation Practices Aug. 1992 8 p (For primary document see N93-10593 01-82)
Copyright Avail: CASI HC A02/MF A02

When the Library stock and layout have been considered, the question of exploiting the collection arises. If money has been invested in stock, staff, and equipment then maximum use must be obtained from them, otherwise the library is failing the parent organization or funder. Full exploitation will produce useful returns on the money invested and further support for library services and future funding. Use of a library means matching users to information in the collection and various library services are available to achieve this. These services are described, highlighting the options, benefits, and problems. It is hoped that the discussion presents a starting point for further investigation of each area. Loans, interlibrary loans, and circulation systems are discussed first followed by information services such as bulletins, inquiry services, online, and current awareness. Author

N93-10603# Federal Armed Forces Documentation and Information Centre, Bonn (Germany).
SECURITY CONSIDERATIONS WITHIN MILITARY INFORMATION SYSTEMS
H. Braun *In* AGARD, Seminar on Basic Documentation Practices Aug. 1992 17 p (For primary document see N93-10593 01-82)
Copyright Avail: CASI HC A03/MF A02

Military information systems, as well as systems operating in a governmental environment, will administer classified information as well as documents, which are not to be released to the public. Such information needs reliable protection against unintentional disclosure and unauthorized access. Advice on the principles of a security risk analysis is presented, and methods for adequate handling of sensitive information are outlined, considering objectives, requirements, and functions of network security. Author

N93-10607# Energy Information Administration, Washington, DC.
EIA PUBLICATIONS DIRECTORY, 1991
19 May 1992 55 p
(DE92-015686; DOE/EIA-0149(91)) Avail: CASI HC A04/MF A01

Enacted in 1977, the Department of Energy (DOE) Organization Act established the Energy Information Administration (EIA) as the Department's independent statistical and analytical agency, with a mandate to collect and publish data and prepare analyses on energy production, consumption, prices, and resources, and projections of energy supply and demand. This edition of the EIA Publications Directory contains titles and abstracts of periodicals and one-time reports produced by the EIA from Jan. to Dec. 1991. This edition supplements EIA Publications Directory 1977-1989 and EIA Publications Directory 1990. The body of the Directory contains citations and abstracts arranged by broad subject categories, such as coal, petroleum, and natural gas and subcategories such as reserves, produces and byproducts, and marketing and economics. All reports are indexed alphabetically by subject and title and numerically by report number. DOE

N93-10610# Advisory Group for Aerospace Research and Development, Neuilly-Sur-Seine (France). Technical Information Panel.
AGARD INDEX OF PUBLICATIONS, 1989-1991 [INDEX DES PUBLICATIONS, 1989-1991]
Jul. 1992 520 p
(AGARD-Index-89-91; ISBN-92-835-0682-0) Copyright Avail: CASI HC A22/MF A04

This volume provides abstracts and indexes for AGARD unclassified publications published during the period 1989-1991. Full bibliographical citations and abstracts for all the documents in this publication are given in the abstract section, which is organized in the major subject divisions and specific categories used by NASA in abstract journals and bibliographies. The major subject divisions are listed, together with a note for each that defines its scope and provides any cross-references. Category breaks in the abstract section are identified by category number and title, and a scope note. Within each category, the abstracts are arranged by series and year. Six indexes -- subject (based on NASA Thesaurus nomenclature), personal author, corporate

source, panel, report/accession number, and accession number -- are included. Sample entries are shown on the first page of each index. Author

N93-10723# Air Force Inst. of Tech., Wright-Patterson AFB, OH.
OBJECT-ORIENTED DESIGN UNIFIES DATABASES AND APPLICATIONS
Douglas E. Dyer and Mark A. Roth 13 Jul. 1992 28 p
(AD-A253313; AFIT/EN-TR-92-2) Avail: CASI HC A03/MF A01

An object-oriented design methodology, such as the object modeling technique (OMT) of Rumbaugh et al., not only unifies database design with applications software design, it abstracts the design process and supports implementation regardless of the data model used. GRA

N93-10788# Oak Ridge National Lab., TN.
SPATIAL MODELS OF ECOLOGICAL SYSTEMS AND PROCESSES: THE ROLE OF GIS
C. T. Hunsaker, M. G. Turner, R. A. Nisbet (California Univ., Santa Barbara.), D. B. Botkin (California Univ., Santa Barbara.), and D. Lam (National Water Research Inst., Burlington, Ontario) 1991 36 p Presented at the Conference on Integrating Geographic Information Systems and Environmental Modeling, Boulder, CO, 15-19 Sep. 1991
(Contract DE-AC05-84OR-21400)
(DE92-016884; CONF-9109345-2) Avail: CASI HC A03/MF A01

This overview paper provides a foundation for the discussion of methods and techniques to integrate spatial ecological models with the technology of geographic information systems (GIS's). A brief review is provided of historical modeling approaches for terrestrial, freshwater, and marine ecosystems that have some spatial component or can be extended into space. Examples of current spatial models are discussed for these ecosystems, and the use of distributional mosaic models for the simulation of broad-scale landscape disturbances such as fire and pests is examined. Spatial modeling is terrestrial and freshwater ecosystems in more advanced than in marine systems; however, marine systems are well suited for the application of GIS's and spatial models. Future needs and directions that will enable ecological models to capitalize on the capabilities of GISs are discussed with regard to the following: data base management; remotely sensed data; landscape-level models; model-based management systems; data and model sensitivity, errors, and uncertainties; and environmental risk assessment. DOE

N93-10801# Royal Signals and Radar Establishment, Malvern (England).
UNIFYING INFORMATION FLOW POLICIES
Simon N. Foley (Cranfield Inst. of Tech., Bedford, England) Oct. 1990 95 p
(RSRE-90020; BR115416) Copyright Avail: CASI HC A05/MF A01

A structure for describing information flow policies that can express transitive, aggregation, and separation (of duty) exceptions is proposed. Operators for comparing, composing, and abstracting flow policies are described. These allow complex policies to be built from simpler policies. Many existing confidentiality (and by using a dual model, integrity) policies can be captured in this framework. A high water mark model is developed that can enforce these information flow policies. This model provides the basis for a taxonomy of existing high water mark mechanisms. Author

N93-10815*# National Aeronautics and Space Administration, Washington, DC.
INDEX TO NASA NEWS RELEASES AND SPEECHES, 1991
Apr. 1992 67 p
(NASA-TM-108004; NAS 1.15:108004) Avail: CASI HC A04/MF A01

This issue of the annual index to NASA Releases and Speeches contains a listing of news releases distributed by the Office of Public Affairs, NASA Headquarters, and a selected listing of speeches presented by members of the Headquarters staff during 1991. The index is arranged in six sections: Subject Index, Personal Name Index, News Release Number Index, Accession Number Index, and Speeches and News Releases Indices. R.L.B.

N93-10821# Royal Signals and Radar Establishment, Malvern (England).
ON THE PROBLEM OF SECURITY IN DATA BASES
Simon Wiseman Jan. 1989 13 p
(RSRE-Memo-4263; BR109899) Copyright Avail: CASI HC A03/MF A01

The fundamental problems of providing multi-level secure data base management systems are addressed. It is shown that the inference problems arises because data is used as an addressing mechanism. Existing solutions are described, but these are shown to have unfortunate consequences for the data base user and so alternatives are suggested. The problems of aggregation and deductions from real world knowledge are also considered. Author

N93-10826# Carnegie-Mellon Univ., Pittsburgh, PA.
TAQL: A PROBLEM SPACE TOOL FOR EXPERT SYSTEM DEVELOPMENT Ph.D. Thesis
Gregg R. Yost 1 May 1992 138 p
(Contract F33615-90-C-1465)
(AD-A253820; CMU-CS-92-134) Avail: CASI HC A07/MF A02

In recent years, the method-based approach to knowledge acquisition has received a great deal of attention. The method-based approach abandons traditional AI programming techniques and languages. Instead, method-based knowledge acquisition tools attempt to interact with the task developer in domain terms rather than computational terms. These tools are built around highly-structured problem-solving methods, and use knowledge of the built-in methods to drive knowledge acquisition. Method-based tools can be quite powerful, but the highly-structured method built into each tool limits its scope to a narrow range of tasks. Furthermore, there are some expert system tasks for which no method-based tool has yet been built, despite serious efforts to do so. SALT, KNACK, and OPAL are well-known method-based knowledge acquisition tools. GRA

N93-10844 Iowa State Univ. of Science and Technology, Ames.
A MULTILEVEL SECURITY MODEL FOR OBJECT-ORIENTED DATABASE SYSTEMS Ph.D. Thesis
Linda M. Null 1991 194 p
Avail: Univ. Microfilms Order No. DA9212173

One of the current research areas is to integrate database technology with object-oriented concepts. The problems involved with object-oriented data models are addressed, and additional proposals for multilevel security in such an environment are provided. A new object-oriented data model is presented, using formal specifications to provide a concise description of the data model, which includes aggregate and composite objects as well as versioning of objects. Multilevel security is addressed with the introduction of a multilevel security policy which describes the security needs and protection requirements of an object-oriented database system. Mandatory security and discretionary security are part of the security model which represents the security policy and specifies security properties that must exist for various entities in an object-oriented system, such as classes, methods and objects. All entities in the system are required to have a security classification level and all users must have a security clearance. In addition, various entities may contain negative authorization lists, specifying restricted access to certain users or groups of users. This security policy, which also addressed information flow violation, is then integrated into the new object-oriented data model. Protection in an object-oriented database system is further extended by providing secure transaction processing. New locking algorithms are introduced to enforce the security policy. At the user level, strategies for secure query processing are addressed. The concept of a virtual class is used to implement a secure view for users. Simple, content-based and context-based security

constraints are enforced by integrating a rule base with the database to perform query modification. The rule base contains security constraints as well as environmental information to protect against user inference. Dissert. Abstr.

N93-10867# EG and G Energy Measurements, Inc., Los Alamos, NM. Remote Sensing Lab.
GEOGRAPHIC INFORMATION SYSTEM (GIS) DEVELOPMENT ASSISTANCE FOR NUCLEAR REGULATORY COMMISSION (NRC) INCIDENT RESPONSE CAPABILITY
R. G. Best and A. L. Guber May 1992 17 p
(Contract DE-AC08-88NV-10617)
(DE92-017595; EGG-10617-1208) Avail: CASI HC A03/MF A01

A plan for managing the development of Geographic Information System (GIS) applications at the Savannah River Site (SRS) in a coordinated, integrated fashion was developed. Included in the plan are discussions on the guidance for GIS activities at the site, the overall strategy for managing GIS applications development, the specific administrative and programmatic tasks with projected completion schedules, and the organizational structure in place to direct this GIS effort. The Department of Energy-Savannah River Field Office (DOE-SR) has encouraged all primary subcontracting organizations at SRS involved with the mapping of spatial data to coordinate their efforts and be more cost effective. This plan provides a description of organized activities in 1992 for establishing a coordinated approach for developing and implementing GIS technology. DOE

N93-10872*# National Aeronautics and Space Administration, Washington, DC.
INDEX TO NASA NEWS RELEASES AND SPEECHES, 1990
Apr. 1991 62 p
(NASA-TM-108003; NAS 1.15:108003) Avail: CASI HC A04/MF A01

This issue of the annual Index to NASA News Releases and Speeches contains a listing of news releases distributed by the Office of Public Affairs, NASA Headquarters, and a selected listing of speeches presented by members of headquarters staff during 1990. The index is arranged in six sections: Subject Index, Personal Names Index, News Release Number Index, Accession Number, Speeches, and New Releases Indices. R.L.B.

N93-10883# Jackson State Univ., MS.
A SPATIAL SIMILARITY MEASURE FOR IMAGE DATABASE APPLICATIONS Interim Technical Report, Jul. 1990 - Sep. 1991
V. N. Gudivada, V. V. Raghavan, and Dwayne Carr 30 Apr. 1992 13 p
(Contract DAAL03-89-G-0118)
(AD-A253570; TR-91-1; ARO-27247.4-MA-SAH) Avail: CASI HC A03/MF A01

Image Retrieval has been considered as an important task in many application areas such as Geographic Information Systems and Computer-Aided Design. Facilitating retrieval of images based on their similarity to a specified image is a desircus feature of a retrieval scheme for an image database. Providing a suitable means for expressing spatial relationships in a query often improves the ease of specifying it. In this report, we propose a similarity retrieval algorithm for use in retrieval by spatial similarity. We also describe the generation of a test bed of images and the user interface development. The proposed method has been applied to a test bed of images comprising of floor and furniture layout designs. Each layout design is generated as an image consisting of several objects such as sofa, chair, and table. The dissimilarity between images is based on the notion of distance. The Euclidean distance is computed between the centroids of the matching pairs of constituent objects in both the images. The sum of all such distances plus a suitable penalty for non matching objects is a quantitative measure of spatial similarity. The experimental results obtained using the spatial similarity algorithm quite well agree with our intuitive ranking of the images in the collection. GRA

N93-10899# Army Engineer Topographic Labs., Fort Belvoir, VA.
A STANDARD FILE FORMAT FOR DATA INTERCHANGE
Michael McDonnel Jul. 1991 11 p
(AD-A254260; TEC-R-165) Avail: CASI HC A03/MF A01

This paper defines a new format and an associated method for encoding data in a set of files. This new format has advantages of simplicity, efficiency, and readability over current formats and their associated methods. A new format is necessary because all current widely available file formats retain restrictions (such as fixed field lengths) that are no longer necessary with modern programming languages. The proposed format has a simple syntax and flexible semantics. The main advantage of PDEF is its lack of fix semantics. This allows unforeseen data types and dependencies to be encoded without modifying the basic format. The PDEF format is efficient both for computers and people. It is efficient for computers because it uses the powerful parsing tools available for the C programming language. It is efficient for people because it encodes data descriptions in a human-readable form, and the content of a data set can be understood without a user's manual. PDEF stands for Protean Data Exchange Format owing to the ability of this format to encode many types of data. GRA

83 ECONOMICS AND COST ANALYSIS

Includes cost effectiveness studies.

No abstracts in this category.

84 LAW, POLITICAL SCIENCE AND SPACE POLICY

Includes NASA appropriation hearings; aviation law; space law and policy; international law; international cooperation; and patent policy.

No abstracts in this category.

85 URBAN TECHNOLOGY AND TRANSPORTATION

Includes applications of space technology to urban problems; technology transfer; technology assessment; and surface and mass transportation.

For related information see also *03 Air Transportation and Safety, 16 Space Transportation,* and *44 Energy Production and Conversion.*

No abstracts in this category.

88 SPACE SCIENCES (GENERAL)

No abstracts in this category.

89 ASTRONOMY

Includes radio, gamma-ray, and infrared astronomy, and astrometry.

N93-10364 Michigan Univ., Ann Arbor.
POWER SPECTRUM OF THE EXTRAGALACTIC BACKGROUND LIGHT Ph.D. Thesis
Jeffrey Robert Youngen 1991 124 p
Avail: Univ. Microfilms Order No. DA9135728

The extragalactic background light (EBL) is the surface brightness of the integrated light from distant unresolved galaxies. Because galaxies tend to cluster, the EBL is anisotropic, and this clustering is reflected in the power spectrum of the extragalactic background light (PSEBL). To measure the PSEBL, observations have been made on four pairs of fields near the galactic poles with a CCD imaging system on angular scales from 2' to 25' at 4400, 5500 and 7000 A. In total, 13 hours of data were collected. In order to collect information from as large a redshift as possible, foreground stars and galaxies brighter than 20.5 magnitudes have been removed from the data. To be sure that the final data is only characteristic of the EBL, specific checks have been made on the contributions to the power spectrum due to instrumental effects, atmospheric variations and zodiacal light, scattering halos of stars and galaxies, and the diffuse galactic light. Most of the data was taken at 7000 A, and the observed PSEBL is well fit by a power law with index -0.84 +/- 0.11. The measured power spectra are compared to a simple model which is based on the two-point galaxy correlation function xi(r). A power law shape for the spatial correlation function, xi(r) varies as r(sup -1.8), implies a power law shape for the angular power spectrum with index -1.2. The amplitude of the observed PSEBL corresponds to fluctuations in the surface brightness which are about 70 percent larger than predicted by the model. However, the amplitude of the power spectra can be explained by including modest luminosity evolution of the galaxy light. Based on the model, it is expected that half of the contributions to the PSEBL comes from beyond a redshift of z approx. 0.55. Dissert. Abstr.

N93-10876 Texas A&M Univ., College Station.
AUTONOMOUS STAR SENSING AND PATTERN RECOGNITION FOR SPACECRAFT ATTITUDE DETERMINATION Ph.D. Thesis
David Stephen Anderson 1991 254 p
Avail: Univ. Microfilms Order No. DA9133905

Autonomous star sensing and pattern recognition for attitude determination provides many technological challenges to modern spacecraft optical sensor design. This is mostly due to the relatively high accuracy requirements coupled with the faintness of many stellar sources, but is also due to real-time processing constraints. The performance of on-orbit star trackers is typically affected by nonlinearities such as lens distortion, coma, and chromatic aberration, as well as atmospheric refraction, thermal cycling, and possibly vibration. Despite these effects, the precise astrometric knowledge of inertially referenced stellar coordinates, along with thermoelectric cooling of the optical sensor, makes accurate star tracker calibration feasible. Land-based camera calibration, while not afflicted by many of the on-orbit difficulties, gives rise to a different set of problems relating to close range photogrammetry. The purpose of this dissertation is to report on the development and implementation of ideas related to near real-time, close range vision-based attitude sensing. The work begins with a survey of the current state of spacecraft attitude determination techniques, along with a discussion of relevant hardware devices. These ideas are extended to the case of close range photogrammetry for use in the laboratory, and a comprehensive discussion of the current experiments is presented. Topics include derivations of stellar and close range collinearity equations, mathematical modelling, CCD camera calibration techniques, resection and parameter estimation, optical aberrations, image processing and pattern recognition techniques, along with hardware and experimental results. Dissert. Abstr.

N93-10884 Oxford Univ. (England).
IMAGING OF BL LAC OBJECTS Ph.D. Thesis
Roberto G. Abraham 1991 166 p
Avail: Univ. Microfilms Order No. BRD-96177

The investigation of the host galaxies of BL Lac objects (BL Lacs) is a promising new field made practical in recent years by advances in detector technology and improved telescope siting. By better understanding the nature of these host galaxies, we can test the standard beaming and lensing models for BL Lacs. The techniques that we have developed for studying the host galaxies of BL Lac objects are described, and the results of a survey of BL Lac host galaxies that we have undertaken with 4.2 m William Herschel Telescope are presented. This survey successfully resolved many new host galaxies, determined the morphology of three BL Lac host galaxies for the first time, and confirmed the morphology of an additional three objects. One BL Lac object, PKS1413 + 135, displayed a number of surprising properties, and was consequently studied in greater detail at multiple wavelengths. These observations are also presented. We conclude with a description of Monte-Carlo simulations that we have undertaken in order to better determine the uncertainty in the results from our survey and to assess the promise of future telescope/instrumentation combinations for host galaxy imaging. Dissert. Abstr.

N93-10902*# Lockheed Aircraft Corp., Palo Alto, CA. Research Lab.
HIGH RESOLUTION OBSERVATIONS: THE STATE OF THE ART AND BEYOND
A. Title, T. Tarbell, R. Shine, K. Topka, and Z. Frank *In* ESA, Solar Physics and Astrophysics at Interferometric Resolution May 1992 p 9-14 Sponsored by NASA, Washington and NSF (For primary document see N93-10901 01-90)
Copyright Avail: CASI HC A02/MF A03

N93-10903# Centre National de la Recherche Scientifique, Verrieres-Le Buisson (France). Inst. d'Astrophysique Spatiale.
PLANNED OBSERVATIONS AT HIGH RESOLUTION FROM SPACE
P. Lemaire and E. Marsch (Max-Planck-Inst. fuer Aeronomie, Katlenburg-Lindau, Germany) *In* ESA, Solar Physics and Astrophysics at Interferometric Resolution May 1992 p 15-20 (For primary document see N93-10901 01-90)
Copyright Avail: CASI HC A02/MF A03

N93-10940# Grenoble-1 Univ. (France). Lab. d'Astrophysique.
SUCCESSES OF AND PROSPECTS FOR GROUND-BASED INTERFEROMETRY
C. Perrier *In* ESA, Solar Physics and Astrophysics at Interferometric Resolution May 1992 p 227-235 (For primary document see N93-10901 01-90)
Copyright Avail: CASI HC A02/MF A03

N93-10941# European Southern Observatory, Garching (Germany).
GROUND-BASED HIGH ANGULAR RESOLUTION OBSERVATION OF THE SUN BY INTERFEROMETRY IN THE VISIBLE
O. vonderLuehe *In* ESA, Solar Physics and Astrophysics at Interferometric Resolution May 1992 p 237-241 (For primary document see N93-10901 01-90)
Copyright Avail: CASI HC A01/MF A03

N93-10942# Observatoire de la Cote d'Azur, Nice (France). Dept. Augustin Fresnel.
THE CHARON PROGRAM
G. Schumacher, P. Cruzalebes, S. Menardi, and Y. Rabbia *In* ESA, Solar Physics and Astrophysics at Interferometric Resolution May 1992 p 243-246 (For primary document see N93-10901 01-90)
Copyright Avail: CASI HC A01/MF A03

N93-10943# European Southern Observatory, Garching (Germany).
INTERFEROMETRY WITH THE VERY LARGE TELESCOPE
O. vonderLuehe, J. M. Beckers, M. Faucherre, B. Koehler, F. Merkle, and N. Zhu *In* ESA, Solar Physics and Astrophysics at Interferometric Resolution May 1992 p 247-254 (For primary document see N93-10901 01-90)
Copyright Avail: CASI HC A02/MF A03

N93-10944# Netherlands Foundation for Radio Astronomy, Dwingelo.
TOWARDS AN ESA STRATEGY FOR OPTICAL INTERFEROMETRY IN SPACE. RECOMMENDATIONS OF THE ESA SPACE INTERFEROMETRY STUDY TEAM (SIST)
J. E. Noordam, P. Y. Bely (Space Telescope Science Inst., Baltimore, MD.), M. Faucherre (European Southern Observatory, Garching, Germany), A. H. Greenaway (Royal Signals and Radar Establishment, Malvern, England), F. Merkle (European Southern Observatory, Garching, Germany), M. A. C. Perryman (European Space Agency. European Space Research and Technology Center, ESTEC, Noordwijk, Netherlands), P. H. Roussel (European Space Agency. European Space Research and Technology Center, ESTEC, Noordwijk, Netherlands), F. Vakili, S. Volonte (European Space Agency, Paris, France), and G. P. Weigelt (Max-Planck-Inst. fuer Radioastronomie, Bonn, Germany) *In* ESA, Solar Physics and Astrophysics at Interferometric Resolution May 1992 p 255-257 (For primary document see N93-10901 01-90)
Copyright Avail: CASI HC A01/MF A03

N93-10945# Imperial Coll. of Science and Technology, London (England).
REPORT OF THE LUNAR INTERFEROMETRY STUDY TEAM (LIST) ACTIVITIES
J. C. Dainty, M. Faucherre (European Southern Observatory, Garching, Germany), A. H. Greenaway (Royal Signals and Radar Establishment, Malvern, England), A. I. Harris (Max-Planck-Inst. fuer Physik und Astrophysik, Garching, Germany), A. Labeyrie (Observatoire de la Cote d'Azur, Nice, France), J. E. Noordam (Netherlands Foundation for Radio Astronomy, Dwingelo.), G. P. Weigelt (Max-Planck-Inst. fuer Radioastronomie, Bonn, Germany), J. Beckers, J. Lequeux (Observatoire de Paris-Meudon, France), and C. M. Fridlund (European Space Agency. European Space Research and Technology Center, ESTEC, Noordwijk, Netherlands) et al *In* ESA, Solar Physics and Astrophysics at Interferometric Resolution May 1992 p 259-266 (For primary document see N93-10901 01-90)
Copyright Avail: CASI HC A02/MF A03

N93-10946# Defence Research Agency, Malvern (England).
GROUND/SPACE CO-OPERATION FOR INTERFEROMETRY
A. H. Greenaway *In* ESA, Solar Physics and Astrophysics at Interferometric Resolution May 1992 p 267-270 (For primary document see N93-10901 01-90)
Copyright Avail: CASI HC A01/MF A03

N93-10947# Centre National de la Recherche Scientifique, Verrieres-Le Buisson (France). Inst. d'Astrophysique Spatiale.
ROTATIONAL APERTURE SYNTHESIS: A PROPOSAL FOR GROUND-BASED OBSERVATIONS
Guy Artzner *In* ESA, Solar Physics and Astrophysics at Interferometric Resolution May 1992 p 273-276 (For primary document see N93-10901 01-90)
Copyright Avail: CASI HC A01/MF A03

N93-10948# Centre National de la Recherche Scientifique, Verrieres-Le Buisson (France). Service d'Aeronomie.
DEMONSTRATION AND PERFORMANCES OF REAL-TIME FRINGE TRACKING: A STEP TOWARDS COPHASED INTERFEROMETERS
L. Dame *In* ESA, Solar Physics and Astrophysics at Interferometric Resolution May 1992 p 277-282 (For primary document see N93-10901 01-90)
(Contract ESA-7978)
Copyright Avail: CASI HC A02/MF A03

N93-10957# Aerospatiale, Cannes (France).
SOME POSSIBLE SPACE INTERFEROMETRY APPLICATIONS
D. Simeoni, B. Koehler, M. Sghedoni, and L. DeSa *In* ESA, Solar Physics and Astrophysics at Interferometric Resolution May 1992 p 309-311 (For primary document see N93-10901 01-90)
Copyright Avail: CASI HC A01/MF A03

90 ASTROPHYSICS

Includes cosmology; celestial mechanics; space plasmas; and interstellar and interplanetary gases and dust.
For related information see also *75 Plasma Physics*.

N93-10067*# National Aeronautics and Space Administration, Washington, DC.
GAMMA RAY ASTROPHYSICS TO THE YEAR 2000. REPORT OF THE NASA GAMMA RAY PROGRAM WORKING GROUP
Oct. 1988 35 p
(NASA-TM-107995; NAS 1.15:107995) Avail: CASI HC A03/MF A01

Important developments in gamma-ray astrophysics up to energies of 100 GeV during the last decade are reviewed. Also, the report seeks to define the major current scientific goals of the field and proposes a vigorous program to pursue them, extending to the year 2000. The goals of gamma-ray astronomy include the study of gamma rays which provide the most direct means of studying many important problems in high energy astrophysics including explosive nucleosynthesis, accelerated particle interactions and sources, and high-energy processes around compact objects. The current research program in gamma-ray astronomy in the U.S. including the space program, balloon program and foreign programs in gamma-ray astronomy is described. The high priority recommendations for future study include an Explorer-class high resolution gamma-ray spectroscopy mission and a Get Away Special cannister (GAS-can) or Scout class multiwavelength experiment for the study of gamma-ray bursts. Continuing programs include an extended Gamma Ray Observatory mission, continuation of the vigorous program of balloon observations of the nearby Supernova 1987A, augmentation of the balloon program to provide for new instruments and rapid scientific results, and continuation of support for theoretical research. Long term recommendations include new space missions using advanced detectors to better study gamma-ray sources, the development of these detectors, continued study for the assembly of large detectors in space, collaboration with the gamma-ray astronomy missions initiated by other countries, and consideration of the Space Station attached payloads for gamma-ray experiments. L.R.R.

N93-10238# Rensselaer Polytechnic Inst., Troy, NY.
PROBING COSMIC INFRARED SOURCES: A COMPUTER MODELING APPROACH Final Technical Report, 1 Nov. 1988 - 30 Apr. 1992
Chun M. Leung Jun. 1992 278 p
(Grant AF-AFOSR-0104-89)
(AD-A253788; AFOSR-92-0759TR) Avail: CASI HC A13/MF A03

Phenomenological computer models were constructed to interpret observations of cosmic infrared sources and to make predictions which would stimulate further studies. The research was divided into four areas: (1) Detailed radiation transport models, incorporating both the equilibrium heating of large dust grains and the transient heating of very small grains, were constructed for interstellar dust clouds and circumstellar dust shells of evolved stars to parameterize the observed radiation characteristics in terms of their physical source properties. (2) Existing methods of analysis (e.g., semi-analytical methods for determining the dust mass, dust temperature, and grain emissivity laws) in infrared astronomy were

critically evaluated to determine the conditions under which these approaches were valid and reliable. Semi-empirical relationships were then developed to facilitate the rapid interpretation of infrared observations. (3) Theoretical models were developed to study various physical phenomena involving dust grains, e.g., molecule formation on grains, grain formation in expanding circumstellar envelopes. (4) Several computational techniques were investigated which could automate and improve the efficiency of existing radiation transport codes for modeling infrared sources. GRA

N93-10296# International Centre for Theoretical Physics, Trieste (Italy).
VECTOR SUPERCONDUCTIVITY IN COSMIC STRINGS
G. R. Dvali and S. M. Mahajan Mar. 1992 11 p
(DE92-634923; IC-92/41) Avail: CASI HC A03/MF A01

We argue that in most realistic cases, the usual Witten-type bosonic superconductivity of the cosmic string is automatically (independent of the existence of superconducting currents) accompanied by the condensation of charged gauge vector bosons in the core giving rise to a new vector type superconductivity. The value of the charged vector condensate is related to the charged scalar expectation value, and vanishes only if the latter goes to zero. The mechanism for the proposed vector superconductivity, differing fundamentally from those in the literature, is delineated using the simplest realistic example of the two Higgs doublet standard model interacting with the extra cosmic string. It is shown that for a wide range of parameters, for which the string becomes scalarly superconducting, W boson condensates (the sources of vector superconductivity) are necessarily excited. DOE

N93-10303 Texas Univ., Austin.
ON THE GRAVITATIONAL POTENTIAL OF TWO ARBITRARY ROTATING BODIES WITH APPLICATIONS TO THE EARTH-MOON SYSTEM Ph.D. Thesis
Curt vonBraun 1991 139 p
Avail: Univ. Microfilms Order No. DA9128388

The improving accuracy of lunar laser range measurements places exacting demands on the theoretical development of models for the lunar orbit, lunar rotation, and earth orientation, which are capable of simulating range effects at one to three centimeter accuracy levels. This study develops a complete rigid body model for the gravitational field of the earth-moon system and establishes the magnitude of the radial, transverse, and normal perturbations due to the geopotential and selenopotential on the orbit of the moon, the influence of the gravitational moments of the earth and sun on the selenopotential, and the contribution of the third degree and order terms in the geopotential to the nutation of the earth. These results are determined by first deriving an expression for the mutual gravitational potential function of two arbitrary rotating bodies and the forces and moments that act between them. Using the appropriate set of equations governing the translational and rotational motion of the moon and the rotational motion of the earth, these are numerically integrated over time to determine the magnitude of the orbit and orientation perturbations due to the harmonic coefficients of both the geopotential and the selenopotential. Dissert. Abstr.

N93-10901# European Space Agency, Paris (France).
SOLAR PHYSICS AND ASTROPHYSICS AT INTERFEROMETRIC RESOLUTION
L. Dame, ed. (Centre National de la Recherche Scientifique, Verrieres-Le Buisson, France) and T.-D. Guyenne, ed. May 1992 293 p Held in Paris, France, 17-19 Feb. 1992
(ESA-SP-344; ISBN-92-9092-218-4; ETN-92-92167) Copyright Avail: CASI HC A13/MF A03

Papers from the conference are given. The scientific aims of the conference include some of the unique possibilities of space interferometry such as ultraviolet spectral line imaging of kilometric size structures on the Sun, and access to reference objects for pointing and cophasing. The ability to maintain phase control over long periods (minutes to hours) is fundamental to the design of space interferometers and a promising method of offset pointing; offset cophasing on a reference field of view was investigated thoroughly in the framework of the Solar Ultraviolet Network (SUN) design. Papers are presented under the following headings: very high resolution solar physics; solar system and galactic astrophysics at high resolution; SIMURIS model payloads, instrumentation and performances; and strategy for interferometry from space. For individual titles, see N93-10902 through N93-10957.

N93-10902*# Lockheed Aircraft Corp., Palo Alto, CA. Research Lab.
HIGH RESOLUTION OBSERVATIONS: THE STATE OF THE ART AND BEYOND **c89**
A. Title, T. Tarbell, R. Shine, K. Topka, and Z. Frank *In* ESA, Solar Physics and Astrophysics at Interferometric Resolution May 1992 p 9-14 Sponsored by NASA, Washington and NSF (For primary document see N93-10901 01-90)
Copyright Avail: CASI HC A02/MF A03

The meaning of high resolution and its scientific importance with regard to solar observations is discussed. The state of the art is reviewed, looking into Solar Optical Universal Polarimeter (SOUP) observations, image selection techniques, and adaptive optics. It is concluded that until there are observations in space, complete understanding of processes in the solar photosphere, chromosphere, transition region, and corona will be impossible. The importance of high resolution is considered with regard to solar surface and convection, solar photosphere inside and outside magnetic fields, and sunspot geometry. ESA

N93-10903# Centre National de la Recherche Scientifique, Verrieres-Le Buisson (France). Inst. d'Astrophysique Spatiale.
PLANNED OBSERVATIONS AT HIGH RESOLUTION FROM SPACE **c89**
P. Lemaire and E. Marsch (Max-Planck-Inst. fuer Aeronomie, Katlenburg-Lindau, Germany) *In* ESA, Solar Physics and Astrophysics at Interferometric Resolution May 1992 p 15-20 (For primary document see N93-10901 01-90)
Copyright Avail: CASI HC A02/MF A03

The performance and ability of solar space instruments launched during the last 20 years are recalled. The main characteristics and parameters of three UV instruments which are part of the Solar and Heliospheric Observatory (Soho) coronal payload are described: SUMER (Solar Ultraviolet Measurement of Emitted Radiations), CDS (Coronal Diagnostic Spectrometer), and EIT (Extreme ultraviolet Imager Telescope). Insight into a few instruments that are in study and which may fly during the next decade are given. ESA

N93-10904# Centre National de la Recherche Scientifique, Verrieres-Le Buisson (France). Service d'Aeronomie.
PROSPECTS WITH SIMURIS **c92**
L. Dame and R. J. Rutten (Astronomical Inst., Utrecht, Netherlands) *In* ESA, Solar Physics and Astrophysics at Interferometric Resolution May 1992 p 21-25 (For primary document see N93-10901 01-90)
Copyright Avail: CASI HC A01/MF A03

The SIMURIS (Solar, solar system and stellar Interferometric Mission for Ultrahigh Resolution Imaging and Spectroscopy) payload is introduced and its goals and concepts outlined. The major goal of SIMURIS is to achieve solar physics at unprecedented image resolution, sufficiently high enough to resolve the fine structuring governed by basic magnetohydrodynamical and plasma physics processes. Requirements of SIMURIS are outlined; these include very high spatial resolution, multiband observation, narrowband imaging, broadband line selection, two dimensional spectrometry, and photon usage versatility. The main instruments on SIMURIS are the Solar Ultraviolet Network (SUN), and the Imaging Fourier Transform Spectrometer (IFTS). The concepts from which these were designed are discussed. ESA

N93-10905# Eidgenoessische Technische Hochschule, Zurich (Switzerland). Inst. of Astronomy.
SMALL-SCALE PHYSICS OF CONVECTION AND MAGNETIC FIELDS **c92**

S. K. Solanki *In* ESA, Solar Physics and Astrophysics at Interferometric Resolution May 1992 p 27-33 (For primary document see N93-10901 01-90)
Copyright Avail: CASI HC A02/MF A03

An overview of current knowledge of the properties and the physics of small scale magnetic features, magnetoconvection and convection, is given. Theoretical aspects are focused upon. Some examples of features or processes which require very high spatial resolution to be observed are given. ESA

N93-10906# Observatoire de Paris-Meudon (France).
CHROMOSPHERIC STRUCTURE AND DYNAMICS **c92**
B. Schmieder *In* ESA, Solar Physics and Astrophysics at Interferometric Resolution May 1992 p 35-42 (For primary document see N93-10901 01-90)
Copyright Avail: CASI HC A02/MF A03

Chromospheric structures are observed up to the limiting resolving power of the instruments (less than 0.5 inches). The magnetic field controls the chromospheric topology both at the large scale, such as canopies, supergranulation, mesogranulation and at the small scale, such as fibrils, mottles, and spicules. Different properties of the chromosphere structure may be deduced from a dynamics study. The role of magnetic and convective forces in oscillatory and nonstationary flows observed in the structures is discussed. Spectroscopic diagnostics are used to derive physical parameters in chromospheric structures. Instruments working in spectroscopic mode with a two dimensional field of view are needed. The multichannel double pass spectrographs (Meudon and Pic du Midi in France and Canary Islands) are particularly well adapted to these observations from the ground. ESA

N93-10907# Hulburt (E. O.) Center for Space Research, Washington, DC.
TRANSITION REGION DYNAMICS **c92**
K. P. Dere *In* ESA, Solar Physics and Astrophysics at Interferometric Resolution May 1992 p 43-48 (For primary document see N93-10901 01-90)
Copyright Avail: CASI HC A02/MF A03

The solar transition region, an ideal testing ground for theories of coronal heating and dynamics, is studied. Strong diagnostic lines formed at transition region temperatures (200,000 to 2,000,000K) are found at VUV wavelengths that are observable with relatively straightforward optical techniques. The transition region is highly dynamic; nonthermal velocities peak at 100,000 K and high velocity explosive events, indicators of magnetic reconnection, are commonly found throughout the quiet and active Sun. The fine scale density and velocity structures indicate that important information will be found at spatial scales below 1 inch. ESA

N93-10908# Florence Univ. (Italy). Dipartimento di Astronomia e Scienza dello Spazio.
ULTRA-HIGH OBSERVATIONS OF THE PROMINENCE-CORONA TRANSITION REGION **c92**
F. C. Chiuderi-Drago *In* ESA, Solar Physics and Astrophysics at Interferometric Resolution May 1992 p 49-51 (For primary document see N93-10901 01-90)
Copyright Avail: CASI HC A01/MF A03

Two models of the Prominence Corona Transition Region (PCTR) are analyzed in view of the possibility of ultrahigh resolution observations of UV lines on filaments and prominence. The first model assumes an isothermal cool filament (T less than 10,000 K) with a PCTR around it, while the second one assumes that a PCTR is present around each one of the thin H(alpha) threads which are usually observed in filaments. In this latter model, dissipation of Alfven waves is invoked to heat the power portion of the PCTR where the magnetic field is perpendicular (upside down Delta) T. ESA

N93-10909# Observatoire de Paris-Meudon (France).
CORONAL AND SOLAR WIND ALFVEN WAVE PROPAGATION **c92**
M. Velli *In* ESA, Solar Physics and Astrophysics at Interferometric Resolution May 1992 p 53-55 (For primary document see N93-10901 01-90)
Copyright Avail: CASI HC A01/MF A03

The transmission of Alfven waves through the solar corona and into the solar wind is discussed for isothermal models with a radial magnetic field. For comparison, the transmission through a static, spherical isothermal corona is also calculated. ESA

N93-10910# Ceskoslovenska Akademie Ved, Ondrejov. Astronomical Inst.
THE FINE STRUCTURE OF PROMINENCES **c92**
P. Heinzel and J.-C. Vial (Centre National de la Recherche Scientifique, Verrieres-Le Buisson, France) *In* ESA, Solar Physics and Astrophysics at Interferometric Resolution May 1992 p 57-64 Sponsored in part by ESA (For primary document see N93-10901 01-90)
(Grant N-30315)
Copyright Avail: CASI HC A02/MF A03

Evidence of the fine structure shown by prominence imaging is discussed, and evidence of small magnetic field structuring is identified. Velocity measurements that point to fine structure are presented. The status of the most recent results in NLTE modeling and the progress made towards realistic radiative transfer computations with numerous fine structures like threads are given. It is shown that the prominence corona transition region is also characterized by small scale structures. The exciting prospects offered by very high resolution observations possible with SIMURUS (Solar, solar system and stellar Interferometric Mission for Ultrahigh Resolution Imaging and Spectroscopy) are considered. ESA

N93-10911# Observatoire de Paris-Meudon (France).
INTENSITY, VELOCITY, AND TURBULENCE IN PROMINENCES OBSERVED WITH THE HRTS **c92**
J. E. Wiik (Oslo Univ., Norway), K. Dere (Naval Research Lab., Washington, DC.), and B. Schmieder *In* ESA, Solar Physics and Astrophysics at Interferometric Resolution May 1992 p 65-68 (For primary document see N93-10901 01-90)
Copyright Avail: CASI HC A01/MF A03

The moments of UV emission line profiles between 1206 and 1670 A observed in two quiescent prominences with the High Resolution Telescope and Spectrograph (HRTS) are analyzed. Spectral lines in this region of the solar spectrum such as C1, Si2, Si4, He2, and C4 provide information on plasmas in the 10,000 to 200,000 K range. In both prominences, a good correlation is found between the intensities of lines formed at different temperatures. A good correlation is also found between the nonthermal velocities of different lines. Generally, the nonthermal velocity increases with intensity and temperature. The nonthermal velocities are higher in the HRTS 1 prominence. Mean nonthermal velocity is 20 km/s for the HRTS 1 prominence and 10 km/s for the SL2 one. The line of sight velocities are generally well correlated in the HRTS 1 prominence. On the contrary, in the SL2 prominence, poor correlation is found between the line of sight velocities of all lines. ESA

N93-10912# Paris VII Univ. (France). Lab. d'Astrophysique Extragalactique et de Cosmologie.
PHYSICS OF CORONAL LOOPS: HEATING AND RECONNECTION **c92**
J. Heyvaerts (Observatoire de Paris-Meudon, France) *In* ESA, Solar Physics and Astrophysics at Interferometric Resolution May 1992 p 69-72 (For primary document see N93-10901 01-90)
Copyright Avail: CASI HC A01/MF A03

The importance of small scale structures in the current distribution is outlined, and the smallest size that these current structures might have is discussed. It is shown that they must be dynamic, turbulent structures. The physical processes that may be at the origin of the formation of such structures are discussed. The braiding of field lines, the phase mixing of oscillations in inhomogeneous magnetic configurations, and a number of secondary instabilities are likely to be the dominant ones. A self-consistent calculation of a large scale coronal flow with

associated turbulence is described. This parameter free theory gives, as a function of boundary motions which cause it, the rate of coronal heating by fine scaled DC current structures. ESA

N93-10913# Birmingham Univ. (England). Dept. of Physics and Space Research.
ENERGY BUILD-UP, TRANSPORT, AND RELEASE IN SOLAR FLARES **c92**
G. M. Simnett *In* ESA, Solar Physics and Astrophysics at Interferometric Resolution May 1992 p 73-80 (For primary document see N93-10901 01-90)
Copyright Avail: CASI HC A02/MF A03

With the advent of the new observatories, it is becoming more evident that the solar flare is a more global phenomenon than previously thought. It is only the high temperature/high density manifestations that are confined to a small part of an active region. The overall question of the energy buildup, transport, and release is examined from a global perspective. The case of transporting the flare energy via energetic charged particles is discussed. Out of the two possibilities, protons or electrons, it is found that the protons give the more satisfactory account for the observations. ESA

N93-10914# Observatoire de Paris-Meudon (France). Dept. Atomes et Molecules en Astrophysique.
STOKES PARAMETERS OF THE O VI 103.2 nm LINE AS A PROBE OF THE MATTER VELOCITY FIELD VECTOR IN THE SOLAR WIND ACCELERATION REGION **c92**
S. Sahal-Brechot, N. Feautrier, V. Bommier, and A. deKertanguy *In* ESA, Solar Physics and Astrophysics at Interferometric Resolution May 1992 p 81-85 (For primary document see N93-10901 01-90)
Copyright Avail: CASI HC A01/MF A03

A theoretical method to determine the matter velocity field vector in the solar wind acceleration region is presented. The O VI 103.2 nm line should be observed high in the corona in the solar wind acceleration region. Preliminary results show that the interpretation of polarimetric data, associated to the shift and the Doppler dimming effect, provided that the partial anisotropy of the incidence radiation field be taken into account, should offer a method of diagnostic of the complete velocity field vector which is currently missing and which is indispensable to understand the acceleration mechanisms of the solar wind and to develop a dynamical modelization of the solar structures. ESA

N93-10915# Centre National de la Recherche Scientifique, Verrieres-Le Buisson (France). Inst. d'Astrophysique Spatiale.
EVIDENCE OF PLASMOID EJECTION IN THE CORONA FROM 1991 ECLIPSE OBSERVATIONS WITH THE CANADA-FRANCE-HAWAII TELESCOPE **c92**
J.-C. Vial, S. Koutchmy (Institut d'Astrophysique, Paris, France), G. Monnet (Canada-France-Hawaii Telescope Corp., Waimea, HI.), J. Sovka (Canada-France-Hawaii Telescope Corp., Waimea, HI.), C. Clark (Canada-France-Hawaii Telescope Corp., Waimea, HI.), D. Salmon (Canada-France-Hawaii Telescope Corp., Waimea, HI.), N. Purves (Canada-France-Hawaii Telescope Corp., Waimea, HI.), P. Sydserff (Canada-France-Hawaii Telescope Corp., Waimea, HI.), R. Coulder (Sacramento Peak Observatory, Sunspot, NM.), and L. November (Sacramento Peak Observatory, Sunspot, NM.) et al *In* ESA, Solar Physics and Astrophysics at Interferometric Resolution May 1992 p 87-90 (For primary document see N93-10901 01-90)
Copyright Avail: CASI HC A01/MF A03

Observations of the solar corona with a large telescope at high altitude was fully exploited with the 3.60 m CFHT (Canada France Hawaii Telescope) in Hawaii, during the 11 Jul. 1991 eclipse, are reported. Different instruments set up for the eclipse and preliminary results are given. The moving feature in the corona is focused upon. Physical conditions in this plasmoid and its origins are discussed. One of the four cameras installed in the primary focus was a video charge coupled device camera with a red filter at 637 nm selecting the red line. The power of the telescope allowed for a good signal in a pixel as small as 0.12 arcsec and a very good time resolution. The spectral resolution as measured at the Moon limb was better than one arcsec. During the three minute long sequence, 6000 video images were obtained. Among the fine structures recorded, a plasmoid about 1500 km wide was seen to ascend and dilute in the corona. Possible emission mechanisms are discussed. It was found that both low and relatively high temperature plasmas can be confined in this ejected plasmoid. Such a small scale phenomenon could be important for the heating of the corona and should be observed in UV emission lines in a wide range of temperatures. The high spatial resolution achieved by Solar Interferometric Mission for Ultrahigh Resolution Imaging and Spectroscopy (SIMURIS) allows to study the shape, stability and the diagnostics of such plasmoids in the corona. ESA

N93-10916# Rutherford Appleton Lab., Chilton (England).
HIGH RESOLUTION OBSERVATIONS OF SOLAR EJECTA **c92**
Richard A. Harrison *In* ESA, Solar Physics and Astrophysics at Interferometric Resolution May 1992 p 91-94 (For primary document see N93-10901 01-90)
Copyright Avail: CASI HC A01/MF A03

Requirements for detailed observation of ejecta and flows in the solar atmosphere are examined and the potential for observations of such phenomena using SIMURIS (Solar Interferometric Mission for Ultrahigh Resolution Imaging and Spectroscopy) are addressed. The solar atmosphere displays various ejection phenomena, with varying sizes, speeds, and characteristic time scales, presumably, resulting from various physical processes. These phenomena include the so called high velocity events detected in the transition region and the corona, chromospheric ejecta known as sprays and surges, and coronal mass ejecta, which include prominence eruptions. The salient observed features are discussed, and a brief description of the outstanding physical problems which govern the observational needs for each event type is given. ESA

N93-10917# Astronomical Inst., Utrecht (Netherlands).
SMALL SCALE PROCESSES IN SOLAR AND STELLAR PLASMAS **c92**
G. H. J. vandenOord *In* ESA, Solar Physics and Astrophysics at Interferometric Resolution May 1992 p 97-104 Sponsored by ESA and Royal Netherlands Academy of Arts and Sciences (For primary document see N93-10901 01-90)
Copyright Avail: CASI HC A02/MF A03

Small scale processes which occur in the magnetically dominated outer layers of the Sun are reviewed. The transport coefficients for the thermal and the electrical conductivity in the classical limit and in the limit of anomalous processes are discussed. It is demonstrated that the corona and the chromosphere must have a filamentary structure. Various heating mechanisms which are based on small scale dissipation of magnetic energy are discussed. The observational requirements for improved modeling of the transition region and the chromosphere are formulated and the consequences of high resolution observations for flare models are pointed out. ESA

N93-10918# Sussex Univ., Brighton (England). Astronomy Centre.
STELLAR AND CIRCUMSTELLAR EVOLUTION AND ACTIVITY
A. Collier-Cameron *In* ESA, Solar Physics and Astrophysics at Interferometric Resolution May 1992 p 105-108 (For primary document see N93-10901 01-90)
Copyright Avail: CASI HC A01/MF A03

Evidence for solar-like magnetic activity on other stars is discussed. This evidence can reveal much about the way in which magnetic activity levels depend on global stellar parameters. Conversely, it now seems that dynamo-generated stellar magnetic fields may themselves modify the rotational evolution of solar type stars significantly. The use of time resolved UV spectroscopy and high resolution imaging with the Solar Interferometric Mission for Ultrahigh Resolution, Imaging and Spectroscopy (SIMURIS) to advance understanding of the structure and evolution of local

magnetic structures in stellar environments, on scales from fractions of a stellar radius to a few tens of AU, are discussed.
ESA

N93-10919# Utrecht State Univ. (Netherlands). Inst. of Astronomy.
YELLOW HYPERGIANT INTERFEROMETRY: A CLUE TO UNDERSTANDING EVOLUTIONARY INSTABILITY
Cornelis deJager and Hans Nieuwenhuijzen *In* ESA, Solar Physics and Astrophysics at Interferometric Resolution May 1992 p 109-111 Prepared in cooperation with Space Research Organization Netherlands, Utrecht (For primary document see N93-10901 01-90)
Copyright Avail: CASI HC A01/MF A03

The importance of interferometry of yellow hypergiants is stressed because of their presumable evolutionary performance in relation to the 'yellow evolutionary void'. The large scale motion field due to nonlinear pulsations, the evolutionary atmospheric instability, the mass loss, and the formation of a 'decretion' disk are discussed. Yellow supergiants are stars with nearly unstable atmospheres, characterized by strong low mode non radial pulsations and intense mass loss. In the Hertzprung Russel diagram, they are located at the cool side of a region where atmospheres are unstable. The atmospheric pulsations should manifest themselves as hot and cool areas in the disk. The strong mass loss will lead to a rather dense equatorial decretion disk that should be observable interferometrically. Many other types of stars may have similar properties. ESA

N93-10920# Centre National de la Recherche Scientifique, Orsay (France). Inst. d'Astrophysique Spatiale.
TOMOGRAPHIC/INTERFEROMETRIC STUDIES OF ACTIVE STARS AND BINARIES
S. Jankov (Astronomical Observatory, Belgrade, Yugoslavia), S. Char (La Serena Univ., Chile), and Bernard H. Foing *In* ESA, Solar Physics and Astrophysics at Interferometric Resolution May 1992 p 113-121 (For primary document see N93-10901 01-90)
Copyright Avail: CASI HC A02/MF A03

The principle of indirect imaging of stellar surfaces, based on spectroscopic and photometric rotation modulation is described, and application and results of Doppler imaging of spotted stars are presented. The common problem of regularization of the inverse problem for the interferometric and tomographic methods is discussed. The applicability of both methods to different phenomena of stellar activity is compared. It is concluded that space interferometry and tomographic imaging methods should be used to produce complementary results in order to have an access to phenomena of different temporal and spatial behavior.
ESA

N93-10921# Centre National de la Recherche Scientifique, Verrieres-Le Buisson (France). Inst. d'Astrophysique Spatiale.
PROSPECTS IN STELLAR AND GALACTIC OBSERVATIONS WITH SIMURIS
Bernard H. Foing *In* ESA, Solar Physics and Astrophysics at Interferometric Resolution May 1992 p 123-130 (For primary document see N93-10901 01-90)
Copyright Avail: CASI HC A02/MF A03

The ability of the Solar Interferometric Mission for Ultrahigh Resolution Imaging and Spectroscopy (SIMURIS) instruments to access nonsolar objects, with an interesting resolution for several stellar programs in preparation for future long baseline interferometers in space or on the Moon is considered. Stellar angular diameters can be measured below the Rayleigh resolution of the Solar Ultraviolet Network (SUN) interferometer, by calibration of the point spread function and by differential interferometric centroid measurements in the blue and red wings of a given spectral line. Using both SUN spatial resolution and Imaging Fourier Transform Spectrometer (IFTS) spectral resolution, the separations and velocity curves of binary stars can be determined at several wavelengths. In particular, separations of binaries including cepheids or supergiants brighter than 12 and a hotter companion brighter than 15 at 180 nm can be obtained down to 0.1 arcsec up to 2 kpc in the galaxy, thus allowing the masses and distances of the components to be solved. Stellar magnetic activity phenomena can be traced ideally in the UV and XUV, through chromospheric, transition region, and coronal lines. Rotational modulation, Doppler tomography, and differential interferometric imaging can be combined to provide a map of active stars in different lines formed at different temperatures and height, giving a three dimensional view of the global activity phenomena on nearby stars and binaries. SIMURIS will also be able to address the diagnostics of stellar flares, extended coronal structures, or for their circumstellar environment and mass transfer phenomena.
ESA

N93-10922# Centre National de la Recherche Scientifique, Verrieres-Le Buisson (France). Inst. d'Astrophysique.
MAGNETOSPHERES AND ATMOSPHERES OF PLANETS c91
Renee Prange *In* ESA, Solar Physics and Astrophysics at Interferometric Resolution May 1992 p 131-138 (For primary document see N93-10901 01-90)
Copyright Avail: CASI HC A02/MF A03

A review of planetary magnetospheres, which depend upon a few key parameters such as the magnetic dipole strength, the planetary rotation rate, and the strength of the internal plasma sources, is given. Present knowledge of the large scale circulation of magnetospheric plasma is rather poor. It is shown how understanding of their dynamics could benefit from high spectral and spatial resolution sensing in the UV to near IR range. The planetary atmospheric constituents are also observable in this wavelength range from the cloud level to the planetary exospheres. New insights on the composition (and the atmospheric formation and evolution processes), the large scale circulation patterns, the stratospheric dynamics and chemistry, and the interaction of the upper stratospheres-exospheres with their plasma environment, which can be derived from high resolution observations, are discussed, including scans of the planetary limb with a resolution better than the scale height of the atmospheric constituents.
ESA

N93-10923# Florence Univ. (Italy). Dipartimento di Astronomia.
OBSERVATION OF SOLAR FLARES AT HIGH RESOLUTION c92
G. Cauzzi, A. Falchi (Osservatorio Astrofisico di Arcetri, Florence, Italy), R. Falciani, and L. A. Smaldone (Naples Univ., Italy) *In* ESA, Solar Physics and Astrophysics at Interferometric Resolution May 1992 p 141-143 Sponsored in part by CNR (For primary document see N93-10901 01-90)
Copyright Avail: CASI HC A01/MF A03

Some preliminary results of the observation of a flare performed with very good spatial resolution (6 to 7 inches) are presented. The flare occurred on 7 Jun. 1991 at about 13:43 UT in the NOAA region 6659, showing an unusual high activity. A small region, about 3 inches wide, shows strong blue shifts (of the order of the sound speed) in some metallic lines formed in the high photosphere, during the flare impulsive phase. These observations show the importance of having measurements at higher spatial and temporal resolution for an effective improvement of the knowledge of the fundamental dynamic of active regions and flares.
ESA

N93-10924# Etablissement Technique Central de l'Armement, Arcueil (France).
PATTERN RECOGNITION APPLIED TO H(SUB ALPHA) SPECTROHELIOGRAMS SOLAR ROTATION AND MERIDIONAL CIRCULATION c92
B. Collin and E. Nesme-Ribes (Observatoire de Paris-Meudon, France) *In* ESA, Solar Physics and Astrophysics at Interferometric Resolution May 1992 p 145-148 (For primary document see N93-10901 01-90)
Copyright Avail: CASI HC A01/MF A03

The surface rotation of the Sun can be investigated by observing the motions of magnetic features observed in the solar atmosphere and embedded in the interior. These tracers are sunspots, bright

facula, and dark H (alpha) features called filaments. To observe their dynamics with high resolution, pattern recognition methods have to be used. A pattern recognition procedure for extracting and tracking filaments which derives rotational and meridional motions with unequalled accuracy is described. The resolution is limited only by the spatial resolution of the image. ESA

N93-10925# Sofia Univ. (Bulgaria). Dept. of Astronomy.
ON THE NATURE OF THE SMALL-SCALE PLASMA STRUCTURES IN THE SOLAR ACTIVE PHENOMENA **c92**
V. N. Dermendjiev *In* ESA, Solar Physics and Astrophysics at Interferometric Resolution May 1992 p 149-152 (For primary document see N93-10901 01-90)
(Grant F50/1991)
Copyright Avail: CASI HC A01/MF A03

High resolution observations of solar active phenomena which have lead to the conclusion that small scale dynamic plasma structures usually occur a short time after a process of energy release are discussed. The formation of these dynamic plasma structures are obviously due to some kind of short lasting small scale magnetohydrodynamic process. Such structures could be described as a small scale plasma volume with imposed helicity and possibility for creation of currents and generation of small scale magnetic field. ESA

N93-10926# Observatoire de Paris-Meudon (France).
MSDP IMAGING SPECTROSCOPY FOR HIGH RESOLUTION SOLAR PHYSICS **c92**
P. Mein *In* ESA, Solar Physics and Astrophysics at Interferometric Resolution May 1992 p 153-155 (For primary document see N93-10901 01-90)
Copyright Avail: CASI HC A01/MF A03

Capabilities of imaging spectroscopy with Multichannel Subtractive Double Pass (MSPD) spectrographs are recalled. The imaging spectroscopy with MSDP spectrographs allows very high spatial resolution and fast time sequences over two dimensional solar targets. It is shown that the MSDP are very suitable for coordinated experiments between ground based and space observations. ESA

N93-10927# Florence Univ. (Italy). Dipartimento di Astronomia e Scienza dello Spazio.
HIGH RESOLUTION GRANULATION SPECTROPHOTOMETRY WITH A UBF AND A FP INTERFEROMETER IN TANDEM **c92**
G. Salucci, L. Bertello, D. Bonaccini (Osservatorio Astrofisico di Arcetri, Florence, Italy), F. Cavallini (Osservatorio Astrofisico di Arcetri, Florence, Italy), G. Ceppatelli (Osservatorio Astrofisico di Arcetri, Florence, Italy), and A. Righini *In* ESA, Solar Physics and Astrophysics at Interferometric Resolution May 1992 p 157-159 (For primary document see N93-10901 01-90)
Copyright Avail: CASI HC A01/MF A03

Recent studies showed that in solar granulation, granules sizes lower than 3 inches may be considered as turbulent eddies. However, this result is in contradiction with morphological studies carried out by other authors. The spatial domain, the autocorrelation, and crosscorrelation functions of the velocity and of the intensity fields at several depths in the solar atmosphere are analyzed using narrow band filtergrams obtained by vacuum tower telescope with a Universal Birefringent Filter (UBF) and a Fabry-Perot (FP) interferometer mounted in tandem. The results show that the granular motion is turbulent for heights larger than 170 km while at lower heights is convective. ESA

N93-10928# Academy of Sciences (USSR), Irkutsk. Siberian Inst. of Terrestrial Magnetism, Ionosphere and Radio Wave Propagation.
SPATIAL DISTRIBUTION OF LINE-OF-SIGHT VELOCITIES IN A QUIESCENT PROMINENCE **c92**
S. A. Druzhinin, A. A. Pevtsov, and G. P. Mashnich *In* ESA, Solar Physics and Astrophysics at Interferometric Resolution May 1992 p 161-164 (For primary document see N93-10901 01-90)
Copyright Avail: CASI HC A01/MF A03

Doppler velocity observations in a quiescent prominence were performed. A device based on an image dissector (television tube) was used, and the Doppler velocity profile in prominence height was measured quasi-simultaneously at two intensity levels in the line H (beta) 486.1 nm. It was found that through the entire height of the prominence, there are 3 to 4 elements with quasi-hourly oscillations. Relative to each other, the oscillations in these elements show a random phase. The distance between such elements is about 20 inches. Quasi-five-minute oscillations have a train like character and a random phase at neighboring points of the prominence (separation about 4 inches). ESA

N93-10929# European Space Agency, Paris (France).
ATTACHED PAYLOADS ON SPACE STATION FREEDOM AND COLUMBUS **c19**
G. P. Haskell and H. Olthof *In its* Solar Physics and Astrophysics at Interferometric Resolution May 1992 p 167-169 (For primary document see N93-10901 01-90)
Copyright Avail: CASI HC A01/MF A03

Plans for accommodation of attached payloads on Space Station Freedom are reviewed. The Columbus Attached laboratory external viewing platform and the Japanese experiment module are considered, and diagrams showing their configurations are given. A diagram of the attached payload truss locations is also given. ESA

N93-10930# Centre National de la Recherche Scientifique, Verrieres-Le Buisson (France). Service d'Aeronomie.
SUN: THE SOLAR ULTRAVIOLET NETWORK **c92**
L. Dame *In* ESA, Solar Physics and Astrophysics at Interferometric Resolution May 1992 p 171-180 (For primary document see N93-10901 01-90)
Copyright Avail: CASI HC A02/MF A03

Reasons for the design choices of SUN, a space interferometer to observe the solar fine structure from the photosphere to the corona, are given. The current status of the instrument definition and performances are presented. SUN is a compact optical interferometer formed with four telescopes of 20 cm diameter distributed non-redundantly on a linear baseline of 2 m. In addition to its intrinsic high spatial resolution (10 km on the Sun at wavelength 120 nm), SUN has an elaborate focal plane instrument, a subtractive double monochromator, that provides 6 simultaneous images of high spectral resolution and is tunable from the far UV (1175 A) to the near IR (1.1 micrometers). Central to SUN imaging capabilities is a powerful, real time, metrology control of the phase error and beam pointing. The compact array configuration, the co-phased recording of fringes, and the spectral properties of the double monochromator of SUN allow interferometric imaging of the complex and extended solar structure with exceptional detail. ESA

N93-10931# Technische Physische Dienst TNO-TH, Delft (Netherlands).
THE SOLAR ULTRAVIOLET NETWORK SUBTRACTIVE DOUBLE MONOCHROMATOR **c92**
B. Kruizinga, B. C. Braam, B. Snijders, and H. Visser *In* ESA, Solar Physics and Astrophysics at Interferometric Resolution May 1992 p 181-184 (For primary document see N93-10901 01-90)
Copyright Avail: CASI HC A01/MF A03

Various aspects of the Subtractive Double Monochromator (SDM), the most critical channel (117.5 to 200 nm) of the six channel spectrometer which is the focal instrument of the Solar Ultraviolet Network (SUN), are discussed. The image is diffraction limited over the 4 by 4 sq arcsec field of view, and the spectral resolution is 0.1 nm. The key components of a SDM are formed by two dispersive elements (gratings in this case) that are mounted in a subtractive configuration in order to achieve dispersion compensation on the output beam. A dispersed image is formed in the SDM slit. Grating pitch and slit size are optimized for spectral resolution and image size across the slit. The zero order beam is relayed to subsequent spectrometer channels by means of a mirror on a Wadsworth mounting. The efficiency of the instrument is

optimized by applying a blaze to the gratings and introducing anamorphosis in the input beam. The resulting design is promising in terms of meeting the specifications. ESA

N93-10932# Centre National de la Recherche Scientifique, Verrieres-Le Buisson (France). Service d'Aeronomie.
INTERFEROMETRIC IMAGING WITH THE SOLAR ULTRAVIOLET NETWORK **c92**
L. Dame and T. J. Cornwell (National Radio Astronomy Observatory, Socorro, NM.) *In* ESA, Solar Physics Astrophysics at Interferometric Resolution May 1992 p 185-189 (For primary document see N93-10901 01-90)
(Contracts ESA-7978; ESA-9301)
Copyright Avail: CASI HC A01/MF A03

Extensive simulations to investigate the image reconstruction potential of the Solar Ultraviolet Network (SUN) were performed. They establish that excellent images are obtained with compact optical arrays despite errors in visibility data caused by photon noise, beam mispointing, and residual phase errors. Imaging fidelity in optical interferometry, with emphasis on extended objects, is a complex function of flux level, source complexity, recombination errors (pointing and phase), and spatial frequency coverage of the so called u,v plane. 'Holes' in the u,v coverage would result in artifacts and in a significant degradation of the quality of the complex and extended images which could be reconstructed from the data. SUN's emphasis on high resolution imaging of an extended field of view (6 by 6 inches) implies that the interferometer has to be compact, i.e., without zeroes in the u,v plane coverage, and controlled to fraction of a wavelength ('cophased'). In these conditions, interferometric imaging quality can be compared to full aperture single dish imaging. ESA

N93-10933# Imperial Coll. of Science and Technology, London (England).
IFTS: THE IMAGING FOURIER TRANSFORM SPECTROMETER **c19**
A. P. Thorne *In* ESA, Solar Physics and Astrophysics at Interferometric Resolution May 1992 p 191-195 (For primary document see N93-10901 01-90)
Copyright Avail: CASI HC A01/MF A03

The IFTS in SIMURIS (Solar Interferometric Mission Ultrahigh Resolution Imaging and Spectroscopy) is described. IFTS is an imaging spectrometer designed to combine two dimensional spatial resolution with high spectral resolution over a scan time of a few seconds. This is done by forming an image of the entrance aperture on an array detector at the output of a scanning interferometer. Each pixel of the detector records an independent interferogram, which can then be Fourier transformed to give the spectrum. The principles, design, problems, and projected performance of IFTS with respect to the SIMURIS objectives, primarily in the wavelength region from 1800 A to Lyman alpha, but also with an alternative mode of operation at increased spectral resolution in the visible region are discussed. ESA

N93-10934# Eidgenoessische Technische Hochschule, Zurich (Switzerland). Inst. of Astronomy.
POLARIMETRY WITH AN IMAGING FTS **c19**
J. O. Stenflo and S. K. Solanki *In* ESA, Solar Physics and Astrophysics at Interferometric Resolution May 1992 p 197-200 (For primary document see N93-10901 01-90)
Copyright Avail: CASI HC A01/MF A03

The concept of an imaging Fourier Transform Spectrometer (FTS) polarimeter based on piezoelastic modulation and direct demodulation in partially masked Charge Coupled Devices (CCD's) is outlined. The currently operational FTS polarimeter at the McMath telescope as well as the detection scheme of the ETH polarimeter, based on partially masked CCD cameras, are outlined to illustrate its principle. ESA

N93-10935# Norges Tekniske Hoegskole, Trondheim.
FOURIER TRANSFORM SPECTROMETER PROCESSING: DATA REDUCTION AND PROCESSOR DESIGN **c19**
K. Andreassen and P. A. Armbruster (European Space Agency. European Space Research and Technology Center, ESTEC, Noordwijk, Netherlands) *In* ESA, Solar Physics and Astrophysics at Interferometric Resolution May 1992 p 201-204 (For primary document see N93-10901 01-90)
Copyright Avail: CASI HC A01/MF A03

A laboratory model of a flexible processing and data handling module for the Imaging Fourier Transform Spectrometer (IFTS) is described. The IFTS is one of the instruments under the Solar Interferometeric Mission for Ultrahigh Resolution Imaging Spectroscopy (SIMURIS) mission. The purpose of the data handling module is to do data compression and to select the data to be transmitted for each observation program. The interferogram time-series-out from the optical filter and the IFTS is selected by demodulation and filtered by a set of multirate filters. The bandwidths of the compressed interferograms is close to the optical bandwidths, and they can be transmitted with reduced bit rates. The short Fourier transformation of these bands is left for ground based preprocessing. The data handling module consists of standard 6U VME boards. Each board has a TMS320C30 signal processor and a special purpose input processor. A complete data handling module would consist of between 5 and 10 boards for a 400 by 400 array with 0.05 arcsec pixels. The model consists of two boards, of which one functions as an input data generator. ESA

N93-10936# Institut d'Astrophysique, Paris (France).
FIRST RESULTS OF AN IMAGING FTS WITH A NICMOS CAMERA **c35**
J. P. Maillard and D. Simons (Canada-France-Hawaii Telescope Corp., Kamuela, HI.) *In* ESA, Solar Physics and Astrophysics at Interferometric Resolution May 1992 p 205-210 (For primary document see N93-10901 01-90)
Copyright Avail: CASI HC A02/MF A03

Results of tests and details from a project which coupled a 256 by 256 NICMOS camera to a Fourier Transform Spectrometer (FTS) are reported. As a result of this successful coupling, spectroimaging in any bandpass between 1 and 2.5 micrometers of each point within a circular 24 arcsec field of view was permitted. The first tests were not too ambitious and limited to data cube of about 350 frames, enough to yield a spectral resolution of several thousands. The main limitation of the system was found to be the overhead time of the camera, which should be improved with a new camera. Analysis of the signal to noise ratios in reference stars, which showed an excess of noise compared to what is expected from a pure photon noise statistics, is discussed. Results of scans made of the planetary nebula NGC 7027 at 2.12 micrometers and of the dark side of Venus at 1.27 and 1.18 micrometers, are presented to illustrate this novel instrument. ESA

N93-10937# Rutherford Appleton Lab., Chilton (England).
DETECTORS FOR THE SIMURIS PAYLOAD **c19**
B. E. Patchett, M. K. Carter, and P. D. Read *In* ESA, Solar Physics and Astrophysics at Interferometric Resolution May 1992 p 211-213 (For primary document see N93-10901 01-90)
Copyright Avail: CASI HC A01/MF A03

Detectors for the Solar Ultraviolet Network (SUN) and Imaging Fourier Transform Spectrometer (IFTS) instruments, which are particularly challenging due to the requirements for high total count rate, high pixel count rate, and far UV sensitivity, are discussed. Count rates are exceptionally high for active regions, but with a spatial resolution of 0.001 inches it is also possible that high individual pixel counts will occur even on 'quiet' Sun observations. On the other hand it is planned to use the Solar Interferometric Mission for Ultrahigh Resolution Imaging and Spectroscopy (SIMURIS) for planetary observations where the detectors will be required to work efficiently and with very low noise levels. It seems unlikely that any one detector would suffice for all channels, and in any case this could potentially represent a single point of failure. The design and performance of a range of modular detectors which are built specifically with solar UV observing in mind are discussed along with plans for their future development. ESA

N93-10938# Turin Univ. (Italy). Ist. di Fisica.
EUV COMPLEMENTARY INSTRUMENTATION FOR SIMURIS **c19**
Ester Antonucci *In* ESA, Solar Physics and Astrophysics at Interferometric Resolution May 1992 p 215-220 (For primary document see N93-10901 01-90)
Copyright Avail: CASI HC A02/MF A03

The design, instrument requirements, and scientific objectives of the X-ray Ultraviolet Imager, a normal incidence telescope with mirrors coated with multilayers, designed to provide observations at the sub arcsecond spatial resolution in the X-ray/XUV domain are considered. The instrument could provide high resolution imaging of the high temperature solar atmosphere. The X-ray Ultraviolet Imager is a multimirror telescope with a number of independent channels imaging at different wavelengths. Each channel is optimized to select a narrow spectroscopic band in the 40 to 400 A region, which is rich in diagnostic lines formed at quite different temperatures. The number of channels is chosen in such a way to cover the entire temperature range observed on the solar outer atmosphere, from 100,000 to about 10(exp 7) K. The instrument consists of two complementary imaging systems: a high resolution telescope with subarcsecond resolution on a limited field of view; and a wide field telescope imaging the whole Sun within 2.5 solar radii from Sun center. ESA

N93-10939*# Harvard-Smithsonian Center for Astrophysics, Cambridge, MA.
OBTAINING HIGH RESOLUTION XUV CORONAL IMAGES **c19**
L. Golub and E. Spiller (IBM Watson Research Center, Yorktown Heights, NY.) *In* ESA, Solar Physics and Astrophysics at Interferometric Resolution May 1992 p 221-224 Sponsored by NASA, Washington (For primary document see N93-10901 01-90)
Copyright Avail: CASI HC A01/MF A03

Photographs obtained during three flights of an 11 inch diameter normal incident soft X-ray (wavelength 63.5 A) telescope are analyzed and the data are compared to the results expected from tests of the mirror surfaces. Multilayer coated X ray telescopes have the potential for 0.01 arcsec resolution, and there is optimism that such high quality mirrors can be built. Some of the factors which enter into the performance actually achieved in practice are as follows: quality of the mirror substrate, quality of the multilayer coating, and number of photons collected. Measurements of multilayer mirrors show that the actual performance achieved in the solar X-ray images demonstrates a reduction in the scattering compared to that calculated from the topography of the top surface of the multilayer. In the brief duration of a rocket flight, the resolution is also limited by counting statistics from the number of photons collected. At X-ray Ultraviolet (XUV) wavelengths from 171 to 335 A the photon flux should be greater than 10(exp 10) ph/sec, so that a resolution better than 0.1 arcsec might be achieved, if mirror quality does not provide a limit first. In a satellite, a large collecting area will be needed for the highest resolution. ESA

N93-10940# Grenoble-1 Univ. (France). Lab. d'Astrophysique.
SUCCESSES OF AND PROSPECTS FOR GROUND-BASED INTERFEROMETRY **c89**
C. Perrier *In* ESA, Solar Physics and Astrophysics at Interferometric Resolution May 1992 p 227-235 (For primary document see N93-10901 01-90)
Copyright Avail: CASI HC A02/MF A03

The development of optical interferometric techniques over the past twenty years is outlined, and future objectives are discussed. These techniques, still ground based, spanning from speckle imaging to long baseline direct beam recombination and analysis, are producing more and more scientific results. New techniques, such as adaptive optics, are continuously developed to take benefit of technical progress in detectors, sensors, and real time control. Part of the most recent results is due to critical progress in the visibility calibration. The range of scientific applications is already wide with results in binary stars, circumstellar envelopes, stellar diameters, solar system bodies, some atypical sources, a few extragalactic objects, and wide angle astrometry. Additionally, a deep knowledge was acquired on the atmospheric turbulence laws. The use of interferometry in the study of binary stars, circumstellar envelopes and stellar diameters is discussed. ESA

N93-10941# European Southern Observatory, Garching (Germany).
GROUND-BASED HIGH ANGULAR RESOLUTION OBSERVATION OF THE SUN BY INTERFEROMETRY IN THE VISIBLE **c89**
O. vonderLuehe *In* ESA, Solar Physics and Astrophysics at Interferometric Resolution May 1992 p 237-241 (For primary document see N93-10901 01-90)
Copyright Avail: CASI HC A01/MF A03

Interferometric imaging of the solar surface which can produce diffraction limited pictures with ground based telescopes, despite the deleterious effects of the Earth's atmosphere is considered. Speckle imaging in broad bands, successful in broad spectral bands for a number of years, is discussed. Recent advances in the methodology show that speckle techniques can succeed at a spectral resolution good enough to permit meaningful spectroscopic observations. Some results in speckle imaging are presented. Fizeau stellar interferometry applied to solar structure is investigated, and its potential and limitations are demonstrated. ESA

N93-10942# Observatoire de la Cote d'Azur, Nice (France). Dept. Augustin Fresnel.
THE CHARON PROGRAM **c89**
G. Schumacher, P. Cruzalebes, S. Menardi, and Y. Rabbia *In* ESA, Solar Physics and Astrophysics at Interferometric Resolution May 1992 p 243-246 (For primary document see N93-10901 01-90)
Copyright Avail: CASI HC A01/MF A03

The concept and current status of CHARON (Calern High Angular Resolution Optical Network), a French ground based imaging stellar interferometer project to provide two dimensional high resolution images by aperture synthesis at visible wavelengths, are discussed. CHARON is a prototype intended to demonstrate the feasibility of phase closure with independent telescopes. The instrument consists of three 26 cm telescopes movable on 100 m baselines and three optical delay lines to compensate the optical paths. The recombining optics included a three channel image tracker and a fringe tracker. The image reconstruction is done by an original method including bispectral analysis and avoiding the use of any a priori model. CHARON is also a test bench for some aspects of the interferometric mode of the very large telescope. The first visibility measurements with two telescopes and two delay lines are reported. ESA

N93-10943# European Southern Observatory, Garching (Germany).
INTERFEROMETRY WITH THE VERY LARGE TELESCOPE **c89**
O. vonderLuehe, J. M. Beckers, M. Faucherre, B. Koehler, F. Merkle, and N. Zhu *In* ESA, Solar Physics and Astrophysics at Interferometric Resolution May 1992 p 247-254 (For primary document see N93-10901 01-90)
Copyright Avail: CASI HC A02/MF A03

An overview of the Very Large Telescope (VLT) interferometer is presented, its characteristics are highlighted and an update on its status is given. One of the observing modes available with the VLT will be coherent combination of the light received by up to four 8 m diameter unit telescopes and several 1.8 m diameter auxiliary telescopes. While the location of the main telescopes is fixed, auxilliary telescopes can be moved among some 30 observing stations designed to efficiently complement the unit telescopes as well as to function as an independent interferometric array. A distinct feature of the VLT interferometer will be its sensitivity due to the large diameter of the unit telescopes and due to the adaptive optics which will remove instrumental and atmospheric wavefront disturbances in the near infrared spectral regime. ESA

N93-10944# Netherlands Foundation for Radio Astronomy, Dwingelo.

TOWARDS AN ESA STRATEGY FOR OPTICAL INTERFEROMETRY IN SPACE. RECOMMENDATIONS OF THE ESA SPACE INTERFEROMETRY STUDY TEAM (SIST) **c89**

J. E. Noordam, P. Y. Bely (Space Telescope Science Inst., Baltimore, MD.), M. Faucherre (European Southern Observatory, Garching, Germany), A. H. Greenaway (Royal Signals and Radar Establishment, Malvern, England), F. Merkle (European Southern Observatory, Garching, Germany), M. A. C. Perryman (European Space Agency. European Space Research and Technology Center, ESTEC, Noordwijk, Netherlands), P. H. Roussel (European Space Agency. European Space Research and Technology Center, ESTEC, Noordwijk, Netherlands), F. Vakili, S. Volonte (European Space Agency, Paris, France), and G. P. Weigelt (Max-Planck-Inst. fuer Radioastronomie, Bonn, Germany) *In* ESA, Solar Physics and Astrophysics at Interferometric Resolution May 1992 p 255-257 (For primary document see N93-10901 01-90)

Copyright Avail: CASI HC A01/MF A03

The conclusions, recommendations, and target design parameters for a 100 m class optical space interferometer recommended for launch by the ESA around the year 2005 are summarized. A successful Solar Interferometric Mission for Ultrahigh Resolution Imaging Spectroscopy (SIMURIS) mission will help the cause of space interferometry in many ways. Since the SIMURIS design cannot easily be extended to long baselines and faint objects, it should be seen as a direct precursor to a 'stellar' interferometer. ESA

N93-10945# Imperial Coll. of Science and Technology, London (England).

REPORT OF THE LUNAR INTERFEROMETRY STUDY TEAM (LIST) ACTIVITIES **c89**

J. C. Dainty, M. Faucherre (European Southern Observatory, Garching, Germany), A. H. Greenaway (Royal Signals and Radar Establishment, Malvern, England), A. I. Harris (Max-Planck-Inst. fuer Physik und Astrophysik, Garching, Germany), A. Labeyrie (Observatoire de la Cote d'Azur, Nice, France), J. E. Noordam (Netherlands Foundation for Radio Astronomy, Dwingelo.), G. P. Weigelt (Max-Planck-Inst. fuer Radioastronomie, Bonn, Germany), J. Beckers, J. Lequeux (Observatoire de Paris-Meudon, France), and C. M. Fridlund (European Space Agency. European Space Research and Technology Center, ESTEC, Noordwijk, Netherlands) et al *In* ESA, Solar Physics and Astrophysics at Interferometric Resolution May 1992 p 259-266 (For primary document see N93-10901 01-90)

Copyright Avail: CASI HC A02/MF A03

Earth based high angular resolution interferometry is discussed together with space and lunar based interferometry (with emphasis on the latter). The scientific goals of optical and sub-milimeter interferometry in astrometry and imaging are described and some aspects of astronomy and astrophysics that will benefit from interferometry are presented. The advantages of lunar interferometry are summarized. A strategy for the development of such a lunar interferometry program is also summarized. ESA

N93-10946# Defence Research Agency, Malvern (England).

GROUND/SPACE CO-OPERATION FOR INTERFEROMETRY **c89**

A. H. Greenaway *In* ESA, Solar Physics and Astrophysics at Interferometric Resolution May 1992 p 267-270 (For primary document see N93-10901 01-90)

Copyright Avail: CASI HC A01/MF A03

The use of PHAROS (Proposal for a High Resolution Optical Survey) for daytime observations and for solar studies is explained. This proposal would launch several low power (about 2 mW) lasers on a satellite in a highly eccentric orbit and use these lasers to provide a calibration source for both adaptive optics correction in large aperture telescopes and for interferometric studies over baselines of up to kilometric dimensions. Diffraction limited imaging of unresolved sources as faint as +30 could be achieved using PHAROS for calibration of night time observations on an 8 m telescope. ESA

N93-10947# Centre National de la Recherche Scientifique, Verrieres-Le Buisson (France). Inst. d'Astrophysique Spatiale.

ROTATIONAL APERTURE SYNTHESIS: A PROPOSAL FOR GROUND-BASED OBSERVATIONS **c89**

Guy Artzner *In* ESA, Solar Physics and Astrophysics at Interferometric Resolution May 1992 p 273-276 (For primary document see N93-10901 01-90)

Copyright Avail: CASI HC A01/MF A03

Attention is drawn to the existence of three axes equatorial mounts for ground based observing. The additional third axis with respect to a conventional two axes equatorial or altitude-azimuth mount allows the position angle to be set at almost any predetermined value when observing close to the zenith. In addition to that, the quasi-total absence of cantilever parts is an asset for interferometric stability. The SIMURIS strategy uses some breadboard for fine structure imaging on the ground in the visible domain as an intermediate step between laboratory developments and flight operations; tactics for solar or stellar interferometric observations are investigated. ESA

N93-10948# Centre National de la Recherche Scientifique, Verrieres-Le Buisson (France). Service d'Aeronomie.

DEMONSTRATION AND PERFORMANCES OF REAL-TIME FRINGE TRACKING: A STEP TOWARDS COPHASED INTERFEROMETERS **c89**

L. Dame *In* ESA, Solar Physics and Astrophysics at Interferometric Resolution May 1992 p 277-282 (For primary document see N93-10901 01-90)

(Contract ESA-7978)

Copyright Avail: CASI HC A02/MF A03

Imaging of complex and extended objects by the Solar Ultraviolet Network (SUN) requires a real time monitoring of the coalignment and cophasing functions of the interferometer. The cophasing of the input beams, i.e., the equalization (zeroing) of the optical path delays, is specific to interferometry and is required to high precision if diffraction limited imaging with the interferometer is expected (wavelength/8 or so at the shortest wavelength). Preliminary results in fringe pattern acquisition and stabilization as performed in a Mach-Zehnder set up representative of the interferometer cophasing system are reported. The system algorithm is based on 'white light' fringe tracking controlled in a reference interferometer by a synchronous detection. This servosystem drives a two stage delay line for real time compensation of the optical path delays. Acquisition capacities and stability possibilities are investigated as a function of flux and noise levels. ESA

N93-10949# Rutherford Appleton Lab., Chilton (England). Space Science Dept.

INVESTIGATIONS OF THE EFFECTS OF CONTAMINATION ON UV OPTICS **c74**

Barry J. Kent *In* ESA, Solar Physics and Astrophysics at Interferometric Resolution May 1992 p 283-285 (For primary document see N93-10901 01-90)

Copyright Avail: CASI HC A01/MF A03

Highly complex instruments, such as SIMURIS (Solar Interferomertric Mission for Ultrahigh Resolution Imaging and Spectroscopy), with many optical surfaces are particularly vulnerable to molecular contamination from outgassing of materials used in their construction. Theoretical predictions of optical performance based on outgas data can be unsatisfactory owing to the difficulty of simulating the precise conditions under which contamination occurs and the problem of modeling the particular contaminant composition and distribution. A study program whose aim was to identify typical contaminants found in space instrumentation, to understand and characterize their properties, and to investigate the optical effects of such contaminants produced from material outgassing under high vacuum conditions, is described. ESA

N93-10950# Technische Physische Dienst TNO-TH, Delft (Netherlands).
THE SOLAR ULTRAVIOLET NETWORK: PERFORMANCE AND TOLERANCE ANALYSIS **c92**
B. Kruizinga, B. C. Braam, and B. Snijders *In* ESA, Solar Physics and Astrophysics at Interferometric Resolution May 1992 p 287 (For primary document see N93-10901 01-90)
Copyright Avail: CASI HC A01/MF A03

An abstract and an outline of a paper on the Solar Ultraviolet Network (SUN), one of the core instruments of SIMURIS (Solar Interferometric Mission for Ultrahigh Resolution Imaging and Spectroscopy), is presented. An analysis of the instrument performance and tolerances was evaluated and its system layout considered. A thermal and vibration analysis was performed using the finite element method. ESA

N93-10951# Technische Physische Dienst TNO-TH, Delft (Netherlands).
THE IMAGING FOURIER TRANSFORM SPECTROMETER OPTICAL DESIGN **c74**
B. Kruizinga, B. Snijders, B. C. Braam, A. P. Thorne (Imperial Coll. of Science and Technology, London, England), J. Maxwell (Imperial Coll. of Science and Technology, London, England), and L. Dame (Centre National de la Recherche Scientifique, Verrieres-Le Buisson, France) *In* ESA, Solar Physics and Astrophysics at Interferometric Resolution May 1992 p 288-289 (For primary document see N93-10901 01-90)
Copyright Avail: CASI HC A01/MF A03

An abstract and an outline of a paper on the optical design of the Imaging Fourier Transform Spectrometer (IFTS), one of the two main instruments of SIMURIS (Solar Interferometric Mission for Ultrahigh Resolution Spectroscopy) is presented. The following were studied: the modes of operation, based on the scientific requirements; the preliminary design of the telescope and the pointing system; a design of one of the prefilters, the subtractive double monochromator; the implementation of the FI and the imaging camera; photometry and the detection system; the instruments housing, mechanisms, and other mechanical aspects. The optimum quality of the entire system was determined by an extensive ray tracing analysis. A preliminary outline of the instrument's mechanical structure was generated. ESA

N93-10952# Technische Physische Dienst TNO-TH, Delft (Netherlands).
THE IMAGING FOURIER TRANSFORM SPECTROMETER: PERFORMANCE AND TOLERANCE ANALYSIS **c35**
B. Kruizinga, B. Snijders, B. C. Braam, A. P. Thorne (Imperial Coll. of Science and Technology, London, England), J. Maxwell (Imperial Coll. of Science and Technology, London, England), and L. Dame (Centre National de la Recherche Scientifique, Verrieres-Le Buisson, France) *In* ESA, Solar Physics and Astrophysics at Interferometric Resolution May 1992 p 290 (For primary document see N93-10901 01-90)
Copyright Avail: CASI HC A01/MF A03

An abstract and an outline of an analysis of the Imaging Fourier Transform Spectrometer (IFTS), one of the core instruments of SIMURIS (Solar Interferometric Mission for Ultrahigh Resolution Imaging and Spectroscopy), is given. The quality of the optical system (including diffraction effects and aberrations of the nominal system) were evaluated. The performance figures were determined in the course of the instrument design process. Detailed information on components and other instrumental considerations lead to a readjustment of some of the requirements. The tolerance analysis and its implications were addressed. The influence of component manufacturing errors, assembly and alignment errors, and environmental disturbances on the optical quality were evaluated. The quality of the instrument including tolerances was determined in terms of the following: spot sizes in the detector, wavefront errors of interfering beams, pointing errors, and accuracy of the selected center wavelength. For each of these aspects the contributing optical components were identified. The permissable error budget was distributed over these components. The component tolerances were calculated. ESA

N93-10953# Imperial Coll. of Science and Technology, London (England).
A MULTIPURPOSE VACUUM-ULTRAVIOLET TEST FACILITY **c14**
R. C. M. Learner, A. Thorne, J. Maxwell, C. R. Young (Chelsea Instruments Ltd., East Molesey, England), and R. P. Glover (RGC Technical Consultancy, London, England) *In* ESA, Solar Physics and Astrophysics at Interferometric Resolution May 1992 p 291-294 Sponsored in part by ESTEC (For primary document see N93-10901 01-90)
Copyright Avail: CASI HC A01/MF A03

The design for a vacuum ultraviolet test facility is described. The initial purpose is for measuring refractive indices and optical homogeneity of substrate materials, and testing and aligning components used in the SIMURIS (Solar Interferometric Mission for Ultrahigh Resolution Imaging and Spectroscopy) IFTS (Imaging Fourier Transform Spectrometer). The IFTS beamsplitter is used as an example. The design features several operating modes including interferometry, Schlieren testing, and refractometry. A UV camera and fringe analysis software facilitates measurements. A progressive self testing scheme is described for commissioning the system. The much more general use for optical testing of samples and assemblies at wavelengths down to 120 nm is discussed. ESA

N93-10954# Messerschmitt-Boelkow-Blohm G.m.b.H., Munich (Germany).
ACCOMMODATION ASPECTS OF SIMURIS ON SPACE STATION FREEDOM **c19**
U. Lemmer, E. Schulz-Luepertz, and K. Thoermer *In* ESA, Solar Physics and Astrophysics at Interferometric Resolution May 1992 p 295-297 (For primary document see N93-10901 01-90)
Copyright Avail: CASI HC A01/MF A03

General aspects for the installation and operation of observatory instruments on possible Space Station Freedom (SSF) viewing platforms or exposed facilities are investigated. As far as the SIMURIS (Solar Interferometric Mission for Ultrahigh Resolution Imaging and Spectroscopy) instrument package is concerned, the Space Station requires a specific accommodation analysis with respect to viewing limitations, pointing, and contamination by the SSF environment and instrument operation. These requirements are considered. ESA

N93-10955# Imperial Coll. of Science and Technology, London (England).
INTERFEROMETER OPTICAL DESIGN FOR THE IMAGING FOURIER TRANSFORM SPECTROMETER (IFTS) **c74**
J. Maxwell, A. P. Thorne, J. Wheaton (Chelsea Instruments Ltd., East Molesey, England), and R. P. Glover (RGC Technical Consultancy, London, England) *In* ESA, Solar Physics and Astrophysics at Interferometric Resolution May 1992 p 299-301 Sponsored in part by ESTEC (For primary document see N93-10901 01-90)
Copyright Avail: CASI HC A01/MF A03

An optical design for the imaging interferometer to be used in the Solar Interferometric Mission for Ultrahigh Resolution Imaging Spectroscopy (SIMURIS) is presented. A significant requirement is the VUV performance (down to 120 nm) which is beyond what has been achieved to date. It is based on the UV Fourier Transform Spectrometer. The most critical aspects of the design are the beamsplitter and the general optical surface tolerances, both of which put the instrument at the limit of today's technology. ESA

N93-10956# European Space Agency. European Space Research and Technology Center, ESTEC, Noordwijk (Netherlands). Structures and Mechanisms Div.
MECHANICAL AND THERMAL DESIGN OF THE SUN INSTRUMENT **c19**
J. Pang and R. Bureo *In its* Solar Physics and Astrophysics at Interferometric Resolution May 1992 p 303-308 (For primary document see N93-10901 01-90)
Copyright Avail: CASI HC A02/MF A03

The mechanical design feasibility of the SUN (Solar Ultraviolet Network) instrument structure is presented. SUN is one of the core instruments of the SIMURIS (Solar, solar system, and stellar Interferometric Mission for Ultrahigh Resolution Imaging and Spectroscopy) mission. The SUN instrument structure has to accommodate adequately the optical systems and their mechanisms and to be certain that all optical systems are well accessible and flexible during integration and assembly procedures. A modular design approach, in which seven subdivisions were identified, was adopted. Verification of the suitability of the preliminary conceptual design is important. A finite element model of the SUN instrument was developed and subsequently, mechanical/thermal analyses were performed to evaluate the adequacy of the payload performance. ESA

N93-10957# Aerospatiale, Cannes (France).
SOME POSSIBLE SPACE INTERFEROMETRY APPLICATIONS
c89
D. Simeoni, B. Koehler, M. Sghedoni, and L. DeSa *In* ESA, Solar Physics and Astrophysics at Interferometric Resolution May 1992 p 309-311 (For primary document see N93-10901 01-90)
Copyright Avail: CASI HC A01/MF A03

Some aspects of interferometry applications dealing with the trend of both high spatial resolution and high spectral resolution are presented. Three technical points of interferometry are summarized: the optical delay line of an I2T (Interferometer with two Telescopes) stellar interferometer; the overall architecture of HSRS (High Spectral Resolution Sounder), a passive atmospheric sounder for the MSG (Meteosat Second Generation) geostationary platform; and an improved version of the field widened interferometer, part of an imaging Fourier transform spectrometer onboard a low orbit payload. These applications demonstrate the possible adaptation of ground experiments to space missions and the translation from a laboratory 'culture' to the space industry. ESA

N93-10113*# Paris VII Univ. (France).
CARBON AND OXYGEN ISOTOPE STUDY OF CARBONATES FROM HIGHLY SHOCKED CLASTS OF THE POLYMICT BRECCIA OF THE HAUGHTON CRATER (CANADA)
P. Agrinier, I. Martinez, M. Javoy, and U. Schaerer *In* Lunar and Planetary Inst., International Conference on Large Meteorite Impacts and Planetary Evolution 1992 p 1-2 (For primary document see N93-10112 01-46)
Avail: CASI HC A01/MF A01

N93-10114*# Geological Survey, Iowa City, IA.
RESEARCH CORE DRILLING IN THE MANSON IMPACT STRUCTURE, IOWA
R. R. Anderson, J. B. Hartung, D. J. Roddy (Geological Survey, Flagstaff, AZ.), and E. M. Shoemaker (Geological Survey, Flagstaff, AZ.) *In* Lunar and Planetary Inst., International Conference on Large Meteorite Impacts and Planetary Evolution 1992 p 2-3 (For primary document see N93-10112 01-46)
Avail: CASI HC A01/MF A01

N93-10120*# Geological Survey, Denver, CO.
LARGE METEORITE IMPACTS: THE K/T MODEL
B. F. Bohor *In* Lunar and Planetary Inst., International Conference on Large Meteorite Impacts and Planetary Evolution 1992 p 8-9 (For primary document see N93-10112 01-46)
(NASA Order T-5715-P)
Avail: CASI HC A01/MF A01

N93-10121*# Geological Survey, Denver, CO.
SHOCKED ZIRCONS IN THE ONAPING FORMATION: FURTHER PROOF OF IMPACT ORIGIN
B. F. Bohor and W. J. Betterton *In* Lunar and Planetary Inst., International Conference on Large Meteorite Impacts and Planetary Evolution 1992 p 9-10 (For primary document see N93-10112 01-46)
Avail: CASI HC A01/MF A01

N93-10125*# National Aeronautics and Space Administration. Lyndon B. Johnson Space Center, Houston, TX.
MELT PRODUCTION IN LARGE-SCALE IMPACT EVENTS: CALCULATIONS OF IMPACT-MELT VOLUMES AND CRATER SCALING
Mark J. Cintala and Richard A. F. Grieve (Geological Survey of Canada, Toronto, Ontario) *In* Lunar and Planetary Inst., International Conference on Large Meteorite Impacts and Planetary Evolution 1992 p 13-14 (For primary document see N93-10112 01-46)
Avail: CASI HC A01/MF A01

N93-10126*# National Aeronautics and Space Administration. Lyndon B. Johnson Space Center, Houston, TX.
MELT PRODUCTION IN LARGE-SCALE IMPACT EVENTS: PLANETARY OBSERVATIONS AND IMPLICATIONS
Mark J. Cintala and Richard A. F. Grieve (Geological Survey of Canada, Toronto, Ontario) *In* Lunar and Planetary Inst., International Conference on Large Meteorite Impacts and Planetary Evoluation 1992 p 14-16 (For primary document see N93-10112 01-46)
Avail: CASI HC A01/MF A01

N93-10143*# Lawrence Livermore National Lab., CA.
SIMULATED METEORITE IMPACTS AND VOLCANIC EXPLOSIONS: EJECTA ANALYSES AND PLANETARY IMPLICATIONS
A. J. Gratz and W. J. Nellis *In* Lunar and Planetary Inst., International Conference on Large Meteorite Impacts and Planetary Evolution 1992 p 31-32 (For primary document see N93-10112 01-46)
Avail: CASI HC A01/MF A01

N93-10154*# Wien Univ. (Austria). Inst. of Geochemistry.
TEKTITE ORIGIN BY HYPERVELOCITY ASTEROIDAL OR COMETARY IMPACT: THE QUEST FOR THE SOURCE CRATERS
Christian Koeberl *In* Lunar and Planetary Inst., International Conference on Large Meteorite Impacts and Planetary Evolution 1992 p 42-43 (For primary document see N93-10112 01-46)
Avail: CASI HC A01/MF A01

N93-10155*# Wien Univ. (Austria). Inst. of Geochemistry.
EARLY ARCHEAN SPHERULE BEDS OF POSSIBLE IMPACT ORIGIN FROM BARBERTON, SOUTH AFRICA: A DETAILED MINERALOGICAL AND GEOCHEMICAL STUDY
Christian Koeberl, Wolf Uwe Reimold (Witwatersrand Univ., Johannesburg, South Africa), and Rudolf H. Boer (Witwatersrand Univ., Johannesburg, South Africa) *In* Lunar and Planetary Inst., International Conference on Large Meteorite Impacts and Planetary Evolution 1992 p 44 (For primary document see N93-10112 01-46)
Avail: CASI HC A01/MF A01

N93-10158*# Cornell Univ., Ithaca, NY. Dept. of Astronomy.
SEARCH FOR A METEORITIC COMPONENT AT THE BEAVERHEAD IMPACT STRUCTURE, MONTANA
Pascal Lee and Robert W. Kay *In* Lunar and Planetary Inst., International Conference on Large Meteorite Impacts and Planetary Evolution 1992 p 47 (For primary document see N93-10112 01-46)
Avail: CASI HC A01/MF A01

N93-10164*# Karpinsky Geological Research Inst., Saint Petersburg (USSR).
IMPACTITES FROM POPIGAI CRATER
V. L. Masaitis *In* Lunar and Planetary Inst., International Conference on Large Meteorite Impacts and Planetary Evolution 1992 p 51 (For primary document see N93-10112 01-46)
Avail: CASI HC A01/MF A01

91 LUNAR AND PLANETARY EXPLORATION

Includes planetology; and manned and unmanned flights. For spacecraft design or space stations see *18 Spacecraft Design, Testing and Performance.*

N93-10064*# Lunar and Planetary Inst., Houston, TX. MSATT Study Group.
WORKSHOP ON THE EVOLUTION OF THE MARTIAN ATMOSPHERE
J. G. Luhmann, ed. and B. M. Jakosky, ed. 1992 13 p Workshop held at Kona, HI, 29 Jun. - 1 Jul. 1992
(Contract NASw-4574)
(NASA-CR-190730; NAS 1.26:190730; LPI-TR-92-05) Avail: CASI HC A03/MF A01

Thirty-three papers based on the state of our knowledge prior to the anticipated new results from Mars Observer were presented at the workshop. Because of the nature of the subject, the scope of the papers covered a broad disciplinary range encompassing astronomy and solar physics, geology and geophysics, climatology, atmospheric science, aeronomy, and space physics. The 42 participants heard about topics from the evolution of solar-type stars to candidate instrumentation for measuring escape to space on yet-unscheduled future missions. Author

N93-10378 Oxford Univ. (England).
REMOTE SOUNDING OF THE MARTIAN ATMOSPHERE Ph.D. Thesis
P. G. J. Irwin 1991 256 p
Avail: Univ. Microfilms Order No. BRDX96205

This thesis describes the development and characterization of the optical elements for six channels of the Pressure Modulated Infrared Radiometer (PMIRR) due for launch on Mars Observer in 1992. This instrument uses two pressure modulators, one containing CO2 for temperature sounding and the other containing H2O. The CO2 gas sample is enriched in some isotopes to allow sounding of the deep atmosphere. The dynamic equilibrium between these isotopes was investigated using infrared spectroscopy to measure surface effects, reaction rates and stability. The reaction rate was found to be increased by the presence of a sieve and having verified the flight mixture to be in stable equilibrium, the composition was determined. The fabrication of the filters for two longest wave channels was not possible using conventional multi-layer dielectric techniques. Thus the extension of far-infrared/microwave mesh filter design was investigated. Test filters were designed and fabricated and, using their measured transmission spectra, a new model of the behavior of meshes in both air and dielectrics was developed. The low transmission of these filters made them unsuitable for PMIRR but the model will be important for future designs if a new, less absorbing, dielectric can be found. To verify the spectroscopy and the modelled behavior of the pressure modulated cells (PMC's), the waveforms and phases of the transmission, emission, pressure and piston cycles were simultaneously measured for the first time for any PMC, together with the mean absorption. Although anomalies were seen in the H2O PMC driving frequency, as have been observed by other authors, none were evident in the cell waveforms. A thermal diffusion model was developed and used to calculate temperature cycles throughout the cells. These were in good agreement with emission measurements made using the cylindrical H2O cell and acceptable for the conical CO2 cell. Dissert. Abstr.

N93-10406# Army Construction Engineering Research Lab., Champaign, IL.
PROCEEDINGS OF THE FY 1990 WORKSHOP ON EXTRATERRESTRIAL MINING AND CONSTRUCTION Special Report
Alvin Smith Apr. 1992 175 p Workshop held 7-9 Aug. 1990
(AD-A253399; CERL-SR-M-92/14) Avail: CASI HC A08/MF A02

This report documents the proceedings of a workshop on issues involved in extraterrestrial planet surface activities involving mining and construction. In this second workshop dedicated to the subject, participants formed three discussion groups: (1) construction and mining concepts and equipment designs; (2) design standards and codes; and (3) operations and performance. Mining and construction tasks were categorized into 11 primary functions. Several equipment types and designs were reviewed for specific surface tasks, and surface and underground mining techniques were reviewed. It was noted that there is a need to develop separate codes and specifications for extraterrestrial construction, although earth-based codes provide a good starting point, and the existing Corps of Engineers Construction Criteria and Specifications may be a good model on which to base the new codes. Several key operational tasks, and concepts for accomplishing them were developed. One such important principle is to progress from simple to complex. Any lunar base should begin construction with modular, self-contained units, and gradually progress to more complex construction using locally derived/developed materials. All groups emphasized that mission plans should be formed as concretely as possible, including crew size and mission timetable, to help establish realistic operations and performance criteria. GRA

N93-10832*# National Aeronautics and Space Administration, Washington, DC.
INDEXES OF MAPS OF THE PLANETS AND SATELLITES, 1992
J. L. Inge and R. M. Batson Aug. 1992 188 p
(NASA Order W-15814)
(NASA-TM-4395; NAS 1.15:4395) Avail: CASI HC A09/MF A02

More than 1,600 maps of the surfaces of planets and satellites of the solar system have been produced by the U.S. geological survey and by the defense mapping agency. This collection of maps is a unique research that has been derived from maps and data returned by a series of remarkably successful space missions. These indexes have been compiled to provide a comprehensive listing of all published maps. Many maps are out of print but copies reside in many libraries and regional planetary imaging facilities. These indexes are a valuable resource for studies of the planets and satellites, and are an important starting point for the acquisition of cartographic data. Author

N93-10145*# Geological Survey, Denver, CO.
VENUSIAN IMPACT BASINS AND CRATERED TERRAINS
Warren B. Hamilton *In* Lunar and Planetary Inst., International Conference on Large Meteorite Impacts and Planetary Evolution 1992 p 33-35 (For primary document see N93-10112 01-46)
Avail: CASI HC A01/MF A01

N93-10148*# Hawaii Univ., Honolulu. Dept. of Planetary Geosciences.
THE DISTRIBUTION AND MODES OF OCCURRENCE OF IMPACT MELT AT LUNAR CRATERS
B. Ray Hawke and J. W. Head (Brown Univ., Providence, RI.) *In* Lunar and Planetary Inst., International Conference on Large Meteorite Impacts and Planetary Evolution 1992 p 37-38 (For primary document see N93-10112 01-46)
Avail: CASI HC A01/MF A01

N93-10166*# Washington Univ., Saint Louis, MO. Dept. of Earth and Planetary Sciences.
WHAT CAN WE LEARN ABOUT IMPACT MECHANICS FROM LARGE CRATERS ON VENUS?
William B. McKinnon and J. S. Alexopoulos *In* Lunar and Planetary Inst., International Conference on Large Meteorite Impacts and Planetary Evolution 1992 p 52-53 (For primary document see N93-10112 01-46)
Avail: CASI HC A01/MF A01

N93-10176*# Lunar and Planetary Inst., Houston, TX.
APOLLO 15 IMPACT MELTS, THE AGE OF IMBRIUM, AND THE EARTH-MOON IMPACT CATACLYSM

Graham Ryder and G. Brent Dalrymple (Geological Survey, Menlo Park, CA.) *In its* International Conference on Large Meteorite Impacts and Planetary Evolution 1992 p 62-63 (For primary document see N93-10112 01-46)
Avail: CASI HC A01/MF A01

N93-10179*# Lunar and Planetary Inst., Houston, TX.
PARADIGM LOST: VENUS CRATER DEPTHS AND THE ROLE OF GRAVITY IN CRATER MODIFICATION
Virgil L. Sharpton *In its* International Conference on Large Meteorite Impacts and Planetary Evolution 1992 p 65-66 (For primary document see N93-10112 01-46)
Avail: CASI HC A01/MF A01

N93-10184*# Lunar and Planetary Inst., Houston, TX.
THE LARGE IMPACT PROCESS INFERRED FROM THE GEOLOGY OF LUNAR MULTIRING BASINS
Paul D. Spudis *In its* International Conference on Large Meteorite Impacts and Planetary Evolution 1992 p 69-71 (For primary document see N93-10112 01-46)
Avail: CASI HC A01/MF A01

N93-10922# Centre National de la Recherche Scientifique, Verrieres-Le Buisson (France). Inst. d'Astrophysique.
MAGNETOSPHERES AND ATMOSPHERES OF PLANETS
Renee Prange *In* ESA, Solar Physics and Astrophysics at Interferometric Resolution May 1992 p 131-138 (For primary document see N93-10901 01-90)
Copyright Avail: CASI HC A02/MF A03

92 SOLAR PHYSICS

Includes solar activity, solar flares, solar radiation and sunspots.

For related information see *93 Space Radiation.*

N93-10767# Smithsonian Astrophysical Observatory, Cambridge, MA.
HIGH RESOLUTIONS STUDIES OF THE STRUCTURE OF THE SOLAR ATMOSPHERE Annual Report No. 1, 1 Jul. 1991 - 30 Jun. 1992
Shadia R. Habbal 30 Jun. 1992 10 p
(Grant AF-AFOSR-0244-91)
(AD-A254292; AFOSR-92-0791TR) Avail: CASI HC A02/MF A01

During this first year, we have concentrated on the analysis, and the image enhancement and processing of an extensive set of the EUV/Skylab data for the search of empirical characteristics of coronal heating in different scale magnetic regions on the Sun. Student involvement in our research projects has been quite successful. GRA

N93-10771# National Geophysical Data Center, Boulder, CO.
SOLAR-GEOPHYSICAL DATA NUMBER 569, JANUARY 1992. PART 1: (PROMPT REPORTS). DATA FOR DECEMBER, NOVEMBER 1991, AND LATE DATA
Helen E. Coffey, ed. Jan. 1992 141 p
(PB92-158880; SGD-569-Pt-1) Avail: CASI HC A07/MF A02

This report contains the following sections: Detailed index for 1991; Data for December 1991--Solar terrestrial environment, Solar activity indices, Solar flares, Solar radio emission, Stanford mean solar magnetic field; Data for November 1991--Solar active regions, Sudden ionospheric disturbances, Solar radio spectral observations by neutron monitor, Geomagnetic indices; Late data--Geomagnetic activity indices October 1991. GRA

N93-10773# National Geophysical Data Center, Boulder, CO.
SOLAR-GEOPHYSICAL DATA NUMBER 570, FEBRUARY 1992. PART 1: (PROMPT REPORTS). DATA FOR JANUARY 1992, DECEMBER 1991, AND LATE DATA
Helen E. Coffey Feb. 1992 173 p
(PB92-170380; SGD-570-Pt-1) Avail: CASI HC A08/MF A02

This report contains the following sections: Detailed index for 1991 - 1992; Data for January 1992 -- Solar-terrestrial environment, IUWDS alert periods (Advance and worldwide), Solar activity indices, Solar flares, Solar radio emission, Stanford mean solar magnetic field; Data for December 1991 -- Solar active regions, Sudden ionospheric disturbances, Solar radio spectral observations, Cosmic ray measurements by neutron monitor, Geomagnetic indices; Late data -- IUWDS alert periods (Advance and worldwide) December 1991, Geomagnetic activity indices November 1991; Errata -- Cosmic ray measurements by neutron monitor. GRA

N93-10774# National Geophysical Data Center, Boulder, CO.
SOLAR-GEOPHYSICAL DATA NUMBER 570, FEBRUARY 1992. PART 2: (COMPREHENSIVE REPORTS). DATA FOR AUGUST 1991 AND MISCELLANEOUS
Helen E. Coffey Feb. 1992 132 p
(PB92-170398; SGD-570-Pt-2) Avail: CASI HC A07/MF A02

This report contains the following sections: Detailed index for 1991 - 1992; Data for August 1991 -- Solar flares, Solar radio bursts at fixed frequencies, Solar x-ray radiation from GOES satellite, Mass ejections from the sun, Active prominences and filaments; Miscellaneous data -- IMP-8 interplanetary solar particle graphs Dec. 88-Oct. 89. GRA

N93-10775# National Geophysical Data Center, Boulder, CO.
SOLAR-GEOPHYSICAL DATA NUMBER 571, MARCH 1992. PART 1: (PROMPT REPORTS). DATA FOR FEBRUARY, JANUARY 1992, AND LATE DATA
Helen E. Coffey Mar. 1992 154 p
(PB92-177062; SGD-571-Pt-1) Avail: CASI HC A08/MF A02

This report contains the following sections: Detailed index for 1991-1992; Data for February 1992--Solar-terrestrial environment, IUWDS alert periods (advance and worldwide), Solar activity indices, Solar flares, Solar radio emission, Stanford mean solar magnetic field; Data for January 1992--Solar active regions, Sudden ionospheric disturbances, Solar radio spectral observations, Cosmic ray measurements by neutron monitor, Geomagnetic indices; Late data--Cosmic rays Climax and Huancayo Jul.-Dec. 91, Sudden Commencements Jun.-Aug. 91, and Geomagnetic indices Dec. 91. GRA

N93-10776# National Geophysical Data Center, Boulder, CO.
SOLAR-GEOPHYSICAL DATA NUMBER 571, MARCH 1992. PART 2: (COMPREHENSIVE REPORTS). DATA FOR SEPTEMBER 1991 AND MISCELLANEOUS
Helen E. Coffey Mar. 1992 87 p
(PB92-177070; SGD-572-Pt-2) Avail: CASI HC A05/MF A01

This report contains the following sections: Detailed index for 1991-1992; Data for September 1991--Solar flares, Solar radio bursts at fixed frequencies, Solar x-ray radiation from GOES satellite, Mass ejections from the sun, active prominences and filaments; Miscellaneous data--SMM Total Solar Irradiance Feb. 80-Jun. 89. GRA

N93-10904# Centre National de la Recherche Scientifique, Verrieres-Le Buisson (France). Service d'Aeronomie.
PROSPECTS WITH SIMURIS
L. Dame and R. J. Rutten (Astronomical Inst., Utrecht, Netherlands) *In* ESA, Solar Physics and Astrophysics at Interferometric Resolution May 1992 p 21-25 (For primary document see N93-10901 01-90)
Copyright Avail: CASI HC A01/MF A03

N93-10905# Eidgenoessische Technische Hochschule, Zurich (Switzerland). Inst. of Astronomy.
SMALL-SCALE PHYSICS OF CONVECTION AND MAGNETIC FIELDS
S. K. Solanki *In* ESA, Solar Physics and Astrophysics at Interferometric Resolution May 1992 p 27-33 (For primary document see N93-10901 01-90)
Copyright Avail: CASI HC A02/MF A03

N93-10906# Observatoire de Paris-Meudon (France).
CHROMOSPHERIC STRUCTURE AND DYNAMICS
B. Schmieder *In* ESA, Solar Physics and Astrophysics at

Interferometric Resolution May 1992 p 35-42 (For primary document see N93-10901 01-90)
Copyright Avail: CASI HC A02/MF A03

N93-10907# Hulburt (E. O.) Center for Space Research, Washington, DC.
TRANSITION REGION DYNAMICS
K. P. Dere *In* ESA, Solar Physics and Astrophysics at Interferometric Resolution May 1992 p 43-48 (For primary document see N93-10901 01-90)
Copyright Avail: CASI HC A02/MF A03

N93-10908# Florence Univ. (Italy). Dipartimento di Astronomia e Scienza dello Spazio.
ULTRA-HIGH OBSERVATIONS OF THE PROMINENCE-CORONA TRANSITION REGION
F. C. Chiuderi-Drago *In* ESA, Solar Physics and Astrophysics at Interferometric Resolution May 1992 p 49-51 (For primary document see N93-10901 01-90)
Copyright Avail: CASI HC A01/MF A03

N93-10909# Observatoire de Paris-Meudon (France).
CORONAL AND SOLAR WIND ALFVEN WAVE PROPAGATION
M. Velli *In* ESA, Solar Physics and Astrophysics at Interferometric Resolution May 1992 p 53-55 (For primary document see N93-10901 01-90)
Copyright Avail: CASI HC A01/MF A03

N93-10910# Ceskoslovenska Akademie Ved, Ondrejov. Astronomical Inst.
THE FINE STRUCTURE OF PROMINENCES
P. Heinzel and J.-C. Vial (Centre National de la Recherche Scientifique, Verrieres-Le Buisson, France) *In* ESA, Solar Physics and Astrophysics at Interferometric Resolution May 1992 p 57-64 Sponsored in part by ESA (For primary document see N93-10901 01-90)
(Grant N-30315)
Copyright Avail: CASI HC A02/MF A03

N93-10911# Observatoire de Paris-Meudon (France).
INTENSITY, VELOCITY, AND TURBULENCE IN PROMINENCES OBSERVED WITH THE HRTS
J. E. Wiik (Oslo Univ., Norway), K. Dere (Naval Research Lab., Washington, DC.), and B. Schmieder *In* ESA, Solar Physics and Astrophysics at Interferometric Resolution May 1992 p 65-68 (For primary document see N93-10901 01-90)
Copyright Avail: CASI HC A01/MF A03

N93-10912# Paris VII Univ. (France). Lab. d'Astrophysique Extragalactique et de Cosmologie.
PHYSICS OF CORONAL LOOPS: HEATING AND RECONNECTION
J. Heyvaerts (Observatoire de Paris-Meudon, France) *In* ESA, Solar Physics and Astrophysics at Interferometric Resolution May 1992 p 69-72 (For primary document see N93-10901 01-90)
Copyright Avail: CASI HC A01/MF A03

N93-10913# Birmingham Univ. (England). Dept. of Physics and Space Research.
ENERGY BUILD-UP, TRANSPORT, AND RELEASE IN SOLAR FLARES
G. M. Simnett *In* ESA, Solar Physics and Astrophysics at Interferometric Resolution May 1992 p 73-80 (For primary document see N93-10901 01-90)
Copyright Avail: CASI HC A02/MF A03

N93-10914# Observatoire de Paris-Meudon (France). Dept. Atomes et Molecules en Astrophysique.
STOKES PARAMETERS OF THE O VI 103.2 nm LINE AS A PROBE OF THE MATTER VELOCITY FIELD VECTOR IN THE SOLAR WIND ACCELERATION REGION
S. Sahal-Brechot, N. Feautrier, V. Bommier, and A. deKertanguy *In* ESA, Solar Physics and Astrophysics at Interferometric Resolution May 1992 p 81-85 (For primary document see N93-10901 01-90)
Copyright Avail: CASI HC A01/MF A03

N93-10915# Centre National de la Recherche Scientifique, Verrieres-Le Buisson (France). Inst. d'Astrophysique Spatiale.
EVIDENCE OF PLASMOID EJECTION IN THE CORONA FROM 1991 ECLIPSE OBSERVATIONS WITH THE CANADA-FRANCE-HAWAII TELESCOPE
J.-C. Vial, S. Koutchmy (Institut d'Astrophysique, Paris, France), G. Monnet (Canada-France-Hawaii Telescope Corp., Waimea, HI.), J. Sovka (Canada-France-Hawaii Telescope Corp., Waimea, HI.), C. Clark (Canada-France-Hawaii Telescope Corp., Waimea, HI.), D. Salmon (Canada-France-Hawaii Telescope Corp., Waimea, HI.), N. Purves (Canada-France-Hawaii Telescope Corp., Waimea, HI.), P. Sydserff (Canada-France-Hawaii Telescope Corp., Waimea, HI.), R. Coulder (Sacramento Peak Observatory, Sunspot, NM.), and L. November (Sacramento Peak Observatory, Sunspot, NM.) et al *In* ESA, Solar Physics and Astrophysics at Interferometric Resolution May 1992 p 87-90 (For primary document see N93-10901 01-90)
Copyright Avail: CASI HC A01/MF A03

N93-10916# Rutherford Appleton Lab., Chilton (England).
HIGH RESOLUTION OBSERVATIONS OF SOLAR EJECTA
Richard A. Harrison *In* ESA, Solar Physics and Astrophysics at Interferometric Resolution May 1992 p 91-94 (For primary document see N93-10901 01-90)
Copyright Avail: CASI HC A01/MF A03

N93-10917# Astronomical Inst., Utrecht (Netherlands).
SMALL SCALE PROCESSES IN SOLAR AND STELLAR PLASMAS
G. H. J. vandenOord *In* ESA, Solar Physics and Astrophysics at Interferometric Resolution May 1992 p 97-104 Sponsored by ESA and Royal Netherlands Academy of Arts and Sciences (For primary document see N93-10901 01-90)
Copyright Avail: CASI HC A02/MF A03

N93-10923# Florence Univ. (Italy). Dipartimento di Astronomia.
OBSERVATION OF SOLAR FLARES AT HIGH RESOLUTION
G. Cauzzi, A. Falchi (Osservatorio Astrofisico di Arcetri, Florence, Italy), R. Falciani, and L. A. Smaldone (Naples Univ., Italy) *In* ESA, Solar Physics and Astrophysics at Interferometric Resolution May 1992 p 141-143 Sponsored in part by CNR (For primary document see N93-10901 01-90)
Copyright Avail: CASI HC A01/MF A03

N93-10924# Etablissement Technique Central de l'Armement, Arcueil (France).
PATTERN RECOGNITION APPLIED TO H(SUB ALPHA) SPECTROHELIOGRAMS SOLAR ROTATION AND MERIDIONAL CIRCULATION
B. Collin and E. Nesme-Ribes (Observatoire de Paris-Meudon, France) *In* ESA, Solar Physics and Astrophysics at Interferometric Resolution May 1992 p 145-148 (For primary document see N93-10901 01-90)
Copyright Avail: CASI HC A01/MF A03

N93-10925# Sofia Univ. (Bulgaria). Dept. of Astronomy.
ON THE NATURE OF THE SMALL-SCALE PLASMA STRUCTURES IN THE SOLAR ACTIVE PHENOMENA
V. N. Dermendjiev *In* ESA, Solar Physics and Astrophysics at Interferometric Resolution May 1992 p 149-152 (For primary document see N93-10901 01-90)
(Grant F50/1991)
Copyright Avail: CASI HC A01/MF A03

N93-10926# Observatoire de Paris-Meudon (France).
MSDP IMAGING SPECTROSCOPY FOR HIGH RESOLUTION SOLAR PHYSICS
P. Mein *In* ESA, Solar Physics and Astrophysics at Interferometric Resolution May 1992 p 153-155 (For primary document see

N93-10901 01-90)
Copyright Avail: CASI HC A01/MF A03

N93-10927# Florence Univ. (Italy). Dipartimento di Astronomia e Scienza dello Spazio.
HIGH RESOLUTION GRANULATION SPECTROPHOTOMETRY WITH A UBF AND A FP INTERFEROMETER IN TANDEM
G. Salucci, L. Bertello, D. Bonaccini (Osservatorio Astrofisico di Arcetri, Florence, Italy), F. Cavallini (Osservatorio Astrofisico di Arcetri, Florence, Italy), G. Ceppatelli (Osservatorio Astrofisico di Arcetri, Florence, Italy), and A. Righini *In* ESA, Solar Physics and Astrophysics at Interferometric Resolution May 1992 p 157-159 (For primary document see N93-10901 01-90)
Copyright Avail: CASI HC A01/MF A03

N93-10928# Academy of Sciences (USSR), Irkutsk. Siberian Inst. of Terrestrial Magnetism, Ionosphere and Radio Wave Propagation.
SPATIAL DISTRIBUTION OF LINE-OF-SIGHT VELOCITIES IN A QUIESCENT PROMINENCE
S. A. Druzhinin, A. A. Pevtsov, and G. P. Mashnich *In* ESA, Solar Physics and Astrophysics at Interferometric Resolution May 1992 p 161-164 (For primary document see N93-10901 01-90)
Copyright Avail: CASI HC A01/MF A03

N93-10930# Centre National de la Recherche Scientifique, Verrieres-Le Buisson (France). Service d'Aeronomie.
SUN: THE SOLAR ULTRAVIOLET NETWORK
L. Dame *In* ESA, Solar Physics and Astrophysics at Interferometric Resolution May 1992 p 171-180 (For primary document see N93-10901 01-90)
Copyright Avail: CASI HC A02/MF A03

N93-10931# Technische Physische Dienst TNO-TH, Delft (Netherlands).
THE SOLAR ULTRAVIOLET NETWORK SUBTRACTIVE DOUBLE MONOCHROMATOR
B. Kruizinga, B. C. Braam, B. Snijders, and H. Visser *In* ESA, Solar Physics and Astrophysics at Interferometric Resolution May 1992 p 181-184 (For primary document see N93-10901 01-90)
Copyright Avail: CASI HC A01/MF A03

N93-10932# Centre National de la Recherche Scientifique, Verrieres-Le Buisson (France). Service d'Aeronomie.
INTERFEROMETRIC IMAGING WITH THE SOLAR ULTRAVIOLET NETWORK
L. Dame and T. J. Cornwell (National Radio Astronomy Observatory, Socorro, NM.) *In* ESA, Solar Physics Astrophysics at Interferometric Resolution May 1992 p 185-189 (For primary document see N93-10901 01-90)
(Contracts ESA-7978; ESA-9301)
Copyright Avail: CASI HC A01/MF A03

N93-10950# Technische Physische Dienst TNO-TH, Delft (Netherlands).
THE SOLAR ULTRAVIOLET NETWORK: PERFORMANCE AND TOLERANCE ANALYSIS
B. Kruizinga, B. C. Braam, and B. Snijders *In* ESA, Solar Physics and Astrophysics at Interferometric Resolution May 1992 p 287 (For primary document see N93-10901 01-90)
Copyright Avail: CASI HC A01/MF A03

93 SPACE RADIATION

Includes cosmic radiation; and inner and outer earth's radiation belts.

For biological effects of radiation see *52 Aerospace Medicine*. For theory see *73 Nuclear and High-Energy Physics*.

N93-10616# Florida Univ., Gainesville. Dept. of Physics.
COSMIC MICROWAVE BACKGROUND ANISOTROPIES FROM PLAUSIBLE DOUBLE INFLATION
J. N. Fry and Yun Wang 1992 11 p
(Contract DE-FG05-86ER-40272)
(DE92-016195; DOE/ER-40272/153; UFIFT-HEP-92-6) Avail: CASI HC A03/MF A01

We study the anisotropies in the cosmic microwave background radiation (CMBR) from certain inflationary models containing two scalar fields, one inflaton and one dilaton. These models can give rise to inflation that occurs in two stages: a first power-law stage during which density fluctuations with a non-scale-invariant power spectrum are generated; and a second slow roll-over stage when the dilaton field evolves toward its global minimum, after the inflaton field has settled down in its true vacuum. The transition can occur on a scale of cosmological interest, lambda(sub f) is approximately 1-1000 Mpc. We find that when normalized to yield a quadrupole moment of order 3(10)(exp -5), the features of the power spectrum can significantly alter the angular correlation function of CMBR anisotropies. In particular, a non-scale-invariant spectrum or/and larger amplitudes on large scales can reduce small-scale CMBR anisotropies significantly, while maintaining the observational bound on the quadrupole moment. DOE

99 GENERAL

N93-10640 Aerospace Industries Association of Canada, Ottawa (Ontario).
AEROSPACE INDUSTRIES ASSOCIATION OF CANADA Annual Report, 1990
1991 49 p Original contains color illustrations
(CTN-92-60345) Avail: CASI HC A03/MF A01

The Aerospace Industries Association of Canada aims to promote the health of the Canadian aerospace industry by providing an industry voice to government agencies, the press, and the public, by developing and coordinating aerospace industry views and encouraging discussion of problems within the industry, by advising governments in developing and programs and policies, by initiating proposals to government which enhance the future of the industry, and, in general, in promoting a harmonious relationship with governments. Descriptions of the activities of the various subcommittees of the association are presented. Industry statistics for the past three years with a projection for 1993 are presented. These show a general pattern of growth in the industry in the past three years. A listing of member companies is provided.
CISTI

N93-10654# Manitoba Industry, Trade and Tourism, Winnipeg.
THE TECHNOLOGY ADVANTAGE: A GUIDE TO SCIENCE, TECHNOLOGY, AND INNOVATION IN MANITOBA
1992 33 p Original contains color illustrations
(CTN-92-60571) Avail: CASi HC A03/MF A01

A directory is provided of organizations in Manitoba that operate in various fields of science, technology, and innovation. The organizations include the following: provincial government agencies and laboratories; universities and colleges; federal government research organizations and facilities; non-profit organizations in the fields of health, environment, aerospace, manufacturing, and industry; and professional organizations. Under each organization a brief description of activities and capabilities is given, along with address and phone number. CISTI

N93-10655# Manitoba Industry, Trade and Tourism, Winnipeg.
MANITOBA AEROSPACE TECHNOLOGY: CAPABILITY DIRECTORY
1991 41 p Original contains color illustrations
(CTN-92-60572) Avail: CASI HC A03/MF A01

A directory is provided to illustrate the potential of Manitoba industry in the aerospace sector. The directory presents information on contractors and subcontractors, manufacturers, consultants, service companies, research organizations, and universities. Under each directory listing, this information includes a description of the company or organization, facilities available, quality standards, featured equipment, major clients, number of employees, addresses, and phone numbers. The industry sectors covered by the directory include remote sensing, communications, electronics, biotechnology, software, metals and composites, fabrications, materials and coatings, engineering consulting, research and development laboratories, project management, testing services, manufacturing of aircraft and spacecraft components, repair and overhaul, and environmental services. CISTI

Typical Subject Index Listing

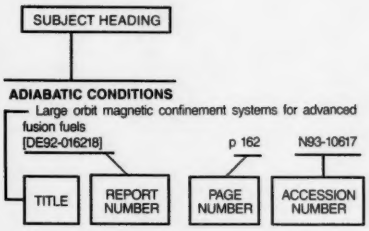

The subject heading is a key to the subject content of the document. Titles, report numbers, and accession numbers of pertinent documents are provided under each subject heading. When the title is insufficiently descriptive of the document content, a title extension has been added, separated from the title by three hyphens. The report number helps to indicate the type of document cited (e.g., NASA report, NASA translation, NASA contractor report). The accession number is the number by which the document abstracts are arranged in this journal and by which the document is sold or requested. The page number helps you locate the the citation in the abstract section. The titles, with title extensions if present, are arranged under each subject heading in ascending accession number order. The subject headings have been selected from the latest revision of the *NASA Thesaurus*.

A

ABIOGENESIS
Self-programming of matter and the evolution of proto-biological organizations
[DE92-015244] p 129 N93-10628
ABLATION
Documentation of the detailed radiation property data for the radiation-ablation code RASLE
[NASA-TM-103848] p 28 N93-10742
ABLATIVE MATERIALS
Feasibility evaluation of the monolithic braided ablative nozzle p 19 N93-10023
Documentation of the detailed radiation property data for the radiation-ablation code RASLE
[NASA-TM-103848] p 28 N93-10742
ABSORPTION
Dermal exposure assessment: Principles and applications
[PB92-205665] p 131 N93-10438
ABSORPTION COOLING
Heat transfer additives for absorption cooling system fluids
[PB92-190354] p 169 N93-10249
ABSORPTION SPECTROSCOPY
Alternate spectrometric oil analysis techniques
[AD-A253355] p 29 N93-10101
Epitaxial growth and dopant incorporation in diamond
[AD-A253636] p 165 N93-10206
ABSTRACTS
EIA publications directory, 1991
[DE92-015686] p 174 N93-10607
ACCELEROMETERS
Design, test, and evaluation of three active flutter suppression controllers
[NASA-TM-4338] p 10 N93-10070
ACCOMMODATION
Attached payloads on Space Station Freedom and Columbus p 14 N93-10929
Accommodation aspects of SIMURIS on Space Station Freedom p 14 N93-10954
ACCURACY
An assessment of the correspondence principle in comparison to nonlinear viscoelastic theory: A case study p 51 N93-10501
ACETATES
Biological production of ethanol from coal
[DE92-016116] p 41 N93-10216
ACHIEVEMENT
The levels of mathematics achievement: Initial performance standards for the 1990 NAEP mathematics assessment, volume 3
[PB92-199421] p 134 N93-10341
ACIDOSIS
Metabolic factors influencing myocardial recovery from acidosis (CiC3)
[AD-A252376] p 132 N93-10796
ACOUSTIC COUPLING
Nozzle installation effects on the noise from supersonic exhaust plumes p 150 N93-10681
Combustion noise and combustion instabilities in propulsion systems p 150 N93-10682
ACOUSTIC EXCITATION
Probability density functions for random nonlinear oscillation p 55 N93-10522
ACOUSTIC INSTABILITY
The prediction of noise radiation from supersonic elliptic jets p 151 N93-10684
ACOUSTIC PROPERTIES
Acoustic noise generation at the air/ocean boundary
[DREA-CR-90-445] p 147 N93-10642
Combustion noise and combustion instabilities in propulsion systems p 150 N93-10682
ACOUSTIC VELOCITY
SBS applications study
[AD-A253779] p 102 N93-10234
ACQUISITION
Acquisition 1: Stock acquisition processes in defence and aerospace documentation centres p 173 N93-10598
Acquisition 2: Procurement, acquisition, and maintenance of configuration management documentation in support of a CIS system p 173 N93-10599
ACTIVATION ENERGY
Transition metal activation and functionalization of carbon-hydrogen bonds
[DE92-014809] p 30 N93-10400
Mobility of toluene in polystyrene-toluene solutions: A NMR study
[AD-A253203] p 31 N93-10794
ACTIVE CONTROL
Numerical simulation of large actively controlled space structures p 13 N93-10308
Characterization of and active control of flexible structures, using piezoceramics as sensors and actuators p 10 N93-10319
Reduction of propeller noise by active noise control p 152 N93-10692
ACTUATORS
Sensor and actuator materials for high performance composites
[AD-A254178] p 27 N93-10254
A study upon structural optimization of elastic rotors for mechanical systems
[INPE-5376-TDI/471] p 94 N93-10310
Characterization of and active control of flexible structures, using piezoceramics as sensors and actuators p 10 N93-10319
Control of panel flutter at high supersonic speed p 9 N93-10900
ADA (PROGRAMMING LANGUAGE)
Ada validation tests for rate monotonic scheduling algorithms
[AD-A253325] p 136 N93-10300
ADAPTATION
Molecular biology in studies of oceanic primary production
[DE92-016101] p 128 N93-10283
Biological and theoretical studies of adaptive networks: The conditioned response
[AD-A253329] p 142 N93-10354
ADAPTIVE FILTERS
Convergence performance of adaptive detectors, part 3
[AD-A248415] p 143 N93-10275
ADAPTIVE OPTICS
Ground/space co-operation for interferometry p 178 N93-10946
ADDITIVES
Heat transfer additives for absorption cooling system fluids
[PB92-190354] p 169 N93-10249
Polynitro polycyclic cage compounds
[AD-A252889] p 42 N93-10268
ADHESION
The development of computational methods of adhesion and adhesive science and technology
[AD-A253758] p 92 N93-10740
ADHESIVE BONDING
Experimental and theoretical behavior of adhesively bonded composite structures under tensile stress at the edge vicinity p 53 N93-10515
Experimental and numeric analysis of constraints in a bonded stepped lap joint subjected to traction p 54 N93-10516
The development of computational methods of adhesion and adhesive science and technology
[AD-A253758] p 92 N93-10740
ADHESIVES
The effect of elevated temperatures on the properties of thermally stable silicon-based elastomers for adhesives, sealants, and insulator applications p 15 N93-10006
Identification and evaluation of lubricants, adhesives, and seals used on LDEF p 39 N93-10588
The development of computational methods of adhesion and adhesive science and technology
[AD-A253758] p 92 N93-10740
ADIABATIC CONDITIONS
Large orbit magnetic confinement systems for advanced fusion fuels
[DE92-016218] p 162 N93-10617
ADIABATIC EQUATIONS
On the measurement of time-dependent quantum phases
[DE92-630206] p 170 N93-10387
ADIPOSE TISSUES
A prospective evaluation of stress fractures/overuse injuries in a population of West Point cadets
[AD-A252427] p 132 N93-10709
ADSORPTION
Nonlinear studies of surface and interfaces of advanced semiconductor materials
[AD-A253365] p 164 N93-10105
Comparison of Cl and HCl adsorption on Si(100)-(2 x 1)
[AD-A252802] p 30 N93-10281
Hydrocarbon surface chemistry on Si(100)
[AD-A252803] p 27 N93-10465
ADVANCED LAUNCH SYSTEM (STS)
Molded nozzle technology for large solid rocket motors p 19 N93-10024
Space Transportation Engine Program (STEP), phase B
[NASA-CR-184062] p 25 N93-10350
ADVANCED TEST REACTORS
D-He-3 spherical torus fusion reactor system study
[AD-A253358] p 155 N93-10102
ADVECTION
The role of eddy fluxes in the response of the atmosphere to tropical thermal forcing p 124 N93-10318
AERIAL PHOTOGRAPHY
Stereoscopy and paralax in the vertical distances determination using aerial photographs
[INPE-5363-PUD/049] p 102 N93-10063
AERIAL RECONNAISSANCE
Open Skies Treaty imaging radar technology issues
[DE92-016548] p 68 N93-10394
AEROACOUSTICS
Tilt rotor hover aeroacoustics
[NASA-CR-177598] p 147 N93-10458
Comparison of flyover noise data from aircraft at high subsonic speeds with prediction p 149 N93-10674

Supersonic acoustic source mechanisms for free jets of various geometries p 150 N93-10680
Nozzle installation effects on the noise from supersonic exhaust plumes p 150 N93-10681
Prediction of jet mixing noise for high subsonic flight speeds p 151 N93-10685
Identifying the principal noise sources of fixed-wing combat aircraft in high-speed flight p 151 N93-10686
Mechanisms of sound generation in subsonic jets p 152 N93-10688

AERODYNAMIC BALANCE
Pitch control trimming system for canard design aircraft
[CA-PATENT-APPL-SN-2013236] p 10 N93-10374
Arguments concerning wind tunnel test studies of the trim characteristics of objects with small asymmetries'
[AD-A254111] p 5 N93-10858

AERODYNAMIC CHARACTERISTICS
The integration of geometric modeling into an inverse design method and application of a PC-based inverse design method and comparison with test results p 78 N93-10058
Computational fluid dynamics capability for internally carried store separation
[AD-A253671] p 79 N93-10297
Forced unsteady separated flows on a 45 degree delta wing p 80 N93-10305
Wind tunnel spin data reduction to obtain aerodynamic spin damping coefficients by using nonlinear equation of motion
[AD-A253880] p 4 N93-10811
Effect of planform and body on supersonic aerodynamics of multibody configurations
[NASA-TP-3212] p 4 N93-10824
Development of nonlinear aerodynamic models for unsteady responses p 4 N93-10845

AERODYNAMIC COEFFICIENTS
A method of testing two-dimensional airfoils
[AD-A253210] p 4 N93-10375
Harmonic analysis of the aerodynamic forces on a Darrieus rotor p 6 N93-10551
Wind tunnel spin data reduction to obtain aerodynamic spin damping coefficients by using nonlinear equation of motion
[AD-A253880] p 4 N93-10811
Development of nonlinear aerodynamic models for unsteady responses p 4 N93-10845
Arguments concerning wind tunnel test studies of the trim characteristics of objects with small asymmetries'
[AD-A254111] p 5 N93-10858

AERODYNAMIC DRAG
Control of lift and drag in unsteady flows
[AD-A253146] p 3 N93-10340
A method of testing two-dimensional airfoils
[AD-A253210] p 4 N93-10375
Experimental investigation of flows behind different Large-Eddy Breakup (LEBU) devices in thick boundary layers p 6 N93-10550
Development of nonlinear aerodynamic models for unsteady responses p 4 N93-10845
Characteristics of separated flows including cavitation effects p 84 N93-10874

AERODYNAMIC FORCES
Computational fluid dynamics capability for internally carried store separation
[AD-A253671] p 79 N93-10297
Methods of guidance flight dynamics
[AD-A254248] p 10 N93-10704
Research on the asymmetrical aerodynamic forces of reentry vehicles
[AD-A254307] p 4 N93-10707

AERODYNAMIC HEATING
One type of automatically adjusted difference scheme with artificial viscosity to calculate ablated exterior shapes
[AD-A254108] p 5 N93-10856

AERODYNAMIC INTERFERENCE
Characteristics of separated flows including cavitation effects p 84 N93-10874

AERODYNAMIC LOADS
Performance parameters and assessment p 77 N93-10052
Measurement of aerodynamic shear stress using side chain liquid crystal polymers
[AD-A254312] p 40 N93-10770

AERODYNAMIC NOISE
Non-propulsive aerodynamic noise p 149 N93-10673
Comparison of flyover noise data from aircraft at high subsonic speeds with prediction p 149 N93-10674
Supersonic acoustic source mechanisms for free jets of various geometries p 150 N93-10680
The prediction of noise radiation from supersonic elliptic jets p 151 N93-10684
Prediction of jet mixing noise for high subsonic flight speeds p 151 N93-10685
Identifying the principal noise sources of fixed-wing combat aircraft in high-speed flight p 151 N93-10686
Mechanisms of sound generation in subsonic jets p 152 N93-10688
Reduction of propeller noise by active noise control p 152 N93-10692

AERODYNAMIC STABILITY
Research on the asymmetrical aerodynamic forces of reentry vehicles
[AD-A254307] p 4 N93-10707

AERODYNAMIC STALLING
A comparative study of semi-empirical dynamic stall models p 5 N93-10544
Harmonic analysis of the aerodynamic forces on a Darrieus rotor p 6 N93-10551

AERODYNAMICS
Aerodynamic investigation of radial turbines using computational methods p 78 N93-10056
Aeronautical engineering: A continuing bibliography with indexes (supplement 276)
[NASA-SP-7037(276)] p 1 N93-10073
Aeronautical engineering: A continuing bibliography with indexes (supplement 279)
[NASA-SP-7037(279)] p 1 N93-10074
Aeronautical engineering: A cumulative index to a continuing bibliography (supplement 274)
[NASA-SP-7037(274)] p 1 N93-10351
Aeronautical engineering: A continuing bibliography with indexes (supplement 281)
[NASA-SP-7037(281)] p 1 N93-10352
Aeronautical technologies for the twenty-first century
[NASA-CR-190918] p 1 N93-10647
Methods of guidance flight dynamics
[AD-A254248] p 10 N93-10704

AEROELASTICITY
Navier-Stokes dynamics and aeroelastic computations for vortical flows, buffet and aeroelastic applications
[NASA-CR-190692] p 2 N93-10098
Nonlinear aeroelasticity of composite structures
[AD-A254285] p 8 N93-10842

AERONAUTICAL ENGINEERING
Aeronautical engineering: A continuing bibliography with indexes (supplement 276)
[NASA-SP-7037(276)] p 1 N93-10073
Aeronautical engineering: A continuing bibliography with indexes (supplement 279)
[NASA-SP-7037(279)] p 1 N93-10074
Aeronautical engineering: A cumulative index to a continuing bibliography (supplement 274)
[NASA-SP-7037(274)] p 1 N93-10351
Aeronautical engineering: A continuing bibliography with indexes (supplement 281)
[NASA-SP-7037(281)] p 1 N93-10352
Aeronautical technologies for the twenty-first century
[NASA-CR-190918] p 1 N93-10647

AERONAUTICS
AGARD index of publications, 1989-1991
[AGARD-INDEX-89-91] p 174 N93-10610
Index to NASA news releases and speeches, 1991
[NASA-TM-108004] p 175 N93-10815
Index to NASA news releases and speeches, 1990
[NASA-TM-108003] p 176 N93-10872

AERONOMY
Workshop on the evolution of the Martian atmosphere
[NASA-CR-190730] p 189 N93-10064

AEROSOLS
Laser and optical physics
[AD-A253619] p 88 N93-10251

AEROSPACE ENGINEERING
NASA patent abstracts bibliography: A continuing bibliography. Section 1: Abstracts (supplement 41)
[NASA-SP-7039(41)-SECT-1] p 171 N93-10078
Reliability assurance requirements for ESA space systems
[ESA-PSS-01-30-ISSUE-2] p 94 N93-10317
AGARD index of publications, 1989-1991
[AGARD-INDEX-89-91] p 174 N93-10610
Index to NASA news releases and speeches, 1991
[NASA-TM-108004] p 175 N93-10815
Index to NASA news releases and speeches, 1990
[NASA-TM-108003] p 176 N93-10872

AEROSPACE INDUSTRY
The development of optical techniques for component inspection in the aerospace industry p 93 N93-10307
Aerospace Industries Association of Canada
[CTN-92-60345] p 192 N93-10640
Aerospace Industries Association of Canada
[CTN-92-60590] p 1 N93-10644
Aerospace industry profile, 1990-1991
[CTN-92-60513] p 1 N93-10651
Aerospace and defence-related industries statistical survey report, 1991
[CTN-92-60514] p 2 N93-10652
The technology advantage: A guide to science, technology, and innovation in Manitoba
[CTN-92-60571] p 192 N93-10654

AEROSPACE MEDICINE
Aerospace medicine and biology: A continuing bibliography with indexes (supplement 365)
[NASA-SP-7011(365)] p 130 N93-10075
Aerospace medicine and biology: A continuing bibliography with indexes (supplement 360)
[NASA-SP-7011(360)] p 130 N93-10076
Aerospace medicine and biology: A continuing bibliography with indexes (supplement 364)
[NASA-SP-7011(364)] p 130 N93-10077
Aerospace medicine and biology: A continuing bibliography with indexes (supplement 366)
[NASA-SP-7011(366)] p 130 N93-10079
Aerospace medicine and biology: A continuing bibliography with indexes (supplement 367)
[NASA-SP-7011(367)] p 130 N93-10080
DoD space radiation concerns
[AD-A253135] p 131 N93-10613

AEROSPACE PLANES
A configuration development strategy for the NASP p 9 N93-10011

AEROSPACE SCIENCES
Acquisition 1: Stock acquisition processes in defence and aerospace documentation centres p 173 N93-10598
AGARD index of publications, 1989-1991
[AGARD-INDEX-89-91] p 174 N93-10610
Index to NASA news releases and speeches, 1991
[NASA-TM-108004] p 175 N93-10815
Index to NASA news releases and speeches, 1990
[NASA-TM-108003] p 176 N93-10872

AEROSPACE TECHNOLOGY TRANSFER
AGARD index of publications, 1989-1991
[AGARD-INDEX-89-91] p 174 N93-10610

AGENTS
Developmental research on ultra abrasion-resistant materials
[DE92-531066] p 36 N93-10287

AGGREGATES
Stability of open-graded bases under wheel loads using a model testing approach
[AD-A253209] p 66 N93-10710

AGING (MATERIALS)
Review and analysis of check valve failure data
[DE92-014462] p 91 N93-10381
Chronorheological characterization of elastomers p 46 N93-10476

AGREEMENTS
Open Skies Treaty imaging radar technology issues
[DE92-016548] p 68 N93-10394

AGRICULTURE
Remote sensing data for monitoring and evaluating burned areas: Case of Emas National Park (GO)
[INPE-5312-PRE/1709] p 102 N93-10373

AH-64 HELICOPTER
Operator workload predictions for the revised AH-64A workload prediction model, volume 1
[AD-A254198] p 133 N93-10261

AIR CONDITIONING EQUIPMENT
ARTI Refrigerant Database
[DE92-015122] p 30 N93-10401

AIR CURRENTS
Heat transfer and pressure drop for air flow through enhanced passages
[DE92-016597] p 82 N93-10612

AIR DEFENSE
Combat aircraft operations: Training requirements for the German Air Force tactical flying units and the noise problem p 148 N93-10667
Combat aircraft noise: The operator's perspective p 148 N93-10669

AIR FLOW
Heat transfer and pressure drop for air flow through enhanced passages
[DE92-016597] p 82 N93-10612

AIR LAUNCHING
Computational fluid dynamics capability for internally carried store separation
[AD-A253671] p 79 N93-10297

AIR NAVIGATION
Rotorcraft en route ATC route standards
[AD-A249129] p 6 N93-10323

AIR POLLUTION
The current and future environmental role of atmospheric methane: Model studies and uncertainties
[NASA-CR-190662] p 104 N93-10256
Gridded Model Information Support System (GMISS) user's guide. Volume 3: Model concentration data retrieval subsystem
[PB92-190263] p 171 N93-10257
Analysis of air pollution and greenhouse gases
[DE92-014955] p 104 N93-10384

AIR TRAFFIC CONTROL
Advanced terrain displays to transport category aircraft
[PB92-197136] p 6 N93-10065

A new test of scanning and monitoring ability: Methods and initial results
| AD-A249123 | p 132 N93-10321
Rotorcraft en route ATC route standards
| AD-A249129 | p 6 N93-10323
Air traffic control visual scanning
| DOT/FAA/CT-TN92/16 | p 7 N93-10459
Defence electronics industry profile, 1990-1991
| CTN-92-60515 | p 66 N93-10653
A description of the Mode Select beacon system (Mode S) and its associated benefits to the National Airspace System (NAS)
| DOT/FAA/SE-92/6 | p 7 N93-10738

AIR TRAFFIC CONTROLLERS (PERSONNEL)
A new test of scanning and monitoring ability: Methods and initial results
| AD-A249123 | p 132 N93-10321
Air traffic control visual scanning
| DOT/FAA/CT-TN92/16 | p 7 N93-10459

AIR WATER INTERACTIONS
Air-sea interaction and remote sensing
| NASA-CR-190913 | p 128 N93-10068
Acoustic noise generation at the air/ocean boundary
| DREA-CR-90-445 | p 147 N93-10642
Air-sea interaction in regions of varying surface conditions
| AD-A253182 | p 128 N93-10791

AIRBORNE/SPACEBORNE COMPUTERS
Requirements analysis notebook for the flight data systems definition in the Real-Time Systems Engineering Laboratory (RSEL)
| NASA-CR-185698 | p 14 N93-10960

AIRCRAFT CONFIGURATIONS
A configuration development strategy for the NASP
p 9 N93-10011

AIRCRAFT CONTROL
Pitch control trimming system for canard design aircraft
| CA-PATENT-APPL-SN-2013236 | p 10 N93-10374
Initial piloted simulation study of geared flap control for tilt-wing V/STOL aircraft
| NASA-TM-103872 | p 11 N93-10741

AIRCRAFT DESIGN
Maintaining future military aircraft design capability
| AD-A253963 | p 8 N93-10420

AIRCRAFT ENGINES
LV software for supersonic flow analysis
| NASA-CR-190911 | p 2 N93-10069
SAPNEW: Parallel finite element code for thin shell structures on the Alliant FX/80
| NASA-CR-190663 | p 94 N93-10372
Technical measures for the attenuation of aircraft noise and their applicability to GAF combat aircraft
p 152 N93-10690

AIRCRAFT INDUSTRY
Maintaining future military aircraft design capability
| AD-A253963 | p 8 N93-10420

AIRCRAFT MAINTENANCE
Maintaining future military aircraft design capability
| AD-A253963 | p 8 N93-10420

AIRCRAFT MANEUVERS
Forced unsteady separated flows on a 45 degree delta wing p 80 N93-10305
Flight test and analysis procedures for new handling criteria
| RAE-TM-FM-26 | p 8 N93-10803

AIRCRAFT NOISE
Tilt rotor hover aeroacoustics
| NASA-CR-177598 | p 147 N93-10458
Combat Aircraft Noise
| AGARD-CP-512 | p 148 N93-10666
Combat aircraft noise: The operator's perspective
p 148 N93-10669
Non-propulsive aerodynamic noise
p 149 N93-10673
Comparison of flyover noise data from aircraft at high subsonic speeds with prediction p 149 N93-10674
A brief review of the source noise technology applicable to fixed-wing military aircraft p 150 N93-10678
Reduction of propeller noise by active noise control
p 152 N93-10692

AIRCRAFT PERFORMANCE
Technical measures for the attenuation of aircraft noise and their applicability to GAF combat aircraft
p 152 N93-10690

AIRCRAFT PILOTS
Operator workload predictions for the revised AH-64A workload prediction model, volume 1
| AD-A254198 | p 133 N93-10261

AIRCRAFT POWER SUPPLIES
Air cell --- model aircraft power supplies
| CA-PATENT-APPL-SN-2001346 | p 72 N93-10368

AIRCRAFT STRUCTURES
An evaluation of a method of reconstituting fatigue loading from Rainflow counting
| RAE-TR-89057 | p 94 N93-10198

AIRDROPS
Relating flying hours to aircrew performance: Evidence for attack and transport missions
| AD-A253988 | p 133 N93-10719

AIRFOIL OSCILLATIONS
A comparative study of semi-empirical dynamic stall models p 5 N93-10544
Stream function-vorticity finite element formulations of unsteady incompressible Navier-Stokes equations
p 60 N93-10545

AIRFOILS
Effect of passive flow-control devices on turbulent low-speed base flow p 79 N93-10304
A method of testing two-dimensional airfoils
| AD-A253210 | p 4 N93-10375
Nonlinear aeroelasticity of composite structures
| AD-A254285 | p 8 N93-10842

AIRFRAMES
Non-propulsive aerodynamic noise
p 149 N93-10673
Contributions to the experimental investigation of rotor/body aerodynamic interactions p 5 N93-10877

AIRPORTS
Noise of combat aircraft in proximity to air bases: Review of the possibilities of noise reduction at the source
p 148 N93-10671
A brief review of the source noise technology applicable to fixed-wing military aircraft p 150 N93-10678

AIRSPACE
Rotorcraft en route ATC route standards
| AD-A249129 | p 6 N93-10323

ALCOHOLS
NQR-NMR studies of higher alcohol synthesis Cu-Co catalysts
| DE92-015783 | p 31 N93-10460

ALGEBRA
A look at scalable dense linear algebra libraries
| DE92-017805 | p 143 N93-10285
Computer algebra and the elliptic restricted problem of three bodies p 11 N93-10499
A look at scalable dense linear algebra libraries
| DE92-017161 | p 139 N93-10816
Algebra-geometric and differential geometric methods in solid geometric modeling
| AD-A253669 | p 145 N93-10870

ALGORITHMS
Numerical simulation of unsteady flow in a nozzle
p 16 N93-10008
A simplified model for hybrid rocket performance prediction p 19 N93-10022
Center for Intelligent Control Systems, Brown University component: Graduate research fellowships
| AD-A253620 | p 141 N93-10095
Unstructured mesh algorithms for aerodynamic calculations
| NASA-CR-189685 | p 2 N93-10097
Unifying the landmark developments in optimal bounding ellipsoid identification
| AD-A253502 | p 143 N93-10200
An implementation of the MVDR beamformer on the Intel iWarp system
| AD-A253641 | p 140 N93-10209
Interactive animation of fault tolerant parallel algorithms
| AD-A253349 | p 135 N93-10212
Fault-tolerant and efficient parallel computation
| AD-A253350 | p 140 N93-10213
Test range tracking network processors
| AD-A253511 | p 140 N93-10219
Implementation of parallel algorithms
| AD-A253638 | p 140 N93-10227
Convergence performance of adaptive detectors, part 3
| AD-A248415 | p 143 N93-10275
Eye movements and visual information processing
| AD-A250198 | p 132 N93-10278
Development of parallel architectures for sensor array processing algorithms
| AD-A253660 | p 141 N93-10299
Ada validation tests for rate monotonic scheduling algorithms
| AD-A253325 | p 136 N93-10300
A globally well-posed accurate and efficient finite element CFD algorithm for compressible aerodynamics
p 3 N93-10306
Numerical simulation of large actively controlled space structures p 13 N93-10308
Improved numerical simulation of Euler equations
p 80 N93-10309
Parallel sparse Cholesky factorization algorithms for shared-memory multiprocessor systems
| DE92-016829 | p 141 N93-10334
On the evaluation of Bessel functions
| AD-A253129 | p 143 N93-10339
Algorithms for multichannel optical processor
| AD-A254009 | p 158 N93-10360
Nonlinear signal processing schemes for robust target detection and automatic clutter rejection in radar
| AD-A253546 | p 68 N93-10380
Box counting multifractal analysis
| AD-A253960 | p 144 N93-10419
Smart algorithms and adaptive methods in computational fluid dynamics p 44 N93-10469
Experimental demonstration of offset control with an application to the tethered payload p 14 N93-10521
An adaptive mesh-management algorithm for three-dimensional automatic finite element analysis
p 61 N93-10554
Numerical considerations for structural system identification from modal information p 63 N93-10564
A boundary element super-element method for coupling with the finite element method of substructures
p 64 N93-10566
Partial solution of the generalized eigenvalue problem using the Woodbury transformation p 64 N93-10567
Optimal robot trajectory planning p 65 N93-10570
Effective formulation of the dynamics of a manipulator based on the Appell equations p 65 N93-10571
The mechanical verification of a simple control system
| ORA-TR-89-5443-04 | p 142 N93-10641
AMR on the CM-2
| NASA-CR-190747 | p 138 N93-10736
A multilevel security model for object-oriented database systems p 175 N93-10844
Modelling of 3-D electromagnetic responses using the time-wavenumber method
| DE92-017025 | p 70 N93-10865
RHALE: A MMALE shock physics code for arbitrary meshes
| DE92-017051 | p 139 N93-10866
A spatial similarity measure for image database applications
| AD-A253570 | p 176 N93-10883

ALKALI METALS
Activated transport in AMTEC electrodes
| DE92-016810 | p 75 N93-10786

ALKYL COMPOUNDS
Improved gallium nitride and aluminum nitride electronic materials
| AD-A253785 | p 76 N93-10888

ALLOYING
A study of the effect of nitrogen and molybdenum in the corrosion inhibition of austenitic stainless steel
| AD-A253354 | p 33 N93-10100
Effect of alloying elements on passivity and breakdown of passivity of Fe- and Ni-based alloys mechanistics aspects
| DE92-017316 | p 33 N93-10395
Inhibiting corrosion in Gr/Al and Gr/Mg metal matrix composites using nonequilibrium alloying techniques
| AD-A253923 | p 34 N93-10752

ALTIMETERS
Comparison of wind speed measurements over the oceans with the Special Sensor Microwave/Imager and the Geosat altimeter p 127 N93-10850

ALTITUDE
Altitude compensating nozzle evaluation
p 22 N93-10037

ALUMINUM
Determination of Sandoz black aluminum coloring dye, olive aluminum coloring dye, and sodium dichromate aluminum sealing solutions by UV-visible spectrophotometry
| AD-A253639 | p 29 N93-10207
A computational study of projectile melt in impact with typical Whipple shields
| DE92-017137 | p 92 N93-10635

ALUMINUM ALLOYS
Tensile properties of cast titanium alloys: Titanium-6Al-4V ELI and Titanium-5Al-2.5Sn ELI
| NASA-TP-3288 | p 33 N93-10072
Fatigue crack propagation in the presence of shot-peening residual stresses p 59 N93-10542
Plasticity of single crystalline Al3X intermetallic compounds
| AD-A254282 | p 40 N93-10786
The microstructural characterization of an Al-Li-Cu-Mg alloy (8090) metal-matrix composite
| RAE-TM-MAT/STR-1139 | p 34 N93-10802

ALUMINUM GALLIUM ARSENIDES
Spatial light modulators with arbitrary quantum well profiles
| AD-A253637 | p 165 N93-10210
Novel optoelectronic devices based on combining GaAs and InP on Si
| AD-A253781 | p 165 N93-10235

ALUMINUM GRAPHITE COMPOSITES
Inhibiting corrosion in Gr/Al and Gr/Mg metal matrix composites using nonequilibrium alloying techniques
| AD-A253923 | p 34 N93-10752

ALUMINUM ISOTOPES
Particle production at high p(sub (perpendicular)) in (sup 28)Si + A collisions at 14.6 A x GeV/c
[DE92-016939] p 154 N93-10402
ALUMINUM NITRIDES
Reactions of Ti and Zr with AlN and Al2O3
[DE92-016234] p 28 N93-10391
Improved gallium nitride and aluminum nitride electronic materials
[AD-A253785] p 76 N93-10888
ALUMINUM OXIDES
Reactions of Ti and Zr with AlN and Al2O3
[DE92-016234] p 28 N93-10391
Mechanical behavior of open cell ceramics
[PB92-212984] p 37 N93-10439
Template-synthesis of infrared-transparent metal microcylinders: Comparison of optical properties with the predictions of effective medium theory
[AD-A253267] p 158 N93-10694
A fundamental understanding of the effects of ceramic processing on product microstructure
[AD-A253660] p 41 N93-10779
Single crystal growth of beta-Al2O3 for iso-index filters
[AD-A252259] p 169 N93-10879
AMMONIA
Investigation of the stimulated release of gaseous ammonia from ammonium perchlorate by HTPB solid propellant bonding agents p 19 N93-10026
A 26 kW arcjet system for on-orbit demonstration p 21 N93-10031
AMMONIUM NITRATES
Theory of combustion of liquid propellants based on hydroxylammonium nitrate
[AD-A248445] p 42 N93-10267
AMMONIUM PERCHLORATES
Investigation of the stimulated release of gaseous ammonia from ammonium perchlorate by HTPB solid propellant bonding agents p 19 N93-10026
Multidimensional effects in composite propellant combustion p 42 N93-10313
AMORPHOUS MATERIALS
The third Workshop on Non-Crystalline Solids, programme and abstracts
[AD-A250739] p 36 N93-10244
AMORPHOUS SEMICONDUCTORS
Theory of transport for interacting many-body systems
[AD-A253789] p 169 N93-10871
AMORPHOUS SILICON
Signal and noise analysis of a-Si:H radiation detector-amplifier system
[DE92-016928] p 75 N93-10790
AMPLIFICATION
Subpicosecond resolved incipient laser damage
[AD-A253624] p 87 N93-10202
ANALOG TO DIGITAL CONVERTERS
Subpicosecond resolved incipient laser damage
[AD-A253624] p 87 N93-10202
Orientation and pair correlation at high density by superresolution holography
[AD-A254034] p 85 N93-10239
ANALYSIS (MATHEMATICS)
Acoustic noise generation at the air/ocean boundary
[DREA-CR-90-445] p 147 N93-10642
ANALYSIS OF VARIANCE
On Watson's ANOVA for directions
[AD-A253576] p 146 N93-10700
ANELASTICITY
Anelastic modelling of explosive cyclogenesis p 126 N93-10377
ANGLE OF ATTACK
Arguments concerning wind tunnel test studies of the trim characteristics of objects with small asymmetries'
[AD-A254111] p 5 N93-10858
ANGLES (GEOMETRY)
Variation in multiring basic structures as a function of impact angle p 123 N93-10194
A new ellipsometry technique for interface analysis: Application to Si-SiO2
[AD-A253143] p 167 N93-10415
ANGULAR DISTRIBUTION
Polarimetry of motional Stark effect and determination of current profiles in D3-D
[DE92-016258] p 161 N93-10393
ANGULAR RESOLUTION
Ground-based high angular resolution observation of the Sun by interferometry in the visible p 177 N93-10941
ANIMALS
Biological and theoretical studies of adaptive networks: The conditioned response
[AD-A253329] p 142 N93-10354
ANISOTROPIC PLATES
Development in the elastic analysis of laminated plates p 44 N93-10468
ANISOTROPY
Cosmic microwave background anisotropies from plausible double inflation
[DE92-016195] p 192 N93-10616
ANNEALING
Tensile properties of cast titanium alloys: Titanium-6Al-4V ELI and Titanium-5Al-2.5Sn ELI
[NASA-TP-3288] p 33 N93-10072
Optical and TEM study of shock metamorphism from the Sedan test site p 111 N93-10142
Implanted contacts for diamond semiconductor devices
[AD-A245568] p 165 N93-10274
Pre-oxidation anneal kinetics: Interface degradation of thin SiO2 films on silicon
[AD-A253142] p 30 N93-10414
A new ellipsometry technique for interface analysis: Application to Si-SiO2
[AD-A253143] p 167 N93-10415
Spectroscopic differential reflectance as an analytical probe for microelectronic processing
[AD-A253134] p 73 N93-10656
ANNUAL VARIATIONS
Atlas of Southern Hemisphere 500 mb teleconnection patterns derived from National Meteorological Center analyses
[PB92-203892] p 126 N93-10337
Meteorological and site influences affecting the comparison of nephelometer and photographic determinations of light extinction at rural sites in the Eastern US
[PB92-195999] p 126 N93-10433
ANNULAR FLOW
Experimental study of the flow field inside a whirling annular seal p 92 N93-10892
ANODES
Effects of anode material on arcjet performance p 23 N93-10044
Effects of anode material on arcjet performance
[NASA-TM-105799] p 25 N93-10197
ANOMALIES
Atlas of Southern Hemisphere 500 mb teleconnection patterns derived from National Meteorological Center analyses
[PB92-203892] p 126 N93-10337
ANTENNA ARRAYS
Proceedings of the Antenna Applications Symposium, volume 1
[AD-A253681] p 68 N93-10301
Proceedings of the Antenna Applications Symposium, volume 2
[AD-A253682] p 68 N93-10302
ANTENNA COMPONENTS
Lightweight deployable antenna system
[AD-D015291] p 67 N93-10096
ANTENNA DESIGN
Lightweight deployable antenna system
[AD-D015291] p 67 N93-10096
Beam forming antenna system
[PATENT-1-265-236] p 67 N93-10111
ANTICLINES
Effects of gravity in folding --- of geological layers p 124 N93-10324
ANTIFERROMAGNETISM
Covalent electron transfer theory of superconductivity
[AD-A253975] p 74 N93-10718
ANTIMISSILE DEFENSE
Critical engine system design characteristics for SSTO vehicles p 17 N93-10014
An indicator of message quality for a single optical sensor using a template based tracking algorithm
[AD-A252704] p 139 N93-10881
ANTINEUTRINOS
Coherent production of pions and rho mesons in neutrino charged current interactions on neon nuclei at the Fermilab Tevatron
[DE92-015674] p 154 N93-10606
APPLICATION SPECIFIC INTEGRATED CIRCUITS
Development of parallel architectures for sensor array processing algorithms
[AD-A253680] p 141 N93-10299
APPLICATIONS PROGRAMS (COMPUTERS)
A building-block approach for turbulence model validation/upgrade focussed on high-speed jet flowfields p 16 N93-10010
Issues and techniques of CASE integration with configuration management
[AD-A253323] p 136 N93-10298
Numerical simulation of large actively controlled space structures p 13 N93-10308
Interactive grid generation program for CAP-TSD
[NASA-TM-102705] p 3 N93-10349
Nonlinear dynamics underlying atmospheric predictability
[AD-A254042] p 126 N93-10363
LABAN-PEL: A two-dimensional, multigroup diffusion, high-order response matrix code
[DE92-626845] p 144 N93-10624
ACIRF user's guide for the general model (Version 3.5)
[AD-A254068] p 69 N93-10657
VLSI design for reliability - hot electron
[AD-A253942] p 74 N93-10715
Object-oriented design unifies databases and applications
[AD-A253313] p 175 N93-10723
APPROXIMATION
A new non-Gausssian approximation technique for random vibration of general hysteresis p 50 N93-10496
AQUIFERS
FLASH: A finite element computer code for variably saturated flow
[DE92-018038] p 84 N93-10868
ARC JET ENGINES
Electric Propulsion Space Experiment (ESEX): Spacecraft design issues for high-power electric propulsion p 21 N93-10030
A 26 kW arcjet system for on-orbit demonstration p 21 N93-10031
Power conditioning unit for 30 kWe class arcjet flight experiment p 21 N93-10032
10 kW power electronics for hydrogen arcjets p 21 N93-10033
Effects of anode material on arcjet performance p 23 N93-10044
Effects of anode material on arcjet performance
[NASA-TM-105799] p 25 N93-10197
ARCHITECTURE (COMPUTERS)
Investigation of a possible stochastic model for the IEEE P896.1 (Futurebus+) protocol, including the proposed enhanced distributed arbiter
[CTN-92-60593] p 135 N93-10088
A look at scalable dense linear algebra libraries
[DE92-017805] p 143 N93-10285
Development of parallel architectures for sensor array processing algorithms
[AD-A253680] p 141 N93-10299
Instrument driver for general purpose interface bus (IEEE-488)
[AD-A253947] p 138 N93-10716
Requirements analysis notebook for the flight data systems definition in the Real-Time Systems Engineering Laboratory (RSEL)
[NASA-CR-185698] p 14 N93-10960
ARGON
Pitot survey of exhaust flow field of a 2-D scramjet nozzle at Mach 6 with air or freon and argon used for exhaust simulation
[NASA-TM-4361] p 2 N93-10071
ARGON ISOTOPES
Ar-40 to Ar-39 dating of pseudotachylites from the Witwatersrand basin, South Africa, with implications for the formation of the Vredefort Dome p 122 N93-10189
ARGON PLASMA
Langmuir probe and optical emission studies of Ar, O2, and N2 plasmas produced by an ECR microwave source
[AD-A253138] p 162 N93-10615
ARMOR
Determination of the dynamic unload/reload characteristics of ceramics
[AD-A253513] p 35 N93-10221
ARRAYS
Development of parallel architectures for sensor array processing algorithms
[AD-A253680] p 141 N93-10299
Field-emitter arrays for RF vacuum microelectronics
[AD-A253396] p 73 N93-10405
ARTIFICIAL INTELLIGENCE
Center for Intelligent Control Systems, Brown University component: Graduate research fellowships
[AD-A253620] p 141 N93-10095
Mesoscale severe weather development under orographic influences
[AD-A253630] p 125 N93-10204
Artificial intelligence technical paper abstracts, 1991
[AD-A253340] p 141 N93-10269
Analysis of observation report databases/knowledge bases
[AD-A252636] p 172 N93-10428
Smart algorithms and adaptive methods in computational fluid dynamics p 44 N93-10469
Selective perception for robot driving
[AD-A253740] p 142 N93-10749
TAQL: A problem space tool for expert system development
[AD-A253820] p 175 N93-10826
Symbolic Boolean manipulation with ordered binary decision diagrams
[AD-A253822] p 142 N93-10828

ARTIFICIAL SATELLITES
Proceedings of the Antenna Applications Symposium, volume 1
| AD-A253681 | p 68 N93-10301
Dynamic positioning systems photogrammetric
| AD-A254250 | p 8 N93-10898
ASSEMBLIES
Effects of long-term exposure on LDEF fastener assemblies p 39 N93-10590
ASSEMBLING
Automated handling and assembling of non-rigid objects
| AD-A253605 | p 66 N93-10649
ASSESSMENTS
The levels of mathematics achievement: Initial performance standards for the 1990 NAEP mathematics assessment, volume 3
| PB92-199421 | p 134 N93-10341
ASSUMPTIONS
The mechanical verification of a simple control system
| ORA-TR-89-5443-04 | p 142 N93-10641
ASTEROIDS
Asteroids and Archaean crustal evolution: Tests of possible genetic links between major mantle/crust melting events and clustered extraterrestrial bombardments p 110 N93-10140
Tektite origin by hypervelocity asteroidal or cometary impact: The quest for the source craters p 114 N93-10154
Ar-40 to Ar-39 ages of the large impact structures Kara and Manicouagan and their relevance to the Cretaceous-Tertiary and the Triassic-Jurassic boundary p 122 N93-10188
ASTRIONICS
Requirements analysis notebook for the flight data systems definition in the Real-Time Systems Engineering Laboratory (RSEL)
| NASA-CR-185698 | p 14 N93-10960
ASTROMETRY
Successes of and prospects for ground-based interferometry p 177 N93-10940
Report of the Lunar Interferometry Study Team (LIST) activities p 178 N93-10945
ASTRONAUTICS
AGARD index of publications, 1989-1991
| AGARD-INDEX-89-91 | p 174 N93-10610
ASTRONOMICAL MODELS
Quantum tunneling and the change in the signature of the spacetime metric
| DE92-634877 | p 165 N93-10225
Probing cosmic infrared sources: A computer modeling approach
| AD-A253788 | p 178 N93-10238
ASTRONOMICAL OBSERVATORIES
Interferometry with the Very Large Telescope p 178 N93-10943
ASTRONOMICAL SPECTROSCOPY
The fine structure of prominences p 180 N93-10910
ASTRONOMY
Workshop on the evolution of the Martian atmosphere
| NASA-CR-190730 | p 189 N93-10064
ASTROPHYSICS
Gamma ray astrophysics to the year 2000. Report of the NASA Gamma Ray Program Working Group
| NASA-TM-107995 | p 178 N93-10067
Research in theoretical particle physics
| DE92-016181 | p 154 N93-10605
Research program in experimental and theoretical high energy physics
| DE92-016219 | p 156 N93-10618
ASYMMETRY
Research on the asymmetrical aerodynamic forces of reentry vehicles
| AD-A254307 | p 4 N93-10707
ASYMPTOTIC METHODS
Mathematical analysis of strong fluid mechanical effects at high Mach number in reactive and nonreactive flow
| AD-A253617 | p 79 N93-10094
The problem of the selection of an a-posteriori error indicator based on smoothening techniques
| AD-A253401 | p 144 N93-10407
ASYMPTOTIC SERIES
On the evaluation of Bessel functions
| AD-A253129 | p 143 N93-10339
ATMOSPHERIC CHEMISTRY
Workshop on the evolution of the Martian atmosphere
| NASA-CR-190730 | p 189 N93-10064
The current and future environmental role of atmospheric methane: Model studies and uncertainties
| NASA-CR-190662 | p 104 N93-10256
Gridded Model Information Support System (GMISS) user's guide. Volume 3: Model concentration data retrieval subsystem
| PB92-190263 | p 171 N93-10257
ATMOSPHERIC CIRCULATION
The role of eddy fluxes in the response of the atmosphere to tropical thermal forcing p 124 N93-10318
Nonlinear dynamics underlying atmospheric predictability
| AD-A254042 | p 126 N93-10363
Adequate sampling of a chaotic time series
| AD-A254170 | p 127 N93-10664
Air-sea interaction in regions of varying surface conditions
| AD-A253182 | p 128 N93-10791
Magnetospheres and atmospheres of planets p 182 N93-10922
ATMOSPHERIC COMPOSITION
Guidelines for developing spacecraft maximum allowable concentrations for Space Station contaminants
| NASA-CR-190748 | p 13 N93-10737
Climate Monitoring and Diagnostics Laboratory
| PB92-162346 | p 105 N93-10772
Magnetospheres and atmospheres of planets p 182 N93-10922
ATMOSPHERIC MODELS
Mesoscale severe weather development under orographic influences
| AD-A253630 | p 125 N93-10204
The role of eddy fluxes in the response of the atmosphere to tropical thermal forcing p 124 N93-10318
Nonlinear dynamics underlying atmospheric predictability
| AD-A254042 | p 126 N93-10363
Anelastic modelling of explosive cyclogenesis p 126 N93-10377
Sensitivity of modeled ozone concentrations to uncertainties in biogenic emissions
| PB92-192202 | p 105 N93-10432
Adequate sampling of a chaotic time series
| AD-A254170 | p 127 N93-10664
ATMOSPHERIC MOISTURE
Microwave radiometer studies of atmospheric water over the oceans, volume 2
| NASA-CR-190343 | p 127 N93-10848
Satellite derived integrated water vapor and rain intensity patterns: Indicators of rapid cyclogenesis p 127 N93-10849
ATMOSPHERIC PHYSICS
Workshop on the evolution of the Martian atmosphere
| NASA-CR-190730 | p 189 N93-10064
High-power microwave breakdown of dielectric interfaces
| AD-A254200 | p 124 N93-10262
ATMOSPHERIC RADIATION
Air-sea interaction and remote sensing
| NASA-CR-190913 | p 128 N93-10068
Climate Monitoring and Diagnostics Laboratory
| PB92-162346 | p 105 N93-10772
ATMOSPHERIC SOUNDING
Remote sounding of the Martian atmosphere p 189 N93-10378
Comparison of wind speed measurements over the oceans with the Special Sensor Microwave/Imager and the Geosat altimeter p 127 N93-10850
Morning-evening differences in global and regional oceanic precipitation as observed by the SSM/I p 127 N93-10851
Some possible space interferometry applications p 178 N93-10957
ATMOSPHERIC TEMPERATURE
Remote sounding of the Martian atmosphere p 189 N93-10378
ATOMIC BEAMS
Matter-wave interferometry with laser cooled atoms
| AD-A254000 | p 89 N93-10720
Laser cooling and trapping of neutral atoms
| AD-A253730 | p 155 N93-10885
ATOMIC COLLISIONS
Electron transfer, ionization, and excitation in atomic collisions
| DE92-017300 | p 154 N93-10435
ATOMIC ENERGY LEVELS
Coherent production of pions and rho mesons in neutrino charged current interactions on neon nuclei at the Fermilab Tevatron
| DE92-015674 | p 154 N93-10606
ATOMIC EXCITATIONS
Development of laser excited atomic fluorescence and ionization methods
| DE92-016199 | p 89 N93-10611
ATOMIC PHYSICS
Basic and applied research in the field of electronics and communications
| AD-A253593 | p 67 N93-10092
Experimental plasma research project summaries
| DE92-016274 | p 162 N93-10464
Laser cooling and trapping of neutral atoms
| AD-A253730 | p 155 N93-10885
ATOMIC SPECTRA
Development of laser excited atomic fluorescence and ionization methods
| DE92-016199 | p 89 N93-10611
ATOMIC STRUCTURE
Epitaxial growth and dopant incorporation in diamond
| AD-A253636 | p 165 N93-10206
Electronic structure of highly correlated structures
| DE92-017017 | p 155 N93-10863
ATOMS
Atomic short range order and spin density wave propagation in CuMn
| DE92-016903 | p 34 N93-10789
ATTACHMENT
Novel seals and specialty component attachment mechanisms for Respiratory Protection system (RESPO 21)
| AD-A253395 | p 91 N93-10290
ATTACKING (ASSAULTING)
Relating flying hours to aircrew performance: Evidence for attack and transport missions
| AD-A253988 | p 133 N93-10719
ATTITUDE CONTROL
A study upon structural optimization of elastic rotors for mechanical systems
| INPE-5376-TDI/471 | p 94 N93-10310
AUDIO FREQUENCIES
Evaluation of lightweight and low profile communications devices for Respiratory Protective system 21 (RESPO 21)
| AD-A253393 | p 133 N93-10217
AUDITORY PERCEPTION
Auditory processing of complex sounds across frequency channels
| AD-A253612 | p 131 N93-10650
AUSTENITIC STAINLESS STEELS
A study of the effect of nitrogen and molybdenum in the corrosion inhibition of austenitic stainless steel
| AD-A253354 | p 33 N93-10100
AUSTRALIA
The Acraman impact and its widespread ejecta, South Australia p 111 N93-10141
Geological evidence for a 2.6-Ga strewn field of impact spherules in the Hamersley Basin of Western Australia p 120 N93-10181
A late Devonian impact event and its association with a possible extinction event on Eastern Gondwana p 122 N93-10191
Meteor burst communications system trial, 1990-1991
| AD-A253625 | p 67 N93-10203
AUTOMATED EN ROUTE ATC
Rotorcraft en route ATC route standards
| AD-A249129 | p 6 N93-10323
AUTOMATIC CONTROL
A seam tracking modulated infrared optical sensor for use in welding
| AD-A254103 | p 159 N93-10812
AUTOMOBILES
Selective perception for robot driving
| AD-A253740 | p 142 N93-10749
AUXILIARY POWER SOURCES
Comparison of all-electric secondary power systems for civil subsonic transports
| NASA-TM-105852 | p 9 N93-10456
AVIONICS
Aeronautical technologies for the twenty-first century
| NASA-CR-190918 | p 1 N93-10647
KC-135 crew reduction feasibility demonstration simulation study. Volume 3: Test and evaluation
| AD-A253931 | p 134 N93-10713
Requirements analysis notebook for the flight data systems definition in the Real-Time Systems Engineering Laboratory (RSEL)
| NASA-CR-185698 | p 14 N93-10960
AXISYMMETRIC BODIES
A study upon structural optimization of elastic rotors for mechanical systems
| INPE-5376-TDI/471 | p 94 N93-10310
AXISYMMETRIC FLOW
A building-block approach for turbulence model validation/upgrade focussed on high-speed jet flowfields p 16 N93-10010
AZIMUTH
GPS azimuth determination using short baseline carrier wave interferometry
| AD-A254257 | p 6 N93-10265

B

BACKGROUND RADIATION
Power spectrum of the extragalactic background light p 177 N93-10364

Cosmic microwave background anisotropies from plausible double inflation
[DE92-016195] p 192 N93-10616

BACKSCATTERING
Millimeter wave measurement and modeling of terrain scattering
[AD-A253525] p 67 N93-10223
Studies impacting the designs of free electron lasers
[AD-A254293] p 90 N93-10768

BACKUPS
Emergency Diesel Generator reliability at Department of Energy (DOE) facilities
[DE92-011888] p 91 N93-10622

BACKWARD FACING STEPS
Effect of passive flow-control devices on turbulent low-speed base flow p 79 N93-10304
Characteristics of separated flows including cavitation effects p 84 N93-10874
The effects of streamline curvature and swirl on turbulent flows in curved ducts p 84 N93-10875

BACTERIA
Biological production of ethanol from coal
[DE92-016116] p 41 N93-10216

BAGS
Research and development of two marine-degradable biopolymers
[AD-A254051] p 41 N93-10783

BALLISTIC MISSILES
Burn phase corrections of maneuver ballistic missiles with star light
[AD-A254105] p 12 N93-10814

BALLISTIC TRAJECTORIES
Methods of guidance flight dynamics
[AD-A254248] p 10 N93-10704
An indicator of message quality for a single optical sensor using a template based tracking algorithm
[AD-A252704] p 139 N93-10881

BALLOONING MODES
Global Alfven eigenmodes in D3-D
[DE92-016250] p 163 N93-10760

BALTIC SHIELD (EUROPE)
Large impacts in the Baltic shield with special attention to the Uppland structure p 113 N93-10149

BAND STRUCTURE OF SOLIDS
Implanted contacts for diamond semiconductor devices
[AD-A245568] p 165 N93-10274

BANDPASS FILTERS
Design and implementation of digital filters for analysis of F/A-18 flight test data
[AD-A253447] p 3 N93-10342
Thermal, structural, and diffraction analyses of a gallium-cooled x ray monochromator
[DE92-017063] p 157 N93-10837

BAROCLINIC INSTABILITY
The role of eddy fluxes in the response of the atmosphere to tropical thermal forcing p 124 N93-10318

BASALT
Noril'sk/Siberian plateau basalts and Bahama hot spot: Impact triggered? p 109 N93-10132
Geochemical aspect of impact cratering: Studies in Vernadsky Institute p 123 N93-10196

BASE FLOW
Effect of passive flow-control devices on turbulent low-speed base flow p 79 N93-10304

BATCH PROCESSING
Implementation of parallel algorithms
[AD-A253638] p 140 N93-10227

BATHOLITHS
Hong Kong is an impact crater: Proof from the geomorphological and geological evidence p 107 N93-10124
Thermobarometric studies on the Levack Gneisses: Footwall rocks to the Sudbury Igneous Complex p 114 N93-10152

BAYES THEOREM
De Finetti representations of survival functions level to a product measure
[AD-A253623] p 146 N93-10107
Automatic cloud classification from multi-spectral satellite data over oceanic regions
[AD-A253670] p 126 N93-10292
Inspection and repair decisions for hydraulic structures under symmetric deterioration
[AD-A253621] p 96 N93-10797

BEAM CURRENTS
Advanced transport systems for electron beams in high-brightness accelerators and FEL's
[AD-A253314] p 88 N93-10286

BEAM INJECTION
Simulation study of interactions of Space Shuttle-generated electron beams with ambient plasmas
[NASA-CR-190843] p 159 N93-10066
Divertor heat flux reduction by D2 injection in DIII-D
[DE92-014232] p 160 N93-10326
Fast magnetic field penetration into an intense neutralized ion beam
[DE92-016861] p 156 N93-10633
Magnetic fusion with high energy self-colliding ion beams
[DE92-016860] p 156 N93-10643

BEAM INTERACTIONS
Simulation study of interactions of Space Shuttle-generated electron beams with ambient plasmas
[NASA-CR-190843] p 159 N93-10066
Magnetic fusion with high energy self-colliding ion beams
[DE92-016860] p 156 N93-10643

BEAMFORMING
Beam forming antenna system
[PATENT-1-265-236] p 67 N93-10111
Simulation of electron beam transport in ion-focused regime conditioning cells
[AD-A253352] p 70 N93-10215

BEAMS (SUPPORTS)
Lightweight deployable antenna system
[AD-D015291] p 67 N93-10096
Elasticity analysis of orthotropic beams under three-part bending p 52 N93-10507
Effect of mounting offset on the dynamics of deploying flexible appendages p 54 N93-10520
Vibration of a damped double-beam system p 56 N93-10527
Flexural vibration of beams with varying section properties p 57 N93-10531
Vibration frequencies of a constrained cantilever wedge p 57 N93-10534
A spline finite strip method for analysing local and distortional buckling of thin-walled beams under arbitrary loading p 58 N93-10538
Design optimization for uniform dynamic strength under multi-modal response p 62 N93-10555

BEDS (GEOLOGY)
Structural aspects of the Araguainha impact structure (Brazil) p 106 N93-10118
Suevite superposition on the Bunte breccia in Noerdlinger Ries, Germany: New findings on the transport mechanism of impactites p 107 N93-10122
A comparison of the chemistry of pseudotachylyte breccias in the Archean Levack Gneisses of the Sudbury structure, Ontario p 122 N93-10187

BENDING
Characterization of and active control of flexible structures, using piezoceramics as sensors and actuators p 10 N93-10319
On the behavior of a higher-order plate bending element p 47 N93-10481
Response of a beam to transverse impulsive and high frequency loads p 56 N93-10526
Evaluation of the triangular plate element of Zienkiewcz and Lefebvre p 63 N93-10562

BENDING THEORY
Evaluation of the triangular plate element of Zienkiewcz and Lefebvre p 63 N93-10562

BERMUDA
Air-sea interaction in regions of varying surface conditions
[AD-A253182] p 128 N93-10791

BESSEL FUNCTIONS
On the evaluation of Bessel functions
[AD-A253129] p 143 N93-10339

BIBLIOGRAPHIES
Aeronautical engineering: A continuing bibliography with indexes (supplement 276)
[NASA-SP-7037(276)] p 1 N93-10073
Aeronautical engineering: A continuing bibliography with indexes (supplement 279)
[NASA-SP-7037(279)] p 1 N93-10074
Aerospace medicine and biology: A continuing bibliography with indexes (supplement 365)
[NASA-SP-7011(365)] p 130 N93-10075
Aerospace medicine and biology: A continuing bibliography with indexes (supplement 360)
[NASA-SP-7011(360)] p 130 N93-10076
Aerospace medicine and biology: A continuing bibliography with indexes (supplement 364)
[NASA-SP-7011(364)] p 130 N93-10077
NASA patent abstracts bibliography: A continuing bibliography. Section 1: Abstracts (supplement 41)
[NASA-SP-7039(41)-SECT-1] p 171 N93-10078
Aerospace medicine and biology: A continuing bibliography with indexes (supplement 366)
[NASA-SP-7011(366)] p 130 N93-10079
Aerospace medicine and biology: A continuing bibliography with indexes (supplement 367)
[NASA-SP-7011(367)] p 130 N93-10080
Aeronautical engineering: A cumulative index to a continuing bibliography (supplement 274)
[NASA-SP-7037(274)] p 1 N93-10351
Aeronautical engineering: A continuing bibliography with indexes (supplement 281)
[NASA-SP-7037(281)] p 1 N93-10352
Document processing p 174 N93-10600
Research in theoretical particle physics
[DE92-016181] p 154 N93-10605
AGARD index of publications, 1989-1991
[AGARD-INDEX-89-91] p 174 N93-10610

BIG BANG COSMOLOGY
Cosmic microwave background anisotropies from plausible double inflation
[DE92-016195] p 192 N93-10616

BINARY ALLOYS
Effect of alloying elements on passivity and breakdown of passivity of Fe- and Ni-based alloys mechanistics aspects
[DE92-017316] p 33 N93-10395
Fatigue crack propagation in the presence of shot-peening residual stresses p 59 N93-10542

BINARY DATA
Symbolic Boolean manipulation with ordered binary decision diagrams
[AD-A253822] p 142 N93-10828

BINARY STARS
Tomographic/interferometric studies of active stars and binaries p 182 N93-10920

BINAURAL HEARING
Auditory processing of complex sounds across frequency channels
[AD-A253612] p 131 N93-10650

BIOASTRONAUTICS
Aerospace medicine and biology: A continuing bibliography with indexes (supplement 365)
[NASA-SP-7011(365)] p 130 N93-10075
Aerospace medicine and biology: A continuing bibliography with indexes (supplement 360)
[NASA-SP-7011(360)] p 130 N93-10076
Aerospace medicine and biology: A continuing bibliography with indexes (supplement 364)
[NASA-SP-7011(364)] p 130 N93-10077
Aerospace medicine and biology: A continuing bibliography with indexes (supplement 366)
[NASA-SP-7011(366)] p 130 N93-10079
Aerospace medicine and biology: A continuing bibliography with indexes (supplement 367)
[NASA-SP-7011(367)] p 130 N93-10080

BIOCHEMISTRY
Numerical modelling of fringing fields and their use for complex permittivity measurements at high frequencies
[AD-A253994] p 72 N93-10359
Interdisciplinary research and training program in the plant sciences
[DE92-015919] p 130 N93-10835

BIODEGRADABILITY
Research and development of two marine-degradable biopolymers
[AD-A254051] p 41 N93-10783

BIODEGRADATION
Research and development of two marine-degradable biopolymers
[AD-A254051] p 41 N93-10783

BIOGEOCHEMISTRY
Molecular biology in studies of oceanic primary production
[DE92-016101] p 128 N93-10283
The 200th American Chemical Society Geochemistry Division Symposium on Progress in Marine Chemistry
[AD-A253757] p 129 N93-10887

BIOLOGICAL EFFECTS
Aerospace medicine and biology: A continuing bibliography with indexes (supplement 365)
[NASA-SP-7011(365)] p 130 N93-10075
Aerospace medicine and biology: A continuing bibliography with indexes (supplement 360)
[NASA-SP-7011(360)] p 130 N93-10076
Aerospace medicine and biology: A continuing bibliography with indexes (supplement 364)
[NASA-SP-7011(364)] p 130 N93-10077
Aerospace medicine and biology: A continuing bibliography with indexes (supplement 366)
[NASA-SP-7011(366)] p 130 N93-10079
Aerospace medicine and biology: A continuing bibliography with indexes (supplement 367)
[NASA-SP-7011(367)] p 130 N93-10080
Molecular biology in studies of oceanic primary production
[DE92-016101] p 128 N93-10283
Understanding mechanisms of carcinogenesis using rat tracheal epithelial cells in vitro
[DE92-013510] p 131 N93-10626

BIOLOGICAL EVOLUTION
Self-programming of matter and the evolution of proto-biological organizations
[DE92-015244] p 129 N93-10628

BIOMASS
Molecular biology in studies of oceanic primary production
| DE92-016101 | p 128 N93-10283
BIOMASS ENERGY PRODUCTION
Biological production of ethanol from coal
| DE92-016116 | p 41 N93-10216
BIOMEDICAL DATA
DoD space radiation concerns
| AD-A253135 | p 131 N93-10613
BIOPOLYMERS
Research and development of two marine-degradable biopolymers
| AD-A254051 | p 41 N93-10783
BIOREACTORS
Method for culturing mammalian cells in a perfused bioreactor
| NASA-CASE-MSC-21293-2 | p 129 N93-10109
Method for culturing mammalian cells in a horizontally rotated bioreactor
| NASA-CASE-MSC-21294-2 | p 129 N93-10110
BIOSYNTHESIS
Interaction of electromagnetic fields with chondrocytes in gel culture
| AD-A253727 | p 70 N93-10747
Interdisciplinary research and training program in the plant sciences
| DE92-015919 | p 130 N93-10835
BIREFRINGENT COATINGS
Measurement of aerodynamic shear stress using side chain liquid crystal polymers
| AD-A254312 | p 40 N93-10770
BISMUTH OXIDES
Development of garnet films for magnetostatic wave channelized receivers
| AD-A252812 | p 166 N93-10335
BISTATIC REFLECTIVITY
Analytical characterization of bistatic scattering from Gaussian distributed surfaces
| AD-A254253 | p 159 N93-10724
BIT ERROR RATE
Analysis of reception variability due to terrain multipath on microwave common carrier links
| NTIA-92-283 | p 69 N93-10430
BL LACERTAE OBJECTS
Imaging of BL Lac objects p 177 N93-10884
BLOWERS
Evaluation of an electronics system concept for Respiratory Protection system (RESPO 21)
| AD-A253394 | p 134 N93-10288
BLUFF BODIES
Characteristics of separated flows including cavitation effects p 84 N93-10874
BLUNT BODIES
Effect of passive flow-control devices on turbulent low-speed base flow p 79 N93-10304
Improved numerical simulation of Euler equations p 80 N93-10309
High-speed viscous flows past blunt bodies and compression corners with flux-split methods
| AD-A253413 | p 81 N93-10410
BODIES OF REVOLUTION
Analysis of a medium size BOR radome
| AD-A253954 | p 69 N93-10418
BODY KINEMATICS
Effective formulation of the dynamics of a manipulator based on the Appell equations p 65 N93-10571
BODY-WING CONFIGURATIONS
Analysis of wing-body junction flowfields using the incompressible Navier-Stokes equations, volumes 1 and 2 p 3 N93-10320
Effect of planform and body on supersonic aerodynamics of multibody configurations
| NASA-TP-3212 | p 4 N93-10824
BOLIDES
Structural review of the Vredefort dome p 108 N93-10127
BOND GRAPHS
Modelling of flexible multibody dynamics and a computer method via the bond graph method p 65 N93-10573
Automated multi-body system dynamics via bond graph modelling and interactive graphics p 66 N93-10576
BONDING
Investigation of the stimulated release of gaseous ammonia from ammonium perchlorate by HTPB solid propellant bonding agents p 19 N93-10026
Transformation of Cl bonding structures on Si(100)-(2x1)
| AD-A253739 | p 40 N93-10748
BONES
A prospective evaluation of stress fractures/overuse injuries in a population of West Point cadets
| AD-A252427 | p 132 N93-10709
BOOLEAN ALGEBRA
Symbolic Boolean manipulation with ordered binary decision diagrams
| AD-A253822 | p 142 N93-10828
BOOLEAN FUNCTIONS
Symbolic Boolean manipulation with ordered binary decision diagrams
| AD-A253822 | p 142 N93-10828
BOOSTER ROCKET ENGINES
Combustion-wave ignition for rocket engines p 17 N93-10016
Molded nozzle technology for large solid rocket motors p 19 N93-10024
BOREHOLES
Gradiometer antennas for tunnel detection
| PB92-205400 | p 69 N93-10440
BORON
Additional results on space environmental effects on polymer matrix composites: Experiment A0180 p 38 N93-10586
Boronization in D3-D
| DE92-016249 | p 163 N93-10759
BORON CARBIDES
Oxidation protection systems for carbon-carbon composites formed by chemical vapor deposition and plasma assisted chemical vapor deposition techniques
| AD-A253450 | p 28 N93-10344
BORON NITRIDES
Developmental research on ultra abrasion-resistant materials
| DE92-531066 | p 36 N93-10287
BOSONS
Vector superconductivity in cosmic strings
| DE92-634923 | p 179 N93-10296
A measurement of the Z(sup 0) hadronic branching fraction to bottom quarks and the charged multiplicity of bottom quark events using precision vertex detectors at E(sub cm) = 91 GeV
| DE92-018236 | p 154 N93-10820
BOULES
Single crystal growth of beta-Al2O3 for iso-index filters
| AD-A252259 | p 169 N93-10879
BOUNDARY ELEMENT METHOD
Nonstationary random variations of moderately thick plates using BEM p 48 N93-10487
A boundary element and mathematical programming approach for unilateral contact problems p 62 N93-10558
On the use of coupled finite element boundary element models in numerical design analysis p 63 N93-10563
A boundary element super-element method for coupling with the finite element method of substructures p 64 N93-10566
BOUNDARY LAYER CONTROL
Experimental investigation of flows behind different Large-Eddy Breakup (LEBU) devices in thick boundary layers p 6 N93-10550
BOUNDARY LAYER FLOW
Nonlinear dynamics underlying atmospheric predictability
| AD-A254042 | p 126 N93-10363
Study of a viscous sublayer model in the analysis of 3-D shock/boundary layer interaction flow fields
| AD-A253731 | p 84 N93-10886
BOUNDARY LAYER SEPARATION
Study of a viscous sublayer model in the analysis of 3-D shock/boundary layer interaction flow fields
| AD-A253731 | p 84 N93-10886
High-resolution TVD schemes for the analysis of: 1. Inviscid supersonic and transonic flows. 2. Viscous flows with shock-induced separation and heat transfer p 5 N93-10889
BOUNDARY LAYER STABILITY
On the coupling between a supersonic boundary layer and a flexible surface
| NASA-CR-189697 | p 82 N93-10757
BOUNDARY LAYER TRANSITION
Flow over a leading edge with distributed roughness p 6 N93-10549
BOUNDARY VALUE PROBLEMS
Interface cracks in an orthotropic layered half-space under impact loading p 47 N93-10482
An improved technique for determining higher order eigenvector coefficients p 64 N93-10565
A solution scheme for the deflection equations of flexible arms with time-dependent boundary conditions p 66 N93-10575
BOUSSINESQ APPROXIMATION
Numerical study of the small scale structures in Boussinesq convection
| NASA-CR-189695 | p 145 N93-10758
BRAGG CELLS
Magnetostatic waves-based integrated optic Bragg cell modules with applications to RF signal processing
| AD-A254035 | p 71 N93-10240
BRAIN
Cognition in the brain: Investigations using positron emission tomography
| AD-A254280 | p 132 N93-10765
BRANCHING (PHYSICS)
Study on the pi(sup -)p yields eta' pi(sup 0)n reaction at 38 and 100 GeV/c momenta
| DE92-624593 | p 153 N93-10328
Dynamic crack division in brittle solids p 48 N93-10489
A measurement of the Z(sup 0) hadronic branching fraction to bottom quarks and the charged multiplicity of bottom quark events using precision vertex detectors at E(sub cm) = 91 GeV
| DE92-018236 | p 154 N93-10820
BRAZIL
Structural aspects of the Araguainha impact structure (Brazil) p 106 N93-10118
Remote sensing data for monitoring and evaluating burned areas: Case of Emas National Park (GO)
| INPE-5312-PRE/1709 | p 102 N93-10373
BREATHING
Evaluation of an electronics system concept for Respiratory Protection system (RESPO 21)
| AD-A253394 | p 134 N93-10288
BRECCIA
Carbon and oxygen isotope study of carbonates from highly shocked clasts of the polymict breccia of the Haughton Crater (Canada) p 105 N93-10113
Research core drilling in the Manson impact structure, Iowa p 105 N93-10114
Sudbury project (University of Muenster-Ontario Geological Survey): Origin of the polymict, allochthonous breccias of the Onaping Formation p 106 N93-10116
Sudbury project (University of Muenster-Ontario Geological Survey): Summary of results - an updated impact model p 106 N93-10117
Sudbury project (University of Muenster-Ontario Geological Survey): Field studies 1984-1989 - summary of results p 107 N93-10119
Suevite superposition on the Bunte breccia in Noerdlinger Ries, Germany: New findings on the transport mechanism of impactites p 107 N93-10122
Sudbury project (University of Muenster-Ontario Geological Survey): Sr-Nd in heterolithic breccias and gabbroic dikes p 107 N93-10123
Impactite and pseudotachylite from Roter Kamm Crater, Namibia p 109 N93-10130
Sudbury project (University of Muenster-Ontario Geological Survey): Isotope systematics support the impact origin p 109 N93-10131
Diaplectic transformation of minerals: Vorotilov drill core, Puchezh-Katunki impact crater, Russia p 110 N93-10136
Breccia dikes from the Beaverhead Impact structure, southwest Montana p 110 N93-10137
Search for a meteoritic component at the Beaverhead impact structure, Montana p 116 N93-10158
Sudbury Breccia and suevite as glacial indicators transported 800 km to Kentland Astrobleme, Indiana p 117 N93-10165
Sudbury project (University of Muenster-Ontario Geological Survey): New investigations on Sudbury breccia p 118 N93-10167
Bohemian circular structure, Czechoslovakia: Search for the impact evidence p 119 N93-10172
The pseudotachylites from the Vredefort structure and the Witwatersrand basin p 119 N93-10174
Viscosity determinations of some frictionally generated silicate melts: Implications for slip zone rheology during impact-induced faulting p 121 N93-10183
Sudbury project (University of Muenster-Ontario Geological Survey): Petrology, chemistry, and origin of breccia formations p 121 N93-10185
A comparison of the chemistry of pseudotachylyte breccias in the Archean Levack Gneisses of the Sudbury structure, Ontario p 122 N93-10187
BREEDER REACTORS
D-He-3 spherical torus fusion reactor system study
| AD-A253358 | p 155 N93-10102
BRIGHTNESS
Advanced transport systems for electron beams in high-brightness accelerators and FEL's
| AD-A253314 | p 88 N93-10286
Perception of lightness and brightness in complex patterns
| AD-A254093 | p 133 N93-10658
BRILLOUIN EFFECT
SBS applications study
| AD-A253779 | p 102 N93-10234
BRITTLE MATERIALS
Determination of the dynamic unload/reload characteristics of ceramics
| AD-A253513 | p 35 N93-10221

BRITTLENESS
Structural review of the Vredefort dome
p 108 N93-10127
BROADBAND
Proceedings of the Antenna Applications Symposium, volume 1
[AD-A253681] p 68 N93-10301
Proceedings of the Antenna Applications Symposium, volume 2
[AD-A253682] p 68 N93-10302
BROKEN SYMMETRY
Symmetry breaking and localization in quantum chaotic systems
[DE92-634890] p 170 N93-10294
BUBBLE CHAMBERS
The development of optical techniques for component inspection in the aerospace industry p 93 N93-10307
BUCKLING
Effects of gravity in folding --- of geological layers
p 124 N93-10324
Compression buckling of thick orthotropic plates with a step thickness change p 46 N93-10478
Comparison of full 3-D, thin-film 3-D, and thin-film plate analyses of a postbuckled embedded delamination
p 47 N93-10480
A spline finite strip method for analysing local and distortional buckling of thin-walled beams under arbitrary loading p 58 N93-10538
BUFFETING
Navier-Stokes dynamics and aeroelastic computations for vortical flows, buffet and aeroelastic applications
[NASA-CR-190692] p 2 N93-10098
BUOYANCY
Combustion in turbulent jets and buoyant flames
[PB92-211481] p 31 N93-10437
BURNING RATE
Effects of the RSRM grain deformation on ballistic performance p 20 N93-10027
Multidimensional effects in composite propellant combustion p 42 N93-10313
BURNING TIME
Effects of the RSRM grain deformation on ballistic performance p 20 N93-10027
BUS CONDUCTORS
Instrument driver for general purpose interface bus (IEEE-488)
[AD-A253947] p 138 N93-10716
BY-PRODUCTS
Investigation of the stimulated release of gaseous ammonia from ammonium perchlorate by HTPB solid propellant bonding agents p 19 N93-10026

C

C (PROGRAMMING LANGUAGE)
Computational fluid dynamics capability for internally carried store separation
[AD-A253671] p 79 N93-10297
A standard file format for data interchange
[AD-A254260] p 176 N93-10899
C++ (PROGRAMMING LANGUAGE)
An MCM/chip concurrent engineering validation
[AD-A253783] p 136 N93-10237
Instrument driver for general purpose interface bus (IEEE-488)
[AD-A253947] p 138 N93-10716
C-135 AIRCRAFT
KC-135 crew reduction feasibility demonstration simulation study. Volume 3: Test and evaluation
[AD-A253931] p 134 N93-10713
CALCIUM FLUORIDES
Atomic force microscope studies of CuCl island formation on CaF2(111) substrates
[AD-A252499] p 34 N93-10880
CALCULUS OF VARIATIONS
Consistent shear constitutive relations for laminated plates p 28 N93-10509
Variational formulation of a mixed method for second order frame analysis p 62 N93-10556
A variational approach for coupled creeping-flow problems p 62 N93-10557
CALIBRATING
A method of testing two-dimensional airfoils
[AD-A253210] p 4 N93-10375
Ground/space co-operation for interferometry
p 178 N93-10946
CAMBODIA
Report on the international Cambodian crater expedition, 1992 p 113 N93-10147
CAMERAS
First results of an imaging FTS with a NICMOS camera p 86 N93-10936
CANADA
International Conference on Large Meteorite Impacts and Planetary Evolution
[NASA-CR-190677] p 105 N93-10112
Phase transformations in 40-60-GPa shocked gneisses from the Haughton Crater (Canada): An Analytical Transmission Electron Microscopy (ATEM) study
p 117 N93-10163
Sudbury Igneous Complex: Impact melt or igneous rock? Implications for lunar magmatism p 118 N93-10169
The Vredefort Dome: Review of geology and deformation phenomena and status report on current knowledge and remaining problematics (five years after the cryptoexplosion workshop) p 119 N93-10173
Aerospace Industries Association of Canada
[CTN-92-60345] p 192 N93-10640
Aerospace Industries Association of Canada
[CTN-92-60590] p 1 N93-10644
Aerospace industry profile, 1990-1991
[CTN-92-60513] p 1 N93-10651
Aerospace and defence-related industries statistical survey report, 1991
[CTN-92-60514] p 2 N93-10652
Defence electronics industry profile, 1990-1991
[CTN-92-60515] p 66 N93-10653
CANARD CONFIGURATIONS
Pitch control trimming system for canard design aircraft
[CA-PATENT-APPL-SN-2013236] p 10 N93-10374
Hydrodynamic investigation of vortical flows for an ATTAC configuration with canards
[AD-A253928] p 4 N93-10753
CANCELLATION
Convergence performance of adaptive detectors, part 3
[AD-A248415] p 143 N93-10275
CANCER
Understanding mechanisms of carcinogenesis using rat tracheal epithelial cells in vitro
[DE92-013510] p 131 N93-10626
CANOPIES (VEGETATION)
Millimeter wave measurement and modeling of terrain scattering
[AD-A253525] p 67 N93-10223
CAPACITANCE
Semiconductor phase conjugation
[AD-A253684] p 166 N93-10345
CAPACITORS
Development of electrosupercapacitors
[AD-A252208] p 71 N93-10250
Critical technology demonstration of plasma focus type MPD thrusters
[AD-A252428] p 26 N93-10638
CAPILLARY FLOW
Structure of thermocapillary flow in narrow cavities
p 61 N93-10552
CARBON CYCLE
Molecular biology in studies of oceanic primary production
[DE92-016101] p 128 N93-10283
CARBON DIOXIDE
Carbon and oxygen isotope study of carbonates from highly shocked clasts of the polymict breccia of the Haughton Crater (Canada) p 105 N93-10113
Resource capture by single leaves
[DE92-015847] p 129 N93-10461
Measurements of surface ocean carbon dioxide partial pressure during WOCE
[DE92-011856] p 128 N93-10621
CARBON DIOXIDE LASERS
Thermo-optical switching in Si based etalons
[AD-A253139] p 88 N93-10412
Influence of flow velocity on the output power of high pressure CW CO2 lasers
[AD-A254240] p 89 N93-10722
CARBON ISOTOPES
A late Devonian impact event and its association with a possible extinction event on Eastern Gondwana
p 122 N93-10191
CARBON STEELS
Fatigue crack propagation in the presence of shot-peening residual stresses p 59 N93-10542
CARBON 13
Carbon and oxygen isotope study of carbonates from highly shocked clasts of the polymict breccia of the Haughton Crater (Canada) p 105 N93-10113
Temperature-programmed oxidation of ethane and ethylene in the presence and absence of C-13 labeled methane
[DE92-015048] p 42 N93-10329
CARBON-CARBON COMPOSITES
Oxidation protection systems for carbon-carbon composites formed by chemical vapor deposition and plasma assisted chemical vapor deposition techniques
[AD-A253450] p 28 N93-10344
CARBONATES
Carbon and oxygen isotope study of carbonates from highly shocked clasts of the polymict breccia of the Haughton Crater (Canada) p 105 N93-10113
CARBONYL COMPOUNDS
A time-resolved two-laser probe of Cr(CO)6 photodissociation dynamics
[AD-A250930] p 88 N93-10247
CARDIOVASCULAR SYSTEM
Metabolic factors influencing myocardial recovery from acidosis (CiC3)
[AD-A252376] p 132 N93-10796
CARRIER DENSITY (SOLID STATE)
Growth, nitrogen vacancy reduction, and solid solution formation in cubic GaN thin films and the subsequent fabrication of superlattice structures using AlN and InN
[AD-A253331] p 166 N93-10356
CARRIER WAVES
GPS azimuth determination using short baseline carrier wave interferometry
[AD-A254257] p 6 N93-10265
CARTILAGE
Interaction of electromagnetic fields with chondrocytes in gel culture
[AD-A253727] p 70 N93-10747
CASCADE FLOW
Explicit Navier-Stokes computation of turbomachinery flows p 81 N93-10370
CAST ALLOYS
Tensile properties of cast titanium alloys: Titanium-6Al-4V ELI and Titanium-5Al-2.5Sn ELI
[NASA-TP-3288] p 33 N93-10072
CATALOGS
Worldwide seismic catalog and the nature of seismic coupling p 124 N93-10376
CATALYSIS
Transition metal activation and functionalization of carbon-hydrogen bonds
[DE92-014809] p 30 N93-10400
Advanced materials development for fossil energy conversion applications
[DE92-015762] p 104 N93-10729
CATALYSTS
Reinforcements for high temperature ceramics
[DE92-014815] p 35 N93-10082
NQR-NMR studies of higher alcohol synthesis Cu-Co catalysts
[DE92-015783] p 31 N93-10460
Advanced materials development for fossil energy conversion applications
[DE92-015762] p 104 N93-10729
CATHODOLUMINESCENCE
Improved gallium nitride and aluminum nitride electronic materials
[AD-A253785] p 76 N93-10888
CAUSTICS (OPTICS)
Dynamic measurement of the J integral in ductile metals using the optical method of caustics p 49 N93-10492
CAVITATION FLOW
Characteristics of separated flows including cavitation effects p 84 N93-10874
CAVITIES
Advanced transport systems for electron beams in high-brightness accelerators and FEL's
[AD-A253314] p 88 N93-10286
Failure processes in elastomeric composites
p 46 N93-10475
Non-propulsive aerodynamic noise
p 149 N93-10673
CAVITY RESONATORS
A new model for interpreting experimental data from a circular waveguide cavity
[AD-A254067] p 75 N93-10785
Extended-interaction klystron for the AN/TPS-43-E radar system
[AD-A253166] p 76 N93-10882
CELLS (BIOLOGY)
Method for culturing mammalian cells in a perfused bioreactor
[NASA-CASE-MSC-21293-2] p 129 N93-10109
Method for culturing mammalian cells in a horizontally rotated bioreactor
[NASA-CASE-MSC-21294-2] p 129 N93-10110
Interdisciplinary research and training program in the plant sciences
[DE92-015919] p 130 N93-10835
CELLULOSE
Research and development of two marine-degradable biopolymers
[AD-A254051] p 41 N93-10783
CENSORED DATA (MATHEMATICS)
The total time on test statistic and age-dependent censoring
[AD-A253622] p 147 N93-10798

CENTRIFUGAL COMPRESSORS
A survey of instabilities within centrifugal pumps and concepts for improving the flow range of pumps in rocket engines p 23 N93-10039
CENTRIFUGAL FORCE
Axisymmetric vibrations of rotating circular plates using characteristic orthogonal polynomials p 45 N93-10470
CENTRIFUGAL PUMPS
A survey of instabilities within centrifugal pumps and concepts for improving the flow range of pumps in rocket engines p 23 N93-10039
CENTRIPETAL FORCE
Chaotic oscillation of a high speed flexible arm robot p 65 N93-10574
CERAMIC MATRIX COMPOSITES
Sensor and actuator materials for high performance composites
| AD-A254178 | p 27 N93-10254
Oxygen barrier oxides
| AD-A253683 | p 36 N93-10343
Analysis of failure modes in ceramic matrix composite p 28 N93-10508
High temperature fatigue crack growth in ceramics and ceramic composites
| DE92-016835 | p 40 N93-10632
CERAMICS
Reinforcements for high temperature ceramics
| DE92-014815 | p 35 N93-10082
Development of physical and mathematical models for the Porous Ceramic Tube Plant Nutrification System (PCTPNS)
| NASA-TM-107551 | p 129 N93-10085
Ceramic transactions. Volume 21: Proceedings of the Symposium on Microwave Theory and Application in Materials Processing Annual Meeting No. 23 io on april 29-may 3 1991
| AD-A253631 | p 35 N93-10205
Determination of the dynamic unload/reload characteristics of ceramics
| AD-A253513 | p 35 N93-10221
Intense ion beam research at Los Alamos
| DE92-015240 | p 155 N93-10333
Oxygen barrier oxides
| AD-A253683 | p 36 N93-10343
Reactions of Ti and Zr with AlN and Al2O3
| DE92-016234 | p 28 N93-10391
Mechanical behavior of open cell ceramics
| PB92-212984 | p 37 N93-10439
High temperature fatigue crack growth in ceramics and ceramic composites
| DE92-016835 | p 40 N93-10632
A fundamental understanding of the effects of ceramic processing on product microstructure
| AD-A253660 | p 41 N93-10779
CERTIFICATION
Operationally efficient space-based integrated propulsion module p 22 N93-10035
CHANGE DETECTION
Remote sensing data for monitoring and evaluating burned areas: Case of Emas National Park (GO)
| INPE-5312-PRE/1709 | p 102 N93-10373
Change analysis
| AD-A253567 | p 146 N93-10795
CHANNEL FLOW
Thermal stratification potential in rocket engine coolant channels p 18 N93-10019
Numerical study of wall turbulence
| ONERA-RSF-21/3419-AY-126 | p 83 N93-10859
Direct simulation of turbulent pulsed plane channel flows p 84 N93-10860
CHANNELS (DATA TRANSMISSION)
Development of garnet films for magnetostatic wave channelized receivers
| AD-A252812 | p 166 N93-10335
ACIRF user's guide for the general model (Version 3.5)
| AD-A254068 | p 69 N93-10657
Instrument driver for general purpose interface bus (IEEE-488)
| AD-A253947 | p 138 N93-10716
CHAOS
Semiclassical quantization of chaotic billiards
| DE92-634888 | p 169 N93-10226
Parallel processing and learning: Variability and chaos in self-organization of activity in groups of neurons
| AD-A250290 | p 140 N93-10242
Symmetry breaking and localization in quantum chaotic systems
| DE92-634890 | p 170 N93-10294
Chaotic oscillation of a high speed flexible arm robot p 65 N93-10574
Adequate sampling of a chaotic time series
| AD-A254170 | p 127 N93-10664
CHARACTER RECOGNITION
Optimization of neural network topology and information content using Boltzman methods
| PB92-205418 | p 142 N93-10450
CHARACTERIZATION
Synthesis and characterization of energetic polymers p 15 N93-10005
The microstructural characterization of an Al-Li-Cu-Mg alloy (8090) metal-matrix composite
| RAE-TM-MAT/STR-1139 | p 34 N93-10802
CHARGE EXCHANGE
Helium transport in enhanced confinement regimes on the TEXTOR and D3-D tokamaks
| DE92-016247 | p 160 N93-10293
CHARGE TRANSFER
Theoretical analysis of discharges in copper vapor lasers: A comparison of Ne and He
| DE92-014739 | p 87 N93-10083
Study on the pi(sup -)p yields eta' pi(sup 0)n reaction at 38 and 100 GeV/c momenta
| DE92-624593 | p 153 N93-10328
CHARGED PARTICLES
Radiation damage to DNA
| DE92-015760 | p 130 N93-10834
CHARM (PARTICLE PHYSICS)
Two-photon couplings of quarkonia with arbitrary J(sup PC)
| DE92-016525 | p 153 N93-10332
CHEMICAL ANALYSIS
Sudbury project (University of Muenster-Ontario Geological Survey): Petrology, chemistry, and origin of breccia formations p 121 N93-10185
CHEMICAL BONDS
Comparison of Cl and HCl adsorption on Si(100)-(2 x 1)
| AD-A252802 | p 30 N93-10281
Transition metal activation and functionalization of carbon-hydrogen bonds
| DE92-014809 | p 30 N93-10400
Hydrocarbon surface chemistry on Si(100)
| AD-A252803 | p 27 N93-10465
Transformation of Cl bonding structures on Si(100)-(2x1)
| AD-A253739 | p 40 N93-10748
CHEMICAL COMPOSITION
Carbon and oxygen isotope study of carbonates from highly shocked clasts of the polymict breccia of the Haughton Crater (Canada) p 105 N93-10113
Apollo 15 impact melts, the age of Imbrium, and the Earth-Moon impact cataclysm p 120 N93-10176
Protective coatings for niobium alloys and their properties
| AD-A254252 | p 33 N93-10706
Analysis of interplanetary dust experiment detectors and other witness plates
| NASA-CR-190818 | p 32 N93-10852
CHEMICAL ELEMENTS
Elemental analyses of hypervelocity microparticle impact sites on interplanetary dust experiment sensor surfaces p 32 N93-10853
CHEMICAL EQUILIBRIUM
Study of improved methods for predicting chemical equilibria
| DE92-016974 | p 31 N93-10436
APOLLO: A computer program for the calculation of chemical equilibrium and reaction kinetics of chemical systems
| DE92-017864 | p 139 N93-10817
CHEMICAL EVOLUTION
Self-programming of matter and the evolution of proto-biological organizations
| DE92-015244 | p 129 N93-10628
CHEMICAL EXPLOSIONS
Molecular dynamics of shocks in crystals with defects
| AD-A253353 | p 164 N93-10099
CHEMICAL PROPERTIES
Numerical modelling of fringing fields and their use for complex permittivity measurements at high frequencies
| AD-A253994 | p 72 N93-10359
CHEMICAL PROPULSION
The 1992 JANNAF Propulsion Meeting, volume 1
| CPIA-PUBL-580-VOL-1 | p 15 N93-10001
CHEMICAL REACTIONS
Molecular dynamics of shocks in crystals with defects
| AD-A253353 | p 164 N93-10099
Biological production of ethanol from coal
| DE92-016116 | p 41 N93-10216
Rate constants for reactions of hydrazine fuels with O(P-3)
| AD-A252813 | p 42 N93-10336
Chemical and thermal stability of refrigerant-lubricant mixture with metal
| DE92-015117 | p 44 N93-10398
Cluster beam studies of metal combustion
| AD-A253952 | p 30 N93-10416
CHEMILUMINESCENCE
Shock enhancement and control of hypersonic combustion
| AD-A254295 | p 31 N93-10843
CHEMISORPTION
Comparison of Cl and HCl adsorption on Si(100)-(2 x 1)
| AD-A252802 | p 30 N93-10281
Hydrocarbon surface chemistry on Si(100)
| AD-A252803 | p 27 N93-10465
Transformation of Cl bonding structures on Si(100)-(2x1)
| AD-A253739 | p 40 N93-10748
CHINA
A late Devonian impact event and its association with a possible extinction event on Eastern Gondwana p 122 N93-10191
Chinese Space Science and Technology (selected articles)
| AD-A254099 | p 69 N93-10701
A personal viewpoint on the development of China's liquid propellant rocket engines
| AD-A254104 | p 27 N93-10813
CHIPS (ELECTRONICS)
An MCM/chip concurrent engineering validation
| AD-A253783 | p 136 N93-10237
Methodology for the computer-aided design of silicon micromachined devices in a standard CMOS process
| PB92-191246 | p 136 N93-10248
Holographic optical interconnects for multichip modules
| AD-A253403 | p 86 N93-10408
CHLORINE
Comparison of Cl and HCl adsorption on Si(100)-(2 x 1)
| AD-A252802 | p 30 N93-10281
Transformation of Cl bonding structures on Si(100)-(2x1)
| AD-A253739 | p 40 N93-10748
CHLOROFLUOROCARBONS
Materials compatibility and lubricants research on CFC-refrigerant substitute: Miscibility of lubricants with refrigerants
| DE92-015118 | p 35 N93-10084
Chemical and thermal stability of refrigerant-lubricant mixture with metal
| DE92-015117 | p 44 N93-10398
CHLOROPHYLLS
Molecular biology in studies of oceanic primary production
| DE92-016101 | p 128 N93-10283
CHOKED FLOW
Mathematical analysis of reactive multiphase flows
| AD-A253854 | p 83 N93-10810
CHOLESKY FACTORIZATION
An implementation of the MVDR beamformer on the Intel iWarp system
| AD-A253641 | p 140 N93-10209
Parallel sparse Cholesky factorization algorithms for shared-memory multiprocessor systems
| DE92-016829 | p 141 N93-10334
CHONDRITES
Ruthenium/iridium ratios in the Cretaceous-Tertiary boundary clay: Implications for global dispersal and fractionation within the ejecta cloud p 109 N93-10135
CHROMATES
Determination of Sandoz black aluminum coloring dye, olive aluminum coloring dye, and sodium dichromate aluminum sealing solutions by UV-visible spectrophotometry
| AD-A253639 | p 29 N93-10207
CHROMIUM
Changes in oxidation state of chromium during LDEF exposure p 34 N93-10581
CHROMIUM ALLOYS
Ohmic contacts to compound semiconductors p 76 N93-10830
CHROMIUM COMPOUNDS
A time-resolved two-laser probe of Cr(CO)6 photodissociation dynamics
| AD-A250930 | p 88 N93-10247
CHROMOSPHERE
Chromospheric structure and dynamics p 180 N93-10906
Small scale processes in solar and stellar plasmas p 181 N93-10917
Observation of solar flares at high resolution p 182 N93-10923
CIRCADIAN RHYTHMS
Effects of early bright, late bright and dim illumination upon circadian neuroendocrine, electrophysiological and behavioral responses
| AD-A254129 | p 131 N93-10661
NASA Space Human Factors Program
| NASA-TM-108005 | p 134 N93-10890

CIRCUIT BOARDS
A four channel 250 MHz visual counter
[DE92-016920] p 86 N93-10444
CIRCUIT PROTECTION
Design and evaluation of a quasi-active delay-line limiter/filter RF protection device
[AD-A254179] p 71 N93-10255
CIRCUIT RELIABILITY
VLSI design for reliability - hot electron
[AD-A253942] p 74 N93-10715
CIRCUITS
Vortices in long Josephson junctions
[AD-A253230] p 167 N93-10404
Holographic optical interconnects for multichip modules
[AD-A253403] p 86 N93-10408
CIRCULAR CYLINDERS
Computational studies of vortex breakdown
[AD-A253759] p 79 N93-10232
CIRCULAR PLATES
Axisymmetric vibrations of rotating circular plates using characteristic orthogonal polynomials
p 45 N93-10470
Orthotropic circular plate on nonlinear elastic subgrade p 53 N93-10513
The vibrations of annular discs: A comparison of experimental and two analytical techniques
p 58 N93-10536
Linear and nonlinear analyses of thick composite circular plates using the finite element method
p 96 N93-10873
CIRCULAR WAVEGUIDES
A new model for interpreting experimental data from a circular waveguide cavity
[AD-A254067] p 75 N93-10785
CIVIL AVIATION
A brief review of the source noise technology applicable to fixed-wing military aircraft p 150 N93-10678
CLAMPS
Effects of long-term exposure on LDEF fastener assemblies p 39 N93-10590
CLASSICAL MECHANICS
Semiclassical quantization of interacting anyons in a strong magnetic field
[DE92-634889] p 169 N93-10229
Local-equilibrium formalism applied to mechanics of solids
[DE92-016852] p 170 N93-10787
CLASSIFICATIONS
Automatic cloud classification from multi-spectral satellite data over oceanic regions
[AD-A253670] p 126 N93-10292
Dynamics of systems with time-varying inertial properties p 54 N93-10517
CLASSIFYING
Implementation of parallel algorithms
[AD-A253638] p 140 N93-10227
CLAYS
Ruthenium/iridium ratios in the Cretaceous-Tertiary boundary clay: Implications for global dispersal and fractionation within the ejecta cloud p 109 N93-10135
Ar-40 to Ar-39 ages of the large impact structures Kara and Manicouagan and their relevance to the Cretaceous-Tertiary and the Triassic-Jurassic boundary
p 122 N93-10188
CLIMATE
Shortened Test Heating Season (STHS)
p 43 N93-10314
Climate Monitoring and Diagnostics Laboratory
[PB92-162346] p 105 N93-10772
CLIMATE CHANGE
The current and future environmental role of atmospheric methane: Model studies and uncertainties
[NASA-CR-190662] p 104 N93-10256
Evaluation of Seasat/Geosat orbits and altimetry with application to long-term sea level changes in the North Pacific p 103 N93-10847
CLIMATOLOGY
Workshop on the evolution of the Martian atmosphere
[NASA-CR-190730] p 189 N93-10064
Atlas of Southern Hemisphere 500 mb teleconnection patterns derived from National Meteorological Center analyses
[PB92-203892] p 126 N93-10337
CLIMBING FLIGHT
An experimental and a theoretical investigation of rotor pitch damping using a model rotor p 8 N93-10322
CLOSTRIDIUM
Biological production of ethanol from coal
[DE92-016116] p 41 N93-10216
Biological production of ethanol from coal
[DE92-016114] p 43 N93-10608
CLOUD COVER
Automatic cloud classification from multi-spectral satellite data over oceanic regions
[AD-A253670] p 126 N93-10292
CLOUDS (METEOROLOGY)
Automatic cloud classification from multi-spectral satellite data over oceanic regions
[AD-A253670] p 126 N93-10292
CLUSTERS
The magnetochemistry of supramolecular particles: The transition from the molecular to the solid-state
[AD-A253126] p 153 N93-10338
CLUTTER
Millimeter wave measurement and modeling of terrain scattering
[AD-A253525] p 67 N93-10223
Nonlinear signal processing schemes for robust target detection and automatic clutter rejection in radar
[AD-A253546] p 68 N93-10380
Analytical characterization of bistatic scattering from Gaussian distributed surfaces
[AD-A254253] p 159 N93-10724
CMOS
Development of 6H-SiC CMOS transistors for insertion into a 350 C operational amplifier
[AD-A253760] p 70 N93-10233
Methodology for the computer-aided design of silicon micromachined devices in a standard CMOS process
[PB92-191246] p 136 N93-10248
VLSI design for reliability - hot electron
[AD-A253942] p 74 N93-10715
COAL
Biological production of ethanol from coal
[DE92-016116] p 41 N93-10216
Reserves in western basins
[DE92-014429] p 102 N93-10625
COAL GASIFICATION
Biological production of ethanol from coal
[DE92-016114] p 43 N93-10608
COAL LIQUEFACTION
Biological production of ethanol from coal
[DE92-016114] p 43 N93-10608
Advanced materials development for fossil energy conversion applications
[DE92-015762] p 104 N93-10729
COAL UTILIZATION
MHD Integrated Topping Cycle Project
[DE92-016610] p 164 N93-10861
COATINGS
Investigations of the dynamics and thermodynamics of the mesosphere lower thermosphere and upper thermosphere at the polar regions with optical ground-based remote sensing
[AD-A253228] p 125 N93-10711
UV spectrum splitting mirror
[DE92-018057] p 159 N93-10818
COAXIAL CABLES
Lightweight deployable antenna system
[AD-D015291] p 67 N93-10096
Numerical modelling of fringing fields and their use for complex permittivity measurements at high frequencies
[AD-A253994] p 72 N93-10359
COBALT
NQR-NMR studies of higher alcohol synthesis Cu-Co catalysts
[DE92-015783] p 31 N93-10460
COCKPIT SIMULATORS
Advanced terrain displays to transport category aircraft
[PB92-197136] p 6 N93-10065
KC-135 crew reduction feasibility demonstration simulation study. Volume 3: Test and evaluation
[AD-A253931] p 134 N93-10713
COCKPITS
Mental workload assessment in the cockpit: Feasibility of using electrophysiological measurements, phase 1
[AD-A254138] p 133 N93-10662
KC-135 crew reduction feasibility demonstration' simulation study. Volume 3: Test and evaluation
[AD-A253931] p 134 N93-10713
CODING
Recovery techniques for real time electronic systems
[AD-A254010] p 136 N93-10361
A standard file format for data interchange
[AD-A254260] p 176 N93-10899
COEFFICIENTS
An improved technique for determining higher order eigenvector coefficients p 64 N93-10565
A semiempirical formula for calculating the coefficients for field emission tip forms
[AD-A254109] p 145 N93-10857
COESITE
Electron petrography of silica polymorphs associated with pseudotachylite, Vredefort structure, South Africa
p 123 N93-10192
COGNITION
Eye movements and visual information processing
[AD-A250198] p 132 N93-10278
Cognition in the brain: Investigations using positron emission tomography
[AD-A254280] p 132 N93-10765
COGNITIVE PSYCHOLOGY
Cognition in the brain: Investigations using positron emission tomography
[AD-A254280] p 132 N93-10765
COHERENT LIGHT
Polarized light scattering from perfect and perturbed surfaces and fundamental scattering systems
[AD-A253186] p 158 N93-10445
COHERENT SCATTERING
Polarized light scattering from perfect and perturbed surfaces and fundamental scattering systems
[AD-A253186] p 158 N93-10445
COLD FLOW TESTS
Facility for cold flow testing of solid rocket motor models p 11 N93-10021
COLLAGENS
Hierarchical structure in polymeric solid and its influence on properties
[AD-A253818] p 41 N93-10825
COLLIMATION
An implementation of the MVDR beamformer on the Intel iWarp system
[AD-A253641] p 140 N93-10209
COLOR
Perception of lightness and brightness in complex patterns
[AD-A254093] p 133 N93-10658
COLORADO
Reserves in western basins
[DE92-014429] p 102 N93-10625
COLUMBUS SPACE STATION
Attached payloads on Space Station Freedom and Columbus p 14 N93-10929
Accommodation aspects of SIMURIS on Space Station Freedom p 14 N93-10954
COMBAT
Combat aircraft operations: Training requirements for the German Air Force tactical flying units and the noise problem p 148 N93-10667
COMBUSTIBLE FLOW
Theory of combustion of liquid propellants based on hydroxylammonium nitrate
[AD-A248445] p 42 N93-10267
Dispersion of seed vapor and gas ionization in an MHD second stage combustor and channel
[DE92-016699] p 163 N93-10645
Mathematical analysis of reactive multiphase flows
[AD-A253854] p 83 N93-10810
COMBUSTION
MHD Integrated Topping Cycle Project
[DE92-016610] p 164 N93-10861
COMBUSTION CHAMBERS
Formed platelets for low cost regeneratively cooled rocket combustion chambers p 18 N93-10018
Hot fire test results of subscale tubular combustion chambers p 18 N93-10020
Hot fire fatigue testing results for the compliant combustion chamber p 22 N93-10038
Turbulence modeling of the flow field in combustors using the non-linear k-epsilon model
[DE92-014745] p 80 N93-10330
Mass transfer in oscillating flows: Efficient drying via pulse combustors
[PB92-204403] p 81 N93-10449
Dispersion of seed vapor and gas ionization in an MHD second stage combustor and channel
[DE92-016699] p 163 N93-10645
Combustion noise and combustion instabilities in propulsion systems p 150 N93-10682
Studies on the combustion efficiency of liquid fuel rockets with variable thrust
[AD-A254232] p 26 N93-10721
Hot fire fatigue testing results for the compliant combustion chamber
[NASA-TP-3223] p 26 N93-10743
Magnetohydrodynamic projects at the CDIF
[DE92-018190] p 164 N93-10819
Shock enhancement and control of hypersonic combustion
[AD-A254295] p 31 N93-10843
COMBUSTION CHEMISTRY
Cluster beam studies of metal combustion
[AD-A253952] p 30 N93-10416
Studies on the combustion efficiency of liquid fuel rockets with variable thrust
[AD-A254232] p 26 N93-10721
An infrared free-electron laser for the Chemical Dynamics Research Laboratory
[DE92-017018] p 90 N93-10864
COMBUSTION CONTROL
Pulsed jet plume combustion: An exothermic process under fluid mechanical control p 32 N93-10553

COMBUSTION EFFICIENCY
Studies on the combustion efficiency of liquid fuel rockets with variable thrust
[AD-A254232] p 26 N93-10721
COMBUSTION PHYSICS
Cluster beam studies of metal combustion
[AD-A253952] p 30 N93-10416
A multi-fluid model of turbulence for Li-SF6 submerged combustion
[AD-A253973] p 31 N93-10423
Studies on the combustion efficiency of liquid fuel rockets with variable thrust
[AD-A254232] p 26 N93-10721
COMBUSTION PRODUCTS
Altitude compensating nozzle evaluation
p 22 N93-10037
COMBUSTION STABILITY
Alternatives in clean propellants for large scale man-rated solid rocket motors p 20 N93-10028
Combustion noise and combustion instabilities in propulsion systems p 150 N93-10682
Studies on the combustion efficiency of liquid fuel rockets with variable thrust
[AD-A254232] p 26 N93-10721
COMETS
Tektite origin by hypervelocity asteroidal or cometary impact: The quest for the source craters
p 114 N93-10154
K/T boundary stratigraphy: Evidence for multiple impacts and a possible comet stream p 120 N93-10180
COMMAND AND CONTROL
Analysis of observation report databases/knowledge bases
[AD-A252636] p 172 N93-10428
COMMERCE
A change of course: The importance to DoD of international standards for electronic commerce
[AD-A253199] p 75 N93-10792
COMMERCIAL AIRCRAFT
Comparison of all-electric secondary power systems for civil subsonic transports
[NASA-TM-105852] p 9 N93-10456
COMMUNICATION EQUIPMENT
Basic and applied research in the field of electronics and communications
[AD-A253593] p 67 N93-10092
Evaluation of lightweight and low profile communications devices for Respiratory Protective system 21 (RESPO 21)
[AD-A253393] p 133 N93-10217
Link-11 communications --- computer-to-computer communications exchange network
[AD-A252766] p 68 N93-10260
Defence electronics industry profile, 1990-1991
[CTN-92-60515] p 66 N93-10653
COMMUNICATION NETWORKS
Analysis of reservation-based dual-link networks for real-time applications
[AD-A254176] p 67 N93-10253
Link-11 communications --- computer-to-computer communications exchange network
[AD-A252766] p 68 N93-10260
SPOT panchromatic band simulation by linear combination of multispectral bands
[INPE-5295-PRE/1650] p 157 N93-10311
Documentation practices: The national scene (Greece)
p 173 N93-10595
Technology for libraries and information centers: A seminar in Greece, Portugal, and Turkey
p 174 N93-10601
Security considerations within military information systems p 174 N93-10603
Architecture and device development for optical networks
[AD-A253247] p 158 N93-10693
Network stability under viral attack: A game entitled, God and the Devil
[RSRE-MEMO-4405] p 147 N93-10822
Weather Message Switching Center Replacement (WMSCR) Operational Test and Evaluation (OT/E)/integration test plan
[DOT/FAA/CT-TN90/59] p 7 N93-10833
COMMUNICATION SATELLITES
Chinese Space Science and Technology (selected articles)
[AD-A254099] p 69 N93-10701
COMPARISON
Selection of rocket propulsion systems
p 22 N93-10034
A comparison of multimegawatt electric propulsion options for Mars missions p 23 N93-10043
Comparison of full 3-D, thin-film 3-D, and thin-film plate analyses of a postbuckled embedded delamination
p 47 N93-10480
Numerical simulation of transient crack growth
p 48 N93-10488
Comparison of the maximum stress and the stress intensity approach in the analysis of bonded joints
p 53 N93-10514
COMPATIBILITY
The application of liquid crystal polymers to turbomachinery p 23 N93-10040
Materials compatibility and lubricants research on CFC-refrigerant substitute: Miscibility of lubricants with refrigerants
[DE92-015118] p 35 N93-10084
ARTI Refrigerant Database
[DE92-015122] p 30 N93-10401
A boundary element super-element method for coupling with the finite element method of substructures
p 64 N93-10566
Extravehicular activity compatibility evaluation of developmental hardware for assembly and repair of precision reflectors
[NASA-TP-3246] p 13 N93-10744
COMPLEX COMPOUNDS
Transition metal activation and functionalization of carbon-hydrogen bonds
[DE92-014809] p 30 N93-10400
COMPLEX SYSTEMS
Operationally efficient space-based integrated propulsion module p 22 N93-10035
COMPONENT RELIABILITY
Advanced technology component derating
[AD-A253334] p 72 N93-10357
COMPOSITE MATERIALS
Piezoelectric and electrostrictive materials for transducers applications, volume 1
[AD-A250889] p 71 N93-10273
Piezoelectric and electrostrictive materials for transducers applications, volume 2
[AD-A250890] p 71 N93-10276
Composite failure analysis handbook. Volume 2: Technical handbook. Part 2: Atlas of fractographs
[AD-A249130] p 28 N93-10325
Vibration of orthotropic cylindrical shell panels with arbitrary supported curved edges p 45 N93-10471
Vibration of laminated composite plates using various plate theories: Analytical and finite element results
p 45 N93-10473
An open or closed crack terminating at a bi-material interface: Power-logarithmic singularities
p 47 N93-10483
Enriched element analysis of bimaterial interface cracks p 47 N93-10484
Singular stress distributions at circular holes in composite laminates p 51 N93-10503
Thermal buckling of heated laminated composite circular cylindrical shells p 51 N93-10504
Failure analysis of laminated composites by using iterative three-dimensional finite element method
p 51 N93-10505
Orthotropic circular plate on nonlinear elastic subgrade p 53 N93-10513
COMPOSITE PROPELLANTS
Impact sensitivity reduction via exo-electron control
p 15 N93-10004
Investigation of the stimulated release of gaseous ammonia from ammonium perchlorate by HTPB solid propellant bonding agents p 19 N93-10026
Multidimensional effects in composite propellant combustion p 42 N93-10313
COMPOSITE STRUCTURES
Instrumented propellant block test and stress analysis comparison p 15 N93-10002
Composite failure analysis handbook. Volume 2: Technical handbook. Part 2: Atlas of fractographs
[AD-A249130] p 28 N93-10325
Contact problem in delamination-buckling of laminated composite shells p 46 N93-10479
On the behavior of a higher-order plate bending element p 47 N93-10481
Analysis of a buffer strip laminate with a cutout
p 52 N93-10506
Elasticity analysis of orthotropic beams under three-part bending p 52 N93-10507
Investigation of laminated composite plates under impact dynamic loading by using a three-dimensional hybrid stress finite element method p 29 N93-10510
Experimental and theoretical behavior of adhesively bonded composite structures under tensile stress at the edge vicinity p 53 N93-10515
Dynamic stability of laminated transversely-isotropic composite plates subjected to parametric excitations
p 29 N93-10525
Natural vibrations of multilayered doubly curved shells
p 57 N93-10532
Modelling and control of robotic arms fabricated from orthotropic materials p 65 N93-10572
Space environmental effects on LDEF low Earth orbit exposed graphite reinforced polymer matrix composites
p 38 N93-10585
Nonlinear aeroelasticity of composite structures
[AD-A254285] p 8 N93-10842
Mechanics of composite materials for spacecraft
[AD-A254217] p 28 N93-10896
COMPRESSIBLE BOUNDARY LAYER
Evaluation and application of the Baldwin-Lomax turbulence model in two-dimensional, unsteady, compressible boundary layers with and without separation in engine inlets
[NASA-TM-105810] p 79 N93-10087
COMPRESSIBLE FLOW
High-speed viscous flows past blunt bodies and compression corners with flux-split methods
[AD-A253413] p 81 N93-10410
AMR on the CM-2
[NASA-CR-190747] p 138 N93-10736
Turbulent mixing in compressible free shear layers
p 83 N93-10846
COMPRESSIBLE FLUIDS
Compressible and incompressible fluid seals: Influence on rotordynamic response and stability
[NASA-CR-190746] p 92 N93-10891
COMPRESSION LOADS
Compression buckling of thick orthotropic plates with a step thickness change p 46 N93-10478
Dynamic stability of laminated transversely-isotropic composite plates subjected to parametric excitations
p 29 N93-10525
COMPRESSION TESTS
Transverse tension, transverse compression, and inplane shear JANNAF round robin test methods standardization results p 16 N93-10007
COMPRESSOR ROTORS
Theoretical and experimental investigations concerning the structural integrity of aeroengine compressor discs
p 10 N93-10539
COMPRESSORS
Theoretical and experimental investigations concerning the structural integrity of aeroengine compressor discs
p 10 N93-10539
COMPTON EFFECT
Studies impacting the designs of free electron lasers
[AD-A254293] p 90 N93-10768
COMPUTATION
Fault-tolerant and efficient parallel computation
[AD-A253350] p 140 N93-10213
Calculation of stress intensity factors in an isotropic multicracked plate: Part 2: Symbolic/numeric implementation
[NASA-TM-105823] p 95 N93-10453
Mechanics of composite materials for spacecraft
[AD-A254217] p 28 N93-10896
COMPUTATIONAL FLUID DYNAMICS
A building-block approach for turbulence model validation/upgrade focussed on high-speed jet flowfields
p 16 N93-10010
Radial Turbines
[VKI-LS-1992-05] p 77 N93-10050
Numerical methods for inviscid and viscous flow analysis p 77 N93-10055
Aerodynamic investigation of radial turbines using computational methods p 78 N93-10056
An inverse design method for radial turbomachines
p 78 N93-10057
LV software for supersonic flow analysis
[NASA-CR-190911] p 2 N93-10069
Species and temperature measurement in H2/O2 rocket flow fields by means of Raman scattering diagnostics
[NASA-CR-189217] p 25 N93-10086
Unstructured mesh algorithms for aerodynamic calculations
[NASA-CR-189685] p 2 N93-10097
Navier-Stokes dynamics and aeroelastic computations for vortical flows, buffet and aeroelastic applications
[NASA-CR-190692] p 2 N93-10098
Finite difference methods for incompressible viscous flow in scientific computing
[AD-A253512] p 79 N93-10220
Computational studies of vortex breakdown
[AD-A253759] p 79 N93-10232
Computational fluid dynamics capability for internally carried store separation
[AD-A253671] p 79 N93-10297
A globally well-posed accurate and efficient finite element CFD algorithm for compressible aerodynamics
p 3 N93-10306
Improved numerical simulation of Euler equations
p 80 N93-10309
Analysis of wing-body junction flowfields using the incompressible Navier-Stokes equations, volumes 1 and 2 p 3 N93-10320
Interactive grid generation program for CAP-TSD
[NASA-TM-102705] p 3 N93-10349
Development of the finite analytic method for turbulent forced and free convection p 80 N93-10369

Explicit Navier-Stokes computation of turbomachinery flows p 81 N93-10370
New directions in computational mechanics p 44 N93-10467
Smart algorithms and adaptive methods in computational fluid dynamics p 44 N93-10469
A field panel method for transonic flows p 6 N93-10547
A least-squares finite element method for incompressible Navier-Stokes problem p 60 N93-10548
Analysis and control of grid quality in computational simulation
[AD-A253723] p 138 N93-10746
Numerical solution of three-dimensional unsteady viscous flows
[AD-A253202] p 83 N93-10793

COMPUTATIONAL GEOMETRY
Algebra-geometric and differential geometric methods in solid geometric modeling
[AD-A253669] p 145 N93-10870

COMPUTATIONAL GRIDS
Numerical simulation of unsteady flow in a nozzle p 16 N93-10008
Unstructured mesh algorithms for aerodynamic calculations
[NASA-CR-189685] p 2 N93-10097
New directions in computational mechanics p 44 N93-10467
Smart algorithms and adaptive methods in computational fluid dynamics p 44 N93-10469
Evolution of hybrid-Trefftz FE model: State of the art and future trends p 49 N93-10494
An adaptive mesh-management algorithm for three-dimensional automatic finite element analysis p 61 N93-10554
AMR on the CM-2
[NASA-CR-190747] p 138 N93-10736
Analysis and control of grid quality in computational simulation
[AD-A253723] p 138 N93-10746
RHALE: A MMALE shock physics code for arbitrary meshes
[DE92-017051] p 139 N93-10866

COMPUTER AIDED DESIGN
Proceedings of the CASE Adoption Workshop
[AD-A253362] p 135 N93-10104
An MCM/chip concurrent engineering validation
[AD-A253783] p 136 N93-10237
Methodology for the computer-aided design of silicon micromachined devices in a standard CMOS process
[PB92-191246] p 136 N93-10248
Issues and techniques of CASE integration with configuration management
[AD-A253323] p 136 N93-10298
Development of parallel architectures for sensor array processing algorithms
[AD-A253680] p 141 N93-10299
SAPNEW: Parallel finite element code for thin shell structures on the Alliant FX/80
[NASA-CR-190663] p 94 N93-10372
Proceedings of the FY 1990 Workshop on Extraterrestrial Mining and Construction
[AD-A253399] p 189 N93-10406
Parallels in computer-aided design framework and software development environment efforts
[AD-A253327] p 137 N93-10448
VLSI design for reliability - hot electron
[AD-A253942] p 74 N93-10715
A spatial similarity measure for image database applications
[AD-A253570] p 176 N93-10883
Requirements analysis notebook for the flight data systems definition in the Real-Time Systems Engineering Laboratory (RSEL)
[NASA-CR-185698] p 14 N93-10960

COMPUTER AIDED MANUFACTURING
Instrument driver for general purpose interface bus (IEEE-488)
[AD-A253947] p 138 N93-10716

COMPUTER AIDED MAPPING
System integration issues in digital photogrammetric mapping
[AD-A254046] p 103 N93-10781

COMPUTER AIDED TOMOGRAPHY
Center for Intelligent Control Systems, Brown University component: Graduate research fellowships
[AD-A253620] p 141 N93-10095
Emission tomography of sodium in a hydrogen-air flame
[AD-A253530] p 29 N93-10224

COMPUTER GRAPHICS
Interactive animation of fault tolerant parallel algorithms
[AD-A253349] p 135 N93-10212
Moire-fringe images of twin boundaries in chemical vapor deposited diamond
[AD-A253729] p 35 N93-10231
Raster graphics validation
[PB92-196070] p 137 N93-10441
Automated multi-body system dynamics via bond graph modelling and interactive graphics p 66 N93-10576
Advanced Scientific Computing Environment Team
[DE92-016714] p 137 N93-10631
Instrument driver for general purpose interface bus (IEEE-488)
[AD-A253947] p 138 N93-10716
A spatial similarity measure for image database applications
[AD-A253570] p 176 N93-10883

COMPUTER INFORMATION SECURITY
Security considerations within military information systems p 174 N93-10603
Unifying information flow policies
[RSRE-90020] p 175 N93-10801
An example secure system specified using the Terry-Wiseman approach
[RSRE-90011] p 134 N93-10804
Causing and preventing viruses in computer systems
[AD-A208591] p 139 N93-10806
The Terry-Wiseman security policy model and examples of its use
[RSRE-90001] p 134 N93-10807
On the problem of security in data bases
[RSRE-MEMO-4263] p 175 N93-10821
Network stability under viral attack: A game entitled, God and the Devil
[RSRE-MEMO-4405] p 147 N93-10822
Lattices for security policies
[RSRE-90005] p 139 N93-10823
A multilevel security model for object-oriented database systems p 175 N93-10844

COMPUTER NETWORKS
Link-11 communications --- computer-to-computer communications exchange network
[AD-A252766] p 68 N93-10260
Technology for libraries and information centers: A seminar in Greece, Portugal, and Turkey p 174 N93-10601
Security considerations within military information systems p 174 N93-10603
Artificial neural network system for memory modification
[AD-D015354] p 142 N93-10958
Memory modification of artificial neural networks
[AD-D015356] p 143 N93-10959

COMPUTER PROGRAM INTEGRITY
Recovery techniques for real time electronic systems
[AD-A254010] p 136 N93-10361

COMPUTER PROGRAMMING
Space Station: NASA's software development approach increases safety and cost risks. Report to the Chairman, Committee on Science, Space, and Technology, House of Representatives
[GAO/IMTEC-92-39] p 12 N93-10081
Proceedings of the CASE Adoption Workshop
[AD-A253362] p 135 N93-10104
An MCM/chip concurrent engineering validation
[AD-A253783] p 136 N93-10237
Issues and techniques of CASE integration with configuration management
[AD-A253323] p 136 N93-10298
Introduction to software process improvement
[AD-A253326] p 137 N93-10447
Parallels in computer-aided design framework and software development environment efforts
[AD-A253327] p 137 N93-10448
A standard file format for data interchange
[AD-A254260] p 176 N93-10899

COMPUTER PROGRAMS
A simplified model for hybrid rocket performance prediction p 19 N93-10022
LV software for supersonic flow analysis
[NASA-CR-190911] p 2 N93-10069
Space Station: NASA's software development approach increases safety and cost risks. Report to the Chairman, Committee on Science, Space, and Technology, House of Representatives
[GAO/IMTEC-92-39] p 12 N93-10081
Integrated vision system for a target seeker
[AD-A253359] p 135 N93-10103
An implementation of the MVDR beamformer on the Intel iWarp system
[AD-A253641] p 140 N93-10209
Resonance apparatus operating manual
[AD-A254040] p 71 N93-10241
Ada validation tests for rate monotonic scheduling algorithms
[AD-A253325] p 136 N93-10300
Design and implementation of digital filters for analysis of F/A-18 flight test data
[AD-A253447] p 3 N93-10342
Recovery techniques for real time electronic systems
[AD-A254010] p 136 N93-10361
Proceedings of the FY 1990 Workshop on Extraterrestrial Mining and Construction
[AD-A253399] p 189 N93-10406
Handbook for operating the OWLKNEST technology
[AD-A253412] p 137 N93-10409
PRODIGY4.0: The manual and tutorial
[AD-A253970] p 137 N93-10422
An adaptive mesh-management algorithm for three-dimensional automatic finite element analysis p 61 N93-10554
Automated multi-body system dynamics via bond graph modelling and interactive graphics p 66 N93-10576
The mechanical verification of a simple control system
[ORA-TR-89-5443-04] p 142 N93-10641
DYNA2D: A nonlinear, explicit, two-dimensional finite element code for solid mechanics: User manual
[DE92-017310] p 95 N93-10646
Modeling of HF propagation and heating in the ionosphere
[AD-A253941] p 125 N93-10714
Instrument driver for general purpose interface bus (IEEE-488)
[AD-A253947] p 138 N93-10716
APOLLO: A computer program for the calculation of chemical equilibrium and reaction kinetics of chemical systems
[DE92-017864] p 139 N93-10817
FLASH: A finite element computer code for variably saturated flow
[DE92-018038] p 84 N93-10868
A standard file format for data interchange
[AD-A254260] p 176 N93-10899

COMPUTER SYSTEMS DESIGN
Ada validation tests for rate monotonic scheduling algorithms
[AD-A253325] p 136 N93-10300
Advanced Scientific Computing Environment Team
[DE92-016714] p 137 N93-10631
Object-oriented design unifies databases and applications
[AD-A253313] p 175 N93-10723
An example secure system specified using the Terry-Wiseman approach
[RSRE-90011] p 134 N93-10804
The Terry-Wiseman security policy model and examples of its use
[RSRE-90001] p 134 N93-10807

COMPUTER SYSTEMS PERFORMANCE
Fault-tolerant and efficient parallel computation
[AD-A253350] p 140 N93-10213

COMPUTER TECHNIQUES
Proceedings of the CASE Adoption Workshop
[AD-A253362] p 135 N93-10104
Computer algebra and the elliptic restricted problem of three bodies p 11 N93-10499
The development of computational methods of adhesion and adhesive science and technology
[AD-A253758] p 92 N93-10740

COMPUTER VIRUSES
Causing and preventing viruses in computer systems
[AD-A208591] p 139 N93-10806
Network stability under viral attack: A game entitled, God and the Devil
[RSRE-MEMO-4405] p 147 N93-10822

COMPUTER VISION
Integrated vision system for a target seeker
[AD-A253359] p 135 N93-10103
The development of optical techniques for component inspection in the aerospace industry p 93 N93-10307
A new test of scanning and monitoring ability: Methods and initial results
[AD-A249123] p 132 N93-10321
Automated handling and assembling of non-rigid objects
[AD-A253605] p 66 N93-10649

COMPUTERIZED SIMULATION
Numerical simulation of unsteady flow in a nozzle p 16 N93-10008
Simulation of electron beam transport in ion-focused regime conditioning cells
[AD-A253352] p 70 N93-10215
Probing cosmic infrared sources: A computer modeling approach
[AD-A253788] p 178 N93-10238
Parallel processing and learning: Variability and chaos in self-organization of activity in groups of neurons
[AD-A250290] p 140 N93-10242
Operator workload predictions for the revised AH-64A workload prediction model, volume 1
[AD-A254198] p 133 N93-10261

Computer simulations of object discrimination by visual cortex
[AD-A253345] p 131 N93-10271
Computational fluid dynamics capability for internally carried store separation
[AD-A253671] p 79 N93-10297
Development of parallel architectures for sensor array processing algorithms
[AD-A253680] p 141 N93-10299
Numerical simulation of transient crack growth
p 48 N93-10488
Numerical simulation of the propagation of coupled thermomechanical waves in inelastic solids
p 64 N93-10568
Self-programming of matter and the evolution of proto-biological organizations
[DE92-015244] p 129 N93-10628
Advanced Scientific Computing Environment Team
[DE92-016714] p 137 N93-10631
A computational study of projectile melt in impact with typical Whipple shields
[DE92-017137] p 92 N93-10635
Dispersion of seed vapor and gas ionization in an MHD second stage combustor and channel
[DE92-016699] p 163 N93-10645
Documentation of the detailed radiation property data for the radiation-ablation code RASLE
[NASA-TM-103848] p 28 N93-10742
Variational full wave calculation of fast wave current drive in D3-D using the ALCYON code
[DE92-016572] p 163 N93-10761
Direct simulation of turbulent pulsed plane channel flows p 84 N93-10860
Investigations of the motion of discrete-velocity gases
[AD-A253728] p 84 N93-10895

COMPUTERS
Causing and preventing viruses in computer systems
[AD-A208591] p 139 N93-10806

CONCURRENT PROCESSING
A look at scalable dense linear algebra libraries
[DE92-017805] p 143 N93-10285

CONDENSED MATTER PHYSICS
Subpicosecond resolved incipient laser damage
[AD-A253624] p 87 N93-10202

CONDITIONING (LEARNING)
Biological and theoretical studies of adaptive networks: The conditioned response
[AD-A253329] p 142 N93-10354

CONDUCTING POLYMERS
Infrared investigations of pristine polypyrrole. Is the polymer called polypyrrole really Poly (Pyrrole-Co-Hydroxypyrrole)?
[AD-A249746] p 36 N93-10243
Development of electrosupercapacitors
[AD-A252208] p 71 N93-10250

CONDUCTION BANDS
Optimization of resonant interband tunnel devices
[AD-A252401] p 168 N93-10637

CONDUCTIVE HEAT TRANSFER
Internal explosion in laser ablation of superconducting targets
[AD-A253701] p 90 N93-10799
FLASH: A finite element computer code for variably saturated flow
[DE92-018038] p 84 N93-10868

CONDUCTORS
Gradiometer antennas for tunnel detection
[PB92-205400] p 69 N93-10440

CONFERENCES
The 1992 JANNAF Propulsion Meeting, volume 1
[CPIA-PUBL-580-VOL-1] p 15 N93-10001
International Conference on Large Meteorite Impacts and Planetary Evolution
[NASA-CR-190677] p 105 N93-10112
Transducer workshop no. 16
[AD-A248047] p 12 N93-10236
The third Workshop on Non-Crystalline Solids, programme and abstracts
[AD-A250739] p 36 N93-10244
The Deposition and Fate of Trace Metals in our Environment: Symposium proceedings
[PB92-189216] p 104 N93-10289
Proceedings of the Antenna Applications Symposium, volume 1
[AD-A253681] p 68 N93-10301
Proceedings of the Antenna Applications Symposium, volume 2
[AD-A253682] p 68 N93-10302
Proceedings of the Twelfth Canadian Congress of Applied Mechanics, volumes 1 and 2
[ISBN-0920049-03] p 44 N93-10466
LDEF Materials Workshop 1991, part 2
[NASA-CP-3162-PT-2] p 37 N93-10578
Seminar on Basic Documentation Practices
[AGARD-R-788] p 172 N93-10593
Advanced processing and characterization technologies. Fabrication and characterization of semiconductor optoelectronic devices and integrated circuits. Final Conference Proceedings No. 10
[AD-A254162] p 73 N93-10663
Combat Aircraft Noise
[AGARD-CP-512] p 148 N93-10666

CONFIGURATION INTERACTION
Modelling of flexible multibody dynamics and a computer method via the bond graph method p 65 N93-10573

CONFIGURATION MANAGEMENT
Issues and techniques of CASE integration with configuration management
[AD-A253323] p 136 N93-10298
Parallels in computer-aided design framework and software development environment efforts
[AD-A253327] p 137 N93-10448
Acquisition 2: Procurement, acquisition, and maintenance of configuration management documentation in support of a CIS system p 173 N93-10599
The past, present, and future of configuration management
[AD-A254175] p 138 N93-10665

CONFINEMENT
Supersonic confined jet nozzles p 16 N93-10009
Helium transport in enhanced confinement regimes on the TEXTOR and D3-D tokamaks
[DE92-016247] p 160 N93-10293
Investigation of the effect of large core changes in toroidal plasma rotation and radial electric field on confinement in H-mode discharges in the D3-D tokamak
[DE92-016252] p 161 N93-10392
VH-mode discharges in the D3-D tokamak
[DE92-016257] p 161 N93-10463
Experimental plasma research project summaries
[DE92-016274] p 162 N93-10464
The effect of current profile changes on confinement in the D3-D tokamak
[DE92-016256] p 163 N93-10620

CONJUGATE GRADIENT METHOD
Optimization of neural network topology and information content using Boltzman methods
[PB92-205418] p 142 N93-10450
Solving large linearized systems in mechanics
[AD-A252723] p 144 N93-10639

CONNECTORS
Lightweight deployable antenna system
[AD-D015291] p 67 N93-10096

CONSERVATION EQUATIONS
Improved numerical simulation of Euler equations
p 80 N93-10309

CONSERVATION LAWS
Improved numerical simulation of Euler equations
p 80 N93-10309

CONSTITUTIVE EQUATIONS
Chronorheological characterization of elastomers
p 46 N93-10476
Consistent shear constitutive relations for laminated plates p 28 N93-10509

CONSTRAINTS
Design optimization for uniform dynamic strength under multi-modal response p 62 N93-10555
A solution scheme for the deflection equations of flexible arms with time-dependent boundary conditions
p 66 N93-10575

CONSTRICTORS
Effects of anode material on arcjet performance
p 23 N93-10044
Effects of anode material on arcjet performance
[NASA-TM-105799] p 25 N93-10197

CONSTRUCTION
Proceedings of the FY 1990 Workshop on Extraterrestrial Mining and Construction
[AD-A253399] p 189 N93-10406
Extravehicular activity compatibility evaluation of developmental hardware for assembly and repair of precision reflectors
[NASA-TP-3246] p 13 N93-10744

CONTACT LOADS
Investigation of laminated composite plates under impact dynamic loading by using a three-dimensional hybrid stress finite element method p 29 N93-10510
A boundary element and mathematical programming approach for unilateral contact problems
p 62 N93-10558

CONTACT RESISTANCE
Ohmic contacts to compound semiconductors
p 76 N93-10830

CONTAMINANTS
The Deposition and Fate of Trace Metals in our Environment: Symposium proceedings
[PB92-189216] p 104 N93-10289
Electrical resistance tomography used in environmental restoration
[DE92-018003] p 103 N93-10763
Analysis of interplanetary dust experiment detectors and other witness plates
[NASA-CR-190818] p 32 N93-10852
Contaminant interferences with SIMS analyses of microparticle impactor residues on LDEF surfaces
p 32 N93-10854

CONTAMINATION
Investigations of the effects of contamination on UV optics p 159 N93-10949
Accommodation aspects of SIMURIS on Space Station Freedom p 14 N93-10954

CONTINUOUS WAVE LASERS
4.5 micron laser source
[AD-A253367] p 87 N93-10090
Influence of flow velocity on the output power of high pressure CW CO2 lasers
[AD-A254240] p 89 N93-10722

CONTINUUM MECHANICS
A multilayered shell finite element p 49 N93-10495
Entropy of disorder in thermomechanics of damage in heterogeneous solids p 50 N93-10498
Damage due to plastic deformation in elastic-plastic materials: The thermodynamical connection
p 51 N93-10502

CONTINUUM MODELING
Mathematical analysis of reactive multiphase flows
[AD-A253854] p 83 N93-10810

CONTRACTORS
Manitoba aerospace technology: Capability directory
[CTN-92-60572] p 193 N93-10655
MHD Integrated Topping Cycle Project
[DE92-016610] p 164 N93-10861

CONTROL EQUIPMENT
LAM actuated propellant flow control device
p 18 N93-10017
Effect of passive flow-control devices on turbulent low-speed base flow p 79 N93-10304
Steering system of a vehicle, such as a snow removing machine for airfields
[CA-PATENT-APPL-SN-1293201] p 91 N93-10367
Pitch control trimming system for canard design aircraft
[CA-PATENT-APPL-SN-2013236] p 10 N93-10374

CONTROL SIMULATION
Numerical simulation of large actively controlled space structures p 13 N93-10308

CONTROL STABILITY
Numerical simulation of large actively controlled space structures p 13 N93-10308
Experimental demonstration of offset control with an application to the tethered payload p 14 N93-10521

CONTROL SURFACES
Design, test, and evaluation of three active flutter suppression controllers
[NASA-TM-4338] p 10 N93-10070

CONTROL SYSTEMS DESIGN
Pneumatic motor powered Thrust Vector Control (TVC) for liquid propelled launch vehicles p 17 N93-10015
Center for Intelligent Control Systems, Brown University component: Graduate research fellowships
[AD-A253620] p 141 N93-10095
Optimal sample policies for multirate digital control
p 141 N93-10346
Model reference adaptive control in large space structures p 13 N93-10365
System model development for nuclear thermal propulsion
[NASA-TM-105761] p 25 N93-10457
Optimal robot trajectory planning p 65 N93-10570
The mechanical verification of a simple control system
[ORA-TR-89-5443-04] p 142 N93-10641
Power system monitoring and source control of the Space Station Freedom DC power system testbed
[NASA-TM-105841] p 26 N93-10734

CONTROL THEORY
Design, test, and evaluation of three active flutter suppression controllers
[NASA-TM-4338] p 10 N93-10070

CONTROL VALVES
Review and analysis of check valve failure data
[DE92-014462] p 91 N93-10381

CONTROLLABILITY
Flight test and analysis procedures for new handling criteria
[RAE-TM-FM-26] p 8 N93-10803

CONTROLLED FUSION
D-He-3 spherical torus fusion reactor system study
[AD-A253358] p 155 N93-10102
A formula for efficiency of fast wave current drive in fusion devices
[DE92-016152] p 160 N93-10390

CONTROLLERS
Optimal sample policies for multirate digital control
p 141 N93-10346
Model reference adaptive control in large space structures p 13 N93-10365

CONVECTION
Small-scale physics of convection and magnetic fields p 179 N93-10905
High resolution granulation spectrophotometry with a UBF and a FP interferometer in tandem p 183 N93-10927

CONVECTIVE FLOW
Development of the finite analytic method for turbulent forced and free convection p 80 N93-10369
Structure of thermocapillary flow in narrow cavities p 61 N93-10552
Numerical study of the small scale structures in Boussinesq convection [NASA-CR-189695] p 145 N93-10758

CONVERGENCE
Three dimensional curved beam elements with large translations and rotations p 63 N93-10560
Partial solution of the generalized eigenvalue problem using the Woodbury transformation p 64 N93-10567

COOLING
Tank chilldown analysis and verification with a flightweight, 175 cu ft tank under normal gravity with liquid hydrogen p 24 N93-10045
Radial turbine cooling p 78 N93-10061
Matter-wave interferometry with laser cooled atoms [AD-A254000] p 89 N93-10720
Laser cooling and trapping of neutral atoms [AD-A253730] p 155 N93-10885

COOLING SYSTEMS
Heat transfer additives for absorption cooling system fluids [PB92-190354] p 169 N93-10249
Assessment study of superconducting fault-current limiters operating at 77 K [DE92-015273] p 76 N93-10831
Laser Journal [AD-A254106] p 90 N93-10855

COORDINATE TRANSFORMATIONS
A derivation for the kinematic equations of flexible robots with appropriate transformation matrices p 66 N93-10577

COORDINATION
Pseudomorphic semiconducting heterostructures from combinations of AlN, GaN, and selected SiC polytypes: Theoretical advancement and its coordination with experimental studies of nucleation, growth, characterization, and device development [AD-A253330] p 166 N93-10355

COPOLYMERS
The effect of elevated temperatures on the properties of thermally stable silicon-based elastomers for adhesives, sealants, and insulator applications p 15 N93-10006

COPPER
Theoretical analysis of discharges in copper vapor lasers: A comparison of Ne and He [DE92-014739] p 87 N93-10083
NQR-NMR studies of higher alcohol synthesis Cu-Co catalysts [DE92-015783] p 31 N93-10460
Some results of the oxidation investigation of copper and silver samples flown on LDEF p 34 N93-10580

COPPER ALLOYS
Atomic short range order and spin density wave propagation in CuMn [DE92-016903] p 34 N93-10789
The microstructural characterization of an Al-Li-Cu-Mg alloy (8090) metal-matrix composite [RAE-TM-MAT/STR-1139] p 34 N93-10802

COPPER CHLORIDES
Atomic force microscope studies of CuCl island formation on CaF2(111) substrates [AD-A252499] p 34 N93-10880

COPPER OXIDES
Covalent electron transfer theory of superconductivity [AD-A253975] p 74 N93-10718

CORE SAMPLING
Diapiectic transformation of minerals: Vorotilov drill core, Puchezh-Katunki impact crater, Russia p 110 N93-10136

CORIOLIS EFFECT
Chaotic oscillation of a high speed flexible arm robot p 65 N93-10574

CORNER FLOW
High-speed viscous flows past blunt bodies and compression corners with flux-split methods [AD-A253413] p 81 N93-10410

CORONAL LOOPS
Physics of coronal loops: Heating and reconnection p 180 N93-10912

CORRECTION
Burn phase corrections of maneuver ballistic missiles with star light [AD-A254105] p 12 N93-10814

CORRELATION
Orientation and pair correlation at high density by superresolution holography [AD-A254034] p 85 N93-10239

CORRELATORS
Demonstration and performances of real-time fringe tracking: A step towards cophased interferometers p 178 N93-10948

CORROSION PREVENTION
A study of the effect of nitrogen and molybdenum in the corrosion inhibition of austenitic stainless steel [AD-A253354] p 33 N93-10100

CORROSION RESISTANCE
A study of the effect of nitrogen and molybdenum in the corrosion inhibition of austenitic stainless steel [AD-A253354] p 33 N93-10100
Effect of alloying elements on passivity and breakdown of passivity of Fe- and Ni-based alloys mechanistics aspects [DE92-017316] p 33 N93-10395
Inhibiting corrosion in Gr/Al and Gr/Mg metal matrix composites using nonequilibrium alloying techniques [AD-A253923] p 34 N93-10752

COSMIC DUST
Probing cosmic infrared sources: A computer modeling approach [AD-A253788] p 178 N93-10238

COSMIC PLASMA
Vector superconductivity in cosmic strings [DE92-634923] p 179 N93-10296

COSMIC RAYS
Vector superconductivity in cosmic strings [DE92-634923] p 179 N93-10296
Some results of the oxidation investigation of copper and silver samples flown on LDEF p 34 N93-10580
Solar-geophysical data number 570, February 1992. Part 1: (Prompt reports). Data for January 1992, December 1991, and late data [PB92-170380] p 190 N93-10773
Solar-geophysical data number 571, March 1992. Part 1: (Prompt reports). Data for February, January 1992, and late data [PB92-177062] p 190 N93-10775

COSMOLOGY
Quantum tunneling and the change in the signature of the spacetime metric [DE92-634877] p 165 N93-10225
Vector superconductivity in cosmic strings [DE92-634923] p 179 N93-10296
Wiggly relativistic strings [DE92-016461] p 170 N93-10434
Research in theoretical particle physics [DE92-016181] p 154 N93-10605
Research program in elementary particle theory [DE92-017399] p 155 N93-10840

COST ANALYSIS
Space Station: NASA's software development approach increases safety and cost risks. Report to the Chairman, Committee on Science, Space, and Technology, House of Representatives [GAO/IMTEC-92-39] p 12 N93-10081

COST REDUCTION
A change of course: The importance to DoD of international standards for electronic commerce [AD-A253199] p 75 N93-10792
Inspection and repair decisions for hydraulic structures under symmetric deterioration [AD-A253621] p 96 N93-10797

COSTS
Semiconductor phase conjugation [AD-A253684] p 166 N93-10345

COUETTE FLOW
Numerical study of wall turbulence [ONERA-RSF-21/3419-AY-126] p 83 N93-10859

COUNTERS
A four channel 250 MHz visual counter [DE92-016920] p 86 N93-10444

COUNTING
Box counting multifractal analysis [AD-A253960] p 144 N93-10419

COUPLING
Mode localization in a simple continuum model p 56 N93-10529

COVALENCE
Covalent electron transfer theory of superconductivity [AD-A253975] p 74 N93-10718

CRACK CLOSURE
Indentation of a precompressed penny-shaped crack p 48 N93-10486

CRACK GEOMETRY
Indentation of a precompressed penny-shaped crack p 48 N93-10486
Improvements to the AC potential drop method of crack measurement p 59 N93-10543

CRACK INITIATION
Failure processes in elastomeric composites p 46 N93-10475
Stress patterns in the dynamic tear test p 49 N93-10491
Dynamic measurement of the J integral in ductile metals using the optical method of caustics p 49 N93-10492

CRACK PROPAGATION
An evaluation of a method of reconstituting fatigue loading from Rainflow counting [RAE-TR-89057] p 94 N93-10198
Composite failure analysis handbook. Volume 2: Technical handbook. Part 2: Atlas of fractographs [AD-A249130] p 28 N93-10325
Mechanical behavior of open cell ceramics [PB92-212984] p 37 N93-10439
Calculation of stress intensity factors in an isotropic multicracked plate: Part 2: Symbolic/numeric implementation [NASA-TM-105823] p 95 N93-10453
Failure processes in elastomeric composites p 46 N93-10475
Contact problem in delamination-buckling of laminated composite shells p 46 N93-10479
Indentation of a precompressed penny-shaped crack p 48 N93-10486
Numerical simulation of transient crack growth p 48 N93-10488
Dynamic crack division in brittle solids p 48 N93-10489
Integral transform approach to an inertial viscoelastic problem involving moving singularities p 49 N93-10490
Status of dynamic fracture in brittle solids p 49 N93-10493
Analysis of a buffer strip laminate with a cutout p 52 N93-10506
Fatigue crack propagation in the presence of shot-peening residual stresses p 59 N93-10542
High temperature fatigue crack growth in ceramics and ceramic composites [DE92-016835] p 40 N93-10632
Mechanisms and modelling of environment-dependent fatigue crack growth in a nickel based superalloy [AD-A253967] p 33 N93-10717

CRACK TIPS
A three-dimensional analysis of the effect of local stress distribution near crack tip p 15 N93-10003
Calculation of stress intensity factors in an isotropic multicracked plate: Part 2: Symbolic/numeric implementation [NASA-TM-105823] p 95 N93-10453
Calculation of stress intensity factors in an isotropic multicracked plate. Part 1: Theoretical development [NASA-TM-105766] p 95 N93-10455
An open or closed crack terminating at a bi-material interface: Power-logarithmic singularities p 47 N93-10483
Enriched element analysis of bimaterial interface cracks p 47 N93-10484
Numerical simulation of transient crack growth p 48 N93-10488
Dynamic crack division in brittle solids p 48 N93-10489
Integral transform approach to an inertial viscoelastic problem involving moving singularities p 49 N93-10490
Dynamic measurement of the J integral in ductile metals using the optical method of caustics p 49 N93-10492
Status of dynamic fracture in brittle solids p 49 N93-10493
Mechanisms and modelling of environment-dependent fatigue crack growth in a nickel based superalloy [AD-A253967] p 33 N93-10717

CRACKING (FRACTURING)
Status of dynamic fracture in brittle solids p 49 N93-10493
Analysis of failure modes in ceramic matrix composite p 28 N93-10508
Stress modified welding process for irradiated materials [DE92-017131] p 92 N93-10634

CRACKS
Interface cracks in an orthotropic layered half-space under impact loading p 47 N93-10482
Elastic wave scattering by an interfacial crack in a plate p 48 N93-10485
Improvements to the AC potential drop method of crack measurement p 59 N93-10543

CRATERING
Melt production in large-scale impact events: Calculations of impact-melt volumes and crater scaling p 108 N93-10125
Melt production in large-scale impact events: Planetary observations and implications p 108 N93-10126

New perspectives on the Popigai impact structure
p 110 N93-10138
Simulated meteorite impacts and volcanic explosions: Ejecta analyses and planetary implications
p 111 N93-10143
Geomechanical models of impact cratering: Puchezh-Katunki structure p 114 N93-10151
A history of the Lonar crater, India: An overview
p 118 N93-10168
Self-organized rock textures and multiring structure in the Duolun crater p 123 N93-10195
Geochemical aspect of impact cratering: Studies in Vernadsky Institute p 123 N93-10196

CRATONS
A quasi-Hertzian stress field from an internal source: A possible working model for the Vredefort structure
p 106 N93-10115
Does the Bushveld-Vredefort system (South Africa) record the largest known terrestrial impact catastrophe?
p 109 N93-10134

CREEP ANALYSIS
An evaluation of the cumulative damage effect under creep loading p 58 N93-10540
A variational approach for coupled creeping-flow problems p 62 N93-10557

CREEP PROPERTIES
Damage accumulation process in advanced metal matrix composite under thermal cycling
[AD-A248674] p 27 N93-10277
Unified viscoplastic behavior of metal matrix composites
[NASA-TM-105819] p 96 N93-10777

CRETACEOUS-TERTIARY BOUNDARY
Research core drilling in the Manson impact structure, Iowa p 105 N93-10114
Large meteorite impacts: The K/T model
p 107 N93-10120
Ruthenium/iridium ratios in the Cretaceous-Tertiary boundary clay: Implications for global dispersal and fractionation within the ejecta cloud p 109 N93-10135
The Cretaceous-Tertiary (K/T) impact: One or more source craters? p 114 N93-10153
Ar-40 to Ar-39 ages of the large impact structures Kara and Manicouagan and their relevance to the Cretaceous-Tertiary and the Triassic-Jurassic boundary
p 122 N93-10188

CRITICAL EXPERIMENTS
Data reduction analysis for the Stanford relativity gyroscope experiment p 86 N93-10347

CRITICAL LOADING
Failure processes in elastomeric composites
p 46 N93-10475
Failure analysis of laminated composites by using iterative three-dimensional finite element method
p 51 N93-10505

CRITICAL TEMPERATURE
Thermal buckling of heated laminated composite circular cylindrical shells p 51 N93-10504
Mechanisms and modelling of environment-dependent fatigue crack growth in a nickel based superalloy
[AD-A253967] p 33 N93-10717

CROSS CORRELATION
Mathematical analysis of multi-sensor cross-correlation processing for source localization
[DREA-CR-89-433] p 68 N93-10366

CROSS SECTIONS
Glenn T. Seaborg and heavy ion nuclear science
[DE92-016943] p 156 N93-10762

CRYOGENIC FLUID STORAGE
Tank chilldown analysis and verification with a flightweight, 175 cu ft tank under normal gravity with liquid hydrogen p 24 N93-10045

CRYOGENIC FLUIDS
Tank chilldown analysis and verification with a flightweight, 175 cu ft tank under normal gravity with liquid hydrogen p 24 N93-10045

CRYOGENIC ROCKET PROPELLANTS
The application of liquid crystal polymers to turbomachinery p 23 N93-10040

CRYOGENIC WIND TUNNELS
Further noise measurements in a slotted cryogenic wind tunnel
[RAE-TM-AERO-2201] p 153 N93-10805

CRYSTAL DEFECTS
Molecular dynamics of shocks in crystals with defects
[AD-A253353] p 164 N93-10099
Atomic approaches to defect thermochemistry
[AD-A254278] p 167 N93-10425
Spectroscopic differential reflectance as an analytical probe for microelectronic processing
[AD-A253134] p 73 N93-10656
Growth defects in diamond films
[AD-A253618] p 40 N93-10778

CRYSTAL DISLOCATIONS
Plasticity of single crystalline Al3X intermetallic compounds
[AD-A254282] p 40 N93-10766

CRYSTAL GROWTH
Reinforcements for high temperature ceramics
[DE92-014815] p 35 N93-10082
Kinetics of oxidation of silicon by electron cyclotron resonance plasmas
[AD-A253140] p 161 N93-10413
Atomic approaches to defect thermochemistry
[AD-A254278] p 167 N93-10425
Structure of thermocapillary flow in narrow cavities
p 61 N93-10552
Advanced processing and characterization technologies. Fabrication and characterization of semiconductor optoelectronic devices and integrated circuits. Final Conference Proceedings No. 10
[AD-A254162] p 73 N93-10663
Growth defects in diamond films
[AD-A253618] p 40 N93-10778
Single crystal growth of beta-Al2O3 for iso-index filters
[AD-A252259] p 169 N93-10879

CRYSTAL LATTICES
Molecular dynamics of shocks in crystals with defects
[AD-A253353] p 164 N93-10099
Moire-fringe images of twin boundaries in chemical vapor deposited diamond
[AD-A253729] p 35 N93-10231
Oxygen barrier oxides
[AD-A253683] p 36 N93-10343
Statics and kinetics of oxygen ordering in the oxide superconductor YBa2Cu3O(z)
[DE92-017001] p 167 N93-10403
Reliability of sublattice occupancies determined by ALCHEMI
[DE92-014592] p 168 N93-10623
Single crystal growth of beta-Al2O3 for iso-index filters
[AD-A252259] p 169 N93-10879

CRYSTAL STRUCTURE
Statics and kinetics of oxygen ordering in the oxide superconductor YBa2Cu3O(z)
[DE92-017001] p 167 N93-10403
Plasticity of single crystalline Al3X intermetallic compounds
[AD-A254282] p 40 N93-10766
Atomic short range order and spin density wave propagation in CuMn
[DE92-016903] p 34 N93-10789

CRYSTAL SURFACES
Nonlinear studies of surface and interfaces of advanced semiconductor materials
[AD-A253365] p 164 N93-10105

CRYSTALLIZATION
Research core drilling in the Manson impact structure, Iowa p 105 N93-10114

CRYSTALS
Atomic approaches to defect thermochemistry
[AD-A254278] p 167 N93-10425
Spectroscopic ellipsometric measurements of the dielectric function of germanium dioxide films on crystal germanium
[AD-A253137] p 168 N93-10614

CULTURE TECHNIQUES
Method for culturing mammalian cells in a perfused bioreactor
[NASA-CASE-MSC-21293-2] p 129 N93-10109
Method for culturing mammalian cells in a horizontally rotated bioreactor
[NASA-CASE-MSC-21294-2] p 129 N93-10110
Biological production of ethanol from coal
[DE92-016116] p 41 N93-10216

CUMULATIVE DAMAGE
An evaluation of a method of reconstituting fatigue loading from Rainflow counting
[RAE-TR-89057] p 94 N93-10198
An evaluation of the cumulative damage effect under creep loading p 58 N93-10540

CURRENT DENSITY
The effect of current profile changes on confinement in the D3-D tokamak
[DE92-016256] p 163 N93-10620
Covalent electron transfer theory of superconductivity
[AD-A253975] p 74 N93-10718
Variational full wave calculation of fast wave current drive in D3-D using the ALCYON code
[DE92-016572] p 163 N93-10761
Assessment study of superconducting fault-current limiters operating at 77 K
[DE92-015273] p 76 N93-10831
Modelling of 3-D electromagnetic responses using the time-wavenumber method
[DE92-017025] p 70 N93-10865

CURRENT DISTRIBUTION
Far-zone field of a monopole element on a disk ground plane above flat earth
[AD-A253580] p 70 N93-10091

CURVATURE
The effects of streamline curvature and swirl on turbulent flows in curved ducts p 84 N93-10875

CURVED BEAMS
Three dimensional curved beam elements with large translations and rotations p 63 N93-10560

CURVES (GEOMETRY)
The integration of geometric modeling into an inverse design method and application of a PC-based inverse design method and comparison with test results
p 78 N93-10058

CUTTERS
Developmental research on ultra abrasion-resistant materials
[DE92-531066] p 36 N93-10287

CYCLIC ACCELERATORS
A four channel 250 MHz visual counter
[DE92-016920] p 86 N93-10444

CYCLIC COMPOUNDS
Polynitro polycyclic cage compounds
[AD-A252889] p 42 N93-10268

CYCLIC LOADS
An evaluation of a method of reconstituting fatigue loading from Rainflow counting
[RAE-TR-89057] p 94 N93-10198
Interface cracks in an orthotropic layered half-space under impact loading p 47 N93-10482

CYCLOGENESIS
Anelastic modelling of explosive cyclogenesis
p 126 N93-10377
Satellite derived integrated water vapor and rain intensity patterns: Indicators of rapid cyclogenesis
p 127 N93-10849

CYCLONES
Anelastic modelling of explosive cyclogenesis
p 126 N93-10377
Satellite derived integrated water vapor and rain intensity patterns: Indicators of rapid cyclogenesis
p 127 N93-10849

CYCLOTRON RADIATION
Langmuir probe and optical emission studies of Ar, O2, and N2 plasmas produced by an ECR microwave source
[AD-A253138] p 162 N93-10615

CYCLOTRON RESONANCE
Kinetics of oxidation of silicon by electron cyclotron resonance plasmas
[AD-A253140] p 161 N93-10413

CYLINDRICAL BODIES
Computational studies of vortex breakdown
[AD-A253759] p 79 N93-10232
Template-synthesis of infrared-transparent metal microcylinders: Comparison of optical properties with the predictions of effective medium theory
[AD-A253267] p 158 N93-10694

CYLINDRICAL SHELLS
A study upon structural optimization of elastic rotors for mechanical systems
[INPE-5376-TDI/471] p 94 N93-10310
A nonlinear oscillatory problem
[DE92-630203] p 95 N93-10385
Vibration of orthotropic cylindrical shell panels with arbitrary supported curved edges p 45 N93-10471
Thermal buckling of heated laminated composite circular cylindrical shells p 51 N93-10504
Free vibrations of the thick circular cylindrical shells and rings p 57 N93-10533

CZECHOSLOVAKIA
Bohemian circular structure, Czechoslovakia: Search for the impact evidence p 119 N93-10172

D

DAMAGE
List of publications, 1969-1991. Panel on wind and seismic effects
[PB92-201102] p 125 N93-10089
Damage accumulation process in advanced metal matrix composite under thermal cycling
[AD-A248674] p 27 N93-10277
Entropy of disorder in thermomechanics of damage in heterogeneous solids p 50 N93-10498
Damage due to plastic deformation in elastic-plastic materials: The thermodynamical connection
p 51 N93-10502

DAMAGE ASSESSMENT
A three-dimensional analysis of the effect of local stress distribution near crack tip p 15 N93-10003
An evaluation of a method of reconstituting fatigue loading from Rainflow counting
[RAE-TR-89057] p 94 N93-10198

Damage accumulation process in advanced metal matrix composite under thermal cycling
[AD-A248674] p 27 N93-10277
LDEF Materials Workshop 1991, part 2
[NASA-CP-3162-PT-2] p 37 N93-10578
Additional results on space environmental effects on polymer matrix composites: Experiment A0180 p 38 N93-10586
Proposed test program and data base for LDEF polymer matrix composites p 38 N93-10587
Effects of long-term exposure on LDEF fastener assemblies p 39 N93-10590
Results from testing and analysis of solar cells flown on LDEF p 39 N93-10591
System related testing and analysis of FRECOPA p 39 N93-10592
Spectroscopic differential reflectance as an analytical probe for microelectronic processing
[AD-A253134] p 73 N93-10656
Inspection and repair decisions for hydraulic structures under symmetric deterioration
[AD-A253821] p 96 N93-10797

DAMPING
Experimental demonstration of offset control with an application to the tethered payload p 14 N93-10521
Wind tunnel spin data reduction to obtain aerodynamic spin damping coefficients by using nonlinear equation of motion
[AD-A253880] p 4 N93-10811

DATA ACQUISITION
Quality assurance practices for data entry and electronic data transfer
[DE92-014804] p 172 N93-10396
Results from the testing and analysis of LDEF batteries p 39 N93-10589
Instrument driver for general purpose interface bus (IEEE-488)
[AD-A253947] p 138 N93-10716
Long-term data collection and empirical background temperature modeling
[AD-A254044] p 127 N93-10780
First results of an imaging FTS with a NICMOS camera p 86 N93-10936

DATA BASE MANAGEMENT SYSTEMS
Format and structure of a database on health and environmental impacts of different energy systems for electricity generation
[DE92-634160] p 130 N93-10222
Gridded Model Information Support System (GMISS) user's guide. Volume 3: Model concentration data retrieval subsystem
[PB92-190263] p 171 N93-10257
A survey of commercial object-oriented database management systems
[NASA-CR-190645] p 172 N93-10452
On the problem of security in data bases
[RSRE-MEMO-4263] p 175 N93-10821
Geographic Information System (GIS) development assistance for Nuclear Regulatory Commission (NRC) incident response capability
[DE92-017595] p 176 N93-10867

DATA BASES
Mesoscale severe weather development under orographic influences
[AD-A253630] p 125 N93-10204
Format and structure of a database on health and environmental impacts of different energy systems for electricity generation
[DE92-634160] p 130 N93-10222
Composite failure analysis handbook. Volume 2: Technical handbook. Part 2: Atlas of fractographs
[AD-A249130] p 28 N93-10325
Quality assurance practices for data entry and electronic data transfer
[DE92-014804] p 172 N93-10396
ARTI Refrigerant Database
[DE92-015122] p 30 N93-10401
Analysis of observation report databases/knowledge bases
[AD-A252636] p 172 N93-10428
NASA Electronic Library System (NELS) database schema, version 1.2
[NASA-CR-190643] p 172 N93-10451
A survey of commercial object-oriented database management systems
[NASA-CR-190645] p 172 N93-10452
LDEF Materials Workshop 1991, part 2
[NASA-CP-3162-PT-2] p 37 N93-10578
Long Duration Exposure Facility (LDEF) optical systems SIG summary and database p 38 N93-10583
Proposed test program and data base for LDEF polymer matrix composites p 38 N93-10587
Seminar on Basic Documentation Practices
[AGARD-R-788] p 172 N93-10593
Scientific and Technical Information (STI) towards technological and industrial development: The case of Portugal p 173 N93-10596
Document processing p 174 N93-10600
Technology for libraries and information centers: A seminar in Greece, Portugal, and Turkey p 174 N93-10601
Services: User services in defence and aerospace documentation centres p 174 N93-10602
Security considerations within military information systems p 174 N93-10603
Object-oriented design unifies databases and applications
[AD-A253313] p 175 N93-10723
Appraisal of digital terrain elevation data for low-altitude flight
[NASA-TM-103896] p 7 N93-10745
On the problem of security in data bases
[RSRE-MEMO-4263] p 175 N93-10821
A multilevel security model for object-oriented database systems p 175 N93-10844
A spatial similarity measure for image database applications
[AD-A253570] p 176 N93-10883

DATA CORRELATION
Atlas of Southern Hemisphere 500 mb teleconnection patterns derived from National Meteorological Center analyses
[PB92-203892] p 126 N93-10337

DATA FLOW ANALYSIS
Architecture and device development for optical networks
[AD-A253247] p 158 N93-10693

DATA INTEGRATION
A standard file format for data interchange
[AD-A254260] p 176 N93-10899

DATA LINKS
Link-11 communications --- computer-to-computer communications exchange network
[AD-A252766] p 68 N93-10260
A description of the Mode Select beacon system (Mode S) and its associated benefits to the National Airspace System (NAS)
[DOT/FAA/SE-92/6] p 7 N93-10738

DATA MANAGEMENT
Advanced Scientific Computing Environment Team
[DE92-016714] p 137 N93-10631

DATA PROCESSING
Two-dimensional signal processing, optical information storage and processing, and electromagnetic measurements
[AD-A253953] p 73 N93-10417
Raster graphics validation
[PB92-196070] p 137 N93-10441
A standard file format for data interchange
[AD-A254260] p 176 N93-10899

DATA PROCESSING EQUIPMENT
Algorithms for multichannel optical processor
[AD-A254009] p 158 N93-10360
Fourier transform spectrometer processing: Data reduction and processor design p 14 N93-10935

DATA REDUCTION
Data reduction analysis for the Stanford relativity gyroscope experiment p 86 N93-10347
Global positioning systems technology and its application in environmental programs
[PB92-169358] p 7 N93-10442
EIA publications directory, 1991
[DE92-015686] p 174 N93-10607
Wind tunnel spin data reduction to obtain aerodynamic spin damping coefficients by using nonlinear equation of motion
[AD-A253880] p 4 N93-10811
Fourier transform spectrometer processing: Data reduction and processor design p 14 N93-10935

DATA RETRIEVAL
Gridded Model Information Support System (GMISS) user's guide. Volume 3: Model concentration data retrieval subsystem
[PB92-190263] p 171 N93-10257

DATA SAMPLING
Optimal sample policies for multirate digital control p 141 N93-10346

DATA STORAGE
Two-dimensional signal processing, optical information storage and processing, and electromagnetic measurements
[AD-A253953] p 73 N93-10417

DATA STRUCTURES
Format and structure of a database on health and environmental impacts of different energy systems for electricity generation
[DE92-634160] p 130 N93-10222
An adaptive mesh-management algorithm for three-dimensional automatic finite element analysis p 61 N93-10554
Symbolic Boolean manipulation with ordered binary decision diagrams
[AD-A253822] p 142 N93-10828

DATA SYSTEMS
Results from the testing and analysis of LDEF batteries p 39 N93-10589
Requirements analysis notebook for the flight data systems definition in the Real-Time Systems Engineering Laboratory (RSEL)
[NASA-CR-185698] p 14 N93-10960

DATA TRANSFER (COMPUTERS)
Investigation of a possible stochastic model for the IEEE P896.1 (Futurebus+) protocol, including the proposed enhanced distributed arbiter
[CTN-92-60593] p 135 N93-10088
Quality assurance practices for data entry and electronic data transfer
[DE92-014804] p 172 N93-10396

DECARBONATION
Carbon and oxygen isotope study of carbonates from highly shocked clasts of the polymict breccia of the Haughton Crater (Canada) p 105 N93-10113

DECISION MAKING
Format and structure of a database on health and environmental impacts of different energy systems for electricity generation
[DE92-634160] p 130 N93-10222
Probability forecasting: A guide for forecasters and staff weather officers
[AD-A254216] p 126 N93-10264

DECOMPOSITION
A look at scalable dense linear algebra libraries
[DE92-017161] p 139 N93-10816

DEFECTS
Effect of alloying elements on passivity and breakdown of passivity of Fe- and Ni-based alloys mechanistics aspects
[DE92-017316] p 33 N93-10395
Semiconductor-metal eutectic composites for high power switching
[AD-A253930] p 74 N93-10755

DEFENSE INDUSTRY
Accelerator Technology Division
[DE92-016023] p 156 N93-10462
Aerospace and defence-related industries statistical survey report, 1991
[CTN-92-60514] p 2 N93-10652
Defence electronics industry profile, 1990-1991
[CTN-92-60515] p 66 N93-10653

DEFENSE PROGRAM
Raster graphics validation
[PB92-196070] p 137 N93-10441
A change of course: The importance to DoD of international standards for electronic commerce
[AD-A253199] p 75 N93-10792

DEFLAGRATION
Impact sensitivity reduction via exo-electron control p 15 N93-10004
Theory of combustion of liquid propellants based on hydroxylammonium nitrate
[AD-A248445] p 42 N93-10267

DEFLECTION
A solution scheme for the deflection equations of flexible arms with time-dependent boundary conditions p 66 N93-10575

DEFORMATION
Effects of the RSRM grain deformation on ballistic performance p 20 N93-10027
Structural review of the Vredefort dome p 108 N93-10127
Non-linear thermoelasticity of rubberlike solids p 45 N93-10474
Integrated finite element model of composite materials p 46 N93-10477
Status of dynamic fracture in brittle solids p 49 N93-10493
A multilayered shell finite element p 49 N93-10495
Linear and nonlinear analyses of thick composite circular plates using the finite element method p 96 N93-10873

DEGRADATION
Divertor heat flux reduction by D2 injection in DIII-D
[DE92-014232] p 160 N93-10326
VLSI design for reliability - hot electron
[AD-A253942] p 74 N93-10715

DELAMINATING
Contact problem in delamination-buckling of laminated composite shells p 46 N93-10479
Comparison of full 3-D, thin-film 3-D, and thin-film plate analyses of a postbuckled embedded delamination p 47 N93-10480
Elastic wave scattering by an interfacial crack in a plate p 48 N93-10485

DELAY LINES
Design and evaluation of a quasi-active delay-line limiter/filter RF protection device
[AD-A254179] p 71 N93-10255
Novel Si-YBCuO reactive patterning technique for manufacture of large area high Tc superconducting electronic devices
[AD-A250740] p 73 N93-10426
Demonstration and performances of real-time fringe tracking: A step towards cophased interferometers
p 178 N93-10948

DELTA WINGS
Forced unsteady separated flows on a 45 degree delta wing p 80 N93-10305
Control of lift and drag in unsteady flows
[AD-A253146] p 3 N93-10340
Development of nonlinear aerodynamic models for unsteady responses p 4 N93-10845

DEMAND (ECONOMICS)
EIA publications directory, 1991
[DE92-015686] p 174 N93-10607

DEMOGRAPHY
TIGER5: Extraction of geographic information from the TIGER system
[DE92-014935] p 171 N93-10382

DEMULTIPLEXING
Architecture and device development for optical networks
[AD-A253247] p 158 N93-10693

DENSE PLASMAS
Synchrotron radiation considerations in the Dense Plasma Focus (DPF) Magnetoplasmadynamic (MPD) thruster
[AD-A254188] p 25 N93-10258

DENSIFICATION
Oxidation protection systems for carbon-carbon composites formed by chemical vapor deposition and plasma assisted chemical vapor deposition techniques
[AD-A253450] p 28 N93-10344
A fundamental understanding of the effects of ceramic processing on product microstructure
[AD-A253660] p 41 N93-10779

DEOXYRIBONUCLEIC ACID
Radiation damage to DNA
[DE92-015760] p 130 N93-10834

DEPLOYMENT
A new deployable mast p 14 N93-10511

DEPOSITION
Hydrocarbon surface chemistry on Si(100)
[AD-A252803] p 27 N93-10465

DEPTH
Paradigm lost: Venus crater depths and the role of gravity in crater modification p 120 N93-10179
Stability of open-graded bases under wheel loads using a model testing approach
[AD-A253209] p 66 N93-10710

DEPTH MEASUREMENT
Improvements to the AC potential drop method of crack measurement p 59 N93-10543

DERIVATION
Hexagonal and octagonal finite elements
p 50 N93-10500

DESCENT TRAJECTORIES
Computational fluid dynamics capability for internally carried store separation
[AD-A253671] p 79 N93-10297

DESIGN ANALYSIS
Plug nozzle propulsion system p 17 N93-10013
Critical engine system design characteristics for SSTO vehicles p 17 N93-10014
LAM actuated propellant flow control device
p 18 N93-10017
A 26 kW arcjet system for on-orbit demonstration
p 21 N93-10031
Power conditioning unit for 30 kWe class arcjet flight experiment p 21 N93-10032
Radial Turbines
[VKI-LS-1992-05] p 77 N93-10050
Introduction to radial turbine technology
p 77 N93-10051
Performance parameters and assessment
p 77 N93-10052
Non-dimensional conceptual design of radial inflow turbines. Part A: Application of fundamental fluid mechanics p 77 N93-10053
Non-dimensional conceptual design of radial inflow turbines. Part B: Application of empirical correlations
p 77 N93-10054
Numerical methods for inviscid and viscous flow analysis p 77 N93-10055
Aerodynamic investigation of radial turbines using computational methods p 78 N93-10056
An inverse design method for radial turbomachines
p 78 N93-10057
The integration of geometric modeling into an inverse design method and application of a PC-based inverse design method and comparison with test results
p 78 N93-10058
Spatial light modulators with arbitrary quantum well profiles
[AD-A253637] p 165 N93-10210
Interactive animation of fault tolerant parallel algorithms
[AD-A253349] p 135 N93-10212
Space Transportation Engine Program (STEP), phase B
[NASA-CR-184062] p 25 N93-10350
SAPNEW: Parallel finite element code for thin shell structures on the Alliant FX/80
[NASA-CR-190663] p 94 N93-10372
Design optimization for uniform dynamic strength under multi-modal response p 62 N93-10555
On the use of coupled finite element boundary element models in numerical design analysis p 63 N93-10563
VLSI design for reliability - hot electron
[AD-A253942] p 74 N93-10715
The solar ultraviolet network subtractive double monochromator p 183 N93-10931
Interferometric imaging with the solar ultraviolet network p 184 N93-10932
IFTS: The Imaging Fourier Transform Spectrometer
p 14 N93-10933
First results of an imaging FTS with a NICMOS camera p 86 N93-10936
Detectors for the SIMURIS payload
p 14 N93-10937

DESORPTION
Nonlinear studies of surface and interfaces of advanced semiconductor materials
[AD-A253365] p 164 N93-10105
Atomic hydrogen: A reagent for the extraction of chemical species from silicon surfaces
[AD-A252804] p 30 N93-10266
Hydrocarbon surface chemistry on Si(100)
[AD-A252803] p 27 N93-10465

DESTRUCTIVE TESTS
Hot fire test results of subscale tubular combustion chambers p 18 N93-10020

DESULFURIZING
Advanced materials development for fossil energy conversion applications
[DE92-015762] p 104 N93-10729

DETECTION
Mathematical analysis of multi-sensor cross-correlation processing for source localization
[DREA-CR-89-433] p 68 N93-10366
Change analysis
[AD-A253567] p 146 N93-10795

DETONATION
Impact sensitivity reduction via exo-electron control
p 15 N93-10004
Molecular dynamics of shocks in crystals with defects
[AD-A253353] p 164 N93-10099
Mathematical analysis of reactive multiphase flows
[AD-A253854] p 83 N93-10810

DEUTERIUM
Divertor heat flux reduction by D2 injection in DIII-D
[DE92-014232] p 160 N93-10326

DIAMOND FILMS
Growth defects in diamond films
[AD-A253618] p 40 N93-10778

DIAMONDS
Epitaxial growth and dopant incorporation in diamond
[AD-A253636] p 165 N93-10206
Moire-fringe images of twin boundaries in chemical vapor deposited diamond
[AD-A253729] p 35 N93-10231
Implanted contacts for diamond semiconductor devices
[AD-A245568] p 165 N93-10274
Developmental research on ultra abrasion-resistant materials
[DE92-531066] p 36 N93-10287
A five-channel, diamond photoconducting x ray detector array for z-pinch experiments
[DE92-017345] p 164 N93-10839

DIELECTRIC PROPERTIES
Application of volumetric multiple-scattering approximations to foliage media
[AD-A253337] p 68 N93-10358
Spectroscopic ellipsometric measurements of the dielectric function of germanium dioxide films on crystal germanium
[AD-A253137] p 168 N93-10614

DIELECTRICS
Ceramic transactions. Volume 21: Proceedings of the Symposium on Microwave Theory and Application in Materials Processing Annual Meeting No. 23 io on april 29-may 3 1991
[AD-A253631] p 35 N93-10205
High-power microwave breakdown of dielectric interfaces
[AD-A254200] p 124 N93-10262
Application of volumetric multiple-scattering approximations to foliage media
[AD-A253337] p 68 N93-10358
Numerical modelling of fringing fields and their use for complex permittivity measurements at high frequencies
[AD-A253994] p 72 N93-10359
Pre-oxidation anneal kinetics: Interface degradation of thin SiO2 films on silicon
[AD-A253142] p 30 N93-10414
Analysis of a medium size BOR radome
[AD-A253954] p 69 N93-10418

DIELS-ALDER REACTIONS
Study of improved methods for predicting chemical equilibria
[DE92-016974] p 31 N93-10436

DIESEL ENGINES
Compound cycle engine for helicopter application
[NASA-CR-180824] p 9 N93-10348
Emergency Diesel Generator reliability at Department of Energy (DOE) facilities
[DE92-011888] p 91 N93-10622

DIFFERENCE EQUATIONS
Progress in multi-dimensional upwind differencing
[NASA-CR-189708] p 83 N93-10808
One type of automatically adjusted difference scheme with artificial viscosity to calculate ablated exterior shapes
[AD-A254108] p 5 N93-10856

DIFFERENTIAL GEOMETRY
Algebra-geometric and differential geometric methods in solid geometric modeling
[AD-A253669] p 145 N93-10870

DIFFRACTION
Geometrical transformation of linear diode-laser arrays for longitudinal pumping of solid-state lasers
[AD-A253415] p 87 N93-10218

DIFFRACTION PATTERNS
Novel Si-YBCuO reactive patterning technique for manufacture of large area high Tc superconducting electronic devices
[AD-A250740] p 73 N93-10426
Demonstration and performances of real-time fringe tracking: A step towards cophased interferometers
p 178 N93-10948

DIFFUSION
Atomic approaches to defect thermochemistry
[AD-A254278] p 167 N93-10425
Stochastic diffusion and Kolmogorov entropy in regular and random Hamiltonians
[DE92-016179] p 170 N93-10604
Modelling of 3-D electromagnetic responses using the time-wavenumber method
[DE92-017025] p 70 N93-10865

DIFFUSION COEFFICIENT
Electron transfer reactions in microporous solids
[DE92-016222] p 166 N93-10284
Oxygen barrier oxides
[AD-A253683] p 36 N93-10343

DIFFUSION FLAMES
A multi-fluid model of turbulence for Li-SF6 submerged combustion
[AD-A253973] p 31 N93-10423
Combustion in turbulent jets and buoyant flames
[PB92-211481] p 31 N93-10437

DIFFUSION LENGTH
Atomic force microscope studies of CuCl island formation on CaF2(111) substrates
[AD-A252499] p 34 N93-10880

DIFFUSION THEORY
Multidimensional deterministic electron transport calculations
[AD-A254021] p 154 N93-10362

DIFFUSIVITY
Oxygen barrier oxides
[AD-A253683] p 36 N93-10343

DIGITAL DATA
Instrument driver for general purpose interface bus (IEEE-488)
[AD-A253947] p 138 N93-10716
Appraisal of digital terrain elevation data for low-altitude flight
[NASA-TM-103896] p 7 N93-10745
System integration issues in digital photogrammetric mapping
[AD-A254046] p 103 N93-10781

DIGITAL FILTERS
Design and implementation of digital filters for analysis of F/A-18 flight test data
[AD-A253447] p 3 N93-10342

DIGITAL SIMULATION
SPOT panchromatic band simulation by linear combination of multispectral bands
[INPE-5295-PRE/1650] p 157 N93-10311

On techniques for digital simulation of random response of nonlinear oscillators p 55 N93-10523
ACIRF user's guide for the general model (Version 3.5)
[AD-A254068] p 69 N93-10657
DIGITAL SYSTEMS
Optimal sample policies for multirate digital control p 141 N93-10346
DIGITAL TECHNIQUES
Measurement of acceleration using an instrumented railgun projectile
[AD-A253366] p 12 N93-10106
The development of optical techniques for component inspection in the aerospace industry p 93 N93-10307
DIMENSIONAL ANALYSIS
Fractals and multifractals in fracture p 50 N93-10497
DIMENSIONLESS NUMBERS
Non-dimensional conceptual design of radial inflow turbines. Part A: Application of fundamental fluid mechanics p 77 N93-10053
Non-dimensional conceptual design of radial inflow turbines. Part B: Application of empirical correlations p 77 N93-10054
DIOXIDES
Spectroscopic ellipsometric measurements of the dielectric function of germanium dioxide films on crystal germanium
[AD-A253137] p 168 N93-10614
DIPOLE ANTENNAS
Gradiometer antennas for tunnel detection
[PB92-205400] p 69 N93-10440
DIPOLES
Lightweight deployable antenna system
[AD-D015291] p 67 N93-10096
DIRAC EQUATION
Finite group actions and elliptic genera
[DE92-630207] p 170 N93-10388
DIRECTIVITY
Combat aircraft jet engine noise studies p 150 N93-10679
DIRECTORIES
EIA publications directory, 1991
[DE92-015686] p 174 N93-10607
The technology advantage: A guide to science, technology, and innovation in Manitoba
[CTN-92-60571] p 192 N93-10654
Manitoba aerospace technology: Capability directory
[CTN-92-60572] p 193 N93-10655
DIRICHLET PROBLEM
Nonlinear dynamics underlying atmospheric predictability
[AD-A254042] p 126 N93-10363
DISCOLORATION
Changes in oxidation state of chromium during LDEF exposure p 34 N93-10581
DISCONTINUITY
Discontinuous initial value problem of nonlinear elasticity by similarity approach p 64 N93-10569
DISCRIMINANT ANALYSIS (STATISTICS)
Misclassification rates of likelihood and predictive discriminant functions for small samples
[AD-A253640] p 146 N93-10208
Resistive Grid Kernel Estimator (RGKE)
[AD-A253520] p 147 N93-10869
DISORDERS
Symmetry breaking and localization in quantum chaotic systems
[DE92-634890] p 170 N93-10294
DISPLACEMENT
On the behavior of a higher-order plate bending element p 47 N93-10481
Interface cracks in an orthotropic layered half-space under impact loading p 47 N93-10482
Evolution of hybrid-Trefftz FE model: State of the art and future trends p 49 N93-10494
A new quadrilateral element for the elastic and plastic analysis of shells p 62 N93-10559
An improved technique for determining higher order eigenvector coefficients p 64 N93-10565
DISPLAY DEVICES
Advanced terrain displays to transport category aircraft
[PB92-197136] p 6 N93-10065
Air traffic control visual scanning
[DOT/FAA/CT-TN92/16] p 7 N93-10459
Comparative study of the MTFA, ICS, and SQRI image quality metrics for visual display systems
[AD-A252116] p 158 N93-10708
KC-135 crew reduction feasibility demonstration simulation study. Volume 3: Test and evaluation
[AD-A253931] p 134 N93-10713
DISTANCE
Stereoscopy and paralax in the vertical distances determination using aerial photographs
[INPE-5363-PUD/049] p 102 N93-10063
A spatial similarity measure for image database applications
[AD-A253570] p 176 N93-10883
DISTANCE MEASURING EQUIPMENT
Stereoscopy and paralax in the vertical distances determination using aerial photographs
[INPE-5363-PUD/049] p 102 N93-10063
DISTRIBUTED PROCESSING
Implementation of parallel algorithms
[AD-A253638] p 140 N93-10227
A look at scalable dense linear algebra libraries
[DE92-017805] p 143 N93-10285
Ada validation tests for rate monotonic scheduling algorithms
[AD-A253325] p 136 N93-10300
A look at scalable dense linear algebra libraries
[DE92-017161] p 139 N93-10816
DISTRIBUTION (PROPERTY)
On the use of coupled finite element boundary element models in numerical design analysis p 63 N93-10563
DISTRIBUTION FUNCTIONS
Data synthesis and display programs for wave distribution function analysis
[NASA-TM-108009] p 70 N93-10800
DIURNAL VARIATIONS
Effects of early bright, late bright and dim illumination upon circadian neuroendocrine, electrophysiological and behavioral responses
[AD-A254129] p 131 N93-10661
Morning-evening differences in global and regional oceanic precipitation as observed by the SSM/I p 127 N93-10851
DIVERTERS
Divertor heat flux reduction by D2 injection in DIII-D
[DE92-014232] p 160 N93-10326
VH-mode discharges in the D3-D tokamak
[DE92-016257] p 161 N93-10463
The effect of current profile changes on confinement in the D3-D tokamak
[DE92-016256] p 163 N93-10620
DMSP SATELLITES
Microwave radiometer studies of atmospheric water over the oceans, volume 2
[NASA-CR-190343] p 127 N93-10848
DOCUMENT STORAGE
Seminar on Basic Documentation Practices
[AGARD-R-788] p 172 N93-10593
Document processing p 174 N93-10600
Security considerations within military information systems p 174 N93-10603
DOCUMENTATION
Seminar on Basic Documentation Practices
[AGARD-R-788] p 172 N93-10593
Documentation practices: The national scene (Greece) p 173 N93-10595
Establishing a scientific and technical information program: Planning and resource management p 173 N93-10597
Acquisition 1: Stock acquisition processes in defence and aerospace documentation centres p 173 N93-10598
Document processing p 174 N93-10600
DOCUMENTS
Seminar on Basic Documentation Practices
[AGARD-R-788] p 172 N93-10593
National scene in information and documentation activities and recent developments in the Documentation Center of TUBITAK (TURDOK) p 173 N93-10594
Documentation practices: The national scene (Greece) p 173 N93-10595
Acquisition 1: Stock acquisition processes in defence and aerospace documentation centres p 173 N93-10598
Document processing p 174 N93-10600
Services: User services in defence and aerospace documentation centres p 174 N93-10602
DOMES (GEOLOGY)
The Vredefort Dome: Review of geology and deformation phenomena and status report on current knowledge and remaining problematics (five years after the cryptoexplosion workshop) p 119 N93-10173
Bronzite Granophyre: New insight on Vredefort p 121 N93-10186
Electron petrography of silica polymorphs associated with pseudotachylite, Vredefort structure, South Africa p 123 N93-10192
DOMES (STRUCTURAL FORMS)
Structural review of the Vredefort dome p 108 N93-10127
Ar-40 to Ar-39 dating of pseudotachylites from the Witwatersrand basin, South Africa, with implications for the formation of the Vredefort Dome p 122 N93-10189
DOPED CRYSTALS
Epitaxial growth and dopant incorporation in diamond
[AD-A253636] p 165 N93-10206
Pseudomorphic semiconducting heterostructures from combinations of AlN, GaN, and selected SiC polytypes: Theoretical advancement and its coordination with experimental studies of nucleation, growth, characterization, and device development
[AD-A253330] p 166 N93-10355
Spectroscopic differential reflectance as an analytical probe for microelectronic processing
[AD-A253134] p 73 N93-10656
DOSAGE
Limited toxicity and mutagenicity testing of five unicharge propellant compounds
[AD-A252339] p 43 N93-10636
DOWNWASH
Acoustic noise generation at the air/ocean boundary
[DREA-CR-90-445] p 147 N93-10642
DRAG
A method of testing two-dimensional airfoils
[AD-A253210] p 4 N93-10375
DRAG COEFFICIENTS
A method of testing two-dimensional airfoils
[AD-A253210] p 4 N93-10375
DRAG REDUCTION
Experimental investigation of flows behind different Large-Eddy Breakup (LEBU) devices in thick boundary layers p 6 N93-10550
DRILLING
Research core drilling in the Manson impact structure, Iowa p 105 N93-10114
DRYING
Mass transfer in oscillating flows: Efficient drying via pulse combustors
[PB92-204403] p 81 N93-10449
DUCTED FLOW
The effects of streamline curvature and swirl on turbulent flows in curved ducts p 84 N93-10875
DUCTILITY
Tensile properties of cast titanium alloys: Titanium-6Al-4V ELI and Titanium-5Al-2.5Sn ELI
[NASA-TP-3288] p 33 N93-10072
Plasticity of single crystalline Al3X intermetallic compounds
[AD-A254282] p 40 N93-10766
DYE LASERS
Subpicosecond resolved incipient laser damage
[AD-A253624] p 87 N93-10202
Resonance ionization of rubidium using sequential diode laser-driven transitions
[DE92-014468] p 89 N93-10429
DYES
Determination of Sandoz black aluminum coloring dye, olive aluminum coloring dye, and sodium dichromate aluminum sealing solutions by UV-visible spectrophotometry
[AD-A253639] p 29 N93-10207
DYNAMIC CHARACTERISTICS
Molecular dynamics of shocks in crystals with defects
[AD-A253353] p 164 N93-10099
Determination of the dynamic unload/reload characteristics of ceramics
[AD-A253513] p 35 N93-10221
An elastic oblate axisymmetric reference gyro for attitude studies p 54 N93-10518
DYNAMIC CONTROL
Numerical simulation of large actively controlled space structures p 13 N93-10308
Characterization of and active control of flexible structures, using piezoceramics as sensors and actuators p 10 N93-10319
Model reference adaptive control in large space structures p 13 N93-10365
Experimental demonstration of offset control with an application to the tethered payload p 14 N93-10521
DYNAMIC MODELS
A comparative study of semi-empirical dynamic stall models p 5 N93-10544
Modelling and control of robotic arms fabricated from orthotropic materials p 65 N93-10572
DYNAMIC PRESSURE
Monitoring structural response in pressurized environments. Part 2: Applications
[DE92-015034] p 94 N93-10327
DYNAMIC RESPONSE
Monitoring structural response in pressurized environments. Part 2: Applications
[DE92-015034] p 94 N93-10327
Orthotropic circular plate on nonlinear elastic subgrade p 53 N93-10513
Dynamics of an orbiting flexible manipulator p 54 N93-10519
Effect of mounting offset on the dynamics of deploying flexible appendages p 54 N93-10520
Probability density functions for random nonlinear oscillation p 55 N93-10522
Response of a beam to transverse impulsive and high frequency loads p 56 N93-10526

Compressible and incompressible fluid seals: Influence on rotordynamic response and stability
[NASA-CR-190746] p 92 N93-10891

DYNAMIC STABILITY
Stability of coupled semiconductor diode lasers
p 88 N93-10379
Dynamic stability of laminated transversely-isotropic composite plates subjected to parametric excitations
p 29 N93-10525
Compressible and incompressible fluid seals: Influence on rotordynamic response and stability
[NASA-CR-190746] p 92 N93-10891

DYNAMIC STRUCTURAL ANALYSIS
Numerical simulation of large actively controlled space structures p 13 N93-10308
Characterization of and active control of flexible structures, using piezoceramics as sensors and actuators p 10 N93-10319
SAPNEW: Parallel finite element code for thin shell structures on the Alliant FX/80
[NASA-CR-190663] p 94 N93-10372
New directions in computational mechanics
p 44 N93-10467
Dynamic crack division in brittle solids
p 48 N93-10489
Vibrations of a flexible Timoshenko beam under gravity p 53 N93-10512
Dynamics of systems with time-varying inertial properties p 54 N93-10517
Dynamics of an orbiting flexible manipulator
p 54 N93-10519
Evolutionary spectra of time-dependent discretized systems to time-frequency modulated random excitations p 55 N93-10524
Dynamic stability of laminated transversely-isotropic composite plates subjected to parametric excitations
p 29 N93-10525
Vibration of a damped double-beam system
p 56 N93-10527
Mode localization in a simple continuum model
p 56 N93-10529
Flexural vibration of beams with varying section properties p 57 N93-10531
Natural vibrations of multilayered doubly curved shells
p 57 N93-10532
Free vibrations of the thick circular cylindrical shells and rings p 57 N93-10533
Vibration frequencies of a constrained cantilever wedge p 57 N93-10534
On the vibration of axisymmetric shells
p 57 N93-10535
The vibrations of annular discs: A comparison of experimental and two analytical techniques
p 58 N93-10536
Partial solution of the generalized eigenvalue problem using the Woodbury transformation p 64 N93-10567
Effective formulation of the dynamics of a manipulator based on the Appell equations p 65 N93-10571
Automated multi-body system dynamics via bond graph modelling and interactive graphics p 66 N93-10576
A derivation for the kinematic equations of flexible robots with appropriate transformation matrices
p 66 N93-10577
DYNA2D: A nonlinear, explicit, two-dimensional finite element code for solid mechanics: User manual
[DE92-017310] p 95 N93-10646

DYNAMICAL SYSTEMS
On techniques for digital simulation of random response of nonlinear oscillators p 55 N93-10523
Self-programming of matter and the evolution of proto-biological organizations
[DE92-015244] p 129 N93-10628
Singular perturbation methods for nonlinear dynamical systems and waves
[AD-A254116] p 144 N93-10660

DYNAMOMETERS
Testing techniques p 78 N93-10060

E

EARTH CRUST
Structural review of the Vredefort dome
p 108 N93-10127
Asteroids and Archaean crustal evolution: Tests of possible genetic links between major mantle/crust melting events and clustered extraterrestrial bombardments
p 110 N93-10140
The Acraman impact and its widespread ejecta, South Australia p 111 N93-10141
Simulated meteorite impacts and volcanic explosions: Ejecta analyses and planetary implications
p 111 N93-10143
Where's the Beaverhead beef? --- meteorite impact structure p 112 N93-10146
SAR in support of geological investigations of the Sudbury structure p 103 N93-10182
Effects of gravity in folding --- of geological layers
p 124 N93-10324

EARTH IONOSPHERE
Simulation study of interactions of Space Shuttle-generated electron beams with ambient plasmas
[NASA-CR-190843] p 159 N93-10066

EARTH MANTLE
Asteroids and Archaean crustal evolution: Tests of possible genetic links between major mantle/crust melting events and clustered extraterrestrial bombardments
p 110 N93-10140

EARTH ORBITAL ENVIRONMENTS
LDEF Materials Workshop 1991, part 2
[NASA-CP-3162-PT-2] p 37 N93-10578
Selected results for metals from LDEF experiment A0171 p 34 N93-10579
Some results of the oxidation investigation of copper and silver samples flown on LDEF p 34 N93-10580
Changes in oxidation state of chromium during LDEF exposure p 34 N93-10581
Effect of space exposure on pyroelectric infrared detectors p 38 N93-10582
Long Duration Exposure Facility (LDEF) optical systems SIG summary and database p 38 N93-10583
Polymer matrix composites on LDEF experiments M0003-9 and M0003-10 p 38 N93-10584
Space environmental effects on LDEF low Earth orbit exposed graphite reinforced polymer matrix composites
p 38 N93-10585
Additional results on space environmental effects on polymer matrix composites: Experiment A0180
p 38 N93-10586
Proposed test program and data base for LDEF polymer matrix composites p 38 N93-10587
Effects of long-term exposure on LDEF fastener assemblies p 39 N93-10590
Results from testing and analysis of solar cells flown on LDEF p 39 N93-10591
System related testing and analysis of FRECOPA
p 39 N93-10592

EARTH PLANETARY STRUCTURE
Asteroids and Archaean crustal evolution: Tests of possible genetic links between major mantle/crust melting events and clustered extraterrestrial bombardments
p 110 N93-10140

EARTH RESOURCES
Stereoscopy and paralax in the vertical distances determination using aerial photographs
[INPE-5363-PUD/049] p 102 N93-10063
Reserves in western basins
[DE92-014429] p 102 N93-10625

EARTH-MOON SYSTEM
On the gravitational potential of two arbitrary rotating bodies with applications to the Earth-Moon system
p 179 N93-10303

EARTHQUAKES
List of publications, 1969-1991. Panel on wind and seismic effects
[PB92-201102] p 125 N93-10089
Worldwide seismic catalog and the nature of seismic coupling p 124 N93-10376

ECOLOGY
The Deposition and Fate of Trace Metals in our Environment: Symposium proceedings
[PB92-189216] p 104 N93-10289

ECONOMIC ANALYSIS
Analysis of air pollution and greenhouse gases
[DE92-014955] p 104 N93-10384

ECOSYSTEMS
Spatial models of ecological systems and processes: The role of GIS
[DE92-016884] p 175 N93-10788

EDDY CURRENTS
Experimental investigation of flows behind different Large-Eddy Breakup (LEBU) devices in thick boundary layers p 6 N93-10550

EDDY VISCOSITY
The effects of streamline curvature and swirl on turbulent flows in curved ducts p 84 N93-10875

EDGES
Singular stress distributions at circular holes in composite laminates p 51 N93-10503

EDUCATION
Center for Intelligent Control Systems, Brown University component: Graduate research fellowships
[AD-A253620] p 141 N93-10095
Total Quality Management (TQM) concepts applied to instruction
[DE92-013399] p 171 N93-10270
The levels of mathematics achievement: Initial performance standards for the 1990 NAEP mathematics assessment, volume 3
[PB92-199421] p 134 N93-10341
Interdisciplinary research and training program in the plant sciences
[DE92-015919] p 130 N93-10835

EFFICIENCY
Introduction to radial turbine technology
p 77 N93-10051

EIGENVALUES
Axisymmetric vibrations of rotating circular plates using characteristic orthogonal polynomials
p 45 N93-10470
Vibration of orthotropic cylindrical shell panels with arbitrary supported curved edges p 45 N93-10471
Experimental investigation of simple support condition in free vibration analysis of plates p 56 N93-10530
An improved technique for determining higher order eigenvector coefficients p 64 N93-10565
Partial solution of the generalized eigenvalue problem using the Woodbury transformation p 64 N93-10567
LABAN-PEL: A two-dimensional, multigroup diffusion, high-order response matrix code
[DE92-626845] p 144 N93-10624
Global Alfven eigenmodes in D3-D
[DE92-016250] p 163 N93-10760

EIGENVECTORS
On the measurement of time-dependent quantum phases
[DE92-630206] p 170 N93-10387
An improved technique for determining higher order eigenvector coefficients p 64 N93-10565
Partial solution of the generalized eigenvalue problem using the Woodbury transformation p 64 N93-10567

EJECTA
Large meteorite impacts: The K/T model
p 107 N93-10120
Shocked zircons in the Onaping Formation: Further proof of impact origin p 107 N93-10121
Suevite superposition on the Bunte breccia in Noerdlinger Ries, Germany: New findings on the transport mechanism of impactites p 107 N93-10122
Mobilization of the platinum group elements by low-temperature fluids: Implications for mineralization and the iridium controversy p 109 N93-10133
Ruthenium/iridium ratios in the Cretaceous-Tertiary boundary clay: Implications for global dispersal and fractionation within the ejecta cloud p 109 N93-10135
Breccia dikes from the Beaverhead Impact structure, southwest Montana p 110 N93-10137
The Zhamanshin impact feature: A new class of complex crater? p 110 N93-10139
The Acraman impact and its widespread ejecta, South Australia p 111 N93-10141
Simulated meteorite impacts and volcanic explosions: Ejecta analyses and planetary implications
p 111 N93-10143
Venusian impact basins and cratered terrains
p 112 N93-10145
Report on the international Cambodian crater expedition, 1992 p 113 N93-10147
Tektite origin by hypervelocity asteroidal or cometary impact: The quest for the source craters
p 114 N93-10154
U-Pb isotopic results for single shocked and polycrystalline zircons record 550-65.5-Ma ages for a K-T target site and 2700-1850-Ma ages for the Sudbury impact event p 115 N93-10156
Impactites from Popigai Crater p 117 N93-10164
The large impact process inferred from the geology of lunar multiring basins p 121 N93-10184

ELASTIC BENDING
Elasticity analysis of orthotropic beams under three-part bending p 52 N93-10507

ELASTIC DEFORMATION
Simple shearing flow of a 3D foam
[DE92-011151] p 36 N93-10399
Development in the elastic analysis of laminated plates p 44 N93-10468
Orthotropic circular plate on nonlinear elastic subgrade p 53 N93-10513
An elastic oblate axisymmetric reference gyro for attitude studies p 54 N93-10518
A new quadrilateral element for the elastic and plastic analysis of shells p 62 N93-10559

ELASTIC MEDIA
Pulse propagation in random media
[AD-A254294] p 152 N93-10769

ELASTIC PLATES
Evaluation of the triangular plate element of Zienkiewcz and Lefebvre p 63 N93-10562

ELASTIC PROPERTIES
Hot fire fatigue testing results for the compliant combustion chamber p 22 N93-10038
Calculation of stress intensity factors in an isotropic multicracked plate. Part 1: Theoretical development
[NASA-TM-105766] p 95 N93-10455
Development in the elastic analysis of laminated plates p 44 N93-10468

Elasticity analysis of orthotropic beams under three-part bending p 52 N93-10507
Hot fire fatigue testing results for the compliant combustion chamber
[NASA-TP-3223] p 26 N93-10743
Mechanics of composite materials for spacecraft
[AD-A254217] p 28 N93-10896

ELASTIC SCATTERING
Pion- and proton-nucleus interactions at intermediate energy
[DE92-017980] p 157 N93-10838

ELASTIC WAVES
Calculation of elastic-plastic wave propagation on the connection machine
[AD-A252429] p 95 N93-10427

ELASTOMERS
The effect of elevated temperatures on the properties of thermally stable silicon-based elastomers for adhesives, sealants, and insulator applications p 15 N93-10006
Non-linear thermoelasticity of rubberlike solids p 45 N93-10474
Failure processes in elastomeric composites p 46 N93-10475
Chronorheological characterization of elastomers p 46 N93-10476

ELECTRIC ARCS
A seam tracking modulated infrared optical sensor for use in welding
[AD-A254103] p 159 N93-10812

ELECTRIC BATTERIES
Results from the testing and analysis of LDEF batteries p 39 N93-10589

ELECTRIC CHARGE
Theoretical analysis of discharges in copper vapor lasers: A comparison of Ne and He
[DE92-014739] p 87 N93-10083

ELECTRIC CONDUCTORS
Conductive titanate fiber and its production method
[DE92-014738] p 39 N93-10627

ELECTRIC CONTACTS
Implanted contacts for diamond semiconductor devices
[AD-A245568] p 165 N93-10274
Ohmic contacts to compound semiconductors p 76 N93-10830

ELECTRIC CURRENT
Theory of light-induced drift of electrons in coupled quantum wells
[AD-A253609] p 164 N93-10093

ELECTRIC DIPOLES
Gradiometer antennas for tunnel detection
[PB92-205400] p 69 N93-10440

ELECTRIC DISCHARGES
Theoretical analysis of discharges in copper vapor lasers: A comparison of Ne and He
[DE92-014739] p 87 N93-10083

ELECTRIC FIELDS
Method and apparatus for determining return stroke polarity of distant lightning
[NASA-CASE-MFS-26102-2-CU] p 125 N93-10108
Investigation of the effect of large core changes in toroidal plasma rotation and radial electric field on confinement in H-mode discharges in the D3-D tokamak
[DE92-016252] p 161 N93-10392
Polarimetry of motional Stark effect and determination of current profiles in D3-D
[DE92-016258] p 161 N93-10393
Investigations of the dynamics and thermodynamics of the mesosphere lower thermosphere and upper thermosphere at the polar regions with optical ground-based remote sensing
[AD-A253228] p 125 N93-10711
Interaction of electromagnetic fields with chondrocytes in gel culture
[AD-A253727] p 70 N93-10747

ELECTRIC FILTERS
Order statistics and nonparametric statistics
[AD-A253574] p 146 N93-10699

ELECTRIC GENERATORS
Format and structure of a database on health and environmental impacts of different energy systems for electricity generation
[DE92-634160] p 130 N93-10222
Comparison of all-electric secondary power systems for civil subsonic transports
[NASA-TM-105852] p 9 N93-10456
Emergency Diesel Generator reliability at Department of Energy (DOE) facilities
[DE92-011888] p 91 N93-10622
Chinese Space Science and Technology (selected articles)
[AD-A254099] p 69 N93-10701

ELECTRIC POTENTIAL
Effects of anode material on arcjet performance p 23 N93-10044
Effects of anode material on arcjet performance
[NASA-TM-105799] p 25 N93-10197
Thermal management in high average power pulsed compression systems
[DE92-017055] p 76 N93-10836

ELECTRIC POWER PLANTS
Chinese Space Science and Technology (selected articles)
[AD-A254099] p 69 N93-10701

ELECTRIC POWER SUPPLIES
Comparison of all-electric secondary power systems for civil subsonic transports
[NASA-TM-105852] p 9 N93-10456
Emergency Diesel Generator reliability at Department of Energy (DOE) facilities
[DE92-011888] p 91 N93-10622

ELECTRIC PROPULSION
The 1992 JANNAF Propulsion Meeting, volume 1
[CPIA-PUBL-580-VOL-1] p 15 N93-10001
Electric propulsion applications p 20 N93-10029
Electric Propulsion Space Experiment (ESEX): Spacecraft design issues for high-power electric propulsion p 21 N93-10030
A 26 kW arcjet system for on-orbit demonstration p 21 N93-10031
Selection of rocket propulsion systems p 22 N93-10034

ELECTRIC SWITCHES
Twenty-five KA, 5000V solid state opening switch for inductive energy stores
[AD-A253968] p 73 N93-10421

ELECTRICAL FAULTS
High-power microwave breakdown of dielectric interfaces
[AD-A254200] p 124 N93-10262

ELECTRICAL IMPEDANCE
Far-zone field of a monopole element on a disk ground plane above flat earth
[AD-A253580] p 70 N93-10091

ELECTRICAL MEASUREMENT
Method and apparatus for determining return stroke polarity of distant lightning
[NASA-CASE-MFS-26102-2-CU] p 125 N93-10108
Numerical modelling of fringing fields and their use for complex permittivity measurements at high frequencies
[AD-A253994] p 72 N93-10359
Vortices in long Josephson junctions
[AD-A253230] p 167 N93-10404
Improvements to the AC potential drop method of crack measurement p 59 N93-10543
Spectroscopic ellipsometric measurements of the dielectric function of germanium dioxide films on crystal germanium
[AD-A253137] p 168 N93-10614
Ohmic contacts to compound semiconductors p 76 N93-10830

ELECTRICAL PROPERTIES
Advanced technology component derating
[AD-A253334] p 72 N93-10357
Activated transport in AMTEC electrodes
[DE92-016810] p 75 N93-10786

ELECTRICAL RESISTANCE
Electrical resistance tomography used in environmental restoration
[DE92-018003] p 103 N93-10763

ELECTRICAL RESISTIVITY
Growth, nitrogen vacancy reduction, and solid solution formation in cubic GaN thin films and the subsequent fabrication of superlattice structures using AlN and InN
[AD-A253331] p 166 N93-10356
Modelling of 3-D electromagnetic responses using the time-wavenumber method
[DE92-017025] p 70 N93-10865

ELECTROCATALYSTS
Advanced materials development for fossil energy conversion applications
[DE92-015762] p 104 N93-10729

ELECTRODE MATERIALS
Advanced materials development for fossil energy conversion applications
[DE92-015762] p 104 N93-10729

ELECTRODEPOSITION
Template-synthesis of infrared-transparent metal microcylinders: Comparison of optical properties with the predictions of effective medium theory
[AD-A253267] p 158 N93-10694

ELECTRODES
Critical technology demonstration of plasma focus type MPD thrusters
[AD-A252428] p 26 N93-10638
Activated transport in AMTEC electrodes
[DE92-016810] p 75 N93-10786

ELECTROLYTES
Development of electrosupercapacitors
[AD-A252208] p 71 N93-10250

ELECTROMAGNETIC ACCELERATION
Twenty-five KA, 5000V solid state opening switch for inductive energy stores
[AD-A253968] p 73 N93-10421

ELECTROMAGNETIC FIELDS
Basic and applied research in the field of electronics and communications
[AD-A253593] p 67 N93-10092
Interaction of electromagnetic fields with chondrocytes in gel culture
[AD-A253727] p 70 N93-10747
Modelling of 3-D electromagnetic responses using the time-wavenumber method
[DE92-017025] p 70 N93-10865

ELECTROMAGNETIC INTERACTIONS
The interaction of UV-Laser radiation with metal and semiconductor surfaces
[AD-A253510] p 87 N93-10201

ELECTROMAGNETIC MEASUREMENT
Two-dimensional signal processing, optical information storage and processing, and electromagnetic measurements
[AD-A253953] p 73 N93-10417
Gradiometer antennas for tunnel detection
[PB92-205400] p 69 N93-10440

ELECTROMAGNETIC PROPULSION
Measurement of acceleration using an instrumented railgun projectile
[AD-A253366] p 12 N93-10106

ELECTROMAGNETIC PULSES
Pulse propagation in random media
[AD-A254294] p 152 N93-10769

ELECTROMAGNETIC RADIATION
Modeling of HF propagation and heating in the ionosphere
[AD-A253941] p 125 N93-10714

ELECTROMAGNETIC SCATTERING
Application of volumetric multiple-scattering approximations to foliage media
[AD-A253337] p 68 N93-10358

ELECTROMAGNETIC WAVE TRANSMISSION
Application of volumetric multiple-scattering approximations to foliage media
[AD-A253337] p 68 N93-10358
Design of laser optical systems
[AD-A254247] p 89 N93-10703
Modeling of HF propagation and heating in the ionosphere
[AD-A253941] p 125 N93-10714
Joint Services Electronics Program
[AD-A253842] p 76 N93-10829

ELECTROMAGNETISM
Basic and applied research in the field of electronics and communications
[AD-A253593] p 67 N93-10092

ELECTROMETERS
Acceptance testing of the prototype electrometer for the SAMPIE flight experiment
[NASA-TM-105880] p 13 N93-10841

ELECTRON ACCELERATORS
Advanced transport systems for electron beams in high-brightness accelerators and FEL's
[AD-A253314] p 88 N93-10286

ELECTRON BEAMS
Simulation study of interactions of Space Shuttle-generated electron beams with ambient plasmas
[NASA-CR-190843] p 159 N93-10066
Moire-fringe images of twin boundaries in chemical vapor deposited diamond
[AD-A253729] p 35 N93-10231
High-power microwave breakdown of dielectric interfaces
[AD-A254200] p 124 N93-10262
Advanced transport systems for electron beams in high-brightness accelerators and FEL's
[AD-A253314] p 88 N93-10286
Thermal management in high average power pulsed compression systems
[DE92-017055] p 76 N93-10836
A semiempirical formula for calculating the coefficients for field emission tip forms
[AD-A254109] p 145 N93-10857
Recent developments in stored polarized electron positron beams
[DE92-016965] p 157 N93-10862
Extended-interaction klystron for the AN/TPS-43-E radar system
[AD-A253166] p 76 N93-10882

ELECTRON CYCLOTRON HEATING
Langmuir probe and optical emission studies of Ar, O2, and N2 plasmas produced by an ECR microwave source
[AD-A253138] p 162 N93-10615

ELECTRON DENSITY (CONCENTRATION)
Divertor heat flux reduction by D2 injection in DIII-D
[DE92-014232] p 160 N93-10326

Electronic and structural properties of metallic microclusters
[DE92-016917] p 33 N93-10411

ELECTRON DIFFUSION
Multidimensional deterministic electron transport calculations
[AD-A254021] p 154 N93-10362

ELECTRON EMISSION
Impact sensitivity reduction via exo-electron control
p 15 N93-10004

ELECTRON ENERGY
Helium transport in enhanced confinement regimes on the TEXTOR and D3-D tokamaks
[DE92-016247] p 160 N93-10293
Multidimensional deterministic electron transport calculations
[AD-A254021] p 154 N93-10362
Variational full wave calculation of fast wave current drive in D3-D using the ALCYON code
[DE92-016572] p 163 N93-10761

ELECTRON GAS
Theory of light-induced drift of electrons in coupled quantum wells
[AD-A253609] p 164 N93-10093

ELECTRON GUNS
Extended-interaction klystron for the AN/TPS-43-E radar system
[AD-A253166] p 76 N93-10882

ELECTRON MICROSCOPY
Phase transformations in 40-60-GPa shocked gneisses from the Haughton Crater (Canada): An Analytical Transmission Electron Microscopy (ATEM) study
p 117 N93-10163
The microstructural characterization of an Al-Li-Cu-Mg alloy (8090) metal-matrix composite
[RAE-TM-MAT/STR-1139] p 34 N93-10802

ELECTRON SCATTERING
Multidimensional deterministic electron transport calculations
[AD-A254021] p 154 N93-10362

ELECTRON STATES
Theory of transport for interacting many-body systems
[AD-A253789] p 169 N93-10871

ELECTRON TRANSFER
Theoretical analysis of discharges in copper vapor lasers: A comparison of Ne and He
[DE92-014739] p 87 N93-10083
Electron transfer reactions in microporous solids
[DE92-016222] p 166 N93-10284
Multidimensional deterministic electron transport calculations
[AD-A254021] p 154 N93-10362
Electron transfer, ionization, and excitation in atomic collisions
[DE92-017300] p 154 N93-10435
Covalent electron transfer theory of superconductivity
[AD-A253975] p 74 N93-10718

ELECTRON TRANSITIONS
Theory of light-induced drift of electrons in coupled quantum wells
[AD-A253609] p 164 N93-10093

ELECTRON TUNNELING
Theory of light-induced drift of electrons in coupled quantum wells
[AD-A253609] p 164 N93-10093

ELECTRONIC COUNTERMEASURES
Convergence performance of adaptive detectors, part 3
[AD-A248415] p 143 N93-10275

ELECTRONIC EQUIPMENT
Resonance apparatus operating manual
[AD-A254040] p 71 N93-10241
Advanced technology component derating
[AD-A253334] p 72 N93-10357
Defence electronics industry profile, 1990-1991
[CTN-92-60515] p 66 N93-10653

ELECTRONIC EQUIPMENT TESTS
Evaluation of an electronics system concept for Respiratory Protection system (RESPO 21)
[AD-A253394] p 134 N93-10288
Advanced technology component derating
[AD-A253334] p 72 N93-10357
Twenty-five KA, 5000V solid state opening switch for inductive energy stores
[AD-A253968] p 73 N93-10421
High sensitivity probes for silicon VLSI internal node testing
[AD-A253924] p 169 N93-10764

ELECTRONIC MAIL
Technology for libraries and information centers: A seminar in Greece, Portugal, and Turkey
p 174 N93-10601
A change of course: The importance to DoD of international standards for electronic commerce
[AD-A253199] p 75 N93-10792

ELECTRONIC MODULES
An MCM/chip concurrent engineering validation
[AD-A253783] p 136 N93-10237
Magnetostatic waves-based integrated optic Bragg cell modules with applications to RF signal processing
[AD-A254035] p 71 N93-10240
Holographic optical interconnects for multichip modules
[AD-A253403] p 86 N93-10408

ELECTRONS
Theory of light-induced drift of electrons in coupled quantum wells
[AD-A253609] p 164 N93-10093
Fellowship in physics/modern optics and quantum electronics
[AD-A253666] p 87 N93-10228
Multidimensional deterministic electron transport calculations
[AD-A254021] p 154 N93-10362
Radiation damage to DNA
[DE92-015760] p 130 N93-10834
Electronic structure of highly correlated structures
[DE92-017017] p 155 N93-10863

ELECTROPHYSIOLOGY
Effects of early bright, late bright and dim illumination upon circadian neuroendocrine, electrophysiological and behavioral responses
[AD-A254129] p 131 N93-10661
Mental workload assessment in the cockpit: Feasibility of using electrophysiological measurements, phase 1
[AD-A254138] p 133 N93-10662

ELECTROSTATIC PROBES
Langmuir probe and optical emission studies of Ar, O2, and N2 plasmas produced by an ECR microwave source
[AD-A253138] p 162 N93-10615

ELECTROSTRICTION
Piezoelectric and electrostrictive materials for transducers applications, volume 1
[AD-A250889] p 71 N93-10273
Piezoelectric and electrostrictive materials for transducers applications, volume 2
[AD-A250890] p 71 N93-10276
Piezoelectric and electrostrictive materials for transducers applications, volume 3
[AD-A250891] p 72 N93-10280
Piezoelectric and electrostrictive materials for transducers applications, volume 4
[AD-A250892] p 72 N93-10282

ELEMENTARY EXCITATIONS
Semiclassical quantization of interacting anyons in a strong magnetic field
[DE92-634889] p 169 N93-10229
Semiclassical quantization of integrable systems of few interacting anyons in a strong magnetic field
[DE92-634892] p 170 N93-10295
Research program in elementary particle theory
[DE92-017399] p 155 N93-10840

ELEMENTARY PARTICLES
Mass and mixing angle patterns in the standard model and its material supersymmetric extension
[DE92-016197] p 153 N93-10291
Particle production at high p(sub (perpendicular)) in (sup 28)Si + A collisions at 14.6 A x GeV/c
[DE92-016939] p 154 N93-10402

ELLIPSOIDS
Unifying the landmark developments in optimal bounding ellipsoid identification
[AD-A253502] p 143 N93-10200
A semiempirical formula for calculating the coefficients for field emission tip forms
[AD-A254109] p 145 N93-10857

ELLIPSOMETRY
A new ellipsometry technique for interface analysis: Application to Si-SiO2
[AD-A253143] p 167 N93-10415
Spectroscopic ellipsometric measurements of the dielectric function of germanium dioxide films on crystal germanium
[AD-A253137] p 168 N93-10614

ELLIPTIC DIFFERENTIAL EQUATIONS
Nonlinear dynamics underlying atmospheric predictability
[AD-A254042] p 126 N93-10363
Numerical solution of three-dimensional unsteady viscous flows
[AD-A253202] p 83 N93-10793

ELLIPTICAL ORBITS
Computer algebra and the elliptic restricted problem of three bodies p 11 N93-10499

ELONGATION
Experimental and numeric analysis of constraints in a bonded stepped lap joint subjected to traction
p 54 N93-10516

EMBRITTLEMENT
Stress modified welding process for irradiated materials
[DE92-017131] p 92 N93-10634

EMERGENCIES
Hubble Space telescope thermal cycle test report for large solar array samples with BSFR cells (Sample numbers 703 and 704)
[NASA-TM-108373] p 104 N93-10809

EMISSION SPECTRA
Alternate spectrometric oil analysis techniques
[AD-A253355] p 29 N93-10101
Emission tomography of sodium in a hydrogen-air flame
[AD-A253530] p 29 N93-10224
Intensity, velocity, and turbulence in prominences observed with the HRTS p 180 N93-10911
High resolution observations of solar ejecta
p 181 N93-10916

EMITTANCE
Studies impacting the designs of free electron lasers
[AD-A254293] p 90 N93-10768

EMITTERS
Field-emitter arrays for RF vacuum microelectronics
[AD-A253396] p 73 N93-10405

ENCAPSULATING
APOLLO: A computer program for the calculation of chemical equilibrium and reaction kinetics of chemical systems
[DE92-017864] p 139 N93-10817

ENERGY BANDS
Implanted contacts for diamond semiconductor devices
[AD-A245568] p 165 N93-10274

ENERGY CONSUMPTION
EIA publications directory, 1991
[DE92-015686] p 174 N93-10607

ENERGY CONVERSION
Advanced materials development for fossil energy conversion applications
[DE92-015762] p 104 N93-10729

ENERGY DISSIPATION
Fractals and multifractals in fracture
p 50 N93-10497
Numerical considerations for structural system identification from modal information p 63 N93-10564
Global Alfven eigenmodes in D3-D
[DE92-016250] p 163 N93-10760

ENERGY DISTRIBUTION
Intense ion beam research at Los Alamos
[DE92-015240] p 155 N93-10333

ENERGY GAPS (SOLID STATE)
Implanted contacts for diamond semiconductor devices
[AD-A245568] p 165 N93-10274

ENERGY LEVELS
Semiclassical quantization of interacting anyons in a strong magnetic field
[DE92-634889] p 169 N93-10229
Resonance ionization of rubidium using sequential diode laser-driven transitions
[DE92-014468] p 89 N93-10429

ENERGY METHODS
Thermal buckling of heated laminated composite circular cylindrical shells p 51 N93-10504
The vibrations of annular discs: A comparison of experimental and two analytical techniques
p 58 N93-10536
Variational formulation of a mixed method for second order frame analysis p 62 N93-10556

ENERGY SPECTRA
Low-frequency noise reduction in SQUID measurements using laser switching
[AD-A253821] p 90 N93-10827

ENERGY STORAGE
Twenty-five KA, 5000V solid state opening switch for inductive energy stores
[AD-A253968] p 73 N93-10421

ENERGY TECHNOLOGY
EIA publications directory, 1991
[DE92-015686] p 174 N93-10607

ENERGY TRANSFER
Multidimensional deterministic electron transport calculations
[AD-A254021] p 154 N93-10362
A new energy transfer model for turbulent free shear flow
[NASA-TM-105854] p 81 N93-10454
Experimental plasma research project summaries
[DE92-016274] p 162 N93-10464
Energy build-up, transport, and release in solar flares
p 181 N93-10913

ENGINE AIRFRAME INTEGRATION
A configuration development strategy for the NASP
p 9 N93-10011

ENGINE COOLANTS
Thermal stratification potential in rocket engine coolant channels p 18 N93-10019
ENGINE DESIGN
LV software for supersonic flow analysis
[NASA-CR-190911] p 2 N93-10069
Compound cycle engine for helicopter application
[NASA-CR-180824] p 9 N93-10348
SAPNEW: Parallel finite element code for thin shell structures on the Alliant FX/80
[NASA-CR-190663] p 94 N93-10372
ENGINE INLETS
Evaluation and application of the Baldwin-Lomax turbulence model in two-dimensional, unsteady, compressible boundary layers with and without separation in engine inlets
[NASA-TM-105810] p 79 N93-10087
ENGINE NOISE
Combat aircraft jet engine noise studies p 150 N93-10679
Supersonic acoustic source mechanisms for free jets of various geometries p 150 N93-10680
Nozzle installation effects on the noise from supersonic exhaust plumes p 150 N93-10681
Combustion noise and combustion instabilities in propulsion systems p 150 N93-10682
Combat aircraft noise reduction by technical measures p 152 N93-10689
Technical measures for the attenuation of aircraft noise and their applicability to GAF combat aircraft p 152 N93-10690
Study results on combat aircraft source noise reduction p 152 N93-10691
Reduction of propeller noise by active noise control p 152 N93-10692
ENGINE PARTS
Uprated OMS engine status: Altitude testing results p 22 N93-10036
Theoretical and experimental investigations concerning the structural integrity of aeroengine compressor discs p 10 N93-10539
ENGINE TESTS
Noise studies for environmental impact assessment of an outdoor engine test facility p 149 N93-10672
ENTHALPY
Study of improved methods for predicting chemical equilibria
[DE92-016974] p 31 N93-10436
ENTROPY
Study of improved methods for predicting chemical equilibria
[DE92-016974] p 31 N93-10436
Entropy of disorder in thermomechanics of damage in heterogeneous solids p 50 N93-10498
Stochastic diffusion and Kolmogorov entropy in regular and random Hamiltonians
[DE92-016179] p 170 N93-10604
ENVIRONMENT EFFECTS
Format and structure of a database on health and environmental impacts of different energy systems for electricity generation
[DE92-634160] p 130 N93-10222
The Deposition and Fate of Trace Metals in our Environment: Symposium proceedings
[PB92-189216] p 104 N93-10289
Analysis of air pollution and greenhouse gases
[DE92-014955] p 104 N93-10384
ENVIRONMENT MANAGEMENT
Quality assurance practices for data entry and electronic data transfer
[DE92-014804] p 172 N93-10396
ENVIRONMENT MODELS
Gridded Model Information Support System (GMISS) user's guide. Volume 3: Model concentration data retrieval subsystem
[PB92-190263] p 171 N93-10257
Spatial models of ecological systems and processes: The role of GIS
[DE92-016684] p 175 N93-10788
ENVIRONMENT POLLUTION
Format and structure of a database on health and environmental impacts of different energy systems for electricity generation
[DE92-634160] p 130 N93-10222
Remote sensing data for monitoring and evaluating burned areas: Case of Emas National Park (GO)
[INPE-5312-PRE/1709] p 102 N93-10373
ENVIRONMENT PROTECTION
Remote sensing data for monitoring and evaluating burned areas: Case of Emas National Park (GO)
[INPE-5312-PRE/1709] p 102 N93-10373
Sensitivity of modeled ozone concentrations to uncertainties in biogenic emissions
[PB92-192202] p 105 N93-10432
ENVIRONMENTAL CONTROL
Rotorcraft en route ATC route standards
[AD-A249129] p 6 N93-10323
ENVIRONMENTAL MONITORING
Quality assurance practices for data entry and electronic data transfer
[DE92-014804] p 172 N93-10396
Climate Monitoring and Diagnostics Laboratory
[PB92-162346] p 105 N93-10772
ENVIRONMENTAL SURVEYS
Stereoscopy and paralax in the vertical distances determination using aerial photographs
[INPE-5363-PUD/049] p 102 N93-10063
Noise studies for environmental impact assessment of an outdoor engine test facility p 149 N93-10672
ENVIRONMENTAL TESTS
LDEF Materials Workshop 1991, part 2
[NASA-CP-3162-PT-2] p 37 N93-10578
Selected results for metals from LDEF experiment A0171 p 34 N93-10579
Some results of the oxidation investigation of copper and silver samples flown on LDEF p 34 N93-10580
Changes in oxidation state of chromium during LDEF exposure p 34 N93-10581
Effect of space exposure on pyroelectric infrared detectors p 38 N93-10582
Long Duration Exposure Facility (LDEF) optical systems SIG summary and database p 38 N93-10583
Polymer matrix composites on LDEF experiments M0003-9 and M0003-10 p 38 N93-10584
Space environmental effects on LDEF low Earth orbit exposed graphite reinforced polymer matrix composites p 38 N93-10585
Additional results on space environmental effects on polymer matrix composites: Experiment A0180 p 38 N93-10586
Proposed test program and data base for LDEF polymer matrix composites p 38 N93-10587
Effects of long-term exposure on LDEF fastener assemblies p 39 N93-10590
Results from testing and analysis of solar cells flown on LDEF p 39 N93-10591
System related testing and analysis of FRECOPA p 39 N93-10592
EPITAXY
Epitaxial growth and dopant incorporation in diamond
[AD-A253636] p 165 N93-10206
Spectroscopic differential reflectance as an analytical probe for microelectronic processing
[AD-A253134] p 73 N93-10656
Scanning tunneling microscopy of semiconductor surfaces
[AD-A246853] p 168 N93-10726
Improved gallium nitride and aluminum nitride electronic materials
[AD-A253785] p 76 N93-10888
EPITHELIUM
Understanding mechanisms of carcinogenesis using rat tracheal epithelial cells in vitro
[DE92-013510] p 131 N93-10626
EPOXY MATRIX COMPOSITES
Additional results on space environmental effects on polymer matrix composites: Experiment A0180 p 38 N93-10586
EQUATIONS OF MOTION
On the gravitational potential of two arbitrary rotating bodies with applications to the Earth-Moon system p 179 N93-10303
Wiggly relativistic strings
[DE92-016461] p 170 N93-10434
Effective formulation of the dynamics of a manipulator based on the Appell equations p 65 N93-10571
RHALE: A MMALE shock physics code for arbitrary meshes
[DE92-017051] p 139 N93-10866
EQUATIONS OF STATE
Calculation of elastic-plastic wave propagation on the connection machine
[AD-A252429] p 95 N93-10427
Wiggly relativistic strings
[DE92-016461] p 170 N93-10434
Investigations of the motion of discrete-velocity gases
[AD-A253728] p 84 N93-10895
EQUILIBRIUM EQUATIONS
An elastic oblate axisymmetric reference gyro for attitude studies p 54 N93-10518
EQUILIBRIUM METHODS
A reappraisal of compound equilibrium finite elements p 63 N93-10561
EROSION
The Zhamanshin impact feature: A new class of complex crater? p 110 N93-10139
Fundamental studies on erosion in MPD thrusters
[AD-A253900] p 159 N93-10252
ERROR ANALYSIS
A new test of scanning and monitoring ability: Methods and initial results
[AD-A249123] p 132 N93-10321
Data reduction analysis for the Stanford relativity gyroscope experiment p 86 N93-10347
The problem of the selection of an a-posteriori error indicator based on smoothening techniques
[AD-A253401] p 144 N93-10407
Artificial neural network system for memory modification
[AD-D015354] p 142 N93-10958
Memory modification of artificial neural networks
[AD-D015356] p 143 N93-10959
ERROR CORRECTING CODES
The mechanical verification of a simple control system
[ORA-TR-89-5443-04] p 142 N93-10641
ERROR FUNCTIONS
Comparative study of the MTFA, ICS, and SQRI image quality metrics for visual display systems
[AD-A252116] p 158 N93-10708
ERRORS
The problem of the selection of an a-posteriori error indicator based on smoothening techniques
[AD-A253401] p 144 N93-10407
Air traffic control visual scanning
[DOT/FAA/CT-TN92/16] p 7 N93-10459
ESSENTIALLY NON-OSCILLATORY SCHEMES
Computational fluid dynamics capability for internally carried store separation
[AD-A253671] p 79 N93-10297
Numerical study of the small scale structures in Boussinesq convection
[NASA-CR-189695] p 145 N93-10758
ESTERS
Materials compatibility and lubricants research on CFC-refrigerant substitute: Miscibility of lubricants with refrigerants
[DE92-015118] p 35 N93-10084
ESTIMATING
Resistive Grid Kernel Estimator (RGKE)
[AD-A253520] p 147 N93-10869
ESTIMATORS
The problem of the selection of an a-posteriori error indicator based on smoothening techniques
[AD-A253401] p 144 N93-10407
ETALONS
Thermo-optical switching in Si based etalons
[AD-A253139] p 88 N93-10412
Investigations of the dynamics and thermodynamics of the mesosphere lower thermosphere and upper thermosphere at the polar regions with optical ground-based remote sensing
[AD-A253228] p 125 N93-10711
ETCHING
Comparison of Cl and HCl adsorption on Si(100)-(2 x 1)
[AD-A252802] p 30 N93-10281
Pre-oxidation anneal kinetics: Interface degradation of thin SiO2 films on silicon
[AD-A253142] p 30 N93-10414
ETHANE
Temperature-programmed oxidation of ethane and ethylene in the presence and absence of C-13 labeled methane
[DE92-015048] p 42 N93-10329
ETHYL ALCOHOL
Biological production of ethanol from coal
[DE92-016116] p 41 N93-10216
Biological production of ethanol from coal
[DE92-016114] p 43 N93-10608
ETHYLENE
Temperature-programmed oxidation of ethane and ethylene in the presence and absence of C-13 labeled methane
[DE92-015048] p 42 N93-10329
EUCLIDEAN GEOMETRY
Quantum tunneling and the change in the signature of the spacetime metric
[DE92-634877] p 165 N93-10225
EULER EQUATIONS OF MOTION
Improved numerical simulation of Euler equations p 80 N93-10309
Progress in multi-dimensional upwind differencing
[NASA-CR-189708] p 83 N93-10808
EULER-LAGRANGE EQUATION
Numerical simulation of unsteady flow in a nozzle p 16 N93-10008
Three dimensional curved beam elements with large translations and rotations p 63 N93-10560
EUROPEAN SPACE AGENCY
Guide to the user requirements definition phase
[ESA-PSS-05-02-ISSUE-1] p 136 N93-10315
Guide to the software requirements definition phase
[ESA-PSS-05-03-ISSUE-1] p 136 N93-10316

Reliability assurance requirements for ESA space systems
[ESA-PSS-01-30-ISSUE-2] p 94 N93-10317

EUTECTIC COMPOSITES
Semiconductor-metal eutectic composites for high power switching
[AD-A253930] p 74 N93-10755

EUTECTICS
Reactions of Ti and Zr with AlN and Al2O3
[DE92-016234] p 28 N93-10391

EVALUATION
Research in the optical sciences
[AD-A253188] p 158 N93-10446
Order statistics and nonparametric statistics
[AD-A253574] p 146 N93-10699
KC-135 crew reduction feasibility demonstration simulation study. Volume 3: Test and evaluation
[AD-A253931] p 134 N93-10713

EXCAVATION
The large impact process inferred from the geology of lunar multiring basins p 121 N93-10184

EXCIMER LASERS
The interaction of UV-Laser radiation with metal and semiconductor surfaces
[AD-A253510] p 87 N93-10201

EXCITATION
Advanced transport systems for electron beams in high-brightness accelerators and FEL's
[AD-A253314] p 88 N93-10286
Electron transfer, ionization, and excitation in atomic collisions
[DE92-017300] p 154 N93-10435
Evolutionary spectra of time-dependent discretized systems to time-frequency modulated random excitations p 55 N93-10524

EXHAUST GASES
Alternatives in clean propellants for large scale man-rated solid rocket motors p 20 N93-10028
Pitot survey of exhaust flow field of a 2-D scramjet nozzle at Mach 6 with air or freon and argon used for exhaust simulation
[NASA-TM-4361] p 2 N93-10071

EXHAUST NOZZLES
Altitude compensating nozzle evaluation p 22 N93-10037
Pitot survey of exhaust flow field of a 2-D scramjet nozzle at Mach 6 with air or freon and argon used for exhaust simulation
[NASA-TM-4361] p 2 N93-10071
Supersonic acoustic source mechanisms for free jets of various geometries p 150 N93-10680
Nozzle installation effects on the noise from supersonic exhaust plumes p 150 N93-10681

EXOBIOLOGY
Aerospace medicine and biology: A continuing bibliography with indexes (supplement 365)
[NASA-SP-7011(365)] p 130 N93-10075
Aerospace medicine and biology: A continuing bibliography with indexes (supplement 360)
[NASA-SP-7011(360)] p 130 N93-10076
Aerospace medicine and biology: A continuing bibliography with indexes (supplement 364)
[NASA-SP-7011(364)] p 130 N93-10077
Aerospace medicine and biology: A continuing bibliography with indexes (supplement 366)
[NASA-SP-7011(366)] p 130 N93-10079
Aerospace medicine and biology: A continuing bibliography with indexes (supplement 367)
[NASA-SP-7011(367)] p 130 N93-10080

EXOTHERMIC REACTIONS
Pulsed jet plume combustion: An exothermic process under fluid mechanical control p 32 N93-10553

EXPANDABLE STRUCTURES
A new deployable mast p 14 N93-10511
Effect of mounting offset on the dynamics of deploying flexible appendages p 54 N93-10520

EXPANSION
Effect of mounting offset on the dynamics of deploying flexible appendages p 54 N93-10520

EXPERIMENTATION
Numerical simulation of transient crack growth p 48 N93-10488

EXPERT SYSTEMS
Automatic cloud classification from multi-spectral satellite data over oceanic regions
[AD-A253670] p 126 N93-10292
Handbook for operating the OWLKNEST technology
[AD-A253412] p 137 N93-10409
PRODIGY4.0: The manual and tutorial
[AD-A253970] p 137 N93-10422
Analysis of observation report databases/knowledge bases
[AD-A252636] p 172 N93-10428
TAQL: A problem space tool for expert system development
[AD-A253820] p 175 N93-10826

EXPLOSIONS
Simulated meteorite impacts and volcanic explosions: Ejecta analyses and planetary implications p 111 N93-10143
Internal explosion in laser ablation of superconducting targets
[AD-A253701] p 90 N93-10799

EXPLOSIVES
Impact sensitivity reduction via exo-electron control p 15 N93-10004

EXPOSURE
Dermal exposure assessment: Principles and applications
[PB92-205665] p 131 N93-10438

EXTERNAL STORE SEPARATION
Computational fluid dynamics capability for internally carried store separation
[AD-A253671] p 79 N93-10297

EXTINCTION
Noril'sk/Siberian plateau basalts and Bahama hot spot: Impact triggered? p 109 N93-10132
Meteorological and site influences affecting the comparison of nephelometer and photographic determinations of light extinction at rural sites in the Eastern US
[PB92-195999] p 126 N93-10433

EXTRATERRESTRIAL RADIATION
Power spectrum of the extragalactic background light p 177 N93-10364

EXTRAVEHICULAR ACTIVITY
Extravehicular activity compatibility evaluation of developmental hardware for assembly and repair of precision reflectors
[NASA-TP-3246] p 13 N93-10744

EXTREME ULTRAVIOLET RADIATION
EUV complementary instrumentation for SIMURIS p 14 N93-10938

EYE (ANATOMY)
Eye movements and visual information processing
[AD-A250198] p 132 N93-10278

EYE MOVEMENTS
Eye movements and visual information processing
[AD-A250198] p 132 N93-10278

F

F-18 AIRCRAFT
Design and implementation of digital filters for analysis of F/A-18 flight test data
[AD-A253447] p 3 N93-10342

FABRICATION
Formed platelets for low cost regeneratively cooled rocket combustion chambers p 18 N93-10018
Feasibility evaluation of the monolithic braided ablative nozzle p 19 N93-10023
Effects of anode material on arcjet performance
[NASA-TM-105799] p 25 N93-10197
Ceramic transactions. Volume 21: Proceedings of the Symposium on Microwave Theory and Application in Materials Processing Annual Meeting No. 23 io on april 29-may 3 1991
[AD-A253631] p 35 N93-10205
Methodology for the computer-aided design of silicon micromachined devices in a standard CMOS process
[PB92-191246] p 136 N93-10248
Air cell --- model aircraft power supplies
[CA-PATENT-APPL-SN-2001346] p 72 N93-10368
Conductive titanate fiber and its production method
[DE92-014738] p 39 N93-10627
Automated handling and assembling of non-rigid objects
[AD-A253605] p 66 N93-10649
Advanced processing and characterization technologies. Fabrication and characterization of semiconductor optoelectronic devices and integrated circuits. Final Conference Proceedings No. 10
[AD-A254162] p 73 N93-10663

FABRY-PEROT INTERFEROMETERS
High resolution granulation spectrophotometry with a UBF and a FP interferometer in tandem p 183 N93-10927

FACSIMILE COMMUNICATION
Technology for libraries and information centers: A seminar in Greece, Portugal, and Turkey p 174 N93-10601

FACTORIZATION
An implementation of the MVDR beamformer on the Intel iWarp system
[AD-A253641] p 140 N93-10209
A look at scalable dense linear algebra libraries
[DE92-017805] p 143 N93-10285
The class of the paths in the Feynman path integral on the phase space
[DE92-630205] p 170 N93-10386

FAILURE
Review and analysis of check valve failure data
[DE92-014462] p 91 N93-10381

FAILURE ANALYSIS
Hot fire test results of subscale tubular combustion chambers p 18 N93-10020
Composite failure analysis handbook. Volume 2: Technical handbook. Part 2: Atlas of fractographs
[AD-A249130] p 28 N93-10325
Failure processes in elastomeric composites p 46 N93-10475
Damage due to plastic deformation in elastic-plastic materials: The thermodynamical connection p 51 N93-10502
Failure analysis of laminated composites by using iterative three-dimensional finite element method p 51 N93-10505
Analysis of failure modes in ceramic matrix composite p 28 N93-10508
Identification and evaluation of lubricants, adhesives, and seals used on LDEF p 39 N93-10588
Emergency Diesel Generator reliability at Department of Energy (DOE) facilities
[DE92-011888] p 91 N93-10622
Inspection and repair decisions for hydraulic structures under symmetric deterioration
[AD-A253621] p 96 N93-10797
The total time on test statistic and age-dependent censoring
[AD-A253622] p 147 N93-10798
Linear and nonlinear analyses of thick composite circular plates using the finite element method p 96 N93-10873

FAILURE MODES
System model development for nuclear thermal propulsion
[NASA-TM-105761] p 25 N93-10457
Failure analysis of laminated composites by using iterative three-dimensional finite element method p 51 N93-10505
Analysis of failure modes in ceramic matrix composite p 28 N93-10508
A spline finite strip method for analysing local and distortional buckling of thin-walled beams under arbitrary loading p 58 N93-10538

FAR FIELDS
Far-zone field of a monopole element on a disk ground plane above flat earth
[AD-A253580] p 70 N93-10091

FAR ULTRAVIOLET RADIATION
UV/XUV FEL storage ring and linac
[AD-A253307] p 89 N93-10697
Photoionization dynamics and cation spectroscopy with coherent VUV radiation
[DE92-015841] p 154 N93-10730
A multipurpose vacuum-ultraviolet test facility p 11 N93-10953

FARM CROPS
Resource capture by single leaves
[DE92-015847] p 129 N93-10461

FAST FOURIER TRANSFORMATIONS
Nonlinear signal processing schemes for robust target detection and automatic clutter rejection in radar
[AD-A253546] p 68 N93-10380

FASTENERS
Effects of long-term exposure on LDEF fastener assemblies p 39 N93-10590

FATIGUE (MATERIALS)
Experimental and numeric analysis of constraints in a bonded stepped lap joint subjected to traction p 54 N93-10516
Mechanisms and modelling of environment-dependent fatigue crack growth in a nickel based superalloy
[AD-A253967] p 33 N93-10717

FATIGUE LIFE
Hot fire test results of subscale tubular combustion chambers p 18 N93-10020
Hot fire fatigue testing results for the compliant combustion chamber p 22 N93-10038
Structural analysis: Fatigue life assessment p 78 N93-10062
An evaluation of a method of reconstituting fatigue loading from Rainflow counting
[RAE-TR-89057] p 94 N93-10198
A finite element method for nonlinear panel flutter p 45 N93-10472
An evaluation of the cumulative damage effect under creep loading p 58 N93-10540
Fatigue crack propagation in the presence of shot-peening residual stresses p 59 N93-10542
Hot fire fatigue testing results for the compliant combustion chamber
[NASA-TP-3223] p 26 N93-10743

FATIGUE TESTS
Improvements to the AC potential drop method of crack measurement p 59 N93-10543

FAULT TOLERANCE
Interactive animation of fault tolerant parallel algorithms
[AD-A253349] p 135 N93-10212
Fault-tolerant and efficient parallel computation
[AD-A253350] p 140 N93-10213
Recovery techniques for real time electronic systems
[AD-A254010] p 136 N93-10361

FEASIBILITY ANALYSIS
Feasibility evaluation of the monolithic braided ablative nozzle p 19 N93-10023
Molded nozzle technology for large solid rocket motors p 19 N93-10024
Mental workload assessment in the cockpit: Feasibility of using electrophysiological measurements, phase 1
[AD-A254138] p 133 N93-10662
KC-135 crew reduction feasibility demonstration simulation study. Volume 3: Test and evaluation
[AD-A253931] p 134 N93-10713

FEEDBACK CONTROL
Design, test, and evaluation of three active flutter suppression controllers
[NASA-TM-4338] p 10 N93-10070
Numerical simulation of large actively controlled space structures p 13 N93-10308
Optimal sample policies for multirate digital control p 141 N93-10346

FELDSPARS
Optical and TEM study of shock metamorphism from the Sedan test site p 111 N93-10142

FERMENTATION
Biological production of ethanol from coal
[DE92-016116] p 41 N93-10216
Biological production of ethanol from coal
[DE92-016114] p 43 N93-10608

FERMI SURFACES
Atomic short range order and spin density wave propagation in CuMn
[DE92-016903] p 34 N93-10789

FERMIONS
Electronic structure of highly correlated structures
[DE92-017017] p 155 N93-10863

FERROELECTRICITY
Piezoelectric and electrostrictive materials for transducers applications, volume 1
[AD-A250889] p 71 N93-10273
Piezoelectric and electrostrictive materials for transducers applications, volume 2
[AD-A250890] p 71 N93-10276
Piezoelectric and electrostrictive materials for transducers applications, volume 3
[AD-A250891] p 72 N93-10280
Piezoelectric and electrostrictive materials for transducers applications, volume 4
[AD-A250892] p 72 N93-10282

FEYNMAN DIAGRAMS
The class of the paths in the Feynman path integral on the phase space
[DE92-630205] p 170 N93-10386

FIBER COMPOSITES
Sensor and actuator materials for high performance composites
[AD-A254178] p 27 N93-10254
Ultrasonic characterization of highly attenuative thick composites
[AD-A253347] p 27 N93-10272
Damage accumulation process in advanced metal matrix composite under thermal cycling
[AD-A248674] p 27 N93-10277
Composite failure analysis handbook. Volume 2: Technical handbook. Part 2: Atlas of fractographs
[AD-A249130] p 28 N93-10325
Integrated finite element model of composite materials p 46 N93-10477
Compression buckling of thick orthotropic plates with a step thickness change p 46 N93-10478
Analysis of failure modes in ceramic matrix composite p 28 N93-10508
Inhibiting corrosion in Gr/Al and Gr/Mg metal matrix composites using nonequilibrium alloying techniques
[AD-A253923] p 34 N93-10752
Mechanics of composite materials for spacecraft
[AD-A254217] p 28 N93-10896

FIBER OPTICS
Geometrical transformation of linear diode-laser arrays for longitudinal pumping of solid-state lasers
[AD-A253415] p 87 N93-10218

FIBERS
Conductive titanate fiber and its production method
[DE92-014738] p 39 N93-10627

FIELD EFFECT TRANSISTORS
Development of 6H-SiC CMOS transistors for insertion into a 350 C operational amplifier
[AD-A253760] p 70 N93-10233
VLSI design for reliability - hot electron
[AD-A253942] p 74 N93-10715

FIELD EMISSION
Field emission current-voltage curves as a diagnostic for scanning tunneling microscope tips
[AD-A251171] p 165 N93-10245
Field-emitter arrays for RF vacuum microelectronics
[AD-A253396] p 73 N93-10405
A semiempirical formula for calculating the coefficients for field emission tip forms
[AD-A254109] p 145 N93-10857

FIELD THEORY (PHYSICS)
Semiclassical quantization of interacting anyons in a strong magnetic field
[DE92-634889] p 169 N93-10229
Symmetry breaking and localization in quantum chaotic systems
[DE92-634890] p 170 N93-10294
Wiggly relativistic strings
[DE92-016461] p 170 N93-10434
Research in particle physics beyond the standard model
[DE92-012240] p 155 N93-10878

FIGHTER AIRCRAFT
Combat Aircraft Noise
[AGARD-CP-512] p 148 N93-10666
Combat aircraft noise: The operator's perspective p 148 N93-10669
Combat aircraft jet engine noise studies p 150 N93-10679
Supersonic acoustic source mechanisms for free jets of various geometries p 150 N93-10680
Identifying the principal noise sources of fixed-wing combat aircraft in high-speed flight p 151 N93-10686
Measurement and prediction of noise from low-altitude military aircraft operations p 151 N93-10687
Combat aircraft noise reduction by technical measures p 152 N93-10689
Technical measures for the attenuation of aircraft noise and their applicability to GAF combat aircraft p 152 N93-10690
Study results on combat aircraft source noise reduction p 152 N93-10691
Hydrodynamic investigation of vortical flows for an ATTAC configuration with canards
[AD-A253928] p 4 N93-10753

FILAMENT WINDING
Transverse tension, transverse compression, and inplane shear JANNAF round robin test methods standardization results p 16 N93-10007

FILE MAINTENANCE (COMPUTERS)
A standard file format for data interchange
[AD-A254260] p 176 N93-10899

FILM BOILING
Boiling behavior of sodium-potassium alloy in a bench-scale solar receiver
[DE92-014947] p 103 N93-10383

FILM THICKNESS
Thermo-optical switching in Si based etalons
[AD-A253139] p 88 N93-10412

FILTERS
Single crystal growth of beta-Al2O3 for iso-index filters
[AD-A252259] p 169 N93-10879

FILTRATION
Alternate spectrometric oil analysis techniques
[AD-A253355] p 29 N93-10101

FINE STRUCTURE
Epitaxial growth and dopant incorporation in diamond
[AD-A253636] p 165 N93-10206
Chromospheric structure and dynamics p 180 N93-10906
The fine structure of prominences p 180 N93-10910
Evidence of plasmoid ejection in the corona from 1991 eclipse observations with the Canada-France-Hawaii telescope p 181 N93-10915

FINITE DIFFERENCE THEORY
Finite difference methods for incompressible viscous flow in scientific computing
[AD-A253512] p 79 N93-10220
Numerical simulation of the propagation of coupled thermomechanical waves in inelastic solids p 64 N93-10568
Progress in multi-dimensional upwind differencing
[NASA-CR-189708] p 83 N93-10808
Investigations of the motion of discrete-velocity gases
[AD-A253728] p 84 N93-10895

FINITE ELEMENT METHOD
Instrumented propellant block test and stress analysis comparison p 15 N93-10002
A three-dimensional analysis of the effect of local stress distribution near crack tip p 15 N93-10003
Numerical simulation of unsteady flow in a nozzle p 16 N93-10008
LAM actuated propellant flow control device p 18 N93-10017
What can we learn about impact mechanics from large craters on Venus? p 118 N93-10166
A globally well-posed accurate and efficient finite element CFD algorithm for compressible aerodynamics p 3 N93-10306
Numerical simulation of large actively controlled space structures p 13 N93-10308
Effects of gravity in folding --- of geological layers p 124 N93-10324
SAPNEW: Parallel finite element code for thin shell structures on the Alliant FX/80
[NASA-CR-190663] p 94 N93-10372
The problem of the selection of an a-posteriori error indicator based on smoothening techniques
[AD-A253401] p 144 N93-10407
A finite element method for nonlinear panel flutter p 45 N93-10472
Vibration of laminated composite plates using various plate theories: Analytical and finite element results p 45 N93-10473
Integrated finite element model of composite materials p 46 N93-10477
Contact problem in delamination-buckling of laminated composite shells p 46 N93-10479
On the behavior of a higher-order plate bending element p 47 N93-10481
Enriched element analysis of bimaterial interface cracks p 47 N93-10484
Evolution of hybrid-Trefftz FE model: State of the art and future trends p 49 N93-10494
A multilayered shell finite element p 49 N93-10495
Hexagonal and octagonal finite elements p 50 N93-10500
Singular stress distributions at circular holes in composite laminates p 51 N93-10503
Failure analysis of laminated composites by using iterative three-dimensional finite element method p 51 N93-10505
Investigation of laminated composite plates under impact dynamic loading by using a three-dimensional hybrid stress finite element method p 29 N93-10510
Vibrations of a flexible Timoshenko beam under gravity p 53 N93-10512
Natural vibrations of multilayered doubly curved shells p 57 N93-10532
On the vibration of axisymmetric shells p 57 N93-10535
The vibrations of annular discs: A comparison of experimental and two analytical techniques p 58 N93-10536
A spline finite strip method for analysing local and distortional buckling of thin-walled beams under arbitrary loading p 58 N93-10538
Stream function-vorticity finite element formulations of unsteady incompressible Navier-Stokes equations p 60 N93-10545
A least-squares finite element method for incompressible Navier-Stokes problem p 60 N93-10548
An adaptive mesh-management algorithm for three-dimensional automatic finite element analysis p 61 N93-10554
Variational formulation of a mixed method for second order frame analysis p 62 N93-10556
A new quadrilateral element for the elastic and plastic analysis of shells p 62 N93-10559
Three dimensional curved beam elements with large translations and rotations p 63 N93-10560
A reappraisal of compound equilibrium finite elements p 63 N93-10561
Evaluation of the triangular plate element of Zienkiewcz and Lefebvre p 63 N93-10562
On the use of coupled finite element boundary element models in numerical design analysis p 63 N93-10563
A boundary element super-element method for coupling with the finite element method of substructures p 64 N93-10566
Solving large linearized systems in mechanics
[AD-A252723] p 144 N93-10639
DYNA2D: A nonlinear, explicit, two-dimensional finite element code for solid mechanics: User manual
[DE92-017310] p 95 N93-10646
FLASH: A finite element computer code for variably saturated flow
[DE92-018038] p 84 N93-10868
Linear and nonlinear analyses of thick composite circular plates using the finite element method p 96 N93-10873

FINITE VOLUME METHOD
Analysis of wing-body junction flowfields using the incompressible Navier-Stokes equations, volumes 1 and 2 p 3 N93-10320
High-speed viscous flows past blunt bodies and compression corners with flux-split methods
[AD-A253413] p 81 N93-10410
Progress in multi-dimensional upwind differencing
[NASA-CR-189708] p 83 N93-10808

FINLAND
Impact cratering record of Fennoscandia
p 119 N93-10171
FIR FILTERS
Design and implementation of digital filters for analysis of F/A-18 flight test data
[AD-A253447] p 3 N93-10342
FIRES
Remote sensing data for monitoring and evaluating burned areas: Case of Emas National Park (GO)
[INPE-5312-PRE/1709] p 102 N93-10373
FIXED WINGS
A brief review of the source noise technology applicable to fixed-wing military aircraft p 150 N93-10678
FIZEAU EFFECT
Ground-based high angular resolution observation of the Sun by interferometry in the visible p 177 N93-10941
FLAME IONIZATION
Development of laser excited atomic fluorescence and ionization methods
[DE92-016199] p 89 N93-10611
FLAME PROPAGATION
Combustion-wave ignition for rocket engines
p 17 N93-10016
FLAME TEMPERATURE
Alternatives in clean propellants for large scale man-rated solid rocket motors p 20 N93-10028
FLAMES
Emission tomography of sodium in a hydrogen-air flame
[AD-A253530] p 29 N93-10224
Combustion in turbulent jets and buoyant flames
[PB92-211481] p 31 N93-10437
FLAPS (CONTROL SURFACES)
Initial piloted simulation study of geared flap control for tilt-wing V/STOL aircraft
[NASA-TM-103872] p 11 N93-10741
FLASHOVER
High-power microwave breakdown of dielectric interfaces
[AD-A254200] p 124 N93-10262
FLAT PLATES
Dynamic stability of laminated transversely-isotropic composite plates subjected to parametric excitations
p 29 N93-10525
FLEXIBLE BODIES
Characterization of and active control of flexible structures, using piezoceramics as sensors and actuators p 10 N93-10319
Vibrations of a flexible Timoshenko beam under gravity p 53 N93-10512
Dynamics of an orbiting flexible manipulator
p 54 N93-10519
Effect of mounting offset on the dynamics of deploying flexible appendages p 54 N93-10520
Modelling of flexible multibody dynamics and a computer method via the bond graph method p 65 N93-10573
Chaotic oscillation of a high speed flexible arm robot
p 65 N93-10574
Automated handling and assembling of non-rigid objects
[AD-A253605] p 66 N93-10649
FLEXIBLE SPACECRAFT
A solution scheme for the deflection equations of flexible arms with time-dependent boundary conditions
p 66 N93-10575
FLEXIBLE WINGS
Design, test, and evaluation of three active flutter suppression controllers
[NASA-TM-4338] p 10 N93-10070
FLIGHT CONDITIONS
Weather Message Switching Center Replacement (WMSCR) Operational Test and Evaluation (OT/E)/integration test plan
[DOT/FAA/CT-TN90/59] p 7 N93-10833
FLIGHT CREWS
Operator workload predictions for the revised AH-64A workload prediction model, volume 1
[AD-A254198] p 133 N93-10261
Combat aircraft operations: Training requirements for the German Air Force tactical flying units and the noise problem p 148 N93-10667
Possibilities and limitations of flying training in the German Air Force p 11 N93-10668
KC-135 crew reduction feasibility demonstration simulation study. Volume 3: Test and evaluation
[AD-A253931] p 134 N93-10713
Relating flying hours to aircrew performance: Evidence for attack and transport missions
[AD-A253988] p 133 N93-10719
FLIGHT MECHANICS
Methods of guidance flight dynamics
[AD-A254248] p 10 N93-10704
FLIGHT OPERATIONS
Combat aircraft operations: Training requirements for the German Air Force tactical flying units and the noise problem p 148 N93-10667
Measurement and prediction of noise from low-altitude military aircraft operations p 151 N93-10687
FLIGHT SIMULATION
Possibilities and limitations of flying training in the German Air Force p 11 N93-10668
KC-135 crew reduction feasibility demonstration simulation study. Volume 3: Test and evaluation
[AD-A253931] p 134 N93-10713
Initial piloted simulation study of geared flap control for tilt-wing V/STOL aircraft
[NASA-TM-103872] p 11 N93-10741
FLIGHT TESTS
Computational fluid dynamics capability for internally carried store separation
[AD-A253671] p 79 N93-10297
Design and implementation of digital filters for analysis of F/A-18 flight test data
[AD-A253447] p 3 N93-10342
Identifying the principal noise sources of fixed-wing combat aircraft in high-speed flight p 151 N93-10686
Appraisal of digital terrain elevation data for low-altitude flight
[NASA-TM-103896] p 7 N93-10745
Flight test and analysis procedures for new handling criteria
[RAE-TM-FM-26] p 8 N93-10803
FLIGHT TIME
Relating flying hours to aircrew performance: Evidence for attack and transport missions
[AD-A253988] p 133 N93-10719
FLIGHT TRAINING
Combat aircraft operations: Training requirements for the German Air Force tactical flying units and the noise problem p 148 N93-10667
Possibilities and limitations of flying training in the German Air Force p 11 N93-10668
Combat aircraft noise: The operator's perspective
p 148 N93-10669
Human noise exposure criteria for combat aircraft training areas p 148 N93-10670
KC-135 crew reduction feasibility demonstration simulation study. Volume 3: Test and evaluation
[AD-A253931] p 134 N93-10713
FLOW CHARACTERISTICS
Hypersonic inlet efficiency revisited p 5 N93-10012
The structure and development of streamwise vortex arrays embedded in a turbulent boundary layer
p 81 N93-10371
A study of flow properties of wet solids using laser induced photochemical anemometry
[DE92-015483] p 82 N93-10629
Hydrodynamic investigation of vortical flows for an ATTAC configuration with canards
[AD-A253928] p 4 N93-10753
Characteristics of separated flows including cavitation effects p 84 N93-10874
FLOW COEFFICIENTS
Performance parameters and assessment
p 77 N93-10052
FLOW DISTRIBUTION
A building-block approach for turbulence model validation/upgrade focussed on high-speed jet flowfields
p 16 N93-10010
Facility for cold flow testing of solid rocket motor models p 11 N93-10021
Introduction to radial turbine technology
p 77 N93-10051
An inverse design method for radial turbomachines
p 78 N93-10057
The integration of geometric modeling into an inverse design method and application of a PC-based inverse design method and comparison with test results
p 78 N93-10058
Pitot survey of exhaust flow field of a 2-D scramjet nozzle at Mach 6 with air or freon and argon used for exhaust simulation
[NASA-TM-4361] p 2 N93-10071
Species and temperature measurement in H2/O2 rocket flow fields by means of Raman scattering diagnostics
[NASA-CR-189217] p 25 N93-10086
Forced unsteady separated flows on a 45 degree delta wing p 80 N93-10305
Analysis of wing-body junction flowfields using the incompressible Navier-Stokes equations, volumes 1 and 2 p 3 N93-10320
Explicit Navier-Stokes computation of turbomachinery flows p 81 N93-10370
LDV Measurements of unsteady flow fields in radial turbine
[AD-A253592] p 4 N93-10648
Echo characteristic analysis of the nonequilibrium wakes of reentry vehicle
[AD-A254249] p 13 N93-10705
Effect of planform and body on supersonic aerodynamics of multibody configurations
[NASA-TP-3212] p 4 N93-10824
The effects of streamline curvature and swirl on turbulent flows in curved ducts p 84 N93-10875
Study of a viscous sublayer model in the analysis of 3-D shock/boundary layer interaction flow fields
[AD-A253731] p 84 N93-10886
Compressible and incompressible fluid seals: Influence on rotordynamic response and stability
[NASA-CR-190746] p 92 N93-10891
Experimental study of the flow field inside a whirling annular seal p 92 N93-10892
Turbulence measurements of high shear flow fields in a turbomachine seal configuration p 93 N93-10893
An experimental technique for performing 3-D LDA measurements inside whirling annular seals
p 93 N93-10894
FLOW EQUATIONS
Navier-Stokes turbine heat transfer predictions using two-equation turbulence
[NASA-TM-105817] p 82 N93-10735
FLOW GEOMETRY
A new energy transfer model for turbulent free shear flow
[NASA-TM-105854] p 81 N93-10454
Structure of thermocapillary flow in narrow cavities
p 61 N93-10552
FLOW MEASUREMENT
LV software for supersonic flow analysis
[NASA-CR-190911] p 2 N93-10069
A study of flow properties of wet solids using laser induced photochemical anemometry
[DE92-015483] p 82 N93-10629
Turbulence measurements of high shear flow fields in a turbomachine seal configuration p 93 N93-10893
An experimental technique for performing 3-D LDA measurements inside whirling annular seals
p 93 N93-10894
FLOW STABILITY
Mathematical analysis of strong fluid mechanical effects at high Mach number in reactive and nonreactive flow
[AD-A253617] p 79 N93-10094
Turbulent mixing in compressible free shear layers
p 83 N93-10846
FLOW VELOCITY
A study of flow properties of wet solids using laser induced photochemical anemometry
[DE92-015483] p 82 N93-10629
Influence of flow velocity on the output power of high pressure CW CO2 lasers
[AD-A254240] p 89 N93-10722
Numerical solution of three-dimensional unsteady viscous flows
[AD-A253202] p 83 N93-10793
Experimental study of the flow field inside a whirling annular seal p 92 N93-10892
FLOW VISUALIZATION
Tilt rotor hover aeroacoustics
[NASA-CR-177598] p 147 N93-10458
Hydrodynamic investigation of vortical flows for an ATTAC configuration with canards
[AD-A253928] p 4 N93-10753
FLUID DYNAMICS
Molecular dynamics of shocks in crystals with defects
[AD-A253353] p 164 N93-10099
Nonlinear dynamics underlying atmospheric predictability
[AD-A254042] p 126 N93-10363
FLUID FLOW
Mathematical analysis of strong fluid mechanical effects at high Mach number in reactive and nonreactive flow
[AD-A253617] p 79 N93-10094
Monitoring structural response in pressurized environments. Part 2: Applications
[DE92-015034] p 94 N93-10327
Simple shearing flow of a 3D foam
[DE92-011151] p 36 N93-10399
FLUID MANAGEMENT
Tank chilldown analysis and verification with a flightweight, 175 cu ft tank under normal gravity with liquid hydrogen p 24 N93-10045
Review and analysis of check valve failure data
[DE92-014462] p 91 N93-10381
FLUID PRESSURE
Heat transfer and pressure drop for air flow through enhanced passages
[DE92-016597] p 82 N93-10612
Numerical solution of three-dimensional unsteady viscous flows
[AD-A253202] p 83 N93-10793

FLUID-SOLID INTERACTIONS
Evaluation of the triangular plate element of Zienkiewcz and Lefebvre p 63 N93-10562
FLUOROCARBONS
Chemical and thermal stability of refrigerant-lubricant mixture with metal
[DE92-015117] p 44 N93-10398
FLUTTER ANALYSIS
A finite element method for nonlinear panel flutter p 45 N93-10472
Control of panel flutter at high supersonic speed p 9 N93-10900
FLUX (RATE)
Multidimensional deterministic electron transport calculations
[AD-A254021] p 154 N93-10362
FLUX PINNING
Model for the reversible magnetization of high-(kappa) type-2 superconductors: Application to high-temperature superconductor
[DE92-016297] p 167 N93-10609
FLUX VECTOR SPLITTING
A globally well-posed accurate and efficient finite element CFD algorithm for compressible aerodynamics p 3 N93-10306
High-speed viscous flows past blunt bodies and compression corners with flux-split methods
[AD-A253413] p 81 N93-10410
FLYWHEELS
A study upon structural optimization of elastic rotors for mechanical systems
[INPE-5376-TDI/471] p 94 N93-10310
FOAMS
Simple shearing flow of a 3D foam
[DE92-011151] p 36 N93-10399
Mechanical behavior of open cell ceramics
[PB92-212984] p 37 N93-10439
FOCUSING
Simulation of electron beam transport in ion-focused regime conditioning cells
[AD-A253352] p 70 N93-10215
FOLDING
Effects of gravity in folding --- of geological layers p 124 N93-10324
FOLIAGE
Application of volumetric multiple-scattering approximations to foliage media
[AD-A253337] p 68 N93-10358
FORCE DISTRIBUTION
Harmonic analysis of the aerodynamic forces on a Darrieus rotor p 6 N93-10551
FORCED CONVECTION
Development of the finite analytic method for turbulent forced and free convection p 80 N93-10369
FORCED VIBRATION
Nonstationary random variations of moderately thick plates using BEM p 48 N93-10487
Dynamic stability of laminated transversely-isotropic composite plates subjected to parametric excitations p 29 N93-10525
Response of a beam to transverse impulsive and high frequency loads p 56 N93-10526
Vibration of a damped double-beam system p 56 N93-10527
Development of nonlinear aerodynamic models for unsteady responses p 4 N93-10845
FORMALISM
Local-equilibrium formalism applied to mechanics of solids
[DE92-016852] p 170 N93-10787
FORMAT
A standard file format for data interchange
[AD-A254260] p 176 N93-10899
FOURIER ANALYSIS
Nonlinear aeroelasticity of composite structures
[AD-A254285] p 8 N93-10842
Development of nonlinear aerodynamic models for unsteady responses p 4 N93-10845
FOURIER TRANSFORMATION
IFTS: The Imaging Fourier Transform Spectrometer p 14 N93-10933
Polarimetry with an imaging FTS p 14 N93-10934
Fourier transform spectrometer processing: Data reduction and processor design p 14 N93-10935
First results of an imaging FTS with a NICMOS camera p 86 N93-10936
The imaging Fourier transform spectrometer optical design p 159 N93-10951
The imaging Fourier transform spectrometer: Performance and tolerance analysis p 86 N93-10952
FRACTALS
Box counting multifractal analysis
[AD-A253960] p 144 N93-10419
Fractals and multifractals in fracture p 50 N93-10497
Entropy of disorder in thermomechanics of damage in heterogeneous solids p 50 N93-10498
FRACTIONATION
Ruthenium/iridium ratios in the Cretaceous-Tertiary boundary clay: Implications for global dispersal and fractionation within the ejecta cloud p 109 N93-10135
FRACTOGRAPHY
Composite failure analysis handbook. Volume 2: Technical handbook. Part 2: Atlas of fractographs
[AD-A249130] p 28 N93-10325
FRACTURE MECHANICS
A quasi-Hertzian stress field from an internal source: A possible working model for the Vredefort structure p 106 N93-10115
Composite failure analysis handbook. Volume 2: Technical handbook. Part 2: Atlas of fractographs
[AD-A249130] p 28 N93-10325
Calculation of stress intensity factors in an isotropic multicracked plate: Part 2: Symbolic/numeric implementation
[NASA-TM-105823] p 95 N93-10453
Calculation of stress intensity factors in an isotropic multicracked plate. Part 1: Theoretical development
[NASA-TM-105766] p 95 N93-10455
Enriched element analysis of bimaterial interface cracks p 47 N93-10484
Dynamic crack division in brittle solids p 48 N93-10489
Stress patterns in the dynamic tear test p 49 N93-10491
Fractals and multifractals in fracture p 50 N93-10497
Experimental and numeric analysis of constraints in a bonded stepped lap joint subjected to traction p 54 N93-10516
Mechanisms and modelling of environment-dependent fatigue crack growth in a nickel based superalloy
[AD-A253967] p 33 N93-10717
FRACTURE STRENGTH
Dynamic measurement of the J integral in ductile metals using the optical method of caustics p 49 N93-10492
On the development of a new fracture toughness procedure p 59 N93-10541
Strength-toughness requirements for thick-walled high pressure vessels
[AD-A253756] p 95 N93-10750
FRACTURING
Fractals and multifractals in fracture p 50 N93-10497
Strength-toughness requirements for thick-walled high pressure vessels
[AD-A253756] p 95 N93-10750
FREE CONVECTION
Development of the finite analytic method for turbulent forced and free convection p 80 N93-10369
FREE ELECTRON LASERS
Advanced transport systems for electron beams in high-brightness accelerators and FEL's
[AD-A253314] p 88 N93-10286
UV/XUV FEL storage ring and linac
[AD-A253307] p 89 N93-10697
Studies impacting the designs of free electron lasers
[AD-A254293] p 90 N93-10768
An infrared free-electron laser for the Chemical Dynamics Research Laboratory
[DE92-017018] p 90 N93-10864
FREE ENERGY
Study of improved methods for predicting chemical equilibria
[DE92-016974] p 31 N93-10436
FREE FLOW
Hypersonic inlet efficiency revisited p 5 N93-10012
FREE JETS
Supersonic acoustic source mechanisms for free jets of various geometries p 150 N93-10680
FREE VIBRATION
Axisymmetric vibrations of rotating circular plates using characteristic orthogonal polynomials p 45 N93-10470
Vibrations of a flexible Timoshenko beam under gravity p 53 N93-10512
Free vibrations of the thick circular cylindrical shells and rings p 57 N93-10533
Vibration frequencies of a constrained cantilever wedge p 57 N93-10534
FREON
Pitot survey of exhaust flow field of a 2-D scramjet nozzle at Mach 6 with air or freon and argon used for exhaust simulation
[NASA-TM-4361] p 2 N93-10071
FREQUENCIES
Nonlinear signal processing schemes for robust target detection and automatic clutter rejection in radar
[AD-A253546] p 68 N93-10380
Optical metrology of magnetically trapped hydrogen
[AD-A253229] p 31 N93-10712
FREQUENCY MULTIPLIERS
4.5 micron laser source
[AD-A253367] p 87 N93-10090
FREQUENCY SCANNING
A new test of scanning and monitoring ability: Methods and initial results
[AD-A249123] p 132 N93-10321
FRESH WATER
Spatial models of ecological systems and processes: The role of GIS
[DE92-016884] p 175 N93-10788
FRICTION
The pseudotachylites from the Vredefort structure and the Witwatersrand basin p 119 N93-10174
Viscosity determinations of some frictionally generated silicate melts: Implications for slip zone rheology during impact-induced faulting p 121 N93-10183
A boundary element and mathematical programming approach for unilateral contact problems p 62 N93-10558
FRICTION FACTOR
A boundary element and mathematical programming approach for unilateral contact problems p 62 N93-10558
FRONTS (METEOROLOGY)
Air-sea interaction in regions of varying surface conditions
[AD-A253182] p 128 N93-10791
FUEL CELLS
Advanced materials development for fossil energy conversion applications
[DE92-015762] p 104 N93-10729
FUEL COMBUSTION
Analysis of air pollution and greenhouse gases
[DE92-014955] p 104 N93-10384
Cluster beam studies of metal combustion
[AD-A253952] p 30 N93-10416
Pulsed jet plume combustion: An exothermic process under fluid mechanical control p 32 N93-10553
Studies on the combustion efficiency of liquid fuel rockets with variable thrust
[AD-A254232] p 26 N93-10721
FUEL CONSUMPTION
Compound cycle engine for helicopter application
[NASA-CR-180824] p 9 N93-10348
FUEL INJECTION
Pulsed jet plume combustion: An exothermic process under fluid mechanical control p 32 N93-10553
FUEL PRODUCTION
Biological production of ethanol from coal
[DE92-016114] p 43 N93-10608
FUEL TANK PRESSURIZATION
Loading operations for spacecraft propulsion subsystems p 11 N93-10047
FUNCTION GENERATORS
Artificial neural network system for memory modification
[AD-D015354] p 142 N93-10958
Memory modification of artificial neural networks
[AD-D015356] p 143 N93-10959
FUNCTION SPACE
Finite group actions and elliptic genera
[DE92-630207] p 170 N93-10388
FUNCTIONAL ANALYSIS
Data synthesis and display programs for wave distribution function analysis
[NASA-TM-108009] p 70 N93-10800
FUNCTIONAL DESIGN SPECIFICATIONS
KC-135 crew reduction feasibility demonstration simulation study. Volume 3: Test and evaluation
[AD-A253931] p 134 N93-10713
FUNCTIONS (MATHEMATICS)
Hexagonal and octagonal finite elements p 50 N93-10500
FUNNELS
Matter-wave interferometry with laser cooled atoms
[AD-A254000] p 89 N93-10720
FUSION REACTORS
D-He-3 spherical torus fusion reactor system study
[AD-A253358] p 155 N93-10102
Large orbit magnetic confinement systems for advanced fusion fuels
[DE92-016218] p 162 N93-10617
FUZZY SYSTEMS
Mesoscale severe weather development under orographic influences
[AD-A253630] p 125 N93-10204

G

GALACTIC RADIATION
Power spectrum of the extragalactic background light p 177 N93-10364

GALACTIC STRUCTURE
Prospects in stellar and galactic observations with SIMURIS p 182 N93-10921
GALAXIES
Imaging of BL Lac objects p 177 N93-10884
GALLIUM ARSENIDES
Theory of light-induced drift of electrons in coupled quantum wells
[AD-A253609] p 164 N93-10093
Novel optoelectronic devices based on combining GaAs and InP on Si
[AD-A253781] p 165 N93-10235
Ohmic contacts to compound semiconductors p 76 N93-10830
GALLIUM COMPOUNDS
4.5 micron laser source
[AD-A253367] p 87 N93-10090
GALLIUM NITRIDES
Improved gallium nitride and aluminum nitride electronic materials
[AD-A253785] p 76 N93-10888
GAMMA RAY ASTRONOMY
Gamma ray astrophysics to the year 2000. Report of the NASA Gamma Ray Program Working Group
[NASA-TM-107995] p 178 N93-10067
Physical implementations of an antimask in URA based coded mask systems
[INPE-5338-PRE/1737] p 153 N93-10312
GAMMA RAY OBSERVATORY
Gamma ray astrophysics to the year 2000. Report of the NASA Gamma Ray Program Working Group
[NASA-TM-107995] p 178 N93-10067
GAMMA RAY TELESCOPES
Physical implementations of an antimask in URA based coded mask systems
[INPE-5338-PRE/1737] p 153 N93-10312
GAMMA RAYS
Gamma ray astrophysics to the year 2000. Report of the NASA Gamma Ray Program Working Group
[NASA-TM-107995] p 178 N93-10067
GAPS (GEOLOGY)
Stability of open-graded bases under wheel loads using a model testing approach
[AD-A253209] p 66 N93-10710
GARNETS
Epitaxial magnetic oxides
[AD-A253667] p 35 N93-10230
Development of garnet films for magnetostatic wave channelized receivers
[AD-A252812] p 166 N93-10335
GAS ANALYSIS
Emission tomography of sodium in a hydrogen-air flame
[AD-A253530] p 29 N93-10224
GAS COMPOSITION
Sensitivity of modeled ozone concentrations to uncertainties in biogenic emissions
[PB92-192202] p 105 N93-10432
GAS DYNAMICS
Investigations of the motion of discrete-velocity gases
[AD-A253728] p 84 N93-10895
GAS FLOW
Emission tomography of sodium in a hydrogen-air flame
[AD-A253530] p 29 N93-10224
Influence of flow velocity on the output power of high pressure CW CO2 lasers
[AD-A254240] p 89 N93-10722
Investigations of the motion of discrete-velocity gases
[AD-A253728] p 84 N93-10895
GAS GENERATORS
Uprated OMS engine status: Altitude testing results p 22 N93-10036
The integration of geometric modeling into an inverse design method and application of a PC-based inverse design method and comparison with test results p 78 N93-10058
GAS INJECTION
Measurement of acceleration using an instrumented railgun projectile
[AD-A253366] p 12 N93-10106
Divertor heat flux reduction by D2 injection in DIII-D
[DE92-014232] p 160 N93-10326
GAS IONIZATION
Dispersion of seed vapor and gas ionization in an MHD second stage combustor and channel
[DE92-016699] p 163 N93-10645
GAS JETS
Mechanisms of sound generation in subsonic jets p 152 N93-10688
GAS TURBINE ENGINES
Compound cycle engine for helicopter application
[NASA-CR-180824] p 9 N93-10348
Noise studies for environmental impact assessment of an outdoor engine test facility p 149 N93-10672
GASEOUS ROCKET PROPELLANTS
Combustion-wave ignition for rocket engines p 17 N93-10016
GATES (CIRCUITS)
VLSI design for reliability - hot electron
[AD-A253942] p 74 N93-10715
GAUGE THEORY
Vector superconductivity in cosmic strings
[DE92-634923] p 179 N93-10296
The class of the paths in the Feynman path integral on the phase space
[DE92-630205] p 170 N93-10386
GELS
Novel seals and specialty component attachment mechanisms for Respiratory Protection system (RESPO 21)
[AD-A253395] p 91 N93-10290
GENERAL AVIATION AIRCRAFT
Analysis of wing-body junction flowfields using the incompressible Navier-Stokes equations, volumes 1 and 2 p 3 N93-10320
GENETICS
Interdisciplinary research and training program in the plant sciences
[DE92-015919] p 130 N93-10835
GEOCHEMISTRY
Carbon and oxygen isotope study of carbonates from highly shocked clasts of the polymict breccia of the Haughton Crater (Canada) p 105 N93-10113
Sudbury project (University of Muenster-Ontario Geological Survey): Summary of results - an updated impact model p 106 N93-10117
Early Archean spherule beds of possible impact origin from Barberton, South Africa: A detailed mineralogical and geochemical study p 115 N93-10155
Sudbury project (University of Muenster-Ontario Geological Survey): Petrology, chemistry, and origin of breccia formations p 121 N93-10185
A comparison of the chemistry of pseudotachylyte breccias in the Archean Levack Gneisses of the Sudbury structure, Ontario p 122 N93-10187
A late Devonian impact event and its association with a possible extinction event on Eastern Gondwana p 122 N93-10191
Geochemical aspect of impact cratering: Studies in Vernadsky Institute p 123 N93-10196
GEOCHRONOLOGY
Large meteorite impacts: The K/T model p 107 N93-10120
Shocked zircons in the Onaping Formation: Further proof of impact origin p 107 N93-10121
Sudbury project (University of Muenster-Ontario Geological Survey): Sr-Nd in heterolithic breccias and gabbroic dikes p 107 N93-10123
Noril'sk/Siberian plateau basalts and Bahama hot spot: Impact triggered? p 109 N93-10132
Does the Bushveld-Vredefort system (South Africa) record the largest known terrestrial impact catastrophe? p 109 N93-10134
U-Pb isotopic results for single shocked and polycrystalline zircons record 550-65.5-Ma ages for a K-T target site and 2700-1850-Ma ages for the Sudbury impact event p 115 N93-10156
Apollo 15 impact melts, the age of Imbrium, and the Earth-Moon impact cataclysm p 120 N93-10176
K/T boundary stratigraphy: Evidence for multiple impacts and a possible comet stream p 120 N93-10180
Ar-40 to Ar-39 dating of pseudotachylites from the Witwatersrand basin, South Africa, with implications for the formation of the Vredefort Dome p 122 N93-10189
GEODETIC SURVEYS
GPS Army research and applications
[AD-A254262] p 7 N93-10424
GEODYNAMICS
Effects of gravity in folding --- of geological layers p 124 N93-10324
GEOGRAPHIC INFORMATION SYSTEMS
TIGER5: Extraction of geographic information from the TIGER system
[DE92-014935] p 171 N93-10382
Global positioning systems technology and its application in environmental programs
[PB92-169358] p 7 N93-10442
System integration issues in digital photogrammetric mapping
[AD-A254046] p 103 N93-10781
Spatial models of ecological systems and processes: The role of GIS
[DE92-016884] p 175 N93-10788
Geographic Information System (GIS) development assistance for Nuclear Regulatory Commission (NRC) incident response capability
[DE92-017595] p 176 N93-10867
A spatial similarity measure for image database applications
[AD-A253570] p 176 N93-10883
GEOGRAPHY
TIGER5: Extraction of geographic information from the TIGER system
[DE92-014935] p 171 N93-10382
GEOLOGICAL FAULTS
SAR in support of geological investigations of the Sudbury structure p 103 N93-10182
FLASH: A finite element computer code for variably saturated flow
[DE92-018038] p 84 N93-10868
GEOLOGICAL SURVEYS
Sudbury project (University of Muenster-Ontario Geological Survey): Origin of the polymict, allochthonous breccias of the Onaping Formation p 106 N93-10116
Sudbury project (University of Muenster-Ontario Geological Survey): Summary of results - an updated impact model p 106 N93-10117
Sudbury project (University of Muenster-Ontario Geological Survey): Field studies 1984-1989 - summary of results p 107 N93-10119
Sudbury project (University of Muenster-Ontario Geological Survey): Sr-Nd in heterolithic breccias and gabbroic dikes p 107 N93-10123
Sudbury project (University of Muenster-Ontario Geological Survey): Isotope systematics support the impact origin p 109 N93-10131
SAR in support of geological investigations of the Sudbury structure p 103 N93-10182
Sudbury project (University of Muenster-Ontario Geological Survey): Petrology, chemistry, and origin of breccia formations p 121 N93-10185
Al Umchaimin depression, Western Iraq: An impact structure? p 122 N93-10190
GEOMETRICAL OPTICS
Geometrical transformation of linear diode-laser arrays for longitudinal pumping of solid-state lasers
[AD-A253415] p 87 N93-10218
Modeling of HF propagation and heating in the ionosphere
[AD-A253941] p 125 N93-10714
GEOMETRY
Hexagonal and octagonal finite elements p 50 N93-10500
Singular stress distributions at circular holes in composite laminates p 51 N93-10503
GEOMORPHOLOGY
Structural aspects of the Araguainha impact structure (Brazil) p 106 N93-10118
Suevite superposition on the Bunte breccia in Noerdlinger Ries, Germany: New findings on the transport mechanism of impactites p 107 N93-10122
Hong Kong is an impact crater: Proof from the geomorphological and geological evidence p 107 N93-10124
Melt production in large-scale impact events: Planetary observations and implications p 108 N93-10126
Noril'sk/Siberian plateau basalts and Bahama hot spot: Impact triggered? p 109 N93-10132
Does the Bushveld-Vredefort system (South Africa) record the largest known terrestrial impact catastrophe? p 109 N93-10134
New perspectives on the Popigai impact structure p 110 N93-10138
The Zhamanshin impact feature: A new class of complex crater? p 110 N93-10139
Sudbury Igneous Complex: Impact melt or igneous rock? Implications for lunar magmatism p 118 N93-10169
Melting and its relationship to impact crater morphology p 119 N93-10170
Impact cratering record of Fennoscandia p 119 N93-10171
The large impact process inferred from the geology of lunar multiring basins p 121 N93-10184
Electron petrography of silica polymorphs associated with pseudotachylite, Vredefort structure, South Africa p 123 N93-10192
GEOPHYSICS
Workshop on the evolution of the Martian atmosphere
[NASA-CR-190730] p 189 N93-10064
The Zhamanshin impact feature: A new class of complex crater? p 110 N93-10139
Solar-geophysical data number 569, January 1992. Part 1: (Prompt reports). Data for December, November 1991, and late data
[PB92-158880] p 190 N93-10771
Solar-geophysical data number 570, February 1992. Part 1: (Prompt reports). Data for January 1992, December 1991, and late data
[PB92-170380] p 190 N93-10773
Solar-geophysical data number 570, February 1992. Part 2: (Comprehensive reports). Data for August 1991 and miscellaneous
[PB92-170398] p 190 N93-10774

Solar-geophysical data number 571, March 1992. Part 1: (Prompt reports). Data for February, January 1992, and late data
[PB92-177062] p 190 N93-10775
Solar-geophysical data number 571, March 1992. Part 2: (Comprehensive reports). Data for September 1991 and miscellaneous
[PB92-177070] p 190 N93-10776
Modelling of 3-D electromagnetic responses using the time-wavenumber method
[DE92-017025] p 70 N93-10865

GEOPOTENTIAL
On the gravitational potential of two arbitrary rotating bodies with applications to the Earth-Moon system
p 179 N93-10303

GEOPOTENTIAL HEIGHT
Atlas of Southern Hemisphere 500 mb teleconnection patterns derived from National Meteorological Center analyses
[PB92-203892] p 126 N93-10337

GEOSAT SATELLITES
Comparison of wind speed measurements over the oceans with the Special Sensor Microwave/Imager and the Geosat altimeter p 127 N93-10850

GEOSTROPHIC WIND
Air-sea interaction in regions of varying surface conditions
[AD-A253182] p 128 N93-10791

GERMANIUM
Spectroscopic ellipsometric measurements of the dielectric function of germanium dioxide films on crystal germanium
[AD-A253137] p 168 N93-10614

GERMANIUM OXIDES
Spectroscopic ellipsometric measurements of the dielectric function of germanium dioxide films on crystal germanium
[AD-A253137] p 168 N93-10614

GERMANY
Suevite superposition on the Bunte breccia in Noerdlinger Ries, Germany: New findings on the transport mechanism of impactites p 107 N93-10122

GIANT STARS
Yellow hypergiant interferometry: A clue to understanding evolutionary instability
p 182 N93-10919

GLACIAL DRIFT
Sudbury Breccia and suevite as glacial indicators transported 800 km to Kentland Astrobleme, Indiana
p 117 N93-10165

GLASS
Bohemian circular structure, Czechoslovakia: Search for the impact evidence p 119 N93-10172
Viscosity determinations of some frictionally generated silicate melts: Implications for slip zone rheology during impact-induced faulting p 121 N93-10183
A late Devonian impact event and its association with a possible extinction event on Eastern Gondwana
p 122 N93-10191
Electron petrography of silica polymorphs associated with pseudotachylite, Vredefort structure, South Africa
p 123 N93-10192
Self-organized rock textures and multiring structure in the Duolun crater p 123 N93-10195
The third Workshop on Non-Crystalline Solids, programme and abstracts
[AD-A250739] p 36 N93-10244
APOLLO: A computer program for the calculation of chemical equilibrium and reaction kinetics of chemical systems
[DE92-017864] p 139 N93-10817

GLOBAL POSITIONING SYSTEM
GPS azimuth determination using short baseline carrier wave interferometry
[AD-A254257] p 6 N93-10265
GPS Army research and applications
[AD-A254262] p 7 N93-10424
Global positioning systems technology and its application in environmental programs
[PB92-169358] p 7 N93-10442
Dynamic positioning systems photogrammetric
[AD-A254250] p 8 N93-10898

GLUONS
Two-photon couplings of quarkonia with arbitrary J(sup PC)
[DE92-016525] p 153 N93-10332

GLYCIDYL AZIDE POLYMER
GAP benefits p 19 N93-10025

GLYCOLS
Materials compatibility and lubricants research on CFC-refrigerant substitute: Miscibility of lubricants with refrigerants
[DE92-015118] p 35 N93-10084

GLYCOLYSIS
Metabolic factors influencing myocardial recovery from acidosis (CiC3)
[AD-A252376] p 132 N93-10796

GNEISS
A quasi-Hertzian stress field from an internal source: A possible working model for the Vredefort structure
p 106 N93-10115
Thermobarometric studies on the Levack Gneisses: Footwall rocks to the Sudbury Igneous Complex
p 114 N93-10152
Phase transformations in 40-60-GPa shocked gneisses from the Haughton Crater (Canada): An Analytical Transmission Electron Microscopy (ATEM) study
p 117 N93-10163
A comparison of the chemistry of pseudotachylyte breccias in the Archean Levack Gneisses of the Sudbury structure, Ontario p 122 N93-10187

GOLD
Template-synthesis of infrared-transparent metal microcylinders: Comparison of optical properties with the predictions of effective medium theory
[AD-A253267] p 158 N93-10694

GOLD ISOTOPES
Particle production at high p(sub (perpendicular)) in (sup 28)Si + A collisions at 14.6 A x GeV/c
[DE92-016939] p 154 N93-10402

GOODNESS OF FIT
Change analysis
[AD-A253567] p 146 N93-10795

GOVERNMENT/INDUSTRY RELATIONS
Aerospace Industries Association of Canada
[CTN-92-60345] p 192 N93-10640
Aerospace Industries Association of Canada
[CTN-92-60590] p 1 N93-10644

GOVERNMENTS
National scene in information and documentation activities and recent developments in the Documentation Center of TUBITAK (TURDOK) p 173 N93-10594

GRADE
Stability of open-graded bases under wheel loads using a model testing approach
[AD-A253209] p 66 N93-10710

GRADIENTS
Analysis of reception variability due to terrain multipath on microwave common carrier links
[NTIA-92-283] p 69 N93-10430

GRADIOMETERS
Gradiometer antennas for tunnel detection
[PB92-205400] p 69 N93-10440

GRAIN BOUNDARIES
Reactions of Ti and Zr with AlN and Al2O3
[DE92-016234] p 28 N93-10391
Activated transport in AMTEC electrodes
[DE92-016810] p 75 N93-10786

GRAIN SIZE
Probing cosmic infrared sources: A computer modeling approach
[AD-A253788] p 178 N93-10238

GRANITE
A quasi-Hertzian stress field from an internal source: A possible working model for the Vredefort structure
p 106 N93-10115
Hong Kong is an impact crater: Proof from the geomorphological and geological evidence
p 107 N93-10124
Bronzite Granophyre: New insight on Vredefort
p 121 N93-10186
Geochemical aspect of impact cratering: Studies in Vernadsky Institute p 123 N93-10196

GRANULAR MATERIALS
Mathematical analysis of reactive multiphase flows
[AD-A253854] p 83 N93-10810

GRAPH THEORY
Symbolic Boolean manipulation with ordered binary decision diagrams
[AD-A253822] p 142 N93-10828

GRAPHITE
Epitaxial growth and dopant incorporation in diamond
[AD-A253636] p 165 N93-10206
Space environmental effects on LDEF low Earth orbit exposed graphite reinforced polymer matrix composites
p 38 N93-10585

GRAPHITE-EPOXY COMPOSITES
Additional results on space environmental effects on polymer matrix composites: Experiment A0180
p 38 N93-10586
Nonlinear aeroelasticity of composite structures
[AD-A254265] p 8 N93-10842

GRAPHS (CHARTS)
TIGER5: Extraction of geographic information from the TIGER system
[DE92-014935] p 171 N93-10382

GRATINGS (SPECTRA)
The solar ultraviolet network subtractive double monochromator p 183 N93-10931

GRAVITATIONAL EFFECTS
Melt production in large-scale impact events: Planetary observations and implications p 108 N93-10126
Paradigm lost: Venus crater depths and the role of gravity in crater modification p 120 N93-10179
Effects of gravity in folding --- of geological layers
p 124 N93-10324
Vibrations of a flexible Timoshenko beam under gravity p 53 N93-10512

GRAVITATIONAL FIELDS
Development of physical and mathematical models for the Porous Ceramic Tube Plant Nutrification System (PCTPNS)
[NASA-TM-107551] p 129 N93-10085
On the gravitational potential of two arbitrary rotating bodies with applications to the Earth-Moon system
p 179 N93-10303

GRAVITY WAVES
Yellow hypergiant interferometry: A clue to understanding evolutionary instability
p 182 N93-10919

GREECE
Documentation practices: The national scene (Greece)
p 173 N93-10595

GREEN'S FUNCTIONS
Global structure of a polynomial autonomous system on the plane
[DE92-630230] p 144 N93-10389

GREENHOUSE EFFECT
The current and future environmental role of atmospheric methane: Model studies and uncertainties
[NASA-CR-190662] p 104 N93-10256
Analysis of air pollution and greenhouse gases
[DE92-014955] p 104 N93-10384

GREENLAND
Eleven years of ionospheric scintillation fading data from twenty Greenlandic stations
[AD-A253271] p 69 N93-10695

GRID GENERATION (MATHEMATICS)
Unstructured mesh algorithms for aerodynamic calculations
[NASA-CR-189685] p 2 N93-10097
Interactive grid generation program for CAP-TSD
[NASA-TM-102705] p 3 N93-10349
Analysis and control of grid quality in computational simulation
[AD-A253723] p 138 N93-10746

GROUND STATIONS
Appraisal of digital terrain elevation data for low-altitude flight
[NASA-TM-103896] p 7 N93-10745

GROUND SUPPORT EQUIPMENT
Generic Propellant Transfer Unit p 11 N93-10046
Steering system of a vehicle, such as a snow removing machine for airfields
[CA-PATENT-APPL-SN-1293201] p 91 N93-10367

GROUND SUPPORT SYSTEMS
Generic Propellant Transfer Unit p 11 N93-10046
Loading operations for spacecraft propulsion subsystems p 11 N93-10047

GROUND TESTS
A 26 kW arcjet system for on-orbit demonstration
p 21 N93-10031
Accelerator Technology Division
[DE92-016023] p 156 N93-10462

GROUND WATER
FLASH: A finite element computer code for variably saturated flow
[DE92-018038] p 84 N93-10868

GROUND WAVE PROPAGATION
Software for prediction and analysis of ground wave propagation loss
[AD-A253474] p 67 N93-10199

GROUP THEORY
Finite group actions and elliptic genera
[DE92-630207] p 170 N93-10388

GUN LAUNCHERS
Twenty-five KA, 5000V solid state opening switch for inductive energy stores
[AD-A253968] p 73 N93-10421

GUN PROPELLANTS
The 1992 JANNAF Propulsion Meeting, volume 1
[CPIA-PUBL-580-VOL-1] p 15 N93-10001

GYROSCOPES
Data reduction analysis for the Stanford relativity gyroscope experiment p 86 N93-10347
An elastic oblate axisymmetric reference gyro for attitude studies p 54 N93-10518

H

H ALPHA LINE
Pattern recognition applied to H(sub alpha) spectroheliograms solar rotation and meridional circulation p 182 N93-10924

HADRONS
A measurement of the Z(sup 0) hadronic branching fraction to bottom quarks and the charged multiplicity of bottom quark events using precision vertex detectors at E(sub cm) = 91 GeV
[DE92-018236] p 154 N93-10820
HALF PLANES
Elasticity analysis of orthotropic beams under three-part bending p 52 N93-10507
HALF SPACES
Interface cracks in an orthotropic layered half-space under impact loading p 47 N93-10482
HALL EFFECT
Fast magnetic field penetration into an intense neutralized ion beam
[DE92-016861] p 156 N93-10633
HALOGENS
Atomic hydrogen: A reagent for the extraction of chemical species from silicon surfaces
[AD-A252804] p 30 N93-10266
HAMILTONIAN FUNCTIONS
Semiclassical quantization of chaotic billiards
[DE92-634888] p 169 N93-10226
Symmetry breaking and localization in quantum chaotic systems
[DE92-634890] p 170 N93-10294
Stochastic diffusion and Kolmogorov entropy in regular and random Hamiltonians
[DE92-016179] p 170 N93-10604
Electronic structure of highly correlated structures
[DE92-017017] p 155 N93-10863
HANDBOOKS
Handbook for operating the OWLKNEST technology
[AD-A253412] p 137 N93-10409
Acquisition 2: Procurement, acquisition, and maintenance of configuration management documentation in support of a CIS system p 173 N93-10599
HARMONIC ANALYSIS
Harmonic analysis of the aerodynamic forces on a Darrieus rotor p 6 N93-10551
HARMONIC EXCITATION
Nonstationary random variations of moderately thick plates using BEM p 48 N93-10487
HARMONIC OSCILLATION
Development of nonlinear aerodynamic models for unsteady responses p 4 N93-10845
HAZARDS
A brief review of the source noise technology applicable to fixed-wing military aircraft p 150 N93-10678
HEALTH
A new test of scanning and monitoring ability: Methods and initial results
[AD-A249123] p 132 N93-10321
HEAT BUDGET
Anelastic modelling of explosive cyclogenesis p 126 N93-10377
HEAT FLUX
Divertor heat flux reduction by D2 injection in DIII-D
[DE92-014232] p 160 N93-10326
HEAT PIPES
Changes in oxidation state of chromium during LDEF exposure p 34 N93-10581
HEAT RESISTANT ALLOYS
Mechanisms and modelling of environment-dependent fatigue crack growth in a nickel based superalloy
[AD-A253967] p 33 N93-10717
HEAT SHIELDING
Documentation of the detailed radiation property data for the radiation-ablation code RASLE
[NASA-TM-103848] p 28 N93-10742
HEAT TRANSFER
Thermal stratification potential in rocket engine coolant channels p 18 N93-10019
Radial turbine cooling p 78 N93-10061
Heat transfer additives for absorption cooling system fluids
[PB92-190354] p 169 N93-10249
Shortened Test Heating Season (STHS) p 43 N93-10314
Flow over a leading edge with distributed roughness p 6 N93-10549
Navier-Stokes turbine heat transfer predictions using two-equation turbulence
[NASA-TM-105817] p 82 N93-10735
Thermal management in high average power pulsed compression systems
[DE92-017055] p 76 N93-10836
Investigations of the motion of discrete-velocity gases
[AD-A253728] p 84 N93-10895
HEAT TRANSFER COEFFICIENTS
Thermal management in high average power pulsed compression systems
[DE92-017055] p 76 N93-10836
HEATING
Shortened Test Heating Season (STHS) p 43 N93-10314
HEAVY IONS
Two-photon physics and the coming generation of heavy ion colliders
[DE92-015850] p 156 N93-10732
Glenn T. Seaborg and heavy ion nuclear science
[DE92-016943] p 156 N93-10762
HELICOPTER CONTROL
Flight test and analysis procedures for new handling criteria
[RAE-TM-FM-26] p 8 N93-10803
HELICOPTER PERFORMANCE
Flight test and analysis procedures for new handling criteria
[RAE-TM-FM-26] p 8 N93-10803
HELICOPTER WAKES
Acoustic noise generation at the air/ocean boundary
[DREA-CR-90-445] p 147 N93-10642
HELICOPTERS
Rotorcraft en route ATC route standards
[AD-A249129] p 6 N93-10323
Compound cycle engine for helicopter application
[NASA-CR-180824] p 9 N93-10348
Appraisal of digital terrain elevation data for low-altitude flight
[NASA-TM-103896] p 7 N93-10745
Flight test and analysis procedures for new handling criteria
[RAE-TM-FM-26] p 8 N93-10803
Contributions to the experimental investigation of rotor/body aerodynamic interactions p 5 N93-10877
HELIOSEISMOLOGY
Transition region dynamics p 180 N93-10907
HELIUM
Helium transport in enhanced confinement regimes on the TEXTOR and D3-D tokamaks
[DE92-016247] p 160 N93-10293
Stress modified welding process for irradiated materials
[DE92-017131] p 92 N93-10634
HELIUM-NEON LASERS
Stress and strain of slab type amplifiers
[AD-A254246] p 74 N93-10702
HEMISPHERE CYLINDER BODIES
Shock wave diffractions over semi-circular and half-diamond cylinders p 60 N93-10546
HETEROJUNCTIONS
Atomic approaches to defect thermochemistry
[AD-A254278] p 167 N93-10425
HIERARCHIES
Hierarchical structure in polymeric solid and its influence on properties
[AD-A253818] p 41 N93-10825
HIGH CURRENT
Long conduction time plasma opening switch experiments at Sandia National Labs
[DE92-015003] p 72 N93-10279
HIGH ENERGY INTERACTIONS
Research in theoretical particle physics
[DE92-016181] p 154 N93-10605
Research program in experimental and theoretical high energy physics
[DE92-016219] p 156 N93-10618
HIGH FREQUENCIES
Numerical modelling of fringing fields and their use for complex permittivity measurements at high frequencies
[AD-A253994] p 72 N93-10359
HIGH PASS FILTERS
Design and implementation of digital filters for analysis of F/A-18 flight test data
[AD-A253447] p 3 N93-10342
HIGH PRESSURE
High pressure and synchrotron radiation studies of solid state electronic instabilities
[DE92-015661] p 168 N93-10630
Influence of flow velocity on the output power of high pressure CW CO2 lasers
[AD-A254240] p 89 N93-10722
Strength-toughness requirements for thick-walled high pressure vessels
[AD-A253756] p 95 N93-10750
HIGH RESOLUTION
High resolutions studies of the structure of the solar atmosphere
[AD-A254292] p 190 N93-10767
High-resolution TVD schemes for the analysis of: 1. Inviscid supersonic and transonic flows. 2. Viscous flows with shock-induced separation and heat transfer p 5 N93-10889
Solar Physics and Astrophysics at Interferometric Resolution
[ESA-SP-344] p 179 N93-10901
High resolution observations: The state of the art and beyond p 177 N93-10902
Planned observations at high resolution from space p 177 N93-10903
Prospects with SIMURIS p 179 N93-10904
Ultra-high observations of the prominence-corona transition region p 180 N93-10908
Intensity, velocity, and turbulence in prominences observed with the HRTS p 180 N93-10911
Small scale processes in solar and stellar plasmas p 181 N93-10917
Stellar and circumstellar evolution and activity p 181 N93-10918
Prospects in stellar and galactic observations with SIMURIS p 182 N93-10921
Magnetospheres and atmospheres of planets p 182 N93-10922
Observation of solar flares at high resolution p 182 N93-10923
MSDP imaging spectroscopy for high resolution solar physics p 183 N93-10926
High resolution granulation spectrophotometry with a UBF and a FP interferometer in tandem p 183 N93-10927
SUN: The Solar Ultraviolet Network p 183 N93-10930
IFTS: The Imaging Fourier Transform Spectrometer p 14 N93-10933
EUV complementary instrumentation for SIMURIS p 14 N93-10938
Obtaining high resolution XUV coronal images p 14 N93-10939
HIGH REYNOLDS NUMBER
Mathematical analysis of strong fluid mechanical effects at high Mach number in reactive and nonreactive flow
[AD-A253617] p 79 N93-10094
Study of a viscous sublayer model in the analysis of 3-D shock/boundary layer interaction flow fields
[AD-A253731] p 84 N93-10886
HIGH SPEED
A building-block approach for turbulence model validation/upgrade focussed on high-speed jet flowfields p 16 N93-10010
High-speed viscous flows past blunt bodies and compression corners with flux-split methods
[AD-A253413] p 81 N93-10410
Identifying the principal noise sources of fixed-wing combat aircraft in high-speed flight p 151 N93-10686
HIGH SPEED CAMERAS
Research in the optical sciences
[AD-A253188] p 158 N93-10446
HIGH TEMPERATURE
The effect of elevated temperatures on the properties of thermally stable silicon-based elastomers for adhesives, sealants, and insulator applications p 15 N93-10006
Reinforcements for high temperature ceramics
[DE92-014815] p 35 N93-10082
Mechanisms and modelling of environment-dependent fatigue crack growth in a nickel based superalloy
[AD-A253967] p 33 N93-10717
EUV complementary instrumentation for SIMURIS p 14 N93-10938
HIGH TEMPERATURE PLASMAS
VH-mode discharges in the D3-D tokamak
[DE92-016257] p 161 N93-10463
Experimental plasma research project summaries
[DE92-016274] p 162 N93-10464
HIGH TEMPERATURE SUPERCONDUCTORS
Vortices in long Josephson junctions
[AD-A253230] p 167 N93-10404
Novel Si-YBCuO reactive patterning technique for manufacture of large area high Tc superconducting electronic devices
[AD-A250740] p 73 N93-10426
Model for the reversible magnetization of high-(kappa) type-2 superconductors: Application to high-temperature superconductor
[DE92-016297] p 167 N93-10609
High pressure and synchrotron radiation studies of solid state electronic instabilities
[DE92-015661] p 168 N93-10630
Covalent electron transfer theory of superconductivity
[AD-A253975] p 74 N93-10718
Development of high temperature superconductors for magnetic field applications
[DE92-015930] p 168 N93-10733
Prototype superconducting planar transformers using high-Tc thin and thick films
[AD-A254230] p 77 N93-10897
HIGH TEMPERATURE TESTS
Materials compatibility and lubricants research on CFC-refrigerant substitute: Miscibility of lubricants with refrigerants
[DE92-015118] p 35 N93-10084
HIGH VOLTAGES
Semiconductor-metal eutectic composites for high power switching
[AD-A253930] p 74 N93-10755
HMX
Impact sensitivity reduction via exo-electron control p 15 N93-10004

HOLOGRAPHY
Orientation and pair correlation at high density by superresolution holography
[AD-A254034] p 85 N93-10239
Holographic optical interconnects for multichip modules
[AD-A253403] p 86 N93-10408
HOMING DEVICES
Integrated vision system for a target seeker
[AD-A253359] p 135 N93-10103
HONG KONG
Hong Kong is an impact crater: Proof from the geomorphological and geological evidence
p 107 N93-10124
HORIZONTAL FLIGHT
An experimental and a theoretical investigation of rotor pitch damping using a model rotor p 8 N93-10322
Contributions to the experimental investigation of rotor/body aerodynamic interactions p 5 N93-10877
HORIZONTAL SPACECRAFT LANDING
Critical engine system design characteristics for SSTO vehicles p 17 N93-10014
HOT ELECTRONS
VLSI design for reliability - hot electron
[AD-A253942] p 74 N93-10715
HOT ISOSTATIC PRESSING
Tensile properties of cast titanium alloys: Titanium-6Al-4V ELI and Titanium-5Al-2.5Sn ELI
[NASA-TP-3288] p 33 N93-10072
HOVERING
An experimental and a theoretical investigation of rotor pitch damping using a model rotor p 8 N93-10322
Tilt rotor hover aeroacoustics
[NASA-CR-177598] p 147 N93-10458
Contributions to the experimental investigation of rotor/body aerodynamic interactions p 5 N93-10877
HTPB PROPELLANTS
Investigation of the stimulated release of gaseous ammonia from ammonium perchlorate by HTPB solid propellant bonding agents p 19 N93-10026
HUBBLE SPACE TELESCOPE
Hubble Space telescope thermal cycle test report for large solar array samples with BSFR cells (Sample numbers 703 and 704)
[NASA-TM-108373] p 104 N93-10809
HUMAN BEINGS
A prospective evaluation of stress fractures/overuse injuries in a population of West Point cadets
[AD-A252427] p 132 N93-10709
HUMAN FACTORS ENGINEERING
KC-135 crew reduction feasibility demonstration simulation study. Volume 3: Test and evaluation
[AD-A253931] p 134 N93-10713
NASA Space Human Factors Program
[NASA-TM-108005] p 134 N93-10890
HUMAN PERFORMANCE
Handbook for operating the OWLKNEST technology
[AD-A253412] p 137 N93-10409
Effects of early bright, late bright and dim illumination upon circadian neuroendocrine, electrophysiological and behavioral responses
[AD-A254129] p 131 N93-10661
Guidelines for developing spacecraft maximum allowable concentrations for Space Station contaminants
[NASA-CR-190748] p 13 N93-10737
NASA Space Human Factors Program
[NASA-TM-108005] p 134 N93-10890
HUMAN REACTIONS
Human noise exposure criteria for combat aircraft training areas p 148 N93-10670
Noise emission of low flying military airplanes p 149 N93-10675
Boom and the problems related to the supersonic flights of military aircraft p 149 N93-10677
HUMAN TOLERANCES
Human noise exposure criteria for combat aircraft training areas p 148 N93-10670
Noise of combat aircraft in proximity to air bases: Review of the possibilities of noise reduction at the source p 148 N93-10671
Noise emission of low flying military airplanes p 149 N93-10675
HYBRID CIRCUITS
Semiconductor phase conjugation
[AD-A253684] p 166 N93-10345
HYBRID PROPELLANT ROCKET ENGINES
A simplified model for hybrid rocket performance prediction p 19 N93-10022
HYDRAULIC EQUIPMENT
Inspection and repair decisions for hydraulic structures under symmetric deterioration
[AD-A253621] p 96 N93-10797
HYDRAZINE ENGINES
Long life monopropellant hydrazine thruster evaluation for Space Station Freedom application p 23 N93-10042
Design and operation of the US Space Station Freedom propulsion system p 24 N93-10049
HYDRAZINES
Long life monopropellant hydrazine thruster evaluation for Space Station Freedom application p 23 N93-10042
DSP propulsion system launch configuration and related testing p 24 N93-10048
Rate constants for reactions of hydrazine fuels with O(P-3)
[AD-A252813] p 42 N93-10336
HYDROCARBON FUEL PRODUCTION
Temperature-programmed oxidation of ethane and ethylene in the presence and absence of C-13 labeled methane
[DE92-015048] p 42 N93-10329
HYDROCARBON FUELS
Cluster beam studies of metal combustion
[AD-A253952] p 30 N93-10416
HYDROCARBONS
Transition metal activation and functionalization of carbon-hydrogen bonds
[DE92-014809] p 30 N93-10400
Sensitivity of modeled ozone concentrations to uncertainties in biogenic emissions
[PB92-192202] p 105 N93-10432
Hydrocarbon surface chemistry on Si(100)
[AD-A252803] p 27 N93-10465
HYDROCHLORIC ACID
Alternatives in clean propellants for large scale man-rated solid rocket motors p 20 N93-10028
Comparison of Cl and HCl adsorption on Si(100)-(2 x 1)
[AD-A252802] p 30 N93-10281
HYDRODYNAMIC EQUATIONS
Calculation of elastic-plastic wave propagation on the connection machine
[AD-A252429] p 95 N93-10427
HYDRODYNAMICS
RHALE: A MMALE shock physics code for arbitrary meshes
[DE92-017051] p 139 N93-10866
HYDROGEN
10 kW power electronics for hydrogen arcjets p 21 N93-10033
Optical metrology of magnetically trapped hydrogen
[AD-A253229] p 31 N93-10712
HYDROGEN ATOMS
Atomic hydrogen: A reagent for the extraction of chemical species from silicon surfaces
[AD-A252804] p 30 N93-10266
HYDROGEN OXYGEN ENGINES
Plug nozzle propulsion system p 17 N93-10013
Critical engine system design characteristics for SSTO vehicles p 17 N93-10014
Combustion-wave ignition for rocket engines p 17 N93-10016
Hot fire test results of subscale tubular combustion chambers p 18 N93-10020
Species and temperature measurement in H2/O2 rocket flow fields by means of Raman scattering diagnostics
[NASA-CR-189217] p 25 N93-10086
Space Transportation Engine Program (STEP), phase B
[NASA-CR-184062] p 25 N93-10350
HYDROLOGY
FLASH: A finite element computer code for variably saturated flow
[DE92-018038] p 84 N93-10868
HYDROSTATIC PRESSURE
Monitoring structural response in pressurized environments. Part 2: Applications
[DE92-015034] p 94 N93-10327
HYDROSTATICS
Monitoring structural response in pressurized environments. Part 2: Applications
[DE92-015034] p 94 N93-10327
HYDROXYL COMPOUNDS
Theory of combustion of liquid propellants based on hydroxylammonium nitrate
[AD-A248445] p 42 N93-10267
HYPERBOLIC FUNCTIONS
Discontinuous initial value problem of nonlinear elasticity by similarity approach p 64 N93-10569
HYPERCUBE MULTIPROCESSORS
Calculation of elastic-plastic wave propagation on the connection machine
[AD-A252429] p 95 N93-10427
HYPERGOLIC ROCKET PROPELLANTS
Generic Propellant Transfer Unit p 11 N93-10046
HYPERSONIC COMBUSTION
Shock enhancement and control of hypersonic combustion
[AD-A254295] p 31 N93-10843
HYPERSONIC FLIGHT
Hypersonic inlet efficiency revisited p 5 N93-10012
HYPERSONIC FLOW
A globally well-posed accurate and efficient finite element CFD algorithm for compressible aerodynamics p 3 N93-10306
HYPERSONIC INLETS
Hypersonic inlet efficiency revisited p 5 N93-10012
HYPERSONIC SPEED
Pitot survey of exhaust flow field of a 2-D scramjet nozzle at Mach 6 with air or freon and argon used for exhaust simulation
[NASA-TM-4361] p 2 N93-10071
HYPERSONIC VEHICLES
Documentation of the detailed radiation property data for the radiation-ablation code RASLE
[NASA-TM-103848] p 28 N93-10742
HYPERVELOCITY IMPACT
International Conference on Large Meteorite Impacts and Planetary Evolution
[NASA-CR-190677] p 105 N93-10112
Large meteorite impacts: The K/T model p 107 N93-10120
Enhanced magnetic field production during oblique hypervelocity impacts p 108 N93-10129
Simulated meteorite impacts and volcanic explosions: Ejecta analyses and planetary implications p 111 N93-10143
Melt production in large-scale impact events: Implications and observations at terrestrial craters p 112 N93-10144
Tektite origin by hypervelocity asteroidal or cometary impact: The quest for the source craters p 114 N93-10154
Early Archean spherule beds of possible impact origin from Barberton, South Africa: A detailed mineralogical and geochemical study p 115 N93-10155
What can we learn about impact mechanics from large craters on Venus? p 118 N93-10166
Melting and its relationship to impact crater morphology p 119 N93-10170
Impact cratering record of Fennoscandia p 119 N93-10171
Search for the 700,000-year-old source crater of the Australasian tektite strewn field p 120 N93-10177
Recognizing impactor signatures in the planetary record p 120 N93-10178
Paradigm lost: Venus crater depths and the role of gravity in crater modification p 120 N93-10179
K/T boundary stratigraphy: Evidence for multiple impacts and a possible comet stream p 120 N93-10180
Ar-40 to Ar-39 ages of the large impact structures Kara and Manicouagan and their relevance to the Cretaceous-Tertiary and the Triassic-Jurassic boundary p 122 N93-10188
Al Umchaimin depression, Western Iraq: An impact structure? p 122 N93-10190
A late Devonian impact event and its association with a possible extinction event on Eastern Gondwana p 122 N93-10191
Floor-fractured crater models of the Sudbury structure, Canada p 123 N93-10193
Variation in multiring basic structures as a function of impact angle p 123 N93-10194
Self-organized rock textures and multiring structure in the Duolun crater p 123 N93-10195
Additional results on space environmental effects on polymer matrix composites: Experiment A0180 p 38 N93-10586
Proposed test program and data base for LDEF polymer matrix composites p 38 N93-10587
Results from testing and analysis of solar cells flown on LDEF p 39 N93-10591
System related testing and analysis of FRECOPA p 39 N93-10592
A computational study of projectile melt in impact with typical Whipple shields
[DE92-017137] p 92 N93-10635
Analysis of interplanetary dust experiment detectors and other witness plates
[NASA-CR-190818] p 32 N93-10852
Elemental analyses of hypervelocity microparticle impact sites on interplanetary dust experiment sensor surfaces p 32 N93-10853
Contaminant interferences with SIMS analyses of microparticle impactor residues on LDEF surfaces p 32 N93-10854
HYPOTHESES
The Zhamanshin impact feature: A new class of complex crater? p 110 N93-10139
A measurement of the Z(sup 0) hadronic branching fraction to bottom quarks and the charged multiplicity of bottom quark events using precision vertex detectors at E(sub cm) = 91 GeV
[DE92-018236] p 154 N93-10820

HYPOXIA
Metabolic factors influencing myocardial recovery from acidosis (CiC3)
[AD-A252376] p 132 N93-10796
HYSTERESIS
A new non-Gausssian approximation technique for random vibration of general hysteresis
p 50 N93-10496

I

IDENTIFYING
A new test of scanning and monitoring ability: Methods and initial results
[AD-A249123] p 132 N93-10321
IGNEOUS ROCKS
Research core drilling in the Manson impact structure, Iowa p 105 N93-10114
A quasi-Hertzian stress field from an internal source: A possible working model for the Vredefort structure
p 106 N93-10115
Sudbury project (University of Muenster-Ontario Geological Survey): Field studies 1984-1989 - summary of results p 107 N93-10119
Hong Kong is an impact crater: Proof from the geomorphological and geological evidence
p 107 N93-10124
Melt production in large-scale impact events: Calculations of impact-melt volumes and crater scaling
p 108 N93-10125
Sudbury project (University of Muenster-Ontario Geological Survey): Isotope systematics support the impact origin p 109 N93-10131
Sudbury Igneous Complex: Impact melt or igneous rock? Implications for lunar magmatism p 118 N93-10169
Bronzite Granophyre: New insight on Vredefort
p 121 N93-10186
A comparison of the chemistry of pseudotachylyte breccias in the Archean Levack Gneisses of the Sudbury structure, Ontario p 122 N93-10187
IGNITION
Combustion-wave ignition for rocket engines
p 17 N93-10016
Shock enhancement and control of hypersonic combustion
[AD-A254295] p 31 N93-10843
ILLUMINATION
Effects of early bright, late bright and dim illumination upon circadian neuroendocrine, electrophysiological and behavioral responses
[AD-A254129] p 131 N93-10661
IMAGE ANALYSIS
Moire-fringe images of twin boundaries in chemical vapor deposited diamond
[AD-A253729] p 35 N93-10231
The development of optical techniques for component inspection in the aerospace industry p 93 N93-10307
System integration issues in digital photogrammetric mapping
[AD-A254046] p 103 N93-10781
IMAGE CONTRAST
Comparative study of the MTFA, ICS, and SQRI image quality metrics for visual display systems
[AD-A252116] p 158 N93-10708
IMAGE ENHANCEMENT
Physical implementations of an antimask in URA based coded mask systems
[INPE-5338-PRE/1737] p 153 N93-10312
High resolutions studies of the structure of the solar atmosphere
[AD-A254292] p 190 N93-10767
IMAGE INTENSIFIERS
Comparative study of the MTFA, ICS, and SQRI image quality metrics for visual display systems
[AD-A252116] p 158 N93-10708
IMAGE PROCESSING
Center for Intelligent Control Systems, Brown University component: Graduate research fellowships
[AD-A253620] p 141 N93-10095
Integrated vision system for a target seeker
[AD-A253359] p 135 N93-10103
Automatic cloud classification from multi-spectral satellite data over oceanic regions
[AD-A253670] p 126 N93-10292
The development of optical techniques for component inspection in the aerospace industry p 93 N93-10307
SPOT panchromatic band simulation by linear combination of multispectral bands
[INPE-5295-PRE/1650] p 157 N93-10311
Two-dimensional signal processing, optical information storage and processing, and electromagnetic measurements
[AD-A253953] p 73 N93-10417
High resolutions studies of the structure of the solar atmosphere
[AD-A254292] p 190 N93-10767
A spatial similarity measure for image database applications
[AD-A253570] p 176 N93-10883
IMAGE RECONSTRUCTION
Orientation and pair correlation at high density by superresolution holography
[AD-A254034] p 85 N93-10239
Interferometric imaging with the solar ultraviolet network p 184 N93-10932
The CHARON program p 177 N93-10942
IMAGE RESOLUTION
Comparative study of the MTFA, ICS, and SQRI image quality metrics for visual display systems
[AD-A252116] p 158 N93-10708
IMAGES
A spatial similarity measure for image database applications
[AD-A253570] p 176 N93-10883
IMAGING RADAR
Open Skies Treaty imaging radar technology issues
[DE92-016548] p 68 N93-10394
IMAGING SPECTROMETERS
Solar Physics and Astrophysics at Interferometric Resolution
[ESA-SP-344] p 179 N93-10901
Prospects with SIMURIS p 179 N93-10904
Prospects in stellar and galactic observations with SIMURIS p 182 N93-10921
MSDP imaging spectroscopy for high resolution solar physics p 183 N93-10926
IFTS: The Imaging Fourier Transform Spectrometer
p 14 N93-10933
Polarimetry with an imaging FTS p 14 N93-10934
Fourier transform spectrometer processing: Data reduction and processor design p 14 N93-10935
First results of an imaging FTS with a NICMOS camera p 86 N93-10936
Detectors for the SIMURIS payload
p 14 N93-10937
The imaging Fourier transform spectrometer optical design p 159 N93-10951
The imaging Fourier transform spectrometer: Performance and tolerance analysis p 86 N93-10952
A multipurpose vacuum-ultraviolet test facility
p 11 N93-10953
Interferometer optical design for the Imaging Fourier Transform Spectrometer (IFTS) p 159 N93-10955
Mechanical and thermal design of the SUN instrument
p 14 N93-10956
Some possible space interferometry applications
p 178 N93-10957
IMAGING TECHNIQUES
Electrical resistance tomography used in environmental restoration
[DE92-018003] p 103 N93-10763
Imaging of BL Lac objects p 177 N93-10884
High resolution observations: The state of the art and beyond p 177 N93-10902
Fourier transform spectrometer processing: Data reduction and processor design p 14 N93-10935
Report of the Lunar Interferometry Study Team (LIST) activities p 178 N93-10945
IMPACT DAMAGE
Carbon and oxygen isotope study of carbonates from highly shocked clasts of the polymict breccia of the Haughton Crater (Canada) p 105 N93-10113
Large meteorite impacts: The K/T model
p 107 N93-10120
Shocked zircons in the Onaping Formation: Further proof of impact origin p 107 N93-10121
Melt production in large-scale impact events: Calculations of impact-melt volumes and crater scaling
p 108 N93-10125
Melt production in large-scale impact events: Planetary observations and implications p 108 N93-10126
Diaplectic transformation of minerals: Vorotilov drill core, Puchezh-Katunki impact crater, Russia
p 110 N93-10136
Apollo 15 impact melts, the age of Imbrium, and the Earth-Moon impact cataclysm p 120 N93-10176
Additional results on space environmental effects on polymer matrix composites: Experiment A0180
p 38 N93-10586
Proposed test program and data base for LDEF polymer matrix composites p 38 N93-10587
Results from testing and analysis of solar cells flown on LDEF p 39 N93-10591
System related testing and analysis of FRECOPA
p 39 N93-10592
Analysis of interplanetary dust experiment detectors and other witness plates
[NASA-CR-190818] p 32 N93-10852
Elemental analyses of hypervelocity microparticle impact sites on interplanetary dust experiment sensor surfaces
p 32 N93-10853
IMPACT LOADS
Optical and TEM study of shock metamorphism from the Sedan test site p 111 N93-10142
Geomechanical models of impact cratering: Puchezh-Katunki structure p 114 N93-10151
Interface cracks in an orthotropic layered half-space under impact loading p 47 N93-10482
Investigation of laminated composite plates under impact dynamic loading by using a three-dimensional hybrid stress finite element method p 29 N93-10510
Overview of the vibroimpact damping of packaged particles p 56 N93-10528
IMPACT MELTS
Research core drilling in the Manson impact structure, Iowa p 105 N93-10114
Sudbury project (University of Muenster-Ontario Geological Survey): Origin of the polymict, allochthonous breccias of the Onaping Formation p 106 N93-10116
Sudbury project (University of Muenster-Ontario Geological Survey): Summary of results - an updated impact model p 106 N93-10117
Sudbury project (University of Muenster-Ontario Geological Survey): Field studies 1984-1989 - summary of results p 107 N93-10119
Sudbury project (University of Muenster-Ontario Geological Survey): Sr-Nd in heterolithic breccias and gabbroic dikes p 107 N93-10123
Hong Kong is an impact crater: Proof from the geomorphological and geological evidence
p 107 N93-10124
Melt production in large-scale impact events: Calculations of impact-melt volumes and crater scaling
p 108 N93-10125
Melt production in large-scale impact events: Planetary observations and implications p 108 N93-10126
Intrusive origin of the Sudbury Igneous Complex: Structural and sedimentological evidence
p 108 N93-10128
Impactite and pseudotachylite from Roter Kamm Crater, Namibia p 109 N93-10130
Sudbury project (University of Muenster-Ontario Geological Survey): Isotope systematics support the impact origin p 109 N93-10131
Noril'sk/Siberian plateau basalts and Bahama hot spot: Impact triggered? p 109 N93-10132
New perspectives on the Popigai impact structure
p 110 N93-10138
Melt production in large-scale impact events: Implications and observations at terrestrial craters
p 112 N93-10144
The distribution and modes of occurrence of impact melt at lunar craters p 113 N93-10148
Search for a meteoritic component at the Beaverhead impact structure, Montana p 116 N93-10158
Impactites from Popigai Crater p 117 N93-10164
Sudbury Igneous Complex: Impact melt or igneous rock? Implications for lunar magmatism p 118 N93-10169
Melting and its relationship to impact crater morphology p 119 N93-10170
Impact cratering record of Fennoscandia
p 119 N93-10171
Bohemian circular structure, Czechoslovakia: Search for the impact evidence p 119 N93-10172
The pseudotachylites from the Vredefort structure and the Witwatersrand basin p 119 N93-10174
Coincidences in time of the Imbrium Basin impact and Apollo 15 KREEP volcanic series: Impact-induced melting? p 119 N93-10175
Apollo 15 impact melts, the age of Imbrium, and the Earth-Moon impact cataclysm p 120 N93-10176
Paradigm lost: Venus crater depths and the role of gravity in crater modification p 120 N93-10179
Geological evidence for a 2.6-Ga strewn field of impact spherules in the Hamersley Basin of Western Australia
p 120 N93-10181
Bronzite Granophyre: New insight on Vredefort
p 121 N93-10186
Ar-40 to Ar-39 ages of the large impact structures Kara and Manicouagan and their relevance to the Cretaceous-Tertiary and the Triassic-Jurassic boundary
p 122 N93-10188
Electron petrography of silica polymorphs associated with pseudotachylite, Vredefort structure, South Africa
p 123 N93-10192
Self-organized rock textures and multiring structure in the Duolun crater p 123 N93-10195
Geochemical aspect of impact cratering: Studies in Vernadsky Institute p 123 N93-10196
A computational study of projectile melt in impact with typical Whipple shields
[DE92-017137] p 92 N93-10635

IMPACT RESISTANCE
Impact sensitivity reduction via exo-electron control p 15 N93-10004
IMPACT TESTS
Determination of the dynamic unload/reload characteristics of ceramics [AD-A253513] p 35 N93-10221
Stress patterns in the dynamic tear test p 49 N93-10491
A computational study of projectile melt in impact with typical Whipple shields [DE92-017137] p 92 N93-10635
IMPURITIES
Boronization in D3-D [DE92-016249] p 163 N93-10759
INCIDENCE
A new ellipsometry technique for interface analysis: Application to Si-SiO2 [AD-A253143] p 167 N93-10415
INCLUSIONS
Ruthenium/iridium ratios in the Cretaceous-Tertiary boundary clay: Implications for global dispersal and fractionation within the ejecta cloud p 109 N93-10135
Failure processes in elastomeric composites p 46 N93-10475
INCOMPRESSIBLE FLOW
Finite difference methods for incompressible viscous flow in scientific computing [AD-A253512] p 79 N93-10220
Improved numerical simulation of Euler equations p 80 N93-10309
Analysis of wing-body junction flowfields using the incompressible Navier-Stokes equations, volumes 1 and 2 p 3 N93-10320
Stream function-vorticity finite element formulations of unsteady incompressible Navier-Stokes equations p 60 N93-10545
A least-squares finite element method for incompressible Navier-Stokes problem p 60 N93-10548
Numerical solution of three-dimensional unsteady viscous flows [AD-A253202] p 83 N93-10793
INCOMPRESSIBLE FLUIDS
Compressible and incompressible fluid seals: Influence on rotordynamic response and stability [NASA-CR-190746] p 92 N93-10891
INDENTATION
Indentation of a precompressed penny-shaped crack p 48 N93-10486
INDEXES (DOCUMENTATION)
Aeronautical engineering: A continuing bibliography with indexes (supplement 276) [NASA-SP-7037(276)] p 1 N93-10073
Aeronautical engineering: A continuing bibliography with indexes (supplement 279) [NASA-SP-7037(279)] p 1 N93-10074
Aeronautical engineering: A cumulative index to a continuing bibliography (supplement 274) [NASA-SP-7037(274)] p 1 N93-10351
Aeronautical engineering: A continuing bibliography with indexes (supplement 281) [NASA-SP-7037(281)] p 1 N93-10352
Document processing p 174 N93-10600
AGARD index of publications, 1989-1991 [AGARD-INDEX-89-91] p 174 N93-10610
Index to NASA news releases and speeches, 1991 [NASA-TM-108004] p 175 N93-10815
Indexes of maps of the planets and satellites, 1992 [NASA-TM-4395] p 189 N93-10832
Index to NASA news releases and speeches, 1990 [NASA-TM-108003] p 176 N93-10872
INDIA
A history of the Lonar crater, India: An overview p 118 N93-10168
INDIUM ARSENIDES
Novel optoelectronic devices based on combining GaAs and InP on Si [AD-A253781] p 165 N93-10235
INDIUM GALLIUM ARSENIDES
Spatial light modulators with arbitrary quantum well profiles [AD-A253637] p 165 N93-10210
INDIUM PHOSPHIDES
Novel optoelectronic devices based on combining GaAs and InP on Si [AD-A253781] p 165 N93-10235
INDUCTANCE
An analytic determination of beta poloidal and internal inductance in an elongated tokamak from magnetic probe measurements [DE92-016294] p 160 N93-10331
INDUSTRIAL PLANTS
Accelerator Technology Division [DE92-016023] p 156 N93-10462
INDUSTRIES
Manitoba aerospace technology: Capability directory [CTN-92-60572] p 193 N93-10655
INELASTIC SCATTERING
Glenn T. Seaborg and heavy ion nuclear science [DE92-016943] p 156 N93-10762
INERTIA
Dynamics of systems with time-varying inertial properties p 54 N93-10517
INERTIAL CONFINEMENT FUSION
Future directions in pulsed power driven ICF [DE92-016233] p 161 N93-10443
INERTIAL GUIDANCE
Methods of guidance flight dynamics [AD-A254248] p 10 N93-10704
Burn phase corrections of maneuver ballistic missiles with star light [AD-A254105] p 12 N93-10814
INERTIAL NAVIGATION
Burn phase corrections of maneuver ballistic missiles with star light [AD-A254105] p 12 N93-10814
INFORMATION
Optimization of neural network topology and information content using Boltzman methods [PB92-205418] p 142 N93-10450
INFORMATION DISSEMINATION
Seminar on Basic Documentation Practices [AGARD-R-788] p 172 N93-10593
National scene in information and documentation activities and recent developments in the Documentation Center of TUBITAK (TURDOK) p 173 N93-10594
Documentation practices: The national scene (Greece) p 173 N93-10595
Scientific and Technical Information (STI) towards technological and industrial development: The case of Portugal p 173 N93-10596
Establishing a scientific and technical information program: Planning and resource management p 173 N93-10597
Acquisition 1: Stock acquisition processes in defence and aerospace documentation centres p 173 N93-10598
Services: User services in defence and aerospace documentation centres p 174 N93-10602
EIA publications directory, 1991 [DE92-015686] p 174 N93-10607
The technology advantage: A guide to science, technology, and innovation in Manitoba [CTN-92-60571] p 192 N93-10654
INFORMATION FLOW
Unifying information flow policies [RSRE-90020] p 175 N93-10801
Lattices for security policies [RSRE-90005] p 139 N93-10823
A multilevel security model for object-oriented database systems p 175 N93-10844
INFORMATION MANAGEMENT
Analysis of observation report databases/knowledge bases [AD-A252636] p 172 N93-10428
A survey of commercial object-oriented database management systems [NASA-CR-190645] p 172 N93-10452
Seminar on Basic Documentation Practices [AGARD-R-788] p 172 N93-10593
National scene in information and documentation activities and recent developments in the Documentation Center of TUBITAK (TURDOK) p 173 N93-10594
Documentation practices: The national scene (Greece) p 173 N93-10595
Scientific and Technical Information (STI) towards technological and industrial development: The case of Portugal p 173 N93-10596
Establishing a scientific and technical information program: Planning and resource management p 173 N93-10597
Acquisition 1: Stock acquisition processes in defence and aerospace documentation centres p 173 N93-10598
Acquisition 2: Procurement, acquisition, and maintenance of configuration management documentation in support of a CIS system p 173 N93-10599
Document processing p 174 N93-10600
Technology for libraries and information centers: A seminar in Greece, Portugal, and Turkey p 174 N93-10601
Services: User services in defence and aerospace documentation centres p 174 N93-10602
Security considerations within military information systems p 174 N93-10603
INFORMATION PROCESSING (BIOLOGY)
Parallel processing and learning: Variability and chaos in self-organization of activity in groups of neurons [AD-A250290] p 140 N93-10242
Auditory processing of complex sounds across frequency channels [AD-A253612] p 131 N93-10650
Cognition in the brain: Investigations using positron emission tomography [AD-A254280] p 132 N93-10765
INFORMATION RETRIEVAL
A survey of commercial object-oriented database management systems [NASA-CR-190645] p 172 N93-10452
Seminar on Basic Documentation Practices [AGARD-R-788] p 172 N93-10593
Document processing p 174 N93-10600
Technology for libraries and information centers: A seminar in Greece, Portugal, and Turkey p 174 N93-10601
INFORMATION SYSTEMS
Format and structure of a database on health and environmental impacts of different energy systems for electricity generation [DE92-634160] p 130 N93-10222
Gridded Model Information Support System (GMISS) user's guide. Volume 3: Model concentration data retrieval subsystem [PB92-190263] p 171 N93-10257
Seminar on Basic Documentation Practices [AGARD-R-788] p 172 N93-10593
National scene in information and documentation activities and recent developments in the Documentation Center of TUBITAK (TURDOK) p 173 N93-10594
Documentation practices: The national scene (Greece) p 173 N93-10595
Scientific and Technical Information (STI) towards technological and industrial development: The case of Portugal p 173 N93-10596
Establishing a scientific and technical information program: Planning and resource management p 173 N93-10597
Acquisition 2: Procurement, acquisition, and maintenance of configuration management documentation in support of a CIS system p 173 N93-10599
Document processing p 174 N93-10600
Technology for libraries and information centers: A seminar in Greece, Portugal, and Turkey p 174 N93-10601
Services: User services in defence and aerospace documentation centres p 174 N93-10602
Security considerations within military information systems p 174 N93-10603
INFORMATION TRANSFER
Scientific and Technical Information (STI) towards technological and industrial development: The case of Portugal p 173 N93-10596
Services: User services in defence and aerospace documentation centres p 174 N93-10602
A change of course: The importance to DoD of international standards for electronic commerce [AD-A253199] p 75 N93-10792
INFRARED ASTRONOMY
Probing cosmic infrared sources: A computer modeling approach [AD-A253788] p 178 N93-10238
INFRARED DETECTORS
Semiconductor phase conjugation [AD-A253684] p 166 N93-10345
Effect of space exposure on pyroelectric infrared detectors p 38 N93-10582
Quantum 1/f noise in high technology applications including ultrasmall structures and devices [AD-A253922] p 74 N93-10751
A seam tracking modulated infrared optical sensor for use in welding [AD-A254103] p 159 N93-10812
INFRARED LASERS
An infrared free-electron laser for the Chemical Dynamics Research Laboratory [DE92-017018] p 90 N93-10864
INFRARED RADIATION
Probing cosmic infrared sources: A computer modeling approach [AD-A253788] p 178 N93-10238
Laser and optical physics [AD-A253619] p 88 N93-10251
INFRARED RADIOMETERS
Remote sounding of the Martian atmosphere p 189 N93-10378
INFRARED SIGNATURES
Air-sea interaction and remote sensing [NASA-CR-190913] p 128 N93-10068
INFRARED SPECTRA
Infrared investigations of pristine polypyrrole. Is the polymer called polypyrrole really Poly (Pyrrole-Co-Hydroxypyrrole)? [AD-A249746] p 36 N93-10243

Measurement of aerodynamic shear stress using side chain liquid crystal polymers
[AD-A254312] p 40 N93-10770
An infrared free-electron laser for the Chemical Dynamics Research Laboratory
[DE92-017018] p 90 N93-10864

INFRARED SPECTROSCOPY
Remote sounding of the Martian atmosphere
p 189 N93-10378

INJURIES
A prospective evaluation of stress fractures/overuse injuries in a population of West Point cadets
[AD-A252427] p 132 N93-10709

INLET FLOW
Radial Turbines
[VKI-LS-1992-05] p 77 N93-10050
Non-dimensional conceptual design of radial inflow turbines. Part A: Application of fundamental fluid mechanics p 77 N93-10053
Non-dimensional conceptual design of radial inflow turbines. Part B: Application of empirical correlations
p 77 N93-10054

INSPECTION
Inspection and repair decisions for hydraulic structures under symmetric deterioration
[AD-A253621] p 96 N93-10797

INSTALLING
Stress and strain of slab type amplifiers
[AD-A254246] p 74 N93-10702

INSTRUMENT FLIGHT RULES
Rotorcraft en route ATC route standards
[AD-A249129] p 6 N93-10323

INSULATORS
The effect of elevated temperatures on the properties of thermally stable silicon-based elastomers for adhesives, sealants, and insulator applications p 15 N93-10006
Template-synthesis of infrared-transparent metal microcylinders: Comparison of optical properties with the predictions of effective medium theory
[AD-A253267] p 158 N93-10694

INTEGRAL EQUATIONS
The class of the paths in the Feynman path integral on the phase space
[DE92-630205] p 170 N93-10386
Global structure of a polynomial autonomous system on the plane
[DE92-630230] p 144 N93-10389

INTEGRAL TRANSFORMATIONS
Integral transform approach to an inertial viscoelastic problem involving moving singularities
p 49 N93-10490

INTEGRATED CIRCUITS
Development of 6H-SiC CMOS transistors for insertion into a 350 C operational amplifier
[AD-A253760] p 70 N93-10233
Advanced processing and characterization technologies. Fabrication and characterization of semiconductor optoelectronic devices and integrated circuits. Final Conference Proceedings No. 10
[AD-A254162] p 73 N93-10663

INTERACTIONAL AERODYNAMICS
Effect of planform and body on supersonic aerodynamics of multibody configurations
[NASA-TP-3212] p 4 N93-10824
Contributions to the experimental investigation of rotor/body aerodynamic interactions p 5 N93-10877

INTERCEPTORS
An indicator of message quality for a single optical sensor using a template based tracking algorithm
[AD-A252704] p 139 N93-10881

INTERCONTINENTAL BALLISTIC MISSILES
Integrated vision system for a target seeker
[AD-A253359] p 135 N93-10103

INTERFACIAL TENSION
Development of physical and mathematical models for the Porous Ceramic Tube Plant Nutrification System (PCTPNS)
[NASA-TM-107551] p 129 N93-10085
Structure of thermocapillary flow in narrow cavities
p 61 N93-10552

INTERFEROMETERS
New developments in atom interferometry
[AD-A254094] p 158 N93-10659
SUN: The Solar Ultraviolet Network
p 183 N93-10930

INTERFEROMETRY
GPS azimuth determination using short baseline carrier wave interferometry
[AD-A254257] p 6 N93-10265
New developments in atom interferometry
[AD-A254094] p 158 N93-10659
Matter-wave interferometry with laser cooled atoms
[AD-A254000] p 89 N93-10720
Solar Physics and Astrophysics at Interferometric Resolution
[ESA-SP-344] p 179 N93-10901
Prospects with SIMURIS p 179 N93-10904
Yellow hypergiant interferometry: A clue to understanding evolutionary instability
p 182 N93-10919
Tomographic/interferometric studies of active stars and binaries p 182 N93-10920
Prospects in stellar and galactic observations with SIMURIS p 182 N93-10921
Interferometric imaging with the solar ultraviolet network p 184 N93-10932
Detectors for the SIMURIS payload
p 14 N93-10937
The CHARON program p 177 N93-10942
Interferometry with the Very Large Telescope
p 178 N93-10943
Towards an ESA strategy for optical interferometry in space. Recommendations of the ESA Space Interferometry Study Team (SIST) p 178 N93-10944
Ground/space co-operation for interferometry
p 178 N93-10946
Rotational aperture synthesis: A proposal for ground-based observations p 178 N93-10947
Demonstration and performances of real-time fringe tracking: A step towards cophased interferometers
p 178 N93-10948
A multipurpose vacuum-ultraviolet test facility
p 11 N93-10953
Interferometer optical design for the Imaging Fourier Transform Spectrometer (IFTS) p 159 N93-10955
Some possible space interferometry applications
p 178 N93-10957

INTERGRANULAR CORROSION
Mechanisms and modelling of environment-dependent fatigue crack growth in a nickel based superalloy
[AD-A253967] p 33 N93-10717

INTERIOR BALLISTICS
Measurement of acceleration using an instrumented railgun projectile
[AD-A253366] p 12 N93-10106

INTERMETALLICS
The third Workshop on Non-Crystalline Solids, programme and abstracts
[AD-A250739] p 36 N93-10244
Reliability of sublattice occupancies determined by ALCHEMI
[DE92-014592] p 168 N93-10623
Plasticity of single crystalline Al3X intermetallic compounds
[AD-A254282] p 40 N93-10766

INTERNAL COMBUSTION ENGINES
Pulsed jet plume combustion: An exothermic process under fluid mechanical control p 32 N93-10553

INTERNAL ENERGY
Local-equilibrium formalism applied to mechanics of solids
[DE92-016852] p 170 N93-10787

INTERNAL WAVES
SBS applications study
[AD-A253779] p 102 N93-10234

INTERNATIONAL COOPERATION
List of publications, 1969-1991. Panel on wind and seismic effects
[PB92-201102] p 125 N93-10089
Open Skies Treaty imaging radar technology issues
[DE92-016548] p 68 N93-10394

INTERNATIONAL RELATIONS
Open Skies Treaty imaging radar technology issues
[DE92-016548] p 68 N93-10394

INTERNATIONAL TRADE
Aerospace industry profile, 1990-1991
[CTN-92-60513] p 1 N93-10651
Aerospace and defence-related industries statistical survey report, 1991
[CTN-92-60514] p 2 N93-10652
Defence electronics industry profile, 1990-1991
[CTN-92-60515] p 66 N93-10653

INTERPLANETARY DUST
Analysis of interplanetary dust experiment detectors and other witness plates
[NASA-CR-190818] p 32 N93-10852
Elemental analyses of hypervelocity microparticle impact sites on interplanetary dust experiment sensor surfaces
p 32 N93-10853

INTERPOLATION
Computational fluid dynamics capability for internally carried store separation
[AD-A253671] p 79 N93-10297

INTERSTELLAR MATTER
Probing cosmic infrared sources: A computer modeling approach
[AD-A253788] p 178 N93-10238

INTESTINES
Hierarchical structure in polymeric solid and its influence on properties
[AD-A253818] p 41 N93-10825

INTRUSION
Intrusive origin of the Sudbury Igneous Complex: Structural and sedimentological evidence
p 108 N93-10128

INVISCID FLOW
Numerical methods for inviscid and viscous flow analysis p 77 N93-10055
AMR on the CM-2
[NASA-CR-190747] p 138 N93-10736
High-resolution TVD schemes for the analysis of: 1. Inviscid supersonic and transonic flows. 2. Viscous flows with shock-induced separation and heat transfer
p 5 N93-10889

ION ACCELERATORS
Reflection of plasma ions from metals (and its use as a hyperthermal neutral beam source)
p 160 N93-10353

ION ATOM INTERACTIONS
Electron transfer, ionization, and excitation in atomic collisions
[DE92-017300] p 154 N93-10435

ION BEAMS
Intense ion beam research at Los Alamos
[DE92-015240] p 155 N93-10333
Reflection of plasma ions from metals (and its use as a hyperthermal neutral beam source)
p 160 N93-10353
Cluster beam studies of metal combustion
[AD-A253952] p 30 N93-10416
Future directions in pulsed power driven ICF
[DE92-016233] p 161 N93-10443
Fast magnetic field penetration into an intense neutralized ion beam
[DE92-016861] p 156 N93-10633
Magnetic fusion with high energy self-colliding ion beams
[DE92-016860] p 156 N93-10643
Merged beam studies of laser stimulated radiative recombination
[AD-A253308] p 89 N93-10698

ION ENGINES
Electric propulsion applications p 20 N93-10029

ION IMPLANTATION
Implanted contacts for diamond semiconductor devices
[AD-A245568] p 165 N93-10274

ION RECOMBINATION
Helium transport in enhanced confinement regimes on the TEXTOR and D3-D tokamaks
[DE92-016247] p 160 N93-10293
Merged beam studies of laser stimulated radiative recombination
[AD-A253308] p 89 N93-10698

ION SOURCES
Intense ion beam research at Los Alamos
[DE92-015240] p 155 N93-10333
Reflection of plasma ions from metals (and its use as a hyperthermal neutral beam source)
p 160 N93-10353

ION TEMPERATURE
Intense ion beam research at Los Alamos
[DE92-015240] p 155 N93-10333
Edge ion dynamics in H-mode discharges in D3-D
[DE92-016255] p 162 N93-10619
Boronization in D3-D
[DE92-016249] p 163 N93-10759

IONIC COLLISIONS
Two-photon physics and the coming generation of heavy ion colliders
[DE92-015850] p 156 N93-10732

IONIC DIFFUSION
Single crystal growth of beta-Al2O3 for iso-index filters
[AD-A252259] p 169 N93-10879

IONIZATION
Resonance ionization of rubidium using sequential diode laser-driven transitions
[DE92-014468] p 89 N93-10429
Electron transfer, ionization, and excitation in atomic collisions
[DE92-017300] p 154 N93-10435

IONIZING RADIATION
DoD space radiation concerns
[AD-A253135] p 131 N93-10613
Radiation damage to DNA
[DE92-015760] p 130 N93-10834

IONOSPHERIC DISTURBANCES
Eleven years of ionospheric scintillation fading data from twenty Greenlandic stations
[AD-A253271] p 69 N93-10695
Modeling of HF propagation and heating in the ionosphere
[AD-A253941] p 125 N93-10714

IONOSPHERIC HEATING
Modeling of HF propagation and heating in the ionosphere
[AD-A253941] p 125 N93-10714

IONOSPHERIC PROPAGATION
ACIRF user's guide for the general model (Version 3.5)
[AD-A254068] p 69 N93-10657
Modeling of HF propagation and heating in the ionosphere
[AD-A253941] p 125 N93-10714
IRAQ
Al Umchaimin depression, Western Iraq: An impact structure? p 122 N93-10190
IRIDIUM
Mobilization of the platinum group elements by low-temperature fluids: Implications for mineralization and the iridium controversy p 109 N93-10133
IRON
Alternate spectrometric oil analysis techniques
[AD-A253355] p 29 N93-10101
IRON COMPOUNDS
The magnetochemistry of supramolecular particles: The transition from the molecular to the solid-state
[AD-A253126] p 153 N93-10338
IRON OXIDES
Development of garnet films for magnetostatic wave channelized receivers
[AD-A252812] p 166 N93-10335
IRRADIANCE
Measurements and modeling of laser irradiance in the high-power third-harmonic Nova focus. Volume A: Report
[DE92-016746] p 90 N93-10739
ISING MODEL
Statics and kinetics of oxygen ordering in the oxide superconductor YBa2Cu3O(z)
[DE92-017001] p 167 N93-10403
ISOTHERMAL PROCESSES
Damage due to plastic deformation in elastic-plastic materials: The thermodynamical connection p 51 N93-10502
ISOTOPES
U-Pb isotopic results for single shocked and polycrystalline zircons record 550-65.5-Ma ages for a K-T target site and 2700-1850-Ma ages for the Sudbury impact event p 115 N93-10156
ISOTOPIC LABELING
Temperature-programmed oxidation of ethane and ethylene in the presence and absence of C-13 labeled methane
[DE92-015048] p 42 N93-10329
ISOTROPIC MEDIA
Dynamic stability of laminated transversely-isotropic composite plates subjected to parametric excitations p 29 N93-10525
ISOTROPY
Calculation of stress intensity factors in an isotropic multicracked plate: Part 2: Symbolic/numeric implementation
[NASA-TM-105823] p 95 N93-10453
Calculation of stress intensity factors in an isotropic multicracked plate. Part 1: Theoretical development
[NASA-TM-105766] p 95 N93-10455
ITERATIVE SOLUTION
Parallel sparse Cholesky factorization algorithms for shared-memory multiprocessor systems
[DE92-016829] p 141 N93-10334

J

J INTEGRAL
Dynamic measurement of the J integral in ductile metals using the optical method of caustics p 49 N93-10492
JAPAN
List of publications, 1969-1991. Panel on wind and seismic effects
[PB92-201102] p 125 N93-10089
JET AIRCRAFT NOISE
Combat Aircraft Noise
[AGARD-CP-512] p 148 N93-10666
Human noise exposure criteria for combat aircraft training areas p 148 N93-10670
Noise of combat aircraft in proximity to air bases: Review of the possibilities of noise reduction at the source p 148 N93-10671
Comparison of flyover noise data from aircraft at high subsonic speeds with prediction p 149 N93-10674
Noise emission of low flying military airplanes p 149 N93-10675
Combat aircraft noise p 149 N93-10676
Boom and the problems related to the supersonic flights of military aircraft p 149 N93-10677
Combat aircraft jet engine noise studies p 150 N93-10679
Supersonic acoustic source mechanisms for free jets of various geometries p 150 N93-10680
Nozzle installation effects on the noise from supersonic exhaust plumes p 150 N93-10681
Combustion noise and combustion instabilities in propulsion systems p 150 N93-10682
Audibility-based annoyance prediction modeling p 151 N93-10683
The prediction of noise radiation from supersonic elliptic jets p 151 N93-10684
Prediction of jet mixing noise for high subsonic flight speeds p 151 N93-10685
Identifying the principal noise sources of fixed-wing combat aircraft in high-speed flight p 151 N93-10686
Measurement and prediction of noise from low-altitude military aircraft operations p 151 N93-10687
Mechanisms of sound generation in subsonic jets p 152 N93-10688
Combat aircraft noise reduction by technical measures p 152 N93-10689
Technical measures for the attenuation of aircraft noise and their applicability to GAF combat aircraft p 152 N93-10690
Study results on combat aircraft source noise reduction p 152 N93-10691
JET ENGINES
Evaluation and application of the Baldwin-Lomax turbulence model in two-dimensional, unsteady, compressible boundary layers with and without separation in engine inlets
[NASA-TM-105810] p 79 N93-10087
Mechanisms and modelling of environment-dependent fatigue crack growth in a nickel based superalloy
[AD-A253967] p 33 N93-10717
JET FLOW
A building-block approach for turbulence model validation/upgrade focussed on high-speed jet flowfields p 16 N93-10010
JET IMPINGEMENT
Nozzle installation effects on the noise from supersonic exhaust plumes p 150 N93-10681
JET MIXING FLOW
Pulsed jet plume combustion: An exothermic process under fluid mechanical control p 32 N93-10553
The prediction of noise radiation from supersonic elliptic jets p 151 N93-10684
Prediction of jet mixing noise for high subsonic flight speeds p 151 N93-10685
Identifying the principal noise sources of fixed-wing combat aircraft in high-speed flight p 151 N93-10686
Mechanisms of sound generation in subsonic jets p 152 N93-10688
Combat aircraft noise reduction by technical measures p 152 N93-10689
JET NOZZLES
Supersonic confined jet nozzles p 16 N93-10009
JET THRUST
Supersonic confined jet nozzles p 16 N93-10009
JFET
A novel charge sensitive preamplifier without the feedback resistor
[DE92-015842] p 74 N93-10731
JOINTS (JUNCTIONS)
Vibration of a damped double-beam system p 56 N93-10527
JOSEPHSON JUNCTIONS
Vortices in long Josephson junctions
[AD-A253230] p 167 N93-10404
JOURNAL BEARINGS
An experimental technique for performing 3-D LDA measurements inside whirling annular seals p 93 N93-10894
JUNCTION TRANSISTORS
Vortices in long Josephson junctions
[AD-A253230] p 167 N93-10404

K

K-EPSILON TURBULENCE MODEL
Turbulence modeling of the flow field in combustors using the non-linear k-epsilon model
[DE92-014745] p 80 N93-10330
Development of the finite analytic method for turbulent forced and free convection p 80 N93-10369
Explicit Navier-Stokes computation of turbomachinery flows p 81 N93-10370
Navier-Stokes turbine heat transfer predictions using two-equation turbulence
[NASA-TM-105817] p 82 N93-10735
The effects of streamline curvature and swirl on turbulent flows in curved ducts p 84 N93-10875
KALMAN FILTERS
Data reduction analysis for the Stanford relativity gyroscope experiment p 86 N93-10347
KARMAN VORTEX STREET
Effect of passive flow-control devices on turbulent low-speed base flow p 79 N93-10304
KERNEL FUNCTIONS
Resistive Grid Kernel Estimator (RGKE)
[AD-A253520] p 147 N93-10869
KEVLAR (TRADEMARK)
Additional results on space environmental effects on polymer matrix composites: Experiment A0180 p 38 N93-10586
KINEMATIC EQUATIONS
A derivation for the kinematic equations of flexible robots with appropriate transformation matrices p 66 N93-10577
KINEMATICS
Numerical solution of three-dimensional unsteady viscous flows
[AD-A253202] p 83 N93-10793
KINETIC ENERGY
A new energy transfer model for turbulent free shear flow
[NASA-TM-105854] p 81 N93-10454
KINETIC EQUATIONS
Effective formulation of the dynamics of a manipulator based on the Appell equations p 65 N93-10571
Methods of guidance flight dynamics
[AD-A254248] p 10 N93-10704
KLYSTRONS
Extended-interaction klystron for the AN/TPS-43-E radar system
[AD-A253166] p 76 N93-10882
KNOWLEDGE BASES (ARTIFICIAL INTELLIGENCE)
Analysis of observation report databases/knowledge bases
[AD-A252636] p 172 N93-10428
KOLMOGOROFF THEORY
Stochastic diffusion and Kolmogorov entropy in regular and random Hamiltonians
[DE92-016179] p 170 N93-10604
KREEP
Coincidences in time of the Imbrium Basin impact and Apollo 15 KREEP volcanic series: Impact-induced melting? p 119 N93-10175

L

LABOR
Aerospace industry profile, 1990-1991
[CTN-92-60513] p 1 N93-10651
LABORATORY EQUIPMENT
Instrument driver for general purpose interface bus (IEEE-488)
[AD-A253947] p 138 N93-10716
LABYRINTH SEALS
An experimental technique for performing 3-D LDA measurements inside whirling annular seals p 93 N93-10894
LAKES
Air-sea interaction and remote sensing
[NASA-CR-190913] p 128 N93-10068
LAMINAR BOUNDARY LAYER
On the coupling between a supersonic boundary layer and a flexible surface
[NASA-CR-189697] p 82 N93-10757
LAMINAR FLOW
Heat transfer and pressure drop for air flow through enhanced passages
[DE92-016597] p 82 N93-10612
Numerical study of wall turbulence
[ONERA-RSF-21/3419-AY-126] p 83 N93-10859
LAMINAR HEAT TRANSFER
High-resolution TVD schemes for the analysis of: 1. Inviscid supersonic and transonic flows. 2. Viscous flows with shock-induced separation and heat transfer p 5 N93-10889
LAMINATES
Multidimensional effects in composite propellant combustion p 42 N93-10313
Development in the elastic analysis of laminated plates p 44 N93-10468
Vibration of orthotropic cylindrical shell panels with arbitrary supported curved edges p 45 N93-10471
Vibration of laminated composite plates using various plate theories: Analytical and finite element results p 45 N93-10473
Contact problem in delamination-buckling of laminated composite shells p 46 N93-10479
Interface cracks in an orthotropic layered half-space under impact loading p 47 N93-10482
An open or closed crack terminating at a bi-material interface: Power-logarithmic singularities p 47 N93-10483
Enriched element analysis of bimaterial interface cracks p 47 N93-10484
Failure analysis of laminated composites by using iterative three-dimensional finite element method p 51 N93-10505

Analysis of a buffer strip laminate with a cutout
p 52 N93-10506
Consistent shear constitutive relations for laminated plates
p 28 N93-10509
Investigation of laminated composite plates under impact dynamic loading by using a three-dimensional hybrid stress finite element method
p 29 N93-10510
Dynamic stability of laminated transversely-isotropic composite plates subjected to parametric excitations
p 29 N93-10525
Natural vibrations of multilayered doubly curved shells
p 57 N93-10532
Linear and nonlinear analyses of thick composite circular plates using the finite element method
p 96 N93-10873

LANDAU DAMPING
A formula for efficiency of fast wave current drive in fusion devices
[DE92-016152] p 160 N93-10390

LANDFORMS
The Zhamanshin impact feature: A new class of complex crater?
p 110 N93-10139

LANTHANUM OXIDES
Oxygen barrier oxides
[AD-A253683] p 36 N93-10343

LAOS
Search for the 700,000-year-old source crater of the Australasian tektite strewn field
p 120 N93-10177

LAP JOINTS
An assessment of the correspondence principle in comparison to nonlinear viscoelastic theory: A case study
p 51 N93-10501
Comparison of the maximum stress and the stress intensity approach in the analysis of bonded joints
p 53 N93-10514
Experimental and theoretical behavior of adhesively bonded composite structures under tensile stress at the edge vicinity
p 53 N93-10515
Experimental and numeric analysis of constraints in a bonded stepped lap joint subjected to traction
p 54 N93-10516

LARGE SPACE STRUCTURES
Numerical simulation of large actively controlled space structures
p 13 N93-10308
Model reference adaptive control in large space structures
p 13 N93-10365

LASER ABLATION
The interaction of UV-Laser radiation with metal and semiconductor surfaces
[AD-A253510] p 87 N93-10201
Internal explosion in laser ablation of superconducting targets
[AD-A253701] p 90 N93-10799

LASER ANEMOMETERS
A study of flow properties of wet solids using laser induced photochemical anemometry
[DE92-015483] p 82 N93-10629
Experimental study of the flow field inside a whirling annular seal
p 92 N93-10892
An experimental technique for performing 3-D LDA measurements inside whirling annular seals
p 93 N93-10894

LASER ANNEALING
Novel Si-YBCuO reactive patterning technique for manufacture of large area high Tc superconducting electronic devices
[AD-A250740] p 73 N93-10426

LASER APPLICATIONS
Holographic optical interconnects for multichip modules
[AD-A253403] p 86 N93-10408
Accelerator Technology Division
[DE92-016023] p 156 N93-10462
Merged beam studies of laser stimulated radiative recombination
[AD-A253308] p 89 N93-10698
Design of laser optical systems
[AD-A254247] p 89 N93-10703
Matter-wave interferometry with laser cooled atoms
[AD-A254000] p 89 N93-10720
Laser cooling and trapping of neutral atoms
[AD-A253730] p 155 N93-10885
Ground/space co-operation for interferometry
p 178 N93-10946

LASER ARRAYS
Novel optoelectronic devices based on combining GaAs and InP on Si
[AD-A253781] p 165 N93-10235

LASER BEAMS
4.5 micron laser source
[AD-A253367] p 87 N93-10090
Subpicosecond resolved incipient laser damage
[AD-A253624] p 87 N93-10202
SBS applications study
[AD-A253779] p 102 N93-10234
Stress and strain of slab type amplifiers
[AD-A254246] p 74 N93-10702
Design of laser optical systems
[AD-A254247] p 89 N93-10703
Optical metrology of magnetically trapped hydrogen
[AD-A253229] p 31 N93-10712
Matter-wave interferometry with laser cooled atoms
[AD-A254000] p 89 N93-10720
System design and relaxation oscillations of a titanium-sapphire laser
[AD-A254264] p 89 N93-10725
Measurements and modeling of laser irradiance in the high-power third-harmonic Nova focus. Volume A: Report
[DE92-016746] p 90 N93-10739

LASER CAVITIES
Spatial light modulators with arbitrary quantum well profiles
[AD-A253637] p 165 N93-10210
Merged beam studies of laser stimulated radiative recombination
[AD-A253308] p 89 N93-10698
System design and relaxation oscillations of a titanium-sapphire laser
[AD-A254264] p 89 N93-10725
Laser Journal
[AD-A254106] p 90 N93-10855

LASER DAMAGE
The interaction of UV-Laser radiation with metal and semiconductor surfaces
[AD-A253510] p 87 N93-10201
Subpicosecond resolved incipient laser damage
[AD-A253624] p 87 N93-10202

LASER DOPPLER VELOCIMETERS
LV software for supersonic flow analysis
[NASA-CR-190911] p 2 N93-10069
LDV Measurements of unsteady flow fields in radial turbine
[AD-A253592] p 4 N93-10648
Experimental study of the flow field inside a whirling annular seal
p 92 N93-10892
An experimental technique for performing 3-D LDA measurements inside whirling annular seals
p 93 N93-10894

LASER INDUCED FLUORESCENCE
A time-resolved two-laser probe of Cr(CO)6 photodissociation dynamics
[AD-A250930] p 88 N93-10247
Vibrational relaxation of H2O by H2, HCl, and H2O at 295 K
[AD-A252800] p 29 N93-10263
Development of laser excited atomic fluorescence and ionization methods
[DE92-016199] p 89 N93-10611

LASER MATERIALS
Long wavelength multiple quantum well lasers for high-speed modulation applications
[AD-A253348] p 87 N93-10211

LASER OUTPUTS
4.5 micron laser source
[AD-A253367] p 87 N93-10090
Laser and optical physics
[AD-A253619] p 88 N93-10251
Stability of coupled semiconductor diode lasers
p 88 N93-10379
Stress and strain of slab type amplifiers
[AD-A254246] p 74 N93-10702
Optical metrology of magnetically trapped hydrogen
[AD-A253229] p 31 N93-10712
Influence of flow velocity on the output power of high pressure CW CO2 lasers
[AD-A254240] p 89 N93-10722
Measurements and modeling of laser irradiance in the high-power third-harmonic Nova focus. Volume A: Report
[DE92-016746] p 90 N93-10739
Studies impacting the designs of free electron lasers
[AD-A254293] p 90 N93-10768

LASER PUMPING
Subpicosecond resolved incipient laser damage
[AD-A253624] p 87 N93-10202
Geometrical transformation of linear diode-laser arrays for longitudinal pumping of solid-state lasers
[AD-A253415] p 87 N93-10218

LASER RANGE FINDERS
Dynamic positioning systems photogrammetric
[AD-A254250] p 8 N93-10898

LASER SPECTROSCOPY
Rate constants for reactions of hydrazine fuels with O(P-3)
[AD-A252813] p 42 N93-10336
Optical metrology of magnetically trapped hydrogen
[AD-A253229] p 31 N93-10712

LASER STABILITY
System design and relaxation oscillations of a titanium-sapphire laser
[AD-A254264] p 89 N93-10725

LASER TARGETS
Internal explosion in laser ablation of superconducting targets
[AD-A253701] p 90 N93-10799

LASERS
Basic and applied research in the field of electronics and communications
[AD-A253593] p 67 N93-10092
Laser and optical physics
[AD-A253619] p 88 N93-10251
Optical metrology of magnetically trapped hydrogen
[AD-A253229] p 31 N93-10712

LAUNCH VEHICLES
Pneumatic motor powered Thrust Vector Control (TVC) for liquid propelled launch vehicles
p 17 N93-10015
Electric propulsion applications
p 20 N93-10029
Operationally efficient space-based integrated propulsion module
p 22 N93-10035
A personal viewpoint on the development of China's liquid propellant rocket engines
[AD-A254104] p 27 N93-10813

LAVA
Coincidences in time of the Imbrium Basin impact and Apollo 15 KREEP volcanic series: Impact-induced melting?
p 119 N93-10175

LAW (JURISPRUDENCE)
The levels of mathematics achievement: Initial performance standards for the 1990 NAEP mathematics assessment, volume 3
[PB92-199421] p 134 N93-10341

LEAD ZIRCONATE TITANATES
Piezoelectric and electrostrictive materials for transducers applications, volume 2
[AD-A250890] p 71 N93-10276
Piezoelectric and electrostrictive materials for transducers applications, volume 3
[AD-A250891] p 72 N93-10280
Characterization of and active control of flexible structures, using piezoceramics as sensors and actuators
p 10 N93-10319

LEADING EDGE SWEEP
Effect of planform and body on supersonic aerodynamics of multibody configurations
[NASA-TP-3212] p 4 N93-10824

LEADING EDGES
Hypersonic inlet efficiency revisited
p 5 N93-10012
Flow over a leading edge with distributed roughness
p 6 N93-10549

LEARNING
Parallel processing and learning: Variability and chaos in self-organization of activity in groups of neurons
[AD-A250290] p 140 N93-10242
The levels of mathematics achievement: Initial performance standards for the 1990 NAEP mathematics assessment, volume 3
[PB92-199421] p 134 N93-10341

LEAST SQUARES METHOD
Unifying the landmark developments in optimal bounding ellipsoid identification
[AD-A253502] p 143 N93-10200
A least-squares finite element method for incompressible Navier-Stokes problem
p 60 N93-10548

LEAVES
Resource capture by single leaves
[DE92-015847] p 129 N93-10461

LECTURES
Index to NASA news releases and speeches, 1991
[NASA-TM-108004] p 175 N93-10815
Index to NASA news releases and speeches, 1990
[NASA-TM-108003] p 176 N93-10872

LEPTONS
Mass and mixing angle patterns in the standard model and its material supersymmetric extension
[DE92-016197] p 153 N93-10291

LETHALITY
Limited toxicity and mutagenicity testing of five unicharge propellant compounds
[AD-A252339] p 43 N93-10636

LIBRARIES
A look at scalable dense linear algebra libraries
[DE92-017805] p 143 N93-10285
NASA Electronic Library System (NELS) database schema, version 1.2
[NASA-CR-190643] p 172 N93-10451
Seminar on Basic Documentation Practices
[AGARD-R-788] p 172 N93-10593
Documentation practices: The national scene (Greece)
p 173 N93-10595
Scientific and Technical Information (STI) towards technological and industrial development: The case of Portugal
p 173 N93-10596

Acquisition 1: Stock acquisition processes in defence and aerospace documentation centres p 173 N93-10598
Technology for libraries and information centers: A seminar in Greece, Portugal, and Turkey p 174 N93-10601
Services: User services in defence and aerospace documentation centres p 174 N93-10602
A look at scalable dense linear algebra libraries [DE92-017161] p 139 N93-10816

LIFE (DURABILITY)
The total time on test statistic and age-dependent censoring [AD-A253622] p 147 N93-10798

LIFE CYCLE COSTS
Feasibility evaluation of the monolithic braided ablative nozzle p 19 N93-10023

LIFE SCIENCES
Aerospace medicine and biology: A continuing bibliography with indexes (supplement 365) [NASA-SP-7011(365)] p 130 N93-10075
Aerospace medicine and biology: A continuing bibliography with indexes (supplement 360) [NASA-SP-7011(360)] p 130 N93-10076
Aerospace medicine and biology: A continuing bibliography with indexes (supplement 364) [NASA-SP-7011(364)] p 130 N93-10077
Aerospace medicine and biology: A continuing bibliography with indexes (supplement 366) [NASA-SP-7011(366)] p 130 N93-10079
Aerospace medicine and biology: A continuing bibliography with indexes (supplement 367) [NASA-SP-7011(367)] p 130 N93-10080

LIFE SUPPORT SYSTEMS
Guidelines for developing spacecraft maximum allowable concentrations for Space Station contaminants [NASA-CR-190748] p 13 N93-10737

LIFT
Forced unsteady separated flows on a 45 degree delta wing p 80 N93-10305
Control of lift and drag in unsteady flows [AD-A253146] p 3 N93-10340
A method of testing two-dimensional airfoils [AD-A253210] p 4 N93-10375

LIGANDS
Transition metal activation and functionalization of carbon-hydrogen bonds [DE92-014809] p 30 N93-10400

LIGHT AIRCRAFT
Analysis of wing-body junction flowfields using the incompressible Navier-Stokes equations, volumes 1 and 2 p 3 N93-10320

LIGHT AMPLIFIERS
Stress and strain of slab type amplifiers [AD-A254246] p 74 N93-10702

LIGHT BEAMS
Optical metrology of magnetically trapped hydrogen [AD-A253229] p 31 N93-10712

LIGHT EMISSION
Langmuir probe and optical emission studies of Ar, O2, and N2 plasmas produced by an ECR microwave source [AD-A253138] p 162 N93-10615

LIGHT IONS
Future directions in pulsed power driven ICF [DE92-016233] p 161 N93-10443

LIGHT MODULATION
Spatial light modulators with arbitrary quantum well profiles [AD-A253637] p 165 N93-10210
Comparison of optically-addressed spatial light modulators [AD-A254189] p 157 N93-10259

LIGHT SCATTERING
SBS applications study [AD-A253779] p 102 N93-10234
Laser and optical physics [AD-A253619] p 88 N93-10251
Polarized light scattering from perfect and perturbed surfaces and fundamental scattering systems [AD-A253186] p 158 N93-10445

LIGHT SOURCES
A seam tracking modulated infrared optical sensor for use in welding [AD-A254103] p 159 N93-10812

LIGHT TRANSMISSION
UV spectrum splitting mirror [DE92-018057] p 159 N93-10818

LIGHT VALVES
Comparison of optically-addressed spatial light modulators [AD-A254189] p 157 N93-10259

LIGHTNING
Method and apparatus for determining return stroke polarity of distant lightning [NASA-CASE-MFS-26102-2-CU] p 125 N93-10108

LIMITER CIRCUITS
Design and evaluation of a quasi-active delay-line limiter/filter RF protection device [AD-A254179] p 71 N93-10255

LINE SPECTRA
Emission tomography of sodium in a hydrogen-air flame [AD-A253530] p 29 N93-10224

LINEAR ACCELERATORS
Advanced transport systems for electron beams in high-brightness accelerators and FEL's [AD-A253314] p 88 N93-10286
UV/XUV FEL storage ring and linac [AD-A253307] p 89 N93-10697

LINEAR AMPLIFIERS
Extended-interaction klystron for the AN/TPS-43-E radar system [AD-A253166] p 76 N93-10882

LINEAR ARRAYS
Geometrical transformation of linear diode-laser arrays for longitudinal pumping of solid-state lasers [AD-A253415] p 87 N93-10218

LINEAR EQUATIONS
Solving large linearized systems in mechanics [AD-A252723] p 144 N93-10639

LINEAR QUADRATIC GAUSSIAN CONTROL
Design, test, and evaluation of three active flutter suppression controllers [NASA-TM-4338] p 10 N93-10070

LINEAR SYSTEMS
Calculation of stress intensity factors in an isotropic multicracked plate. Part 1: Theoretical development [NASA-TM-105766] p 95 N93-10455

LINEARIZATION
An assessment of the correspondence principle in comparison to nonlinear viscoelastic theory: A case study p 51 N93-10501
Solving large linearized systems in mechanics [AD-A252723] p 144 N93-10639

LIPID METABOLISM
Interdisciplinary research and training program in the plant sciences [DE92-015919] p 130 N93-10835

LIQUID CRYSTALS
The application of liquid crystal polymers to turbomachinery p 23 N93-10040
Comparison of optically-addressed spatial light modulators [AD-A254189] p 157 N93-10259
Synthesis of side chain liquid crystal polymerization by living ring opening metathesis polymerization. Report 1: Influence of molecular weight, polydispersity, and flexible spacer length (n=2-8) on the thermotropic behavior of the resulting polymers [AD-A248699] p 40 N93-10727
Measurement of aerodynamic shear stress using side chain liquid crystal polymers [AD-A254312] p 40 N93-10770

LIQUID FUELS
Temperature-programmed oxidation of ethane and ethylene in the presence and absence of C-13 labeled methane [DE92-015048] p 42 N93-10329
Biological production of ethanol from coal [DE92-016114] p 43 N93-10608
Studies on the combustion efficiency of liquid fuel rockets with variable thrust [AD-A254232] p 26 N93-10721

LIQUID HYDROGEN
Tank chilldown analysis and verification with a flightweight, 175 cu ft tank under normal gravity with liquid hydrogen p 24 N93-10045
Tensile properties of cast titanium alloys: Titanium-6Al-4V ELI and Titanium-5Al-2.5Sn ELI [NASA-TP-3288] p 33 N93-10072

LIQUID METALS
A multi-fluid model of turbulence for Li-SF6 submerged combustion [AD-A253973] p 31 N93-10423

LIQUID PHASE EPITAXY
Epitaxial magnetic oxides [AD-A253667] p 35 N93-10230
Development of garnet films for magnetostatic wave channelized receivers [AD-A252812] p 166 N93-10335

LIQUID PHASES
Tank chilldown analysis and verification with a flightweight, 175 cu ft tank under normal gravity with liquid hydrogen p 24 N93-10045
Electronic and structural properties of metallic microclusters [DE92-016917] p 33 N93-10411
Study of improved methods for predicting chemical equilibria [DE92-016974] p 31 N93-10436

LIQUID PROPELLANT ROCKET ENGINES
The 1992 JANNAF Propulsion Meeting, volume 1 [CPIA-PUBL-580-VOL-1] p 15 N93-10001
Pneumatic motor powered Thrust Vector Control (TVC) for liquid propelled launch vehicles p 17 N93-10015
LAM actuated propellant flow control device p 18 N93-10017
Selection of rocket propulsion systems p 22 N93-10034
A personal viewpoint on the development of China's liquid propellant rocket engines [AD-A254104] p 27 N93-10813

LIQUID ROCKET PROPELLANTS
NLS cargo transfer vehicle propulsion system p 23 N93-10041
Loading operations for spacecraft propulsion subsystems p 11 N93-10047
Theory of combustion of liquid propellants based on hydroxylammonium nitrate [AD-A248445] p 42 N93-10267
Rate constants for reactions of hydrazine fuels with O(P-3) [AD-A252813] p 42 N93-10336

LIQUID-SOLID INTERFACES
Structure of thermocapillary flow in narrow cavities p 61 N93-10552

LITHIUM ALLOYS
The microstructural characterization of an Al-Li-Cu-Mg alloy (8090) metal-matrix composite [RAE-TM-MAT/STR-1139] p 34 N93-10802

LITHOLOGY
Sudbury project (University of Muenster-Ontario Geological Survey): Sr-Nd in heterolithic breccias and gabbroic dikes p 107 N93-10123
Viscosity determinations of some frictionally generated silicate melts: Implications for slip zone rheology during impact-induced faulting p 121 N93-10183
A comparison of the chemistry of pseudotachylyte breccias in the Archean Levack Gneisses of the Sudbury structure, Ontario p 122 N93-10187

LOAD DISTRIBUTION (FORCES)
Investigation of laminated composite plates under impact dynamic loading by using a three-dimensional hybrid stress finite element method p 29 N93-10510

LOAD TESTS
Transverse tension, transverse compression, and inplane shear JANNAF round robin test methods standardization results p 16 N93-10007
On the development of a new fracture toughness procedure p 59 N93-10541

LOADING OPERATIONS
Loading operations for spacecraft propulsion subsystems p 11 N93-10047

LOADS (FORCES)
An evaluation of a method of reconstituting fatigue loading from Rainflow counting [RAE-TR-89057] p 94 N93-10198
A spline finite strip method for analysing local and distortional buckling of thin-walled beams under arbitrary loading p 58 N93-10538
An evaluation of the cumulative damage effect under creep loading p 58 N93-10540
Stability of open-graded bases under wheel loads using a model testing approach [AD-A253209] p 66 N93-10710
Power system monitoring and source control of the Space Station Freedom DC power system testbed [NASA-TM-105841] p 26 N93-10734

LOGISTICS MANAGEMENT
A change of course: The importance to DoD of international standards for electronic commerce [AD-A253199] p 75 N93-10792

LONG DURATION EXPOSURE FACILITY
LDEF Materials Workshop 1991, part 2 [NASA-CP-3162-PT-2] p 37 N93-10578
Selected results for metals from LDEF experiment A0171 p 34 N93-10579
Some results of the oxidation investigation of copper and silver samples flown on LDEF p 34 N93-10580
Changes in oxidation state of chromium during LDEF exposure p 34 N93-10581
Effect of space exposure on pyroelectric infrared detectors p 38 N93-10582
Long Duration Exposure Facility (LDEF) optical systems SIG summary and database p 38 N93-10583
Polymer matrix composites on LDEF experiments M0003-9 and M0003-10 p 38 N93-10584
Space environmental effects on LDEF low Earth orbit exposed graphite reinforced polymer matrix composites p 38 N93-10585
Proposed test program and data base for LDEF polymer matrix composites p 38 N93-10587
Identification and evaluation of lubricants, adhesives, and seals used on LDEF p 39 N93-10588
Results from the testing and analysis of LDEF batteries p 39 N93-10589

Effects of long-term exposure on LDEF fastener assemblies p 39 N93-10590
Results from testing and analysis of solar cells flown on LDEF p 39 N93-10591
System related testing and analysis of FRECOPA p 39 N93-10592
Analysis of interplanetary dust experiment detectors and other witness plates [NASA-CR-190818] p 32 N93-10852
Elemental analyses of hypervelocity microparticle impact sites on interplanetary dust experiment sensor surfaces p 32 N93-10853
Contaminant interferences with SIMS analyses of microparticle impactor residues on LDEF surfaces p 32 N93-10854

LONG DURATION SPACE FLIGHT
Aerospace medicine and biology: A continuing bibliography with indexes (supplement 366) [NASA-SP-7011(366)] p 130 N93-10079
Aerospace medicine and biology: A continuing bibliography with indexes (supplement 367) [NASA-SP-7011(367)] p 130 N93-10080

LONGITUDINAL CONTROL
Pitch control trimming system for canard design aircraft [CA-PATENT-APPL-SN-2013236] p 10 N93-10374

LORAN C
Rotorcraft en route ATC route standards [AD-A249129] p 6 N93-10323

LOSSES
Software for prediction and analysis of ground wave propagation loss [AD-A253474] p 67 N93-10199

LOW ALTITUDE
Combat aircraft operations: Training requirements for the German Air Force tactical flying units and the noise problem p 148 N93-10667
Combat aircraft noise: The operator's perspective p 148 N93-10669
Noise emission of low flying military airplanes p 149 N93-10675
Measurement and prediction of noise from low-altitude military aircraft operations p 151 N93-10687
Appraisal of digital terrain elevation data for low-altitude flight [NASA-TM-103896] p 7 N93-10745

LOW COST
Formed platelets for low cost regeneratively cooled rocket combustion chambers p 18 N93-10018
Global positioning systems technology and its application in environmental programs [PB92-169358] p 7 N93-10442

LOW FREQUENCIES
Low-frequency noise reduction in SQUID measurements using laser switching [AD-A253821] p 90 N93-10827

LOW SPEED
Effect of passive flow-control devices on turbulent low-speed base flow p 79 N93-10304
An experimental and a theoretical investigation of rotor pitch damping using a model rotor p 8 N93-10322

LOW TEMPERATURE
Mobilization of the platinum group elements by low-temperature fluids: Implications for mineralization and the iridium controversy p 109 N93-10133

LOW THRUST
Electric Propulsion Space Experiment (ESEX): Spacecraft design issues for high-power electric propulsion p 21 N93-10030

LUBRICANTS
Materials compatibility and lubricants research on CFC-refrigerant substitute: Miscibility of lubricants with refrigerants [DE92-015118] p 35 N93-10084
Materials compatibility and lubricants research on CFC-refrigerant substitutes: Thermophysical properties [DE92-015116] p 43 N93-10397
Chemical and thermal stability of refrigerant-lubricant mixture with metal [DE92-015117] p 44 N93-10398
ARTI Refrigerant Database [DE92-015122] p 30 N93-10401
Identification and evaluation of lubricants, adhesives, and seals used on LDEF p 39 N93-10588

LUNAR BASED EQUIPMENT
Proceedings of the FY 1990 Workshop on Extraterrestrial Mining and Construction [AD-A253399] p 189 N93-10406
Report of the Lunar Interferometry Study Team (LIST) activities p 178 N93-10945

LUNAR BASES
Proceedings of the FY 1990 Workshop on Extraterrestrial Mining and Construction [AD-A253399] p 189 N93-10406

LUNAR CONSTRUCTION EQUIPMENT
Proceedings of the FY 1990 Workshop on Extraterrestrial Mining and Construction [AD-A253399] p 189 N93-10406

LUNAR CRATERS
The distribution and modes of occurrence of impact melt at lunar craters p 113 N93-10148
Apollo 15 impact melts, the age of Imbrium, and the Earth-Moon impact cataclysm p 120 N93-10176

LUNAR CRUST
Enhanced magnetic field production during oblique hypervelocity impacts p 108 N93-10129
Sudbury Igneous Complex: Impact melt or igneous rock? Implications for lunar magmatism p 118 N93-10169
Coincidences in time of the Imbrium Basin impact and Apollo 15 KREEP volcanic series: Impact-induced melting? p 119 N93-10175

LUNAR EVOLUTION
Enhanced magnetic field production during oblique hypervelocity impacts p 108 N93-10129

LUNAR EXCAVATION EQUIPMENT
Proceedings of the FY 1990 Workshop on Extraterrestrial Mining and Construction [AD-A253399] p 189 N93-10406

LUNAR GEOLOGY
Enhanced magnetic field production during oblique hypervelocity impacts p 108 N93-10129
The distribution and modes of occurrence of impact melt at lunar craters p 113 N93-10148
Coincidences in time of the Imbrium Basin impact and Apollo 15 KREEP volcanic series: Impact-induced melting? p 119 N93-10175
The large impact process inferred from the geology of lunar multiring basins p 121 N93-10184

LUNAR GRAVITATION
On the gravitational potential of two arbitrary rotating bodies with applications to the Earth-Moon system p 179 N93-10303

LUNAR MAGNETIC FIELDS
Enhanced magnetic field production during oblique hypervelocity impacts p 108 N93-10129

LUNAR MARIA
Coincidences in time of the Imbrium Basin impact and Apollo 15 KREEP volcanic series: Impact-induced melting? p 119 N93-10175
Apollo 15 impact melts, the age of Imbrium, and the Earth-Moon impact cataclysm p 120 N93-10176
Variation in multiring basic structures as a function of impact angle p 123 N93-10194

LUNAR ROCKS
The distribution and modes of occurrence of impact melt at lunar craters p 113 N93-10148

LUNAR SURFACE
Enhanced magnetic field production during oblique hypervelocity impacts p 108 N93-10129
Apollo 15 impact melts, the age of Imbrium, and the Earth-Moon impact cataclysm p 120 N93-10176
The large impact process inferred from the geology of lunar multiring basins p 121 N93-10184

LUTETIUM COMPOUNDS
Development of garnet films for magnetostatic wave channelized receivers [AD-A252812] p 166 N93-10335

M

MACH NUMBER
Pitot survey of exhaust flow field of a 2-D scramjet nozzle at Mach 6 with air or freon and argon used for exhaust simulation [NASA-TM-4361] p 2 N93-10071
Mathematical analysis of strong fluid mechanical effects at high Mach number in reactive and nonreactive flow [AD-A253617] p 79 N93-10094
High-speed viscous flows past blunt bodies and compression corners with flux-split methods [AD-A253413] p 81 N93-10410
Effect of planform and body on supersonic aerodynamics of multibody configurations [NASA-TP-3212] p 4 N93-10824

MACHINE LEARNING
Artificial intelligence technical paper abstracts, 1991 [AD-A253340] p 141 N93-10269
PRODIGY4.0: The manual and tutorial [AD-A253970] p 137 N93-10422

MACHINE TOOLS
Developmental research on ultra abrasion-resistant materials [DE92-531066] p 36 N93-10287

MAGMA
Sudbury project (University of Muenster-Ontario Geological Survey): Isotope systematics support the impact origin p 109 N93-10131
Sudbury Igneous Complex: Impact melt or igneous rock? Implications for lunar magmatism p 118 N93-10169
Bronzite Granophyre: New insight on Vredefort p 121 N93-10186
Al Umchaimin depression, Western Iraq: An impact structure? p 122 N93-10190

MAGNESIUM
Development of garnet films for magnetostatic wave channelized receivers [AD-A252812] p 166 N93-10335

MAGNESIUM ALLOYS
The microstructural characterization of an Al-Li-Cu-Mg alloy (8090) metal-matrix composite [RAE-TM-MAT/STR-1139] p 34 N93-10802

MAGNETIC COMPRESSION
Thermal management in high average power pulsed compression systems [DE92-017055] p 76 N93-10836

MAGNETIC CORES
Investigation of the effect of large core changes in toroidal plasma rotation and radial electric field on confinement in H-mode discharges in the D3-D tokamak [DE92-016252] p 161 N93-10392

MAGNETIC DIPOLES
Gradiometer antennas for tunnel detection [PB92-205400] p 69 N93-10440
Modelling of 3-D electromagnetic responses using the time-wavenumber method [DE92-017025] p 70 N93-10865

MAGNETIC ENERGY STORAGE
Long conduction time plasma opening switch experiments at Sandia National Labs [DE92-015003] p 72 N93-10279

MAGNETIC FIELD CONFIGURATIONS
An analytic determination of beta poloidal and internal inductance in an elongated tokamak from magnetic probe measurements [DE92-016294] p 160 N93-10331

MAGNETIC FIELD RECONNECTION
Physics of coronal loops: Heating and reconnection p 180 N93-10912

MAGNETIC FIELDS
Semiclassical quantization of interacting anyons in a strong magnetic field [DE92-634889] p 169 N93-10229
Long conduction time plasma opening switch experiments at Sandia National Labs [DE92-015003] p 72 N93-10279
Advanced transport systems for electron beams in high-brightness accelerators and FEL's [AD-A253314] p 88 N93-10286
Semiclassical quantization of integrable systems of few interacting anyons in a strong magnetic field [DE92-634892] p 170 N93-10295
Vector superconductivity in cosmic strings [DE92-634923] p 179 N93-10296
An analytic determination of beta poloidal and internal inductance in an elongated tokamak from magnetic probe measurements [DE92-016294] p 160 N93-10331
Investigation of the effect of large core changes in toroidal plasma rotation and radial electric field on confinement in H-mode discharges in the D3-D tokamak [DE92-016252] p 161 N93-10392
Polarimetry of motional Stark effect and determination of current profiles in D3-D [DE92-016258] p 161 N93-10393
Gradiometer antennas for tunnel detection [PB92-205400] p 69 N93-10440
Model for the reversible magnetization of high-(kappa) type-2 superconductors: Application to high-temperature superconductor [DE92-016297] p 167 N93-10609
Fast magnetic field penetration into an intense neutralized ion beam [DE92-016861] p 156 N93-10633
Optical metrology of magnetically trapped hydrogen [AD-A253229] p 31 N93-10712
Covalent electron transfer theory of superconductivity [AD-A253975] p 74 N93-10718
Development of high temperature superconductors for magnetic field applications [DE92-015930] p 168 N93-10733
Stellar and circumstellar evolution and activity p 181 N93-10918

MAGNETIC FLUX
Variational full wave calculation of fast wave current drive in D3-D using the ALCYON code [DE92-016572] p 163 N93-10761

MAGNETIC MATERIALS
Epitaxial magnetic oxides [AD-A253667] p 35 N93-10230

MAGNETIC MEASUREMENT
An analytic determination of beta poloidal and internal inductance in an elongated tokamak from magnetic probe measurements [DE92-016294] p 160 N93-10331

MAGNETIC MOMENTS
Electronic structure of highly correlated structures
[DE92-017017] p 155 N93-10863
MAGNETIC PROBES
An analytic determination of beta poloidal and internal inductance in an elongated tokamak from magnetic probe measurements
[DE92-016294] p 160 N93-10331
High sensitivity probes for silicon VLSI internal node testing
[AD-A253924] p 169 N93-10764
MAGNETIC PROPERTIES
The magnetochemistry of supramolecular particles: The transition from the molecular to the solid-state
[AD-A253126] p 153 N93-10338
NQR-NMR studies of higher alcohol synthesis Cu-Co catalysts
[DE92-015783] p 31 N93-10460
MAGNETICALLY TRAPPED PARTICLES
Matter-wave interferometry with laser cooled atoms
[AD-A254000] p 89 N93-10720
MAGNETIZATION
Enhanced magnetic field production during oblique hypervelocity impacts p 108 N93-10129
Model for the reversible magnetization of high-(kappa) type-2 superconductors: Application to high-temperature superconductor
[DE92-016297] p 167 N93-10609
MAGNETO-OPTICS
Epitaxial magnetic oxides
[AD-A253667] p 35 N93-10230
Magnetostatic waves-based integrated optic Bragg cell modules with applications to RF signal processing
[AD-A254035] p 71 N93-10240
Matter-wave interferometry with laser cooled atoms
[AD-A254000] p 89 N93-10720
MAGNETOHYDRODYNAMIC GENERATORS
Dispersion of seed vapor and gas ionization in an MHD second stage combustor and channel
[DE92-016699] p 163 N93-10645
Magnetohydrodynamic projects at the CDIF
[DE92-018190] p 164 N93-10819
MHD Integrated Topping Cycle Project
[DE92-016610] p 164 N93-10861
MAGNETOHYDRODYNAMIC STABILITY
D-He-3 spherical torus fusion reactor system study
[AD-A253358] p 155 N93-10102
Investigation of the effect of large core changes in toroidal plasma rotation and radial electric field on confinement in H-mode discharges in the D3-D tokamak
[DE92-016252] p 161 N93-10392
Future directions in pulsed power driven ICF
[DE92-016233] p 161 N93-10443
VH-mode discharges in the D3-D tokamak
[DE92-016257] p 161 N93-10463
Large orbit magnetic confinement systems for advanced fusion fuels
[DE92-016218] p 162 N93-10617
Global Alfven eigenmodes in D3-D
[DE92-016250] p 163 N93-10760
MAGNETOHYDRODYNAMIC WAVES
A formula for efficiency of fast wave current drive in fusion devices
[DE92-016152] p 160 N93-10390
Global Alfven eigenmodes in D3-D
[DE92-016250] p 163 N93-10760
Variational full wave calculation of fast wave current drive in D3-D using the ALCYON code
[DE92-016572] p 163 N93-10761
Ultra-high observations of the prominence-corona transition region p 180 N93-10908
Coronal and solar wind Alfven wave propagation p 180 N93-10909
MAGNETOHYDRODYNAMICS
Fast magnetic field penetration into an intense neutralized ion beam
[DE92-016861] p 156 N93-10633
MAGNETOMETERS
Enhanced magnetic field production during oblique hypervelocity impacts p 108 N93-10129
MAGNETOPLASMADYNAMICS
Fundamental studies on erosion in MPD thrusters
[AD-A253900] p 159 N93-10252
Synchrotron radiation considerations in the Dense Plasma Focus (DPF) Magnetoplasmadynamic (MPD) thruster
[AD-A254188] p 25 N93-10258
MAGNETOSHEATH
Simulation study of interactions of Space Shuttle-generated electron beams with ambient plasmas
[NASA-CR-190843] p 159 N93-10066
MAGNETOSTATICS
Magnetostatic waves-based integrated optic Bragg cell modules with applications to RF signal processing
[AD-A254035] p 71 N93-10240
Development of garnet films for magnetostatic wave channelized receivers
[AD-A252812] p 166 N93-10335
MAGNETS
High-power microwave breakdown of dielectric interfaces
[AD-A254200] p 124 N93-10262
MAGNITUDE
Worldwide seismic catalog and the nature of seismic coupling p 124 N93-10376
MAGNONS
Atomic short range order and spin density wave propagation in CuMn
[DE92-016903] p 34 N93-10789
MAINTENANCE
Acquisition 2: Procurement, acquisition, and maintenance of configuration management documentation in support of a CIS system p 173 N93-10599
Inspection and repair decisions for hydraulic structures under symmetric deterioration
[AD-A253621] p 96 N93-10797
MAN MACHINE SYSTEMS
Maintaining future military aircraft design capability
[AD-A253963] p 8 N93-10420
KC-135 crew reduction feasibility demonstration simulation study. Volume 3: Test and evaluation
[AD-A253931] p 134 N93-10713
MAN-COMPUTER INTERFACE
Ada validation tests for rate monotonic scheduling algorithms
[AD-A253325] p 136 N93-10300
MANAGEMENT INFORMATION SYSTEMS
Space Station: NASA's software development approach increases safety and cost risks. Report to the Chairman, Committee on Science, Space, and Technology, House of Representatives
[GAO/IMTEC-92-39] p 12 N93-10081
MANAGEMENT METHODS
Space Station: NASA's software development approach increases safety and cost risks. Report to the Chairman, Committee on Science, Space, and Technology, House of Representatives
[GAO/IMTEC-92-39] p 12 N93-10081
MANAGEMENT PLANNING
Total Quality Management (TQM) concepts applied to instruction
[DE92-013399] p 171 N93-10270
MANEUVERABILITY
Flight test and analysis procedures for new handling criteria
[RAE-TM-FM-26] p 8 N93-10803
MANGANESE ALLOYS
Atomic short range order and spin density wave propagation in CuMn
[DE92-016903] p 34 N93-10789
MANIPULATORS
Dynamics of an orbiting flexible manipulator p 54 N93-10519
Effective formulation of the dynamics of a manipulator based on the Appell equations p 65 N93-10571
A solution scheme for the deflection equations of flexible arms with time-dependent boundary conditions p 66 N93-10575
A derivation for the kinematic equations of flexible robots with appropriate transformation matrices p 66 N93-10577
MANITOBA
The technology advantage: A guide to science, technology, and innovation in Manitoba
[CTN-92-60571] p 192 N93-10654
Manitoba aerospace technology: Capability directory
[CTN-92-60572] p 193 N93-10655
MANNED MARS MISSIONS
A comparison of multimegawatt electric propulsion options for Mars missions p 23 N93-10043
MANNED SPACE FLIGHT
DoD space radiation concerns
[AD-A253135] p 131 N93-10613
MANUALS
Probability forecasting: A guide for forecasters and staff weather officers
[AD-A254216] p 126 N93-10264
MANUFACTURING
Semiconductor phase conjugation
[AD-A253684] p 166 N93-10345
Automated handling and assembling of non-rigid objects
[AD-A253605] p 66 N93-10649
Manitoba aerospace technology: Capability directory
[CTN-92-60572] p 193 N93-10655
MANY BODY PROBLEM
Automated multi-body system dynamics via bond graph modelling and interactive graphics p 66 N93-10576
Theory of transport for interacting many-body systems
[AD-A253789] p 169 N93-10871
MAPPING
Geographic Information System (GIS) development assistance for Nuclear Regulatory Commission (NRC) incident response capability
[DE92-017595] p 176 N93-10867
MAPS
Indexes of maps of the planets and satellites, 1992
[NASA-TM-4395] p 189 N93-10832
MARANGONI CONVECTION
Structure of thermocapillary flow in narrow cavities p 61 N93-10552
MARINE BIOLOGY
Molecular biology in studies of oceanic primary production
[DE92-016101] p 128 N93-10283
MARINE CHEMISTRY
The 200th American Chemical Society Geochemistry Division Symposium on Progress in Marine Chemistry
[AD-A253757] p 129 N93-10887
MARINE ENVIRONMENTS
Spatial models of ecological systems and processes: The role of GIS
[DE92-016884] p 175 N93-10788
MARINE METEOROLOGY
Air-sea interaction in regions of varying surface conditions
[AD-A253182] p 128 N93-10791
Microwave radiometer studies of atmospheric water over the oceans, volume 2
[NASA-CR-190343] p 127 N93-10848
Comparison of wind speed measurements over the oceans with the Special Sensor Microwave/Imager and the Geosat altimeter p 127 N93-10850
Morning-evening differences in global and regional oceanic precipitation as observed by the SSM/I p 127 N93-10851
MARKET RESEARCH
Defence electronics industry profile, 1990-1991
[CTN-92-60515] p 66 N93-10653
MARKETING
EIA publications directory, 1991
[DE92-015686] p 174 N93-10607
MARS (PLANET)
A comparison of multimegawatt electric propulsion options for Mars missions p 23 N93-10043
MARS ATMOSPHERE
Workshop on the evolution of the Martian atmosphere
[NASA-CR-190730] p 189 N93-10064
Remote sounding of the Martian atmosphere p 189 N93-10378
MARS OBSERVER
Remote sounding of the Martian atmosphere p 189 N93-10378
MARTENSITIC TRANSFORMATION
Electronic and structural properties of metallic microclusters
[DE92-016917] p 33 N93-10411
MASKS
Evaluation of lightweight and low profile communications devices for Respiratory Protective system 21 (RESPO 21)
[AD-A253393] p 133 N93-10217
Evaluation of an electronics system concept for Respiratory Protection system (RESPO 21)
[AD-A253394] p 134 N93-10288
Novel seals and specialty component attachment mechanisms for Respiratory Protection system (RESPO 21)
[AD-A253395] p 91 N93-10290
MASS FLOW
Performance parameters and assessment p 77 N93-10052
MASS SPECTRA
Study on the pi(sup -)p yields eta' pi(sup 0)n reaction at 38 and 100 GeV/c momenta
[DE92-624593] p 153 N93-10328
MASS SPECTROMETERS
Portable tandem mass spectrometer analyzer
[AD-A254065] p 125 N93-10784
MASS TRANSFER
Mass transfer in oscillating flows: Efficient drying via pulse combustors
[PB92-204403] p 81 N93-10449
MASSIFS
Bohemian circular structure, Czechoslovakia: Search for the impact evidence p 119 N93-10172
Variation in multiring basic structures as a function of impact angle p 123 N93-10194
MASSIVELY PARALLEL PROCESSORS
Calculation of elastic-plastic wave propagation on the connection machine
[AD-A252429] p 95 N93-10427
AMR on the CM-2
[NASA-CR-190747] p 138 N93-10736

MATERIALS TESTS
LDEF Materials Workshop 1991, part 2
[NASA-CP-3162-PT-2] p 37 N93-10578
Stability of open-graded bases under wheel loads using a model testing approach
[AD-A253209] p 66 N93-10710
MATHEMATICAL LOGIC
Symbolic Boolean manipulation with ordered binary decision diagrams
[AD-A253822] p 142 N93-10828
MATHEMATICAL MODELS
A simplified model for hybrid rocket performance prediction p 19 N93-10022
An inverse design method for radial turbomachines p 78 N93-10057
Development of physical and mathematical models for the Porous Ceramic Tube Plant Nutrification System (PCTPNS)
[NASA-TM-107551] p 129 N93-10085
Mathematical analysis of strong fluid mechanical effects at high Mach number in reactive and nonreactive flow
[AD-A253617] p 79 N93-10094
What can we learn about impact mechanics from large craters on Venus? p 118 N93-10166
Probing cosmic infrared sources: A computer modeling approach
[AD-A253788] p 178 N93-10238
Convergence performance of adaptive detectors, part 3
[AD-A248415] p 143 N93-10275
On the gravitational potential of two arbitrary rotating bodies with applications to the Earth-Moon system p 179 N93-10303
The role of eddy fluxes in the response of the atmosphere to tropical thermal forcing p 124 N93-10318
An experimental and a theoretical investigation of rotor pitch damping using a model rotor p 8 N93-10322
Effects of gravity in folding --- of geological layers p 124 N93-10324
Monitoring structural response in pressurized environments. Part 2: Applications
[DE92-015034] p 94 N93-10327
Semiconductor phase conjugation
[AD-A253684] p 166 N93-10345
Numerical modelling of fringing fields and their use for complex permittivity measurements at high frequencies
[AD-A253994] p 72 N93-10359
Materials compatibility and lubricants research on CFC-refrigerant substitutes: Thermophysical properties
[DE92-015116] p 43 N93-10397
Simple shearing flow of a 3D foam
[DE92-011151] p 36 N93-10399
A multi-fluid model of turbulence for Li-SF6 submerged combustion
[AD-A253973] p 31 N93-10423
New directions in computational mechanics p 44 N93-10467
Non-linear thermoelasticity of rubberlike solids p 45 N93-10474
Integrated finite element model of composite materials p 46 N93-10477
Contact problem in delamination-buckling of laminated composite shells p 48 N93-10479
Comparison of full 3-D, thin-film 3-D, and thin-film plate analyses of a postbuckled embedded delamination p 47 N93-10480
On the behavior of a higher-order plate bending element p 47 N93-10481
Enriched element analysis of bimaterial interface cracks p 47 N93-10484
Elastic wave scattering by an interfacial crack in a plate p 48 N93-10485
Nonstationary random variations of moderately thick plates using BEM p 48 N93-10487
Numerical simulation of transient crack growth p 48 N93-10488
Dynamic crack division in brittle solids p 48 N93-10489
Stress patterns in the dynamic tear test p 49 N93-10491
A multilayered shell finite element p 49 N93-10495
A new non-Gausssian approximation technique for random vibration of general hysteresis p 50 N93-10496
Orthotropic circular plate on nonlinear elastic subgrade p 53 N93-10513
An elastic oblate axisymmetric reference gyro for attitude studies p 54 N93-10518
Vibration of a damped double-beam system p 56 N93-10527
On the vibration of axisymmetric shells p 57 N93-10535
A comparative study of semi-empirical dynamic stall models p 5 N93-10544
A reappraisal of compound equilibrium finite elements p 63 N93-10561
On the use of coupled finite element boundary element models in numerical design analysis p 63 N93-10563
Numerical considerations for structural system identification from modal information p 63 N93-10564
A boundary element super-element method for coupling with the finite element method of substructures p 64 N93-10566
Partial solution of the generalized eigenvalue problem using the Woodbury transformation p 64 N93-10567
Numerical simulation of the propagation of coupled thermomechanical waves in inelastic solids p 64 N93-10568
Optimal robot trajectory planning p 65 N93-10570
Modelling and control of robotic arms fabricated from orthotropic materials p 65 N93-10572
Modelling of flexible multibody dynamics and a computer method via the bond graph method p 65 N93-10573
Automated multi-body system dynamics via bond graph modelling and interactive graphics p 66 N93-10576
Self-programming of matter and the evolution of proto-biological organizations
[DE92-015244] p 129 N93-10628
Combustion noise and combustion instabilities in propulsion systems p 150 N93-10682
Modeling of HF propagation and heating in the ionosphere
[AD-A253941] p 125 N93-10714
Analytical characterization of bistatic scattering from Gaussian distributed surfaces
[AD-A254253] p 159 N93-10724
The development of computational methods of adhesion and adhesive science and technology
[AD-A253758] p 92 N93-10740
Unified viscoplastic behavior of metal matrix composites
[NASA-TM-105819] p 96 N93-10777
Air-sea interaction in regions of varying surface conditions
[AD-A253182] p 128 N93-10791
Inspection and repair decisions for hydraulic structures under symmetric deterioration
[AD-A253621] p 96 N93-10797
The total time on test statistic and age-dependent censoring
[AD-A253622] p 147 N93-10798
An example secure system specified using the Terry-Wiseman approach
[RSRE-90011] p 134 N93-10804
The Terry-Wiseman security policy model and examples of its use
[RSRE-90001] p 134 N93-10807
Development of nonlinear aerodynamic models for unsteady responses p 4 N93-10845
Arguments concerning wind tunnel test studies of the trim characteristics of objects with small asymmetries'
[AD-A254111] p 5 N93-10858
Numerical study of wall turbulence
[ONERA-RSF-21/3419-AY-126] p 83 N93-10859
Study of a viscous sublayer model in the analysis of 3-D shock/boundary layer interaction flow fields
[AD-A253731] p 84 N93-10886
Mechanics of composite materials for spacecraft
[AD-A254217] p 28 N93-10896
Small scale processes in solar and stellar plasmas p 181 N93-10917
MATHEMATICAL PROGRAMMING
A boundary element and mathematical programming approach for unilateral contact problems p 62 N93-10558
MATHEMATICS
The levels of mathematics achievement: Initial performance standards for the 1990 NAEP mathematics assessment, volume 3
[PB92-199421] p 134 N93-10341
MATRICES (MATHEMATICS)
A look at scalable dense linear algebra libraries
[DE92-017805] p 143 N93-10285
Numerical simulation of large actively controlled space structures p 13 N93-10308
Recovery techniques for real time electronic systems
[AD-A254010] p 136 N93-10361
Variational formulation of a mixed method for second order frame analysis p 62 N93-10556
Numerical simulation of the propagation of coupled thermomechanical waves in inelastic solids p 64 N93-10568
LABAN-PEL: A two-dimensional, multigroup diffusion, high-order response matrix code
[DE92-626845] p 144 N93-10624
A look at scalable dense linear algebra libraries
[DE92-017161] p 139 N93-10816
MATRIX MATERIALS
Space environmental effects on LDEF low Earth orbit exposed graphite reinforced polymer matrix composites p 38 N93-10585
Proposed test program and data base for LDEF polymer matrix composites p 38 N93-10587
MATRIX METHODS
Variational formulation of a mixed method for second order frame analysis p 62 N93-10556
Partial solution of the generalized eigenvalue problem using the Woodbury transformation p 64 N93-10567
A derivation for the kinematic equations of flexible robots with appropriate transformation matrices p 66 N93-10577
LABAN-PEL: A two-dimensional, multigroup diffusion, high-order response matrix code
[DE92-626845] p 144 N93-10624
MAXIMA
An assessment of the correspondence principle in comparison to nonlinear viscoelastic theory: A case study p 51 N93-10501
Comparison of the maximum stress and the stress intensity approach in the analysis of bonded joints p 53 N93-10514
MAXIMUM LIKELIHOOD ESTIMATES
Test range tracking network processors
[AD-A253511] p 140 N93-10219
MAXWELL EQUATION
System design and relaxation oscillations of a titanium-sapphire laser
[AD-A254264] p 89 N93-10725
MECHANICAL ENGINEERING
Proceedings of the Twelfth Canadian Congress of Applied Mechanics, volumes 1 and 2
[ISBN-0920049-03] p 44 N93-10466
Inspection and repair decisions for hydraulic structures under symmetric deterioration
[AD-A253621] p 96 N93-10797
Mechanical and thermal design of the SUN instrument p 14 N93-10956
MECHANICAL PROPERTIES
Transverse tension, transverse compression, and inplane shear JANNAF round robin test methods standardization results p 16 N93-10007
GAP benefits p 19 N93-10025
Effects of the RSRM grain deformation on ballistic performance p 20 N93-10027
Resonance apparatus operating manual
[AD-A254040] p 71 N93-10241
Damage accumulation process in advanced metal matrix composite under thermal cycling
[AD-A248674] p 27 N93-10277
Composite failure analysis handbook. Volume 2: Technical handbook. Part 2: Atlas of fractographs
[AD-A249130] p 28 N93-10325
Advanced technology component derating
[AD-A253334] p 72 N93-10357
Mechanical behavior of open cell ceramics
[PB92-212984] p 37 N93-10439
Protective coatings for niobium alloys and their properties
[AD-A254252] p 33 N93-10706
Hierarchical structure in polymeric solid and its influence on properties
[AD-A253818] p 41 N93-10825
MEDIAN (STATISTICS)
Order statistics and nonparametric statistics
[AD-A253574] p 146 N93-10699
MEDICAL PHENOMENA
A new test of scanning and monitoring ability: Methods and initial results
[AD-A249123] p 132 N93-10321
MELTING
Nonlinear studies of surface and interfaces of advanced semiconductor materials
[AD-A253365] p 164 N93-10105
Asteroids and Archaean crustal evolution: Tests of possible genetic links between major mantle/crust melting events and clustered extraterrestrial bombardments p 110 N93-10140
Electronic and structural properties of metallic microclusters
[DE92-016917] p 33 N93-10411
MELTS (CRYSTAL GROWTH)
Viscosity determinations of some frictionally generated silicate melts: Implications for slip zone rheology during impact-induced faulting p 121 N93-10183
MEMBRANE STRUCTURES
Template-synthesis of infrared-transparent metal microcylinders: Comparison of optical properties with the predictions of effective medium theory
[AD-A253267] p 158 N93-10694
MEMBRANES
Research in the optical sciences
[AD-A253188] p 158 N93-10446

Chronorheological characterization of elastomers p 46 N93-10476

MEMORY
Parallel processing and learning: Variability and chaos in self-organization of activity in groups of neurons [AD-A250290] p 140 N93-10242

MEMORY (COMPUTERS)
Parallel sparse Cholesky factorization algorithms for shared-memory multiprocessor systems [DE92-016829] p 141 N93-10334
Artificial neural network system for memory modification [AD-D015354] p 142 N93-10958
Memory modification of artificial neural networks [AD-D015356] p 143 N93-10959

MENTAL PERFORMANCE
Effects of early bright, late bright and dim illumination upon circadian neuroendocrine, electrophysiological and behavioral responses [AD-A254129] p 131 N93-10861
Mental workload assessment in the cockpit: Feasibility of using electrophysiological measurements, phase 1 [AD-A254138] p 133 N93-10862
NASA Space Human Factors Program [NASA-TM-108005] p 134 N93-10890

MERIDIONAL FLOW
Pattern recognition applied to H(sub alpha) spectroheliograms: solar rotation and meridional circulation p 182 N93-10924

MESOMETEOROLOGY
Mesoscale severe weather development under orographic influences [AD-A253630] p 125 N93-10204

MESOSCALE PHENOMENA
Mesoscale severe weather development under orographic influences [AD-A253630] p 125 N93-10204

MESOSPHERE
Investigations of the dynamics and thermodynamics of the mesosphere lower thermosphere and upper thermosphere at the polar regions with optical ground-based remote sensing [AD-A253228] p 125 N93-10711

MESSAGE PROCESSING
Weather Message Switching Center Replacement (WMSCR) Operational Test and Evaluation (OT/E)/integration test plan [DOT/FAA/CT-TN90/59] p 7 N93-10833
An indicator of message quality for a single optical sensor using a template based tracking algorithm [AD-A252704] p 139 N93-10881

MESSAGES
Investigation of a possible stochastic model for the IEEE P896.1 (Futurebus+) protocol, including the proposed enhanced distributed arbiter [CTN-92-60593] p 135 N93-10088
A change of course: The importance to DoD of international standards for electronic commerce [AD-A253199] p 75 N93-10792

METABOLISM
Interaction of electromagnetic fields with chondrocytes in gel culture [AD-A253727] p 70 N93-10747
Metabolic factors influencing myocardial recovery from acidosis (CiC3) [AD-A252376] p 132 N93-10796

METAL AIR BATTERIES
Air cell --- model aircraft power supplies [CA-PATENT-APPL-SN-2001346] p 72 N93-10368

METAL BONDING
Experimental and numeric analysis of constraints in a bonded stepped lap joint subjected to traction p 54 N93-10516

METAL COMBUSTION
Cluster beam studies of metal combustion [AD-A253952] p 30 N93-10416
A multi-fluid model of turbulence for Li-SF6 submerged combustion [AD-A253973] p 31 N93-10423

METAL FATIGUE
Fatigue crack propagation in the presence of shot-peening residual stresses p 59 N93-10542
Improvements to the AC potential drop method of crack measurement p 59 N93-10543

METAL FILMS
Intense ion beam research at Los Alamos [DE92-015240] p 155 N93-10333
Scanning tunneling microscopy of semiconductor surfaces [AD-A246853] p 168 N93-10726

METAL MATRIX COMPOSITES
Sensor and actuator materials for high performance composites [AD-A254178] p 27 N93-10254
Damage accumulation process in advanced metal matrix composite under thermal cycling [AD-A248674] p 27 N93-10277
Inhibiting corrosion in Gr/Al and Gr/Mg metal matrix composites using nonequilibrium alloying techniques [AD-A253923] p 34 N93-10752
Unified viscoplastic behavior of metal matrix composites [NASA-TM-105819] p 96 N93-10777
The microstructural characterization of an Al-Li-Cu-Mg alloy (8090) metal-matrix composite [RAE-TM-MAT/STR-1139] p 34 N93-10802
Mechanics of composite materials for spacecraft [AD-A254217] p 28 N93-10896

METAL OXIDE SEMICONDUCTORS
Development of 6H-SiC CMOS transistors for insertion into a 350 C operational amplifier [AD-A253760] p 70 N93-10233
Electron transfer reactions in microporous solids [DE92-016222] p 166 N93-10284

METAL OXIDES
Development of high temperature superconductors for magnetic field applications [DE92-015930] p 168 N93-10733

METAL PARTICLES
Alternate spectrometric oil analysis techniques [AD-A253355] p 29 N93-10101

METAL PROPELLANTS
Cluster beam studies of metal combustion [AD-A253952] p 30 N93-10416

METAL SURFACES
Activated transport in AMTEC electrodes [DE92-016810] p 75 N93-10786

METAL VAPOR LASERS
Theoretical analysis of discharges in copper vapor lasers: A comparison of Ne and He [DE92-014739] p 87 N93-10083

METALLIC GLASSES
The third Workshop on Non-Crystalline Solids, programme and abstracts [AD-A250739] p 36 N93-10244

METALORGANIC CHEMICAL VAPOR DEPOSITION
Atomic approaches to defect thermochemistry [AD-A254278] p 167 N93-10425

METALS
The Deposition and Fate of Trace Metals in our Environment: Symposium proceedings [PB92-189216] p 104 N93-10289
Chemical and thermal stability of refrigerant-lubricant mixture with metal [DE92-015117] p 44 N93-10398
ARTI Refrigerant Database [DE92-015122] p 30 N93-10401
Selected results for metals from LDEF experiment A0171 p 34 N93-10579
Mechanics of composite materials for spacecraft [AD-A254217] p 28 N93-10896

METAMORPHIC ROCKS
Research core drilling in the Manson impact structure, Iowa p 105 N93-10114
Diaplectic transformation of minerals: Vorotilov drill core, Puchezh-Katunki impact crater, Russia p 110 N93-10136
Self-organized rock textures and multiring structure in the Duolun crater p 123 N93-10195

METAMORPHISM (GEOLOGY)
A quasi-Hertzian stress field from an internal source: A possible working model for the Vredefort structure p 106 N93-10115
Shocked zircons in the Onaping Formation: Further proof of impact origin p 107 N93-10121
Sudbury project (University of Muenster-Ontario Geological Survey): Sr-Nd in heterolithic breccias and gabbroic dikes p 107 N93-10123
Hong Kong is an impact crater: Proof from the geomorphological and geological evidence p 107 N93-10124
Intrusive origin of the Sudbury Igneous Complex: Structural and sedimentological evidence p 108 N93-10128
Does the Bushveld-Vredefort system (South Africa) record the largest known terrestrial impact catastrophe? p 109 N93-10134
Breccia dikes from the Beaverhead Impact structure, southwest Montana p 110 N93-10137
Optical and TEM study of shock metamorphism from the Sedan test site p 111 N93-10142
Report on the international Cambodian crater expedition, 1992 p 113 N93-10147
Thermobarometric studies on the Levack Gneisses: Footwall rocks to the Sudbury Igneous Complex p 114 N93-10152
Influence of the preshock temperature on shock effects in quartz p 115 N93-10157
Phase transformations in 40-60-GPa shocked gneisses from the Haughton Crater (Canada): An Analytical Transmission Electron Microscopy (ATEM) study p 117 N93-10163
Impactites from Popigai Crater p 117 N93-10164

METASTABLE STATE
Effect of alloying elements on passivity and breakdown of passivity of Fe- and Ni-based alloys mechanistics aspects [DE92-017316] p 33 N93-10395

METATHESIS
Synthesis of side chain liquid crystal polymerization by living ring opening metathesis polymerization. Report 1: Influence of molecular weight, polydispersity, and flexible spacer length (n=2-8) on the thermotropic behavior of the resulting polymers [AD-A248699] p 40 N93-10727

METEOR TRAILS
Meteor burst communications system trial, 1990-1991 [AD-A253625] p 67 N93-10203

METEORITE COLLISIONS
International Conference on Large Meteorite Impacts and Planetary Evolution [NASA-CR-190677] p 105 N93-10112
Large meteorite impacts: The K/T model p 107 N93-10120
Shocked zircons in the Onaping Formation: Further proof of impact origin p 107 N93-10121
Impactite and pseudotachylite from Roter Kamm Crater, Namibia p 109 N93-10130
Noril'sk/Siberian plateau basalts and Bahama hot spot: Impact triggered? p 109 N93-10132
Mobilization of the platinum group elements by low-temperature fluids: Implications for mineralization and the iridium controversy p 109 N93-10133
Does the Bushveld-Vredefort system (South Africa) record the largest known terrestrial impact catastrophe? p 109 N93-10134
Ruthenium/iridium ratios in the Cretaceous-Tertiary boundary clay: Implications for global dispersal and fractionation within the ejecta cloud p 109 N93-10135
Diaplectic transformation of minerals: Vorotilov drill core, Puchezh-Katunki impact crater, Russia p 110 N93-10136
Breccia dikes from the Beaverhead Impact structure, southwest Montana p 110 N93-10137
New perspectives on the Popigai impact structure p 110 N93-10138
Asteroids and Archaean crustal evolution: Tests of possible genetic links between major mantle/crust melting events and clustered extraterrestrial bombardments p 110 N93-10140
The Acraman impact and its widespread ejecta, South Australia p 111 N93-10141
Optical and TEM study of shock metamorphism from the Sedan test site p 111 N93-10142
Simulated meteorite impacts and volcanic explosions: Ejecta analyses and planetary implications p 111 N93-10143
Melt production in large-scale impact events: Implications and observations at terrestrial craters p 112 N93-10144
Where's the Beaverhead beef? --- meteorite impact structure p 112 N93-10146
Report on the international Cambodian crater expedition, 1992 p 113 N93-10147
The distribution and modes of occurrence of impact melt at lunar craters p 113 N93-10148
Large impacts in the Baltic shield with special attention to the Uppland structure p 113 N93-10149
Geomechanical models of impact cratering: Puchezh-Katunki structure p 114 N93-10151
Thermobarometric studies on the Levack Gneisses: Footwall rocks to the Sudbury Igneous Complex p 114 N93-10152
The Cretaceous-Tertiary (K/T) impact: One or more source craters? p 114 N93-10153
Tektite origin by hypervelocity asteroidal or cometary impact: The quest for the source craters p 114 N93-10154
Early Archean spherule beds of possible impact origin from Barberton, South Africa: A detailed mineralogical and geochemical study p 115 N93-10155
U-Pb isotopic results for single shocked and polycrystalline zircons record 550-65.5-Ma ages for a K-T target site and 2700-1850-Ma ages for the Sudbury impact event p 115 N93-10156
Influence of the preshock temperature on shock effects in quartz p 115 N93-10157
Search for a meteoritic component at the Beaverhead impact structure, Montana p 116 N93-10158
Ordovician impacts at sea in Baltoscandia p 116 N93-10159
Does the sedimentology of the Chelmsford formation provide evidence for a meteorite impact origin of the Sudbury structure? p 116 N93-10160

Impact origin of the Sudbury structure: Evolution of a theory p 116 N93-10161
What can we learn about impact mechanics from large craters on Venus? p 118 N93-10166
A history of the Lonar crater, India: An overview p 118 N93-10168
Melting and its relationship to impact crater morphology p 119 N93-10170
Impact cratering record of Fennoscandia p 119 N93-10171
Bohemian circular structure, Czechoslovakia: Search for the impact evidence p 119 N93-10172
The Vredefort Dome: Review of geology and deformation phenomena and status report on current knowledge and remaining problematics (five years after the cryptoexplosion workshop) p 119 N93-10173
The pseudotachylites from the Vredefort structure and the Witwatersrand basin p 119 N93-10174
Apollo 15 impact melts, the age of Imbrium, and the Earth-Moon impact cataclysm p 120 N93-10176
Recognizing impactor signatures in the planetary record p 120 N93-10178
Paradigm lost: Venus crater depths and the role of gravity in crater modification p 120 N93-10179
K/T boundary stratigraphy: Evidence for multiple impacts and a possible comet stream p 120 N93-10180
Bronzite Granophyre: New insight on Vredefort p 121 N93-10186
Ar-40 to Ar-39 ages of the large impact structures Kara and Manicouagan and their relevance to the Cretaceous-Tertiary and the Triassic-Jurassic boundary p 122 N93-10188
Ar-40 to Ar-39 dating of pseudotachylites from the Witwatersrand basin, South Africa, with implications for the formation of the Vredefort Dome p 122 N93-10189
Al Umchaimin depression, Western Iraq: An impact structure? p 122 N93-10190
A late Devonian impact event and its association with a possible extinction event on Eastern Gondwana p 122 N93-10191
Floor-fractured crater models of the Sudbury structure, Canada p 123 N93-10193
Variation in multiring basic structures as a function of impact angle p 123 N93-10194
Self-organized rock textures and multiring structure in the Duolun crater p 123 N93-10195

METEORITE CRATERS

International Conference on Large Meteorite Impacts and Planetary Evolution [NASA-CR-190677] p 105 N93-10112
Research core drilling in the Manson impact structure, Iowa p 105 N93-10114
A quasi-Hertzian stress field from an internal source: A possible working model for the Vredefort structure p 106 N93-10115
Sudbury project (University of Muenster-Ontario Geological Survey): Origin of the polymict, allochthonous breccias of the Onaping Formation p 106 N93-10116
Sudbury project (University of Muenster-Ontario Geological Survey): Summary of results - an updated impact model p 106 N93-10117
Structural aspects of the Araguainha impact structure (Brazil) p 106 N93-10118
Large meteorite impacts: The K/T model p 107 N93-10120
Suevite superposition on the Bunte breccia in Noerdlinger Ries, Germany: New findings on the transport mechanism of impactites p 107 N93-10122
Sudbury project (University of Muenster-Ontario Geological Survey): Sr-Nd in heterolithic breccias and gabbroic dikes p 107 N93-10123
Hong Kong is an impact crater: Proof from the geomorphological and geological evidence p 107 N93-10124
Melt production in large-scale impact events: Calculations of impact-melt volumes and crater scaling p 108 N93-10125
Melt production in large-scale impact events: Planetary observations and implications p 108 N93-10126
Impactite and pseudotachylite from Roter Kamm Crater, Namibia p 109 N93-10130
Mobilization of the platinum group elements by low-temperature fluids: Implications for mineralization and the iridium controversy p 109 N93-10133
Diaplectic transformation of minerals: Vorotilov drill core, Puchezh-Katunki impact crater, Russia p 110 N93-10136
The Zhamanshin impact feature: A new class of complex crater? p 110 N93-10139
Simulated meteorite impacts and volcanic explosions: Ejecta analyses and planetary implications p 111 N93-10143
Melt production in large-scale impact events: Implications and observations at terrestrial craters p 112 N93-10144
Venusian impact basins and cratered terrains p 112 N93-10145
Report on the international Cambodian crater expedition, 1992 p 113 N93-10147
The distribution and modes of occurrence of impact melt at lunar craters p 113 N93-10148
Large impacts in the Baltic shield with special attention to the Uppland structure p 113 N93-10149
The Panther Mountain circular structure, a possible buried meteorite crater p 113 N93-10150
Geomechanical models of impact cratering: Puchezh-Katunki structure p 114 N93-10151
The Cretaceous-Tertiary (K/T) impact: One or more source craters? p 114 N93-10153
Tektite origin by hypervelocity asteroidal or cometary impact: The quest for the source craters p 114 N93-10154
Ordovician impacts at sea in Baltoscandia p 116 N93-10159
Does the sedimentology of the Chelmsford formation provide evidence for a meteorite impact origin of the Sudbury structure? p 116 N93-10160
Impact origin of the Sudbury structure: Evolution of a theory p 116 N93-10161
Imaging radar investigations of the Sudbury structure p 117 N93-10162
Phase transformations in 40-60-GPa shocked gneisses from the Haughton Crater (Canada): An Analytical Transmission Electron Microscopy (ATEM) study p 117 N93-10163
Impactites from Popigai Crater p 117 N93-10164
Sudbury Breccia and suevite as glacial indicators transported 800 km to Kentland Astroblème, Indiana p 117 N93-10165
What can we learn about impact mechanics from large craters on Venus? p 118 N93-10166
Sudbury project (University of Muenster-Ontario Geological Survey): New investigations on Sudbury breccia p 118 N93-10167
A history of the Lonar crater, India: An overview p 118 N93-10168
Sudbury Igneous Complex: Impact melt or igneous rock? Implications for lunar magmatism p 118 N93-10169
Melting and its relationship to impact crater morphology p 119 N93-10170
Impact cratering record of Fennoscandia p 119 N93-10171
Bohemian circular structure, Czechoslovakia: Search for the impact evidence p 119 N93-10172
The Vredefort Dome: Review of geology and deformation phenomena and status report on current knowledge and remaining problematics (five years after the cryptoexplosion workshop) p 119 N93-10173
Search for the 700,000-year-old source crater of the Australasian tektite strewn field p 120 N93-10177
Recognizing impactor signatures in the planetary record p 120 N93-10178
Paradigm lost: Venus crater depths and the role of gravity in crater modification p 120 N93-10179
The large impact process inferred from the geology of lunar multiring basins p 121 N93-10184
Ar-40 to Ar-39 ages of the large impact structures Kara and Manicouagan and their relevance to the Cretaceous-Tertiary and the Triassic-Jurassic boundary p 122 N93-10188
Ar-40 to Ar-39 dating of pseudotachylites from the Witwatersrand basin, South Africa, with implications for the formation of the Vredefort Dome p 122 N93-10189
A late Devonian impact event and its association with a possible extinction event on Eastern Gondwana p 122 N93-10191
Electron petrography of silica polymorphs associated with pseudotachylite, Vredefort structure, South Africa p 123 N93-10192
Floor-fractured crater models of the Sudbury structure, Canada p 123 N93-10193
Variation in multiring basic structures as a function of impact angle p 123 N93-10194
Self-organized rock textures and multiring structure in the Duolun crater p 123 N93-10195
Geochemical aspect of impact cratering: Studies in Vernadsky Institute p 123 N93-10196

METEORITIC COMPOSITION

Ruthenium/iridium ratios in the Cretaceous-Tertiary boundary clay: Implications for global dispersal and fractionation within the ejecta cloud p 109 N93-10135
Bohemian circular structure, Czechoslovakia: Search for the impact evidence p 119 N93-10172
The Vredefort Dome: Review of geology and deformation phenomena and status report on current knowledge and remaining problematics (five years after the cryptoexplosion workshop) p 119 N93-10173
Search for the 700,000-year-old source crater of the Australasian tektite strewn field p 120 N93-10177

METEORITIC DAMAGE

Noril'sk/Siberian plateau basalts and Bahama hot spot: Impact triggered? p 109 N93-10132
Diaplectic transformation of minerals: Vorotilov drill core, Puchezh-Katunki impact crater, Russia p 110 N93-10136
Breccia dikes from the Beaverhead impact structure, southwest Montana p 110 N93-10137
Melting and its relationship to impact crater morphology p 119 N93-10170
Impact cratering record of Fennoscandia p 119 N93-10171
Bohemian circular structure, Czechoslovakia: Search for the impact evidence p 119 N93-10172
The pseudotachylites from the Vredefort structure and the Witwatersrand basin p 119 N93-10174
Coincidences in time of the Imbrium Basin impact and Apollo 15 KREEP volcanic series: Impact-induced melting? p 119 N93-10175
Apollo 15 impact melts, the age of Imbrium, and the Earth-Moon impact cataclysm p 120 N93-10176
Search for the 700,000-year-old source crater of the Australasian tektite strewn field p 120 N93-10177
Recognizing impactor signatures in the planetary record p 120 N93-10178
Ar-40 to Ar-39 ages of the large impact structures Kara and Manicouagan and their relevance to the Cretaceous-Tertiary and the Triassic-Jurassic boundary p 122 N93-10188
Floor-fractured crater models of the Sudbury structure, Canada p 123 N93-10193
Variation in multiring basic structures as a function of impact angle p 123 N93-10194

METEOROID SHOWERS

Meteor burst communications system trial, 1990-1991 [AD-A253625] p 67 N93-10203

METEOROLOGICAL PARAMETERS

Shortened Test Heating Season (STHS) p 43 N93-10314
Meteorological and site influences affecting the comparison of nephelometer and photographic determinations of light extinction at rural sites in the Eastern US [PB92-195999] p 126 N93-10433
Long-term data collection and empirical background temperature modeling [AD-A254044] p 127 N93-10780
Microwave radiometer studies of atmospheric water over the oceans, volume 2 [NASA-CR-190343] p 127 N93-10848
Comparison of wind speed measurements over the oceans with the Special Sensor Microwave/Imager and the Geosat altimeter p 127 N93-10850

METEOROLOGICAL SATELLITES

Automatic cloud classification from multi-spectral satellite data over oceanic regions [AD-A253670] p 126 N93-10292

METEOROLOGICAL SERVICES

Mesoscale severe weather development under orographic influences [AD-A253630] p 125 N93-10204
Weather Message Switching Center Replacement (WMSCR) Operational Test and Evaluation (OT/E)/integration test plan [DOT/FAA/CT-TN90/59] p 7 N93-10833

METEOROLOGY

Workshop on the evolution of the Martian atmosphere [NASA-CR-190730] p 189 N93-10064
Atlas of Southern Hemisphere 500 mb teleconnection patterns derived from National Meteorological Center analyses [PB92-203892] p 126 N93-10337
Meteorological and site influences affecting the comparison of nephelometer and photographic determinations of light extinction at rural sites in the Eastern US [PB92-195999] p 126 N93-10433

METHANE

The current and future environmental role of atmospheric methane: Model studies and uncertainties [NASA-CR-190662] p 104 N93-10256
Temperature-programmed oxidation of ethane and ethylene in the presence and absence of C-13 labeled methane [DE92-015048] p 42 N93-10329

METHOD OF MOMENTS

Far-zone field of a monopole element on a disk ground plane above flat earth [AD-A253580] p 70 N93-10091
Analysis of a medium size BOR radome [AD-A253954] p 69 N93-10418

METHYLHYDRAZINE

Rate constants for reactions of hydrazine fuels with O(P-3) [AD-A252813] p 42 N93-10336

METRIC SPACE
Quantum tunneling and the change in the signature of the spacetime metric
[DE92-634877] p 165 N93-10225
METROLOGY
Optical metrology of magnetically trapped hydrogen
[AD-A253229] p 31 N93-10712
MICROANALYSIS
Reliability of sublattice occupancies determined by ALCHEMI
[DE92-014592] p 168 N93-10623
MICROCRACKS
Calculation of stress intensity factors in an isotropic multicracked plate: Part 2: Symbolic/numeric implementation
[NASA-TM-105823] p 95 N93-10453
Calculation of stress intensity factors in an isotropic multicracked plate. Part 1: Theoretical development
[NASA-TM-105766] p 95 N93-10455
MICROELECTRONICS
Multidimensional deterministic electron transport calculations
[AD-A254021] p 154 N93-10362
Field-emitter arrays for RF vacuum microelectronics
[AD-A253396] p 73 N93-10405
Spectroscopic differential reflectance as an analytical probe for microelectronic processing
[AD-A253134] p 73 N93-10656
MICROMECHANICS
Failure processes in elastomeric composites
p 46 N93-10475
Integrated finite element model of composite materials
p 46 N93-10477
Dynamic crack division in brittle solids
p 48 N93-10489
Status of dynamic fracture in brittle solids
p 49 N93-10493
Entropy of disorder in thermomechanics of damage in heterogeneous solids p 50 N93-10498
Analysis of failure modes in ceramic matrix composite
p 28 N93-10508
Mechanics of composite materials for spacecraft
[AD-A254217] p 28 N93-10896
MICROMETEOROIDS
System related testing and analysis of FRECOPA
p 39 N93-10592
Elemental analyses of hypervelocity microparticle impact sites on interplanetary dust experiment sensor surfaces
p 32 N93-10853
Contaminant interferences with SIMS analyses of microparticle impactor residues on LDEF surfaces
p 32 N93-10854
MICROPARTICLES
Analysis of interplanetary dust experiment detectors and other witness plates
[NASA-CR-190818] p 32 N93-10852
Elemental analyses of hypervelocity microparticle impact sites on interplanetary dust experiment sensor surfaces
p 32 N93-10853
Contaminant interferences with SIMS analyses of microparticle impactor residues on LDEF surfaces
p 32 N93-10854
MICROPHONES
Evaluation of an electronics system concept for Respiratory Protection system (RESPO 21)
[AD-A253394] p 134 N93-10288
MICROPOROSITY
Electron transfer reactions in microporous solids
[DE92-016222] p 166 N93-10284
MICROPROCESSORS
Instrument driver for general purpose interface bus (IEEE-488)
[AD-A253947] p 138 N93-10716
MICROSCOPES
Field emission current-voltage curves as a diagnostic for scanning tunneling microscope tips
[AD-A251171] p 165 N93-10245
MICROSCOPY
Atomic force microscope studies of CuCl island formation on CaF2(111) substrates
[AD-A252499] p 34 N93-10880
MICROSTRIP ANTENNAS
Proceedings of the Antenna Applications Symposium, volume 1
[AD-A253681] p 68 N93-10301
Proceedings of the Antenna Applications Symposium, volume 2
[AD-A253682] p 68 N93-10302
MICROSTRIP TRANSMISSION LINES
Proceedings of the Antenna Applications Symposium, volume 2
[AD-A253682] p 68 N93-10302
Field-emitter arrays for RF vacuum microelectronics
[AD-A253396] p 73 N93-10405
MICROSTRUCTURE
Optical and TEM study of shock metamorphism from the Sedan test site p 111 N93-10142
Epitaxial growth and dopant incorporation in diamond
[AD-A253636] p 165 N93-10206
Damage accumulation process in advanced metal matrix composite under thermal cycling
[AD-A248674] p 27 N93-10277
Oxygen barrier oxides
[AD-A253683] p 36 N93-10343
Growth defects in diamond films
[AD-A253618] p 40 N93-10778
A fundamental understanding of the effects of ceramic processing on product microstructure
[AD-A253660] p 41 N93-10779
The microstructural characterization of an Al-Li-Cu-Mg alloy (8090) metal-matrix composite
[RAE-TM-MAT/STR-1139] p 34 N93-10802
MICROWAVE AMPLIFIERS
Extended-interaction klystron for the AN/TPS-43-E radar system
[AD-A253166] p 76 N93-10882
MICROWAVE ATTENUATION
Microwave propagation and attenuation in magnetoplasmas
[AD-A250197] p 69 N93-10728
MICROWAVE EMISSION
Cosmic microwave background anisotropies from plausible double inflation
[DE92-016195] p 192 N93-10616
MICROWAVE EQUIPMENT
Basic and applied research in the field of electronics and communications
[AD-A253593] p 67 N93-10092
Ceramic transactions. Volume 21: Proceedings of the Symposium on Microwave Theory and Application in Materials Processing Annual Meeting No. 23 io on april 29-may 3 1991
[AD-A253631] p 35 N93-10205
Field-emitter arrays for RF vacuum microelectronics
[AD-A253396] p 73 N93-10405
A new model for interpreting experimental data from a circular waveguide cavity
[AD-A254067] p 75 N93-10785
MICROWAVE FILTERS
Design and evaluation of a quasi-active delay-line limiter/filter RF protection device
[AD-A254179] p 71 N93-10255
MICROWAVE FREQUENCIES
Advanced transport systems for electron beams in high-brightness accelerators and FEL's
[AD-A253314] p 88 N93-10286
MICROWAVE IMAGERY
Microwave radiometer studies of atmospheric water over the oceans, volume 2
[NASA-CR-190343] p 127 N93-10848
Satellite derived integrated water vapor and rain intensity patterns: Indicators of rapid cyclogenesis
p 127 N93-10849
Comparison of wind speed measurements over the oceans with the Special Sensor Microwave/Imager and the Geosat altimeter p 127 N93-10850
Morning-evening differences in global and regional oceanic precipitation as observed by the SSM/I
p 127 N93-10851
MICROWAVE OSCILLATORS
Extended-interaction klystron for the AN/TPS-43-E radar system
[AD-A253166] p 76 N93-10882
MICROWAVE RADIOMETERS
Microwave radiometer studies of atmospheric water over the oceans, volume 2
[NASA-CR-190343] p 127 N93-10848
Satellite derived integrated water vapor and rain intensity patterns: Indicators of rapid cyclogenesis
p 127 N93-10849
MICROWAVE SENSORS
Comparison of wind speed measurements over the oceans with the Special Sensor Microwave/Imager and the Geosat altimeter p 127 N93-10850
MICROWAVE SPECTRA
Cosmic microwave background anisotropies from plausible double inflation
[DE92-016195] p 192 N93-10616
MICROWAVE TRANSMISSION
Analysis of reception variability due to terrain multipath on microwave common carrier links
[NTIA-92-283] p 69 N93-10430
Microwave propagation and attenuation in magnetoplasmas
[AD-A250197] p 69 N93-10728
MICROWAVES
Basic and applied research in the field of electronics and communications
[AD-A253593] p 67 N93-10092
Ceramic transactions. Volume 21: Proceedings of the Symposium on Microwave Theory and Application in Materials Processing Annual Meeting No. 23 io on april 29-may 3 1991
[AD-A253631] p 35 N93-10205
High-power microwave breakdown of dielectric interfaces
[AD-A254200] p 124 N93-10262
Langmuir probe and optical emission studies of Ar, O2, and N2 plasmas produced by an ECR microwave source
[AD-A253138] p 162 N93-10615
MILITARY HELICOPTERS
Compound cycle engine for helicopter application
[NASA-CR-180824] p 9 N93-10348
MILITARY OPERATIONS
DoD space radiation concerns
[AD-A253135] p 131 N93-10613
Combat aircraft operations: Training requirements for the German Air Force tactical flying units and the noise problem p 148 N93-10667
Possibilities and limitations of flying training in the German Air Force p 11 N93-10668
Human noise exposure criteria for combat aircraft training areas p 148 N93-10670
Noise of combat aircraft in proximity to air bases: Review of the possibilities of noise reduction at the source
p 148 N93-10671
Noise emission of low flying military airplanes
p 149 N93-10675
Combat aircraft noise p 149 N93-10676
Boom and the problems related to the supersonic flights of military aircraft p 149 N93-10677
A brief review of the source noise technology applicable to fixed-wing military aircraft p 150 N93-10678
Audibility-based annoyance prediction modeling
p 151 N93-10683
Relating flying hours to aircrew performance: Evidence for attack and transport missions
[AD-A253988] p 133 N93-10719
MILITARY TECHNOLOGY
Open Skies Treaty imaging radar technology issues
[DE92-016548] p 68 N93-10394
Acquisition 1: Stock acquisition processes in defence and aerospace documentation centres
p 173 N93-10598
Security considerations within military information systems p 174 N93-10603
MILLIMETER WAVES
Millimeter wave measurement and modeling of terrain scattering
[AD-A253525] p 67 N93-10223
Epitaxial magnetic oxides
[AD-A253667] p 35 N93-10230
MIM (SEMICONDUCTORS)
Template-synthesis of infrared-transparent metal microcylinders: Comparison of optical properties with the predictions of effective medium theory
[AD-A253267] p 158 N93-10694
MINERAL DEPOSITS
Geological evidence for a 2.6-Ga strewn field of impact spherules in the Hamersley Basin of Western Australia
p 120 N93-10181
A comparison of the chemistry of pseudotachylyte breccias in the Archean Levack Gneisses of the Sudbury structure, Ontario p 122 N93-10187
MINERAL OILS
Chemical and thermal stability of refrigerant-lubricant mixture with metal
[DE92-015117] p 44 N93-10398
MINERALOGY
Early Archean spherule beds of possible impact origin from Barberton, South Africa: A detailed mineralogical and geochemical study p 115 N93-10155
MINERALS
Shocked zircons in the Onaping Formation: Further proof of impact origin p 107 N93-10121
Diaplectic transformation of minerals: Vorotilov drill core, Puchezh-Katunki impact crater, Russia
p 110 N93-10136
U-Pb isotopic results for single shocked and polycrystalline zircons record 550-65.5-Ma ages for a K-T target site and 2700-1850-Ma ages for the Sudbury impact event p 115 N93-10156
Electron transfer reactions in microporous solids
[DE92-016222] p 166 N93-10284
MINING
Proceedings of the FY 1990 Workshop on Extraterrestrial Mining and Construction
[AD-A253399] p 189 N93-10406
MIRRORS
Research in the optical sciences
[AD-A253188] p 158 N93-10446
UV spectrum splitting mirror
[DE92-018057] p 159 N93-10818

MISALIGNMENT
Studies impacting the designs of free electron lasers
[AD-A254293] p 90 N93-10768
MISSILE TRACKING
An indicator of message quality for a single optical sensor using a template based tracking algorithm
[AD-A252704] p 139 N93-10881
MISSILE TRAJECTORIES
Computational fluid dynamics capability for internally carried store separation
[AD-A253671] p 79 N93-10297
Research on the asymmetrical aerodynamic forces of reentry vehicles
[AD-A254307] p 4 N93-10707
MISSION PLANNING
Selection of rocket propulsion systems
p 22 N93-10034
Solar Physics and Astrophysics at Interferometric Resolution
[ESA-SP-344] p 179 N93-10901
Prospects with SIMURIS p 179 N93-10904
Attached payloads on Space Station Freedom and Columbus p 14 N93-10929
MITOCHONDRIA
Metabolic factors influencing myocardial recovery from acidosis (CiC3)
[AD-A252376] p 132 N93-10796
MIXED OXIDES
Oxygen barrier oxides
[AD-A253683] p 36 N93-10343
MIXING LAYERS (FLUIDS)
A new energy transfer model for turbulent free shear flow
[NASA-TM-105854] p 81 N93-10454
MOBILITY
Mobility of toluene in polystyrene-toluene solutions: A NMR study
[AD-A253203] p 31 N93-10794
MODAL RESPONSE
Vibration of orthotropic cylindrical shell panels with arbitrary supported curved edges p 45 N93-10471
Dynamics of an orbiting flexible manipulator
p 54 N93-10519
Response of a beam to transverse impulsive and high frequency loads p 56 N93-10526
Mode localization in a simple continuum model
p 56 N93-10529
Free vibrations of the thick circular cylindrical shells and rings p 57 N93-10533
Vibrations of nonlinearly pretwisted asymmetrical thick turbine blades p 9 N93-10537
Design optimization for uniform dynamic strength under multi-modal response p 62 N93-10555
Numerical considerations for structural system identification from modal information p 63 N93-10564
MODEL REFERENCE ADAPTIVE CONTROL
Model reference adaptive control in large space structures p 13 N93-10365
MODULARITY
Mechanical and thermal design of the SUN instrument
p 14 N93-10956
MODULATION TRANSFER FUNCTION
Comparative study of the MTFA, ICS, and SQRI image quality metrics for visual display systems
[AD-A252116] p 158 N93-10708
MODULATORS
Spatial light modulators with arbitrary quantum well profiles
[AD-A253637] p 165 N93-10210
Comparison of optically-addressed spatial light modulators
[AD-A254189] p 157 N93-10259
MOIRE FRINGES
Moire-fringe images of twin boundaries in chemical vapor deposited diamond
[AD-A253729] p 35 N93-10231
MOISTURE CONTENT
Development of physical and mathematical models for the Porous Ceramic Tube Plant Nutrification System (PCTPNS)
[NASA-TM-107551] p 129 N93-10085
Resource capture by single leaves
[DE92-015847] p 129 N93-10461
MOLECULAR BEAM EPITAXY
Spatial light modulators with arbitrary quantum well profiles
[AD-A253637] p 165 N93-10210
Atomic force microscope studies of CuCl island formation on CaF2(111) substrates
[AD-A252499] p 34 N93-10880
MOLECULAR BIOLOGY
Molecular biology in studies of oceanic primary production
[DE92-016101] p 128 N93-10283
MOLECULAR CHAINS
The application of liquid crystal polymers to turbomachinery p 23 N93-10040
MOLECULAR ENERGY LEVELS
Vibrational relaxation of H2O by H2, HCl, and H2O at 295 K
[AD-A252800] p 29 N93-10263
MOLECULAR IONS
Merged beam studies of laser stimulated radiative recombination
[AD-A253308] p 89 N93-10698
MOLECULAR PHYSICS
Molecular dynamics of shocks in crystals with defects
[AD-A253353] p 164 N93-10099
MOLECULAR RELAXATION
Vibrational relaxation of H2O by H2, HCl, and H2O at 295 K
[AD-A252800] p 29 N93-10263
MOLECULAR SPECTROSCOPY
Photoionization dynamics and cation spectroscopy with coherent VUV radiation
[DE92-015841] p 154 N93-10730
MOLECULAR WEIGHT
Synthesis of side chain liquid crystal polymerization by living ring opening metathesis polymerization. Report 1: Influence of molecular weight, polydispersity, and flexible spacer length (n=2-8) on the thermotropic behavior of the resulting polymers
[AD-A248699] p 40 N93-10727
MOLECULES
The magnetochemistry of supramolecular particles: The transition from the molecular to the solid-state
[AD-A253126] p 153 N93-10338
Radiation damage to DNA
[DE92-015760] p 130 N93-10834
MOLYBDENUM
A study of the effect of nitrogen and molybdenum in the corrosion inhibition of austenitic stainless steel
[AD-A253354] p 33 N93-10100
MOMENT DISTRIBUTION
A method of testing two-dimensional airfoils
[AD-A253210] p 4 N93-10375
Development of nonlinear aerodynamic models for unsteady responses p 4 N93-10845
MOMENTS
A reappraisal of compound equilibrium finite elements
p 63 N93-10561
MOMENTS OF INERTIA
Dynamics of systems with time-varying inertial properties p 54 N93-10517
MOMENTUM TRANSFER
Divertor heat flux reduction by D2 injection in DIII-D
[DE92-014232] p 160 N93-10326
MONOCHROMATORS
Thermal, structural, and diffraction analyses of a gallium-cooled x ray monochromator
[DE92-017063] p 157 N93-10837
The solar ultraviolet network subtractive double monochromator p 183 N93-10931
MONOPOLES
Far-zone field of a monopole element on a disk ground plane above flat earth
[AD-A253580] p 70 N93-10091
MONOPROPELLANTS
Long life monopropellant hydrazine thruster evaluation for Space Station Freedom application
p 23 N93-10042
DSP propulsion system launch configuration and related testing p 24 N93-10048
MONOTONE FUNCTIONS
De Finetti representations of survival functions level to a product measure
[AD-A253623] p 146 N93-10107
MONTANA
Search for a meteoritic component at the Beaverhead impact structure, Montana p 116 N93-10158
MONTE CARLO METHOD
Statics and kinetics of oxygen ordering in the oxide superconductor YBa2Cu3O(z)
[DE92-017001] p 167 N93-10403
Imaging of BL Lac objects p 177 N93-10884
Investigations of the motion of discrete-velocity gases
[AD-A253728] p 84 N93-10895
MOTOR VEHICLES
Steering system of a vehicle, such as a snow removing machine for airfields
[CA-PATENT-APPL-SN-1293201] p 91 N93-10367
MOUNTAINS
The Panther Mountain circular structure, a possible buried meteorite crater p 113 N93-10150
MOUNTING
Effect of mounting offset on the dynamics of deploying flexible appendages p 54 N93-10520
MRCA AIRCRAFT
Identifying the principal noise sources of fixed-wing combat aircraft in high-speed flight p 151 N93-10686
MULTIBEAM ANTENNAS
Beam forming antenna system
[PATENT-1-265-236] p 67 N93-10111
Proceedings of the Antenna Applications Symposium, volume 1
[AD-A253681] p 68 N93-10301
Proceedings of the Antenna Applications Symposium, volume 2
[AD-A253682] p 68 N93-10302
MULTIPATH TRANSMISSION
Algorithms for multichannel optical processor
[AD-A254009] p 158 N93-10360
Analysis of reception variability due to terrain multipath on microwave common carrier links
[NTIA-92-283] p 69 N93-10430
MULTIPHASE FLOW
A study of flow properties of wet solids using laser induced photochemical anemometry
[DE92-015483] p 82 N93-10629
Mathematical analysis of reactive multiphase flows
[AD-A253854] p 83 N93-10810
MULTIPHOTON ABSORPTION
A time-resolved two-laser probe of Cr(CO)6 photodissociation dynamics
[AD-A250930] p 88 N93-10247
Resonance ionization of rubidium using sequential diode laser-driven transitions
[DE92-014468] p 89 N93-10429
MULTIPROCESSING (COMPUTERS)
Fault-tolerant and efficient parallel computation
[AD-A253350] p 140 N93-10213
A look at scalable dense linear algebra libraries
[DE92-017805] p 143 N93-10285
Parallel sparse Cholesky factorization algorithms for shared-memory multiprocessor systems
[DE92-016829] p 141 N93-10334
Two-dimensional signal processing, optical information storage and processing, and electromagnetic measurements
[AD-A253953] p 73 N93-10417
A look at scalable dense linear algebra libraries
[DE92-017161] p 139 N93-10816
MULTISENSOR APPLICATIONS
Mathematical analysis of multi-sensor cross-correlation processing for source localization
[DREA-CR-89-433] p 68 N93-10366
MULTISPECTRAL BAND SCANNERS
SPOT panchromatic band simulation by linear combination of multispectral bands
[INPE-5295-PRE/1650] p 157 N93-10311
MUSCLES
A prospective evaluation of stress fractures/overuse injuries in a population of West Point cadets
[AD-A252427] p 132 N93-10709
MUTAGENS
Limited toxicity and mutagenicity testing of five unicharge propellant compounds
[AD-A252339] p 43 N93-10636
MYOCARDIUM
Metabolic factors influencing myocardial recovery from acidosis (CiC3)
[AD-A252376] p 132 N93-10796

N

N-TYPE SEMICONDUCTORS
VLSI design for reliability - hot electron
[AD-A253942] p 74 N93-10715
Ohmic contacts to compound semiconductors
p 76 N93-10830
NAP-OF-THE-EARTH NAVIGATION
Flight test and analysis procedures for new handling criteria
[RAE-TM-FM-26] p 8 N93-10803
NASA PROGRAMS
NASA patent abstracts bibliography: A continuing bibliography. Section 1: Abstracts (supplement 41)
[NASA-SP-7039(41)-SECT-1] p 171 N93-10078
Space Transportation Engine Program (STEP), phase B
[NASA-CR-184062] p 25 N93-10350
NASA Electronic Library System (NELS) database schema, version 1.2
[NASA-CR-190643] p 172 N93-10451
Aeronautical technologies for the twenty-first century
[NASA-CR-190918] p 1 N93-10647
Index to NASA news releases and speeches, 1991
[NASA-TM-108004] p 175 N93-10815
Index to NASA news releases and speeches, 1990
[NASA-TM-108003] p 176 N93-10872
NASA SPACE PROGRAMS
NASA Space Human Factors Program
[NASA-TM-108005] p 134 N93-10890

NATIONAL AEROSPACE PLANE PROGRAM
A configuration development strategy for the NASP p 9 N93-10011

NATIONAL AIRSPACE SYSTEM
A description of the Mode Select beacon system (Mode S) and its associated benefits to the National Airspace System (NAS)
[DOT/FAA/SE-92/6] p 7 N93-10738
Weather Message Switching Center Replacement (WMSCR) Operational Test and Evaluation (OT/E)/integration test plan
[DOT/FAA/CT-TN90/59] p 7 N93-10833

NATIONAL LAUNCH VEHICLE PROGRAM
NLS cargo transfer vehicle propulsion system p 23 N93-10041

NATIONAL PARKS
Remote sensing data for monitoring and evaluating burned areas: Case of Emas National Park (GO)
[INPE-5312-PRE/1709] p 102 N93-10373

NATURAL GAS
Temperature-programmed oxidation of ethane and ethylene in the presence and absence of C-13 labeled methane
[DE92-015048] p 42 N93-10329
Combustion in turbulent jets and buoyant flames
[PB92-211481] p 31 N93-10437
Reserves in western basins
[DE92-014429] p 102 N93-10625

NATURAL LANGUAGE (COMPUTERS)
Artificial intelligence technical paper abstracts, 1991
[AD-A253340] p 141 N93-10269

NATURAL SATELLITES
Indexes of maps of the planets and satellites, 1992
[NASA-TM-4395] p 189 N93-10832

NAVIER-STOKES EQUATION
Navier-Stokes dynamics and aeroelastic computations for vortical flows, buffet and aeroelastic applications
[NASA-CR-190692] p 2 N93-10098
Finite difference methods for incompressible viscous flow in scientific computing
[AD-A253512] p 79 N93-10220
A globally well-posed accurate and efficient finite element CFD algorithm for compressible aerodynamics p 3 N93-10306
Analysis of wing-body junction flowfields using the incompressible Navier-Stokes equations, volumes 1 and 2 p 3 N93-10320
Development of the finite analytic method for turbulent forced and free convection p 80 N93-10369
Explicit Navier-Stokes computation of turbomachinery flows p 81 N93-10370
High-speed viscous flows past blunt bodies and compression corners with flux-split methods
[AD-A253413] p 81 N93-10410
Stream function-vorticity finite element formulations of unsteady incompressible Navier-Stokes equations p 60 N93-10545
A least-squares finite element method for incompressible Navier-Stokes problem p 60 N93-10548
Navier-Stokes turbine heat transfer predictions using two-equation turbulence
[NASA-TM-105817] p 82 N93-10735
On the coupling between a supersonic boundary layer and a flexible surface
[NASA-CR-189697] p 82 N93-10757

NAVIGATION
GPS Army research and applications
[AD-A254262] p 7 N93-10424

NAVIGATION AIDS
Appraisal of digital terrain elevation data for low-altitude flight
[NASA-TM-103896] p 7 N93-10745

NAVIGATION SATELLITES
GPS azimuth determination using short baseline carrier wave interferometry
[AD-A254257] p 6 N93-10265

NAVSTAR SATELLITES
GPS Army research and applications
[AD-A254262] p 7 N93-10424

NEAR INFRARED RADIATION
First results of an imaging FTS with a NICMOS camera p 86 N93-10936

NEODYMIUM ISOTOPES
Sudbury project (University of Muenster-Ontario Geological Survey): Isotope systematics support the impact origin p 109 N93-10131

NEODYMIUM LASERS
Thermo-optical switching in Si based etalons
[AD-A253139] p 88 N93-10412
Laser Journal
[AD-A254106] p 90 N93-10855

NEON
Coherent production of pions and rho mesons in neutrino charged current interactions on neon nuclei at the Fermilab Tevatron
[DE92-015674] p 154 N93-10606

NEOPLASMS
Understanding mechanisms of carcinogenesis using rat tracheal epithelial cells in vitro
[DE92-013510] p 131 N93-10626

NEPHELOMETERS
Meteorological and site influences affecting the comparison of nephelometer and photographic determinations of light extinction at rural sites in the Eastern US
[PB92-195999] p 126 N93-10433

NETWORK ANALYSIS
Analysis of reservation-based dual-link networks for real-time applications
[AD-A254176] p 67 N93-10253

NEUMANN PROBLEM
Nonlinear dynamics underlying atmospheric predictability
[AD-A254042] p 126 N93-10363

NEURAL NETS
Integrated vision system for a target seeker
[AD-A253359] p 135 N93-10103
Biological and theoretical studies of adaptive networks: The conditioned response
[AD-A253329] p 142 N93-10354
Optimization of neural network topology and information content using Boltzman methods
[PB92-205418] p 142 N93-10450
Joint Services Electronics Program
[AD-A253842] p 76 N93-10829
Resistive Grid Kernel Estimator (RGKE)
[AD-A253520] p 147 N93-10869
Artificial neural network system for memory modification
[AD-D015354] p 142 N93-10958
Memory modification of artificial neural networks
[AD-D015356] p 143 N93-10959

NEURONS
Parallel processing and learning: Variability and chaos in self-organization of activity in groups of neurons
[AD-A250290] p 140 N93-10242
Biological and theoretical studies of adaptive networks: The conditioned response
[AD-A253329] p 142 N93-10354

NEUROPHYSIOLOGY
Parallel processing and learning: Variability and chaos in self-organization of activity in groups of neurons
[AD-A250290] p 140 N93-10242
Computer simulations of object discrimination by visual cortex
[AD-A253345] p 131 N93-10271
Biological and theoretical studies of adaptive networks: The conditioned response
[AD-A253329] p 142 N93-10354
Auditory processing of complex sounds across frequency channels
[AD-A253612] p 131 N93-10650

NEUTRAL ATOMS
Laser cooling and trapping of neutral atoms
[AD-A253730] p 155 N93-10885

NEUTRAL BEAMS
Intense ion beam research at Los Alamos
[DE92-015240] p 155 N93-10333
Reflection of plasma ions from metals (and its use as a hyperthermal neutral beam source) p 160 N93-10353
Fast magnetic field penetration into an intense neutralized ion beam
[DE92-016861] p 156 N93-10633

NEUTRAL BUOYANCY SIMULATION
Extravehicular activity compatibility evaluation of developmental hardware for assembly and repair of precision reflectors
[NASA-TP-3246] p 13 N93-10744

NEUTRINOS
Coherent production of pions and rho mesons in neutrino charged current interactions on neon nuclei at the Fermilab Tevatron
[DE92-015674] p 154 N93-10606

NEUTRON IRRADIATION
Stress modified welding process for irradiated materials
[DE92-017131] p 92 N93-10634

NEUTRON SCATTERING
Atomic short range order and spin density wave propagation in CuMn
[DE92-016903] p 34 N93-10789

NEUTRON SOURCES
Accelerator Technology Division
[DE92-016023] p 156 N93-10462

NEWS
Index to NASA news releases and speeches, 1991
[NASA-TM-108004] p 175 N93-10815
Index to NASA news releases and speeches, 1990
[NASA-TM-108003] p 176 N93-10872

NEWTONIAN FLUIDS
Effects of gravity in folding --- of geological layers p 124 N93-10324
Investigations into swirling flows of Newtonian and non-Newtonian fluids
[AD-A253298] p 82 N93-10696

NICKEL ALLOYS
Mechanisms and modelling of environment-dependent fatigue crack growth in a nickel based superalloy
[AD-A253967] p 33 N93-10717
Ohmic contacts to compound semiconductors p 76 N93-10830

NIMBUS 7 SATELLITE
Microwave radiometer studies of atmospheric water over the oceans, volume 2
[NASA-CR-190343] p 127 N93-10848

NIOBIUM ALLOYS
Protective coatings for niobium alloys and their properties
[AD-A254252] p 33 N93-10706

NITRATES
A study of the effect of nitrogen and molybdenum in the corrosion inhibition of austenitic stainless steel
[AD-A253354] p 33 N93-10100

NITRIDES
Pseudomorphic semiconducting heterostructures from combinations of AlN, GaN, and selected SiC polytypes: Theoretical advancement and its coordination with experimental studies of nucleation, growth, characterization, and device development
[AD-A253330] p 166 N93-10355

NITRITES
A study of the effect of nitrogen and molybdenum in the corrosion inhibition of austenitic stainless steel
[AD-A253354] p 33 N93-10100

NITRO COMPOUNDS
Polynitro polycyclic cage compounds
[AD-A252889] p 42 N93-10268

NITROGEN
A study of the effect of nitrogen and molybdenum in the corrosion inhibition of austenitic stainless steel
[AD-A253354] p 33 N93-10100
Growth, nitrogen vacancy reduction, and solid solution formation in cubic GaN thin films and the subsequent fabrication of superlattice structures using AlN and InN
[AD-A253331] p 166 N93-10356

NITROGEN PLASMA
Langmuir probe and optical emission studies of Ar, O2, and N2 plasmas produced by an ECR microwave source
[AD-A253138] p 162 N93-10615

NITROUS OXIDES
Theory of combustion of liquid propellants based on hydroxylammonium nitrate
[AD-A248445] p 42 N93-10267

NODES (STANDING WAVES)
Mode localization in a simple continuum model p 56 N93-10529

NOISE GENERATORS
Combat Aircraft Noise
[AGARD-CP-512] p 148 N93-10666

NOISE INTENSITY
Noise of combat aircraft in proximity to air bases: Review of the possibilities of noise reduction at the source p 148 N93-10671
Noise studies for environmental impact assessment of an outdoor engine test facility p 149 N93-10672
Noise emission of low flying military airplanes p 149 N93-10675
Combat aircraft noise p 149 N93-10676
Boom and the problems related to the supersonic flights of military aircraft p 149 N93-10677
A brief review of the source noise technology applicable to fixed-wing military aircraft p 150 N93-10678
Supersonic acoustic source mechanisms for free jets of various geometries p 150 N93-10680
Audibility-based annoyance prediction modeling p 151 N93-10683
Identifying the principal noise sources of fixed-wing combat aircraft in high-speed flight p 151 N93-10686
Measurement and prediction of noise from low-altitude military aircraft operations p 151 N93-10687
Low-frequency noise reduction in SQUID measurements using laser switching
[AD-A253821] p 90 N93-10827

NOISE MEASUREMENT
Combat Aircraft Noise
[AGARD-CP-512] p 148 N93-10666
Human noise exposure criteria for combat aircraft training areas p 148 N93-10670
Comparison of flyover noise data from aircraft at high subsonic speeds with prediction p 149 N93-10674

Noise emission of low flying military airplanes
p 149 N93-10675
Measurement and prediction of noise from low-altitude military aircraft operations p 151 N93-10687
Further noise measurements in a slotted cryogenic wind tunnel
[RAE-TM-AERO-2201] p 153 N93-10805

NOISE POLLUTION
Audibility-based annoyance prediction modeling
p 151 N93-10683

NOISE PREDICTION (AIRCRAFT)
Tilt rotor hover aeroacoustics
[NASA-CR-177598] p 147 N93-10458
Noise studies for environmental impact assessment of an outdoor engine test facility p 149 N93-10672
Non-propulsive aerodynamic noise
p 149 N93-10673
Comparison of flyover noise data from aircraft at high subsonic speeds with prediction p 149 N93-10674
Boom and the problems related to the supersonic flights of military aircraft p 149 N93-10677
Combat aircraft jet engine noise studies
p 150 N93-10679
Combustion noise and combustion instabilities in propulsion systems p 150 N93-10682
Audibility-based annoyance prediction modeling
p 151 N93-10683
The prediction of noise radiation from supersonic elliptic jets p 151 N93-10684
Prediction of jet mixing noise for high subsonic flight speeds p 151 N93-10685
Measurement and prediction of noise from low-altitude military aircraft operations p 151 N93-10687

NOISE REDUCTION
Convergence performance of adaptive detectors, part 3
[AD-A248415] p 143 N93-10275
Combat Aircraft Noise
[AGARD-CP-512] p 148 N93-10666
Combat aircraft noise: The operator's perspective
p 148 N93-10669
Noise of combat aircraft in proximity to air bases: Review of the possibilities of noise reduction at the source
p 148 N93-10671
Non-propulsive aerodynamic noise
p 149 N93-10673
Combat aircraft noise p 149 N93-10676
Boom and the problems related to the supersonic flights of military aircraft p 149 N93-10677
Combat aircraft jet engine noise studies
p 150 N93-10679
Supersonic acoustic source mechanisms for free jets of various geometries p 150 N93-10680
Combat aircraft noise reduction by technical measures
p 152 N93-10689
Technical measures for the attenuation of aircraft noise and their applicability to GAF combat aircraft
p 152 N93-10690
Study results on combat aircraft source noise reduction p 152 N93-10691
Reduction of propeller noise by active noise control
p 152 N93-10692
Low-frequency noise reduction in SQUID measurements using laser switching
[AD-A253821] p 90 N93-10827

NOISE SPECTRA
Signal and noise analysis of a-Si:H radiation detector-amplifier system
[DE92-016928] p 75 N93-10790
Low-frequency noise reduction in SQUID measurements using laser switching
[AD-A253821] p 90 N93-10827

NOISE TOLERANCE
Human noise exposure criteria for combat aircraft training areas p 148 N93-10670
Noise of combat aircraft in proximity to air bases: Review of the possibilities of noise reduction at the source
p 148 N93-10671
Audibility-based annoyance prediction modeling
p 151 N93-10683

NONADIABATIC CONDITIONS
Hypersonic inlet efficiency revisited p 5 N93-10012

NONDESTRUCTIVE TESTS
Ultrasonic characterization of highly attenuative thick composites
[AD-A253347] p 27 N93-10272
The development of optical techniques for component inspection in the aerospace industry p 93 N93-10307
Elastic wave scattering by an interfacial crack in a plate p 48 N93-10485

NONEQUILIBRIUM FLOW
Echo characteristic analysis of the nonequilibrium wakes of reentry vehicle
[AD-A254249] p 13 N93-10705

NONHOLONOMIC EQUATIONS
Effective formulation of the dynamics of a manipulator based on the Appell equations p 65 N93-10571

NONLINEAR EQUATIONS
Improved numerical simulation of Euler equations
p 80 N93-10309
An assessment of the correspondence principle in comparison to nonlinear viscoelastic theory: A case study p 51 N93-10501
On techniques for digital simulation of random response of nonlinear oscillators p 55 N93-10523
Discontinuous initial value problem of nonlinear elasticity by similarity approach p 64 N93-10569
Solving large linearized systems in mechanics
[AD-A252723] p 144 N93-10639
Singular perturbation methods for nonlinear dynamical systems and waves
[AD-A254116] p 144 N93-10660
Wind tunnel spin data reduction to obtain aerodynamic spin damping coefficients by using nonlinear equation of motion
[AD-A253880] p 4 N93-10811
Development of nonlinear aerodynamic models for unsteady responses p 4 N93-10845

NONLINEAR OPTICS
4.5 micron laser source
[AD-A253367] p 87 N93-10090
Investigations of the dynamics and thermodynamics of the mesosphere lower thermosphere and upper thermosphere at the polar regions with optical ground-based remote sensing
[AD-A253228] p 125 N93-10711

NONLINEAR SYSTEMS
A study upon structural optimization of elastic rotors for mechanical systems
[INPE-5376-TDI/471] p 94 N93-10310
The role of eddy fluxes in the response of the atmosphere to tropical thermal forcing
p 124 N93-10318
Nonlinear signal processing schemes for robust target detection and automatic clutter rejection in radar
[AD-A253546] p 68 N93-10380
A nonlinear oscillatory problem
[DE92-630203] p 95 N93-10385
New directions in computational mechanics
p 44 N93-10467
Probability density functions for random nonlinear oscillation p 55 N93-10522
On techniques for digital simulation of random response of nonlinear oscillators p 55 N93-10523
Vibrations of nonlinearly pretwisted asymmetrical thick turbine blades p 9 N93-10537
Chaotic oscillation of a high speed flexible arm robot
p 65 N93-10574
DYNA2D: A nonlinear, explicit, two-dimensional finite element code for solid mechanics: User manual
[DE92-017310] p 95 N93-10646
Singular perturbation methods for nonlinear dynamical systems and waves
[AD-A254116] p 144 N93-10660
Combustion noise and combustion instabilities in propulsion systems p 150 N93-10682
Nonlinear aeroelasticity of composite structures
[AD-A254285] p 8 N93-10842

NONLINEARITY
Nonlinear studies of surface and interfaces of advanced semiconductor materials
[AD-A253365] p 164 N93-10105
Turbulence modeling of the flow field in combustors using the non-linear k-epsilon model
[DE92-014745] p 80 N93-10330
Nonlinear dynamics underlying atmospheric predictability
[AD-A254042] p 126 N93-10363
A nonlinear oscillatory problem
[DE92-630203] p 95 N93-10385
A new energy transfer model for turbulent free shear flow
[NASA-TM-105854] p 81 N93-10454
A finite element method for nonlinear panel flutter
p 45 N93-10472
Non-linear thermoelasticity of rubberlike solids
p 45 N93-10474
Chronorheological characterization of elastomers
p 46 N93-10476
Fractals and multifractals in fracture
p 50 N93-10497
Failure analysis of laminated composites by using iterative three-dimensional finite element method
p 51 N93-10505
A field panel method for transonic flows
p 6 N93-10547
Three dimensional curved beam elements with large translations and rotations p 63 N93-10560

NONNEWTONIAN FLOW
Investigations into swirling flows of Newtonian and non-Newtonian fluids
[AD-A253298] p 82 N93-10696

NONNEWTONIAN FLUIDS
Investigations into swirling flows of Newtonian and non-Newtonian fluids
[AD-A253298] p 82 N93-10696

NONPARAMETRIC STATISTICS
Order statistics and nonparametric statistics
[AD-A253574] p 146 N93-10699
Change analysis
[AD-A253567] p 146 N93-10795

NONUNIFORM FLOW
Hypersonic inlet efficiency revisited p 5 N93-10012

NORMAL DENSITY FUNCTIONS
Analytical characterization of bistatic scattering from Gaussian distributed surfaces
[AD-A254253] p 159 N93-10724

NORTH AMERICA
K/T boundary stratigraphy: Evidence for multiple impacts and a possible comet stream p 120 N93-10180

NORTHERN HEMISPHERE
Morning-evening differences in global and regional oceanic precipitation as observed by the SSM/I
p 127 N93-10851

NORWAY
Impact cratering record of Fennoscandia
p 119 N93-10171

NOSE TIPS
One type of automatically adjusted difference scheme with artificial viscosity to calculate ablated exterior shapes
[AD-A254108] p 5 N93-10856

NOTCH STRENGTH
Analysis of a buffer strip laminate with a cutout
p 52 N93-10506

NOTCH TESTS
Stress patterns in the dynamic tear test
p 49 N93-10491
On the development of a new fracture toughness procedure p 59 N93-10541

NOVA LASER SYSTEM
Measurements and modeling of laser irradiance in the high-power third-harmonic Nova focus. Volume A: Report
[DE92-016746] p 90 N93-10739

NOWCASTING
Mesoscale severe weather development under orographic influences
[AD-A253630] p 125 N93-10204

NOZZLE DESIGN
Altitude compensating nozzle evaluation
p 22 N93-10037
Supersonic acoustic source mechanisms for free jets of various geometries p 150 N93-10680
Nozzle installation effects on the noise from supersonic exhaust plumes p 150 N93-10681
Study results on combat aircraft source noise reduction p 152 N93-10691

NOZZLE EFFICIENCY
Altitude compensating nozzle evaluation
p 22 N93-10037

NOZZLE FLOW
Numerical simulation of unsteady flow in a nozzle
p 16 N93-10008
Supersonic confined jet nozzles p 16 N93-10009
Altitude compensating nozzle evaluation
p 22 N93-10037
Introduction to radial turbine technology
p 77 N93-10051

NOZZLE GEOMETRY
Altitude compensating nozzle evaluation
p 22 N93-10037
Pitot survey of exhaust flow field of a 2-D scramjet nozzle at Mach 6 with air or freon and argon used for exhaust simulation
[NASA-TM-4361] p 2 N93-10071
Supersonic acoustic source mechanisms for free jets of various geometries p 150 N93-10680
Nozzle installation effects on the noise from supersonic exhaust plumes p 150 N93-10681
Combat aircraft noise reduction by technical measures
p 152 N93-10689

NUCLEAR ELECTRIC PROPULSION
A comparison of multimegawatt electric propulsion options for Mars missions p 23 N93-10043

NUCLEAR FUELS
Large orbit magnetic confinement systems for advanced fusion fuels
[DE92-016218] p 162 N93-10617

NUCLEAR FUSION
Experimental plasma research project summaries
[DE92-016274] p 162 N93-10464

Magnetic fusion with high energy self-colliding ion beams
[DE92-016860] p 156 N93-10643
NUCLEAR INTERACTIONS
Glenn T. Seaborg and heavy ion nuclear science
[DE92-016943] p 156 N93-10762
NUCLEAR MAGNETIC RESONANCE
NQR-NMR studies of higher alcohol synthesis Cu-Co catalysts
[DE92-015783] p 31 N93-10460
Mobility of toluene in polystyrene-toluene solutions: A NMR study
[AD-A253203] p 31 N93-10794
NUCLEAR POWER PLANTS
Review and analysis of check valve failure data
[DE92-014462] p 91 N93-10381
NUCLEAR PROPULSION
Synchrotron radiation considerations in the Dense Plasma Focus (DPF) Magnetoplasmadynamic (MPD) thruster
[AD-A254188] p 25 N93-10258
System model development for nuclear thermal propulsion
[NASA-TM-105761] p 25 N93-10457
Critical technology demonstration of plasma focus type MPD thrusters
[AD-A252428] p 26 N93-10638
NUCLEAR QUADRUPOLE RESONANCE
NQR-NMR studies of higher alcohol synthesis Cu-Co catalysts
[DE92-015783] p 31 N93-10460
NUCLEAR REACTIONS
Study on the pi(sup -)p yields eta' pi(sup 0)n reaction at 38 and 100 GeV/c momenta
[DE92-624593] p 153 N93-10328
Particle production at high p(sub (perpendicular)) in (sup 28)Si + A collisions at 14.6 A x GeV/c
[DE92-016939] p 154 N93-10402
NUCLEAR RESEARCH
Geographic Information System (GIS) development assistance for Nuclear Regulatory Commission (NRC) incident response capability
[DE92-017595] p 176 N93-10867
NUCLEAR STRUCTURE
Pion- and proton-nucleus interactions at intermediate energy
[DE92-017980] p 157 N93-10838
NUCLEATION
Pseudomorphic semiconducting heterostructures from combinations of AlN, GaN, and selected SiC polytypes: Theoretical advancement and its coordination with experimental studies of nucleation, growth, characterization, and device development
[AD-A253330] p 166 N93-10355
Boiling behavior of sodium-potassium alloy in a bench-scale solar receiver
[DE92-014947] p 103 N93-10383
NUMERICAL ANALYSIS
Numerical methods for inviscid and viscous flow analysis p 77 N93-10055
Computational studies of vortex breakdown
[AD-A253759] p 79 N93-10232
Convergence performance of adaptive detectors, part 3
[AD-A248415] p 143 N93-10275
NUMERICAL CONTROL
Optimal sample policies for multirate digital control p 141 N93-10346

O

OBJECT PROGRAMS
A survey of commercial object-oriented database management systems
[NASA-CR-190645] p 172 N93-10452
OBJECT-ORIENTED PROGRAMMING
Mesoscale severe weather development under orographic influences
[AD-A253630] p 125 N93-10204
A look at scalable dense linear algebra libraries
[DE92-017805] p 143 N93-10285
A survey of commercial object-oriented database management systems
[NASA-CR-190645] p 172 N93-10452
Object-oriented design unifies databases and applications
[AD-A253313] p 175 N93-10723
A multilevel security model for object-oriented database systems p 175 N93-10844
OBSERVATION
High resolution observations: The state of the art and beyond p 177 N93-10902
OCCLUSION
The development of optical techniques for component inspection in the aerospace industry p 93 N93-10307
OCEAN SURFACE
Air-sea interaction and remote sensing
[NASA-CR-190913] p 128 N93-10068
Acoustic noise generation at the air/ocean boundary
[DREA-CR-90-445] p 147 N93-10642
Air-sea interaction in regions of varying surface conditions
[AD-A253182] p 128 N93-10791
OCEANOGRAPHY
Air-sea interaction and remote sensing
[NASA-CR-190913] p 128 N93-10068
OCEANS
Search for the 700,000-year-old source crater of the Australasian tektite strewn field p 120 N93-10177
Molecular biology in studies of oceanic primary production
[DE92-016101] p 128 N93-10283
Automatic cloud classification from multi-spectral satellite data over oceanic regions
[AD-A253670] p 126 N93-10292
OCULOMETERS
Air traffic control visual scanning
[DOT/FAA/CT-TN92/16] p 7 N93-10459
OILS
Alternate spectrometric oil analysis techniques
[AD-A253355] p 29 N93-10101
Mechanical behavior of open cell ceramics
[PB92-212984] p 37 N93-10439
ON-LINE SYSTEMS
Interactive animation of fault tolerant parallel algorithms
[AD-A253349] p 135 N93-10212
Scientific and Technical Information (STI) towards technological and industrial development: The case of Portugal p 173 N93-10596
Technology for libraries and information centers: A seminar in Greece, Portugal, and Turkey p 174 N93-10601
Services: User services in defence and aerospace documentation centres p 174 N93-10602
ONTARIO
Sudbury Breccia and suevite as glacial indicators transported 800 km to Kentland Astrobleme, Indiana p 117 N93-10165
The pseudotachylites from the Vredefort structure and the Witwatersrand basin p 119 N93-10174
SAR in support of geological investigations of the Sudbury structure p 103 N93-10182
Sudbury project (University of Muenster-Ontario Geological Survey): Petrology, chemistry, and origin of breccia formations p 121 N93-10185
A comparison of the chemistry of pseudotachylyte breccias in the Archean Levack Gneisses of the Sudbury structure, Ontario p 122 N93-10187
Floor-fractured crater models of the Sudbury structure, Canada p 123 N93-10193
OPERATING COSTS
Comparison of all-electric secondary power systems for civil subsonic transports
[NASA-TM-105852] p 9 N93-10456
Assessment study of superconducting fault-current limiters operating at 77 K
[DE92-015273] p 76 N93-10831
OPERATING SYSTEMS (COMPUTERS)
Issues and techniques of CASE integration with configuration management
[AD-A253323] p 136 N93-10298
OPERATIONAL AMPLIFIERS
Development of 6H-SiC CMOS transistors for insertion into a 350 C operational amplifier
[AD-A253760] p 70 N93-10233
OPERATIONAL PROBLEMS
Operationally efficient space-based integrated propulsion module p 22 N93-10035
OPERATORS (MATHEMATICS)
On the measurement of time-dependent quantum phases
[DE92-630206] p 170 N93-10387
OPTICAL COMMUNICATION
Soviet optical processing research. FSAC Technical Assessment Report (TAR)
[PB92-195569] p 172 N93-10431
Architecture and device development for optical networks
[AD-A253247] p 158 N93-10693
OPTICAL COMPUTERS
Algorithms for multichannel optical processor
[AD-A254009] p 158 N93-10360
OPTICAL CORRELATORS
Comparison of optically-addressed spatial light modulators
[AD-A254189] p 157 N93-10259
OPTICAL COUPLING
Stability of coupled semiconductor diode lasers p 88 N93-10379
Holographic optical interconnects for multichip modules
[AD-A253403] p 86 N93-10408
OPTICAL DATA PROCESSING
Comparison of optically-addressed spatial light modulators
[AD-A254189] p 157 N93-10259
Algorithms for multichannel optical processor
[AD-A254009] p 158 N93-10360
Two-dimensional signal processing, optical information storage and processing, and electromagnetic measurements
[AD-A253953] p 73 N93-10417
Soviet optical processing research. FSAC Technical Assessment Report (TAR)
[PB92-195569] p 172 N93-10431
Architecture and device development for optical networks
[AD-A253247] p 158 N93-10693
OPTICAL EQUIPMENT
The development of optical techniques for component inspection in the aerospace industry p 93 N93-10307
Soviet optical processing research. FSAC Technical Assessment Report (TAR)
[PB92-195569] p 172 N93-10431
Long Duration Exposure Facility (LDEF) optical systems SIG summary and database p 38 N93-10583
Design of laser optical systems
[AD-A254247] p 89 N93-10703
Thermal, structural, and diffraction analyses of a gallium-cooled x ray monochromator
[DE92-017063] p 157 N93-10837
SUN: The Solar Ultraviolet Network p 183 N93-10930
Investigations of the effects of contamination on UV optics p 159 N93-10949
The imaging Fourier transform spectrometer optical design p 159 N93-10951
Mechanical and thermal design of the SUN instrument p 14 N93-10956
OPTICAL MATERIALS
Epitaxial magnetic oxides
[AD-A253667] p 35 N93-10230
Soviet optical processing research. FSAC Technical Assessment Report (TAR)
[PB92-195569] p 172 N93-10431
Measurement of aerodynamic shear stress using side chain liquid crystal polymers
[AD-A254312] p 40 N93-10770
OPTICAL MEASUREMENT
Interferometry with the Very Large Telescope p 178 N93-10943
Towards an ESA strategy for optical interferometry in space. Recommendations of the ESA Space Interferometry Study Team (SIST) p 178 N93-10944
Report of the Lunar Interferometry Study Team (LIST) activities p 178 N93-10945
A multipurpose vacuum-ultraviolet test facility p 11 N93-10953
Interferometer optical design for the Imaging Fourier Transform Spectrometer (IFTS) p 159 N93-10955
OPTICAL MEASURING INSTRUMENTS
A seam tracking modulated infrared optical sensor for use in welding
[AD-A254103] p 159 N93-10812
An indicator of message quality for a single optical sensor using a template based tracking algorithm
[AD-A252704] p 139 N93-10881
The solar ultraviolet network subtractive double monochromator p 183 N93-10931
OPTICAL MEMORY (DATA STORAGE)
TIGER5: Extraction of geographic information from the TIGER system
[DE92-014935] p 171 N93-10382
Two-dimensional signal processing, optical information storage and processing, and electromagnetic measurements
[AD-A253953] p 73 N93-10417
OPTICAL PATHS
The CHARON program p 177 N93-10942
OPTICAL PROPERTIES
Selected results for metals from LDEF experiment A0171 p 34 N93-10579
Template-synthesis of infrared-transparent metal microcylinders: Comparison of optical properties with the predictions of effective medium theory
[AD-A253267] p 158 N93-10694
Measurement of aerodynamic shear stress using side chain liquid crystal polymers
[AD-A254312] p 40 N93-10770
OPTICAL PUMPING
Theoretical analysis of discharges in copper vapor lasers: A comparison of Ne and He
[DE92-014739] p 87 N93-10083

OPTICAL SWITCHING
Low-frequency noise reduction in SQUID measurements using laser switching
[AD-A253821] p 90 N93-10827
OPTICAL THICKNESS
Thermo-optical switching in Si based etalons
[AD-A253139] p 88 N93-10412
OPTICAL TRACKING
An indicator of message quality for a single optical sensor using a template based tracking algorithm
[AD-A252704] p 139 N93-10881
OPTIMIZATION
Unifying the landmark developments in optimal bounding ellipsoid identification
[AD-A253502] p 143 N93-10200
Optimization of neural network topology and information content using Boltzman methods
[PB92-205418] p 142 N93-10450
Smart algorithms and adaptive methods in computational fluid dynamics p 44 N93-10469
An adaptive mesh-management algorithm for three-dimensional automatic finite element analysis p 61 N93-10554
OPTOELECTRONIC DEVICES
Novel optoelectronic devices based on combining GaAs and InP on Si
[AD-A253781] p 165 N93-10235
Advanced processing and characterization technologies. Fabrication and characterization of semiconductor optoelectronic devices and integrated circuits. Final Conference Proceedings No. 10
[AD-A254162] p 73 N93-10663
ORBIT MANEUVERING ENGINE (SPACE SHUTTLE)
Uprated OMS engine status: Altitude testing results p 22 N93-10036
ORBIT PERTURBATION
On the gravitational potential of two arbitrary rotating bodies with applications to the Earth-Moon system p 179 N93-10303
ORBIT TRANSFER VEHICLES
Electric propulsion applications p 20 N93-10029
Electric Propulsion Space Experiment (ESEX): Spacecraft design issues for high-power electric propulsion p 21 N93-10030
A 26 kW arcjet system for on-orbit demonstration p 21 N93-10031
Power conditioning unit for 30 kWe class arcjet flight experiment p 21 N93-10032
ORBITAL ASSEMBLY
Extravehicular activity compatibility evaluation of developmental hardware for assembly and repair of precision reflectors
[NASA-TP-3246] p 13 N93-10744
ORBITAL MECHANICS
Semiclassical quantization of chaotic billiards
[DE92-634888] p 169 N93-10226
Computer algebra and the elliptic restricted problem of three bodies p 11 N93-10499
ORGANIC CHEMISTRY
The 200th American Chemical Society Geochemistry Division Symposium on Progress in Marine Chemistry
[AD-A253757] p 129 N93-10887
ORGANIZATIONS
Aerospace Industries Association of Canada
[CTN-92-60590] p 1 N93-10644
ORGANOMETALLIC COMPOUNDS
A time-resolved two-laser probe of Cr(CO)6 photodissociation dynamics
[AD-A250930] p 88 N93-10247
Transition metal activation and functionalization of carbon-hydrogen bonds
[DE92-014809] p 30 N93-10400
Atomic approaches to defect thermochemistry
[AD-A254278] p 167 N93-10425
ORGANOMETALLIC POLYMERS
Water soluble polysiloxanes with pendant 1-oxypyridin-3-yl groups
[AD-A250637] p 36 N93-10246
ORTHOGONAL FUNCTIONS
Axisymmetric vibrations of rotating circular plates using characteristic orthogonal polynomials p 45 N93-10470
ORTHOTROPIC PLATES
Compression buckling of thick orthotropic plates with a step thickness change p 46 N93-10478
Interface cracks in an orthotropic layered half-space under impact loading p 47 N93-10482
Consistent shear constitutive relations for laminated plates p 28 N93-10509
Orthotropic circular plate on nonlinear elastic subgrade p 53 N93-10513
ORTHOTROPIC SHELLS
A nonlinear oscillatory problem
[DE92-630203] p 95 N93-10385
Vibration of orthotropic cylindrical shell panels with arbitrary supported curved edges p 45 N93-10471
OSCILLATING FLOW
Forced unsteady separated flows on a 45 degree delta wing p 80 N93-10305
Mass transfer in oscillating flows: Efficient drying via pulse combustors
[PB92-204403] p 81 N93-10449
Investigations into swirling flows of Newtonian and non-Newtonian fluids
[AD-A253298] p 82 N93-10696
OSCILLATION DAMPERS
Overview of the vibroimpact damping of packaged particles p 56 N93-10528
OSCILLATIONS
A nonlinear oscillatory problem
[DE92-630203] p 95 N93-10385
Chaotic oscillation of a high speed flexible arm robot p 65 N93-10574
System design and relaxation oscillations of a titanium-sapphire laser
[AD-A254264] p 89 N93-10725
OSCILLATORS
On techniques for digital simulation of random response of nonlinear oscillators p 55 N93-10523
Singular perturbation methods for nonlinear dynamical systems and waves
[AD-A254116] p 144 N93-10660
OSCILLOSCOPES
Instrument driver for general purpose interface bus (IEEE-488)
[AD-A253947] p 138 N93-10716
OUTGASSING
Investigations of the effects of contamination on UV optics p 159 N93-10949
OVER-THE-HORIZON RADAR
Modeling of HF propagation and heating in the ionosphere
[AD-A253941] p 125 N93-10714
OXIDATION
Temperature-programmed oxidation of ethane and ethylene in the presence and absence of C-13 labeled methane
[DE92-015048] p 42 N93-10329
Kinetics of oxidation of silicon by electron cyclotron resonance plasmas
[AD-A253140] p 161 N93-10413
Pre-oxidation anneal kinetics: Interface degradation of thin SiO2 films on silicon
[AD-A253142] p 30 N93-10414
A new ellipsometry technique for interface analysis: Application to Si-SiO2
[AD-A253143] p 167 N93-10415
Selected results for metals from LDEF experiment A0171 p 34 N93-10579
Some results of the oxidation investigation of copper and silver samples flown on LDEF p 34 N93-10580
Changes in oxidation state of chromium during LDEF exposure p 34 N93-10581
Additional results on space environmental effects on polymer matrix composites: Experiment A0180 p 38 N93-10586
Mechanisms and modelling of environment-dependent fatigue crack growth in a nickel based superalloy
[AD-A253967] p 33 N93-10717
OXIDATION RESISTANCE
Oxidation protection systems for carbon-carbon composites formed by chemical vapor deposition and plasma assisted chemical vapor deposition techniques
[AD-A253450] p 28 N93-10344
OXIDATION-REDUCTION REACTIONS
The 200th American Chemical Society Geochemistry Division Symposium on Progress in Marine Chemistry
[AD-A253757] p 129 N93-10887
OXIDE FILMS
Kinetics of oxidation of silicon by electron cyclotron resonance plasmas
[AD-A253140] p 161 N93-10413
Pre-oxidation anneal kinetics: Interface degradation of thin SiO2 films on silicon
[AD-A253142] p 30 N93-10414
Spectroscopic ellipsometric measurements of the dielectric function of germanium dioxide films on crystal germanium
[AD-A253137] p 168 N93-10614
OXIDES
Epitaxial magnetic oxides
[AD-A253667] p 35 N93-10230
VLSI design for reliability - hot electron
[AD-A253942] p 74 N93-10715
OXIDIZERS
Alternatives in clean propellants for large scale man-rated solid rocket motors p 20 N93-10028
A multi-fluid model of turbulence for Li-SF6 submerged combustion
[AD-A253973] p 31 N93-10423
Sensitivity of modeled ozone concentrations to uncertainties in biogenic emissions
[PB92-192202] p 105 N93-10432
OXYGEN
Rate constants for reactions of hydrazine fuels with O(P-3)
[AD-A252813] p 42 N93-10336
Statics and kinetics of oxygen ordering in the oxide superconductor YBa2Cu3O(z)
[DE92-017001] p 167 N93-10403
OXYGEN ATOMS
Selected results for metals from LDEF experiment A0171 p 34 N93-10579
Additional results on space environmental effects on polymer matrix composites: Experiment A0180 p 38 N93-10586
Proposed test program and data base for LDEF polymer matrix composites p 38 N93-10587
Results from testing and analysis of solar cells flown on LDEF p 39 N93-10591
OXYGEN PLASMA
Langmuir probe and optical emission studies of Ar, O2, and N2 plasmas produced by an ECR microwave source
[AD-A253138] p 162 N93-10615
OXYGEN 18
Carbon and oxygen isotope study of carbonates from highly shocked clasts of the polymict breccia of the Haughton Crater (Canada) p 105 N93-10113
OZONE
Sensitivity of modeled ozone concentrations to uncertainties in biogenic emissions
[PB92-192202] p 105 N93-10432

P

P-I-N JUNCTIONS
Signal and noise analysis of a-Si:H radiation detector-amplifier system
[DE92-016928] p 75 N93-10790
P-TYPE SEMICONDUCTORS
Impact sensitivity reduction via exo-electron control p 15 N93-10004
Ohmic contacts to compound semiconductors p 76 N93-10830
PACIFIC OCEAN
Measurements of surface ocean carbon dioxide partial pressure during WOCE
[DE92-011856] p 128 N93-10621
Evaluation of Seasat/Geosat orbits and altimetry with application to long-term sea level changes in the North Pacific p 103 N93-10847
PACKING DENSITY
Electronic and structural properties of metallic microclusters
[DE92-016917] p 33 N93-10411
PANEL FLUTTER
A finite element method for nonlinear panel flutter p 45 N93-10472
Control of panel flutter at high supersonic speed p 9 N93-10900
PANEL METHOD (FLUID DYNAMICS)
A field panel method for transonic flows p 6 N93-10547
PARABOLIC DIFFERENTIAL EQUATIONS
Numerical solution of three-dimensional unsteady viscous flows
[AD-A253202] p 83 N93-10793
PARALLAX
Stereoscopy and paralax in the vertical distances determination using aerial photographs
[INPE-5363-PUD/049] p 102 N93-10063
PARALLEL PROCESSING (COMPUTERS)
An implementation of the MVDR beamformer on the Intel iWarp system
[AD-A253641] p 140 N93-10209
Fault-tolerant and efficient parallel computation
[AD-A253350] p 140 N93-10213
Test range tracking network processors
[AD-A253511] p 140 N93-10219
Implementation of parallel algorithms
[AD-A253638] p 140 N93-10227
A look at scalable dense linear algebra libraries
[DE92-017805] p 143 N93-10285
Development of parallel architectures for sensor array processing algorithms
[AD-A253680] p 141 N93-10299
SAPNEW: Parallel finite element code for thin shell structures on the Alliant FX/80
[NASA-CR-190663] p 94 N93-10372
AMR on the CM-2
[NASA-CR-190747] p 138 N93-10736
PARAMETER IDENTIFICATION
Stokes parameters of the O VI 103.2 nm line as a probe of the matter velocity field vector in the solar wind acceleration region p 181 N93-10914

PARAMETERIZATION
A reappraisal of compound equilibrium finite elements p 63 N93-10561
On the use of coupled finite element boundary element models in numerical design analysis p 63 N93-10563
The mechanical verification of a simple control system [ORA-TR-89-5443-04] p 142 N93-10641

PARTIAL DIFFERENTIAL EQUATIONS
Theoretical analysis of discharges in copper vapor lasers: A comparison of Ne and He [DE92-014739] p 87 N93-10083
Improved numerical simulation of Euler equations p 80 N93-10309
Nonlinear dynamics underlying atmospheric predictability [AD-A254042] p 126 N93-10363
Discontinuous initial value problem of nonlinear elasticity by similarity approach p 64 N93-10569
Numerical solution of three-dimensional unsteady viscous flows [AD-A253202] p 83 N93-10793

PARTIAL PRESSURE
Partial admission and unsteady flow in radial turbines p 78 N93-10059
Measurements of surface ocean carbon dioxide partial pressure during WOCE [DE92-011856] p 128 N93-10621

PARTICLE ACCELERATOR TARGETS
Particle production at high p(sub (perpendicular)) in (sup 28)Si + A collisions at 14.6 A x GeV/c [DE92-016939] p 154 N93-10402
Future directions in pulsed power driven ICF [DE92-016233] p 161 N93-10443
Pion- and proton-nucleus interactions at intermediate energy [DE92-017980] p 157 N93-10838
Recent developments in stored polarized electron positron beams [DE92-016965] p 157 N93-10862

PARTICLE ACCELERATORS
Future directions in pulsed power driven ICF [DE92-016233] p 161 N93-10443

PARTICLE DIFFUSION
LABAN-PEL: A two-dimensional, multigroup diffusion, high-order response matrix code [DE92-626845] p 144 N93-10624

PARTICLE INTERACTIONS
Semiclassical quantization of interacting anyons in a strong magnetic field [DE92-634889] p 169 N93-10229
Mass and mixing angle patterns in the standard model and its material supersymmetric extension [DE92-016197] p 153 N93-10291
Semiclassical quantization of integrable systems of few interacting anyons in a strong magnetic field [DE92-634892] p 170 N93-10295
Vector superconductivity in cosmic strings [DE92-634923] p 179 N93-10296
Study on the pi(sup -)p yields eta' pi(sup 0)n reaction at 38 and 100 GeV/c momenta [DE92-624593] p 153 N93-10328
Two-photon couplings of quarkonia with arbitrary J(sup PC) [DE92-016525] p 153 N93-10332
Two-photon physics and the coming generation of heavy ion colliders [DE92-015850] p 156 N93-10732

PARTICLE MASS
Mass and mixing angle patterns in the standard model and its material supersymmetric extension [DE92-016197] p 153 N93-10291

PARTICLE MOTION
Recent developments in stored polarized electron positron beams [DE92-016965] p 157 N93-10862

PARTICLE PRODUCTION
Study on the pi(sup -)p yields eta' pi(sup 0)n reaction at 38 and 100 GeV/c momenta [DE92-624593] p 153 N93-10328
Particle production at high p(sub (perpendicular)) in (sup 28)Si + A collisions at 14.6 A x GeV/c [DE92-016939] p 154 N93-10402
Two-photon physics and the coming generation of heavy ion colliders [DE92-015850] p 156 N93-10732
A measurement of the Z(sup 0) hadronic branching fraction to bottom quarks and the charged multiplicity of bottom quark events using precision vertex detectors at E(sub cm) = 91 GeV [DE92-018236] p 154 N93-10820

PARTICLE THEORY
Mass and mixing angle patterns in the standard model and its material supersymmetric extension [DE92-016197] p 153 N93-10291
Semiclassical quantization of integrable systems of few interacting anyons in a strong magnetic field [DE92-634892] p 170 N93-10295
Vector superconductivity in cosmic strings [DE92-634923] p 179 N93-10296
Research program in elementary particle theory [DE92-017399] p 155 N93-10840
Research in particle physics beyond the standard model [DE92-012240] p 155 N93-10878

PARTITIONS (STRUCTURES)
Interdisciplinary research and training program in the plant sciences [DE92-015919] p 130 N93-10835

PASSIVITY
Effect of alloying elements on passivity and breakdown of passivity of Fe- and Ni-based alloys mechanistics aspects [DE92-017316] p 33 N93-10395

PATENT POLICY
NASA patent abstracts bibliography: A continuing bibliography. Section 1: Abstracts (supplement 41) [NASA-SP-7039(41)-SECT-1] p 171 N93-10078

PATHOGENESIS
Understanding mechanisms of carcinogenesis using rat tracheal epithelial cells in vitro [DE92-013510] p 131 N93-10626
Interdisciplinary research and training program in the plant sciences [DE92-015919] p 130 N93-10835

PATTERN RECOGNITION
Integrated vision system for a target seeker [AD-A253359] p 135 N93-10103
Misclassification rates of likelihood and predictive discriminant functions for small samples [AD-A253640] p 146 N93-10208
The development of optical techniques for component inspection in the aerospace industry p 93 N93-10307
Optimization of neural network topology and information content using Boltzman methods [PB92-205418] p 142 N93-10450
Joint Services Electronics Program [AD-A253842] p 76 N93-10829
Resistive Grid Kernel Estimator (RGKE) [AD-A253520] p 147 N93-10869
Autonomous star sensing and pattern recognition for spacecraft attitude determination p 177 N93-10876
A spatial similarity measure for image database applications [AD-A253570] p 176 N93-10883
Pattern recognition applied to H(sub alpha) spectroheliograms solar rotation and meridional circulation p 182 N93-10924

PAVEMENTS
Stability of open-graded bases under wheel loads using a model testing approach [AD-A253209] p 66 N93-10710

PAYLOAD INTEGRATION
Attached payloads on Space Station Freedom and Columbus p 14 N93-10929

PAYLOAD TRANSFER
Attached payloads on Space Station Freedom and Columbus p 14 N93-10929

PAYLOADS
Attached payloads on Space Station Freedom and Columbus p 14 N93-10929
Accommodation aspects of SIMURIS on Space Station Freedom p 14 N93-10954

PERFORATED PLATES
Singular stress distributions at circular holes in composite laminates p 51 N93-10503

PERFORMANCE PREDICTION
A simplified model for hybrid rocket performance prediction p 19 N93-10022
Effects of the RSRM grain deformation on ballistic performance p 20 N93-10027

PERFORMANCE TESTS
Uprated OMS engine status: Altitude testing results p 22 N93-10036
Testing techniques p 78 N93-10060
Results from the testing and analysis of LDEF batteries p 39 N93-10589
Activated transport in AMTEC electrodes [DE92-016810] p 75 N93-10786
Acceptance testing of the prototype electrometer for the SAMPIE flight experiment [NASA-TM-105880] p 13 N93-10841
The solar ultraviolet network: Performance and tolerance analysis p 187 N93-10950
The imaging Fourier transform spectrometer: Performance and tolerance analysis p 86 N93-10952

PERIODICALS
EIA publications directory, 1991 [DE92-015686] p 174 N93-10607

PERMITTIVITY
Application of volumetric multiple-scattering approximations to foliage media [AD-A253337] p 68 N93-10358
Numerical modelling of fringing fields and their use for complex permittivity measurements at high frequencies [AD-A253994] p 72 N93-10359

PEROVSKITES
Covalent electron transfer theory of superconductivity [AD-A253975] p 74 N93-10718

PERSONAL COMPUTERS
The integration of geometric modeling into an inverse design method and application of a PC-based inverse design method and comparison with test results p 78 N93-10058

PERSONNEL SELECTION
A new test of scanning and monitoring ability: Methods and initial results [AD-A249123] p 132 N93-10321

PERTURBATION
Computer algebra and the elliptic restricted problem of three bodies p 11 N93-10499

PERTURBATION THEORY
Chaotic oscillation of a high speed flexible arm robot p 65 N93-10574
Singular perturbation methods for nonlinear dynamical systems and waves [AD-A254116] p 144 N93-10660

PETN
Impact sensitivity reduction via exo-electron control p 15 N93-10004

PETROGRAPHY
Sudbury project (University of Muenster-Ontario Geological Survey): Summary of results - an updated impact model p 106 N93-10117
Impactite and pseudotachylite from Roter Kamm Crater, Namibia p 109 N93-10130
Phase transformations in 40-60-GPa shocked gneisses from the Haughton Crater (Canada): An Analytical Transmission Electron Microscopy (ATEM) study p 117 N93-10163
Sudbury project (University of Muenster-Ontario Geological Survey): Petrology, chemistry, and origin of breccia formations p 121 N93-10185
Electron petrography of silica polymorphs associated with pseudotachylite, Vredefort structure, South Africa p 123 N93-10192

PETROLOGY
Impactites from Popigai Crater p 117 N93-10164
Sudbury Breccia and suevite as glacial indicators transported 800 km to Kentland Astrobleme, Indiana p 117 N93-10165
Sudbury project (University of Muenster-Ontario Geological Survey): Petrology, chemistry, and origin of breccia formations p 121 N93-10185

PHASE CONJUGATION
Semiconductor phase conjugation [AD-A253684] p 166 N93-10345

PHASE DIAGRAMS
Electronic and structural properties of metallic microclusters [DE92-016917] p 33 N93-10411

PHASE TRANSFORMATIONS
Phase transformations in 40-60-GPa shocked gneisses from the Haughton Crater (Canada): An Analytical Transmission Electron Microscopy (ATEM) study p 117 N93-10163

PHASE VELOCITY
A formula for efficiency of fast wave current drive in fusion devices [DE92-016152] p 160 N93-10390

PHASED ARRAYS
Proceedings of the Antenna Applications Symposium, volume 1 [AD-A253681] p 68 N93-10301
Proceedings of the Antenna Applications Symposium, volume 2 [AD-A253682] p 68 N93-10302

PHENOLIC RESINS
Feasibility evaluation of the monolithic braided ablative nozzle p 19 N93-10023

PHONONS
Subpicosecond resolved incipient laser damage [AD-A253624] p 87 N93-10202
Laser and optical physics [AD-A253619] p 88 N93-10251

PHOTOCHEMICAL OXIDANTS
Sensitivity of modeled ozone concentrations to uncertainties in biogenic emissions [PB92-192202] p 105 N93-10432

PHOTOCHEMICAL REACTIONS
Electron transfer reactions in microporous solids [DE92-016222] p 166 N93-10284
The 200th American Chemical Society Geochemistry Division Symposium on Progress in Marine Chemistry [AD-A253757] p 129 N93-10887

PHOTOCONDUCTORS
A five-channel, diamond photoconducting x ray detector array for z-pinch experiments
[DE92-017345] p 164 N93-10839
PHOTODIODES
Subpicosecond resolved incipient laser damage
[AD-A253624] p 87 N93-10202
PHOTODISSOCIATION
A time-resolved two-laser probe of Cr(CO)6 photodissociation dynamics
[AD-A250930] p 88 N93-10247
PHOTOELECTRIC EMISSION
Theory of light-induced drift of electrons in coupled quantum wells
[AD-A253609] p 164 N93-10093
PHOTOELECTRON SPECTROSCOPY
Photoionization dynamics and cation spectroscopy with coherent VUV radiation
[DE92-015841] p 154 N93-10730
PHOTOGRAMMETRY
Stereoscopy and paralax in the vertical distances determination using aerial photographs
[INPE-5363-PUD/049] p 102 N93-10063
System integration issues in digital photogrammetric mapping
[AD-A254046] p 103 N93-10781
Autonomous star sensing and pattern recognition for spacecraft attitude determination p 177 N93-10876
Dynamic positioning systems photogrammetric
[AD-A254250] p 8 N93-10898
PHOTOGRAPHIC MEASUREMENT
Meteorological and site influences affecting the comparison of nephelometer and photographic determinations of light extinction at rural sites in the Eastern US
[PB92-195999] p 126 N93-10433
PHOTOGRAPHS
Meteorological and site influences affecting the comparison of nephelometer and photographic determinations of light extinction at rural sites in the Eastern US
[PB92-195999] p 126 N93-10433
PHOTOINTERPRETATION
System integration issues in digital photogrammetric mapping
[AD-A254046] p 103 N93-10781
PHOTOIONIZATION
Development of laser excited atomic fluorescence and ionization methods
[DE92-016199] p 89 N93-10611
Photoionization dynamics and cation spectroscopy with coherent VUV radiation
[DE92-015841] p 154 N93-10730
PHOTOLYSIS
Electron transfer reactions in microporous solids
[DE92-016222] p 166 N93-10284
Rate constants for reactions of hydrazine fuels with O(P-3)
[AD-A252813] p 42 N93-10336
PHOTOMAPPING
System integration issues in digital photogrammetric mapping
[AD-A254046] p 103 N93-10781
PHOTOMASKS
Physical implementations of an antimask in URA based coded mask systems
[INPE-5338-PRE/1737] p 153 N93-10312
PHOTOMETERS
Holographic optical interconnects for multichip modules
[AD-A253403] p 86 N93-10408
PHOTOMICROGRAPHY
Moire-fringe images of twin boundaries in chemical vapor deposited diamond
[AD-A253729] p 35 N93-10231
PHOTONS
Laser and optical physics
[AD-A253619] p 88 N93-10251
Two-photon physics and the coming generation of heavy ion colliders
[DE92-015850] p 156 N93-10732
PHOTOSPHERE
High resolution granulation spectrophotometry with a UBF and a FP interferometer in tandem
p 183 N93-10927
PHOTOSYNTHESIS
Molecular biology in studies of oceanic primary production
[DE92-016101] p 128 N93-10283
Resource capture by single leaves
[DE92-015847] p 129 N93-10461
PHYSICAL CHEMISTRY
The 200th American Chemical Society Geochemistry Division Symposium on Progress in Marine Chemistry
[AD-A253757] p 129 N93-10887
PHYSICAL OPTICS
Laser and optical physics
[AD-A253619] p 88 N93-10251
PHYSIOLOGICAL EFFECTS
Boom and the problems related to the supersonic flights of military aircraft p 149 N93-10677
A prospective evaluation of stress fractures/overuse injuries in a population of West Point cadets
[AD-A252427] p 132 N93-10709
Metabolic factors influencing myocardial recovery from acidosis (CiC3)
[AD-A252376] p 132 N93-10796
PHYSIOLOGICAL RESPONSES
Eye movements and visual information processing
[AD-A250198] p 132 N93-10278
PHYTOPLANKTON
Molecular biology in studies of oceanic primary production
[DE92-016101] p 128 N93-10283
PIEZOELECTRIC CERAMICS
Piezoelectric and electrostrictive materials for transducers applications, volume 1
[AD-A250889] p 71 N93-10273
Piezoelectric and electrostrictive materials for transducers applications, volume 2
[AD-A250890] p 71 N93-10276
Piezoelectric and eiectrostrictive materials for transducers applications, volume 3
[AD-A250891] p 72 N93-10280
Piezoelectric and electrostrictive materials for transducers applications, volume 4
[AD-A250892] p 72 N93-10282
Characterization of and active control of flexible structures, using piezoceramics as sensors and actuators p 10 N93-10319
PIEZOELECTRIC TRANSDUCERS
Piezoelectric and electrostrictive materials for transducers applications, volume 1
[AD-A250889] p 71 N93-10273
Piezoelectric and electrostrictive materials for transducers applications, volume 2
[AD-A250890] p 71 N93-10276
Piezoelectric and electrostrictive materials for transducers applications, volume 3
[AD-A250891] p 72 N93-10280
Piezoelectric and electrostrictive materials for transducers applications, volume 4
[AD-A250892] p 72 N93-10282
PIEZOELECTRICITY
Control of panel flutter at high supersonic speed
p 9 N93-10900
PILOT PERFORMANCE
Advanced terrain displays to transport category aircraft
[PB92-197136] p 6 N93-10065
Mental workload assessment in the cockpit: Feasibility of using electrophysiological measurements, phase 1
[AD-A254138] p 133 N93-10662
KC-135 crew reduction feasibility demonstration simulation study. Volume 3: Test and evaluation
[AD-A253931] p 134 N93-10713
Relating flying hours to aircrew performance: Evidence for attack and transport missions
[AD-A253988] p 133 N93-10719
PILOT TRAINING
Combat aircraft operations: Training requirements for the German Air Force tactical flying units and the noise problem p 148 N93-10667
Possibilities and limitations of flying training in the German Air Force p 11 N93-10668
Combat aircraft noise: The operator's perspective
p 148 N93-10669
Human noise exposure criteria for combat aircraft training areas p 148 N93-10670
PILOTLESS AIRCRAFT
Air cell --- model aircraft power supplies
[CA-PATENT-APPL-SN-2001346] p 72 N93-10368
PION BEAMS
Pion- and proton-nucleus interactions at intermediate energy
[DE92-017980] p 157 N93-10838
PIONS
Coherent production of pions and rho mesons in neutrino charged current interactions on neon nuclei at the Fermilab Tevatron
[DE92-015674] p 154 N93-10606
Pion- and proton-nucleus interactions at intermediate energy
[DE92-017980] p 157 N93-10838
PIPE FLOW
Investigations into swirling flows of Newtonian and non-Newtonian fluids
[AD-A253298] p 82 N93-10696
PIPES (TUBES)
Monitoring structural response in pressurized environments. Part 2: Applications
[DE92-015034] p 94 N93-10327
PITCH (INCLINATION)
An experimental and a theoretical investigation of rotor pitch damping using a model rotor p 8 N93-10322
PITCHING MOMENTS
A method of testing two-dimensional airfoils
[AD-A253210] p 4 N93-10375
PITOT TUBES
Pitot survey of exhaust flow field of a 2-D scramjet nozzle at Mach 6 with air or freon and argon used for exhaust simulation
[NASA-TM-4361] p 2 N93-10071
PITTING
Effect of alloying elements on passivity and breakdown of passivity of Fe- and Ni-based alloys mechanistics aspects
[DE92-017316] p 33 N93-10395
PLANAR STRUCTURES
Indentation of a precompressed penny-shaped crack
p 48 N93-10486
Numerical simulation of transient crack growth
p 48 N93-10488
A new deployable mast p 14 N93-10511
PLANE STRAIN
On the development of a new fracture toughness procedure p 59 N93-10541
PLANE WAVES
On the coupling between a supersonic boundary layer and a flexible surface
[NASA-CR-189697] p 82 N93-10757
Pulse propagation in random media
[AD-A254294] p 152 N93-10769
PLANETARY ATMOSPHERES
Magnetospheres and atmospheres of planets
p 182 N93-10922
PLANETARY CRATERS
Melt production in large-scale impact events: Planetary observations and implications p 108 N93-10126
What can we learn about impact mechanics from large craters on Venus? p 118 N93-10166
Recognizing impactor signatures in the planetary record p 120 N93-10178
Paradigm lost: Venus crater depths and the role of gravity in crater modification p 120 N93-10179
A late Devonian impact event and its association with a possible extinction event on Eastern Gondwana
p 122 N93-10191
Geochemical aspect of impact cratering: Studies in Vernadsky Institute p 123 N93-10196
PLANETARY CRUSTS
Venusian impact basins and cratered terrains
p 112 N93-10145
PLANETARY EVOLUTION
Workshop on the evolution of the Martian atmosphere
[NASA-CR-190730] p 189 N93-10064
International Conference on Large Meteorite Impacts and Planetary Evolution
[NASA-CR-190677] p 105 N93-10112
Asteroids and Archaean crustal evolution: Tests of possible genetic links between major mantle/crust melting events and clustered extraterrestrial bombardments
p 110 N93-10140
Paradigm lost: Venus crater depths and the role of gravity in crater modification p 120 N93-10179
The large impact process inferred from the geology of lunar multiring basins p 121 N93-10184
PLANETARY GEOLOGY
Workshop on the evolution of the Martian atmosphere
[NASA-CR-190730] p 189 N93-10064
Structural aspects of the Araguainha impact structure (Brazil) p 106 N93-10118
Melting and its relationship to impact crater morphology p 119 N93-10170
The Vredefort Dome: Review of geology and deformation phenomena and status report on current knowledge and remaining problematics (five years after the cryptoexplosion workshop) p 119 N93-10173
Geological evidence for a 2.6-Ga strewn field of impact spherules in the Hamersley Basin of Western Australia
p 120 N93-10181
SAR in support of geological investigations of the Sudbury structure p 103 N93-10182
Ar-40 to Ar-39 dating of pseudotachylites from the Witwatersrand basin, South Africa, with implications for the formation of the Vredefort Dome
p 122 N93-10189
Floor-fractured crater models of the Sudbury structure, Canada p 123 N93-10193
Geochemical aspect of impact cratering: Studies in Vernadsky Institute p 123 N93-10196
PLANETARY GRAVITATION
Paradigm lost: Venus crater depths and the role of gravity in crater modification p 120 N93-10179

PLANETARY MAGNETOSPHERES
Magnetospheres and atmospheres of planets
p 182 N93-10922
PLANETARY SURFACES
Indexes of maps of the planets and satellites, 1992
[NASA-TM-4395] p 189 N93-10832
PLANETS
Indexes of maps of the planets and satellites, 1992
[NASA-TM-4395] p 189 N93-10832
PLANFORMS
Effect of planform and body on supersonic aerodynamics of multibody configurations
[NASA-TP-3212] p 4 N93-10824
PLANT DISEASES
Interdisciplinary research and training program in the plant sciences
[DE92-015919] p 130 N93-10835
PLANTS (BOTANY)
Resource capture by single leaves
[DE92-015847] p 129 N93-10461
PLASMA ACCELERATION
Reflection of plasma ions from metals (and its use as a hyperthermal neutral beam source)
p 160 N93-10353
Stokes parameters of the O VI 103.2 nm line as a probe of the matter velocity field vector in the solar wind acceleration region p 181 N93-10914
High resolution observations of solar ejecta
p 181 N93-10916
PLASMA COMPOSITION
Boronization in D3-D
[DE92-016249] p 163 N93-10759
PLASMA CONTROL
D-He-3 spherical torus fusion reactor system study
[AD-A253358] p 155 N93-10102
Fundamental studies on erosion in MPD thrusters
[AD-A253900] p 159 N93-10252
Investigation of the effect of large core changes in toroidal plasma rotation and radial electric field on confinement in H-mode discharges in the D3-D tokamak
[DE92-016252] p 161 N93-10392
Large orbit magnetic confinement systems for advanced fusion fuels
[DE92-016218] p 162 N93-10617
Edge ion dynamics in H-mode discharges in D3-D
[DE92-016255] p 162 N93-10619
The effect of current profile changes on confinement in the D3-D tokamak
[DE92-016256] p 163 N93-10620
Boronization in D3-D
[DE92-016249] p 163 N93-10759
PLASMA CURRENTS
A formula for efficiency of fast wave current drive in fusion devices
[DE92-016152] p 160 N93-10390
Polarimetry of motional Stark effect and determination of current profiles in D3-D
[DE92-016258] p 161 N93-10393
The effect of current profile changes on confinement in the D3-D tokamak
[DE92-016256] p 163 N93-10620
Acceptance testing of the prototype electrometer for the SAMPIE flight experiment
[NASA-TM-105880] p 13 N93-10841
PLASMA DENSITY
Helium transport in enhanced confinement regimes on the TEXTOR and D3-D tokamaks
[DE92-016247] p 160 N93-10293
PLASMA DIAGNOSTICS
Helium transport in enhanced confinement regimes on the TEXTOR and D3-D tokamaks
[DE92-016247] p 160 N93-10293
Intense ion beam research at Los Alamos
[DE92-015240] p 155 N93-10333
Future directions in pulsed power driven ICF
[DE92-016233] p 161 N93-10443
Langmuir probe and optical emission studies of Ar, O2, and N2 plasmas produced by an ECR microwave source
[AD-A253138] p 162 N93-10615
Edge ion dynamics in H-mode discharges in D3-D
[DE92-016255] p 162 N93-10619
Measurements and modeling of laser irradiance in the high-power third-harmonic Nova focus. Volume A: Report
[DE92-016746] p 90 N93-10739
A five-channel, diamond photoconducting x ray detector array for z-pinch experiments
[DE92-017345] p 164 N93-10839
PLASMA DYNAMICS
On the nature of the small-scale plasma structures in the solar active phenomena p 183 N93-10925
PLASMA ELECTRODES
Fundamental studies on erosion in MPD thrusters
[AD-A253900] p 159 N93-10252
PLASMA ENGINES
Fundamental studies on erosion in MPD thrusters
[AD-A253900] p 159 N93-10252
Basic processes of plasma propulsion
[AD-A253929] p 163 N93-10754
PLASMA EQUILIBRIUM
Large orbit magnetic confinement systems for advanced fusion fuels
[DE92-016218] p 162 N93-10617
PLASMA FOCUS
Synchrotron radiation considerations in the Dense Plasma Focus (DPF) Magnetoplasmadynamic (MPD) thruster
[AD-A254188] p 25 N93-10258
Critical technology demonstration of plasma focus type MPD thrusters
[AD-A252428] p 26 N93-10638
PLASMA HEATING
A formula for efficiency of fast wave current drive in fusion devices
[DE92-016152] p 160 N93-10390
Polarimetry of motional Stark effect and determination of current profiles in D3-D
[DE92-016258] p 161 N93-10393
Experimental plasma research project summaries
[DE92-016274] p 162 N93-10464
Small scale processes in solar and stellar plasmas
p 181 N93-10917
PLASMA INTERACTION EXPERIMENT
Acceptance testing of the prototype electrometer for the SAMPIE flight experiment
[NASA-TM-105880] p 13 N93-10841
PLASMA INTERACTIONS
Simulation study of interactions of Space Shuttle-generated electron beams with ambient plasmas
[NASA-CR-190843] p 159 N93-10066
PLASMA JETS
Fundamental studies on erosion in MPD thrusters
[AD-A253900] p 159 N93-10252
PLASMA LAYERS
Transition region dynamics p 180 N93-10907
Ultra-high observations of the prominence-corona transition region p 180 N93-10908
PLASMA PHYSICS
Experimental plasma research project summaries
[DE92-016274] p 162 N93-10464
Stochastic diffusion and Kolmogorov entropy in regular and random Hamiltonians
[DE92-016179] p 170 N93-10604
Solar Physics and Astrophysics at Interferometric Resolution
[ESA-SP-344] p 179 N93-10901
PLASMA PROPULSION
Fundamental studies on erosion in MPD thrusters
[AD-A253900] p 159 N93-10252
Basic processes of plasma propulsion
[AD-A253929] p 163 N93-10754
PLASMA TURBULENCE
Microwave propagation and attenuation in magnetoplasmas
[AD-A250197] p 69 N93-10728
Intensity, velocity, and turbulence in prominences observed with the HRTS p 180 N93-10911
PLASMA WAVES
Modeling of HF propagation and heating in the ionosphere
[AD-A253941] p 125 N93-10714
Data synthesis and display programs for wave distribution function analysis
[NASA-TM-108009] p 70 N93-10800
PLASMA-ELECTROMAGNETIC INTERACTION
Microwave propagation and attenuation in magnetoplasmas
[AD-A250197] p 69 N93-10728
PLASMAS (PHYSICS)
Long conduction time plasma opening switch experiments at Sandia National Labs
[DE92-015003] p 72 N93-10279
Helium transport in enhanced confinement regimes on the TEXTOR and D3-D tokamaks
[DE92-016247] p 160 N93-10293
Divertor heat flux reduction by D2 injection in DIII-D
[DE92-014232] p 160 N93-10326
An analytic determination of beta poloidal and internal inductance in an elongated tokamak from magnetic probe measurements
[DE92-016294] p 160 N93-10331
Kinetics of oxidation of silicon by electron cyclotron resonance plasmas
[AD-A253140] p 161 N93-10413
A new ellipsometry technique for interface analysis: Application to Si-SiO2
[AD-A253143] p 167 N93-10415
Variational full wave calculation of fast wave current drive in D3-D using the ALCYON code
[DE92-016572] p 163 N93-10761
PLASTIC DEFORMATION
Simple shearing flow of a 3D foam
[DE92-011151] p 36 N93-10399
Integrated finite element model of composite materials
p 46 N93-10477
Damage due to plastic deformation in elastic-plastic materials: The thermodynamical connection
p 51 N93-10502
A new quadrilateral element for the elastic and plastic analysis of shells p 62 N93-10559
PLASTIC FLOW
A variational approach for coupled creeping-flow problems p 62 N93-10557
PLASTIC PROPERTIES
Plasticity of single crystalline Al3X intermetallic compounds
[AD-A254282] p 40 N93-10766
Unified viscoplastic behavior of metal matrix composites
[NASA-TM-105819] p 96 N93-10777
PLASTICIZERS
GAP benefits p 19 N93-10025
PLASTICS
Research and development of two marine-degradable biopolymers
[AD-A254051] p 41 N93-10783
PLATE THEORY
On the behavior of a higher-order plate bending element p 47 N93-10481
Evaluation of the triangular plate element of Zienkiewcz and Lefebvre p 63 N93-10562
Linear and nonlinear analyses of thick composite circular plates using the finite element method
p 96 N93-10873
PLATEAUS
Noril'sk/Siberian plateau basalts and Bahama hot spot: Impact triggered? p 109 N93-10132
PLATES (STRUCTURAL MEMBERS)
Calculation of stress intensity factors in an isotropic multicracked plate: Part 2: Symbolic/numeric implementation
[NASA-TM-105823] p 95 N93-10453
Calculation of stress intensity factors in an isotropic multicracked plate. Part 1: Theoretical development
[NASA-TM-105766] p 95 N93-10455
Development in the elastic analysis of laminated plates p 44 N93-10468
Nonstationary random variations of moderately thick plates using BEM p 48 N93-10487
PLATES (TECTONICS)
Worldwide seismic catalog and the nature of seismic coupling p 124 N93-10376
PLATINUM
Mobilization of the platinum group elements by low-temperature fluids: Implications for mineralization and the iridium controversy p 109 N93-10133
PLENUM CHAMBERS
Further noise measurements in a slotted cryogenic wind tunnel
[RAE-TM-AERO-2201] p 153 N93-10805
PLUG NOZZLES
Plug nozzle propulsion system p 17 N93-10013
Critical engine system design characteristics for SSTO vehicles p 17 N93-10014
PLUMES
Pitot survey of exhaust flow field of a 2-D scramjet nozzle at Mach 6 with air or freon and argon used for exhaust simulation
[NASA-TM-4361] p 2 N93-10071
Species and temperature measurement in H2/O2 rocket flow fields by means of Raman scattering diagnostics
[NASA-CR-189217] p 25 N93-10086
A multi-fluid model of turbulence for Li-SF6 submerged combustion
[AD-A253973] p 31 N93-10423
Nozzle installation effects on the noise from supersonic exhaust plumes p 150 N93-10681
PNEUMATIC CONTROL
Pneumatic motor powered Thrust Vector Control (TVC) for liquid propelled launch vehicles p 17 N93-10015
PNEUMATIC EQUIPMENT
Pneumatic motor powered Thrust Vector Control (TVC) for liquid propelled launch vehicles p 17 N93-10015
POINTING CONTROL SYSTEMS
Accommodation aspects of SIMURIS on Space Station Freedom p 14 N93-10954
POLAR REGIONS
Eleven years of ionospheric scintillation fading data from twenty Greenlandic stations
[AD-A253271] p 69 N93-10695
Investigations of the dynamics and thermodynamics of the mesosphere lower thermosphere and upper thermosphere at the polar regions with optical ground-based remote sensing
[AD-A253228] p 125 N93-10711

POLARIMETRY
Polarimetry of motional Stark effect and determination of current profiles in D3-D
[DE92-016258] p 161 N93-10393
Polarimetry with an imaging FTS p 14 N93-10934
POLARITY
Method and apparatus for determining return stroke polarity of distant lightning
[NASA-CASE-MFS-26102-2-CU] p 125 N93-10108
POLARIZATION (SPIN ALIGNMENT)
Recent developments in stored polarized electron positron beams
[DE92-016965] p 157 N93-10862
POLARIZED LIGHT
Polarized light scattering from perfect and perturbed surfaces and fundamental scattering systems
[AD-A253186] p 158 N93-10445
POLARIZED RADIATION
Recent developments in stored polarized electron positron beams
[DE92-016965] p 157 N93-10862
POLARONS
Covalent electron transfer theory of superconductivity
[AD-A253975] p 74 N93-10718
Theory of transport for interacting many-body systems
[AD-A253789] p 169 N93-10871
POLICIES
The levels of mathematics achievement: Initial performance standards for the 1990 NAEP mathematics assessment, volume 3
[PB92-199421] p 134 N93-10341
Raster graphics validation
[PB92-196070] p 137 N93-10441
Aerospace Industries Association of Canada
[CTN-92-60345] p 192 N93-10640
Aerospace Industries Association of Canada
[CTN-92-60590] p 1 N93-10644
POLLUTION
The Deposition and Fate of Trace Metals in our Environment: Symposium proceedings
[PB92-189216] p 104 N93-10289
POLLUTION CONTROL
Format and structure of a database on health and environmental impacts of different energy systems for electricity generation
[DE92-634160] p 130 N93-10222
POLLUTION MONITORING
The Deposition and Fate of Trace Metals in our Environment: Symposium proceedings
[PB92-189216] p 104 N93-10289
Portable tandem mass spectrometer analyzer
[AD-A254065] p 125 N93-10784
POLYACRYLONITRILE
Molded nozzle technology for large solid rocket motors p 19 N93-10024
POLYATOMIC MOLECULES
Photoionization dynamics and cation spectroscopy with coherent VUV radiation
[DE92-015841] p 154 N93-10730
POLYCRYSTALS
Growth, nitrogen vacancy reduction, and solid solution formation in cubic GaN thin films and the subsequent fabrication of superlattice structures using AlN and InN
[AD-A253331] p 166 N93-10356
POLYESTERS
Synthesis and characterization of energetic polymers p 15 N93-10005
POLYETHER RESINS
Synthesis and characterization of energetic polymers p 15 N93-10005
POLYGONS
Hexagonal and octagonal finite elements p 50 N93-10500
POLYMER CHEMISTRY
Synthesis and characterization of energetic polymers p 15 N93-10005
POLYMER MATRIX COMPOSITES
Polymer matrix composites on LDEF experiments M0003-9 and M0003-10 p 38 N93-10584
Space environmental effects on LDEF low Earth orbit exposed graphite reinforced polymer matrix composites p 38 N93-10585
Additional results on space environmental effects on polymer matrix composites: Experiment A0180 p 38 N93-10586
Proposed test program and data base for LDEF polymer matrix composites p 38 N93-10587
POLYMERIC FILMS
Development of electrosupercapacitors
[AD-A252208] p 71 N93-10250
Research and development of two marine-degradable biopolymers
[AD-A254051] p 41 N93-10783
POLYMERIZATION
Synthesis and characterization of energetic polymers p 15 N93-10005
Synthesis of side chain liquid crystal polymerization by living ring opening metathesis polymerization. Report 1: Influence of molecular weight, polydispersity, and flexible spacer length (n=2-8) on the thermotropic behavior of the resulting polymers
[AD-A248699] p 40 N93-10727
POLYMERS
Measurement of aerodynamic shear stress using side chain liquid crystal polymers
[AD-A254312] p 40 N93-10770
POLYMORPHISM
Electron petrography of silica polymorphs associated with pseudotachylite, Vredefort structure, South Africa p 123 N93-10192
POLYNOMIALS
Interactive grid generation program for CAP-TSD
[NASA-TM-102705] p 3 N93-10349
Global structure of a polynomial autonomous system on the plane
[DE92-630230] p 144 N93-10389
Axisymmetric vibrations of rotating circular plates using characteristic orthogonal polynomials p 45 N93-10470
Algebra-geometric and differential geometric methods in solid geometric modeling
[AD-A253669] p 145 N93-10870
POLYPROPYLENE
Materials compatibility and lubricants research on CFC-refrigerant substitute: Miscibility of lubricants with refrigerants
[DE92-015118] p 35 N93-10084
POLYSILOXANES
Water soluble polysiloxanes with pendant 1-oxypyridin-3-yl groups
[AD-A250637] p 36 N93-10246
POLYSTYRENE
Mobility of toluene in polystyrene-toluene solutions: A NMR study
[AD-A253203] p 31 N93-10794
POPULATIONS
Noise of combat aircraft in proximity to air bases: Review of the possibilities of noise reduction at the source p 148 N93-10671
POROSITY
Development of physical and mathematical models for the Porous Ceramic Tube Plant Nutrification System (PCTPNS)
[NASA-TM-107551] p 129 N93-10085
Oxygen barrier oxides
[AD-A253683] p 36 N93-10343
Template-synthesis of infrared-transparent metal microcylinders: Comparison of optical properties with the predictions of effective medium theory
[AD-A253267] p 158 N93-10694
Activated transport in AMTEC electrodes
[DE92-016810] p 75 N93-10786
POROUS MATERIALS
Electron transfer reactions in microporous solids
[DE92-016222] p 166 N93-10284
PORTABLE EQUIPMENT
Resonance apparatus operating manual
[AD-A254040] p 71 N93-10241
Portable tandem mass spectrometer analyzer
[AD-A254065] p 125 N93-10784
PORTUGAL
Scientific and Technical Information (STI) towards technological and industrial development: The case of Portugal p 173 N93-10596
POSITION (LOCATION)
Symmetry breaking and localization in quantum chaotic systems
[DE92-634890] p 170 N93-10294
Global positioning systems technology and its application in environmental programs
[PB92-169358] p 7 N93-10442
POSITION INDICATORS
Dynamic positioning systems photogrammetric
[AD-A254250] p 8 N93-10898
POSITIONING
Mathematical analysis of multi-sensor cross-correlation processing for source localization
[DREA-CR-89-433] p 68 N93-10366
GPS Army research and applications
[AD-A254262] p 7 N93-10424
POSITRONS
Cognition in the brain: Investigations using positron emission tomography
[AD-A254280] p 132 N93-10765
Recent developments in stored polarized electron positron beams
[DE92-016965] p 157 N93-10862
POSTFLIGHT ANALYSIS
LDEF Materials Workshop 1991, part 2
[NASA-CP-3162-PT-2] p 37 N93-10578
Results from the testing and analysis of LDEF batteries p 39 N93-10589
Effects of long-term exposure on LDEF fastener assemblies p 39 N93-10590
Results from testing and analysis of solar cells flown on LDEF p 39 N93-10591
System related testing and analysis of FRECOPA p 39 N93-10592
Analysis of interplanetary dust experiment detectors and other witness plates
[NASA-CR-190818] p 32 N93-10852
Elemental analyses of hypervelocity microparticle impact sites on interplanetary dust experiment sensor surfaces p 32 N93-10853
Contaminant interferences with SIMS analyses of microparticle impactor residues on LDEF surfaces p 32 N93-10854
POTASSIUM ALLOYS
Boiling behavior of sodium-potassium alloy in a bench-scale solar receiver
[DE92-014947] p 103 N93-10383
POTENTIAL FLOW
Aerodynamic investigation of radial turbines using computational methods p 78 N93-10056
POWDER (PARTICLES)
Developmental research on ultra abrasion-resistant materials
[DE92-531066] p 36 N93-10287
POWER CONDITIONING
A 26 kW arcjet system for on-orbit demonstration p 21 N93-10031
Power conditioning unit for 30 kWe class arcjet flight experiment p 21 N93-10032
Design and operation of the US Space Station Freedom propulsion system p 24 N93-10049
MHD Integrated Topping Cycle Project
[DE92-016610] p 164 N93-10861
POWER EFFICIENCY
10 kW power electronics for hydrogen arcjets p 21 N93-10033
Non-dimensional conceptual design of radial inflow turbines. Part A: Application of fundamental fluid mechanics p 77 N93-10053
POWER SERIES
Finite group actions and elliptic genera
[DE92-630207] p 170 N93-10388
POWER SPECTRA
Power spectrum of the extragalactic background light p 177 N93-10364
POWER SUPPLY CIRCUITS
Evaluation of an electronics system concept for Respiratory Protection system (RESPO 21)
[AD-A253394] p 134 N93-10288
PREAMPLIFIERS
A novel charge sensitive preamplifier without the feedback resistor
[DE92-015842] p 74 N93-10731
PRECAMBRIAN PERIOD
Mobilization of the platinum group elements by low-temperature fluids: Implications for mineralization and the iridium controversy p 109 N93-10133
Asteroids and Archaean crustal evolution: Tests of possible genetic links between major mantle/crust melting events and clustered extraterrestrial bombardments p 110 N93-10140
The Acraman impact and its widespread ejecta, South Australia p 111 N93-10141
Early Archean spherule beds of possible impact origin from Barberton, South Africa: A detailed mineralogical and geochemical study p 115 N93-10155
PRECIPITATES
Plasticity of single crystalline Al3X intermetallic compounds
[AD-A254282] p 40 N93-10766
PRECIPITATION (METEOROLOGY)
Analysis of air pollution and greenhouse gases
[DE92-014955] p 104 N93-10384
Morning-evening differences in global and regional oceanic precipitation as observed by the SSM/I p 127 N93-10851
PREDICTION ANALYSIS TECHNIQUES
Instrumented propellant block test and stress analysis comparison p 15 N93-10002
A simplified model for hybrid rocket performance prediction p 19 N93-10022
Misclassification rates of likelihood and predictive discriminant functions for small samples
[AD-A253640] p 146 N93-10208
Advanced technology component derating
[AD-A253334] p 72 N93-10357
Nonlinear dynamics underlying atmospheric predictability
[AD-A254042] p 126 N93-10363
Handbook for operating the OWLKNEST technology
[AD-A253412] p 137 N93-10409
Navier-Stokes turbine heat transfer predictions using two-equation turbulence
[NASA-TM-105817] p 82 N93-10735

Improve SSME power balance model
[NASA-CR-184464] p 26 N93-10756
PREDICTIONS
Operator workload predictions for the revised AH-64A workload prediction model, volume 1
[AD-A254198] p 133 N93-10261
Study of improved methods for predicting chemical equilibria
[DE92-016974] p 31 N93-10436
PRESSURE DISTRIBUTION
Analysis of wing-body junction flowfields using the incompressible Navier-Stokes equations, volumes 1 and 2 p 3 N93-10320
PRESSURE EFFECTS
Monitoring structural response in pressurized environments. Part 2: Applications
[DE92-015034] p 94 N93-10327
PRESSURE OSCILLATIONS
Further noise measurements in a slotted cryogenic wind tunnel
[RAE-TM-AERO-2201] p 153 N93-10805
PRESSURE VESSELS
Strength-toughness requirements for thick-walled high pressure vessels
[AD-A253756] p 95 N93-10750
PRINTED CIRCUITS
A four channel 250 MHz visual counter
[DE92-016920] p 86 N93-10444
PROBABILITY DENSITY FUNCTIONS
A new non-Gausssian approximation technique for random vibration of general hysteresis p 50 N93-10496
Probability density functions for random nonlinear oscillation p 55 N93-10522
Resistive Grid Kernel Estimator (RGKE)
[AD-A253520] p 147 N93-10869
PROBABILITY DISTRIBUTION FUNCTIONS
Change analysis
[AD-A253567] p 146 N93-10795
PROBABILITY THEORY
Probability forecasting: A guide for forecasters and staff weather officers
[AD-A254216] p 126 N93-10264
Convergence performance of adaptive detectors, part 3
[AD-A248415] p 143 N93-10275
Change analysis
[AD-A253567] p 146 N93-10795
Radiation damage to DNA
[DE92-015760] p 130 N93-10834
Resistive Grid Kernel Estimator (RGKE)
[AD-A253520] p 147 N93-10869
PROBLEM SOLVING
PRODIGY4.0: The manual and tutorial
[AD-A253970] p 137 N93-10422
Smart algorithms and adaptive methods in computational fluid dynamics p 44 N93-10469
TAQL: A problem space tool for expert system development
[AD-A253820] p 175 N93-10826
PROCEDURES
Quality assurance practices for data entry and electronic data transfer
[DE92-014804] p 172 N93-10396
PROCESS CONTROL (INDUSTRY)
Introduction to software process improvement
[AD-A253326] p 137 N93-10447
PROCUREMENT
Acquisition 2: Procurement, acquisition, and maintenance of configuration management documentation in support of a CIS system p 173 N93-10599
PRODUCT DEVELOPMENT
Aerospace industry profile, 1990-1991
[CTN-92-60513] p 1 N93-10651
Manitoba aerospace technology: Capability directory
[CTN-92-60572] p 193 N93-10655
PRODUCTION ENGINEERING
Ceramic transactions. Volume 21: Proceedings of the Symposium on Microwave Theory and Application in Materials Processing Annual Meeting No. 23 io on april 29-may 3 1991
[AD-A253631] p 35 N93-10205
PRODUCTION MANAGEMENT
Introduction to software process improvement
[AD-A253326] p 137 N93-10447
PROGRAM VERIFICATION (COMPUTERS)
A building-block approach for turbulence model validation/upgrade focussed on high-speed jet flowfields p 16 N93-10010
Ada validation tests for rate monotonic scheduling algorithms
[AD-A253325] p 136 N93-10300
PROJECT MANAGEMENT
Total Quality Management (TQM) concepts applied to instruction
[DE92-013399] p 171 N93-10270
Establishing a scientific and technical information program: Planning and resource management p 173 N93-10597
Manitoba aerospace technology: Capability directory
[CTN-92-60572] p 193 N93-10655
PROJECT PLANNING
Establishing a scientific and technical information program: Planning and resource management p 173 N93-10597
Weather Message Switching Center Replacement (WMSCR) Operational Test and Evaluation (OT/E)/integration test plan
[DOT/FAA/CT-TN90/59] p 7 N93-10833
PROJECTILES
Measurement of acceleration using an instrumented railgun projectile
[AD-A253366] p 12 N93-10106
PROMINENCES
Spatial distribution of line-of-sight velocities in a quiescent prominence p 183 N93-10928
PROPAGATION MODES
Status of dynamic fracture in brittle solids p 49 N93-10493
Modeling of HF propagation and heating in the ionosphere
[AD-A253941] p 125 N93-10714
PROPELLANT ADDITIVES
Impact sensitivity reduction via exo-electron control p 15 N93-10004
PROPELLANT CHEMISTRY
Synthesis and characterization of energetic polymers p 15 N93-10005
Theory of combustion of liquid propellants based on hydroxylammonium nitrate
[AD-A248445] p 42 N93-10267
Polynitro polycyclic cage compounds
[AD-A252889] p 42 N93-10268
PROPELLANT COMBUSTION
Combustion-wave ignition for rocket engines p 17 N93-10016
Theory of combustion of liquid propellants based on hydroxylammonium nitrate
[AD-A248445] p 42 N93-10267
PROPELLANT GRAINS
The 1992 JANNAF Propulsion Meeting, volume 1
[CPIA-PUBL-580-VOL-1] p 15 N93-10001
Effects of the RSRM grain deformation on ballistic performance p 20 N93-10027
PROPELLANT PROPERTIES
Synthesis and characterization of energetic polymers p 15 N93-10005
Effects of the RSRM grain deformation on ballistic performance p 20 N93-10027
PROPELLANT SENSITIVITY
Impact sensitivity reduction via exo-electron control p 15 N93-10004
PROPELLANT TANKS
Loading operations for spacecraft propulsion subsystems p 11 N93-10047
PROPELLANT TESTS
Instrumented propellant block test and stress analysis comparison p 15 N93-10002
Multidimensional effects in composite propellant combustion p 42 N93-10313
PROPELLANT TRANSFER
Generic Propellant Transfer Unit p 11 N93-10046
Loading operations for spacecraft propulsion subsystems p 11 N93-10047
PROPELLANTS
Polynitro polycyclic cage compounds
[AD-A252889] p 42 N93-10268
Limited toxicity and mutagenicity testing of five unicharge propellant compounds
[AD-A252339] p 43 N93-10636
PROPELLER NOISE
Reduction of propeller noise by active noise control p 152 N93-10692
PROPULSION
Aeronautical technologies for the twenty-first century
[NASA-CR-190918] p 1 N93-10647
PROPULSION SYSTEM CONFIGURATIONS
The 1992 JANNAF Propulsion Meeting, volume 1
[CPIA-PUBL-580-VOL-1] p 15 N93-10001
Plug nozzle propulsion system p 17 N93-10013
Electric propulsion applications p 20 N93-10029
Electric Propulsion Space Experiment (ESEX): Spacecraft design issues for high-power electric propulsion p 21 N93-10030
10 kW power electronics for hydrogen arcjets p 21 N93-10033
Selection of rocket propulsion systems p 22 N93-10034
Operationally efficient space-based integrated propulsion module p 22 N93-10035
NLS cargo transfer vehicle propulsion system p 23 N93-10041
DSP propulsion system launch configuration and related testing p 24 N93-10048
LV software for supersonic flow analysis
[NASA-CR-190911] p 2 N93-10069
Measurement of acceleration using an instrumented railgun projectile
[AD-A253366] p 12 N93-10106
A personal viewpoint on the development of China's liquid propellant rocket engines
[AD-A254104] p 27 N93-10813
PROPULSION SYSTEM PERFORMANCE
The 1992 JANNAF Propulsion Meeting, volume 1
[CPIA-PUBL-580-VOL-1] p 15 N93-10001
Supersonic confined jet nozzles p 16 N93-10009
Plug nozzle propulsion system p 17 N93-10013
Hot fire test results of subscale tubular combustion chambers p 18 N93-10020
A simplified model for hybrid rocket performance prediction p 19 N93-10022
Electric propulsion applications p 20 N93-10029
Electric Propulsion Space Experiment (ESEX): Spacecraft design issues for high-power electric propulsion p 21 N93-10030
Power conditioning unit for 30 kWe class arcjet flight experiment p 21 N93-10032
10 kW power electronics for hydrogen arcjets p 21 N93-10033
Selection of rocket propulsion systems p 22 N93-10034
Operationally efficient space-based integrated propulsion module p 22 N93-10035
Uprated OMS engine status: Altitude testing results p 22 N93-10036
Long life monopropellant hydrazine thruster evaluation for Space Station Freedom application p 23 N93-10042
DSP propulsion system launch configuration and related testing p 24 N93-10048
Design and operation of the US Space Station Freedom propulsion system p 24 N93-10049
LV software for supersonic flow analysis
[NASA-CR-190911] p 2 N93-10069
Measurement of acceleration using an instrumented railgun projectile
[AD-A253366] p 12 N93-10106
A personal viewpoint on the development of China's liquid propellant rocket engines
[AD-A254104] p 27 N93-10813
PROPULSIVE EFFICIENCY
Hypersonic inlet efficiency revisited p 5 N93-10012
PROTECTION
Novel seals and specialty component attachment mechanisms for Respiratory Protection system (RESPO 21)
[AD-A253395] p 91 N93-10290
Combat aircraft noise p 149 N93-10676
Power system monitoring and source control of the Space Station Freedom DC power system testbed
[NASA-TM-105841] p 26 N93-10734
PROTECTIVE CLOTHING
Evaluation of lightweight and low profile communications devices for Respiratory Protective system 21 (RESPO 21)
[AD-A253393] p 133 N93-10217
PROTECTIVE COATINGS
Oxidation protection systems for carbon-carbon composites formed by chemical vapor deposition and plasma assisted chemical vapor deposition techniques
[AD-A253450] p 28 N93-10344
Protective coatings for niobium alloys and their properties
[AD-A254252] p 33 N93-10706
Boronization in D3-D
[DE92-016249] p 163 N93-10759
PROTECTORS
Evaluation of an electronics system concept for Respiratory Protection system (RESPO 21)
[AD-A253394] p 134 N93-10288
PROTEINS
Interaction of electromagnetic fields with chondrocytes in gel culture
[AD-A253727] p 70 N93-10747
Hierarchical structure in polymeric solid and its influence on properties
[AD-A253818] p 41 N93-10825
PROTOCOL (COMPUTERS)
Investigation of a possible stochastic model for the IEEE P896.1 (Futurebus+) protocol, including the proposed enhanced distributed arbiter
[CTN-92-60593] p 135 N93-10088
Ada validation tests for rate monotonic scheduling algorithms
[AD-A253325] p 136 N93-10300
PROTON BEAMS
Future directions in pulsed power driven ICF
[DE92-016233] p 161 N93-10443

Pion- and proton-nucleus interactions at intermediate energy
[DE92-017980] p 157 N93-10838

PROTOTYPES
Investigations of the dynamics and thermodynamics of the mesosphere lower thermosphere and upper thermosphere at the polar regions with optical ground-based remote sensing
[AD-A253228] p 125 N93-10711
Prototype superconducting planar transformers using high-Tc thin and thick films
[AD-A254230] p 77 N93-10897

PSEUDOPOTENTIALS
Electronic and structural properties of metallic microclusters
[DE92-016917] p 33 N93-10411

PSYCHOPHYSIOLOGY
Perception of lightness and brightness in complex patterns
[AD-A254093] p 133 N93-10658

PUBLIC HEALTH
Format and structure of a database on health and environmental impacts of different energy systems for electricity generation
[DE92-634160] p 130 N93-10222

PUBLIC RELATIONS
Index to NASA news releases and speeches, 1991
[NASA-TM-108004] p 175 N93-10815
Index to NASA news releases and speeches, 1990
[NASA-TM-108003] p 176 N93-10872

PULSE AMPLITUDE
Numerical study of wall turbulence
[ONERA-RSF-21/3419-AY-126] p 83 N93-10859

PULSE COMMUNICATION
Architecture and device development for optical networks
[AD-A253247] p 158 N93-10693

PULSED LASERS
Long wavelength multiple quantum well lasers for high-speed modulation applications
[AD-A253348] p 87 N93-10211
Fellowship in physics/modern optics and quantum electronics
[AD-A253666] p 87 N93-10228
Studies impacting the designs of free electron lasers
[AD-A254293] p 90 N93-10768
Internal explosion in laser ablation of superconducting targets
[AD-A253701] p 90 N93-10799

PULSED RADIATION
Pulse propagation in random media
[AD-A254294] p 152 N93-10769

PULSES
Pulsed jet plume combustion: An exothermic process under fluid mechanical control p 32 N93-10553

PUMP IMPELLERS
Tensile properties of cast titanium alloys: Titanium-6Al-4V ELI and Titanium-5Al-2.5Sn ELI
[NASA-TP-3288] p 33 N93-10072

PYROELECTRICITY
Effect of space exposure on pyroelectric infrared detectors p 38 N93-10582

PYRROLES
Infrared investigations of pristine polypyrrole. Is the polymer called polypyrrole really Poly (Pyrrole-Co-Hydroxypyrrole)?
[AD-A249746] p 36 N93-10243

Q

Q FACTORS
A new model for interpreting experimental data from a circular waveguide cavity
[AD-A254067] p 75 N93-10785

QUALITY CONTROL
Quality assurance practices for data entry and electronic data transfer
[DE92-014804] p 172 N93-10396
Introduction to software process improvement
[AD-A253326] p 137 N93-10447

QUANTITATIVE ANALYSIS
Atomic force microscope studies of CuCl island formation on CaF2(111) substrates
[AD-A252499] p 34 N93-10880

QUANTUM CHROMODYNAMICS
Two-photon couplings of quarkonia with arbitrary J(sup PC)
[DE92-016525] p 153 N93-10332
Research in theoretical particle physics
[DE92-016181] p 154 N93-10605
Research program in elementary particle theory
[DE92-017399] p 155 N93-10840

QUANTUM ELECTRODYNAMICS
Quantum 1/f noise in high technology applications including ultrasmall structures and devices
[AD-A253922] p 74 N93-10751

QUANTUM ELECTRONICS
Basic and applied research in the field of electronics and communications
[AD-A253593] p 67 N93-10092
Theory of light-induced drift of electrons in coupled quantum wells
[AD-A253609] p 164 N93-10093
Fellowship in physics/modern optics and quantum electronics
[AD-A253666] p 87 N93-10228
Quantum 1/f noise in high technology applications including ultrasmall structures and devices
[AD-A253922] p 74 N93-10751
Joint Services Electronics Program
[AD-A253842] p 76 N93-10829
Theory of transport for interacting many-body systems
[AD-A253789] p 169 N93-10871

QUANTUM MECHANICS
Quantum tunneling and the change in the signature of the spacetime metric
[DE92-634877] p 165 N93-10225
Semiclassical quantization of chaotic billiards
[DE92-634888] p 169 N93-10226
Semiclassical quantization of interacting anyons in a strong magnetic field
[DE92-634889] p 169 N93-10229
Symmetry breaking and localization in quantum chaotic systems
[DE92-634890] p 170 N93-10294
Semiclassical quantization of integrable systems of few interacting anyons in a strong magnetic field
[DE92-634892] p 170 N93-10295
Vector superconductivity in cosmic strings
[DE92-634923] p 179 N93-10296
The class of the paths in the Feynman path integral on the phase space
[DE92-630205] p 170 N93-10386
On the measurement of time-dependent quantum phases
[DE92-630206] p 170 N93-10387

QUANTUM NUMBERS
Merged beam studies of laser stimulated radiative recombination
[AD-A253308] p 89 N93-10698

QUANTUM STATISTICS
Semiclassical quantization of integrable systems of few interacting anyons in a strong magnetic field
[DE92-634892] p 170 N93-10295

QUANTUM THEORY
Semiclassical quantization of chaotic billiards
[DE92-634888] p 169 N93-10226
Semiclassical quantization of interacting anyons in a strong magnetic field
[DE92-634889] p 169 N93-10229
Mass and mixing angle patterns in the standard model and its material supersymmetric extension
[DE92-016197] p 153 N93-10291
Symmetry breaking and localization in quantum chaotic systems
[DE92-634890] p 170 N93-10294
Semiclassical quantization of integrable systems of few interacting anyons in a strong magnetic field
[DE92-634892] p 170 N93-10295
Vector superconductivity in cosmic strings
[DE92-634923] p 179 N93-10296
Theory of transport for interacting many-body systems
[AD-A253789] p 169 N93-10871

QUANTUM WELLS
Theory of light-induced drift of electrons in coupled quantum wells
[AD-A253609] p 164 N93-10093
Spatial light modulators with arbitrary quantum well profiles
[AD-A253637] p 165 N93-10210
Long wavelength multiple quantum well lasers for high-speed modulation applications
[AD-A253348] p 87 N93-10211
Novel optoelectronic devices based on combining GaAs and InP on Si
[AD-A253781] p 165 N93-10235
Laser and optical physics
[AD-A253619] p 88 N93-10251
Theory of transport for interacting many-body systems
[AD-A253789] p 169 N93-10871

QUARK MODELS
Two-photon couplings of quarkonia with arbitrary J(sup PC)
[DE92-016525] p 153 N93-10332

QUARKS
Mass and mixing angle patterns in the standard model and its material supersymmetric extension
[DE92-016197] p 153 N93-10291
Two-photon couplings of quarkonia with arbitrary J(sup PC)
[DE92-016525] p 153 N93-10332
A measurement of the Z(sup 0) hadronic branching fraction to bottom quarks and the charged multiplicity of bottom quark events using precision vertex detectors at E(sub cm) = 91 GeV
[DE92-018236] p 154 N93-10820

QUARTZ
Optical and TEM study of shock metamorphism from the Sedan test site p 111 N93-10142
Influence of the preshock temperature on shock effects in quartz p 115 N93-10157
Quantum 1/f noise in high technology applications including ultrasmall structures and devices
[AD-A253922] p 74 N93-10751

QUEUEING THEORY
Investigation of a possible stochastic model for the IEEE P896.1 (Futurebus+) protocol, including the proposed enhanced distributed arbiter
[CTN-92-60593] p 135 N93-10088

R

RADAR BEACONS
A description of the Mode Select beacon system (Mode S) and its associated benefits to the National Airspace System (NAS)
[DOT/FAA/SE-92/6] p 7 N93-10738

RADAR CLUTTER MAPS
Nonlinear signal processing schemes for robust target detection and automatic clutter rejection in radar
[AD-A253546] p 68 N93-10380

RADAR CROSS SECTIONS
Analysis of a medium size BOR radome
[AD-A253954] p 69 N93-10418
Echo characteristic analysis of the nonequilibrium wakes of reentry vehicle
[AD-A254249] p 13 N93-10705

RADAR DETECTION
Nonlinear signal processing schemes for robust target detection and automatic clutter rejection in radar
[AD-A253546] p 68 N93-10380

RADAR ECHOES
Echo characteristic analysis of the nonequilibrium wakes of reentry vehicle
[AD-A254249] p 13 N93-10705

RADAR EQUIPMENT
Extended-interaction klystron for the AN/TPS-43-E radar system
[AD-A253166] p 76 N93-10882

RADAR IMAGERY
Imaging radar investigations of the Sudbury structure p 117 N93-10162
Open Skies Treaty imaging radar technology issues
[DE92-016548] p 68 N93-10394

RADAR MEASUREMENT
SAR in support of geological investigations of the Sudbury structure p 103 N93-10182

RADAR NETWORKS
Software for prediction and analysis of ground wave propagation loss
[AD-A253474] p 67 N93-10199

RADAR REFLECTORS
Proceedings of the Antenna Applications Symposium, volume 1
[AD-A253681] p 68 N93-10301
Proceedings of the Antenna Applications Symposium, volume 2
[AD-A253682] p 68 N93-10302

RADAR SCATTERING
Millimeter wave measurement and modeling of terrain scattering
[AD-A253525] p 67 N93-10223
Echo characteristic analysis of the nonequilibrium wakes of reentry vehicle
[AD-A254249] p 13 N93-10705
Analytical characterization of bistatic scattering from Gaussian distributed surfaces
[AD-A254253] p 159 N93-10724

RADAR TARGETS
Test range tracking network processors
[AD-A253511] p 140 N93-10219
Nonlinear signal processing schemes for robust target detection and automatic clutter rejection in radar
[AD-A253546] p 68 N93-10380

RADAR TRANSMITTERS
Mathematical analysis of multi-sensor cross-correlation processing for source localization
[DREA-CR-89-433] p 68 N93-10366

RADIAL FLOW
Radial Turbines
[VKI-LS-1992-05] p 77 N93-10050
Introduction to radial turbine technology p 77 N93-10051

Performance parameters and assessment
p 77 N93-10052
Non-dimensional conceptual design of radial inflow turbines. Part A: Application of fundamental fluid mechanics p 77 N93-10053
Non-dimensional conceptual design of radial inflow turbines. Part B: Application of empirical correlations
p 77 N93-10054
Numerical methods for inviscid and viscous flow analysis p 77 N93-10055
Aerodynamic investigation of radial turbines using computational methods p 78 N93-10056
An inverse design method for radial turbomachines
p 78 N93-10057
The integration of geometric modeling into an inverse design method and application of a PC-based inverse design method and comparison with test results
p 78 N93-10058
Partial admission and unsteady flow in radial turbines
p 78 N93-10059
Testing techniques p 78 N93-10060
Radial turbine cooling p 78 N93-10061

RADIAL VELOCITY
Experimental study of the flow field inside a whirling annular seal p 92 N93-10892

RADIATION COUNTERS
A novel charge sensitive preamplifier without the feedback resistor
[DE92-015842] p 74 N93-10731

RADIATION DAMAGE
Proposed test program and data base for LDEF polymer matrix composites p 38 N93-10587
Results from testing and analysis of solar cells flown on LDEF p 39 N93-10591
System related testing and analysis of FRECOPA
p 39 N93-10592
Stress modified welding process for irradiated materials
[DE92-017131] p 92 N93-10634
Radiation damage to DNA
[DE92-015760] p 130 N93-10834

RADIATION DETECTORS
Signal and noise analysis of a-Si:H radiation detector-amplifier system
[DE92-016928] p 75 N93-10790

RADIATION DISTRIBUTION
Modeling of HF propagation and heating in the ionosphere
[AD-A253941] p 125 N93-10714

RADIATION DOSAGE
System related testing and analysis of FRECOPA
p 39 N93-10592
DoD space radiation concerns
[AD-A253135] p 131 N93-10613

RADIATION EFFECTS
DoD space radiation concerns
[AD-A253135] p 131 N93-10613
Understanding mechanisms of carcinogenesis using rat tracheal epithelial cells in vitro
[DE92-013510] p 131 N93-10626
Stress modified welding process for irradiated materials
[DE92-017131] p 92 N93-10634
Interaction of electromagnetic fields with chondrocytes in gel culture
[AD-A253727] p 70 N93-10747

RADIATION SOURCES
Accelerator Technology Division
[DE92-016023] p 156 N93-10462
Thermal, structural, and diffraction analyses of a gallium-cooled x ray monochromator
[DE92-017063] p 157 N93-10837
An infrared free-electron laser for the Chemical Dynamics Research Laboratory
[DE92-017018] p 90 N93-10864

RADIATION THERAPY
Center for Intelligent Control Systems, Brown University component: Graduate research fellowships
[AD-A253620] p 141 N93-10095

RADIATION TOLERANCE
Signal and noise analysis of a-Si:H radiation detector-amplifier system
[DE92-016928] p 75 N93-10790

RADIATION TRANSPORT
Probing cosmic infrared sources: A computer modeling approach
[AD-A253788] p 178 N93-10238

RADIATIVE HEAT TRANSFER
Documentation of the detailed radiation property data for the radiation-ablation code RASLE
[NASA-TM-103848] p 28 N93-10742

RADIATIVE RECOMBINATION
Merged beam studies of laser stimulated radiative recombination
[AD-A253308] p 89 N93-10698

RADIATIVE TRANSFER
Emission tomography of sodium in a hydrogen-air flame
[AD-A253530] p 29 N93-10224
The fine structure of prominences
p 180 N93-10910

RADIO ALTIMETERS
Appraisal of digital terrain elevation data for low-altitude flight
[NASA-TM-103896] p 7 N93-10745

RADIO COMMUNICATION
Meteor burst communications system trial, 1990-1991
[AD-A253625] p 67 N93-10203
Defence electronics industry profile, 1990-1991
[CTN-92-60515] p 66 N93-10653
Eleven years of ionospheric scintillation fading data from twenty Greenlandic stations
[AD-A253271] p 69 N93-10695

RADIO EQUIPMENT
Basic and applied research in the field of electronics and communications
[AD-A253593] p 67 N93-10092
Meteor burst communications system trial, 1990-1991
[AD-A253625] p 67 N93-10203
High-power microwave breakdown of dielectric interfaces
[AD-A254200] p 124 N93-10262

RADIO FILTERS
Design and evaluation of a quasi-active delay-line limiter/filter RF protection device
[AD-A254179] p 71 N93-10255

RADIO FREQUENCIES
Magnetostatic waves-based integrated optic Bragg cell modules with applications to RF signal processing
[AD-A254035] p 71 N93-10240
High-power microwave breakdown of dielectric interfaces
[AD-A254200] p 124 N93-10262
Field-emitter arrays for RF vacuum microelectronics
[AD-A253396] p 73 N93-10405

RADIO PHYSICS
Data synthesis and display programs for wave distribution function analysis
[NASA-TM-108009] p 70 N93-10800

RADIO TRANSMISSION
Meteor burst communications system trial, 1990-1991
[AD-A253625] p 67 N93-10203
ACIRF user's guide for the general model (Version 3.5)
[AD-A254068] p 69 N93-10657

RADIOACTIVE AGE DETERMINATION
U-Pb isotopic results for single shocked and polycrystalline zircons record 550-65.5-Ma ages for a K-T target site and 2700-1850-Ma ages for the Sudbury impact event p 115 N93-10156
Ar-40 to Ar-39 dating of pseudotachylites from the Witwatersrand basin, South Africa, with implications for the formation of the Vredefort Dome
p 122 N93-10189

RADIOACTIVE WASTES
APOLLO: A computer program for the calculation of chemical equilibrium and reaction kinetics of chemical systems
[DE92-017864] p 139 N93-10817

RADIOBIOLOGY
DoD space radiation concerns
[AD-A253135] p 131 N93-10613
Interaction of electromagnetic fields with chondrocytes in gel culture
[AD-A253727] p 70 N93-10747

RADIOCHEMISTRY
Glenn T. Seaborg and heavy ion nuclear science
[DE92-016943] p 156 N93-10762

RADIOLOGY
Quality assurance practices for data entry and electronic data transfer
[DE92-014804] p 172 N93-10396

RADOMES
Analysis of a medium size BOR radome
[AD-A253954] p 69 N93-10418

RAILGUN ACCELERATORS
Measurement of acceleration using an instrumented railgun projectile
[AD-A253366] p 12 N93-10106
Twenty-five KA, 5000V solid state opening switch for inductive energy stores
[AD-A253968] p 73 N93-10421

RAIN
Satellite derived integrated water vapor and rain intensity patterns: Indicators of rapid cyclogenesis
p 127 N93-10849
Morning-evening differences in global and regional oceanic precipitation as observed by the SSM/I
p 127 N93-10851

RAMAN SPECTRA
Species and temperature measurement in H2/O2 rocket flow fields by means of Raman scattering diagnostics
[NASA-CR-189217] p 25 N93-10086

RAMAN SPECTROSCOPY
Species and temperature measurement in H2/O2 rocket flow fields by means of Raman scattering diagnostics
[NASA-CR-189217] p 25 N93-10086

RANDOM LOADS
Evolutionary spectra of time-dependent discretized systems to time-frequency modulated random excitations p 55 N93-10524

RANDOM NOISE
Probability density functions for random nonlinear oscillation p 55 N93-10522

RANDOM PROCESSES
Entropy of disorder in thermomechanics of damage in heterogeneous solids p 50 N93-10498
On techniques for digital simulation of random response of nonlinear oscillators p 55 N93-10523
Evolutionary spectra of time-dependent discretized systems to time-frequency modulated random excitations p 55 N93-10524

RANDOM VIBRATION
Nonstationary random variations of moderately thick plates using BEM p 48 N93-10487
A new non-Gausssian approximation technique for random vibration of general hysteresis
p 50 N93-10496

RANDOM WALK
Change analysis
[AD-A253567] p 146 N93-10795

RANGE FINDERS
Dynamic positioning systems photogrammetric
[AD-A254250] p 8 N93-10898

RANGEFINDING
Dynamic positioning systems photogrammetric
[AD-A254250] p 8 N93-10898

RANKINE CYCLE
Compound cycle engine for helicopter application
[NASA-CR-180824] p 9 N93-10348

RARE EARTH COMPOUNDS
Oxygen barrier oxides
[AD-A253683] p 36 N93-10343

RARE EARTH ELEMENTS
Electronic structure of highly correlated structures
[DE92-017017] p 155 N93-10863

RARE GASES
Theoretical analysis of discharges in copper vapor lasers: A comparison of Ne and He
[DE92-014739] p 87 N93-10083

RAREFIED GAS DYNAMICS
Investigations of the motion of discrete-velocity gases
[AD-A253728] p 84 N93-10895

RAY TRACING
Modeling of HF propagation and heating in the ionosphere
[AD-A253941] p 125 N93-10714

RAYLEIGH SCATTERING
Polarized light scattering from perfect and perturbed surfaces and fundamental scattering systems
[AD-A253186] p 158 N93-10445
Shock enhancement and control of hypersonic combustion
[AD-A254295] p 31 N93-10843

RAYLEIGH-BENARD CONVECTION
Adequate sampling of a chaotic time series
[AD-A254170] p 127 N93-10664

RAYLEIGH-RITZ METHOD
Nonlinear aeroelasticity of composite structures
[AD-A254285] p 8 N93-10842

RDX
Impact sensitivity reduction via exo-electron control
p 15 N93-10004

REACTING FLOW
Mathematical analysis of strong fluid mechanical effects at high Mach number in reactive and nonreactive flow
[AD-A253617] p 79 N93-10094

REACTION KINETICS
Species and temperature measurement in H2/O2 rocket flow fields by means of Raman scattering diagnostics
[NASA-CR-189217] p 25 N93-10086
Biological production of ethanol from coal
[DE92-016116] p 41 N93-10216
Electron transfer reactions in microporous solids
[DE92-016222] p 166 N93-10284
Temperature-programmed oxidation of ethane and ethylene in the presence and absence of C-13 labeled methane
[DE92-015048] p 42 N93-10329
Rate constants for reactions of hydrazine fuels with O(P-3)
[AD-A252813] p 42 N93-10336
Transition metal activation and functionalization of carbon-hydrogen bonds
[DE92-014809] p 30 N93-10400

Statics and kinetics of oxygen ordering in the oxide superconductor YBa2Cu3O(z)
[DE92-017001] p 167 N93-10403
Kinetics of oxidation of silicon by electron cyclotron resonance plasmas
[AD-A253140] p 161 N93-10413
Pre-oxidation anneal kinetics: Interface degradation of thin SiO2 films on silicon
[AD-A253142] p 30 N93-10414
Mobility of toluene in polystyrene-toluene solutions: A NMR study
[AD-A253203] p 31 N93-10794
APOLLO: A computer program for the calculation of chemical equilibrium and reaction kinetics of chemical systems
[DE92-017864] p 139 N93-10817
An infrared free-electron laser for the Chemical Dynamics Research Laboratory
[DE92-017018] p 90 N93-10864

REACTION PRODUCTS
Reactions of Ti and Zr with AlN and Al2O3
[DE92-016234] p 28 N93-10391

REACTIVITY
Investigation of the stimulated release of gaseous ammonia from ammonium perchlorate by HTPB solid propellant bonding agents p 19 N93-10026
Temperature-programmed oxidation of ethane and ethylene in the presence and absence of C-13 labeled methane
[DE92-015048] p 42 N93-10329
Mathematical analysis of reactive multiphase flows
[AD-A253854] p 83 N93-10810

REACTOR MATERIALS
Stress modified welding process for irradiated materials
[DE92-017131] p 92 N93-10634

REACTOR TECHNOLOGY
D-He-3 spherical torus fusion reactor system study
[AD-A253358] p 155 N93-10102

READ-ONLY MEMORY DEVICES
TIGER5: Extraction of geographic information from the TIGER system
[DE92-014935] p 171 N93-10382
Scientific and Technical Information (STI) towards technological and industrial development: The case of Portugal p 173 N93-10596
Technology for libraries and information centers: A seminar in Greece, Portugal, and Turkey p 174 N93-10601
Services: User services in defence and aerospace documentation centres p 174 N93-10602

READOUT
Semiconductor phase conjugation
[AD-A253684] p 166 N93-10345

REAGENTS
Atomic hydrogen: A reagent for the extraction of chemical species from silicon surfaces
[AD-A252804] p 30 N93-10266

REAL TIME OPERATION
Integrated vision system for a target seeker
[AD-A253359] p 135 N93-10103
Mesoscale severe weather development under orographic influences
[AD-A253630] p 125 N93-10204
Test range tracking network processors
[AD-A253511] p 140 N93-10219
Analysis of reservation-based dual-link networks for real-time applications
[AD-A254176] p 67 N93-10253
Biological and theoretical studies of adaptive networks: The conditioned response
[AD-A253329] p 142 N93-10354
Recovery techniques for real time electronic systems
[AD-A254010] p 136 N93-10361
GPS Army research and applications
[AD-A254262] p 7 N93-10424
Dynamic positioning systems photogrammetric
[AD-A254250] p 8 N93-10898
Demonstration and performances of real-time fringe tracking: A step towards cophased interferometers p 178 N93-10948
Requirements analysis notebook for the flight data systems definition in the Real-Time Systems Engineering Laboratory (RSEL)
[NASA-CR-185698] p 14 N93-10960

RECEIVERS
Development of garnet films for magnetostatic wave channelized receivers
[AD-A252812] p 166 N93-10335

RECIRCULATIVE FLUID FLOW
Experimental study of the flow field inside a whirling annular seal p 92 N93-10892
Turbulence measurements of high shear flow fields in a turbomachine seal configuration p 93 N93-10893

RECRYSTALLIZATION
Bohemian circular structure, Czechoslovakia: Search for the impact evidence p 119 N93-10172

RECTANGULAR PLATES
Vibration of laminated composite plates using various plate theories: Analytical and finite element results p 45 N93-10473
Compression buckling of thick orthotropic plates with a step thickness change p 46 N93-10478
Singular stress distributions at circular holes in composite laminates p 51 N93-10503
Investigation of laminated composite plates under impact dynamic loading by using a three-dimensional hybrid stress finite element method p 29 N93-10510
Experimental investigation of simple support condition in free vibration analysis of plates p 56 N93-10530
Nonlinear aeroelasticity of composite structures
[AD-A254285] p 8 N93-10842

RECURSIVE FUNCTIONS
Unifying the landmark developments in optimal bounding ellipsoid identification
[AD-A253502] p 143 N93-10200

REDUCED GRAVITY
Tank chilldown analysis and verification with a flightweight, 175 cu ft tank under normal gravity with liquid hydrogen p 24 N93-10045
Structure of thermocapillary flow in narrow cavities p 61 N93-10552
NASA Space Human Factors Program
[NASA-TM-108005] p 134 N93-10890

REENTRY EFFECTS
One type of automatically adjusted difference scheme with artificial viscosity to calculate ablated exterior shapes
[AD-A254108] p 5 N93-10856

REENTRY VEHICLES
Plug nozzle propulsion system p 17 N93-10013
Echo characteristic analysis of the nonequilibrium wakes of reentry vehicle
[AD-A254249] p 13 N93-10705
Research on the asymmetrical aerodynamic forces of reentry vehicles
[AD-A254307] p 4 N93-10707

REFLECTANCE
Spectroscopic differential reflectance as an analytical probe for microelectronic processing
[AD-A253134] p 73 N93-10656

REFLECTION
Reflection of plasma ions from metals (and its use as a hyperthermal neutral beam source) p 160 N93-10353
Polarized light scattering from perfect and perturbed surfaces and fundamental scattering systems
[AD-A253186] p 158 N93-10445

REFLECTOR ANTENNAS
Proceedings of the Antenna Applications Symposium, volume 1
[AD-A253681] p 68 N93-10301
Proceedings of the Antenna Applications Symposium, volume 2
[AD-A253682] p 68 N93-10302

REFLECTORS
Extravehicular activity compatibility evaluation of developmental hardware for assembly and repair of precision reflectors
[NASA-TP-3246] p 13 N93-10744

REFRACTIVITY
A new ellipsometry technique for interface analysis: Application to Si-SiO2
[AD-A253143] p 167 N93-10415
Analysis of reception variability due to terrain multipath on microwave common carrier links
[NTIA-92-283] p 69 N93-10430
A multipurpose vacuum-ultraviolet test facility p 11 N93-10953

REFRACTORIES
U-Pb isotopic results for single shocked and polycrystalline zircons record 550-65.5-Ma ages for a K-T target site and 2700-1850-Ma ages for the Sudbury impact event p 115 N93-10156

REFRACTORY MATERIALS
Geochemical aspect of impact cratering: Studies in Vernadsky Institute p 123 N93-10196
Documentation of the detailed radiation property data for the radiation-ablation code RASLE
[NASA-TM-103848] p 28 N93-10742

REFRIGERANTS
Materials compatibility and lubricants research on CFC-refrigerant substitute: Miscibility of lubricants with refrigerants
[DE92-015118] p 35 N93-10084
Materials compatibility and lubricants research on CFC-refrigerant substitutes: Thermophysical properties
[DE92-015116] p 43 N93-10397
Chemical and thermal stability of refrigerant-lubricant mixture with metal
[DE92-015117] p 44 N93-10398
ARTI Refrigerant Database
[DE92-015122] p 30 N93-10401

REFRIGERATING
Assessment study of superconducting fault-current limiters operating at 77 K
[DE92-015273] p 76 N93-10831

REFRIGERATORS
ARTI Refrigerant Database
[DE92-015122] p 30 N93-10401

REGENERATIVE COOLING
Formed platelets for low cost regeneratively cooled rocket combustion chambers p 18 N93-10018

REGULATIONS
Combat aircraft noise: The operator's perspective p 148 N93-10669

REINFORCING FIBERS
Sensor and actuator materials for high performance composites
[AD-A254178] p 27 N93-10254
Damage accumulation process in advanced metal matrix composite under thermal cycling
[AD-A248674] p 27 N93-10277

RELATIVISTIC EFFECTS
Data reduction analysis for the Stanford relativity gyroscope experiment p 86 N93-10347

RELATIVISTIC ELECTRON BEAMS
Simulation of electron beam transport in ion-focused regime conditioning cells
[AD-A253352] p 70 N93-10215

RELATIVISTIC THEORY
Wiggly relativistic strings
[DE92-016461] p 170 N93-10434

RELATIVITY
Data reduction analysis for the Stanford relativity gyroscope experiment p 86 N93-10347

RELAXATION TIME
Mobility of toluene in polystyrene-toluene solutions: A NMR study
[AD-A253203] p 31 N93-10794

RELIABILITY
Review and analysis of check valve failure data
[DE92-014462] p 91 N93-10381

RELIABILITY ANALYSIS
Theoretical and experimental investigations concerning the structural integrity of aeroengine compressor discs p 10 N93-10539
VLSI design for reliability - hot electron
[AD-A253942] p 74 N93-10715

RELIABILITY ENGINEERING
Reliability assurance requirements for ESA space systems
[ESA-PSS-01-30-ISSUE-2] p 94 N93-10317

RELIC RADIATION
Cosmic microwave background anisotropies from plausible double inflation
[DE92-016195] p 192 N93-10616

REMANENCE
Enhanced magnetic field production during oblique hypervelocity impacts p 108 N93-10129

REMOTE MANIPULATOR SYSTEM
Modelling and control of robotic arms fabricated from orthotropic materials p 65 N93-10572
Modelling of flexible multibody dynamics and a computer method via the bond graph method p 65 N93-10573

REMOTE SENSING
Stereoscopy and paralax in the vertical distances determination using aerial photographs
[INPE-5363-PUD/049] p 102 N93-10063
Air-sea interaction and remote sensing
[NASA-CR-190913] p 128 N93-10068
Imaging radar investigations of the Sudbury structure p 117 N93-10162
SAR in support of geological investigations of the Sudbury structure p 103 N93-10182
SBS applications study
[AD-A253779] p 102 N93-10234
Molecular biology in studies of oceanic primary production
[DE92-016101] p 128 N93-10283
Automatic cloud classification from multi-spectral satellite data over oceanic regions
[AD-A253670] p 126 N93-10292
Monitoring structural response in pressurized environments. Part 2: Applications
[DE92-015034] p 94 N93-10327
Remote sensing data for monitoring and evaluating burned areas: Case of Emas National Park (GO)
[INPE-5312-PRE/1709] p 102 N93-10373
Investigations of the dynamics and thermodynamics of the mesosphere lower thermosphere and upper thermosphere at the polar regions with optical ground-based remote sensing
[AD-A253228] p 125 N93-10711

Microwave radiometer studies of atmospheric water over the oceans, volume 2
[NASA-CR-190343] p 127 N93-10848
Magnetospheres and atmospheres of planets
p 182 N93-10922

REMOTE SENSORS
Remote sounding of the Martian atmosphere
p 189 N93-10378

RENORMALIZATION GROUP METHODS
Mass and mixing angle patterns in the standard model and its material supersymmetric extension
[DE92-016197] p 153 N93-10291

REPUBLIC OF SOUTH AFRICA
Early Archean spherule beds of possible impact origin from Barberton, South Africa: A detailed mineralogical and geochemical study p 115 N93-10155
The Vredefort Dome: Review of geology and deformation phenomena and status report on current knowledge and remaining problematics (five years after the cryptoexplosion workshop) p 119 N93-10173
The pseudotachylites from the Vredefort structure and the Witwatersrand basin p 119 N93-10174
Bronzite Granophyre: New insight on Vredefort
p 121 N93-10186
Ar-40 to Ar-39 dating of pseudotachylites from the Witwatersrand basin, South Africa, with implications for the formation of the Vredefort Dome
p 122 N93-10189

REQUIREMENTS
Rotorcraft en route ATC route standards
[AD-A249129] p 6 N93-10323
Demonstration and performances of real-time fringe tracking: A step towards cophased interferometers
p 178 N93-10948

RESEARCH AND DEVELOPMENT
Accelerator Technology Division
[DE92-016023] p 156 N93-10462
Establishing a scientific and technical information program: Planning and resource management
p 173 N93-10597
The technology advantage: A guide to science, technology, and innovation in Manitoba
[CTN-92-60571] p 192 N93-10654
Chinese Space Science and Technology (selected articles)
[AD-A254099] p 69 N93-10701
High resolutions studies of the structure of the solar atmosphere
[AD-A254292] p 190 N93-10767

RESEARCH FACILITIES
Emergency Diesel Generator reliability at Department of Energy (DOE) facilities
[DE92-011888] p 91 N93-10622
An infrared free-electron laser for the Chemical Dynamics Research Laboratory
[DE92-017018] p 90 N93-10864
Geographic Information System (GIS) development assistance for Nuclear Regulatory Commission (NRC) incident response capability
[DE92-017595] p 176 N93-10867

RESEARCH MANAGEMENT
Research program in experimental and theoretical high energy physics
[DE92-016219] p 156 N93-10618
Research program in elementary particle theory
[DE92-017399] p 155 N93-10840

RESEARCH PROJECTS
Gamma ray astrophysics to the year 2000. Report of the NASA Gamma Ray Program Working Group
[NASA-TM-107995] p 178 N93-10067
Center for Intelligent Control Systems, Brown University component: Graduate research fellowships
[AD-A253620] p 141 N93-10095
Research in particle physics beyond the standard model
[DE92-012240] p 155 N93-10878

RESERVES
Reserves in western basins
[DE92-014429] p 102 N93-10625

RESIDUAL STRESS
Sensor and actuator materials for high performance composites
[AD-A254178] p 27 N93-10254
Fatigue crack propagation in the presence of shot-peening residual stresses p 59 N93-10542

RESIDUES
Analysis of interplanetary dust experiment detectors and other witness plates
[NASA-CR-190818] p 32 N93-10852
Contaminant interferences with SIMS analyses of microparticle impactor residues on LDEF surfaces
p 32 N93-10854

RESISTOJET ENGINES
Design and operation of the US Space Station Freedom propulsion system p 24 N93-10049

RESONANCE
Resonance apparatus operating manual
[AD-A254040] p 71 N93-10241
Resonance ionization of rubidium using sequential diode laser-driven transitions
[DE92-014468] p 89 N93-10429

RESONANCE FLUORESCENCE
Rate constants for reactions of hydrazine fuels with O(P-3)
[AD-A252813] p 42 N93-10336

RESONANT TUNNELING
Optimization of resonant interband tunnel devices
[AD-A252401] p 168 N93-10637

RESONANT VIBRATION
Axisymmetric vibrations of rotating circular plates using characteristic orthogonal polynomials
p 45 N93-10470
Vibration of orthotropic cylindrical shell panels with arbitrary supported curved edges p 45 N93-10471
Flexural vibration of beams with varying section properties p 57 N93-10531
Natural vibrations of multilayered doubly curved shells
p 57 N93-10532
Free vibrations of the thick circular cylindrical shells and rings p 57 N93-10533
Vibration frequencies of a constrained cantilever wedge p 57 N93-10534
The vibrations of annular discs: A comparison of experimental and two analytical techniques
p 58 N93-10536
Vibrations of nonlinearly pretwisted asymmetrical thick turbine blades p 9 N93-10537
Numerical considerations for structural system identification from modal information p 63 N93-10564

RESONATORS
Quantum 1/f noise in high technology applications including ultrasmall structures and devices
[AD-A253922] p 74 N93-10751

RESPIRATION
Metabolic factors influencing myocardial recovery from acidosis (CiC3)
[AD-A252376] p 132 N93-10796

RESPIRATORY SYSTEM
Evaluation of lightweight and low profile communications devices for Respiratory Protective system 21 (RESPO 21)
[AD-A253393] p 133 N93-10217
Evaluation of an electronics system concept for Respiratory Protection system (RESPO 21)
[AD-A253394] p 134 N93-10288
Novel seals and specialty component attachment mechanisms for Respiratory Protection system (RESPO 21)
[AD-A253395] p 91 N93-10290

RESTORATION
Electrical resistance tomography used in environmental restoration
[DE92-018003] p 103 N93-10763

REVERSE FIELD PINCH
Magnetic fusion with high energy self-colliding ion beams
[DE92-016860] p 156 N93-10643

REVISIONS
Artificial neural network system for memory modification
[AD-D015354] p 142 N93-10958
Memory modification of artificial neural networks
[AD-D015356] p 143 N93-10959

REYNOLDS NUMBER
Pitot survey of exhaust flow field of a 2-D scramjet nozzle at Mach 6 with air or freon and argon used for exhaust simulation
[NASA-TM-4361] p 2 N93-10071
Mathematical analysis of strong fluid mechanical effects at high Mach number in reactive and nonreactive flow
[AD-A253617] p 79 N93-10094
Turbulence measurements of high shear flow fields in a turbomachine seal configuration p 93 N93-10893

REYNOLDS STRESS
Explicit Navier-Stokes computation of turbomachinery flows p 81 N93-10370

RHEOLOGY
What can we learn about impact mechanics from large craters on Venus? p 118 N93-10166
Viscosity determinations of some frictionally generated silicate melts: Implications for slip zone rheology during impact-induced faulting p 121 N93-10183
Simple shearing flow of a 3D foam
[DE92-011151] p 36 N93-10399
Chronorheological characterization of elastomers
p 46 N93-10476

RIBBONS
Selected results for metals from LDEF experiment A0171 p 34 N93-10579

RIEMANN MANIFOLD
Quantum tunneling and the change in the signature of the spacetime metric
[DE92-634877] p 165 N93-10225

RIGID STRUCTURES
Numerical simulation of the propagation of coupled thermomechanical waves in inelastic solids
p 64 N93-10568

RING STRUCTURES
Free vibrations of the thick circular cylindrical shells and rings p 57 N93-10533
The vibrations of annular discs: A comparison of experimental and two analytical techniques
p 58 N93-10536

ROBOT CONTROL
Modelling and control of robotic arms fabricated from orthotropic materials p 65 N93-10572

ROBOT DYNAMICS
Effective formulation of the dynamics of a manipulator based on the Appeli equations p 65 N93-10571
Modelling and control of robotic arms fabricated from orthotropic materials p 65 N93-10572
Automated multi-body system dynamics via bond graph modelling and interactive graphics p 66 N93-10576
A derivation for the kinematic equations of flexible robots with appropriate transformation matrices
p 66 N93-10577

ROBOT SENSORS
Selective perception for robot driving
[AD-A253740] p 142 N93-10749

ROBOTICS
Artificial intelligence technical paper abstracts, 1991
[AD-A253340] p 141 N93-10269
Modelling and control of robotic arms fabricated from orthotropic materials p 65 N93-10572
A derivation for the kinematic equations of flexible robots with appropriate transformation matrices
p 66 N93-10577
Automated handling and assembling of non-rigid objects
[AD-A253605] p 66 N93-10649
Selective perception for robot driving
[AD-A253740] p 142 N93-10749

ROBOTS
Optimal robot trajectory planning p 65 N93-10570

ROBUSTNESS (MATHEMATICS)
Design, test, and evaluation of three active flutter suppression controllers
[NASA-TM-4338] p 10 N93-10070
Nonlinear signal processing schemes for robust target detection and automatic clutter rejection in radar
[AD-A253546] p 68 N93-10380

ROCK INTRUSIONS
Sudbury project (University of Muenster-Ontario Geological Survey): Sr-Nd in heterolithic breccias and gabbroic dikes p 107 N93-10123
Breccia dikes from the Beaverhead Impact structure, southwest Montana p 110 N93-10137
Bronzite Granophyre: New insight on Vredefort
p 121 N93-10186

ROCKET ENGINE CASES
Instrumented propellant block test and stress analysis comparison p 15 N93-10002

ROCKET ENGINE DESIGN
Critical engine system design characteristics for SSTO vehicles p 17 N93-10014
LAM actuated propellant flow control device
p 18 N93-10017
Power conditioning unit for 30 kWe class arcjet flight experiment p 21 N93-10032
A survey of instabilities within centrifugal pumps and concepts for improving the flow range of pumps in rocket engines p 23 N93-10039
Design and operation of the US Space Station Freedom propulsion system p 24 N93-10049
Space Transportation Engine Program (STEP), phase B
[NASA-CR-184062] p 25 N93-10350

ROCKET ENGINES
Formed platelets for low cost regeneratively cooled rocket combustion chambers p 18 N93-10018
Thermal stratification potential in rocket engine coolant channels p 18 N93-10019
Operationally efficient space-based integrated propulsion module p 22 N93-10035
A survey of instabilities within centrifugal pumps and concepts for improving the flow range of pumps in rocket engines p 23 N93-10039
Studies on the combustion efficiency of liquid fuel rockets with variable thrust
[AD-A254232] p 26 N93-10721

ROCKET LININGS
Formed platelets for low cost regeneratively cooled rocket combustion chambers p 18 N93-10018
Hot fire test results of subscale tubular combustion chambers p 18 N93-10020

ROCKET NOZZLES
The 1992 JANNAF Propulsion Meeting, volume 1
[CPIA-PUBL-580-VOL-1] p 15 N93-10001
Critical engine system design characteristics for SSTO vehicles p 17 N93-10014
Facility for cold flow testing of solid rocket motor models p 11 N93-10021
Feasibility evaluation of the monolithic braided ablative nozzle p 19 N93-10023
Molded nozzle technology for large solid rocket motors p 19 N93-10024
ROCKET OXIDIZERS
Multidimensional effects in composite propellant combustion p 42 N93-10313
ROCKET PROPELLANTS
Design and operation of the US Space Station Freedom propulsion system p 24 N93-10049
ROCKET VEHICLES
Methods of guidance flight dynamics
[AD-A254248] p 10 N93-10704
ROOM TEMPERATURE
Rate constants for reactions of hydrazine fuels with O(P-3)
[AD-A252813] p 42 N93-10336
ROTARY WING AIRCRAFT
Rotorcraft en route ATC route standards
[AD-A249129] p 6 N93-10323
ROTATING BODIES
On the gravitational potential of two arbitrary rotating bodies with applications to the Earth-Moon system p 179 N93-10303
An experimental technique for performing 3-D LDA measurements inside whirling annular seals p 93 N93-10894
ROTATING DISKS
Axisymmetric vibrations of rotating circular plates using characteristic orthogonal polynomials p 45 N93-10470
Theoretical and experimental investigations concerning the structural integrity of aeroengine compressor discs p 10 N93-10539
ROTATING FLUIDS
Investigations into swirling flows of Newtonian and non-Newtonian fluids
[AD-A253298] p 82 N93-10696
ROTATING PLASMAS
Large orbit magnetic confinement systems for advanced fusion fuels
[DE92-016218] p 162 N93-10617
ROTATING SHAFTS
Experimental study of the flow field inside a whirling annular seal p 92 N93-10892
Turbulence measurements of high shear flow fields in a turbomachine seal configuration p 93 N93-10893
ROTATION
Effect of mounting offset on the dynamics of deploying flexible appendages p 54 N93-10520
Mobility of toluene in polystyrene-toluene solutions: A NMR study
[AD-A253203] p 31 N93-10794
ROTOR AERODYNAMICS
Radial turbine cooling p 78 N93-10061
Explicit Navier-Stokes computation of turbomachinery flows p 81 N93-10370
Tilt rotor hover aeroacoustics
[NASA-CR-177598] p 147 N93-10458
Harmonic analysis of the aerodynamic forces on a Darrieus rotor p 6 N93-10551
LDV Measurements of unsteady flow fields in radial turbine
[AD-A253592] p 4 N93-10648
ROTOR BLADES (TURBOMACHINERY)
An inverse design method for radial turbomachines p 78 N93-10057
Structural analysis: Fatigue life assessment p 78 N93-10062
ROTOR BODY INTERACTIONS
An experimental and a theoretical investigation of rotor pitch damping using a model rotor p 8 N93-10322
Contributions to the experimental investigation of rotor/body aerodynamic interactions p 5 N93-10877
ROTOR DYNAMICS
Radial Turbines
[VKI-LS-1992-05] p 77 N93-10050
An experimental and a theoretical investigation of rotor pitch damping using a model rotor p 8 N93-10322
Vibrations of nonlinearly pretwisted asymmetrical thick turbine blades p 9 N93-10537
Compressible and incompressible fluid seals: Influence on rotordynamic response and stability
[NASA-CR-190746] p 92 N93-10891
ROTOR SPEED
An experimental and a theoretical investigation of rotor pitch damping using a model rotor p 8 N93-10322
ROTORS
A study upon structural optimization of elastic rotors for mechanical systems
[INPE-5376-TDI/471] p 94 N93-10310
An experimental and a theoretical investigation of rotor pitch damping using a model rotor p 8 N93-10322
RUBIDIUM
Resonance ionization of rubidium using sequential diode laser-driven transitions
[DE92-014468] p 89 N93-10429
Matter-wave interferometry with laser cooled atoms
[AD-A254000] p 89 N93-10720
RUNGE-KUTTA METHOD
A globally well-posed accurate and efficient finite element CFD algorithm for compressible aerodynamics p 3 N93-10306
Analysis of wing-body junction flowfields using the incompressible Navier-Stokes equations, volumes 1 and 2 p 3 N93-10320
Nonlinear aeroelasticity of composite structures
[AD-A254285] p 8 N93-10842

S

S MATRIX THEORY
Polarized light scattering from perfect and perturbed surfaces and fundamental scattering systems
[AD-A253186] p 158 N93-10445
S WAVES
Elastic wave scattering by an interfacial crack in a plate p 48 N93-10485
Progress in multi-dimensional upwind differencing
[NASA-CR-189708] p 83 N93-10808
SACCADIC EYE MOVEMENTS
Eye movements and visual information processing
[AD-A250198] p 132 N93-10278
Air traffic control visual scanning
[DOT/FAA/CT-TN92/16] p 7 N93-10459
SAFETY
Generic Propellant Transfer Unit p 11 N93-10046
Computational fluid dynamics capability for internally carried store separation
[AD-A253671] p 79 N93-10297
SAMPLING
Adequate sampling of a chaotic time series
[AD-A254170] p 127 N93-10664
SANDSTONES
Does the sedimentology of the Chelmsford formation provide evidence for a meteorite impact origin of the Sudbury structure? p 116 N93-10160
SANDWICH STRUCTURES
Multidimensional effects in composite propellant combustion p 42 N93-10313
SAPPHIRE
System design and relaxation oscillations of a titanium-sapphire laser
[AD-A254264] p 89 N93-10725
SATELLITE ALTIMETRY
Evaluation of Seasat/Geosat orbits and altimetry with application to long-term sea level changes in the North Pacific p 103 N93-10647
SATELLITE ANTENNAS
Proceedings of the Antenna Applications Symposium, volume 1
[AD-A253681] p 68 N93-10301
Proceedings of the Antenna Applications Symposium, volume 2
[AD-A253682] p 68 N93-10302
SATELLITE ATTITUDE CONTROL
Autonomous star sensing and pattern recognition for spacecraft attitude determination p 177 N93-10876
SATELLITE COMMUNICATION
SPOT panchromatic band simulation by linear combination of multispectral bands
[INPE-5295-PRE/1650] p 157 N93-10311
Eleven years of ionospheric scintillation fading data from twenty Greenlandic stations
[AD-A253271] p 69 N93-10695
Chinese Space Science and Technology (selected articles)
[AD-A254099] p 69 N93-10701
SATELLITE DESIGN
Chinese Space Science and Technology (selected articles)
[AD-A254099] p 69 N93-10701
SATELLITE IMAGERY
Stereoscopy and paralax in the vertical distances determination using aerial photographs
[INPE-5363-PUD/049] p 102 N93-10063
Imaging radar investigations of the Sudbury structure p 117 N93-10162
Molecular biology in studies of oceanic primary production
[DE92-016101] p 128 N93-10283
Automatic cloud classification from multi-spectral satellite data over oceanic regions
[AD-A253670] p 126 N93-10292
SPOT panchromatic band simulation by linear combination of multispectral bands
[INPE-5295-PRE/1650] p 157 N93-10311
Microwave radiometer studies of atmospheric water over the oceans, volume 2
[NASA-CR-190343] p 127 N93-10848
Satellite derived integrated water vapor and rain intensity patterns: Indicators of rapid cyclogenesis p 127 N93-10849
Comparison of wind speed measurements over the oceans with the Special Sensor Microwave/Imager and the Geosat altimeter p 127 N93-10850
Morning-evening differences in global and regional oceanic precipitation as observed by the SSM/I p 127 N93-10851
SATELLITE NAVIGATION SYSTEMS
GPS Army research and applications
[AD-A254262] p 7 N93-10424
SATELLITE OBSERVATION
Imaging radar investigations of the Sudbury structure p 117 N93-10162
Ground/space co-operation for interferometry p 178 N93-10946
SATELLITE SURFACES
Indexes of maps of the planets and satellites, 1992
[NASA-TM-4395] p 189 N93-10832
SATELLITE TRACKING
Dynamic positioning systems photogrammetric
[AD-A254250] p 8 N93-10896
SCALE MODELS
Boiling behavior of sodium-potassium alloy in a bench-scale solar receiver
[DE92-014947] p 103 N93-10383
SCALING
A look at scalable dense linear algebra libraries
[DE92-017805] p 143 N93-10285
SCALING LAWS
Melt production in large-scale impact events: Calculations of impact-melt volumes and crater scaling p 108 N93-10125
A look at scalable dense linear algebra libraries
[DE92-017805] p 143 N93-10285
A look at scalable dense linear algebra libraries
[DE92-017161] p 139 N93-10816
SCANNING TUNNELING MICROSCOPY
Field emission current-voltage curves as a diagnostic for scanning tunneling microscope tips
[AD-A251171] p 165 N93-10245
Scanning tunneling microscopy of semiconductor surfaces
[AD-A246853] p 168 N93-10726
SCATTERING
Semiclassical quantization of chaotic billiards
[DE92-634888] p 169 N93-10226
SCATTERING CROSS SECTIONS
Echo characteristic analysis of the nonequilibrium wakes of reentry vehicle
[AD-A254249] p 13 N93-10705
Pion- and proton-nucleus interactions at intermediate energy
[DE92-017980] p 157 N93-10638
SCHEDULING
Ada validation tests for rate monotonic scheduling algorithms
[AD-A253325] p 136 N93-10300
Noise studies for environmental impact assessment of an outdoor engine test facility p 149 N93-10672
SCHOTTKY DIODES
Implanted contacts for diamond semiconductor devices
[AD-A245568] p 165 N93-10274
SCIENTISTS
Glenn T. Seaborg and heavy ion nuclear science
[DE92-016943] p 156 N93-10762
SCINTILLATION
Eleven years of ionospheric scintillation fading data from twenty Greenlandic stations
[AD-A253271] p 69 N93-10695
SEA LEVEL
Evaluation of Seasat/Geosat orbits and altimetry with application to long-term sea level changes in the North Pacific p 103 N93-10647
SEA STATES
Air-sea interaction and remote sensing
[NASA-CR-190913] p 128 N93-10068
SEA SURFACE TEMPERATURE
Air-sea interaction and remote sensing
[NASA-CR-190913] p 128 N93-10068
Air-sea interaction in regions of varying surface conditions
[AD-A253182] p 128 N93-10791

SEA WATER
Ordovician impacts at sea in Baltoscandia p 116 N93-10159
Measurements of surface ocean carbon dioxide partial pressure during WOCE
[DE92-011856] p 128 N93-10621
SEALERS
The effect of elevated temperatures on the properties of thermally stable silicon-based elastomers for adhesives, sealants, and insulator applications p 15 N93-10006
Determination of Sandoz black aluminum coloring dye, olive aluminum coloring dye, and sodium dichromate aluminum sealing solutions by UV-visible spectrophotometry
[AD-A253639] p 29 N93-10207
SEALING
Novel seals and specialty component attachment mechanisms for Respiratory Protection system (RESPO 21)
[AD-A253395] p 91 N93-10290
SEALS (STOPPERS)
Identification and evaluation of lubricants, adhesives, and seals used on LDEF p 39 N93-10588
Compressible and incompressible fluid seals: Influence on rotordynamic response and stability
[NASA-CR-190746] p 92 N93-10891
Experimental study of the flow field inside a whirling annular seal p 92 N93-10892
Turbulence measurements of high shear flow fields in a turbomachine seal configuration p 93 N93-10893
An experimental technique for performing 3-D LDA measurements inside whirling annular seals p 93 N93-10894
SEAMS (JOINTS)
A seam tracking modulated infrared optical sensor for use in welding
[AD-A254103] p 159 N93-10812
SEASAT SATELLITES
Microwave radiometer studies of atmospheric water over the oceans, volume 2
[NASA-CR-190343] p 127 N93-10848
SECONDARY ION MASS SPECTROMETRY
Elemental analyses of hypervelocity microparticle impact sites on interplanetary dust experiment sensor surfaces p 32 N93-10853
Contaminant interferences with SIMS analyses of microparticle impactor residues on LDEF surfaces p 32 N93-10854
SEDIMENTARY ROCKS
Sudbury project (University of Muenster-Ontario Geological Survey): Origin of the polymict, allochthonous breccias of the Onaping Formation p 106 N93-10116
Does the sedimentology of the Chelmsford formation provide evidence for a meteorite impact origin of the Sudbury structure? p 116 N93-10160
SEISMIC ENERGY
Worldwide seismic catalog and the nature of seismic coupling p 124 N93-10376
SEISMIC WAVES
List of publications, 1969-1991. Panel on wind and seismic effects
[PB92-201102] p 125 N93-10089
Worldwide seismic catalog and the nature of seismic coupling p 124 N93-10376
SEISMOLOGY
List of publications, 1969-1991. Panel on wind and seismic effects
[PB92-201102] p 125 N93-10089
Worldwide seismic catalog and the nature of seismic coupling p 124 N93-10376
SELECTIVE DISSEMINATION OF INFORMATION
Security considerations within military information systems p 174 N93-10603
Unifying information flow policies
[RSRE-90020] p 175 N93-10801
The Terry-Wiseman security policy model and examples of its use
[RSRE-90001] p 134 N93-10807
Lattices for security policies
[RSRE-90005] p 139 N93-10823
A multilevel security model for object-oriented database systems p 175 N93-10844
SELENIDES
4.5 micron laser source
[AD-A253367] p 87 N93-10090
SELF DIFFUSION (SOLID STATE)
Mobility of toluene in polystyrene-toluene solutions: A NMR study
[AD-A253203] p 31 N93-10794
SELF EXCITATION
Chaotic oscillation of a high speed flexible arm robot p 65 N93-10574
SELF ORGANIZING SYSTEMS
Smart algorithms and adaptive methods in computational fluid dynamics p 44 N93-10469
SEMICONDUCTING FILMS
Pseudomorphic semiconducting heterostructures from combinations of AlN, GaN, and selected SiC polytypes: Theoretical advancement and its coordination with experimental studies of nucleation, growth, characterization, and device development
[AD-A253330] p 166 N93-10355
Pre-oxidation anneal kinetics: Interface degradation of thin SiO2 films on silicon
[AD-A253142] p 30 N93-10414
SEMICONDUCTOR DEVICES
Semiconductor phase conjugation
[AD-A253684] p 166 N93-10345
Twenty-five KA, 5000V solid state opening switch for inductive energy stores
[AD-A253968] p 73 N93-10421
Optimization of resonant interband tunnel devices
[AD-A252401] p 168 N93-10637
Advanced processing and characterization technologies. Fabrication and characterization of semiconductor optoelectronic devices and integrated circuits. Final Conference Proceedings No. 10
[AD-A254162] p 73 N93-10663
Quantum 1/f noise in high technology applications including ultrasmall structures and devices
[AD-A253922] p 74 N93-10751
Theory of transport for interacting many-body systems
[AD-A253789] p 169 N93-10871
SEMICONDUCTOR DIODES
Geometrical transformation of linear diode-laser arrays for longitudinal pumping of solid-state lasers
[AD-A253415] p 87 N93-10218
Stability of coupled semiconductor diode lasers p 88 N93-10379
Holographic optical interconnects for multichip modules
[AD-A253403] p 86 N93-10408
Resonance ionization of rubidium using sequential diode laser-driven transitions
[DE92-014468] p 89 N93-10429
SEMICONDUCTOR LASERS
Long wavelength multiple quantum well lasers for high-speed modulation applications
[AD-A253348] p 87 N93-10211
Fellowship in physics/modern optics and quantum electronics
[AD-A253666] p 87 N93-10228
Stability of coupled semiconductor diode lasers p 88 N93-10379
Holographic optical interconnects for multichip modules
[AD-A253403] p 86 N93-10408
SEMICONDUCTORS (MATERIALS)
Nonlinear studies of surface and interfaces of advanced semiconductor materials
[AD-A253365] p 164 N93-10105
The interaction of UV-Laser radiation with metal and semiconductor surfaces
[AD-A253510] p 87 N93-10201
Spatial light modulators with arbitrary quantum well profiles
[AD-A253637] p 165 N93-10210
Fellowship in physics/modern optics and quantum electronics
[AD-A253666] p 87 N93-10228
Novel optoelectronic devices based on combining GaAs and InP on Si
[AD-A253781] p 165 N93-10235
Atomic hydrogen: A reagent for the extraction of chemical species from silicon surfaces
[AD-A252804] p 30 N93-10266
Implanted contacts for diamond semiconductor devices
[AD-A245568] p 165 N93-10274
Comparison of Cl and HCl adsorption on Si(100)-(2 x 1)
[AD-A252802] p 30 N93-10281
A new ellipsometry technique for interface analysis: Application to Si-SiO2
[AD-A253143] p 167 N93-10415
Two-dimensional signal processing, optical information storage and processing, and electromagnetic measurements
[AD-A253953] p 73 N93-10417
Atomic approaches to defect thermochemistry
[AD-A254278] p 167 N93-10425
Hydrocarbon surface chemistry on Si(100)
[AD-A252803] p 27 N93-10465
Advanced processing and characterization technologies. Fabrication and characterization of semiconductor optoelectronic devices and integrated circuits. Final Conference Proceedings No. 10
[AD-A254162] p 73 N93-10663
Scanning tunneling microscopy of semiconductor surfaces
[AD-A246853] p 168 N93-10726
Semiconductor-metal eutectic composites for high power switching
[AD-A253930] p 74 N93-10755
Theory of transport for interacting many-body systems
[AD-A253789] p 169 N93-10871
SENSITIVITY
Sensitivity of modeled ozone concentrations to uncertainties in biogenic emissions
[PB92-192202] p 105 N93-10432
SENSORS
Development of parallel architectures for sensor array processing algorithms
[AD-A253680] p 141 N93-10299
SEPARATED FLOW
Effect of passive flow-control devices on turbulent low-speed base flow p 79 N93-10304
Forced unsteady separated flows on a 45 degree delta wing p 80 N93-10305
Characteristics of separated flows including cavitation effects p 84 N93-10874
The effects of streamline curvature and swirl on turbulent flows in curved ducts p 84 N93-10875
Study of a viscous sublayer model in the analysis of 3-D shock/boundary layer interaction flow fields
[AD-A253731] p 84 N93-10886
High-resolution TVD schemes for the analysis of: 1. Inviscid supersonic and transonic flows. 2. Viscous flows with shock-induced separation and heat transfer p 5 N93-10889
SERVICE LIFE
An evaluation of a method of reconstituting fatigue loading from Rainflow counting
[RAE-TR-89057] p 94 N93-10198
An evaluation of the cumulative damage effect under creep loading p 58 N93-10540
SERVOMECHANISMS
Pneumatic motor powered Thrust Vector Control (TVC) for liquid propelled launch vehicles p 17 N93-10015
Optical metrology of magnetically trapped hydrogen
[AD-A253229] p 31 N93-10712
SHAFTS (MACHINE ELEMENTS)
Characterization of and active control of flexible structures, using piezoceramics as sensors and actuators p 10 N93-10319
SHALES
The Acraman impact and its widespread ejecta, South Australia p 111 N93-10141
SHAPES
Hexagonal and octagonal finite elements p 50 N93-10500
One type of automatically adjusted difference scheme with artificial viscosity to calculate ablated exterior shapes
[AD-A254108] p 5 N93-10856
A semiempirical formula for calculating the coefficients for field emission tip forms
[AD-A254109] p 145 N93-10857
SHATTER CONES
Sudbury project (University of Muenster-Ontario Geological Survey): Field studies 1984-1989 - summary of results p 107 N93-10119
Breccia dikes from the Beaverhead impact structure, southwest Montana p 110 N93-10137
Where's the Beaverhead beef? --- meteorite impact structure p 112 N93-10146
Search for a meteoritic component at the Beaverhead impact structure, Montana p 116 N93-10158
SHEAR FLOW
Simple shearing flow of a 3D foam
[DE92-011151] p 36 N93-10399
A new energy transfer model for turbulent free shear flow
[NASA-TM-105854] p 81 N93-10454
Investigations into swirling flows of Newtonian and non-Newtonian fluids
[AD-A253298] p 82 N93-10696
Turbulent mixing in compressible free shear layers p 83 N93-10846
Direct simulation of turbulent pulsed plane channel flows p 84 N93-10860
Turbulence measurements of high shear flow fields in a turbomachine seal configuration p 93 N93-10893
SHEAR LAYERS
Shock enhancement and control of hypersonic combustion
[AD-A254295] p 31 N93-10843
Turbulent mixing in compressible free shear layers p 83 N93-10846
SHEAR PROPERTIES
Transverse tension, transverse compression, and inplane shear JANNAF round robin test methods standardization results p 16 N93-10007
Sensor and actuator materials for high performance composites
[AD-A254178] p 27 N93-10254

Consistent shear constitutive relations for laminated plates p 28 N93-10509
Shock enhancement and control of hypersonic combustion
[AD-A254295] p 31 N93-10843

SHEAR STRENGTH
Determination of the dynamic unload/reload characteristics of ceramics
[AD-A253513] p 35 N93-10221

SHEAR STRESS
Sensor and actuator materials for high performance composites
[AD-A254178] p 27 N93-10254
Compression buckling of thick orthotropic plates with a step thickness change p 46 N93-10478
An assessment of the correspondence principle in comparison to nonlinear viscoelastic theory: A case study p 51 N93-10501
Analysis of a buffer strip laminate with a cutout p 52 N93-10506
Measurement of aerodynamic shear stress using side chain liquid crystal polymers
[AD-A254312] p 40 N93-10770
Linear and nonlinear analyses of thick composite circular plates using the finite element method p 96 N93-10873

SHEARING
Dynamic stability of laminated transversely-isotropic composite plates subjected to parametric excitations p 29 N93-10525

SHELL THEORY
A multilayered shell finite element p 49 N93-10495
Thermal buckling of heated laminated composite circular cylindrical shells p 51 N93-10504
Natural vibrations of multilayered doubly curved shells p 57 N93-10532
A new quadrilateral element for the elastic and plastic analysis of shells p 62 N93-10559

SHELLS (STRUCTURAL FORMS)
Contact problem in delamination-buckling of laminated composite shells p 46 N93-10479
Natural vibrations of multilayered doubly curved shells p 57 N93-10532
On the vibration of axisymmetric shells p 57 N93-10535

SHOCK LAYERS
Documentation of the detailed radiation property data for the radiation-ablation code RASLE
[NASA-TM-103848] p 28 N93-10742

SHOCK LOADS
Carbon and oxygen isotope study of carbonates from highly shocked clasts of the polymict breccia of the Haughton Crater (Canada) p 105 N93-10113
Shocked zircons in the Onaping Formation: Further proof of impact origin p 107 N93-10121
Optical and TEM study of shock metamorphism from the Sedan test site p 111 N93-10142

SHOCK RESISTANCE
Mechanical behavior of open cell ceramics
[PB92-212984] p 37 N93-10439

SHOCK TESTS
Influence of the preshock temperature on shock effects in quartz p 115 N93-10157

SHOCK TUBES
Shock enhancement and control of hypersonic combustion
[AD-A254295] p 31 N93-10843

SHOCK WAVE INTERACTION
Shock wave diffractions over semi-circular and half-diamond cylinders p 60 N93-10546
RHALE: A MMALE shock physics code for arbitrary meshes
[DE92-017051] p 139 N93-10866
Study of a viscous sublayer model in the analysis of 3-D shock/boundary layer interaction flow fields
[AD-A253731] p 84 N93-10886
High-resolution TVD schemes for the analysis of: 1. Inviscid supersonic and transonic flows. 2. Viscous flows with shock-induced separation and heat transfer p 5 N93-10889

SHOCK WAVE PROPAGATION
Numerical simulation of the propagation of coupled thermomechanical waves in inelastic solids p 64 N93-10568

SHOCK WAVES
Pitot survey of exhaust flow field of a 2-D scramjet nozzle at Mach 6 with air or freon and argon used for exhaust simulation
[NASA-TM-4361] p 2 N93-10071
Molecular dynamics of shocks in crystals with defects
[AD-A253353] p 164 N93-10099
Shock wave diffractions over semi-circular and half-diamond cylinders p 60 N93-10546
Progress in multi-dimensional upwind differencing
[NASA-CR-189708] p 83 N93-10808
RHALE: A MMALE shock physics code for arbitrary meshes
[DE92-017051] p 139 N93-10866
Investigations of the motion of discrete-velocity gases
[AD-A253728] p 84 N93-10895
Yellow hypergiant interferometry: A clue to understanding evolutionary instability p 182 N93-10919

SHORT HAUL AIRCRAFT
Aeronautical technologies for the twenty-first century
[NASA-CR-190918] p 1 N93-10647

SHORT WAVE RADIATION
Modeling of HF propagation and heating in the ionosphere
[AD-A253941] p 125 N93-10714

SHOT PEENING
Fatigue crack propagation in the presence of shot-peening residual stresses p 59 N93-10542

SIDE-LOOKING RADAR
Open Skies Treaty imaging radar technology issues
[DE92-016548] p 68 N93-10394

SIGNAL ANALYSIS
Nonlinear signal processing schemes for robust target detection and automatic clutter rejection in radar
[AD-A253546] p 68 N93-10380
Signal and noise analysis of a-Si:H radiation detector-amplifier system
[DE92-016928] p 75 N93-10790

SIGNAL DETECTION
Subpicosecond resolved incipient laser damage
[AD-A253624] p 87 N93-10202
Convergence performance of adaptive detectors, part 3
[AD-A248415] p 143 N93-10275
Two-dimensional signal processing, optical information storage and processing, and electromagnetic measurements
[AD-A253953] p 73 N93-10417

SIGNAL DETECTORS
Convergence performance of adaptive detectors, part 3
[AD-A248415] p 143 N93-10275

SIGNAL FADING
Eleven years of ionospheric scintillation fading data from twenty Greenlandic stations
[AD-A253271] p 69 N93-10695

SIGNAL GENERATORS
High-power microwave breakdown of dielectric interfaces
[AD-A254200] p 124 N93-10262

SIGNAL PROCESSING
Magnetostatic waves-based integrated optic Bragg cell modules with applications to RF signal processing
[AD-A254035] p 71 N93-10240
Development of parallel architectures for sensor array processing algorithms
[AD-A253680] p 141 N93-10299
Algorithms for multichannel optical processor
[AD-A254009] p 158 N93-10360
Nonlinear signal processing schemes for robust target detection and automatic clutter rejection in radar
[AD-A253546] p 68 N93-10380
Two-dimensional signal processing, optical information storage and processing, and electromagnetic measurements
[AD-A253953] p 73 N93-10417
Instrument driver for general purpose interface bus (IEEE-488)
[AD-A253947] p 138 N93-10716
Signal and noise analysis of a-Si:H radiation detector-amplifier system
[DE92-016928] p 75 N93-10790

SIGNAL TO NOISE RATIOS
Convergence performance of adaptive detectors, part 3
[AD-A248415] p 143 N93-10275

SIGNAL TRANSMISSION
An implementation of the MVDR beamformer on the Intel iWarp system
[AD-A253641] p 140 N93-10209

SIGNATURE ANALYSIS
Air-sea interaction and remote sensing
[NASA-CR-190913] p 128 N93-10068
Recognizing impactor signatures in the planetary record p 120 N93-10178

SIGNATURES
Recognizing impactor signatures in the planetary record p 120 N93-10178
Quantum tunneling and the change in the signature of the spacetime metric
[DE92-634877] p 165 N93-10225

SILICATES
Viscosity determinations of some frictionally generated silicate melts: Implications for slip zone rheology during impact-induced faulting p 121 N93-10183

SILICON
The effect of elevated temperatures on the properties of thermally stable silicon-based elastomers for adhesives, sealants, and insulator applications p 15 N93-10006
Methodology for the computer-aided design of silicon micromachined devices in a standard CMOS process
[PB92-191246] p 136 N93-10248
Atomic hydrogen: A reagent for the extraction of chemical species from silicon surfaces
[AD-A252804] p 30 N93-10266
Comparison of Cl and HCl adsorption on Si(100)-(2 x 1)
[AD-A252802] p 30 N93-10281
Semiconductor phase conjugation
[AD-A253684] p 166 N93-10345
Thermo-optical switching in Si based etalons
[AD-A253139] p 88 N93-10412
Hydrocarbon surface chemistry on Si(100)
[AD-A252803] p 27 N93-10465
Spectroscopic differential reflectance as an analytical probe for microelectronic processing
[AD-A253134] p 73 N93-10656
Scanning tunneling microscopy of semiconductor surfaces
[AD-A246853] p 168 N93-10726
Transformation of Cl bonding structures on Si(100)-(2x1)
[AD-A253739] p 40 N93-10748
High sensitivity probes for silicon VLSI internal node testing
[AD-A253924] p 169 N93-10764

SILICON CARBIDES
Oxidation protection systems for carbon-carbon composites formed by chemical vapor deposition and plasma assisted chemical vapor deposition techniques
[AD-A253450] p 28 N93-10344
High temperature fatigue crack growth in ceramics and ceramic composites
[DE92-016835] p 40 N93-10632
Ohmic contacts to compound semiconductors p 76 N93-10830

SILICON DIOXIDE
Bronzite Granophyre: New insight on Vredefort p 121 N93-10186
Electron petrography of silica polymorphs associated with pseudotachylite, Vredefort structure, South Africa p 123 N93-10192
Kinetics of oxidation of silicon by electron cyclotron resonance plasmas
[AD-A253140] p 161 N93-10413
Pre-oxidation anneal kinetics: Interface degradation of thin SiO2 films on silicon
[AD-A253142] p 30 N93-10414
A new ellipsometry technique for interface analysis: Application to Si-SiO2
[AD-A253143] p 167 N93-10415

SILICON FILMS
Kinetics of oxidation of silicon by electron cyclotron resonance plasmas
[AD-A253140] p 161 N93-10413
Novel Si-YBCuO reactive patterning technique for manufacture of large area high Tc superconducting electronic devices
[AD-A250740] p 73 N93-10426

SILICON ISOTOPES
Particle production at high p(sub (perpendicular)) in (sup 28)Si + A collisions at 14.6 A x GeV/c
[DE92-016939] p 154 N93-10402

SILICON NITRIDES
Thermo-optical switching in Si based etalons
[AD-A253139] p 88 N93-10412

SILVER
Some results of the oxidation investigation of copper and silver samples flown on LDEF p 34 N93-10580

SILVER COMPOUNDS
4.5 micron laser source
[AD-A253367] p 87 N93-10090

SINGLE CRYSTALS
Molecular dynamics of shocks in crystals with defects
[AD-A253353] p 164 N93-10099
The interaction of UV-Laser radiation with metal and semiconductor surfaces
[AD-A253510] p 87 N93-10201
Development of garnet films for magnetostatic wave channelized receivers
[AD-A252812] p 166 N93-10335
Plasticity of single crystalline Al3X intermetallic compounds
[AD-A254282] p 40 N93-10766
Thermal, structural, and diffraction analyses of a gallium-cooled x ray monochromator
[DE92-017083] p 157 N93-10837
Single crystal growth of beta-Al2O3 for iso-index filters
[AD-A252259] p 169 N93-10879

SINGLE STAGE TO ORBIT VEHICLES
Plug nozzle propulsion system p 17 N93-10013

Critical engine system design characteristics for SSTO vehicles p 17 N93-10014
SINGULARITY (MATHEMATICS)
An open or closed crack terminating at a bi-material interface: Power-logarithmic singularities p 47 N93-10483
Enriched element analysis of bimaterial interface cracks p 47 N93-10484
Integral transform approach to an inertial viscoelastic problem involving moving singularities p 49 N93-10490
Singular stress distributions at circular holes in composite laminates p 51 N93-10503
A variational approach for coupled creeping-flow problems p 62 N93-10557
SINTERING
Ceramic transactions. Volume 21: Proceedings of the Symposium on Microwave Theory and Application in Materials Processing Annual Meeting No. 23 io on april 29-may 3 1991
[AD-A253631] p 35 N93-10205
Developmental research on ultra abrasion-resistant materials
[DE92-531066] p 36 N93-10287
A fundamental understanding of the effects of ceramic processing on product microstructure
[AD-A253660] p 41 N93-10779
SKIN (ANATOMY)
Dermal exposure assessment: Principles and applications
[PB92-205665] p 131 N93-10438
SLABS
Stress and strain of slab type amplifiers
[AD-A254246] p 74 N93-10702
Laser Journal
[AD-A254106] p 90 N93-10855
SLEEP
NASA Space Human Factors Program
[NASA-TM-108005] p 134 N93-10890
SLOTTED WIND TUNNELS
Further noise measurements in a slotted cryogenic wind tunnel
[RAE-TM-AERO-2201] p 153 N93-10805
SMART STRUCTURES
Sensor and actuator materials for high performance composites
[AD-A254178] p 27 N93-10254
SMOOTHING
The problem of the selection of an a-posteriori error indicator based on smoothening techniques
[AD-A253401] p 144 N93-10407
SODIUM
Emission tomography of sodium in a hydrogen-air flame
[AD-A253530] p 29 N93-10224
Laser cooling and trapping of neutral atoms
[AD-A253730] p 155 N93-10885
SODIUM ALLOYS
Boiling behavior of sodium-potassium alloy in a bench-scale solar receiver
[DE92-014947] p 103 N93-10383
SODIUM COMPOUNDS
Determination of Sandoz black aluminum coloring dye, olive aluminum coloring dye, and sodium dichromate aluminum sealing solutions by UV-visible spectrophotometry
[AD-A253639] p 29 N93-10207
SOFTWARE ENGINEERING
Proceedings of the CASE Adoption Workshop
[AD-A253362] p 135 N93-10104
An analysis technique for examining integration in a project support environment
[AD-A253351] p 135 N93-10214
Guide to the user requirements definition phase
[ESA-PSS-05-02-ISSUE-1] p 136 N93-10315
Guide to the software requirements definition phase
[ESA-PSS-05-03-ISSUE-1] p 136 N93-10316
Reliability assurance requirements for ESA space systems
[ESA-PSS-01-30-ISSUE-2] p 94 N93-10317
The past, present, and future of configuration management
[AD-A254175] p 138 N93-10665
Software support for programming in the large
[AD-A254050] p 138 N93-10782
Requirements analysis notebook for the flight data systems definition in the Real-Time Systems Engineering Laboratory (RSEL)
[NASA-CR-185698] p 14 N93-10960
SOFTWARE TOOLS
Space Station: NASA's software development approach increases safety and cost risks. Report to the Chairman, Committee on Science, Space, and Technology, House of Representatives
[GAO/IMTEC-92-39] p 12 N93-10081
Interactive animation of fault tolerant parallel algorithms
[AD-A253349] p 135 N93-10212
An analysis technique for examining integration in a project support environment
[AD-A253351] p 135 N93-10214
Handbook for operating the OWLKNEST technology
[AD-A253412] p 137 N93-10409
Parallels in computer-aided design framework and software development environment efforts
[AD-A253327] p 137 N93-10448
Software support for programming in the large
[AD-A254050] p 138 N93-10782
Requirements analysis notebook for the flight data systems definition in the Real-Time Systems Engineering Laboratory (RSEL)
[NASA-CR-185698] p 14 N93-10960
SOILS
APOLLO: A computer program for the calculation of chemical equilibrium and reaction kinetics of chemical systems
[DE92-017864] p 139 N93-10817
FLASH: A finite element computer code for variably saturated flow
[DE92-018038] p 84 N93-10868
SOLAR ACTIVITY
High resolutions studies of the structure of the solar atmosphere
[AD-A254292] p 190 N93-10767
Solar-geophysical data number 569, January 1992. Part 1: (Prompt reports). Data for December, November 1991, and late data
[PB92-158880] p 190 N93-10771
Solar-geophysical data number 570, February 1992. Part 1: (Prompt reports). Data for January 1992, December 1991, and late data
[PB92-170380] p 190 N93-10773
Solar-geophysical data number 570, February 1992. Part 2: (Comprehensive reports). Data for August 1991 and miscellaneous
[PB92-170398] p 190 N93-10774
Solar-geophysical data number 571, March 1992. Part 1: (Prompt reports). Data for February, January 1992, and late data
[PB92-177062] p 190 N93-10775
Solar-geophysical data number 571, March 1992. Part 2: (Comprehensive reports). Data for September 1991 and miscellaneous
[PB92-177070] p 190 N93-10776
On the nature of the small-scale plasma structures in the solar active phenomena p 183 N93-10925
Rotational aperture synthesis: A proposal for ground-based observations p 178 N93-10947
SOLAR ACTIVITY EFFECTS
Eleven years of ionospheric scintillation fading data from twenty Greenlandic stations
[AD-A253271] p 69 N93-10695
SOLAR ARRAYS
Hubble Space telescope thermal cycle test report for large solar array samples with BSFR cells (Sample numbers 703 and 704)
[NASA-TM-108373] p 104 N93-10809
Acceptance testing of the prototype electrometer for the SAMPIE flight experiment
[NASA-TM-105880] p 13 N93-10841
SOLAR ATMOSPHERE
High resolutions studies of the structure of the solar atmosphere
[AD-A254292] p 190 N93-10767
EUV complementary instrumentation for SIMURIS p 14 N93-10938
SOLAR CELLS
Results from testing and analysis of solar cells flown on LDEF p 39 N93-10591
Hubble Space telescope thermal cycle test report for large solar array samples with BSFR cells (Sample numbers 703 and 704)
[NASA-TM-108373] p 104 N93-10809
SOLAR COLLECTORS
Boiling behavior of sodium-potassium alloy in a bench-scale solar receiver
[DE92-014947] p 103 N93-10383
Changes in oxidation state of chromium during LDEF exposure p 34 N93-10581
SOLAR CORONA
High resolutions studies of the structure of the solar atmosphere
[AD-A254292] p 190 N93-10767
Planned observations at high resolution from space p 177 N93-10903
Transition region dynamics p 180 N93-10907
Ultra-high observations of the prominence-corona transition region p 180 N93-10908
Coronal and solar wind Alfven wave propagation p 180 N93-10909
Evidence of plasmoid ejection in the corona from 1991 eclipse observations with the Canada-France-Hawaii telescope p 181 N93-10915
High resolution observations of solar ejecta p 181 N93-10916
EUV complementary instrumentation for SIMURIS p 14 N93-10938
Obtaining high resolution XUV coronal images p 14 N93-10939
SOLAR ECLIPSES
Evidence of plasmoid ejection in the corona from 1991 eclipse observations with the Canada-France-Hawaii telescope p 181 N93-10915
SOLAR ELECTRIC PROPULSION
10 kW power electronics for hydrogen arcjets p 21 N93-10033
A comparison of multimegawatt electric propulsion options for Mars missions p 23 N93-10043
SOLAR ENERGY CONVERSION
Boiling behavior of sodium-potassium alloy in a bench-scale solar receiver
[DE92-014947] p 103 N93-10383
SOLAR FLARES
Solar-geophysical data number 569, January 1992. Part 1: (Prompt reports). Data for December, November 1991, and late data
[PB92-158880] p 190 N93-10771
Solar-geophysical data number 570, February 1992. Part 1: (Prompt reports). Data for January 1992, December 1991, and late data
[PB92-170380] p 190 N93-10773
Solar-geophysical data number 570, February 1992. Part 2: (Comprehensive reports). Data for August 1991 and miscellaneous
[PB92-170398] p 190 N93-10774
Solar-geophysical data number 571, March 1992. Part 1: (Prompt reports). Data for February, January 1992, and late data
[PB92-177062] p 190 N93-10775
Solar-geophysical data number 571, March 1992. Part 2: (Comprehensive reports). Data for September 1991 and miscellaneous
[PB92-177070] p 190 N93-10776
Energy build-up, transport, and release in solar flares p 181 N93-10913
Small scale processes in solar and stellar plasmas p 181 N93-10917
Observation of solar flares at high resolution p 182 N93-10923
On the nature of the small-scale plasma structures in the solar active phenomena p 183 N93-10925
MSDP imaging spectroscopy for high resolution solar physics p 183 N93-10926
SOLAR GRANULATION
High resolution granulation spectrophotometry with a UBF and a FP interferometer in tandem p 183 N93-10927
SOLAR HEATING
High resolutions studies of the structure of the solar atmosphere
[AD-A254292] p 190 N93-10767
Physics of coronal loops: Heating and reconnection p 180 N93-10912
SOLAR INSTRUMENTS
Solar Physics and Astrophysics at Interferometric Resolution
[ESA-SP-344] p 179 N93-10901
High resolution observations: The state of the art and beyond p 177 N93-10902
SUN: The Solar Ultraviolet Network p 183 N93-10930
Detectors for the SIMURIS payload p 14 N93-10937
EUV complementary instrumentation for SIMURIS p 14 N93-10938
Investigations of the effects of contamination on UV optics p 159 N93-10949
The solar ultraviolet network: Performance and tolerance analysis p 187 N93-10950
Accommodation aspects of SIMURIS on Space Station Freedom p 14 N93-10954
Interferometer optical design for the Imaging Fourier Transform Spectrometer (IFTS) p 159 N93-10955
Mechanical and thermal design of the SUN instrument p 14 N93-10956
SOLAR MAGNETIC FIELD
Solar-geophysical data number 569, January 1992. Part 1: (Prompt reports). Data for December, November 1991, and late data
[PB92-158880] p 190 N93-10771
Solar-geophysical data number 570, February 1992. Part 1: (Prompt reports). Data for January 1992, December 1991, and late data
[PB92-170380] p 190 N93-10773

Solar-geophysical data number 571, March 1992. Part 1: (Prompt reports). Data for February, January 1992, and late data
[PB92-177062] p 190 N93-10775
Small-scale physics of convection and magnetic fields
p 179 N93-10905
Stellar and circumstellar evolution and activity
p 181 N93-10918
Polarimetry with an imaging FTS p 14 N93-10934

SOLAR OSCILLATIONS
Spatial distribution of line-of-sight velocities in a quiescent prominence p 183 N93-10928

SOLAR PHYSICS
Workshop on the evolution of the Martian atmosphere
[NASA-CR-190730] p 189 N93-10064
Solar Physics and Astrophysics at Interferometric Resolution
[ESA-SP-344] p 179 N93-10901
High resolution observations: The state of the art and beyond p 177 N93-10902
Prospects with SIMURIS p 179 N93-10904
Small-scale physics of convection and magnetic fields
p 179 N93-10905
Chromospheric structure and dynamics
p 180 N93-10906
Physics of coronal loops: Heating and reconnection
p 180 N93-10912
MSDP imaging spectroscopy for high resolution solar physics p 183 N93-10926
SUN: The Solar Ultraviolet Network
p 183 N93-10930
Interferometric imaging with the solar ultraviolet network p 184 N93-10932

SOLAR PROMINENCES
Ultra-high observations of the prominence-corona transition region p 180 N93-10908
The fine structure of prominences
p 180 N93-10910
Intensity, velocity, and turbulence in prominences observed with the HRTS p 180 N93-10911
Spatial distribution of line-of-sight velocities in a quiescent prominence p 183 N93-10928

SOLAR PROTONS
Energy build-up, transport, and release in solar flares
p 181 N93-10913

SOLAR RADIATION
Detectors for the SIMURIS payload
p 14 N93-10937
Ground-based high angular resolution observation of the Sun by interferometry in the visible p 177 N93-10941

SOLAR RADIO BURSTS
Solar-geophysical data number 570, February 1992. Part 2: (Comprehensive reports). Data for August 1991 and miscellaneous
[PB92-170398] p 190 N93-10774
Solar-geophysical data number 571, March 1992. Part 2: (Comprehensive reports). Data for September 1991 and miscellaneous
[PB92-177070] p 190 N93-10776

SOLAR RADIO EMISSION
Solar-geophysical data number 569, January 1992. Part 1: (Prompt reports). Data for December, November 1991, and late data
[PB92-158880] p 190 N93-10771
Solar-geophysical data number 570, February 1992. Part 1: (Prompt reports). Data for January 1992, December 1991, and late data
[PB92-170380] p 190 N93-10773
Solar-geophysical data number 571, March 1992. Part 1: (Prompt reports). Data for February, January 1992, and late data
[PB92-177062] p 190 N93-10775

SOLAR ROTATION
Pattern recognition applied to H(sub alpha) spectroheliograms solar rotation and meridional circulation p 182 N93-10924

SOLAR SPECTRA
Transition region dynamics p 180 N93-10907
Observation of solar flares at high resolution
p 182 N93-10923
MSDP imaging spectroscopy for high resolution solar physics p 183 N93-10926

SOLAR SPECTROMETERS
Solar Physics and Astrophysics at Interferometric Resolution
[ESA-SP-344] p 179 N93-10901
Planned observations at high resolution from space
p 177 N93-10903
The solar ultraviolet network subtractive double monochromator p 183 N93-10931
IFTS: The Imaging Fourier Transform Spectrometer
p 14 N93-10933
Detectors for the SIMURIS payload
p 14 N93-10937

SOLAR WIND
Transition region dynamics p 180 N93-10907
Coronal and solar wind Alfven wave propagation
p 180 N93-10909
Stokes parameters of the O VI 103.2 nm line as a probe of the matter velocity field vector in the solar wind acceleration region p 181 N93-10914
Evidence of plasmoid ejection in the corona from 1991 eclipse observations with the Canada-France-Hawaii telescope p 181 N93-10915
High resolution observations of solar ejecta
p 181 N93-10916
Small scale processes in solar and stellar plasmas
p 181 N93-10917
On the nature of the small-scale plasma structures in the solar active phenomena p 183 N93-10925

SOLAR WIND VELOCITY
Intensity, velocity, and turbulence in prominences observed with the HRTS p 180 N93-10911
Stokes parameters of the O VI 103.2 nm line as a probe of the matter velocity field vector in the solar wind acceleration region p 181 N93-10914

SOLAR X-RAYS
Solar-geophysical data number 570, February 1992. Part 2: (Comprehensive reports). Data for August 1991 and miscellaneous
[PB92-170398] p 190 N93-10774
Solar-geophysical data number 571, March 1992. Part 2: (Comprehensive reports). Data for September 1991 and miscellaneous
[PB92-177070] p 190 N93-10776

SOLID MECHANICS
Local-equilibrium formalism applied to mechanics of solids
[DE92-016852] p 170 N93-10787

SOLID PROPELLANT COMBUSTION
Multidimensional effects in composite propellant combustion p 42 N93-10313

SOLID PROPELLANT ROCKET ENGINES
The 1992 JANNAF Propulsion Meeting, volume 1
[CPIA-PUBL-580-VOL-1] p 15 N93-10001
Instrumented propellant block test and stress analysis comparison p 15 N93-10002
Facility for cold flow testing of solid rocket motor models p 11 N93-10021
Feasibility evaluation of the monolithic braided ablative nozzle p 19 N93-10023
Molded nozzle technology for large solid rocket motors p 19 N93-10024
Effects of the RSRM grain deformation on ballistic performance p 20 N93-10027
Alternatives in clean propellants for large scale man-rated solid rocket motors p 20 N93-10028
Selection of rocket propulsion systems
p 22 N93-10034

SOLID PROPELLANTS
Investigation of the stimulated release of gaseous ammonia from ammonium perchlorate by HTPB solid propellant bonding agents p 19 N93-10026
Alternatives in clean propellants for large scale man-rated solid rocket motors p 20 N93-10028

SOLID ROCKET BINDERS
Synthesis and characterization of energetic polymers
p 15 N93-10005
Multidimensional effects in composite propellant combustion p 42 N93-10313

SOLID ROCKET PROPELLANTS
Instrumented propellant block test and stress analysis comparison p 15 N93-10002
Synthesis and characterization of energetic polymers
p 15 N93-10005

SOLID SOLUTIONS
Pseudomorphic semiconducting heterostructures from combinations of AlN, GaN, and selected SiC polytypes: Theoretical advancement and its coordination with experimental studies of nucleation, growth, characterization, and device development
[AD-A253330] p 166 N93-10355
Growth, nitrogen vacancy reduction, and solid solution formation in cubic GaN thin films and the subsequent fabrication of superlattice structures using AlN and InN
[AD-A253331] p 166 N93-10356

SOLID STATE
The magnetochemistry of supramolecular particles: The transition from the molecular to the solid-state
[AD-A253126] p 153 N93-10338
Twenty-five KA, 5000V solid state opening switch for inductive energy stores
[AD-A253968] p 73 N93-10421

SOLID STATE LASERS
Geometrical transformation of linear diode-laser arrays for longitudinal pumping of solid-state lasers
[AD-A253415] p 87 N93-10218
System design and relaxation oscillations of a titanium-sapphire laser
[AD-A254264] p 89 N93-10725

SOLID STATE PHYSICS
The third Workshop on Non-Crystalline Solids, programme and abstracts
[AD-A250739] p 36 N93-10244
The magnetochemistry of supramolecular particles: The transition from the molecular to the solid-state
[AD-A253126] p 153 N93-10338
High pressure and synchrotron radiation studies of solid state electronic instabilities
[DE92-015661] p 168 N93-10630

SOLID SURFACES
The interaction of UV-Laser radiation with metal and semiconductor surfaces
[AD-A253510] p 87 N93-10201

SOLID-SOLID INTERFACES
Interface cracks in an orthotropic layered half-space under impact loading p 47 N93-10482
An open or closed crack terminating at a bi-material interface: Power-logarithmic singularities
p 47 N93-10483
Enriched element analysis of bimaterial interface cracks p 47 N93-10484
Elastic wave scattering by an interfacial crack in a plate p 48 N93-10485

SOLIDS
Electron transfer reactions in microporous solids
[DE92-016222] p 166 N93-10284

SOLIDS FLOW
A study of flow properties of wet solids using laser induced photochemical anemometry
[DE92-015483] p 82 N93-10629

SOLUBILITY
Materials compatibility and lubricants research on CFC-refrigerant substitute: Miscibility of lubricants with refrigerants
[DE92-015118] p 35 N93-10084
Water soluble polysiloxanes with pendant 1-oxypyridin-3-yl groups
[AD-A250637] p 36 N93-10246
Effect of alloying elements on passivity and breakdown of passivity of Fe- and Ni-based alloys mechanistics aspects
[DE92-017316] p 33 N93-10395

SOLUTIONS
Mobility of toluene in polystyrene-toluene solutions: A NMR study
[AD-A253203] p 31 N93-10794

SONIC BOOMS
Boom and the problems related to the supersonic flights of military aircraft p 149 N93-10677

SOUND GENERATORS
Combat aircraft jet engine noise studies
p 150 N93-10679

SOUND INTENSITY
Acoustic noise generation at the air/ocean boundary
[DREA-CR-90-445] p 147 N93-10642

SOUND PRESSURE
Prediction of jet mixing noise for high subsonic flight speeds p 151 N93-10685

SOUND PROPAGATION
Noise studies for environmental impact assessment of an outdoor engine test facility p 149 N93-10672

SOUND WAVES
An implementation of the MVDR beamformer on the Intel iWarp system
[AD-A253641] p 140 N93-10209
SBS applications study
[AD-A253779] p 102 N93-10234
On the coupling between a supersonic boundary layer and a flexible surface
[NASA-CR-189697] p 82 N93-10757
Pulse propagation in random media
[AD-A254294] p 152 N93-10769

SOUTHERN HEMISPHERE
Atlas of Southern Hemisphere 500 mb teleconnection patterns derived from National Meteorological Center analyses
[PB92-203892] p 126 N93-10337

SPACE COMMUNICATION
Chinese Space Science and Technology (selected articles)
[AD-A254099] p 69 N93-10701

SPACE DEBRIS
Contaminant interferences with SIMS analyses of microparticle impactor residues on LDEF surfaces
p 32 N93-10854

SPACE ERECTABLE STRUCTURES
A new deployable mast p 14 N93-10511

SPACE EXPLORATION
A comparison of multimegawatt electric propulsion options for Mars missions p 23 N93-10043
Aerospace medicine and biology: A continuing bibliography with indexes (supplement 366)
[NASA-SP-7011(366)] p 130 N93-10079

System model development for nuclear thermal propulsion
[NASA-TM-105761] p 25 N93-10457
SPACE FLIGHT STRESS
DoD space radiation concerns
[AD-A253135] p 131 N93-10613
NASA Space Human Factors Program
[NASA-TM-108005] p 134 N93-10890
SPACE OBSERVATIONS (FROM EARTH)
Successes of and prospects for ground-based interferometry p 177 N93-10940
Ground-based high angular resolution observation of the Sun by interferometry in the visible p 177 N93-10941
The CHARON program p 177 N93-10942
Ground/space co-operation for interferometry p 178 N93-10946
Rotational aperture synthesis: A proposal for ground-based observations p 178 N93-10947
SPACE PERCEPTION
Eye movements and visual information processing
[AD-A250198] p 132 N93-10278
SPACE PLASMAS
Simulation study of interactions of Space Shuttle-generated electron beams with ambient plasmas
[NASA-CR-190843] p 159 N93-10066
Echo characteristic analysis of the nonequilibrium wakes of reentry vehicle
[AD-A254249] p 13 N93-10705
Data synthesis and display programs for wave distribution function analysis
[NASA-TM-108009] p 70 N93-10800
SPACE SHUTTLE MAIN ENGINE
Formed platelets for low cost regeneratively cooled rocket combustion chambers p 18 N93-10018
Improve SSME power balance model
[NASA-CR-184464] p 26 N93-10756
SPACE STATION FREEDOM
Long life monopropellant hydrazine thruster evaluation for Space Station Freedom application p 23 N93-10042
Design and operation of the US Space Station Freedom propulsion system p 24 N93-10049
Space Station: NASA's software development approach increases safety and cost risks. Report to the Chairman, Committee on Science, Space, and Technology, House of Representatives
[GAO/IMTEC-92-39] p 12 N93-10081
Power system monitoring and source control of the Space Station Freedom DC power system testbed
[NASA-TM-105841] p 26 N93-10734
Guidelines for developing spacecraft maximum allowable concentrations for Space Station contaminants
[NASA-CR-190748] p 13 N93-10737
SPACE STATION POWER SUPPLIES
Power system monitoring and source control of the Space Station Freedom DC power system testbed
[NASA-TM-105841] p 26 N93-10734
SPACE STATION PROPULSION
Design and operation of the US Space Station Freedom propulsion system p 24 N93-10049
SPACE STATIONS
Space Station: NASA's software development approach increases safety and cost risks. Report to the Chairman, Committee on Science, Space, and Technology, House of Representatives
[GAO/IMTEC-92-39] p 12 N93-10081
SPACE TOOLS
TAQL: A problem space tool for expert system development
[AD-A253820] p 175 N93-10626
SPACE TRANSPORTATION SYSTEM
Space Transportation Engine Program (STEP), phase B
[NASA-CR-184062] p 25 N93-10350
SPACE WEAPONS
An indicator of message quality for a single optical sensor using a template based tracking algorithm
[AD-A252704] p 139 N93-10881
SPACE-TIME FUNCTIONS
Quantum tunneling and the change in the signature of the spacetime metric
[DE92-634877] p 165 N93-10225
SPACEBORNE ASTRONOMY
Solar Physics and Astrophysics at Interferometric Resolution
[ESA-SP-344] p 179 N93-10901
Planned observations at high resolution from space p 177 N93-10903
Prospects with SIMURIS p 179 N93-10904
Stellar and circumstellar evolution and activity p 181 N93-10918
Tomographic/interferometric studies of active stars and binaries p 182 N93-10920
Prospects in stellar and galactic observations with SIMURIS p 182 N93-10921
Towards an ESA strategy for optical interferometry in space. Recommendations of the ESA Space Interferometry Study Team (SIST) p 178 N93-10944
Report of the Lunar Interferometry Study Team (LIST) activities p 178 N93-10945
Some possible space interferometry applications p 178 N93-10957
SPACEBORNE EXPERIMENTS
Electric Propulsion Space Experiment (ESEX): Spacecraft design issues for high-power electric propulsion p 21 N93-10030
A 26 kW arcjet system for on-orbit demonstration p 21 N93-10031
Structure of thermocapillary flow in narrow cavities p 61 N93-10552
LDEF Materials Workshop 1991, part 2
[NASA-CP-3162-PT-2] p 37 N93-10578
Some results of the oxidation investigation of copper and silver samples flown on LDEF p 34 N93-10580
Polymer matrix composites on LDEF experiments M0003-9 and M0003-10 p 38 N93-10584
Space environmental effects on LDEF low Earth orbit exposed graphite reinforced polymer matrix composites p 38 N93-10585
Acceptance testing of the prototype electrometer for the SAMPIE flight experiment
[NASA-TM-105880] p 13 N93-10841
SPACEBORNE TELESCOPES
EUV complementary instrumentation for SIMURIS p 14 N93-10938
SPACECRAFT CABIN ATMOSPHERES
Guidelines for developing spacecraft maximum allowable concentrations for Space Station contaminants
[NASA-CR-190748] p 13 N93-10737
SPACECRAFT CONFIGURATIONS
A configuration development strategy for the NASP p 9 N93-10011
SPACECRAFT CONSTRUCTION MATERIALS
LDEF Materials Workshop 1991, part 2
[NASA-CP-3162-PT-2] p 37 N93-10578
Space environmental effects on LDEF low Earth orbit exposed graphite reinforced polymer matrix composites p 38 N93-10585
Identification and evaluation of lubricants, adhesives, and seals used on LDEF p 39 N93-10588
Mechanics of composite materials for spacecraft
[AD-A254217] p 28 N93-10896
SPACECRAFT CONTAMINATION
Guidelines for developing spacecraft maximum allowable concentrations for Space Station contaminants
[NASA-CR-190748] p 13 N93-10737
SPACECRAFT CONTROL
NLS cargo transfer vehicle propulsion system p 23 N93-10041
Numerical simulation of large actively controlled space structures p 13 N93-10308
SPACECRAFT DESIGN
Plug nozzle propulsion system p 17 N93-10013
SPACECRAFT ELECTRONIC EQUIPMENT
Requirements analysis notebook for the flight data systems definition in the Real-Time Systems Engineering Laboratory (RSEL)
[NASA-CR-185698] p 14 N93-10960
SPACECRAFT INSTRUMENTS
Remote sounding of the Martian atmosphere p 189 N93-10378
Autonomous star sensing and pattern recognition for spacecraft attitude determination p 177 N93-10876
Planned observations at high resolution from space p 177 N93-10903
SPACECRAFT MAINTENANCE
Generic Propellant Transfer Unit p 11 N93-10046
Extravehicular activity compatibility evaluation of developmental hardware for assembly and repair of precision reflectors
[NASA-TP-3246] p 13 N93-10744
SPACECRAFT MANEUVERS
Electric propulsion applications p 20 N93-10029
NLS cargo transfer vehicle propulsion system p 23 N93-10041
SPACECRAFT PERFORMANCE
Uprated OMS engine status: Altitude testing results p 22 N93-10036
SPACECRAFT POWER SUPPLIES
Results from the testing and analysis of LDEF batteries p 39 N93-10589
SPACECRAFT PROPULSION
Power conditioning unit for 30 kWe class arcjet flight experiment p 21 N93-10032
NLS cargo transfer vehicle propulsion system p 23 N93-10041
Loading operations for spacecraft propulsion subsystems p 11 N93-10047
DSP propulsion system launch configuration and related testing p 24 N93-10048
LV software for supersonic flow analysis
[NASA-CR-190911] p 2 N93-10069
Synchrotron radiation considerations in the Dense Plasma Focus (DPF) Magnetoplasmadynamic (MPD) thruster
[AD-A254188] p 25 N93-10258
System model development for nuclear thermal propulsion
[NASA-TM-105761] p 25 N93-10457
Basic processes of plasma propulsion
[AD-A253929] p 163 N93-10754
SPACECRAFT RELIABILITY
Molded nozzle technology for large solid rocket motors p 19 N93-10024
SPACECRAFT SHIELDING
A computational study of projectile melt in impact with typical Whipple shields
[DE92-017137] p 92 N93-10635
SPATIAL DEPENDENCIES
A solution scheme for the deflection equations of flexible arms with time-dependent boundary conditions p 66 N93-10575
SPATIAL DISTRIBUTION
Enhanced magnetic field production during oblique hypervelocity impacts p 108 N93-10129
Spatial distribution of line-of-sight velocities in a quiescent prominence p 183 N93-10928
SPATIAL RESOLUTION
Edge ion dynamics in H-mode discharges in D3-D
[DE92-016255] p 162 N93-10619
Some possible space interferometry applications p 178 N93-10957
SPECIFIC HEAT
Assessment study of superconducting fault-current limiters operating at 77 K
[DE92-015273] p 76 N93-10831
SPECIFIC IMPULSE
Electric Propulsion Space Experiment (ESEX): Spacecraft design issues for high-power electric propulsion p 21 N93-10030
10 kW power electronics for hydrogen arcjets p 21 N93-10033
Long life monopropellant hydrazine thruster evaluation for Space Station Freedom application p 23 N93-10042
SPECIFICATIONS
Raster graphics validation
[PB92-196070] p 137 N93-10441
SPECKLE INTERFEROMETRY
Successes of and prospects for ground-based interferometry p 177 N93-10940
Ground-based high angular resolution observation of the Sun by interferometry in the visible p 177 N93-10941
SPECTRA
Automatic cloud classification from multi-spectral satellite data over oceanic regions
[AD-A253670] p 126 N93-10292
UV spectrum splitting mirror
[DE92-018057] p 159 N93-10818
SPECTRAL BANDS
SPOT panchromatic band simulation by linear combination of multispectral bands
[INPE-5295-PRE/1650] p 157 N93-10311
SPECTRAL ENERGY DISTRIBUTION
Design optimization for uniform dynamic strength under multi-modal response p 62 N93-10555
SPECTRAL METHODS
Numerical study of the small scale structures in Boussinesq convection
[NASA-CR-189695] p 145 N93-10758
SPECTRAL REFLECTANCE
UV spectrum splitting mirror
[DE92-018057] p 159 N93-10818
SPECTRAL RESOLUTION
Some possible space interferometry applications p 178 N93-10957
SPECTROGRAMS
Pattern recognition applied to H(sub alpha) spectroheliograms solar rotation and meridional circulation p 182 N93-10924
SPECTROGRAPHS
MSDP imaging spectroscopy for high resolution solar physics p 183 N93-10926
SPECTROPHOTOMETERS
Determination of Sandoz black aluminum coloring dye, olive aluminum coloring dye, and sodium dichromate aluminum sealing solutions by UV-visible spectrophotometry
[AD-A253639] p 29 N93-10207
SPECTROPHOTOMETRY
Determination of Sandoz black aluminum coloring dye, olive aluminum coloring dye, and sodium dichromate aluminum sealing solutions by UV-visible spectrophotometry
[AD-A253639] p 29 N93-10207

SPECTROSCOPIC ANALYSIS
Alternate spectrometric oil analysis techniques
[AD-A253355] p 29 N93-10101
Infrared investigations of pristine polypyrrole. Is the polymer called polypyrrole really Poly (Pyrrole-Co-Hydroxypyrrole)?
[AD-A249746] p 36 N93-10243
A new ellipsometry technique for interface analysis: Application to Si-SiO2
[AD-A253143] p 167 N93-10415
Spectroscopic ellipsometric measurements of the dielectric function of germanium dioxide films on crystal germanium
[AD-A253137] p 168 N93-10614
Spectroscopic differential reflectance as an analytical probe for microelectronic processing
[AD-A253134] p 73 N93-10656
The microstructural characterization of an Al-Li-Cu-Mg alloy (8090) metal-matrix composite
[RAE-TM-MAT/STR-1139] p 34 N93-10802
Analysis of interplanetary dust experiment detectors and other witness plates
[NASA-CR-190818] p 32 N93-10852
Elemental analyses of hypervelocity microparticle impact sites on interplanetary dust experiment sensor surfaces
p 32 N93-10853
Contaminant interferences with SIMS analyses of microparticle impactor residues on LDEF surfaces
p 32 N93-10854

SPECTROSCOPY
Chromospheric structure and dynamics
p 180 N93-10906

SPECTRUM ANALYSIS
Evolutionary spectra of time-dependent discretized systems to time-frequency modulated random excitations p 55 N93-10524

SPHERES
Laser and optical physics
[AD-A253619] p 88 N93-10251
Polarized light scattering from perfect and perturbed surfaces and fundamental scattering systems
[AD-A253186] p 158 N93-10445

SPHERICAL COORDINATES
A globally well-posed accurate and efficient finite element CFD algorithm for compressible aerodynamics
p 3 N93-10306

SPHERICAL SHELLS
Analysis of a medium size BOR radome
[AD-A253954] p 69 N93-10418

SPHERICAL WAVES
Epitaxial growth and dopant incorporation in diamond
[AD-A253636] p 165 N93-10206

SPHERULES
Early Archean spherule beds of possible impact origin from Barberton, South Africa: A detailed mineralogical and geochemical study p 115 N93-10155
Geological evidence for a 2.6-Ga strewn field of impact spherules in the Hamersley Basin of Western Australia
p 120 N93-10181

SPLINE FUNCTIONS
A spline finite strip method for analysing local and distortional buckling of thin-walled beams under arbitrary loading p 58 N93-10538

SPLINES
Algebra-geometric and differential geometric methods in solid geometric modeling
[AD-A253669] p 145 N93-10870

SPOT (FRENCH SATELLITE)
SPOT panchromatic band simulation by linear combination of multispectral bands
[INPE-5295-PRE/1650] p 157 N93-10311

SPUTTERING
Implanted contacts for diamond semiconductor devices
[AD-A245568] p 165 N93-10274

SQUID (DETECTORS)
Low-frequency noise reduction in SQUID measurements using laser switching
[AD-A253821] p 90 N93-10827

STABILITY
Global structure of a polynomial autonomous system on the plane
[DE92-630230] p 144 N93-10389
Yellow hypergiant interferometry: A clue to understanding evolutionary instability
p 182 N93-10919

STABILITY AUGMENTATION
Experimental demonstration of offset control with an application to the tethered payload p 14 N93-10521

STABILITY DERIVATIVES
Research on the asymmetrical aerodynamic forces of reentry vehicles
[AD-A254307] p 4 N93-10707

STABILITY TESTS
Chemical and thermal stability of refrigerant-lubricant mixture with metal
[DE92-015117] p 44 N93-10398
Stability of open-graded bases under wheel loads using a model testing approach
[AD-A253209] p 66 N93-10710

STABILIZATION
Advanced transport systems for electron beams in high-brightness accelerators and FEL's
[AD-A253314] p 88 N93-10286

STAGNATION FLOW
Flow over a leading edge with distributed roughness
p 6 N93-10549

STAINLESS STEELS
Stress modified welding process for irradiated materials
[DE92-017131] p 92 N93-10634

STANDARDIZATION
Transverse tension, transverse compression, and inplane shear JANNAF round robin test methods standardization results p 16 N93-10007
Advanced technology component derating
[AD-A253334] p 72 N93-10357

STANDARDS
Guide to the software requirements definition phase
[ESA-PSS-05-03-ISSUE-1] p 136 N93-10316
Reliability assurance requirements for ESA space systems
[ESA-PSS-01-30-ISSUE-2] p 94 N93-10317
On the development of a new fracture toughness procedure p 59 N93-10541
A change of course: The importance to DoD of international standards for electronic commerce
[AD-A253199] p 75 N93-10792

STANDING WAVES
The role of eddy fluxes in the response of the atmosphere to tropical thermal forcing
p 124 N93-10318

STAR TRACKERS
Burn phase corrections of maneuver ballistic missiles with star light
[AD-A254105] p 12 N93-10814
Autonomous star sensing and pattern recognition for spacecraft attitude determination p 177 N93-10876

STARK EFFECT
Polarimetry of motional Stark effect and determination of current profiles in D3-D
[DE92-016258] p 161 N93-10393

STATE ESTIMATION
Power system monitoring and source control of the Space Station Freedom DC power system testbed
[NASA-TM-105841] p 26 N93-10734

STATIC DEFORMATION
A variational approach for coupled creeping-flow problems p 62 N93-10557

STATICS
Statics and kinetics of oxygen ordering in the oxide superconductor YBa2Cu3O(z)
[DE92-017001] p 167 N93-10403

STATISTICAL ANALYSIS
The problem of the selection of an a-posteriori error indicator based on smoothening techniques
[AD-A253401] p 144 N93-10407
Order statistics and nonparametric statistics
[AD-A253574] p 146 N93-10699
Air-sea interaction in regions of varying surface conditions
[AD-A253182] p 128 N93-10791
Change analysis
[AD-A253567] p 146 N93-10795

STATISTICAL DISTRIBUTIONS
Noise emission of low flying military airplanes
p 149 N93-10675
Analytical characterization of bistatic scattering from Gaussian distributed surfaces
[AD-A254253] p 159 N93-10724
Change analysis
[AD-A253567] p 146 N93-10795

STATISTICAL TESTS
The total time on test statistic and age-dependent censoring
[AD-A253622] p 147 N93-10798

STATISTICAL WEATHER FORECASTING
Probability forecasting: A guide for forecasters and staff weather officers
[AD-A254216] p 126 N93-10264

STEADY STATE
System model development for nuclear thermal propulsion
[NASA-TM-105761] p 25 N93-10457

STEEPEST DESCENT METHOD
Artificial neural network system for memory modification
[AD-D015354] p 142 N93-10958
Memory modification of artificial neural networks
[AD-D015356] p 143 N93-10959

STEERING
Steering system of a vehicle, such as a snow removing machine for airfields
[CA-PATENT-APPL-SN-1293201] p 91 N93-10367

STELLAR ACTIVITY
Stellar and circumstellar evolution and activity
p 181 N93-10918
Tomographic/interferometric studies of active stars and binaries p 182 N93-10920
Prospects in stellar and galactic observations with SIMURIS p 182 N93-10921

STELLAR ENVELOPES
Probing cosmic infrared sources: A computer modeling approach
[AD-A253788] p 178 N93-10238

STELLAR EVOLUTION
Workshop on the evolution of the Martian atmosphere
[NASA-CR-190730] p 189 N93-10064
Stellar and circumstellar evolution and activity
p 181 N93-10918
Yellow hypergiant interferometry: A clue to understanding evolutionary instability
p 182 N93-10919

STELLAR MASS EJECTION
Evidence of plasmoid ejection in the corona from 1991 eclipse observations with the Canada-France-Hawaii telescope p 181 N93-10915
High resolution observations of solar ejecta
p 181 N93-10916

STELLAR MODELS
Ultra-high observations of the prominence-corona transition region p 180 N93-10908

STELLAR PHYSICS
High resolutions studies of the structure of the solar atmosphere
[AD-A254292] p 190 N93-10767
The CHARON program p 177 N93-10942

STELLAR SPECTROPHOTOMETRY
High resolution granulation spectrophotometry with a UBF and a FP interferometer in tandem
p 183 N93-10927

STEREOSCOPIC VISION
Stereoscopy and paralax in the vertical distances determination using aerial photographs
[INPE-5363-PUD/049] p 102 N93-10063
Automated handling and assembling of non-rigid objects
[AD-A253605] p 66 N93-10649

STEREOSCOPY
Stereoscopy and paralax in the vertical distances determination using aerial photographs
[INPE-5363-PUD/049] p 102 N93-10063

STIFFNESS
Compression buckling of thick orthotropic plates with a step thickness change p 46 N93-10478
An elastic oblate axisymmetric reference gyro for attitude studies p 54 N93-10518
A new quadrilateral element for the elastic and plastic analysis of shells p 62 N93-10559

STIFFNESS MATRIX
On the behavior of a higher-order plate bending element p 47 N93-10481

STIMULATED EMISSION
SBS applications study
[AD-A253779] p 102 N93-10234

STIRLING ENGINES
Boiling behavior of sodium-potassium alloy in a bench-scale solar receiver
[DE92-014947] p 103 N93-10383

STISHOVITE
Electron petrography of silica polymorphs associated with pseudotachylite, Vredefort structure, South Africa
p 123 N93-10192

STOCHASTIC PROCESSES
Investigation of a possible stochastic model for the IEEE P896.1 (Futurebus+) protocol, including the proposed enhanced distributed arbiter
[CTN-92-60593] p 135 N93-10088
Unifying the landmark developments in optimal bounding ellipsoid identification
[AD-A253502] p 143 N93-10200
Chaotic oscillation of a high speed flexible arm robot
p 65 N93-10574
Stochastic diffusion and Kolmogorov entropy in regular and random Hamiltonians
[DE92-016179] p 170 N93-10604

STOICHIOMETRY
Statics and kinetics of oxygen ordering in the oxide superconductor YBa2Cu3O(z)
[DE92-017001] p 167 N93-10403

STOKES FLOW
A variational approach for coupled creeping-flow problems p 62 N93-10557

Direct simulation of turbulent pulsed plane channel flows p 84 N93-10860

STOKES THEOREM (VECTOR CALCULUS)

Stokes parameters of the O VI 103.2 nm line as a probe of the matter velocity field vector in the solar wind acceleration region p 181 N93-10914

STORABLE PROPELLANTS

LAM actuated propellant flow control device p 18 N93-10017

Uprated OMS engine status: Altitude testing results p 22 N93-10036

The application of liquid crystal polymers to turbomachinery p 23 N93-10040

STORAGE RINGS (PARTICLE ACCELERATORS)

UV/XUV FEL storage ring and linac [AD-A253307] p 89 N93-10697

Recent developments in stored polarized electron positron beams [DE92-016965] p 157 N93-10862

STORAGE TANKS

Tank chilldown analysis and verification with a flightweight, 175 cu ft tank under normal gravity with liquid hydrogen p 24 N93-10045

STORM SURGES

List of publications, 1969-1991. Panel on wind and seismic effects [PB92-201102] p 125 N93-10089

STRAIN DISTRIBUTION

Comparison of full 3-D, thin-film 3-D, and thin-film plate analyses of a postbuckled embedded delamination p 47 N93-10480

STRAIN ENERGY METHODS

Comparison of full 3-D, thin-film 3-D, and thin-film plate analyses of a postbuckled embedded delamination p 47 N93-10480

Design optimization for uniform dynamic strength under multi-modal response p 62 N93-10555

STRAIN ENERGY RELEASE RATE

Cluster beam studies of metal combustion [AD-A253952] p 30 N93-10416

Comparison of full 3-D, thin-film 3-D, and thin-film plate analyses of a postbuckled embedded delamination p 47 N93-10480

STRAIN GAGES

A method of testing two-dimensional airfoils [AD-A253210] p 4 N93-10375

STRAIN RATE

Viscosity determinations of some frictionally generated silicate melts: Implications for slip zone rheology during impact-induced faulting p 121 N93-10183

STRATA

Sudbury project (University of Muenster-Ontario Geological Survey): Origin of the polymict, allochthonous breccias of the Onaping Formation p 106 N93-10116

Structural review of the Vredefort dome p 108 N93-10127

Intrusive origin of the Sudbury Igneous Complex: Structural and sedimentological evidence p 108 N93-10128

K/T boundary stratigraphy: Evidence for multiple impacts and a possible comet stream p 120 N93-10180

Geological evidence for a 2.6-Ga strewn field of impact spherules in the Hamersley Basin of Western Australia p 120 N93-10181

Ar-40 to Ar-39 ages of the large impact structures Kara and Manicouagan and their relevance to the Cretaceous-Tertiary and the Triassic-Jurassic boundary p 122 N93-10188

STRATIFICATION

Thermal stratification potential in rocket engine coolant channels p 18 N93-10019

STRATIFIED FLOW

Thermal stratification potential in rocket engine coolant channels p 18 N93-10019

STRATIGRAPHY

A quasi-Hertzian stress field from an internal source: A possible working model for the Vredefort structure p 106 N93-10115

Sudbury project (University of Muenster-Ontario Geological Survey): Origin of the polymict, allochthonous breccias of the Onaping Formation p 106 N93-10116

Sudbury project (University of Muenster-Ontario Geological Survey): Summary of results - an updated impact model p 106 N93-10117

Sudbury project (University of Muenster-Ontario Geological Survey): Field studies 1984-1989 - summary of results p 107 N93-10119

Intrusive origin of the Sudbury Igneous Complex: Structural and sedimentological evidence p 108 N93-10128

Ordovician impacts at sea in Baltoscandia p 116 N93-10159

Does the sedimentology of the Chelmsford formation provide evidence for a meteorite impact origin of the Sudbury structure? p 116 N93-10160

K/T boundary stratigraphy: Evidence for multiple impacts and a possible comet stream p 120 N93-10180

Geological evidence for a 2.6-Ga strewn field of impact spherules in the Hamersley Basin of Western Australia p 120 N93-10181

Sudbury project (University of Muenster-Ontario Geological Survey): Petrology, chemistry, and origin of breccia formations p 121 N93-10185

A late Devonian impact event and its association with a possible extinction event on Eastern Gondwana p 122 N93-10191

STRESS (PHYSIOLOGY)

A prospective evaluation of stress fractures/overuse injuries in a population of West Point cadets [AD-A252427] p 132 N93-10709

STRESS (PSYCHOLOGY)

DoD space radiation concerns [AD-A253135] p 131 N93-10613

STRESS ANALYSIS

Instrumented propellant block test and stress analysis comparison p 15 N93-10002

A three-dimensional analysis of the effect of local stress distribution near crack tip p 15 N93-10003

Determination of the dynamic unload/reload characteristics of ceramics [AD-A253513] p 35 N93-10221

Sensor and actuator materials for high performance composites [AD-A254178] p 27 N93-10254

Development in the elastic analysis of laminated plates p 44 N93-10468

Numerical simulation of transient crack growth p 48 N93-10488

An assessment of the correspondence principle in comparison to nonlinear viscoelastic theory: A case study p 51 N93-10501

Elasticity analysis of orthotropic beams under three-part bending p 52 N93-10507

Analysis of failure modes in ceramic matrix composite p 28 N93-10508

Experimental and theoretical behavior of adhesively bonded composite structures under tensile stress at the edge vicinity p 53 N93-10515

An improved technique for determining higher order eigenvector coefficients p 64 N93-10565

A prospective evaluation of stress fractures/overuse injuries in a population of West Point cadets [AD-A252427] p 132 N93-10709

STRESS CONCENTRATION

Analysis of a buffer strip laminate with a cutout p 52 N93-10506

Elasticity analysis of orthotropic beams under three-part bending p 52 N93-10507

Comparison of the maximum stress and the stress intensity approach in the analysis of bonded joints p 53 N93-10514

Experimental and theoretical behavior of adhesively bonded composite structures under tensile stress at the edge vicinity p 53 N93-10515

STRESS DISTRIBUTION

Instrumented propellant block test and stress analysis comparison p 15 N93-10002

A three-dimensional analysis of the effect of local stress distribution near crack tip p 15 N93-10003

A quasi-Hertzian stress field from an internal source: A possible working model for the Vredefort structure p 106 N93-10115

Enriched element analysis of bimaterial interface cracks p 47 N93-10484

Integral transform approach to an inertial viscoelastic problem involving moving singularities p 49 N93-10490

Stress patterns in the dynamic tear test p 49 N93-10491

Status of dynamic fracture in brittle solids p 49 N93-10493

Evolution of hybrid-Trefftz FE model: State of the art and future trends p 49 N93-10494

Singular stress distributions at circular holes in composite laminates p 51 N93-10503

Theoretical and experimental investigations concerning the structural integrity of aeroengine compressor discs p 10 N93-10539

Flow over a leading edge with distributed roughness p 6 N93-10549

Design optimization for uniform dynamic strength under multi-modal response p 62 N93-10555

A boundary element and mathematical programming approach for unilateral contact problems p 62 N93-10558

A reappraisal of compound equilibrium finite elements p 63 N93-10561

STRESS INTENSITY FACTORS

A three-dimensional analysis of the effect of local stress distribution near crack tip p 15 N93-10003

Calculation of stress intensity factors in an isotropic multicracked plate: Part 2: Symbolic/numeric implementation [NASA-TM-105823] p 95 N93-10453

Calculation of stress intensity factors in an isotropic multicracked plate. Part 1: Theoretical development [NASA-TM-105766] p 95 N93-10455

Indentation of a precompressed penny-shaped crack p 48 N93-10486

Numerical simulation of transient crack growth p 48 N93-10488

Stress patterns in the dynamic tear test p 49 N93-10491

Comparison of the maximum stress and the stress intensity approach in the analysis of bonded joints p 53 N93-10514

STRESS MEASUREMENT

Instrumented propellant block test and stress analysis comparison p 15 N93-10002

Measurement of aerodynamic shear stress using side chain liquid crystal polymers [AD-A254312] p 40 N93-10770

STRESS RELAXATION

Chronorheological characterization of elastomers p 46 N93-10476

STRESS-STRAIN RELATIONSHIPS

Integrated finite element model of composite materials p 46 N93-10477

Stress and strain of slab type amplifiers [AD-A254246] p 74 N93-10702

STRESS-STRAIN-TIME RELATIONS

Chronorheological characterization of elastomers p 46 N93-10476

STRESSES

Non-linear thermoelasticity of rubberlike solids p 45 N93-10474

Evolution of hybrid-Trefftz FE model: State of the art and future trends p 49 N93-10494

STRING THEORY

Vector superconductivity in cosmic strings [DE92-634923] p 179 N93-10296

Wiggly relativistic strings [DE92-016461] p 170 N93-10434

Research in particle physics beyond the standard model [DE92-012240] p 155 N93-10878

STRIP TRANSMISSION LINES

Proceedings of the Antenna Applications Symposium, volume 1 [AD-A253681] p 68 N93-10301

STRONTIUM ISOTOPES

Sudbury project (University of Muenster-Ontario Geological Survey): Isotope systematics support the impact origin p 109 N93-10131

STRUCTURAL ANALYSIS

Instrumented propellant block test and stress analysis comparison p 15 N93-10002

A three-dimensional analysis of the effect of local stress distribution near crack tip p 15 N93-10003

The integration of geometric modeling into an inverse design method and application of a PC-based inverse design method and comparison with test results p 78 N93-10058

Radial turbine cooling p 78 N93-10061

Structural analysis: Fatigue life assessment p 78 N93-10062

Proceedings of the Twelfth Canadian Congress of Applied Mechanics, volumes 1 and 2 [ISBN-0920049-03] p 44 N93-10466

A multilayered shell finite element p 49 N93-10495

Variational formulation of a mixed method for second order frame analysis p 62 N93-10556

Evaluation of the triangular plate element of Zienkiewcz and Lefebvre p 63 N93-10562

A boundary element super-element method for coupling with the finite element method of substructures p 64 N93-10566

Numerical simulation of the propagation of coupled thermomechanical waves in inelastic solids p 64 N93-10568

Modelling of flexible multibody dynamics and a computer method via the bond graph method p 65 N93-10573

Solving large linearized systems in mechanics [AD-A252723] p 144 N93-10639

STRUCTURAL BASINS

Shocked zircons in the Onaping Formation: Further proof of impact origin p 107 N93-10121

New perspectives on the Popigai impact structure p 110 N93-10138

Venusian impact basins and cratered terrains p 112 N93-10145

Does the sedimentology of the Chelmsford formation provide evidence for a meteorite impact origin of the Sudbury structure? p 116 N93-10160

Impact origin of the Sudbury structure: Evolution of a theory p 116 N93-10161

Imaging radar investigations of the Sudbury structure
p 117 N93-10162
Sudbury Breccia and suevite as glacial indicators transported 800 km to Kentland Astrobleme, Indiana
p 117 N93-10165
What can we learn about impact mechanics from large craters on Venus?
p 118 N93-10166
Sudbury project (University of Muenster-Ontario Geological Survey): New investigations on Sudbury breccia
p 118 N93-10167
The pseudotachylites from the Vredefort structure and the Witwatersrand basin
p 119 N93-10174
Coincidences in time of the Imbrium Basin impact and Apollo 15 KREEP volcanic series: Impact-induced melting?
p 119 N93-10175
Apollo 15 impact melts, the age of Imbrium, and the Earth-Moon impact cataclysm
p 120 N93-10176
Recognizing impactor signatures in the planetary record
p 120 N93-10178
K/T boundary stratigraphy: Evidence for multiple impacts and a possible comet stream
p 120 N93-10180
Geological evidence for a 2.6-Ga strewn field of impact spherules in the Hamersley Basin of Western Australia
p 120 N93-10181
The large impact process inferred from the geology of lunar multiring basins
p 121 N93-10184
Sudbury project (University of Muenster-Ontario Geological Survey): Petrology, chemistry, and origin of breccia formations
p 121 N93-10185
Ar-40 to Ar-39 dating of pseudotachylites from the Witwatersrand basin, South Africa, with implications for the formation of the Vredefort Dome
p 122 N93-10189
Al Umchaimin depression, Western Iraq: An impact structure?
p 122 N93-10190
Variation in multiring basic structures as a function of impact angle
p 123 N93-10194
Self-organized rock textures and multiring structure in the Duolun crater
p 123 N93-10195

STRUCTURAL DESIGN
A new deployable mast
p 14 N93-10511

STRUCTURAL DESIGN CRITERIA
Structural analysis: Fatigue life assessment
p 78 N93-10062

STRUCTURAL ENGINEERING
List of publications, 1969-1991. Panel on wind and seismic effects
[PB92-201102]
p 125 N93-10089
Inspection and repair decisions for hydraulic structures under symmetric deterioration
[AD-A253621]
p 96 N93-10797

STRUCTURAL FAILURE
A spline finite strip method for analysing local and distortional buckling of thin-walled beams under arbitrary loading
p 58 N93-10538

STRUCTURAL MEMBERS
Lightweight deployable antenna system
[AD-D015291]
p 67 N93-10096

STRUCTURAL PROPERTIES (GEOLOGY)
Sudbury project (University of Muenster-Ontario Geological Survey): Origin of the polymict, allochthonous breccias of the Onaping Formation
p 106 N93-10116
Sudbury project (University of Muenster-Ontario Geological Survey): Summary of results - an updated impact model
p 106 N93-10117
Structural aspects of the Araguainha impact structure (Brazil)
p 106 N93-10118
Sudbury project (University of Muenster-Ontario Geological Survey): Field studies 1984-1989 - summary of results
p 107 N93-10119
Suevite superposition on the Bunte breccia in Noerdlinger Ries, Germany: New findings on the transport mechanism of impactites
p 107 N93-10122
Hong Kong is an impact crater: Proof from the geomorphological and geological evidence
p 107 N93-10124
Structural review of the Vredefort dome
p 108 N93-10127
Intrusive origin of the Sudbury Igneous Complex: Structural and sedimentological evidence
p 108 N93-10128
Does the Bushveld-Vredefort system (South Africa) record the largest known terrestrial impact catastrophe?
p 109 N93-10134
New perspectives on the Popigai impact structure
p 110 N93-10138
Asteroids and Archaean crustal evolution: Tests of possible genetic links between major mantle/crust melting events and clustered extraterrestrial bombardments
p 110 N93-10140
Venusian impact basins and cratered terrains
p 112 N93-10145
Where's the Beaverhead beef? --- meteorite impact structure
p 112 N93-10146
Large impacts in the Baltic shield with special attention to the Uppland structure
p 113 N93-10149
The Panther Mountain circular structure, a possible buried meteorite crater
p 113 N93-10150
Impact origin of the Sudbury structure: Evolution of a theory
p 116 N93-10161
Sudbury project (University of Muenster-Ontario Geological Survey): New investigations on Sudbury breccia
p 118 N93-10167
A history of the Lonar crater, India: An overview
p 118 N93-10168
SAR in support of geological investigations of the Sudbury structure
p 103 N93-10182
Ar-40 to Ar-39 ages of the large impact structures Kara and Manicouagan and their relevance to the Cretaceous-Tertiary and the Triassic-Jurassic boundary
p 122 N93-10188

STRUCTURAL RELIABILITY
Theoretical and experimental investigations concerning the structural integrity of aeroengine compressor discs
p 10 N93-10539

STRUCTURAL STABILITY
A multilayered shell finite element
p 49 N93-10495

STRUCTURAL VIBRATION
Characterization of and active control of flexible structures, using piezoceramics as sensors and actuators
p 10 N93-10319
Design and implementation of digital filters for analysis of F/A-18 flight test data
[AD-A253447]
p 3 N93-10342
Proceedings of the Twelfth Canadian Congress of Applied Mechanics, volumes 1 and 2
[ISBN-0920049-03]
p 44 N93-10466
Vibration of laminated composite plates using various plate theories: Analytical and finite element results
p 45 N93-10473
Vibrations of a flexible Timoshenko beam under gravity
p 53 N93-10512
Overview of the vibroimpact damping of packaged particles
p 56 N93-10528
Mode localization in a simple continuum model
p 56 N93-10529
Experimental investigation of simple support condition in free vibration analysis of plates
p 56 N93-10530
Flexural vibration of beams with varying section properties
p 57 N93-10531
Natural vibrations of multilayered doubly curved shells
p 57 N93-10532
Free vibrations of the thick circular cylindrical shells and rings
p 57 N93-10533
Vibration frequencies of a constrained cantilever wedge
p 57 N93-10534
On the vibration of axisymmetric shells
p 57 N93-10535
The vibrations of annular discs: A comparison of experimental and two analytical techniques
p 58 N93-10536
Characteristics of separated flows including cavitation effects
p 84 N93-10874

STRUTS
Mechanical behavior of open cell ceramics
[PB92-212984]
p 37 N93-10439

STUDENTS
The levels of mathematics achievement: Initial performance standards for the 1990 NAEP mathematics assessment, volume 3
[PB92-199421]
p 134 N93-10341
Change analysis
[AD-A253567]
p 146 N93-10795

STYROFOAM (TRADEMARK)
Nonlinear aeroelasticity of composite structures
[AD-A254285]
p 8 N93-10842

SUBDUCTION (GEOLOGY)
Worldwide seismic catalog and the nature of seismic coupling
p 124 N93-10376

SUBSONIC FLOW
Improved numerical simulation of Euler equations
p 80 N93-10309
Mechanisms of sound generation in subsonic jets
p 152 N93-10688

SUBSONIC SPEED
Non-propulsive aerodynamic noise
p 149 N93-10673
Prediction of jet mixing noise for high subsonic flight speeds
p 151 N93-10685

SUBSONIC WIND TUNNELS
Further noise measurements in a slotted cryogenic wind tunnel
[RAE-TM-AERO-2201]
p 153 N93-10805

SUBSTRATES
UV spectrum splitting mirror
[DE92-018057]
p 159 N93-10818
Atomic force microscope studies of CuCl island formation on CaF2(111) substrates
[AD-A252499]
p 34 N93-10880

SUMMER
Atlas of Southern Hemisphere 500 mb teleconnection patterns derived from National Meteorological Center analyses
[PB92-203892]
p 126 N93-10337
Morning-evening differences in global and regional oceanic precipitation as observed by the SSM/I
p 127 N93-10651

SUN
Ground-based high angular resolution observation of the Sun by interferometry in the visible
p 177 N93-10941

SUPERCONDUCTING FILMS
Vortices in long Josephson junctions
[AD-A253230]
p 167 N93-10404
Prototype superconducting planar transformers using high-Tc thin and thick films
[AD-A254230]
p 77 N93-10897

SUPERCONDUCTING MAGNETS
Development of high temperature superconductors for magnetic field applications
[DE92-015930]
p 168 N93-10733

SUPERCONDUCTIVITY
Semiclassical quantization of interacting anyons in a strong magnetic field
[DE92-634889]
p 169 N93-10229
Semiclassical quantization of integrable systems of few interacting anyons in a strong magnetic field
[DE92-634892]
p 170 N93-10295
Vector superconductivity in cosmic strings
[DE92-634923]
p 179 N93-10296
Covalent electron transfer theory of superconductivity
[AD-A253975]
p 74 N93-10718

SUPERCONDUCTORS
Internal explosion in laser ablation of superconducting targets
[AD-A253701]
p 90 N93-10799
Assessment study of superconducting fault-current limiters operating at 77 K
[DE92-015273]
p 76 N93-10831
Electronic structure of highly correlated structures
[DE92-017017]
p 155 N93-10863

SUPERLATTICES
Growth, nitrogen vacancy reduction, and solid solution formation in cubic GaN thin films and the subsequent fabrication of superlattice structures using AlN and InN
[AD-A253331]
p 166 N93-10356

SUPERPOSITION (MATHEMATICS)
Elasticity analysis of orthotropic beams under three-part bending
p 52 N93-10507

SUPERSONIC AIRCRAFT
LV software for supersonic flow analysis
[NASA-CR-190911]
p 2 N93-10069

SUPERSONIC BOUNDARY LAYERS
On the coupling between a supersonic boundary layer and a flexible surface
[NASA-CR-189697]
p 82 N93-10757

SUPERSONIC COMBUSTION RAMJET ENGINES
A configuration development strategy for the NASP
p 9 N93-10011
Hypersonic inlet efficiency revisited
p 5 N93-10012
Pitot survey of exhaust flow field of a 2-D scramjet nozzle at Mach 6 with air or freon and argon used for exhaust simulation
[NASA-TM-4361]
p 2 N93-10071

SUPERSONIC COMPRESSORS
Explicit Navier-Stokes computation of turbomachinery flows
p 81 N93-10370

SUPERSONIC FLIGHT
Boom and the problems related to the supersonic flights of military aircraft
p 149 N93-10677

SUPERSONIC FLOW
Supersonic confined jet nozzles
p 16 N93-10009
LV software for supersonic flow analysis
[NASA-CR-190911]
p 2 N93-10069
A finite element method for nonlinear panel flutter
p 45 N93-10472
High-resolution TVD schemes for the analysis of: 1. Inviscid supersonic and transonic flows. 2. Viscous flows with shock-induced separation and heat transfer
p 5 N93-10889

SUPERSONIC INLETS
Evaluation and application of the Baldwin-Lomax turbulence model in two-dimensional, unsteady, compressible boundary layers with and without separation in engine inlets
[NASA-TM-105810]
p 79 N93-10087

SUPERSONIC JET FLOW
Supersonic confined jet nozzles
p 16 N93-10009
Supersonic acoustic source mechanisms for free jets of various geometries
p 150 N93-10680
Nozzle installation effects on the noise from supersonic exhaust plumes
p 150 N93-10681
The prediction of noise radiation from supersonic elliptic jets
p 151 N93-10684

SUPERSONIC SPEED
Control of panel flutter at high supersonic speed
p 9 N93-10900
SUPERSONICS
Effect of planform and body on supersonic aerodynamics of multibody configurations
[NASA-TP-3212] p 4 N93-10824
SUPERSYMMETRY
Mass and mixing angle patterns in the standard model and its material supersymmetric extension
[DE92-016197] p 153 N93-10291
SUPPLYING
EIA publications directory, 1991
[DE92-015686] p 174 N93-10607
SUPPORT SYSTEMS
An analysis technique for examining integration in a project support environment
[AD-A253351] p 135 N93-10214
Software support for programming in the large
[AD-A254050] p 138 N93-10782
SUPPORTS
Experimental investigation of simple support condition in free vibration analysis of plates p 56 N93-10530
SURFACE DIFFUSION
Atomic force microscope studies of CuCl island formation on CaF2(111) substrates
[AD-A252499] p 34 N93-10880
SURFACE EMITTING LASERS
Spatial light modulators with arbitrary quantum well profiles
[AD-A253637] p 165 N93-10210
SURFACE PROPERTIES
Nonlinear studies of surface and interfaces of advanced semiconductor materials
[AD-A253365] p 164 N93-10105
The interaction of UV-Laser radiation with metal and semiconductor surfaces
[AD-A253510] p 87 N93-10201
SURFACE REACTIONS
Atomic hydrogen: A reagent for the extraction of chemical species from silicon surfaces
[AD-A252804] p 30 N93-10266
Comparison of Cl and HCl adsorption on Si(100)-(2 x 1)
[AD-A252802] p 30 N93-10281
Hydrocarbon surface chemistry on Si(100)
[AD-A252803] p 27 N93-10465
SURFACE ROUGHNESS
Pre-oxidation anneal kinetics: Interface degradation of thin SiO2 films on silicon
[AD-A253142] p 30 N93-10414
Fractals and multifractals in fracture
p 50 N93-10497
Shock wave diffractions over semi-circular and half-diamond cylinders p 60 N93-10546
Flow over a leading edge with distributed roughness
p 6 N93-10549
Analytical characterization of bistatic scattering from Gaussian distributed surfaces
[AD-A254253] p 159 N93-10724
SURFACE TEMPERATURE
Long-term data collection and empirical background temperature modeling
[AD-A254044] p 127 N93-10780
SURVEILLANCE
Semiconductor phase conjugation
[AD-A253684] p 166 N93-10345
SURVEILLANCE RADAR
Beam forming antenna system
[PATENT-1-265-236] p 67 N93-10111
A description of the Mode Select beacon system (Mode S) and its associated benefits to the National Airspace System (NAS)
[DOT/FAA/SE-92/6] p 7 N93-10738
SURVEYS
TIGER5: Extraction of geographic information from the TIGER system
[DE92-014935] p 171 N93-10382
A survey of commercial object-oriented database management systems
[NASA-CR-190645] p 172 N93-10452
Aerospace and defence-related industries statistical survey report, 1991
[CTN-92-60514] p 2 N93-10652
SURVIVAL
De Finetti representations of survival functions level to a product measure
[AD-A253623] p 146 N93-10107
SWAZILAND
Early Archean spherule beds of possible impact origin from Barberton, South Africa: A detailed mineralogical and geochemical study p 115 N93-10155
SWEDEN
Impact cratering record of Fennoscandia
p 119 N93-10171
SWEPT WINGS
Effect of planform and body on supersonic aerodynamics of multibody configurations
[NASA-TP-3212] p 4 N93-10824
SWIRLING
Turbulence modeling of the flow field in combustors using the non-linear k-epsilon model
[DE92-014745] p 80 N93-10330
Investigations into swirling flows of Newtonian and non-Newtonian fluids
[AD-A253298] p 82 N93-10696
The effects of streamline curvature and swirl on turbulent flows in curved ducts p 84 N93-10875
SWITCHES
Long conduction time plasma opening switch experiments at Sandia National Labs
[DE92-015003] p 72 N93-10279
SWITCHING
Architecture and device development for optical networks
[AD-A253247] p 158 N93-10693
SWITCHING CIRCUITS
Twenty-five KA, 5000V solid state opening switch for inductive energy stores
[AD-A253968] p 73 N93-10421
Semiconductor-metal eutectic composites for high power switching
[AD-A253930] p 74 N93-10755
SYMBOLIC PROGRAMMING
Calculation of stress intensity factors in an isotropic multicracked plate: Part 2: Symbolic/numeric implementation
[NASA-TM-105823] p 95 N93-10453
SYMMETRICAL BODIES
Improved numerical simulation of Euler equations
p 80 N93-10309
SYNCHROTRON RADIATION
Synchrotron radiation considerations in the Dense Plasma Focus (DPF) Magnetoplasmadynamic (MPD) thruster
[AD-A254188] p 25 N93-10258
High pressure and synchrotron radiation studies of solid state electronic instabilities
[DE92-015661] p 168 N93-10630
UV/XUV FEL storage ring and linac
[AD-A253307] p 89 N93-10697
Thermal, structural, and diffraction analyses of a gallium-cooled x ray monochromator
[DE92-017063] p 157 N93-10837
SYNCHROTRONS
Particle production at high p(sub (perpendicular)) in (sup 28)Si + A collisions at 14.6 A x GeV/c
[DE92-016939] p 154 N93-10402
SYNTHESIS (CHEMISTRY)
Synthesis and characterization of energetic polymers
p 15 N93-10005
Biological production of ethanol from coal
[DE92-016116] p 41 N93-10216
Water soluble polysiloxanes with pendant 1-oxypyridin-3-yl groups
[AD-A250637] p 36 N93-10246
Development of electrosupercapacitors
[AD-A252208] p 71 N93-10250
Polynitro polycyclic cage compounds
[AD-A252889] p 42 N93-10268
Developmental research on ultra abrasion-resistant materials
[DE92-531066] p 36 N93-10287
SYNTHETIC APERTURE RADAR
SAR in support of geological investigations of the Sudbury structure p 103 N93-10182
Open Skies Treaty imaging radar technology issues
[DE92-016548] p 68 N93-10394
SYNTHETIC APERTURES
Rotational aperture synthesis: A proposal for ground-based observations p 178 N93-10947
SYSTEM IDENTIFICATION
The mechanical verification of a simple control system
[ORA-TR-89-5443-04] p 142 N93-10641
SYSTEMS ENGINEERING
Recovery techniques for real time electronic systems
[AD-A254010] p 136 N93-10361
Maintaining future military aircraft design capability
[AD-A253963] p 8 N93-10420
System model development for nuclear thermal propulsion
[NASA-TM-105761] p 25 N93-10457
TAQL: A problem space tool for expert system development
[AD-A253820] p 175 N93-10826
A spatial similarity measure for image database applications
[AD-A253570] p 176 N93-10883
SUN: The Solar Ultraviolet Network
p 183 N93-10930
The solar ultraviolet network: Performance and tolerance analysis p 187 N93-10950
The imaging Fourier transform spectrometer optical design p 159 N93-10951
Interferometer optical design for the Imaging Fourier Transform Spectrometer (IFTS) p 159 N93-10955
Requirements analysis notebook for the flight data systems definition in the Real-Time Systems Engineering Laboratory (RSEL)
[NASA-CR-185698] p 14 N93-10960
SYSTEMS INTEGRATION
Reliability assurance requirements for ESA space systems
[ESA-PSS-01-30-ISSUE-2] p 94 N93-10317
Holographic optical interconnects for multichip modules
[AD-A253403] p 86 N93-10408
System integration issues in digital photogrammetric mapping
[AD-A254046] p 103 N93-10781
SYSTEMS MANAGEMENT
Power system monitoring and source control of the Space Station Freedom DC power system testbed
[NASA-TM-105841] p 26 N93-10734
SYSTEMS STABILITY
A survey of instabilities within centrifugal pumps and concepts for improving the flow range of pumps in rocket engines p 23 N93-10039
A nonlinear oscillatory problem
[DE92-630203] p 95 N93-10385
Network stability under viral attack: A game entitled, God and the Devil
[RSRE-MEMO-4405] p 147 N93-10822

T

TAIL ASSEMBLIES
Design and implementation of digital filters for analysis of F/A-18 flight test data
[AD-A253447] p 3 N93-10342
TARGET ACQUISITION
Integrated vision system for a target seeker
[AD-A253359] p 135 N93-10103
Mathematical analysis of multi-sensor cross-correlation processing for source localization
[DREA-CR-89-433] p 68 N93-10366
Nonlinear signal processing schemes for robust target detection and automatic clutter rejection in radar
[AD-A253546] p 68 N93-10380
TARGET RECOGNITION
Integrated vision system for a target seeker
[AD-A253359] p 135 N93-10103
TASKS
Operator workload predictions for the revised AH-64A workload prediction model, volume 1
[AD-A254198] p 133 N93-10261
TAYLOR SERIES
On the evaluation of Bessel functions
[AD-A253129] p 143 N93-10339
TECHNOLOGY ASSESSMENT
Testing techniques p 78 N93-10060
Structural analysis: Fatigue life assessment
p 78 N93-10062
Soviet optical processing research. FSAC Technical Assessment Report (TAR)
[PB92-195569] p 172 N93-10431
TECHNOLOGY TRANSFER
List of publications, 1969-1991. Panel on wind and seismic effects
[PB92-201102] p 125 N93-10089
TECTONICS
Structural review of the Vredefort dome
p 108 N93-10127
Impactite and pseudotachylite from Roter Kamm Crater, Namibia p 109 N93-10130
The pseudotachylites from the Vredefort structure and the Witwatersrand basin p 119 N93-10174
Bronzite Granophyre: New insight on Vredefort
p 121 N93-10186
Ar-40 to Ar-39 dating of pseudotachylites from the Witwatersrand basin, South Africa, with implications for the formation of the Vredefort Dome
p 122 N93-10189
Floor-fractured crater models of the Sudbury structure, Canada p 123 N93-10193
Variation in multiring basic structures as a function of impact angle p 123 N93-10194
Worldwide seismic catalog and the nature of seismic coupling p 124 N93-10376
TEKTITES
Tektite origin by hypervelocity asteroidal or cometary impact: The quest for the source craters
p 114 N93-10154
Search for the 700,000-year-old source crater of the Australasian tektite strewn field p 120 N93-10177

TELECOMMUNICATION
Acquisition 2: Procurement, acquisition, and maintenance of configuration management documentation in support of a CIS system p 173 N93-10599
TELECONNECTIONS (METEOROLOGY)
Atlas of Southern Hemisphere 500 mb teleconnection patterns derived from National Meteorological Center analyses
[PB92-203892] p 126 N93-10337
TELESCOPES
Evidence of plasmoid ejection in the corona from 1991 eclipse observations with the Canada-France-Hawaii telescope p 181 N93-10915
The CHARON program p 177 N93-10942
Interferometry with the Very Large Telescope p 178 N93-10943
Ground/space co-operation for interferometry p 178 N93-10946
Mechanical and thermal design of the SUN instrument p 14 N93-10956
TEMPERATURE CONTROL
Thermal management in high average power pulsed compression systems
[DE92-017055] p 76 N93-10836
SUN: The Solar Ultraviolet Network p 183 N93-10930
TEMPERATURE DEPENDENCE
Oxygen barrier oxides
[AD-A253683] p 36 N93-10343
Covalent electron transfer theory of superconductivity
[AD-A253975] p 74 N93-10718
Activated transport in AMTEC electrodes
[DE92-016810] p 75 N93-10786
TEMPERATURE DISTRIBUTION
Thermal stratification potential in rocket engine coolant channels p 18 N93-10019
TEMPERATURE EFFECTS
The effect of elevated temperatures on the properties of thermally stable silicon-based elastomers for adhesives, sealants, and insulator applications p 15 N93-10006
Influence of the preshock temperature on shock effects in quartz p 115 N93-10157
Temperature-programmed oxidation of ethane and ethylene in the presence and absence of C-13 labeled methane
[DE92-015048] p 42 N93-10329
Chemical and thermal stability of refrigerant-lubricant mixture with metal
[DE92-015117] p 44 N93-10398
Heat transfer and pressure drop for air flow through enhanced passages
[DE92-016597] p 82 N93-10612
High temperature fatigue crack growth in ceramics and ceramic composites
[DE92-016835] p 40 N93-10632
TEMPERATURE MEASUREMENT
Species and temperature measurement in H2/O2 rocket flow fields by means of Raman scattering diagnostics
[NASA-CR-189217] p 25 N93-10086
TEMPERATURE PROFILES
Internal explosion in laser ablation of superconducting targets
[AD-A253701] p 90 N93-10799
TEMPLATES
An indicator of message quality for a single optical sensor using a template based tracking algorithm
[AD-A252704] p 139 N93-10881
TEMPORAL DISTRIBUTION
Mathematical analysis of multi-sensor cross-correlation processing for source localization
[DREA-CR-89-433] p 68 N93-10366
TEMPORAL RESOLUTION
Observation of solar flares at high resolution p 182 N93-10923
TENSILE DEFORMATION
Experimental and numeric analysis of constraints in a bonded stepped lap joint subjected to traction p 54 N93-10516
TENSILE PROPERTIES
Tensile properties of cast titanium alloys: Titanium-6Al-4V ELI and Titanium-5Al-2.5Sn ELI
[NASA-TP-3288] p 33 N93-10072
TENSILE STRESS
Experimental and theoretical behavior of adhesively bonded composite structures under tensile stress at the edge vicinity p 53 N93-10515
TENSILE TESTS
Transverse tension, transverse compression, and inplane shear JANNAF round robin test methods standardization results p 16 N93-10007
TERMINAL BALLISTICS
Determination of the dynamic unload/reload characteristics of ceramics
[AD-A253513] p 35 N93-10221
TERNARY ALLOYS
Theory of transport for interacting many-body systems
[AD-A253789] p 169 N93-10871
TERRAIN
Advanced terrain displays to transport category aircraft
[PB92-197136] p 6 N93-10065
Millimeter wave measurement and modeling of terrain scattering
[AD-A253525] p 67 N93-10223
Analysis of reception variability due to terrain multipath on microwave common carrier links
[NTIA-92-283] p 69 N93-10430
System integration issues in digital photogrammetric mapping
[AD-A254046] p 103 N93-10781
TERRAIN FOLLOWING AIRCRAFT
Appraisal of digital terrain elevation data for low-altitude flight
[NASA-TM-103896] p 7 N93-10745
TEST EQUIPMENT
High sensitivity probes for silicon VLSI internal node testing
[AD-A253924] p 169 N93-10764
TEST FACILITIES
Facility for cold flow testing of solid rocket motor models p 11 N93-10021
Noise studies for environmental impact assessment of an outdoor engine test facility p 149 N93-10672
Improve SSME power balance model
[NASA-CR-184464] p 26 N93-10756
Magnetohydrodynamic projects at the CDIF
[DE92-018190] p 164 N93-10819
An experimental technique for performing 3-D LDA measurements inside whirling annular seals p 93 N93-10894
A multipurpose vacuum-ultraviolet test facility p 11 N93-10953
TEST FIRING
Hot fire test results of subscale tubular combustion chambers p 18 N93-10020
TEST RANGES
Test range tracking network processors
[AD-A253511] p 140 N93-10219
TEST STANDS
Testing techniques p 78 N93-10060
TESTING TIME
System model development for nuclear thermal propulsion
[NASA-TM-105761] p 25 N93-10457
TESTS
Change analysis
[AD-A253567] p 146 N93-10795
TETHERLINES
Experimental demonstration of offset control with an application to the tethered payload p 14 N93-10521
TEXTURES
Self-organized rock textures and multiring structure in the Duolun crater p 123 N93-10195
THAILAND
Search for the 700,000-year-old source crater of the Australasian tektite strewn field p 120 N93-10177
THEOREM PROVING
Global structure of a polynomial autonomous system on the plane
[DE92-630230] p 144 N93-10389
THEORETICAL PHYSICS
Research in theoretical particle physics
[DE92-016181] p 154 N93-10605
Research program in experimental and theoretical high energy physics
[DE92-016219] p 156 N93-10618
THERMAL ANALYSIS
Tank chilldown analysis and verification with a flightweight, 175 cu ft tank under normal gravity with liquid hydrogen p 24 N93-10045
Shortened Test Heating Season (STHS) p 43 N93-10314
The solar ultraviolet network: Performance and tolerance analysis p 187 N93-10950
Mechanical and thermal design of the SUN instrument p 14 N93-10956
THERMAL BUCKLING
Thermal buckling of heated laminated composite circular cylindrical shells p 51 N93-10504
THERMAL CONTROL COATINGS
Changes in oxidation state of chromium during LDEF exposure p 34 N93-10581
THERMAL CYCLING TESTS
Hot fire fatigue testing results for the compliant combustion chamber p 22 N93-10038
Damage accumulation process in advanced metal matrix composite under thermal cycling
[AD-A248674] p 27 N93-10277
Hot fire fatigue testing results for the compliant combustion chamber
[NASA-TP-3223] p 26 N93-10743
Hubble Space telescope thermal cycle test report for large solar array samples with BSFR cells (Sample numbers 703 and 704)
[NASA-TM-108373] p 104 N93-10809
THERMAL DECOMPOSITION
Epitaxial magnetic oxides
[AD-A253667] p 35 N93-10230
THERMAL ENERGY
VH-mode discharges in the D3-D tokamak
[DE92-016257] p 161 N93-10463
THERMAL EXPANSION
Hot fire fatigue testing results for the compliant combustion chamber p 22 N93-10038
Hot fire fatigue testing results for the compliant combustion chamber
[NASA-TP-3223] p 26 N93-10743
THERMAL FATIGUE
Hot fire fatigue testing results for the compliant combustion chamber p 22 N93-10038
High temperature fatigue crack growth in ceramics and ceramic composites
[DE92-016835] p 40 N93-10632
Mechanisms and modelling of environment-dependent fatigue crack growth in a nickel based superalloy
[AD-A253967] p 33 N93-10717
Hot fire fatigue testing results for the compliant combustion chamber
[NASA-TP-3223] p 26 N93-10743
THERMAL SHOCK
Mechanical behavior of open cell ceramics
[PB92-212984] p 37 N93-10439
THERMAL STABILITY
The effect of elevated temperatures on the properties of thermally stable silicon-based elastomers for adhesives, sealants, and insulator applications p 15 N93-10006
Chemical and thermal stability of refrigerant-lubricant mixture with metal
[DE92-015117] p 44 N93-10398
THERMAL STRESSES
Effects of anode material on arcjet performance p 23 N93-10044
Effects of anode material on arcjet performance
[NASA-TM-105799] p 25 N93-10197
Damage accumulation process in advanced metal matrix composite under thermal cycling
[AD-A248674] p 27 N93-10277
THERMIONIC EMISSION
Fundamental studies on erosion in MPD thrusters
[AD-A253900] p 159 N93-10252
THERMOCHEMISTRY
Atomic approaches to defect thermochemistry
[AD-A254278] p 167 N93-10425
THERMODYNAMIC CYCLES
Magnetohydrodynamic projects at the CDIF
[DE92-018190] p 164 N93-10819
MHD Integrated Topping Cycle Project
[DE92-016610] p 164 N93-10861
THERMODYNAMIC PROPERTIES
A globally well-posed accurate and efficient finite element CFD algorithm for compressible aerodynamics p 3 N93-10306
Transition metal activation and functionalization of carbon-hydrogen bonds
[DE92-014809] p 30 N93-10400
THERMODYNAMICS
Compound cycle engine for helicopter application
[NASA-CR-180824] p 9 N93-10348
Atomic approaches to defect thermochemistry
[AD-A254278] p 167 N93-10425
Entropy of disorder in thermomechanics of damage in heterogeneous solids p 50 N93-10498
Damage due to plastic deformation in elastic-plastic materials: The thermodynamical connection p 51 N93-10502
Investigations of the dynamics and thermodynamics of the mesosphere lower thermosphere and upper thermosphere at the polar regions with optical ground-based remote sensing
[AD-A253228] p 125 N93-10711
Local-equilibrium formalism applied to mechanics of solids
[DE92-016852] p 170 N93-10787
THERMOELASTICITY
Non-linear thermoelasticity of rubberlike solids p 45 N93-10474
THERMOELECTRIC GENERATORS
Activated transport in AMTEC electrodes
[DE92-016810] p 75 N93-10786
THERMOPHYSICAL PROPERTIES
Materials compatibility and lubricants research on CFC-refrigerant substitutes: Thermophysical properties
[DE92-015116] p 43 N93-10397

THERMOPLASTICITY
Mechanics of composite materials for spacecraft
[AD-A254217] p 28 N93-10896
THERMOSPHERE
Investigations of the dynamics and thermodynamics of the mesosphere lower thermosphere and upper thermosphere at the polar regions with optical ground-based remote sensing
[AD-A253228] p 125 N93-10711
THESAURI
Document processing p 174 N93-10600
THICK FILMS
Piezoelectric and electrostrictive materials for transducers applications, volume 4
[AD-A250892] p 72 N93-10282
Prototype superconducting planar transformers using high-Tc thin and thick films
[AD-A254230] p 77 N93-10897
THICK PLATES
Compression buckling of thick orthotropic plates with a step thickness change p 46 N93-10478
Nonstationary random variations of moderately thick plates using BEM p 48 N93-10487
Linear and nonlinear analyses of thick composite circular plates using the finite element method
p 96 N93-10873
THICKNESS
Ultrasonic characterization of highly attenuative thick composites
[AD-A253347] p 27 N93-10272
THIN FILMS
Nonlinear studies of surface and interfaces of advanced semiconductor materials
[AD-A253365] p 164 N93-10105
Piezoelectric and electrostrictive materials for transducers applications, volume 1
[AD-A250889] p 71 N93-10273
Piezoelectric and electrostrictive materials for transducers applications, volume 2
[AD-A250890] p 71 N93-10276
Piezoelectric and electrostrictive materials for transducers applications, volume 4
[AD-A250892] p 72 N93-10282
Intense ion beam research at Los Alamos
[DE92-015240] p 155 N93-10333
Pseudomorphic semiconducting heterostructures from combinations of AlN, GaN, and selected SiC polytypes: Theoretical advancement and its coordination with experimental studies of nucleation, growth, characterization, and device development
[AD-A253330] p 166 N93-10355
Growth, nitrogen vacancy reduction, and solid solution formation in cubic GaN thin films and the subsequent fabrication of superlattice structures using AlN and InN
[AD-A253331] p 166 N93-10356
Simple shearing flow of a 3D foam
[DE92-011151] p 36 N93-10399
Vortices in long Josephson junctions
[AD-A253230] p 167 N93-10404
Pre-oxidation anneal kinetics: Interface degradation of thin SiO2 films on silicon
[AD-A253142] p 30 N93-10414
Novel Si-YBCuO reactive patterning technique for manufacture of large area high Tc superconducting electronic devices
[AD-A250740] p 73 N93-10426
Hydrocarbon surface chemistry on Si(100)
[AD-A252803] p 27 N93-10465
Spectroscopic ellipsometric measurements of the dielectric function of germanium dioxide films on crystal germanium
[AD-A253137] p 168 N93-10614
Spectroscopic differential reflectance as an analytical probe for microelectronic processing
[AD-A253134] p 73 N93-10656
Semiconductor-metal eutectic composites for high power switching
[AD-A253930] p 74 N93-10755
Boronization in D3-D
[DE92-016249] p 163 N93-10759
Signal and noise analysis of a-Si:H radiation detector-amplifier system
[DE92-016928] p 75 N93-10790
Atomic force microscope studies of CuCl island formation on CaF2(111) substrates
[AD-A252499] p 34 N93-10880
Prototype superconducting planar transformers using high-Tc thin and thick films
[AD-A254230] p 77 N93-10897
THIN PLATES
On the behavior of a higher-order plate bending element p 47 N93-10481
THIN WALLED SHELLS
SAPNEW: Parallel finite element code for thin shell structures on the Alliant FX/80
[NASA-CR-190663] p 94 N93-10372
THOMSON SCATTERING
Helium transport in enhanced confinement regimes on the TEXTOR and D3-D tokamaks
[DE92-016247] p 160 N93-10293
Studies impacting the designs of free electron lasers
[AD-A254293] p 90 N93-10768
THREE BODY PROBLEM
Computer algebra and the elliptic restricted problem of three bodies p 11 N93-10499
THREE DIMENSIONAL BODIES
Three dimensional curved beam elements with large translations and rotations p 63 N93-10560
THREE DIMENSIONAL BOUNDARY LAYER
Study of a viscous sublayer model in the analysis of 3-D shock/boundary layer interaction flow fields
[AD-A253731] p 84 N93-10886
THREE DIMENSIONAL FLOW
Unstructured mesh algorithms for aerodynamic calculations
[NASA-CR-189685] p 2 N93-10097
Analysis of wing-body junction flowfields using the incompressible Navier-Stokes equations, volumes 1 and 2 p 3 N93-10320
Numerical solution of three-dimensional unsteady viscous flows
[AD-A253202] p 83 N93-10793
THROTTLING
A survey of instabilities within centrifugal pumps and concepts for improving the flow range of pumps in rocket engines p 23 N93-10039
THRUST CHAMBERS
Hot fire fatigue testing results for the compliant combustion chamber p 22 N93-10038
Hot fire fatigue testing results for the compliant combustion chamber
[NASA-TP-3223] p 26 N93-10743
THRUST VECTOR CONTROL
Supersonic confined jet nozzles p 16 N93-10009
Critical engine system design characteristics for SSTO vehicles p 17 N93-10014
Pneumatic motor powered Thrust Vector Control (TVC) for liquid propelled launch vehicles p 17 N93-10015
THRUSTORS
Fundamental studies on erosion in MPD thrusters
[AD-A253900] p 159 N93-10252
TIDAL WAVES
List of publications, 1969-1991. Panel on wind and seismic effects
[PB92-201102] p 125 N93-10089
TILT ROTOR AIRCRAFT
Tilt rotor hover aeroacoustics
[NASA-CR-177598] p 147 N93-10458
TILT WING AIRCRAFT
Initial piloted simulation study of geared flap control for tilt-wing V/STOL aircraft
[NASA-TM-103872] p 11 N93-10741
TIME DEPENDENCE
On the measurement of time-dependent quantum phases
[DE92-630206] p 170 N93-10387
An assessment of the correspondence principle in comparison to nonlinear viscoelastic theory: A case study p 51 N93-10501
A solution scheme for the deflection equations of flexible arms with time-dependent boundary conditions
p 66 N93-10575
Relating flying hours to aircrew performance: Evidence for attack and transport missions
[AD-A253988] p 133 N93-10719
TIME DIVISION MULTIPLE ACCESS
Architecture and device development for optical networks
[AD-A253247] p 158 N93-10693
TIME LAG
Mathematical analysis of multi-sensor cross-correlation processing for source localization
[DREA-CR-89-433] p 68 N93-10366
TIME MARCHING
On techniques for digital simulation of random response of nonlinear oscillators p 55 N93-10523
TIME MEASUREMENT
GPS Army research and applications
[AD-A254262] p 7 N93-10424
TIME SERIES ANALYSIS
Adequate sampling of a chaotic time series
[AD-A254170] p 127 N93-10664
TIME TEMPERATURE PARAMETER
Reactions of Ti and Zr with AlN and Al2O3
[DE92-016234] p 28 N93-10391
TIMOSHENKO BEAMS
Vibrations of a flexible Timoshenko beam under gravity p 53 N93-10512
Response of a beam to transverse impulsive and high frequency loads p 56 N93-10526
TIN ALLOYS
Tensile properties of cast titanium alloys: Titanium-6Al-4V ELI and Titanium-5Al-2.5Sn ELI
[NASA-TP-3288] p 33 N93-10072
TIRES
Stability of open-graded bases under wheel loads using a model testing approach
[AD-A253209] p 66 N93-10710
TISSUES (BIOLOGY)
Method for culturing mammalian cells in a perfused bioreactor
[NASA-CASE-MSC-21293-2] p 129 N93-10109
Method for culturing mammalian cells in a horizontally rotated bioreactor
[NASA-CASE-MSC-21294-2] p 129 N93-10110
Interaction of electromagnetic fields with chondrocytes in gel culture
[AD-A253727] p 70 N93-10747
TITAN LAUNCH VEHICLES
Pneumatic motor powered Thrust Vector Control (TVC) for liquid propelled launch vehicles p 17 N93-10015
TITANATES
Conductive titanate fiber and its production method
[DE92-014738] p 39 N93-10627
TITANIUM
System design and relaxation oscillations of a titanium-sapphire laser
[AD-A254264] p 89 N93-10725
TITANIUM ALLOYS
Tensile properties of cast titanium alloys: Titanium-6Al-4V ELI and Titanium-5Al-2.5Sn ELI
[NASA-TP-3288] p 33 N93-10072
Reactions of Ti and Zr with AlN and Al2O3
[DE92-016234] p 28 N93-10391
Plasticity of single crystalline Al3X intermetallic compounds
[AD-A254282] p 40 N93-10766
Ohmic contacts to compound semiconductors
p 76 N93-10830
TITANIUM BORIDES
Reinforcements for high temperature ceramics
[DE92-014815] p 35 N93-10082
TOKAMAK DEVICES
D-He-3 spherical torus fusion reactor system study
[AD-A253358] p 155 N93-10102
Helium transport in enhanced confinement regimes on the TEXTOR and D3-D tokamaks
[DE92-016247] p 160 N93-10293
An analytic determination of beta poloidal and internal inductance in an elongated tokamak from magnetic probe measurements
[DE92-016294] p 160 N93-10331
Intense ion beam research at Los Alamos
[DE92-015240] p 155 N93-10333
A formula for efficiency of fast wave current drive in fusion devices
[DE92-016152] p 160 N93-10390
Investigation of the effect of large core changes in toroidal plasma rotation and radial electric field on confinement in H-mode discharges in the D3-D tokamak
[DE92-016252] p 161 N93-10392
Polarimetry of motional Stark effect and determination of current profiles in D3-D
[DE92-016258] p 161 N93-10393
VH-mode discharges in the D3-D tokamak
[DE92-016257] p 161 N93-10463
Edge ion dynamics in H-mode discharges in D3-D
[DE92-016255] p 162 N93-10619
The effect of current profile changes on confinement in the D3-D tokamak
[DE92-016256] p 163 N93-10620
Magnetic fusion with high energy self-colliding ion beams
[DE92-016860] p 156 N93-10643
Boronization in D3-D
[DE92-016249] p 163 N93-10759
Global Alfven eigenmodes in D3-D
[DE92-016250] p 163 N93-10760
Variational full wave calculation of fast wave current drive in D3-D using the ALCYON code
[DE92-016572] p 163 N93-10761
TOLERANCES (MECHANICS)
The solar ultraviolet network: Performance and tolerance analysis p 187 N93-10950
The imaging Fourier transform spectrometer: Performance and tolerance analysis p 86 N93-10952
TOLLMIEN-SCHLICHTING WAVES
On the coupling between a supersonic boundary layer and a flexible surface
[NASA-CR-189697] p 82 N93-10757
TOLUENE
Mobility of toluene in polystyrene-toluene solutions: A NMR study
[AD-A253203] p 31 N93-10794

TOMOGRAPHY
Electrical resistance tomography used in environmental restoration
[DE92-018003] p 103 N93-10763
Cognition in the brain: Investigations using positron emission tomography
[AD-A254280] p 132 N93-10765
Tomographic/interferometric studies of active stars and binaries p 182 N93-10920
TOPOGRAPHY
New perspectives on the Popigai impact structure p 110 N93-10138
The Zhamanshin impact feature: A new class of complex crater? p 110 N93-10139
TOPOLOGY
Global structure of a polynomial autonomous system on the plane
[DE92-630230] p 144 N93-10389
TOROIDAL PLASMAS
Investigation of the effect of large core changes in toroidal plasma rotation and radial electric field on confinement in H-mode discharges in the D3-D tokamak
[DE92-016252] p 161 N93-10392
Edge ion dynamics in H-mode discharges in D3-D
[DE92-016255] p 162 N93-10619
TORQUE
A boundary element and mathematical programming approach for unilateral contact problems p 62 N93-10558
TORSION
Characterization of and active control of flexible structures, using piezoceramics as sensors and actuators p 10 N93-10319
TOTAL QUALITY MANAGEMENT
Total Quality Management (TQM) concepts applied to instruction
[DE92-013399] p 171 N93-10270
Space Transportation Engine Program (STEP), phase B
[NASA-CR-184062] p 25 N93-10350
TOUGHNESS
Strength-toughness requirements for thick-walled high pressure vessels
[AD-A253756] p 95 N93-10750
TOXICITY
Limited toxicity and mutagenicity testing of five unicharge propellant compounds
[AD-A252339] p 43 N93-10636
TOXICOLOGY
Guidelines for developing spacecraft maximum allowable concentrations for Space Station contaminants
[NASA-CR-190748] p 13 N93-10737
TRACE CONTAMINANTS
Guidelines for developing spacecraft maximum allowable concentrations for Space Station contaminants
[NASA-CR-190748] p 13 N93-10737
TRACE ELEMENTS
The Deposition and Fate of Trace Metals in our Environment: Symposium proceedings
[PB92-189216] p 104 N93-10289
TRACKING (POSITION)
Eye movements and visual information processing
[AD-A250198] p 132 N93-10278
TRACKING NETWORKS
Test range tracking network processors
[AD-A253511] p 140 N93-10219
TRACTION
A boundary element and mathematical programming approach for unilateral contact problems p 62 N93-10558
TRAFFIC
Stability of open-graded bases under wheel loads using a model testing approach
[AD-A253209] p 66 N93-10710
Selective perception for robot driving
[AD-A253740] p 142 N93-10749
TRAFFIC CONTROL
A new test of scanning and monitoring ability: Methods and initial results
[AD-A249123] p 132 N93-10321
TRAILERS
Generic Propellant Transfer Unit p 11 N93-10046
TRAILING EDGES
Effect of passive flow-control devices on turbulent low-speed base flow p 79 N93-10304
TRAINING SIMULATORS
Possibilities and limitations of flying training in the German Air Force p 11 N93-10668
TRAJECTORY ANALYSIS
Anelastic modelling of explosive cyclogenesis p 126 N93-10377
Computer algebra and the elliptic restricted problem of three bodies p 11 N93-10499
Optimal robot trajectory planning p 65 N93-10570
Research on the asymmetrical aerodynamic forces of reentry vehicles
[AD-A254307] p 4 N93-10707
TRAJECTORY CONTROL
Optimal robot trajectory planning p 65 N93-10570
TRAJECTORY PLANNING
Optimal robot trajectory planning p 65 N93-10570
TRANSDUCERS
Instrumented propellant block test and stress analysis comparison p 15 N93-10002
Transducer workshop no. 16
[AD-A248047] p 12 N93-10236
Piezoelectric and electrostrictive materials for transducers applications, volume 1
[AD-A250889] p 71 N93-10273
Piezoelectric and electrostrictive materials for transducers applications, volume 2
[AD-A250890] p 71 N93-10276
Piezoelectric and electrostrictive materials for transducers applications, volume 3
[AD-A250891] p 72 N93-10280
Piezoelectric and electrostrictive materials for transducers applications, volume 4
[AD-A250892] p 72 N93-10282
Instrument driver for general purpose interface bus (IEEE-488)
[AD-A253947] p 138 N93-10716
TRANSFORMATIONS (MATHEMATICS)
The development of optical techniques for component inspection in the aerospace industry p 93 N93-10307
Discontinuous initial value problem of nonlinear elasticity by similarity approach p 64 N93-10569
Design of laser optical systems
[AD-A254247] p 89 N93-10703
TRANSFORMERS
Prototype superconducting planar transformers using high-Tc thin and thick films
[AD-A254230] p 77 N93-10897
TRANSIENT LOADS
Integral transform approach to an inertial viscoelastic problem involving moving singularities p 49 N93-10490
TRANSISTOR AMPLIFIERS
Development of 6H-SiC CMOS transistors for insertion into a 350 C operational amplifier
[AD-A253760] p 70 N93-10233
Vortices in long Josephson junctions
[AD-A253230] p 167 N93-10404
TRANSISTORS
Development of 6H-SiC CMOS transistors for insertion into a 350 C operational amplifier
[AD-A253760] p 70 N93-10233
A four channel 250 MHz visual counter
[DE92-016920] p 86 N93-10444
TRANSITION FLOW
Flow over a leading edge with distributed roughness p 6 N93-10549
TRANSITION METALS
Transition metal activation and functionalization of carbon-hydrogen bonds
[DE92-014809] p 30 N93-10400
TRANSITION PROBABILITIES
Electron transfer, ionization, and excitation in atomic collisions
[DE92-017300] p 154 N93-10435
TRANSMISSION LOSS
Software for prediction and analysis of ground wave propagation loss
[AD-A253474] p 67 N93-10199
TRANSMITTANCE
UV spectrum splitting mirror
[DE92-018057] p 159 N93-10818
TRANSMITTER RECEIVERS
Software for prediction and analysis of ground wave propagation loss
[AD-A253474] p 67 N93-10199
TRANSONIC FLOW
Interactive grid generation program for CAP-TSD
[NASA-TM-102705] p 3 N93-10349
A field panel method for transonic flows p 6 N93-10547
High-resolution TVD schemes for the analysis of: 1. Inviscid supersonic and transonic flows. 2. Viscous flows with shock-induced separation and heat transfer p 5 N93-10889
TRANSONIC WIND TUNNELS
Further noise measurements in a slotted cryogenic wind tunnel
[RAE-TM-AERO-2201] p 153 N93-10805
TRANSPORT AIRCRAFT
Advanced terrain displays to transport category aircraft
[PB92-197136] p 6 N93-10065
Comparison of all-electric secondary power systems for civil subsonic transports
[NASA-TM-105852] p 9 N93-10456
Aeronautical technologies for the twenty-first century
[NASA-CR-190918] p 1 N93-10647
Relating flying hours to aircrew performance: Evidence for attack and transport missions
[AD-A253988] p 133 N93-10719
Initial piloted simulation study of geared flap control for tilt-wing V/STOL aircraft
[NASA-TM-103872] p 11 N93-10741
TRANSPORT PROPERTIES
Mathematical analysis of strong fluid mechanical effects at high Mach number in reactive and nonreactive flow
[AD-A253617] p 79 N93-10094
Helium transport in enhanced confinement regimes on the TEXTOR and D3-D tokamaks
[DE92-016247] p 160 N93-10293
A formula for efficiency of fast wave current drive in fusion devices
[DE92-016152] p 160 N93-10390
Materials compatibility and lubricants research on CFC-refrigerant substitutes: Thermophysical properties
[DE92-015116] p 43 N93-10397
Theory of transport for interacting many-body systems
[AD-A253789] p 169 N93-10871
TRANSPORT THEORY
Multidimensional deterministic electron transport calculations
[AD-A254021] p 154 N93-10362
A formula for efficiency of fast wave current drive in fusion devices
[DE92-016152] p 160 N93-10390
Theory of transport for interacting many-body systems
[AD-A253789] p 169 N93-10871
TRANSPORTATION
Generic Propellant Transfer Unit p 11 N93-10046
TRANSVERSE OSCILLATION
A solution scheme for the deflection equations of flexible arms with time-dependent boundary conditions p 66 N93-10575
TRAPPING
Laser cooling and trapping of neutral atoms
[AD-A253730] p 155 N93-10885
TRAPS
Optical metrology of magnetically trapped hydrogen
[AD-A253229] p 31 N93-10712
TRAVELING WAVE TUBES
Extended-interaction klystron for the AN/TPS-43-E radar system
[AD-A253166] p 76 N93-10882
TREES (PLANTS)
Millimeter wave measurement and modeling of terrain scattering
[AD-A253525] p 67 N93-10223
TRIANGLES
Evaluation of the triangular plate element of Zienkiewcz and Lefebvre p 63 N93-10562
TROPICAL REGIONS
The role of eddy fluxes in the response of the atmosphere to tropical thermal forcing p 124 N93-10318
TRUSSES
Characterization of and active control of flexible structures, using piezoceramics as sensors and actuators p 10 N93-10319
TUNGSTEN
Effects of anode material on arcjet performance p 23 N93-10044
TUNGSTEN ALLOYS
Ohmic contacts to compound semiconductors p 76 N93-10830
TUNNEL DIODES
Optimization of resonant interband tunnel devices
[AD-A252401] p 168 N93-10637
TUNNELING
Quantum tunneling and the change in the signature of the spacetime metric
[DE92-634877] p 165 N93-10225
TUNNELS
Gradiometer antennas for tunnel detection
[PB92-205400] p 69 N93-10440
TURBINE BLADES
Vibrations of nonlinearly pretwisted asymmetrical thick turbine blades p 9 N93-10537
Navier-Stokes turbine heat transfer predictions using two-equation turbulence
[NASA-TM-105817] p 82 N93-10735
TURBINE PUMPS
Uprated OMS engine status: Altitude testing results p 22 N93-10036
A survey of instabilities within centrifugal pumps and concepts for improving the flow range of pumps in rocket engines p 23 N93-10039
The application of liquid crystal polymers to turbomachinery p 23 N93-10040
Tensile properties of cast titanium alloys: Titanium-6Al-4V ELI and Titanium-5Al-2.5Sn ELI
[NASA-TP-3288] p 33 N93-10072

Improve SSME power balance model
[NASA-CR-184464] p 26 N93-10756
TURBINE WHEELS
Structural analysis: Fatigue life assessment
p 78 N93-10062
TURBINES
Radial Turbines
[VKI-LS-1992-05] p 77 N93-10050
Introduction to radial turbine technology
p 77 N93-10051
Performance parameters and assessment
p 77 N93-10052
Non-dimensional conceptual design of radial inflow turbines. Part A: Application of fundamental fluid mechanics p 77 N93-10053
Non-dimensional conceptual design of radial inflow turbines. Part B: Application of empirical correlations
p 77 N93-10054
Numerical methods for inviscid and viscous flow analysis p 77 N93-10055
Aerodynamic investigation of radial turbines using computational methods p 78 N93-10056
An inverse design method for radial turbomachines
p 78 N93-10057
The integration of geometric modeling into an inverse design method and application of a PC-based inverse design method and comparison with test results
p 78 N93-10058
Partial admission and unsteady flow in radial turbines
p 78 N93-10059
Testing techniques p 78 N93-10060
Radial turbine cooling p 78 N93-10061
LDV Measurements of unsteady flow fields in radial turbine
[AD-A253592] p 4 N93-10648
Navier-Stokes turbine heat transfer predictions using two-equation turbulence
[NASA-TM-105817] p 82 N93-10735
TURBOFAN ENGINES
SAPNEW: Parallel finite element code for thin shell structures on the Alliant FX/80
[NASA-CR-190663] p 94 N93-10372
TURBOMACHINERY
Structural analysis: Fatigue life assessment
p 78 N93-10062
Compound cycle engine for helicopter application
[NASA-CR-180824] p 9 N93-10348
Explicit Navier-Stokes computation of turbomachinery flows p 81 N93-10370
SAPNEW: Parallel finite element code for thin shell structures on the Alliant FX/80
[NASA-CR-190663] p 94 N93-10372
Turbulence measurements of high shear flow fields in a turbomachine seal configuration p 93 N93-10893
TURBULENCE
A multi-fluid model of turbulence for Li-SF6 submerged combustion
[AD-A253973] p 31 N93-10423
Navier-Stokes turbine heat transfer predictions using two-equation turbulence
[NASA-TM-105817] p 82 N93-10735
Air-sea interaction in regions of varying surface conditions
[AD-A253182] p 128 N93-10791
Experimental study of the flow field inside a whirling annular seal p 92 N93-10892
TURBULENCE MODELS
A building-block approach for turbulence model validation/upgrade focussed on high-speed jet flowfields
p 16 N93-10010
Evaluation and application of the Baldwin-Lomax turbulence model in two-dimensional, unsteady, compressible boundary layers with and without separation in engine inlets
[NASA-TM-105810] p 79 N93-10087
Unstructured mesh algorithms for aerodynamic calculations
[NASA-CR-189685] p 2 N93-10097
Combustion in turbulent jets and buoyant flames
[PB92-211481] p 31 N93-10437
Turbulent mixing in compressible free shear layers
p 83 N93-10846
Direct simulation of turbulent pulsed plane channel flows p 84 N93-10860
TURBULENT BOUNDARY LAYER
The structure and development of streamwise vortex arrays embedded in a turbulent boundary layer
p 81 N93-10371
Air-sea interaction in regions of varying surface conditions
[AD-A253182] p 128 N93-10791
TURBULENT COMBUSTION
Combustion in turbulent jets and buoyant flames
[PB92-211481] p 31 N93-10437
TURBULENT FLOW
A building-block approach for turbulence model validation/upgrade focussed on high-speed jet flowfields
p 16 N93-10010
LV software for supersonic flow analysis
[NASA-CR-190911] p 2 N93-10069
Mathematical analysis of strong fluid mechanical effects at high Mach number in reactive and nonreactive flow
[AD-A253617] p 79 N93-10094
Effect of passive flow-control devices on turbulent low-speed base flow p 79 N93-10304
Turbulence modeling of the flow field in combustors using the non-linear k-epsilon model
[DE92-014745] p 80 N93-10330
Development of the finite analytic method for turbulent forced and free convection p 80 N93-10369
Explicit Navier-Stokes computation of turbomachinery flows p 81 N93-10370
Combustion in turbulent jets and buoyant flames
[PB92-211481] p 31 N93-10437
A new energy transfer model for turbulent free shear flow
[NASA-TM-105854] p 81 N93-10454
Heat transfer and pressure drop for air flow through enhanced passages
[DE92-016597] p 82 N93-10612
Air-sea interaction in regions of varying surface conditions
[AD-A253182] p 128 N93-10791
Numerical solution of three-dimensional unsteady viscous flows
[AD-A253202] p 83 N93-10793
Turbulent mixing in compressible free shear layers
p 83 N93-10846
Numerical study of wall turbulence
[ONERA-RSF-21/3419-AY-126] p 83 N93-10859
Direct simulation of turbulent pulsed plane channel flows p 84 N93-10860
The effects of streamline curvature and swirl on turbulent flows in curved ducts p 84 N93-10875
Turbulence measurements of high shear flow fields in a turbomachine seal configuration p 93 N93-10893
TURBULENT HEAT TRANSFER
Heat transfer and pressure drop for air flow through enhanced passages
[DE92-016597] p 82 N93-10612
High-resolution TVD schemes for the analysis of: 1. Inviscid supersonic and transonic flows. 2. Viscous flows with shock-induced separation and heat transfer
p 5 N93-10889
TURBULENT JETS
Combustion in turbulent jets and buoyant flames
[PB92-211481] p 31 N93-10437
Pulsed jet plume combustion: An exothermic process under fluid mechanical control p 32 N93-10553
Mechanisms of sound generation in subsonic jets
p 152 N93-10688
TURBULENT MIXING
Turbulent mixing in compressible free shear layers
p 83 N93-10846
TURBULENT WAKES
Echo characteristic analysis of the nonequilibrium wakes of reentry vehicle
[AD-A254249] p 13 N93-10705
TURKEY
National scene in information and documentation activities and recent developments in the Documentation Center of TUBITAK (TURDOK) p 173 N93-10594
TVD SCHEMES
High-resolution TVD schemes for the analysis of: 1. Inviscid supersonic and transonic flows. 2. Viscous flows with shock-induced separation and heat transfer
p 5 N93-10889
TWINNING
Plasticity of single crystalline Al3X intermetallic compounds
[AD-A254282] p 40 N93-10766
TWISTING
Vibrations of nonlinearly pretwisted asymmetrical thick turbine blades p 9 N93-10537
TWO DIMENSIONAL BOUNDARY LAYER
Evaluation and application of the Baldwin-Lomax turbulence model in two-dimensional, unsteady, compressible boundary layers with and without separation in engine inlets
[NASA-TM-105810] p 79 N93-10087
On the coupling between a supersonic boundary layer and a flexible surface
[NASA-CR-189697] p 82 N93-10757
TWO DIMENSIONAL FLOW
A globally well-posed accurate and efficient finite element CFD algorithm for compressible aerodynamics
p 3 N93-10306
Improved numerical simulation of Euler equations
p 80 N93-10309
A method of testing two-dimensional airfoils
[AD-A253210] p 4 N93-10375
A field panel method for transonic flows
p 6 N93-10547
FLASH: A finite element computer code for variably saturated flow
[DE92-018038] p 84 N93-10868
Characteristics of separated flows including cavitation effects p 84 N93-10874
TWO DIMENSIONAL MODELS
Statics and kinetics of oxygen ordering in the oxide superconductor YBa2Cu3O(z)
[DE92-017001] p 167 N93-10403

U

U.S.S.R.
Geomechanical models of impact cratering: Puchezh-Katunki structure p 114 N93-10151
Soviet optical processing research. FSAC Technical Assessment Report (TAR)
[PB92-195569] p 172 N93-10431
ULLAGE
DSP propulsion system launch configuration and related testing p 24 N93-10048
ULTRAHIGH FREQUENCIES
Dynamic positioning systems photogrammetric
[AD-A254250] p 8 N93-10898
ULTRASONIC RADIATION
Instrument driver for general purpose interface bus (IEEE-488)
[AD-A253947] p 138 N93-10716
ULTRASONIC TESTS
Ultrasonic characterization of highly attenuative thick composites
[AD-A253347] p 27 N93-10272
ULTRASONICS
Elastic wave scattering by an interfacial crack in a plate p 48 N93-10485
ULTRAVIOLET DETECTORS
Detectors for the SIMURIS payload
p 14 N93-10937
ULTRAVIOLET LASERS
The interaction of UV-Laser radiation with metal and semiconductor surfaces
[AD-A253510] p 87 N93-10201
UV/XUV FEL storage ring and linac
[AD-A253307] p 89 N93-10697
ULTRAVIOLET PHOTOGRAPHY
Obtaining high resolution XUV coronal images
p 14 N93-10939
ULTRAVIOLET RADIATION
Results from testing and analysis of solar cells flown on LDEF p 39 N93-10591
ULTRAVIOLET SPECTRA
Intensity, velocity, and turbulence in prominences observed with the HRTS p 180 N93-10911
ULTRAVIOLET TELESCOPES
SUN: The Solar Ultraviolet Network
p 183 N93-10930
EUV complementary instrumentation for SIMURIS
p 14 N93-10938
The solar ultraviolet network: Performance and tolerance analysis p 187 N93-10950
UNDERWATER ACOUSTICS
SBS applications study
[AD-A253779] p 102 N93-10234
UNDERWATER VEHICLES
A multi-fluid model of turbulence for Li-SF6 submerged combustion
[AD-A253973] p 31 N93-10423
UNITED STATES
List of publications, 1969-1991. Panel on wind and seismic effects
[PB92-201102] p 125 N93-10089
UNIVERSITIES
Manitoba aerospace technology: Capability directory
[CTN-92-60572] p 193 N93-10655
UNSTEADY AERODYNAMICS
Forced unsteady separated flows on a 45 degree delta wing p 80 N93-10305
Control of lift and drag in unsteady flows
[AD-A253148] p 3 N93-10340
Further noise measurements in a slotted cryogenic wind tunnel
[RAE-TM-AERO-2201] p 153 N93-10805
UNSTEADY FLOW
Numerical simulation of unsteady flow in a nozzle
p 16 N93-10008
Radial Turbines
[VKI-LS-1992-05] p 77 N93-10050
Partial admission and unsteady flow in radial turbines
p 78 N93-10059
Testing techniques p 78 N93-10060

Forced unsteady separated flows on a 45 degree delta wing p 80 N93-10305
Control of lift and drag in unsteady flows [AD-A253146] p 3 N93-10340
Interactive grid generation program for CAP-TSD [NASA-TM-102705] p 3 N93-10349
Stream function-vorticity finite element formulations of unsteady incompressible Navier-Stokes equations p 60 N93-10545
LDV Measurements of unsteady flow fields in radial turbine [AD-A253592] p 4 N93-10648
Numerical solution of three-dimensional unsteady viscous flows [AD-A253202] p 83 N93-10793

URBAN TRANSPORTATION
Selective perception for robot driving [AD-A253740] p 142 N93-10749

USER MANUALS (COMPUTER PROGRAMS)
Resonance apparatus operating manual [AD-A254040] p 71 N93-10241
Handbook for operating the OWLKNEST technology [AD-A253412] p 137 N93-10409
PRODIGY4.0: The manual and tutorial [AD-A253970] p 137 N93-10422
DYNA2D: A nonlinear, explicit, two-dimensional finite element code for solid mechanics: User manual [DE92-017310] p 95 N93-10646
ACIRF user's guide for the general model (Version 3.5) [AD-A254068] p 69 N93-10657
A standard file format for data interchange [AD-A254260] p 176 N93-10899

USER REQUIREMENTS
Guide to the user requirements definition phase [ESA-PSS-05-02-ISSUE-1] p 136 N93-10315
Guide to the software requirements definition phase [ESA-PSS-05-03-ISSUE-1] p 136 N93-10316

UTAH
Reserves in western basins [DE92-014429] p 102 N93-10625

V

V/STOL AIRCRAFT
Initial piloted simulation study of geared flap control for tilt-wing V/STOL aircraft [NASA-TM-103872] p 11 N93-10741

VACUUM
Field-emitter arrays for RF vacuum microelectronics [AD-A253396] p 73 N93-10405

VACUUM TESTS
A multipurpose vacuum-ultraviolet test facility p 11 N93-10953

VAPOR DEPOSITION
Long wavelength multiple quantum well lasers for high-speed modulation applications [AD-A253348] p 87 N93-10211
Moire-fringe images of twin boundaries in chemical vapor deposited diamond [AD-A253729] p 35 N93-10231
Intense ion beam research at Los Alamos [DE92-015240] p 155 N93-10333
Oxidation protection systems for carbon-carbon composites formed by chemical vapor deposition and plasma assisted chemical vapor deposition techniques [AD-A253450] p 28 N93-10344
Boronization in D3-D [DE92-016249] p 163 N93-10759
Growth defects in diamond films [AD-A253618] p 40 N93-10778

VAPORIZING
Geochemical aspect of impact cratering: Studies in Vernadsky Institute p 123 N93-10196

VARIABILITY
Analysis of reception variability due to terrain multipath on microwave common carrier links [NTIA-92-283] p 69 N93-10430

VARIABLE THRUST
Studies on the combustion efficiency of liquid fuel rockets with variable thrust [AD-A254232] p 26 N93-10721

VARIANCE (STATISTICS)
On Watson's ANOVA for directions [AD-A253576] p 146 N93-10700

VECTOR ANALYSIS
On Watson's ANOVA for directions [AD-A253576] p 146 N93-10700

VECTOR CURRENTS
Modelling of 3-D electromagnetic responses using the time-wavenumber method [DE92-017025] p 70 N93-10865

VECTOR DOMINANCE MODEL
Vector superconductivity in cosmic strings [DE92-634923] p 179 N93-10296
Coherent production of pions and rho mesons in neutrino charged current interactions on neon nuclei at the Fermilab Tevatron [DE92-015674] p 154 N93-10606

VECTOR PROCESSING (COMPUTERS)
SAPNEW: Parallel finite element code for thin shell structures on the Alliant FX/80 [NASA-CR-190663] p 94 N93-10372

VEGETATION
Application of volumetric multiple-scattering approximations to foliage media [AD-A253337] p 68 N93-10358

VELOCITY DISTRIBUTION
The structure and development of streamwise vortex arrays embedded in a turbulent boundary layer p 81 N93-10371
Experimental study of the flow field inside a whirling annular seal p 92 N93-10892
Stokes parameters of the O VI 103.2 nm line as a probe of the matter velocity field vector in the solar wind acceleration region p 181 N93-10914
Spatial distribution of line-of-sight velocities in a quiescent prominence p 183 N93-10928

VELOCITY MEASUREMENT
Comparison of wind speed measurements over the oceans with the Special Sensor Microwave/Imager and the Geosat altimeter p 127 N93-10850

VENUS (PLANET)
Paradigm lost: Venus crater depths and the role of gravity in crater modification p 120 N93-10179

VENUS SURFACE
Venusian impact basins and cratered terrains p 112 N93-10145
What can we learn about impact mechanics from large craters on Venus? p 118 N93-10166

VERTICAL MOTION SIMULATORS
Initial piloted simulation study of geared flap control for tilt-wing V/STOL aircraft [NASA-TM-103872] p 11 N93-10741

VERTICAL TAKEOFF AIRCRAFT
Critical engine system design characteristics for SSTO vehicles p 17 N93-10014

VERY LARGE SCALE INTEGRATION
Integrated vision system for a target seeker [AD-A253359] p 135 N93-10103
Development of parallel architectures for sensor array processing algorithms [AD-A253680] p 141 N93-10299
VLSI design for reliability - hot electron [AD-A253942] p 74 N93-10715
High sensitivity probes for silicon VLSI internal node testing [AD-A253924] p 169 N93-10784
Joint Services Electronics Program [AD-A253842] p 76 N93-10829

VERY LONG BASE INTERFEROMETRY
Successes of and prospects for ground-based interferometry p 177 N93-10940
Report of the Lunar Interferometry Study Team (LIST) activities p 178 N93-10945

VIBRATION DAMPING
Design, test, and evaluation of three active flutter suppression controllers [NASA-TM-4338] p 10 N93-10070
Nonstationary random variations of moderately thick plates using BEM p 48 N93-10487
Dynamics of an orbiting flexible manipulator p 54 N93-10519
Vibration of a damped double-beam system p 56 N93-10527
Overview of the vibroimpact damping of packaged particles p 56 N93-10528
Control of panel flutter at high supersonic speed p 9 N93-10900

VIBRATION MODE
A study upon structural optimization of elastic rotors for mechanical systems [INPE-5376-TDI/471] p 94 N93-10310
Response of a beam to transverse impulsive and high frequency loads p 56 N93-10526
Nonlinear aeroelasticity of composite structures [AD-A254285] p 8 N93-10842

VIBRATION TESTS
Numerical considerations for structural system identification from modal information p 63 N93-10564

VIBRATIONAL SPECTRA
Improved gallium nitride and aluminum nitride electronic materials [AD-A253785] p 76 N93-10888

VIDEO EQUIPMENT
Research in the optical sciences [AD-A253188] p 158 N93-10446

VISCOELASTICITY
Chronorheological characterization of elastomers p 46 N93-10476

VISCOPLASTICITY
Unified viscoplastic behavior of metal matrix composites [NASA-TM-105819] p 96 N93-10777
Mechanics of composite materials for spacecraft [AD-A254217] p 26 N93-10896

VISCOSITY
Viscosity determinations of some frictionally generated silicate melts: Implications for slip zone rheology during impact-induced faulting p 121 N93-10183
One type of automatically adjusted difference scheme with artificial viscosity to calculate ablated exterior shapes [AD-A254108] p 5 N93-10856
RHALE: A MMALE shock physics code for arbitrary meshes [DE92-017051] p 139 N93-10866

VISCOUS DAMPING
An experimental and a theoretical investigation of rotor pitch damping using a model rotor p 8 N93-10322
Response of a beam to transverse impulsive and high frequency loads p 56 N93-10526

VISCOUS FLOW
Numerical methods for inviscid and viscous flow analysis p 77 N93-10055
Finite difference methods for incompressible viscous flow in scientific computing [AD-A253512] p 79 N93-10220
High-speed viscous flows past blunt bodies and compression corners with flux-split methods [AD-A253413] p 81 N93-10410
Numerical solution of three-dimensional unsteady viscous flows [AD-A253202] p 83 N93-10793
Study of a viscous sublayer model in the analysis of 3-D shock/boundary layer interaction flow fields [AD-A253731] p 84 N93-10886
High-resolution TVD schemes for the analysis of: 1. Inviscid supersonic and transonic flows. 2. Viscous flows with shock-induced separation and heat transfer p 5 N93-10889

VISION
Eye movements and visual information processing [AD-A250198] p 132 N93-10278
A new test of scanning and monitoring ability: Methods and initial results [AD-A249123] p 132 N93-10321

VISUAL ACUITY
Comparative study of the MTFA, ICS, and SQRI image quality metrics for visual display systems [AD-A252116] p 158 N93-10708

VISUAL DISCRIMINATION
Computer simulations of object discrimination by visual cortex [AD-A253345] p 131 N93-10271

VISUAL FIELDS
Eye movements and visual information processing [AD-A250198] p 132 N93-10278

VISUAL FLIGHT RULES
Rotorcraft en route ATC route standards [AD-A249129] p 6 N93-10323

VISUAL PERCEPTION
Eye movements and visual information processing [AD-A250198] p 132 N93-10278
Perception of lightness and brightness in complex patterns [AD-A254093] p 133 N93-10658
Effects of early bright, late bright and dim illumination upon circadian neuroendocrine, electrophysiological and behavioral responses [AD-A254129] p 131 N93-10661

VITRIFICATION
APOLLO: A computer program for the calculation of chemical equilibrium and reaction kinetics of chemical systems [DE92-017864] p 139 N93-10817

VOICE COMMUNICATION
Evaluation of lightweight and low profile communications devices for Respiratory Protective system 21 (RESPO 21) [AD-A253393] p 133 N93-10217
Evaluation of an electronics system concept for Respiratory Protection system (RESPO 21) [AD-A253394] p 134 N93-10288

VOLCANOES
Simulated meteorite impacts and volcanic explosions: Ejecta analyses and planetary implications p 111 N93-10143
Ar-40 to Ar-39 dating of pseudotachylites from the Witwatersrand basin, South Africa, with implications for the formation of the Vredefort Dome p 122 N93-10189
Floor-fractured crater models of the Sudbury structure, Canada p 123 N93-10193

VOLCANOLOGY
Coincidences in time of the Imbrium Basin impact and Apollo 15 KREEP volcanic series: Impact-induced melting? p 119 N93-10175
Geological evidence for a 2.6-Ga strewn field of impact spherules in the Hamersley Basin of Western Australia p 120 N93-10181
Al Umchaimin depression, Western Iraq: An impact structure? p 122 N93-10190
Floor-fractured crater models of the Sudbury structure, Canada p 123 N93-10193
Variation in multiring basic structures as a function of impact angle p 123 N93-10194
VOLT-AMPERE CHARACTERISTICS
Field emission current-voltage curves as a diagnostic for scanning tunneling microscope tips
[AD-A251171] p 165 N93-10245
VORTEX ALLEVIATION
Experimental investigation of flows behind different Large-Eddy Breakup (LEBU) devices in thick boundary layers p 6 N93-10550
VORTEX BREAKDOWN
Computational studies of vortex breakdown
[AD-A253759] p 79 N93-10232
Control of lift and drag in unsteady flows
[AD-A253146] p 3 N93-10340
VORTEX FILAMENTS
Mathematical analysis of strong fluid mechanical effects at high Mach number in reactive and nonreactive flow
[AD-A253617] p 79 N93-10094
VORTEX GENERATORS
Effect of passive flow-control devices on turbulent low-speed base flow p 79 N93-10304
VORTEX SHEETS
Mathematical analysis of strong fluid mechanical effects at high Mach number in reactive and nonreactive flow
[AD-A253617] p 79 N93-10094
VORTICES
Navier-Stokes dynamics and aeroelastic computations for vortical flows, buffet and aeroelastic applications
[NASA-CR-190692] p 2 N93-10098
Computational studies of vortex breakdown
[AD-A253759] p 79 N93-10232
Forced unsteady separated flows on a 45 degree delta wing p 80 N93-10305
The role of eddy fluxes in the response of the atmosphere to tropical thermal forcing p 124 N93-10318
Control of lift and drag in unsteady flows
[AD-A253146] p 3 N93-10340
The structure and development of streamwise vortex arrays embedded in a turbulent boundary layer p 81 N93-10371
Vortices in long Josephson junctions
[AD-A253230] p 167 N93-10404
Investigations into swirling flows of Newtonian and non-Newtonian fluids
[AD-A253298] p 82 N93-10696
Hydrodynamic investigation of vortical flows for an ATTAC configuration with canards
[AD-A253928] p 4 N93-10753
Shock enhancement and control of hypersonic combustion
[AD-A254295] p 31 N93-10843
The effects of streamline curvature and swirl on turbulent flows in curved ducts p 84 N93-10875
Contributions to the experimental investigation of rotor/body aerodynamic interactions p 5 N93-10877
VORTICITY
Anelastic modelling of explosive cyclogenesis p 126 N93-10377
Numerical solution of three-dimensional unsteady viscous flows
[AD-A253202] p 83 N93-10793
VORTICITY EQUATIONS
RHALE: A MMALE shock physics code for arbitrary meshes
[DE92-017051] p 139 N93-10866

W

WAKES
Contributions to the experimental investigation of rotor/body aerodynamic interactions p 5 N93-10877
WALL FLOW
Numerical study of wall turbulence
[ONERA-RSF-21/3419-AY-126] p 83 N93-10859
Direct simulation of turbulent pulsed plane channel flows p 84 N93-10860
Characteristics of separated flows including cavitation effects p 84 N93-10874
Study of a viscous sublayer model in the analysis of 3-D shock/boundary layer interaction flow fields
[AD-A253731] p 84 N93-10886
WALL TEMPERATURE
Thermal stratification potential in rocket engine coolant channels p 18 N93-10019
WALLS
Heat transfer and pressure drop for air flow through enhanced passages
[DE92-016597] p 82 N93-10612
WARNING SYSTEMS
Advanced terrain displays to transport category aircraft
[PB92-197136] p 6 N93-10065
WASTE DISPOSAL
Ceramic transactions. Volume 21: Proceedings of the Symposium on Microwave Theory and Application in Materials Processing Annual Meeting No. 23 io on april 29-may 3 1991
[AD-A253631] p 35 N93-10205
WASTE TREATMENT
Ceramic transactions. Volume 21: Proceedings of the Symposium on Microwave Theory and Application in Materials Processing Annual Meeting No. 23 io on april 29-may 3 1991
[AD-A253631] p 35 N93-10205
APOLLO: A computer program for the calculation of chemical equilibrium and reaction kinetics of chemical systems
[DE92-017864] p 139 N93-10817
WATER
Vibrational relaxation of H2O by H2, HCl, and H2O at 295 K
[AD-A252800] p 29 N93-10263
Electron transfer reactions in microporous solids
[DE92-016222] p 166 N93-10284
WATER IMMERSION
Mechanical behavior of open cell ceramics
[PB92-212984] p 37 N93-10439
WATER TUNNEL TESTS
Hydrodynamic investigation of vortical flows for an ATTAC configuration with canards
[AD-A253928] p 4 N93-10753
WATER VAPOR
Satellite derived integrated water vapor and rain intensity patterns: Indicators of rapid cyclogenesis p 127 N93-10849
WAVE DEGRADATION
A new non-Gausssian approximation technique for random vibration of general hysteresis p 50 N93-10496
WAVE DIFFRACTION
Elastic wave scattering by an interfacial crack in a plate p 48 N93-10485
Shock wave diffractions over semi-circular and half-diamond cylinders p 60 N93-10546
WAVE FUNCTIONS
Semiclassical quantization of integrable systems of few interacting anyons in a strong magnetic field
[DE92-634892] p 170 N93-10295
Two-photon couplings of quarkonia with arbitrary J(sup PC)
[DE92-016525] p 153 N93-10332
Data synthesis and display programs for wave distribution function analysis
[NASA-TM-108009] p 70 N93-10800
WAVE PROPAGATION
Software for prediction and analysis of ground wave propagation loss
[AD-A253474] p 67 N93-10199
Calculation of elastic-plastic wave propagation on the connection machine
[AD-A252429] p 95 N93-10427
Modeling of HF propagation and heating in the ionosphere
[AD-A253941] p 125 N93-10714
Pulse propagation in random media
[AD-A254294] p 152 N93-10769
Atomic short range order and spin density wave propagation in CuMn
[DE92-016903] p 34 N93-10789
Progress in multi-dimensional upwind differencing
[NASA-CR-189708] p 83 N93-10808
Coronal and solar wind Alfven wave propagation p 180 N93-10909
WAVEGUIDES
High-power microwave breakdown of dielectric interfaces
[AD-A254200] p 124 N93-10262
Pulse propagation in random media
[AD-A254294] p 152 N93-10769
Extended-interaction klystron for the AN/TPS-43-E radar system
[AD-A253166] p 76 N93-10882
WEAPON SYSTEMS
Maintaining future military aircraft design capability
[AD-A253963] p 8 N93-10420
WEAR RESISTANCE
Developmental research on ultra abrasion-resistant materials
[DE92-531066] p 36 N93-10287
WEATHER
Weather Message Switching Center Replacement (WMSCR) Operational Test and Evaluation (OT/E)/integration test plan
[DOT/FAA/CT-TN90/59] p 7 N93-10833
WEATHER FORECASTING
Satellite derived integrated water vapor and rain intensity patterns: Indicators of rapid cyclogenesis p 127 N93-10849
WEATHER STATIONS
Eleven years of ionospheric scintillation fading data from twenty Greenlandic stations
[AD-A253271] p 69 N93-10695
WEDGES
An open or closed crack terminating at a bi-material interface: Power-logarithmic singularities p 47 N93-10483
Vibration frequencies of a constrained cantilever wedge p 57 N93-10534
Shock wave diffractions over semi-circular and half-diamond cylinders p 60 N93-10546
WEIGHT (MASS)
A prospective evaluation of stress fractures/overuse injuries in a population of West Point cadets
[AD-A252427] p 132 N93-10709
WEIGHT REDUCTION
Selected results for metals from LDEF experiment A0171 p 34 N93-10579
WEIGHTING FUNCTIONS
Unifying the landmark developments in optimal bounding ellipsoid identification
[AD-A253502] p 143 N93-10200
WELDING
Stress modified welding process for irradiated materials
[DE92-017131] p 92 N93-10634
A seam tracking modulated infrared optical sensor for use in welding
[AD-A254103] p 159 N93-10812
WENTZEL-KRAMER-BRILLOUIN METHOD
Semiclassical quantization of interacting anyons in a strong magnetic field
[DE92-634889] p 169 N93-10229
Semiclassical quantization of integrable systems of few interacting anyons in a strong magnetic field
[DE92-634892] p 170 N93-10295
WHEELS
Stability of open-graded bases under wheel loads using a model testing approach
[AD-A253209] p 66 N93-10710
WHISKER COMPOSITES
High temperature fatigue crack growth in ceramics and ceramic composites
[DE92-016835] p 40 N93-10632
WHISKERS (CRYSTALS)
Reinforcements for high temperature ceramics
[DE92-014815] p 35 N93-10082
WHITE NOISE
Probability density functions for random nonlinear oscillation p 55 N93-10522
Low-frequency noise reduction in SQUID measurements using laser switching
[AD-A253821] p 90 N93-10827
WIND (METEOROLOGY)
List of publications, 1969-1991. Panel on wind and seismic effects
[PB92-201102] p 125 N93-10089
WIND TUNNEL MODELS
Design, test, and evaluation of three active flutter suppression controllers
[NASA-TM-4338] p 10 N93-10070
Arguments concerning wind tunnel test studies of the trim characteristics of objects with small asymmetries'
[AD-A254111] p 5 N93-10858
WIND TUNNEL TESTS
Design, test, and evaluation of three active flutter suppression controllers
[NASA-TM-4338] p 10 N93-10070
Pitot survey of exhaust flow field of a 2-D scramjet nozzle at Mach 6 with air or freon and argon used for exhaust simulation
[NASA-TM-4361] p 2 N93-10071
Effect of passive flow-control devices on turbulent low-speed base flow p 79 N93-10304
A method of testing two-dimensional airfoils
[AD-A253210] p 4 N93-10375
Experimental investigation of flows behind different Large-Eddy Breakup (LEBU) devices in thick boundary layers p 6 N93-10550

Wind tunnel spin data reduction to obtain aerodynamic spin damping coefficients by using nonlinear equation of motion
[AD-A253880] p 4 N93-10811
Effect of planform and body on supersonic aerodynamics of multibody configurations
[NASA-TP-3212] p 4 N93-10824
Shock enhancement and control of hypersonic combustion
[AD-A254295] p 31 N93-10843
Arguments concerning wind tunnel test studies of the trim characteristics of objects with small asymmetries'
[AD-A254111] p 5 N93-10858

WIND TUNNELS
Non-propulsive aerodynamic noise
p 149 N93-10673

WIND VELOCITY
Acoustic noise generation at the air/ocean boundary
[DREA-CR-90-445] p 147 N93-10642
Comparison of wind speed measurements over the oceans with the Special Sensor Microwave/Imager and the Geosat altimeter p 127 N93-10850

WING PLANFORMS
Effect of planform and body on supersonic aerodynamics of multibody configurations
[NASA-TP-3212] p 4 N93-10824

WINGS
Control of lift and drag in unsteady flows
[AD-A253146] p 3 N93-10340
Nonlinear aeroelasticity of composite structures
[AD-A254285] p 8 N93-10842

WINTER
Atlas of Southern Hemisphere 500 mb teleconnection patterns derived from National Meteorological Center analyses
[PB92-203892] p 126 N93-10337
Morning-evening differences in global and regional oceanic precipitation as observed by the SSM/I
p 127 N93-10851

WIRE
Lightweight deployable antenna system
[AD-D015291] p 67 N93-10096

WORK FUNCTIONS
Effects of anode material on arcjet performance
p 23 N93-10044
Effects of anode material on arcjet performance
[NASA-TM-105799] p 25 N93-10197

WORKING FLUIDS
The application of liquid crystal polymers to turbomachinery p 23 N93-10040
Heat transfer additives for absorption cooling system fluids
[PB92-190354] p 169 N93-10249

WORKLOADS (PSYCHOPHYSIOLOGY)
Operator workload predictions for the revised AH-64A workload prediction model, volume 1
[AD-A254198] p 133 N93-10261
Handbook for operating the OWLKNEST technology
[AD-A253412] p 137 N93-10409
Mental workload assessment in the cockpit: Feasibility of using electrophysiological measurements, phase 1
[AD-A254138] p 133 N93-10662
KC-135 crew reduction feasibility demonstration simulation study. Volume 3: Test and evaluation
[AD-A253931] p 134 N93-10713
NASA Space Human Factors Program
[NASA-TM-108005] p 134 N93-10890

WORKSTATIONS
TIGER5: Extraction of geographic information from the TIGER system
[DE92-014935] p 171 N93-10382

WYOMING
Reserves in western basins
[DE92-014429] p 102 N93-10625

X

X RAY ABSORPTION
Epitaxial growth and dopant incorporation in diamond
[AD-A253636] p 165 N93-10206

X RAY ASTRONOMY
Physical implementations of an antimask in URA based coded mask systems
[INPE-5338-PRE/1737] p 153 N93-10312

X RAY DETECTORS
A five-channel, diamond photoconducting x ray detector array for z-pinch experiments
[DE92-017345] p 164 N93-10839

X RAY DIFFRACTION
Thermal, structural, and diffraction analyses of a gallium-cooled x ray monochromator
[DE92-017063] p 157 N93-10837

X RAY IMAGERY
Physical implementations of an antimask in URA based coded mask systems
[INPE-5338-PRE/1737] p 153 N93-10312
Obtaining high resolution XUV coronal images
p 14 N93-10939

X RAY SPECTROSCOPY
Reliability of sublattice occupancies determined by ALCHEMI
[DE92-014592] p 168 N93-10623

X RAY TELESCOPES
Physical implementations of an antimask in URA based coded mask systems
[INPE-5338-PRE/1737] p 153 N93-10312
EUV complementary instrumentation for SIMURIS
p 14 N93-10938

X RAYS
Studies impacting the designs of free electron lasers
[AD-A254293] p 90 N93-10768

XV-15 AIRCRAFT
Tilt rotor hover aeroacoustics
[NASA-CR-177598] p 147 N93-10458

Y

YAG LASERS
Thermo-optical switching in Si based etalons
[AD-A253139] p 88 N93-10412
Laser Journal
[AD-A254106] p 90 N93-10855

YBCO SUPERCONDUCTORS
Statics and kinetics of oxygen ordering in the oxide superconductor YBa2Cu3O(z)
[DE92-017001] p 167 N93-10403

YIELD STRENGTH
Damage due to plastic deformation in elastic-plastic materials: The thermodynamical connection
p 51 N93-10502
Strength-toughness requirements for thick-walled high pressure vessels
[AD-A253756] p 95 N93-10750

YTTRIUM COMPOUNDS
Novel Si-YBCuO reactive patterning technique for manufacture of large area high Tc superconducting electronic devices
[AD-A250740] p 73 N93-10426

YTTRIUM OXIDES
Oxygen barrier oxides
[AD-A253683] p 36 N93-10343

YTTRIUM-IRON GARNET
Development of garnet films for magnetostatic wave channelized receivers
[AD-A252812] p 166 N93-10335

Z

ZEOLITES
Electron transfer reactions in microporous solids
[DE92-016222] p 166 N93-10284

ZETA PINCH
A five-channel, diamond photoconducting x ray detector array for z-pinch experiments
[DE92-017345] p 164 N93-10839

ZINC ALLOYS
Fatigue crack propagation in the presence of shot-peening residual stresses p 59 N93-10542

ZIRCONATES
Oxygen barrier oxides
[AD-A253683] p 36 N93-10343

ZIRCONIUM ALLOYS
Reactions of Ti and Zr with AlN and Al2O3
[DE92-016234] p 28 N93-10391

ZIRCONIUM CARBIDES
Oxidation protection systems for carbon-carbon composites formed by chemical vapor deposition and plasma assisted chemical vapor deposition techniques
[AD-A253450] p 28 N93-10344

Typical Personal Author Index Listing

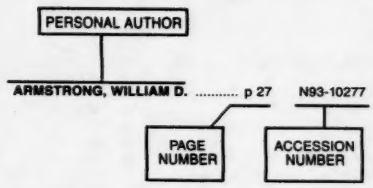

Listings in this index are arranged alphabetically by personal author. The page number helps you locate the citation in the abstract section. The accession number denotes the number by which the citation is identified.

A

AADLAND, R. S. ..... p 21 N93-10031
ABFALTER, G. ..... p 35 N93-10221
ABOU-AMER, SEOUD AHMED ..... p 9 N93-10900
ABOU-ELLAIL, M. M. ..... p 31 N93-10423
ABRAHAM, JACOB A. ..... p 136 N93-10361
ABRAHAM, ROBERTO G. ..... p 177 N93-10884
ACHAREKAR, M. A. ..... p 87 N93-10090
ACKERS, DEANE E. ..... p 63 N93-10560
ADAIR, J. H. ..... p 71 N93-10273
p 71 N93-10276
p 72 N93-10280
p 72 N93-10282
ADAMS, WILLIAM M., JR. ..... p 10 N93-10070
AGER, SCOTT A. ..... p 12 N93-10106
AGRINIER, P. ..... p 105 N93-10113
AHRENS, THOMAS J. ..... p 119 N93-10170
AIELLO, PETER F. ..... p 19 N93-10025
AILEY-TRENT, K. S. ..... p 166 N93-10355
p 166 N93-10356
AL-KHAYAT, I. A. ..... p 45 N93-10471
ALDE, D. ..... p 153 N93-10328
ALEXANDER, D. W. ..... p 104 N93-10809
ALEXANDER, MICHAEL G. ..... p 4 N93-10753
ALEXOPOULOS, J. S. ..... p 118 N93-10166
ALLEN, JONATHAN ..... p 67 N93-10092
ALME, M. L. ..... p 92 N93-10835
ALPERT, NATHANIEL M. ..... p 132 N93-10765
ALSTON, S. G. ..... p 154 N93-10435
AMEEL, T. A. ..... p 169 N93-10249
AMERI, ALI A. ..... p 82 N93-10735
ANDERSON, DAVID STEPHEN ..... p 177 N93-10876
ANDERSON, DUANE L. ..... p 135 N93-10088
ANDERSON, R. R. ..... p 105 N93-10114
ANDERSON, SCOTT L. ..... p 30 N93-10416
ANDES, DAVID K. ..... p 142 N93-10958
p 143 N93-10959
ANDRADY, ANTHONY L. ..... p 41 N93-10783
ANDRAKA, C. E. ..... p 103 N93-10383
ANDREASSEN, K. ..... p 14 N93-10935
ANINI, Y. I. ..... p 165 N93-10225
ANTOINE, L. A. G. ..... p 106 N93-10115
ANTONUCCI, ESTER ..... p 14 N93-10938
APGAR, SCOTT W. ..... p 135 N93-10212
AREND, LAWRENCE E., JR. ..... p 133 N93-10658
ARMALE, R. ..... p 156 N93-10633
ARMBRUSTER, P. A. ..... p 14 N93-10935
ARMSTRONG, WILLIAM D. ..... p 27 N93-10277
ARNOLD, S. M. ..... p 95 N93-10453
p 95 N93-10455
p 96 N93-10777
ARNONE, ANDREA ..... p 82 N93-10735
ARPACI, V. S. ..... p 81 N93-10449
ARTZNER, GUY ..... p 178 N93-10947
ARVAS, E. ..... p 69 N93-10418
ASH, R. M. ..... p 87 N93-10211
ATAKTUERK, SERHAD S. ..... p 128 N93-10068
ATKINS, JOHN ..... p 172 N93-10452
ATTARD, ALFRED E. ..... p 172 N93-10431
AU, M. C. ..... p 48 N93-10486
AVERILL, R. C. ..... p 47 N93-10481
AVERMANN, M. ..... p 106 N93-10117
p 121 N93-10185
AVERMANN, M. E. ..... p 106 N93-10116
p 107 N93-10119
AZIZ, OMER ..... p 62 N93-10559

B

BABUSKA, IVO M. ..... p 144 N93-10407
BACA, R. G. ..... p 84 N93-10868
BACCHUS, D. L. ..... p 11 N93-10021
BAEK, W. Y. ..... p 160 N93-10293
BAER, ERIC ..... p 41 N93-10825
BAEZ, ANASTACIO N. ..... p 26 N93-10734
BAHEI-EL-DIN, YEHIA A. ..... p 28 N93-10896
BAINES, N. C. ..... p 77 N93-10051
p 77 N93-10052
p 78 N93-10059
p 78 N93-10060
BAJAJ, KRISHAN K. ..... p 165 N93-10210
BALACHANDAR, RAMASWAMI ..... p 84 N93-10874
BALACHANDRAN, A. P. ..... p 155 N93-10840
BALDWIN, JAMES C. ..... p 15 N93-10006
BANON, GERALD JEAN FRANCIS ..... p 157 N93-10311
BARBIERI, JAMES F. ..... p 142 N93-10958
p 143 N93-10959
BARNABA, JAMES M. ..... p 134 N93-10713
BARNES, T. ..... p 153 N93-10332
BARRY, BERNARD F. ..... p 151 N93-10687
BARTELS, P. ..... p 152 N93-10691
BARTOLOTTA, P. A. ..... p 96 N93-10777
BARTSCH, R. R. ..... p 155 N93-10333
BARUT, A. O. ..... p 170 N93-10387
BASILEVSKY, A. T. ..... p 123 N93-10196
BASKI, A. A. ..... p 168 N93-10726
BATCHELOR, D. ..... p 32 N93-10854
BATES, J. L. ..... p 104 N93-10729
BATRA, NARENDRA K. ..... p 27 N93-10272
BATSON, R. M. ..... p 189 N93-10832
BAUER, STEVEN X. S. ..... p 4 N93-10824
BAYLISS, ALVIN ..... p 82 N93-10757
BAZHENOV, S. ..... p 41 N93-10825
BEATON, R. J. ..... p 158 N93-10708
BECHHOEFER, ERIC R. ..... p 139 N93-10881
BECKERS, J. ..... p 178 N93-10945
BECKERS, J. M. ..... p 178 N93-10943
BECOULET, A. ..... p 163 N93-10761
BEETZ, C. P., JR. ..... p 165 N93-10274
BELIVEAU, JEAN-GUY ..... p 63 N93-10564
p 64 N93-10567
BELL, A. E. ..... p 104 N93-10729
BELL, GERALD D. ..... p 126 N93-10337
BELL, R. ..... p 59 N93-10543
BELL, WILLIAM A. ..... p 2 N93-10069
BELT, R. F. ..... p 166 N93-10335
p 169 N93-10879
BELY, P. Y. ..... p 178 N93-10944
BELZER, M. ..... p 140 N93-10219
BENKOVITZ, C. M. ..... p 104 N93-10384
BENNER, WILLIAM ..... p 7 N93-10833
BENTLEY, J. ..... p 168 N93-10623
BERGER, MARSHA J. ..... p 138 N93-10736
BERKENBOSCH, L. ..... p 35 N93-10084
BERMAN, N. S. ..... p 169 N93-10249
BERNARD, M. ..... p 59 N93-10541
BERNATZ, RICHARD ALLEN ..... p 80 N93-10369
BERTELLO, L. ..... p 183 N93-10927
BERTUCCIO, G. ..... p 74 N93-10731
BEST, R. G. ..... p 176 N93-10867
BETTERTON, W. J. ..... p 107 N93-10121
BETTES, P. ..... p 63 N93-10562
BEYER, JAMES B. ..... p 167 N93-10404
BHALLA, A. S. ..... p 71 N93-10273
p 71 N93-10276
p 72 N93-10280
p 72 N93-10282
BHAT, R. B. ..... p 45 N93-10470
BHAT, THONSE R. S. ..... p 151 N93-10684
BI, NAIPEI ..... p 5 N93-10877
BICKEL, WILLIAM S. ..... p 158 N93-10445
BIERBAUM, CARL R. ..... p 133 N93-10261
BIGGER, CHRIS ..... p 173 N93-10598
p 174 N93-10602
BILGUTAY, NIHAT M. ..... p 68 N93-10380
BILLINGHURST, E. E., JR. ..... p 33 N93-10072
BINIENDA, W. K. ..... p 95 N93-10453
p 95 N93-10455
BINON, F. ..... p 153 N93-10328
BIRON, A. ..... p 58 N93-10540
BISCHOFF, L. ..... p 106 N93-10117
p 106 N93-10118
p 107 N93-10119
BLADOS, WALTER R. ..... p 173 N93-10597
BLAECK, S. ..... p 152 N93-10690
BLAIR, CHRISTOPHER ..... p 38 N93-10584
BLAKESLEE, RICHARD J. ..... p 125 N93-10108
BLAND, SAMUEL R. ..... p 3 N93-10349
BLANDO, P. ..... p 86 N93-10444
BLUEMEL, R. ..... p 170 N93-10294
BLUM, FRANK D. ..... p 31 N93-10794
BLYTHE, JIM ..... p 137 N93-10422
BOER, R. H. ..... p 122 N93-10189
BOER, RUDOLF H. ..... p 115 N93-10155
BOETTCHER, JAN ..... p 149 N93-10674
p 151 N93-10685
BOGG, R. ..... p 148 N93-10669
BOHNHOFF-HLAVACEK, GAIL ..... p 38 N93-10583
BOHOR, B. F. ..... p 107 N93-10120
p 107 N93-10121
p 115 N93-10156
BOLT, SCOTT ..... p 28 N93-10638
BOMMIER, V. ..... p 181 N93-10914
BONACCINI, D. ..... p 183 N93-10927
BONCEK, RAYMOND K. ..... p 158 N93-10693
BORCHERS, I. U. ..... p 152 N93-10691
BORIS, JAY P. ..... p 164 N93-10099
BORNSCHAUER, KARL-HEINZ ..... p 76 N93-10888
BOSSERT, DAVID JEROME ..... p 88 N93-10379
BOTEZ, R. ..... p 5 N93-10544
BOTKIN, D. B. ..... p 175 N93-10788
BOUILLARD, J. X. ..... p 163 N93-10645
BOUKSOUR, OTMANE ..... p 51 N93-10503
BOURQUE, MARY LYN ..... p 134 N93-10341
BOWEN, A. W. ..... p 34 N93-10802
BOWLES, E. ..... p 73 N93-10421
BOZIC, M. ..... p 170 N93-10387
BRAAM, B. C. ..... p 183 N93-10931
p 187 N93-10950
p 159 N93-10951
p 86 N93-10952
BRADLEY, CURTISS ..... p 9 N93-10348
BRAGA, JOAO ..... p 153 N93-10312
BRAINARD, GEORGE ..... p 131 N93-10661
BRAKE, M. L. ..... p 88 N93-10286
BRANDENBERGER, R. ..... p 156 N93-10618
BRAR, N. ..... p 35 N93-10221
BRATTON, R. L. ..... p 48 N93-10485
BRAUN, H. ..... p 174 N93-10600
p 174 N93-10603
BRICMAN, C. ..... p 153 N93-10328
BRIGGS, J. S ..... p 77 N93-10897
BRINGEMEIER, D. ..... p 107 N93-10122
BROADWELL, JAMES E. ..... p 31 N93-10437
BROCKMEYER, P. ..... p 106 N93-10117
p 106 N93-10118
p 107 N93-10119
p 107 N93-10123
p 109 N93-10131
p 121 N93-10185
BRON, W. E. ..... p 87 N93-10202
BROOK, MARX ..... p 125 N93-10108
BROWN, ALAN W. ..... p 135 N93-10214
BROWNLEE, D. E. ..... p 32 N93-10853
BRUCKER, DAVID ..... p 80 N93-10309
BRUEHL, CHRISTOPH H. ..... p 104 N93-10256
BRUUN, A. ..... p 116 N93-10159
BRYANT, RANDAL E. ..... p 142 N93-10828
BRYCE, W. D. ..... p 151 N93-10686
BSCHORR, O. ..... p 152 N93-10692
BUCHAL, R. O. ..... p 65 N93-10570
BUCHANAN, P. C. ..... p 109 N93-10130

BUCHENAUER, D. ..... p 160 N93-10326
BUCINELL, RON B. ..... p 16 N93-10007
BUDGE, K. G. ..... p 139 N93-10866
BUECHNER, S. ..... p 82 N93-10629
BUHL, D. ..... p 106 N93-10117
p 107 N93-10123
p 109 N93-10131
BUI-QUOC, T. ..... p 58 N93-10540
BUKSA, JOHN H. ..... p 25 N93-10457
BUREO, R. ..... p 14 N93-10956
BURKHARDT, WENDEL M. ..... p 18 N93-10018
BURNLEY, V. ..... p 150 N93-10682
BURNS, T. M. ..... p 73 N93-10656
BURRELL, K. H. ..... p 161 N93-10463
p 162 N93-10619
p 163 N93-10759
BUSCHMANN, MICHAEL D. ..... p 70 N93-10747
BUSH, HAROLD G. ..... p 13 N93-10744
BUTLER, M. ..... p 76 N93-10836
BYERS, CURTIS ..... p 64 N93-10565
BYRNE, MARK T. ..... p 134 N93-10288

C

CABLE, J. W. ..... p 34 N93-10789
CABRERA, BLAS ..... p 90 N93-10827
CALDWELL, R. H. ..... p 102 N93-10625
CALM, J. M. ..... p 30 N93-10401
CAMPBELL, R. B. ..... p 160 N93-10326
CAMPOS, E. ..... p 152 N93-10688
CARBONELL, JAIME G. ..... p 137 N93-10422
CARDARELLI, J. J. ..... p 172 N93-10396
CARPENTER, WILLIAM C. ..... p 53 N93-10514
p 64 N93-10565
CARR, DWAYNE ..... p 176 N93-10883
CARTER, J. A. ..... p 7 N93-10442
CARTER, M. K. ..... p 14 N93-10937
CASADA, D. A. ..... p 91 N93-10381
CASSADY, R. JOE ..... p 21 N93-10031
CASTOR, JERE ..... p 9 N93-10348
CAUZZI, G. ..... p 182 N93-10923
CAVALLINI, F. ..... p 183 N93-10927
CEDER, G. ..... p 167 N93-10403
CEPPATELLI, G. ..... p 183 N93-10927
CHAI, L. ..... p 28 N93-10508
CHAKRAVARTHY, SUKUMAR R. ..... p 79 N93-10297
CHAN, CHU-LOK ..... p 107 N93-10124
CHAN, J. K. ..... p 54 N93-10519
CHAN, S. ..... p 14 N93-10521
CHAN, S. H. ..... p 31 N93-10423
CHANCE, M. S. ..... p 163 N93-10760
CHANDRASHEKHARA, K. ..... p 57 N93-10532
p 65 N93-10572
CHANG, FUKUO ..... p 46 N93-10479
CHANG, S. L. ..... p 163 N93-10645
CHAR, S. ..... p 182 N93-10920
CHARLTON, M. T. ..... p 8 N93-10803
CHAU, D. S. C. ..... p 169 N93-10249
CHAU, NGUYEN VAN ..... p 144 N93-10389
CHEHIL, D. S. ..... p 57 N93-10531
CHEN, E. P. ..... p 47 N93-10484
CHEN, ERGANG ..... p 145 N93-10857
CHEN, H. ..... p 77 N93-10052
CHEN, LIYIN ..... p 89 N93-10722
CHEN, P. J. ..... p 30 N93-10281
CHEN, QIZHI ..... p 26 N93-10721
CHEN, WUZHU ..... p 159 N93-10812
CHEN, YUNQIN ..... p 26 N93-10721
CHENG, C. C. ..... p 30 N93-10266
p 30 N93-10281
p 27 N93-10465
p 40 N93-10748
CHENG, CHIH-HSIUNG GARY ..... p 84 N93-10875
CHEVACHAROEUKUL, S. ..... p 73 N93-10656
CHICK, L. A. ..... p 104 N93-10729
CHIN, B. A. ..... p 92 N93-10634
CHIN, SUEI ..... p 4 N93-10845
CHIU, S. C. ..... p 160 N93-10390
CHIUDERI-DRAGO, F. C. ..... p 180 N93-10908
CHO, GYUSEONG ..... p 75 N93-10790
CHO, Y. ..... p 140 N93-10219
CHOHAN, HARPAL S. ..... p 28 N93-10509
CHONG, S. ..... p 140 N93-10219
CHONGSAWANGVIROD, S. ..... p 168 N93-10614
CHOW, R. ..... p 159 N93-10818
CHOYKE, W. J. ..... p 30 N93-10266
p 30 N93-10281
p 40 N93-10748
p 76 N93-10888
CHRIST, RICHARD E. ..... p 137 N93-10409
CHRISTHILF, DAVID M. ..... p 10 N93-10070
CHU, M. S. ..... p 163 N93-10760
CHU, ZEXIANG ..... p 89 N93-10722
CHURCH, J. P. ..... p 137 N93-10631
CHURCH, THOMAS M. ..... p 129 N93-10887
CINTALA, MARK J. ..... p 108 N93-10125
p 108 N93-10126
p 112 N93-10144
CIOFALO, VINCENT B. ..... p 43 N93-10636
CISZEWSKI, D. ..... p 56 N93-10530
CLARK, C. ..... p 181 N93-10915
CLARK, DAVID E. ..... p 35 N93-10205
CLARK, KENNETH C. ..... p 125 N93-10711
CLARKE, D. R. ..... p 27 N93-10254
CLAYTON, CLIVE R. ..... p 33 N93-10100
CLEMEN, M. L. ..... p 27 N93-10465
CLINE, JAMES ..... p 41 N93-10779
COFFEN, CHARLES DAVID ..... p 147 N93-10458
COFFEY, HELEN E. ..... p 190 N93-10771
p 190 N93-10773
p 190 N93-10774
p 190 N93-10775
p 190 N93-10776
COLAIANNI, M. L. ..... p 30 N93-10266
COLLIER-CAMERON, A. ..... p 181 N93-10918
COLLIN, B. ..... p 182 N93-10924
COLLIN, D. ..... p 148 N93-10671
COLLINS, DANIEL L. ..... p 131 N93-10613
COLLISTON, W. P. ..... p 106 N93-10115
p 108 N93-10127
p 119 N93-10174
COOK, D. ..... p 161 N93-10443
COOK, JOSEPH C. ..... p 23 N93-10042
COOKE, ROGER M. ..... p 146 N93-10107
p 147 N93-10798
COOKSON, THOMAS ..... p 38 N93-10584
COOPER, G. W. ..... p 72 N93-10279
CORLISS, LLOYD D. ..... p 11 N93-10741
CORNETTE, JAMES B. ..... p 73 N93-10421
CORNWELL, T. J. ..... p 184 N93-10932
CORREIA, ANA MARIA RAMALHO
p 173 N93-10596
COTE, P. J. ..... p 144 N93-10419
COTTER, GLADYS A. ..... p 174 N93-10601
COTTON, B. W. ..... p 102 N93-10625
COULDER, R. ..... p 181 N93-10915
COWAN, E. J. ..... p 108 N93-10128
COX, LARRY T., JR. ..... p 25 N93-10258
CRAVER, W. LIONEL, JR. ..... p 57 N93-10534
CRAWFORD, D. A. ..... p 108 N93-10129
CRAWFORD, H. ..... p 86 N93-10444
CRAWFORD, MARK ..... p 124 N93-10262
CREAMER, J. E. ..... p 169 N93-10879
CROFT, M. C. ..... p 168 N93-10630
CROFTON, JOHN BERNARD ..... p 76 N93-10830
CRONIN-GOLOMB, MARK ..... p 172 N93-10431
CROSS, L. E. ..... p 71 N93-10273
p 71 N93-10276
p 72 N93-10280
p 72 N93-10282
CRUZALEBES, P. ..... p 177 N93-10942
CULICK, F. E. C. ..... p 150 N93-10682
CURRAN, F. M. ..... p 23 N93-10044
CURRAN, FRANK M. ..... p 25 N93-10197
CUST, KEVIN M. ..... p 18 N93-10017
CUTHBERTSON, JOHN WILLIAM ..... p 160 N93-10353
CUTTS, D. ..... p 156 N93-10618

D

DACOSTAPEREIRA, MARCOS ..... p 102 N93-10373
DAI, LIA ..... p 172 N93-10396
DAILY, W. ..... p 103 N93-10763
DAINTY, J. C. ..... p 178 N93-10945
DALLMANN, U. ..... p 6 N93-10549
DALRYMPLE, G. BRENT ..... p 120 N93-10176
DAMAREN, C. J. ..... p 56 N93-10529
DAME, L. ..... p 179 N93-10901
p 179 N93-10904
p 183 N93-10930
p 184 N93-10932
p 178 N93-10948
p 159 N93-10951
p 86 N93-10952
DANA, ROGER A. ..... p 69 N93-10657
DANGTRAN, K. ..... p 84 N93-10860
DARLING, DOUGLAS ..... p 79 N93-10087
DART, SUSAN A. ..... p 137 N93-10448
p 138 N93-10665
DASGUPTA, GAUTAM ..... p 50 N93-10500
DASH, STANFORD M. ..... p 16 N93-10010
DATTA, S. K. ..... p 48 N93-10485
DAVID, H. A. ..... p 146 N93-10699
DAVIES, HUW G. ..... p 55 N93-10522
DAVILA, CARLOS G. ..... p 46 N93-10478
DAVIS, CHUCK L. ..... p 11 N93-10046
DAVIS, H. A. ..... p 155 N93-10333
DAVIS, J. A. ..... p 5 N93-10012
DAVIS, ROBERT F. ..... p 166 N93-10355
p 166 N93-10356
DAVOODI, H. ..... p 50 N93-10496
DAY, R. ..... p 15 N93-10005
DEBOO, J. C. ..... p 161 N93-10463
p 163 N93-10759
DEFONTAINE, D. ..... p 167 N93-10403
DEGENHARDT, J. J., JR. ..... p 109 N93-10130
DEGIORGI, V. GENSHEIMER ..... p 49 N93-10491
DEGROOT, WIM A. ..... p 25 N93-10086
DEHNHARD, D. ..... p 157 N93-10838
DEINO, A. L. ..... p 110 N93-10138
DEITZ, R. S. ..... p 109 N93-10132
DEJAGER, CORNELIS ..... p 182 N93-10919
DEKERTANGUY, A. ..... p 181 N93-10914
DELEON, ROBERT ..... p 88 N93-10247
DELLER, J. R., JR. ..... p 143 N93-10200
DELVENTHAL, REX A. ..... p 24 N93-10049
DEMANDANTE, CARLO G. ..... p 40 N93-10770
DEMEESTER, P. ..... p 165 N93-10235
DEMPSEY, JOHN P. ..... p 47 N93-10483
p 48 N93-10489
DEOTTE, ROBERT E., JR. ..... p 92 N93-10892
p 93 N93-10893
p 93 N93-10894
DEPITRE, A. ..... p 149 N93-10676
DERE, K. ..... p 180 N93-10911
DERE, K. P. ..... p 180 N93-10907
DERMENDJIEV, V. N. ..... p 183 N93-10925
DEROOIJ, A. ..... p 34 N93-10580
DESA, L. ..... p 178 N93-10957
DEUTSCH, A. ..... p 106 N93-10117
p 107 N93-10123
p 109 N93-10131
p 115 N93-10157
p 121 N93-10185
DEVATY, R. P. ..... p 76 N93-10888
DEVOTO, J. A. ..... p 170 N93-10388
DHARANI, L. R. ..... p 52 N93-10506
p 28 N93-10508
DIAZ, CARLOS ..... p 74 N93-10715
DICKINSON, J. ..... p 6 N93-10550
DIETZ, ROBERT S. ..... p 117 N93-10165
DIMOTAKIS, PAUL E. ..... p 31 N93-10437
DING, LIMING ..... p 74 N93-10702
DIONNE, GERALD F. ..... p 74 N93-10718
DIPPEL, K. H. ..... p 160 N93-10293
DIPPREY, NEIL F. ..... p 24 N93-10048
DIRECTOR, MARK N. ..... p 19 N93-10023
DISPERATI, ATTILIO ANTONIO ..... p 102 N93-10063
DITCHEK, B. M. ..... p 74 N93-10755
DOBRANICH, DEAN ..... p 25 N93-10457
DOERS, JESSE ..... p 132 N93-10796
DON, JARLEN ..... p 28 N93-10344
DONGARRA, J. J. ..... p 143 N93-10285
p 139 N93-10816
DONOHUE, KEVIN D. ..... p 68 N93-10380
DORAN, JEFFREY A. ..... p 127 N93-10664
DORON, E. ..... p 169 N93-10226
DOUGHERTY, J. P. ..... p 71 N93-10273
p 71 N93-10276
p 72 N93-10280
p 72 N93-10282
DOWLING, KIM ..... p 109 N93-10133
DOWNEY, P. J. ..... p 20 N93-10027
DRESCHEL, T. W. ..... p 129 N93-10085
DRESSLER, B. ..... p 107 N93-10123
DRESSLER, B. O. ..... p 106 N93-10117
p 107 N93-10119
p 103 N93-10182
DREZNER, JEFFREY A. ..... p 8 N93-10420
DRIVER, MARK ANTHONY ..... p 5 N93-10889
DRUZHININ, S. A. ..... p 183 N93-10928
DUBEY, R. N. ..... p 66 N93-10575
p 66 N93-10577
DUDLEY, ROSS A. ..... p 134 N93-10713
DUGUNDJI, JOHN ..... p 8 N93-10842
DUMAS, R. ..... p 15 N93-10005
DUNEEN, R. J. ..... p 113 N93-10150
DUNN, MARTY ..... p 27 N93-10277
DUNN, PETER E. ..... p 8 N93-10842
DUONG, H. ..... p 163 N93-10760
DURIN, CHRISTIAN ..... p 39 N93-10592
DURSCH, HARRY ..... p 39 N93-10589
p 39 N93-10590
p 39 N93-10591
DUTTON, E. J. ..... p 69 N93-10430
DVALI, G. R. ..... p 179 N93-10296
DVORAK, GEORGE J. ..... p 28 N93-10896
DVORSKY, JAMES E. ..... p 133 N93-10217
DYE, RAYMOND H. ..... p 131 N93-10650
DYER, DOUGLAS E. ..... p 175 N93-10723

E

EDWARDS, DANIEL ..... p 103 N93-10781
EDWARDS, DOREEN ..... p 36 N93-10343

EGGLESTON, DEBRA S. p 15 N93-10001
EKMANN, J. M. p 80 N93-10330
ELKINS, NANCY p 132 N93-10796
ELLISON, J. R. p 11 N93-10047
ELMARAGHY, W. H. p 66 N93-10576
ELSTON, W. E. p 109 N93-10134
ELTGROTH, P. G. p 92 N93-10635
EMBID, PEDRO F. p 83 N93-10810
ENGELAGE, J. p 86 N93-10444
ENGELMANN, B. E. p 95 N93-10646
ENOMOTO, RYO p 39 N93-10627
EPSTEIN, MARCELO p 49 N93-10495
ERICKSON, C. p 22 N93-10035
ERIKSON, WILLIAM L. p 89 N93-10725
ERKI, M. A. p 44 N93-10466
ESEN, E. B. p 82 N93-10612
ETZIONI, OREN p 137 N93-10422
EURINGER, H. p 160 N93-10293
EVANS, A. G. p 27 N93-10254
EVANS, E. G. p 126 N93-10433
EVANS, NOREEN JOYCE p 109 N93-10135
EVANS, P. S. p 17 N93-10015

F

FAEHL, R. J. p 155 N93-10333
FALCHI, A. p 182 N93-10923
FALCIANI, R. p 182 N93-10923
FALCO, R. E. p 82 N93-10629
FALICOV, L. M. p 155 N93-10863
FALKOWSKI, P. G. p 128 N93-10283
FANCIULLO, THOMAS J. p 17 N93-10014
FARABAUGH, E. N. p 40 N93-10778
FARLEY, W. W. p 158 N93-10708
FAUCHERRE, M. p 178 N93-10943
p 178 N93-10944
p 178 N93-10945
FEAUTRIER, N. p 181 N93-10914
FEI, YE p 89 N93-10703
FEILER, PETER H. p 135 N93-10214
FELDBERG, RASMA p 129 N93-10628
FELDMAN, A. p 35 N93-10231
p 40 N93-10778
FELDMAN, MICHAEL R. p 86 N93-10408
FELDMAN, V. I. p 110 N93-10136
FENG, MINGXI p 5 N93-10858
FENG, S. T. p 88 N93-10412
FENG, WILLIAM W. p 46 N93-10476
FERGUSON, ELDON E. p 105 N93-10772
FERNANDEZ, MICHAEL J. p 12 N93-10106
FERNSLER, R. F. p 70 N93-10215
FERRON, J. R. p 163 N93-10620
FIDELL, SANFORD p 151 N93-10683
FIFE, WILMER K. p 36 N93-10246
FILIPPONE, W. L. p 154 N93-10362
FINEGOLD, LAWRENCE S. p 151 N93-10683
FINKEL, LEIF H. p 131 N93-10271
FINKEN, K. H. p 160 N93-10293
FISHER, A. p 156 N93-10643
FISHER, J. R. p 21 N93-10032
FISHER, L. T. p 7 N93-10442
FISKE, P. S. p 110 N93-10137
FITZ-SIMONS, T. p 126 N93-10433
FIZIEV, P. P. p 170 N93-10386
FLODEN, T. p 116 N93-10159
FLORES, I. p 86 N93-10444
FLORYAN, J. M. p 6 N93-10549
p 61 N93-10552
FLUCKS, M. p 109 N93-10131
FLUEGEL, BRIAN p 87 N93-10228
FOING, BERNARD H. p 182 N93-10920
p 182 N93-10921
FOLEY, S. N. p 139 N93-10823
FOLEY, SIMON N. p 175 N93-10801
FONSECA, LEILA MARIA GARCIA p 157 N93-10311
FOSS, C. A., JR. p 158 N93-10694
FOURNIER, G. p 150 N93-10679
FOX, MARK L. p 19 N93-10024
FRANK, Z. p 177 N93-10902
FRANKE, MILT E. p 16 N93-10009
FREERICKS, J. K. p 155 N93-10863
FRENCH, JONATHAN p 131 N93-10661
FRENDI, ABDELKADER p 82 N93-10757
FRIDLUND, C. M. p 178 N93-10945
FRIED, H. M. p 156 N93-10618
FRISBEE, ROBERT H. p 23 N93-10043
FRISE, P. R. p 59 N93-10543
FRY, J. N. p 192 N93-10616
FRYDRYCHOWICZ, W. p 64 N93-10569
FUJITA, KATSUHIDE p 65 N93-10573

G

GABRIEL, CAMELIA p 72 N93-10359
GAC, FRANK D. p 35 N93-10205
GAETA, R. J., JR. p 5 N93-10012
GAITAN, MICHAEL p 136 N93-10248
GAITONDE, DATTA p 81 N93-10410
GAKWAYA, A. p 62 N93-10558
GANAPOL, B. D. p 154 N93-10362
GAO, Q. p 30 N93-10266
p 30 N93-10281
p 40 N93-10748
GARVEY, JAMES F. p 88 N93-10247
GARVIN, J. B. p 110 N93-10138
p 110 N93-10139
p 120 N93-10177
GATLIN, B. p 138 N93-10746
GAULT, DONALD E. p 120 N93-10178
GAUTIER, CATHERINE p 126 N93-10292
GAUTIER, D. C. p 155 N93-10333
GAVIN, D. p 15 N93-10005
GEIDER, R. p 128 N93-10283
GELDSETZER, H. H. J. p 122 N93-10191
GEMMEN, R. p 81 N93-10449
GENT, A. N. p 46 N93-10475
GEORGE, PETE p 38 N93-10585
p 38 N93-10587
GEORGE, THOMAS F. p 164 N93-10093
p 90 N93-10799
GEORGIADIS, H. G. p 49 N93-10490
GERASEVA, YE. L. p 33 N93-10706
GERLACH, KARL p 143 N93-10275
GEVINS, A. S. p 133 N93-10662
GHALY, W. p 60 N93-10545
GHONEM, H. p 33 N93-10717
GIBSON, WILLIAM p 131 N93-10661
GIESE, R. F. p 76 N93-10831
GIESS, S. C. p 147 N93-10822
GIL, YOLANDA p 137 N93-10422
GILGENBACH, R. M. p 88 N93-10286
GILIBERT, Y. p 53 N93-10515
GILIBERT, YVON p 54 N93-10516
GILMORE, C. J. p 34 N93-10802
GIRIDHARAN, MANAMPATHY G. p 83 N93-10846
GLASS, I. I. p 60 N93-10546
GLENN, CHANCE M. p 71 N93-10255
GLIKSON, A. Y. p 110 N93-10140
GLOVER, R. P. p 11 N93-10953
p 159 N93-10955
GLUZBAND, YEHEZKIEL A. p 70 N93-10747
GOHIL, P. p 162 N93-10619
GOLDAK, J. A. p 61 N93-10554
GOLDEN, C. M. p 21 N93-10032
GOLDEN, JOHNNY L. p 34 N93-10581
GOLIGHTLY, MICHAEL J. p 131 N93-10613
GOLNARAGHI, M. F. p 65 N93-10574
GOLTSOS, W. C. p 87 N93-10218
GOLUB, L. p 14 N93-10939
GOMUC, R. p 58 N93-10540
GONZALEZ, CARLOS R. p 66 N93-10710
GOODENOUGH, JOHN B. p 136 N93-10300
GOODFELLOW, W. D. p 109 N93-10135
GORE, J. C. p 172 N93-10396
GOSTIN, V. A. p 111 N93-10141
GOSTIN, VICTOR A. p 109 N93-10133
GOTO, N. p 87 N93-10083
GRAINGER, D. W. p 104 N93-10729
GRANT, E. R. p 154 N93-10730
GRATZ, A. J. p 111 N93-10142
p 111 N93-10143
GRAY, CARL E., JR. p 45 N93-10472
GREEN, D. J. p 37 N93-10439
GREENAWAY, A. H. p 178 N93-10944
p 178 N93-10945
p 178 N93-10946
GREENE, J. M. p 163 N93-10760
GREENFIELD, C. M. p 161 N93-10463
p 163 N93-10759
GREENLY, J. B. p 155 N93-10333
GREGOIRE, D. C. p 109 N93-10135
GREGORY, DON A. p 157 N93-10259
GREINER, L. p 86 N93-10444
GRIEVE, RICHARD p 103 N93-10182
GRIEVE, RICHARD A. F. p 108 N93-10125
p 108 N93-10126
p 112 N93-10144
GRIFFIS, D. P. p 32 N93-10852
p 32 N93-10853
p 32 N93-10854
GRIGG, PHILIP p 166 N93-10355
GRODZINSKY, ALAN J. p 70 N93-10747
GROEBNER, R. J. p 160 N93-10326
p 161 N93-10392
p 162 N93-10619
p 163 N93-10759
GROSSBECK, M. L. p 92 N93-10634
GRYDER, R. K. p 171 N93-10382
GUBER, A. L. p 176 N93-10867
GUDIVADA, V. N. p 176 N93-10883
GUERRERO, LOURDES M. p 11 N93-10741
GUPTA, A. p 141 N93-10334
GURALNIK, G. p 156 N93-10618
GURAN, A. p 54 N93-10518
GUTLEBEN, H. p 27 N93-10465
GUYENNE, T.-D. p 179 N93-10901
GUYOT, F. p 117 N93-10163

H

HABBAL, SHADIA R. p 190 N93-10767
HABERMAN, RICHARD p 144 N93-10660
HACKSTEIN, H. J. p 152 N93-10691
HACKWORTH, JOHN A. p 67 N93-10203
HAIL, M. p 125 N93-10784
HAINES, BRUCE JOSEPH p 103 N93-10847
HAJJ, IBRAHIM p 74 N93-10715
HAMBLETON, RONALD K. p 134 N93-10341
HAMILTON, DAVID B. p 133 N93-10261
HAMILTON, WARREN B. p 112 N93-10145
HAMLEY, JOHN A. p 21 N93-10033
HAMMON, COLIN P. p 133 N93-10719
HAN, SEUNGEUK p 4 N93-10811
HANDEL, PETER H. p 74 N93-10751
HANI, R. p 15 N93-10005
HANNAN, NELSON A. p 25 N93-10457
HANNON, PATRICK R. p 131 N93-10661
HANSMAN, R. J. p 6 N93-10065
HAO, ZHIDONG p 167 N93-10609
HARGRAVES, R. B. p 110 N93-10137
p 112 N93-10146
HARJES, H. C. p 76 N93-10836
HARMON, TIMOTHY p 22 N93-10035
HARRIS, A. I. p 178 N93-10945
HARRIS, ANTHONY L. p 151 N93-10687
HARRIS, C. STANLEY p 148 N93-10670
HARRIS, REGINA M. p 137 N93-10409
HARRISON, RICHARD A. p 181 N93-10916
HARROLD, C. L. p 134 N93-10804
p 134 N93-10807
HARTMAN, RICHARD L. p 172 N93-10431
HARTUNG, J. p 113 N93-10147
HARTUNG, J. B. p 105 N93-10114
HARVEY, R. W. p 160 N93-10390
HASEGANU-ZAMFIRESCU, E. p 58 N93-10536
HASKELL, G. P. p 14 N93-10929
HASSOUN, JOHN A. p 134 N93-10713
HATFIELD, L. L. p 124 N93-10262
HAWKE, B. RAY p 113 N93-10148
HAWKER, MAHLON C. p 6 N93-10265
HE, FANGDIAN p 159 N93-10812
HE, JUN p 28 N93-10344
HEAD, J. W. p 113 N93-10148
HEALD, DAN A. p 17 N93-10013
HEARD, WALTER L., JR. p 13 N93-10744
HEARN, HANK C. p 23 N93-10041
HEDLEY, MARK p 126 N93-10377
HEIDARI-MIANDOAB, FARID p 79 N93-10304
HEIDBRINK, W. W. p 163 N93-10760
HEINIG, K. p 152 N93-10689
HEINZEL, P. p 180 N93-10910
HENINS, I. p 155 N93-10333
HENKEL, H. p 113 N93-10149
p 119 N93-10171
HENLINE, WILLIAM D. p 28 N93-10742
HEO, E. p 170 N93-10604
HEPPLER, G. R. p 57 N93-10535
HERBEIN, WILLIAM C. p 46 N93-10477
HERNANDEZ, G. p 125 N93-10711
HEUER, R. p 48 N93-10487
HEWITT, M. J. p 7 N93-10442
HEYSE, MARK W. p 73 N93-10421
HEYVAERTS, J. p 180 N93-10912
HICKSON, A. J. p 63 N93-10563
HILL, D. N. p 160 N93-10326
HILL, DAVID A. p 69 N93-10440
HILL, GERALD M. p 21 N93-10033
HILL, O. E. p 11 N93-10021
HILL, SUSAN G. p 137 N93-10409
HILLARD, G. BARRY p 13 N93-10841
HILLIS, D. L. p 160 N93-10293
HILTNER, A. p 41 N93-10825
HINKEL, DENISE p 125 N93-10714
HO, CHIH-MING p 3 N93-10340
HODAPP, T. p 163 N93-10759
HODGKINS, P. DOUGLAS p 7 N93-10738
HOGAN, J. T. p 160 N93-10293
HOLLOWAY, PAUL H. p 73 N93-10663
HOMEYER, W. G. p 73 N93-10421
HONG, JOOYOO p 170 N93-10434
HONG, SOON-JO p 28 N93-10509
HOOPLE, T. G. p 69 N93-10430
HOPSON, MARGARET p 131 N93-10661
HORGAN, LUCILLE E. p 8 N93-10420
HOROWITZ, STANLEY A. p 133 N93-10719

HORTON, W. p 170 N93-10604
HORWITZ, SUSAN p 138 N93-10782
HOUGEN, S. B. p 110 N93-10137
HOUSTON, S. S. p 8 N93-10803
HOWELL, DOROTHY T. p 4 N93-10824
HRUDEY, T. M. p 62 N93-10556
HU, S. p 52 N93-10507
HU, Y. Z. p 161 N93-10413
p 168 N93-10614
p 162 N93-10615
HUBBARD, R. F. p 70 N93-10215
HUCK, RONALD P. p 134 N93-10288
HUDSON, ROGER D. p 12 N93-10106
HUDSON, T. D. p 157 N93-10259
HUFF, CLIFF p 135 N93-10104
HUGHES, THOMAS J. R. p 44 N93-10467
HUMPHREY, WATTS S. p 137 N93-10447
HUNSAKER, C. T. p 175 N93-10788
HUNTER, J. L. p 32 N93-10853
p 32 N93-10854
HURST, J. K. p 104 N93-10729
HUTCHINSON, JAMES R. p 56 N93-10526
HUTCHISON, BOYD J. p 20 N93-10027
HUTCHISON, J. L. p 35 N93-10231
p 40 N93-10778
HUTING, WILLIAM A. p 75 N93-10785
HUTTENLOCHER, D. F. p 44 N93-10398
HUYER, STEPHEN ALBERT p 80 N93-10305
HWANG, C. C. p 80 N93-10330
HWANG, W. C. p 51 N93-10505
HYATT, A. W. p 161 N93-10392

I

IANNELLI, GIUSEPPE SETTIMO p 3 N93-10306
INGE, J. L. p 189 N93-10832
INGER, GEORGE R. p 84 N93-10886
INGS, J. B. p 166 N93-10335
INIGO, RAFAEL M. p 135 N93-10103
IRANI, Z. R. p 54 N93-10520
IRENE, E. A. p 88 N93-10412
p 161 N93-10413
p 30 N93-10414
p 167 N93-10415
p 168 N93-10614
p 162 N93-10615
p 73 N93-10656
IRSCHIK, H. p 48 N93-10487
IRVING, PAUL ANTHONY p 93 N93-10307
IRWIN, P. G. J. p 189 N93-10378
ISACHSEN, Y. W. p 113 N93-10150
ISICHENKO, M. B. p 170 N93-10604
IVANOV, B. A. p 114 N93-10151
IZETT, G. A. p 120 N93-10180

J

JACKSON, G. L. p 161 N93-10463
p 163 N93-10759
JACKSON, M. C. p 122 N93-10189
JAIN, RAKESH KUMAR p 53 N93-10513
JAKOSKY, B. M. p 189 N93-10064
JAMALI, M. M. p 141 N93-10299
JAMES, R. S. p 114 N93-10152
JAMISON, KEITH A. p 12 N93-10106
JANKOV, S. p 182 N93-10920
JANKOVSKY, ROBERT S. p 18 N93-10020
p 22 N93-10038
p 26 N93-10743
JATEGAONKAR, R. p 57 N93-10531
JAVOY, M. p 105 N93-10113
JAYANTHI, UDAYA BHASKARAM p 153 N93-10312
JEFFRIES-NAKAMURA, B. p 75 N93-10786
JENCHEN, U. p 106 N93-10118
JENNINGS, TIMOTHY A. p 72 N93-10357
JENSEN, J. KERMIT p 13 N93-10744
JERTZ, W. p 148 N93-10667
JESSBERGER, E. K. p 122 N93-10188
p 122 N93-10189
JEVICKI, A. p 156 N93-10618
JIANG, BONAN p 60 N93-10548
JIAYU, NIU p 13 N93-10705
JIROUSEK, J. p 49 N93-10494
JOHNS, STEVEN T. p 158 N93-10693
JOHNS, WILLIAM E. p 92 N93-10740
JOHNSON, ALLEN L. p 69 N93-10695
JOHNSON, CHRIS p 39 N93-10589
JOHNSON, ERIC R. p 46 N93-10478
JOHNSON, L. J. p 77 N93-10897
JOHNSON, M. A. p 144 N93-10419
JOHNSON, MARK C. p 93 N93-10894
JOHNSON, MATUSZAK K. p 125 N93-10784
JONES, T. E. p 77 N93-10897
JONES, W. D. p 30 N93-10400
JONKOUSKI, JILL p 36 N93-10343
JOSEPH, J. p 161 N93-10413
JOSEPH, ROBERT p 137 N93-10422
JOYCE, G. p 70 N93-10215
JOYCE, RICHARD K. p 4 N93-10375
JUDD, D. C. p 17 N93-10014
JULLIARD, J. p 148 N93-10671
JURICK, D. p 35 N93-10221

K

KACA, J. p 60 N93-10546
KACYNSKI, KENNETH J. p 18 N93-10019
KAILASANATH, K. p 16 N93-10008
KALAYCIOGLU, B. A. p 54 N93-10520
KALAYCIOGLU, S. p 54 N93-10520
KAMAT, MANOHAR P. p 94 N93-10372
KAMMASH, T. p 88 N93-10286
KAMO, S. L. p 115 N93-10156
KANDIL, OSAMA A. p 2 N93-10098
KANG, SUNG-MO p 74 N93-10715
KAPP, JOSEPH A. p 95 N93-10750
KAR, R. J. p 28 N93-10325
KARADAG, V. p 9 N93-10537
KARIM, M. R. p 47 N93-10482
KARNEY, C. F. F. p 160 N93-10390
KARNOPP, B. H. p 56 N93-10527
KARR, GERALD R. p 26 N93-10756
KATSAROS, KRISTINA p 127 N93-10849
KATSAROS, KRISTINA B. p 128 N93-10068
p 127 N93-10848
p 127 N93-10850
p 127 N93-10851
KAUFFMAN, ROBERT E. p 29 N93-10101
KAUSHAL, A. p 45 N93-10470
KAWASE, TAKEHIKO p 65 N93-10573
KAY, ROBERT J. p 21 N93-10032
KAY, ROBERT W. p 116 N93-10158
KAYSER, R. F. p 43 N93-10397
KAZAROFF, JOHN M. p 18 N93-10020
p 22 N93-10038
p 26 N93-10743
KEAYS, R. R. p 111 N93-10141
KEAYS, REID R. p 109 N93-10133
KELLMAN, A. G. p 163 N93-10759
KENNEPOHL, F. p 152 N93-10689
KENT, BARRY J. p 159 N93-10949
KEOUGH, BRUCE p 39 N93-10588
KERN, SCOTT p 166 N93-10355
KESTER, DANIEL p 166 N93-10356
KESTIN, J. p 170 N93-10787
KEVAN, STEPHEN D. p 164 N93-10105
KHDEIR, A. A. p 45 N93-10473
KHOO, IAM-CHOON p 166 N93-10345
KIKKERT, S. p 75 N93-10786
KIM, D. E. p 170 N93-10604
KIM, DONGGIL p 33 N93-10100
KIM, J. p 162 N93-10619
KIM, JAEWAN p 170 N93-10434
KIM, K. p 169 N93-10249
KIM, YOUNG K. p 166 N93-10355
KIMES, KENNETH L. p 134 N93-10288
KIMNACH, GREG L. p 26 N93-10734
KIMSEY, KENT D. p 95 N93-10427
KING, K. p 156 N93-10618
KINGSLEY, J. J. p 104 N93-10729
KIRKHOPE, J. p 44 N93-10466
KIRSCH, JAMES C. p 157 N93-10259
KISLEV, HANOCH p 26 N93-10638
KITSON, S. T. p 78 N93-10056
KLARSFELD, S. p 170 N93-10387
KLEIN, MICHEL L. L. p 53 N93-10515
KLEPPER, C. C. p 160 N93-10293
KLEPPNER, DANIEL p 31 N93-10712
KNAUSS, W. G. p 49 N93-10493
KNUDSEN, CARSTEN p 129 N93-10628
KO, S. p 86 N93-10444
KOEBERL, C. p 113 N93-10147
KOEBERL, CHRISTIAN p 114 N93-10153
p 114 N93-10154
p 115 N93-10155
KOEHLER, B. p 178 N93-10943
p 178 N93-10957
KOETKE, D. S. p 154 N93-10820
KOHLER, WERNER p 152 N93-10769
KOHOUT, KEITH A. p 136 N93-10300
KOMIYA, ZEN p 40 N93-10727
KORNBLITH, JEFFREY p 67 N93-10096
KOSSECKA, ELZBIETA p 43 N93-10314
KOUSKY, VERNON E. p 126 N93-10337
KOUTCHMY, S. p 181 N93-10915
KOWLER, EILEEN p 132 N93-10278
KOZLOVA, M. N. p 33 N93-10706
KRAYNIK, A. M. p 36 N93-10399
KREBS, G. p 86 N93-10444
KRIEBEL, MARY M. p 21 N93-10030
KRISHNAMURTHY, K. p 65 N93-10572
KRISHNAPPA, G. p 149 N93-10672
KRISTIANSEN, M. p 124 N93-10262
KROGH, T. E. p 115 N93-10156
KROL, J. p 61 N93-10552
KROL, MARK F. p 158 N93-10693
KRUIZINGA, B. p 183 N93-10931
p 187 N93-10950
p 159 N93-10951
p 86 N93-10952
KRUSINGER, ALAN E. p 127 N93-10780
KRYDER, M. H. p 35 N93-10230
KUBANKE, D. p 152 N93-10692
KUCERA, RICHARD F. p 132 N93-10796
KUCHAR, J. K. p 6 N93-10065
KUNDU, T. p 47 N93-10482
KUNZ, J. p 122 N93-10189
KUNZ, ROBERT FRANCIS p 81 N93-10370
KURTZ, HELMUT L. p 163 N93-10754
KUTLU, ZAFER p 46 N93-10479
KUTSCHENREUTER, PAUL H. p 5 N93-10012
KWAN, A. p 14 N93-10511
KWATRA, S. C. p 141 N93-10299
KYRIACOU, C. I. p 35 N93-10082

L

LABEYRIE, A. p 178 N93-10945
LABRECQUE, D. p 103 N93-10763
LAHAYE, R. J. p 161 N93-10392
LAHOUD, ANTOINE E. p 51 N93-10503
LAIT, ANDREW J. p 67 N93-10111
LAKE, MARK S. p 13 N93-10744
LAKOMY, R. p 106 N93-10117
p 107 N93-10119
p 107 N93-10123
p 109 N93-10131
p 121 N93-10185
LAKSHMANAN, P. K. p 14 N93-10521
LAM, D. p 175 N93-10788
LAMARCHE, L. p 6 N93-10547
LAMBERT, D. p 62 N93-10558
LAMPE, M. p 70 N93-10215
LANEVILLE, ANDRE p 6 N93-10551
LANG, VALERIE I. p 42 N93-10336
LANGENHORST, F. p 115 N93-10157
LANGFORD, G. K. p 23 N93-10041
LANOU, R. E. p 156 N93-10618
LAO, L. L. p 161 N93-10393
p 161 N93-10463
p 163 N93-10620
p 163 N93-10760
LARAMEE, R. C. p 19 N93-10024
LARBALESTIER, D. C. p 168 N93-10733
LAROCHE, J. p 128 N93-10283
LARSON, C. A. p 23 N93-10044
p 25 N93-10197
LASHKO, N. F. p 33 N93-10706
LAUGHLIN, D. E. p 35 N93-10230
LAX, MELVIN p 88 N93-10251
LE, MINH D. p 15 N93-10003
LEARNER, R. C. M. p 11 N93-10953
LEBLEBICI, YUSUF p 74 N93-10715
LECOMTE, CLAUDE p 149 N93-10677
LEE, DAVID CHUNG LIANG p 102 N93-10373
LEE, GILBERT F. p 71 N93-10241
LEE, JOHN N. p 172 N93-10431
LEE, MIN-CHANG p 69 N93-10728
LEE, P. p 113 N93-10147
LEE, PASCAL p 116 N93-10158
LEE, R. p 163 N93-10759
LEE, ROBERT A. p 148 N93-10670
LEE, S. p 70 N93-10865
LEE, SUNG-TAICK p 42 N93-10313
LEGER, J. R. p 87 N93-10218
LEI, JUNTING p 36 N93-10243
LEMAIRE, P. p 177 N93-10903
LEMMER, U. p 14 N93-10954
LENZ, T. G. p 31 N93-10436
LEONARD, A. W. p 160 N93-10326
LEONG, H. M. p 133 N93-10662
LEQUEUX, J. p 178 N93-10945
LEUNG, CHUN M. p 178 N93-10238
LEVESQUE, B. p 65 N93-10571
LEVINSON, M. p 74 N93-10755
LEVIT, S. p 169 N93-10229
p 170 N93-10295
LEWY, S. p 150 N93-10679
LI, J. X. p 41 N93-10825
LI, PING p 74 N93-10715
LI, X. p 90 N93-10799
LIANG, SHIN-CHING p 13 N93-10365
LIBRESCU, L. p 29 N93-10525
LICKLIDER, ROBERT A. p 142 N93-10958
p 143 N93-10959

LILLJEQUIST, R. p 113 N93-10149
LIN, CHIN S. p 159 N93-10066
LIN, D. L. p 90 N93-10799
LINDSTROEM, M. p 116 N93-10159
LINTON, T. W. p 155 N93-10333
LIOU, LARRY C. p 17 N93-10016
LIOU, W. J. p 29 N93-10510
LIOU, WILLIAM W.-W. p 81 N93-10454
LIPPMAN, S. I. p 163 N93-10759
LIPPMANN, S. I. p 160 N93-10326
LITTRELL, DONALD M. p 12 N93-10106
LIU, CHI-TSIEH p 15 N93-10003
LIU, M. S. p 143 N93-10200
LIU, NING p 172 N93-10396
LIU, QIANG p 55 N93-10522
LIU, Z. D. p 90 N93-10799
LOEHMAN, R. E. p 28 N93-10391
LOEHNER, R. p 16 N93-10008
LONG, D. G. F. p 116 N93-10160
LONG, GABRIELLE p 41 N93-10779
LONG, S. P. p 129 N93-10461
LONGVAL, J. R. p 6 N93-10550
LOOMIS, G. E. p 159 N93-10818
LOSKOT, KRZYSZTOF p 43 N93-10314
LOTTES, S. A. p 163 N93-10645
LOU, J. Z. p 140 N93-10209
LOVELAND, W. p 156 N93-10762
LOW, K. H. p 66 N93-10575
p 66 N93-10577
LOWMAN, P. D. p 117 N93-10162
LOWMAN, PAUL D., JR. p 116 N93-10161
LU, YANGSHAN p 57 N93-10534
LUCHINI, P. p 62 N93-10557
LUHMANN, J. G. p 189 N93-10064
LUO, XIUQUAN p 107 N93-10124
LUZZI, D. E. p 40 N93-10766
LYSAGHT, ROBERT J. p 137 N93-10409

M

MA, S. F. p 51 N93-10504
MABEY, D. G. p 153 N93-10805
MACDONALD, DIGBY D. p 71 N93-10250
MACKUSE, FRANCES A. p 7 N93-10833
MACON, WILLIAM A., JR. p 155 N93-10102
MACRANDER, A. T. p 157 N93-10837
MADEY, JOHN M. p 89 N93-10697
MAESTRELLO, LUCIO p 82 N93-10757
MAGLICH, B. p 156 N93-10643
MAGNUSON, S. O. p 84 N93-10868
MAHAJAN, S. M. p 179 N93-10296
MAHDAVI, A. M. p 160 N93-10326
MAILLARD, J. P. p 86 N93-10936
MAITI, A. p 33 N93-10411
MAJDA, ANDREW J. p 79 N93-10094
MALLEN, F. p 152 N93-10688
MALLORY, VICTOR T. p 43 N93-10636
MALLOUK, T. E. p 166 N93-10284
MALONE, MARK C. p 17 N93-10015
MANZARA, ANTHONY P. p 19 N93-10025
MARBLE, FRANK E. p 31 N93-10843
MARCAS, GEORGE N. p 165 N93-10210
MARCHAND, O. p 5 N93-10544
p 6 N93-10547
MARCOS, B. p 64 N93-10567
MARIC, Z. p 170 N93-10387
MAROHN, H.-D. p 149 N93-10675
MARSCH, E. p 177 N93-10903
MARSCHER, WILLIAM D. p 78 N93-10062
MARSHALL, JANET C. p 136 N93-10248
MARTH, RICHARD B., SR. p 7 N93-10424
MARTIN, C. R. p 158 N93-10694
MARTIN, CHARLES R. p 36 N93-10243
MARTIN, JOHN p 9 N93-10348
MARTINEZ, I. p 105 N93-10113
p 117 N93-10163
MASAITIS, V. L. p 117 N93-10164
MASCARENHAS, NELSON DELFINO DAVILA
p 157 N93-10311
MASHNICH, G. P. p 183 N93-10928
MASSON, C. p 6 N93-10547
MASSOUDI, M. p 80 N93-10330
MASTIN, C. W. p 138 N93-10746
MASTURZO, D. E. p 29 N93-10263
MATSUNO, YOSHIYA p 39 N93-10627
MATTHEWS, RAYMOND H. p 6 N93-10323
MATVIYENKO, GREGORY p 143 N93-10339
MAU, T. K. p 160 N93-10390
MAUNDER, E. A. W. p 63 N93-10561
MAVRIPLIS, D. J. p 2 N93-10097
MAXWELL, J. p 159 N93-10951
p 86 N93-10952
p 11 N93-10953
p 159 N93-10955
MAYES, PAUL p 68 N93-10301
p 68 N93-10302
MAZOUZI, ABDELKRIM p 6 N93-10551
MCCLURE, DONALD E. p 141 N93-10095
MCCOMB, JAMES C. p 19 N93-10026
p 20 N93-10028
MCCORMACK, R. p 167 N93-10403
MCCORMICK, M. p 132 N93-10796
MCDILL, J. M. p 61 N93-10554
MCDONNEL, MICHAEL p 176 N93-10899
MCGIMPSEY, SUE p 172 N93-10396
MCGINNIS, W. C. p 77 N93-10897
MCGUIRE, G. E. p 73 N93-10656
MCHONE, J. F. p 109 N93-10132
MCHONE, JOHN F. p 117 N93-10165
MCINNIS, J. B. p 66 N93-10576
MCINTYRE, DAVID p 89 N93-10720
MCKAY, D. W. p 154 N93-10605
MCKINNON, WILLIAM B. p 118 N93-10166
MCLAIN, M. G. p 20 N93-10029
MCMILLIN, S. NAOMI p 4 N93-10824
MCMURDIE, LYNN p 127 N93-10849
MCPHEE, JOHN J. p 54 N93-10517
MCPHERSON, DOUGLASS J., SR. p 19 N93-10023
MCVEY, E. S. p 135 N93-10103
MEGUID, S. A. p 10 N93-10539
p 59 N93-10542
MEI, CHUH p 45 N93-10472
MEIN, P. p 183 N93-10926
MEISEL, L. V. p 144 N93-10419
MELEBECK, CLOVIS J. p 172 N93-10451
MENARDI, S. p 177 N93-10942
MENKEN, C. M. p 58 N93-10538
MERKLE, F. p 178 N93-10943
p 178 N93-10944
MEYER, E. S. p 52 N93-10506
MEYER, J. A. p 165 N93-10245
MEYER, KENT p 136 N93-10300
MICHEL, ULF p 149 N93-10674
p 151 N93-10685
MILESKI, PAUL p 67 N93-10096
MILEY, GEORGE H. p 26 N93-10638
MILLER, J. H. p 130 N93-10834
MILLS, D. M. p 157 N93-10837
MINKEL, DONALD HOWE p 124 N93-10324
MIODUSZEWSKI, P. K. p 160 N93-10293
MISRA, A. K. p 54 N93-10520
p 14 N93-10521
MISRA, V. p 32 N93-10853
p 32 N93-10854
MITCHELL, J. B. p 89 N93-10698
MODI, V. J. p 54 N93-10519
p 14 N93-10521
MOGNARD, NELLY M. p 127 N93-10850
MONAHAN, S. P. p 154 N93-10362
MONNET, G. p 181 N93-10915
MONTA, WILLIAM J. p 2 N93-10071
MONTGOMERY, J. p 87 N93-10090
MOORE, JOHN W. p 142 N93-10354
MORANO, JOSEPH S. p 24 N93-10049
MOREAU, D. p 163 N93-10761
MORENO, HECTOR p 136 N93-10237
MORENO, J. B. p 103 N93-10383
MORRIS, ED p 135 N93-10104
MORRIS, G. MICHAEL p 172 N93-10431
MORRIS, PHILIP J. p 151 N93-10684
MORRISON, GERALD L. p 92 N93-10892
p 93 N93-10893
p 93 N93-10894
MOSHIER, W. C. p 34 N93-10752
MOSS, T. A. p 103 N93-10383
MOUSKOS, S. C. p 49 N93-10490
MOY, D. p 16 N93-10007
MPITSOS, GEORGE J. p 140 N93-10242
MUELLER-MOHR, V. p 106 N93-10117
p 107 N93-10119
p 118 N93-10167
p 121 N93-10185
MUELLER, E. Z. p 144 N93-10624
MUELLER, MARK A. p 23 N93-10040
MUENCHAUSEN, R. E. p 155 N93-10333
MUKHOPADHYAY, VIVEK p 10 N93-10070
MUNCZEK, H. p 154 N93-10605
MURATOV, LEONID S. p 164 N93-10093
MUSSAKOWSKI, R. p 103 N93-10182

N

NADLER, JONATHON p 26 N93-10638
NAKANO, HIDEO p 65 N93-10573
NANAGARA, BYAPRORN p 31 N93-10794
NARANG, SUBHASH C. p 71 N93-10250
NARIGON, MICHAEL LEE p 141 N93-10346
NATH, YOGENDRA p 53 N93-10513
NAYAK, V. K. p 118 N93-10168
NAYERI, M. p 143 N93-10200
NEAU, E. L. p 76 N93-10836
NECESSARY, J. p 15 N93-10005
p 79 N93-10232
NEITZEL, G. P. p 111 N93-10143
NELLIS, W. J. p 87 N93-10083
NEMOTO, K. p 182 N93-10924
NESME-RIBES, E. p 71 N93-10273
NEWNHAM, R. E. p 71 N93-10276
p 72 N93-10280
p 72 N93-10282
NEXON, J. W. p 172 N93-10396
NG, CHIU H. p 4 N93-10811
NG, E. p 141 N93-10334
NGUYEN, H. D. p 139 N93-10817
NGUYEN, Q. p 74 N93-10755
NGUYEN, V. D. p 6 N93-10550
NIEUWENHUIJZEN, HANS p 182 N93-10919
NILES, ANTHONY p 8 N93-10698
NISBET, R. A. p 175 N93-10788
NOCERA, D. G. p 82 N93-10629
NOFAL, MOSTAFA p 62 N93-10559
NOORDAM, J. E. p 178 N93-10944
p 178 N93-10945
NOORI, M. p 50 N93-10496
NORDENG, H. O. p 11 N93-10047
NORDMAN, JAMES E. p 167 N93-10404
NORMAN, MARC D. p 118 N93-10169
NOUR-OMID, B. p 144 N93-10639
NOVEMBER, L. p 181 N93-10915
NUCCIO, E. J. p 171 N93-10270
NULL, LINDA M. p 175 N93-10844

O

OBOT, N. T. p 82 N93-10612
OBRIEN, C. J. p 17 N93-10014
OCONNOR, D. p 75 N93-10786
OCONNOR, ROBERT D. p 31 N93-10794
ODDY, A. S. p 81 N93-10554
OGDEN, R. W. p 45 N93-10474
OKAMURA, OKIYOSHI p 72 N93-10368
OKEEFE, JOHN D. p 119 N93-10170
OKOS, M. R. p 129 N93-10085
OLSON, MARK A. p 95 N93-10427
OLSON, TODD M. p 41 N93-10783
OLTHOF, H. p 14 N93-10929
OMIDVAR, O. M. p 142 N93-10450
OPPENHEIM, A. K. p 32 N93-10553
ORAN, ELAINE S. p 164 N93-10099
ORENSTEIN, R. M. p 37 N93-10439
ORISAMOLU, I. R. p 64 N93-10568
OSBORNE, T. H. p 161 N93-10483
OSGOOD, RICHARD M., JR. p 87 N93-10201
OSTOJA-STARZEWSKI, MARTIN p 50 N93-10498

P

PACHECO, JAVIER FRANCISCO p 124 N93-10376
PADMANABLAN, M. K. p 62 N93-10555
PAGLIETTI, A. p 51 N93-10502
PAGNACITH, KUHN p 113 N93-10147
PAISLEY, MICHAEL J. p 166 N93-10356
PALMOUR, JOHN W. p 70 N93-10233
PANG, C. p 56 N93-10528
PANG, J. p 14 N93-10956
PAPAEFTHYMIOU, GEORGIA C. p 153 N93-10338
PAPARIZOS, L. p 150 N93-10682
PARASCHIVOIU, I. p 5 N93-10544
p 60 N93-10545
p 6 N93-10547
PARMESWARAN, M. p 136 N93-10248
PARSLEY, R. C. p 22 N93-10037
PARTLOW, W. D. p 76 N93-10888
PARTRIDGE, R. p 156 N93-10618
PARZEN, EMANUEL p 146 N93-10795
PASIN, M. p 4 N93-10648
PATCHETT, B. E. p 14 N93-10937
PATE, B. B. p 165 N93-10206
PATE, LEAH R. p 23 N93-10042
PATE, M. B. p 35 N93-10084
PATRINOS, D. p 173 N93-10595
PAUCKERT, R. p 22 N93-10035
PAUL, BERNARD P., JR. p 3 N93-10320
PAVLI, AL J. p 22 N93-10038
PAVLI, ALBERT J. p 18 N93-10020
p 26 N93-10743
PAYNE, JUDITH E. p 75 N93-10792
PAYNE, RICHARD C. p 151 N93-10687
PEDERSON, L. R. p 104 N93-10729
PEERY, J. S. p 139 N93-10866
PEGRAM, JAN E. p 41 N93-10783
PEIFER, WILLIAM R. p 88 N93-10247
PELLEGRINO, S. p 14 N93-10511
PENN, K. J. p 76 N93-10836
PEREDERY, W. p 114 N93-10152

PEREDERY, WALTER V. p 117 N93-10165
PERKINS, KEN R. p 25 N93-10457
PERKINS, STEVEN E. p 15 N93-10002
PERRETT, B. H. E. p 94 N93-10198
PERRIER, C. p 177 N93-10940
PERRY, BILL p 166 N93-10356
PERRYMAN, M. A. C. p 178 N93-10944
PESEUX, B. p 63 N93-10562
PESONEN, L. J. p 119 N93-10171
PETRIE, T. W. p 160 N93-10326
PETTENSKI, THOMAS A. p 91 N93-10290
PETTY, GRANT W. p 127 N93-10851
PEVTSOV, A. A. p 183 N93-10928
PEYTON, B. p 141 N93-10334
PFEFFER, RICHARD L. p 126 N93-10363
PHELPS, JAMES E. p 13 N93-10744
PHILLIPS, J. p 163 N93-10759
PHILLIPS, LEE p 164 N93-10099
PHILLIPS, W. J. p 29 N93-10224
PHILLIPS, WILLIAM D. p 155 N93-10885
PIANKO, M. p 150 N93-10679
PICHA, R. J. p 14 N93-10521
PIFER, J. H. p 168 N93-10630
PINCKNEY, S. ZANE p 9 N93-10011
PINERO, LUIS R. p 21 N93-10033
PING, ZHANG p 89 N93-10703
PINKER, R. A. p 150 N93-10678
p 151 N93-10686
PINTO, JOSEPH P. p 104 N93-10256
POETZ, W. p 169 N93-10871
POLAR, J. C. p 30 N93-10414
PONTON, MICHAEL K. p 150 N93-10680
PONZONI, FLAVIO JORGE p 102 N93-10063
POOL, R. p 173 N93-10599
POPE, D. P. p 40 N93-10766
POPP, CHRISTOPHER G. p 23 N93-10042
POPPLEWELL, N. p 56 N93-10528
POSPIESZCYK, A. p 160 N93-10293
POSTON, WENDY p 147 N93-10869
POVINELLI, LOUIS A. p 60 N93-10548
POZZI, A. p 62 N93-10557
PRABHU, M. S. S. p 62 N93-10555
PRANGE, RENEE p 182 N93-10922
PRETCZYNSKI, ZBIGNIEW p 43 N93-10314
PRICE, M. A. p 68 N93-10366
PRIEBE, CAREY p 147 N93-10869
PRITCHARD, DAVID E. p 158 N93-10659
PROVAN, J. W. p 59 N93-10541
PRUCNAL, PAUL R. p 158 N93-10693
PUBLICO, ANDRE p 50 N93-10500
PUGH, COLEEN p 40 N93-10727
PURCELL, ANTHONY J. p 147 N93-10642
PUROHIT, G. P. p 11 N93-10047
PURVES, N. p 181 N93-10915
PUTERSKI, R. p 7 N93-10442
PUURA, V. p 116 N93-10159

Q

QIN, XINHUA p 86 N93-10347
QUAN, RALPH W. p 13 N93-10308
QUATE, C. F. p 168 N93-10726
QUEVAT, J. P. p 63 N93-10562

R

RABBIA, Y. p 177 N93-10942
RAGHAVAN, V. V. p 176 N93-10883
RAGLAND, BRENDA L. p 23 N93-10042
RAHHALARABI, A. p 69 N93-10418
RAJAGOPAL, DOCOTR p 82 N93-10696
RAJLICH, PETR p 119 N93-10172
RALSTON, J. p 154 N93-10605
RAMAMURTI, RAVI p 16 N93-10008
RAMESH, M. p 35 N93-10230
RAMIREZ, A. L. p 103 N93-10763
RAMOND, P. p 153 N93-10291
RAMOS, JEFFREY W. p 20 N93-10029
RAMSEY, J. M. p 89 N93-10429
RANANAVARE, S. B. p 104 N93-10729
RAND, RICHARD H. p 11 N93-10499
RANDLES, M. H. p 169 N93-10879
RANTALAHTI, ESKO T. p 91 N93-10367
RASMUSSEN, P. G. p 132 N93-10321
RASMUSSEN, STEEN p 129 N93-10628
RAUFASTE, NOEL J. p 125 N93-10089
RAVI-CHANDAR, K. p 48 N93-10488
RAZAQPUR, A. GHANI p 62 N93-10559
READ, P. D. p 14 N93-10937
REDDY, J. N. p 45 N93-10473
p 47 N93-10481
REECE, DOUGLAS A. p 142 N93-10749
REED, K. W. p 76 N93-10836
REED, RUSSELL p 15 N93-10004
REHAK, P. p 74 N93-10731
REID, A. M. p 109 N93-10130
p 121 N93-10186
REIF, JOHN H. p 140 N93-10227
REIMOLD, W. U. p 106 N93-10115
p 108 N93-10127
p 119 N93-10173
p 119 N93-10174
p 122 N93-10189
REIMOLD, WOLF UWE p 115 N93-10155
REINELT, D. A. p 36 N93-10399
REINICKE, ROBERT H. p 18 N93-10017
REITER, ELMAR R. p 125 N93-10204
REJ, D. J. p 155 N93-10333
RENNER, G. F. p 133 N93-10217
RENZ, DAVID D. p 9 N93-10456
REPS, THOMAS p 138 N93-10782
RETTIG, C. p 161 N93-10463
REVETTA, F. A. p 113 N93-10150
REVZIN, A. M. p 132 N93-10321
RHEIN, ROBERT A. p 15 N93-10004
p 15 N93-10006
RHOADES-BROWN, M. J. p 156 N93-10732
RHOADES, C. E., JR. p 92 N93-10635
RHODES, WILLIAM T. p 172 N93-10431
RICHARD, M. J. p 65 N93-10571
RICHMOND, GERALDINE L. p 164 N93-10105
RICHTER, R. p 152 N93-10690
RICKS, D. A. p 32 N93-10853
p 32 N93-10854
RIDA, S. p 83 N93-10859
p 84 N93-10860
RIGHINI, A. p 183 N93-10927
RIGOLOT, ALAIN p 54 N93-10516
RIMROTT, F. P. J. p 54 N93-10518
RIOU, G. p 148 N93-10671
RITTER, JOSE p 41 N93-10779
ROACH, D. P. p 94 N93-10327
ROACH, ROBERT L. p 79 N93-10087
ROADIFER, M. P. p 69 N93-10430
ROBBINS, D. J. p 87 N93-10211
ROBERTODOSSANTOS, JOAO p 102 N93-10373
ROBERTSON, JAMES B. p 38 N93-10582
ROBINS, L. H. p 40 N93-10778
ROBINSON, D. N. p 96 N93-10777
RODDY, D. J. p 105 N93-10114
RODRIGUES, ROGERIO LACOURT p 94 N93-10310
RODRIGUEZ, RODOLFO p 144 N93-10407
ROELKE, RICHARD J. p 78 N93-10061
ROGERS, C. S. p 157 N93-10837
ROGERS, CURT p 8 N93-10420
ROGERS, GEORGE p 147 N93-10869
ROGERS, LAWRENCE W. p 4 N93-10753
ROSAKIS, ARES J. p 49 N93-10492
ROSELLE, S. J. p 105 N93-10432
ROSENGREEN, A. p 73 N93-10405
ROSENZWEIG, C. p 155 N93-10840
ROSSMANITH, R. p 157 N93-10862
ROSSON, RITA M. p 105 N93-10772
ROSSONI, P. p 74 N93-10755
ROSTOKER, N. p 162 N93-10617
p 156 N93-10633
p 156 N93-10643
ROTH, MARK A. p 175 N93-10723
ROTHBERG, E. p 141 N93-10334
ROTHGERY, EUGENE p 15 N93-10005
ROUSSEL, P. H. p 178 N93-10944
ROY, S. p 65 N93-10572
RUBINSZTAJN, SLAWOMIR p 36 N93-10246
RUEB, JUSTIN D. p 134 N93-10713
RUEGGEBERG, H. p 11 N93-10668
RUNDE, M. p 76 N93-10831
RUTTEN, R. J. p 179 N93-10904
RYAN, M. A. p 75 N93-10786
RYDER, GRAHAM p 119 N93-10175
p 120 N93-10176

S

SAALTINK, MARK p 142 N93-10641
SABA, COSTANDY S. p 29 N93-10101
SAGER, J. C. p 129 N93-10085
SAHAL-BRECHOT, S. p 181 N93-10914
SAIYED, NASEEM H. p 24 N93-10045
SAJDA, PAUL p 131 N93-10271
SAKOWSKI, BARBARA p 79 N93-10087
SALIBA, H. T. p 56 N93-10530
SALMON, D. p 181 N93-10915
SALOMONS, E. p 167 N93-10403
SALTZMAN, JEFF S. p 138 N93-10736
SALUCCI, G. p 183 N93-10927
SAMBATH, TOUCH p 113 N93-10147
SAMUEL, S. p 155 N93-10878
SANCAKTAR, E. p 51 N93-10501
SANDHU, RANBIR S. p 28 N93-10509
SANDOVAL, M. B. p 68 N93-10394
SANIIE, JAFAR p 68 N93-10380
SANKAR, B. V. p 52 N93-10507
SANKAR, LAKSHMI N. p 83 N93-10793
SANKOVIC, JOHN M. p 23 N93-10044
p 25 N93-10197
SANKS, TERRY M. p 21 N93-10030
SATHAYE, SHIRISH S. p 67 N93-10253
SAVAGE, M. E. p 72 N93-10279
SAWYER, BRIAN M. p 6 N93-10323
SCHAERER, U. p 105 N93-10113
p 117 N93-10163
SCHAFER, R. W. p 73 N93-10417
SCHECHTER, J. p 155 N93-10840
SCHISSEL, D. P. p 161 N93-10463
SCHLEGEL, V. p 54 N93-10518
SCHMIDT, ED E. p 23 N93-10040
SCHMIDT, RACHEL p 8 N93-10420
SCHMIEDER, B. p 180 N93-10906
p 180 N93-10911
SCHNETZLER, C. C. p 110 N93-10139
p 120 N93-10177
SCHOENBERG, RICHARD J. p 22 N93-10036
SCHRADE, HERBERT O. p 163 N93-10754
SCHRECENGOST, T. R. p 34 N93-10752
SCHROCK, RICHARD R. p 40 N93-10727
SCHULTZ, P. H. p 108 N93-10129
p 123 N93-10193
p 123 N93-10194
SCHULTZ, PETER H. p 120 N93-10178
SCHULZ-LUEPERTZ, E. p 14 N93-10954
SCHUMACHER, G. p 177 N93-10942
SCHWARZ, RAY P. p 129 N93-10109
p 129 N93-10110
SCHWERDTNER, W. M. p 108 N93-10128
SCOTT, PETER D. p 85 N93-10239
SCOVILLE, J. T. p 161 N93-10392
SEGAWA, Y. p 34 N93-10880
SEINER, J. M. p 16 N93-10010
SEINER, JOHN M. p 150 N93-10680
SELVADURAI, A. P. S. p 48 N93-10486
SEMERCIGIL, S. E. p 56 N93-10528
SEPULVEDA, J. L. p 35 N93-10082
SERAYDARIAN, R. P. p 162 N93-10619
SGARBOZZA, M. p 149 N93-10676
SGHEDONI, M. p 178 N93-10957
SHA, LUI p 67 N93-10253
SHAH, A. H. p 48 N93-10485
SHAMSI, A. p 42 N93-10329
SHANNON, R. R. p 158 N93-10446
SHAPIRO, JOSEPH I. p 132 N93-10796
SHARMA, C. B. p 45 N93-10471
SHARPE, LISA M. p 159 N93-10724
SHARPTON, VIRGIL L. p 120 N93-10179
SHATAS, A. A. p 162 N93-10615
SHAW, B. A. p 34 N93-10752
SHAW, R. W. p 89 N93-10429
SHECHTMAN, D. p 35 N93-10231
p 40 N93-10778
SHEIKH, M. A. p 63 N93-10563
p 64 N93-10566
SHEN, GONGXUN p 12 N93-10814
SHEN, M. p 15 N93-10005
SHEPHARD, MARK S. p 28 N93-10896
SHI, YONGYI p 28 N93-10344
SHIMABUKURO, YOSIO EDEMIR p 102 N93-10373
SHINE, R. p 177 N93-10902
SHIUE, T.-J. p 48 N93-10488
SHOEMAKER, E. M. p 105 N93-10114
p 120 N93-10180
SHOFNER, WILLIAM P. p 131 N93-10650
SHOUCRI, MERIT p 125 N93-10714
SHU, CHI-WANG p 145 N93-10758
SHVARTSMAN, ALEXANDER A. p 140 N93-10213
SIKIVIE, P. p 170 N93-10434
SIMENSEN, THOR A. p 68 N93-10260
SIMEONI, D. p 178 N93-10957
SIMNETT, G. M. p 181 N93-10913
SIMON, C. G. p 32 N93-10853
p 32 N93-10854
SIMONS, D. p 86 N93-10936
SIMONSON, BRUCE M. p 120 N93-10181
SIMPSON, W. W. p 72 N93-10279
SINCEBAUGH, PATRICK J. p 138 N93-10716
SINGAL, R. K. p 57 N93-10533
p 58 N93-10536
SINGH, B. M. p 48 N93-10486
SINGH, M. C. p 64 N93-10568
p 64 N93-10569
SINGHROY, V. p 103 N93-10182
SINGHROY, V. H. p 117 N93-10162
SINKOVITS, ROBERT S. p 164 N93-10099
SIVAN, N. p 169 N93-10229
p 170 N93-10295
SKOE, IVAR HELGE p 78 N93-10058
SLANEY, V. R. p 117 N93-10162

SLEZIONA, P. C. ..... p 163 N93-10754
SLINKER, S. P. ..... p 70 N93-10215
SMALDONE, L. A. ..... p 182 N93-10923
SMILANSKY, U. ..... p 169 N93-10226
p 170 N93-10294
SMITH, ALVIN ..... p 189 N93-10406
SMITH, DENNIS ..... p 135 N93-10104
SMITH, GILES K. ..... p 8 N93-10420
SMITH, HOOVER A. ..... p 29 N93-10101
SMITH, TIMOTHY ..... p 125 N93-10714
SNIJDERS, B. ..... p 183 N93-10931
p 187 N93-10950
p 159 N93-10951
p 86 N93-10952
SNYDER, CURTIS D. ..... p 9 N93-10011
SNYDER, E. J. ..... p 34 N93-10880
SOKOLOV, A. N. ..... p 33 N93-10706
SOLANKI, S. K. ..... p 179 N93-10905
p 14 N93-10934
SOLKA, JEFFREY ..... p 147 N93-10869
SOLOMON, MARVIN ..... p 138 N93-10782
SONG, HONGJIANG ..... p 145 N93-10857
SOPOK, SAMUEL ..... p 29 N93-10207
SORCI, J. M. ..... p 160 N93-10331
SOREM, ROBERT M. ..... p 63 N93-10560
SOTIRIOU, CONSTANTINOS PANTELI
p 8 N93-10322
SOVKA, J. ..... p 181 N93-10915
SPEAR, STEVE ..... p 39 N93-10589
p 39 N93-10590
SPENCER, A. J. M. ..... p 44 N93-10468
SPIELMAN, F. E. ..... p 137 N93-10441
SPIELMAN, R. B. ..... p 164 N93-10839
SPILLER, E. ..... p 14 N93-10939
SPINDT, C. A. ..... p 73 N93-10405
SPITZ, H. B. ..... p 172 N93-10396
SPRAY, JOHN G. ..... p 121 N93-10183
p 122 N93-10187
SPUDIS, PAUL D. ..... p 121 N93-10184
SRINATHKUMAR, S. ..... p 10 N93-10070
STACY, JOHN L. ..... p 158 N93-10693
STAGE, STEVEN A. ..... p 128 N93-10791
STANCIL, D. D. ..... p 35 N93-10230
STEADMAN, S. G. ..... p 154 N93-10402
STECKEL, GARY L. ..... p 38 N93-10584
p 38 N93-10587
STEIN, BLAND A. ..... p 37 N93-10578
STEIN, EARL S. ..... p 7 N93-10459
STENFLO, J. O. ..... p 14 N93-10934
STEPHENS, M. A. ..... p 146 N93-10700
STEPIEN-OAKES, KIM ..... p 135 N93-10104
STERLING, J. ..... p 150 N93-10682
STILLER, PETER F. ..... p 145 N93-10870
STOCKMAN, MARK I. ..... p 164 N93-10093
STOEFFLER, D. ..... p 106 N93-10117
p 121 N93-10185
STOJAK, JEAN L. ..... p 28 N93-10344
STONE, H. F. ..... p 7 N93-10442
STOREY, L. R. O. ..... p 70 N93-10800
STRAIT, E. J. ..... p 163 N93-10760
STRANGE, P. J. R. ..... p 151 N93-10686
STRANICK, S. J. ..... p 165 N93-10245
STRIKWERDA, JOHN C. ..... p 79 N93-10220
STROSNIDER, JAY K. ..... p 67 N93-10253
STROYEV, A. S. ..... p 33 N93-10706
STURTEVANT, B. ..... p 84 N93-10895
SU, YONG ..... p 159 N93-10812
SUBRAMANIAM, V. V. ..... p 159 N93-10252
SUN, C. T. ..... p 51 N93-10505
p 29 N93-10510
SUNG, CHIA-CHI ..... p 10 N93-10319
SURANA, KARAN S. ..... p 63 N93-10560
SURESH, S. ..... p 40 N93-10632
SURI, SURESH C. ..... p 42 N93-10268
SURYANARAYAN, S. ..... p 62 N93-10555
SUTTON, BENNIE ..... p 171 N93-10257
SUTTON, D. M. ..... p 20 N93-10029
SUTTON, GEORGE P. ..... p 22 N93-10034
SUTTON, WILLARD H. ..... p 35 N93-10205
SWAIN, JAMES H. ..... p 132 N93-10709
SWEENY, J. M. ..... p 114 N93-10152
SWEENY, MARK F. ..... p 168 N93-10637
SWENSON, HARRY N. ..... p 7 N93-10745
SWENSON, RICHARD M. ..... p 142 N93-10958
p 143 N93-10959
SWIETLIK, R.-M. ..... p 106 N93-10118
SYDSERFF, P. ..... p 181 N93-10915
SZEMA, KUO-YEN ..... p 79 N93-10297
SZKLARSKA-AMIALOWSKA, Z. ..... p 33 N93-10395

T

TABAKOFF, W. ..... p 4 N93-10648
TABER, BRADLEY M., III ..... p 138 N93-10716
TACONI, NOLAN E. ..... p 73 N93-10421
TAMANOI, YOSHIHITO ..... p 72 N93-10368
TAMASANIS, DOUGLAS ..... p 68 N93-10358
TAN, C. I. ..... p 156 N93-10618
TAN, H. Q. ..... p 95 N93-10453
p 95 N93-10455
TAN, SOO-HEE ..... p 165 N93-10274
TANG, CHA-MEI ..... p 90 N93-10768
TARBELL, T. ..... p 177 N93-10902
TAYA, MINORU ..... p 27 N93-10277
TAYLOR, KEVIN M. ..... p 133 N93-10217
TAYLOR, P. A. ..... p 27 N93-10465
TAYLOR, T. S. ..... p 161 N93-10463
p 163 N93-10620
p 163 N93-10760
TCHON, K. F. ..... p 60 N93-10545
TEIXEIRA, LUIZ ..... p 125 N93-10204
TEMPLE, BRIAN ..... p 26 N93-10638
TENNYSON, R. C. ..... p 38 N93-10586
p 38 N93-10587
TEPLY, JAN L. ..... p 46 N93-10477
THAMES, H. DAVIS, III ..... p 92 N93-10892
THAMES, H. DAVIS, III. ..... p 93 N93-10893
p 93 N93-10894
THAMES, HOWARD D. ..... p 92 N93-10891
THANGJITHAM, S. ..... p 29 N93-10525
THEOBALD, B. ..... p 10 N93-10539
THERRIAULT, A. M. ..... p 121 N93-10186
THERY, CHRISTIAN ..... p 149 N93-10677
THIEL, GEORGE HENRY ..... p 96 N93-10873
THOERMER, K. ..... p 14 N93-10954
THOMAS, HUGH O. ..... p 10 N93-10374
THOMAS, R. M. ..... p 67 N93-10199
THOMASSEN, DAVID G. ..... p 131 N93-10626
THOMPSON, ANNE M. ..... p 104 N93-10256
THOMPSON, J. F. ..... p 138 N93-10746
THOMPSON, LUCY M. ..... p 122 N93-10187
THOMPSON, RICHARD E. ..... p 15 N93-10002
THORNE, A. ..... p 11 N93-10953
THORNE, A. P. ..... p 14 N93-10933
p 159 N93-10951
p 86 N93-10952
p 159 N93-10955
TIERNEY, M. J. ..... p 158 N93-10694
TINGLE, S. D. ..... p 24 N93-10048
TINKHAM, MICHAEL ..... p 76 N93-10829
TINSLEY ODEN, J. ..... p 44 N93-10469
TITLE, A. ..... p 177 N93-10902
TO, C. W. S. ..... p 55 N93-10523
p 55 N93-10524
TODD, M. D. ..... p 91 N93-10381
TOENSKOETTER, H. ..... p 152 N93-10690
TOMCZAK, L. M. ..... p 172 N93-10396
TOMSIA, A. P. ..... p 28 N93-10391
TONG, W. M. ..... p 34 N93-10880
TONKYN, R. G. ..... p 154 N93-10730
TOPKA, K. ..... p 177 N93-10902
TRACY, MAUREEN B. ..... p 149 N93-10673
TRAYLOR, GERRY ..... p 15 N93-10005
TRIELOFF, M. ..... p 122 N93-10188
p 122 N93-10189
TRINH, TINH T. ..... p 129 N93-10110
TROPP, R. J. ..... p 126 N93-10433
TROWELL, N. F. ..... p 103 N93-10182
TSAI, CHEN S. ..... p 71 N93-10240
TSAO, D. TEH-WEI ..... p 129 N93-10085
TSUNODA, Y. ..... p 34 N93-10789
TURCOTTE, RHEAL ..... p 36 N93-10343
TURNBULL, A. D. ..... p 163 N93-10760
TURNER, M. G. ..... p 175 N93-10788

U

ULABY, FAWWAZ T. ..... p 67 N93-10223
UNDERWOOD, JAMES R., JR. ..... p 122 N93-10190
UNDERWOOD, M. L. ..... p 75 N93-10786
USHER, M. A. ..... p 72 N93-10279

V

VAKIL, S. ..... p 14 N93-10521
VAKILI, F. ..... p 178 N93-10944
VALDMANIS, JANIS A. ..... p 169 N93-10764
VANDEGEIJN, R. ..... p 143 N93-10285
VANDEGEIJN, R. A. ..... p 139 N93-10816
VANDENOORD, G. H. J. ..... p 181 N93-10917
VANDERLUGT, ANTHONY ..... p 172 N93-10431
VANDEWALL, ALLAN ..... p 79 N93-10087
VANDIVER, TERRY ..... p 16 N93-10007
VANERP, G. M. ..... p 58 N93-10538
VANLEER, BRAM ..... p 83 N93-10808
VANNOORTWIJK, JAN M. ..... p 96 N93-10797
VANSTELLE, KENNETH J. ..... p 22 N93-10037
VANVECHTEN, JAMES A. ..... p 167 N93-10425
VARADAN, V. K. ..... p 71 N93-10273
p 71 N93-10276
p 72 N93-10280
p 72 N93-10282
VARADAN, V. V. ..... p 71 N93-10273
p 71 N93-10276
p 72 N93-10280
p 72 N93-10282
VARANI, MAUREEN ..... p 7 N93-10833
VAUDIN, M. D. ..... p 35 N93-10231
VAUGHAN, C. E. ..... p 21 N93-10031
VAUGHAN, D. ..... p 90 N93-10864
VAUGHAN, J. D. ..... p 31 N93-10436
VEIZER, J. ..... p 109 N93-10135
VELLI, M. ..... p 180 N93-10909
VERES, JOSEPH P. ..... p 23 N93-10039
VERMETTE, STEPHEN J. ..... p 104 N93-10289
VERRY, ELON S. ..... p 104 N93-10289
VIAL, J.-C. ..... p 180 N93-10910
p 181 N93-10915
VISSER, G. ..... p 86 N93-10444
VISSER, H. ..... p 183 N93-10931
VISWANADHAM, BHASKAR ..... p 11 N93-10499
VITEK, V. ..... p 40 N93-10766
VITTECOQ, PIERRE ..... p 6 N93-10551
VO-NGOC, D. ..... p 6 N93-10550
VOLONTE, S. ..... p 178 N93-10944
VONBRAUN, CURT ..... p 179 N93-10303
VONDERLUEHE, O. ..... p 177 N93-10941
p 178 N93-10943
VONGIERKE, HENNING E. ..... p 148 N93-10670
VU, H. V. ..... p 56 N93-10527
VU, NGO Q. ..... p 15 N93-10004

W

WAAGEN, DON ..... p 146 N93-10208
WADE, M. R. ..... p 160 N93-10293
WAGANAAR, W. J. ..... p 155 N93-10333
WAGER, JOHN F. ..... p 167 N93-10425
WAGNER, JOHN W. ..... p 19 N93-10022
WAGNER, THOMAS ..... p 125 N93-10714
WAHL, L. ..... p 57 N93-10535
WAKASA, MASAYUKI ..... p 72 N93-10368
WALDMAN, W. ..... p 3 N93-10342
WALI, K. C. ..... p 155 N93-10640
WALKER, B. J. ..... p 16 N93-10010
WALKER, D. W. ..... p 143 N93-10285
p 139 N93-10816
WALKER, R. Y. ..... p 29 N93-10224
WALLACE, M. W. ..... p 111 N93-10141
WALLACE, MALCOLM W. ..... p 109 N93-10133
WALLACE, R. M. ..... p 27 N93-10465
WALLNAU, KURT C. ..... p 136 N93-10298
WALLSOM, RICHARD E. ..... p 13 N93-10744
WALTON, JAMES T. ..... p 25 N93-10457
WANG, C. A. ..... p 92 N93-10634
WANG, J. B. ..... p 165 N93-10245
WANG, K. ..... p 122 N93-10191
WANG, W. ..... p 35 N93-10230
WANG, Y. Q. ..... p 168 N93-10614
WANG, YUN ..... p 192 N93-10616
WANG, ZHI ..... p 145 N93-10857
WARD, G. F. ..... p 134 N93-10713
WASHABAUGH, P. D. ..... p 49 N93-10493
WASZAK, MARTIN R. ..... p 10 N93-10070
WATSON, BRIAN C. ..... p 94 N93-10372
WATSON, JOHN P. ..... p 79 N93-10232
WATSON, M. A. ..... p 35 N93-10082
WAVRIK, R. W. ..... p 76 N93-10836
WEARING, J. L. ..... p 63 N93-10563
p 64 N93-10566
WEBER, G. J. ..... p 76 N93-10836
WEBER, W. J. ..... p 104 N93-10729
WEGMANN, THOMAS ..... p 163 N93-10754
WEGNER, M. ..... p 152 N93-10689
WEGNER, P. ..... p 90 N93-10739
WEIGELT, G. P. ..... p 178 N93-10944
p 178 N93-10945
WEINAN, E. ..... p 145 N93-10758
WEINER, MELVIN M. ..... p 70 N93-10091
WEISS, JONATHAN M. ..... p 25 N93-10086
WEISS, P. S. ..... p 165 N93-10245
WEISS, R. F. ..... p 128 N93-10621
WELSTEAD, STEPHEN T. ..... p 158 N93-10360
WENDT, BRUCE JAMES ..... p 81 N93-10371
WENDT, R. G. ..... p 34 N93-10752
WENXUAN, ZHU ..... p 10 N93-10704
WESSEL, F. ..... p 156 N93-10643
WEST, W. P. ..... p 160 N93-10326
WESTON, RALPH J. ..... p 151 N93-10687
WHEATON, J. ..... p 159 N93-10955
WHIRLEY, R. G. ..... p 95 N93-10646
WHITAKER, ANN F. ..... p 34 N93-10579
WHITCOMB, JOHN D. ..... p 47 N93-10480
WHITE, J. C. ..... p 123 N93-10192
WHITE, M. G. ..... p 154 N93-10730

WHITESIDES, R. HAROLD ..... p 11 N93-10021
WHITFIELD, A. ..... p 77 N93-10053
p 77 N93-10054
WHITINGTON, M. J. ..... p 67 N93-10199
WICHMAN, R. W. ..... p 123 N93-10193
p 123 N93-10194
WIDGOFF, M. ..... p 156 N93-10618
WIEDMANN, R. T. ..... p 154 N93-10730
WIEDNER, BRIAN G. ..... p 93 N93-10894
WIIK, J. E. ..... p 180 N93-10911
WILCOX, MARION W. ..... p 51 N93-10504
WILEY, CATHY J. ..... p 141 N93-10269
WILLIAMS, FORMAN A. ..... p 42 N93-10267
WILLIAMS, K. ..... p 57 N93-10533
p 58 N93-10536
WILLIAMS, R. M. ..... p 75 N93-10786
WILLIAMS, WILLIAM J. ..... p 133 N93-10217
WILLIFORD, R. E. ..... p 50 N93-10497
WILLIMS, R. S. ..... p 34 N93-10880
WILLOCQ, STEPHANE ..... p 154 N93-10606
WILLSHIRE, WILLIAM L., JR. ..... p 149 N93-10673
WILSON, C. L. ..... p 142 N93-10450
WINEFORDNER, J. D. ..... p 89 N93-10611
WINTER, J. ..... p 161 N93-10463
WINTER, T. G. ..... p 154 N93-10435
WISEMAN, J. ..... p 10 N93-10539
WISEMAN, S. R. ..... p 139 N93-10806
WISEMAN, SIMON ..... p 175 N93-10821
WITCHER, DONALD H. ..... p 142 N93-10958
p 143 N93-10959
WLEZIEN, R. W. ..... p 150 N93-10681
WOLF, DAVID A. ..... p 129 N93-10109
p 129 N93-10110
WOLF, ROBERT S. ..... p 19 N93-10022
WOLK, C. P. ..... p 130 N93-10835
WONG, H. ..... p 58 N93-10536
WOOD, A. K. ..... p 87 N93-10211
WOOD, B. D. ..... p 169 N93-10249
WOODRUFF, KENNETH J. ..... p 133 N93-10217
WORLEY, BRIAN A. ..... p 25 N93-10457
WORTMAN, J. J. ..... p 32 N93-10852
p 32 N93-10853
p 32 N93-10854
WRAY, RICHARD B. ..... p 14 N93-10960
WRIGHT, MAURICE A ..... p 28 N93-10344
WRIGHT, S. F. ..... p 113 N93-10150
WROBLEWSKI, D. ..... p 161 N93-10393
WU, HUEY-TZU ..... p 124 N93-10318
WU, MINSHENG ..... p 159 N93-10812
WU, SIBEN ..... p 107 N93-10124
p 123 N93-10195
WU, ZHONGXIANG ..... p 89 N93-10722

X

XI, D. ..... p 74 N93-10731
XIAOBIN, LI ..... p 26 N93-10721
XU, M. H. ..... p 95 N93-10453

Y

YAKOVLEV, O. I. ..... p 123 N93-10196
YAKOVLEV, V. A. ..... p 167 N93-10415
YAN, BINGYI ..... p 159 N93-10812
YANASE, A. ..... p 34 N93-10880
YANG, DEQING ..... p 145 N93-10857
YANG, FUMIN ..... p 74 N93-10702
YANG, MAOZHAO ..... p 5 N93-10856
YATES, J. T., JR. ..... p 30 N93-10266
p 30 N93-10281
p 40 N93-10748
YATES, JOHN T., JR. ..... p 76 N93-10888
YEH, K. J. ..... p 70 N93-10800
YILDIZ, IMRE ..... p 173 N93-10594
YOKAYAMA, T. ..... p 53 N93-10512
YOSHIMURA, HIROAKI ..... p 65 N93-10573
YOST, GREGG R. ..... p 175 N93-10826
YOST, R. ..... p 125 N93-10784
YOST, WILLIAM A. ..... p 131 N93-10650
YOUNG, C. R. ..... p 11 N93-10953
YOUNG, J. P. ..... p 89 N93-10429
YOUNG, PHILIP R. ..... p 37 N93-10578
YOUNGBLOOD, G. E. ..... p 104 N93-10729
YOUNGEN, JEFFREY ROBERT ..... p 177 N93-10364

Z

ZAGHLOUL, MONA E. ..... p 136 N93-10248
ZANGENEH, M. ..... p 77 N93-10055
p 78 N93-10057
ZARRELLA, PAUL ..... p 135 N93-10104
ZEHNDER, ALAN T. ..... p 49 N93-10492
ZELDIN, MARTEL ..... p 36 N93-10246
ZELENKA, RICHARD E. ..... p 7 N93-10745
ZETTLER, J.-T. ..... p 168 N93-10614
ZHANG, D. L. ..... p 60 N93-10546
ZHANG, JIAYUN ..... p 123 N93-10195
ZHANG, LUMIN ..... p 4 N93-10707
ZHANG, S. W. ..... p 55 N93-10523
ZHENG, D. ..... p 33 N93-10717
ZHENG, YUAN F. ..... p 66 N93-10649
ZHOU, QING-QING ..... p 95 N93-10385
ZHOU, ZHIMING ..... p 12 N93-10814
ZHU, G. ..... p 80 N93-10330
ZHU, N. ..... p 178 N93-10943
ZHU, NINCHANG ..... p 27 N93-10813
ZIMCIK, D. G. ..... p 38 N93-10587
ZITTEL, P. F. ..... p 29 N93-10263
ZONDERVAN, K. P. ..... p 20 N93-10029
ZOZ, S. ..... p 35 N93-10084
ZUKOSKI, EDWARD E. ..... p 31 N93-10843

Typical Corporate Source Index Listing

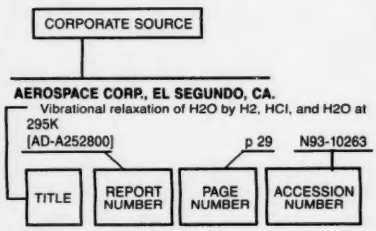

Listings in this index are arranged alphabetically by corporate source. The title of the document provides the user with a brief description of the subject matter. The report number helps to indicate the type of document cited (e.g., NASA report, translation, NASA contractor report). The accession number denotes the number by which the citation is identified. The page number helps you locate the citation in the abstract section. The titles are arranged under each corporate source in ascending accession number order.

A

ACADEMIA SINICA, BEIJING (CHINA).
Self-organized rock textures and multiring structure in the Duolun crater p 123 N93-10195

ACADEMY OF SCIENCES (USSR), IRKUTSK.
Spatial distribution of line-of-sight velocities in a quiescent prominence p 183 N93-10928

ACADEMY OF SCIENCES (USSR), MOSCOW.
Geomechanical models of impact cratering: Puchezh-Katunki structure p 114 N93-10151
Geochemical aspect of impact cratering: Studies in Vernadsky Institute p 123 N93-10196

ADELAIDE UNIV. (AUSTRALIA).
The Acraman impact and its widespread ejecta, South Australia p 111 N93-10141

ADVANCED TECHNOLOGY MATERIALS, INC., DANBURY, CT.
Implanted contacts for diamond semiconductor devices
[AD-A245568] p 165 N93-10274

ADVISORY GROUP FOR AEROSPACE RESEARCH AND DEVELOPMENT, NEUILLY-SUR-SEINE (FRANCE).
Seminar on Basic Documentation Practices
[AGARD-R-788] p 172 N93-10593
AGARD index of publications, 1989-1991
[AGARD-INDEX-89-91] p 174 N93-10610
Combat Aircraft Noise
[AGARD-CP-512] p 148 N93-10666

AEROJET-GENERAL CORP., SACRAMENTO, CA.
Formed platelets for low cost regeneratively cooled rocket combustion chambers p 18 N93-10018

AERONAUTICAL DEVELOPMENT ESTABLISHMENT, BANGALORE (INDIA).
Design optimization for uniform dynamic strength under multi-modal response p 62 N93-10555

AERONAUTICAL RESEARCH LABS., MELBOURNE (AUSTRALIA).
Design and implementation of digital filters for analysis of F/A-18 flight test data
[AD-A253447] p 3 N93-10342

AERONAUTICAL SYSTEMS DIV., WRIGHT-PATTERSON AFB, OH.
KC-135 crew reduction feasibility demonstration simulation study. Volume 3: Test and evaluation
[AD-A253931] p 134 N93-10713

AEROSPACE CORP., EL SEGUNDO, CA.
Vibrational relaxation of H2O by H2, HCl, and H2O at 295 K
[AD-A252800] p 29 N93-10263
Rate constants for reactions of hydrazine fuels with O(P-3)
[AD-A252813] p 42 N93-10336
Polymer matrix composites on LDEF experiments M0003-9 and M0003-10 p 38 N93-10584

AEROSPACE CORP., LOS ANGELES, CA.
Electric propulsion applications p 20 N93-10029

AEROSPACE INDUSTRIES ASSOCIATION OF CANADA, OTTAWA (ONTARIO).
Aerospace Industries Association of Canada
[CTN-92-60345] p 192 N93-10640
Aerospace Industries Association of Canada
[CTN-92-60590] p 1 N93-10644

AEROSPACE MEDICAL RESEARCH LABS., WRIGHT-PATTERSON AFB, OH.
Human noise exposure criteria for combat aircraft training areas p 148 N93-10670

AEROSPATIALE, CANNES (FRANCE).
Some possible space interferometry applications p 178 N93-10957

AIR-CONDITIONING AND REFRIGERATION TECHNOLOGY INST., INC., ARLINGTON, VA.
Materials compatibility and lubricants research on CFC-refrigerant substitute: Miscibility of lubricants with refrigerants
[DE92-015118] p 35 N93-10084
Materials compatibility and lubricants research on CFC-refrigerant substitutes: Thermophysical properties
[DE92-015116] p 43 N93-10397
Chemical and thermal stability of refrigerant-lubricant mixture with metal
[DE92-015117] p 44 N93-10398

AIR FORCE ACADEMY, CO.
A simplified model for hybrid rocket performance prediction p 19 N93-10022

AIR FORCE INST. OF TECH., WRIGHT-PATTERSON AFB, OH.
Supersonic confined jet nozzles p 16 N93-10009
Adequate sampling of a chaotic time series
[AD-A254170] p 127 N93-10664
Chinese Space Science and Technology (selected articles)
[AD-A254099] p 69 N93-10701
Stress and strain of slab type amplifiers
[AD-A254246] p 74 N93-10702
Design of laser optical systems
[AD-A254247] p 89 N93-10703
Methods of guidance flight dynamics
[AD-A254248] p 10 N93-10704
Echo characteristic analysis of the nonequilibrium wakes of reentry vehicle
[AD-A254249] p 13 N93-10705
Protective coatings for niobium alloys and their properties
[AD-A254252] p 33 N93-10706
Research on the asymmetrical aerodynamic forces of reentry vehicles
[AD-A254307] p 4 N93-10707
Studies on the combustion efficiency of liquid fuel rockets with variable thrust
[AD-A254232] p 26 N93-10721
Influence of flow velocity on the output power of high pressure CW CO2 lasers
[AD-A254240] p 89 N93-10722
Object-oriented design unifies databases and applications
[AD-A253313] p 175 N93-10723
System design and relaxation oscillations of a titanium-sapphire laser
[AD-A254264] p 89 N93-10725
Measurement of aerodynamic shear stress using side chain liquid crystal polymers
[AD-A254312] p 40 N93-10770
A seam tracking modulated infrared optical sensor for use in welding
[AD-A254103] p 159 N93-10812
A personal viewpoint on the development of China's liquid propellant rocket engines
[AD-A254104] p 27 N93-10813
Burn phase corrections of maneuver ballistic missiles with star light
[AD-A254105] p 12 N93-10814
Laser Journal
[AD-A254106] p 90 N93-10855
One type of automatically adjusted difference scheme with artificial viscosity to calculate ablated exterior shapes
[AD-A254108] p 5 N93-10856
A semiempirical formula for calculating the coefficients for field emission tip forms
[AD-A254109] p 145 N93-10857
Arguments concerning wind tunnel test studies of the trim characteristics of objects with small asymmetries'
[AD-A254111] p 5 N93-10858
High-resolution TVD schemes for the analysis of: 1. Inviscid supersonic and transonic flows. 2. Viscous flows with shock-induced separation and heat transfer p 5 N93-10889

AIR WEATHER SERVICE, SCOTT AFB, IL.
Probability forecasting: A guide for forecasters and staff weather officers
[AD-A254216] p 126 N93-10264

AKRON UNIV., OH.
Failure processes in elastomeric composites p 46 N93-10475

ALABAMA UNIV., HUNTSVILLE.
Improve SSME power balance model
[NASA-CR-184464] p 26 N93-10756

ALBERTA UNIV., EDMONTON.
A late Devonian impact event and its association with a possible extinction event on Eastern Gondwana p 122 N93-10191
Variational formulation of a mixed method for second order frame analysis p 62 N93-10556

ALCOA FOUNDATION, PITTSBURGH, PA.
Integrated finite element model of composite materials p 46 N93-10477

ALLIANCE TECHNOLOGIES CORP., CHAPEL HILL, NC.
Meteorological and site influences affecting the comparison of nephelometer and photographic determinations of light extinction at rural sites in the Eastern US
[PB92-195999] p 126 N93-10433

AMERICAN CERAMIC SOCIETY, WESTERVILLE, OH.
Ceramic transactions. Volume 21: Proceedings of the Symposium on Microwave Theory and Application in Materials Processing Annual Meeting No. 23 io on april 29-may 3 1991
[AD-A253631] p 35 N93-10205

AMES LAB., IA.
Model for the reversible magnetization of high-(kappa) type-2 superconductors: Application to high-temperature superconductor
[DE92-016297] p 167 N93-10609

ANACAPA SCIENCES, INC., FORT RUCKER, AL.
Operator workload predictions for the revised AH-64A workload prediction model, volume 1
[AD-A254198] p 133 N93-10261

ANALYTICS, INC., WILLOW GROVE, PA.
Handbook for operating the OWLKNEST technology
[AD-A253412] p 137 N93-10409

ARCON CORP., WALTHAM, MA.
Application of volumetric multiple-scattering approximations to foliage media
[AD-A253337] p 68 N93-10358

ARGONNE NATIONAL LAB., IL.
Dispersion of seed vapor and gas ionization in an MHD second stage combustor and channel
[DE92-016699] p 163 N93-10645

Assessment study of superconducting fault-current limiters operating at 77 K
[DE92-015273] p 76 N93-10831
Thermal, structural, and diffraction analyses of a gallium-cooled x ray monochromator
[DE92-017063] p 157 N93-10837

ARIZONA STATE UNIV., TEMPE.
Noril'sk/Siberian plateau basalts and Bahama hot spot: Impact triggered? p 109 N93-10132
Sudbury Breccia and suevite as glacial indicators transported 800 km to Kentland Astrobleme, Indiana p 117 N93-10165
Spatial light modulators with arbitrary quantum well profiles
[AD-A253637] p 165 N93-10210
Heat transfer additives for absorption cooling system fluids
[PB92-190354] p 169 N93-10249

ARIZONA UNIV., TUCSON.
Fellowship in physics/modern optics and quantum electronics
[AD-A253666] p 87 N93-10228
Multidimensional deterministic electron transport calculations
[AD-A254021] p 154 N93-10362
Polarized light scattering from perfect and perturbed surfaces and fundamental scattering systems
[AD-A253186] p 158 N93-10445
Research in the optical sciences
[AD-A253188] p 158 N93-10446
Interface cracks in an orthotropic layered half-space under impact loading p 47 N93-10482

ARKANSAS UNIV., FAYETTEVILLE.
Biological production of ethanol from coal
[DE92-016116] p 41 N93-10216
Biological production of ethanol from coal
[DE92-016114] p 43 N93-10608

ARMED FORCES RADIOBIOLOGY RESEARCH INST., BETHESDA, MD.
DoD space radiation concerns
[AD-A253135] p 131 N93-10613

ARMY ARMAMENT RESEARCH, DEVELOPMENT AND ENGINEERING CENTER, PICATINNY ARSENAL, NJ.
Wind tunnel spin data reduction to obtain aerodynamic spin damping coefficients by using nonlinear equation of motion
[AD-A253880] p 4 N93-10811

ARMY ARMAMENT RESEARCH, DEVELOPMENT AND ENGINEERING CENTER, WATERVLIET, NY.
Determination of Sandoz black aluminum coloring dye, olive aluminum coloring dye, and sodium dichromate aluminum sealing solutions by UV-visible spectrophotometry
[AD-A253639] p 29 N93-10207
Box counting multifractal analysis
[AD-A253960] p 144 N93-10419
Strength-toughness requirements for thick-walled high pressure vessels
[AD-A253756] p 95 N93-10750

ARMY CONSTRUCTION ENGINEERING RESEARCH LAB., CHAMPAIGN, IL.
Proceedings of the FY 1990 Workshop on Extraterrestrial Mining and Construction
[AD-A253399] p 189 N93-10406

ARMY ENGINEER TOPOGRAPHIC LABS., FORT BELVOIR, VA.
GPS azimuth determination using short baseline carrier wave interferometry
[AD-A254257] p 6 N93-10265
GPS Army research and applications
[AD-A254262] p 7 N93-10424
Long-term data collection and empirical background temperature modeling
[AD-A254044] p 127 N93-10780
System integration issues in digital photogrammetric mapping
[AD-A254046] p 103 N93-10781
Dynamic positioning systems photogrammetric
[AD-A254250] p 8 N93-10898
A standard file format for data interchange
[AD-A254260] p 176 N93-10899

ARMY ENGINEER WATERWAYS EXPERIMENT STATION, VICKSBURG, MS.
Stability of open-graded bases under wheel loads using a model testing approach
[AD-A253209] p 66 N93-10710

ARMY LAB. COMMAND, WATERTOWN, MA.
Instrument driver for general purpose interface bus (IEEE-488)
[AD-A253947] p 138 N93-10716

ARMY MEDICAL CENTER, FORT GORDON, GA.
Metabolic factors influencing myocardial recovery from acidosis (CiC3)
[AD-A252376] p 132 N93-10796

ARMY MISSILE COMMAND, REDSTONE ARSENAL, AL.
Comparison of optically-addressed spatial light modulators
[AD-A254189] p 157 N93-10259

ARNOLD ENGINEERING DEVELOPMENT CENTER, ARNOLD AIR FORCE STATION, TN.
Emission tomography of sodium in a hydrogen-air flame
[AD-A253530] p 29 N93-10224

ASPEN SYSTEMS CORP., ROCKVILLE, MD.
The levels of mathematics achievement: Initial performance standards for the 1990 NAEP mathematics assessment, volume 3
[PB92-199421] p 134 N93-10341

ASTRONOMICAL INST., UTRECHT (NETHERLANDS).
Small scale processes in solar and stellar plasmas p 181 N93-10917

ATLANTIC RESEARCH CORP., GAINESVILLE, VA.
Feasibility evaluation of the monolithic braided ablative nozzle p 19 N93-10023

ATOMIC ENERGY CORP. OF SOUTH AFRICA LTD., PRETORIA.
LABAN-PEL: A two-dimensional, multigroup diffusion, high-order response matrix code
[DE92-626845] p 144 N93-10624

AUBURN UNIV., AL.
Ohmic contacts to compound semiconductors p 76 N93-10830

B

BATH UNIV. (ENGLAND).
Non-dimensional conceptual design of radial inflow turbines. Part A: Application of fundamental fluid mechanics p 77 N93-10053
Non-dimensional conceptual design of radial inflow turbines. Part B: Application of empirical correlations p 77 N93-10054

BATTELLE COLUMBUS LABS., OH.
Evaluation of lightweight and low profile communications devices for Respiratory Protective system 21 (RESPO 21)
[AD-A253393] p 133 N93-10217
Evaluation of an electronics system concept for Respiratory Protection system (RESPO 21)
[AD-A253394] p 134 N93-10288
Novel seals and specialty component attachment mechanisms for Respiratory Protection system (RESPO 21)
[AD-A253395] p 91 N93-10290

BIRMINGHAM UNIV. (ENGLAND).
Energy build-up, transport, and release in solar flares p 181 N93-10913

BOCHUM UNIV. (GERMANY).
Sudbury project (University of Muenster-Ontario Geological Survey): Sr-Nd in heterolithic breccias and gabbroic dikes p 107 N93-10123

BOEING AEROSPACE CO., SEATTLE, WA.
Identification and evaluation of lubricants, adhesives, and seals used on LDEF p 39 N93-10588
Results from the testing and analysis of LDEF batteries p 39 N93-10589
Effects of long-term exposure on LDEF fastener assemblies p 39 N93-10590
Results from testing and analysis of solar cells flown on LDEF p 39 N93-10591

BOEING CO., SEATTLE, WA.
Changes in oxidation state of chromium during LDEF exposure p 34 N93-10581
Long Duration Exposure Facility (LDEF) optical systems SIG summary and database p 38 N93-10583
Space environmental effects on LDEF low Earth orbit exposed graphite reinforced polymer matrix composites p 38 N93-10585

BOLT, BERANEK, AND NEWMAN, INC., CANOGA PARK, CA.
Audibility-based annoyance prediction modeling p 151 N93-10683

BRINGEMEIER (D.), CLAUSTHAL-ZELLERFELD, (GERMANY).
Suevite superposition on the Bunte breccia in Noerdlinger Ries, Germany: New findings on the transport mechanism of impactites p 107 N93-10122

BRITISH COLUMBIA UNIV., VANCOUVER.
Dynamics of an orbiting flexible manipulator p 54 N93-10519
Experimental demonstration of offset control with an application to the tethered payload p 14 N93-10521

BROOKHAVEN NATIONAL LAB., UPTON, NY.
Molecular biology in studies of oceanic primary production
[DE92-016101] p 128 N93-10283
Analysis of air pollution and greenhouse gases
[DE92-014955] p 104 N93-10384
Particle production at high p(sub (perpendicular)) in (sup 28)Si + A collisions at 14.6 A x GeV/c
[DE92-016939] p 154 N93-10402
Resource capture by single leaves
[DE92-015847] p 129 N93-10461
Photoionization dynamics and cation spectroscopy with coherent VUV radiation
[DE92-015841] p 154 N93-10730
A novel charge sensitive preamplifier without the feedback resistor
[DE92-015842] p 74 N93-10731
Two-photon physics and the coming generation of heavy ion colliders
[DE92-015850] p 156 N93-10732

BROWN UNIV., PROVIDENCE, RI.
Center for Intelligent Control Systems, Brown University component: Graduate research fellowships
[AD-A253620] p 141 N93-10095
Enhanced magnetic field production during oblique hypervelocity impacts p 108 N93-10129
Recognizing impactor signatures in the planetary record p 120 N93-10178
Floor-fractured crater models of the Sudbury structure, Canada p 123 N93-10193
Variation in multiring basic structures as a function of impact angle p 123 N93-10194
Interactive animation of fault tolerant parallel algorithms
[AD-A253349] p 135 N93-10212
Fault-tolerant and efficient parallel computation
[AD-A253350] p 140 N93-10213
Research program in experimental and theoretical high energy physics
[DE92-016219] p 156 N93-10618
High temperature fatigue crack growth in ceramics and ceramic composites
[DE92-016835] p 40 N93-10632
Local-equilibrium formalism applied to mechanics of solids
[DE92-016852] p 170 N93-10787

BUNDESMINISTERIUM DER VERTEIDIGUNG, BONN (GERMANY).
Combat aircraft operations: Training requirements for the German Air Force tactical flying units and the noise problem p 148 N93-10667

BUREAU OF MINERAL RESOURCES, GEOLOGY AND GEOPHYSICS, CANBERRA (AUSTRALIA).
Asteroids and Archaean crustal evolution: Tests of possible genetic links between major mantle/crust melting events and clustered extraterrestrial bombardments p 110 N93-10140

C

CAGLIARI UNIV. (ITALY).
Damage due to plastic deformation in elastic-plastic materials: The thermodynamical connection p 51 N93-10502

CALGARY UNIV. (ALBERTA).
A multilayered shell finite element p 49 N93-10495
Numerical simulation of the propagation of coupled thermomechanical waves in inelastic solids p 64 N93-10568
Discontinuous initial value problem of nonlinear elasticity by similarity approach p 64 N93-10569

CALIFORNIA COMPUTER PRODUCTS, INC., DOWNEY.
Algebra-geometric and differential geometric methods in solid geometric modeling
[AD-A253669] p 145 N93-10670

CALIFORNIA INST. OF TECH., PASADENA.
Ruthenium/iridium ratios in the Cretaceous-Tertiary boundary clay: Implications for global dispersal and fractionation within the ejecta cloud p 109 N93-10135
Melting and its relationship to impact crater morphology p 119 N93-10170
Combustion in turbulent jets and buoyant flames
[PB92-211481] p 31 N93-10437
Status of dynamic fracture in brittle solids p 49 N93-10493
Combustion noise and combustion instabilities in propulsion systems p 150 N93-10682
Shock enhancement and control of hypersonic combustion
[AD-A254295] p 31 N93-10843
Investigations of the motion of discrete-velocity gases
[AD-A253728] p 84 N93-10895

CALIFORNIA STATE UNIV., LONG BEACH.
Vibration of a damped double-beam system p 56 N93-10527

CALIFORNIA UNIV., BERKELEY.
De Finetti representations of survival functions level to a product measure
[AD-A253623] p 146 N93-10107
Pulsed jet plume combustion: An exothermic process under fluid mechanical control p 32 N93-10553

Inspection and repair decisions for hydraulic structures under symmetric deterioration
[AD-A253621] p 96 N93-10797
The total time on test statistic and age-dependent censoring
[AD-A253622] p 147 N93-10798

CALIFORNIA UNIV., BERKELEY. LAWRENCE BERKELEY LAB.
Statics and kinetics of oxygen ordering in the oxide superconductor YBa2Cu3O(z)
[DE92-017001] p 167 N93-10403
Electronic and structural properties of metallic microclusters
[DE92-016917] p 33 N93-10411
A four channel 250 MHz visual counter
[DE92-016920] p 86 N93-10444
Glenn T. Seaborg and heavy ion nuclear science
[DE92-016943] p 156 N93-10762
Signal and noise analysis of a-Si:H radiation detector-amplifier system
[DE92-016928] p 75 N93-10790
Electronic structure of highly correlated structures
[DE92-017017] p 155 N93-10863
An infrared free-electron laser for the Chemical Dynamics Research Laboratory
[DE92-017018] p 90 N93-10864
Modelling of 3-D electromagnetic responses using the time-wavenumber method
[DE92-017025] p 70 N93-10865

CALIFORNIA UNIV., DAVIS.
Improved numerical simulation of Euler equations
p 80 N93-10309
Response of a beam to transverse impulsive and high frequency loads p 56 N93-10526

CALIFORNIA UNIV., IRVINE.
Subpicosecond resolved incipient laser damage
[AD-A253624] p 87 N93-10202
Magnetostatic waves-based integrated optic Bragg cell modules with applications to RF signal processing
[AD-A254035] p 71 N93-10240
Large orbit magnetic confinement systems for advanced fusion fuels
[DE92-016218] p 162 N93-10617

CALIFORNIA UNIV., LIVERMORE. LAWRENCE LIVERMORE LAB.
Chronorheological characterization of elastomers
p 46 N93-10476

CALIFORNIA UNIV., LOS ANGELES.
Atomic force microscope studies of CuCl island formation on CaF2(111) substrates
[AD-A252499] p 34 N93-10880

CALIFORNIA UNIV., SAN DIEGO.
Theory of combustion of liquid propellants based on hydroxylammonium nitrate
[AD-A248445] p 42 N93-10267

CALIFORNIA UNIV., SANTA BARBARA.
Sensor and actuator materials for high performance composites
[AD-A254178] p 27 N93-10254
Automatic cloud classification from multi-spectral satellite data over oceanic regions
[AD-A253670] p 126 N93-10292

CALM (JAMES M.), ARLINGTON, VA.
ARTI Refrigerant Database
[DE92-015122] p 30 N93-10401

CALSPAN-BUFFALO UNIV. RESEARCH CENTER, NY.
Architecture and device development for optical networks
[AD-A253247] p 158 N93-10693

CAMBRIDGE UNIV. (ENGLAND).
A new deployable mast p 14 N93-10511

CANADA CENTRE FOR REMOTE SENSING, OTTAWA (ONTARIO).
SAR in support of geological investigations of the Sudbury structure p 103 N93-10182

CANADIAN MARCONI CO. LTD., MONTREAL (QUEBEC).
Beam forming antenna system
[PATENT-1-265-236] p 67 N93-10111

CARLETON UNIV., OTTAWA (ONTARIO).
Proceedings of the Twelfth Canadian Congress of Applied Mechanics, volumes 1 and 2
[ISBN-0920049-03] p 44 N93-10466
Indentation of a precompressed penny-shaped crack
p 48 N93-10486
Improvements to the AC potential drop method of crack measurement p 59 N93-10543
An adaptive mesh-management algorithm for three-dimensional automatic finite element analysis
p 61 N93-10554
A new quadrilateral element for the elastic and plastic analysis of shells p 62 N93-10559

CARNEGIE-MELLON UNIV., PITTSBURGH, PA.
Proceedings of the CASE Adoption Workshop
[AD-A253362] p 135 N93-10104
An analysis technique for examining integration in a project support environment
[AD-A253351] p 135 N93-10214
Epitaxial magnetic oxides
[AD-A253667] p 35 N93-10230
Analysis of reservation-based dual-link networks for real-time applications
[AD-A254176] p 67 N93-10253
Issues and techniques of CASE integration with configuration management
[AD-A253323] p 136 N93-10298
Ada validation tests for rate monotonic scheduling algorithms
[AD-A253325] p 136 N93-10300
PRODIGY4.0: The manual and tutorial
[AD-A253970] p 137 N93-10422
Introduction to software process improvement
[AD-A253326] p 137 N93-10447
Parallels in computer-aided design framework and software development environment efforts
[AD-A253327] p 137 N93-10448
The past, present, and future of configuration management
[AD-A254175] p 138 N93-10665
Selective perception for robot driving
[AD-A253740] p 142 N93-10749
TAQL: A problem space tool for expert system development
[AD-A253820] p 175 N93-10826
Symbolic Boolean manipulation with ordered binary decision diagrams
[AD-A253822] p 142 N93-10828

CASE WESTERN RESERVE UNIV., CLEVELAND, OH.
The structure and development of streamwise vortex arrays embedded in a turbulent boundary layer
p 81 N93-10371
Hierarchical structure in polymeric solid and its influence on properties
[AD-A253818] p 41 N93-10825

CENTRE NATIONAL D'ETUDES SPATIALES, TOULOUSE (FRANCE).
System related testing and analysis of FRECOPA
p 39 N93-10592
Comparison of wind speed measurements over the oceans with the Special Sensor Microwave/Imager and the Geosat altimeter p 127 N93-10850

CENTRE NATIONAL DE LA RECHERCHE SCIENTIFIQUE, ORSAY (FRANCE).
Tomographic/interferometric studies of active stars and binaries p 182 N93-10920

CENTRE NATIONAL DE LA RECHERCHE SCIENTIFIQUE, VERRIERES-LE BUISSON (FRANCE).
Planned observations at high resolution from space
p 177 N93-10903
Prospects with SIMURIS p 179 N93-10904
Evidence of plasmoid ejection in the corona from 1991 eclipse observations with the Canada-France-Hawaii telescope p 181 N93-10915
Prospects in stellar and galactic observations with SIMURIS p 182 N93-10921
Magnetospheres and atmospheres of planets
p 182 N93-10922
SUN: The Solar Ultraviolet Network
p 183 N93-10930
Interferometric imaging with the solar ultraviolet network p 184 N93-10932
Rotational aperture synthesis: A proposal for ground-based observations p 178 N93-10947
Demonstration and performances of real-time fringe tracking: A step towards cophased interferometers
p 178 N93-10948

CESKOSLOVENSKA AKADEMIE VED, ONDREJOV.
The fine structure of prominences
p 180 N93-10910

CESKOSLOVENSKA AKADEMIE VED, PRAGUE.
Bohemian circular structure, Czechoslovakia: Search for the impact evidence p 119 N93-10172

CHUNG SHAN INST. OF SCIENCE AND TECHNOLOGY (TAIWAN).
Failure analysis of laminated composites by using iterative three-dimensional finite element method
p 51 N93-10505

CINCINNATI UNIV., OH.
LDV Measurements of unsteady flow fields in radial turbine
[AD-A253592] p 4 N93-10648

CITY COLL. OF THE CITY UNIV. OF NEW YORK, NY.
Research in particle physics beyond the standard model
[DE92-012240] p 155 N93-10878

CITY UNIV. OF NEW YORK, NY.
Laser and optical physics
[AD-A253619] p 88 N93-10251

CLARKSON UNIV., POTSDAM, NY.
An open or closed crack terminating at a bi-material interface: Power-logarithmic singularities
p 47 N93-10483
Dynamic crack division in brittle solids
p 48 N93-10489
An assessment of the correspondence principle in comparison to nonlinear viscoelastic theory: A case study p 51 N93-10501
Heat transfer and pressure drop for air flow through enhanced passages
[DE92-016597] p 82 N93-10612

CLIMATE ANALYSIS CENTER, CAMP SPRINGS, MD.
Atlas of Southern Hemisphere 500 mb teleconnection patterns derived from National Meteorological Center analyses
[PB92-203892] p 126 N93-10337

COLORADO STATE UNIV., FORT COLLINS.
Mesoscale severe weather development under orographic influences
[AD-A253630] p 125 N93-10204
Infrared investigations of pristine polypyrrole. Is the polymer called polypyrrole really Poly (Pyrrole-Co-Hydroxypyrrole)?
[AD-A249746] p 36 N93-10243
Study of improved methods for predicting chemical equilibria
[DE92-016974] p 31 N93-10436
Template-synthesis of infrared-transparent metal microcylinders: Comparison of optical properties with the predictions of effective medium theory
[AD-A253267] p 158 N93-10694

COLORADO UNIV., BOULDER.
Forced unsteady separated flows on a 45 degree delta wing p 80 N93-10305
Numerical simulation of large actively controlled space structures p 13 N93-10308
Model reference adaptive control in large space structures p 13 N93-10365
Elastic wave scattering by an interfacial crack in a plate p 48 N93-10485
Evaluation of Seasat/Geosat orbits and altimetry with application to long-term sea level changes in the North Pacific p 103 N93-10847

COLSA, INC., HUNTSVILLE, AL.
Algorithms for multichannel optical processor
[AD-A254009] p 158 N93-10360

COLUMBIA UNIV., NEW YORK, NY.
The interaction of UV-Laser radiation with metal and semiconductor surfaces
[AD-A253510] p 87 N93-10201
Worldwide seismic catalog and the nature of seismic coupling p 124 N93-10376
Hexagonal and octagonal finite elements
p 50 N93-10500

COMMUNICATIONS RESEARCH CENTRE, OTTAWA (ONTARIO).
Free vibrations of the thick circular cylindrical shells and rings p 57 N93-10533
The vibrations of annular discs: A comparison of experimental and two analytical techniques
p 58 N93-10536

COMPOSITE AIRCRAFT PRODUCTS LTD. (CANADA).
Pitch control trimming system for canard design aircraft
[CA-PATENT-APPL-SN-2013236] p 10 N93-10374

COMPUTER SCIENCES CORP., MINNEAPOLIS, MN.
Calculation of elastic-plastic wave propagation on the connection machine
[AD-A252429] p 95 N93-10427

COMPUTER SCIENCES CORP., RESEARCH TRIANGLE PARK, NC.
Gridded Model Information Support System (GMISS) user's guide. Volume 3: Model concentration data retrieval subsystem
[PB92-190263] p 171 N93-10257

CONCORDIA UNIV., MONTREAL (QUEBEC).
Axisymmetric vibrations of rotating circular plates using characteristic orthogonal polynomials
p 45 N93-10470
Characteristics of separated flows including cavitation effects p 84 N93-10874

CONTINUOUS ELECTRON BEAM ACCELERATOR FACILITY, NEWPORT NEW, VA.
Recent developments in stored polarized electron positron beams
[DE92-016965] p 157 N93-10862

CORNELL UNIV., ITHACA, NY.
Search for a meteoritic component at the Beaverhead impact structure, Montana p 116 N93-10158
Tilt rotor hover aeroacoustics
[NASA-CR-177598] p 147 N93-10458
Dynamic measurement of the J integral in ductile metals using the optical method of caustics p 49 N93-10492
Computer algebra and the elliptic restricted problem of three bodies p 11 N93-10499

COUNCIL FOR NATIONAL ACADEMIC AWARDS (ENGLAND).
The development of optical techniques for component inspection in the aerospace industry p 93 N93-10307
CREE RESEARCH, INC., DURHAM, NC.
Development of 6H-SiC CMOS transistors for insertion into a 350 C operational amplifier
[AD-A253760] p 70 N93-10233

D

DASSAULT (E. M.) CO., SAINT CLOUD (FRANCE).
Combat aircraft noise p 149 N93-10676
DAYTON UNIV., OH.
Determination of the dynamic unload/reload characteristics of ceramics
[AD-A253513] p 35 N93-10221
DAYTON UNIV. RESEARCH INST., OH.
Alternate spectrometric oil analysis techniques
[AD-A253355] p 29 N93-10101
Polynitro polycyclic cage compounds
[AD-A252889] p 42 N93-10268
DEFENCE RESEARCH AGENCY, MALVERN (ENGLAND).
Ground/space co-operation for interferometry
p 178 N93-10946
DELAWARE UNIV., NEWARK.
The 200th American Chemical Society Geochemistry Division Symposium on Progress in Marine Chemistry
[AD-A253757] p 129 N93-10887
DEPARTMENT OF DEFENSE, WASHINGTON, DC.
Emergency Diesel Generator reliability at Department of Energy (DOE) facilities
[DE92-011888] p 91 N93-10622
DEPARTMENT OF ENERGY, WASHINGTON, DC.
Experimental plasma research project summaries
[DE92-016274] p 162 N93-10464
DEPARTMENT OF THE NAVY, WASHINGTON, DC.
Lightweight deployable antenna system
[AD-D015291] p 67 N93-10096
Artificial neural network system for memory modification
[AD-D015354] p 142 N93-10958
Memory modification of artificial neural networks
[AD-D015356] p 143 N93-10959
DEUTSCHE FORSCHUNGSANSTALT FUER LUFT- UND RAUMFAHRT, BERLIN (GERMANY).
Prediction of jet mixing noise for high subsonic flight speeds p 151 N93-10685
DEUTSCHE FORSCHUNGSANSTALT FUER LUFT- UND RAUMFAHRT, BRUNSWICK (GERMANY).
Comparison of flyover noise data from aircraft at high subsonic speeds with prediction p 149 N93-10674
DORNIER LUFTFAHRT G.M.B.H., FRIEDRICHSHAFEN (GERMANY).
Study results on combat aircraft source noise reduction p 152 N93-10691
DRESSER INDUSTRIES, INC., LIBERTY CORNER, NJ.
Structural analysis: Fatigue life assessment
p 78 N93-10062
DREXEL UNIV., PHILADELPHIA, PA.
Nonlinear signal processing schemes for robust target detection and automatic clutter rejection in radar
[AD-A253546] p 68 N93-10380
DUKE UNIV., DURHAM, NC.
Implementation of parallel algorithms
[AD-A253638] p 140 N93-10227
UV/XUV FEL storage ring and linac
[AD-A253307] p 89 N93-10697

E

ECOLE NATIONALE SUPERIEURE DE TECHNIQUES AVANCEES, PARIS (FRANCE).
Experimental and numeric analysis of constraints in a bonded stepped lap joint subjected to traction
p 54 N93-10516
ECOLE POLYTECHNIQUE, MONTREAL (QUEBEC).
An evaluation of the cumulative damage effect under creep loading p 58 N93-10540
On the development of a new fracture toughness procedure p 59 N93-10541
A comparative study of semi-empirical dynamic stall models p 5 N93-10544
Stream function-vorticity finite element formulations of unsteady incompressible Navier-Stokes equations
p 60 N93-10545
A field panel method for transonic flows
p 6 N93-10547
ECOLE POLYTECHNIQUE FEDERALE DE LAUSANNE (SWITZERLAND).
Evolution of hybrid-Trefftz FE model: State of the art and future trends p 49 N93-10494
EDGERTON, GERMESHAUSEN AND GRIER, INC., IDAHO FALLS, ID.
APOLLO: A computer program for the calculation of chemical equilibrium and reaction kinetics of chemical systems
[DE92-017864] p 139 N93-10817
EDGEWATER COMPUTER SYSTEMS, INC., CARP (ONTARIO).
Investigation of a possible stochastic model for the IEEE P896.1 (Futurebus+) protocol, including the proposed enhanced distributed arbiter
[CTN-92-60593] p 135 N93-10088
EG AND G ENERGY MEASUREMENTS, INC., IDAHO FALLS.
FLASH: A finite element computer code for variably saturated flow
[DE92-018038] p 84 N93-10868
EG AND G ENERGY MEASUREMENTS, INC., LOS ALAMOS, NM.
Geographic Information System (GIS) development assistance for Nuclear Regulatory Commission (NRC) incident response capability
[DE92-017595] p 176 N93-10867
EG AND G ROCKY FLATS, INC., GOLDEN, CO.
Total Quality Management (TQM) concepts applied to instruction
[DE92-013399] p 171 N93-10270
EIDGENOESSISCHE TECHNISCHE HOCHSCHULE, ZURICH (SWITZERLAND).
Small-scale physics of convection and magnetic fields
p 179 N93-10905
Polarimetry with an imaging FTS p 14 N93-10934
ELECTRONICS RESEARCH LAB., ADELAIDE (AUSTRALIA).
Meteor burst communications system trial, 1990-1991
[AD-A253625] p 67 N93-10203
ENERGY INFORMATION ADMINISTRATION, WASHINGTON, DC.
EIA publications directory, 1991
[DE92-015686] p 174 N93-10607
ENVIRONMENTAL PROTECTION AGENCY, RESEARCH TRIANGLE PARK, NC.
Sensitivity of modeled ozone concentrations to uncertainties in biogenic emissions
[PB92-192202] p 105 N93-10432
Meteorological and site influences affecting the comparison of nephelometer and photographic determinations of light extinction at rural sites in the Eastern US
[PB92-195999] p 126 N93-10433
ETABLISSEMENT TECHNIQUE CENTRAL DE L'ARMEMENT, ARCUEIL (FRANCE).
Pattern recognition applied to H(sub alpha) spectroheliograms solar rotation and meridional circulation p 182 N93-10924
EUROPEAN SOUTHERN OBSERVATORY, GARCHING (GERMANY).
Ground-based high angular resolution observation of the Sun by interferometry in the visible p 177 N93-10941
Interferometry with the Very Large Telescope
p 178 N93-10943
EUROPEAN SPACE AGENCY, PARIS (FRANCE).
Guide to the user requirements definition phase
[ESA-PSS-05-02-ISSUE-1] p 136 N93-10315
Guide to the software requirements definition phase
[ESA-PSS-05-03-ISSUE-1] p 136 N93-10316
Solar Physics and Astrophysics at Interferometric Resolution
[ESA-SP-344] p 179 N93-10901
Attached payloads on Space Station Freedom and Columbus p 14 N93-10929
EUROPEAN SPACE AGENCY. EUROPEAN SPACE RESEARCH AND TECHNOLOGY CENTER, ESTEC, NOORDWIJK (NETHERLANDS).
Reliability assurance requirements for ESA space systems
[ESA-PSS-01-30-ISSUE-2] p 94 N93-10317
Some results of the oxidation investigation of copper and silver samples flown on LDEF p 34 N93-10580
Mechanical and thermal design of the SUN instrument
p 14 N93-10956
EXETER UNIV. (ENGLAND).
A reappraisal of compound equilibrium finite elements
p 63 N93-10561

F

FEDERAL ARMED FORCES DOCUMENTATION AND INFORMATION CENTRE, BONN (GERMANY).
Document processing p 174 N93-10600
Security considerations within military information systems p 174 N93-10603
FEDERAL AVIATION ADMINISTRATION, ATLANTIC CITY, NJ.
Air traffic control visual scanning
[DOT/FAA/CT-TN92/16] p 7 N93-10459
Weather Message Switching Center Replacement (WMSCR) Operational Test and Evaluation (OT/E)/integration test plan
[DOT/FAA/CT-TN90/59] p 7 N93-10833
FEDERAL AVIATION ADMINISTRATION, CAMBRIDGE, MA.
Advanced terrain displays to transport category aircraft
[PB92-197136] p 6 N93-10065
FEDERAL AVIATION ADMINISTRATION, WASHINGTON, DC.
A new test of scanning and monitoring ability: Methods and initial results
[AD-A249123] p 132 N93-10321
A description of the Mode Select beacon system (Mode S) and its associated benefits to the National Airspace System (NAS)
[DOT/FAA/SE-92/6] p 7 N93-10738
FLORENCE UNIV. (ITALY).
Ultra-high observations of the prominence-corona transition region p 180 N93-10908
Observation of solar flares at high resolution
p 182 N93-10923
High resolution granulation spectrophotometry with a UBF and a FP interferometer in tandem
p 183 N93-10927
FLORIDA STATE UNIV., TALLAHASSEE.
Nonlinear dynamics underlying atmospheric predictability
[AD-A254042] p 126 N93-10363
Air-sea interaction in regions of varying surface conditions
[AD-A253182] p 128 N93-10791
FLORIDA UNIV., GAINESVILLE.
Mass and mixing angle patterns in the standard model and its material supersymmetric extension
[DE92-016197] p 153 N93-10291
Wiggly relativistic strings
[DE92-016461] p 170 N93-10434
Elasticity analysis of orthotropic beams under three-part bending p 52 N93-10507
Investigation of laminated composite plates under impact dynamic loading by using a three-dimensional hybrid stress finite element method p 29 N93-10510
Development of laser excited atomic fluorescence and ionization methods
[DE92-016199] p 89 N93-10611
Cosmic microwave background anisotropies from plausible double inflation
[DE92-016195] p 192 N93-10616
Advanced processing and characterization technologies. Fabrication and characterization of semiconductor optoelectronic devices and integrated circuits. Final Conference Proceedings No. 10
[AD-A254162] p 73 N93-10663
Portable tandem mass spectrometer analyzer
[AD-A254065] p 125 N93-10784

G

GARRETT FLUID SYSTEMS CO., TEMPE, AZ.
Pneumatic motor powered Thrust Vector Control (TVC) for liquid propelled launch vehicles p 17 N93-10015
GARRETT TURBINE ENGINE CO., PHOENIX, AZ.
Compound cycle engine for helicopter application
[NASA-CR-180824] p 9 N93-10348
GEC-MARCONI ELECTRONICS LTD., CHELMSFORD (ENGLAND).
Acquisition 1: Stock acquisition processes in defence and aerospace documentation centres
p 173 N93-10598
Services: User services in defence and aerospace documentation centres p 174 N93-10602
GENCORP AEROJET, SACRAMENTO, CA.
Critical engine system design characteristics for SSTO vehicles p 17 N93-10014
GENERAL ACCOUNTING OFFICE, WASHINGTON, DC.
Space Station: NASA's software development approach increases safety and cost risks. Report to the Chairman, Committee on Science, Space, and Technology, House of Representatives
[GAO/IMTEC-92-39] p 12 N93-10081
GENERAL ATOMIC CO., SAN DIEGO, CA.
Helium transport in enhanced confinement regimes on the TEXTOR and D3-D tokamaks
[DE92-016247] p 160 N93-10293
Divertor heat flux reduction by D2 injection in DIII-D
[DE92-014232] p 160 N93-10326
A formula for efficiency of fast wave current drive in fusion devices
[DE92-016152] p 160 N93-10390

Investigation of the effect of large core changes in toroidal plasma rotation and radial electric field on confinement in H-mode discharges in the D3-D tokamak
[DE92-016252] p 161 N93-10392
Polarimetry of motional Stark effect and determination of current profiles in D3-D
[DE92-016258] p 161 N93-10393
Twenty-five KA, 5000V solid state opening switch for inductive energy stores
[AD-A253968] p 73 N93-10421
VH-mode discharges in the D3-D tokamak
[DE92-016257] p 161 N93-10463
Edge ion dynamics in H-mode discharges in D3-D
[DE92-016255] p 162 N93-10619
The effect of current profile changes on confinement in the D3-D tokamak
[DE92-016256] p 163 N93-10620
Boronization in D3-D
[DE92-016249] p 163 N93-10759
Global Alfven eigenmodes in D3-D
[DE92-016250] p 163 N93-10760
Variational full wave calculation of fast wave current drive in D3-D using the ALCYON code
[DE92-016572] p 163 N93-10761

GENERAL DYNAMICS CORP., SAN DIEGO, CA.
Plug nozzle propulsion system p 17 N93-10013

GENERAL ELECTRIC CO., CINCINNATI, OH.
Hypersonic inlet efficiency revisited p 5 N93-10012

GEOLOGICAL SURVEY, ALBANY, NY.
The Panther Mountain circular structure, a possible buried meteorite crater p 113 N93-10150

GEOLOGICAL SURVEY, DENVER, CO.
Large meteorite impacts: The K/T model p 107 N93-10120
Shocked zircons in the Onaping Formation: Further proof of impact origin p 107 N93-10121
Venusian impact basins and cratered terrains p 112 N93-10145

GEOLOGICAL SURVEY, FLAGSTAFF, AZ.
K/T boundary stratigraphy: Evidence for multiple impacts and a possible comet stream p 120 N93-10180

GEOLOGICAL SURVEY, IOWA CITY, IA.
Research core drilling in the Manson impact structure, Iowa p 105 N93-10114

GEOLOGICAL SURVEY OF FINLAND, ESPOO.
Impact cratering record of Fennoscandia p 119 N93-10171

GEORGIA INST. OF TECH., ATLANTA.
LV software for supersonic flow analysis
[NASA-CR-190911] p 2 N93-10069
Computational studies of vortex breakdown
[AD-A253759] p 79 N93-10232
Multidimensional effects in composite propellant combustion p 42 N93-10313
SAPNEW: Parallel finite element code for thin shell structures on the Alliant FX/80
[NASA-CR-190663] p 94 N93-10372
Two-dimensional signal processing, optical information storage and processing, and electromagnetic measurements
[AD-A253953] p 73 N93-10417
Numerical solution of three-dimensional unsteady viscous flows
[AD-A253202] p 83 N93-10793

GERMAN AIR FORCE, BONN (GERMANY).
Possibilities and limitations of flying training in the German Air Force p 11 N93-10668

GHENT UNIV. (BELGIUM).
Novel optoelectronic devices based on combining GaAs and InP on Si
[AD-A253781] p 165 N93-10235

GLASGOW UNIV. (SCOTLAND).
Non-linear thermoelasticity of rubberlike solids p 45 N93-10474

GOSUDARSTVENNYI KOMITET PO ISPOLZOVANIYU ATOMNOI ENERGII, SERPUKHOV (USSR).
Study on the pi(sup -)p yields eta' pi(sup 0)n reaction at 38 and 100 GeV/c momenta
[DE92-624593] p 153 N93-10328

GRAMBLING STATE UNIV., LA.
NQR-NMR studies of higher alcohol synthesis Cu-Co catalysts
[DE92-015783] p 31 N93-10460

GRENOBLE-1 UNIV. (FRANCE).
Successes of and prospects for ground-based interferometry p 177 N93-10940

GTE GOVERNMENT SYSTEMS CORP., MOUNTAIN VIEW, CA.
SBS applications study
[AD-A253779] p 102 N93-10234

GTE LABS., INC., WALTHAM, MA.
Semiconductor-metal eutectic composites for high power switching
[AD-A253930] p 74 N93-10755

H

HARRY DIAMOND LABS., ADELPHI, MD.
Design and evaluation of a quasi-active delay-line limiter/filter RF protection device
[AD-A254179] p 71 N93-10255

HARTUNG (J.), DES MOINES, IA.
Report on the international Cambodian crater expedition, 1992 p 113 N93-10147

HARVARD-SMITHSONIAN CENTER FOR ASTROPHYSICS, CAMBRIDGE, MA.
Obtaining high resolution XUV coronal images p 14 N93-10939

HARVARD UNIV., CAMBRIDGE, MA.
Joint Services Electronics Program
[AD-A253842] p 76 N93-10829

HAWAII UNIV., HONOLULU.
The distribution and modes of occurrence of impact melt at lunar craters p 113 N93-10148
Sudbury Igneous Complex: Impact melt or igneous rock? Implications for lunar magmatism p 118 N93-10169

HELLENIC AEROSPACE INDUSTRY, SCHIMATARI (GREECE).
Documentation practices: The national scene (Greece) p 173 N93-10595

HOLSET ENGINEERING CO., TURNBRIDGE (ENGLAND).
Aerodynamic investigation of radial turbines using computational methods p 78 N93-10056

HONG KONG AMATEUR ASTRONOMICAL SOCIETY.
Hong Kong is an impact crater: Proof from the geomorphological and geological evidence p 107 N93-10124

HOUSTON UNIV., TX.
Impactite and pseudotachylite from Roter Kamm Crater, Namibia p 109 N93-10130
Bronzite Granophyre: New insight on Vredefort p 121 N93-10186
Numerical simulation of transient crack growth p 48 N93-10488

HUGHES AIRCRAFT CO., CULVER CITY, CA.
Development of parallel architectures for sensor array processing algorithms
[AD-A253680] p 141 N93-10299

HUGHES SPACE AND COMMUNICATIONS GROUP, EL SEGUNDO, CA.
Loading operations for spacecraft propulsion subsystems p 11 N93-10047

HULBURT (E. O.) CENTER FOR SPACE RESEARCH, WASHINGTON, DC.
Transition region dynamics p 180 N93-10907

I

IBIDEN CO. LTD., OGAKI (JAPAN).
Conductive titanate fiber and its production method
[DE92-014738] p 39 N93-10627

ILLINOIS INST. OF TECH., CHICAGO.
Nozzle installation effects on the noise from supersonic exhaust plumes p 150 N93-10681
Control of panel flutter at high supersonic speed p 9 N93-10900

ILLINOIS UNIV., CHAMPAIGN.
Proceedings of the Antenna Applications Symposium, volume 1
[AD-A253681] p 68 N93-10301
Proceedings of the Antenna Applications Symposium, volume 2
[AD-A253682] p 68 N93-10302

ILLINOIS UNIV., CHICAGO.
Theory of transport for interacting many-body systems
[AD-A253789] p 169 N93-10871

ILLINOIS UNIV., URBANA.
VLSI design for reliability - hot electron
[AD-A253942] p 74 N93-10715

ILLINOIS UNIV., URBANA-CHAMPAIGN.
The role of eddy fluxes in the response of the atmosphere to tropical thermal forcing p 124 N93-10318

ILLINOIS UNIV. AT URBANA-CHAMPAIGN, SAVOY.
Linear and nonlinear analyses of thick composite circular plates using the finite element method p 96 N93-10873

IMPERIAL COLL. OF SCIENCE AND TECHNOLOGY, LONDON (ENGLAND).
Introduction to radial turbine technology p 77 N93-10051
Performance parameters and assessment p 77 N93-10052
Partial admission and unsteady flow in radial turbines p 78 N93-10059
Testing techniques p 78 N93-10060
IFTS: The Imaging Fourier Transform Spectrometer p 14 N93-10933
Report of the Lunar Interferometry Study Team (LIST) activities p 178 N93-10945
A multipurpose vacuum-ultraviolet test facility p 11 N93-10953
Interferometer optical design for the Imaging Fourier Transform Spectrometer (IFTS) p 159 N93-10955

INDIAN INST. OF TECH., NEW DELHI.
Orthotropic circular plate on nonlinear elastic subgrade p 53 N93-10513

INDIAN SCHOOL OF MINES, DHANBAD.
A history of the Lonar crater, India: An overview p 118 N93-10168

INDIANA UNIV.-PURDUE UNIV., INDIANAPOLIS.
Water soluble polysiloxanes with pendant 1-oxypyridin-3-yl groups
[AD-A250637] p 36 N93-10246

INDUSTRIAL MARINE PRODUCTS GROUP LTD., HALIFAX (NOVA SCOTIA).
Flexural vibration of beams with varying section properties p 57 N93-10531

INDUSTRIEANLAGEN-BETRIEBSGESELLSCHAFT M.B.H., OTTOBRUNN (GERMANY).
Technical measures for the attenuation of aircraft noise and their applicability to GAF combat aircraft p 152 N93-10690

INDUSTRY, SCIENCE AND TECHNOLOGY CANADA, TORONTO (ONTARIO).
Aerospace industry profile, 1990-1991
[CTN-92-60513] p 1 N93-10651
Aerospace and defence-related industries statistical survey report, 1991
[CTN-92-60514] p 2 N93-10652
Defence electronics industry profile, 1990-1991
[CTN-92-60515] p 66 N93-10653

INHALATION TOXICOLOGY RESEARCH INST., ALBUQUERQUE, NM.
Understanding mechanisms of carcinogenesis using rat tracheal epithelial cells in vitro
[DE92-013510] p 131 N93-10626

INSTITUT D'ASTROPHYSIQUE, PARIS (FRANCE).
First results of an imaging FTS with a NICMOS camera p 86 N93-10936

INSTITUTE FOR COMPUTER APPLICATIONS IN SCIENCE AND ENGINEERING, HAMPTON, VA.
Unstructured mesh algorithms for aerodynamic calculations
[NASA-CR-189685] p 2 N93-10097
On the coupling between a supersonic boundary layer and a flexible surface
[NASA-CR-189697] p 82 N93-10757
Numerical study of the small scale structures in Boussinesq convection
[NASA-CR-189695] p 145 N93-10758
Progress in multi-dimensional upwind differencing
[NASA-CR-189708] p 83 N93-10808

INSTITUTE FOR DEFENSE ANALYSES, ALEXANDRIA, VA.
Relating flying hours to aircrew performance: Evidence for attack and transport missions
[AD-A253988] p 133 N93-10719

INSTITUTE FOR SPACE SCIENCE AND TECHNOLOGY, INC., GAINESVILLE, FL.
Elemental analyses of hypervelocity microparticle impact sites on interplanetary dust experiment sensor surfaces p 32 N93-10853
Contaminant interferences with SIMS analyses of microparticle impactor residues on LDEF surfaces p 32 N93-10854

INSTITUTO DE PESQUISAS ESPACIAIS, SAO JOSE DOS CAMPOS (BRAZIL).
Stereoscopy and paralax in the vertical distances determination using aerial photographs
[INPE-5363-PUD/049] p 102 N93-10063
A study upon structural optimization of elastic rotors for mechanical systems
[INPE-5376-TDI/471] p 94 N93-10310
SPOT panchromatic band simulation by linear combination of multispectral bands
[INPE-5295-PRE/1650] p 157 N93-10311
Physical implementations of an antimask in URA based coded mask systems
[INPE-5338-PRE/1737] p 153 N93-10312
Remote sensing data for monitoring and evaluating burned areas: Case of Emas National Park (GO)
[INPE-5312-PRE/1709] p 102 N93-10373

INSTITUTO NACIONAL DE TECNICA AEROESPACIAL, MADRID (SPAIN).
Mechanisms of sound generation in subsonic jets p 152 N93-10688

INTERNATIONAL ATOMIC ENERGY AGENCY, VIENNA (AUSTRIA).
Format and structure of a database on health and environmental impacts of different energy systems for electricity generation
[DE92-634160] p 130 N93-10222

INTERNATIONAL CENTRE FOR THEORETICAL PHYSICS, TRIESTE (ITALY).
Quantum tunneling and the change in the signature of the spacetime metric
[DE92-634877] p 165 N93-10225
Vector superconductivity in cosmic strings
[DE92-634923] p 179 N93-10296
A nonlinear oscillatory problem
[DE92-630203] p 95 N93-10385
The class of the paths in the Feynman path integral on the phase space
[DE92-630205] p 170 N93-10386
On the measurement of time-dependent quantum phases
[DE92-630206] p 170 N93-10387
Finite group actions and elliptic genera
[DE92-630207] p 170 N93-10388
Global structure of a polynomial autonomous system on the plane
[DE92-630230] p 144 N93-10389
IOWA STATE UNIV. OF SCIENCE AND TECHNOLOGY, AMES.
Materials compatibility and lubricants research on CFC-refrigerant substitute: Miscibility of lubricants with refrigerants
[DE92-015118] p 35 N93-10084
Order statistics and nonparametric statistics
[AD-A253574] p 146 N93-10699
A multilevel security model for object-oriented database systems p 175 N93-10844
Study of a viscous sublayer model in the analysis of 3-D shock/boundary layer interaction flow fields
[AD-A253731] p 84 N93-10886
IOWA UNIV., IOWA CITY.
Development of the finite analytic method for turbulent forced and free convection p 80 N93-10369

J

JACKSON STATE UNIV., MS.
A spatial similarity measure for image database applications
[AD-A253570] p 176 N93-10883
JET PROPULSION LAB., CALIFORNIA INST. OF TECH., PASADENA.
Investigation of the stimulated release of gaseous ammonia from ammonium perchlorate by HTPB solid propellant bonding agents p 19 N93-10026
Alternatives in clean propellants for large scale man-rated solid rocket motors p 20 N93-10028
A comparison of multimegawatt electric propulsion options for Mars missions p 23 N93-10043
Activated transport in AMTEC electrodes
[DE92-016810] p 75 N93-10786
JOHNS HOPKINS UNIV., COLUMBIA, MD.
The 1992 JANNAF Propulsion Meeting, volume 1
[CPIA-PUBL-580-VOL-1] p 15 N93-10001
JOHNS HOPKINS UNIV., LAUREL, MD.
A new model for interpreting experimental data from a circular waveguide cavity
[AD-A254067] p 75 N93-10785

K

KANSAS STATE UNIV., MANHATTAN.
Al Umchaimin depression, Western Iraq: An impact structure? p 122 N93-10190
KANSAS UNIV., LAWRENCE.
Three dimensional curved beam elements with large translations and rotations p 83 N93-10560
Research in theoretical particle physics
[DE92-016181] p 154 N93-10605
Development of nonlinear aerodynamic models for unsteady responses p 4 N93-10845
The effects of streamline curvature and swirl on turbulent flows in curved ducts p 84 N93-10875
KARPINSKY GEOLOGICAL RESEARCH INST., SAINT PETERSBURG (USSR).
Impactites from Popigai Crater p 117 N93-10164
KELLER ARMY COMMUNITY HOSPITAL, WEST POINT, NY.
A prospective evaluation of stress fractures/overuse injuries in a population of West Point cadets
[AD-A252427] p 132 N93-10709
KERAMONT CORP., TUCSON, AZ.
Reinforcements for high temperature ceramics
[DE92-014815] p 35 N93-10082
KEYSTONE ENGINEERING LTD., BLACKSBURG, VA.
Comparative study of the MTFA, ICS, and SQRI image quality metrics for visual display systems
[AD-A252116] p 158 N93-10708
KINGS COLL., LONDON (ENGLAND).
Numerical modelling of fringing fields and their use for complex permittivity measurements at high frequencies
[AD-A253994] p 72 N93-10359
KOA OIL CO. LTD. (JAPAN).
Air cell
[CA-PATENT-APPL-SN-2001346] p 72 N93-10368

L

LABORATORIO NACIONAL DE ENGENHARIA E TECNOLOGIA INDUSTRIAL, LISBON (PORTUGAL).
Scientific and Technical Information (STI) towards technological and industrial development: The case of Portugal p 173 N93-10596
LAKEHEAD UNIV., PORT ARTHUR (ONTARIO).
Experimental investigation of simple support condition in free vibration analysis of plates p 56 N93-10530
LAURENTIAN UNIV. OF SUDBURY (ONTARIO).
Thermobarometric studies on the Levack Gneisses: Footwall rocks to the Sudbury Igneous Complex p 114 N93-10152
Does the sedimentology of the Chelmsford formation provide evidence for a meteorite impact origin of the Sudbury structure? p 116 N93-10160
LAVAL UNIV. (QUEBEC).
A boundary element and mathematical programming approach for unilateral contact problems p 62 N93-10558
Effective formulation of the dynamics of a manipulator based on the Appell equations p 65 N93-10571
LAWRENCE LIVERMORE NATIONAL LAB., CA.
Selection of rocket propulsion systems p 22 N93-10034
Theoretical analysis of discharges in copper vapor lasers: A comparison of Ne and He
[DE92-014739] p 87 N93-10083
Optical and TEM study of shock metamorphism from the Sedan test site p 111 N93-10142
Simulated meteorite impacts and volcanic explosions: Ejecta analyses and planetary implications p 111 N93-10143
A computational study of projectile melt in impact with typical Whipple shields
[DE92-017137] p 92 N93-10635
DYNA2D: A nonlinear, explicit, two-dimensional finite element code for solid mechanics: User manual
[DE92-017310] p 95 N93-10646
Measurements and modeling of laser irradiance in the high-power third-harmonic Nova focus. Volume A: Report
[DE92-016746] p 90 N93-10739
Electrical resistance tomography used in environmental restoration
[DE92-018003] p 103 N93-10763
UV spectrum splitting mirror
[DE92-018057] p 159 N93-10818
LINGUISTIC RESEARCH INST., BOULDER, CO.
Analysis of observation report databases/knowledge bases
[AD-A252636] p 172 N93-10428
LITTON SYSTEMS, INC., CHARLOTTE, NC.
Single crystal growth of beta-Al2O3 for iso-index filters
[AD-A252259] p 169 N93-10879
LITTON SYSTEMS, INC., MORRIS PLAINS, NJ.
Development of garnet films for magnetostatic wave channelized receivers
[AD-A252812] p 166 N93-10335
LOCKHEED AIRCRAFT CORP., PALO ALTO, CA.
High resolution observations: The state of the art and beyond p 177 N93-10902
LOCKHEED ENGINEERING AND SCIENCES CO., HOUSTON, TX.
Requirements analysis notebook for the flight data systems definition in the Real-Time Systems Engineering Laboratory (RSEL)
[NASA-CR-185698] p 14 N93-10960
LOCKHEED ENGINEERING AND SCIENCES CO., LAS VEGAS, NV.
Global positioning systems technology and its application in environmental programs
[PB92-169358] p 7 N93-10442
LOGICON TECHNICAL SERVICES, INC., DAYTON, OH.
Comparative study of the MTFA, ICS, and SQRI image quality metrics for visual display systems
[AD-A252116] p 158 N93-10708
LOS ALAMOS NATIONAL LAB., NM.
Intense ion beam research at Los Alamos
[DE92-015240] p 155 N93-10333
Accelerator Technology Division
[DE92-016023] p 156 N93-10462
Self-programming of matter and the evolution of proto-biological organizations
[DE92-015244] p 129 N93-10628
LOYOLA UNIV., CHICAGO, IL.
Auditory processing of complex sounds across frequency channels
[AD-A253612] p 131 N93-10650
LUNAR AND PLANETARY INST., HOUSTON, TX.
Workshop on the evolution of the Martian atmosphere
[NASA-CR-190730] p 189 N93-10064
International Conference on Large Meteorite Impacts and Planetary Evolution
[NASA-CR-190677] p 105 N93-10112
Coincidences in time of the Imbrium Basin impact and Apollo 15 KREEP volcanic series: Impact-induced melting? p 119 N93-10175
Apollo 15 impact melts, the age of Imbrium, and the Earth-Moon impact cataclysm p 120 N93-10176
Paradigm lost: Venus crater depths and the role of gravity in crater modification p 120 N93-10179
The large impact process inferred from the geology of lunar multiring basins p 121 N93-10184

M

MANCHESTER UNIV. (ENGLAND).
Vibration of orthotropic cylindrical shell panels with arbitrary supported curved edges p 45 N93-10471
MANITOBA INDUSTRY, TRADE AND TOURISM, WINNIPEG.
The technology advantage: A guide to science, technology, and innovation in Manitoba
[CTN-92-60571] p 192 N93-10654
Manitoba aerospace technology: Capability directory
[CTN-92-60572] p 193 N93-10655
MANITOBA UNIV., WINNIPEG.
Overview of the vibroimpact damping of packaged particles p 56 N93-10528
MAROTTA SCIENTIFIC CONTROLS, INC., MONTVILLE, NJ.
LAM actuated propellant flow control device p 18 N93-10017
MAROTTA SCIENTIFIC CONTROLS, INC., TUSTIN, CA.
LAM actuated propellant flow control device p 18 N93-10017
MARYLAND UNIV., COLLEGE PARK.
The problem of the selection of an a-posteriori error indicator based on smoothening techniques
[AD-A253401] p 144 N93-10407
Contributions to the experimental investigation of rotor/body aerodynamic interactions p 5 N93-10877
MASSACHUSETTS GENERAL HOSPITAL, BOSTON.
Cognition in the brain: Investigations using positron emission tomography
[AD-A254280] p 132 N93-10765
MASSACHUSETTS INST. OF TECH., CAMBRIDGE.
Advanced terrain displays to transport category aircraft
[PB92-197136] p 6 N93-10065
Basic and applied research in the field of electronics and communications
[AD-A253593] p 67 N93-10092
An analytic determination of beta poloidal and internal inductance in an elongated tokamak from magnetic probe measurements
[DE92-016294] p 160 N93-10331
The magnetochemistry of supramolecular particles: The transition from the molecular to the solid-state
[AD-A253126] p 153 N93-10338
New developments in atom interferometry
[AD-A254094] p 158 N93-10659
Optical metrology of magnetically trapped hydrogen
[AD-A253229] p 31 N93-10712
Synthesis of side chain liquid crystal polymerization by living ring opening metathesis polymerization. Report 1: Influence of molecular weight, polydispersity, and flexible spacer length (n=2-8) on the thermotropic behavior of the resulting polymers
[AD-A248699] p 40 N93-10727
Microwave propagation and attenuation in magnetoplasmas
[AD-A250197] p 69 N93-10728
Interaction of electromagnetic fields with chondrocytes in gel culture
[AD-A253727] p 70 N93-10747
Nonlinear aeroelasticity of composite structures
[AD-A254285] p 8 N93-10842
MASSACHUSETTS INST. OF TECH., LEXINGTON.
Geometrical transformation of linear diode-laser arrays for longitudinal pumping of solid-state lasers
[AD-A253415] p 87 N93-10218
Covalent electron transfer theory of superconductivity
[AD-A253975] p 74 N93-10718
MASSACHUSETTS UNIV., AMHERST.
Biological and theoretical studies of adaptive networks: The conditioned response
[AD-A253329] p 142 N93-10354

MATERIALS SCIENCES CORP., BLUE BELL, PA.
Transverse tension, transverse compression, and inplane shear JANNAF round robin test methods standardization results p 16 N93-10007
MAX-PLANCK-INST. FUER KERNPHYSIK, HEIDELBERG (GERMANY).
Ar-40 to Ar-39 ages of the large impact structures Kara and Manicouagan and their relevance to the Cretaceous-Tertiary and the Triassic-Jurassic boundary p 122 N93-10188
Ar-40 to Ar-39 dating of pseudotachylites from the Witwatersrand basin, South Africa, with implications for the formation of the Vredefort Dome p 122 N93-10189
MCDONNELL-DOUGLAS CORP., SAINT LOUIS, MO.
Analysis of a buffer strip laminate with a cutout p 52 N93-10506
MCGILL UNIV., MONTREAL (QUEBEC).
Anelastic modelling of explosive cyclogenesis p 126 N93-10377
MELBOURNE UNIV., CARLTON (AUSTRALIA).
Mobilization of the platinum group elements by low-temperature fluids: Implications for mineralization and the iridium controversy p 109 N93-10133
MENTOR TECHNOLOGIES, INC., ROCKVILLE, MD.
Test range tracking network processors [AD-A253511] p 140 N93-10219
MESSERSCHMITT-BOELKOW-BLOHM G.M.B.H., MUNICH (GERMANY).
Accommodation aspects of SIMURIS on Space Station Freedom p 14 N93-10954
MESSERSCHMITT-BOELKOW G.M.B.H., MUNICH (GERMANY).
Reduction of propeller noise by active noise control p 152 N93-10692
MICHIGAN STATE UNIV., EAST LANSING.
Unifying the landmark developments in optimal bounding ellipsoid identification [AD-A253502] p 143 N93-10200
A study of flow properties of wet solids using laser induced photochemical anemometry [DE92-015483] p 82 N93-10629
Interdisciplinary research and training program in the plant sciences [DE92-015919] p 130 N93-10835
MICHIGAN UNIV., ANN ARBOR.
Millimeter wave measurement and modeling of terrain scattering [AD-A253525] p 67 N93-10223
Advanced transport systems for electron beams in high-brightness accelerators and FEL's [AD-A253314] p 88 N93-10286
Power spectrum of the extragalactic background light p 177 N93-10364
Mass transfer in oscillating flows: Efficient drying via pulse combustors [PB92-204403] p 81 N93-10449
High sensitivity probes for silicon VLSI internal node testing [AD-A253924] p 169 N93-10764
MICROELECTRONICS AND COMPUTER TECHNOLOGY CORP., AUSTIN, TX.
An MCM/chip concurrent engineering validation [AD-A253783] p 136 N93-10237
MINNESOTA MINING AND MFG. CO., SAINT PAUL.
GAP benefits p 19 N93-10025
MINNESOTA UNIV., MINNEAPOLIS.
Pion- and proton-nucleus interactions at intermediate energy [DE92-017980] p 157 N93-10838
MISSION RESEARCH CORP., SANTA BARBARA, CA.
ACIRF user's guide for the general model (Version 3.5) [AD-A254068] p 69 N93-10657
MISSISSIPPI STATE UNIV., MISSISSIPPI STATE.
Analysis and control of grid quality in computational simulation [AD-A253723] p 138 N93-10746
MISSOURI UNIV., ROLLA.
Analysis of failure modes in ceramic matrix composite p 28 N93-10508
Natural vibrations of multilayered doubly curved shells p 57 N93-10532
Modelling and control of robotic arms fabricated from orthotropic materials p 65 N93-10572
Mobility of toluene in polystyrene-toluene solutions: A NMR study [AD-A253203] p 31 N93-10794
MISSOURI UNIV., SAINT LOUIS.
Quantum 1/f noise in high technology applications including ultrasmall structures and devices [AD-A253922] p 74 N93-10751
MITRE CORP., BEDFORD, MA.
Far-zone field of a monopole element on a disk ground plane above flat earth [AD-A253580] p 70 N93-10091
MONCTON UNIV., EDMUNDSTON (NEW BRUNSWICK).
Experimental investigation of flows behind different Large-Eddy Breakup (LEBU) devices in thick boundary layers p 6 N93-10550
MORGANTOWN TECHNOLOGY CENTER, WV.
Temperature-programmed oxidation of ethane and ethylene in the presence and absence of C-13 labeled methane [DE92-015048] p 42 N93-10329
MOSCOW STATE UNIV. (USSR).
Diaplectic transformation of minerals: Vorotilov drill core, Puchezh-Katunki impact crater, Russia p 110 N93-10136
MOTOREN- UND TURBINEN-UNION MUENCHEN G.M.B.H. (GERMANY).
Combat aircraft noise reduction by technical measures p 152 N93-10689
MSE, INC., BUTTE, MT.
Magnetohydrodynamic projects at the CDIF [DE92-018190] p 164 N93-10819
MUENSTER UNIV. (GERMANY).
Sudbury project (University of Muenster-Ontario Geological Survey): Origin of the polymict, allochthonous breccias of the Onaping Formation p 106 N93-10116
Sudbury project (University of Muenster-Ontario Geological Survey): Summary of results - an updated impact model p 106 N93-10117
Structural aspects of the Araguainha impact structure (Brazil) p 106 N93-10118
Sudbury project (University of Muenster-Ontario Geological Survey): Field studies 1984-1989 - summary of results p 107 N93-10119
Sudbury project (University of Muenster-Ontario Geological Survey): Isotope systematics support the impact origin p 109 N93-10131
Influence of the preshock temperature on shock effects in quartz p 115 N93-10157
Sudbury project (University of Muenster-Ontario Geological Survey): New investigations on Sudbury breccia p 118 N93-10167
Sudbury project (University of Muenster-Ontario Geological Survey): Petrology, chemistry, and origin of breccia formations p 121 N93-10185

N

NANYANG TECHNOLOGICAL INST. (SINGAPORE).
A derivation for the kinematic equations of flexible robots with appropriate transformation matrices p 66 N93-10577
NANYANG UNIV. (SINGAPORE).
A solution scheme for the deflection equations of flexible arms with time-dependent boundary conditions p 66 N93-10575
NAPLES UNIV. (ITALY).
A variational approach for coupled creeping-flow problems p 62 N93-10557
NATIONAL ACADEMY OF SCIENCES - NATIONAL RESEARCH COUNCIL, WASHINGTON, DC.
Aeronautical technologies for the twenty-first century [NASA-CR-190918] p 1 N93-10647
Guidelines for developing spacecraft maximum allowable concentrations for Space Station contaminants [NASA-CR-190748] p 13 N93-10737
NATIONAL AERO-SPACE PLANE JOINT PROGRAM OFFICE, WRIGHT-PATTERSON AFB, OH.
A configuration development strategy for the NASP p 9 N93-10011
NATIONAL AERONAUTICS AND SPACE ADMINISTRATION, WASHINGTON, DC.
Gamma ray astrophysics to the year 2000. Report of the NASA Gamma Ray Program Working Group [NASA-TM-107995] p 178 N93-10067
Aeronautical engineering: A continuing bibliography with indexes (supplement 276) [NASA-SP-7037(276)] p 1 N93-10073
Aeronautical engineering: A continuing bibliography with indexes (supplement 279) [NASA-SP-7037(279)] p 1 N93-10074
Aerospace medicine and biology: A continuing bibliography with indexes (supplement 365) [NASA-SP-7011(365)] p 130 N93-10075
Aerospace medicine and biology: A continuing bibliography with indexes (supplement 360) [NASA-SP-7011(360)] p 130 N93-10076
Aerospace medicine and biology: A continuing bibliography with indexes (supplement 364) [NASA-SP-7011(364)] p 130 N93-10077
NASA patent abstracts bibliography: A continuing bibliography. Section 1: Abstracts (supplement 41) [NASA-SP-7039(41)-SECT-1] p 171 N93-10078
Aerospace medicine and biology: A continuing bibliography with indexes (supplement 366) [NASA-SP-7011(366)] p 130 N93-10079
Aerospace medicine and biology: A continuing bibliography with indexes (supplement 367) [NASA-SP-7011(367)] p 130 N93-10080
Aeronautical engineering: A cumulative index to a continuing bibliography (supplement 274) [NASA-SP-7037(274)] p 1 N93-10351
Aeronautical engineering: A continuing bibliography with indexes (supplement 281) [NASA-SP-7037(281)] p 1 N93-10352
Establishing a scientific and technical information program: Planning and resource management p 173 N93-10597
Technology for libraries and information centers: A seminar in Greece, Portugal, and Turkey p 174 N93-10601
Index to NASA news releases and speeches, 1991 [NASA-TM-108004] p 175 N93-10815
Indexes of maps of the planets and satellites, 1992 [NASA-TM-4395] p 189 N93-10832
Index to NASA news releases and speeches, 1990 [NASA-TM-108003] p 176 N93-10872
NASA Space Human Factors Program [NASA-TM-108005] p 134 N93-10890
NATIONAL AERONAUTICS AND SPACE ADMINISTRATION. AMES RESEARCH CENTER, MOFFETT FIELD, CA.
Initial piloted simulation study of geared flap control for tilt-wing V/STOL aircraft [NASA-TM-103872] p 11 N93-10741
Documentation of the detailed radiation property data for the radiation-ablation code RASLE [NASA-TM-103848] p 28 N93-10742
Appraisal of digital terrain elevation data for low-altitude flight [NASA-TM-103896] p 7 N93-10745
NATIONAL AERONAUTICS AND SPACE ADMINISTRATION. GODDARD SPACE FLIGHT CENTER, GREENBELT, MD.
New perspectives on the Popigai impact structure p 110 N93-10138
The Zhamanshin impact feature: A new class of complex crater? p 110 N93-10139
Impact origin of the Sudbury structure: Evolution of a theory p 116 N93-10161
Imaging radar investigations of the Sudbury structure p 117 N93-10162
Search for the 700,000-year-old source crater of the Australasian tektite strewn field p 120 N93-10177
The current and future environmental role of atmospheric methane: Model studies and uncertainties [NASA-CR-190662] p 104 N93-10256
Data synthesis and display programs for wave distribution function analysis [NASA-TM-108009] p 70 N93-10800
NATIONAL AERONAUTICS AND SPACE ADMINISTRATION. JOHN F. KENNEDY SPACE CENTER, COCOA BEACH, FL.
Generic Propellant Transfer Unit p 11 N93-10046
NATIONAL AERONAUTICS AND SPACE ADMINISTRATION. LYNDON B. JOHNSON SPACE CENTER, HOUSTON, TX.
Uprated OMS engine status: Altitude testing results p 22 N93-10036
Long life monopropellant hydrazine thruster evaluation for Space Station Freedom application p 23 N93-10042
Design and operation of the US Space Station Freedom propulsion system p 24 N93-10049
Method for culturing mammalian cells in a perfused bioreactor [NASA-CASE-MSC-21293-2] p 129 N93-10109
Method for culturing mammalian cells in a horizontally rotated bioreactor [NASA-CASE-MSC-21294-2] p 129 N93-10110
Melt production in large-scale impact events: Calculations of impact-melt volumes and crater scaling p 108 N93-10125
Melt production in large-scale impact events: Planetary observations and implications p 108 N93-10126
Melt production in large-scale impact events: Implications and observations at terrestrial craters p 112 N93-10144
NATIONAL AERONAUTICS AND SPACE ADMINISTRATION. LANGLEY RESEARCH CENTER, HAMPTON, VA.
A building-block approach for turbulence model validation/upgrade focussed on high-speed jet flowfields p 16 N93-10010
Design, test, and evaluation of three active flutter suppression controllers [NASA-TM-4338] p 10 N93-10070
Pitot survey of exhaust flow field of a 2-D scramjet nozzle at Mach 6 with air or freon and argon used for exhaust simulation [NASA-TM-4361] p 2 N93-10071

Interactive grid generation program for CAP-TSD
[NASA-TM-102705] p 3 N93-10349
Comparison of full 3-D, thin-film 3-D, and thin-film plate analyses of a postbuckled embedded delamination
p 47 N93-10480
LDEF Materials Workshop 1991, part 2
[NASA-CP-3162-PT-2] p 37 N93-10578
Effect of space exposure on pyroelectric infrared detectors p 38 N93-10582
Non-propulsive aerodynamic noise
p 149 N93-10673
Supersonic acoustic source mechanisms for free jets of various geometries p 150 N93-10680
Extravehicular activity compatibility evaluation of developmental hardware for assembly and repair of precision reflectors
[NASA-TP-3246] p 13 N93-10744
Effect of planform and body on supersonic aerodynamics of multibody configurations
[NASA-TP-3212] p 4 N93-10824

NATIONAL AERONAUTICS AND SPACE ADMINISTRATION. LEWIS RESEARCH CENTER, CLEVELAND, OH.
Combustion-wave ignition for rocket engines
p 17 N93-10016
Thermal stratification potential in rocket engine coolant channels p 18 N93-10019
Hot fire test results of subscale tubular combustion chambers p 18 N93-10020
10 kW power electronics for hydrogen arcjets
p 21 N93-10033
Hot fire fatigue testing results for the compliant combustion chamber p 22 N93-10038
A survey of instabilities within centrifugal pumps and concepts for improving the flow range of pumps in rocket engines p 23 N93-10039
Effects of anode material on arcjet performance
p 23 N93-10044
Tank chilldown analysis and verification with a flightweight, 175 cu ft tank under normal gravity with liquid hydrogen p 24 N93-10045
Radial turbine cooling p 78 N93-10061
Evaluation and application of the Baldwin-Lomax turbulence model in two-dimensional, unsteady, compressible boundary layers with and without separation in engine inlets
[NASA-TM-105810] p 79 N93-10087
Effects of anode material on arcjet performance
[NASA-TM-105799] p 25 N93-10197
Calculation of stress intensity factors in an isotropic multicracked plate: Part 2: Symbolic/numeric implementation
[NASA-TM-105823] p 95 N93-10453
A new energy transfer model for turbulent free shear flow
[NASA-TM-105854] p 81 N93-10454
Calculation of stress intensity factors in an isotropic multicracked plate. Part 1: Theoretical development
[NASA-TM-105766] p 95 N93-10455
Comparison of all-electric secondary power systems for civil subsonic transports
[NASA-TM-105852] p 9 N93-10456
System model development for nuclear thermal propulsion
[NASA-TM-105761] p 25 N93-10457
A least-squares finite element method for incompressible Navier-Stokes problem
p 60 N93-10548
Power system monitoring and source control of the Space Station Freedom DC power system testbed
[NASA-TM-105841] p 26 N93-10734
Navier-Stokes turbine heat transfer predictions using two-equation turbulence
[NASA-TM-105817] p 82 N93-10735
Hot fire fatigue testing results for the compliant combustion chamber
[NASA-TP-3223] p 26 N93-10743
Unified viscoplastic behavior of metal matrix composites
[NASA-TM-105819] p 96 N93-10777
Acceptance testing of the prototype electrometer for the SAMPIE flight experiment
[NASA-TM-105880] p 13 N93-10841

NATIONAL AERONAUTICS AND SPACE ADMINISTRATION. MARSHALL SPACE FLIGHT CENTER, HUNTSVILLE, AL.
Facility for cold flow testing of solid rocket motor models p 11 N93-10021
NLS cargo transfer vehicle propulsion system
p 23 N93-10041
Tensile properties of cast titanium alloys: Titanium-6Al-4V ELI and Titanium-5Al-2.5Sn ELI
[NASA-TP-3288] p 33 N93-10072
Method and apparatus for determining return stroke polarity of distant lightning
[NASA-CASE-MFS-26102-2-CU] p 125 N93-10106
Selected results for metals from LDEF experiment A0171 p 34 N93-10579
Hubble Space telescope thermal cycle test report for large solar array samples with BSFR cells (Sample numbers 703 and 704)
[NASA-TM-108373] p 104 N93-10809

NATIONAL ASSESSMENT GOVERNING BOARD, WASHINGTON, DC.
The levels of mathematics achievement: Initial performance standards for the 1990 NAEP mathematics assessment, volume 3
[PB92-199421] p 134 N93-10341

NATIONAL GEOPHYSICAL DATA CENTER, BOULDER, CO.
Solar-geophysical data number 569, January 1992. Part 1: (Prompt reports). Data for December, November 1991, and late data
[PB92-158880] p 190 N93-10771
Solar-geophysical data number 570, February 1992. Part 1: (Prompt reports). Data for January 1992, December 1991, and late data
[PB92-170380] p 190 N93-10773
Solar-geophysical data number 570, February 1992. Part 2: (Comprehensive reports). Data for August 1991 and miscellaneous
[PB92-170398] p 190 N93-10774
Solar-geophysical data number 571, March 1992. Part 1: (Prompt reports). Data for February, January 1992, and late data
[PB92-177062] p 190 N93-10775
Solar-geophysical data number 571, March 1992. Part 2: (Comprehensive reports). Data for September 1991 and miscellaneous
[PB92-177070] p 190 N93-10776

NATIONAL INST. FOR RESEARCH IN INORGANIC MATERIALS, TOKYO (JAPAN).
Developmental research on ultra abrasion-resistant materials
[DE92-531066] p 36 N93-10287

NATIONAL INST. OF STANDARDS AND TECHNOLOGY, BOULDER, CO.
Gradiometer antennas for tunnel detection
[PB92-205400] p 69 N93-10440

NATIONAL INST. OF STANDARDS AND TECHNOLOGY, GAITHERSBURG, MD.
List of publications, 1969-1991. Panel on wind and seismic effects
[PB92-201102] p 125 N93-10089
Moire-fringe images of twin boundaries in chemical vapor deposited diamond
[AD-A253729] p 35 N93-10231
Methodology for the computer-aided design of silicon micromachined devices in a standard CMOS process
[PB92-191246] p 136 N93-10248
Materials compatibility and lubricants research on CFC-refrigerant substitutes: Thermophysical properties
[DE92-015116] p 43 N93-10397
Raster graphics validation
[PB92-196070] p 137 N93-10441
Optimization of neural network topology and information content using Boltzman methods
[PB92-205418] p 142 N93-10450
Growth defects in diamond films
[AD-A253618] p 40 N93-10778
A fundamental understanding of the effects of ceramic processing on product microstructure
[AD-A253660] p 41 N93-10779
Laser cooling and trapping of neutral atoms
[AD-A253730] p 155 N93-10885

NATIONAL OCEANIC AND ATMOSPHERIC ADMINISTRATION, BOULDER, CO.
Climate Monitoring and Diagnostics Laboratory
[PB92-162346] p 105 N93-10772

NATIONAL PHYSICAL LAB., TEDDINGTON (ENGLAND).
Measurement and prediction of noise from low-altitude military aircraft operations p 151 N93-10687

NATIONAL RESEARCH COUNCIL OF CANADA, OTTAWA (ONTARIO).
Noise studies for environmental impact assessment of an outdoor engine test facility p 149 N93-10672

NATIONAL TELECOMMUNICATIONS AND INFORMATION ADMINISTRATION, BOULDER, CO.
Analysis of reception variability due to terrain multipath on microwave common carrier links
[NTIA-92-283] p 69 N93-10430

NAVAL ACADEMY OF GREECE, ATHENS.
Integral transform approach to an inertial viscoelastic problem involving moving singularities
p 49 N93-10490

NAVAL COMMAND, CONTROL AND OCEAN SURVEILLANCE CENTER, SAN DIEGO, CA.
Misclassification rates of likelihood and predictive discriminant functions for small samples
[AD-A253640] p 146 N93-10208
An implementation of the MVDR beamformer on the Intel iWarp system
[AD-A253641] p 140 N93-10209

NAVAL OCEAN SYSTEMS CENTER, SAN DIEGO, CA.
Prototype superconducting planar transformers using high-Tc thin and thick films
[AD-A254230] p 77 N93-10897

NAVAL POSTGRADUATE SCHOOL, MONTEREY, CA.
Link-11 communications
[AD-A252766] p 68 N93-10260
A method of testing two-dimensional airfoils
[AD-A253210] p 4 N93-10375
An indicator of message quality for a single optical sensor using a template based tracking algorithm
[AD-A252704] p 139 N93-10881

NAVAL RESEARCH LAB., WASHINGTON, DC.
Numerical simulation of unsteady flow in a nozzle
p 16 N93-10008
Molecular dynamics of shocks in crystals with defects
[AD-A253353] p 164 N93-10099
Simulation of electron beam transport in ion-focused regime conditioning cells
[AD-A253352] p 70 N93-10215
Artificial intelligence technical paper abstracts, 1991
[AD-A253340] p 141 N93-10269
Ultrasonic characterization of highly attenuative thick composites
[AD-A253347] p 27 N93-10272
Convergence performance of adaptive detectors, part 3
[AD-A248415] p 143 N93-10275
Stress patterns in the dynamic tear test
p 49 N93-10491
Studies impacting the designs of free electron lasers
[AD-A254293] p 90 N93-10768

NAVAL SURFACE WARFARE CENTER, SILVER SPRING, MD.
Resonance apparatus operating manual
[AD-A254040] p 71 N93-10241

NAVAL SURFACE WEAPONS CENTER, DAHLGREN, VA.
Resistive Grid Kernel Estimator (RGKE)
[AD-A253520] p 147 N93-10869

NAVAL WEAPONS CENTER, CHINA LAKE, CA.
Impact sensitivity reduction via exo-electron control
p 15 N93-10004
The effect of elevated temperatures on the properties of thermally stable silicon-based elastomers for adhesives, sealants, and insulator applications p 15 N93-10006

NETHERLANDS FOUNDATION FOR RADIO ASTRONOMY, DWINGELO.
Towards an ESA strategy for optical interferometry in space. Recommendations of the ESA Space Interferometry Study Team (SiST) p 178 N93-10944

NEW BRUNSWICK UNIV., FREDERICTON.
Viscosity determinations of some frictionally generated silicate melts: Implications for slip zone rheology during impact-induced faulting p 121 N93-10183
A comparison of the chemistry of pseudotachylyte breccias in the Archean Levack Gneisses of the Sudbury structure, Ontario p 122 N93-10187
Electron petrography of silica polymorphs associated with pseudotachylite, Vredefort structure, South Africa
p 123 N93-10192
Probability density functions for random nonlinear oscillation p 55 N93-10522

NEW MEXICO UNIV., ALBUQUERQUE.
Does the Bushveld-Vredefort system (South Africa) record the largest known terrestrial impact catastrophe?
p 109 N93-10134
Mathematical analysis of reactive multiphase flows
[AD-A253854] p 83 N93-10810

NEWCASTLE-UPON-TYNE UNIV. (ENGLAND).
Evaluation of the triangular plate element of Zienkiewcz and Lefebvre p 63 N93-10562

NORGES TEKNISKE HOEGSKOLE, TRONDHEIM.
Fourier transform spectrometer processing: Data reduction and processor design p 14 N93-10935

NORTH ATLANTIC TREATY ORGANIZATION, BRUSSELS (BELGIUM).
Acquisition 2: Procurement, acquisition, and maintenance of configuration management documentation in support of a CIS system p 173 N93-10599

NORTH CAROLINA STATE UNIV., RALEIGH.
Pseudomorphic semiconducting heterostructures from combinations of AlN, GaN, and selected SiC polytypes: Theoretical advancement and its coordination with experimental studies of nucleation, growth, characterization, and device development
[AD-A253330] p 166 N93-10355
Growth, nitrogen vacancy reduction, and solid solution formation in cubic GaN thin films and the subsequent fabrication of superlattice structures using AlN and InN
[AD-A253331] p 166 N93-10356

Analysis of interplanetary dust experiment detectors and other witness plates
[NASA-CR-190818] p 32 N93-10852

NORTH CAROLINA UNIV., CHAPEL HILL.
Thermo-optical switching in Si based etalons
[AD-A253139] p 88 N93-10412
Kinetics of oxidation of silicon by electron cyclotron resonance plasmas
[AD-A253140] p 161 N93-10413
Pre-oxidation anneal kinetics: Interface degradation of thin SiO2 films on silicon
[AD-A253142] p 30 N93-10414
A new ellipsometry technique for interface analysis: Application to Si-SiO2
[AD-A253143] p 167 N93-10415
Spectroscopic ellipsometric measurements of the dielectric function of germanium dioxide films on crystal germanium
[AD-A253137] p 168 N93-10614
Langmuir probe and optical emission studies of Ar, O2, and N2 plasmas produced by an ECR microwave source
[AD-A253138] p 162 N93-10615
Spectroscopic differential reflectance as an analytical probe for microelectronic processing
[AD-A253134] p 73 N93-10656

NORTH CAROLINA UNIV., CHARLOTTE.
Holographic optical interconnects for multichip modules
[AD-A253403] p 86 N93-10408

NORTH CENTRAL FOREST EXPERIMENT STATION, SAINT PAUL, MN.
The Deposition and Fate of Trace Metals in our Environment: Symposium proceedings
[PB92-189216] p 104 N93-10289

NORTHROP CORP., HAWTHORNE, CA.
Composite failure analysis handbook. Volume 2: Technical handbook. Part 2: Atlas of fractographs
[AD-A249130] p 28 N93-10325

NORTHWESTERN UNIV., EVANSTON, IL.
Oxygen barrier oxides
[AD-A253683] p 36 N93-10343

NOTTINGHAM UNIV. (ENGLAND).
Development in the elastic analysis of laminated plates p 44 N93-10468

O

OAK RIDGE NATIONAL LAB., TN.
Reinforcements for high temperature ceramics
[DE92-014815] p 35 N93-10082
A look at scalable dense linear algebra libraries
[DE92-017805] p 143 N93-10285
Two-photon couplings of quarkonia with arbitrary J(sup PC)
[DE92-016525] p 153 N93-10332
Parallel sparse Cholesky factorization algorithms for shared-memory multiprocessor systems
[DE92-016829] p 141 N93-10334
Review and analysis of check valve failure data
[DE92-014462] p 91 N93-10381
TIGER5: Extraction of geographic information from the TIGER system
[DE92-014935] p 171 N93-10382
Resonance ionization of rubidium using sequential diode laser-driven transitions
[DE92-014468] p 89 N93-10429
Reliability of sublattice occupancies determined by ALCHEMI
[DE92-014592] p 168 N93-10623
Conductive titanate fiber and its production method
[DE92-014738] p 39 N93-10627
Stress modified welding process for irradiated materials
[DE92-017131] p 92 N93-10634
Spatial models of ecological systems and processes: The role of GIS
[DE92-016884] p 175 N93-10788
Atomic short range order and spin density wave propagation in CuMn
[DE92-016903] p 34 N93-10789
A look at scalable dense linear algebra libraries
[DE92-017161] p 139 N93-10816

OBERLIN COLL., OH.
Geological evidence for a 2.6-Ga strewn field of impact spherules in the Hamersley Basin of Western Australia p 120 N93-10181

OBSERVATOIRE DE LA COTE D'AZUR, NICE (FRANCE).
The CHARON program p 177 N93-10942

OBSERVATOIRE DE PARIS-MEUDON (FRANCE).
Chromospheric structure and dynamics p 180 N93-10906
Coronal and solar wind Alfven wave propagation p 180 N93-10909
Intensity, velocity, and turbulence in prominences observed with the HRTS p 180 N93-10911
Stokes parameters of the O VI 103.2 nm line as a probe of the matter velocity field vector in the solar wind acceleration region p 181 N93-10914
MSDP imaging spectroscopy for high resolution solar physics p 183 N93-10926

ODYSSEY RESEARCH ASSOCIATES, INC., OTTAWA (ONTARIO).
The mechanical verification of a simple control system
[ORA-TR-89-5443-04] p 142 N93-10641

OFFICE NATIONAL D'ETUDES ET DE RECHERCHES AERONAUTIQUES, PARIS (FRANCE).
Boom and the problems related to the supersonic flights of military aircraft p 149 N93-10677
Combat aircraft jet engine noise studies p 150 N93-10679

OFFICE NATIONAL D'ETUDES ET DE RECHERCHES AEROSPATIALES, PARIS (FRANCE).
Numerical study of wall turbulence
[ONERA-RSF-21/3419-AY-126] p 83 N93-10859
Direct simulation of turbulent pulsed plane channel flows p 84 N93-10860

OHIO STATE UNIV., COLUMBUS.
Fundamental studies on erosion in MPD thrusters
[AD-A253900] p 159 N93-10252
Effect of alloying elements on passivity and breakdown of passivity of Fe- and Ni-based alloys mechanistics aspects
[DE92-017316] p 33 N93-10395
Consistent shear constitutive relations for laminated plates p 28 N93-10509
Automated handling and assembling of non-rigid objects
[AD-A253605] p 66 N93-10649

OLD DOMINION UNIV., NORFOLK, VA.
Navier-Stokes dynamics and aeroelastic computations for vortical flows, buffet and aeroelastic applications
[NASA-CR-190692] p 2 N93-10098
Effect of passive flow-control devices on turbulent low-speed base flow p 79 N93-10304
A finite element method for nonlinear panel flutter p 45 N93-10472

OLIN CORP., BRANDENBURG, KY.
Synthesis and characterization of energetic polymers p 15 N93-10005

OLIN CORP., CHESHIRE, CT.
Synthesis and characterization of energetic polymers p 15 N93-10005

ORANGE FREE STATE UNIV., BLOEMFONTEIN (SOUTH AFRICA).
Structural review of the Vredefort dome p 108 N93-10127

OREGON GRADUATE INST. OF SCIENCE AND TECHNOLOGY, BEAVERTON.
Stability of coupled semiconductor diode lasers p 88 N93-10379

OREGON STATE UNIV., CORVALLIS.
Atomic approaches to defect thermochemistry
[AD-A254278] p 167 N93-10425
Matter-wave interferometry with laser cooled atoms
[AD-A254000] p 89 N93-10720

OREGON STATE UNIV., NEWPORT.
Parallel processing and learning: Variability and chaos in self-organization of activity in groups of neurons
[AD-A250290] p 140 N93-10242

OREGON UNIV., EUGENE.
Nonlinear studies of surface and interfaces of advanced semiconductor materials
[AD-A253365] p 164 N93-10105

OSAKA UNIV., SUITA (JAPAN).
Vibrations of a flexible Timoshenko beam under gravity p 53 N93-10512

OXFORD UNIV. (ENGLAND).
Remote sounding of the Martian atmosphere p 189 N93-10378
Imaging of BL Lac objects p 177 N93-10884

P

PACIFIC ELECTRO DYNAMICS, REDMOND, WA.
Power conditioning unit for 30 kWe class arcjet flight experiment p 21 N93-10032

PACIFIC NORTHWEST LAB., RICHLAND, WA.
Fractals and multifractals in fracture p 50 N93-10497
Advanced materials development for fossil energy conversion applications
[DE92-015762] p 104 N93-10729
Radiation damage to DNA
[DE92-015760] p 130 N93-10834

PARIS VII UNIV. (FRANCE).
Carbon and oxygen isotope study of carbonates from highly shocked clasts of the polymict breccia of the Haughton Crater (Canada) p 105 N93-10113
Phase transformations in 40-60-GPa shocked gneisses from the Haughton Crater (Canada): An Analytical Transmission Electron Microscopy (ATEM) study p 117 N93-10163
Physics of coronal loops: Heating and reconnection p 180 N93-10912

PCO, INC., CHATSWORTH, CA.
Long wavelength multiple quantum well lasers for high-speed modulation applications
[AD-A253348] p 87 N93-10211

PENNSYLVANIA STATE UNIV., UNIVERSITY PARK.
Field emission current-voltage curves as a diagnostic for scanning tunneling microscope tips
[AD-A251171] p 165 N93-10245
Piezoelectric and electrostrictive materials for transducers applications, volume 1
[AD-A250889] p 71 N93-10273
Piezoelectric and electrostrictive materials for transducers applications, volume 2
[AD-A250890] p 71 N93-10276
Piezoelectric and electrostrictive materials for transducers applications, volume 3
[AD-A250891] p 72 N93-10280
Piezoelectric and electrostrictive materials for transducers applications, volume 4
[AD-A250892] p 72 N93-10282
Characterization of and active control of flexible structures, using piezoceramics as sensors and actuators p 10 N93-10319
Semiconductor phase conjugation
[AD-A253684] p 166 N93-10345
Explicit Navier-Stokes computation of turbomachinery flows p 81 N93-10370
Electron transfer, ionization, and excitation in atomic collisions
[DE92-017300] p 154 N93-10435
Mechanical behavior of open cell ceramics
[PB92-212984] p 37 N93-10439
The prediction of noise radiation from supersonic elliptic jets p 151 N93-10684
Inhibiting corrosion in Gr/Al and Gr/Mg metal matrix composites using nonequilibrium alloying techniques
[AD-A253923] p 34 N93-10752
Turbulent mixing in compressible free shear layers p 83 N93-10846

PENNSYLVANIA UNIV., PHILADELPHIA.
Computer simulations of object discrimination by visual cortex
[AD-A253345] p 131 N93-10271
Plasticity of single crystalline Al3X intermetallic compounds
[AD-A254282] p 40 N93-10766

PHARMAKON RESEARCH INTERNATIONAL, INC., WAVERLY, PA.
Limited toxicity and mutagenicity testing of five unicharge propellant compounds
[AD-A252339] p 43 N93-10636

PHILLIPS LAB., EDWARDS AFB, CA.
Electric Propulsion Space Experiment (ESEX): Spacecraft design issues for high-power electric propulsion p 21 N93-10030
Synchrotron radiation considerations in the Dense Plasma Focus (DPF) Magnetoplasmadynamic (MPD) thruster
[AD-A254188] p 25 N93-10258

PHILLIPS LAB., HANSCOM AFB, MA.
A three-dimensional analysis of the effect of local stress distribution near crack tip p 15 N93-10003
The application of liquid crystal polymers to turbomachinery p 23 N93-10040

PITTSBURGH ENERGY TECHNOLOGY CENTER, PA.
Turbulence modeling of the flow field in combustors using the non-linear k-epsilon model
[DE92-014745] p 80 N93-10330

PITTSBURGH UNIV., PA.
Atomic hydrogen: A reagent for the extraction of chemical species from silicon surfaces
[AD-A252804] p 30 N93-10266
Comparison of Cl and HCl adsorption on Si(100)-(2 x 1)
[AD-A252802] p 30 N93-10281
Hydrocarbon surface chemistry on Si(100)
[AD-A252803] p 27 N93-10465
Investigations into swirling flows of Newtonian and non-Newtonian fluids
[AD-A253298] p 82 N93-10696
Transformation of Cl bonding structures on Si(100)-(2x1)
[AD-A253739] p 40 N93-10748

POLISH ACADEMY OF SCIENCES, WARSAW.
Shortened Test Heating Season (STHS) p 43 N93-10314

PRATT AND WHITNEY AIRCRAFT, WEST PALM BEACH, FL.
Altitude compensating nozzle evaluation p 22 N93-10037

PRICE (M. A.), WINDSOR JUNCTION (NOVA SCOTIA).
Mathematical analysis of multi-sensor cross-correlation processing for source localization
[DREA-CR-89-433] p 68 N93-10366
PRINCETON UNIV., NJ.
Mathematical analysis of strong fluid mechanical effects at high Mach number in reactive and nonreactive flow
[AD-A253617] p 79 N93-10094
Where's the Beaverhead beef? p 112 N93-10146
Reflection of plasma ions from metals (and its use as a hyperthermal neutral beam source)
p 160 N93-10353
Architecture and device development for optical networks
[AD-A253247] p 158 N93-10693
PUERTO RICO UNIV., MAYAGUEZ.
A new non-Gausssian approximation technique for random vibration of general hysteresis
p 50 N93-10496
PURCELL (ANTHONY) CONSULTANTS, LUENBURG (NOVA SCOTIA).
Acoustic noise generation at the air/ocean boundary
[DREA-CR-90-445] p 147 N93-10642
PURDUE UNIV., WEST LAFAYETTE, IN.
Development of physical and mathematical models for the Porous Ceramic Tube Plant Nutrification System (PCTPNS)
[NASA-TM-107551] p 129 N93-10085
Entropy of disorder in thermomechanics of damage in heterogeneous solids p 50 N93-10498
Morning-evening differences in global and regional oceanic precipitation as observed by the SSM/I
p 127 N93-10851

R

RAHTIKONE OY (FINLAND).
Steering system of a vehicle, such as a snow removing machine for airfields
[CA-PATENT-APPL-SN-1293201] p 91 N93-10367
RAND CORP., SANTA MONICA, CA.
Maintaining future military aircraft design capability
[AD-A253963] p 8 N93-10420
A change of course: The importance to DoD of international standards for electronic commerce
[AD-A253199] p 75 N93-10792
RANGE COMMANDERS COUNCIL, WHITE SANDS MISSILE RANGE, NM.
Transducer workshop no. 16
[AD-A248047] p 12 N93-10236
REIMS UNIV. (FRANCE).
Experimental and theoretical behavior of adhesively bonded composite structures under tensile stress at the edge vicinity p 53 N93-10515
RENSSELAER POLYTECHNIC INST., TROY, NY.
D-He-3 spherical torus fusion reactor system study
[AD-A253358] p 155 N93-10102
Probing cosmic infrared sources: A computer modeling approach
[AD-A253788] p 178 N93-10238
Effects of gravity in folding p 124 N93-10324
Mechanics of composite materials for spacecraft
[AD-A254217] p 28 N93-10896
RESEARCH INST. FOR ADVANCED COMPUTER SCIENCE, MOFFETT FIELD, CA.
AMR on the CM-2
[NASA-CR-190747] p 138 N93-10736
RESEARCH INST. FOR COMPUTING AND INFORMATION SYSTEMS, HOUSTON, TX.
NASA Electronic Library System (NELS) database schema, version 1.2
[NASA-CR-190643] p 172 N93-10451
A survey of commercial object-oriented database management systems
[NASA-CR-190645] p 172 N93-10452
RESEARCH TRIANGLE INST., RESEARCH TRIANGLE PARK, NC.
Research and development of two marine-degradable biopolymers
[AD-A254051] p 41 N93-10783
RETINA FOUNDATION, BOSTON, MA.
Perception of lightness and brightness in complex patterns
[AD-A254093] p 133 N93-10658
RHODE ISLAND UNIV., KINGSTON.
Mechanisms and modelling of environment-dependent fatigue crack growth in a nickel based superalloy
[AD-A253967] p 33 N93-10717
ROCHESTER UNIV., NY.
Transition metal activation and functionalization of carbon-hydrogen bonds
[DE92-014809] p 30 N93-10400
ROCKET RESEARCH CORP., REDMOND, WA.
A 26 kW arcjet system for on-orbit demonstration
p 21 N93-10031
ROCKFORD TECHNOLOGY ASSOCIATES, INC., CHAMPAIGN, IL.
Critical technology demonstration of plasma focus type MPD thrusters
[AD-A252428] p 26 N93-10638
ROCKWELL INTERNATIONAL CORP., CANOGA PARK, CA.
Operationally efficient space-based integrated propulsion module p 22 N93-10035
Space Transportation Engine Program (STEP), phase B
[NASA-CR-184062] p 25 N93-10350
ROCKWELL INTERNATIONAL CORP., THOUSAND OAKS, CA.
Computational fluid dynamics capability for internally carried store separation
[AD-A253671] p 79 N93-10297
ROME LAB., GRIFFISS AFB, NY.
Analytical characterization of bistatic scattering from Gaussian distributed surfaces
[AD-A254253] p 159 N93-10724
ROYAL AIR FORCE, LONDON (ENGLAND).
Combat aircraft noise: The operator's perspective
p 148 N93-10669
ROYAL AIRCRAFT ESTABLISHMENT, FARNBOROUGH (ENGLAND).
An evaluation of a method of reconstituting fatigue loading from Rainflow counting
[RAE-TR-89057] p 94 N93-10198
A brief review of the source noise technology applicable to fixed-wing military aircraft p 150 N93-10678
Identifying the principal noise sources of fixed-wing combat aircraft in high-speed flight p 151 N93-10686
The microstructural characterization of an Al-Li-Cu-Mg alloy (8090) metal-matrix composite
[RAE-TM-MAT/STR-1139] p 34 N93-10802
Flight test and analysis procedures for new handling criteria
[RAE-TM-FM-26] p 8 N93-10803
Further noise measurements in a slotted cryogenic wind tunnel
[RAE-TM-AERO-2201] p 153 N93-10805
ROYAL ONTARIO MUSEUM, TORONTO.
U-Pb isotopic results for single shocked and polycrystalline zircons record 550-65.5-Ma ages for a K-T target site and 2700-1850-Ma ages for the Sudbury impact event p 115 N93-10156
ROYAL SIGNALS AND RADAR ESTABLISHMENT, MALVERN (ENGLAND).
Unifying information flow policies
[RSRE-90020] p 175 N93-10801
An example secure system specified using the Terry-Wiseman approach
[RSRE-90011] p 134 N93-10804
Causing and preventing viruses in computer systems
[AD-A208591] p 139 N93-10806
The Terry-Wiseman security policy model and examples of its use
[RSRE-90001] p 134 N93-10807
On the problem of security in data bases
[RSRE-MEMO-4263] p 175 N93-10821
Network stability under viral attack: A game entitled, God and the Devil
[RSRE-MEMO-4405] p 147 N93-10822
Lattices for security policies
[RSRE-90005] p 139 N93-10823
RUTGERS - THE STATE UNIV., NEW BRUNSWICK, NJ.
Eye movements and visual information processing
[AD-A250198] p 132 N93-10278
High pressure and synchrotron radiation studies of solid state electronic instabilities
[DE92-015661] p 168 N93-10630
RUTHERFORD APPLETON LAB., CHILTON (ENGLAND).
High resolution observations of solar ejecta
p 181 N93-10916
Detectors for the SIMURIS payload
p 14 N93-10937
Investigations of the effects of contamination on UV optics p 159 N93-10949

S

SAM TECHNOLOGY, INC., SAN FRANCISCO, CA.
Mental workload assessment in the cockpit: Feasibility of using electrophysiological measurements, phase 1
[AD-A254138] p 133 N93-10662
SANDIA NATIONAL LABS., ALBUQUERQUE, NM.
Long conduction time plasma opening switch experiments at Sandia National Labs
[DE92-015003] p 72 N93-10279
Monitoring structural response in pressurized environments. Part 2: Applications
[DE92-015034] p 94 N93-10327
Boiling behavior of sodium-potassium alloy in a bench-scale solar receiver
[DE92-014947] p 103 N93-10383
Reactions of Ti and Zr with AlN and Al2O3
[DE92-016234] p 28 N93-10391
Open Skies Treaty imaging radar technology issues
[DE92-016548] p 68 N93-10394
Simple shearing flow of a 3D foam
[DE92-011151] p 36 N93-10399
Future directions in pulsed power driven ICF
[DE92-016233] p 161 N93-10443
Mass transfer in oscillating flows: Efficient drying via pulse combustors
[PB92-204403] p 81 N93-10449
Enriched element analysis of bimaterial interface cracks p 47 N93-10484
Thermal management in high average power pulsed compression systems
[DE92-017055] p 76 N93-10836
A five-channel, diamond photoconducting x ray detector array for z-pinch experiments
[DE92-017345] p 164 N93-10839
RHALE: A MMALE shock physics code for arbitrary meshes
[DE92-017051] p 139 N93-10866
SCHWARTZ ELECTRO-OPTICS, INC., ORLANDO, FL.
4.5 micron laser source
[AD-A253367] p 87 N93-10090
SCIENCE APPLICATIONS INTERNATIONAL CORP., SAN DIEGO, CA.
Soviet optical processing research. FSAC Technical Assessment Report (TAR)
[PB92-195569] p 172 N93-10431
SCIENCE APPLICATIONS INTERNATIONAL CORP., SHALIMAR, FL.
Measurement of acceleration using an instrumented railgun projectile
[AD-A253366] p 12 N93-10106
SCIENTIFIC AND TECHNICAL RESEARCH COUNCIL OF TURKEY, ANKARA.
National scene in information and documentation activities and recent developments in the Documentation Center of TUBITAK (TURDOK) p 173 N93-10594
SCOPUS TECHNOLOGY, INC., EMERYVILLE, CA.
Solving large linearized systems in mechanics
[AD-A252723] p 144 N93-10639
SCOTIA GROUP, INC., DALLAS, TX.
Reserves in western basins
[DE92-014429] p 102 N93-10625
SCRIPPS INSTITUTION OF OCEANOGRAPHY, LA JOLLA, CA.
Measurements of surface ocean carbon dioxide partial pressure during WOCE
[DE92-011856] p 128 N93-10621
SEVILLE UNIV. (SPAIN).
The third Workshop on Non-Crystalline Solids, programme and abstracts
[AD-A250739] p 36 N93-10244
SHEFFIELD UNIV. (ENGLAND).
On the use of coupled finite element boundary element models in numerical design analysis p 63 N93-10563
A boundary element super-element method for coupling with the finite element method of substructures
p 64 N93-10566
SHERBROOKE UNIV. (QUEBEC).
Singular stress distributions at circular holes in composite laminates p 51 N93-10503
Harmonic analysis of the aerodynamic forces on a Darrieus rotor p 6 N93-10551
SMITHSONIAN ASTROPHYSICAL OBSERVATORY, CAMBRIDGE, MA.
High resolutions studies of the structure of the solar atmosphere
[AD-A254292] p 190 N93-10767
SOCIETE NATIONALE D'ETUDE ET DE CONSTRUCTION DE MOTEURS D'AVIATION, VILLAROCHE (FRANCE).
Noise of combat aircraft in proximity to air bases: Review of the possibilities of noise reduction at the source
p 148 N93-10671
SOFIA UNIV. (BULGARIA).
On the nature of the small-scale plasma structures in the solar active phenomena p 183 N93-10925
SOFTWARE KINETICS LTD., STITTSVILLE (ONTARIO).
Investigation of a possible stochastic model for the IEEE P896.1 (Futurebus+) protocol, including the proposed enhanced distributed arbiter
[CTN-92-60593] p 135 N93-10088
SOUTHAMPTON UNIV. (ENGLAND).
An experimental and a theoretical investigation of rotor pitch damping using a model rotor p 8 N93-10322
SOUTHERN METHODIST UNIV., DALLAS, TX.
Thermal buckling of heated laminated composite circular cylindrical shells p 51 N93-10504

Singular perturbation methods for nonlinear dynamical systems and waves
[AD-A254116] p 144 N93-10660

SOUTHWEST RESEARCH INST., SAN ANTONIO, TX.
Simulation study of interactions of Space Shuttle-generated electron beams with ambient plasmas
[NASA-CR-190843] p 159 N93-10066

SPACE RESEARCH ORGANIZATION NETHERLANDS, UTRECHT.
Yellow hypergiant interferometry: A clue to understanding evolutionary instability
p 182 N93-10919

SPAUSCHUS ASSOCIATES, INC., ATLANTA, GA.
Chemical and thermal stability of refrigerant-lubricant mixture with metal
[DE92-015117] p 44 N93-10398

SRI INTERNATIONAL CORP., MENLO PARK, CA.
Development of electrosupercapacitors
[AD-A252208] p 71 N93-10250
Field-emitter arrays for RF vacuum microelectronics
[AD-A253396] p 73 N93-10405

STANFORD LINEAR ACCELERATOR CENTER, CA.
A measurement of the Z(sup 0) hadronic branching fraction to bottom quarks and the charged multiplicity of bottom quark events using precision vertex detectors at E(sub cm) = 91 GeV
[DE92-018236] p 154 N93-10820

STANFORD UNIV., CA.
Breccia dikes from the Beaverhead Impact structure, southwest Montana p 110 N93-10137
Epitaxial growth and dopant incorporation in diamond
[AD-A253636] p 165 N93-10206
Optimal sample policies for multirate digital control
p 141 N93-10346
Data reduction analysis for the Stanford relativity gyroscope experiment p 86 N93-10347
New directions in computational mechanics
p 44 N93-10467
Contact problem in delamination-buckling of laminated composite shells p 46 N93-10479
On Watson's ANOVA for directions
[AD-A253576] p 146 N93-10700
Scanning tunneling microscopy of semiconductor surfaces
[AD-A246853] p 168 N93-10726
Low-frequency noise reduction in SQUID measurements using laser switching
[AD-A253821] p 90 N93-10827

STATE UNIV. OF NEW YORK, BUFFALO.
A time-resolved two-laser probe of Cr(CO)6 photodissociation dynamics
[AD-A250930] p 88 N93-10247

STATE UNIV. OF NEW YORK, STONY BROOK.
A study of the effect of nitrogen and molybdenum in the corrosion inhibition of austenitic stainless steel
[AD-A253354] p 33 N93-10100
Cluster beam studies of metal combustion
[AD-A253952] p 30 N93-10416

STATE UNIV. OF NEW YORK AT BUFFALO, AMHERST.
Orientation and pair correlation at high density by superresolution holography
[AD-A254034] p 85 N93-10239

STOCKHOLM UNIV. (SWEDEN).
Large impacts in the Baltic shield with special attention to the Uppland structure p 113 N93-10149
Ordovician impacts at sea in Baltoscandia
p 116 N93-10159

STUTTGART UNIV. (GERMANY).
Basic processes of plasma propulsion
[AD-A253929] p 163 N93-10754

SURVEILLANCE RESEARCH LAB., SALISBURY (AUSTRALIA).
Software for prediction and analysis of ground wave propagation loss
[AD-A253474] p 67 N93-10199

SUSSEX UNIV., BRIGHTON (ENGLAND).
Stellar and circumstellar evolution and activity
p 181 N93-10918

SVERDRUP TECHNOLOGY, INC., BROOK PARK, OH.
Species and temperature measurement in H2/O2 rocket flow fields by means of Raman scattering diagnostics
[NASA-CR-189217] p 25 N93-10086

SYRACUSE UNIV., NY.
Analysis of a medium size BOR radome
[AD-A253954] p 69 N93-10418
Research program in elementary particle theory
[DE92-017399] p 155 N93-10840

SYSTEMS CONTROL TECHNOLOGY, INC., ARLINGTON, VA.
Rotorcraft en route ATC route standards
[AD-A249129] p 6 N93-10323

T

TECHNICAL UNIV. OF ISTANBUL (TURKEY).
Vibrations of nonlinearly pretwisted asymmetrical thick turbine blades p 9 N93-10537

TECHNISCHE HOCHSCHULE, VIENNA (AUSTRIA).
Nonstationary random variations of moderately thick plates using BEM p 48 N93-10487

TECHNISCHE HOGESCHOOL, EINDHOVEN (NETHERLANDS).
A spline finite strip method for analysing local and distortional buckling of thin-walled beams under arbitrary loading p 58 N93-10538

TECHNISCHE PHYSISCHE DIENST TNO-TH, DELFT (NETHERLANDS).
The solar ultraviolet network subtractive double monochromator p 183 N93-10931
The solar ultraviolet network: Performance and tolerance analysis p 187 N93-10950
The imaging Fourier transform spectrometer optical design p 159 N93-10951
The imaging Fourier transform spectrometer: Performance and tolerance analysis p 86 N93-10952

TECHNISCHE UNIV., BERLIN (GERMANY).
Noise emission of low flying military airplanes
p 149 N93-10675

TECHNISCHE UNIV., HAMBURG (GERMANY).
An elastic oblate axisymmetric reference gyro for attitude studies p 54 N93-10518

TENNESSEE UNIV., KNOXVILLE.
A globally well-posed accurate and efficient finite element CFD algorithm for compressible aerodynamics
p 3 N93-10306
Two-photon couplings of quarkonia with arbitrary J(sup PC)
[DE92-016525] p 153 N93-10332

TEXAS A&M UNIV., COLLEGE STATION.
Analysis of wing-body junction flowfields using the incompressible Navier-Stokes equations, volumes 1 and 2 p 3 N93-10320
Change analysis
[AD-A253567] p 146 N93-10795
Autonomous star sensing and pattern recognition for spacecraft attitude determination p 177 N93-10876
Compressible and incompressible fluid seals: Influence on rotordynamic response and stability
[NASA-CR-190746] p 92 N93-10891
Experimental study of the flow field inside a whirling annular seal p 92 N93-10892
Turbulence measurements of high shear flow fields in a turbomachine seal configuration p 93 N93-10893
An experimental technique for performing 3-D LDA measurements inside whirling annular seals
p 93 N93-10894

TEXAS TECHNOLOGICAL UNIV., LUBBOCK.
High-power microwave breakdown of dielectric interfaces
[AD-A254200] p 124 N93-10262

TEXAS UNIV., AUSTIN.
Electron transfer reactions in microporous solids
[DE92-016222] p 166 N93-10284
On the gravitational potential of two arbitrary rotating bodies with applications to the Earth-Moon system
p 179 N93-10303
Recovery techniques for real time electronic systems
[AD-A254010] p 136 N93-10361
Smart algorithms and adaptive methods in computational fluid dynamics p 44 N93-10469
Stochastic diffusion and Kolmogorov entropy in regular and random Hamiltonians
[DE92-016179] p 170 N93-10604
Fast magnetic field penetration into an intense neutralized ion beam
[DE92-016861] p 156 N93-10633
Magnetic fusion with high energy self-colliding ion beams
[DE92-016860] p 156 N93-10643

TEXAS UNIV., EL PASO.
Vibration frequencies of a constrained cantilever wedge p 57 N93-10534

THIN FILM CONCEPTS, INC., ELMSFORD, NY.
Novel Si-YBCuO reactive patterning technique for manufacture of large area high Tc superconducting electronic devices
[AD-A250740] p 73 N93-10426

THIOKOL CORP., BRIGHAM CITY, UT.
Effects of the RSRM grain deformation on ballistic performance p 20 N93-10027

THIOKOL CORP., HUNTSVILLE, AL.
Molded nozzle technology for large solid rocket motors p 19 N93-10024

THOMSON-CSF, OTTAWA (ONTARIO).
Effect of mounting offset on the dynamics of deploying flexible appendages p 54 N93-10520

TORONTO UNIV. (ONTARIO).
Intrusive origin of the Sudbury Igneous Complex: Structural and sedimentological evidence
p 108 N93-10128
Mode localization in a simple continuum model
p 56 N93-10529
Theoretical and experimental investigations concerning the structural integrity of aeroengine compressor discs
p 10 N93-10539
Fatigue crack propagation in the presence of shot-peening residual stresses p 59 N93-10542
Shock wave diffractions over semi-circular and half-diamond cylinders p 60 N93-10546
Additional results on space environmental effects on polymer matrix composites: Experiment A0180
p 38 N93-10586
Proposed test program and data base for LDEF polymer matrix composites p 38 N93-10587

TRW, INC., REDONDO BEACH, CA.
DSP propulsion system launch configuration and related testing p 24 N93-10048

TRW SPACE AND DEFENSE SECTOR, REDONDO BEACH, CA.
Electric Propulsion Space Experiment (ESEX): Spacecraft design issues for high-power electric propulsion p 21 N93-10030

TRW SPACE TECHNOLOGY LABS., REDONDO BEACH, CA.
Modeling of HF propagation and heating in the ionosphere
[AD-A253941] p 125 N93-10714
MHD Integrated Topping Cycle Project
[DE92-016610] p 164 N93-10861

TUFTS UNIV., MEDFORD, MA.
Coherent production of pions and rho mesons in neutrino charged current interactions on neon nuclei at the Fermilab Tevatron
[DE92-015674] p 154 N93-10606

TURIN UNIV. (ITALY).
EUV complementary instrumentation for SIMURIS
p 14 N93-10938

U

ULSTEIN TURBINE A/S, KONGSBERG (NORWAY).
The integration of geometric modeling into an inverse design method and application of a PC-based inverse design method and comparison with test results
p 78 N93-10058

UNITED TECHNOLOGIES CORP., SAN JOSE, CA.
Instrumented propellant block test and stress analysis comparison p 15 N93-10002

UNIVERSAL ENERGY SYSTEMS, INC., DAYTON, OH.
High-speed viscous flows past blunt bodies and compression corners with flux-split methods
[AD-A253413] p 81 N93-10410

UNIVERSITY COLL., LONDON (ENGLAND).
Numerical methods for inviscid and viscous flow analysis p 77 N93-10055
An inverse design method for radial turbomachines
p 78 N93-10057

UNIVERSITY OF NORTHERN ARIZONA, FLAGSTAFF.
Effects of early bright, late bright and dim illumination upon circadian neuroendocrine, electrophysiological and behavioral responses
[AD-A254129] p 131 N93-10661

UNIVERSITY OF SOUTH FLORIDA, TAMPA.
Comparison of the maximum stress and the stress intensity approach in the analysis of bonded joints
p 53 N93-10514
An improved technique for determining higher order eigenvector coefficients p 64 N93-10565

UNIVERSITY OF SOUTHERN CALIFORNIA, LOS ANGELES.
Control of lift and drag in unsteady flows
[AD-A253146] p 3 N93-10340

UNIVERSITY OF SOUTHERN ILLINOIS, CARBONDALE.
Oxidation protection systems for carbon-carbon composites formed by chemical vapor deposition and plasma assisted chemical vapor deposition techniques
[AD-A253450] p 28 N93-10344

UNIVERSITY OF WESTERN ONTARIO, LONDON.
On techniques for digital simulation of random response of nonlinear oscillators p 55 N93-10523
Evolutionary spectra of time-dependent discretized systems to time-frequency modulated random excitations p 55 N93-10524
Flow over a leading edge with distributed roughness
p 6 N93-10549
Structure of thermocapillary flow in narrow cavities
p 61 N93-10552
Optimal robot trajectory planning p 65 N93-10570
Automated multi-body system dynamics via bond graph modelling and interactive graphics p 66 N93-10576

Merged beam studies of laser stimulated radiative recombination
[AD-A253308] p 89 N93-10698

UTRECHT STATE UNIV. (NETHERLANDS).
Yellow hypergiant interferometry: A clue to understanding evolutionary instability
p 182 N93-10919

V

VARIAN ASSOCIATES, PALO ALTO, CA.
Extended-interaction klystron for the AN/TPS-43-E radar system
[AD-A253166] p 76 N93-10882

VERMONT UNIV., BURLINGTON.
Numerical considerations for structural system identification from modal information p 63 N93-10564
Partial solution of the generalized eigenvalue problem using the Woodbury transformation p 64 N93-10567

VERSAR, INC., SPRINGFIELD, VA.
Dermal exposure assessment: Principles and applications
[PB92-205665] p 131 N93-10438

VIRGINIA POLYTECHNIC INST. AND STATE UNIV., BLACKSBURG.
Vibration of laminated composite plates using various plate theories: Analytical and finite element results
p 45 N93-10473
Compression buckling of thick orthotropic plates with a step thickness change p 46 N93-10478
On the behavior of a higher-order plate bending element p 47 N93-10481
Dynamic stability of laminated transversely-isotropic composite plates subjected to parametric excitations
p 29 N93-10525
Pulse propagation in random media
[AD-A254294] p 152 N93-10769

VIRGINIA UNIV., CHARLOTTESVILLE.
Integrated vision system for a target seeker
[AD-A253359] p 135 N93-10103

VON KARMAN INST. FOR FLUID DYNAMICS, RHODE-SAINT-GENESE (BELGIUM).
Radial Turbines
[VKI-LS-1992-05] p 77 N93-10050

W

WASEDA UNIV., TOKYO (JAPAN).
Modelling of flexible multibody dynamics and a computer method via the bond graph method p 65 N93-10573

WASHINGTON STATE UNIV., PULLMAN.
Theory of light-induced drift of electrons in coupled quantum wells
[AD-A253609] p 164 N93-10093
The development of computational methods of adhesion and adhesive science and technology
[AD-A253758] p 92 N93-10740
Internal explosion in laser ablation of superconducting targets
[AD-A253701] p 90 N93-10799

WASHINGTON UNIV., SAINT LOUIS, MO.
What can we learn about impact mechanics from large craters on Venus? p 118 N93-10166

WASHINGTON UNIV., SEATTLE.
Air-sea interaction and remote sensing
[NASA-CR-190913] p 128 N93-10068
Damage accumulation process in advanced metal matrix composite under thermal cycling
[AD-A248674] p 27 N93-10277
Investigations of the dynamics and thermodynamics of the mesosphere lower thermosphere and upper thermosphere at the polar regions with optical ground-based remote sensing
[AD-A253228] p 125 N93-10711
Microwave radiometer studies of atmospheric water over the oceans, volume 2
[NASA-CR-190343] p 127 N93-10848
Satellite derived integrated water vapor and rain intensity patterns: Indicators of rapid cyclogenesis
p 127 N93-10849

WATERLOO UNIV. (ONTARIO).
Dynamics of systems with time-varying inertial properties p 54 N93-10517
On the vibration of axisymmetric shells
p 57 N93-10535
Chaotic oscillation of a high speed flexible arm robot
p 65 N93-10574

WEIZMANN INST. OF SCIENCE, REHOVOTH (ISRAEL).
Semiclassical quantization of chaotic billiards
[DE92-634888] p 169 N93-10226
Semiclassical quantization of interacting anyons in a strong magnetic field
[DE92-634889] p 169 N93-10229
Symmetry breaking and localization in quantum chaotic systems
[DE92-634890] p 170 N93-10294
Semiclassical quantization of integrable systems of few interacting anyons in a strong magnetic field
[DE92-634892] p 170 N93-10295

WESTINGHOUSE ELECTRIC CORP., BALTIMORE, MD.
Advanced technology component derating
[AD-A253334] p 72 N93-10357

WESTINGHOUSE ENVIRONMENTAL MANAGEMENT CO. OF OHIO, CINCINNATI.
Quality assurance practices for data entry and electronic data transfer
[DE92-014804] p 172 N93-10396

WESTINGHOUSE SAVANNAH RIVER CO., AIKEN, SC.
Advanced Scientific Computing Environment Team
[DE92-016714] p 137 N93-10631

WESTINGHOUSE SCIENCE AND TECHNOLOGY CENTER, PITTSBURGH, PA.
Improved gallium nitride and aluminum nitride electronic materials
[AD-A253785] p 76 N93-10888

WIEN UNIV. (AUSTRIA).
The Cretaceous-Tertiary (K/T) impact: One or more source craters? p 114 N93-10153
Tektite origin by hypervelocity asteroidal or cometary impact: The quest for the source craters
p 114 N93-10154
Early Archean spherule beds of possible impact origin from Barberton, South Africa: A detailed mineralogical and geochemical study p 115 N93-10155

WISCONSIN UNIV., MADISON.
Finite difference methods for incompressible viscous flow in scientific computing
[AD-A253512] p 79 N93-10220
Vortices in long Josephson junctions
[AD-A253230] p 167 N93-10404
Development of high temperature superconductors for magnetic field applications
[DE92-015930] p 168 N93-10733
Software support for programming in the large
[AD-A254050] p 138 N93-10782

WISCONSIN UNIV., MILWAUKEE.
A multi-fluid model of turbulence for Li-SF6 submerged combustion
[AD-A253973] p 31 N93-10423

WITWATERSRAND UNIV., JOHANNESBURG (SOUTH AFRICA).
A quasi-Hertzian stress field from an internal source: A possible working model for the Vredefort structure
p 106 N93-10115
The Vredefort Dome: Review of geology and deformation phenomena and status report on current knowledge and remaining problematics (five years after the cryptoexplosion workshop) p 119 N93-10173
The pseudotachylites from the Vredefort structure and the Witwatersrand basin p 119 N93-10174

WRIGHT LAB., WRIGHT-PATTERSON AFB, OH.
Eleven years of ionospheric scintillation fading data from twenty Greenlandic stations
[AD-A253271] p 69 N93-10695
Hydrodynamic investigation of vortical flows for an ATTAC configuration with canards
[AD-A253928] p 4 N93-10753

Y

YALE UNIV., NEW HAVEN, CT.
On the evaluation of Bessel functions
[AD-A253129] p 143 N93-10339

Z

ZYTRON CORP., SAINT PAUL, MN.
Optimization of resonant interband tunnel devices
[AD-A252401] p 168 N93-10637

Typical Contract Number Index Listing

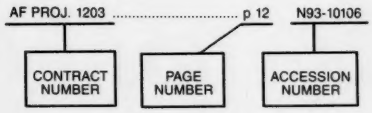

Listings in this index are arranged alphanumerically by contract number. Under each contract number the accession numbers denoting documents that have been produced as a result of research done under that contract are arranged in ascending order. The page number helps to locate the citation in the abstract section. The accession number denotes the number by which the citation is identified.

AF PROJ. 1203 ..... p 12 N93-10106
AF PROJ. 2301 ..... p 89 N93-10698
AF PROJ. 3058 ..... p 25 N93-10258
AF-AFOSR-0029-91 ..... p 132 N93-10765
AF-AFOSR-0045-88 ..... p 82 N93-10696
AF-AFOSR-0047-91 ..... p 79 N93-10232
AF-AFOSR-0049-91 ..... p 84 N93-10886
AF-AFOSR-0052-89 ..... p 167 N93-10404
AF-AFOSR-0062-89 ..... p 40 N93-10766
AF-AFOSR-0063-91 ..... p 138 N93-10736
AF-AFOSR-0090-90 ..... p 145 N93-10758
AF-AFOSR-0097-89 ..... p 35 N93-10230
AF-AFOSR-0104-89 ..... p 178 N93-10238
AF-AFOSR-0118-90 ..... p 165 N93-10210
AF-AFOSR-0118-91 ..... p 163 N93-10754
AF-AFOSR-0122-91 ..... p 72 N93-10359
AF-AFOSR-0127-90 ..... p 31 N93-10712
AF-AFOSR-0130-88 ..... p 28 N93-10344
AF-AFOSR-0134-87 ..... p 144 N93-10660
AF-AFOSR-0137-90 ..... p 152 N93-10769
AF-AFOSR-0143-91 ..... p 126 N93-10292
AF-AFOSR-0153-91 ..... p 70 N93-10747
AF-AFOSR-0171-88 ..... p 132 N93-10278
AF-AFOSR-0229-91 ..... p 35 N93-10205
AF-AFOSR-0234-91 ..... p 27 N93-10277
AF-AFOSR-0243-90 ..... p 158 N93-10445
AF-AFOSR-0244-91 ..... p 190 N93-10767
AF-AFOSR-0260-91 ..... p 124 N93-10262
AF-AFOSR-0262-89 ..... p 140 N93-10242
AF-AFOSR-0263-90 ..... p 69 N93-10728
AF-AFOSR-0271-91 ..... p 131 N93-10661
AF-AFOSR-0285-89 ..... p 33 N93-10717
AF-AFOSR-0309-89 ..... p 167 N93-10425
AF-AFOSR-0316-89 ..... p 125 N93-10711
AF-AFOSR-0327-89 ..... p 89 N93-10698
AF-AFOSR-0335-89 ..... p 131 N93-10650
AF-AFOSR-0360-87 ..... p 159 N93-10252
AF-AFOSR-0369-89 ..... p 84 N93-10895
AF-AFOSR-0377-89 ..... p 133 N93-10658
AF-AFOSR-0391-89 ..... p 142 N93-10354
AF-AFOSR-0416-89 ..... p 74 N93-10751
AF-AFOSR-0462-89 ..... p 126 N93-10363
AF-AFOSR-0804-92 ..... p 31 N93-10843
ARO-MIPR-120-89 ..... p 41 N93-10779
ARO-MIRO-120-90 ..... p 41 N93-10779
ARPA ORDER 6378 ..... p 138 N93-10782
ARPA ORDER 7597 ..... p 137 N93-10422
p 142 N93-10749
ARPA ORDER 8162 ..... p 73 N93-10405
ARPA ORDER 8363 ..... p 136 N93-10237
DA PROJ. 1L1-61102-AH-45 ..... p 9 N93-10348
DA PROJ. 1L1-62618-AH-80 ..... p 95 N93-10427
DA PROJ. 2Q2-63007-A-793 ..... p 133 N93-10261
DA PROJ. 3M2-63002-D-840 ..... p 132 N93-10709
DAAD07-91-C-0153 ..... p 140 N93-10219
DAAL01-88-C-0840 ..... p 71 N93-10250
DAAL03-88-K-0019 ..... p 145 N93-10870
DAAL03-88-K-0097 ..... p 41 N93-10825
DAAL03-88-K-0203 ..... p 35 N93-10221
DAAL03-89-C-0001 ..... p 67 N93-10092
DAAL03-89-C-0088 ..... p 95 N93-10427
DAAL03-89-G-0010 ..... p 141 N93-10095
DAAL03-89-G-0118 ..... p 176 N93-10883
DAAL03-89-K-0010 ..... p 146 N93-10699
DAAL03-89-K-0011 ..... p 42 N93-10267
DAAL03-89-K-0013 ..... p 79 N93-10094
DAAL03-89-K-0028 ..... p 87 N93-10201
DAAL03-89-K-0039 ..... p 145 N93-10758
DAAL03-89-K-0051 ..... p 164 N93-10105
DAAL03-89-K-0056 ..... p 67 N93-10223
DAAL03-89-K-0060 ..... p 87 N93-10202
DAAL03-89-K-0065 ..... p 88 N93-10251
DAAL03-89-K-0082 ..... p 158 N93-10659
DAAL03-90-C-0004 ..... p 73 N93-10417
DAAL03-90-G-0006 ..... p 87 N93-10228
DAAL03-90-G-0069 ..... p 146 N93-10795
DAAL03-90-G-0129 ..... p 4 N93-10648
DAAL03-91-G-0046 ..... p 146 N93-10107
p 96 N93-10797
p 147 N93-10798
DAAL03-91-G-0094 ..... p 79 N93-10220
DAAL03-91-G-0123 ..... p 145 N93-10758
DAAL03-91-G-0142 ..... p 73 N93-10663
DAAL03-91-G-0144 ..... p 85 N93-10239
DAAL03-91-G-0186 ..... p 83 N93-10810
DAAL03-91-G-0216 ..... p 169 N93-10871
DAAL04-89-C-0023 ..... p 16 N93-10007
DAJA45-90-C-0003 ..... p 165 N93-10235
DAMD17-91-C-1140 ..... p 43 N93-10636
DARPA ORDER 7531 ..... p 169 N93-10879
DASG60-88-C-0030 ..... p 135 N93-10103
DASG60-91-C-0025 ..... p 165 N93-10274
DE-AC02-76CH-00016 ..... p 128 N93-10283
p 104 N93-10384
p 154 N93-10402
p 129 N93-10461
p 154 N93-10730
p 74 N93-10731
DE-AC02-76CH-03073 ..... p 156 N93-10732
p 160 N93-10390
DE-AC02-83ER-40107 ..... p 163 N93-10760
DE-AC03-76SF-00098 ..... p 155 N93-10878
p 167 N93-10403
p 33 N93-10411
p 86 N93-10444
p 156 N93-10762
p 75 N93-10790
p 155 N93-10863
p 90 N93-10864
p 70 N93-10865
DE-AC03-76SF-00515 ..... p 154 N93-10820
DE-AC03-89ER-51114 ..... p 160 N93-10293
p 160 N93-10326
p 161 N93-10392
p 161 N93-10393
p 161 N93-10463
p 162 N93-10619
p 163 N93-10620
p 163 N93-10759
p 163 N93-10760
p 163 N93-10761
DE-AC03-89ER-53277 ..... p 160 N93-10390
p 163 N93-10760
DE-AC04-76DP-00789 ..... p 72 N93-10279
p 94 N93-10327
p 103 N93-10383
p 28 N93-10391
p 68 N93-10394
p 36 N93-10399
p 161 N93-10443
p 76 N93-10836
p 164 N93-10839
p 139 N93-10866
DE-AC04-76EV-01013 ..... p 131 N93-10626
DE-AC05-84ER-40150 ..... p 157 N93-10862
DE-AC05-84OR-21400 ..... p 35 N93-10082
p 143 N93-10285
p 160 N93-10293
p 153 N93-10332
p 141 N93-10334
p 91 N93-10381
p 171 N93-10382
p 89 N93-10429
p 168 N93-10623
p 39 N93-10627
p 92 N93-10634
p 175 N93-10788
p 34 N93-10789
p 139 N93-10816
DE-AC05-86OR-21600 ..... p 172 N93-10396
DE-AC06-76RL-01830 ..... p 104 N93-10729
p 130 N93-10834
DE-AC07-76ID-01570 ..... p 139 N93-10817
p 84 N93-10868
DE-AC08-88NV-10617 ..... p 176 N93-10867
DE-AC09-89SR-18035 ..... p 137 N93-10631
DE-AC21-91MC-28130 ..... p 102 N93-10625
DE-AC22-87PC-90274 ..... p 164 N93-10861
DE-AC22-88ID-12735 ..... p 164 N93-10819
DE-AC22-88PC-88948 ..... p 82 N93-10629
DE-AC22-89PC-89876 ..... p 41 N93-10216
p 43 N93-10608
DE-AC34-90DP-62349 ..... p 171 N93-10270
DE-AI01-86CE-90237 ..... p 75 N93-10786
DE-FG02-84ER-45167 ..... p 40 N93-10632
DE-FG02-85ER-40214 ..... p 154 N93-10605
DE-FG02-85ER-40231 ..... p 155 N93-10840
DE-FG02-86ER-13549 ..... p 154 N93-10435
DE-FG02-86ER-13569 ..... p 30 N93-10400
DE-FG02-86ER-13582 ..... p 31 N93-10436
DE-FG02-87ER-13687 ..... p 170 N93-10787
DE-FG02-87ER-40362 ..... p 157 N93-10838
DE-FG02-87ER-45293 ..... p 33 N93-10395
DE-FG02-88ER-25053 ..... p 138 N93-10736
DE-FG02-89CE-90029 ..... p 82 N93-10612
DE-FG02-91CE-23810 ..... p 35 N93-10084
p 43 N93-10397
p 44 N93-10398
p 30 N93-10401
DE-FG02-91ER-20021 ..... p 130 N93-10835
DE-FG02-91ER-40643 ..... p 168 N93-10733
DE-FG02-91ER-40688 ..... p 156 N93-10618
DE-FG02-91ER-54109 ..... p 160 N93-10331
DE-FG02-92ER-40702 ..... p 154 N93-10606
DE-FG03-90ER-54087 ..... p 162 N93-10617
DE-FG03-90ER-60981 ..... p 128 N93-10621
DE-FG05-80ET-53088 ..... p 170 N93-10604
p 156 N93-10633
p 156 N93-10643
DE-FG05-84ER-45081 ..... p 168 N93-10630
DE-FG05-86ER-40272 ..... p 153 N93-10291
p 170 N93-10434
p 192 N93-10616
DE-FG05-87ER-13789 ..... p 166 N93-10284
DE-FG05-88ER-13881 ..... p 89 N93-10611
DE-FG05-91ER-54134 ..... p 92 N93-10634
DE-FG22-89PC-89761 ..... p 31 N93-10460
DLA900-86-C-2045 ..... p 133 N93-10217
p 134 N93-10288
p 91 N93-10290
DNA001-91-C-0010 ..... p 69 N93-10657
DREA-W7707-8-0176 ..... p 68 N93-10366
DREA-W7707-9-0036-01-OSC ..... p 147 N93-10642
DRET-89-34-001 ..... p 83 N93-10859
DSS-W7700-88-72093 ..... p 142 N93-10641
DTFA01-87-C-00014 ..... p 6 N93-10323
DTRS57-88-C-00078 ..... p 6 N93-10065
EPA-68-CO-0050 ..... p 7 N93-10442
EPA-68-D00101 ..... p 131 N93-10438
EPA-68-01-7365 ..... p 171 N93-10257
ESA-7978 ..... p 184 N93-10932
p 178 N93-10948
ESA-9301 ..... p 184 N93-10932
FAA-F2003-C ..... p 7 N93-10459
F04611-87-C-0062 ..... p 15 N93-10002
F04611-87-C-0069 ..... p 22 N93-10037
F04611-88-C-0020 ..... p 42 N93-10268
F04611-90-C-0005 ..... p 21 N93-10030
F04701-85-C-0019 ..... p 17 N93-10015
F04701-88-C-0089 ..... p 29 N93-10263
p 42 N93-10336
p 38 N93-10584
F08630-91-C-0006 ..... p 87 N93-10090
F08635-83-C-0136 ..... p 125 N93-10784
F08635-87-C-0003 ..... p 12 N93-10106
F08635-89-C-0209 ..... p 138 N93-10746
F08635-90-C-0241 ..... p 73 N93-10421

F19628-89-C-0031 ..... p 125 N93-10714
F19628-89-C-0136 ..... p 87 N93-10211
F19628-89-C-0186 ..... p 68 N93-10358
F19628-90-C-0002 ..... p 87 N93-10218
p 74 N93-10718
F19628-90-C-0003 ..... p 135 N93-10104
p 135 N93-10214
p 67 N93-10253
p 138 N93-10298
p 136 N93-10300
p 137 N93-10447
p 137 N93-10448
p 138 N93-10665
F29601-88-K-0028 ..... p 166 N93-10345
F29601-91-C-0036 ..... p 26 N93-10638
F30602-81-C-0185 ..... p 154 N93-10362
F30602-83-C-0161 ..... p 76 N93-10882
F30602-88-D-0026 ..... p 158 N93-10693
F30602-88-D-0028 ..... p 68 N93-10301
p 68 N93-10302
p 158 N93-10360
p 74 N93-10715
p 169 N93-10764
F30602-89-C-0095 ..... p 72 N93-10357
F30602-89-C-0152 ..... p 172 N93-10428
F33615-87-C-2714 ..... p 29 N93-10101
F33615-87-C-5339 ..... p 36 N93-10343
F33615-88-C-2908 ..... p 81 N93-10410
F33615-89-C-0532 ..... p 158 N93-10708
F33615-90-C-1465 ..... p 137 N93-10422
p 142 N93-10749
p 175 N93-10826
F33616-87-C-5212 ..... p 28 N93-10325
F49620-86-C-0066 ..... p 8 N93-10842
F49620-88-C-0009 ..... p 158 N93-10446
F49620-88-C-0100 ..... p 89 N93-10897
F49620-89-C-0036 ..... p 125 N93-10204
F49620-89-C-0262 ..... p 140 N93-10242
F49620-90-C-0038 ..... p 3 N93-10340
F49620-90-C-0077 ..... p 133 N93-10662
F49620-91-C-0003 ..... p 8 N93-10420
F49620-91-C-0032 ..... p 76 N93-10888
F49620-91-C-0043 ..... p 168 N93-10637
F49620-91-C-0089 ..... p 73 N93-10426
F50/1991 ..... p 183 N93-10925
GRI-5084-238-1302 ..... p 37 N93-10439
GRI-5087-260-1467 ..... p 31 N93-10437
GRI-5088-260-1686 ..... p 81 N93-10449
GRI-5089-260-1874 ..... p 169 N93-10249
MDA903-86-C-0384 ..... p 137 N93-10409
MDA903-87-C-0523 ..... p 133 N93-10261
MDA903-89-C-0003 ..... p 133 N93-10719
MDA903-90-C-0004 ..... p 75 N93-10792
MDA972-91-C-0029 ..... p 73 N93-10405
MDA972-92-C-0022 ..... p 136 N93-10237
MIPR-91MM1533 ..... p 132 N93-10796
MIPR-91M1502 ..... p 132 N93-10709
N-30315 ..... p 180 N93-10910
NAGW-1322 ..... p 128 N93-10068
NAGW-1688 ..... p 127 N93-10848
NAGW-1936 ..... p 159 N93-10006
NAGW-2239 ..... p 13 N93-10737
NAG1-1047 ..... p 151 N93-10684
NAG1-1145 ..... p 145 N93-10758
NAG1-1214 ..... p 32 N93-10852
NAG1-648 ..... p 2 N93-10098
NAG2-554 ..... p 147 N93-10458
NAG3-1215 ..... p 2 N93-10089
NAG3-181 ..... p 92 N93-10892
p 93 N93-10893
NAG3-379 ..... p 96 N93-10777
NAG3-895 ..... p 94 N93-10372
NAG5-943 ..... p 127 N93-10851
NASA ORDER C-99066-G ..... p 81 N93-10454
p 82 N93-10735
NASA ORDER T-5715-P ..... p 107 N93-10120
NASA ORDER W-15814 ..... p 189 N93-10832
NASW-3749 ..... p 13 N93-10737
NASW-4003 ..... p 1 N93-10647
NASW-4574 ..... p 189 N93-10064
p 105 N93-10112
NAS1-18605 ..... p 2 N93-10097
p 82 N93-10757
p 145 N93-10758
p 83 N93-10808
NAS1-19480 ..... p 2 N93-10097
p 145 N93-10758
p 83 N93-10808
NAS10-11624 ..... p 129 N93-10085
NAS3-24346 ..... p 9 N93-10348
NAS3-25266 ..... p 25 N93-10086
NAS8-30490 ..... p 20 N93-10027
NAS8-36473 ..... p 127 N93-10849
NAS8-36955 ..... p 26 N93-10756
NAS8-37456 ..... p 18 N93-10018
NAS8-37505 ..... p 11 N93-10021
NAS8-38160 ..... p 25 N93-10350
NAS8-38237 ..... p 19 N93-10023
NAS9-17900 ..... p 14 N93-10960
NCC2-387 ..... p 138 N93-10736
NCC9-16 ..... p 172 N93-10451
p 172 N93-10452
NR PROJ. RM3-3-F-60 ..... p 144 N93-10639
NR PROJ. 3M1-61102-BS-87 ..... p 132 N93-10796
NSF ASC-88-58101 ..... p 138 N93-10736
NSF DMS-89-19074 ..... p 138 N93-10736
NSF DMS-90-12751 ..... p 143 N93-10339
NSF DMS-91-00383 ..... p 145 N93-10758
N00014-82-C-0280 ..... p 30 N93-10266
p 30 N93-10281
p 27 N93-10465
p 40 N93-10748
N00014-82-K-0612 ..... p 36 N93-10243
p 158 N93-10694
N00014-85-K-0437 ..... p 33 N93-10100
N00014-85-K-0678 ..... p 30 N93-10416
N00014-85-K-0733 ..... p 28 N93-10896
N00014-86-C-0595 ..... p 74 N93-10755
N00014-86-K-0520 ..... p 68 N93-10380
N00014-86-K-0686 ..... p 166 N93-10356
N00014-87-K-0262 ..... p 165 N93-10206
N00014-88-K-0483 ..... p 88 N93-10247
N00014-88-K-0590 ..... p 138 N93-10782
N00014-89-C-2228 ..... p 166 N93-10335
N00014-89-J-1023 ..... p 76 N93-10829
N00014-89-J-1178 ..... p 88 N93-10412
p 161 N93-10413
p 30 N93-10414
p 167 N93-10415
p 168 N93-10614
p 162 N93-10615
p 73 N93-10656
N00014-89-J-1267 ..... p 31 N93-10423
N00014-89-J-1274 ..... p 31 N93-10794
N00014-89-J-1319 ..... p 83 N93-10793
N00014-89-J-1542 ..... p 40 N93-10727
N00014-89-J-1660 ..... p 128 N93-10791
N00014-89-J-1689 ..... p 71 N93-10273
p 71 N93-10276
p 72 N93-10280
p 72 N93-10282
N00014-89-J-1779 ..... p 153 N93-10338
N00014-89-K-0089 ..... p 136 N93-10361
N00014-90-C-0006 ..... p 169 N93-10879
N00014-90-F-0002 ..... p 155 N93-10885
N00014-90-F-0011 ..... p 35 N93-10231
p 40 N93-10778
N00014-90-J-1001 ..... p 168 N93-10726
N00014-90-J-1030 ..... p 144 N93-10407
N00014-90-J-1178 ..... p 34 N93-10880
N00014-90-J-1193 ..... p 164 N93-10093
p 90 N93-10799
N00014-90-J-1224 ..... p 69 N93-10418
N00014-90-J-1298 ..... p 92 N93-10740
N00014-90-J-1427 ..... p 166 N93-10355
N00014-90-J-1516 ..... p 66 N93-10649
N00014-90-J-1528 ..... p 90 N93-10827
N00014-90-J-1864 ..... p 131 N93-10271
N00014-90-J-4039 ..... p 71 N93-10240
N00014-91-C-0001 ..... p 15 N93-10001
N00014-91-C-0246 ..... p 102 N93-10234
N00014-91-J-1011 ..... p 141 N93-10299
N00014-91-J-1196 ..... p 34 N93-10752
N00014-91-J-1198 ..... p 89 N93-10720
N00014-91-J-1250 ..... p 129 N93-10887
N00014-91-J-1329 ..... p 143 N93-10200
N00014-91-J-1434 ..... p 36 N93-10246
N00014-91-J-1613 ..... p 135 N93-10212
p 140 N93-10213
N00014-91-J-1630 ..... p 165 N93-10245
N00014-91-J-1941 ..... p 88 N93-10286
N00014-91-J-1985 ..... p 140 N93-10227
N00014-91-J-4022 ..... p 86 N93-10408
N00014-91-J-4024 ..... p 27 N93-10254
N00014-92-C-0053 ..... p 70 N93-10233
N00014-92-J-1254 ..... p 146 N93-10700
N00039-91-C-6099 ..... p 75 N93-10785
N60530-90-C-0393 ..... p 79 N93-10297
PROJ. 6547 ..... p 146 N93-10795
RF PROJ. 4502 ..... p 92 N93-10891
RICIS PROJ. RB-08 ..... p 172 N93-10451
RICIS PROJ. SE-43 ..... p 172 N93-10452
RTOP 474-42-10 ..... p 26 N93-10734
RTOP 505-59-30-01 ..... p 4 N93-10824
RTOP 505-59-40-03 ..... p 2 N93-10071
RTOP 505-61-51 ..... p 11 N93-10741
RTOP 505-62-20 ..... p 79 N93-10087
RTOP 505-62-21 ..... p 81 N93-10454
RTOP 505-62-52 ..... p 82 N93-10735
RTOP 505-63-21-01 ..... p 3 N93-10349
RTOP 505-64-20-01 ..... p 10 N93-10070
RTOP 505-64-36 ..... p 7 N93-10745
RTOP 505-90-52--01 ..... p 82 N93-10757
RTOP 505-90-52-01 ..... p 2 N93-10097
p 145 N93-10758
p 83 N93-10808
RTOP 506-42-31 ..... p 25 N93-10086
p 25 N93-10197
RTOP 506-43-31 ..... p 28 N93-10742
RTOP 506-43-41-02 ..... p 13 N93-10744
RTOP 506-48-91-08 ..... p 37 N93-10578
RTOP 510-01-50 ..... p 95 N93-10453
p 95 N93-10455
p 96 N93-10777
RTOP 538-01-10 ..... p 9 N93-10456
RTOP 589-01-1B ..... p 13 N93-10841
RTOP 593-12-21 ..... p 26 N93-10743
RTOP 593-71-00 ..... p 25 N93-10457
SDIO84-90-C-0030 ..... p 17 N93-10014
SRI PROJ. 2743 ..... p 73 N93-10405
SWRI PROJ. 15-3399 ..... p 159 N93-10066
W-31-109-ENG-38 ..... p 163 N93-10645
p 76 N93-10831
p 157 N93-10837
W-7405-ENG-36 ..... p 155 N93-10333
p 156 N93-10462
p 129 N93-10628
p 138 N93-10736
W-7405-ENG-48 ..... p 87 N93-10083
p 161 N93-10393
p 92 N93-10635
p 95 N93-10646
p 90 N93-10739
p 103 N93-10763
p 159 N93-10818
W-7405-ENG-82 ..... p 167 N93-10609

REPORT NUMBER INDEX

Typical Report Number Index Listing

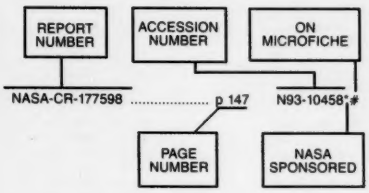

Listings in this index are arranged alphanumerically by report number. The accession number denotes the number by which the citation is identified. The page number helps to locate the citation in the abstract section. An asterisk (*) indicates that the item is a NASA report. A pound sign (#) indicates that the item is available on microfiche.

A-91097 ..... p 28 N93-10742 * #
A-91175 ..... p 11 N93-10741 * #
A-91241 ..... p 7 N93-10745 * #
A-92143 ..... p 147 N93-10458 * #

AD-A208591 ..... p 139 N93-10806 #
AD-A245568 ..... p 165 N93-10274 #
AD-A246853 ..... p 168 N93-10726 #
AD-A248047 ..... p 12 N93-10236 #
AD-A248415 ..... p 143 N93-10275 #
AD-A248445 ..... p 42 N93-10267 #
AD-A248674 ..... p 27 N93-10277 #
AD-A248699 ..... p 40 N93-10727 #
AD-A249123 ..... p 132 N93-10321 #
AD-A249129 ..... p 6 N93-10323 #
AD-A249130 ..... p 28 N93-10325 #
AD-A249746 ..... p 36 N93-10243 #
AD-A250197 ..... p 69 N93-10728 #
AD-A250198 ..... p 132 N93-10278 #
AD-A250290 ..... p 140 N93-10242 #
AD-A250637 ..... p 36 N93-10246 #
AD-A250739 ..... p 36 N93-10244 #
AD-A250740 ..... p 73 N93-10426 #
AD-A250889 ..... p 71 N93-10273 #
AD-A250890 ..... p 71 N93-10276 #
AD-A250891 ..... p 72 N93-10280 #
AD-A250892 ..... p 72 N93-10282 #
AD-A250930 ..... p 88 N93-10247 #
AD-A251171 ..... p 165 N93-10245 #
AD-A252116 ..... p 158 N93-10708 #
AD-A252208 ..... p 71 N93-10250 #
AD-A252259 ..... p 169 N93-10879 #
AD-A252339 ..... p 43 N93-10636 #
AD-A252376 ..... p 132 N93-10796 #
AD-A252401 ..... p 168 N93-10637 #
AD-A252427 ..... p 132 N93-10709 #
AD-A252428 ..... p 26 N93-10638 #
AD-A252429 ..... p 95 N93-10427 #
AD-A252495 ..... p 6 N93-10065 #
AD-A252499 ..... p 34 N93-10880 #
AD-A252636 ..... p 172 N93-10428 #
AD-A252704 ..... p 139 N93-10881 #
AD-A252723 ..... p 144 N93-10639 #
AD-A252766 ..... p 68 N93-10260 #
AD-A252800 ..... p 29 N93-10263 #
AD-A252802 ..... p 30 N93-10281 #
AD-A252803 ..... p 27 N93-10465 #
AD-A252804 ..... p 30 N93-10266 #
AD-A252812 ..... p 166 N93-10335 #
AD-A252813 ..... p 42 N93-10336 #
AD-A252889 ..... p 42 N93-10268 #
AD-A253108 ..... p 148 N93-10666 #
AD-A253126 ..... p 153 N93-10338 #
AD-A253129 ..... p 143 N93-10339 #
AD-A253134 ..... p 73 N93-10656 #
AD-A253135 ..... p 131 N93-10613 #
AD-A253137 ..... p 168 N93-10614 #
AD-A253138 ..... p 162 N93-10615 #
AD-A253139 ..... p 88 N93-10412 #
AD-A253140 ..... p 161 N93-10413 #
AD-A253142 ..... p 30 N93-10414 #
AD-A253143 ..... p 167 N93-10415 #
AD-A253146 ..... p 3 N93-10340 #
AD-A253166 ..... p 76 N93-10882 #
AD-A253182 ..... p 128 N93-10791 #
AD-A253186 ..... p 158 N93-10445 #
AD-A253188 ..... p 158 N93-10446 #
AD-A253199 ..... p 75 N93-10792 #
AD-A253202 ..... p 83 N93-10793 #
AD-A253203 ..... p 31 N93-10794 #
AD-A253209 ..... p 66 N93-10710 #
AD-A253210 ..... p 4 N93-10375 #
AD-A253228 ..... p 125 N93-10711 #
AD-A253229 ..... p 31 N93-10712 #
AD-A253230 ..... p 167 N93-10404 #
AD-A253247 ..... p 158 N93-10693 #
AD-A253267 ..... p 158 N93-10694 #
AD-A253271 ..... p 69 N93-10695 #
AD-A253298 ..... p 82 N93-10696 #
AD-A253307 ..... p 89 N93-10697 #
AD-A253308 ..... p 89 N93-10698 #
AD-A253313 ..... p 175 N93-10723 #
AD-A253314 ..... p 88 N93-10286 #
AD-A253323 ..... p 136 N93-10298 #
AD-A253325 ..... p 136 N93-10300 #
AD-A253326 ..... p 137 N93-10447 #
AD-A253327 ..... p 137 N93-10448 #
AD-A253329 ..... p 142 N93-10354 #
AD-A253330 ..... p 166 N93-10355 #
AD-A253331 ..... p 166 N93-10356 #
AD-A253334 ..... p 72 N93-10357 #
AD-A253337 ..... p 68 N93-10358 #
AD-A253340 ..... p 141 N93-10269 #
AD-A253345 ..... p 131 N93-10271 #
AD-A253347 ..... p 27 N93-10272 #
AD-A253348 ..... p 87 N93-10211 #
AD-A253349 ..... p 135 N93-10212 #
AD-A253350 ..... p 140 N93-10213 #
AD-A253351 ..... p 135 N93-10214 #
AD-A253352 ..... p 70 N93-10215 #
AD-A253353 ..... p 164 N93-10099 #
AD-A253354 ..... p 33 N93-10100 #
AD-A253355 ..... p 29 N93-10101 #
AD-A253358 ..... p 155 N93-10102 #
AD-A253359 ..... p 135 N93-10103 #
AD-A253362 ..... p 135 N93-10104 #
AD-A253365 ..... p 164 N93-10105 #
AD-A253366 ..... p 12 N93-10106 #
AD-A253367 ..... p 87 N93-10090 #
AD-A253393 ..... p 133 N93-10217 #
AD-A253394 ..... p 134 N93-10288 #
AD-A253395 ..... p 91 N93-10290 #
AD-A253396 ..... p 73 N93-10405 #
AD-A253399 ..... p 189 N93-10406 #
AD-A253401 ..... p 144 N93-10407 #
AD-A253403 ..... p 86 N93-10408 #
AD-A253412 ..... p 137 N93-10409 #
AD-A253413 ..... p 81 N93-10410 #
AD-A253415 ..... p 87 N93-10218 #
AD-A253447 ..... p 3 N93-10342 #
AD-A253450 ..... p 28 N93-10344 #
AD-A253474 ..... p 67 N93-10199 #
AD-A253502 ..... p 143 N93-10200 #
AD-A253510 ..... p 87 N93-10201 #
AD-A253511 ..... p 140 N93-10219 #
AD-A253512 ..... p 79 N93-10220 #
AD-A253513 ..... p 35 N93-10221 #
AD-A253520 ..... p 147 N93-10869 #
AD-A253525 ..... p 67 N93-10223 #
AD-A253530 ..... p 29 N93-10224 #
AD-A253546 ..... p 68 N93-10380 #
AD-A253567 ..... p 146 N93-10795 #
AD-A253570 ..... p 176 N93-10883 #
AD-A253574 ..... p 146 N93-10699 #
AD-A253576 ..... p 146 N93-10700 #
AD-A253580 ..... p 70 N93-10091 #
AD-A253592 ..... p 4 N93-10648 #
AD-A253593 ..... p 67 N93-10092 #
AD-A253605 ..... p 66 N93-10649 #
AD-A253609 ..... p 164 N93-10093 #
AD-A253612 ..... p 131 N93-10650 #
AD-A253617 ..... p 79 N93-10094 #
AD-A253618 ..... p 40 N93-10778 #
AD-A253619 ..... p 88 N93-10251 #
AD-A253620 ..... p 141 N93-10095 #
AD-A253621 ..... p 96 N93-10797 #
AD-A253622 ..... p 147 N93-10798 #
AD-A253623 ..... p 146 N93-10107 #
AD-A253624 ..... p 87 N93-10202 #
AD-A253625 ..... p 67 N93-10203 #
AD-A253630 ..... p 125 N93-10204 #
AD-A253631 ..... p 35 N93-10205 #
AD-A253636 ..... p 165 N93-10206 #
AD-A253637 ..... p 165 N93-10210 #
AD-A253638 ..... p 140 N93-10227 #
AD-A253639 ..... p 29 N93-10207 #
AD-A253640 ..... p 146 N93-10208 #
AD-A253641 ..... p 140 N93-10209 #
AD-A253660 ..... p 41 N93-10779 #
AD-A253666 ..... p 87 N93-10228 #
AD-A253667 ..... p 35 N93-10230 #
AD-A253669 ..... p 145 N93-10870 #
AD-A253670 ..... p 126 N93-10292 #
AD-A253671 ..... p 79 N93-10297 #
AD-A253680 ..... p 141 N93-10299 #
AD-A253681 ..... p 68 N93-10301 #
AD-A253682 ..... p 68 N93-10302 #
AD-A253683 ..... p 36 N93-10343 #
AD-A253684 ..... p 166 N93-10345 #
AD-A253701 ..... p 90 N93-10799 #
AD-A253723 ..... p 138 N93-10746 #
AD-A253727 ..... p 70 N93-10747 #
AD-A253728 ..... p 84 N93-10895 #
AD-A253729 ..... p 35 N93-10231 #
AD-A253730 ..... p 155 N93-10885 #
AD-A253731 ..... p 84 N93-10886 #
AD-A253739 ..... p 40 N93-10748 #
AD-A253740 ..... p 142 N93-10749 #
AD-A253756 ..... p 95 N93-10750 #
AD-A253757 ..... p 129 N93-10887 #
AD-A253758 ..... p 92 N93-10740 #
AD-A253759 ..... p 79 N93-10232 #
AD-A253760 ..... p 70 N93-10233 #
AD-A253779 ..... p 102 N93-10234 #
AD-A253781 ..... p 165 N93-10235 #
AD-A253783 ..... p 136 N93-10237 #
AD-A253785 ..... p 76 N93-10888 #
AD-A253788 ..... p 178 N93-10238 #
AD-A253789 ..... p 169 N93-10871 #
AD-A253818 ..... p 41 N93-10825 #
AD-A253820 ..... p 175 N93-10826 #
AD-A253821 ..... p 90 N93-10827 #
AD-A253822 ..... p 142 N93-10828 #
AD-A253842 ..... p 76 N93-10829 #
AD-A253854 ..... p 83 N93-10810 #
AD-A253880 ..... p 4 N93-10811 #
AD-A253900 ..... p 159 N93-10252 #
AD-A253922 ..... p 74 N93-10751 #
AD-A253923 ..... p 34 N93-10752 #
AD-A253924 ..... p 169 N93-10764 #
AD-A253928 ..... p 4 N93-10753 #
AD-A253929 ..... p 163 N93-10754 #
AD-A253930 ..... p 74 N93-10755 #
AD-A253931 ..... p 134 N93-10713 #
AD-A253941 ..... p 125 N93-10714 #
AD-A253942 ..... p 74 N93-10715 #
AD-A253947 ..... p 138 N93-10716 #
AD-A253952 ..... p 30 N93-10416 #
AD-A253953 ..... p 73 N93-10417 #
AD-A253954 ..... p 69 N93-10418 #
AD-A253960 ..... p 144 N93-10419 #
AD-A253963 ..... p 8 N93-10420 #
AD-A253967 ..... p 33 N93-10717 #
AD-A253968 ..... p 73 N93-10421 #
AD-A253970 ..... p 137 N93-10422 #
AD-A253973 ..... p 31 N93-10423 #
AD-A253975 ..... p 74 N93-10718 #
AD-A253988 ..... p 133 N93-10719 #
AD-A253994 ..... p 72 N93-10359 #
AD-A254000 ..... p 89 N93-10720 #
AD-A254009 ..... p 158 N93-10360 #

AD-A254010 ..... p 136 N93-10361 #
AD-A254021 ..... p 154 N93-10362 #
AD-A254034 ..... p 85 N93-10239 #
AD-A254035 ..... p 71 N93-10240 #
AD-A254040 ..... p 71 N93-10241 #
AD-A254042 ..... p 126 N93-10363 #
AD-A254044 ..... p 127 N93-10780 #
AD-A254046 ..... p 103 N93-10781 #
AD-A254050 ..... p 138 N93-10782 #
AD-A254051 ..... p 41 N93-10783 #
AD-A254065 ..... p 125 N93-10784 #
AD-A254067 ..... p 75 N93-10785 #
AD-A254068 ..... p 69 N93-10657 #
AD-A254093 ..... p 133 N93-10658 #
AD-A254094 ..... p 158 N93-10659 #
AD-A254099 ..... p 69 N93-10701 #
AD-A254103 ..... p 159 N93-10812 #
AD-A254104 ..... p 27 N93-10813 #
AD-A254105 ..... p 12 N93-10814 #
AD-A254106 ..... p 90 N93-10855 #
AD-A254108 ..... p 5 N93-10856 #
AD-A254109 ..... p 145 N93-10857 #
AD-A254111 ..... p 5 N93-10858 #
AD-A254116 ..... p 144 N93-10660 #
AD-A254129 ..... p 131 N93-10661 #
AD-A254138 ..... p 133 N93-10662 #
AD-A254162 ..... p 73 N93-10663 #
AD-A254170 ..... p 127 N93-10664 #
AD-A254175 ..... p 138 N93-10665 #
AD-A254176 ..... p 67 N93-10253 #
AD-A254178 ..... p 27 N93-10254 #
AD-A254179 ..... p 71 N93-10255 #
AD-A254188 ..... p 25 N93-10258 #
AD-A254189 ..... p 157 N93-10259 #
AD-A254198 ..... p 133 N93-10261 #
AD-A254200 ..... p 124 N93-10262 #
AD-A254216 ..... p 126 N93-10264 #
AD-A254217 ..... p 28 N93-10896 #
AD-A254230 ..... p 77 N93-10897 #
AD-A254232 ..... p 26 N93-10721 #
AD-A254240 ..... p 89 N93-10722 #
AD-A254246 ..... p 74 N93-10702 #
AD-A254247 ..... p 89 N93-10703 #
AD-A254248 ..... p 10 N93-10704 #
AD-A254249 ..... p 13 N93-10705 #
AD-A254250 ..... p 8 N93-10698 #
AD-A254252 ..... p 33 N93-10706 #
AD-A254253 ..... p 159 N93-10724 #
AD-A254257 ..... p 6 N93-10265 #
AD-A254260 ..... p 176 N93-10899 #
AD-A254262 ..... p 7 N93-10424 #
AD-A254264 ..... p 89 N93-10725 #
AD-A254278 ..... p 167 N93-10425 #
AD-A254280 ..... p 132 N93-10765 #
AD-A254282 ..... p 40 N93-10766 #
AD-A254285 ..... p 8 N93-10842 #
AD-A254292 ..... p 190 N93-10767 #
AD-A254293 ..... p 90 N93-10768 #
AD-A254294 ..... p 152 N93-10769 #
AD-A254295 ..... p 31 N93-10843 #
AD-A254307 ..... p 4 N93-10707 #
AD-A254312 ..... p 40 N93-10770 #

AD-D015291 ..... p 67 N93-10096 #
AD-D015354 ..... p 142 N93-10958
AD-D015356 ..... p 143 N93-10959 #

AD-E201061 ..... p 42 N93-10268 #
AD-E201073 ..... p 166 N93-10345 #
AD-E201089 ..... p 26 N93-10638 #
AD-E201166 ..... p 25 N93-10258 #
AD-E501546 ..... p 133 N93-10719 #
AD-E951861 ..... p 157 N93-10259 #

AEDC-TR-92-2 ..... p 29 N93-10224 #

AFIT/CI/CIA-92-054 ..... p 127 N93-10664 #
AFIT/CI/CIA-92-067 ..... p 40 N93-10770 #
AFIT/CI/CIA-92-072 ..... p 89 N93-10725 #

AFIT/EN-TR-92-2 ..... p 175 N93-10723 #

AFOSR-92-0256TR ..... p 27 N93-10277 #
AFOSR-92-0268TR ..... p 132 N93-10278 #
AFOSR-92-0275TR ..... p 69 N93-10728 #
AFOSR-92-0295TR ..... p 73 N93-10426 #
AFOSR-92-0301TR ..... p 140 N93-10242 #
AFOSR-92-0526TR ..... p 168 N93-10637 #
AFOSR-92-0649TR ..... p 125 N93-10711 #
AFOSR-92-0657TR ..... p 165 N93-10210 #
AFOSR-92-0670TR-VOL-21 ..... p 35 N93-10205 #
AFOSR-92-0675TR ..... p 3 N93-10340 #
AFOSR-92-0677TR ..... p 158 N93-10445 #
AFOSR-92-0678TR ..... p 142 N93-10354 #
AFOSR-92-0684TR ..... p 89 N93-10698 #
AFOSR-92-0688TR ..... p 158 N93-10446 #

AFOSR-92-0693TR ..... p 89 N93-10697 #
AFOSR-92-0695TR ..... p 31 N93-10712 #
AFOSR-92-0696TR ..... p 167 N93-10404 #
AFOSR-92-0700TR ..... p 82 N93-10696 #
AFOSR-92-0714TR ..... p 131 N93-10650 #
AFOSR-92-0720TR ..... p 76 N93-10888 #
AFOSR-92-0721TR ..... p 35 N93-10230 #
AFOSR-92-0724TR ..... p 84 N93-10886 #
AFOSR-92-0726TR ..... p 126 N93-10292 #
AFOSR-92-0730TR ..... p 125 N93-10204 #
AFOSR-92-0741TR ..... p 84 N93-10895 #
AFOSR-92-0742TR ..... p 70 N93-10747 #
AFOSR-92-0746TR ..... p 74 N93-10751 #
AFOSR-92-0758TR ..... p 79 N93-10232 #
AFOSR-92-0759TR ..... p 178 N93-10238 #
AFOSR-92-0765TR ..... p 40 N93-10766 #
AFOSR-92-0766TR ..... p 132 N93-10765 #
AFOSR-92-0767TR ..... p 144 N93-10660 #
AFOSR-92-0778TR ..... p 133 N93-10658 #
AFOSR-92-0779TR ..... p 124 N93-10262 #
AFOSR-92-0782TR ..... p 167 N93-10425 #
AFOSR-92-0785TR ..... p 159 N93-10252 #
AFOSR-92-0787TR ..... p 33 N93-10717 #
AFOSR-92-0791TR ..... p 190 N93-10767 #
AFOSR-92-0793TR ..... p 131 N93-10661 #
AFOSR-92-0796TR ..... p 126 N93-10363 #
AFOSR-92-0801TR ..... p 152 N93-10769 #
AFOSR-92-0804TR ..... p 31 N93-10843 #
AFOSR-92-0807TR ..... p 8 N93-10842 #
AFOSR-92-0809TR ..... p 133 N93-10662 #
AFOSR-97-0747TR ..... p 72 N93-10359 #

AGARD-CP-512 ..... p 148 N93-10666 #

AGARD-INDEX-89-91 ..... p 174 N93-10610 #

AGARD-R-788 ..... p 172 N93-10593 #

AIAA PAPER 92-3353 ..... p 25 N93-10086 * #

AL-TR-1992-0001 ..... p 158 N93-10708 #

AMSMI/TR-RD-WS-92-10 ..... p 157 N93-10259 #

ANL/CP-75447 ..... p 163 N93-10645 #
ANL/CP-75500 ..... p 76 N93-10831 #
ANL/CP-76521 ..... p 157 N93-10837 #

ARAED-TR-92011 ..... p 4 N93-10811 #

ARCCB-MR-92022 ..... p 29 N93-10207 #

ARCCB-TR-92023 ..... p 95 N93-10750 #
ARCCB-TR-92025 ..... p 144 N93-10419 #

ARI-RN-92-49 ..... p 137 N93-10409 #

ARL-STRUC-TM-555 ..... p 3 N93-10342 #

ARO-RN-92-61 ..... p 133 N93-10261 #

ARO-25187.1-MA-R ..... p 145 N93-10870 #
ARO-25193.9-MS ..... p 41 N93-10825 #
ARO-25836.17-MA ..... p 146 N93-10699 #
ARO-25872.11-PH-SAH ..... p 88 N93-10251 #
ARO-26113.19-MS ..... p 79 N93-10094 #
ARO-26126.3-MS ..... p 41 N93-10779 #
ARO-26169.11-MS-A ..... p 35 N93-10221 #
ARO-26191-CH ..... p 164 N93-10105 #
ARO-26211.1-PH ..... p 87 N93-10202 #
ARO-26213.137-EL ..... p 67 N93-10092 #
ARO-26223.2-PH ..... p 87 N93-10201 #
ARO-26224.8-GS ..... p 67 N93-10223 #
ARO-26566.5-PH ..... p 158 N93-10659 #
ARO-26730.1-MA-UIF ..... p 141 N93-10095 #
ARO-27247.4-MA-SAH ..... p 176 N93-10883 #
ARO-27574.9-MA ..... p 146 N93-10795 #
ARO-27587.10-PH-F ..... p 87 N93-10228 #
ARO-27993.2-MA ..... p 147 N93-10798 #
ARO-27993.3-MA ..... p 146 N93-10107 #
ARO-27993.4-MA ..... p 96 N93-10797 #
ARO-28025.4-MA ..... p 79 N93-10220 #
ARO-28359.1-GS ..... p 85 N93-10239 #
ARO-28464.3-PH ..... p 169 N93-10871 #
ARO-28953.1-EL-CF ..... p 73 N93-10663 #
ARO-28980.4-MA ..... p 83 N93-10810 #

ASD-TR-5004-VOL-3 ..... p 134 N93-10713 #

ASE/EM-92-105 ..... p 4 N93-10648 #

ASI690-354-92-I ..... p 133 N93-10261 #

ASU-CR-R-92020 ..... p 169 N93-10249 #

AVSCOM-TR-87-C-30 ..... p 9 N93-10348 * #

AWS/TR-91/001 ..... p 126 N93-10264 #

B-247878 ..... p 12 N93-10081 #

BN-1126 ..... p 144 N93-10407 #

BNL-47274 ..... p 104 N93-10384 #
BNL-47525 ..... p 74 N93-10731 #
BNL-47565 ..... p 156 N93-10732 #
BNL-47574 ..... p 129 N93-10461 #
BNL-47612 ..... p 154 N93-10402 #
BNL-47617 ..... p 154 N93-10730 #
BNL-47654 ..... p 128 N93-10283 #

BRL-TR-3360 ..... p 95 N93-10427 #

BR109824 ..... p 139 N93-10806 #
BR109899 ..... p 175 N93-10821 #
BR111319 ..... p 8 N93-10803 #
BR112718 ..... p 34 N93-10802 #
BR113381 ..... p 94 N93-10198 #
BR114203 ..... p 134 N93-10807 #
BR114204 ..... p 139 N93-10823 #
BR115188 ..... p 147 N93-10822 #
BR115326 ..... p 134 N93-10804 #
BR115416 ..... p 175 N93-10801 #
BR116372 ..... p 153 N93-10805 #

CA-PATENT-APPL-SN-1293201 .. p 91 N93-10367
CA-PATENT-APPL-SN-2001346 .. p 72 N93-10368
CA-PATENT-APPL-SN-2013236 .. p 10 N93-10374

CAM-9007 ..... p 37 N93-10439 #

CEBAF-PR-92-007 ..... p 157 N93-10862 #

CERL-SR-M-92/14 ..... p 189 N93-10406 #

CMOTT-92-09 ..... p 81 N93-10454 * #

CMU-CS-91-162 ..... p 142 N93-10828 #
CMU-CS-92-134 ..... p 175 N93-10826 #
CMU-CS-92-139 ..... p 142 N93-10749 #
CMU-CS-92-150 ..... p 137 N93-10422 #
CMU-CS-92-160 ..... p 142 N93-10828 #

CMU/SEI-91-TR-14 ..... p 135 N93-10104 #
CMU/SEI-92-TR-10 ..... p 67 N93-10253 #
CMU/SEI-92-TR-1 ..... p 136 N93-10300 #
CMU/SEI-92-TR-3 ..... p 135 N93-10214 #
CMU/SEI-92-TR-5 ..... p 136 N93-10298 #
CMU/SEI-92-TR-7 ..... p 137 N93-10447 #
CMU/SEI-92-TR-8 ..... p 138 N93-10665 #
CMU/SEI-92-TR-9 ..... p 137 N93-10448 #

CONF-9106236-3 ..... p 28 N93-10391 #
CONF-9108140-3 ..... p 168 N93-10733 #
CONF-9109345-2 ..... p 175 N93-10788 #
CONF-9110388-1 ..... p 129 N93-10628 #
CONF-9201107-2 ..... p 157 N93-10862 #
CONF-920113-7 ..... p 154 N93-10402 #
CONF-9202107-1 ..... p 131 N93-10626 #
CONF-920299-3 ..... p 74 N93-10731 #
CONF-920305-12 ..... p 167 N93-10403 #
CONF-920311-12 ..... p 160 N93-10326 #
CONF-920311-19 ..... p 163 N93-10759 #
CONF-920311-20 ..... p 160 N93-10293 #
CONF-9203159-2 ..... p 156 N93-10732 #
CONF-9203159-3 ..... p 153 N93-10332 #
CONF-9203160-1 ..... p 129 N93-10461 #
CONF-9203167-1 ..... p 170 N93-10787 #
CONF-920362-34 ..... p 161 N93-10393 #
CONF-9204106-6 ..... p 139 N93-10816 #
CONF-9204144-2 ..... p 130 N93-10834 #
CONF-9204146-3 ..... p 161 N93-10443 #
CONF-9204164-1 ..... p 128 N93-10283 #
CONF-920444-30 ..... p 156 N93-10762 #
CONF-9205123-5 ..... p 104 N93-10729 #
CONF-920515-11 ..... p 155 N93-10333 #
CONF-920515-22 ..... p 156 N93-10643 #
CONF-920515-4 ..... p 72 N93-10279 #
CONF-920574-1 ..... p 89 N93-10429 #
CONF-920574-5 ..... p 154 N93-10730 #
CONF-920584-18 ..... p 102 N93-10625 #
CONF-920584-20 ..... p 42 N93-10329 #
CONF-920610-10 ..... p 163 N93-10760 #
CONF-920610-4 ..... p 161 N93-10392 #
CONF-920610-5 ..... p 162 N93-10619 #
CONF-920610-7 ..... p 163 N93-10620 #
CONF-920610-8 ..... p 161 N93-10463 #
CONF-9206164-1 ..... p 171 N93-10270 #
CONF-9206173-4 ..... p 92 N93-10634 #
CONF-9206179-2 ..... p 68 N93-10394 #
CONF-9206184-2 ..... p 103 N93-10763 #
CONF-9206185-2 ..... p 141 N93-10334 #
CONF-9206185-5 ..... p 139 N93-10866 #

CONF-9206214-1 ..... p 155 N93-10863 #
CONF-920631-39-PT-2 ..... p 94 N93-10327 #
CONF-920671-5 ..... p 76 N93-10836 #
CONF-920677-15 ..... p 163 N93-10645 #
CONF-9207100-1 ..... p 172 N93-10396 #
CONF-920713-1 ..... p 76 N93-10831 #
CONF-920717-1 ..... p 160 N93-10390 #
CONF-920732-3 ..... p 91 N93-10381 #
CONF-920762-3 ..... p 34 N93-10789 #
CONF-920792-8 ..... p 157 N93-10837 #
CONF-920801-3 ..... p 103 N93-10383 #
CONF-920801-8 ..... p 75 N93-10786 #
CONF-920819-18 ..... p 168 N93-10623 #
CONF-920852-3 ..... p 36 N93-10399 #

CPIA-PUBL-580-VOL-1 ..... p 15 N93-10001

CS-92-10 ..... p 135 N93-10212 #
CS-92-23 ..... p 140 N93-10213 #

CSU-TR-67 ..... p 36 N93-10243 #

CTN-91-60130 ..... p 67 N93-10111
CTN-92-60345 ..... p 192 N93-10640
CTN-92-60352 ..... p 142 N93-10641 #
CTN-92-60356 ..... p 68 N93-10366 #
CTN-92-60362 ..... p 10 N93-10374
CTN-92-60365 ..... p 91 N93-10367
CTN-92-60388 ..... p 147 N93-10642 #
CTN-92-60390 ..... p 72 N93-10368
CTN-92-60512 ..... p 44 N93-10466
CTN-92-60513 ..... p 1 N93-10651 #
CTN-92-60514 ..... p 2 N93-10652 #
CTN-92-60515 ..... p 66 N93-10653 #
CTN-92-60571 ..... p 192 N93-10654 #
CTN-92-60572 ..... p 193 N93-10655 #
CTN-92-60590 ..... p 1 N93-10644
CTN-92-60593 ..... p 135 N93-10088

DE92-011151 ..... p 36 N93-10399 #
DE92-011856 ..... p 128 N93-10621 #
DE92-011888 ..... p 91 N93-10622 #
DE92-012240 ..... p 155 N93-10878 #
DE92-013399 ..... p 171 N93-10270 #
DE92-013510 ..... p 131 N93-10626 #
DE92-014232 ..... p 160 N93-10326 #
DE92-014429 ..... p 102 N93-10625 #
DE92-014462 ..... p 91 N93-10381 #
DE92-014468 ..... p 89 N93-10429 #
DE92-014592 ..... p 168 N93-10623 #
DE92-014738 ..... p 39 N93-10627 #
DE92-014739 ..... p 87 N93-10083 #
DE92-014745 ..... p 80 N93-10330 #
DE92-014804 ..... p 172 N93-10396 #
DE92-014809 ..... p 30 N93-10400 #
DE92-014815 ..... p 35 N93-10082 #
DE92-014935 ..... p 171 N93-10382 #
DE92-014947 ..... p 103 N93-10383 #
DE92-014955 ..... p 104 N93-10384 #
DE92-015003 ..... p 72 N93-10279 #
DE92-015034 ..... p 94 N93-10327 #
DE92-015048 ..... p 42 N93-10329 #
DE92-015116 ..... p 43 N93-10397 #
DE92-015117 ..... p 44 N93-10398 #
DE92-015118 ..... p 35 N93-10084 #
DE92-015122 ..... p 30 N93-10401 #
DE92-015240 ..... p 155 N93-10333 #
DE92-015244 ..... p 129 N93-10628 #
DE92-015273 ..... p 76 N93-10831 #
DE92-015483 ..... p 82 N93-10629 #
DE92-015661 ..... p 168 N93-10630 #
DE92-015674 ..... p 154 N93-10606 #
DE92-015686 ..... p 174 N93-10607 #
DE92-015760 ..... p 130 N93-10834 #
DE92-015762 ..... p 104 N93-10729 #
DE92-015783 ..... p 31 N93-10460 #
DE92-015841 ..... p 154 N93-10730 #
DE92-015842 ..... p 74 N93-10731 #
DE92-015847 ..... p 129 N93-10461 #
DE92-015850 ..... p 156 N93-10732 #
DE92-015919 ..... p 130 N93-10835 #
DE92-015930 ..... p 168 N93-10733 #
DE92-016023 ..... p 156 N93-10462 #
DE92-016101 ..... p 128 N93-10283 #
DE92-016114 ..... p 43 N93-10608 #
DE92-016116 ..... p 41 N93-10216 #
DE92-016152 ..... p 160 N93-10390 #
DE92-016179 ..... p 170 N93-10604 #
DE92-016181 ..... p 154 N93-10605 #
DE92-016195 ..... p 192 N93-10616 #
DE92-016197 ..... p 153 N93-10291 #
DE92-016199 ..... p 89 N93-10611 #
DE92-016218 ..... p 162 N93-10617 #
DE92-016219 ..... p 156 N93-10618 #
DE92-016222 ..... p 166 N93-10284 #
DE92-016233 ..... p 161 N93-10443 #
DE92-016234 ..... p 28 N93-10391 #
DE92-016247 ..... p 160 N93-10293 #
DE92-016249 ..... p 163 N93-10759 #
DE92-016250 ..... p 163 N93-10760 #
DE92-016252 ..... p 161 N93-10392 #
DE92-016255 ..... p 162 N93-10619 #
DE92-016256 ..... p 163 N93-10620 #
DE92-016257 ..... p 161 N93-10463 #
DE92-016258 ..... p 161 N93-10393 #
DE92-016274 ..... p 162 N93-10464 #
DE92-016294 ..... p 160 N93-10331 #
DE92-016297 ..... p 167 N93-10609 #
DE92-016461 ..... p 170 N93-10434 #
DE92-016525 ..... p 153 N93-10332 #
DE92-016548 ..... p 68 N93-10394 #
DE92-016572 ..... p 163 N93-10761 #
DE92-016597 ..... p 82 N93-10612 #
DE92-016610 ..... p 164 N93-10861 #
DE92-016699 ..... p 163 N93-10645 #
DE92-016714 ..... p 137 N93-10631 #
DE92-016746 ..... p 90 N93-10739 #
DE92-016810 ..... p 75 N93-10786 #
DE92-016829 ..... p 141 N93-10334 #
DE92-016835 ..... p 40 N93-10632 #
DE92-016852 ..... p 170 N93-10787 #
DE92-016860 ..... p 156 N93-10643 #
DE92-016861 ..... p 156 N93-10633 #
DE92-016884 ..... p 175 N93-10788 #
DE92-016903 ..... p 34 N93-10789 #
DE92-016917 ..... p 33 N93-10411 #
DE92-016920 ..... p 86 N93-10444 #
DE92-016928 ..... p 75 N93-10790 #
DE92-016939 ..... p 154 N93-10402 #
DE92-016943 ..... p 156 N93-10762 #
DE92-016965 ..... p 157 N93-10862 #
DE92-016974 ..... p 31 N93-10436 #
DE92-017001 ..... p 167 N93-10403 #
DE92-017017 ..... p 155 N93-10863 #
DE92-017018 ..... p 90 N93-10864 #
DE92-017025 ..... p 70 N93-10865 #
DE92-017051 ..... p 139 N93-10866 #
DE92-017055 ..... p 76 N93-10836 #
DE92-017063 ..... p 157 N93-10837 #
DE92-017131 ..... p 92 N93-10634 #
DE92-017137 ..... p 92 N93-10635 #
DE92-017161 ..... p 139 N93-10816 #
DE92-017300 ..... p 154 N93-10435 #
DE92-017310 ..... p 95 N93-10646 #
DE92-017316 ..... p 33 N93-10395 #
DE92-017345 ..... p 164 N93-10839 #
DE92-017399 ..... p 155 N93-10840 #
DE92-017595 ..... p 176 N93-10867 #
DE92-017805 ..... p 143 N93-10285 #
DE92-017864 ..... p 139 N93-10817 #
DE92-017980 ..... p 157 N93-10838 #
DE92-018003 ..... p 103 N93-10763 #
DE92-018038 ..... p 84 N93-10868 #
DE92-018057 ..... p 159 N93-10818 #
DE92-018190 ..... p 164 N93-10819 #
DE92-018236 ..... p 154 N93-10820 #
DE92-531066 ..... p 36 N93-10287 #
DE92-624593 ..... p 153 N93-10328 #
DE92-626845 ..... p 144 N93-10624 #
DE92-630203 ..... p 95 N93-10385 #
DE92-630205 ..... p 170 N93-10386 #
DE92-630206 ..... p 170 N93-10387 #
DE92-630207 ..... p 170 N93-10388 #
DE92-630230 ..... p 144 N93-10389 #
DE92-634160 ..... p 130 N93-10222 #
DE92-634877 ..... p 165 N93-10225 #
DE92-634888 ..... p 169 N93-10226 #
DE92-634889 ..... p 169 N93-10229 #
DE92-634890 ..... p 170 N93-10294 #
DE92-634892 ..... p 170 N93-10295 #
DE92-634923 ..... p 179 N93-10296 #

DNA-TR-91-162 ..... p 69 N93-10657 #

DODA-AR-006-678 ..... p 3 N93-10342 #
DODA-AR-006-744 ..... p 67 N93-10199 #
DODA-AR-006-928 ..... p 67 N93-10203 #

DOE/CE-23810/2A ..... p 43 N93-10397 #
DOE/CE-23810/2B ..... p 44 N93-10398 #
DOE/CE-23810/2C ..... p 35 N93-10084 #
DOE/CE-23810/2G ..... p 30 N93-10401 #
DOE/CE-90029/8 ..... p 82 N93-10612 #

DOE/DP-0098T ..... p 91 N93-10622 #

DOE/EIA-0149(91) ..... p 174 N93-10607 #

DOE/ER-0550T ..... p 162 N93-10464 #
DOE/ER-13549/6 ..... p 154 N93-10435 #
DOE/ER-13569/7 ..... p 30 N93-10400 #
DOE/ER-13582/6 ..... p 31 N93-10436 #
DOE/ER-13687/8 ..... p 170 N93-10787 #
DOE/ER-13789/5 ..... p 166 N93-10284 #
DOE/ER-13881/T1 ..... p 89 N93-10611 #
DOE/ER-20021/2 ..... p 130 N93-10835 #
DOE/ER-40107/11(B) ..... p 155 N93-10878 #
DOE/ER-40150/192 ..... p 157 N93-10862 #
DOE/ER-40214/1 ..... p 154 N93-10605 #
DOE/ER-40231/16 ..... p 155 N93-10840 #
DOE/ER-40272/153 ..... p 192 N93-10616 #
DOE/ER-40272/155 ..... p 153 N93-10291 #
DOE/ER-40272/158 ..... p 170 N93-10434 #
DOE/ER-40362/5 ..... p 157 N93-10838 #
DOE/ER-40688/1 ..... p 156 N93-10618 #
DOE/ER-40702/1 ..... p 154 N93-10606 #
DOE/ER-45081/T1 ..... p 168 N93-10630 #
DOE/ER-45167/7 ..... p 40 N93-10632 #
DOE/ER-45293/5 ..... p 33 N93-10395 #
DOE/ER-54087/T1 ..... p 162 N93-10617 #
DOE/ER-54109/T3 ..... p 160 N93-10331 #
DOE/ER-60981/2 ..... p 128 N93-10621 #

DOE/ET-53088/551 ..... p 170 N93-10604 #
DOE/ET-53088/558 ..... p 156 N93-10643 #
DOE/ET-53088/559 ..... p 156 N93-10633 #

DOE/ID-12735/T23 ..... p 164 N93-10819 #

DOE/MC-28130/92/C0020 ..... p 102 N93-10625 #

DOE/METC-C/92/7017 ..... p 42 N93-10329 #

DOE/PC-88948/T15 ..... p 82 N93-10629 #
DOE/PC-89761/T6 ..... p 31 N93-10460 #
DOE/PC-89876/T12 ..... p 43 N93-10608 #
DOE/PC-89876/T14 ..... p 41 N93-10216 #
DOE/PC-90274/T17 ..... p 164 N93-10861 #

DOE/PETC-TR/92/7 ..... p 80 N93-10330 #

DOT-VNTSC-FAA-92-4 ..... p 6 N93-10065 #

DOT/FAA/AM-92/12 ..... p 132 N93-10321 #

DOT/FAA/CT-TN90/59 ..... p 7 N93-10833 #
DOT/FAA/CT-TN92/16 ..... p 7 N93-10459 #

DOT/FAA/CT-91-23-VOL-2-PT-2 p 28 N93-10325 #

DOT/FAA/RD-90/19 ..... p 6 N93-10323 #
DOT/FAA/RD-92/4 ..... p 6 N93-10065 #

DOT/FAA/SE-92/6 ..... p 7 N93-10738 #

DREA-CR-89-433 ..... p 68 N93-10366 #
DREA-CR-90-445 ..... p 147 N93-10642 #

DSPH-2 ..... p 141 N93-10299 #

DTRC/SME-CR-19-90 ..... p 41 N93-10783 #

E-6850 ..... p 26 N93-10743 * #
E-6873 ..... p 25 N93-10197 * #
E-7178 ..... p 25 N93-10457 * #
E-7183 ..... p 95 N93-10455 * #
E-7241 ..... p 79 N93-10087 * #
E-7246 ..... p 25 N93-10086 * #
E-7248 ..... p 82 N93-10735 * #
E-7250 ..... p 96 N93-10777 * #
E-7254 ..... p 95 N93-10453 * #
E-7284 ..... p 26 N93-10734 * #
E-7300 ..... p 9 N93-10456 * #
E-7310 ..... p 81 N93-10454 * #
E-7343 ..... p 13 N93-10841 * #

EGG-GEO-10274 ..... p 84 N93-10868 #

EGG-WTD-9876 ..... p 139 N93-10817 #

EGG-10617-1208 ..... p 176 N93-10867 #

EPA/450/4-91/032-VOL-3 ..... p 171 N93-10257 #
EPA/600/A-92/116 ..... p 104 N93-10256 * #
EPA/600/A-92/139 ..... p 126 N93-10433 #
EPA/600/R-92/036 ..... p 7 N93-10442 #
EPA/600/R-92/067 ..... p 105 N93-10432 #
EPA/600/8-91/011B ..... p 131 N93-10438 #

ERL-0596-RE ..... p 67 N93-10203 #

ESA-PSS-01-30-ISSUE-2 ..... p 94 N93-10317 #
ESA-PSS-05-02-ISSUE-1 ..... p 136 N93-10315 #
ESA-PSS-05-03-ISSUE-1 ..... p 136 N93-10316 #

ESA-SP-344 ..... p 179 N93-10901 #

ESD-TR-91-092 ..... p 74 N93-10718 #

ESD-TR-91-14 ..... p 135 N93-10104 #
ESD-TR-91-250 ..... p 87 N93-10218 #
ESD-TR-92-009 ..... p 137 N93-10448 #
ESD-TR-92-10 ..... p 67 N93-10253 #
ESD-TR-92-5 ..... p 136 N93-10298 #
ESD-TR-92-8 ..... p 138 N93-10665 #

ESD-92-TR-007 ..... p 137 N93-10447 #
ESD-92-TR-1 ..... p 136 N93-10300 #
ESD-92-TR-3 ..... p 135 N93-10214 #

ESL-TR-88-74 ..... p 125 N93-10784 #

ETDE/JP-MF-92531066 ..... p 36 N93-10287 #

ETN-92-91967 ..... p 136 N93-10315 #
ETN-92-91968 ..... p 136 N93-10316 #
ETN-92-91969 ..... p 94 N93-10317 #
ETN-92-92166 ..... p 77 N93-10050 #
ETN-92-92167 ..... p 179 N93-10901 #
ETN-92-92176 ..... p 83 N93-10859 #

FASTC-ID(RS)T-0745-91 ..... p 145 N93-10857 #
FASTC-ID(RS)T-0784-91 ..... p 13 N93-10705 #
FASTC-ID(RS)T-0786-91 ..... p 5 N93-10856 #
FASTC-ID(RS)T-0788-91 ..... p 5 N93-10858 #
FASTC-ID(RS)T-0789-91 ..... p 4 N93-10707 #
FASTC-ID(RS)T-0919-91 ..... p 33 N93-10706 #
FASTC-ID(RS)T-1476-90 ..... p 74 N93-10702 #
FASTC-ID(RS)T-1477-90 ..... p 89 N93-10722 #
FASTC-ID(RS)T-1478-90 ..... p 89 N93-10703 #

FEMP-2265 ..... p 172 N93-10396 #

FSGTR-NC-150 ..... p 104 N93-10289 #

FTD-ID(RS)T-0544-91 ..... p 10 N93-10704 #
FTD-ID(RS)T-0545-91 ..... p 27 N93-10813 #
FTD-ID(RS)T-0571-91 ..... p 26 N93-10721 #
FTD-ID(RS)T-0847-90 ..... p 90 N93-10855 #
FTD-ID(RS)T-1274-90 ..... p 69 N93-10701 #
FTD-ID(RS)T-1431-90 ..... p 159 N93-10812 #
FTD-ID(RS)T-1471-90 ..... p 12 N93-10814 #

F1776 ..... p 76 N93-10882 #

GA-A-20846 ..... p 163 N93-10761 #
GA-A-20873 ..... p 160 N93-10390 #
GA-A-20881 ..... p 161 N93-10393 #
GA-A-20899 ..... p 160 N93-10326 #
GA-A-20901 ..... p 160 N93-10293 #
GA-A-20904 ..... p 163 N93-10759 #
GA-A-20909 ..... p 161 N93-10392 #
GA-A-20912 ..... p 162 N93-10619 #
GA-A-20913 ..... p 163 N93-10620 #
GA-A-20917 ..... p 161 N93-10463 #
GA-A-20935 ..... p 163 N93-10760 #

GAO/IMTEC-92-39 ..... p 12 N93-10081 #

GIS-TM-3 ..... p 7 N93-10442 #

GRI-91/0025 ..... p 37 N93-10439 #
GRI-92/0051 ..... p 169 N93-10249 #
GRI-92/0136 ..... p 81 N93-10449 #
GRI-92/0213 ..... p 31 N93-10437 #

GTEC-21-5854-1 ..... p 9 N93-10348 * #

HDL-TM-92-9 ..... p 71 N93-10255 #

HVE-171-92 ..... p 136 N93-10237 #

IAEA-TECDOC-645 ..... p 130 N93-10222 #

IC-91/332 ..... p 144 N93-10389 #
IC-91/337 ..... p 95 N93-10385 #
IC-91/368 ..... p 170 N93-10386 #
IC-91/382 ..... p 170 N93-10387 #
IC-91/394 ..... p 170 N93-10388 #
IC-92/41 ..... p 179 N93-10296 #
IC-92/46 ..... p 165 N93-10225 #

ICASE-92-35 ..... p 2 N93-10097 * #
ICASE-92-40 ..... p 145 N93-10758 * #
ICASE-92-42 ..... p 82 N93-10757 * #
ICASE-92-43 ..... p 83 N93-10808 * #

ICOMP-92-14 ..... p 82 N93-10735 * #
ICOMP-92-16 ..... p 81 N93-10454 * #

IDA-P-2609 ..... p 133 N93-10719 #

IDA/HQ-91-39384 ..... p 133 N93-10719 #

IFSR-551 ..... p 170 N93-10604 #

IFSR-558 ..... p 156 N93-10643 #
IFSR-559 ..... p 156 N93-10633 #

IFVE-OEF-91-88 ..... p 153 N93-10328 #

INPE-5295-PRE/1650 ..... p 157 N93-10311 #
INPE-5312-PRE/1709 ..... p 102 N93-10373 #
INPE-5338-PRE/1737 ..... p 153 N93-10312 #
INPE-5363-PUD/049 ..... p 102 N93-10063 #
INPE-5376-TDI/471 ..... p 94 N93-10310 #

INT-PATENT-CLASS-B29C-41/18 p 72 N93-10368
INT-PATENT-CLASS-B62D-5/12 . p 91 N93-10367
INT-PATENT-CLASS-B64C-13/00 p 10 N93-10374
INT-PATENT-CLASS-B64C-17/00 p 10 N93-10374
INT-PATENT-CLASS-B64D-27/08 p 10 N93-10374

INT-PATENT-CLASS-C12N-5/02 . p 129 N93-10109 *
INT-PATENT-CLASS-C12N-5/02 . p 129 N93-10110 *

INT-PATENT-CLASS-G01R-31/02 p 125 N93-10108 *
INT-PATENT-CLASS-G01W-1/00 p 125 N93-10108 *

INT-PATENT-CLASS-H01M-12/00 p 72 N93-10368
INT-PATENT-CLASS-H01M-4/04 p 72 N93-10368
INT-PATENT-CLASS-H01Q-25/00 p 67 N93-10111
INT-PATENT-CLASS-H01Q-3/40 . p 67 N93-10111

IS-T-1533 ..... p 167 N93-10609 #

ISBN-0-309-04732-3 ..... p 1 N93-10647 * #
ISBN-0-8330-1168-5 ..... p 75 N93-10792 #
ISBN-0-86960-888-6 ..... p 144 N93-10624 #
ISBN-0920049-03 ..... p 44 N93-10466
ISBN-92-835-0667-7 ..... p 148 N93-10666 #
ISBN-92-835-0681-2 ..... p 172 N93-10593 #
ISBN-92-835-0682-0 ..... p 174 N93-10610 #
ISBN-92-9092-218-4 ..... p 179 N93-10901 #

JHU/APL-TG-1383 ..... p 75 N93-10785 #

L-16976 ..... p 4 N93-10824 * #
L-17021 ..... p 2 N93-10071 * #
L-17041 ..... p 10 N93-10070 * #
L-17062 ..... p 13 N93-10744 * #
L-17135-PT-2 ..... p 37 N93-10578 * #

LA-UR-92-1642 ..... p 155 N93-10333 #
LA-UR-92-1722 ..... p 129 N93-10628 #

LA-12281-PR ..... p 156 N93-10462 #

LBL-PUB-3097 ..... p 86 N93-10444 #
LBL-PUB-5335 ..... p 90 N93-10864 #

LBL-31970 ..... p 70 N93-10865 #
LBL-32164 ..... p 167 N93-10403 #
LBL-32185 ..... p 33 N93-10411 #
LBL-32218 ..... p 75 N93-10790 #
LBL-32317 ..... p 156 N93-10762 #
LBL-32405 ..... p 155 N93-10863 #

LC-92-64197 ..... p 1 N93-10647 * #

LESC-29702 ..... p 14 N93-10960 * #

LPI-CONTRIB-790 ..... p 105 N93-10112 * #

LPI-TR-92-05 ..... p 189 N93-10064 * #

M-699 ..... p 33 N93-10072 * #

MHD-ITC-92-033 ..... p 164 N93-10861 #

MIT-TR-885 ..... p 74 N93-10718 #

MRC-R-1358 ..... p 69 N93-10657 #

MTI-R91-004 ..... p 140 N93-10219 #

MTR-92B0000090 ..... p 70 N93-10091 #

NAS 1.15:102705 ..... p 3 N93-10349 * #
NAS 1.15:103848 ..... p 28 N93-10742 * #
NAS 1.15:103872 ..... p 11 N93-10741 * #
NAS 1.15:103896 ..... p 7 N93-10745 * #
NAS 1.15:105761 ..... p 25 N93-10457 * #
NAS 1.15:105766 ..... p 95 N93-10455 * #
NAS 1.15:105799 ..... p 25 N93-10197 * #
NAS 1.15:105810 ..... p 79 N93-10087 * #
NAS 1.15:105817 ..... p 82 N93-10735 * #
NAS 1.15:105819 ..... p 96 N93-10777 * #
NAS 1.15:105823 ..... p 95 N93-10453 * #
NAS 1.15:105841 ..... p 26 N93-10734 * #
NAS 1.15:105852 ..... p 9 N93-10456 * #
NAS 1.15:105854 ..... p 81 N93-10454 * #
NAS 1.15:105880 ..... p 13 N93-10841 * #
NAS 1.15:107551 ..... p 129 N93-10085 * #
NAS 1.15:107995 ..... p 178 N93-10067 * #
NAS 1.15:108003 ..... p 176 N93-10872 * #
NAS 1.15:108004 ..... p 175 N93-10815 * #
NAS 1.15:108005 ..... p 134 N93-10890 * #
NAS 1.15:108009 ..... p 70 N93-10800 * #
NAS 1.15:108373 ..... p 104 N93-10809 * #
NAS 1.15:4338 ..... p 10 N93-10070 * #
NAS 1.15:4361 ..... p 2 N93-10071 * #
NAS 1.15:4395 ..... p 189 N93-10832 * #
NAS 1.21:7011(360) ..... p 130 N93-10076 *
NAS 1.21:7011(364) ..... p 130 N93-10077 *
NAS 1.21:7011(365) ..... p 130 N93-10075 *
NAS 1.21:7011(366) ..... p 130 N93-10079 *
NAS 1.21:7011(367) ..... p 130 N93-10080 *
NAS 1.21:7037(274) ..... p 1 N93-10351 *
NAS 1.21:7037(276) ..... p 1 N93-10073 *
NAS 1.21:7037(279) ..... p 1 N93-10074 *
NAS 1.21:7037(281) ..... p 1 N93-10352 *
NAS 1.21:7039(41)-SECT-1 ..... p 171 N93-10078 *
NAS 1.26:177598 ..... p 147 N93-10458 * #
NAS 1.26:180824 ..... p 9 N93-10348 * #
NAS 1.26:184062 ..... p 25 N93-10350 * #
NAS 1.26:184464 ..... p 26 N93-10756 * #
NAS 1.26:185698 ..... p 14 N93-10960 * #
NAS 1.26:189217 ..... p 25 N93-10086 * #
NAS 1.26:189685 ..... p 2 N93-10097 * #
NAS 1.26:189695 ..... p 145 N93-10758 * #
NAS 1.26:189697 ..... p 82 N93-10757 * #
NAS 1.26:189708 ..... p 83 N93-10808 * #
NAS 1.26:190343 ..... p 127 N93-10848 * #
NAS 1.26:190643 ..... p 172 N93-10451 * #
NAS 1.26:190645 ..... p 172 N93-10452 * #
NAS 1.26:190662 ..... p 104 N93-10256 * #
NAS 1.26:190663 ..... p 94 N93-10372 * #
NAS 1.26:190677 ..... p 105 N93-10112 * #
NAS 1.26:190692 ..... p 2 N93-10098 * #
NAS 1.26:190730 ..... p 189 N93-10064 * #
NAS 1.26:190746 ..... p 92 N93-10891 * #
NAS 1.26:190747 ..... p 138 N93-10736 * #
NAS 1.26:190748 ..... p 13 N93-10737 * #
NAS 1.26:190818 ..... p 32 N93-10852 * #
NAS 1.26:190843 ..... p 159 N93-10066 * #
NAS 1.26:190911 ..... p 2 N93-10069 * #
NAS 1.26:190913 ..... p 128 N93-10068 * #
NAS 1.26:190918 ..... p 1 N93-10647 * #
NAS 1.55:3162-PT-2 ..... p 37 N93-10578 * #
NAS 1.60:3212 ..... p 4 N93-10824 * #
NAS 1.60:3223 ..... p 26 N93-10743 * #
NAS 1.60:3246 ..... p 13 N93-10744 * #
NAS 1.60:3288 ..... p 33 N93-10072 * #

NASA-CASE-MFS-26102-2-CU .... p 125 N93-10108 *

NASA-CASE-MSC-21293-2 ..... p 129 N93-10109 *
NASA-CASE-MSC-21294-2 ..... p 129 N93-10110 *

NASA-CP-3162-PT-2 ..... p 37 N93-10578 * #

NASA-CR-177598 ..... p 147 N93-10458 * #
NASA-CR-180824 ..... p 9 N93-10348 * #
NASA-CR-184062 ..... p 25 N93-10350 * #
NASA-CR-184464 ..... p 26 N93-10756 * #
NASA-CR-185698 ..... p 14 N93-10960 * #
NASA-CR-189217 ..... p 25 N93-10086 * #
NASA-CR-189685 ..... p 2 N93-10097 * #
NASA-CR-189695 ..... p 145 N93-10758 * #
NASA-CR-189697 ..... p 82 N93-10757 * #
NASA-CR-189708 ..... p 83 N93-10808 * #
NASA-CR-190343 ..... p 127 N93-10848 * #
NASA-CR-190643 ..... p 172 N93-10451 * #
NASA-CR-190645 ..... p 172 N93-10452 * #
NASA-CR-190662 ..... p 104 N93-10256 * #
NASA-CR-190663 ..... p 94 N93-10372 * #
NASA-CR-190677 ..... p 105 N93-10112 * #
NASA-CR-190692 ..... p 2 N93-10098 * #
NASA-CR-190730 ..... p 189 N93-10064 * #
NASA-CR-190746 ..... p 92 N93-10891 * #
NASA-CR-190747 ..... p 138 N93-10736 * #
NASA-CR-190748 ..... p 13 N93-10737 * #
NASA-CR-190818 ..... p 32 N93-10852 * #
NASA-CR-190843 ..... p 159 N93-10066 * #
NASA-CR-190911 ..... p 2 N93-10069 * #
NASA-CR-190913 ..... p 128 N93-10068 * #
NASA-CR-190918 ..... p 1 N93-10647 * #

NASA-SP-7011(360) ..... p 130 N93-10076 *
NASA-SP-7011(364) ..... p 130 N93-10077 *
NASA-SP-7011(365) ..... p 130 N93-10075 *
NASA-SP-7011(366) ..... p 130 N93-10079 *
NASA-SP-7011(367) ..... p 130 N93-10080 *
NASA-SP-7037(274) ..... p 1 N93-10351 *
NASA-SP-7037(276) ..... p 1 N93-10073 *
NASA-SP-7037(279) ..... p 1 N93-10074 *
NASA-SP-7037(281) ..... p 1 N93-10352 *

NASA-SP-7039(41)-SECT-1 ..... p 171 N93-10078 *

NASA-TM-102705 ..... p 3 N93-10349 * #
NASA-TM-103848 ..... p 28 N93-10742 * #
NASA-TM-103872 ..... p 11 N93-10741 * #
NASA-TM-103896 ..... p 7 N93-10745 * #
NASA-TM-105761 ..... p 25 N93-10457 * #
NASA-TM-105766 ..... p 95 N93-10455 * #
NASA-TM-105799 ..... p 25 N93-10197 * #
NASA-TM-105810 ..... p 79 N93-10087 * #
NASA-TM-105817 ..... p 82 N93-10735 * #
NASA-TM-105819 ..... p 96 N93-10777 * #
NASA-TM-105823 ..... p 95 N93-10453 * #
NASA-TM-105841 ..... p 26 N93-10734 * #
NASA-TM-105852 ..... p 9 N93-10456 * #
NASA-TM-105854 ..... p 81 N93-10454 * #
NASA-TM-105880 ..... p 13 N93-10841 * #
NASA-TM-107551 ..... p 129 N93-10085 * #
NASA-TM-107995 ..... p 178 N93-10067 * #
NASA-TM-108003 ..... p 176 N93-10872 * #
NASA-TM-108004 ..... p 175 N93-10815 * #
NASA-TM-108005 ..... p 134 N93-10890 * #
NASA-TM-108009 ..... p 70 N93-10800 * #
NASA-TM-108373 ..... p 104 N93-10809 * #
NASA-TM-4338 ..... p 10 N93-10070 * #
NASA-TM-4361 ..... p 2 N93-10071 * #
NASA-TM-4395 ..... p 189 N93-10832 * #

NASA-TP-3212 ..... p 4 N93-10824 * #
NASA-TP-3223 ..... p 26 N93-10743 * #
NASA-TP-3246 ..... p 13 N93-10744 * #
NASA-TP-3288 ..... p 33 N93-10072 * #

NAVSWCMP91-644 ..... p 71 N93-10241 #

NCEL-CR-92001 ..... p 144 N93-10639 #

NIST-TR-13 ..... p 40 N93-10778 #
NIST-TR-14 ..... p 35 N93-10231 #

NIST/SP-835 ..... p 125 N93-10089 #

NISTIR-3990 ..... p 69 N93-10440 #
NISTIR-4766 ..... p 142 N93-10450 #
NISTIR-4845 ..... p 136 N93-10248 #
NISTIR-4848 ..... p 137 N93-10441 #

NOAA-ATLAS-9 ..... p 126 N93-10337 #

NOSC/TR-1479 ..... p 77 N93-10897 #

NRAD-TD-2277 ..... p 146 N93-10208 #
NRAD-TD-2282 ..... p 140 N93-10209 #

NRL-9370-PT-3 ..... p 143 N93-10275 #

NRL/MR/4440-92-6998 ..... p 164 N93-10099 #
NRL/MR/4790-92-6983 ..... p 70 N93-10215 #
NRL/MR/5510-92-6997 ..... p 141 N93-10269 #
NRL/MR/6385-92-7102 ..... p 27 N93-10272 #

NSSDC/WDC-A-R/S-92-05 ..... p 70 N93-10800 * #

NSWCDD/TR-92/241 ..... p 147 N93-10869 #

NTIA-92-283 ..... p 69 N93-10430 #

NWC-TP-7207 ..... p 79 N93-10297 #

OHEA-E-367 ..... p 131 N93-10438 #

ONERA-RSF-21/3419-AY-126 ..... p 83 N93-10859 #

ORA-TR-89-5443-04 ..... p 142 N93-10641 #

ORNL-CCIP-92-05 ..... p 153 N93-10332 #

ORNL/SUB-90-SB688/1 ..... p 35 N93-10082 #

ORNL/TM-12061 ..... p 171 N93-10382 #
ORNL/TM-12126 ..... p 143 N93-10285 #

ORNL/TR-91/39 ..... p 39 N93-10627 #

PATENT-1-265-236 ..... p 67 N93-10111

PB92-158880 ..... p 190 N93-10771 #
PB92-162346 ..... p 105 N93-10772 #
PB92-169358 ..... p 7 N93-10442 #
PB92-170380 ..... p 190 N93-10773 #
PB92-170398 ..... p 190 N93-10774 #
PB92-177062 ..... p 190 N93-10775 #
PB92-177070 ..... p 190 N93-10776 #
PB92-188820 ..... p 104 N93-10256 * #
PB92-189216 ..... p 104 N93-10289 #
PB92-190263 ..... p 171 N93-10257 #
PB92-190354 ..... p 169 N93-10249 #
PB92-191246 ..... p 136 N93-10248 #
PB92-192202 ..... p 105 N93-10432 #
PB92-195569 ..... p 172 N93-10431 #
PB92-195999 ..... p 126 N93-10433 #
PB92-196070 ..... p 137 N93-10441 #
PB92-197136 ..... p 6 N93-10065 #
PB92-199421 ..... p 134 N93-10341 #
PB92-201102 ..... p 125 N93-10089 #
PB92-203892 ..... p 126 N93-10337 #
PB92-204403 ..... p 81 N93-10449 #
PB92-205400 ..... p 69 N93-10440 #
PB92-205418 ..... p 142 N93-10450 #
PB92-205665 ..... p 131 N93-10438 #
PB92-211481 ..... p 31 N93-10437 #
PB92-212984 ..... p 37 N93-10439 #

PEL-309 ..... p 144 N93-10624 #

PETC-2-2-91 ..... p 43 N93-10608 #
PETC-2-5-91 ..... p 41 N93-10216 #

PFC/RR-92-6 ..... p 160 N93-10331 #

PL-TR-91-1082 ..... p 166 N93-10345 #
PL-TR-91-3089 ..... p 42 N93-10268 #
PL-TR-91-3111 ..... p 26 N93-10638 #
PL-TR-92-3035 ..... p 25 N93-10258 #

PNL-SA-20917 ..... p 104 N93-10729 #
PNL-SA-21039 ..... p 130 N93-10834 #

R/D-6291-EE-01 ..... p 165 N93-10235 #

RAE-TM-AERO-2201 ..... p 153 N93-10805 #

RAE-TM-FM-26 ..... p 8 N93-10803 #

RAE-TM-MAT/STR-1139 ..... p 34 N93-10802 #

RAE-TR-89057 ..... p 94 N93-10198 #

RAND/R-4088-PL ..... p 75 N93-10792 #
RAND/R-4199-AF ..... p 8 N93-10420 #

REPT-026247-1-F ..... p 67 N93-10223 #

RFP-4571 ..... p 171 N93-10270 #

RIACS-TR-92-16 ..... p 138 N93-10736 * #

RL-TR-91-351 ..... p 159 N93-10724 #
RL-TR-91-415 ..... p 172 N93-10428 #
RL-TR-91-433 ..... p 68 N93-10358 #
RL-TR-91-437 ..... p 158 N93-10693 #
RL-TR-92-106 ..... p 74 N93-10715 #
RL-TR-92-11 ..... p 72 N93-10357 #
RL-TR-92-183 ..... p 76 N93-10882 #
RL-TR-92-29 ..... p 125 N93-10714 #
RL-TR-92-2 ..... p 87 N93-10211 #
RL-TR-92-42-VOL-1 ..... p 68 N93-10301 #
RL-TR-92-42-VOL-2 ..... p 68 N93-10302 #
RL-TR-92-47 ..... p 154 N93-10362 #
RL-TR-92-78 ..... p 158 N93-10360 #
RL-TR-92-81 ..... p 169 N93-10764 #

RSRE-MEMO-4261 ..... p 139 N93-10806 #
RSRE-MEMO-4263 ..... p 175 N93-10821 #
RSRE-MEMO-4405 ..... p 147 N93-10822 #

RSRE-90001 ..... p 134 N93-10807 #
RSRE-90005 ..... p 139 N93-10823 #
RSRE-90011 ..... p 134 N93-10804 #
RSRE-90020 ..... p 175 N93-10801 #

SAND-91-1080C ..... p 28 N93-10391 #
SAND-91-2801C ..... p 103 N93-10383 #
SAND-92-0032C ..... p 139 N93-10866 #
SAND-92-0080C ..... p 72 N93-10279 #
SAND-92-0372C ..... p 76 N93-10836 #
SAND-92-0429C ..... p 36 N93-10399 #
SAND-92-0580 ..... p 164 N93-10839 #
SAND-92-0942C ..... p 161 N93-10443 #
SAND-92-1028C ..... p 94 N93-10327 #
SAND-92-1372C ..... p 68 N93-10394 #

SBIL-002 ..... p 30 N93-10416 #

SC-71039-TR ..... p 79 N93-10297 #

SCT-90-RR67 ..... p 6 N93-10323 #

SGD-569-PT-1 ..... p 190 N93-10771 #
SGD-570-PT-1 ..... p 190 N93-10773 #
SGD-570-PT-2 ..... p 190 N93-10774 #
SGD-571-PT-1 ..... p 190 N93-10775 #
SGD-572-PT-2 ..... p 190 N93-10776 #

SRL-0073-TM ..... p 67 N93-10199 #

SSD-TR-92-14 ..... p 29 N93-10263 #
SSD-TR-92-20 ..... p 42 N93-10336 #

SU-GL-4897 ..... p 168 N93-10726 #

SU-SLAC-396 ..... p 154 N93-10820 #

SU-TR-454 ..... p 146 N93-10700 #

TEC-R-155 ..... p 7 N93-10424 #
TEC-R-162 ..... p 127 N93-10780 #
TEC-R-165 ..... p 176 N93-10899 #
TEC-R-172 ..... p 6 N93-10265 #
TEC-R-178 ..... p 8 N93-10898 #

TR-0091(6940-07)-1 ..... p 29 N93-10263 #
TR-0091(6940-07)-2 ..... p 42 N93-10336 #
TR-13-REPT-1 ..... p 40 N93-10727 #
TR-15 ..... p 36 N93-10246 #
TR-172 ..... p 146 N93-10795 #
TR-18 ..... p 34 N93-10880 #
TR-1 ..... p 165 N93-10245 #
TR-29 ..... p 88 N93-10247 #
TR-42 ..... p 162 N93-10615 #
TR-43 ..... p 88 N93-10412 #
TR-44 ..... p 168 N93-10614 #
TR-45 ..... p 161 N93-10413 #
TR-45 ..... p 27 N93-10465 #
TR-46 ..... p 30 N93-10266 #
TR-46 ..... p 167 N93-10415 #
TR-47 ..... p 30 N93-10281 #
TR-47 ..... p 73 N93-10656 #
TR-48 ..... p 30 N93-10414 #
TR-48 ..... p 40 N93-10748 #
TR-76 ..... p 158 N93-10694 #
TR-90 ..... p 90 N93-10799 #
TR-91-1 ..... p 176 N93-10883 #
TR-950 ..... p 87 N93-10218 #

TSL-92-2 ..... p 82 N93-10629 #

T89036 ..... p 87 N93-10083 #

UCRL-CR-108745 ..... p 159 N93-10818 #

UCRL-ID-110480-VOL-A ..... p 90 N93-10739 #
UCRL-ID-110842 ..... p 92 N93-10635 #

UCRL-JC-110356 ..... p 103 N93-10763 #

UCRL-MA-110630 ..... p 95 N93-10646 #

UCRL-TT-108270 ..... p 87 N93-10083 #

UDR-TR-91-156 ..... p 29 N93-10101 #
UDR-TR-91-20 ..... p 42 N93-10268 #
UDR-TR-92-72 ..... p 35 N93-10221 #

UFIFT-HEP-92-10 ..... p 170 N93-10434 #
UFIFT-HEP-92-4 ..... p 153 N93-10291 #
UFIFT-HEP-92-6 ..... p 192 N93-10616 #

UMR-FDB-25 ..... p 31 N93-10794 #

URI-MSL-921 ..... p 33 N93-10717 #

US-PATENT-APPL-SN-213558 ..... p 129 N93-10110 *
US-PATENT-APPL-SN-213559 ..... p 129 N93-10109 *
US-PATENT-APPL-SN-410373 ..... p 143 N93-10959 #
US-PATENT-APPL-SN-545233 ..... p 129 N93-10109 *
US-PATENT-APPL-SN-579455 ..... p 67 N93-10096 #
US-PATENT-APPL-SN-687605 ..... p 129 N93-10110 *
US-PATENT-APPL-SN-722413 ..... p 142 N93-10958
US-PATENT-APPL-SN-776710 ..... p 125 N93-10108 *

US-PATENT-CLASS-324-72 ..... p 125 N93-10108 *
US-PATENT-CLASS-340-601 ..... p 125 N93-10108 *
US-PATENT-CLASS-343-797 ..... p 67 N93-10096 #
US-PATENT-CLASS-395-23 ..... p 143 N93-10959 #
US-PATENT-CLASS-395-24 ..... p 142 N93-10958
US-PATENT-CLASS-435-240.241 p 129 N93-10110 *
US-PATENT-CLASS-435-240.24 .. p 129 N93-10109 *
US-PATENT-CLASS-435-240.24 .. p 129 N93-10110 *
US-PATENT-CLASS-435-240.25 .. p 129 N93-10109 *
US-PATENT-CLASS-435-240.25 .. p 129 N93-10110 *
US-PATENT-CLASS-435-240.46 .. p 129 N93-10109 *
US-PATENT-CLASS-435-240.46 .. p 129 N93-10110 *
US-PATENT-CLASS-435-818 ..... p 129 N93-10110 *

US-PATENT-5,075,868 ..... p 143 N93-10959 #
US-PATENT-5,091,732 ..... p 67 N93-10096 #
US-PATENT-5,103,496 ..... p 142 N93-10958

US-PATENT-5,153,133 ..... p 129 N93-10110 *
US-PATENT-5,153,508 ..... p 125 N93-10108 *
US-PATENT-5,155,035 ..... p 129 N93-10109 *
US-PATENT-7,571,687 ..... p 125 N93-10108 *

UTK-92-3 ..... p 153 N93-10332 #

UW-ME-91-002 ..... p 27 N93-10277 #

VKI-LS-1992-05 ..... p 77 N93-10050 #

WES/MP/GL-92-11 ..... p 66 N93-10710 #

WGD-12523-CE ..... p 76 N93-10888 #

WIS-PH-91-63 ..... p 169 N93-10226 #
WIS-PH-92-13 ..... p 170 N93-10294 #
WIS-PH-92-1 ..... p 169 N93-10229 #
WIS-PH-92-6 ..... p 170 N93-10295 #

WL-TM-92-332 ..... p 4 N93-10753 #

WL-TP-92-006 ..... p 73 N93-10421 #

WL-TR-91-4032-VOL-2-PT-2 ..... p 28 N93-10325 #
WL-TR-91-4059 ..... p 36 N93-10343 #
WL-TR-92-1050 ..... p 69 N93-10695 #
WL-TR-92-2017 ..... p 29 N93-10101 #
WL-TR-92-3018 ..... p 81 N93-10410 #
WL-TR-92-7016 ..... p 87 N93-10090 #

WL/MN-TR-91-76 ..... p 12 N93-10106 #
WL/MN-TR-91-83 ..... p 138 N93-10746 #

WSRC-MS-92-154 ..... p 137 N93-10631 #

WSU/92/89 ..... p 164 N93-10093 #
WSU/92/90 ..... p 90 N93-10799 #

Appendix

NASA SCIENTIFIC AND TECHNICAL INFORMATION PROGRAM PRODUCTS AND SERVICES

The NASA Scientific and Technical Information (STI) Program provides for the collection and announcement of aerospace-related reports and literature obtained worldwide through agreements and exchanges. The result of the collection is the comprehensive NASA STI Database that covers aeronautics, space, and supporting disciplines.

The STI Database, documents generated or obtained by NASA, and products and services derived from or supporting the database are made available to the NASA research community and to the public. Descriptions and sources of these items are presented in the following pages.

Scientific and Technical Aerospace Reports (*STAR*) is an abstract journal, listing citations with abstracts for aerospace-related reports obtained from worldwide sources. *STAR* is issued on the first of each month, and announces current documents that have been entered into the NASA STI Database during the previous month. The reports are of the following types:

- NASA, NASA contractor, and NASA grantee reports;
- Reports issued by other U.S. Government agencies, domestic and foreign institutions, universities, and private firms;
- Translations in report form;
- NASA-owned patents and patent applications;
- Other U.S. Government agency and foreign patents and patent applications;
- Domestic and foreign dissertations and theses.

Journal, book, and conference literature, journal translations, and certain foreign dissertations having the same subject scope as *STAR* are announced in a companion journal, *International Aerospace Abstracts* (*IAA*). *IAA* is issued on the 1st and 15th of each month and is available from the American Institute of Aeronautics and Astronautics, Technical Information Service, 555 West 57th Street, 12th Floor, New York, NY 10019.

ELIGIBILITY AND REGISTRATION FOR NASA STI PRODUCTS AND SERVICES

Organizations of the type listed below that have registered with NASA can receive products and services.

- NASA offices and installations, contractors, subcontractors, grantees, and consultants;
- Other U.S. Government agencies and their contractors;
- Libraries in the United States that have arrangements with NASA to maintain collections of NASA documents for public reference;
- Other organizations in the United States having a need for NASA documents in work related to aeronautics and space research;
- Organizations abroad that have established reciprocal documents exchange arrangements with NASA.

The central service points — central points of document acquisition and control within qualified organizations — or individuals are eligible to register for NASA STI products and services. Domestic organizations or individuals may be eligible to receive various classes of NASA publications and services and should address their requests for registration or further information to:

NASA Center for AeroSpace Information
ATTN: Registration Services
P.O. Box 8757
Baltimore, MD 21240-0757
301-621-0390

Organizations abroad should direct requests to:

National Aeronautics and Space Administration
Scientific and Technical Information Program (JTT)
International STI Program
Washington, DC 20546-0001
USA
703-271-5640

SUBJECT SCOPE

The subject scope of *STAR* and *IAA* includes all aspects of aeronautics and space research and development, supporting basic and applied research, and applications. Aerospace aspects of Earth resources, energy development, conservation, oceanography, environmental protection, urban transportation, and other topics of high national priority are also covered.

HOW TO USE *STAR* SUBJECT CATEGORIES

Abstracts in *STAR* are categorized by 10 major subject divisions that are divided further into 76 specific subject categories. The subject divisions and categories are listed in the Table of Contents together with a note for each that defines its scope and provides any cross-references. For example:

16 SPACE TRANSPORTATION
Includes passenger and cargo space transportation, e.g., shuttle operations; and space rescue techniques. For related information see also *03 Air Transportation and Safety* and *18 Spacecraft Design, Testing and Performance.* For space suits see *54 Man/System Technology and Life Support.*

CROSS-REFERENCES

Individual *STAR* abstracts are not ordinarily cross-referenced, except for certain conference reports or book translations that have had separate abstracts written for their component papers or chapters. Citations and abstracts of the components follow immediately after those of the parent document. When the subject content of a component differs sufficiently from the general content of the parent, a cross-reference citation also is printed at the end of the category to which it normally would have been assigned if it were independent.

DOCUMENTS ON MICROFICHE

Documents available on microfiche are designated by a pound sign (#) following the accession number.

LIMITED REPRODUCIBILITY

A note of limited reproducibility appears in the citation, if there are factors affecting the reproducibility of more than 20% of the document. These factors include faint or broken type, color photographs, black and white photographs, foldouts, dot matrix print, or some other factor that limits the reproducibility of the document. This notation also appears on the microfiche header.

COLOR COPIES

An increasing number of NASA scientific and technical reports are being produced with color graphs, charts, illustrations, and photographs. An indication that a document has color pages follows the source and pricing (SAP) information in the *STAR* citation.

Registered users of the NASA Scientific and Technical Information Program will receive ordered documents with color at no additional cost, as long as stock copies of the document are available. Otherwise, an additional fee of $2.00 per color page will be charged. The NASA Center for AeroSpace Information staff will contact registered users to determine individual user's needs.

NASA PATENTS AND PATENT APPLICATIONS

Patents and patent applications owned by NASA are announced in *STAR* under appropriate subject categories and are referenced in the *STAR* indexes. In the Report/Accession Number Index, patents are indexed by the NASA Case Number, and the U.S. Patent Class. Patent applications are indexed by the NASA Case Number and the U.S. Patent Application Serial Number.

Printed copies of patents (which are not microfiched) are available for purchase from the U.S. Patent and Trademark Office.

When ordering patents, the U.S. Patent Number should be used, and payment must be remitted in advance, by money order or check payable to the Commissioner of Patents and Trademarks. Prepaid purchase coupons for ordering are also available from the U.S. Patent and Trademark Office.

NASA patent application specifications are sold in both paper copy and microfiche by the NASA Center for AeroSpace Information (CASI). The N accession number should be used in ordering either paper copy or microfiche from CASI.

The patents and patent applications announced in *STAR* are owned by NASA and are available for royalty-free licensing. Requests for licensing terms and further information should be addressed to:

National Aeronautics and Space Administration
Associate General Counsel for Intellectual Property
Code GP
Washington, DC 20546-0001

SOURCES FOR DOCUMENTS

One or more sources from which a document announced in *STAR* is available to the public is given in each citation. The most commonly indicated sources and their acronyms or abbreviations are listed below, and their addresses are listed on page A-6. If the publication is available from a source other than those listed, the publisher and address will be displayed on the availability line or in combination with the corporate source line.

Avail: CASI. Sold by the NASA Center for AeroSpace Information. Prices for hard copy (HC) and microfiche (MF) are indicated by a price code following the letters HC or MF in the *STAR* citation. Current values for the price codes are given in the tables on page A-7.

NOTE ON ORDERING DOCUMENTS: When ordering publications from CASI, use the N accession number or other report number. It is also advisable to cite the title and other bibliographic identification.

Avail: SOD (or GPO). Sold by the Superintendent of Documents, U.S. Government Printing Office, in hard copy.

Avail: BLL (formerly NLL): British Library Lending Division, Boston Spa, Wetherby, Yorkshire, England. Photocopies available from this organization at the price shown. (If none is given, address inquiry to the BLL.)

Avail: DOE Depository Libraries. Organizations in U.S. cities and abroad that maintain collections of Department of Energy reports, usually in microfiche form, are listed in *Energy Research Abstracts.* Services available from the DOE and its depositories are described in a booklet, *DOE Technical Information Center - Its Functions and Services* (TID-4660), which may be obtained without charge from the DOE Technical Information Center.

Avail: ESDU. Pricing information on specific data, computer programs, and details on Engineering Sciences Data Unit (ESDU) topic categories can be obtained from ESDU International Ltd. Requesters in North America should use the Virginia address while all other requesters should use the London address, both of which are on page A-6.

Avail: Fachinformationszentrum, Karlsruhe. Gesellschaft für wissenschaftlich-technische Information mbH 7514 Eggenstein-Leopoldshafen 2, Germany.

Avail: HMSO. Publications of Her Majesty's Stationery Office are sold in the U.S. by Pendragon House, Inc. (PHI), Redwood City, CA. The U.S. price (including a service and mailing charge) is given, or a conversion table may be obtained from PHI.

Avail: Issuing Activity, or Corporate Author, or no indication of availability. Inquiries as to the availability of these documents should be addressed to the organization shown in the citation as the corporate author of the document.

Avail: NASA Public Document Rooms. Documents so indicated may be examined at or purchased from the National Aeronautics and Space Administration (JBD-4), Public Documents Room (Room 1H23), Washington, DC 20546-0001, or public document rooms located at NASA installations, and the NASA Pasadena Office at the Jet Propulsion Laboratory.

Avail: NTIS. Sold by the National Technical Information Service. Initially distributed microfiche under the NTIS SRIM (Selected Research in Microfiche) are available. For information concerning this service, consult the NTIS Subscription Section, Springfield, VA 22161.

Avail: Univ. Microfilms. Documents so indicated are dissertations selected from *Dissertation Abstracts* and are sold by University Microfilms as xerographic copy (HC) and microfilm. All requests should cite the author and the Order Number as they appear in the citation.

Avail: US Patent and Trademark Office. Sold by Commissioner of Patents and Trademarks, U.S. Patent and Trademark Office, at the standard price of $1.50 each, postage free. (See discussion of NASA patents and patent applications on page A-3.)

Avail: (US Sales Only). These foreign documents are available to users within the United States from the National Technical Information Service (NTIS). They are available to users outside the United States through the International Nuclear Information Service (INIS) representative in their country, or by applying directly to the issuing organization.

Avail: USGS. Originals of many reports from the U.S. Geological Survey, which may contain color illustrations, or otherwise may not have the quality of illustrations preserved in the microfiche or facsimile reproduction, may be examined by the public at the libraries of the USGS field offices whose addresses are listed on page A-6. The libraries may be queried concerning the availability of specific documents and the possible utilization of local copying services, such as color reproduction.

FEDERAL DEPOSITORY LIBRARIES: To provide the general public with greater access to U.S. Government publications, Congress established the Federal Depository Library Program under the Government Printing Office (GPO), with 53 regional depositories responsible for permanent retention of material, inter-library loan, and reference services. (These libraries are not sales outlets.) At least one copy of nearly every NASA and NASA-sponsored publication, either in printed or microfiche format, is received and retained by the 53 regional depositories. A list of the regional GPO libraries, appears on page A-8. A local library can contact a regional depository library to help locate specific reports, or direct contact may be made by an individual.

PUBLIC COLLECTION OF NASA DOCUMENTS

An extensive collection of NASA and NASA-sponsored publications is maintianed by the British Library Lending Divison, Boston Spa, Wetherby, Yorkshire, England, for public access. The British Library Lending Division also has available many of the non-NASA publications cited in *STAR*.

European requesters may purchase facsimile copy or microfiche of NASA and NASA-sponsored documents, those identified by both the symbols # and * from ESA—Information Retrieval Service, European Space Agency, 8-10 rue Mario-Nikis, 75738 Paris CEDEX 15, France.

SUBMITTING DOCUMENTS

All users of this abstract service are urged to forward reports to be considered for announcement in *STAR*. This will aid NASA in its efforts to provide the fullest possible coverage of all scientific and technical publications that might support aeronautics and space research and development. If you have prepared relevant reports (other than those you will transmit to NASA, DOD, or DOE through the usual contract- or grant-reporting channels), please send them for consideration to the NASA Center for AeroSpace Information, P.O. Box 8757, Baltimore, MD 21240-0757.

Reprints of journal articles, book chapters, and conference papers are also welcome. These will be considered for announcement in *STAR*'s companion journal, *IAA*.

You may specify a particular source to be included in a report announcement if you wish; otherwise the report will be placed on a public sale at the NASA Center for AeroSpace Information. Copyrighted publications will be announced but not distributed or sold.

PURCHASE OF *STAR*

STAR is publicly available on annual subscription from the NASA Center for AeroSpace Information (CASI) at $114.00.

STAR is available to registered users on annual subscription from the NASA Center for AeroSpace Information, ATTN: Registration Services, P.O. Box 8757, Baltimore, MD 21240-0757.

Microfiche of the abstract sections of *STAR* are available, on annual subscription, from CASI. Annual subscription rates are $216.00 North America; $432.00 foreign.

ADDRESSES OF ORGANIZATIONS

American Institute of Aeronautics and Astronautics
Technical Information Service
555 West 57th Street, 12th Floor
New York, New York 10019

British Library Lending Division,
Boston Spa, Wetherby, Yorkshire,
England

Commissioner of Patents and Trademarks
U.S. Patent and Trademark Office
Washington, DC 20231

Department of Energy
Technical Information Center
P.O. Box 62
Oak Ridge, Tennessee 37830

European Space Agency-Information Retrieval Service
ESRIN
Via Galileo Galilei
00044 Frascati (Rome) Italy

Engineering Sciences Data Unit International
P.O. Box 1633
Manassas, Virginia 22110

Engineering Sciences Data Unit International, Ltd.
251-259 Regent Street
London, W1R 7AD, England

Fachinformationszentrum Karlsruhe
Gesellschaft für wissenschaftlich-technische
Information mbH
7514 Eggenstein-Leopoldshafen 2, Germany

Her Majesty's Stationery Office
P.O. Box 569, S.E. 1
London, England

NASA Center for AeroSpace Information
P.O. Box 8757
Baltimore, Maryland 21240-0757

National Aeronautics and Space Administration
Scientific and Technical Information Program (JTT)
Washington, DC 20546-0001

National Technical Information Service
5285 Port Royal Road
Springfield, Virginia 22161

Pendragon House, Inc.
899 Broadway Avenue
Redwood City, California 94063

Superintendent of Documents
U.S. Government Printing Office
Washington, DC 20402

University Microfilms
A Xerox Company
300 North Zeeb Road
Ann Arbor, Michigan 48106

University Microfilms, Ltd.
Tylers Green
London, England

U.S. Geological Survey Library National Center
MS 950
12201 Sunrise Valley Drive
Reston, Virginia 22092

U.S. Geological Survey Library
2255 North Gemini Drive
Flagstaff, Arizona 86001

U.S. Geological Survey
345 Middlefield Road
Menlo Park, California 94025

U.S. Geological Survey Library
Box 25046
Denver Federal Center, MS914
Denver, Colorado 80225

CASI PRICE TABLES

(Effective October 1, 1992)

STANDARD PRICE DOCUMENTS

PRICE CODE	NORTH AMERICAN PRICE	FOREIGN PRICE
A01	$ 9.00	$ 18.00
A02	12.50	25.00
A03	17.00	34.00
A04-A05	19.00	38.00
A06-A09	26.00	52.00
A10-A13	35.00	70.00
A14-A17	43.00	86.00
A18-A21	50.00	100.00
A22-A25	59.00	118.00
A99	69.00	138.00

MICROFICHE

PRICE CODE	NORTH AMERICAN PRICE	FOREIGN PRICE
A01	$ 9.00	$ 18.00
A02	12.50	25.00
A03	17.00	34.00
A04	19.00	38.00
A06	26.00	52.00
A10	35.00	70.00

IMPORTANT NOTICE

CASI Shipping and Handling Charges
U.S. — ADD $3.00 per TOTAL ORDER
Canada and Mexico — ADD $3.50 per TOTAL ORDER
All Other Countries — ADD $7.50 per TOTAL ORDER
Does NOT apply to orders
requesting CASI RUSH HANDLING.
Contact CASI for charge.

FEDERAL REGIONAL DEPOSITORY LIBRARIES

ALABAMA

AUBURN UNIV. AT MONTGOMERY LIBRARY
Documents Dept.
7300 University Drive
Montgomery, AL 36117-3596
(205) 244-3650 FAX: (205) 244-0678

UNIV. OF ALABAMA
Amelia Gayle Gorgas Library
Govt. Documents
Box 870266
Tuscaloosa, AL 35487-0266
(205) 348-6046 FAX: (205) 348-8833

ARIZONA

DEPT. OF LIBRARY, ARCHIVES, AND PUBLIC RECORDS
Federal Documents
Third Floor State Capitol
1700 West Washington
Phoenix, AZ 85007
(602) 542-4121 FAX: (602) 542-4400; 542-4500

ARKANSAS

ARKANSAS STATE LIBRARY
State Library Services
One Capitol Mall
Little Rock, AR 72201.
(501) 682-2869

CALIFORNIA

CALIFORNIA STATE LIBRARY
Govt. Publications Section
914 Capitol Mall - P.O. Box 942837
Sacramento, CA 94237-0001
(916) 322-4572 FAX: (916) 324-8120

COLORADO

UNIV. OF COLORADO - BOULDER
Norlin Library
Govt. Publications
Campus Box 184
Boulder, CO 80309-0184
(303) 492-8834 FAX: (303) 492-2185

DENVER PUBLIC LIBRARY
Govt. Publications Dept. BS/GPD
1357 Broadway
Denver, CO 80203
(303) 571-2135

CONNECTICUT

CONNECTICUT STATE LIBRARY
231 Capitol Avenue
Hartford, CT 06106
(203) 566-4971 FAX: (203) 566-3322

FLORIDA

UNIV. OF FLORIDA LIBRARIES
Documents Dept.
Library West
Gainesville, FL 32611-2048
(904) 392-0366 FAX: (904) 392-7251

GEORGIA

UNIV. OF GEORGIA LIBRARIES
Govt. Documents Dept.
Jackson Street
Athens, GA 30602
(404) 542-8949 FAX: (404) 542-6522

HAWAII

UNIV. OF HAWAII
Hamilton Library
Govt. Documents Collection
2550 The Mall
Honolulu, HI 96822
(808) 948-8230 FAX: (808) 956-5968

IDAHO

UNIV. OF IDAHO LIBRARY
Documents Section
Moscow, ID 83843
(208) 885-6344 FAX: (208) 885-6817

ILLINOIS

ILLINOIS STATE LIBRARY
Reference Dept.
300 South Second
Springfield, IL 62701-1796
(217) 782-7596 FAX: (217) 524-0041

INDIANA

INDIANA STATE LIBRARY
Serials/Documents Section
140 North Senate Avenue
Indianapolis, IN 46204
(317) 232-3678 FAX: (317) 232-3728

IOWA

UNIV. OF IOWA LIBRARIES
Govt. Publications Dept.
Washington & Madison Streets
Iowa City, IA 52242
(319) 335-5926 FAX: (319) 335-5830

KANSAS

UNIV. OF KANSAS
Govt. Documents & Map Library
6001 Malott Hall
Lawrence, KS 66045-2800
(913) 864-4660 FAX: (913) 864-5380

KENTUCKY

UNIV. OF KENTUCKY LIBRARIES
Govt. Publications/Maps Dept.
Lexington, KY 40506-0039
(606) 257-3139 FAX: (606) 257-1563; 257-8379

LOUISIANA

LOUISIANA STATE UNIV.
Middleton Library
Govt. Documents Dept.
Baton Rouge, LA 70803
(504) 388-2570 FAX: (504) 388-6992

LOUISIANA TECHNICAL UNIV.
Prescott Memorial Library
Govt. Documents Dept.
305 Wisteria Street
Ruston, LA 71270-9985
(318) 257-4962 FAX: (318) 257-2447

MAINE

TRI-STATE DOCUMENTS DEPOSITORY
Raymond H. Fogler Library
Govt. Documents & Microforms Dept.
Univ. of Maine
Orono, ME 04469
(207) 581-1680

MARYLAND

UNIV. OF MARYLAND
Hornbake Library
Govt. Documents/Maps Unit
College Park, MD 20742
(301) 454-3034 FAX: (301) 454-4985

MASSACHUSETTS

BOSTON PUBLIC LIBRARY
Govt. Documents Dept.
666 Boylston Street
Boston, MA 02117
(617) 536-5400 ext. 226
FAX: (617) 267-8273; 267-8248

MICHIGAN

DETROIT PUBLIC LIBRARY
5201 Woodward Avenue
Detroit, MI 48202-4093
(313) 833-1440; 833-1409
FAX: (313) 833-5039

LIBRARY OF MICHIGAN
Govt. Documents Unit
P.O. Box 30007
Lansing, MI 48909
(517) 373-0640 FAX: (517) 373-3381

MINNESOTA

UNIV. OF MINNESOTA
Wilson Library
Govt. Publications Library
309 19th Avenue South
Minneapolis, MN 55455
(612) 624-5073 FAX: (612) 626-9353

MISSISSIPPI

UNIV. OF MISSISSIPPI
J.D. Williams Library
Federal Documents Dept.
106 Old Gym Bldg.
University, MS 38677
(601) 232-5857 FAX: (601) 232-5453

MISSOURI

UNIV. OF MISSOURI - COLUMBIA
Ellis Library
Govt. Documents
Columbia, MO 65201
(314) 882-6733 FAX: (314) 882-8044

MONTANA

UNIV. OF MONTANA
Maureen & Mike Mansfield Library
Documents Div.
Missoula, MT 59812-1195
(406) 243-6700 FAX: (406) 243-2060

NEBRASKA

UNIV. OF NEBRASKA - LINCOLN
D.L. Love Memorial Library
Documents Dept.
Lincoln, NE 68588
(402) 472-2562

NEVADA

UNIV. OF NEVADA
Reno Library
Govt. Publications Dept.
Reno, NV 89557
(702) 784-6579 FAX: (702) 784-1751

NEW JERSEY

NEWARK PUBLIC LIBRARY
U.S. Documents Div.
5 Washington Street -
P.O. Box 630
Newark, NJ 07101-0630
(201) 733-7812 FAX: (201) 733-5648

NEW MEXICO

UNIV. OF NEW MEXICO
General Library
Govt. Publications Dept.
Albuquerque, NM 87131-1466
(505) 277-5441 FAX: (505) 277-6019

NEW MEXICO STATE LIBRARY
325 Don Gaspar Avenue
Santa Fe, NM 87503
(505) 827-3826 FAX: (505) 827-3820

NEW YORK

NEW YORK STATE LIBRARY
Documents/Gift & Exchange Section
Federal Depository Program
Cultural Education Center
Albany, NY 12230
(518) 474-5563 FAX: (518) 474-5786

NORTH CAROLINA

UNIV. OF NORTH CAROLINA - CHAPEL HILL
CB#3912, Davis Library
BA/SS Dept.—Documents
Chapel Hill, NC 27599
(919) 962-1151 FAX: (919) 962-0484

NORTH DAKOTA

NORTH DAKOTA STATE UNIV. LIBRARY
Documents Office
Fargo, ND 58105
(701) 237-8886 FAX: (701) 237-7138
In cooperation with Univ. of North Dakota, Chester Fritz Library
Grand Forks

OHIO

STATE LIBRARY OF OHIO
Documents Dept.
65 South Front Street
Columbus, OH 43266
(614) 644-7051 FAX: (614) 752-9178

OKLAHOMA

OKLAHOMA DEPT. OF LIBRARIES
U.S. Govt. Information Div.
200 NE 18th Street
Oklahoma City, OK 73105-3298
(405) 521-2502, ext. 252, 253
FAX: (405) 525-7804

OKLAHOMA STATE UNIV.
Edmon Low Library
Documents Dept.
Stillwater, OK 74078
(405) 744-6546 FAX: (405) 744-5183

OREGON

PORTLAND STATE UNIV.
Millar Library
934 SW Harrison - P.O. Box 1151
Portland, OR 97207
(503) 725-3673 FAX: (503) 725-4527

PENNSYLVANIA

STATE LIBRARY OF PENN.
Govt. Publications Section
Walnut St. & Commonwealth Ave. -
P.O. Box 1601
Harrisburg, PA 17105
(717) 787-3752

SOUTH CAROLINA

CLEMSON UNIV.
Cooper Library
Public Documents Unit
Clemson, SC 29634-3001
(803) 656-5174 FAX: (803) 656-3025
In cooperation with Univ. of South Carolina, Thomas Cooper Library, Columbia

TENNESSEE

MEMPHIS STATE UNIV. LIBRARIES
Govt. Documents
Memphis, TN 38152
(901) 678-2586 FAX: (901) 678-2511

TEXAS

TEXAS STATE LIBRARY
United States Documents
P.O. Box 12927 - 1201 Brazos
Austin, TX 78711
(512) 463-5455 FAX: (512) 463-5436

TEXAS TECH. UNIV. LIBRARY
Documents Dept.
Lubbock, TX 79409
(806) 742-2268 FAX: (806) 742-1920

UTAH

UTAH STATE UNIV.
Merrill Library & Learning Resources Center, UMC-3000
Documents Dept.
Logan, UT 84322-3000
(801) 750-2684 FAX: (801) 750-2677

VIRGINIA

UNIV. OF VIRGINIA
Alderman Library
Govt. Documents
Charlottesville, VA 22903-2498
(804) 924-3133 FAX: (804) 924-4337

WASHINGTON

WASHINGTON STATE LIBRARY
Document Section
MS AJ-11
Olympia, WA 98504-0111
(206) 753-4027 FAX: (206) 753-3546

WEST VIRGINIA

WEST VIRGINIA UNIV. LIBRARY
Govt. Documents Section
P.O. Box 6069
Morgantown, WV 26506
(304) 293-3640

WISCONSIN

ST. HIST. SOC. OF WISCONSIN LIBRARY
Govt. Publications Section
816 State Street
Madison, WI 53706
(608) 262-2781 FAX: (608) 262-4711
In cooperation with Univ. of Wisconsin-Madison, Memorial Library

MILWAUKEE PUBLIC LIBRARY
Documents Div.
814 West Wisconsin Avenue
Milwaukee, WI 53233
(414) 278-2167 FAX: (414) 278-2137

* U.S. G.P.O.:1992-342-599:60025

National Aeronautics and
Space Administration
Code JTT
Washington, D.C.
20546-0001

Official Business
Penalty for Private Use, $300

SPECIAL FOURTH-CLASS RATE
POSTAGE & FEES PAID
NASA
PERMIT No. G27

NASA

POSTMASTER: If Undeliverable (Section 158
Postal Manual) Do Not Return